BOROX CATALYSIS:
A NEW FRONTIER IN CHIRAL BRØNSTED ACID CATALYSIS DERIVED FROM CHIRAL BORATE ANIONS

By

Anil Kumar Gupta

A DISSERTATION

Submitted to
Michigan State University
in partial fulfillment of the requirements
for the degree of

DOCTOR OF PHILOSOPHY

Chemistry

2012

ABSTRACT

BOROX CATALYSIS:
A NEW FRONTIER IN CHIRAL BRØNSTED ACID CATALYSIS DERIVED FROM CHIRAL BORATE ANIONS

By

Anil Kumar Gupta

In this doctoral research, focus has been on the development of the new chiral Brønsted acid catalysts, large-scale synthesis, novel reaction methodologies and understanding their mechanisms by experimental/computational analysis. In due course of time, a pool of unprecedented chiral Brønsted acid catalysts known to be "BOROX" catalysts, were prepared and characterized by NMR spectroscopy and X-ray analysis. These Wulff's BOROX catalysts were then employed on a variety of asymmetric reactions. In particular, the long-lasted problem of the alkyl aziridination has been solved by the development of the first multi-component aziridination reaction using the IMINO-BOROX catalyst. Out of the investigations regarding alkyl aziridination, a novel multi-component asymmetric [3+2] cycloaddition has also been developed. Additionally, an asymmetric epoxidation of aldehydes utilizing an unprecedented chiral SULFOX-BOROX catalyst has been successfully realized. By means of ^{1}H, ^{11}B NMR and computational analysis, the catalytic cycle of a Brønsted acid catalyzed reaction and its intermediates have been characterized using the Wulff aziridination reaction as the template. Interestingly, during this doctoral research, it has been found that the Brønsted acid catalysts derived from chiral borate anions are generated only upon the addition of a base. This was further supported by NMR spectroscopy, computational chemistry and X-ray analysis. Lastly, a

new mechanism has been examined for the imino-aldol reaction using computational chemistry. This mechanism supports the idea of a Lewis acid assisted Brønsted acid catalyzed reaction.

To,

My Family, Friends and Teachers

ACKNOWLEDGEMENTS

A life of a graduate student is full of experiences and mine is no different. A PhD degree is a result of the hard work, the dedication, and foremost the passion for the subject. However, it is impossible to discount the fact that it is one of the perfect examples where continuous support of several people contributes to the progress of one being and the science. I am really blessed in this regard. I would start my acknowledgement by thanking Professor Wulff, my research advisor, for providing an opportunity to work under his guidance. To me, he has always been one of the most simple person, I ever met. I could not have asked for a better person to be my mentor. His intellect, vision and desire to do different from others always inspired me to work hard. When I joined the group, the senior members of the group were in the process of graduating. Hence, I had to go to Dr. Wulff for any problems I had and I was really surprised to see how patiently he used to listen and always had some valuable suggestions to offer. One of the most important things in the Wulff group is the freedom offered by him. The freedom to pursue my own ideas and dreams has allowed me to learn a lot many things in different research areas. I really liked his approach as it provides an opportunity to grow as an independent researcher and to enhance one's creative thinking. Also, his thrust on the minute details about the experimental information has helped me to become a skillful scientist. I would like to thank him for all his teachings about life and chemistry during the last six years. Not only he taught chemistry, but also how to celebrate success and enjoy life in the graduate life. Further, he introduced me to one of the interesting additions to my life i.e. wine. He is real wine connoisseur and loves to share with others. He also introduced me to the Sex, the sparkling

wine. I think, no words can suffice my gratitude to him for being an amazing advisor and a person.

My other committee members were also quite supportive throughout my PhD life. Specially, Dr. Babak Borhan has been very helpful on many occasions. I think, it's the ease with which he let others to interact with him makes him a different person altogether. And, he is such kind of a person who always has a solution irrespective of the problem. I learnt a lot from him thorough personal interactions and of course his spectroscopy course. His continuous support has provided much needed inspiration to keep going at crucial phases of my PhD. Hence I would like to thank him for all his inputs. Although I did not get a chance to interact a lot with Prof. Maleckza, I still found him one of the best teachers and I really enjoyed his course CEM 956. I really appreciate him for his suggestions and recommendations. Also, I would like to thanks Prof. Odom for his suggestions during my second year oral and final oral exams. Although Dr. Jackson is not in my committee, he has been really phenomenal in passing the passion for the understanding the mechanisms of organic reactions to me. I am really thankful to him. I would like to thank Dr. Baker for his smile whenever I met him in the hallway.

I owe special thanks to Dr. Dan Holmes for his time during my NMR studies. He has been really nice to me all the time. I have really bugged him a lot and I dedicate all my NMR studies to him. I also thank Dr. Richard Staples for his efforts towards the determination of the structure and absolute stereochemistry of some of my compounds. Additionally, I thank Ms. Chen Lijun and Dr. Jones for the excellent service they provided at Mass facility at Michigan State University. A special thank to my friend and my collaborator Carmin Burrell. It was really fun working with her and she was phenomenal in finishing up the collaborative project in a short span of time. Also, I would like to thank Jeanne Basnight, staff in Department of

Chemistry at Michigan State University, for her care for me. It was always refreshing to talk about many things including her grandson's funny stories. I would like to take this opportunity to thank Dr. G. B. Bhattacharjee, my advisor in my Masters, for his teachings and guidance. Also, I would like to thanks Dr. Chad Lewis, professor at Cornell University, for being patient and giving me ample time to finish my thesis and giving me an opportunity to work with him as a postdoctoral associate.

I believe that the lab environment is very important for a healthy PhD life. I was fortunate enough to be part of a wonderful group. All past group members were awesome, especially Dr. Zhenjie Lu. She taught me many things during my initial time in the group. Dr. Alex Predesus and Dr. Kostas Rampalakos were really awesome lab mates. Dr. Zhensheng Ding was always the funniest face of the group. Also, I would like to thank Dr. Gang Hu for his suggestions and ideas about research. In the current group, I interacted a lot with Dr. Li Huang and Dr. Dymtro Berbasov. We had so many fruitful and not so fruitful discussions about chemistry, life, and many other silly things. I shared some very good moments with Dr. Li Huang and found her an exceptional chemist and human being. Dr. Dymtro Berbasov is one of the few people who are immensely talented and very nice at the same time. I would like to thank him for teaching me driving and for the parties we had together. Also, I owe a special thanks to Victor Prutyanov for his valuable teachings about computational chemistry. He taught me the minute details of theoretical chemistry. I really had good time with other current group members like Hong Ren, Wenjun Zhao, Xin Zhang, Dr. Yong Guan and Dr. Nilanjana Majumdar in the group meeting and the post-group meeting parties. Hong Ren is one of the most hard working persons, I know. The smile of Wenjun Zhao is always soothing. I really like the simplicity of Xin Zhang. Dr. Yong Guan has been a very good lab mate and very friendly in nature. I am

really grateful to all of them for making a great atmosphere in the lab. It was also wonderful to work with Dr. Mathew Vetticatt, postdoctoral associate, in the Wulff group. I would like to thank him for his help in the KIE studies and his suggestions regarding calculations. I am also thankful to Yubai Zhou and Xiaopeng Yin, new Wulff group members, for their enthusiasm.

Dr. Munmun Mukherjee and Wynter E. Osminski certainly deserve special thanks. Wynter Osminski, a fun person to talk, has always been a quiet admirer of all my silly jokes. She has been a wonderful person to work with and to have long discussions. Especially, I would like to thank her for celebrating my last birthday in East Lansing and for her time during HRMS analysis. I wish her all the best for everything. In the end, I would like to thank Dr. Munmun Mukherjee for everything she did for me for last six years. We moved from Indiana University together and since then she has been always there for me. She is exceptional lab mate, a very close friend and of course, a wonderful human being. I used to have so many long discussions about chemistry and there are many inputs from her in my dissertation. In her defense talk, she mentioned that I helped her even if she did not need it. But, I can say very easily that she always helped me as I always needed her help. I was fortunate to work with Dr. María Pascual and Dr. Roberto Morán-Ramallal, postdoctoral research associates from Spain, during their brief visit. I learned a lot from them. I am also thankful to my undergraduate students Charlie Najt and Leslie Bateman for their help in my research and for the wonderful time we spent together.

I am also fortunate to have lot of friends outside the Wulff Group. Dr. Aman Kulshrestha has been a long time friend and has helped on numerous occasions. Its hard to mention every occasion, yet, she was there for every time I needed her. Specifically, she gave a lot of time during my postdoctoral search. So a big thank to her for all she did for me in last six years. Also, I am thankful to my other friends, Kumar Ashtekar, Carmin Burrell, Camille Watson, Ipek

Yapici, Tanya Berbasova, Atefeh Garzan, Roozbeh Yousefi, Arvind Jaganathan, Dr. Mercy Anyika, Dr. Rahman Saleem, Dr. Luis Mori-Quiroz, Dr. Luis Sanchez and Damith Parera for making my life pleasant by their presence. Specifically, Kumar Ashtekar helped me on many occasions, be it my car related issues or research problems. I am also thankful to him for patiently listening to my crap even if he was busy. I am sure that I am going to miss the big smile of Camille Watson. Her smile has always been the source of inspiration especially in tough times during PhD. Dr. Rahman Saleem and Dr. Luis-Mori Quiroz have also been very close friends. I would like to thank my other friends, Dr. Rupinder Sayal, Puneet Kumar, Dr. Paramita Mukherjee, Krishna Chotnerru, Dr. Kelly Telu, Dr. Abhishek Singh and Dr. Vijoya Sa for their time and help. Also, I would like to thank my friend, Sara Bano for her help and support. Additionally, I am lucky to have numerous good friends from India. Dr. Manish Singh, Abhishek Singh, Sapna Gupta, Aishwarya Kar, Soumitra Kar and Dr. Aditi Singhal, have been really nice and supportive throughout these years. Additionally, I am really thankful to my close friend, Dr. Navratna Vajpai, for helping me in every possible way whenever I needed. It would have been very difficult without his support.

Last but not the least, I would like to thank my family. It's their continuous support and encouragement that helped me to travel so far in life. I owe special thanks to my dad, Ramesh Chandra Gupta and my mom, Maya Gupta. It would not have been possible without them. My brother, Sunil Gupta and sister in law, Gudiya Gupta have been always there when it mattered most. I am also thankful to Nikhil Gupta, my younger brother, for being my best buddy and for listening to all my sorrows in difficult times. Finally, I would like to thank God for being so kind and providing a chance to interact with so many nice people during my journey so far.

TABLE OF CONTENTS

LIST OF TABLES

LIST OF FIGURES

LIST OF SCHEMES

CHAPTER 1

CHIRAL BORATE ANIONS IN ASYMMETRIC BRØNSTED ACID CATALYSIS AND ASYMMETRIC COUNTERANION-DIRECTED CATALYSIS

You should never be ashamed of any reaction you did. A publication is like a movie. A classic movie is not understood completely the first time.

-William D. Wulff

1.1 Chiral anions in asymmetric catalysis and its different classes

Chiral compounds have always an immense impact on every aspect of chemistry. In organic synthesis, there are primarily three ways of synthesizing chiral compounds: chiral pool derived synthesis; chiral auxiliary mediated synthesis and asymmetric catalysis.[1] Nowadays, there are many different kinds of asymmetric catalysis using transition-metal complexes (organometallic catalysis), organic acids or bases/nucleophiles ("organocatalysis"), and enzymes (biocatalysis).[1e] Chiral induction is typically achieved through strongly directional chiral catalyst-substrate interactions. Mostly, these interactions are operating *via* covalent bonds or coordination bonds. They could also be the result of simple Lewis acid/base interactions. However, many reactions might proceed via charged intermediates. In these cases, chirality induction can be achieved either by employing the salt of a chiral cation and an achiral anion or vice versa. The former type of catalysis has been used in organic synthesis for a very long time in the form of phase transfer catalysis.[2] The latter type, which involves the usage of chiral counter-anions, has emerged more recently. Over the past few years, there has been amazing advance in the field of asymmetric catalysis mediated by chiral counter-anions.[3]

Asymmetric catalysis mediated by chiral counter-anions can be classified into five different classes based on the counter-cation and mode of catalysis (Table 1.1). The very first class (I) belongs to the field of asymmetric Brønsted acid catalysis (sometimes called as asymmetric Hydrogen-bond catalysis). The second class (II) comprises chiral counter-anions along with protonated achiral or chiral bases (mostly amine) as the cation. This class can either be included in asymmetric Brønsted acid catalysis or asymmetric counteranion-directed catalysis (sometimes called as asymmetric ion-pairing catalysis or anion binding catalysis) depending upon their catalytic function (see section 1.2). The remaining three classes can be brought under the asymmetric counteranion-directed catalysis. In class III, the ion-pair catalysts consist of chiral anions with achiral or chiral bases with no protons (for instance: tetra-alkylammonium ion). The remaining two classes (IV and V) consist of chiral counter-anions with a) metal only or b) metal with achiral or chiral ligands. The first example of chiral counteranions utilized in transition metal catalysis and organocatalysis were reported in 2000[4] and 2006[5] respectively.

Table 1.1 Different classes of catalysis involving chiral counter-anions[a]

Class	Anion	Counter Cation	Catalyst	Mode of Catalysis
I	X^{*-}	H^+	Brønsted acid	Brønsted acid catalysis
II	X^{*-}	$[B1\text{-}H]^+$ or $[B1^*\text{-}H]^+$	Brønsted acid or Ion-pair	Brønsted acid catalysis and/or ACDC
III	X^{*-}	$[B2]^+$ or $[B2^*]^+$	Ion-pair	ACDC
IV	X^{*-}	M^+	Ion-pair	ACDC in metal catalysis
V	X^{*-}	$M^+(L)$ or $M^+(L^*)$	Ion-pair	ACDC in metal catalysis

[a] X^{*-} = Chiral anion; B1 or B2 = Base; B1* or B2* = Chiral base; M = Metal; L = Ligand; L* = Chiral ligand; ACDC = Asymmetric Counteranion-Directed Catalysis

These chiral anions differ in structure and reactivity. As discussed above, they have been used in both asymmetric Brønsted acid catalysis and asymmetric counteranion-directed catalysis. A list of some of the chiral anions used in asymmetric catalysis is shown in Figure 1.1. The list includes carboxylate,[6] sulfonate,[6c,7] tetracoordinated phosphate,[5,8] disulfonimidate,[9] phosphoramidate,[10] hexacoordinated phosphate[11] and cobaltate[12] anions. More recently, there are reports showcasing the concept of supramolecular chiral anions.[13]

Figure 1.1 Chiral counter-anions used in asymmetric catalysis (blue: asymmetric Brønsted acid catalysis; red: asymmetric counteranion-directed catalysis). For interpretation of the references to color in this and all other figures, the reader is referred to the electronic version of this dissertation.

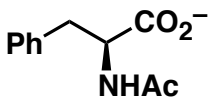

1

Milstein
J. Organomet. Chem. **2004**, *689*, 751

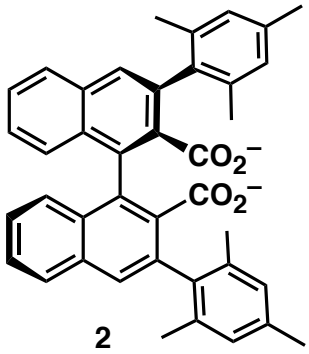

2

Maruoka
J. Am. Chem. Soc. **2007**, *129*, 10054
J. Am. Chem. Soc. **2008**, *130*, 14380

Carboxylate anions

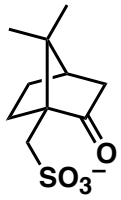

3

Milstein
J. Organomet. Chem. **2004**, *689*, 751

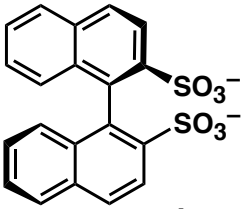

4

Isihara
J. Am. Chem. Soc. **2008**, *130*, 16858
Synlett **2011**, 1247

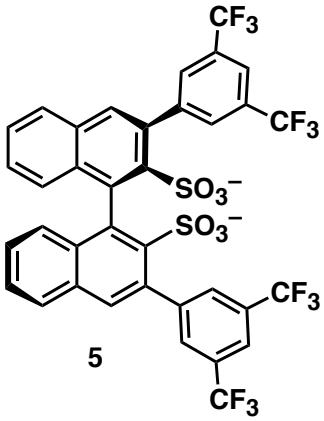

5

Toste
Angew. Chem. Int. Ed. **2010**, *49*, 598

Sulfonate anions

Figure 1.1
cont'd

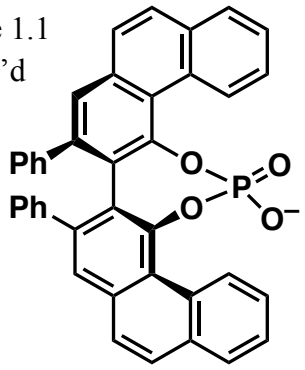

6

Antilla
J. Am. Chem. Soc. **2007**, *129*, 5830
J. Am. Chem. Soc. **2005**, *127*, 15696

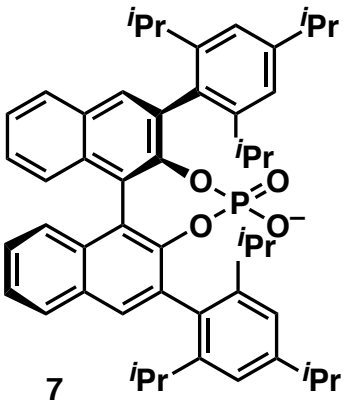

7

List *Angew. Chem. Int. Ed.* **2006**, *45*, 4193
List *J. Am. Chem. Soc.* **2006**, *128*, 13368
Toste *Science* **2007**, *317*, 496
List *Angew. Chem. Int. Ed.* **2010**, *49*, 628
List *Aldrichimica Acta* **2008**, *41*, 31

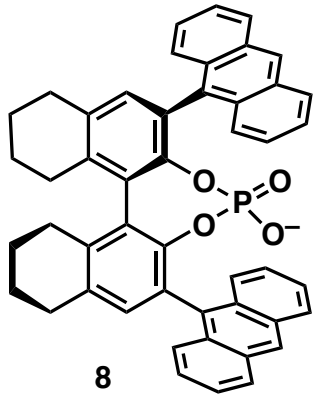

8

List *Chem. Commun.* **2011**, *47*, 10022.
Ding *Eur. J. Org. Chem.* **2011**, 110-116.

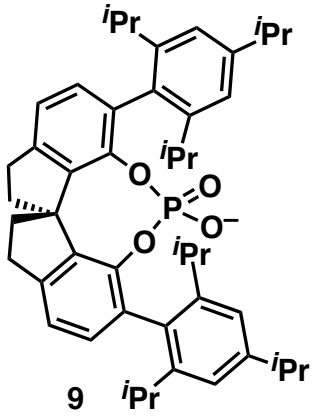

9

List *Chem. Commun.* **2011**, *47*, 10022.
List *J. Am. Chem. Soc.* **2010**, *132*, 17370

Tetracoordinated Phosphate anions

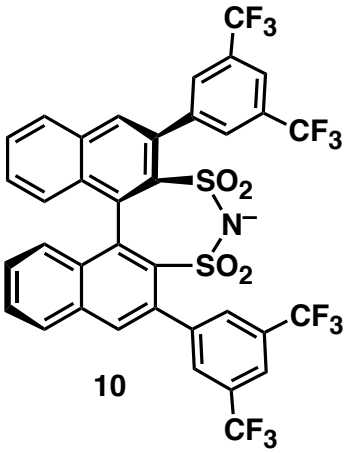

10

Disulfonimidate anion

List *Angew. Chem. Int. Ed.* **2009**, *48*, 4363
List *Angew. Chem. Int. Ed.* **2011**, *50*, 754
Lee *J. Org. Chem.* **2011**, *76*, 7141

Figure 1.1 cont'd

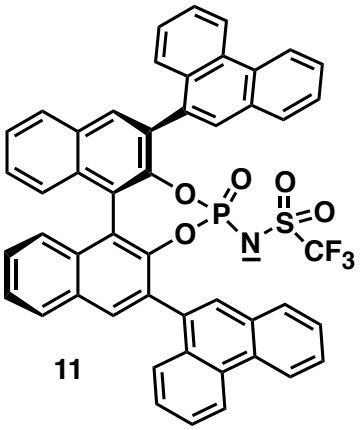

11

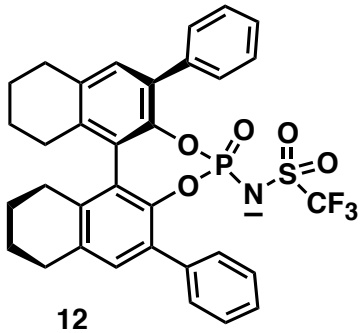

12

Rueping *Angew. Chem. Int. Ed.* **2008**, *47*, 593
Rueping *Chem.–Eur. J.* **2010**, *16*, 13116

Rueping *J. Am. Chem. Soc.* **2011**, *133*, 3732
Rueping *Chem.–Eur. J.* **2010**, *16*, 13116

Phosphoramidate anions

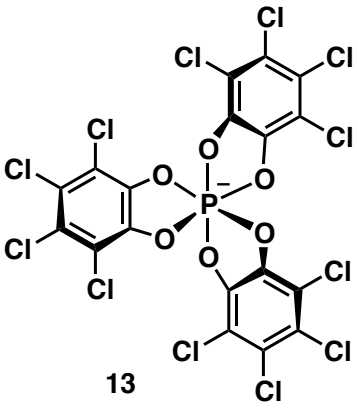

13

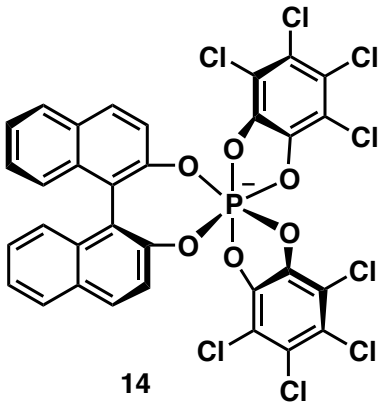

14

Lacour *Tetrahedron Lett.* **2002**, *43*, 8257
Nelson *Tetrahedron Asymmetry.* **2003**, *14*, 1995

Lacour *Chem. Commun.* **2008**, 829

Hexacoordinated Phosphate anions

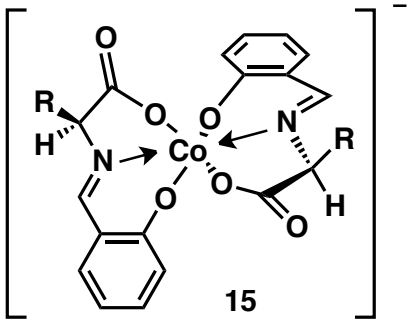

15

Tetrahedron Asymmetry. **2008**, *19*, 822

Cobaltate anion

Figure 1.1 cont'd

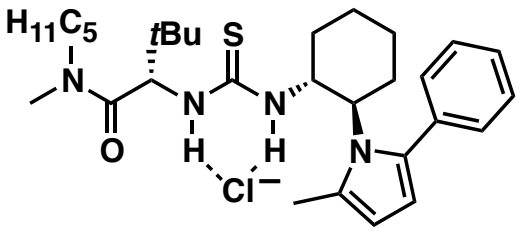

16

Jacobsen
J. Am. Chem. Soc. **2007**, *129*, 13404

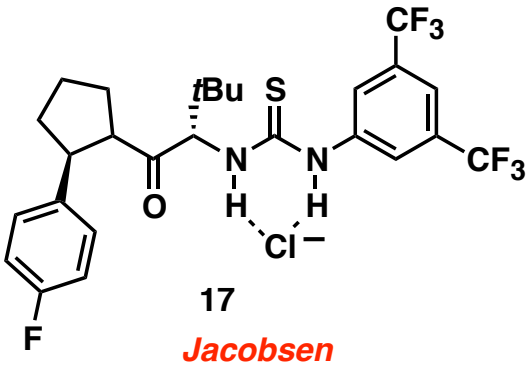

17

Jacobsen
J. Am. Chem. Soc. **2008**, *130*, 7198

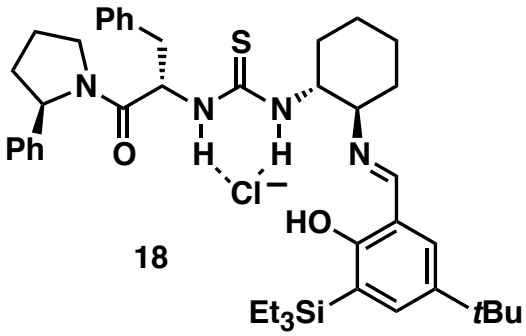

18

Jacobsen
Angew. Chem. Int. Ed. **2009**, *48*, 6328

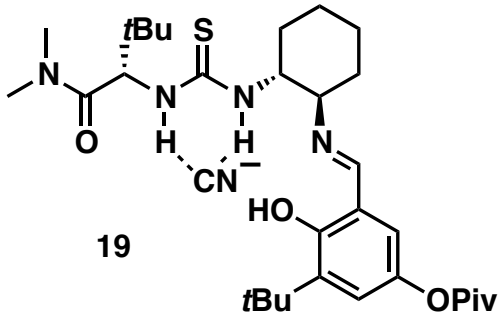

19

List
Chem. Asian J. **2008**, *3*, 430

Supramolecular chiral anions

The present discussion is focused on catalysis that involves chiral borate anions. They have been used in both asymmetric Brønsted acid catalysis (not organocatalysis as it involves boron) and asymmetric counteranion-directed catalysis (transition-metal catalysis). In the case of asymmetric Brønsted acid catalysis, there are three type of chiral borate anions: a) spiroborate[14] (SB) b) fused-spiroborate[15] (FSB) and c) boroxinate[16] (BOROX) (Figure 1.2). However, in the case of asymmetric counteranion-directed catalysis, only spiroborate type anions from BINOL,[4,11b,17] tartaric acid[18] and amino acids[18-19] are reported (Figure 1.2).

Figure 1.2 Chiral borate anions used in (**A**) asymmetric Brønsted acid catalysis (**B**) asymmetric counteranion-directed catalysis

A

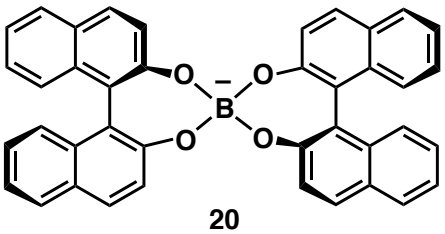

20

Yamamoto, *J. Am. Chem. Soc.* **1994**, *116*, 10520
Nakagawa, *Synlett* **1997**, 761
Nakagawa, *J. Org. Chem.* **1998**, *63*, 6348
James, *Tetrahedron Asymmetry.* **2003**, *14*, 1965

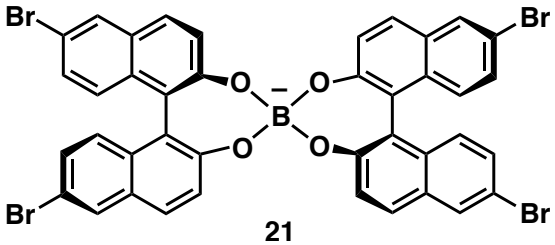

21

Nakagawa
Synlett **1997**, 761
J. Org. Chem. **1998**, *63*, 6348

Spiro-borate anions

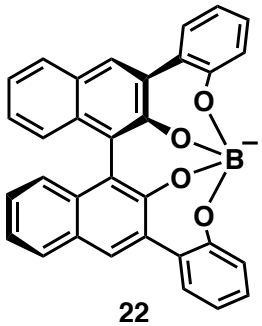

22

Fused-spiroborate anion

Yamamoto, *J. Am. Chem. Soc.* **1994**, *116*, 1561
Yamamoto, *J. Am. Chem. Soc.* **1996**, *118*, 3049
Yamamoto, *J. Am. Chem. Soc.* **1998**, *120*, 6920
Yamamoto, *J. Org. Chem.* **1997**, *62*, 3026
Davies, *Adv. Synth. Catal.* ***2006***, *348, 2449*

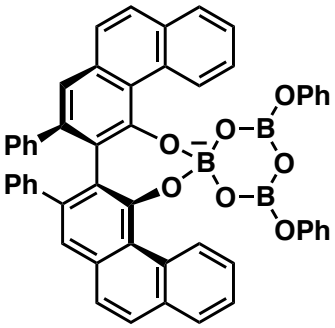

23

Wulff
J. Am. Chem. Soc. **2009**, *131*, 15615
J. Am. Chem. Soc. **2010**, *132*, 14669
J. Org. Chem. **2010**, *75*, 5643
Org. Lett. **2011**, *13*, 5866

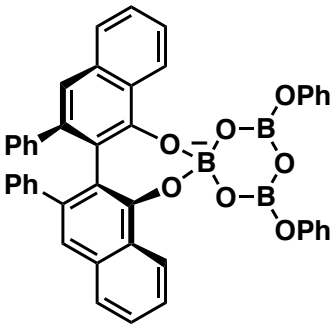

24

Wulff
J. Org. Chem. **2010**, *75*, 5643
J. Am. Chem. Soc. **2010**, *132*, 13100
J. Am. Chem. Soc. **2010**, *132*, 13104
J. Am. Chem. Soc. **2011**, *133*, 5656

Figure 1.2 cont'd

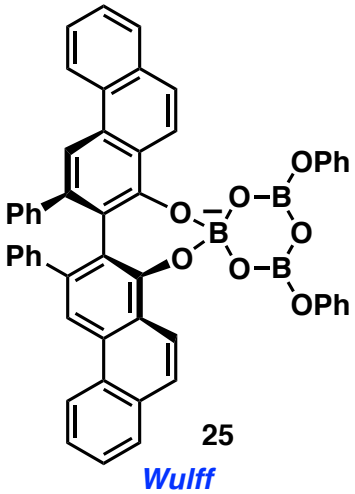

25

Wulff
Unpublished

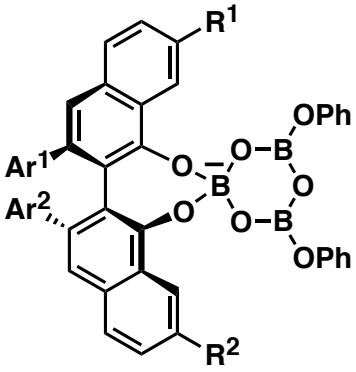

26

Wulff
Unpublished

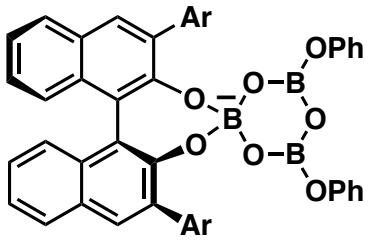

27

Wulff
Unpublished

Boroxinate anions

B

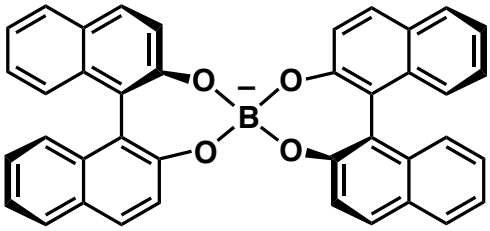

20

Leitner, *Chem. Cat. Chem* **2010**, *2*, 55
Nelson, *Tetrahedron Asymmetry.* **2003**, *14*, 1995
Arndtsen, *Org. Lett.* **2000**, *2*, 4165

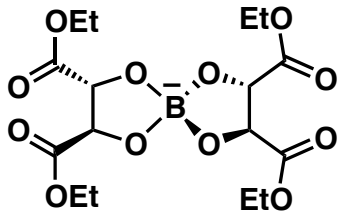

28

Arndtsen
Organometallics. **2004**, *23*, 2838

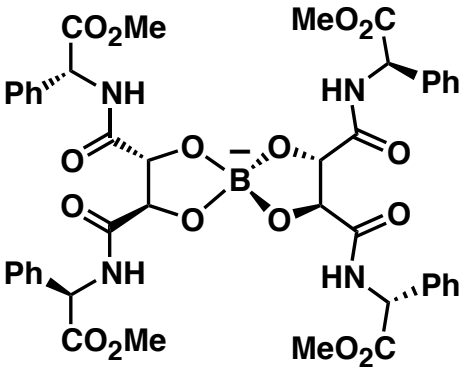

29

Arndtsen
Organometallics. **2004**, *23*, 2838

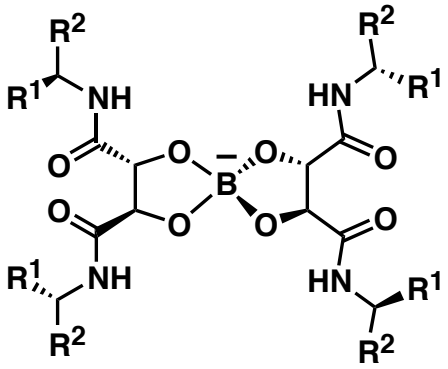

30

Arndtsen
Tetrahedron Asymmetry. **2005**, *16*, 1789

Figure 1.2 cont'd

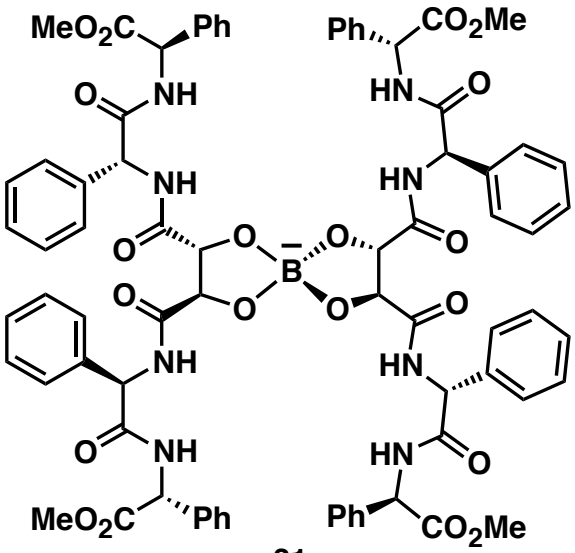

31

Arndtsen

Tetrahedron Asymmetry. **2005**, *16*, 1789

Spiro-borate anions

1.2 Chiral borate anions in asymmetric Brønsted acid catalysis (Class I and II)

In last decade or so, there has been enormous growth in the field of asymmetric Brønsted acid catalysis (Class I). There have been a number of elegant examples demonstrating the magnificent work in asymmetric catalysis utilizing these acids. A brief introduction is given below prior to the discussion of the chiral borate anions in asymmetric Brønsted acid catalysis.

1.2.1 An introduction to asymmetric Brønsted acid catalysis

A number of reviews have been published in the literature showcasing the idea of asymmetric catalysis via chiral Brønsted acid catalyst.[3c,20] The most common Brønsted acids used are chiral phosphoric acids, which has *chiral tetracoordinated phosphate anions*. More specifically, the phosphoric acids derived from BINOL and H8-BINOL are primarily used in

asymmetric catalysis.[21] In 2004, Akiyama and Terada have introduced these kinds of catalysts.[22] The binding of the substrate to the catalyst has been altered to a great deal with the help of 3,3′ or 6,6′ substituents on the BINOL ligand. Additionally, Toste and co-workers have introduced thio-phosphoric acids derived from BINOL derivatives.[23] Also, Terada and coworkers have introduced the concept of chiral bis-phosphoric acid catalyst.[24] In recent years, novel chiral phosphoric acids derived from VANOL,[25] VAPOL,[8a,8b,25-26] SPINOL,[8i,27] and TADDOL[8i,28] have been employed. More recently, metal salts of VAPOL or BINOL phosphoric acids are being used.[29] In recent years, the acidity of these Brønsted acids have been increased to a great extent by utilizing phosphorodiamidic acid,[30] phosphoramides,[10a,10b,31] bis(sufonyl)imides[9a,9b,32] and bis(sulfuryl)imides[33] prepared from BINOL and H8-BINOL.[20a] More recently, List and coworkers have reported a novel class of C_2-symmetric imidodiphosphoric acids.[34] The other group comprises chiral dicarboxylic acids[6a,6b,35] and chiral disulfonic acids.[7,36] *Also, the pKa values of these acids have been reported in DMSO ranging from 1.74±0.08 to 5.74±0.05*.[37] Rueping and co-workers have recently shown asymmetric Brønsted acid catalysis in aqueous solution.[38]

In the case of Brønsted acid catalysis, the mode of substrate activation is either hydrogen bonding or ion-pair formation by the complete proton transfer to the substrate. Recently, it has been demonstrated that both the activation modes are synergistically operational in case of

imines.[39] The population of the substrate in an activation mode would also be governed by the strength of the acid. Weak Brønsted acids are likely to operate *via* hydrogen bonding. Consequently, chiral thioureas like **46**-**47**,[20e,20h,20j,40] TADDOL **48**[41] and chiral BINOL derivatives **49**-**54**[42] have been used as Brønsted acid catalysts (Hydrogen-bond donor catalysts) (Figure 1.3B). In general, diols such as BINOLs **55** and **56**,[43] H8-BINOLs **53** and **57**,[44] VAPOL **58**,[45] VANOL **59**,[45] SPINOL **60**[46] and TADDOL **61**[43a,47] are relatively very weak Brønsted acids when used directly as catalysts, however, they have been extensively used as chiral ligands for various asymmetric reactions. *It is important to note that while the catalyst might exist as the Brønsted acid, their catalytic function could be of Lewis acid type.*[25b,26a,26c,26d,48]

Figure 1.3 A list of various (**A**) chiral phosphoric acids, phosphorodiamidic acid, phosphoramides, imidodiphosphoric acids, disulfonamides, carboxylic and sulfonic acids. (**B**) chiral thioureas and chiral diols

A

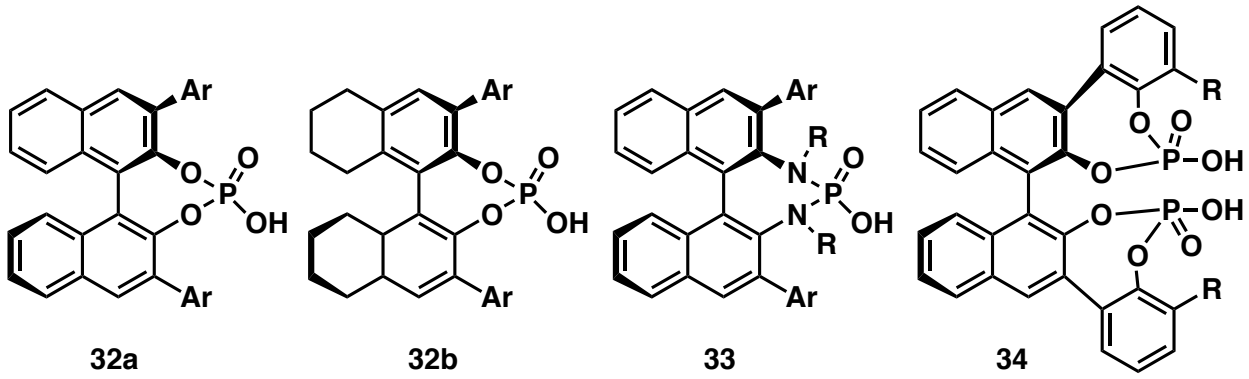

Figure 1.3 cont'd

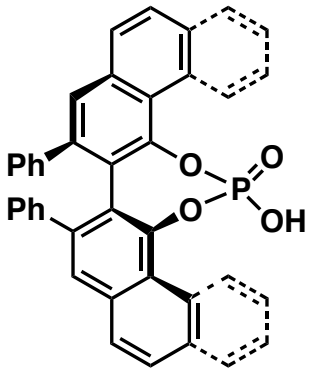

35 (for (S)-VAPOL)
36 (for (S)-VANOL)

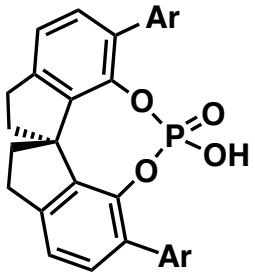

37

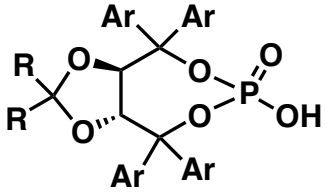

38

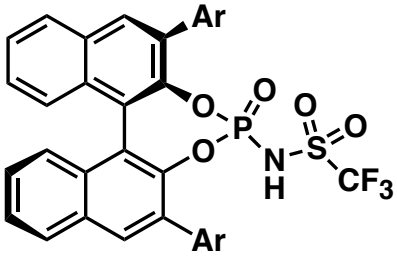

39a

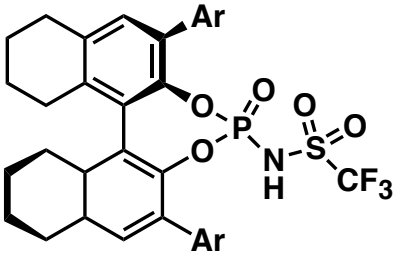

39b

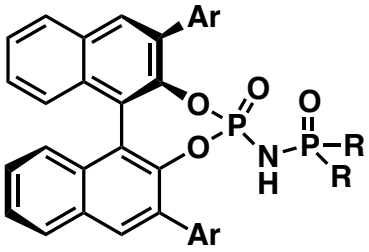

40

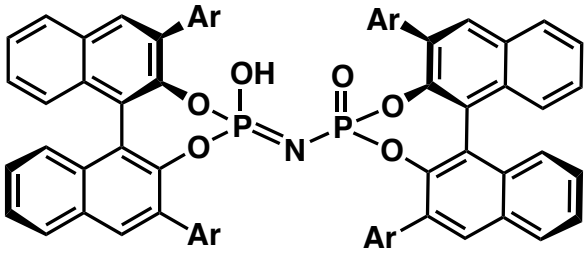

41

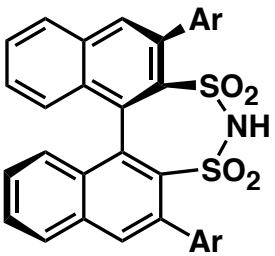

42

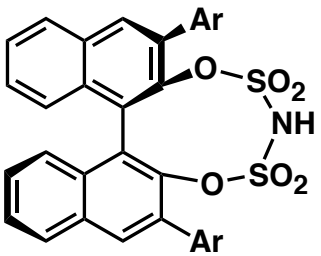

43

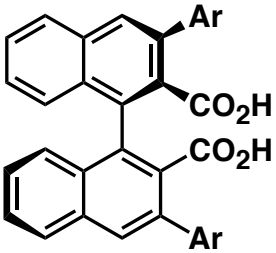

44

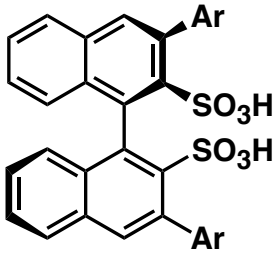

45

Figure 1.3 cont'd

B

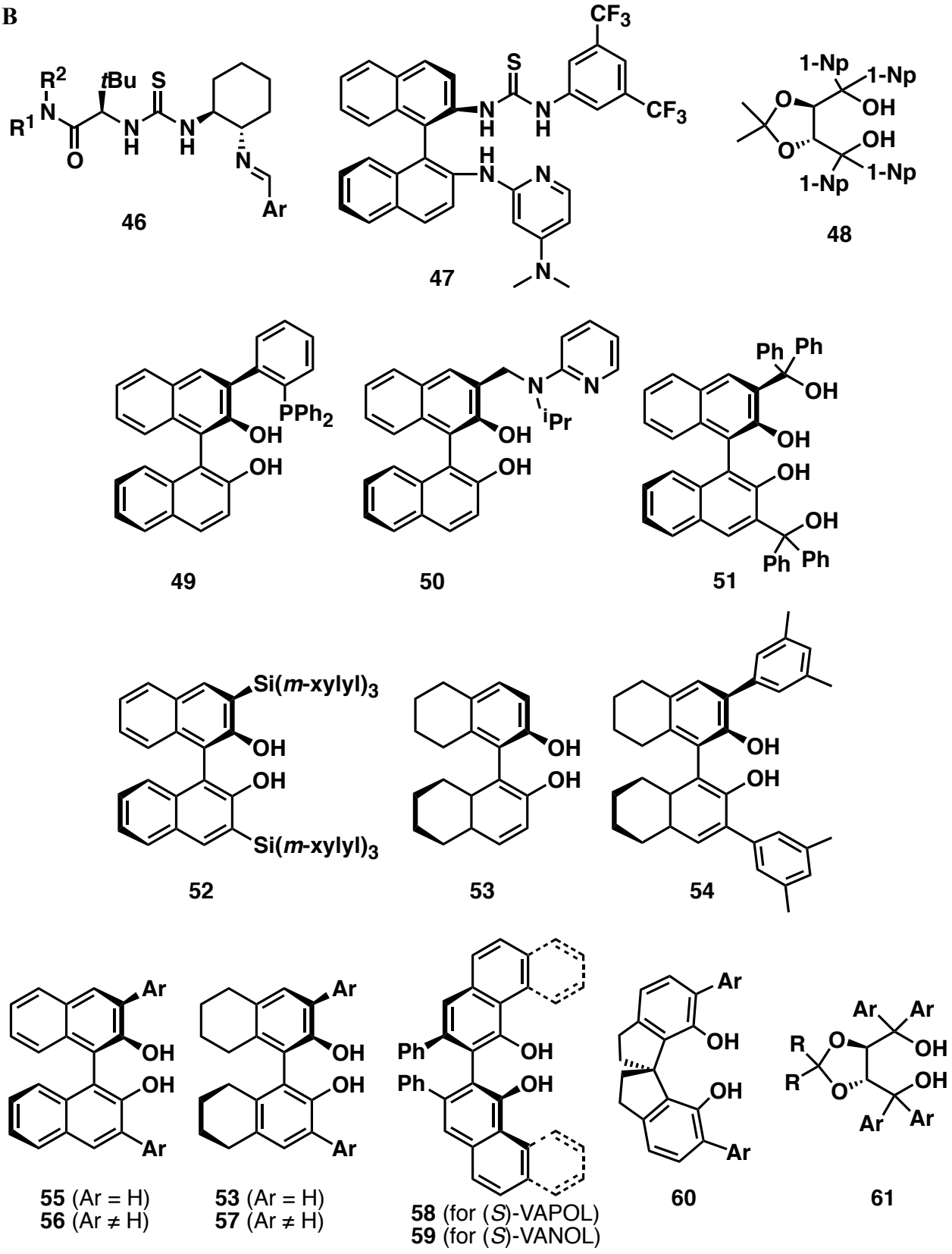

Regarding class II type catalyst, they exist as Brønsted acid catalysts. Depending upon their catalytic function, they belong to either asymmetric Brønsted acid catalysis or asymmetric counteranion-directed catalysis. For instance; if the catalyst looses all protons at the catalytic step, then it can be included in asymmetric counteranion-directed catalysis (Scheme 1.1). In these cases, class II serves as pre-catalyst and the eventually transforms into class III type catalyst during the reaction.

Scheme 1.1 Brønsted acid catalysis[49] verses asymmetric counteranion-directed catalysis[5]

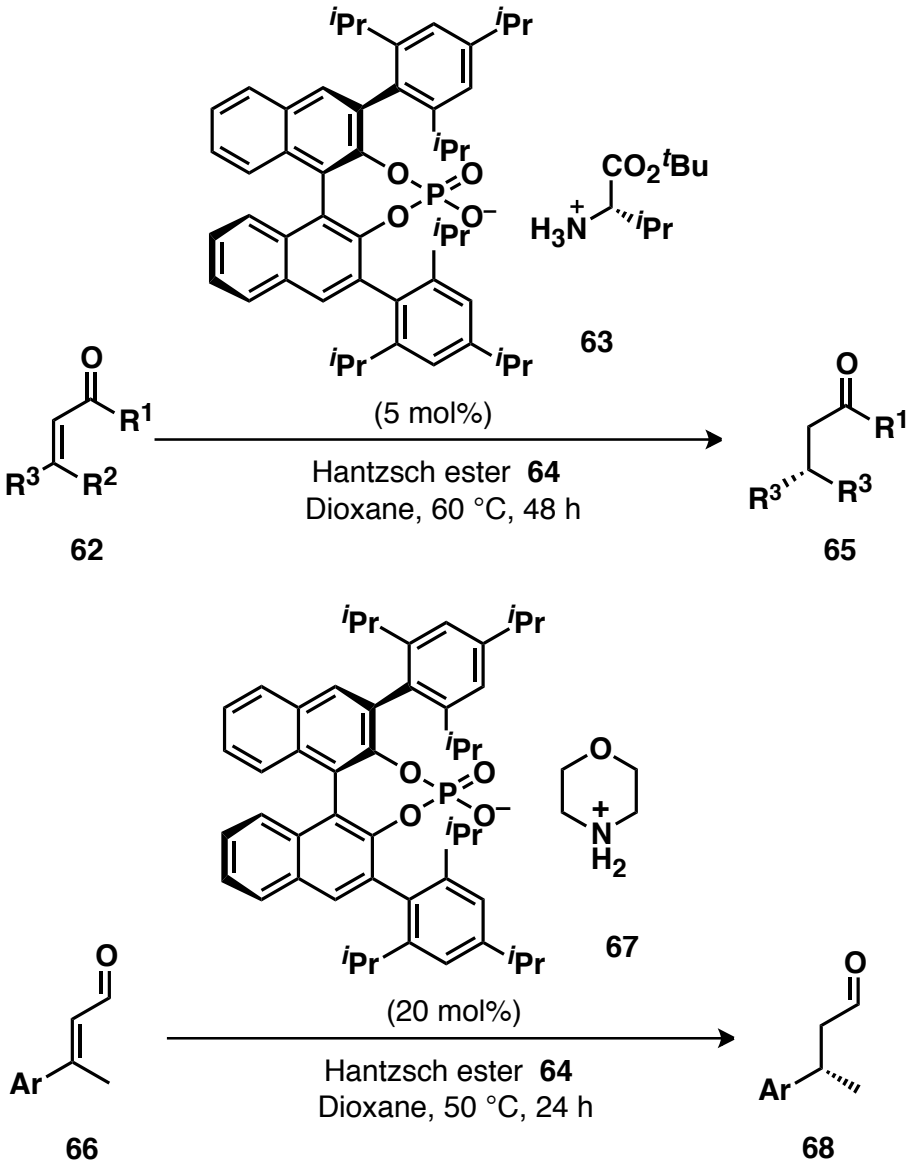

Scheme 1.1 cont'd

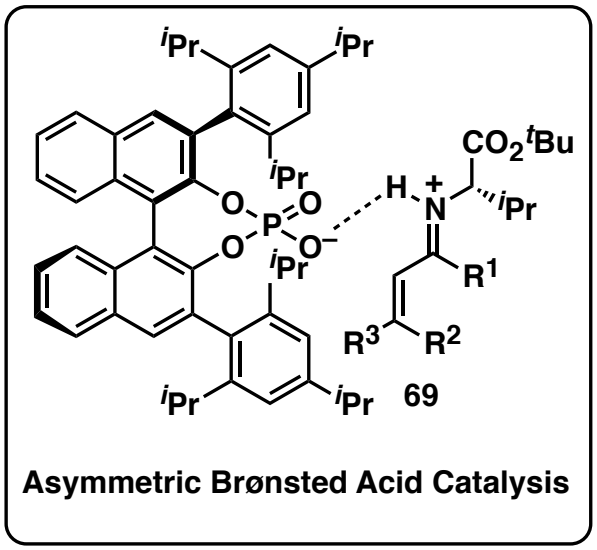

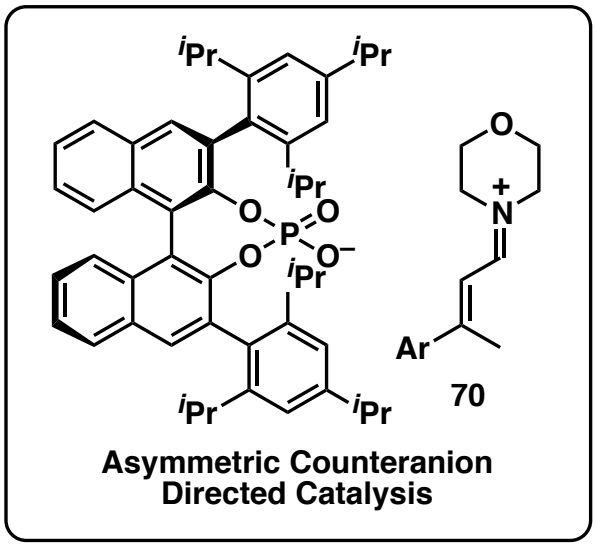

An important class of Brønsted acid catalysts involves chiral borate anions. Catalysts which belong to the class I are supposedly containing spiroborate[14] (SB) or fused-spiroborate[15] (FSB) anions. However these are found to be class II type catalysts (see section 1.2.2 and 1.2.3). Boroxinate[16] (BOROX) anions form the Brønsted acid catalyst only in the presence of a base and hence belong to class II.

1.2.2 Chiral spiroborate anions in asymmetric Brønsted acid catalysis

In 1994, Yamamoto and co-workers reported one of the early examples of chiral borate anions. They utilized spiroborate (SB) anion **20** for Mannich reactions[14a-14c] (Scheme 1.3) and heteroatom Diels-Alder reactions of imines (Scheme 1.4).[14a,14d] In the year 1997, the same catalyst was supposedly used for Pictet-Spengler reaction (Scheme 1.5).[14e,14f] The reported structure represents the catalyst as a Brønsted acid **20**-H containing a tetra-coordinate boron

(Scheme 1.2).[14a,14e] However, the mode of catalysis of **20**-H was assumed to be Brønsted acid assisted Lewis acid (BLA) catalysis. The catalytic function of **20**-H was proposed to be as a chiral Lewis acid where interaction with a Lewis base disrupts one of the boron-oxygen bonds to give Lewis acid-Lewis base complex **71** (Scheme 1.2).[14a,14e] However, we found that there is no tetracoordinated boron atom unless a base is added (see Chapter 4). Hence, catalyst **20**-H exists as Brønsted acid assisted Lewis acid (BLA) **72** with a tri-coordinate boron atom (Scheme 1.2).

Scheme 1.2 Different proposals about catalytic activity of **20**-H (LB = Lewis base)

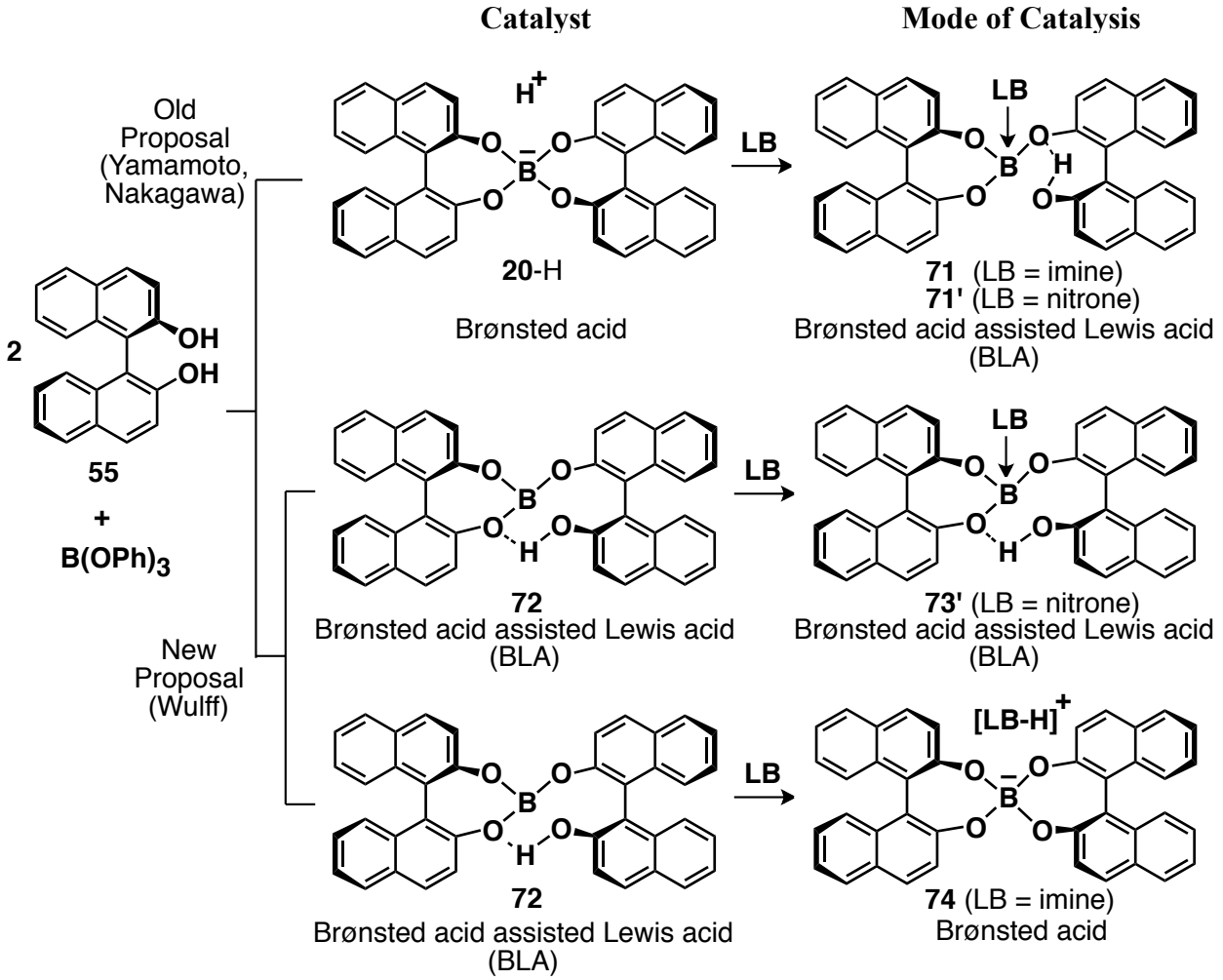

Interestingly, we found that the mode of catalysis (catalytic function) is actually Brønsted acid or hydrogen bond catalysis for imino-aldol reaction of imines and Brønsted acid assisted Lewis acid catalysis for Pictet-Spengler reaction of nitrones (Scheme 1.2). For imino-aldol reaction of imine, the actual catalyst exists as Brønsted acid **74** and belongs to the class II type catalysts where it is formed only upon the addition of chiral or achiral bases (Scheme 1.2). A detailed discussion of this system is given in Chapter 4.

In the case of asymmetric imino-aldol reaction; stoichiometric amount of catalyst **20**-H was utilized and enantioselectivity up to 98% was reported (Scheme 1.3).[14a] Reaction with chiral amine created the environment for matched/mismatched cases resulting in 95% diastereomeric cxcess. Yamamoto and co-workers used the asymmetric imino-aldol reaction in the total synthesis of (+)-(*S*)-Dihydroperiphylline.[14b,14c]

Scheme 1.3 Asymmetric imino-aldol reaction catalyzed by **20**-H

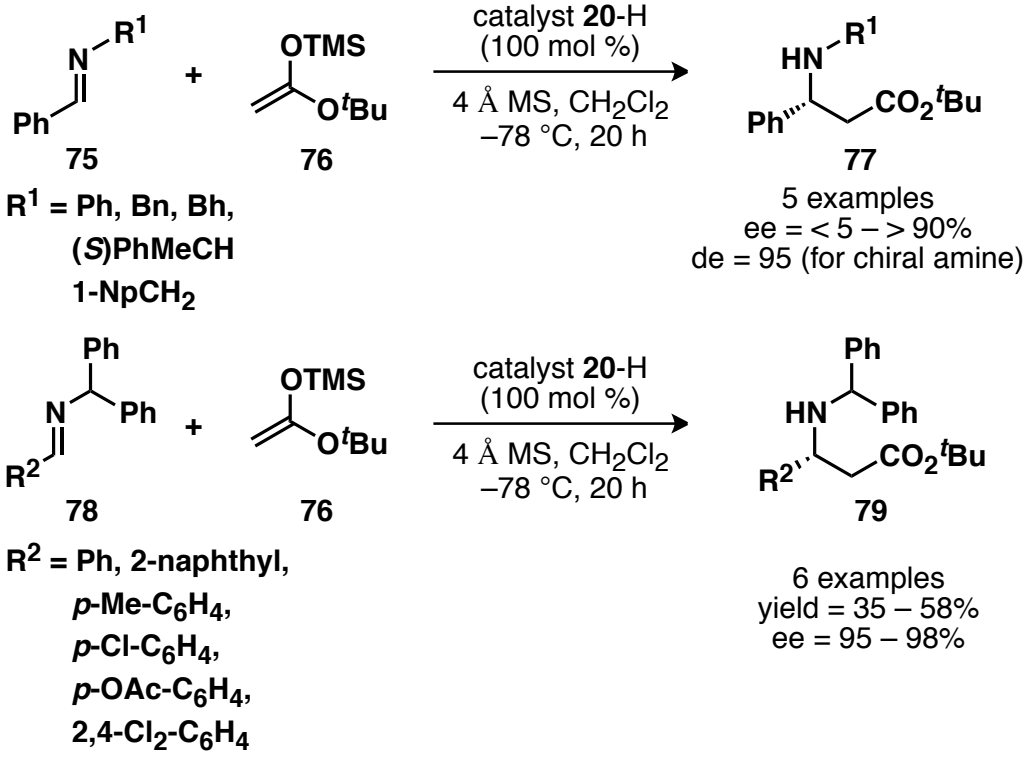

Yamamoto and coworkers reported the asymmetric heteroatom Diels-Alder reaction between imine **75** and Danishefsky diene **80** to give vinylogous amides **81** (Scheme 1.4). They examined different imines derived from benzaldehyde and benzylamine or (*S*)-α-methylbenzylamine. Excellent yields and enantioselectivities and diastereoselectivities were obtained though stoichiometric amount of catalyst used. Results with chiral amine and different enantiomers of catalyst did not show any match or mismatched cases. Our group then thought to examine benzhydryl amine derived imine **78a** as it is the protecting group we utilized for the same reaction with our BOROX catalyst.[16h] A slight increase in ee was observed as compared to the benzyl amine derived imine **75a** although low yield was obtained when 10 mol % catalyst was used instead of 100 mol % (Scheme 1.4).[50]

Scheme 1.4 Asymmetric heteroatom Diels-Alder reaction catalyzed by **20**-H or **74**

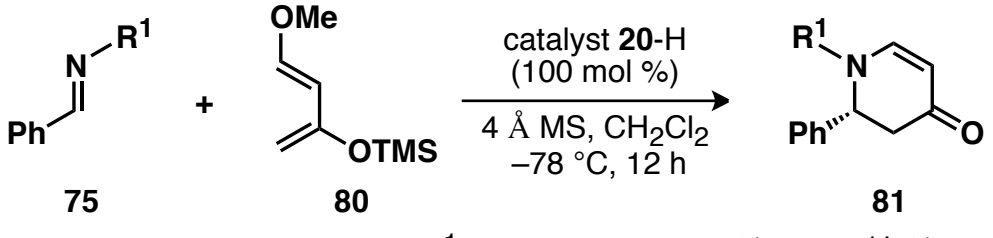

75 **80** **81**

R^1	y%	ee/de%
Bn	78	86
(*S*)PhMeCH	64	99
(*S*)PhMeCH (with *ent*-**20**-H)	49	83

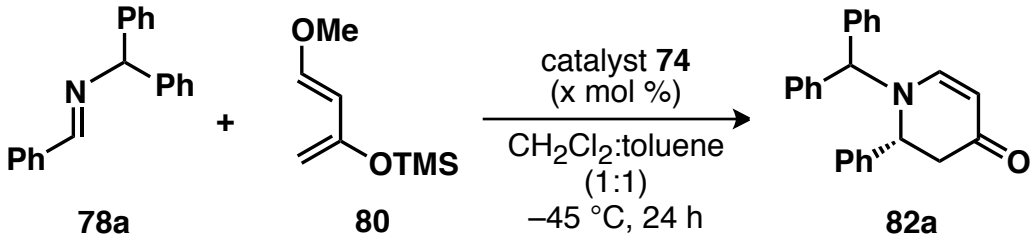

78a **80** **82a**

Catalyst **74** (mol %)	y%	ee%
10	39	93
100	92	89

Regarding the Pictet-Spengler reaction, Nagakawa and coworkers had to utilize two equivalents of the catalyst **20**-H in order to get the turnover as the product **84** was more basic than the reactant **83**.

Scheme 1.5 Asymmetric Pictet-Spengler reaction catalyzed by **20**-H or **21**-H

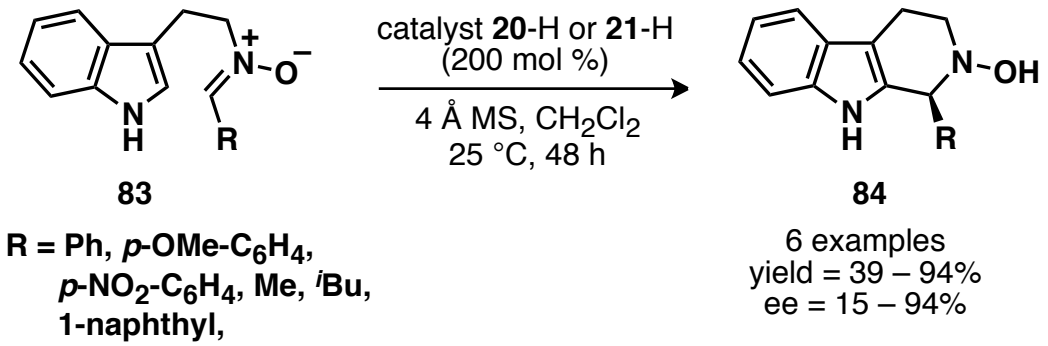

Interestingly, the opposite enantiomer of aziridine **86a** was obtained when (*R*,*R*)-**74a** was employed as compared to a BOROX catalyst generated from (*R*)-VAPOL.[16a,50] Low yields and moderate ees were obtained irrespective of the catalyst loading (Scheme 1.6).

Scheme 1.6 Asymmetric aziridination reaction catalyzed by (*R*,*R*)-**74a**

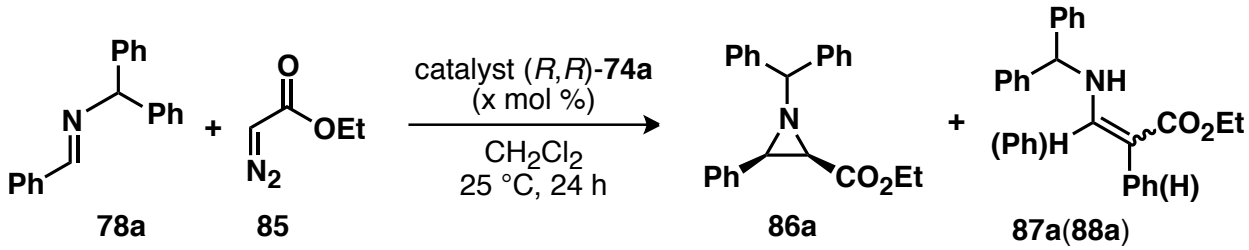

Catalyst **74a** (mol %)	y %	ee %	*cis:trans*	*enamines*
10	47	40	2:1	24(23)
100	8	76	50:1	5(5)

1.2.3 Chiral fused-spiroborate anions in asymmeric Brønsted acid catalysis

Another example reported is the case of fused-spiroborate (FSB) anion **22**. In 1994, Yamamoto and co-workers reported this kind of catalyst for the first time.[15a] They used this catalyst for asymmetric Diels-Alder reaction between dienes and enals (Scheme 1.8). The reported structure represents it as a Brønsted acid containing a tetra-coordinate boron atom (Scheme 1.7).[15] However, it was proposed to function as a Brønsted acid assisted Lewis acid (BLA) catalyst. In this case, we found that it is indeed a BLA type mechanism for aldehydes. However, we found that there is no tetra-coordinated boron unless a base is added. This work is discussed more in detail in Chapter 4.

Scheme 1.7 Proposed catalytic activity of **22**-H

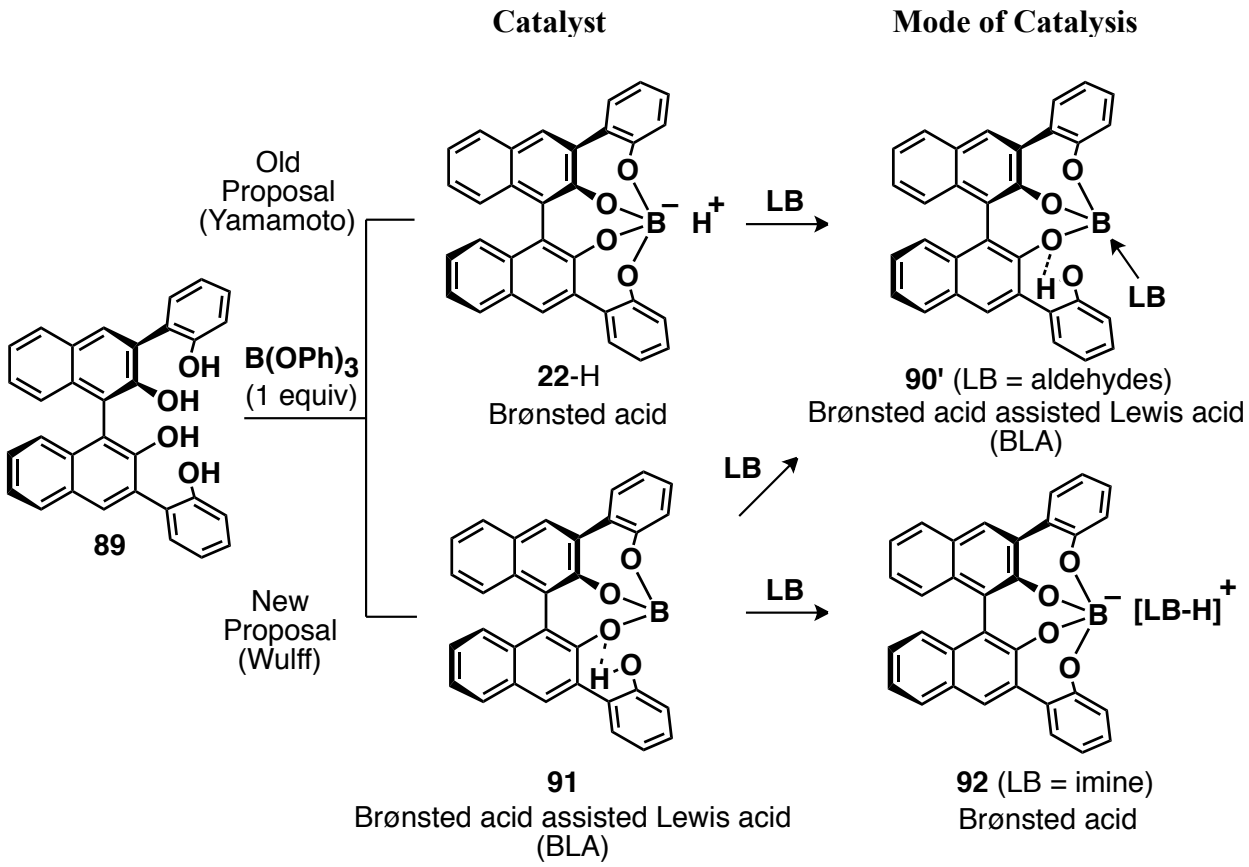

Excellent yields and ees were reported for the Diels-Alder reaction of dienes **93** and enals **94** giving exo isomer as the major product (Scheme 1.8A).[15a] In the years 1996 and 1998, Yamamoto and coworkers designed some modified catalytic systems for Diels-Alder reaction between dienes and enals in order to increase the enantio-induction and broaden the substrate scope (Scheme 1.8B).[15b,15c]

Scheme 1.8 Asymmetric Diels-Alder reaction of dienes and enals catalyzed by (**A**) **22**-H (**B**) **98**-**100**

A

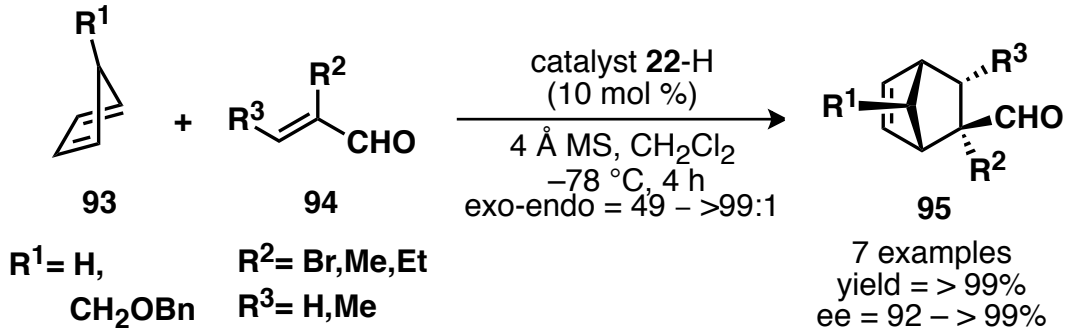

B

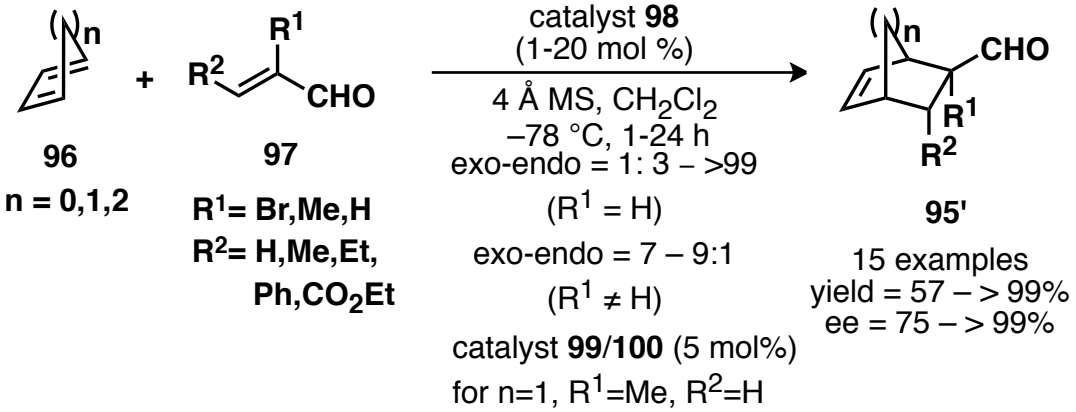

Scheme 1.8 cont'd

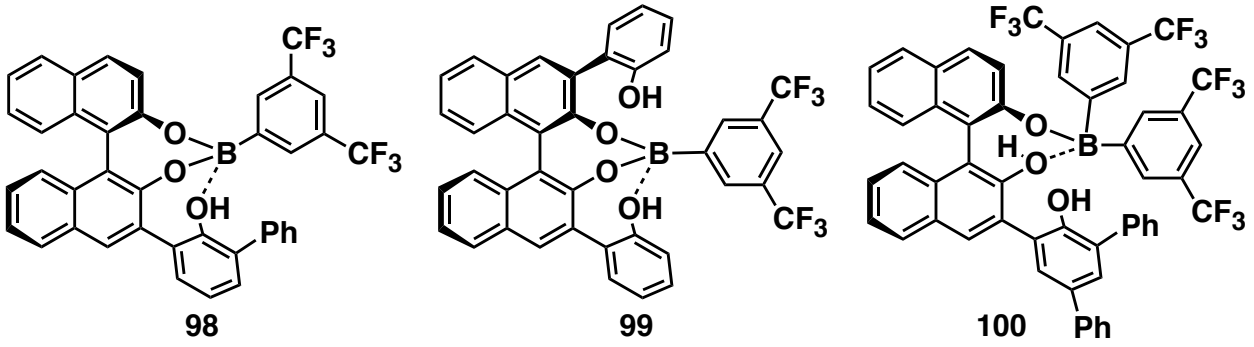

In the year 2006, Davies and coworkers introduced a formal [4+3] cycloaddition by a tandem Diels Alder reaction/ring expansion using **22**-H as the catalyst (Scheme 1.9).[15e]

Scheme 1.9 Formal [4+3] cycloaddition catalyzed by **22**-H

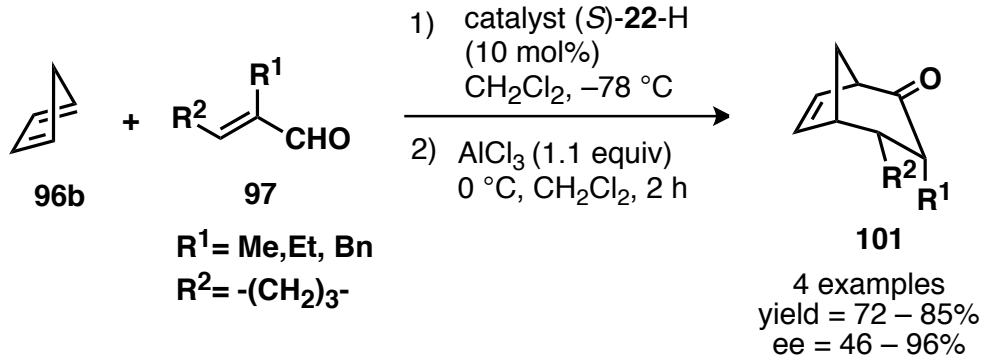

Additionally, Yamamoto and coworkers reported the first enantioselective catalytic Diels-Alder reaction of dienes **96** and acetylenic aldehydes **102** with ee up to 95%.[15d]

Scheme 1.10 Asymmetric Diels-Alder reaction of dienes and alkynals catalyzed by **22**-H or **98**

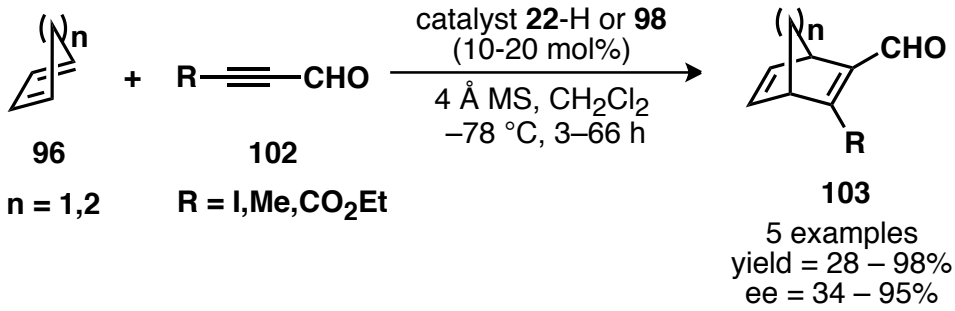

Also, as a part of this doctoral work, a low ee of 48% was observed for aziridine **86a** when (*R*)-**92a** was employed (Scheme 1.11).

Scheme 1.11 Asymmetric aziridination reaction catalyzed by (*R*)-**92a**

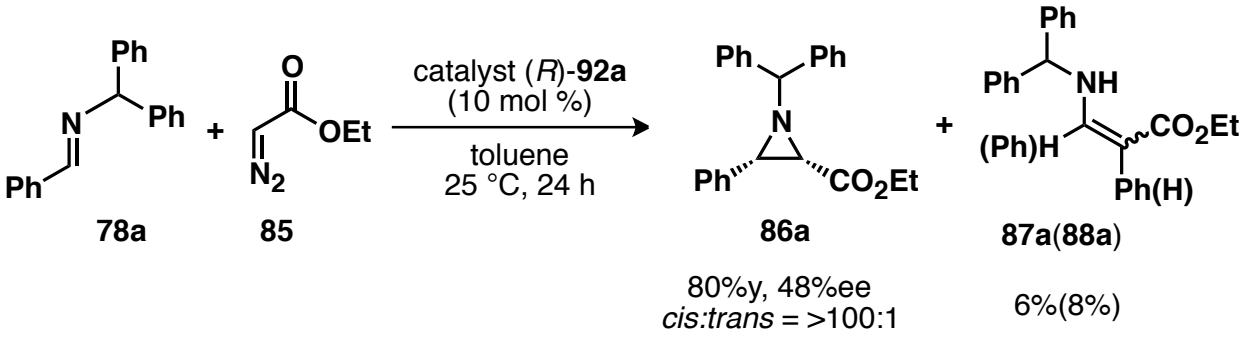

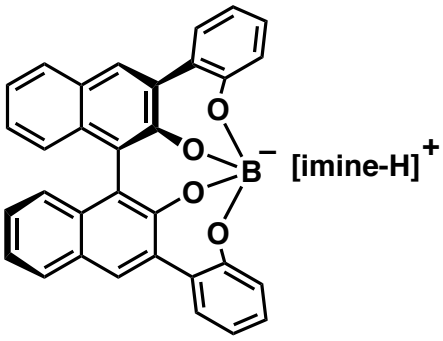

(*R*)-**92a (imine = 78a)**

Brønsted acid

1.2.4 Chiral boroxinate anions in asymmetric Brønsted acid catalysis: BOROX catalysis

So far we have discussed two major kinds of chiral borate anions (SB **20**-H and FSB **22**-H) with free proton supposedly as the cation. Both contain a spiroborate ring as a common feature. However, there is no report of a chiral boroxinate (BOROX) catalyst in literature prior to our work. In the due course of time, we have developed a universal catalytic asymmetric aziridination utilizing a chiral boroxinate catalyst derived from the vaulted ligands such as

VAPOL **58** or VANOL **59** and $B(OPh)_3$.[16] The catalyst consists of a chiral boroxinate anion with a protonated base as the cation. It forms only in the presence of a base and hence it belongs to class II type of catalysts (Table 1.1). It can be generated *via* **B1** and **B2** or directly from the ligands (Scheme 1.12). Since, the borate anion can be seen as a derivative of a boroxine ring, we coined a new term "BOROX catalyst" for this class of catalysts.[16] More recently, we have shown that even some BINOL derivatives form boroxinate anions of type **27** in the presence of base.[51]

Scheme 1.12 Generation of BOROX catalyst **104** and **105**

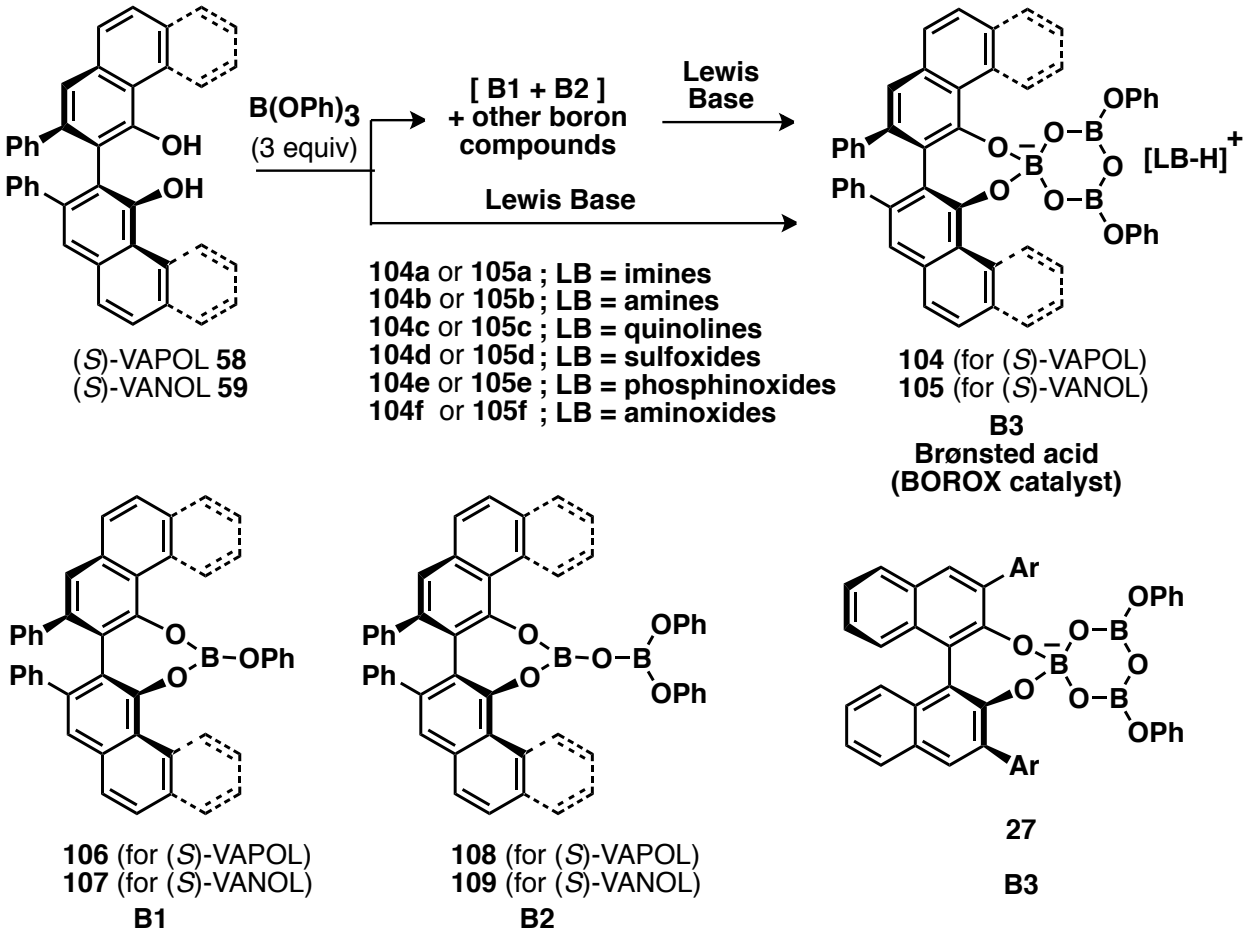

For the past few years, a considerable effort has been given towards the evolution of a universal aziridination reaction. Utilizing BOROX catalysts, a substrate general catalytic asymmetric aziridination reaction for *cis*-[16a-16d,16j,16k,16m] and *trans*-aziridination[16i,16j] has been realized (Scheme 1.13 and 1.14). A unique feature of our catalytic system is that either *cis*- or *trans*-aziridines can be prepared from the same imine and same catalyst **104a**/**105a**. Recently, we accomplished a *cis*-aziridination for alkynyl imines.[52] In all these cases, substrate i.e. imines, acting as the base, induced the formation of the BOROX catalyst of type **104a**/**105a**.

Scheme 1.13 The Wulff asymmetric *cis*-aziridination reaction

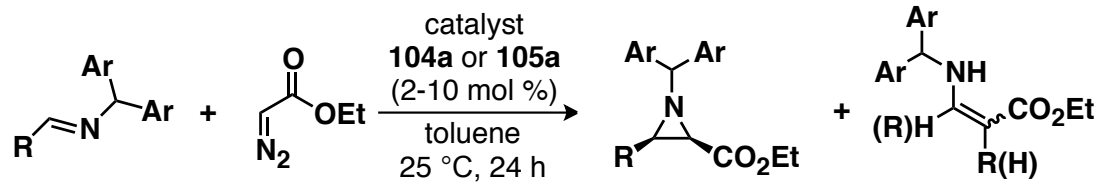

78 (Ar_2CH=Bh) **85**
110 (Ar_2CH=DAM)
111 (Ar_2CH=MEDAM)
112 (Ar_2CH=BUDAM)

R = aryl and alkyl

86 (Ar_2CH=Bh) **87**(**88**) (Ar_2CH=Bh)
113 (Ar_2CH=DAM) **116**(**117**) (Ar_2CH=DAM)
114 (Ar_2CH=MEDAM) **118**(**119**) (Ar_2CH=MEDAM)
115 (Ar_2CH=BUDAM) **120**(**121**) (Ar_2CH=BUDAM)

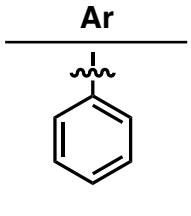

Bh
15 examples
Yield = 54–91%
ee = 90–98%
c/t = 38–50:1

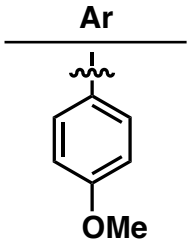

DAM
10 examples
Yield = 11–95%
ee = 52–98%
c/t = 33–50:1

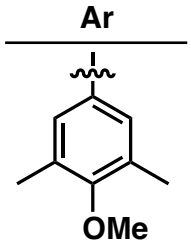

MEDAM
10 examples
Yield = 67–98%
ee = 90–99.5%
c/t = 33–50:1

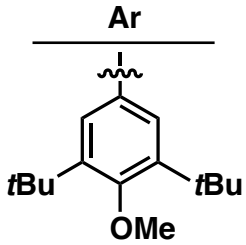

BUDAM
11 examples
Yield = 57–99%
ee = 78–99%
c/t = > 50:1

Scheme 1.13 cont'd

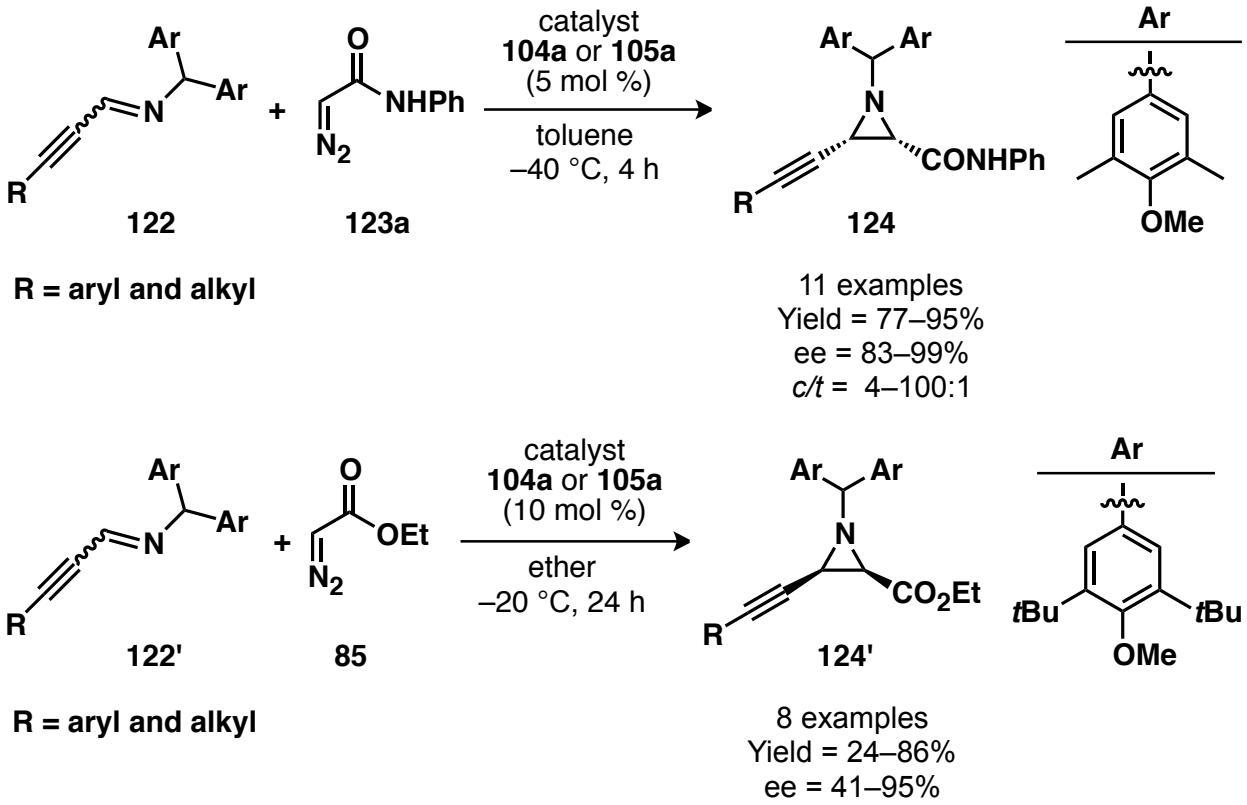

Scheme 1.14 The Wulff asymmetric *trans*-aziridination reaction

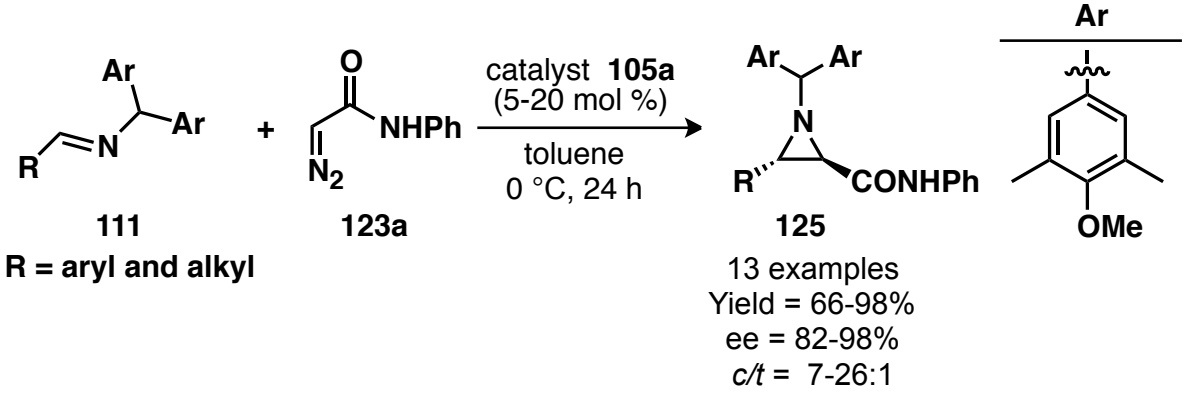

A considerable amount of time during this doctoral research has been spent in the realization of the first catalytic asymmetric multicomponent *cis*- and *trans*-aziridination of aldehydes (Scheme 1.15).[16g] Although, amine **126** induced the generation of a BOROX species,

it was found the reaction was catalyzed by a BOROX catalyst generated from an imine after its complete formation from amine **126** and aldehyde **127**.

Scheme 1.15 Asymmetric multicomponent aziridination reaction catalyzed by **104a** or **105a**

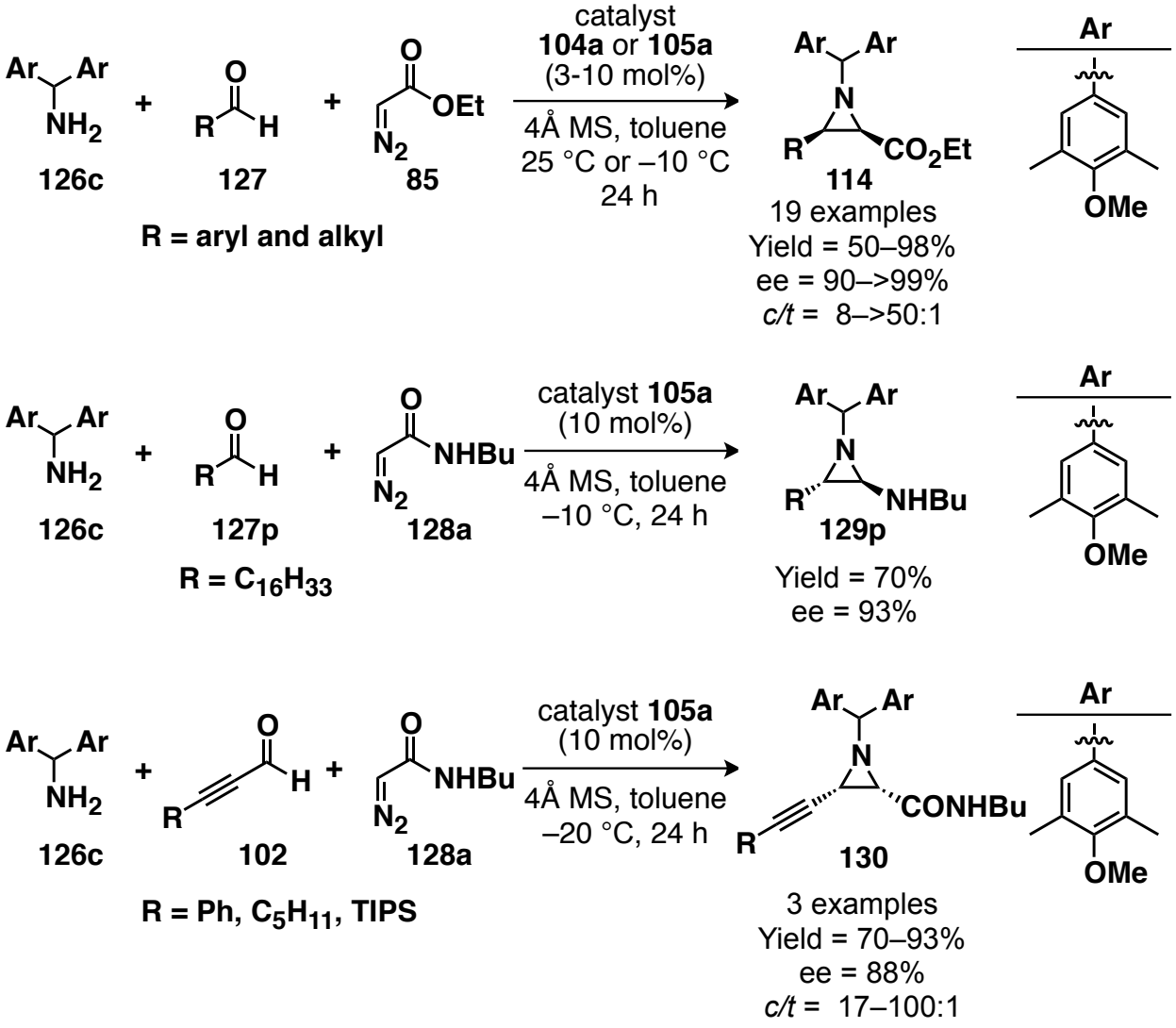

In 2007, our group reported the catalytic asymmetric aza Diels-Alder reactions of imines and Danishefsky diene **80** using a BOROX catalyst. In that case, excess $B(OPh)_3$ was found to be critical in improving the turnover of the catalyst. (Scheme 1.16).[16h]

Scheme 1.16 Asymmetric aza Diels-Alder reaction of imine and Danishefsky diene **80**

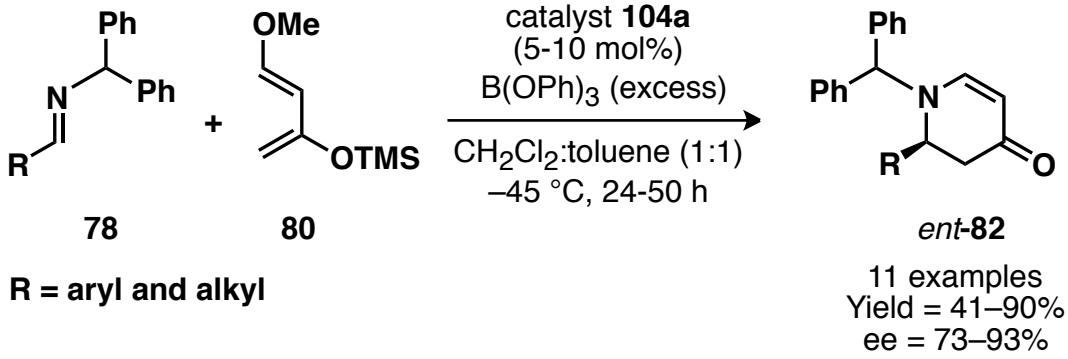

Adding to the versatility of the BOROX catalysts, our group has recently reported an example of catalytic asymmetric aza-Cope rearrangement of imines. Inspired by the multicomponent aziridination reaction, this was then performed in a multicomponent fashion. Interestingly, one equivalent of benzoic acid with respect to the catalyst was found to be synergistic in order to give useful levels of enantioselectivity (Scheme 1.17).[16l]

Scheme 1.17 Asymmetric aza-Cope rearrangement catalyzed by **105a**

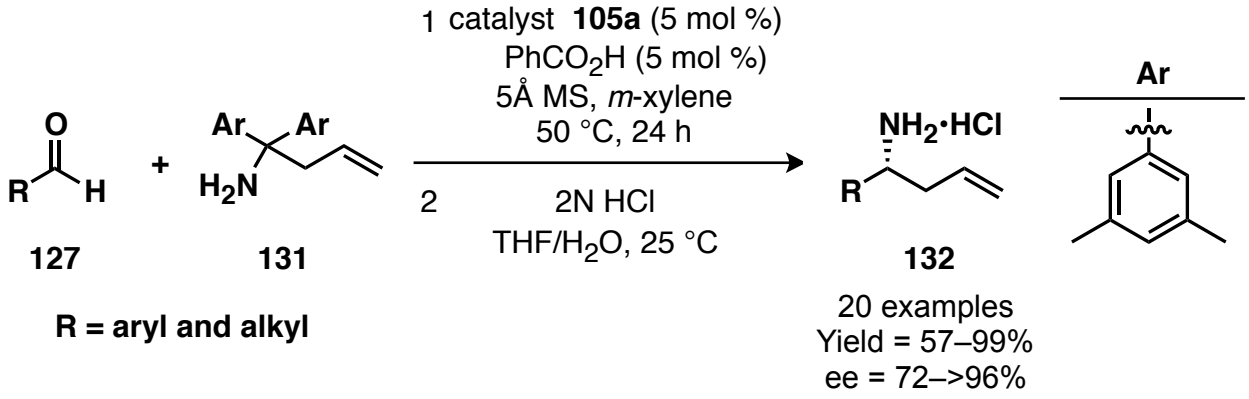

During the optimization of the multicomponent aziridination reaction, a novel [3+2] cycloaddition reaction was discovered (Scheme 1.18). The absolute stereochemistry was not determined. However, due to time constraints, this work has been put on hold.[53]

Scheme 1.18 Asymmetric [3+2] cycloaddition reaction catalyzed by BOROX catalyst **104a**

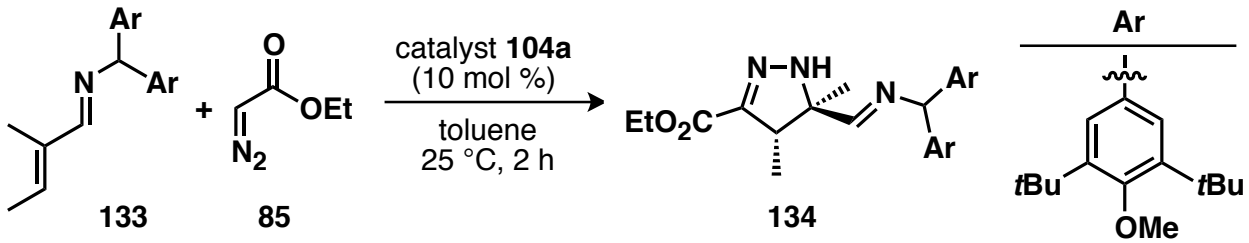

133 **85** **134**

Yield = 59%
ee = 50%

A prominent part of this thesis will focus on the development of a catalytic asymmetric epoxidation reaction. A number of aldehydes were examined and excellent results were obtained (Scheme 1.19).[53]

Scheme 1.19 Asymmetric epoxidation reaction catalyzed by BOROX catalyst **105d**

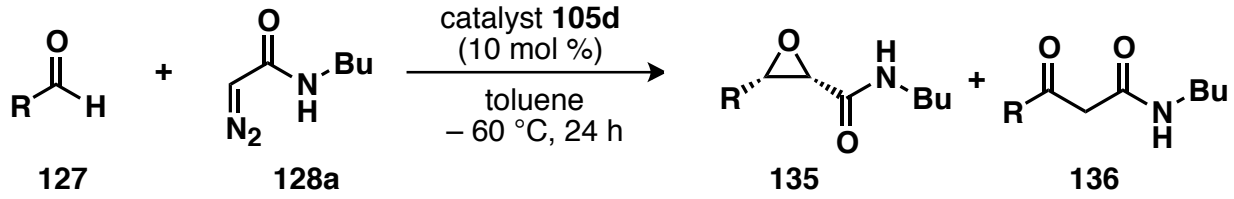

127 **128a** **135** **136**

R = aryl and alkyl

14 examples
Yield = 60–97%
ee = 78–99%
c/t = 13–100:1

Our group has also been able to perform catalytic asymmetric reduction of quinolines (Scheme 1.20).[54] High yields with moderate ees were obtained using BOROX catalyst **104c**.

Scheme 1.20 Catalytic asymmetric reduction of quinolines

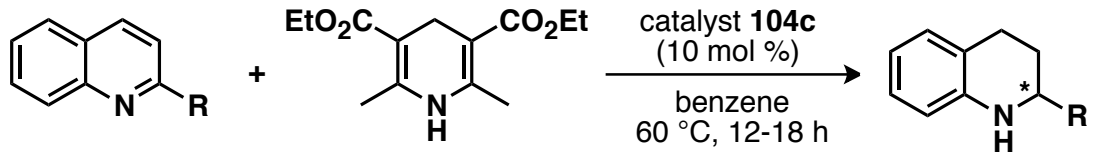

137 **64** **138**

R = Ph, C_5H_{11}

2 examples
Yield = >99%
ee = 67–73%

Last but not the least, substrate-controlled and catalyst-controlled aziridination reactions were examined with our BOROX catalysts and chiral imines made from either chiral amines or chiral aldehydes. Both matched and mismatched cases were observed (Scheme 1.21).[55]

Scheme 1.21 Double stereodifferentiation in catalytic asymmetric aziridination

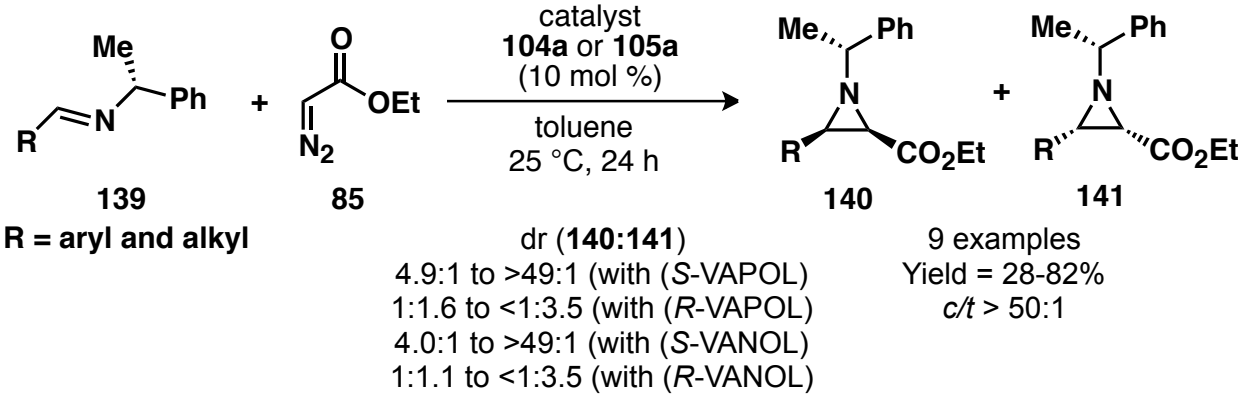

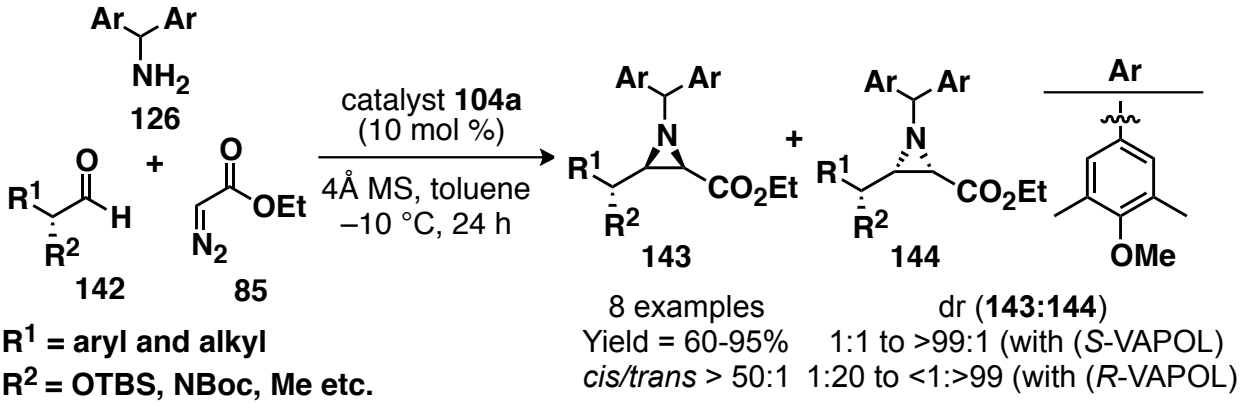

1.3 Chiral borate anions in asymmetric counteranion-directed catalysis (Classes II, III, IV, and V)

Nowadays, a lot of chiral anions are being used in asymmetric counteranion-directed catalysis.[3] As discussed in section 1.2, a class II catalyst can be included in asymmetric counteranion-directed catalysis if the catalyst looses all protons prior to the chirality transfer

step. In these cases, the class II catalyst serves as the pre-catalyst and eventually transforms itself into a class III type catalyst (see Section 1.2, Scheme 1.1). One such kind of catalyst utilizing the chiral spiroborate anion **20** was reported in 2003.[11b] The addition of *N*-methyl indole **145** to an iminium ion **146** and the ring-opening of an aziridinium ion **150** with benzylamine **151** were studied utilizing catalyst **147**.

In these cases, the mode of catalysis is asymmetric counteranion-directed catalysis as depicted in Table 1.2 and 1.3. Various catalysts were generated using different chiral achiral amines as the base. The level of enantioselectivity obtained was very low (< 15%) irrespective of the base used for the generation of the catalyst. Nonetheless this was one of the early examples where chiral borate anions have been used in counteranion-directed catalysis.

Table 1.2 The addition of *N*-methyl indole **145** to an iminium ion **146**

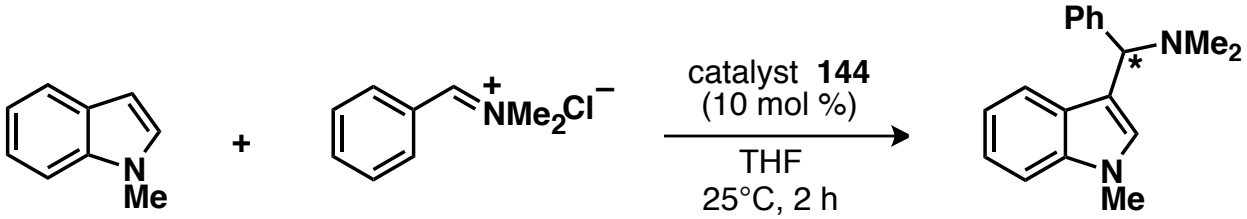

145 **146** **148**

#	Cat	C^+	Yield **148** (%) [a,b]	ee **148** (%)	ee **148** (%) [c]
1	**147a**	$Et_2NH_2^+$	12 [a]	3	–5
2	**147b**	Et_3NH^+	38 [b]	–3	nd
3	**147c**	(*R*)-PhMeCHNH$_3^+$	52 [a]	10	–11
4	**147d**	Na^+	22 [b]	11	nd

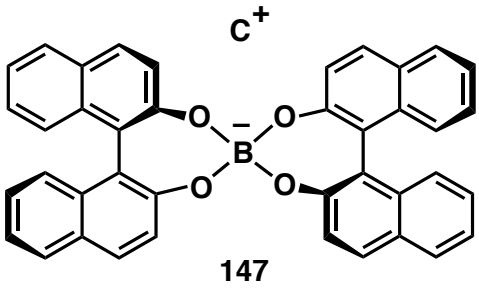

147

[a] Average yield for reactions with catalyst **147** and catalyst *ent*-**147**. [b] Yield for the reaction with catalyst **147**. [c] ee for the reactions with catalyst *ent*-**147**.

Table 1.3 The ring-opening of an aziridinium ion **150** with benzylamine **151**

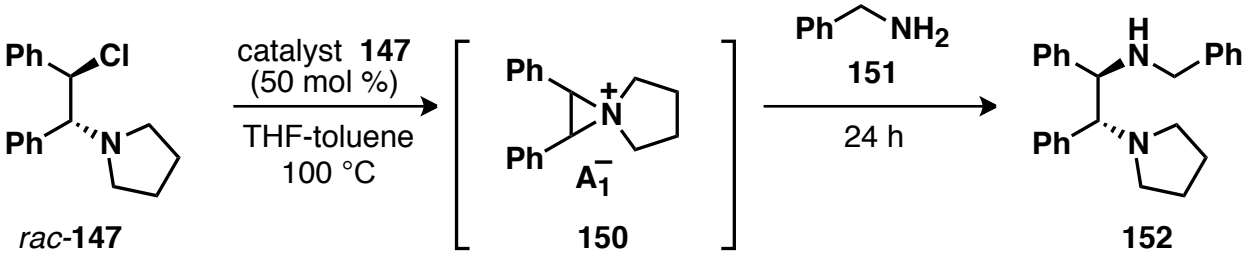

#	Cat	C^+	Yield **152** (%) [a]	ee **152** (%)	ee **152** (%) [b]
1	**147a**	$Et_2NH_2^+$	18	–6	5
2	**147b**	Et_3NH^+	25	13	–15
3	**147c**	(*R*)-$PhMeCHNH_3^+$	12	3	7
4	**147d**	Na^+	12	–7	nd

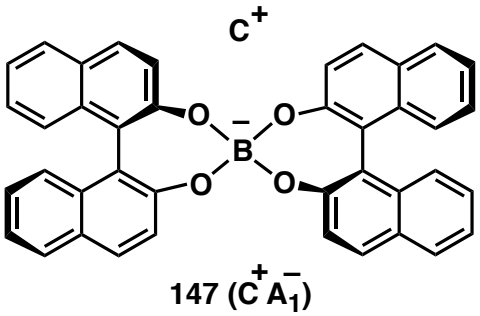

[a] Average yield for reactions with catalyst **147** and catalyst *ent*-**147**. [b] ee for the reactions with catalyst *ent*-**147**.

This work was then extended to a catalyst belonging to class IV (see Table 1.1 for definition of class IV type catalysts). Chiral borate anions along with a metal as the cation have been employed in asymmetric catalysis. With catalyst **147d**, ring-opening of aziridinium ion was performed yielding diamine **152** in 12% yield and 7% ee.[11b] However, the same reaction was reported to afford **156** in 84% yield and 94% ee utilizing TRIP-PO_3Ag **153** (Scheme 1.22).[56]

Scheme 1.22 The ring-opening of an aziridinium ion **150** and **154** with catalysts **147d** and **153**.

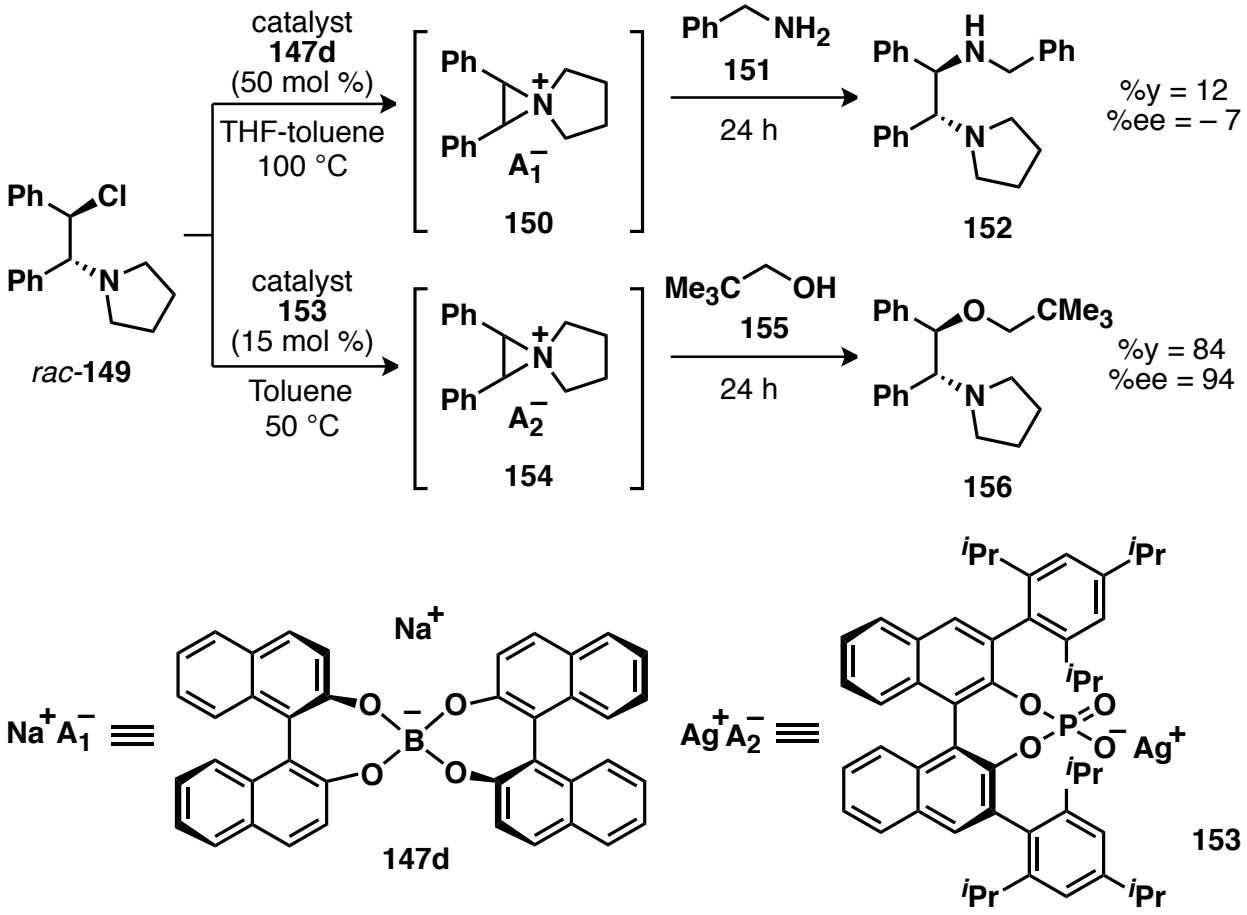

The following section is primarily focused on class V type catalysts (see Table 1.1 for definition of class V type catalysts). Conventionally, chiral ligands are bound to a metal along with an achiral non-coordinating counteranion. In these cases; steric information, which decides facial selectivity, lies within the coordination sphere. Recently, ion-pairs which have achiral ligands bound to the metal along with chiral non-coordinating anions have been utilized in asymmetric catalysis.[4,18-19] In these cases, the factors affecting enantioselection lies outside the coordination sphere. Moreover, a hybrid of chiral ligands and chiral anions provides the opportunity of matched and mismatched cases for catalysis.

Arndtsen and coworkers introduced class V type catalysts in the year 2000.[4] They performed asymmetric aziridination and cyclopropanation of styrene utilizing catalyst **147e**.[4] Low enantioslelectivities were observed in the case of aziridination reaction irrespective of the chiral or achiral ligands used (Table 1.4). In fact, similar results were obtained for the cyclopropanation reaction between styrene and ethyl diazoacetate. In these cases, *cis* isomer was found to be the major isomer (Table 1.5).

Table 1.4 Asymmetric aziridination reaction with spiroborate ion-pair **147e**

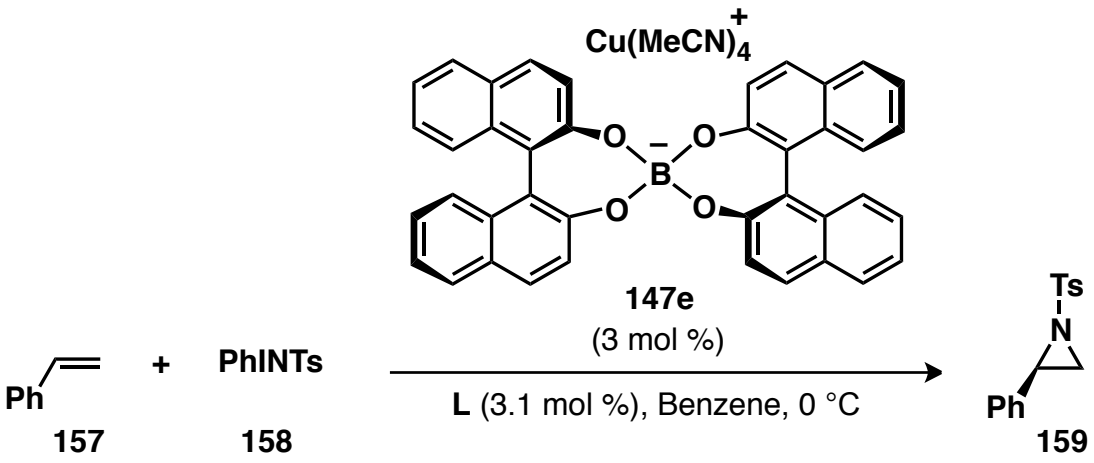

157 158 159

#	L	Yield **159** (%)	ee **159** (%)
1	**160**	75	–22 [a]
2	**160**	85 [b]	–24 [b]
3	**none**	86	7
4	**161**	43	10
5	**162**	41	10
6	**163**	78	<1

[a] –33% ee with 10 mol % $CuPF_6$ and 11 mol % **160**. [b] Results for the reactions with catalyst *ent*-**147e**.

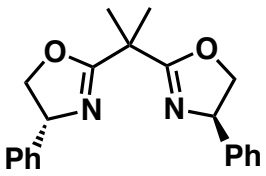

160

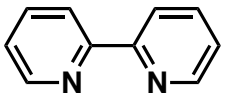

161

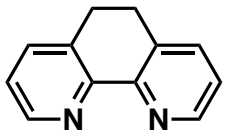

162

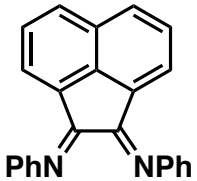

163

Table 1.5 Asymmetric cyclopropanation reaction with spiroborate ion-pair **147e**

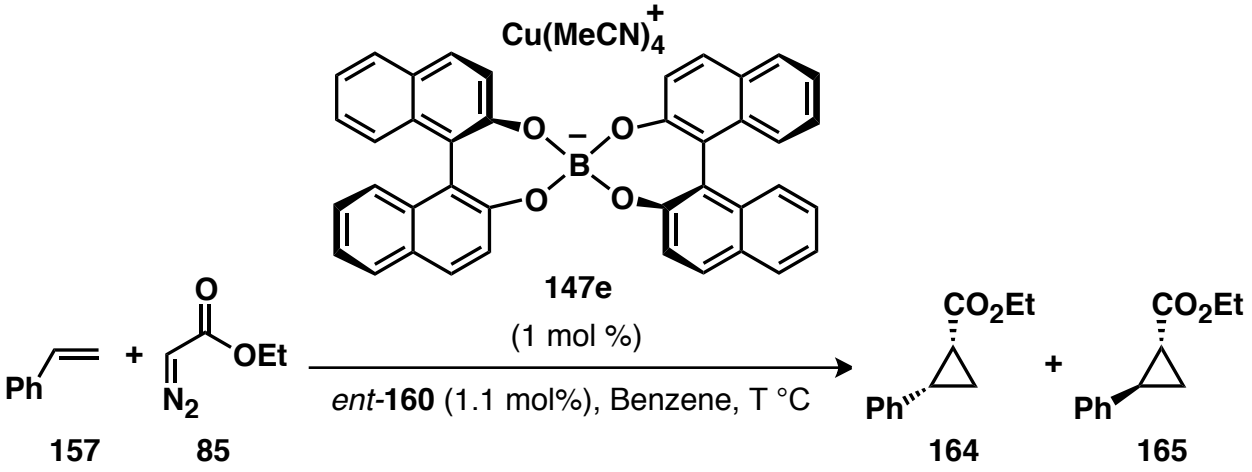

#	T (°C)	*cis*/*trans*	Yield **164+165** (%)	ee **164** (%)	ee **165** (%)
1 [a]	0	1.4:1	12	6	21
2	0	2.2:1	20	–28	10
3 [a]	25	nd	34	6	15
4	25	nd	34	8	12

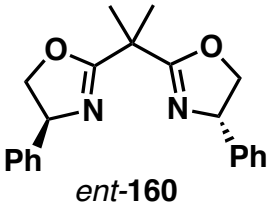

[a] Results for the reactions with catalyst *ent*-**147e**.

In 2004, Arndtsen and coworkers extended the concept of chiral spiroborate counteranion by employing tartrate amides to build the framework of the counteranion.[18-19]

Table 1.6 Asymmetric cyclopropanation with spiroborate ion-pair **166**

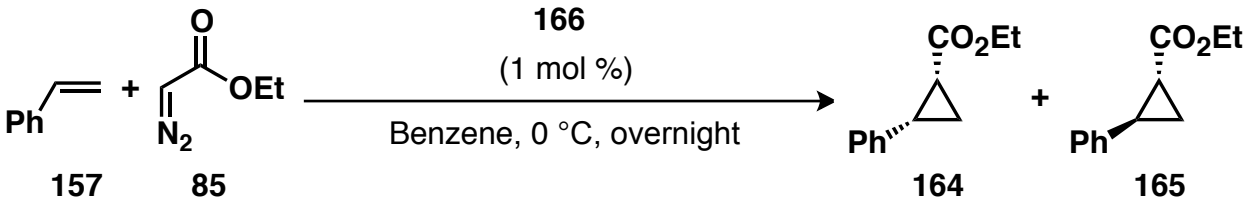

Table 1.6 Cont'd.

#	Cat.	*trans/cis*	Yield **164+165** (%)	ee **165** (%)	ee **164** (%)
1 [a]	**166a**	1.9:1	67	<2	<2
2	**166b**	1.3:1	21	17	26
3	**166c**	1.2:1	36	–23	–19
4	**166d**	1.0:1	3	–34	–19
5	**166e**	1.3:1	32	14	24

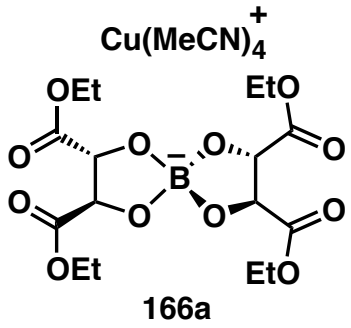

166a

[a] Reaction performed in dichloromethane at room temperature.

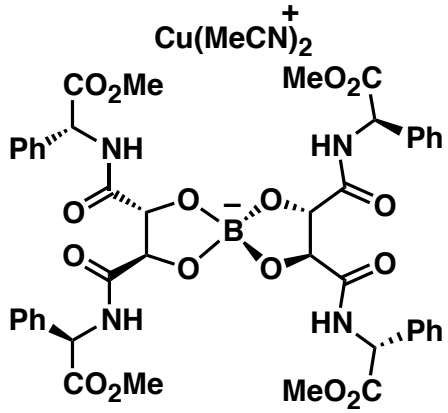

166b

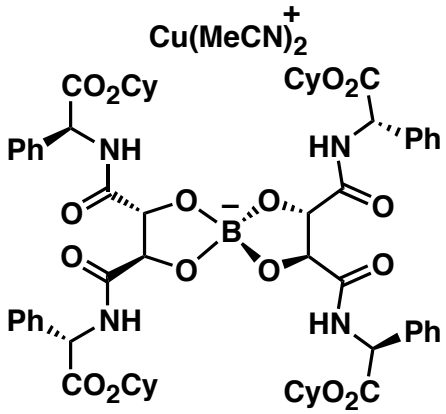

166c

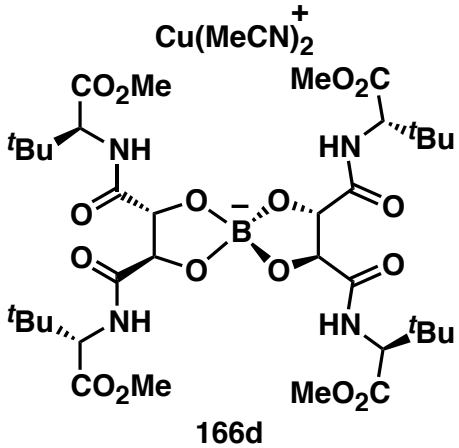

166d

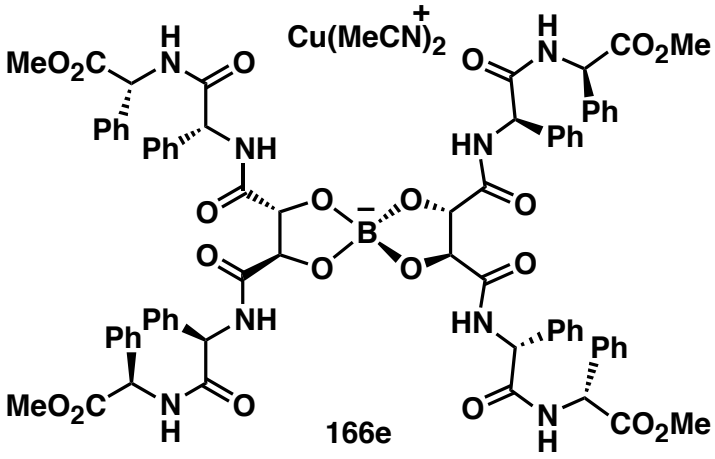

166e

One of the important features of this approach is the availability of the large number of amino acids, thereby generating a large pool of possible catalysts. However, for cyclopropanation reaction, the maximum enantio-induction attained was 34% and 26% for *trans*- and *cis*-isomer respectively (Table 1.6). Interestingly, *trans* isomer was observed to be the major product. They carried out a limited substrate scope with catalyst **166b** (Scheme 1.23).[19]

Scheme 1.23 Asymmetric cyclopropanation reaction with spiroborate ion-pair **166b**

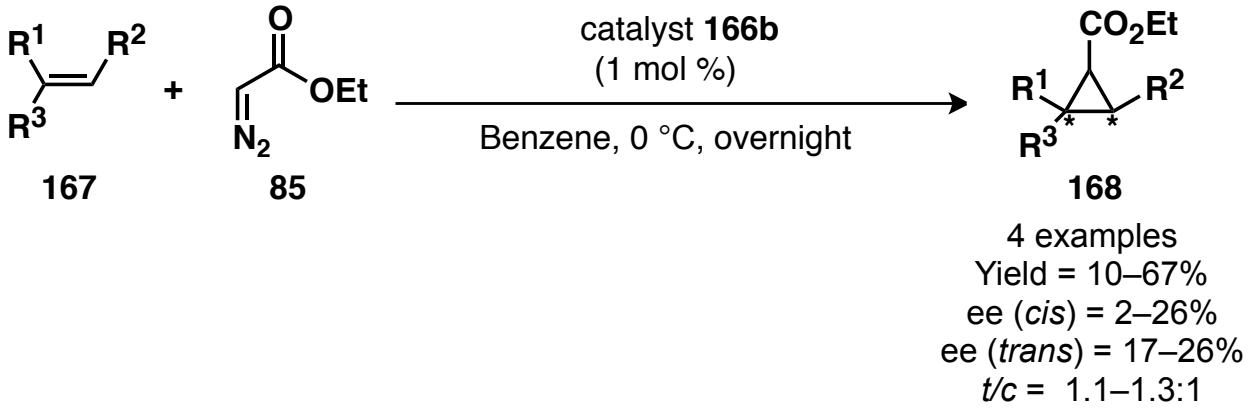

Recently, asymmetric hydrogenation of dimethyl itaconate **169** was reported by utilizing rhodium catalyst with *rac*-BINAP **171** in the presence of the chiral spiroborate ion-pair **147d** (Table 1.7).[17] Enantioselectivity up to 57% ee was observed with BINAP *rac*-**171** and 69% ee with BINAP (*R*)-**171**. Interestingly, the opposite enantiomer of **170** was observed with BINAP (*R*)-**171** alone.

Table 1.7 Asymmetric hydrogenation with spiroborate ion-pair **147d**

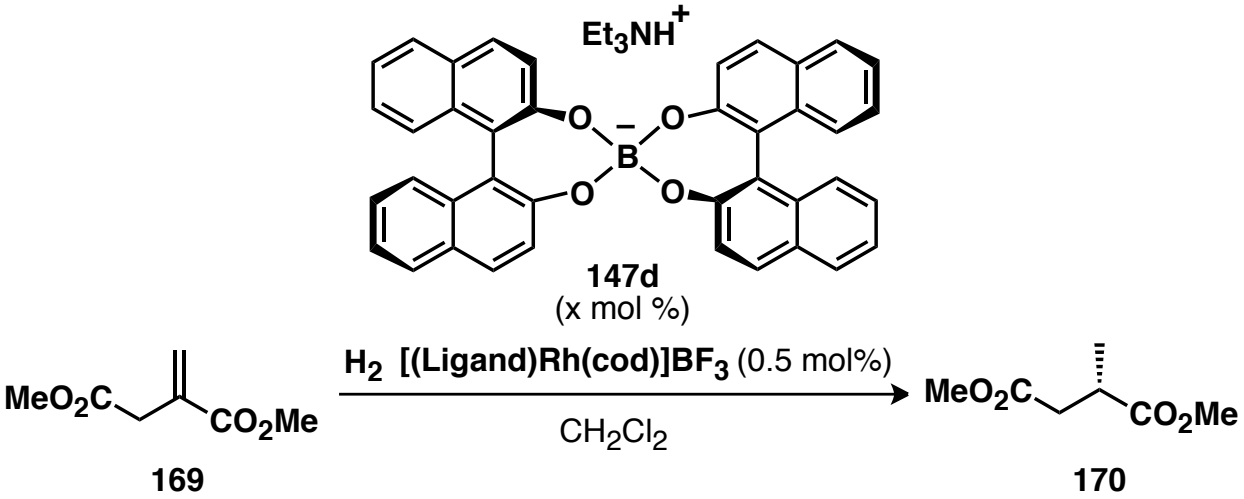

#	Ligand	x	ee **170** (%)
1	(*R*)-**171**	–	–67
2	(*R*)-**171**	5	69
3	(*S*)-**171**	5	73
4	*rac*-**171**	5	40
5	*rac*-**171**	30	57

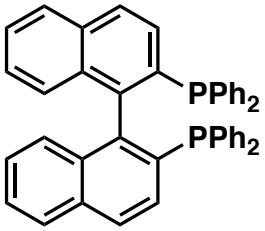

rac-**171**

1.4 Miscellaneous chiral borate anions

There are many chiral borate anions reported in literature that are used for purpose other than asymmetric catalysis. This section will briefly touch on these aspects of chiral borate anions. In 2006, Leitner and co-workers employed chiral ionic liquid (CIL) as a medium for the aza-Baylis-Hillman reaction.[57] The chiral ionic liquid was an ion pair **174** composed of an achiral methyltrioctylammonium cation and a spiroborate anion. They were able to attain enantioselectivity up to 84% ee utilizing this ionic liquid as the chiral reaction medium (Scheme Scheme 1.24).

Scheme 1.24 Chiral reaction medium made of spiroborate ion-pair **174**

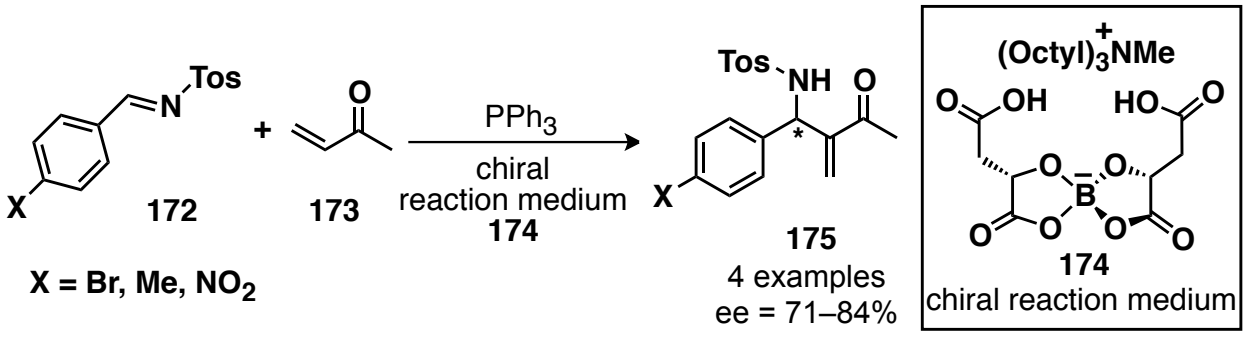

Additionally, some chiral borate anions are used as the vehicle for the resolution of racemic compounds. Periasamy and co-workers reported the resolution of BINOL *rac*-**55** by treating it with chiral amine and boric acid. The stereoselectivity is induced by the steroselective formation of the ion pair **147c** comprised of the spiroborate anion **20** and a chiral ammonium cation (Figure 1.4).[58] More recently, resolution of racemic chiral diamines has been reported *via* an ion pair **176** consisting of a chiral diborate dianion and a protonated achiral diamine as the cation (Figure 1.4).[59]

Figure 1.4 Chiral borate ion-pairs used for resolution of racemic compounds

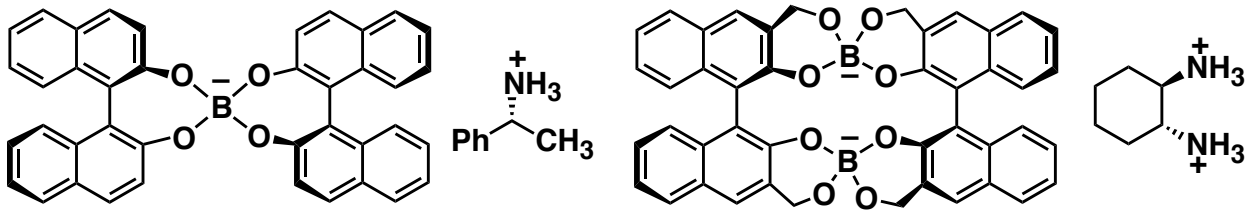

One of the prominent uses of the chiral borate anions has been its use as chiral NMR shift reagents. Arndtsen and co-workers utilized spiroborate **147e** as chiral NMR shift reagent for enantiomeric copper (I) complexes with tol-BINAP and oxazoline ligand (Figure 1.5).[60]

Recently, Glorius and co-workers used chiral dianion **177** as a chiral shift reagent for NMR analysis of triphenylphosphonium salts (Figure 1.5).[59]

Figure 1.5 Chiral borate ion-pairs used as chiral NMR shift reagents.

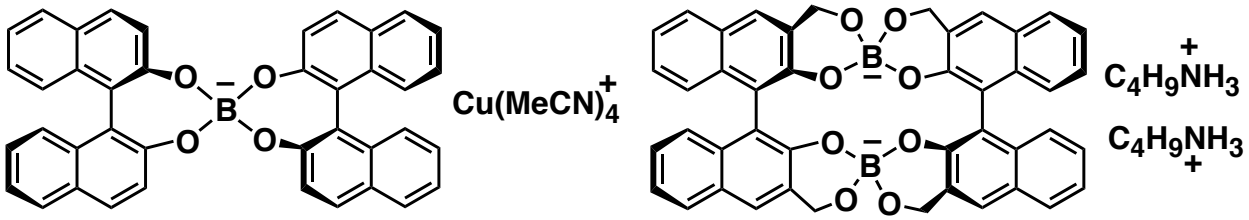

147e **177**

Chiral borate anions have also been used as ligands in asymmetric catalysis. Peng and coworkers developed a new class of chiral spiroborate ligands and used them in enantioselective Nozaki-Hiyama allylation of alkyl and aryl ketones (Figure 1.6).[61]

Figure 1.6 Chiral borate ion-pairs used as chiral ligands.

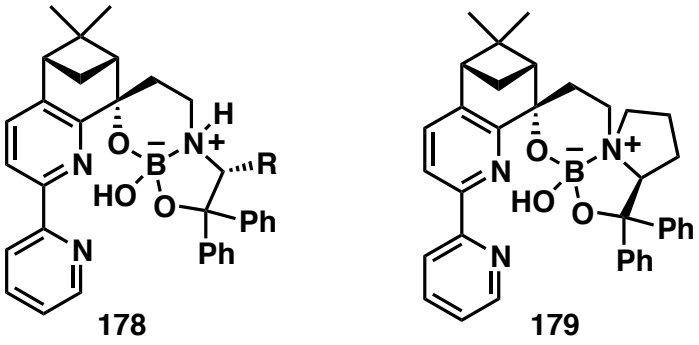

178 **179**

In quest of designing ordered materials with predicable structures and properties, considerable effort has been given to the study of chiral borate anions as a structural unit in solution and in the solid state.[62] Back-to-back twin bowls of D3-symmetry containing tris-(spiroborate) cyclophanes were recently prepared. These compounds have been prepared for

potential iterative host–guest interactions in an effort to generate supramolecular chain structures.[63]

Finally, it is interesting to observe that there are quite a few chiral spiroborate esters exist in nature (Figure 1.7).[64] The first natural product containing boron to be identified was boromycin **180**,[65] a polyether macrolide antibiotic. It was isolated from a culture of *Streptomyces antibioticus* which originated from a terrestrial soil sample from Ivory Coast. It is active against the Gram-positive bacteria. Boromycin affects the cytoplasmic membrane, which results in the release of potassium ions from the cell. Recent studies have suggested that boromycin has potent anti-HIV activity.[66] The total synthesis has been reported by White and coworkers.[67] The second natural product, aplasmomycin **181**, was isolated from a strain of *Streptomyces griseus* obtained from shallow sea and mud.[68] Aplasmomycin inhibits the growth of gram-positive bacteria in vitro and is active against *Plasmodium berghei* in vivo.[68] Its total synthesis has also been reported by a number of groups.[69] Another structurally related natural product is Tartrolon B **182**. It was isolated from Myxobacterium *Sorangium cellulosum* strain.[70] Like other boron containing natural products, it also inhibits gram-positive bacteria and works as ion carriers. A number of syntheses of this compound have been reported in the recent past.[71] In 1994, Moore and co-workers reported borophycin **183**.[72] Borophycin is the potent cytotoxin in the lipophilic extract of a marine strain of the blue-green algae (cyanobacterium) *Nostoc linckia*. No synthesis of borophycin has been reported yet. It showed cytotoxicity against LoVo

(MIC 0.066 μg/mL).[72] Also, the biosyntheses of boromycin,[73] aplasmomycin,[74] tartrolon B[75] and borophycin[72] have also been elucidated. All of these natural products are polyketides and have the same boron-binding substrate C_1-C_7 in each half of the symmetric molecules. Further, a novel AI-2 furanosyl borate diester complex **184** and was originally identified in the bioluminescent marine bacterium *Vibrio harveyi* as one of the two autoinducers that regulate light production in response to sell density.[76] Later on, it has been proposed to serve as universal bacterial quorum sensing signal containing boron for inter bacteria community communication.[77]

Figure 1.7 Chiral borate anions existing in nature

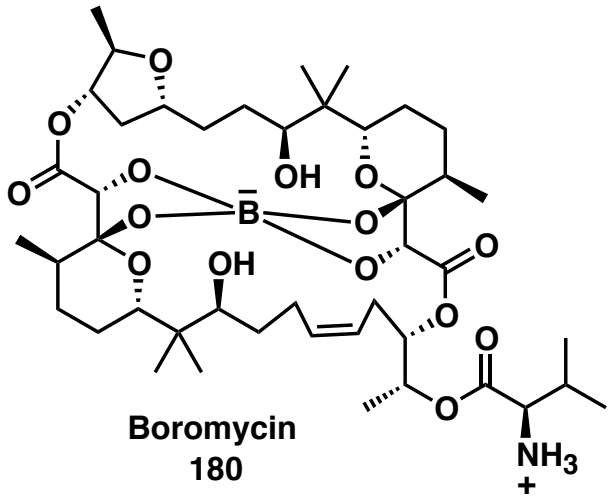

Boromycin
180

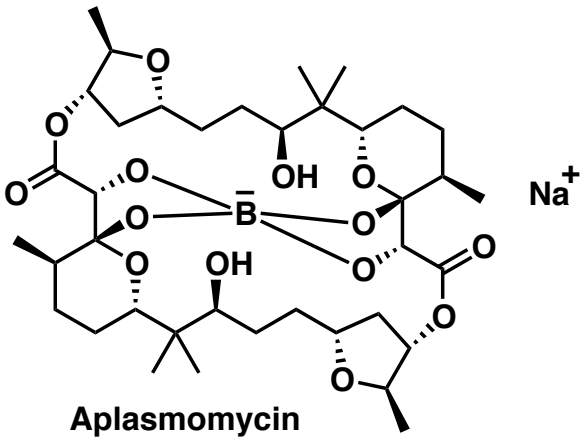

Aplasmomycin
181

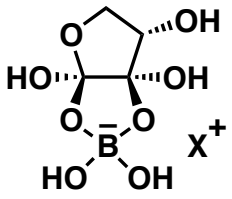

Autoinducer-2
AI-2
184

Figure 1.7 cont'd

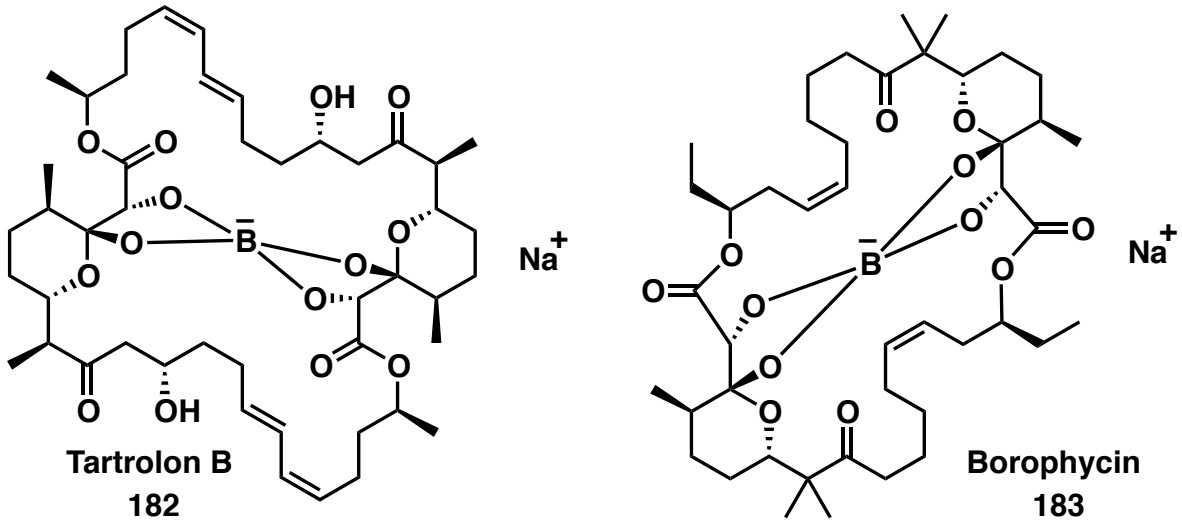

1.5 Conclusions

At the end, it is quite clear that the usage of chiral borate anions has been more prominent in last decade or so. In the field of asymmetric Brønsted acid catalysis, chiral boroxinate (BOROX) anions and other borate anions have been used quite comprehensively for a number of reactions. On the other hand, a lot of work has been done in transition metal catalysis using chiral anions other than borate anions. A significant effort is still needed in order to achieve this goal.

In subsequent chapters, a tale of BOROX catalysis will be told. It involves various aspects of catalysis such as designing new BOROX catalysts, novel reaction methodologies and its mechanistic understanding via NMR spectroscopy and computational chemistry.

REFERENCES

REFERENCES

(1) (a) Hanessian, S. In *Total Synthesis of Natural Products: The 'Chiron' Approach*; Baldwin, J. E., Ed.; Pergamon: Oxford, UK, 1983. (b) Nugent, W. A.; Rajanbabu, T. V.; Burk, M. J. *Science* **1993**, *259*, 479-483. (c) Taylor, M. S.; Jacobsen, E. N. *Proc. Nat. Acad. Sci. U.S.A* **2004**, *101*, 5368-5373. (d) *Catalytic Asymmetric Synthesis, 3rd Ed.*; Ojima, I., Ed.; Wiley-VCH: Weinheim, 2010. (e) *Asymmetric Synthesis: The Essentials, 2nd, Completely Revised Edition*; Christmann, M.; Bräse, S., Eds.; Wiley-VCH: Weinheim, 2007.

(2) *Asymmetric Phase Transfer Catalysis*; Maruoka, K., Ed.; Wiley-VCH Weinheim, 2008.

(3) (a) Lacour, J.; Hebbe-Viton, V. *Chem. Soc. Rev.* **2003**, *32*, 373-382. (b) Lacour, J.; Moraleda, D. *Chem. Commun.* **2009**, 7073-7089. (c) Rueping, M.; Koenigs, R. M.; Atodiresei, I. *Chem.–Eur. J.* **2010**, *16*, 9350-9365.

(4) Llewellyn, D. B.; Adamson, D.; Arndtsen, B. A. *Org. Lett.* **2000**, *2*, 4165-4168.

(5) Mayer, S.; List, B. *Angew. Chem., Int. Ed.* **2006**, *45*, 4193-4195.

(6) (a) Hashimoto, T.; Uchiyama, N.; Maruoka, K. *J. Am. Chem. Soc.* **2008**, *130*, 14380-14381. (b) Hashimoto, T.; Maruoka, K. *J. Am. Chem. Soc.* **2007**, *129*, 10054-10055. (c) Dorta, R.; Shimon, L.; Milstein, D. *J. Organomet. Chem.* **2004**, *689*, 751-758.

(7) (a) Hatano, M.; Sugiura, Y.; Akakura, M.; Ishihara, K. *Synlett* **2011**, 1247-1250. (b) Hatano, M.; Maki, T.; Moriyama, K.; Arinobe, M.; Ishihara, K. *J. Am. Chem. Soc.* **2008**, *130*, 16858-16860.

(8) (a) Li, G.; Liang, Y.; Antilla, J. C. *J. Am. Chem. Soc.* **2007**, *129*, 5830-5831. (b) Rowland, G. B.; Zhang, H.; Rowland, E. B.; Chennamadhavuni, S.; Wang, Y.; Antilla, J. C. *J. Am. Chem. Soc.* **2005**, *127*, 15696-15697. (c) Martin, N. J. A.; List, B. *J. Am. Chem. Soc.* **2006**, *128*, 13368-13369. (d) Liao, S.; List, B. *Angew. Chem., Int. Ed.* **2010**, *49*, 628-631. (e) Hamilton, G. L.; Kang, E. J.; Mba, M.; Toste, F. D. *Science* **2007**, *317*, 496-499. (f) List, B.; Adair, G.; Mukherjee, S. *Aldrichimica Acta* **2008**, *41*, 31-39. (g) Xu, S.; Wang, Z.; Zhang, X.; Ding, K. *Eur. J. Org. Chem.* **2011**, 110-116. (h) Jiang, G.; List, B. *Chem. Commun.* **2011**, *47*, 10022-10024. (i) Coric, I.; Mueller, S.; List, B. *J. Am. Chem. Soc.* **2010**, *132*, 17370-17373.

(9) (a) Chen, L.-Y.; He, H.; Chan, W.-H.; Lee, A. W. M. *J. Org. Chem.* **2011**, *76*, 7141-7147. (b) Ratjen, L.; Garcìa-Garcìa, P.; Lay, F.; Beck, M. E.; List, B. *Angew. Chem., Int. Ed.* **2011**, *50*,

754-758. (c) Garcìa-Garcìa, P.; Lay, F.; Garcìa-Garcìa, P.; Rabalakos, C.; List, B. *Angew. Chem., Int. Ed.* **2009**, *48*, 4363-4366.

(10) (a) Rueping, M.; Uria, U.; Lin, M.-Y.; Atodiresei, I. *J. Am. Chem. Soc.* **2011**, *133*, 3732-3735. (b) Rueping, M.; Nachtsheim, B. J.; Koenigs, R. M.; Ieawsuwan, W. *Chem.–Eur. J.* **2010**, *16*, 13116-13126. (c) Rueping, M.; Nachtsheim, B. J.; Moreth, S. A.; Bolte, M. *Angew. Chem., Int. Ed.* **2008**, *47*, 593-596.

(11) (a) Goncalves-Farbos, M.-H.; Vial, L.; Lacour, J. *Chem. Commun.* **2008**, 829-831. (b) Carter, C.; Fletcher, S.; Nelson, A. *Tetrahedron: Asymmetry* **2003**, *14*, 1995-2004. (c) Lacour, J.; Monchaud, D.; Marsol, C. *Tetrahedron Lett.* **2002**, *43*, 8257-8260.

(12) Belokon, Y. N.; Maleev, V. I.; Kataev, D. A.; Mal'fanov, I. L.; Bulychev, A. G.; Moskalenko, M. A.; Saveleva, T. y. F.; Skrupskaya, T. y. V.; Lyssenko, K. A.; Godovikov, I. A.; North, M. *Tetrahedron: Asymmetry* **2008**, *19*, 822-831.

(13) (a) Peterson, E. A.; Jacobsen, E. N. *Angew. Chem., Int. Ed.* **2009**, *48*, 6328-6331. (b) Reisman, S. E.; Doyle, A. G.; Jacobsen, E. N. *J. Am. Chem. Soc.* **2008**, *130*, 7198-7199. (c) Pan, S. C.; List, B. *Chem.–Asian. J.* **2008**, *3*, 430-437. (d) Raheem, I. T.; Thiara, P. S.; Peterson, E. A.; Jacobsen, E. N. *J. Am. Chem. Soc.* **2007**, *129*, 13404-13405.

(14) (a) Ishihara, K.; Miyata, M.; Hattori, K.; Tada, T.; Yamamoto, H. *J. Am. Chem. Soc.* **1994**, *116*, 10520-10524. (b) Ishihara, K.; Kuroki, Y.; Yamamoto, H. *Synlett* **1995**, 41-42. (c) Kuroki, Y.; Ishihara, K.; Hanaki, N.; Ohara, S.; Yamamoto, H. *Bull. Chem. Soc. Jpn.* **1998**, *71*, 1221-1230. (d) Cros, J. P.; Pérez-Fuertes, Y.; Thatcher, M. J.; Arimori, S.; Bull, S. D.; James, T. D. *Tetrahedron: Asymmetry* **2003**, *14*, 1965-1968. (e) Kawate, T.; Yamada, H.; Matsumizu, M.; Nishida, A.; Nakagawa, M. *Synlett* **1997**, 761-762. (f) Yamada, H.; Kawate, T.; Matsumizu, M.; Nishida, A.; Yamaguchi, K.; Nakagawa, M. *J. Org. Chem.* **1998**, *63*, 6348-6354.

(15) (a) Ishihara, K.; Yamamoto, H. *J. Am. Chem. Soc.* **1994**, *116*, 1561-1562. (b) Ishihara, K.; Kurihara, H.; Yamamoto, H. *J. Am. Chem. Soc.* **1996**, *118*, 3049-3050. (c) Ishihara, K.; Kurihara, H.; Matsumoto, M.; Yamamoto, H. *J. Am. Chem. Soc.* **1998**, *120*, 6920-6930. (d) Ishihara, K.; Kondo, S.; Kurihara, H.; Yamamoto, H.; Ohashi, S.; Inagaki, S. *J. Org. Chem.* **1997**, *62*, 3026-3027. (e) Dai, X.; Davies, H. M. L. *Adv. Synth. Catal.* **2006**, *348*, 2449-2456.

(16) (a) Zhang, Y.; Desai, A.; Lu, A.; Hu, G.; Ding, Z.; Wulff, W. D. *Chem. –Eur. J.* **2008**, *14*, 3785-3803. (b) Zhang, Y.; Lu, Z.; Desai, A.; Wulff, W. D. *Org. Lett.* **2008**, *10*, 5429-5432. (c) Mukherjee, M.; Gupta, A. K.; Lu, Z.; Zhang, Y.; Wulff, W. D. *J. Org. Chem.* **2010**, *75*, 5643-5660. (d) Ren, H.; Wulff, W. D. *Org. Lett.* **2010**, *12*, 4908-4911. (e) Hu, G.; Huang, L.; Huang, R. H.; Wulff, W. D. *J. Am. Chem. Soc.* **2009**, *131*, 15615-15617. (f) Hu, G.; Gupta, A. K.;

Huang, R. H.; Mukherjee, M.; Wulff, W. D. *J. Am. Chem. Soc.* **2010**, *132*, 14669–14675. (g) Gupta, A. K.; Mukherjee, M.; Wulff, W. D. *Org. Lett.* **2011**, *13*, 5866-5869. (h) Newman, C. A.; Antilla, J. C.; Chen, P.; Predeus, A. V.; Fielding, L.; Wulff, W. D. *J. Am. Chem. Soc.* **2007**, *129*, 7216-7217. (i) Desai, A. A.; Wulff, W. D. *J. Am. Chem. Soc.* **2010**, *132*, 13100-13103. (j) Vetticatt, M. J.; Desai, A. A.; Wulff, W. D. *J. Am. Chem. Soc.* **2010**, *132*, 13104-13107. (k) Desai, A. A.; Morán-Ramallal, R.; Wulff, W. D. *Org. Synth.* **2011**, *88*, 224-237. (l) Ren, H.; Wulff, W. D. *J. Am. Chem. Soc.* **2011**, *133*, 5656-5659. (m) Desai, A. A.; Ren, H.; Mukherjee, M.; Wulff, W. D. *Org. Process Res. Dev.* **2011**, *15*, 1108-1115.

(17) Chen, D.; Sundararaju, B.; Krause, R.; Klankermayer, J.; Dixneuf, P. H.; Leitner, W. *ChemCatChem* **2010**, *2*, 55-57.

(18) Llewellyn, D. B.; Arndtsen, B. A. *Organometallics* **2004**, *23*, 2838-2840.

(19) Llewellyn, D. B.; Arndtsen, B. A. *Tetrahedron: Asymmetry* **2005**, *16*, 1789-1799.

(20) (a) Rueping, M.; Nachtsheim, B. J.; Ieawsuwan, W.; Atodiresei, I. *Angew. Chem., Int. Ed.* **2011**, *50*, 6706-6720. (b) Schenker, S.; Zamfir, A.; Freund, M.; Tsogoeva, S. B. *Eur. J. Org. Chem.* **2011**, 2209-2222. (c) Rueping, M.; Kuenkel, A.; Atodiresei, I. *Chem. Soc. Rev.* **2011**, *40*, 4539-4549. (d) List, B.; Kampen, D.; Reisinger, C. M. *Top Curr Chem* **2010**, *291*, 395-456. (e) Sohtome, Y.; Nagasawa, K. *Synlett* **2010**, 1-22. (f) Yamamoto, H.; Payette, J. N. In *Hydrogen Bonding in Organic Synthesis*; Wiley-VCH 2009, p 73-140. (g) Yu, X.; Wang, W. *Chem.–Asian. J.* **2008**, *3*, 516-532. (h) Doyle, A. G.; Jacobsen, E. N. *Chem. Rev.* **2007**, *107*, 5713-5743. (i) Akiyama, T. *Chem. Rev.* **2007**, *107*, 5744-5758. (j) Taylor, M. S. J., E. N. *Angew. Chem., Int. Ed.* **2006**, *45*, 1520-1543. (k) Akiyama, T.; Itoh, J.; Fuchibe, K. *Adv. Synth. Catal.* **2006**, *348*, 999-1010.

(21) (a) Terada, M. *Synthesis* **2010**, 1929-1982. (b) Terada, M. *Bull. Chem. Soc. Jpn.* **2010**, *83*, 101-119. (c) Zamfir, A.; Schenker, S.; Freund, M.; Tsogoeva, S. B. *Org. Biomol. Chem.* **2010**, *8*. (d) Terada, M. *Chem. Commun. (Cambridge, U. K.)* **2008**, 4097-4112. (e) Connon, S. J. *Angew. Chem., Int. Ed.* **2006**, *45*, 3909-3912.

(22) (a) Akiyama, T.; Itoh, J.; Yokota, K.; Fuchibe, K. *Angew. Chem., Int. Ed.* **2004**, *43*, 1566-1568. (b) Uraguchi, D.; Terada, M. *J. Am. Chem. Soc.* **2004**, *126*, 5356-5357.

(23) Shapiro, N. D.; Rauniyar, V.; Hamilton, G. L.; Wu, J.; Toste, F. D. *Nature* **2011**, *470*, 245-249.

(24) Momiyama, N.; Konno, T.; Furiya, Y.; Iwamoto, T.; Terada, M. *J. Am. Chem. Soc.* **2011**, *133*, 19294-19297.

(25) (a) Desai, A. A.; Wulff, W. D. *Synthesis* **2010**, 3670-3680. (b) Rowland, E. B.; Rowland, G. B.; Rivera-Otero, E.; Antilla, J. C. *J. Am. Chem. Soc.* **2007**, *129*, 12084-12085.

(26) (a) Senatore, M.; Lattanzi, A.; Santoro, S.; Santi, C.; Della, S. G. *Org. Biomol. Chem.* **2011**, *9*, 6205-6207. (b) Desai, A. A.; Huang, L.; Wulff, W. D.; Rowland, G. B.; Antilla, J. C. *Synthesis* **2010**, 2106-2109. (c) Larson, S. E.; Baso, J. C.; Li, G.; Antilla, J. C. *Org. Lett.* **2009**, *11*, 5186-5189. (d) Della, S. G.; Lattanzi, A. *Org. Lett.* **2009**, *11*, 3330-3333. (e) Rowland, G. B.; Rowland, E. B.; Liang, Y.; Perman, J. A.; Antilla, J. C. *Org. Lett.* **2007**, *9*, 2609-2611. (f) Liang, Y.; Rowland, E. B.; Rowland, G. B.; Perman, J. A.; Antilla, J. C. *Chem. Commun.* **2007**, 4477-4479.

(27) (a) Xu, B.; Zhu, S.-F.; Xie, X.-L.; Shen, J.-J.; Zhou, Q.-L. *Angew. Chem., Int. Ed.* **2011**, *50*, 11483-11486. (b) Xing, C.-H.; Liao, Y.-X.; Ng, J.; Hu, Q.-S. *J. Org. Chem.* **2011**, *76*, 4125-4131. (c) Müller, S.; Webber, M. J.; List, B. *J. Am. Chem. Soc.* **2011**, *133*, 18534-18537. (d) Huang, D.; Xu, F.; Lin, X.; Wang, Y. Chiral spirocyclic phosphoric acid, its preparation method and application as catalyst CN102030780A Apr 27, 2011. (e) Xu, F.; Huang, D.; Han, C.; Shen, W.; Lin, X.; Wang, Y. *J. Org. Chem.* **2010**, *75*, 8677-8680.

(28) (a) Akiyama, T. Preparation of cyclic erythritol phosphoric acid derivatives as catalysts for asymmetric synthesis WO2006092884A1 . (b) Voituriez, A.; Charette, A. B. *Adv. Synth. Catal.* **2006**, *348*, 2363-2370. (c) Akiyama, T.; Saitoh, Y.; Morita, H.; Fuchibe, K. *Adv. Synth. Catal.* **2005**, *347*, 1523-1526.

(29) (a) Zheng, W.; Zhang, Z.; Kaplan, M. J.; Antilla, J. C. *J. Am. Chem. Soc.* **2011**, *133*, 3339-3341. (b) Zhang, Z.; Zheng, W.; Antilla, J. C. *Angew. Chem., Int. Ed.* **2011**, *50*, 1135-1138. (c) Larson, S. E.; Li, G.; Rowland, G. B.; Junge, D.; Huang, R.; Woodcock, H. L.; Antilla, J. C. *Org. Lett.* **2011**, *13*, 2188-2191. (d) Rueping, M.; Bootwicha, T.; Sugiono, E. *Synlett* **2011**, 323-326. (e) Hatano, M.; Ishihara, K. *Synthesis* **2010**, 3785-3801. (f) Klussmann, M.; Ratjen, L.; Hoffmann, S.; Wakchaure, V.; Goddard, R.; List, B. *Synlett* **2010**, 2189-2192.

(30) Terada, M.; Sorimachi, K.; Uraguchi, D. *Synlett* **2006**, 133-136.

(31) (a) Hashimoto, T.; Nakatsu, H.; Yamamoto, K.; Maruoka, K. *J. Am. Chem. Soc.* **2011**, *133*, 9730-9733. (b) Vellalath, S.; Coric, I.; List, B. *Angew. Chem., Int. Ed.* **2010**, *49*, 9749-9752. (c) Cheon, C. H.; Yamamoto, H. *J. Am. Chem. Soc.* **2008**, *130*, 9246-9247. (d) Rueping, M.; Ieawsuwan, W.; Antonchick, A. P.; Nachtsheim, B. J. *Angew. Chem., Int. Ed.* **2007**, *46*, 2097-2100. (e) Nakashima, D.; Yamamoto, H. *J. Am. Chem. Soc.* **2006**, *128*, 9626-9627.

(32) (a) He, H.; Chen, L.-Y.; Wong, W.-Y.; Chan, W.-H.; Lee, A. W. M. *Eur. J. Org. Chem.* **2010**, 4181-4184. (b) Treskow, M.; Neudoerfl, J.; Giernoth, R. *Eur. J. Org. Chem.* **2009**, 3693-3697.

(33) Berkessel, A.; Christ, P.; Leconte, N.; Neudörfl, J.-M.; Schäfer, M. *Eur. J. Org. Chem.* **2010**, 5165-5170.

(34) Coric, I.; List, B. *Nature* **2012**, *483*, 315-319.

(35) (a) Hashimoto, T.; Omote, M.; Maruoka, K. *Angew. Chem., Int. Ed.* **2011**, *50*, 3489-3492. (b) Hashimoto, T.; Omote, M.; Maruoka, K. *Angew. Chem., Int. Ed.* **2011**, *50*, 8952-8955. (c) Hashimoto, T.; Kimura, H.; Nakatsu, H.; Maruoka, K. *J. Org. Chem.* **2011**, *76*, 6030-6037. (d) Hashimoto, T.; Kimura, H.; Maruoka, K. *Angew. Chem., Int. Ed.* **2010**, *49*, 6844-6847.

(36) Hatano, M.; Sugiura, Y.; Ishihara, K. *Tetrahedron: Asymmetry* **2010**, *21*, 1311-1314.

(37) Christ, P.; Lindsay, A. G.; Vormittag, S. S.; Neudoerfl, J.-M.; Berkessel, A.; O'Donoghue, A. C. *Chem.–Eur. J.* **2011**, *17*, 8524-8528.

(38) Rueping, M.; Theissmann, T. *Chem. Sci.* **2010**, *1*, 473-476.

(39) (a) Fleischmann, M.; Drettwan, D.; Sugiono, E.; Rueping, M.; Gschwind, R. M. *Angew. Chem., Int. Ed.* **2011**, *50*, 6364-6369. (b) Simón, L.; Goodman, J. M. *J. Org. Chem.* **2011**, *76*, 1775-1788.

(40) (a) Takemoto, Y. *Chem. Pharm. Bull.* **2010**, *58*, 593-601. (b) Yoshida, K.; Inokuma, T.; Takasu, K.; Takemoto, Y. *Molecules* **2010**, *15*, 8305-8326. (c) Rodriguez, A. A.; Yoo, H.; Ziller, J. W.; Shea, K. J. *Tetrahedron Lett.* **2009**, *50*, 6830-6833. (d) Connon, S. J. *Chem. Commun.* **2008**. (e) Rampalakos, C.; Wulff, W. D. *Adv. Synth. Catal.* **2008**, *350*, 1785-1790. (f) Connon, S. J. *Chem.–Eur. J.* **2006**, *12*, 5418-5427. (g) Takemoto, Y. *Org. Biomol. Chem.* **2005**, *3*.

(41) (a) Huang, Y.; Unni, A. K.; Thadani, A. N.; Rawal, V. H. *Nature* **2003**, *424*, 146-146. (b) Thadani, A. N.; Stankovic, A. R.; Rawal, V. H. *Proc. Nat. Acad. Sci. U.S.A* **2004**, *101*, 5846-5850. (c) Gondi, V. B.; Gravel, M.; Rawal, V. H. *Org. Lett.* **2005**, *7*, 5657-5660. (d) McGilvra, J. D.; Unni, A. K.; Modi, K.; Rawal, V. H. *Angew. Chem., Int. Ed.* **2006**, *45*, 6130-6133. (e) Gómez-Bengoa, E. *Eur. J. Org. Chem.* **2009**, 1207-1213. (f) Etzenbach-Effers, K.; Berkessel, A. *Top Curr Chem* **2010**, *291*, 1-27.

(42) (a) Tillman, A. L.; Dixon, D. J. *Org. Biomol. Chem.* **2007**, *5*. (b) Momiyama, N.; Yamamoto, Y.; Yamamoto, H. *J. Am. Chem. Soc.* **2007**, *129*, 1190-1195. (c) Matsui, K.; Takizawa, S.; Sasai, H. *Synlett* **2006**, 761-765. (d) Momiyama, N.; Yamamoto, H. *J. Am. Chem. Soc.* **2005**, *127*, 1080-1081. (e) Matsui, K.; Takizawa, S.; Sasai, H. *J. Am. Chem. Soc.* **2005**, *127*, 3680-3681. (f) Dixon, D. J.; Tillman, A. L. *Synlett* **2005**, 2635-2638. (g) McDougal, N. T.; Schaus, S. E. *J. Am. Chem. Soc.* **2003**, *125*, 12094-12095. (h) Dixon, D. J.; Tillman, A. L. *Synlett* **2005**, 2635-2638.

(43) (a) *Privileged Chiral Ligands and Catalysts*; Zhou, Q.-L., Ed.; Wiley-VCH: Weinheim, 2011. (b) Brunel, J. M. *Chem. Rev.* **2008**, *108*, 1170-1170. (c) Chen, Y.; Yekta, S.; Yudin, A. K. *Chem. Rev.* **2003**, *103*, 3155-3211. (d) Jorgensen, K. A.; Simonsen, K. B.; Gothelf, K. V. *J. Org. Chem.* **1998**, *63*, 7536-7538.

(44) (a) Heumann, L. V.; Keck, G. E. *J. Org. Chem.* **2008**, *73*, 4725-4727. (b) Takasaki, M.; Motoyama, Y.; Yoon, S.-H.; Mochida, I.; Nagashima, H. *J. Org. Chem.* **2007**, *72*, 10291-10293. (c) Korostylev, A.; Tararov, V. I.; Fischer, C.; Monsees, A.; Borner, A. *J. Org. Chem.* **2004**, *69*, 3220-3221. (d) Au-Yeung, T. T. L.; Chan, S.-S.; Chan, A. S. C. *Adv. Synth. Catal.* **2003**, *345*, 537-555 and references therein. (e) Ding, K.; Guo, H. *Tetrahedron Lett.* **2000**, *41*, 10061-10064.

(45) Ding, Z.; Osminski, W. E. G.; Ren, H.; Wulff, W. D. *Org. Process Res. Dev.* **2011**, *15*, 1089-1107 and references therein.

(46) (a) Zhou, Q. L.; Xie, J. H. *Top. Organomet. Chem.* **2011**, *36*, 1-28. (b) Ding, K. L.; Han, Z. B.; Wang, Z. *Chem.–Asian. J.* **2009**, *4*, 32-41 and references therein. (c) Cheng, X.; Hou, G. H.; Xie, J. H.; Zhou, Q. L. *Org. Lett.* **2004**, *6*, 2381-2383. (d) Zhu, S. F.; Fu, Y.; Xie, J. H.; Liu, B.; Xing, L.; Zhou, Q. L. *Tetrahedron: Asymmetry* **2003**, *14*, 3219-3224. (e) Zhang, J. H.; Liao, J.; Cui, X.; Yu, K. B.; Zhu, J.; Deng, J. G.; Zhu, S. F.; Wang, L. X.; Zhou, Q. L.; Chung, L. W.; Ye, T. *Tetrahedron: Asymmetry* **2002**, *13*, 1363-1366. (f) Birman, V. B.; L. Rheingold, A.; Lam, K.-C. *Tetrahedron: Asymmetry* **1999**, *10*, 125-131.

(47) (a) Lam, H. W. *Synthesis* **2011**, 2011-2043. (b) Pellissier, H. *Tetrahedron* **2008**, *64*, 10279-10317. (c) Seebach, D.; Beck, A. K.; Heckel, A. *Angew. Chem., Int. Ed.* **2001**, *40*, 92-138.

(48) Zhang, Z.; Jain, P.; Antilla, J. C. *Angew. Chem., Int. Ed.* **2011**, *50*, 10961-10964.

(49) Martin, N. J. A.; List, B. *J. Am. Chem. Soc.* **2006**, *128*, 13368-13369.

(50) Hu, G. PhD Thesis, Michigan State University, 2007.

(51) Hu, G.; Huang, L.; Gupta, A. K.; Huang, R.; Wulff, W. D., *manuscript in preparation.*

(52) Guan, Y.; Wulff, W. D., Unpublished results.

(53) Gupta, A. K.; Wulff, W. D., Unpublished results.

(54) Desai, A.; Wulff, W. D., Unpublished results.

(55) (a) Huang, L.; Zhang, Y.; Staples, R. J.; Huang, R. H.; Wulff, W. D. *Chem.–Eur. J.* **2012**, *18*, 5302-5313. (b) Mukherjee, M. PhD Dissertation, Michigan State University, 2012.

(56) Hamilton, G. L.; Kanai, T.; Toste, F. D. *J. Am. Chem. Soc.* **2008**, *130*, 14984-14986.

(57) Gausepohl, R.; Buskens, P.; Kleinen, J.; Bruckmann, A.; Lehmann, C. W.; Klankermayer, J.; Leitner, W. *Angew. Chem., Int. Ed.* **2006**, *45*, 3689-3692.

(58) Periasamy, M.; Venkatraman, L.; Sivakumar, S.; Sampathkumar, N.; Ramanathan, C. R. *J. Org. Chem.* **1999**, *64*, 7643-7645.

(59) Loewer, Y.; Weiss, C.; Biju, A. T.; Fröhlich, R.; Glorius, F. *J. Org. Chem.* **2011**, *76*, 2324-2327.

(60) Llewellyn, D. B.; Arndtsen, B. A. *Can. J. Chem.* **2003**, *81*, 1280-1284.

(61) Huang, X.-R.; Chen, C.; Lee, G.-H.; Peng, S.-M. *Adv. Synth. Catal.* **2009**, *351*, 3089-3095.

(62) (a) Raskatov, J. A.; Brown, J. M.; Thompson, A. L. *Crystengcomm* **2011**, *13*, 2923-2929. (b) Wrackmeyer, B.; Klimkina, E. V.; Milius, W. *Eur. J. Inorg. Chem.* **2011**, 2164-2171. (c) Tu, T.; Maris, T.; Wuest, J. D. *Cryst. Growth Des.* **2008**, *8*, 1541-1546. (d) Green, S.; Nelson, A.; Warriner, S.; Whittaker, B. *J. Chem. Soc., Perkin Trans. 1* **2000**, 4403-4408.

(63) Danjo, H.; Hirata, K.; Yoshigai, S.; Azumaya, I.; Yamaguchi, K. *J. Am. Chem. Soc.* **2009**, *131*, 1638-1639.

(64) (a) Baker, S. J.; Tomsho, J. W.; Benkovic, S. J. *Chem. Soc. Rev.* **2011**, *40*. (b) Carrano, C.; Schellenberg, S.; Amin, S.; Green, D.; Küpper, F. *Mar. Biotechnol.* **2009**, *11*, 431-440. (c) Dembitsky, V. M.; Smoum, R.; Al-Quntar, A. A.; Ali, H. A.; Pergament, I.; Srebnik, M. *Plant Science* **2002**, *163*, 931-942.

(65) (a) Dunitz, J. D.; Hawley, D. M.; Mikloš, D.; White, D. N. J.; Berlin, Y.; Marušić, R.; Prelog, V. *Helv. Chim. Acta* **1971**, *54*, 1709-1713. (b) Hütter, R.; Keller-Schien, W.; Knüsel, F.; Prelog, V.; Rodgers, G. C.; Suter, P.; Vogel, G.; Voser, W.; Zähner, H. *Helv. Chim. Acta* **1967**, *50*, 1533-1539.

(66) Kohno, J.; Kawahata, T.; Otake, T.; Morimoto, M.; Mori, H.; Ueba, N.; Nishio, M.; Kinumaki, A.; Komatsubara, S.; Kawashima, K. *Biosci. Biotechnol., Biochem.* **1996**, *60*, 1036-1037.

(67) White, J. D.; Avery, M. A.; Choudhry, S. C.; Dhingra, O. P.; Gray, B. D.; Kang, M. C.; Kuo, S. C.; Whittle, A. J. *J. Am. Chem. Soc.* **1989**, *111*, 790-792.

(68) Okami, Y.; Okazaki, T.; KIitahara, T.; Umezawa, H. *J. Antibiot.* **1976**, *29*, 1019-1025.

(69) (a) Matsuda, F.; Tomiyoshi, N.; Yanagiya, M.; Matsumoto, T. *Tetrahedron* **1990**, *46*, 3469-3488. (b) White, J. D.; Vedananda, T. R.; Kang, M. C.; Choudhry, S. C. *J. Am. Chem. Soc.* **1986**, *108*, 8105-8107. (c) Nakata, T.; Saito, K.; Oishi, T. *Tetrahedron Lett.* **1986**, *27*, 6345-6348. (d) Corey, E. J.; Pan, B. C.; Hua, D. H.; Deardorff, D. R. *J. Am. Chem. Soc.* **1982**, *104*, 6816-6818. (e) Corey, E. J.; Hua, D. H.; Pan, B. C.; Seitz, S. P. *J. Am. Chem. Soc.* **1982**, *104*, 6818-6820.

(70) Irschik, H.; Schummer, D.; Gerth, K.; Höfle, G.; Reichenbach, H. *J. Antibiot.* **1977**, *48*, 26-30.

(71) (a) Mulzer, J.; Berger, M. *J. Org. Chem.* **2004**, *69*, 891-898. (b) Berger, M.; Mulzer, J. *J. Am. Chem. Soc.* **1999**, *121*, 8393-8394.

(72) Hemscheidt, T.; Puglisi, M. P.; Larsen, L. K.; Patterson, G. M. L.; Moore, R. E.; Rios, J. L.; Clardy, J. *J. Org. Chem.* **1994**, *59*, 3467-3471.

(73) Chen, T. S. S.; Chang, C.-J.; Floss, H. G. *J. Org. Chem.* **1981**, *46*, 2661-2665.

(74) (a) Lee, J. J.; Dewick, P. M.; Gorst-Allman, C. P.; Spreafico, F.; Kowal, C.; Chang, C. J.; McInnes, A. G.; Walter, J. A.; Keller, P. J.; Floss, H. G. *J. Am. Chem. Soc.* **1987**, *109*, 5426-5432. (b) Chen, T. S. S.; Chang, C.-J.; Floss, H. G. *J. Am. Chem. Soc.* **1981**, *103*, 4565-4568.

(75) Schummer, D.; Schomburg, D.; Irschik, H.; Reichenbach, H.; Höfle, G. *Liebigs Ann. Chem.* **1996**, 965-969.

(76) Bassler, B. L.; Wright, M.; Showalter, R. E.; Silverman, M. R. *Mol. Microbiol.* **1993**, *9*, 773-786.

(77) Chen, X.; Schauder, S.; Potier, N.; Van Dorsselaer, A.; Pelczer, I.; Bassler, B. L.; Hughson, F. M. *Nature* **2002**, *415*, 545-549.

CHAPTER 2

A NEW ARRAY OF BRØNSTED ACID CATALYSTS DERIVED FROM CHIRAL BORATE ANIONS

I think you don't have enough work in the lab. Plus, I think you need another paper.

-William D. Wulff

As discussed in chapter 1, the field of asymmetric Brønsted acid catalysis has made amazing advances over the last few years.[1] Particularly, there has been an exponential growth in the field of chiral phosphoric acids,[2] phosphoramides,[3] bis(sufonyl)imides,[4] bis(sulfuryl)imides,[5] chiral dicarboxylic acids,[6] and chiral disulfonic acids[7] prepared from BINOL and H8-BINOL and their derivatives.[1a] More recently, novel chiral phosphoric acids derived from VANOL,[8] VAPOL,[8-9] SPINOL,[10] and TADDOL[10f,11] have also been employed.

In the case of Brønsted acids derived from chiral borate anions, there is no example reported prior to our work. Although Brønsted acid catalyst derived from spiroborate anions[12] have been reported, they have been proposed to mechanistically function as a Lewis acid until it was found in work for this thesis that they can function as Brønsted acids (Scheme 4.6, Chapter 4). At the present time, there are three different kinds of Brønsted acid catalysts derived from chiral borate anions as shown in Figure 2.1. These are characterized by NMR spectroscopy and are discussed in subsequent sections of this chapter.

Figure 2.1 Brønsted acid catalysts derived from chiral borate anions and imines as the base

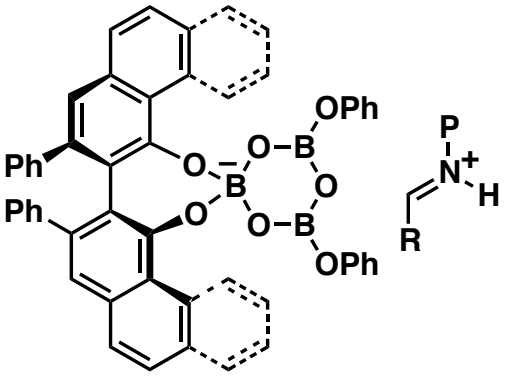

104a/105a

B3 (BOROX)

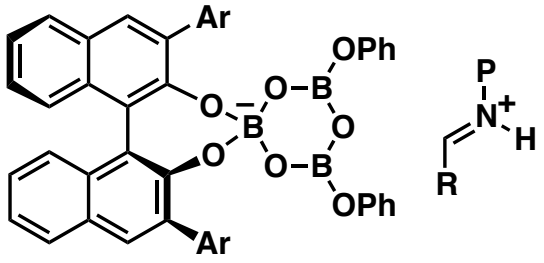

185 (Ar = H)

186 (Ar ≠ H)

B3 (BOROX)

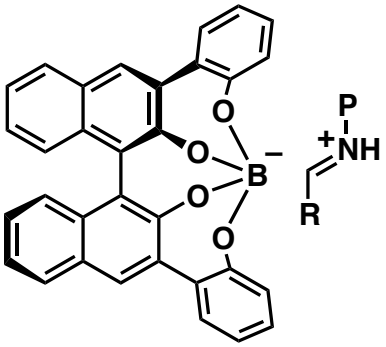

92

B1 (FSB)

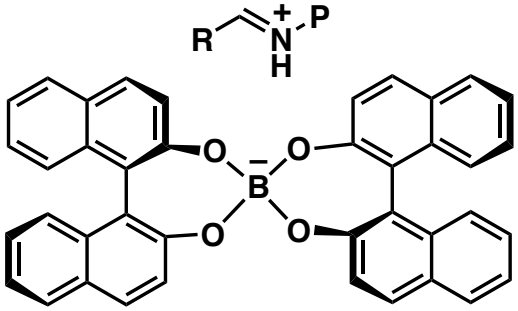

74

B1 (SB)

2.1 B3 or BOROX Catalysts

Prior to our report, a Brønsted acid derived from a chiral boroxinate anion has never been reported (Scheme 2.1).[13] Since the boroxinate anion can be viewed as a derivative of a boroxine ring, we coined a new term "BOROX catalyst" for this class of catalysts. These novel spiroboroxinate catalysts are formed only upon the addition of a base (usually imines) and thus it belongs to class II type catalysts (Table 1.1, Chapter 1). Initially, only imines were used to generate these catalysts. The aim of this part of the project is two fold: a) refinement of the study

towards the discovery of unique chiral boroxinate catalysts generated by imines b) screening other bases and thereby generating an array of novel Brønsted acid catalysts and subsequently their application in asymmetric catalysts. *Hence, a number of novel BOROX catalysts were generated using different bases. These catalysts were characterized by ^{1}H NMR, ^{11}B NMR spectroscopy and computational chemistry. It must be noted that these catalysts could also be chiral Lewis acids as similar NMR behavior is expected in the case of Lewis acids. However, we were able to obtain X-ray crystals of the BOROX catalysts with bases such as imines[13f] and 2,6-lutidine (this work).* The screening of different bases is discussed below.

2.1.1 Imines as the base: IMINO-BOROX catalyst

Over the past few years, we have developed a universal catalytic asymmetric aziridination reaction of imines utilizing a catalyst derived from either of the vaulted ligands VAPOL **58** or VANOL **59** and commercial $B(OPh)_3$ (Chapter 1, Scheme 1.13).[13] Inspired by the work reported by Brookhart and Templeton,[14] we reported the catalytic asymmetric aziridination of imines **78** to afford *cis*-aziridines in 1999 and 2000.[15] Meanwhile, a lot of mechanistic studies were carried out in our group regarding the identification of the structure of the active catalyst. Prior to these studies, it was believed that the active catalyst was B1 **106**/**107** (Scheme 2.1) that was generated from VAPOL or VANOL when reacted with triphenyl borate **187a**. This proposed structure was based on analogous studies carried out by Yamamoto on BINOL **55**,[12a,16] however no spectroscopic evidence was presented by Yamamoto for his proposed structure. Further, Yu Zhang, one of the former group members, found that on the

basis of NMR and MS studies there are two boron species identified as B2 **108**/**109** and B1 **106**/**107** (Scheme 2.1).[13a] Additionally, it was found that the catalyst enriched with B2 **108**/**109** gives higher asymmetric inductions and higher rates in the aziridination reaction compared with catalyst enriched with B1 **106**/**107**. In the continuing effort to probe the mechanistic rationale for the asymmetric inductions observed for catalysts generated from VAPOL and VANOL, a major breakthrough was the identification of the active boroxinate catalyst **188**/**189 (**Scheme 2.1). Surprisingly, the catalyst for the aziridination reaction proved to be a Brønsted acid catalysis in operation contrary to the common belief that a Lewis-acid catalyst was involved. In general, the pKa of protonated imines is approximately 7.[17] This suggests that the pKa value of the protonated boroxinate species should be in the same range i.e. either lower or equal to 7.

Scheme 2.1 The Wulff asymmetric *cis*-aziridination reaction with benzhydryl imines **78**

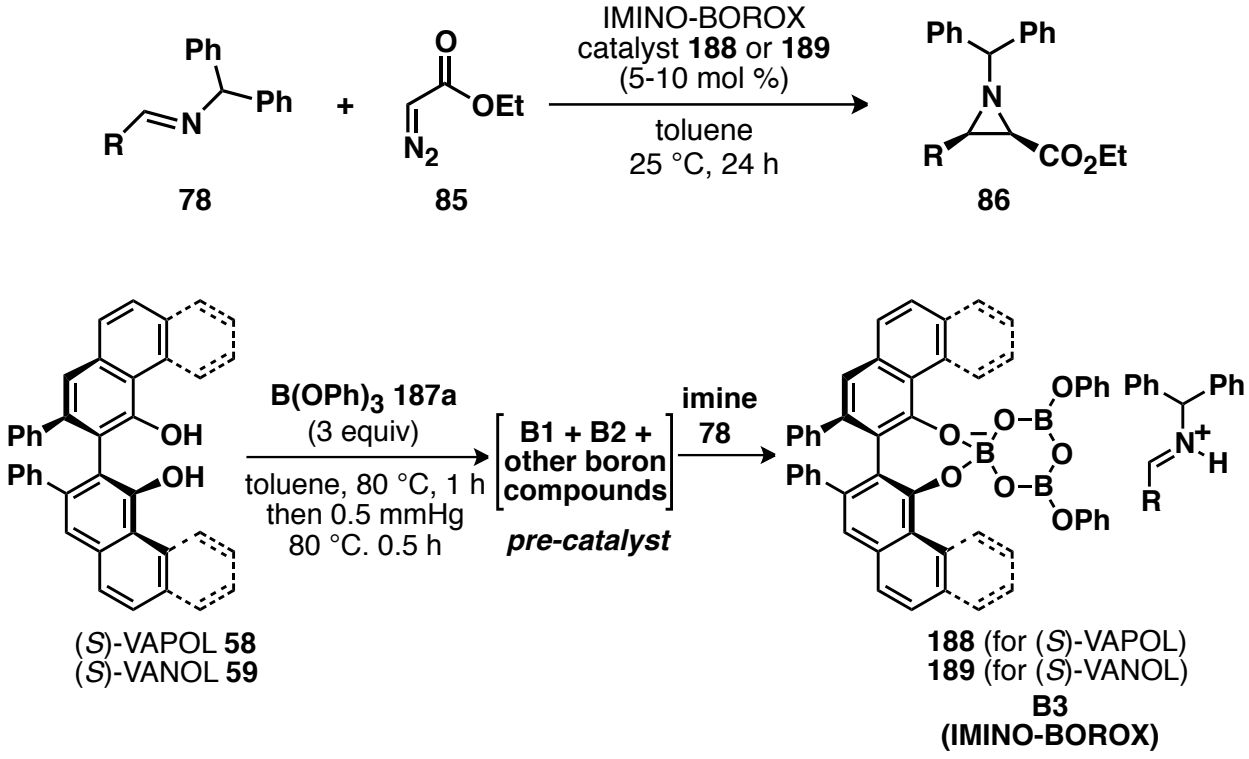

Scheme 2.1 cont'd

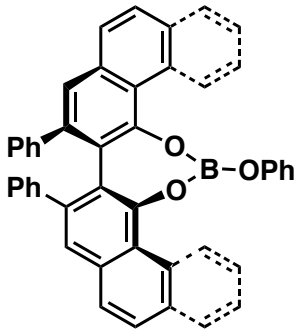

106 (for (*S*)-VAPOL)
107 (for (*S*)-VANOL)
B1

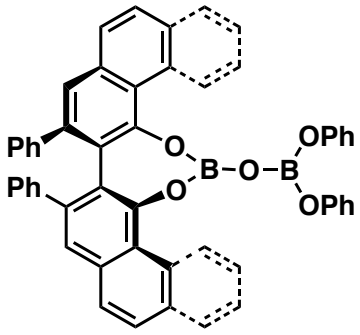

108 (for (*S*)-VAPOL)
109 (for (*S*)-VANOL)
B2

This is the first ever example of a chiral boroxinate catalyst reported in the literature. Gang Hu, one of the former group members, was able to characterize the catalyst by obtaining the X-ray crystal structure of the boroxinate catalyst with the MEDAM phenyl imine **111a**.[13f] The crystal structure of catalyst **190a** showed a complex consisting of a protonated imine and a chiral counteranion in the form of a boroxinate anion derived from (*S*)-VAPOL **58** and commercial $B(OPh)_3$ (Figure 2.2). Apart from the strong hydrogen bond (d_1), a number of important non-covalent interactions (d_2-d_7, CH-π and π-π) were observed as shown in Figure 2.2. The nature of the involvement of the imine suggested that the actual catalyst was formed upon the addition of imine. X-ray structure revealed the presence of a tetra-coordinate boron which was further confirmed by ^{11}B NMR spectroscopy. A ^{1}H NMR study of the crystals revealed that the bay proton (Hb) of VAPOL shifted up field to δ 10.2-10.4 ppm. Our understanding of the catalyst was greatly enhanced since we were able to obtain crystals and structural information about the actual boroxinate catalyst in the aziridination reaction. However, it is not easy to grow crystals on demand. It was then thought to design an NMR

protocol in order to characterize these kinds of catalysts. Gang Hu, a former group member, initiated certain NMR experiments, however, a quantitative assessment of the BOROX catalysts and other VAPOL derivatives was missing.

Figure 2.2 (**A**) Generation of the BOROX catalysts **190a** and **191a**. (B) Diagrammatic representation of the solid-state structure of the chemzyme-substrate complex **190a**.

A

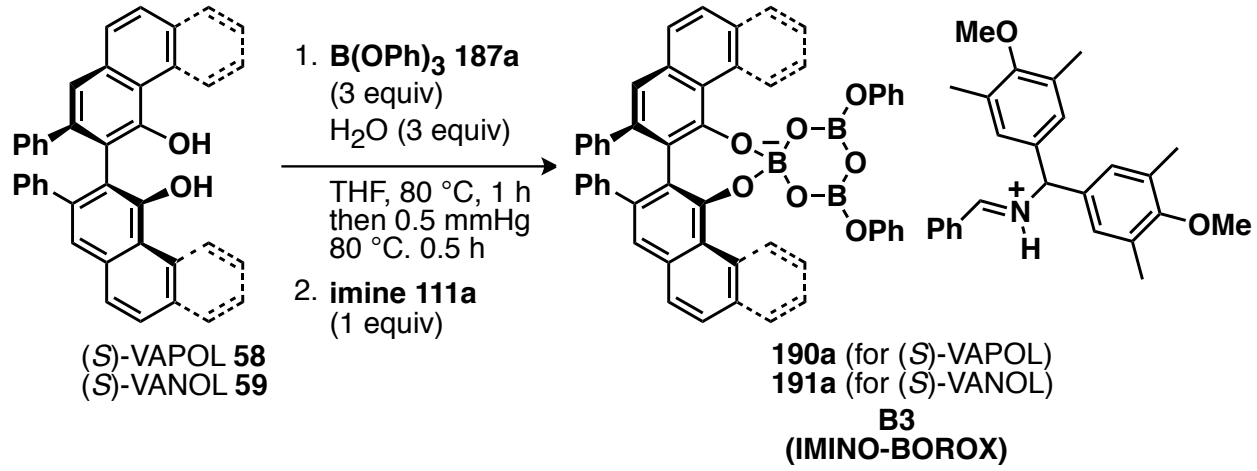

B

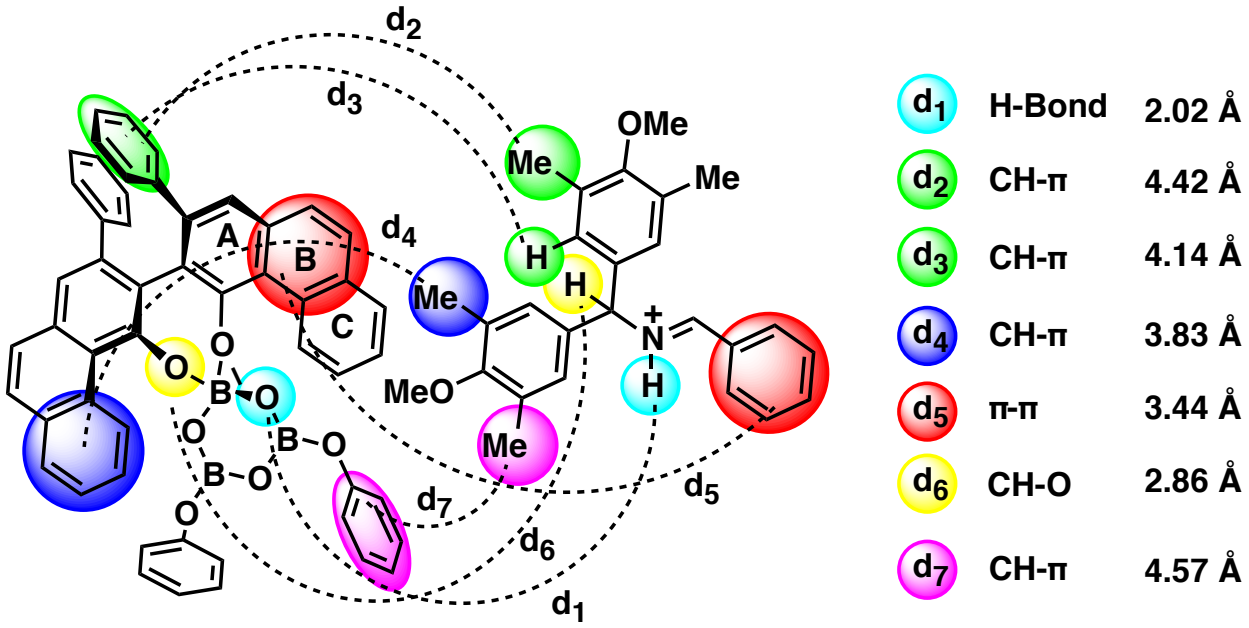

IMINO-BOROX 190a

2.1.1.1 $B(OPh)_3$ as the boron source

A series of NMR experiments were designed to devise the protocol for the characterization of BOROX catalysts generated by vaulted ligands and commercial $B(OPh)_3$. The identification of various species generated in the process is facilitated by the fact that the bay proton (H_b) of VAPOL **58**, its derivatives B1 **106** and B2 **108** along with the IMINO-BOROX catalyst **190a** are quite distinct. The chemical shift of the bay protons for VAPOL is at δ = 9.77 ppm ($CDCl_3$). To begin with, we employed the traditional method for catalyst formation which involves heating (*S*)-VAPOL with 3 equiv of commercial $B(OPh)_3$ at 80 °C. This resulted in the generation of a 53% yield of pyroborate B2 **106** (δ = 9.22 ppm, $CDCl_3$) along with a 6% yield of the meso-borate B1 **104** (δ = 9.55 ppm, $CDCl_3$) and 20% of unreacted VAPOL (entry 1, Figure 2.3B). Treatment of this mixture with 2 equivalents of the imine **111a** at room temperature within a few minutes results in the conversion of the colorless solution of **106** and **108** to a red solution of boroxinate **190a** (δ = 10.26 ppm, $CDCl_3$) in 81% yield (entry 2, Figure 2.3B). Another tool that has been used in the characterization of these catalysts is ^{11}B NMR spectroscopy. Three coordinate aryl borate compounds show very broad absorptions at 16-18 ppm in the ^{11}B NMR spectrum. However, the increased spherical symmetry of a tetra-coordinate boron leads to a sharpening of the absorption and the negative charge of the borate causes an upfield shift. The IMINO-BOROX catalyst **190a** has a sharp absorption at 5.33 ppm (entry 2, Figure 2.3C). The ratio of the tetra-coordinate boron to tri-coordinate boron is found to

be 1:2 which furthers supports the structure of the BOROX catalyst. This study was published in a recent publication.[13f]

Figure 2.3 (**A**) Imine induced boroxinate catalyst formation using commercial $B(OPh)_3$. (**B**)[a] ^1H NMR spectra in $CDCl_3$ with Ph_3CH as internal standard with percent yields of **190a** given parenthesis. (**C**) ^{11}B NMR spectra corresponding to the ^1H NMR spectra in Figure 2.3B

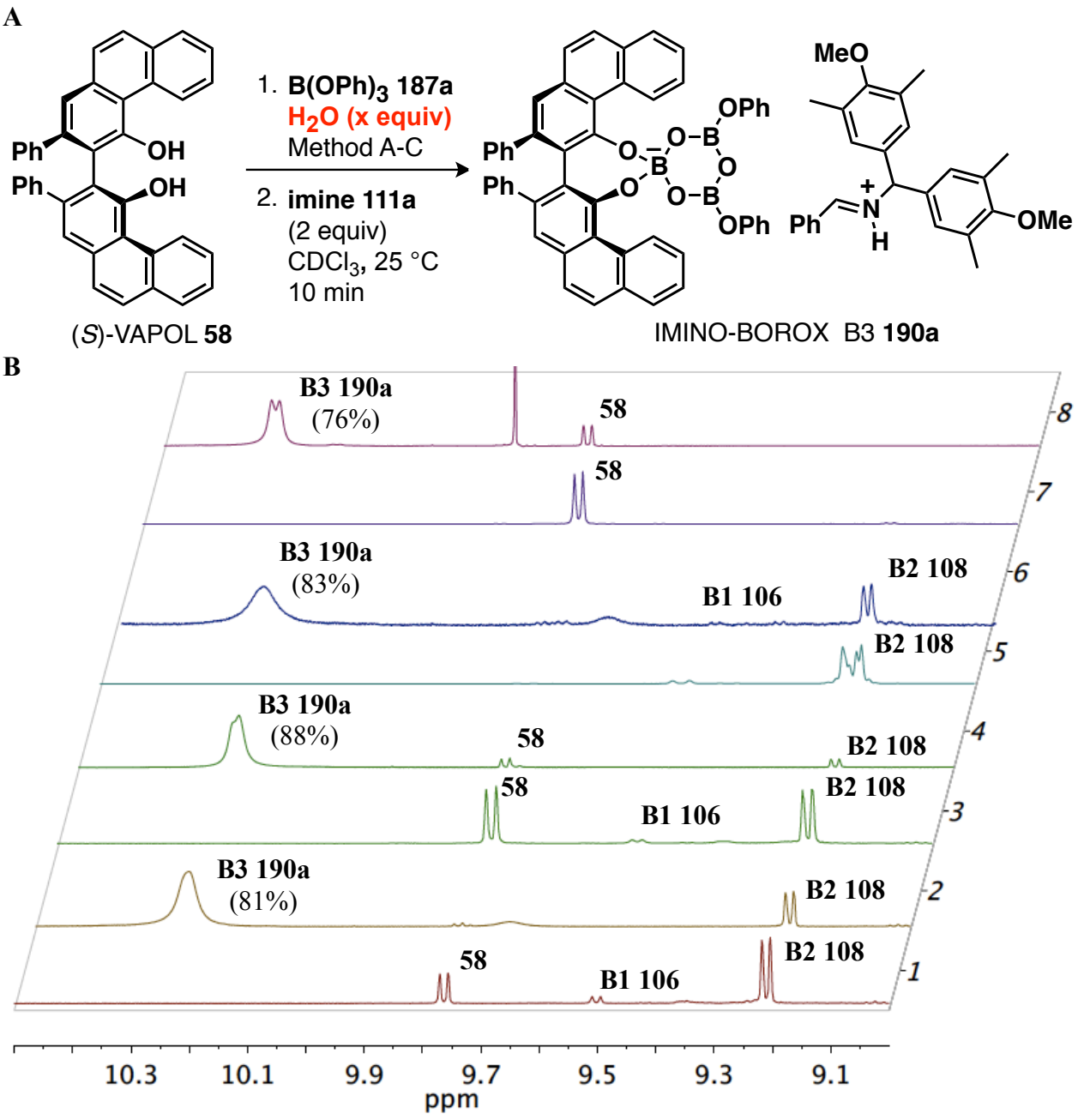

Figure 2.3 cont'd

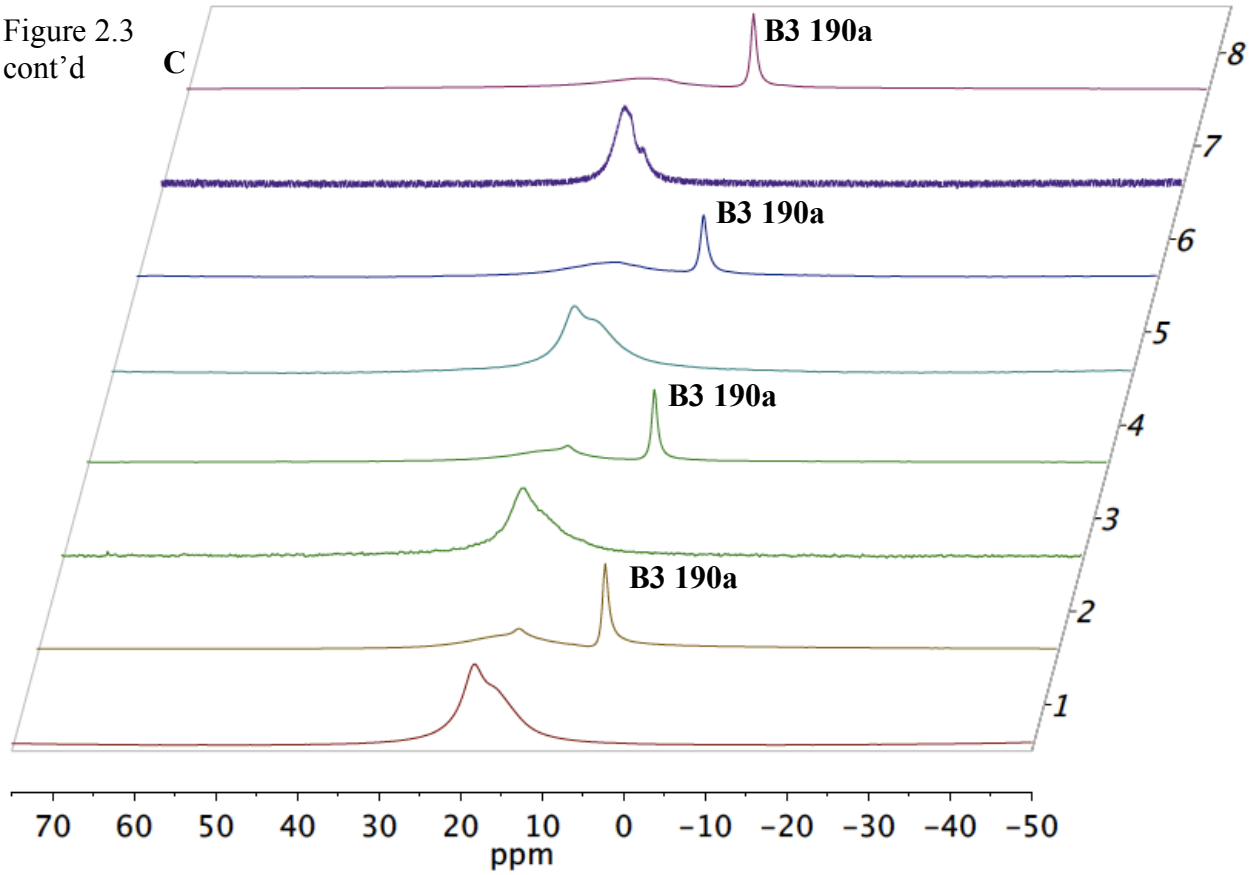

[a] Note for Figure 2.3B: Entry 1: (*S*)-VAPOL (0.1 mmol) plus 3 equiv commercial $B(OPh)_3$ were heated at 80 °C in toluene for 1 h followed by removal of volatiles under vacuum for 0.5 h (method A). Entry 2: 2.0 equiv of imine **111a** added to the solution in entry 1 for 10 min at 25 °C. Entry 3: Same as entry 1 except that 3 equiv of H_2O was also added to make the pre-catalyst in THF (method B). Entry 4: 2.0 equiv of imine **111a** added to the solution in entry 3 for 10 min at 25 °C. Entry 5: Same as entry 1 except that 4 equiv of commercial $B(OPh)_3$ and 1 equiv of H_2O was used to make the pre-catalyst (method C). Entry 6: 2.0 equiv of imine **111a** added to the solution in entry 5 for 10 min at 25 °C. Entry 7: (*S*)-VAPOL (0.1 mmol) plus 3

equiv commercial $B(OPh)_3$ at 25 °C for 10 min. Entry 8: (*S*)-VAPOL (0.1 mmol) plus 3 equiv commercial $B(OPh)_3$ and 2 equiv imine **111a** at 25 °C for 10 min.

The formation of the three B-O-B linkages in the boroxine ring in the BOROX catalyst **190a** requires 3 equivalents of water along with commercial $B(OPh)_3$. *The source of the water in the cases where the water is not added is most probably results from partial hydrolysis of commercial* $B(OPh)_3$.[13f] *Hence, the ratio of* ***190a***, ***106***, ***108***, *and unreacted* ***58*** *may vary significantly depending on the nature and amount of hydrolyzed boron species present in commercially available* $B(OPh)_3$. It must be remembered that no boroxinate catalyst was observed when highly purified $B(OPh)_3$ was employed.[13f] It was then decided to add the 3 equivalents of water to the mixture of VAPOL and commercial $B(OPh)_3$ in order to compensate for any variation in the quality of commercial $B(OPh)_3$ and to study the subsequent effect in the NMR studies. As shown in the third entry of Figure 2.3B, this method for catalyst formation generated the pyroborate B2 **108** and mesoborate B1 **106** in 41% yield and 5% yield respectively. The amount of unreacted VAPOL **58** was found to be 45% as monitored by ^1H NMR spectroscopy. After the addition of 2 equivalents of imine **111a**, an 88% yield of the boroxinate catalyst **190a** was formed (entry 4, Figure 2.3B). Also, the pre-catalyst made from method C ($B(OPh)_3$:H_2O = 4:1) gave B2 **108** in 90% yield and B1 **106** in 5% yield. Subsequent treatment with 2 equiv of imine **111a** resulted in **190a** in 83% yield (entry 6, Figure 2.3B).

Interestingly, we found that the formation of the IMINO-BOROX catalyst **190a** can be observed simply upon the treatment of VAPOL **58** and 3 equivalents of $B(OPh)_3$ with 2 equivalents of imine **111a** at room temperature in 76% yield (entry 8, Figure 2.3B). More interestingly, VAPOL **58** and commercial $B(OPh)_3$ barely react with each other to afford a 3% yield of B2 **108** and this does not change after 24 h (entry 7, Figure 2.3B). However, an 18% yield of B2 **108** was observed with another sample of commercial $B(OPh)_3$.

2.1.1.2 Other boron sources

A special feature of the BOROX catalyst is that a variety of catalysts can be made by utilizing various trialkyl or triaryl borates **187** and different boroxines **191** (Figure 2.5A and 2.5B). However, these approaches are not feasible due to the limited commercial availability of these compounds. This limitation has been solved by employing BH_3•Me_2S **192a**, $B(OH)_3$ **193** and BH_3•THF **192b** in conjunction with different alcohols (Figure 2.5C and 2.5D). A comparison of these boron sources and of $B(OPh)_3$ for catalyst preparation and their impact on the outcome in the aziridination reaction has been presented in Table 2.1.

Table 2.1 Asymmetric aziridination with different boron sources and (*S*)-VAPOL **58** [a]

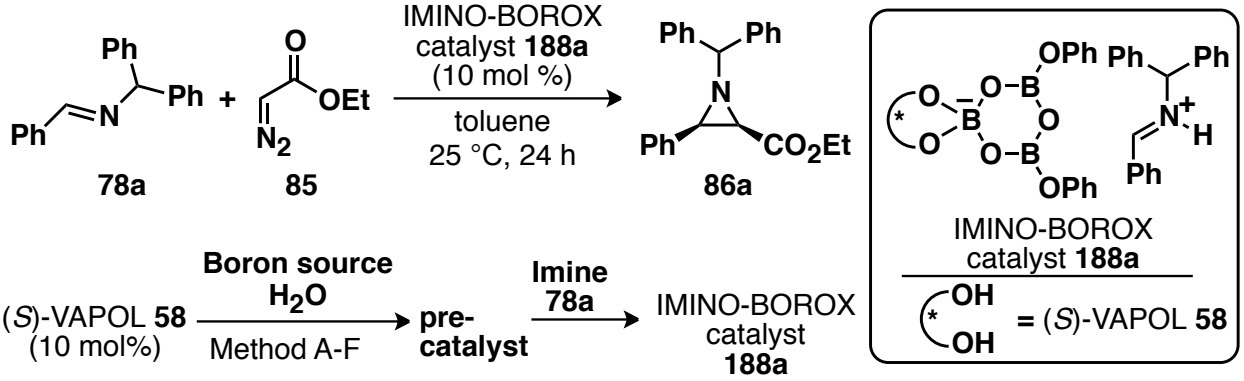

Table 2.1 cont'd

#	Boron Source	Pre-catalyst (method) [b]	Ratio ('B' source: PhOH:H_2O)	Procedure	Yield **86a** (%) [c]	ee **86a** (%) [d]
1	$B(OPh)_3$	A	3:0:0	I	83	91
2	$B(OPh)_3$	– [e]	3:0:0	II	80	92
3	$B(OPh)_3$	B	3:0:3	III	84	92
4	$B(OPh)_3$	C	4:0:1	IV	82 (81) [g]	94 (96) [g]
5	$B(OPh)_3$	– [f]	4:0:0	V	80	92
6	BH_3•Me_2S	E	3:2:3	VI	85 (81) [g]	94 (91) [g]
7	BH_3•Me_2S	F	3:2:3	VII [h]	89	92
8	$B(OH)_3$	G	3:2:0	VIII [i]	85	90
9	BH_3•THF	H	3:2:3	IX	82	94

[a] Unless otherwise specified, all reactions were run with 1 mmol of imine **78a** in toluene (0.5 M in imine **78a**) with 1.2 equiv of **85**. [b] Method A: The pre-catalyst was prepared by heating 1 equiv of (*S*)-VAPOL with 3 equiv of commercial $B(OPh)_3$ in toluene at 80 °C for 1 h, followed by removing all volatiles under high vacuum (0.1 mm Hg) for 0.5 h at 80 °C. Method B: By heating 1 equiv of (*S*)-VAPOL, 3 equiv of commercial $B(OPh)_3$ and 3 equiv of H_2O in THF at 80 °C for 1 h, followed by removing all volatiles under high vacuum (0.1 mm Hg) for 0.5 h at 80 °C. Method C: Same as Method A except 4 equiv of commercial $B(OPh)_3$ with 1 equiv of H_2O was used. Method E: By heating 1 equiv of (*S*)-VAPOL, 3 equiv of BH_3•Me_2S, 2 equiv of PhOH and 3 equiv of H_2O in toluene at 100 °C for 1 h, followed by removing all volatiles under high vacuum (0.1 mm Hg) for 0.5 h at 100 °C. Method F: Same as Method E except removals of volatiles was excluded. Method G: Same as Method A except 3 equiv of $B(OH)_3$ with 2 equiv of PhOH was used. Method H: By mixing 1 equiv of (*S*)-VAPOL, 3 equiv of BH_3•THF, 2 equiv of PhOH and 3 equiv of H_2O in toluene at 25 °C for 15 min followed by removing all volatiles under high vacuum (0.1 mm Hg) for 0.5 h at 25 °C. [c] Isolated yield. [d] Determined by HPLC. [e] In this case, cat **188a** is directly generated by mixing 1 equiv of (*S*)-VAPOL, 3 equiv of $B(OPh)_3$ and 10 equiv of imine **78a** in toluene at 25 °C for 5 min. [f] In this case, cat **188a** is directly generated by heating a mixture of 1 equiv of (*S*)-VAPOL, 4 equiv of $B(OPh)_3$ and 10 equiv of imine **78a** in toluene at 80 °C for 0.5 h. [g] *m*-xylene used as the solvent for results in parenthesis. [h] Data contributed by Wynter Osminski. [i] Data contributed by Li Huang.

It was then decided to carry out NMR analyses in order to quantify the amount of boroxinate catalyst formed in each case. The generation of the BOROX catalyst with 2 equiv of imine **111a** resulted in 55%, 71% and 26% yields of **190a** from triphenoxyboroxine **191a**, BH_3•Me_2S **192a** and $B(OH)_3$ **193**, respectively (entries 2, 4 and 6, Figure 2.4A).

Figure 2.4 Imine induced boroxinate catalyst formation using other boron sources. (**A**)[a] ^1H NMR spectra in $CDCl_3$ with Ph_3CH as internal standard with percent yields of **190a** given in parenthesis. (**B**) ^{11}B NMR spectra corresponding to the ^1H NMR spectra in Figure 2.4A.

A

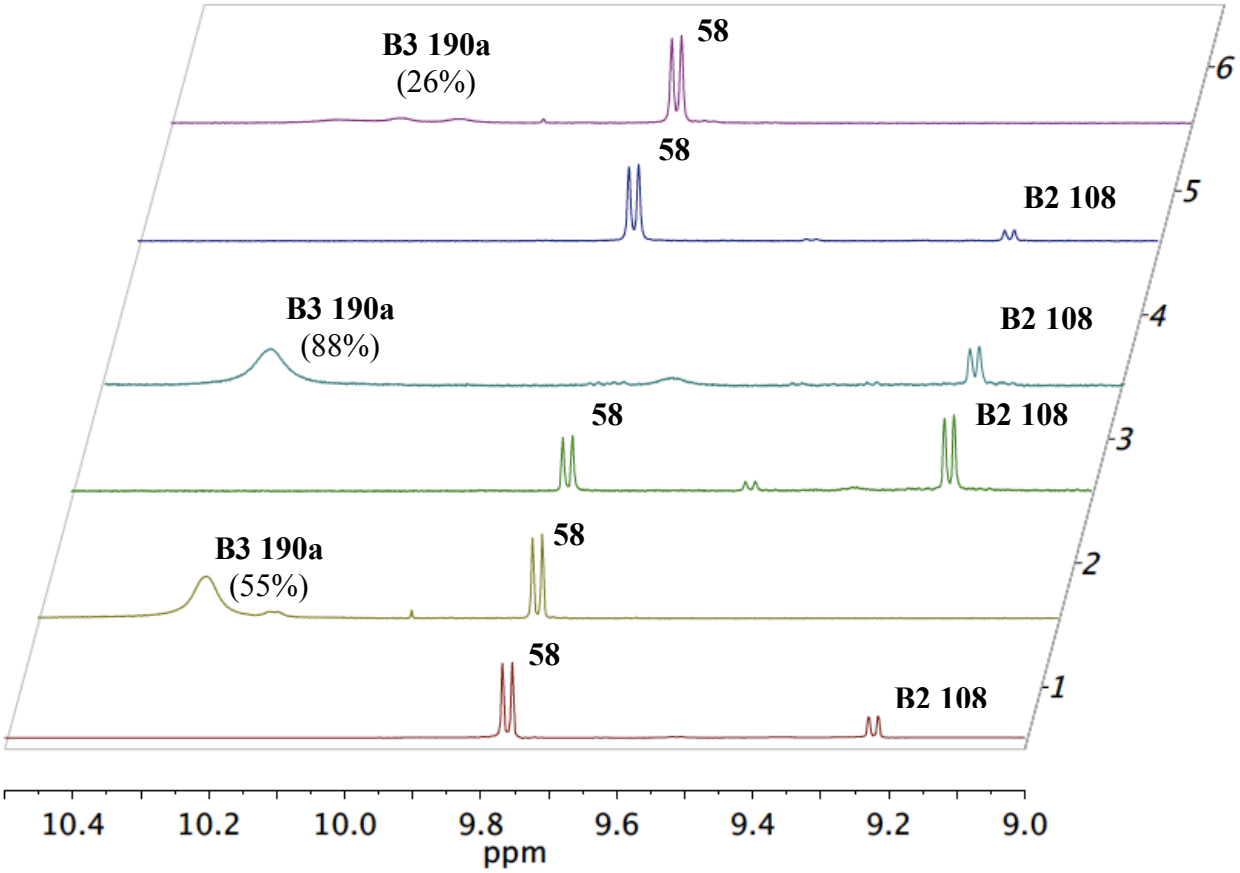

Figure 2.4 cont'd

B

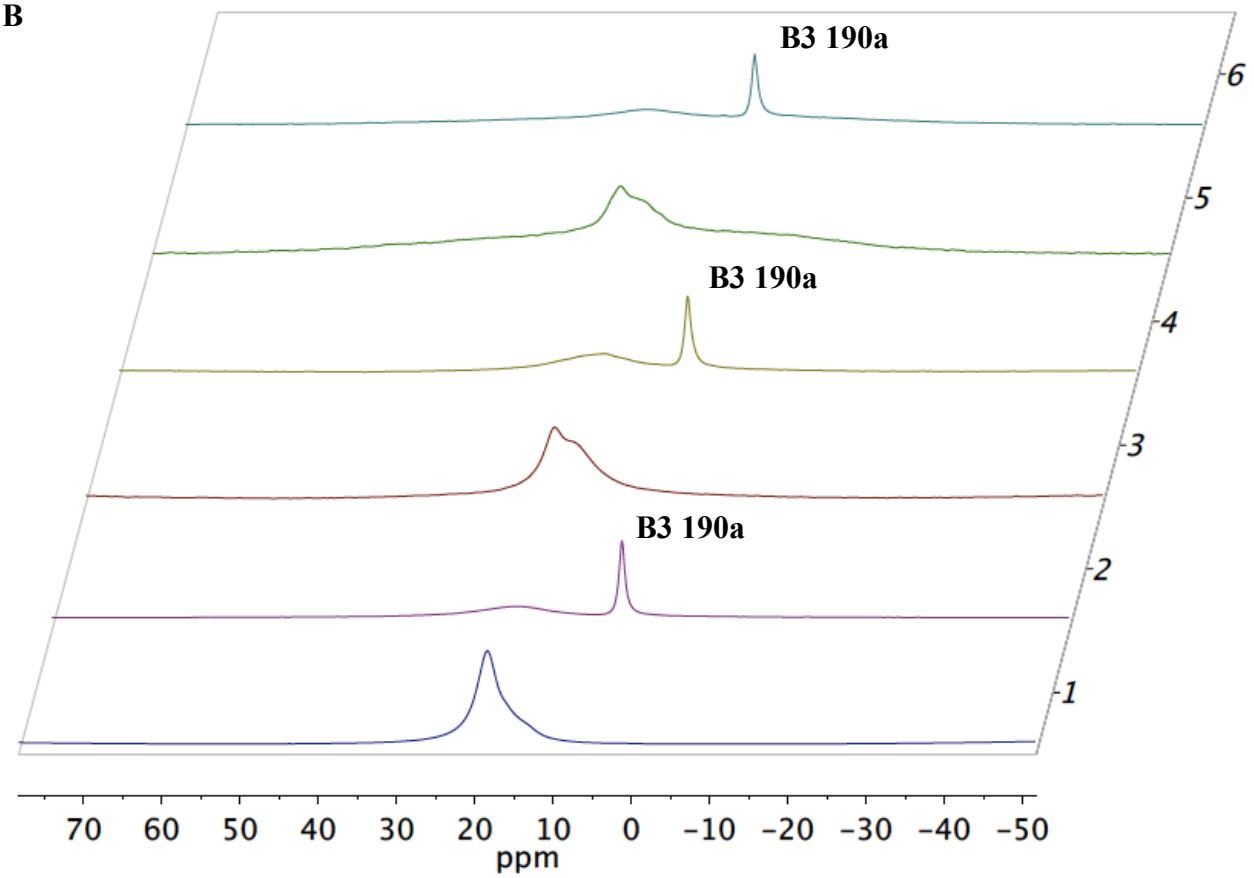

[a] Note for Figure 2.4A: Entry 1: (*S*)-VAPOL (0.1 mmol) plus 1 equiv triphenoxyboroxine **191a** at 25 °C for 10 min (method D). Triphenoxyboroxine **191a** was prepared when a mixture of 3 equiv BH_3•Me_2S **192a**, 3 equiv PhOH and 3 equiv H_2O was heated at 80 °C in toluene for 1 h followed by removal of volatiles under vacuum for 0.5 h (see experimental). Entry 2: 2.0 equiv of imine **111a** added to the solution in entry 1 for 10 min at 25 °C. Entry 3: (*S*)-VAPOL (0.1 mmol) plus 3 equiv BH_3•Me_2S **192a**, 2 equiv PhOH and 3 equiv H_2O were heated at 100 °C in toluene for 1 h followed by removal of volatiles under vacuum for 0.5 h (method E). Entry 4: 2.0 equiv of imine **111a** added to the solution in entry 3 for 10 min at 25 °C. Entry 5: (*S*)-

VAPOL (0.1 mmol) plus 3 equiv $B(OH)_3$ **193** and 2 equiv PhOH were heated at 80 °C in CH_3CN for 1 h followed by removal of volatiles under vacuum for 0.5 h (method G). Entry 6: 2.0 equiv of imine **111a** added to the solution in entry 5 for 10 min at 25 °C.

A detailed summary of the results obtained from the various NMR experiments on mixtures of (*S*)-VAPOL **58**, imine **111a** and various boron sources are presented in Table 2.2.

Table 2.2 NMR Analysis of mixtures of (*S*)-VAPOL **58**, imine **111a** and various boron sources [a]

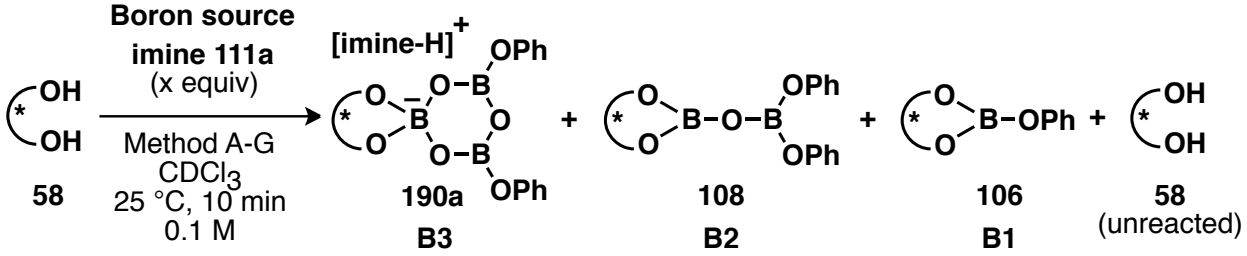

	#	Pre-Cat method [b]	Equiv of imine (x)	Cat. (%)	(*S*)-VAPOL [c,d]	B1 [d]	B2 [d]	B3 [d]	^1H (δ) [e]	^{11}B (δ) [f]
B(OPh)₃ Before imine	1	A	-	-	20	6	53	-		18.29
After imine	2		2	50	2	<1	13	81	10.24	15.92, 5.33
	3		10	10	<1	<1	6	55	10.29	16.73, 5.37
	4		1	100	6	<1	4	90	10.23	15.96, 5.38
	5		0.5	200	41	<1	11	49 [g]	10.23	18.29, 5.42
B(OPh)₃ Before imine	6	B	-	-	45	5	41	-		18.46
After imine	7		2	50	4	<1	4	88	10.23	15.92, 5.36
	8		1	100	1	<1	2	90	10.25	16.00, 5.35

Table 2.2 cont'd

B(OPh)$_3$ Before imine	9	-	-	-	85	<1	3	-		18.24
After imine	10		2	50	11	<1	<1	76	10.31	19.16, 5.51
	11		10	10	11	<1	<1	41	10.41	17.75, 5.52
B(OPh)$_3$ Before imine	12	C	-	-	<1	5	88	-		18.39
After imine	13		2	50	1	<1	15	83	10.26	19.33, 5.42
Boroxine Before imine	14	D	-	-	69	4	23	-		18.39
After imine	15		2	50	19	<1	<1	55	10.25	19.33, 5.42
BH$_3$.Me$_2$S Before imine	16	E	-	-	33	5	53	-		18.27
After imine	17		2	50	<1	<1	20	71	10.26	16.18, 5.50
	18		1	100	<1	<1	30	62	10.28	16.04, 5.45
B(OH)$_3$ Before imine	19	G	-	-	65	2	9	-		18.31
After imine	20		2	50	39	<1	<1	26	10.16	19.13, 5.43
	21		1	100	50	<1	<1	23	10.16	19.49, 5.42

[a] Unless otherwise specified, all NMR samples were prepared from (*S*)-VAPOL (0.1 mmol), boron sources and imine **111a** in $CDCl_3$ (1 mL) utilizing methods A-G for pre-catalyst preparation. [b] See Table 2.1 for various methods. Method D: The pre-catalyst was prepared by simple mixing of 1 equiv of (*S*)-VAPOL and pre-formed triphenoxyboroxine **191a**. [c] Unreacted (*S*)-VAPOL **58**. [d] NMR yield with Ph_3CH as internal standard with ligand as the limiting reagent. [e] Chemical Shift of the peaks observed in the bay region of **190a** in the ^1H NMR spectrum. [f] Chemical Shift of the peaks observed in the ^{11}B NMR spectrum. [g] The NMR yield with Ph_3CH as internal standard with respect to imine is 89%.

Finally, we have four different protocols for the generation of the BOROX catalyst as shown in Figure 2.5.

Figure 2.5 Generation of a BOROX catalyst from (**A**) trialkyl/triaryl borates **187** (**B**) boroxines **191** (**C**) $B(OH)_3$ **193** (D) BH_3•Me_2S complex **192a**

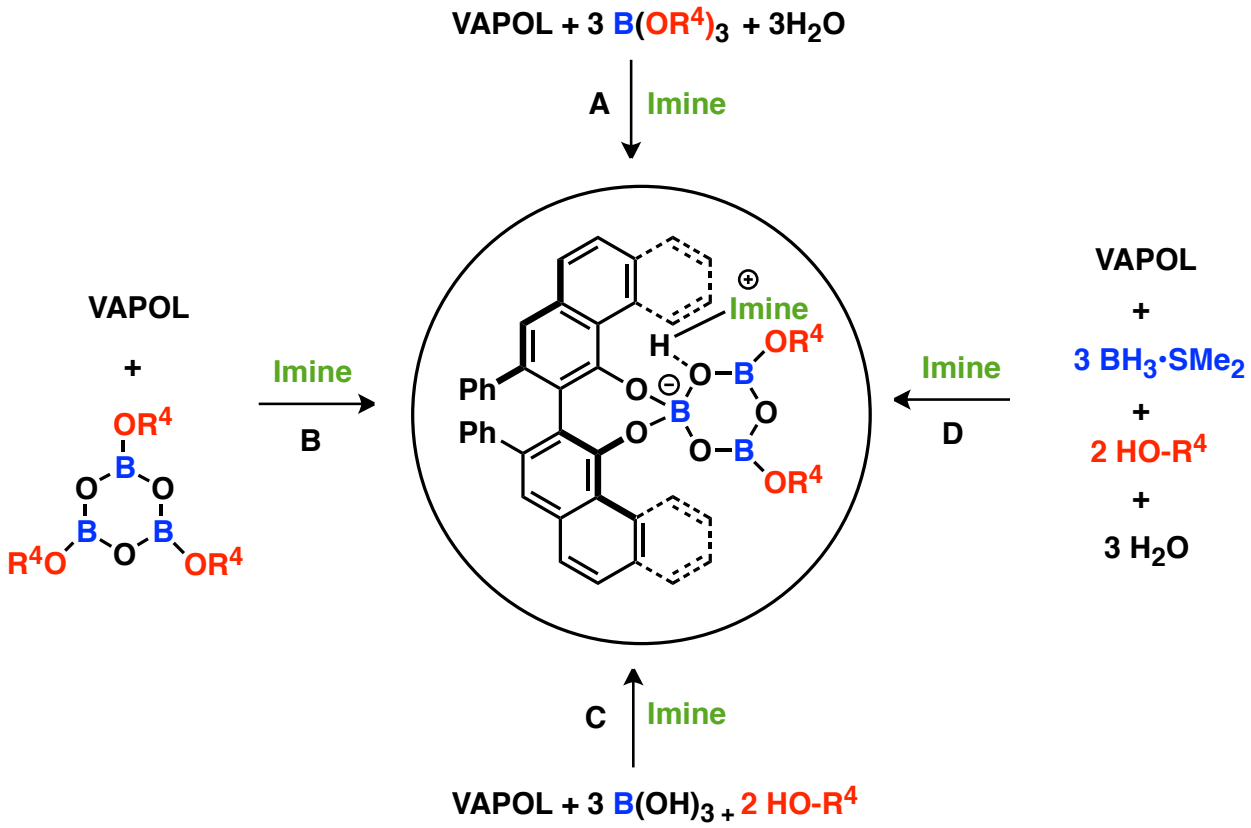

2.1.1.3 Temperature studies of IMINO-BOROX catalyst 190a

A temperature study on the ^{1}H NMR spectrum of the IMINO-BOROX catalyst **190a** provided additional information of the dynamics of this complex. The ^{1}H NMR spectrum of **190a** has only one peak for bay protons (Figure 2.6A, entry 2). This was interpreted to mean that the migration of the protonated imine from top face of the catalyst to the bottom face is fast on the NMR time scale. On decreasing the temperature from 25 ºC to -44 ºC, the two sets of bay

protons in the imine-boroxinate complex **190a** begin to appear (Figure 2.6A, entry 5). This reflects a decreased rate of migration of the iminium on the NMR time scale at low temperature.

Figure 2.6 (**A**)[a] ^{1}H NMR spectra of the bay region of **190a** in $CDCl_3$. (**B**) ^{1}H NMR spectra of the methyl and methoxy regions of **190a** in $CDCl_3$ corresponding to the entries of Figure 2.6A.

A

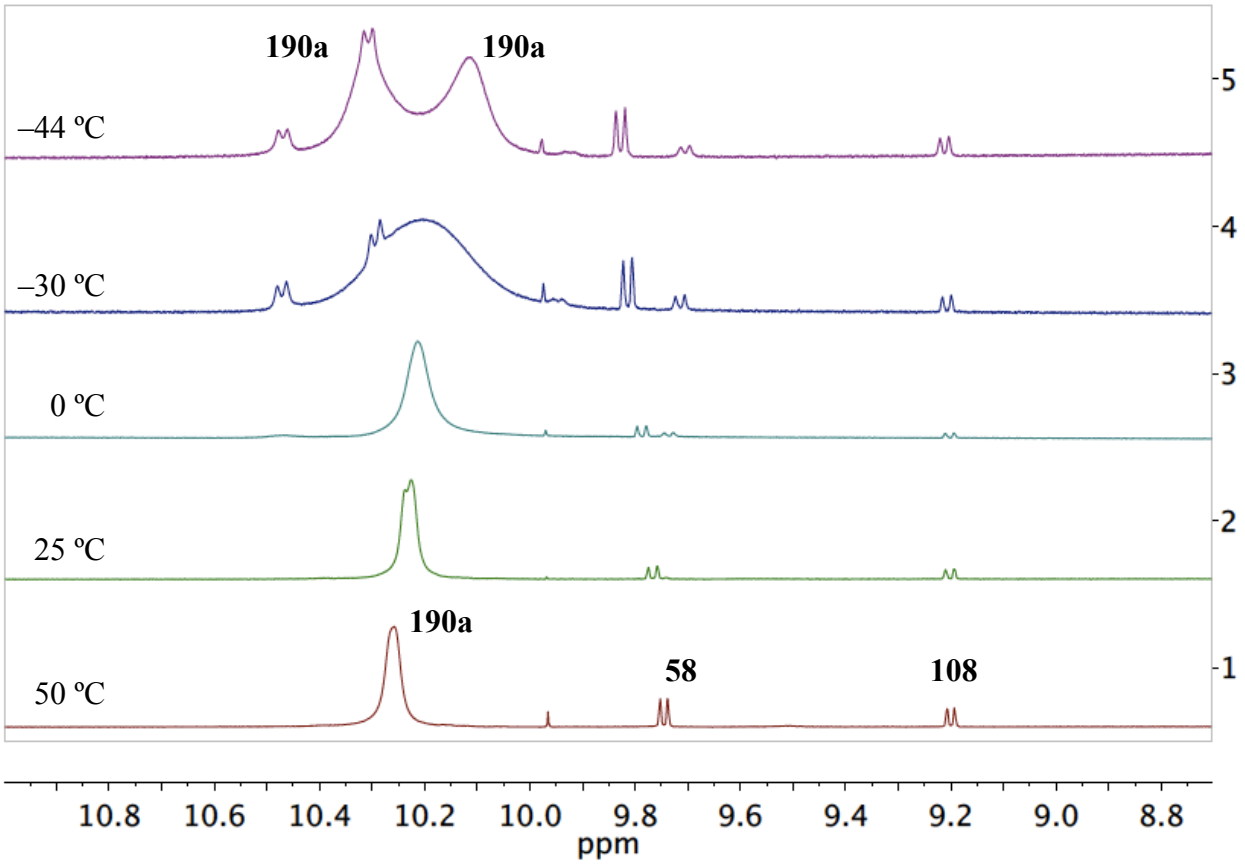

Figure 2.6 cont'd

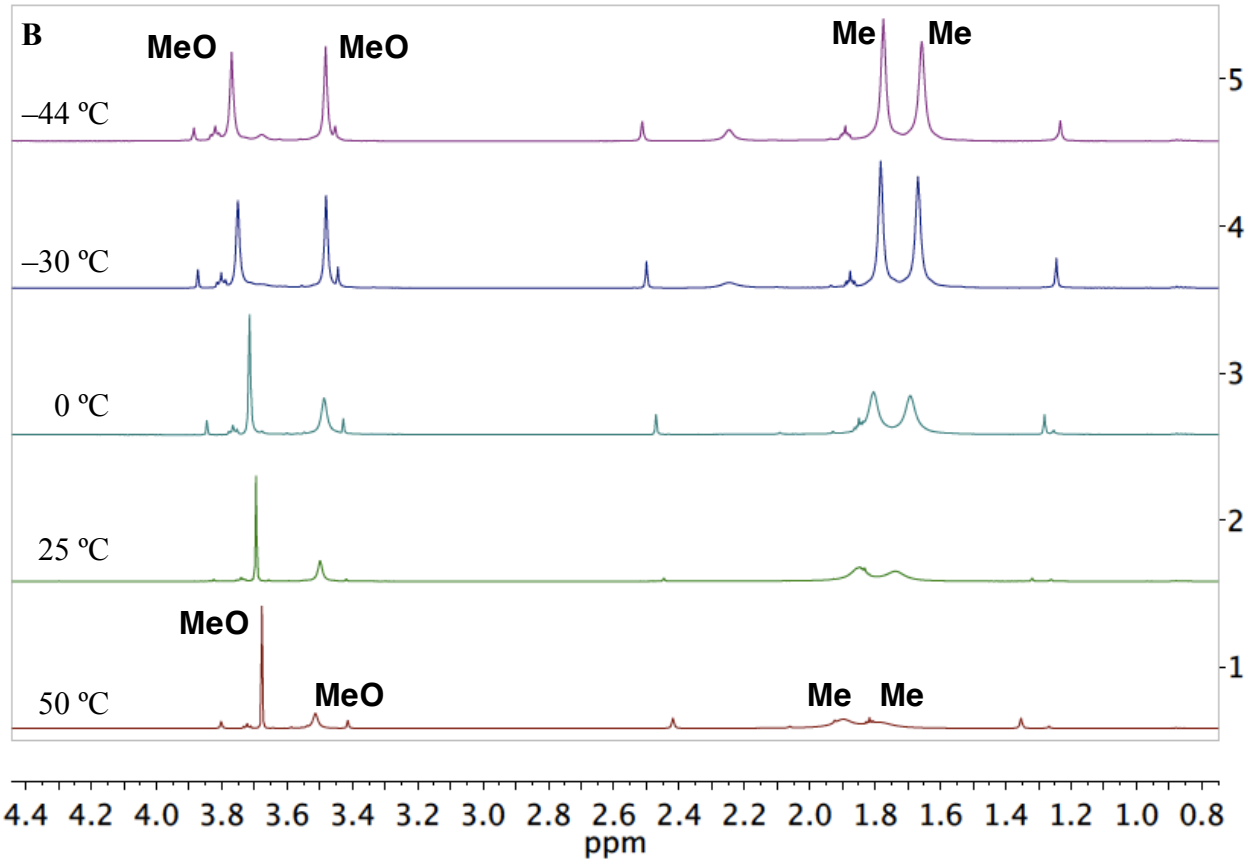

[a] Note for Figure 2.6A: Entry 1: (*S*)-VAPOL (0.1 mmol) plus 3 equiv commercial $B(OPh)_3$ and 3 equiv H_2O were heated at 80 °C in THF for 1 h followed by removal of volatiles under vacuum for 0.5 h. Thereafter, 1.0 equiv of imine **111a** was added to the pre-catalyst followed by the addition of $CDCl_3$ (1 mL) and the stirred for 10 min at 25 °C. The NMR taken at 50 °C. Entry 2: Same as entry 1 but the NMR taken at 25 °C. Entry 3: Same as entry 1 but the NMR taken at 0 °C. Entry 4: Same as entry 1 but the NMR taken at –30 °C. Entry 5: Same as entry 1 but the NMR taken at –44 °C.

Another important observation was made in the methyl and the methoxy region of the boroxinate complex **190a** (Figure 2.6B). At ambient temperature (25 ºC), one of the methoxy groups was found to be much broader than the other. This observation indicates that one of the methoxy groups is more restricted than the other one in complex **190a**. However, at low temperature (–44 ºC), the equivalent methyl and methoxy groups of the free imine **111a** are desymmetrized in the boroxinate **190a** (Figure 2.6B, entry 5). This behavior of boroxinate complex at low temperature is ambiguous and not completely understood at present. Both methyl (δ = 1.85 ppm and 1.74 ppm) and methoxy (δ = 3.70 ppm and 3.49 ppm) groups are substantially shielded as compared to the free imine (δ = 3.69 ppm and δ = 2.26 ppm for methyl and methoxy groups in free imine **111a**, respectively).

2.1.1.4 Multiplex diversity in the generation of BOROX catalyst

As discussed earlier, the diversity of BOROX catalyst is exemplified by the fact that different alcohols, ligands and imines can be employed. These variations can generate a potentially large pool of catalysts and thereby provide new opportunities in asymmetric catalysis. Considerable time was devoted during the course of this doctoral research to the development of these novel catalysts. One of the first variations that were tried was the generation of catalyst **196a** with cubenol **194c**. No significant change in the yield or enantioselectivity was observed in the aziridination reaction (Table 2.3, entry 3). However, this work was carried out in more detail by another group member namely Wynter Osminski. Cyclohexanol **194b** was found to be the optimum alcohol for the Wulff asymmetric aziridination reaction (Table 2.3, entry 2).

Table 2.3 Catalytic asymmetric aziridination with different alcohols and (*S*)-VAPOL [a]

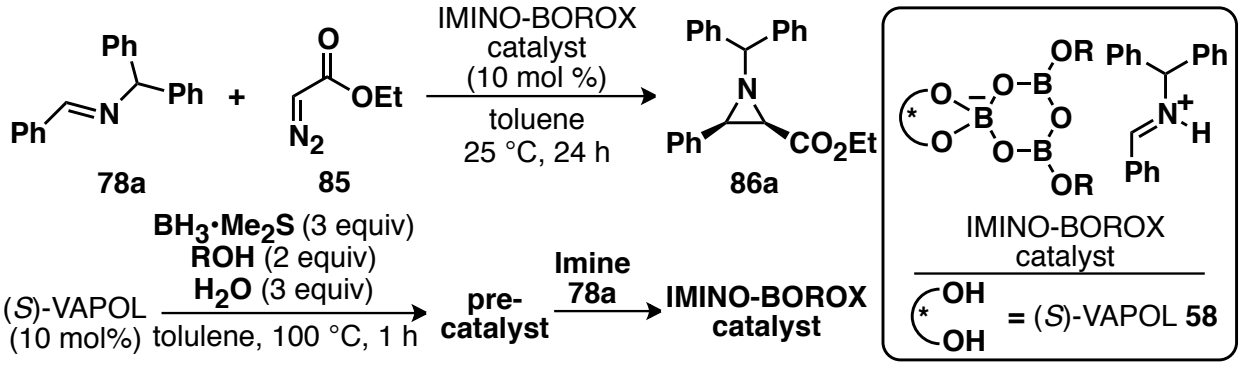

#	Catalyst	Alcohol Source	Yield **86a** (%) [b]	ee **86a** (%) [c]
1	**188a**	 **194a**	89	92
2	**195a**	 **194b**	90	95 [d]
3	**196a**	 **194c** [e]	89	92

[a] Unless otherwise specified, all reactions were performed with 1 mmol of imine **78a** in toluene (0.5 M in imine **78a**) with 1.2 equiv of **85**. The pre-catalyst was prepared heating 1 equiv of (*S*)-VAPOL, 3 equiv of BH_3•Me_2S, 2 equiv of alcohol or phenol and 3 equiv of H_2O in toluene at 100 °C for 1 h, followed by removing all volatiles under high vacuum (0.1 mm Hg) for 0.5 h at 100 °C (method F). [b] Isolated yield. [c] Determined by HPLC. [d] Data contributed by Wynter Osminski. [e] Generously provided by Victor Prutyanov.

A number of comprehensive studies have shown that both VAPOL and VANOL are broadly effective in the asymmetric aziridination reaction.[13] In search of more diversity in the catalyst and in continued improvement in the aziridination with benzhydryl imines **78**, we envisioned the possibility of the (*S*)-ISOVAPOL **197**. The ligand was easily synthesized following the new protocol for the synthesis of VAPOL.[18] The results are discussed in detail in

chapter 5. Unfortunately, no significant improvement was observed when ISOVAPOL was employed in the aziridination reaction (Table 2.4, entry 3). Recently, another group member namely Yong Guan was able to increase the stereo-induction of the aziridines from benzhydryl imines by synthesizing a derivative of VANOL that has *tert*-butyl groups in the 7,7′ positions ((*S*)-7,7′-*t*Bu_2-VANOL **198**, Table 2.4, entry 4). Additionally, another group member, Li Huang found that 3,3′-Ph_2-BINOL **56a** gave satisfactory results. Later on, in order to *investigate the structure of the catalyst*, we screened a number of chiral diols such as BINOL derivatives **56** and TADDOL **61a**. The results and NMR analysis are discussed in detail in chapter 5.

Table 2.4 Catalytic asymmetric aziridination with different ligands [a]

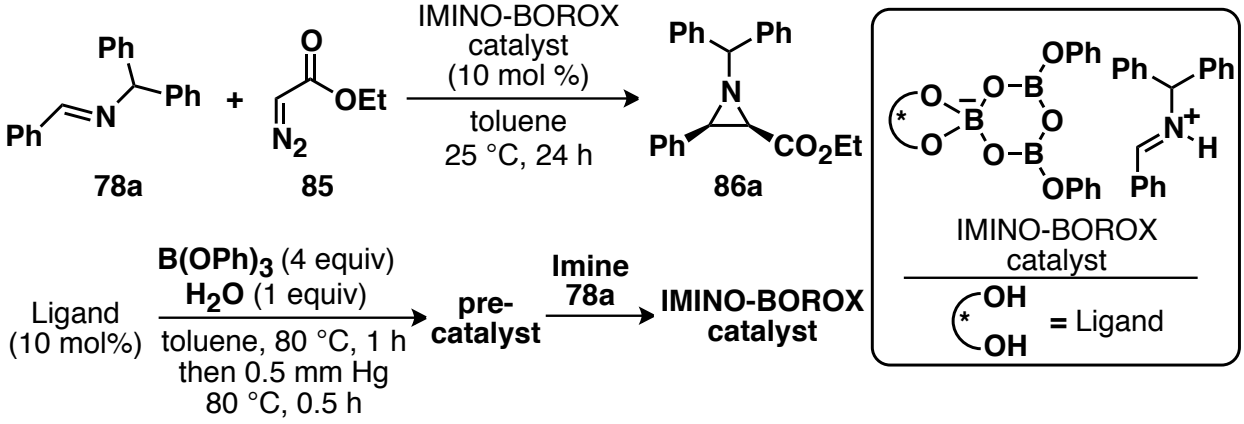

#	Catalyst	Ligand		Yield **86a** (%) [b]	ee **86a** (%) [c]
1	**188a**	(*S*)-VAPOL	**58**	82	94
2	**189a**	(*S*)-VANOL	**59**	87	93
3	**199a**	(*S*)-ISOVAPOL	**197**	82	92
4	**200a**	(*S*)-7,7′-*t*Bu_2-VANOL	**198**	82	98 [d]
5	**201a**	(*R*)-3,3′-Ph_2-BINOL	**56a**	88	–76 [e]
6	**202a**	(*R*)-3,3′-I_2-BINOL	**56e**	80	–51
7	**203a**	(*R*)-BINOL	**55**	66	–13
8	**204a**	(*R*)-3,3′-TRIP_2-BINOL	**56f**	78	2
9	**205a**	(*R, R*)-TADDOL	**61a**	73	<1

Table 2.4 cont'd

[a] Unless otherwise specified, all reactions were performed with 1 mmol of imine **78a** in toluene (0.5 M in imine **78a**) with 1.2 equiv of **85**. The pre-catalyst was prepared by heating 1 equiv of (*S*)-ligand with 4 equiv of commercial $B(OPh)_3$ and 1 equiv of H_2O in toluene at 80 °C for 1 h, followed by removing all volatiles under high vacuum (0.1 mm Hg) for 0.5 h at 80 °C (method C). [b] Isolated Yield. [c] Determined by HPLC. [d] Data contributed by Yong Guan. [e] Data contributed by Li Huang.

Lastly, a variation on the protecting group of the imine was examined (Table 2.5). Prior to this doctoral research, benzyhydryl,[13a] DAM[19] and BUDAM[13b] *N*-protecting groups were already employed in the search for the optimal substituent. Bh and DAM groups were found to be equally good and the BUDAM group was found to be the best for aryl imines. Although DAM imines **110** were already examined by Zhenjie Lu, a former group member, they were needed to be tested under new reaction conditions (toluene as the solvent instead of CCl_4 and a new procedure for catalyst preparation) for the optimization of alkyl imines. We were able to establish a simplified procedure utilizing DAM imines. The results are discussed in detail in chapter 6. Meanwhile, a new protecting group, MEDAM was developed by another group member namely Munmun Mukherjee. This group was found to be the optimal *N*-substituent for the asymmetric aziridination reactions of both aryl and alkyl imines.[13c] In terms of *mechanistic findings*, a combination of results from benzyl, benzhydryl and homo-benzhydryl (this work) protecting groups revealed the requirement for two aromatic rings separated by a methine group, which is directly attached to the nitrogen of the imine (Table 2.5, entries1-3).

Table 2.5 Catalytic asymmetric aziridination with imines from different protecting groups [a]

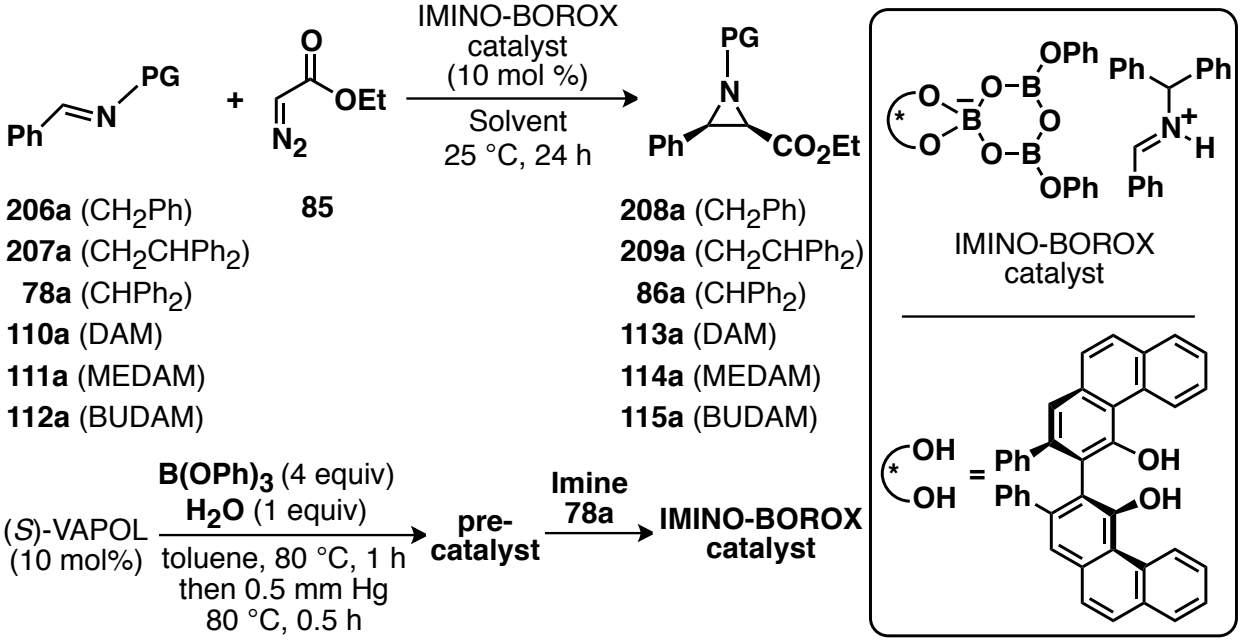

#	cat	Protecting Group (PG)	Solvent					
			$C_6H_5CH_3$		CH_2Cl_2		CCl_4	
			Yield azi (%) [b]	ee azi (%) [c]	Yield azi (%) [b]	ee azi (%) [c]	Yield azi (%) [b]	ee azi (%) [c]
1	**210a**	CH_2Ph	–	–	51 [d]	43 [d]	54 [d]	48 [d]
2	**211a**	CH_2CHPh_2	32	52	35	39	15	54
3	**188a**	$CHPh_2$	82	94	83	89	84	93
4	**212a**	DAM	95	92	80	90	84	94
5	**190a**	MEDAM	98 [e]	99.8 [e]	89 [e]	97.5 [e]	81 [e]	99 [e]
6	**213a**	BUDAM	96 [d]	99 [d]	84 [d]	99 [d]	94 [d]	99 [d]

[a] Unless otherwise specified, all reactions were performed with 1 mmol of imine **78a** in toluene (0.5 M in imine **78a**) with 1.2 equiv of **85**. The pre-catalyst was prepared by heating 1 equiv of (*S*)-VAPOL with 4 equiv of commercial $B(OPh)_3$ and 1 equiv of H_2O in toluene at 80 °C for 1 h, followed by removing all volatiles under high vacuum (0.1 mm Hg) for 0.5 h at 80 °C (method C). The concentration of the reaction was 0.2 M in imine **78a** for entry 2. [b] Isolated Yield. [c] Determined by HPLC. [d] Data contributed by Yu Zhang. [e] Data contributed by Munmun Mukherjee.

A NMR analysis of various imines was then performed and it is shown in Figure 2.7. All the imines show the formation of the boroxinate catalysts.

Figure 2.7 Imine induced boroxinate catalyst formation (See Table 2.5 for structures of different imines used). (**A**)[a] ^{1}H NMR spectra in $CDCl_3$ with Ph_3CH as internal standard. (**B**) ^{11}B NMR spectra corresponding to the ^{1}H NMR spectra in Figure 2.7A.

A

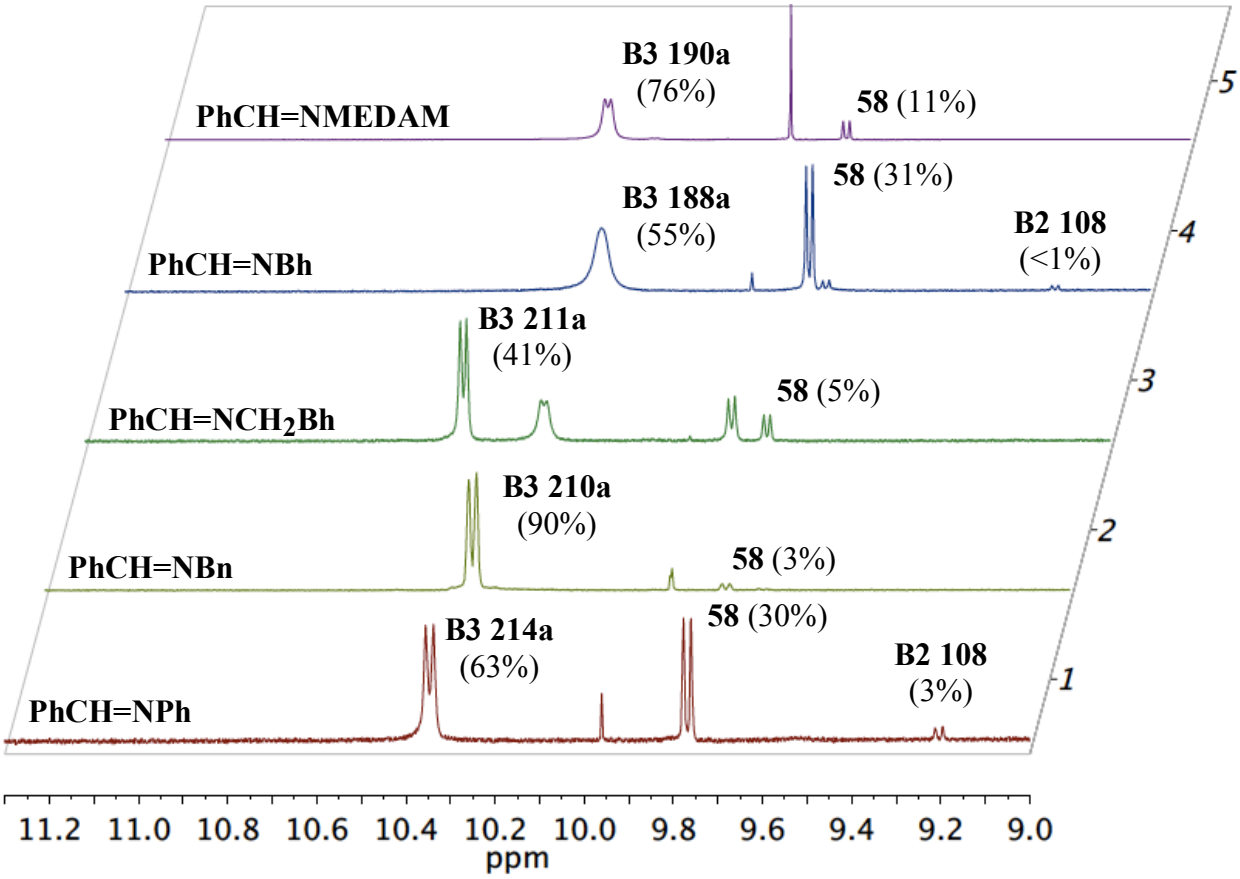

Figure 2.7 cont'd

B

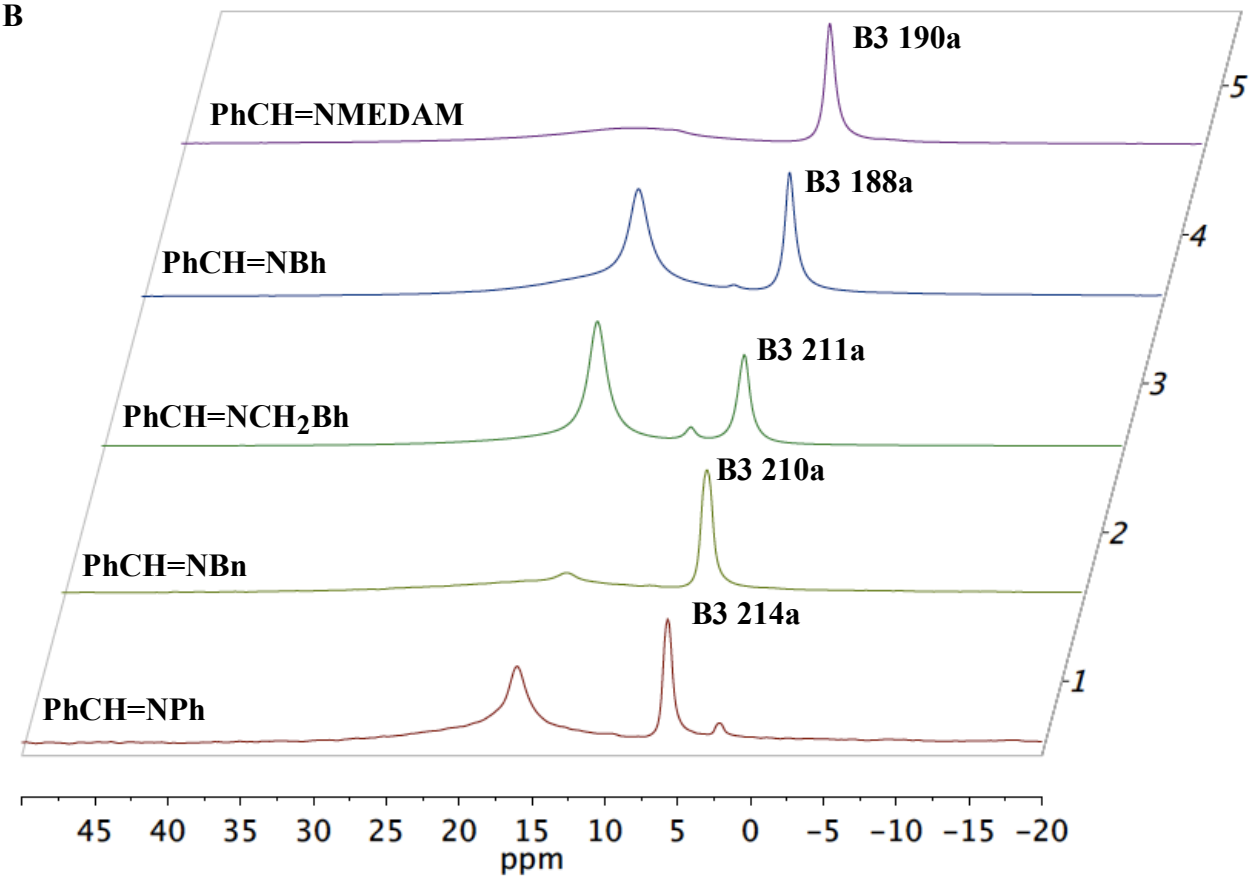

[a] Note for Figure 2.7A: Entry 1: (*S*)-VAPOL (0.1 mmol) plus 3 equiv commercial $B(OPh)_3$ and 2 equiv imine **75a** (PhCH=NPh) at 25 °C for 10 min. Entry 2: same as entry 1 with imine **206a** ($PhCH=NCH_2Ph$). Entry 3: same as entry 2 with imine **207a** ($PhCH=NCH_2CHPh_2$). Entry 4: same as entry 2 with imine **78a** ($PhCH=NCHPh_2$). Entry 5: same as entry 2 with imine **111a** (PhCH=NMEDAM).

2.1.1.5 A comparison of X-ray structure and calculated structure of BOROX catalyst

We have previously reported the solid-state structure of the IMINO-BOROX catalyst-substrate complex **190a**.[13f] The *X*-ray analysis revealed the presence of a number of non-

covalent interactions between the protonated imine substrate as it is bound in the anionic boroxinate catalyst (Figure 2.2B). In the follow-up work where a lot different bases were examined for BOROX complex, we have used computational chemistry to predict the possible structures of the BOROX catalysts with various bases. As a prelude, computations were first performed on the IMINO-BOROX **190a** since the results could be compared with the solid-state structure determined by *X*-ray analysis.[13f] Calculations were preformed using Gaussian ′03 at B3LYP/6-31g* level of theory.[20] The results of DFT calculations on **190a** are shown in Figure 2.8 and are very similar to the structure determined by X-ray. There are some differences as one might expect for a substrate-catalyst complex in the gas phase versus solid state. The strongest non-covalent interaction would be expected to be the H-bond between the protonated iminium and the boroxinate core. As in the solid state this was found to be with O-2 of the boroxinate core with a calculated distance of 1.73 Å vs. 2.02 Å in the solid state (d_1 in Figure 2.8 and Figure 2.2B). Common to both structures is the edge-face interaction (CH-π) between of one of the aryl rings of the MEDAM group with one of the phenyl rings of the VAPOL ligand (d_2 in Figure 2.8 and Figure 2.2B).[21] This distance in the calculated structure is 3.92 Å (Figure 2.8) and it is 4.42 Å (Figure 2.2B) in the solid state. It should be noted that the CH-π interaction distances are by convention indicted as the distance between the carbon bearing the hydrogen and the centroid of the benzene ring participating in the interaction.[22] There are also differences in the orientation of the phenyl group of the benzaldehyde imine relative to one of the phenanthrene walls of the VAPOL ligands (d_5 in Figure 2.8 and Figure 2.2B). The contact distance is about the same (3.56 vs 3.44 Å) but the angle between the planes containing these two rings increases from 4 to 39° in

the calculated structure. This twisting of the phenyl ring in the calculated structure allows for a closer edge-face interaction between one of the phenoxy groups of the boroxinate core and the phenyl group of the benzaldehyde imine (d_8, Figure 2.8). This distance is 4.66 Å in the calculated structure and 5.52 Å in the solid state. This phenoxy group of the boroxinate core in the calculated structure also moves about a half an Angstrom closer for a better CH-π interaction with one of the methyl groups on the back-end aryl substituent of the MEDAM group (d_9 in Figure 2.8). Also, there is another interaction (CH-O) between the methine CH of the iminium and the O-1 of the boroxinate anion (d_6 in Figure 2.8 and Figure 2.2B).

Figure 2.8 Calculated structure of IMINO-BOROX catalyst **190a** using Gaussian ′03. **(A)** Calculated B3LYP/6-31g* structure visualized by the Mercury Program (C, gray; O, red; N, blue; B, yellow; H, white). Hydrogen atoms omitted for clarity (except N-H and C-H). Some secondary interactions are highlighted: d_1 = 1.73 Å (H-bonding), d_2 = 3.92 Å (CH-π), d_5 = 3.56 Å (CH-π or π-π stack), d_6 = 2.53 Å (CH-O), d_8 = 4.66 Å (CH-π), d_9 = 4.02 Å (CH-π). (**B**) Space-filling rendition of **190a** with the same orientation and showing hydrogens. The boroxinate anion is given in green and the iminium cation is in traditional colors.

Figure 2.8 cont'd

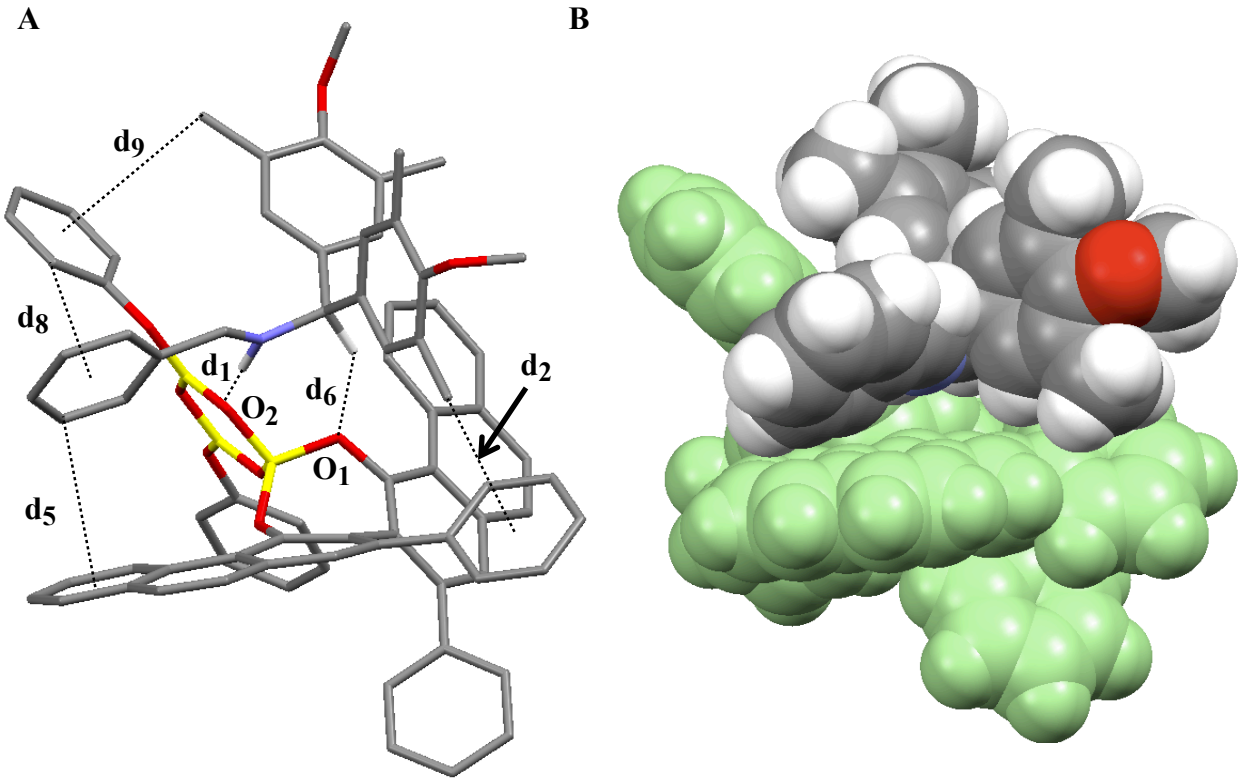

As the complex involves hydrogen bonding, it was also examined with BHandHLYP/6-31g* level of theory and the results were not significantly different from that with B3LYP/6-31g* (Table 2.6).

Table 2.6 Comparison of distances in computed structure **190a** using different levels of theories

Methods	d_1 (Å)	d_2 (Å)	d_5 (Å)	d_6 (Å)	d_8 (Å)	d_9 (Å)
X-ray crystals	2.02	4.42	3.44	2.86	5.52	4.78
B3LYP/3-21g*	1.53	3.89	3.52	2.21	4.42	4.19
B3LYP/6-31g*	1.73	3.92	3.56	2.53	4.66	4.02
BHandHLYP/6-31g*	1.73	3.84	3.52	2.47	4.55	3.88

2.1.2 Amines as the base: AMINO-BOROX catalyst

After establishing the catalytic system where imines are the bases that generate the catalysts, we envisioned to screen other bases in order to broaden the diversity of the BOROX catalyst. To begin with, one of the obvious choices for the base is an amine as they are more basic than imines. An ulterior motive to screening amines was to examine the possibility of developing the first example of a catalytic asymmetric multicomponent aziridination (MCAZ). To our delight, all kinds of aliphatic amines (1°, 2°, 3°) generated B3 catalysts in good yields (Table 2.7, entries 1-5 and Figure 2.9, entries 1-5). The pKa of protonated triethylamine is 10.65 (in water).[23]

Table 2.7 NMR Analysis of a mixture of (*S*)-VAPOL, $B(OPh)_3$ and amines **126** as bases [a]

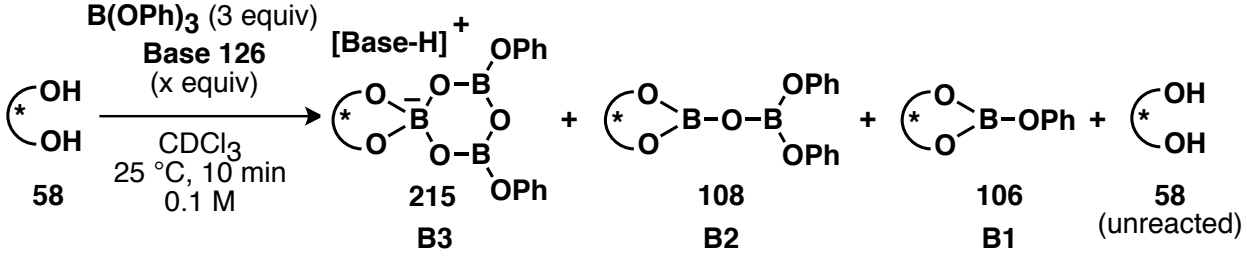

#	series	Base **126** [b]	Equiv of Base	(*S*)-VAPOL *c,d*	B1 **106** *d*	B2 **108** *d*	B3 **215** *d*	^{1}H *e*	^{11}B *f*
1	**a**	Ph_2CHNH_2	2	7	<1	<1	66	10.36	17.77, 5.58
2	**c**	MEDAM-NH_2	2	3	<1	<1	50	10.37	18.48, 5.48
3	**g**	iPr_2NH	2	<1	<1	<1	74	10.31	16.13, 5.18
4 [g]	**h**	Bn_2NH	2	<1	<1	<1	34	10.45	18.25, 5.56
5	**i**	Et_3N	2	8	<1	<1	63	10.25	16.00, 5.37
6 [g]	**j**	4-MeO-$C_6H_4NH_2$	2	5	<1	<1	23	10.30	15.85, 5.49
7	**k**	$C_6H_5NH_2$	2	24	<1	<1	61	10.29	16.04, 5.56
8	**l**	$(C_6H_5)_2NH$	2	51	<1	28	<1	–	16.41
9	–	No base	0	57	5	18	<1	–	16.00

Table 2.7 cont'd

[a] Unless otherwise specified, all NMR samples were prepared by mixing (*S*)-VAPOL **58** (0.1 mmol) and commercial $B(OPh)_3$ (0.3 mmol) and base **126** in $CDCl_3$ (1 mL) at 25 °C and stirring 10 min before spectra were taken. [b] All bases were distilled or sublimed prior to use. [c] Unreacted (*S*)-VAPOL **58**. [d] NMR yield with Ph_3CH as internal standard with ligand as the limiting reagent. [e] Chemical Shift for the bay proton in B3-base complex. [f] Chemical Shift of the peaks observed in ^{11}B NMR spectrum. [g] There is an unknown specie at 10.41 ppm (40% yield, determined by the integration of the bay proton of the new species against the internal standard) for entry 4 and at 9.66 ppm (44% yield, determined by the integration of the bay proton of the new species against the internal standard) for entry 6.

To our surprise, even an aromatic amine such as aniline **126k** (pKa of protonated aniline is 4.62 in water)[24] gave BOROX catalyst **215k** in 61 % yield (Table 2.7, entry 7 and Figure 2.9 entry 7). However, Ph_2NH **126l** (pKa of $Ph_2N^+H_2$ is 0.78 in water) failed to give any boroxinate. After these results, we moved on to develop a true MCAZ reaction and were able to successfully accomplish that goal and this is discussed in detail in Chapter 7.

Figure 2.9 Amine induced boroxinate catalyst formation. (**A**)[a] ^1H NMR spectra in $CDCl_3$ with Ph_3CH as internal standard. (**B**) ^{11}B NMR spectra corresponding to the ^1H NMR spectra in Figure 2.9A.

Figure 2.9 cont'd

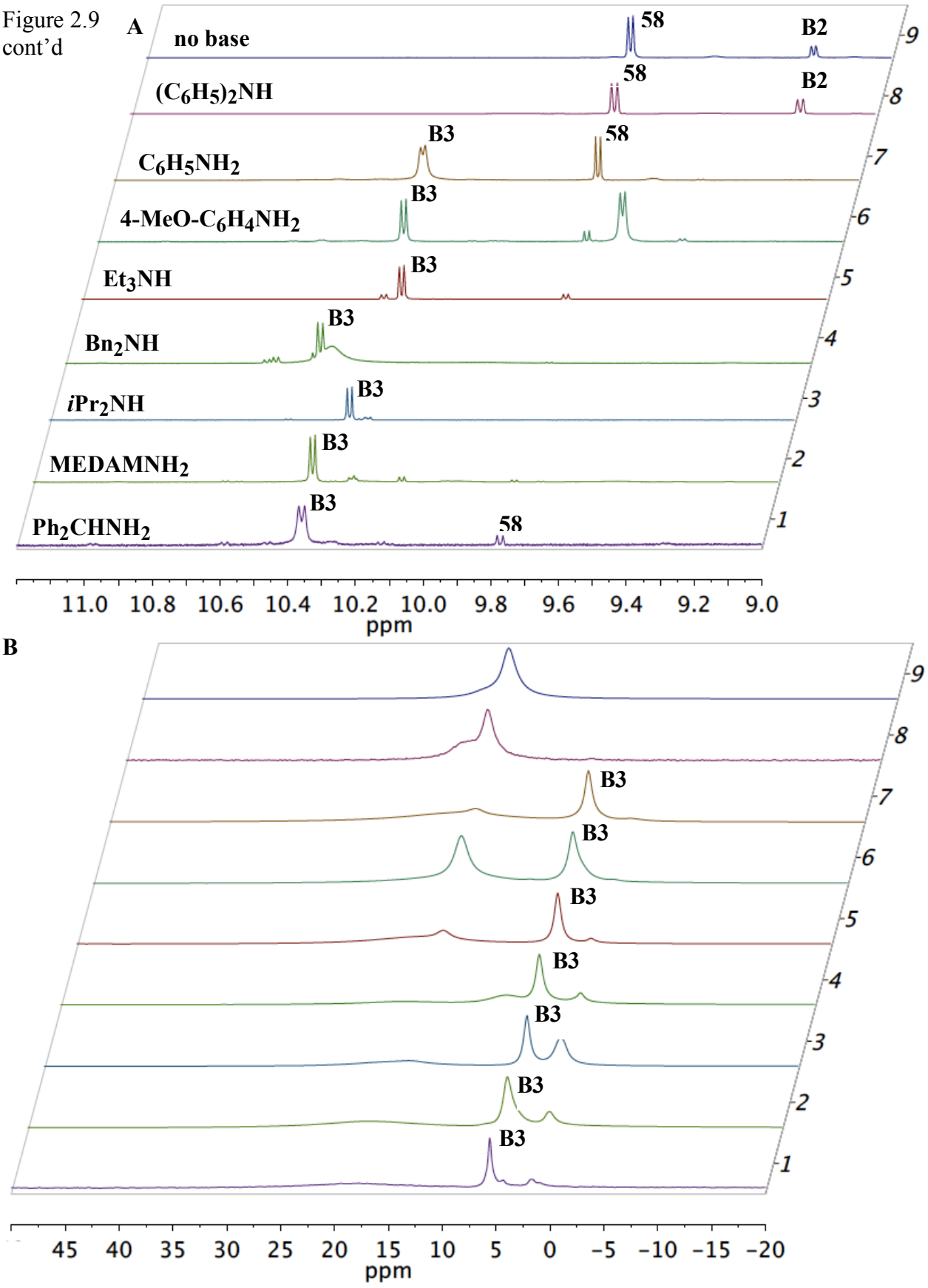

[a] Note for Figure 2.9A: Entry 1: (*S*)-VAPOL (0.1 mmol) plus 3 equiv commercial $B(OPh)_3$ and 2 equiv amine **126a** (Ph_2CHNH_2) at 25 °C for 10 min. Entry 2: same as entry 1 but with amine **126c** (MEDAM-NH_2). Entry 3: same as entry 2 but with amine **126g** (*i*Pr_2NH). Entry 4: same as entry 2 but with amine **126h** (Bn_2NH). Entry 5: same as entry 2 but with amine **126i** (Et_3N). Entry 6: same as entry 2 but with amine **126j** (4-MeO-$C_6H_4NH_2$). Entry 7: same as entry 2 but with amine **126k** ($C_6H_5NH_2$). Entry 8: same as entry 2 but with amine **126l** ($(C_6H_5)_2NH$). Entry 9: (*S*)-VAPOL (0.1 mmol) plus 3 equiv commercial $B(OPh)_3$ at 25 °C for 10 min.

A lot effort has been given to obtain crystals of AMINO-BOROX catalyst. Unfortunately, no success was achieved. Therefore, computational methods were undertaken to explore the possible structures of the AMINO-BOROX **215c** derived from MEDAM amine **126c**. Calculations were preformed using Gaussian ′03 at B3LYP/6-31g* level of theory.[20] The protonated amine **126c**-H should have a very different binding mode in the boroxinate species **215c** due to the absence of the benzylidene group on the nitrogen atom and the presence of an ammonium ion with three hydrogens capable of H-bonding to the anionic boroxinate platform.

The calculated structure for the BOROX species **215c** is presented in Figure 2.10. The key interactions between the cationic protonated amine and the anionic boroxinate core are the two hydrogen bonds from the ammonium ion to O-1 and O-2 of the boroxinated anion (Figure 2.10). The hydrogen bond to O-2 (d_1 = 1.75 Å) is slightly shorter than that to O-1 (d_2 = 1.96 Å) consistent with the computational finding that the electron density of the boroxinate core is

highest at O-2 (see experimental). There is also a short distance between the ammonium nitrogen and the centroid of the A-ring of one of the phenanthrene units in the VAPOL ligand (d_3 = 3.21 Å), which is indicative of an NH-π interaction. The iminium ion in **190a** and the ammonium ion in **215c** both have the protonated nitrogen H-bonded to O-2 of the boroxinate core, but the head groups of the nitrogen substituent (MEDAM group) are on opposite sides of the boroxinate platform. In **190a** the MEDAM group has an edge-face interaction with the phenyl substitutent of VAPOL and in **215c**, the MEDAM group has an edge-face interaction with the C-ring of VAPOL (d_4 = 4.18 Å).

Figure 2.10 Calculated structure of AMINO-BOROX catalyst **215c** (derived from MEDAM amine **126c**) using Gaussian ′03. **(A)** Calculated B3LYP/6-31g* structure visualized by the Mercury Program (C, gray; O, red; N, blue; B, yellow; H, white). Hydrogen atoms omitted for clarity (except N-H). Some secondary interactions are highlighted: d_1 = 1.75 Å (H-bonding), d_2 = 1.96 Å (H-bonding), d_3 = 3.21 Å (NH-π or cation-π), d_4 = 4.18 Å (CH-π). (**B**) Space-filling rendition of **215c** with the same orientation and showing hydrogens. The boroxinate anion is given in green and the ammonium cation is in traditional colors.

Figure 2.10 cont'd

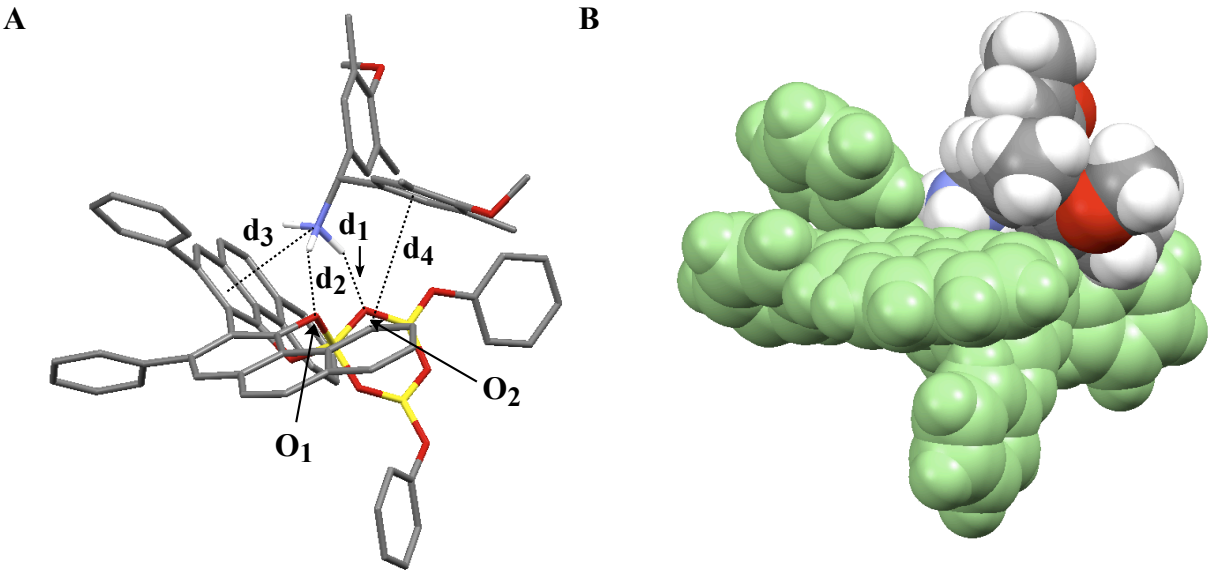

The boroxinate complex **215c** was also examined with BHandHLYP/6-31g* level of theory and the results were not significantly different from that with B3LYP/6-31g* (Table 2.8). In fact, a calculated structure of **215k** (not shown here) derived from aniline **126k** also revealed the presence of dual hydrogen bonding and an NH-π interaction.

Table 2.8 Comparison of distances in computed structure **215c** using different levels of theories

Methods	d_1 (Å)	d_2 (Å)	d_3 (Å)	d_4 (Å)
X-ray crystals	-	-	-	-
B3LYP/3-21g*	1.60	1.86	3.15	4.05
B3LYP/6-31g*	1.75	1.96	3.21	4.18
BHandHLYP/6-31g*	1.74	1.99	3.16	4.13

2.1.3 Pyridines and Quinolines as the base: PYRIDINO- and QUINOLINO-BOROX catalyst

It was interesting to find that heterocyclic bases were also able to generate B3 in good yields. Simple mixing of pyridine **216a** with VAPOL and commercial $B(OPh)_3$ in $CDCl_3$ gave a

white precipitate in the NMR tube (unsuitable for shimming). However, we were able to obtain a good quality ^{1}H NMR and ^{11}B NMR spectra (in d_8-toluene), when the boroxinate catalyst was made via pre-catalyst (Figure 2.11). The boroxinate **217a** was obtained in 85% yield when one equivalent of pyridine was added to the pre-catalyst. The pKa of protonated pyridine is 5.14.[24]

Figure 2.11 Pyridine induced boroxinate catalyst formation. (**A**) ^{1}H NMR spectra of **217a** in d_8-toluene. A mixture of (*S*)-VAPOL (0.1 mmol), 3 equiv commercial $B(OPh)_3$ was heated at 80 °C in toluene for 1 h followed by removal of volatiles under vacuum for 0.5 h (method A). Thereafter, 1.0 equiv of pyridine **216a** was added to the pre-catalyst followed by the addition of d_8-toluene (1 mL) and the stirred for 10 min at 25 °C. (**B**) ^{11}B NMR spectra corresponding to the ^{1}H NMR spectra in Figure 2.11A.

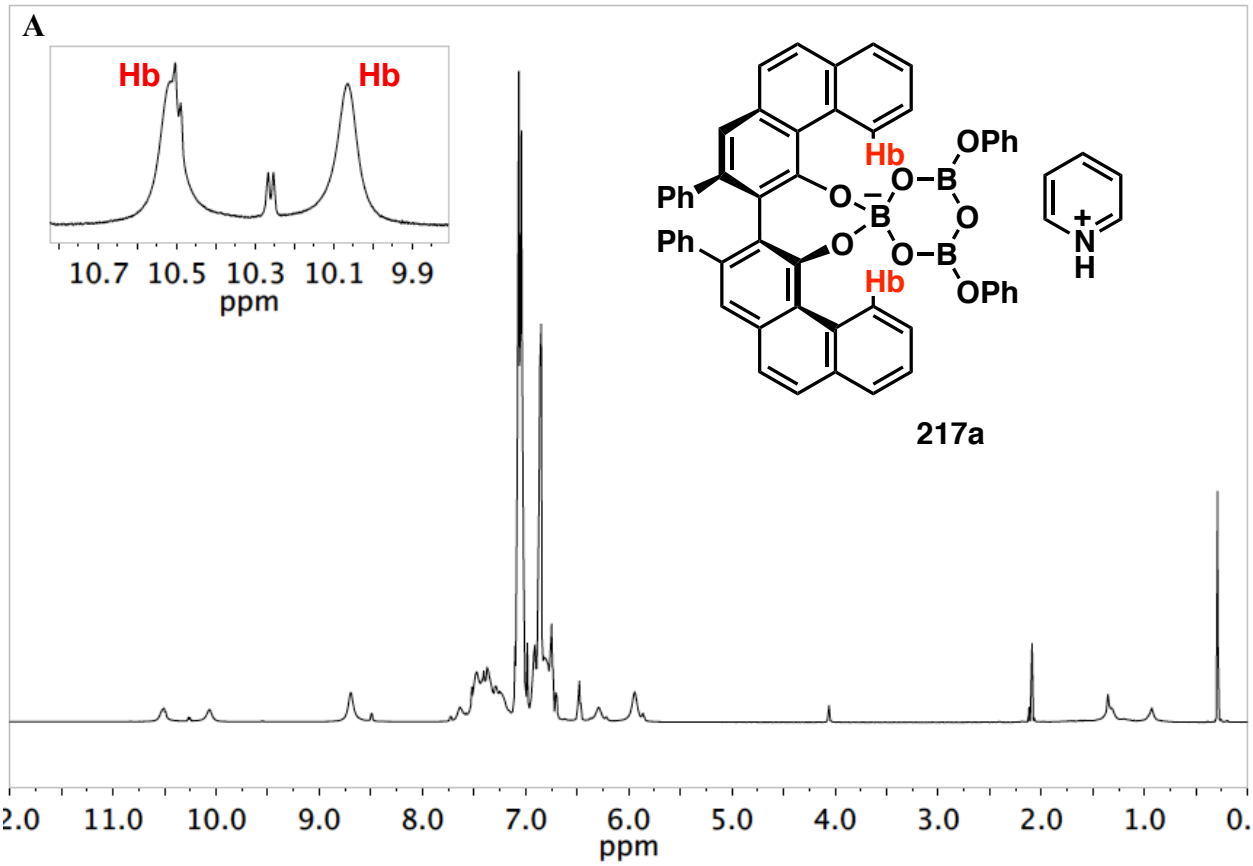

Figure 2.11 cont'd

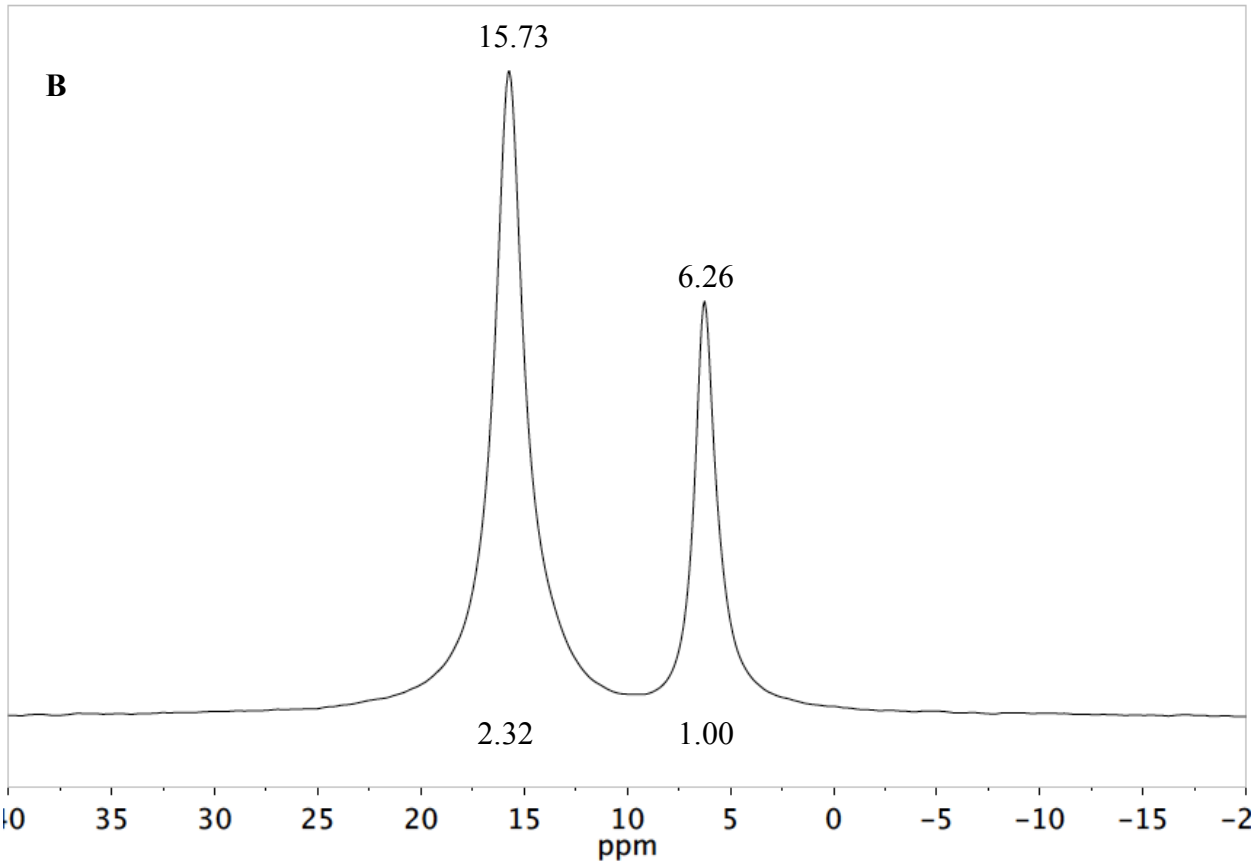

The ^{1}H NMR spectrum of **217a** has two peaks (δ = 10.07 ppm and δ = 10.51 ppm) for the bay protons (Figure 2.11A). This was interpreted to mean that the migration of the protonated pyridine from top face of the catalyst to the bottom face is slow on the NMR time scale. Pyridine derivatives such as 2,6-lutidine **216b** and DMAP **216c** also gave the catalyst in good yields (Table 2.9 and Figure 2.11, entries 1-2). In fact, Gang Hu, a former group member, was able to obtain an X-ray crystal structure of boroxinate **217c**.[13e] A small amount of [DMAP-H]$^{+}$ [B(OPh)$_4$]$^{-}$ **218** (δ=2.30 ppm, ^{11}B NMR) was also observed during the NMR study of **217c** complex. The structure of **218** was confirmed by X-ray analysis and is discussed in chapter 4.

Table 2.9 NMR Analysis of a mixture of (*S*)-VAPOL, $B(OPh)_3$ and pyridine derivatives, pyrrole, imidazole and quinoline derivatives as bases [a]

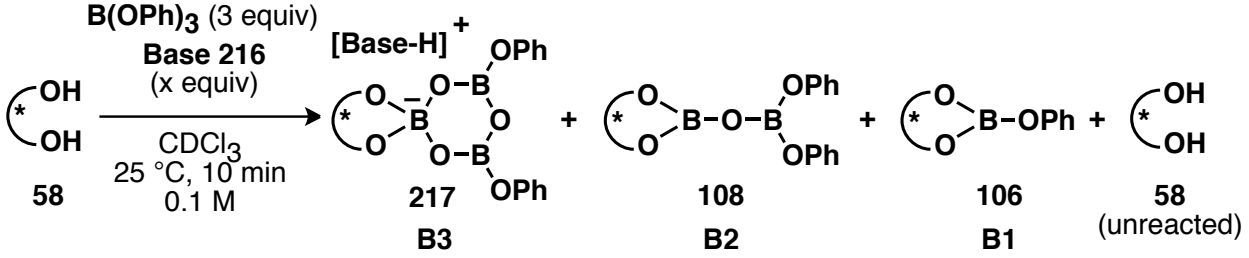

#	series	Base **216** [b]	Equiv of Base	(*S*)-VAPOL *c,d*	B1 **106** *d*	B2 **108** *d*	B3 **217** *d*	^{1}H *e*	^{11}B *f*
1	**b**	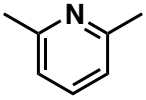	2	<1	<1	<1	74	10.13	13.26, 5.30
2	**c**	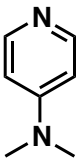	2	<1	<1	<1	78	10.46	17.58, 5.90
3	**d**	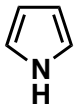	2	65	5	29	<1	–	16.16
4	**e**	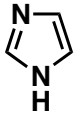	2	nd	<1	<1	nd	nd	nd
5	**f**	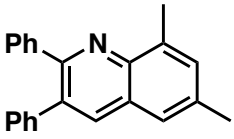	1 2	nd nd	<1 <1	3 3	27 29	10.35 10.35	15.95, 5.38 15.98, 5.44
6	**g**	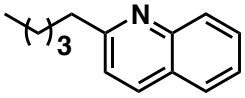	1 2	2 <1	<1 <1	<1 <1	59 59	10.19 10.21	15.79, 5.66 15.45, 5.56
7	**h**	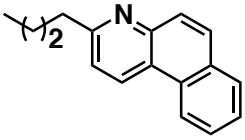	1 2	14 13	<1 <1	<1 <1	65 71	10.19 10.25	15.92, 5.92 15.98, 5.59
8	–	No base	0	57	5	18	<1	–	16.00

Table 2.9 cont'd

[a] Unless otherwise specified, all NMR samples were prepared by mixing (*S*)-VAPOL **58** (0.1 mmol) and commercial $B(OPh)_3$ (0.3 mmol) and base **216** in $CDCl_3$ (1 mL) at 25 °C and stirring 10 min before spectra were taken. Compounds **216f-h** were generously provided by Amila Dissanayake. [b] All bases were distilled or sublimed prior to use. [c] Unreacted (*S*)-VAPOL **58**. [d] NMR yield with Ph_3CH as internal standard with ligand as the limiting reagent. [e] Chemical Shift for the bay proton in B3-base complex. [f] Chemical Shift of the peaks observed in ^{11}B NMR spectrum.

In case of pyrrole **216d**, there was no sign of catalyst formation (Table 2.9 and Figure 2.12, entry 3). This was expected, as the pKa of protonated pyrrole is –3.80.[25] *The case of imidazole **216e** was a little complex as there was no tri-coordinate boron observed in the ^{11}B NMR spectrum (Figure 2.11, entry 4). It might be possible that all three boron atoms are coordinated by imidazole.* Quinoline derivatives were also screened for the generation of QUINOLINO-BOROX catalyst (Table 2.9 and Figure 2.11, entries 5-7). Direct generation of a boroxinate from quinolines lead us to the discovery of another asymmetric reaction mediated by QUINOLINO-BOROX catalyst i.e. asymmetric reduction of quinolines[26] as discussed in Scheme 1.20 of Chapter 1. The pKa of protonated quinoline and 5,6-benzoquinoline are 4.85 and 5.15 respectively.[24]

Figure 2.12 Pyridine and quinoline derivatives in the induction of boroxinate catalyst formation. (**A**)[a] ^1H NMR spectra in $CDCl_3$ with Ph_3CH as internal standard. (**B**) ^{11}B NMR spectra corresponding to the ^1H NMR spectra in Figure 2.12A.

Figure 2.12 cont'd

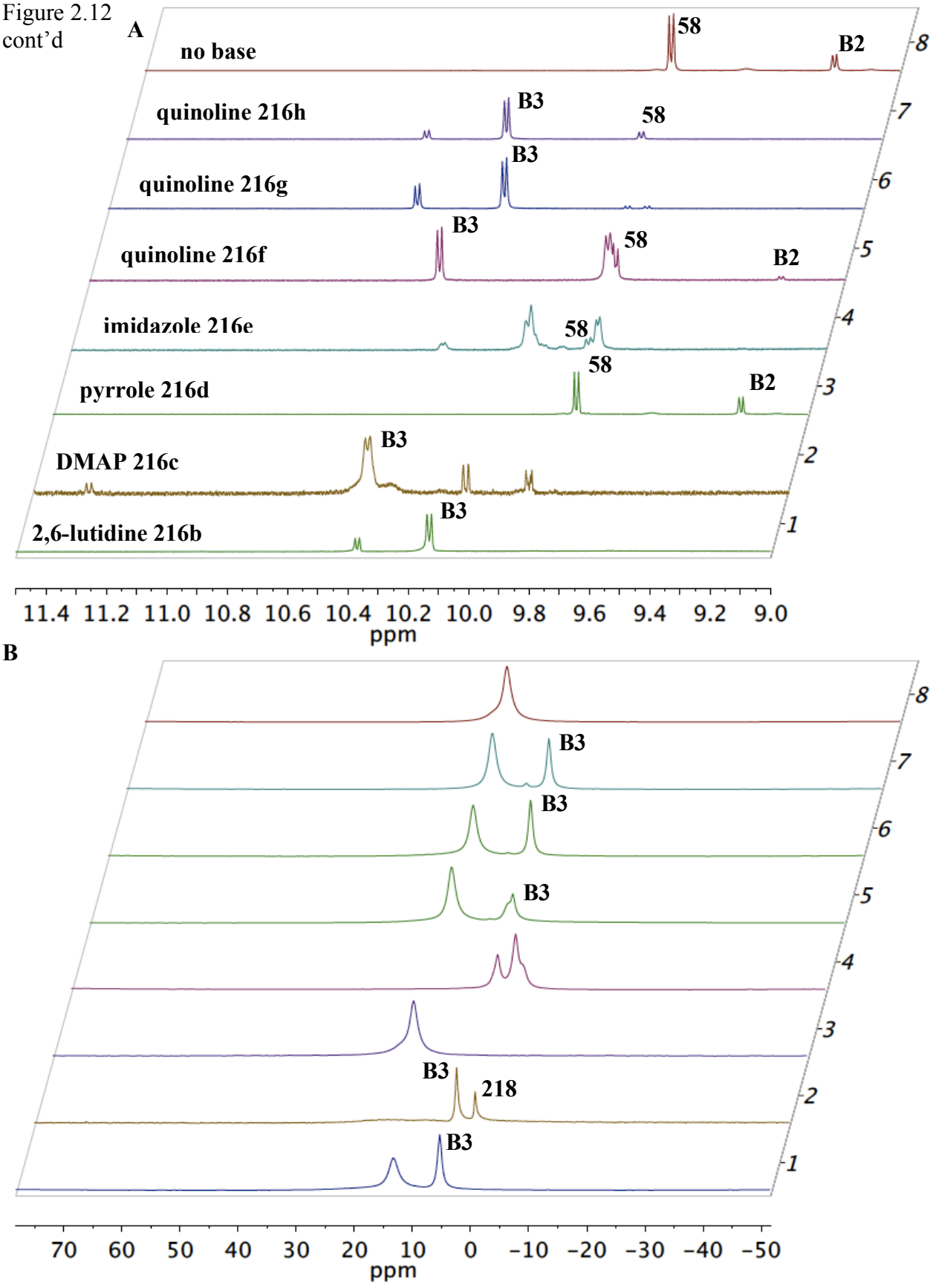

[a] Note for Figure 2.12A: Entry 1: (*S*)-VAPOL (0.1 mmol) plus 3 equiv commercial $B(OPh)_3$ and 2 equiv **216b** at 25 °C for 10 min. Entry 2: same as entry 1 with **216c**. Entry 3: same as entry 2 with **216d**. Entry 4: same as entry 2 with **216e**. Entry 5: same as entry 2 with **216f**. Entry 6: same as entry 2 with **216g**. Entry 7: same as entry 2 with **216h**. Entry 8: (*S*)-VAPOL (0.1 mmol) plus 3 equiv commercial $B(OPh)_3$ at 25 °C for 10 min.

While studying the NMR spectra of the complex **217b** (base = 2,6 lutidine) derived from (*R*)-VAPOL, colorless crystals were serendipitously formed in the NMR tube and thus the opportunity to determine the crystal structure of the LUTIDINO-BOROX complex **217b** presented itself. Structural parameters for **217b** are available free of charge from the Cambridge Cystallographic Data Centre under reference number CCDC. The observed crystal structure is found to be different from crystal structures of all the boroxinates we reported so far. A detailed analysis revealed the presence of two BOROX units (**B3a** and **B3b**) in a single array (Figure 2.13). Each unit consists of a protonated lutidinium ion, a molecule of phenol and the boroxinate anion derived from a boroxine ring in which the tetra-coordinate boron is spiro-fused to the VAPOL ligand. There is no direct H-bonding between the protonated lutidinium and the boroxinate anion, but rather the protonated lutidinium is H-bonded to the phenol (Figure 2.13, d_1 = 1.91 Å in **B3a** and $d_{1'}$ = 1.87 Å in **B3b**), which in turn is H-bonded to the boroxinate anion (Figure 2.13, d_1 = 1.91 Å in **B3a** and $d_{1'}$ = 1.92 Å in **B3b**). It must be noted that the pKa of protonated lutidine is 5.77.[24] Yamamoto and coworkers reported a similar kind of hydrogen bonding interaction incorporating a molecule of phenol in the case of the crystal structure of a

spiroborate anion.[12a] An important difference between the two B3 units (**B3a** and **B3b**) is that they differ at the point of binding of the phenol to the boroxinate: the phenol is H-bonded to O1 in **B3a** and to O2 in **B3b**. It must be remembered that we have always observed the presence of hydrogen bonding to O2 in all boroxinates reported so far.[13e,13f] Similar to the case of imines, there are several non-covalent interactions like CH-π and π-π interactions. One of the important CH-π interactions is from the methyl group on lutidine to the middle ring of the phenantherene unit in the VAPOL ligand (Figure 2.13, d_3 = 3.77 Å in **B3a** and $d_{3'}$ = 4.17 Å in **B3b**).

Figure 2.13 (**A**)[a] Solid state structure of the LUTIDINO-BOROX **217b** visualized by the Mercury Program (C, gray; O, red; N, blue; B, yellow; H, white). Hydrogen atoms omitted for clarity (except N-H and O-H). (**B**) Space-filling rendition of **217b** with the same orientation and showing hydrogens. The boroxinate anion is given in green and the lutidinium cation is in traditional colors. (**C**) Diagrammatic representation of **B3a** and **B3b** in **217b**

A

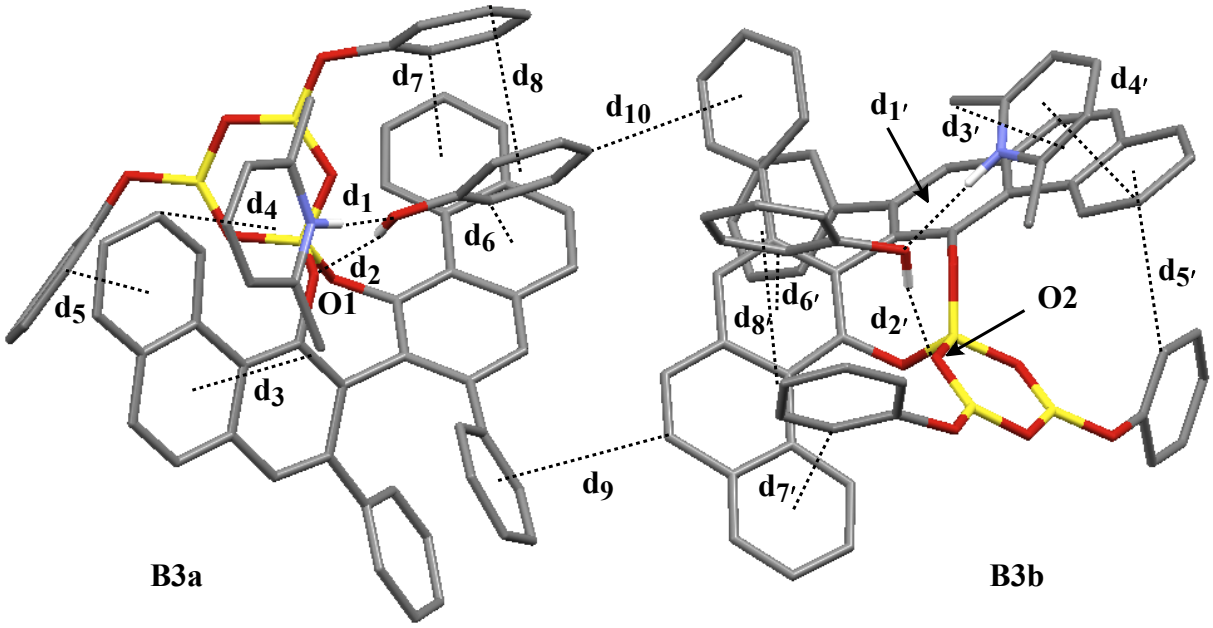

217b

Figure 2.13 cont'd

B

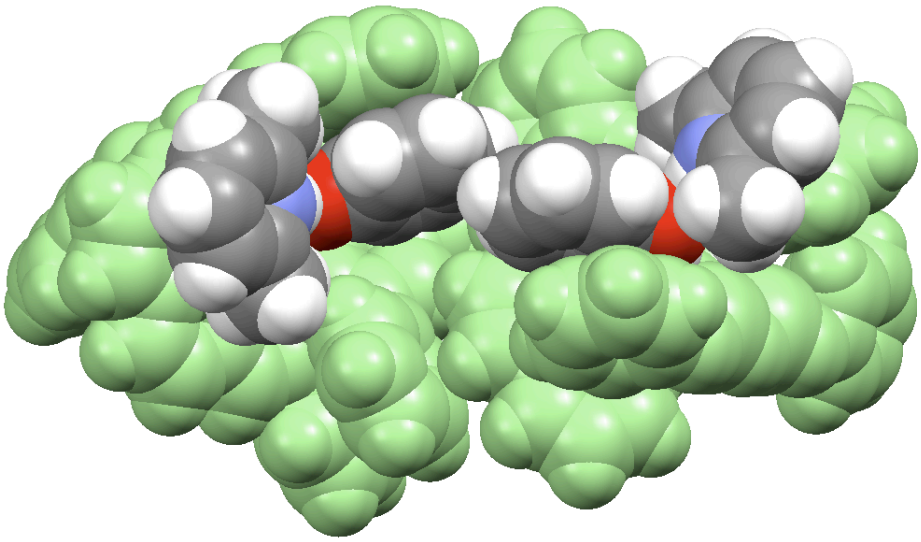

C

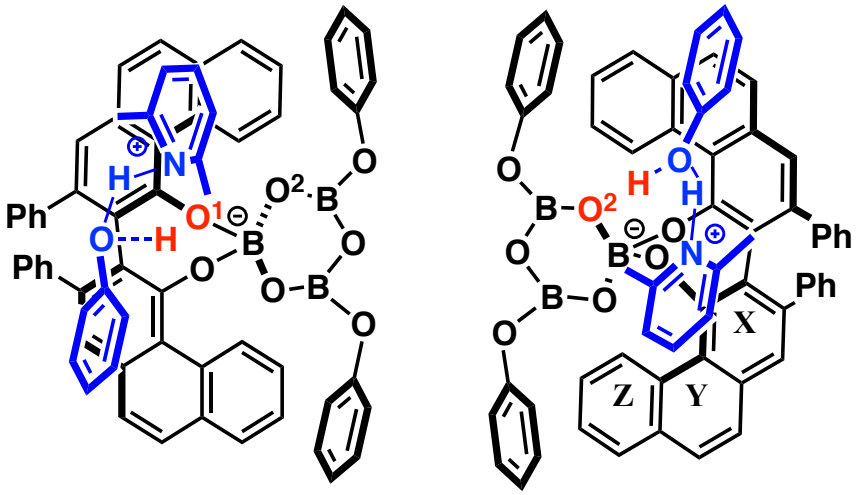

B3a **B3b**

[a] Note for Figure 2.13A: Some secondary interactions are highlighted: d_1 = 1.91 Å (H-bonding), d_2 = 1.91 Å (H-bonding), $d_{1'}$ = 1.87 Å (H-bonding), $d_{2'}$ = 1.92 Å (H-bonding), d_3 = 3.77 Å (CH-π), $d_{3'}$ = 4.17 Å (CH-π), d_4 = 3.54 Å (CH-π or π-π stack), $d_{4'}$ = 3.44 Å (CH-π or π-π stack), d_5 = 3.70 Å (CH-π), $d_{5'}$ = 3.92 Å (CH-π), d_6 = 3.94 Å (CH-π), $d_{6'}$ = 3.50 Å (CH-π), d_7 = 3.54 Å

(CH-π), $d_{7'}$ = 3.43 Å (CH-π), d_8 = 3.40 Å (CH-π or π-π stack), $d_{8'}$ = 3.54 Å (CH-π or π-π stack), d_9 = 3.62 Å (CH-π), d_{10} = 4.25 Å (CH-π).

There are several other CH-π interactions including the two interactions from the phenyl ring of the phenol component of the boroxinate to the end ring of the phenanthrene unit in the VAPOL ligand (Figure 2.13, d_5 = 3.70 and d_7 = 3.54 in **B3a** and $d_{5'}$ = 3.92 and $d_{7'}$ = 3.43 in **B3b**). One of the interesting CH-π interactions is from the external phenol to the middle ring (in case of **B3a**) or X-ring (in case of **B3b**) of the phenanthrene unit in the VAPOL ligand (Figure 2.13, d_6 = 3.94 in **B3a** and $d_{6'}$ = 3.50 in **B3b**). Another important noncovalent interaction between the catalyst and the base is a π-π stacking interaction between the external phenol molecule and the phenyl ring of the phenol component of the boroxinate anion (Figure 2.13, d_8 = 3.40 in **B3a** and $d_{8'}$ = 3.54 in **B3b**). An additional π-π stacking interaction was located between the aryl ring of lutidine and the end ring of the phenanthrene unit in the VAPOL ligand (Figure 2.13, d_4 = 3.54 in **B3a** and $d_{4'}$ = 3.44 in **B3b**). Finally, there are two CH-π interactions, which are possibly holding the two B3 units together (Figure 2.13, d_9 = 3.62 and d_{10} = 4.25 in **B3a** and **B3b**). The crystal structure of **217b** has provided many new details about the nature and binding of the boroxinate catalyst. The presence of two B3 units suggests the idea of possible aggregation of the catalyst in the mechanism of aziridination reaction. Also, the steric bulk of two methyl groups on lutidine might have made it necessary for the external phenol to serve the role of the sandwich for the hydrogen bonding. This suggests that the asymmetric reduction of

quinoline should be tried with an extra molecule of phenol during the preparation of the catalyst as quinoline and lutidine both have steric bulk at the ortho positions.

2.1.4 Amides as the base: AMIDO-BOROX catalyst

The next base examined was amides. The pKa of the protonated *N*, *N* dimethyl acetamide **219** is –0.39.[27] An 18% yield of the catalyst **220** was formed when 2 equiv of **219** was employed based on the integration of the absorption at δ = 10.16 ppm in ^{1}H NMR spectrum (Figure 2.14).

Figure 2.14 Amide induced boroxinate formation. (**A**) ^{1}H NMR spectra in $CDCl_3$ with Ph_3CH as internal standard. (*S*)-VAPOL (0.1 mmol) plus 3 equiv commercial $B(OPh)_3$ and 2 equiv **219** at 25 °C for 10 min. (**B**) ^{11}B NMR spectra corresponding to the ^{1}H NMR spectra in Figure 2.14A.

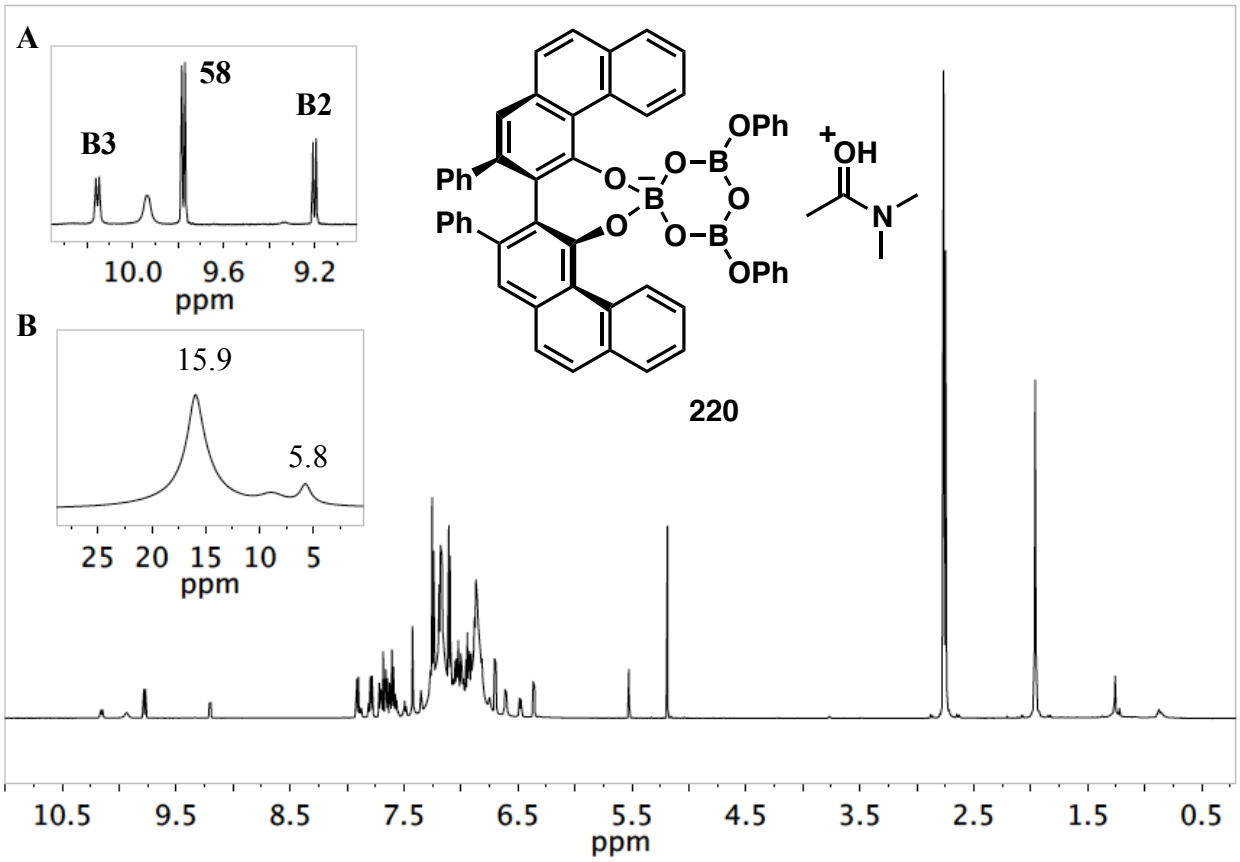

2.1.5 Sulfoxides as the base: SULFOX-BOROX catalyst

In search of a highly acidic BOROX catalyst, we envisioned to employ very weak bases like sulfoxides. It must be noted that the pKa of a protonated dimethyl sulfoxide is –1.8 (in H_2O).[28] To our delight and surprise, when 2 equiv of DMSO **221a** was used as the base the SULFOX-BOROX catalyst **222a** was formed in 66% yield (Table 2.10, entry 1). In fact, good yields of boroxinate catalysts were obtained irrespective of the sulfoxides being acyclic, cyclic, aliphatic or even aromatic (Table 2.10, entries 1-5). Also, mixed sulfoxides like **221e** resulted in 46% yield of the catalyst (Table 2.10, entry 6). The pKa of protonated **221e** is –2.27.[28]

Table 2.10 NMR Analysis of a mixture of (*S*)-VAPOL, $B(OPh)_3$ and sulfoxides as bases [a]

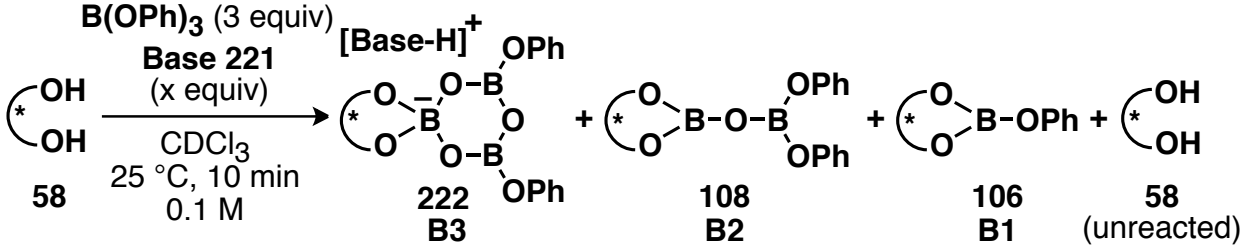

#	series	Base **221** [b]	Equiv of Base	(*S*)-VAPOL *c,d*	B1 **106** *d*	B2 **108** *d*	B3 **222** *d*	^{1}H *e*	^{11}B *f*
1	**a**	Me_2SO	1	21	<1	15	53	9.98	16.03, 6.98
2			2	11	<1	10	66	10.02	15.95, 6.24
3	**b**	$(CH_2)_4SO$	2	8	<1	3	73	10.08	15.78, 5.70
4	**c**	Bn_2SO	2	22	<1	17	38	10.09	15.96, 7.42
5	**d**	Ph_2SO	2	45	<1	21	25	10.01	16.01, 8.57
6	**e**	±Ph(Me)SO	2	22	<1	17	46	9.94	15.96, 7.11
7	**f**	(*R*)-*p*-tol-(Me)SO	1	32	<1	15	47	9.81	15.95, 7.92
8	**f**	(*R*)-*p*-tol-(Me)SO	2	09	<1	17	74	9.87	15.97, 6.73
9 [g]	**g**	(*R*)-*p*-tol-(Me)SO	1	18	<1	08	64	10.01	15.94, 7.66
10 [g]	**g**	(*R*)-*p*-tol-(Me)SO	2	06	<1	13	70	10.08	15.93, 6.43
11	**h**	Me_2SO_2	2	69	07	11	<1	–	15.99
12	**i**	$(CH_2)_4SO_2$	2	58	<1	22	<1	–	15.98

Table 2.10 cont'd

13	–	No base	0	57	5	18	<1	–	16.00

[a] Unless otherwise specified, all NMR samples were prepared by mixing (*S*)-VAPOL **58** (0.1 mmol) and commercial $B(OPh)_3$ (0.3 mmol) and base **221** in $CDCl_3$ (1 mL) at 25 °C and stirring for 10 min before spectra were taken. [b] All bases were distilled or sublimed prior to use. [c] Unreacted (*S*)-VAPOL **58**. [d] NMR yield with Ph_3CH as internal standard with ligand as the limiting reagent. [e] Chemical Shift for the bay proton in B3-base complex. [f] Chemical Shift of the peaks observed in the ^{11}B NMR spectrum. [g] (*R*)-VAPOL used for analysis.

Chiral sulfoxide **221f** was employed with both enantiomers of the ligand. Similar yields were observed in both the cases suggesting the absence of any kind of matched/mismatched case although the bay proton is 0.2 ppm different between the diastereometric SULFOX-BOROX species. Interestingly, sulfones **221h** and **221i** gave no sign of BOROX catalyst. This was expected, as the pKa of the protonated dimethylsulfone **221h** is –12 (in H_2O).[29]

Figure 2.15 Sulfoxide induced boroxinate catalyst formation. (**A**)[a] ^1H NMR spectra in $CDCl_3$ with Ph_3CH as internal standard. (**B**) The alkyl region corresponding to the ^1H NMR spectra in Figure 2.15A. (**C**) ^{11}B NMR spectra corresponding to the ^1H NMR spectra in Figure 2.15A. (**D**)[b] The shift in the methyl region of the dimethylsulfoxide after the formation of **222a**. ^1H NMR spectra in $CDCl_3$. (**E**) The bay region of the ^1H NMR spectra corresponding to the ^1H NMR spectra in Figure 2.15D.

Figure 2.15 cont'd

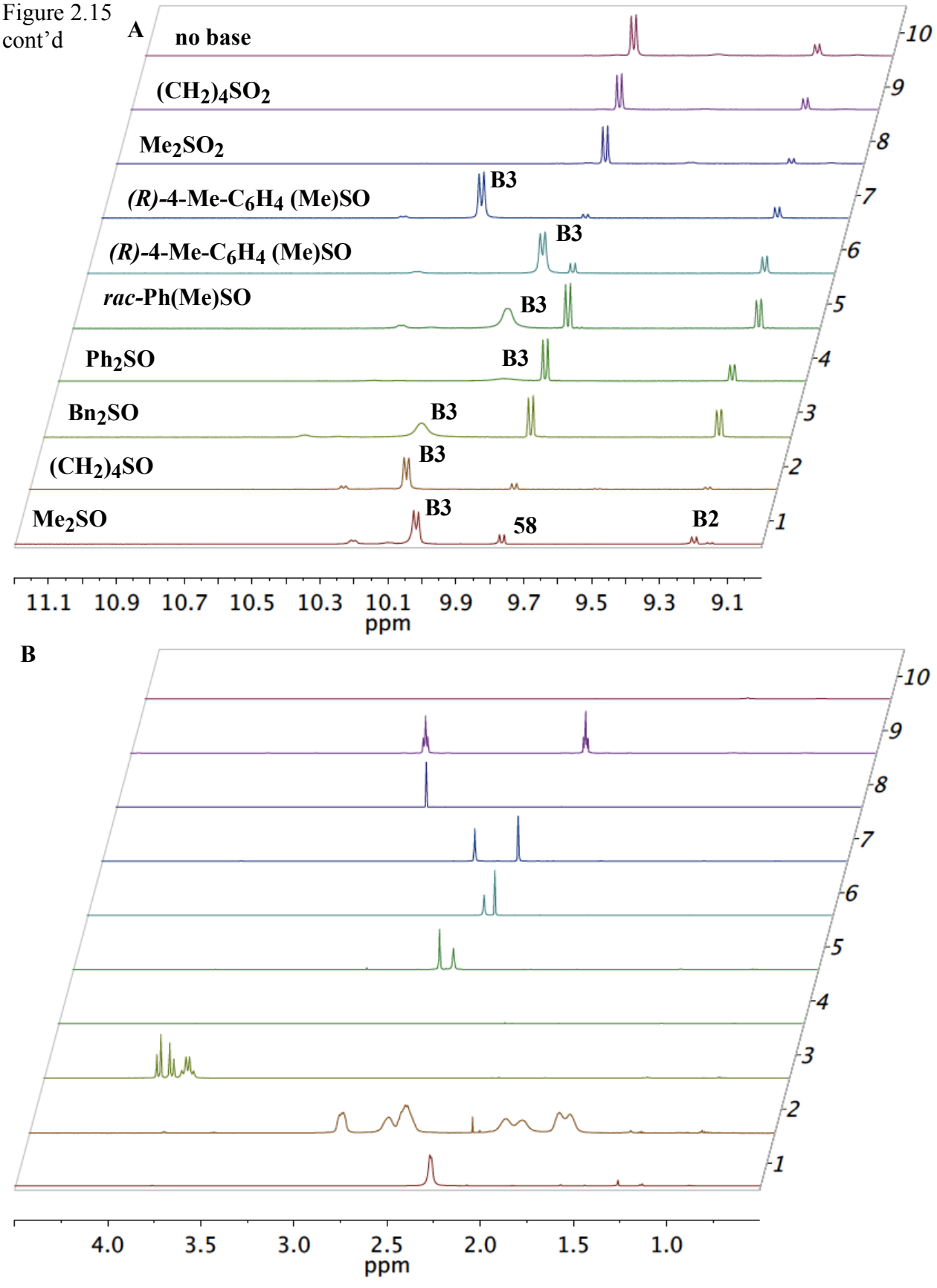

Figure 2.15 cont'd

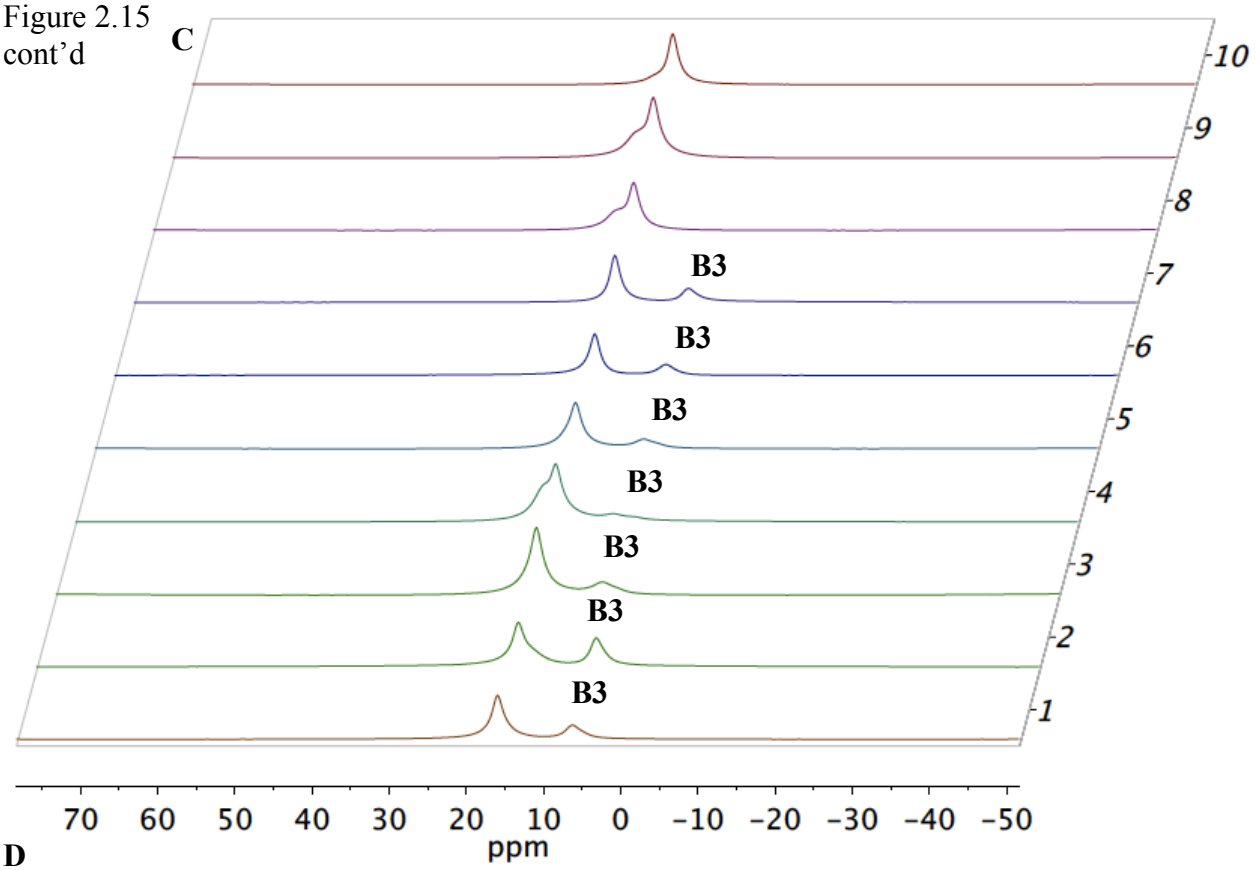

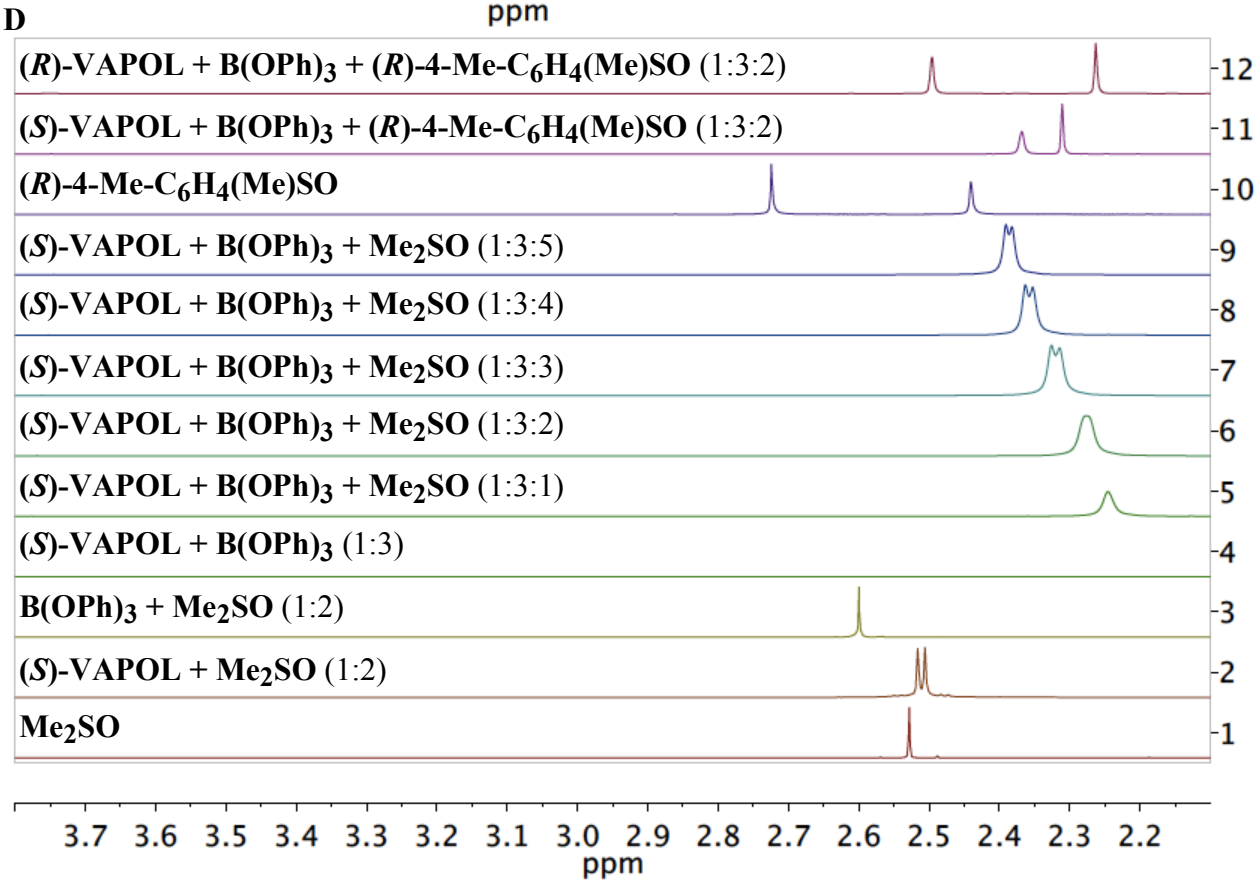

Figure 2.15 cont'd

E

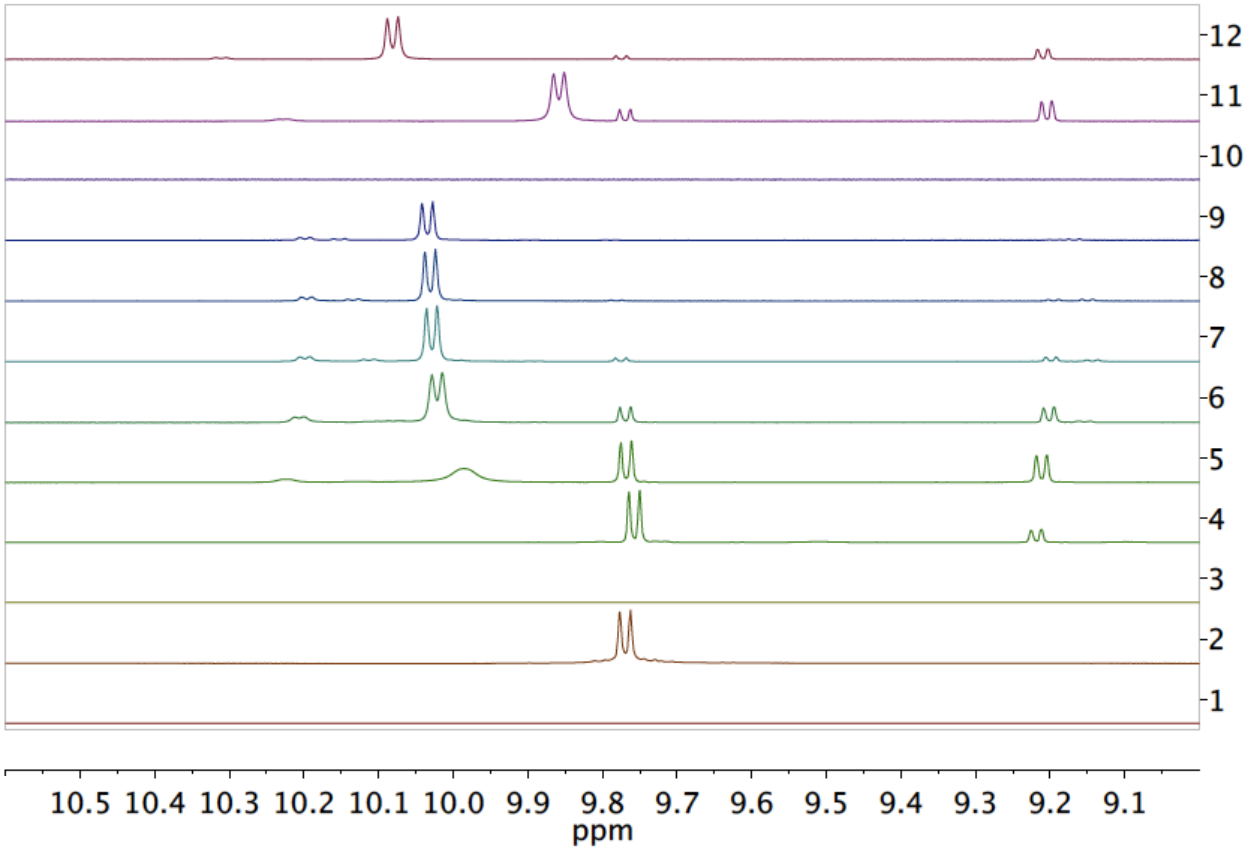

[a] Note for Figure 2.15A: Entry 1: (*S*)-VAPOL (0.1 mmol) plus 3 equiv commercial $B(OPh)_3$ and 2 equiv Me_2SO **221a** at 25 °C for 10 min. Entries 2-6: same as entry 1 with 2 equiv $(CH_2)_4SO$ **221b**, Bn_2SO **221c**, Ph_2SO **221d**, *rac*-Ph(Me)SO **221e** and (*R*)-4-Me-C_6H_4(Me)SO **221f** respectively. Entry 7: (*R*)-VAPOL (0.1 mmol) plus 3 equiv commercial $B(OPh)_3$ and 2 equiv (*R*)-4-Me-C_6H_4(Me)SO **221f** at 25 °C for 10 min. Entries 8-9: same as entry 1 with 2 equiv Me_2SO_2 **221h** and $(CH_2)_4SO_2$ **221i**, respectively. Entry 10: (*S*)-VAPOL (0.1 mmol) plus 3 equiv commercial $B(OPh)_3$ at 25 °C for 10 min. [b] Note for Figure 2.15D: Entry 1: neat

DMSO. Entry 2: (*S*)-VAPOL (0.1 mmol) plus 2 equiv Me_2SO **221a** at 25 °C for 10 min. Entry 3: commercial $B(OPh)_3$ (0.1 mmol) plus 2 equiv Me_2SO **221a** at 25 °C for 10 min. Entry 4: (*S*)-VAPOL (0.1 mmol) plus 3 equiv commercial $B(OPh)_3$ at 25 °C for 10 min. Entry 5: (*S*)-VAPOL (0.1 mmol) plus 3 equiv commercial $B(OPh)_3$ and 1 equiv Me_2SO **221a** at 25 °C for 10 min. Entry 6: same as entry 5 except 2 equiv Me_2SO **221a** used. Entry 7: same as entry 5 except 3 equiv Me_2SO **221a** used. Entry 8: same as entry 5 except 4 equiv Me_2SO **221a** used. Entry 9: same as entry 5 except 5 equiv Me_2SO **221a** used. Entry 10: neat (*R*)-4-Me-C_6H_4(Me)SO **221f**. Entry 11: (*S*)-VAPOL (0.1 mmol) plus 3 equiv commercial $B(OPh)_3$ and 2 equiv (*R*)-4-Me-C_6H_4(Me)SO **221f** at 25 °C for 10 min. Entry 12: (*R*)-VAPOL (0.1 mmol) plus 3 equiv commercial $B(OPh)_3$ and 2 equiv (*R*)-4-Me-C_6H_4(Me)SO **221f** at 25 °C for 10 min.

With the realization of the SULFOX-BOROX catalyst, we decided to computationally explore the complexes of **222a** and **222b** in order to gain some insight into their possible structures. Calculations were preformed using Gaussian 03 at B3LYP/6-31g* level of theory.[20] The resulting structures are presented in Figure 2.16. There is hydrogen bond between the protonated DMSO and the boroxinate core (Figure 2.16A, d_1 = 1.44 Å). One of the intriguing features in the calculated structure was the possible CH-π interaction between the methyl groups of DMSO and the phenanthrene ring of the ligand (Figure 2.16A, d_2 = 3.56 Å and d_3 = 3.80 Å). A careful analysis of the ^{1}H NMR of the SULFOX-BOROX species **222a** (Figure 2.15D, entry 1

vs. 5) revealed an upfield shift of 0.3 ppm when one equiv of DMSO was used to generate **222a**. Although the methyl peak for free DMSO was missing when excess DMSO (up to 5 equivalents) was employed, the difference in chemical shift decreased from 0.3 ppm to 0.15 ppm (Figure 2.15D, entry 1 *vs.* 5-9). This suggests that there is an exchange between bound DMSO and free DMSO. An up field shift for the methyl protons was also observed in the case of the chiral sulfoxide **221f** (Figure 2.15D, entry 10 *vs.* 11-12). Similar observations (experimental and theoretical) were made for the methylene units in the case of **222b** derived from $(CH_2)_4SO$ **221b** (Figure 2.16C and 2.16D). The structure for **222h** was also computed and is discussed in Section 2.2. Also, the rationale of the lack of a match/mismatch relationship in catalyst formation, was also found as the sulfoxide **221f** shifts in such a way that it has the maximum CH-π interaction (not shown here). The SULFOX-BOROX catalyst **222a** was successfully employed for the catalytic asymmetric epoxidation of aldehydes. The details are discussed in Chapter 8.

Figure 2.16 Calculated structure of SULFOX-BOROX catalysts **222a** and **222b** using Gaussian ′03. They are visualized by the Mercury Program (C, gray; O, red; S, orange; B, yellow; H, white). Hydrogen atoms omitted for clarity (except protonated DMSO and TMSO). **(A)** Calculated B3LYP/6-31g* structure of **222a**. Some secondary interactions are highlighted: d_1 = 1.44 Å (H-bonding), d_2 = 3.56 Å (CH-π), d_3 = 3.80 Å (CH-π). (**B**) Space-filling rendition of **222a** with the same orientation and showing hydrogens. The boroxinate anion is given in green and the protonated sulfoxide is in traditional colors. **(C)** Calculated B3LYP/6-31g* structure of **222b**. Some secondary interactions are highlighted: d_1 = 1.44 Å (H-bonding), d_2 = 3.67 Å (CH-π), d_3 = 3.54 Å (CH-π), d_4 = 3.39 Å (CH-O). (**D**) Space-filling rendition of **222b** with the same

Figure 2.16 cont'd

orientation and showing hydrogens. The boroxinate anion is given in green and the protonated sulfoxide is in traditional colors.

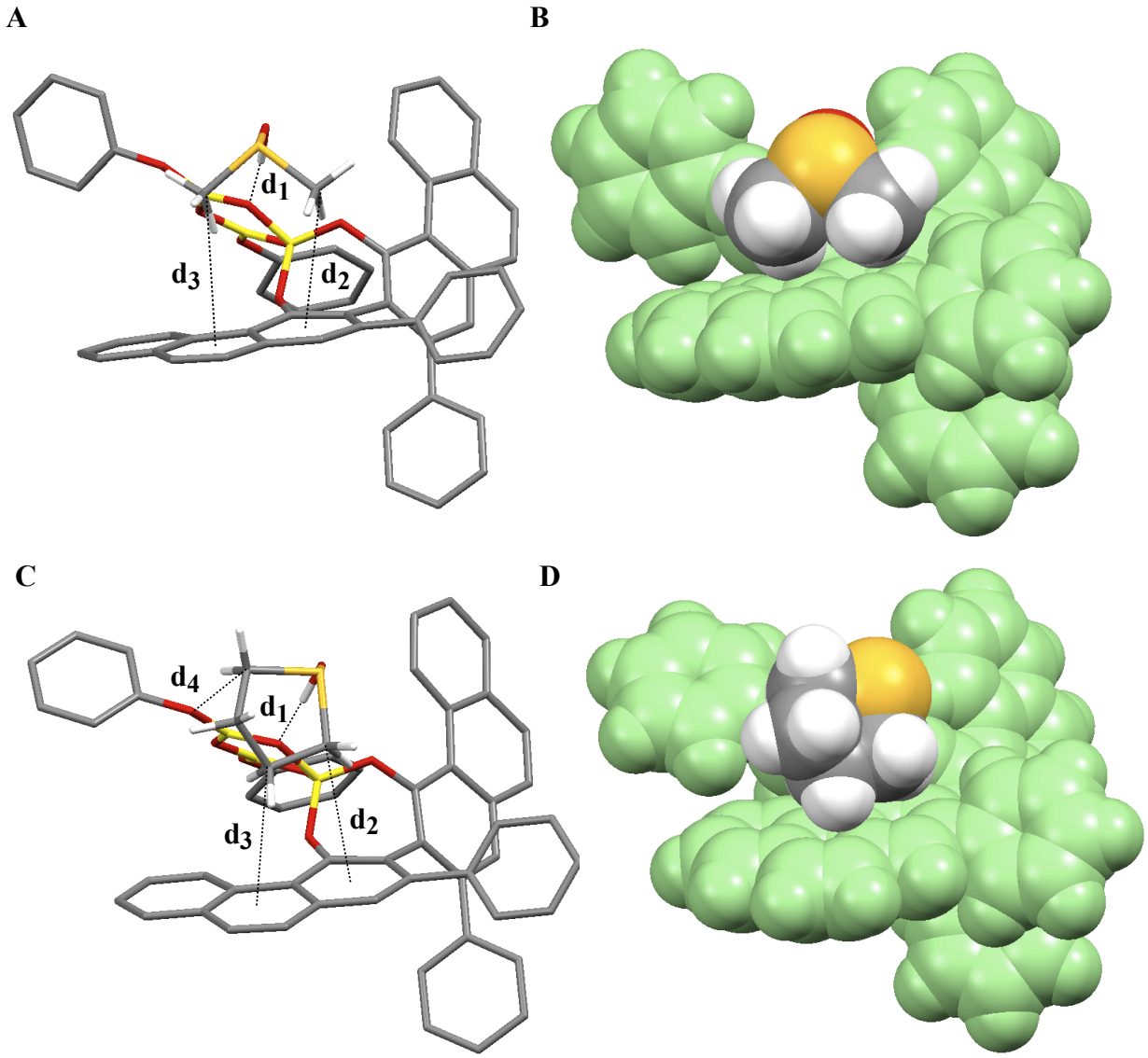

2.1.6 Phosphine-oxides as the base: PHOSPHINOX-BOROX catalyst

Another class of bases examined is phosphine-oxides **223**. As expected, aliphatic phosphine-oxides afforded excellent yields of the boroxinate catalysts **224** (Table 2.11, entries 3-4). The pKa's of protonated $Ph_2P(Me)O$ and $Bu_2P(Me)O$ are –3.2[27] and –1.51±0.29[30]

respectively. This suggested that there is lower probability that Ph_3PO might induce the catalyst formation. In fact, although boroxinate formation did occur with Ph_3PO, the catalyst was generated in lower yields than with Bu_3PO. (Table 2.11, entries 1-2). Additionally, secondary phosphine oxide *m*-$Xyl_2P(H)O$ **223d** was also able to generate the BOROX catalyst as well (Table 2.12, entries 7-8). However, tributyl phosphate **223c** and phosphonate **223e** were found not to be basic enough to give the catalyst (Table 2.11, entries 5-6 and 9-10).

Table 2.11 NMR Analysis of a mixture of (*S*)-VAPOL, $B(OPh)_3$ and phosphine-oxides as bases *a*

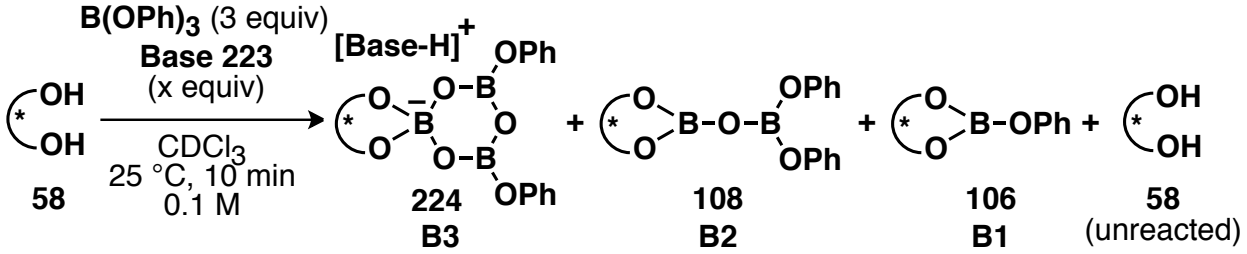

#	series	Base **223** *b*	Equiv of Base	(*S*)-VAPOL *c,d*	B1 **106** *d*	B2 **108** *d*	B3 **224** *d*	^1H *e*	^{11}B *f*
1	**a**	Ph_3PO	1	29	<1	11	37	9.91	15.94, 7.16
2			2	15	<1	11	41	9.96	15.96, 6.59
3	**b**	Bu_3PO	1	10	<1	<1	67	10.25	15.94, 5.13
4			2	<1	<1	<1	94	10.28	14.76, 5.06
5	**c**	$(BuO)_3PO$	1	30	<1	43	<1	–	18.23
6			2	12	<1	30	<1	–	17.57
7	**d**	*m*-$Xyl_2P(H)O$	1	11	<1	7	66	9.98	15.96, 7.11
8			2	05	<1	<1	78	10.01	15.95, 7.92
9	**e**	$(EtO)_2P(H)O$	1	60	<1	10	<1	–	16.00
10			2	44	<1	20	<1	–	15.97
11	–	No base	0	57	5	18	<1	–	16.00

a Unless otherwise specified, all NMR samples were prepared by mixing (*S*)-VAPOL **58** (0.1 mmol) and commercial $B(OPh)_3$ (0.3 mmol) and base **223** in $CDCl_3$ (1 mL) at 25 °C and

Table 2.11 cont'd

stirring for 10 min before spectra were taken. [b] All bases were distilled or sublimed prior to use. [c] Unreacted (*S*)-VAPOL **58**. [d] NMR yield with Ph_3CH as internal standard with ligand as the limiting reagent. [e] Chemical Shift for the bay proton in B3-base complex. [f] Chemical Shift of the peaks observed in the ^{11}B NMR spectrum.

The NMR analysis is given in Figure 2.17. Characteristic peaks were observed in the ^{1}H NMR and ^{11}B NMR spectra in the cases where it formed the boroxinate catalyst. Although, the bay region of the ^{1}H NMR spectra do show some new peaks (Figure 2.17A, entries 7 and 12), no significant change in the alkyl region indicated the absence of any boroxinate species when large excesses of tributyl phosphate **223c** and phosphonate **223e** are used.

Figure 2.17 Phosphine-oxide induced boroxinate catalyst formation. (**A**)[a] ^{1}H NMR spectra in $CDCl_3$ with Ph_3CH as internal standard. (**B**) ^{11}B NMR spectra corresponding to the ^{1}H NMR spectra in Figure 2.17A. (**C**) The alkyl region corresponding to the ^{1}H NMR spectra in Figure 2.17A. (**D**) ^{31}P NMR spectra in $CDCl_3$. The chemical shifts in ^{31}P NMR are referenced with respect to a standard sample of H_3PO_4. Entry 1: pure *m*-$Xyl_2P(H)O$ **223d**. Entry 2: pure *m*-$Xyl_2P(H)O$ **223d** (decoupled). Entry 3: (*S*)-VAPOL (0.1 mmol) plus 3 equiv commercial $B(OPh)_3$ and 2 equiv *m*-$Xyl_2P(H)O$ **223d** at 25 °C for 10 min. Entry 4: same as entry 3 with decoupling.

Figure 2.17 cont'd

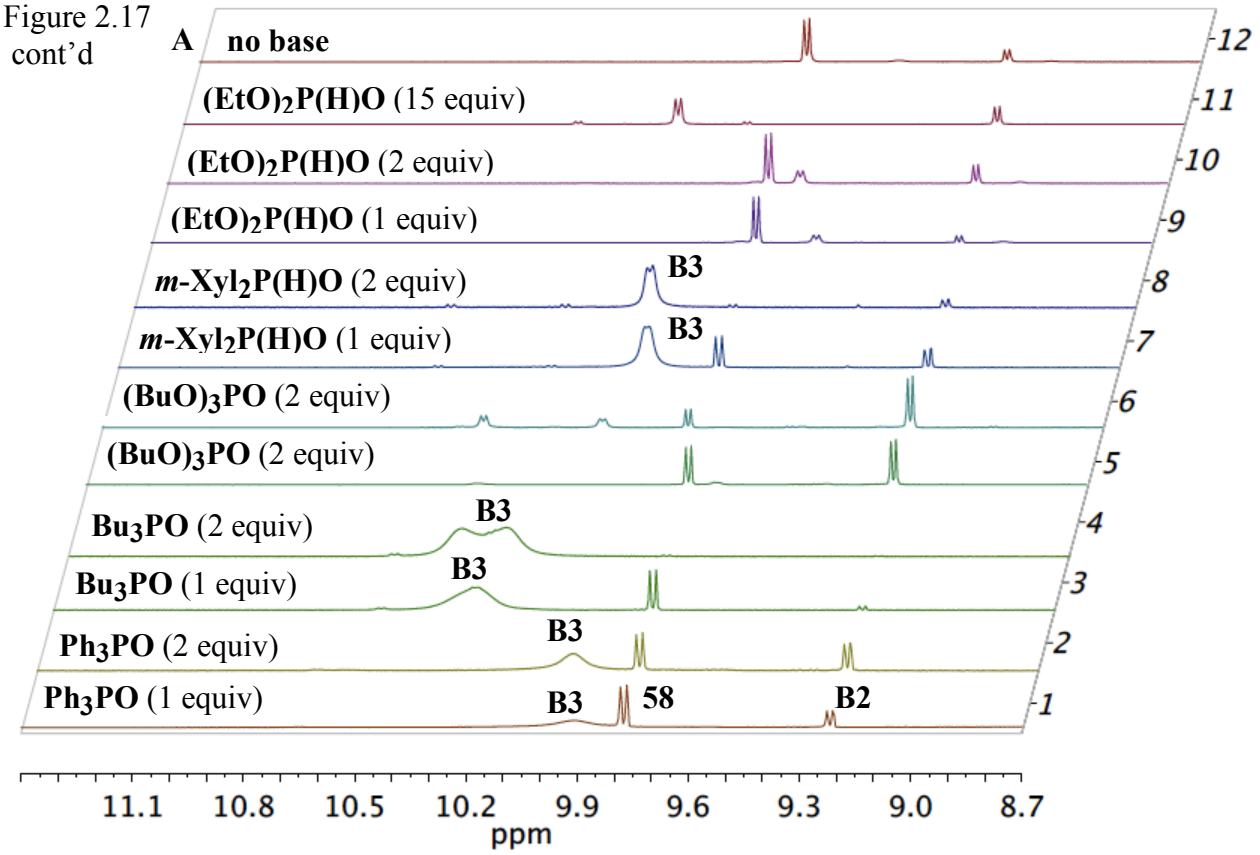

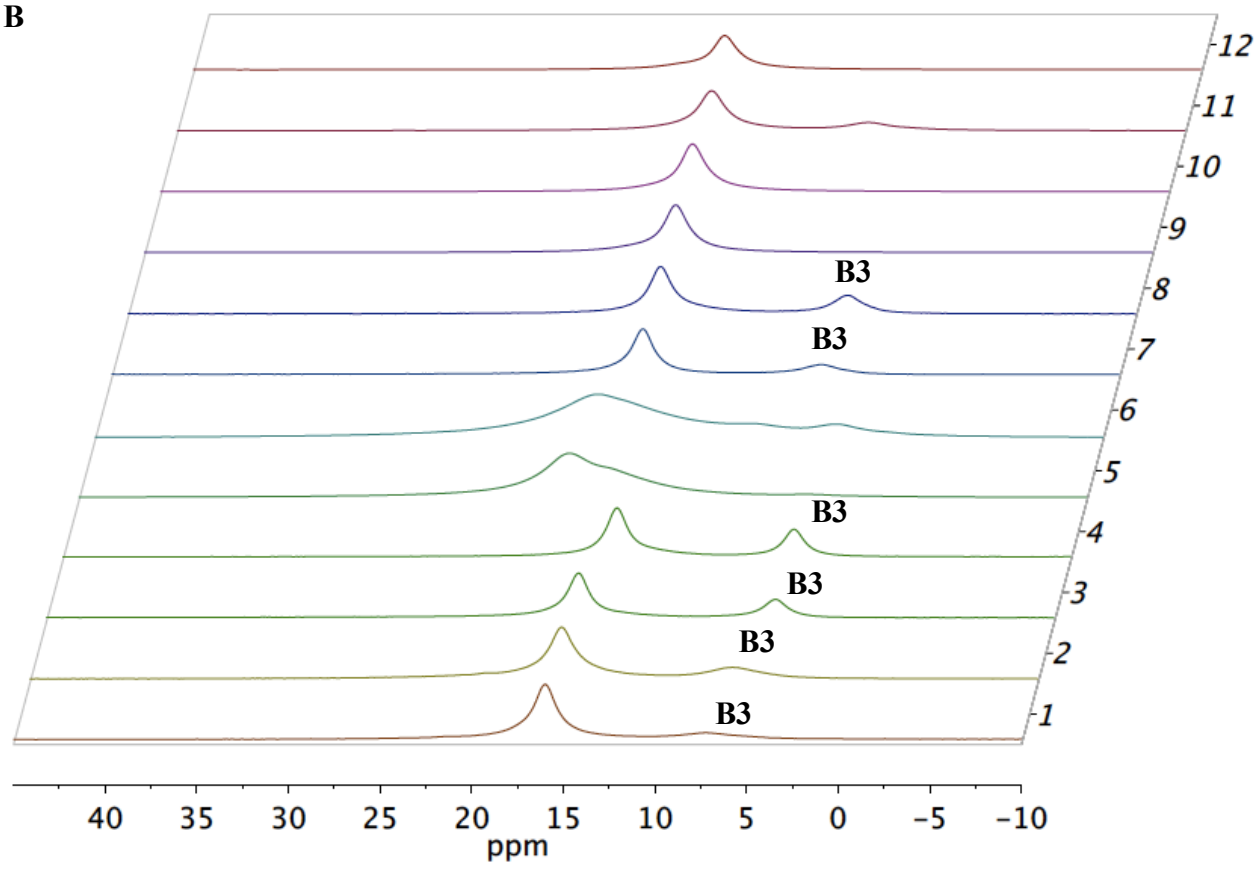

Figure 2.17 cont'd

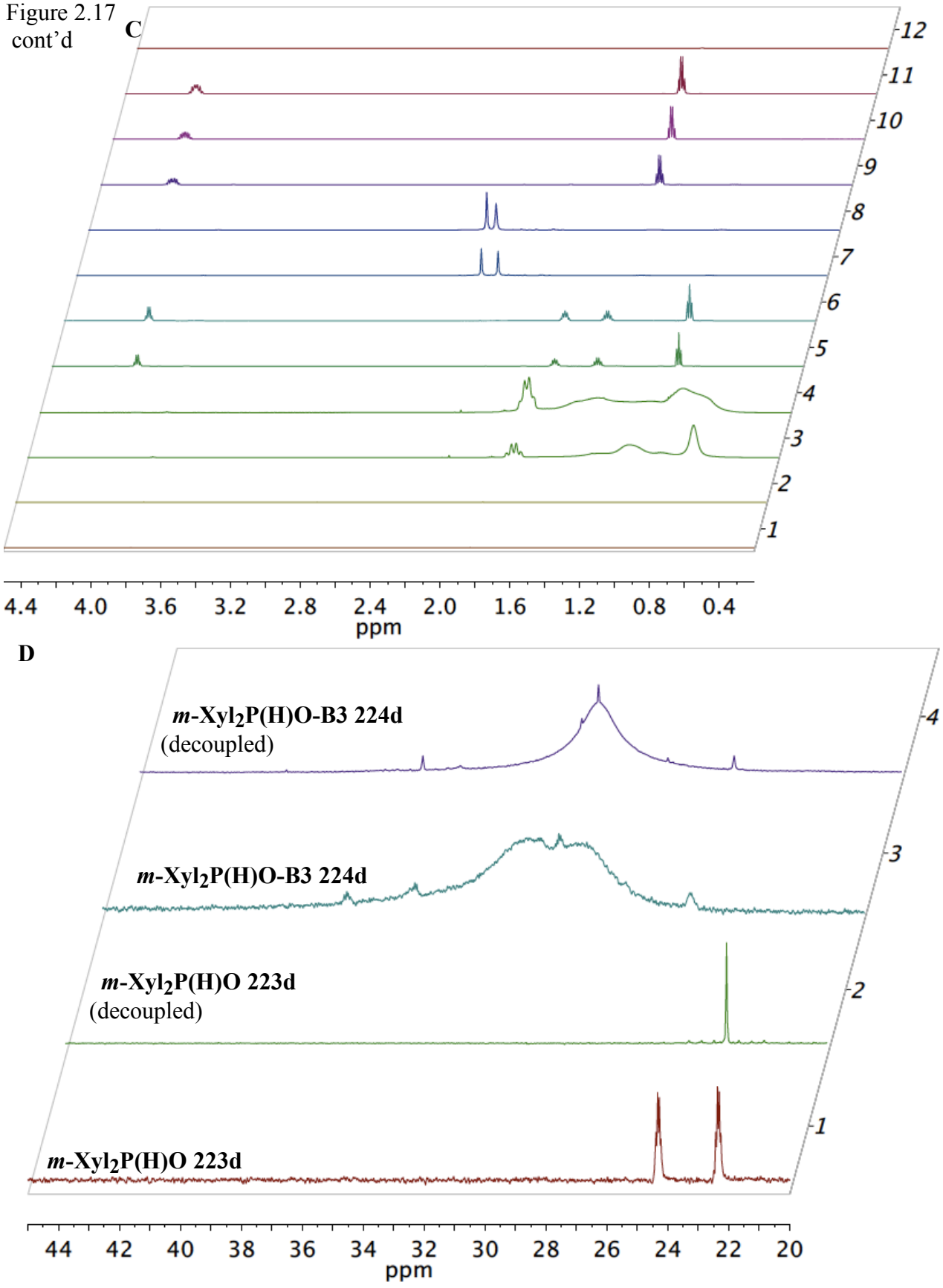

[a] Note for Figure 2.17A: Entry 1: (*S*)-VAPOL (0.1 mmol) plus 3 equiv commercial $B(OPh)_3$ and 1 equiv Ph_3PO **223a** at 25 °C for 10 min. Entry 2: same as entry 1 with 2 equiv Ph_3PO **223a**. Entry 3 and 4: same as entry 1 with 1 and 2 equiv Bu_3PO **223b** respectively. Entry 5 and 6: same as entry 1 with 1 and 2 equiv $(BuO)_3PO$ **223c** respectively. Entry 7 and 8: same as entry 1 with 1 and 2 equiv *m*-$Xyl_2P(H)O$ **223d** respectively. Entry 9, 10 and 11: same as entry 1 with 1, 2 and 15 equiv $(EtO)_2P(H)O$ **223e** respectively. Entry 12: (*S*)-VAPOL (0.1 mmol) plus 3 equiv commercial $B(OPh)_3$ at 25 °C for 10 min.

Also, the BOROX catalyst **224d** was characterized by ^{31}P NMR analysis (Figure 2.17D). The ^{31}P NMR spectrum of pure *m*-$Xyl_2P(H)O$ **223d** exhibits one single peak at $\delta = 23.29$ ppm when the spectrum is proton decoupled. A new broad peak at $\delta = 29.25$ ppm was observed in case of boroxinate **224d**. The chemical shifts in the ^{31}P NMR spectrum are referenced with respect to a standard sample of H_3PO_4.

The computed structure of **224b** reveals the presence of possible CH-π interactions between the alkyl groups of the phosphine oxide and the phenanthrene ring of the ligand (calculated structure not shown).

2.1.7 Amine-oxides as the base: AMINOX-BOROX catalyst

Given the ability of phosphine-oxides to generate boroxinate species, it was natural to consider that amine-oxides could also generate boroxinates, further broadening the scope of

boroxinate catalysts. As documented in the literature, the pKa of protonated Me_3NO is 4.6 (in H_2O)[31] whereas the pKa of protonated pyridine-*N*-oxide is 0.79 (in H_2O).[32] From NMR studies, it seems that boroxinates **226** are generated when 1 equiv of amine oxides are utilized (Table 2.12, entries 1,5-6 and Figure 2.18D, entries 3,7-8). However, they are not generated in a clean fashion in the cases of Me_3NO **225a** and *N*-methyl morpholine oxide **225b** as some additional unknown peaks were observed (Figure 2.18A, entries 3 and 6).

Table 2.12 NMR Analysis of a mixture of (*S*)-VAPOL, $B(OPh)_3$ and amine-oxides as bases [a]

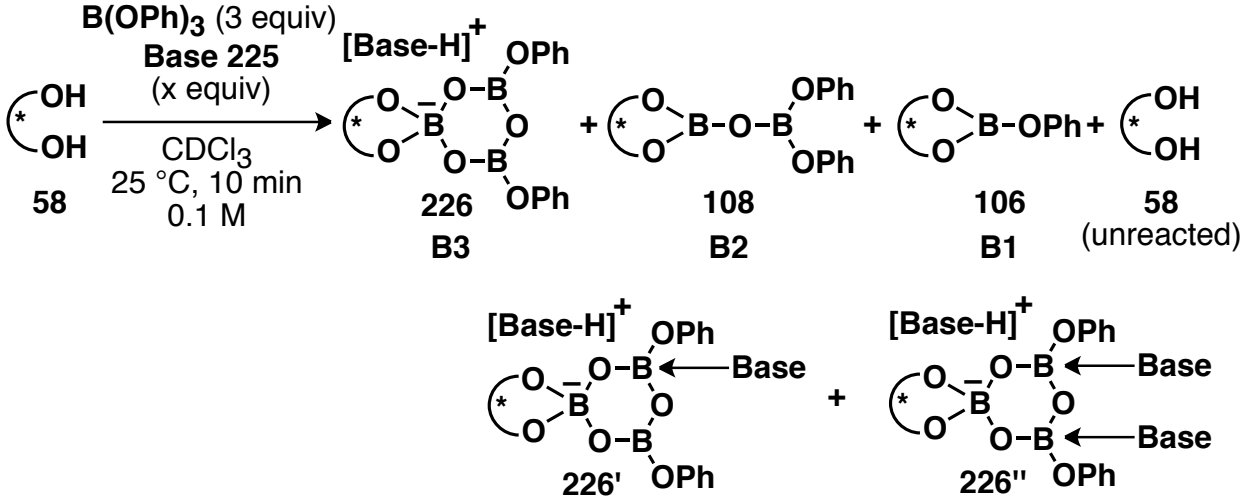

#	series	Base **225** [b]	Equiv of Base	(*S*)-VAPOL *c,d*	B3 **226** *d*	^{1}H *e*	^{11}B *f*	^{11}B *f*
1			1	7	nd	nd	15.70, 5.48	1.8:1.0
2			2	<1	nd	nd	17.08, 5.30	0.2:1.0
3	**a**	Me_3NO	3	<1	nd	nd	17.95, 5.31,2.51	0.8:1.0:1.0
4			3	<1	nd	nd	17.63, 5.31,2.48	0.7:1.0:1.1
5	**b**	NMO	1	15	nd	nd	15.56, 5.50	1.7:1.0
6	**c**	Pyridine-*N*-oxide	1	9	68	9.98	15.66, 6.42	2.2:1.0
7	–	No base	0	57	<1	–	16.00	–

Table 2.12 cont'd

[a] Unless otherwise specified, all NMR samples were prepared by mixing (*S*)-VAPOL **58** (0.1 mmol) and commercial $B(OPh)_3$ (0.3 mmol) and base **225** in $CDCl_3$ (1 mL) at 25 °C and stirring for 10 min before spectra were taken. All but entry 7 have both B1 **106** and B2 **108** <1. Entry 7 has 5% and 18% of **106** and **108** respectively. [b] All bases were distilled or sublimed prior to use. [c] Unreacted (*S*)-VAPOL **58**. [d] NMR yield with Ph_3CH as internal standard with ligand as the limiting reagent. [e] Chemical Shift for the bay proton in B3-base complex. [f] Chemical Shift of the peaks observed in the ^{11}B NMR spectrum. [g] The ratio of peaks observed in the ^{11}B NMR spectrum.

With excess amine oxides (Table 2.12, entries 2-4 and Figure 2.18, entries 4-6), extra coordination of amine oxide to boron seems to be operating giving rise possibly to **226′** or **226′′**(Table 2.12). These structures are suggested by the integration of the peaks in the ^{11}B NMR (Table 2.12). A clean generation of B3 (δ = 9.82 ppm in ^{1}H NMR, 68% yield) was observed when one equiv of pyridine-*N*-oxide **225c** was used (Table 2.12, entry 6 and Figure 2.18, entry 8).

Figure 2.18 Amine-oxide induced boroxinate catalyst formation. (**A**)[a] ^{1}H NMR spectra in $CDCl_3$ with Ph_3CH as internal standard. (**B**) same as in Figure 2.18A with a stacked angle of 15º. (**C**) The alkyl region corresponding to the ^{1}H NMR spectra in Figure 2.18A. (**D**) ^{11}B NMR spectra corresponding to the ^{1}H NMR spectra in Figure 2.18A.

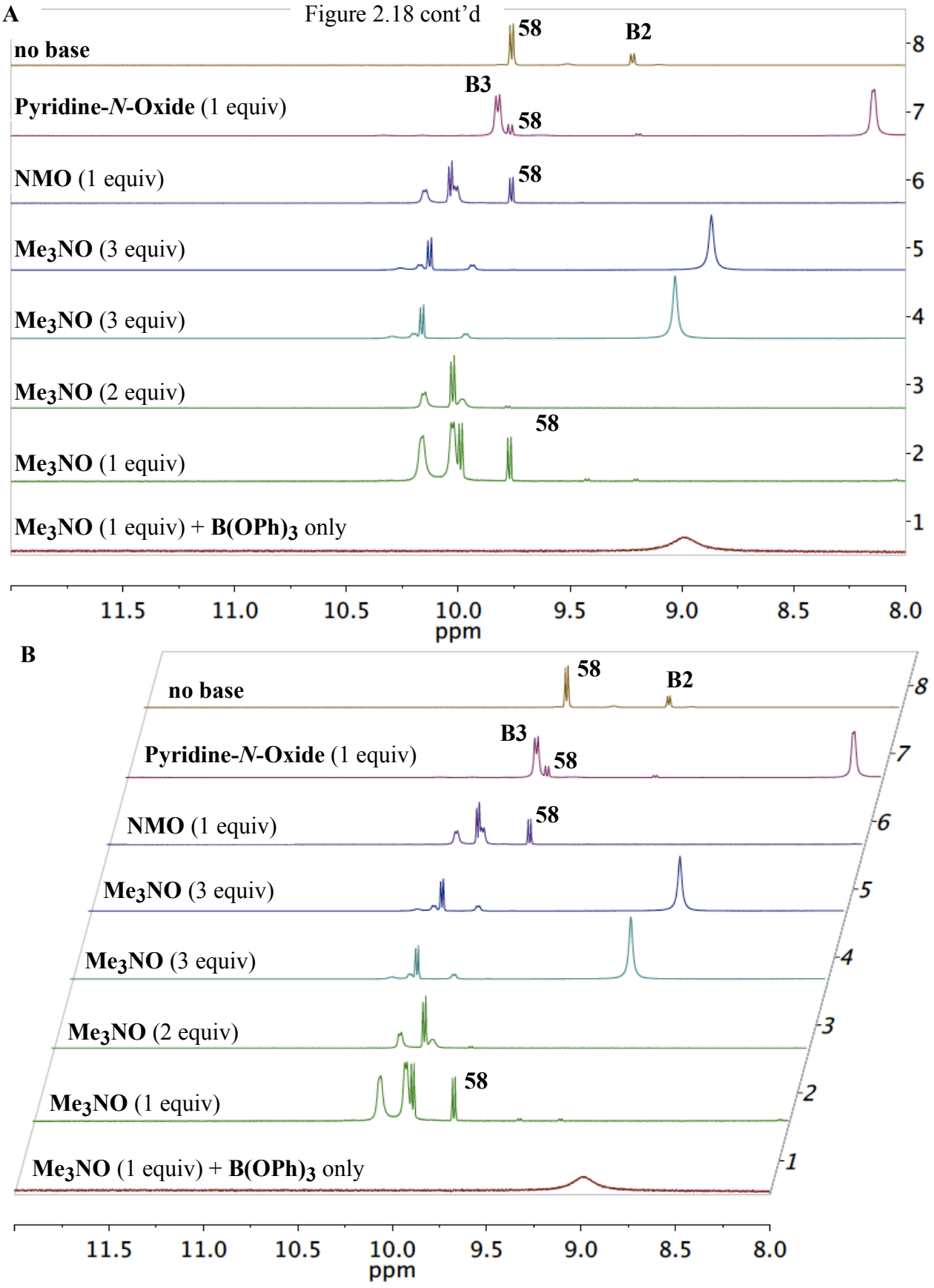

Figure 2.18 cont'd

Figure 2.18 cont'd

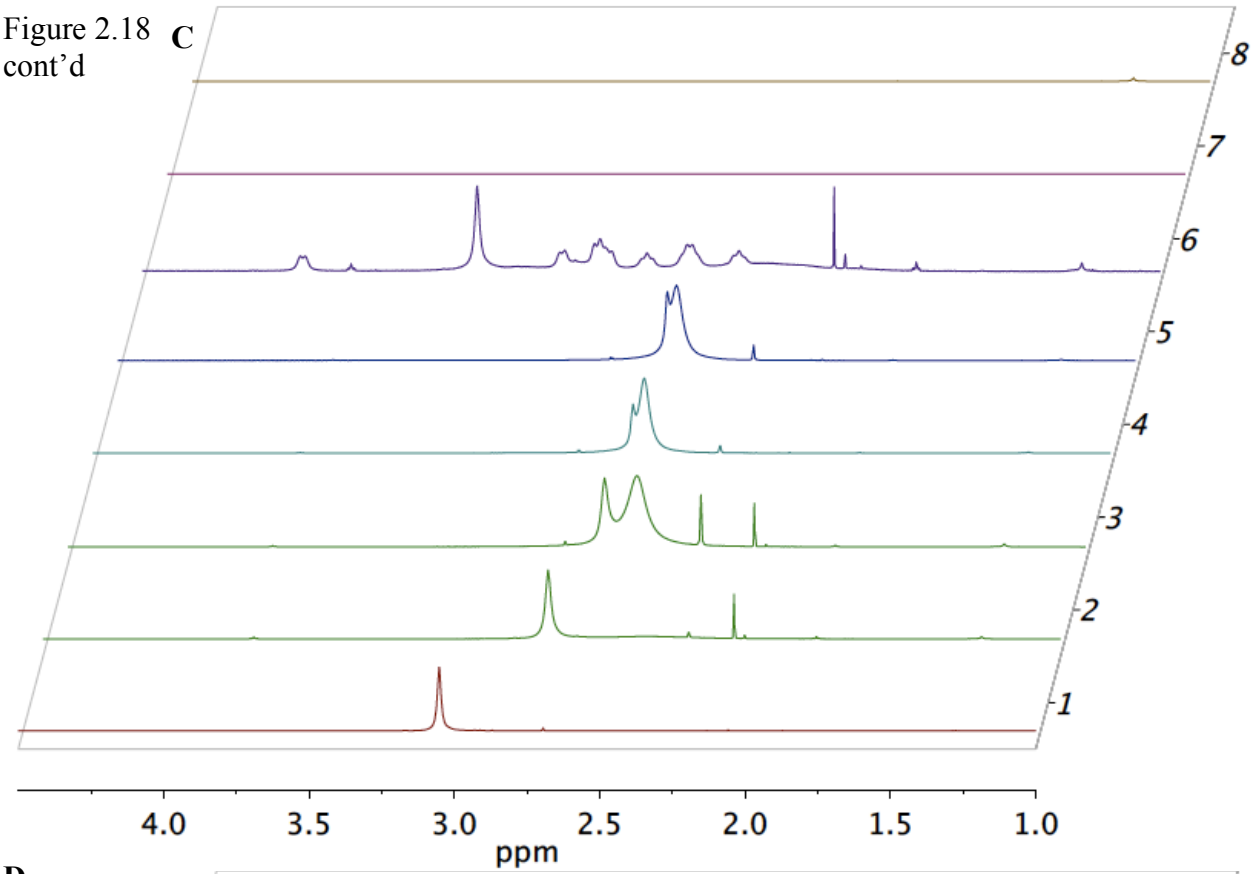

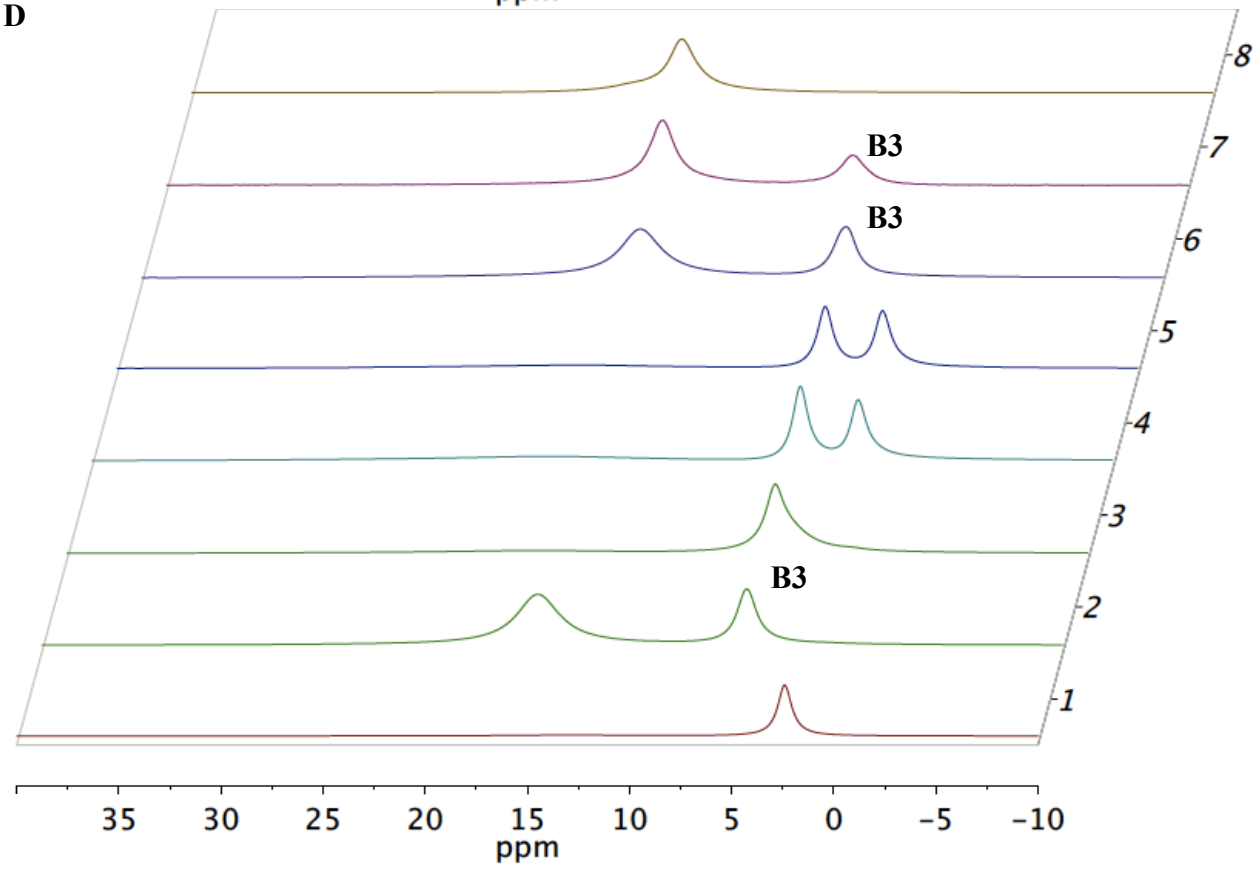

[a] Note for Figure 2.18A: Entry 1: Me_3NO **225a** plus 1 equiv commercial $B(OPh)_3$ at 25 °C for 10 min. Entry 2: (*S*)-VAPOL (0.1 mmol) plus 3 equiv commercial $B(OPh)_3$ and 1 equiv Me_3NO **225a** at 25 °C for 10 min. Entry 3: same as entry 2 with 2 equiv Me_3NO **225a**. Entry 4: same as entry 2 with 3 equiv Me_3NO **225a**. Entry 5: 3 equiv Me_3NO **225a** is added to a pre-formed mixture of (*S*)-VAPOL (0.1 mmol) and 3 equiv commercial $B(OPh)_3$ in $CDCl_3$. Entry 6: same as entry 2 with 1 equiv NMO (*N*-methyl morpholine oxide) **225b**. Entry 7: same as entry 2 with 1 equiv pyridine-*N*-Oxide **225c**. Entry 8: (*S*)-VAPOL (0.1 mmol) plus 3 equiv commercial $B(OPh)_3$ at 25 °C for 10 min.

In some cases, with excess amine oxides, an appreciable amount of an absorption at $\delta = 2.7$ ppm is observed in the ^{11}B NMR spectrum which is tentatively assigned as $[Me_3NO\text{-}H]^+$ $[B(OPh)_4]^-$ **227** or $[Me_3NO \rightarrow B(OPh)_3]$ **227′** from the NMR study of **226a** complex (Figure 2.18, entries 1,4-5). The computed structures of **226a** and **226b** reveal the presence of the possible CH-π and π-π interactions between the alkyl or aryl groups of the oxide and the phenanthrene ring of the ligand (calculated structure not shown). It would be interesting to examine nitrones as the base (not done).

2.1.8 Aldehydes as the base: ALDO-BOROX catalyst

As expected, no sign of any boroxinate was observed when aldehydes **127** were utilized as the bases (Figure 2.19). This is probably due to the high acidity (pKa = –7) of the protonated aldehydes. However, aldehydes with other basic sites do form BOROX catalyst. This is probably due the protonation of the nitrogens attached to these aldehydes (Figure 2.19, entries 5-

7). Surprisingly, 2-methyloxazole-4-carbaldehyde **127n** failed to give any boroxinate even though it has a free basic nitrogen (Figure 2.19, entry 4). In almost all cases, pyroborate B2 **108** was observed.

Figure 2.19 (**A**) Aldehyde induced boroxinate catalyst formation. (**B**)[a] ^{1}H NMR spectra in $CDCl_3$ with Ph_3CH as internal standard. (**C**) ^{11}B NMR spectra corresponding to the ^{1}H NMR spectra in Figure 2.19B.

A

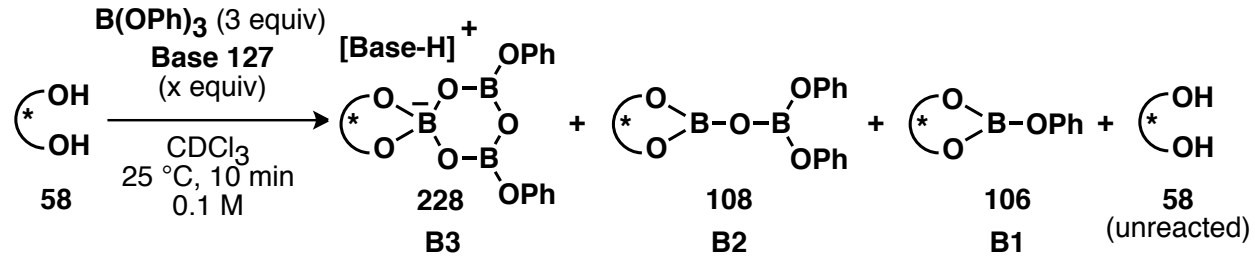

B

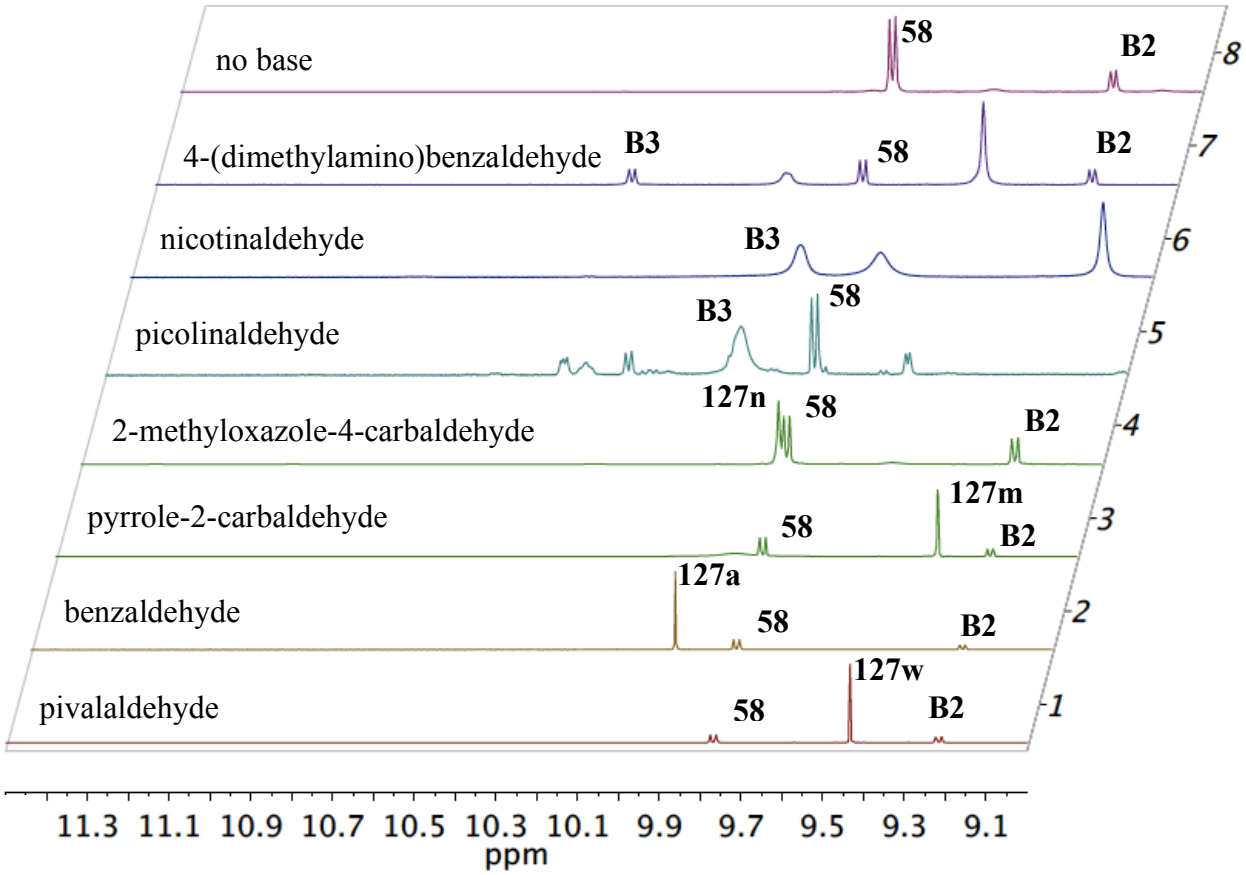

Figure 2.19 cont'd

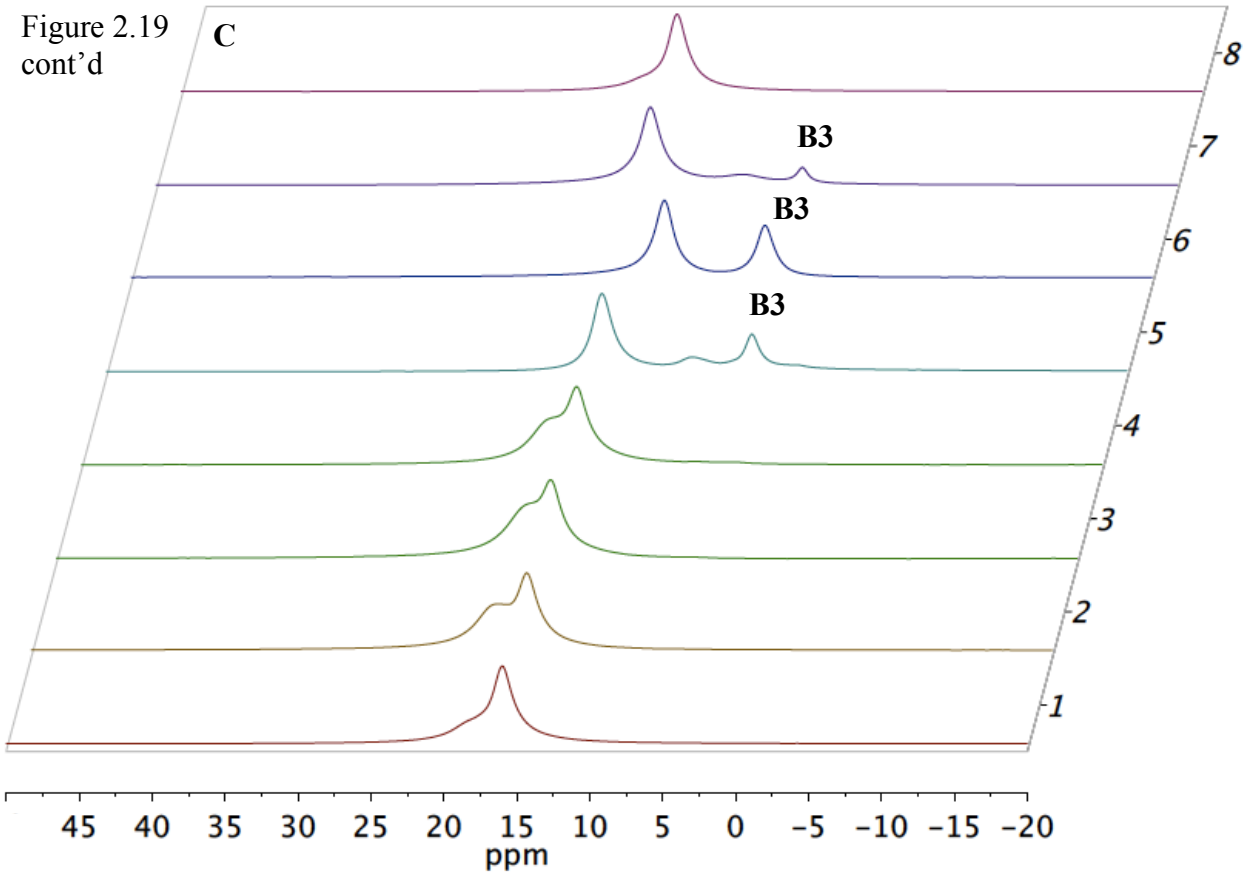

[a] Note for Figure 2.19B: Entry 1: (*S*)-VAPOL (0.1 mmol) plus 3 equiv commercial $B(OPh)_3$ and 2 equiv pivalaldehyde **127w** at 25 °C for 10 min. Entry 2: same as entry 1 with 2 equiv benzaldehyde **127a**. Entry 3: same as entry 1 with 2 equiv pyrrole-2-carbaldehyde **127m**. Entry 4: same as entry 1 with 2 equiv of 2-methyloxazole-4-carbaldehyde **127n**. Entry 5: same as entry 1 with 2 equiv picolinaldehyde **127i**. Entry 6: same as entry 1 with 2 equiv nicotinaldehyde **127j**. Entry 7: same as entry 1 with 2 equiv 4-(dimethylamino)benzaldehyde **127h**. Entry 8: (*S*)-VAPOL (0.1 mmol) plus 3 equiv commercial $B(OPh)_3$ at 25 °C for 10 min.

2.1.9 Diazo as the base: DIAZO-BOROX catalyst

Ethyl diazoacetate **85** was found to be reacting with the VAPOL to afford **230** in 80% yield when tested under conditions optimal for boroxinate generation (Figure 2.20). The mono-

alkylated adduct **230** is often observed at the end of the Wulff catalytic asymmetric aziridination reaction.[13a] There was no sign of any boroxinate **229a**. In a separate experiment, a peak at δ = 5.74 ppm (in ^{11}B NMR) was observed when *N*-benzyl diazoacetamide **128b** was employed as the base (Figure 2.20). However, there is no conclusive evidence for the formation of the boroxinate **229b**. The calculated structure of **229b** supports the presence of the boroxinate (not shown here). Also, there was no sign of adduct **231** under these conditions. It must be remembered that most diazo compounds are more basic at the carbon bearing the leaving group.

Figure 2.20 (**A**) Diazo induced boroxinate catalyst formation. (**B**)[a] ^{1}H NMR spectra in $CDCl_3$ with Ph_3CH as internal standard. (**C**) ^{11}B NMR spectra corresponding to the ^{1}H NMR spectra in Figure 2.20B.

A

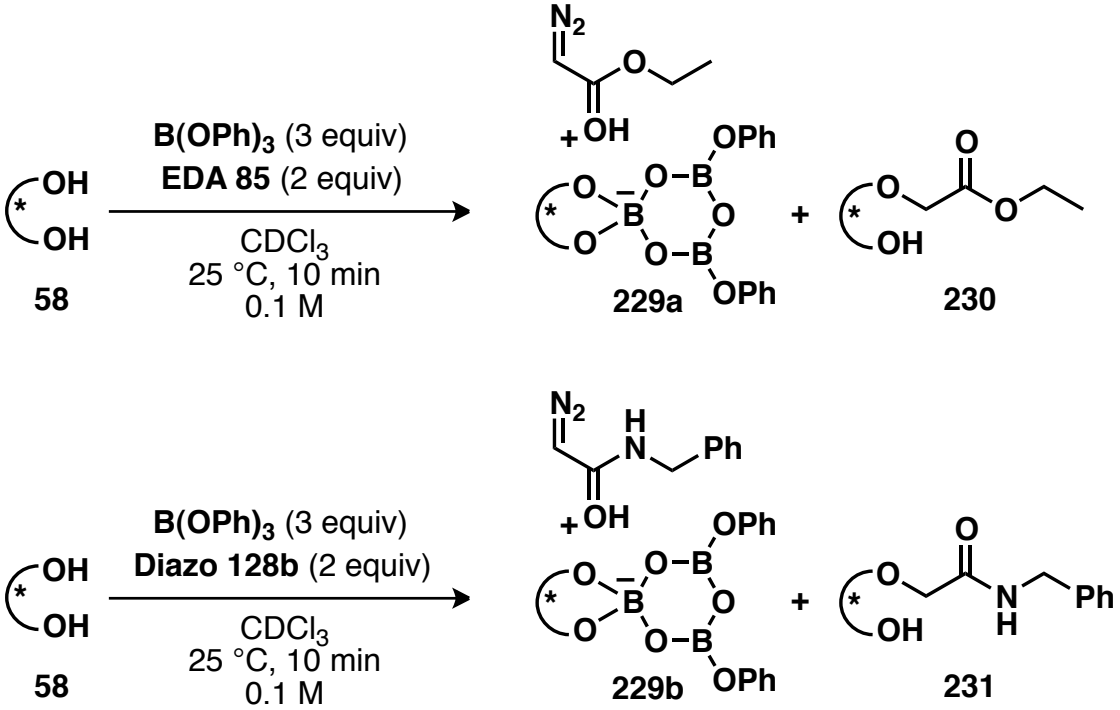

Figure 2.20
cont'd

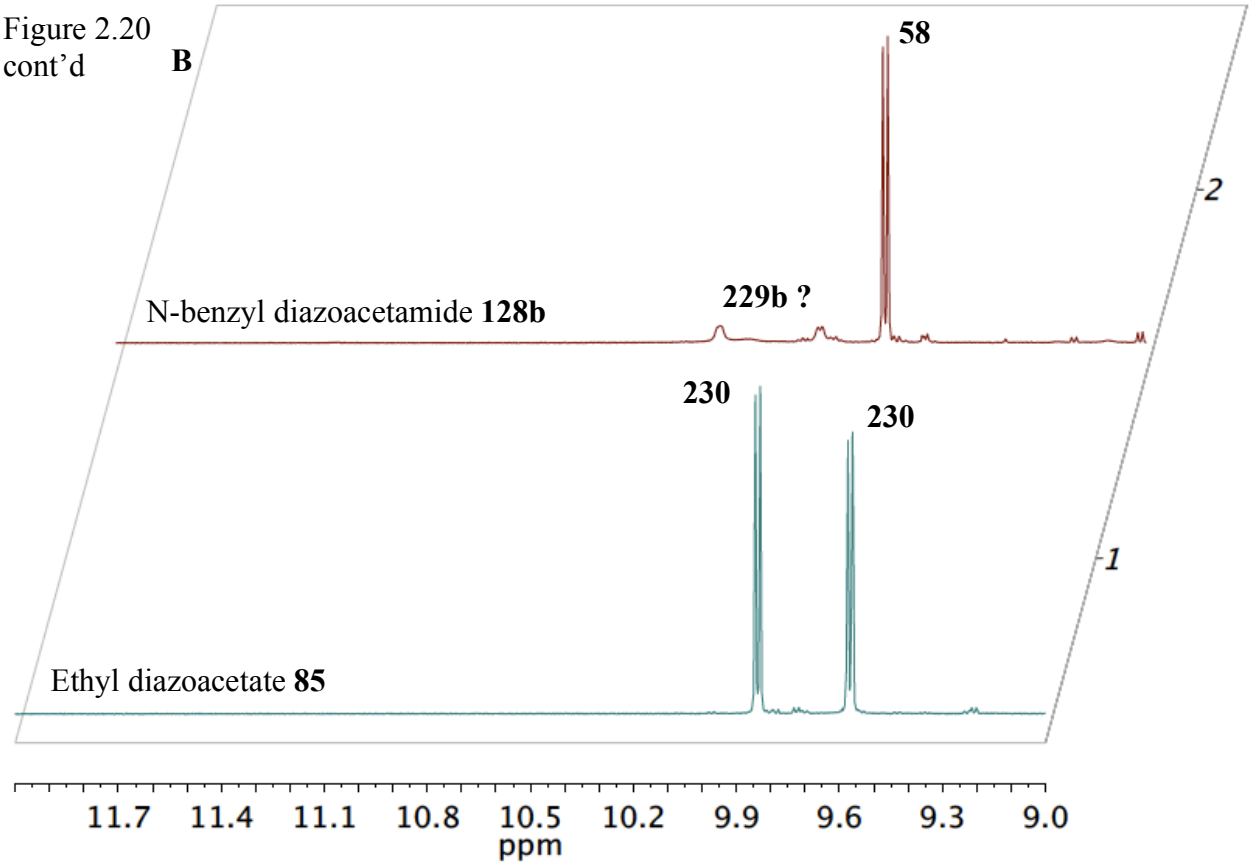

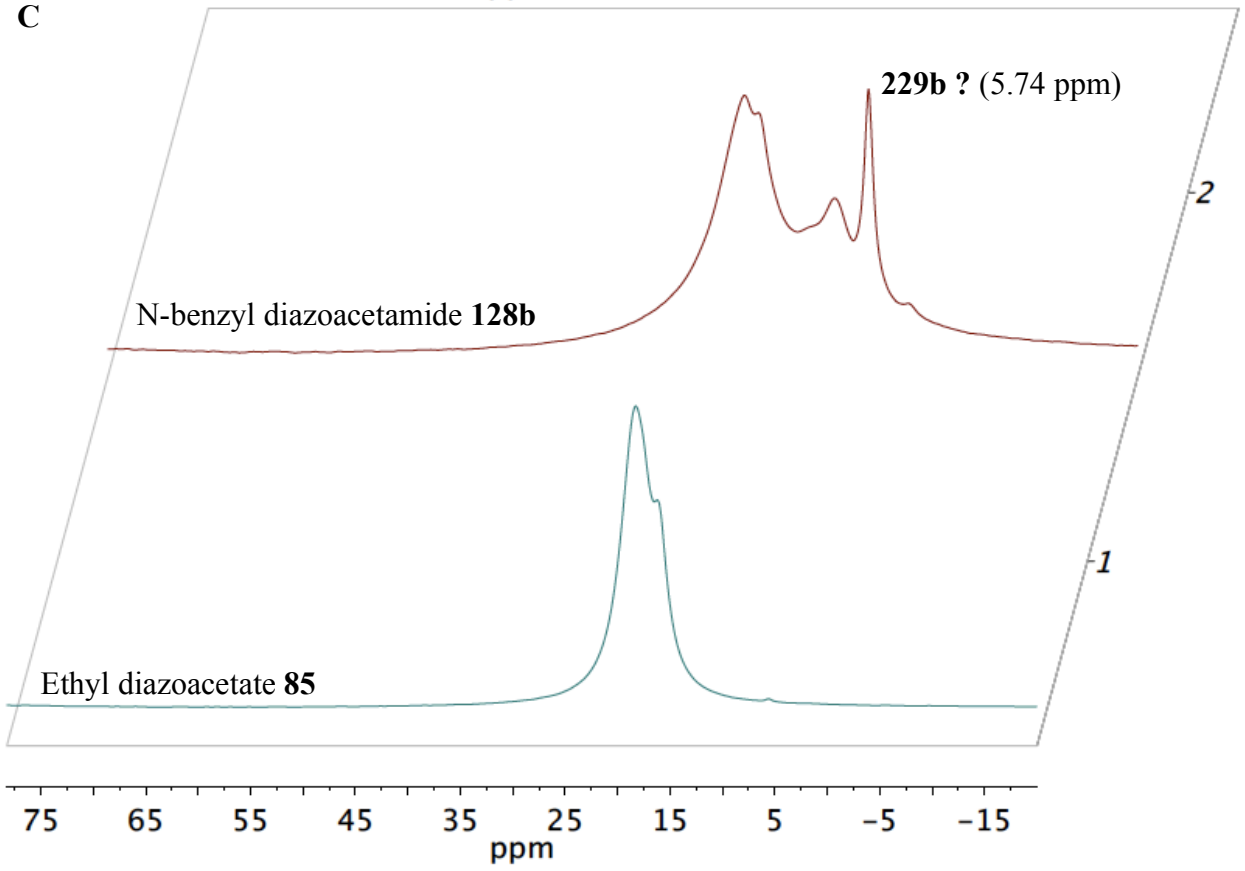

[a] Note for Figure 2.20B: Entry 1: (*S*)-VAPOL (0.1 mmol) plus 3 equiv commercial $B(OPh)_3$ and 2 equiv EDA **85** at 25 °C for 10 min. Entry 2: same as entry 1 with 2 equiv *N*-benzyl diazoacetamide **128b**. (**C**) ^{11}B NMR spectra corresponding to the ^{1}H NMR spectra in.

2.1.10 Miscellaneous bases:

Bases such as methyl carbamate **232a** and THF **232b** failed to give any boroxinate **233** (Figure 2.21). The pKa of protonated THF is –2.02, which is quite similar to DMSO. Hence it is quite interesting to observe the BOROX catalyst with DMSO and not with THF.

Figure 2.21 Miscellaneous bases induced boroxinate catalyst formation. (**A**)[a] ^{1}H NMR spectra in $CDCl_3$ with Ph_3CH as internal standard. (**B**) ^{11}B NMR spectra corresponding to the ^{1}H NMR spectra in Figure 2.21A.

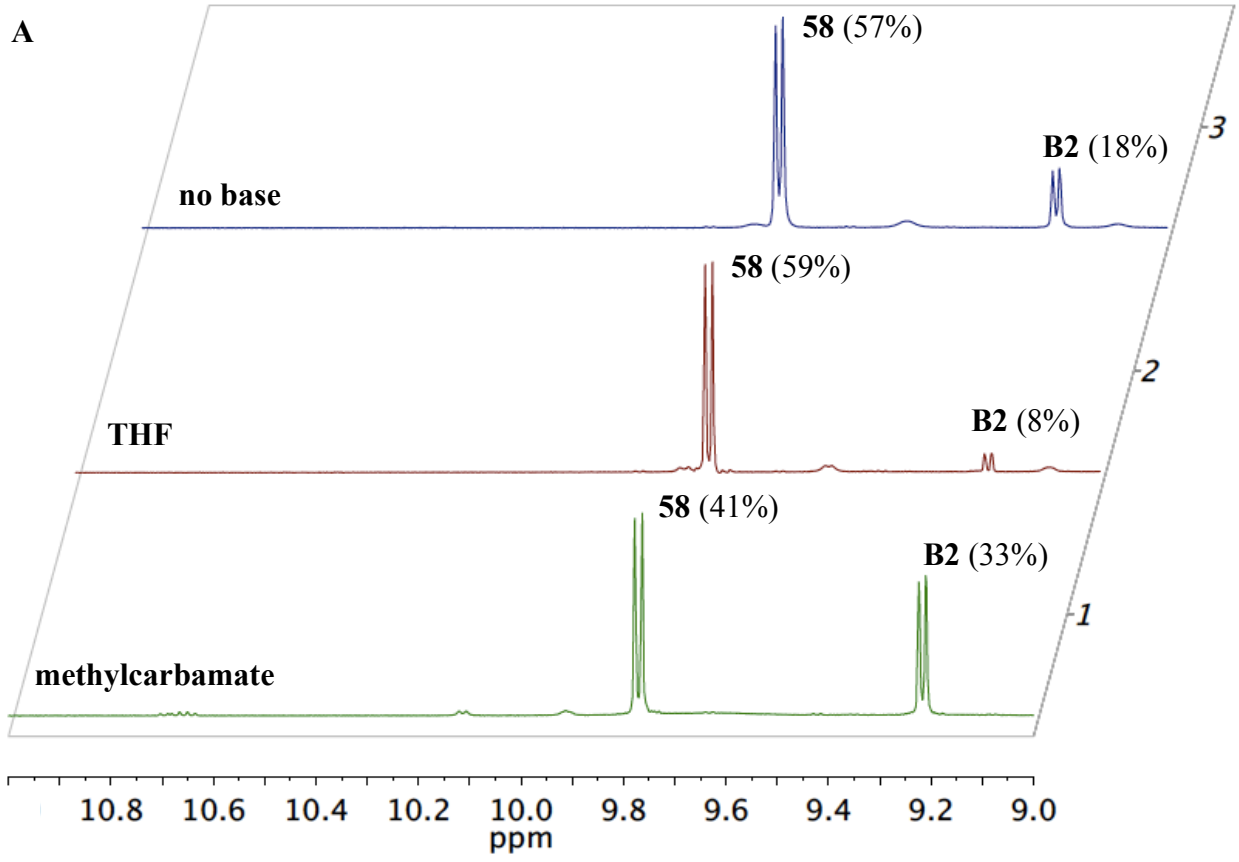

Figure 2.21 cont'd **B**

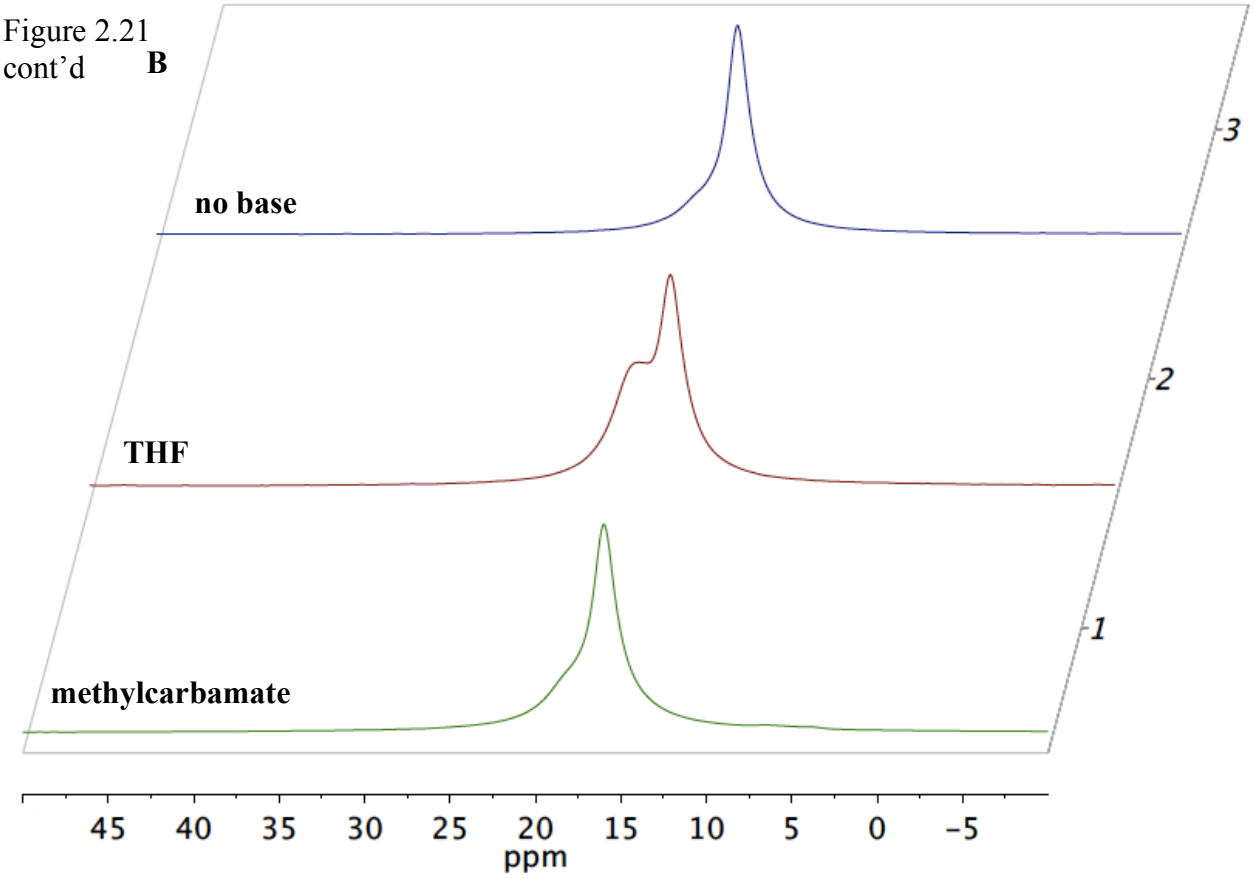

[a] Note for Figure 2.21A: Entry 1: (*S*)-VAPOL (0.1 mmol) plus 3 equiv commercial $B(OPh)_3$ and 2 equiv methyl carbamate **232a** at 25 °C for 10 min. Entry 2: same as entry 1 with 2 equiv THF **232b**. Entry 3: (*S*)-VAPOL (0.1 mmol) plus 3 equiv commercial $B(OPh)_3$ at 25 °C for 10 min.

2.2 Prediction of BOROX catalysts via computational chemistry

During the calculations of the possible BOROX complexes, an interesting observation was made. In all the cases, where no boroxinates were observed, it was found that proton is completely transferred to the O2 and the boroxinate ring is also collapsed (Figure 2.21). Specifically, the bond between O2 and tetra-coordinate boron is broken. This is found in the

cases of bases like PhCHO **127a**, pyrrole **216d**, Me_2SO_2 **221h**, $(CH_2)_4SO_2$ **221i**, BuO_3PO **223c**, THF **232b** etc. A few of calculated structures are presented in Figure 2.21. Hence, we can probably make a guess about the generation of the boroxinate complex even without the NMR study. It must be noted that these calculations are not representative of the actual structures and it should be used as tool to predict the possibility of boroxinate formation. In all cases, the distance (B-O2) between the O-2 and former tetra-coordinate boron was found to more than 1.6 Å. Additionally, the former tetra-coordinate boron is found to be out of the plane by ~ 13º–14º. In the case of the boroxinate anion, the ∠oop and B-O2 was found to be 20.2º and 1.43 Å respectively (not shown here).

Figure 2.22 Calculated structures of boroxinates (**A**) **228b** (base = PhCHO **127a**), (**B**) **217d** (base = pyrrole **216d**), (**C**) **222h** (base = Me_2SO_2 **221h**), (**D**) **222i** (base = $(CH_2)_4SO_2$ **221i**), (**E**) **224c** (base = $(BuO)_3PO$ **223c**) and (**F**) **233b** (base = THF **232b**) using Gaussian ′03. Calculated B3LYP/6-31g* structure visualized by the Mercury Program (C, gray; O, red; N, blue; B, pink, S, orange; H, white). Hydrogen atoms omitted for clarity (except O-H). ∠oop = angle out of plane for the former tetra-coordinate boron, B-O2 = the distance between O-2 and the former tetra-coordinate boron.

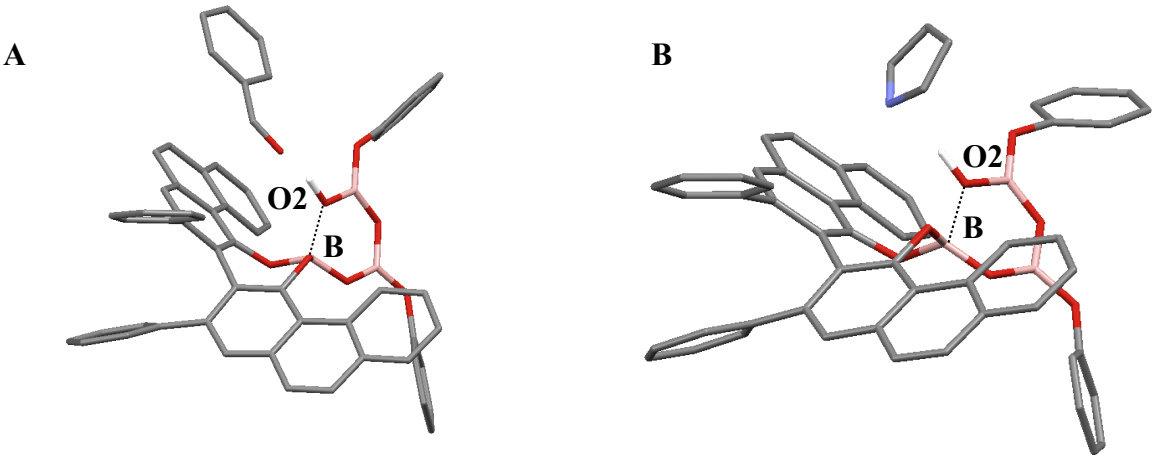

Figure 2.22 cont'd

228a
(∠oop = 13.1°, B-O2 = 1.71 Å)

217d
(∠oop = 13.2°, B-O2 = 1.69 Å)

C

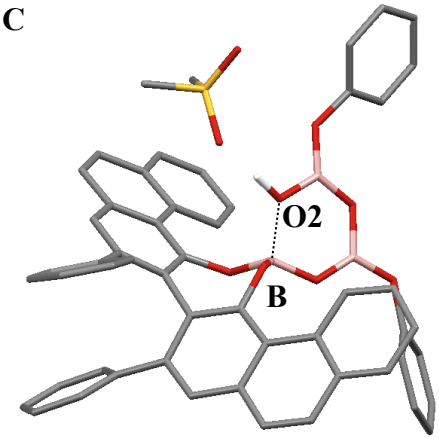

222h
(∠oop = 13.7°, B-O2 = 1.67 Å)

D

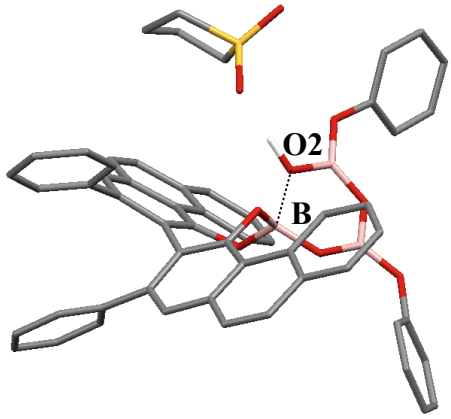

222i
(∠oop = 13.7°, B-O2 = 1.66 Å)

E

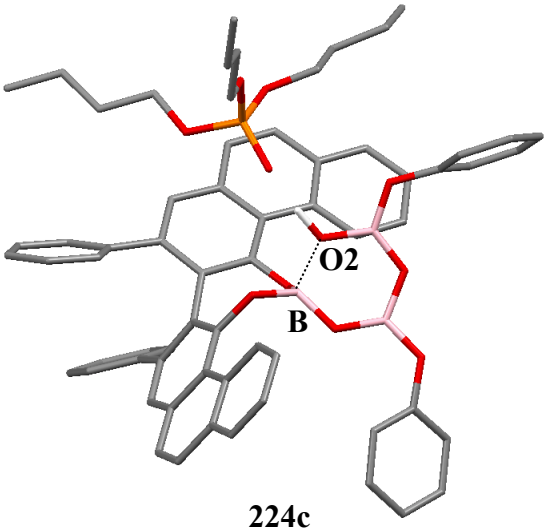

224c
(∠oop = 14.3°, B-O2 = 1.65 Å)

F

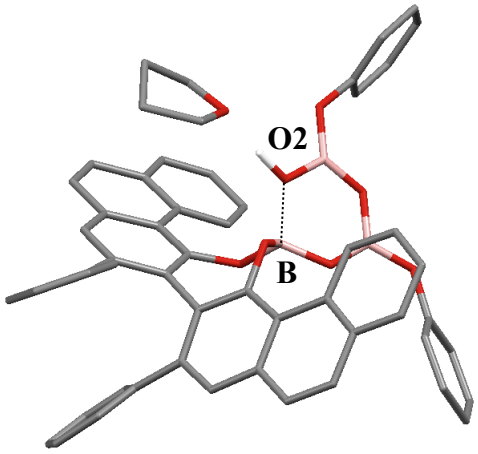

222i
(∠oop = 14.6°, B-O2 = 1.64 Å)

2.3 Possibility of Bench-Top Stable BOROX catalyst

The real application of any catalyst lies in its broad applicability in catalytic asymmetric reactions. This, in turn, requires the catalyst to be easily available specifically on a commercial

scale. There has been a long lasting dream of the feasibility of the commercial BOROX catalyst. There are two problems regarding this possibility. They are discussed below with their probable solutions.

2.3.1 Substrate induced formation of the catalyst

The first problem with our catalyst is its unique characteristic, which is substrate-induced formation of the catalyst. This is a big problem as the commercially available catalyst should ideally be independent of the substrate used. A potential solution of the problem could be that a particular base should be employed to generate the catalyst, which is easily replaced by the substrate without disrupting the catalyst structure. The realization of the SULFOX-BOROX catalyst could be the first step in this direction. In terms of basicity, DMSO should be easily replaced by an imine. In fact, the same was observed when the aziridination reaction was carried out with the pre-formed SULFOX-BOROX catalyst **222a** (Scheme 2.2). The aziridination reaction gave comparable results to the reaction carried out by substrate-induced IMINO-BOROX catalyst **188a**. Later, other boroxinates derived from bases such as aniline and benzhydryl amine were also tried and the results are described in Chapter 7 in detail.

Scheme 2.2 The Wulff asymmetric *cis*-aziridination reaction with benzhydryl imines **78**

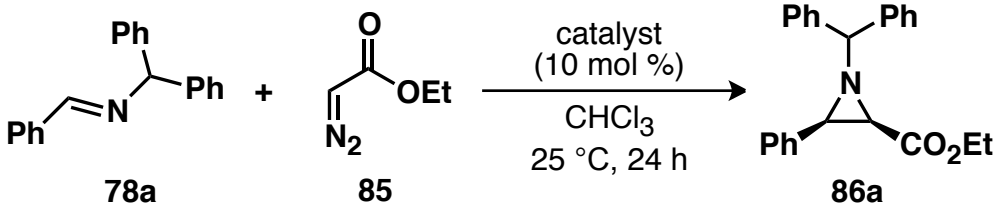

78a **85** **86a**

IMINO-BOROX catalyst **188a**: yield = 82%, ee = 90%
SULFOX-BOROX catalyst **222a**: yield = 86%, ee = 90%

2.3.2 Stability of the BOROX catalyst

The second problem is a typical one for any catalyst i.e. stability of the catalyst. One of the complexities of the BOROX catalyst is that its assembly is dependent on a number of variables. One of the ways to increase the stability is to decrease the number of these variables. This can be done by utilizing one of the components in which there is a pre-installed base. Among all the variables, the two obvious choices are the alcohol component and the borane component. These two modifications were tested and are discussed below.

2.3.2.1 Base incorporated in alcohol

The major advantage of boroxinate catalysts as revealed by the work in this thesis is that now there are many bases from which to choose to generate the boroxinate catalyst. Since sulfoxides can be easily be replaced by imines, it was thought to utilize the alcohol **234a** which has a sulfoxide in the tether. Thereafter, it was utilized and afforded the BOROX catalyst **235a** in 40% NMR yield (δ = 11.06 ppm and 10.44 ppm in ^{1}H NMR and δ = 5.30 in ^{11}B NMR, Figure 2.23B, entry 1). As the structure of this species is not known, the presented structure is an assumption only. Later, two other alcohols **234b** and **234c** were also employed. However, the results were not that conclusive from the ^{11}B NMR spectrum (Figure 2.23, entries 2-3).

Figure 2.23 (**A**) Bases (with pre-installed alcohols) induced boroxinate catalyst formation. (**B**)[a] ^{1}H NMR spectra in $CDCl_3$ with Ph_3CH as internal standard. (**C**) ^{11}B NMR spectra corresponding to the ^{1}H NMR spectra in Figure 2.23B with the highlighted chemical shifts of the various boron species.

Figure 2.23 cont'd

A

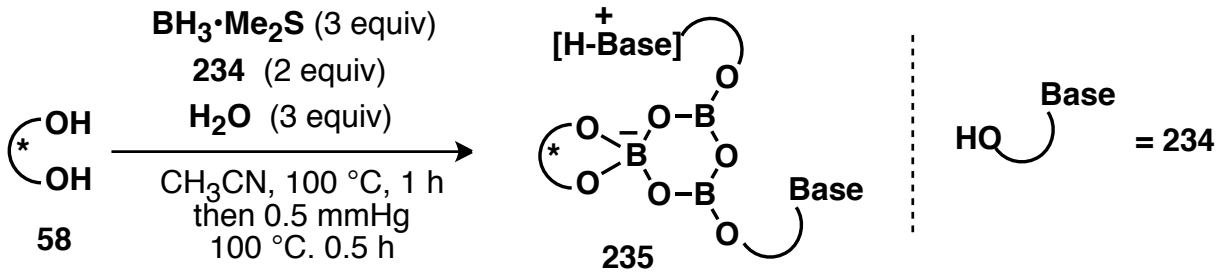

B

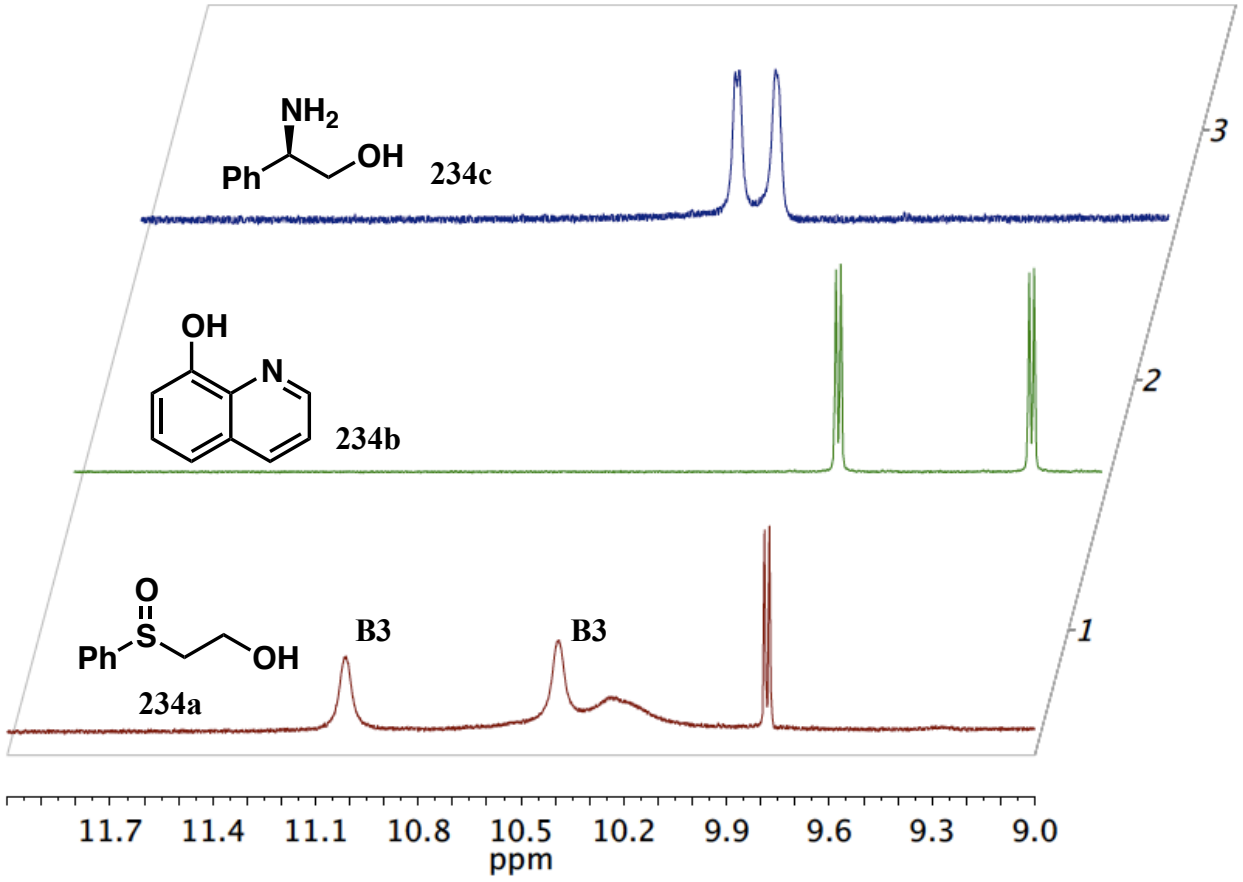

Figure 2.23
cont'd

C

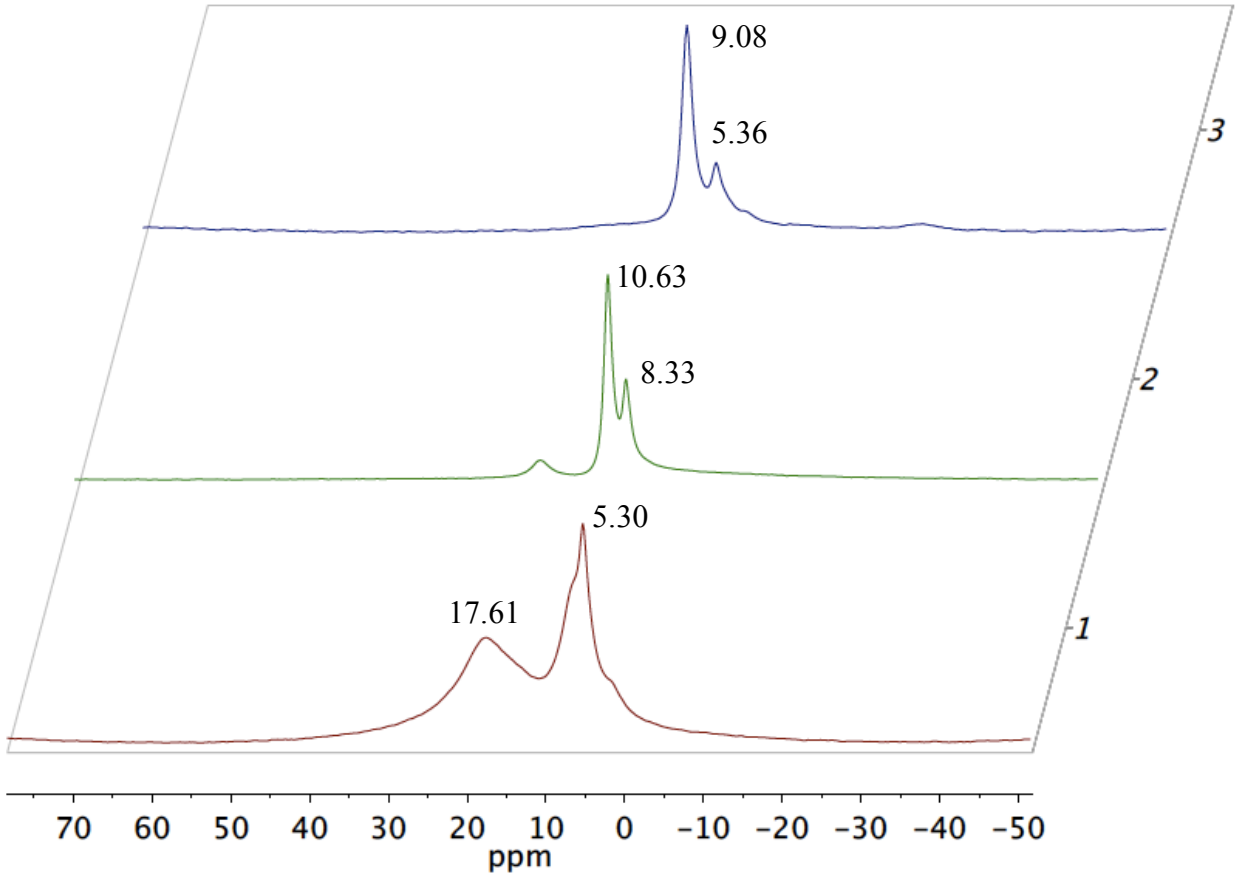

[a] Note for Figure 2.23B: Entry 1: (*S*)-VAPOL (0.1 mmol) plus 3 equiv BH_3•Me_2S **192a**, 2 equiv ROH **234a** and 3 equiv H_2O were heated at 100 °C in CH_3CN for 1 h followed by removal of volatiles under vacuum for 0.5 h. Entry 2: same as entry 1 with 2 equiv ROH **234b**. Entry 3: same as entry 1 with 2 equiv ROH **234c**.

One of the other ways is to utilize a base, which could simply function as the alcohol component. Hence we tried to generate the boroxinate **236** by employing 1 equiv of (S)-VAPOL, 3 equiv of BH3•Me_2S**,** 3 equiv H_2O and 3 equiv aniline **126k**. The result is presented in Figure 2.24. To our delight, boroxinate complex **236** was observed. However, the structure of **236** is not confirmed and must remain a tentative assignment. Peaks at δ = 10.06 ppm and δ = 10.30 ppm (in the ^{1}H NMR spectrum) and δ = 4.35 ppm (in the ^{11}B NMR spectrum) supports the formation of the catalyst **236**.

Figure 2.24 (**A**) Aniline induced boroxinate catalyst formation. (**B**) ^{1}H NMR spectra in $CDCl_3$. (*S*)-VAPOL (0.1 mmol) plus 3 equiv BH_3•Me_2S **192a**, 3 equiv aniline **126k** and 3 equiv H_2O were heated at 100 °C in CH_3CN for 1 h followed by removal of volatiles under vacuum for 0.5 h. Thereafter, the catalyst was dissolved in $CDCl_3$ and subjected to NMR analysis. (**C**) ^{11}B NMR spectra corresponding to the ^{1}H NMR spectra in Figure 2.24B.

A

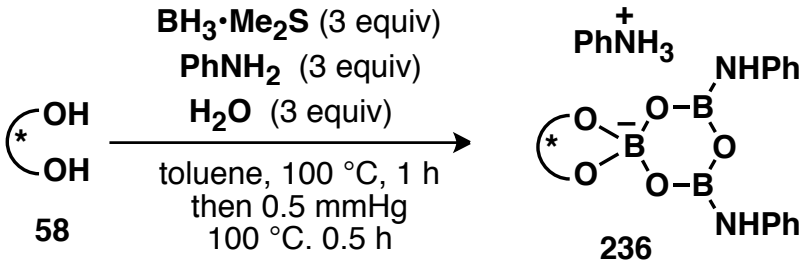

Figure 2.24 cont'd

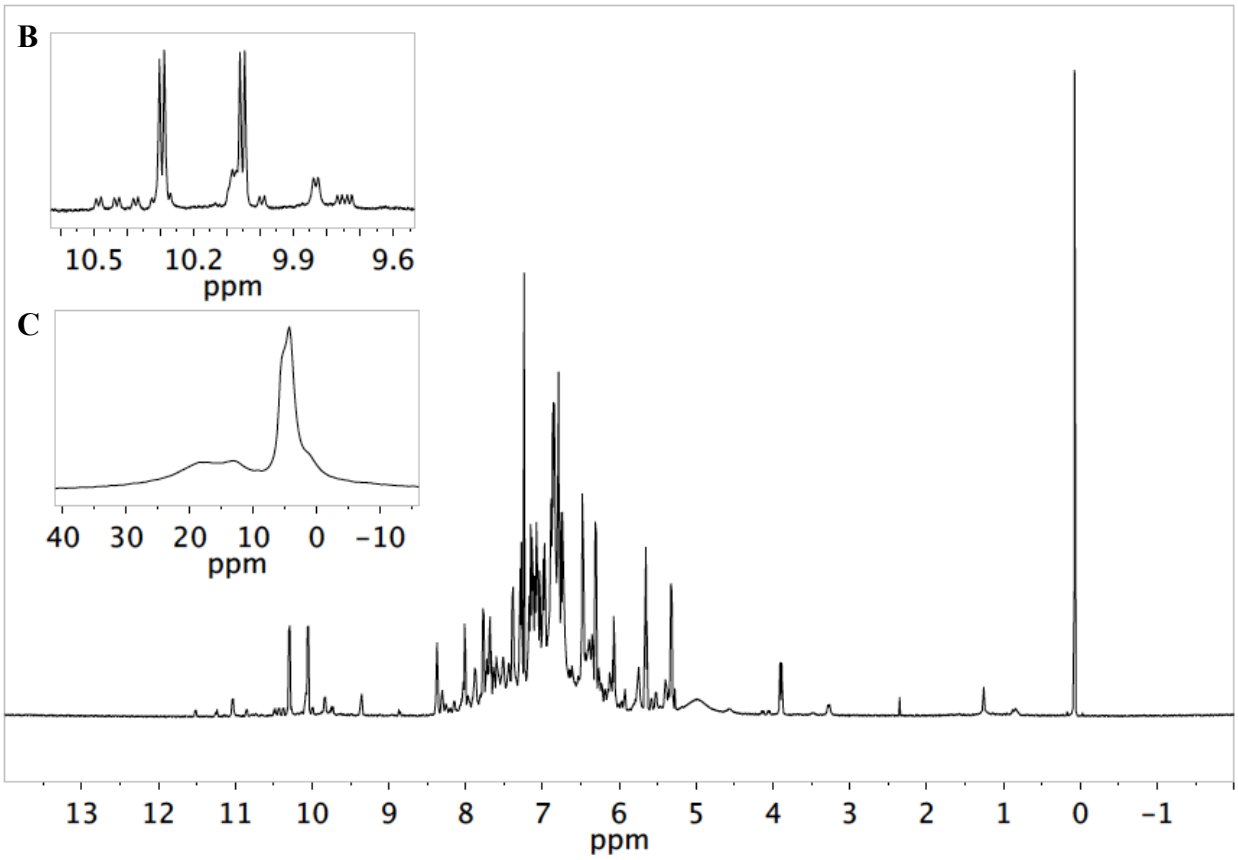

2.3.2.2 Base incorporated in the boron source

Another way is the usage of the borane that has the base installed in it. The base attached to borane should be a weak so that it can be easily be replaced by the substrate i.e. imine. Hence we decided to examine borane like BH_3•PPh_3 **192c** and BH_3•Et_2NPh **192d**. While BH_3•PPh_3 **192c** failed to give any catalyst, boroxinate **237** was obtained when BH_3•Et_2NPh **192d** was employed (Scheme 2.3, NMR not shown). A peak at δ = 10.73 ppm (in ^{1}H NMR) and δ = 5.88 ppm (in ^{11}B NMR) supports the formation of the catalyst **237**. It must be noted that structure of **237** is a tentative assignment.

Scheme 2.3 Boroxinate formation using BH_3•Et_2NPh **192d**

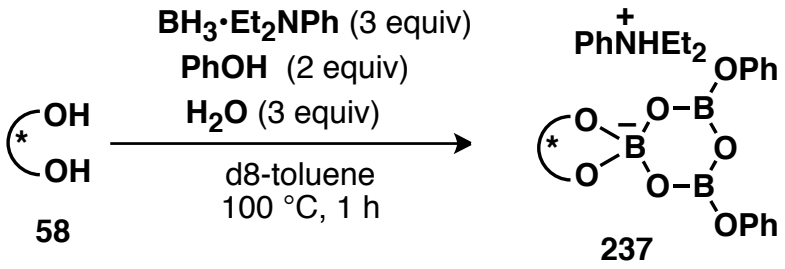

2.4 B1 catalysts

So far we have been focused on the BOROX catalyst, which has three boron atoms involved. Another class of the catalyst could be one, which involves only boron atom in a spiroborate such as **74** and **92** (Figure 2.1). The catalysts **74** and **92** will be discussed in detail in Chapter 4 and 5. Given the existence of **74**, it was wondered that whether a similar catalyst could be made from our VANOL ligand. Although, the structure of **238** is not confirmed, a characteristic peak at δ = 9.55 ppm was observed when VANOL **59** was subjected to conditions suitable for spiroborate formation (Figure 2.25).

Figure 2.25 (**A**) Attempt to generate dimer catalyst **238**. (**B**) ^{1}H NMR spectra in $CDCl_3$. (*S*)-VANOL (0.1 mmol) plus 0.5 equiv BH_3•Me_2S **192a** was heated at 100 °C in toluene for 1 h followed by removal of volatiles under vacuum for 0.5 h. Thereafter, 0.5 equiv of imine **111a** was added. (**C**) ^{11}B NMR spectra corresponding to the ^{1}H NMR spectra in Figure 2.25B.

A

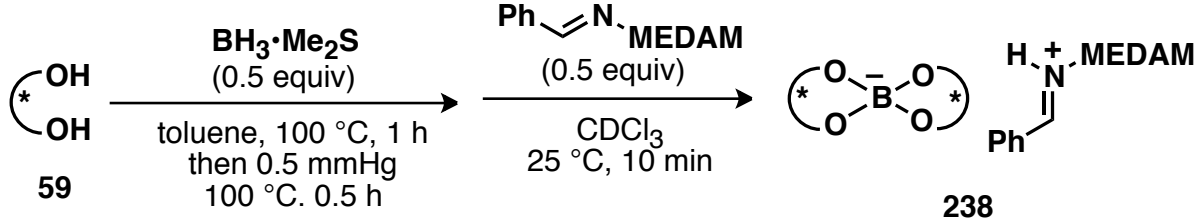

Figure 2.25 cont'd

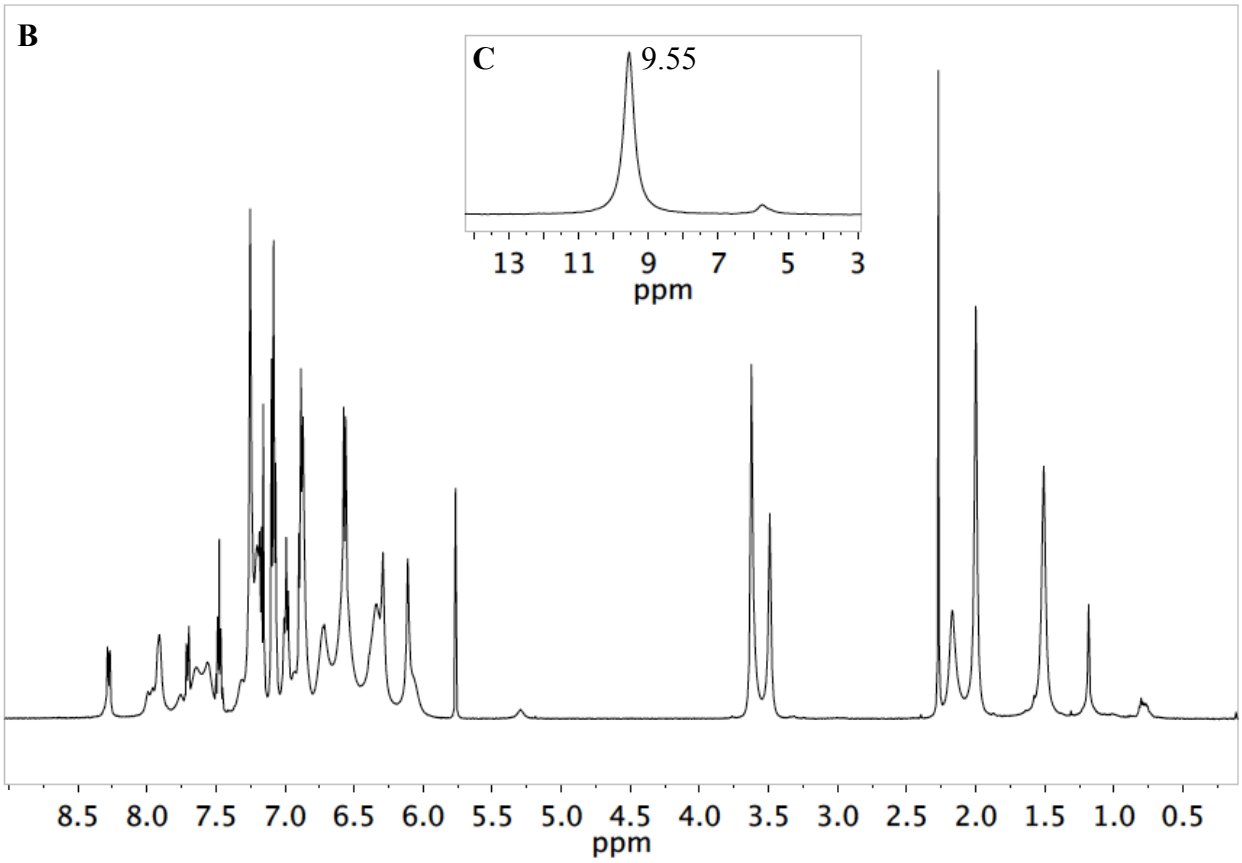

2.5 Conclusions

This chapter describes the generation of novel boroxinate catalysts employing various bases. These catalysts are characterized by ^{1}H NMR and ^{11}B NMR spectroscopy, computational chemistry and X-ray analysis. Some of these catalysts have already been utilized for various catalytic asymmetric reactions such as asymmetric aziridination of imines, multicomponent aziridination of aldehydes, [3+2] cycloaddition of imines and aldehydes, asymmetric reduction of quinolines and asymmetric epoxidation of aldehydes. Hopefully, a variety of new asymmetric reactions will be accomplished utilizing these novel catalysts in the near future.

APPENDIX

2.6 Experimental

2.6.1 General information

All reactions were carried out in flame-dried glassware under an atmosphere of argon unless otherwise indicated. Unless otherwise specified, all solvents were strictly dried before use: dichloromethane and acetonitrile were distilled over calcium hydride under nitrogen; tetrahydrofuran, and ether were distilled from sodium and benzophenone; toluene was distilled from sodium under nitrogen. Hexanes and ethyl acetate were ACS grade and used as purchased.

Melting points were recorded on a Thomas Hoover capillary melting point apparatus and are uncorrected. IR spectra were recorded in KBr matrix (for solids) and on NaCl disc (for liquids) on a Nicolet IR/42 spectrometer. $CDCl_3$ (with TMS) was dried over activated 4Å overnight and distilled. Purified $CDCl_3$ was stored and handled in a glove box. Commercial $CDCl_3$ in ampoule (CIL®, 100%, 0.75 mL) can be directly used in a glove box without further purification. ^{1}H NMR and ^{13}C NMR were recorded on a Varian Inova 300 MHz or Varian Unity Plus 500 MHz or Varian Inova 600 MHz spectrometer using $CDCl_3$ as solvent (unless otherwise noted). The residual peak of $CDCl_3$ or TMS was used as the internal standard for both ^{1}H NMR (δ = 7.24 ppm for $CDCl_3$ or δ = 0 ppm for TMS) and ^{13}C NMR (δ = 77.0 ppm). ^{11}B NMR spectra were recorded on a Varian 500 MHz instrument or Varian Inova 600 MHz spectrometer in $CDCl_3$ unless otherwise noted. ^{11}B NMR was done in a Norell® quartz NMR tube and referenced to external standard $BF_3 \bullet Et_2O$ (δ = 0 ppm). Chemical shifts were reported in parts per million (ppm). Low-resolution Mass Spectrometry and High Resolution Mass Spectrometry were performed in the Department of Chemistry at Michigan State University

Mass Facility. Analytical thin-layer chromatography (TLC) was performed on Silicycle silica gel plates with F-254 indicator. Visualization was by short wave (254 nm) and long wave (365 nm) ultraviolet light, or by staining with phosphomolybdic acid in ethanol or with potassium permanganate. Column chromatography was performed with silica gel 60 (230 – 450 mesh).

HPLC analyses were peformed using a Varian Prostar 210 Solvent Delivery Module with a Prostar 330 PDA Detector and a Prostar Workstation. Chiral HPLC data for the aziridines and epoxides were obtained using a CHIRALCEL OD-H column and PIRKLE COVALENT (R, R) WHELK-O 1 column.

Optical rotations were obtained on a Perkin-Elmer 341 polarimeter at a wavelength of 589 nm (sodium D line) using a 1.0 decimeter cell with a total volume of 1.0 mL. Specific rotations are reported in degrees per decimeter at 20 °C and the concentrations are given in gram per 100 mL in ethyl acetate unless otherwise noted.

All reagents were purified by simple distillation or crystallization with simple solvents unless otherwise indicated. Ethyl diazoacetate **85** and $B(OPh)_3$ (stored in dessicators) are obtained from Aldrich Chemical Co., Inc. and used as received. Amines such as aniline **126k**, benzyl amine **126e**, homo-benzhydrylamine **126f** and benzhydrylamine **126a** (distilled prior to use) are also obtained from Aldrich Chemical Co., Inc. and used as received. (*S*)-VAPOL **58** or (*S*)-VANOL **59** (>99% ee) were made according to published procedure[18] and were dried over P_2O_5 overnight under reduced pressure (0.1 mm Hg) with refluxing hexane in a Abderhalden drying apparatus. These ligands are also commercially available from Aldrich Chemical Co., Inc and Strem Chemicals. bis(4-methoxyphenyl)methanamine (DAM amine) **126b**,[19] bis-(3,5-di-

methyl-4- methoxyphenyl)methanamine (MEDAM amine) **126c**,[13c] bis-(3,5-di-*tert*-butyl-4-methoxyphenyl)methanamine (BUDAM amine) **126d**,[13b] *m*-$Xyl_2P(H)O$ **223d**[33] and sulfoxide **234a**[34] were made according to the published procedure. Unless otherwise noted, all NMR analysis has been carried out using Ph_3CH as the internal standard.

Home-made Schlenk flask:

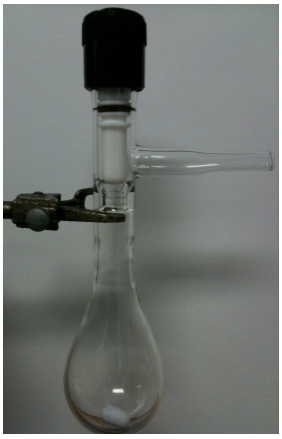

Figure 2.26 The Schlenk flask was prepared from a single-necked 25 mL pear-shaped flask that had its 14/20 glass joint replaced with a high vacuum threaded Teflon valve.

2.6.2 Synthesis of imines 75a, 78a, 110a, 111a, 112a, 206a, 207a, boroxine 191a and diazo 128b

General Procedure for the synthesis of aldimines – Illustrated for the synthesis of *N*-phenylmethylidene-*bis*(4-methoxy-3,5-dimethylphenyl)methylamine 111a.

Benzaldehyde was distilled before use and all imines were could be purified by crystallization.

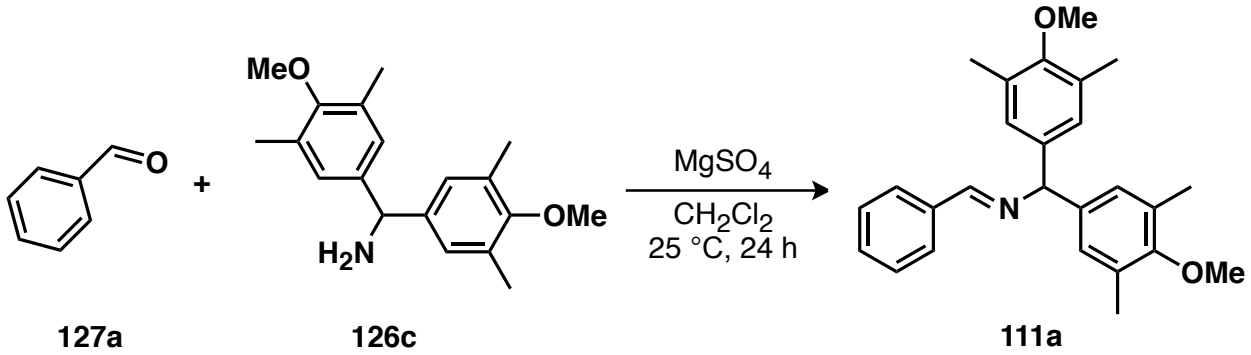

127a **126c** **111a**

***N*-phenylmethylidene-*bis*(4-methoxy-3,5-dimethylphenyl)methylamine 111a:** To a 50 mL flame-dried round bottom flask filled with argon was added bis(2,6-di-methyl-4-methoxyphenyl)methylamine **126c** (1.49 g, 5.00 mmol), $MgSO_4$ (1.0 g, 8.4 mmol, freshly flame-dried) and dry CH_2Cl_2 (15 mL). After stirring for 10 min, benzaldehyde **127a** (0.54 g, 5.05 mmol, 1.01 equiv) was added. The reaction mixture was stirred at room temperature for 24 h. The reaction mixture was filtered through Celite and the Celite bed was washed with CH_2Cl_2 (10 mL × 3) and then the filtrate was concentrated by rotary evaporation to give the crude imine as an off-white solid. Crystallization (1:9 CH_2Cl_2/hexanes) and collection of the first crop afforded **111a** as a white solid (mp 144-146 °C) in 90% isolated yield (1.74 g, 4.5 mmol).

Spectral data for **111a**: ^{1}H NMR ($CDCl_3$, 500 MHz) δ 2.24 (s, 12H), 3.66 (s, 6H), 5.35 (s, 1H), 6.99 (s, 4H), 7.39-7.41 (m, 3H), 7.80–7.82 (m, 2H), 8.35 (s, 1H); ^{13}C ($CDCl_3$, 125 MHz) δ 16.22, 59.59, 77.41, 127.86, 128.46, 128.49, 130.61, 130.63, 136.45, 139.22, 155.84, 160.28; IR (thin film) 2944w, 1643vs, 1483vs cm^{-1}; Mass spectrum: *m/z* (% rel intensity) 387 M+ (3), 283 (100), 40 (17); Anal calcd for $C_{26}H_{29}NO_2$: C, 80.59; H, 7.54; N, 3.61. Found: C, 80.42; H, 7.24;

N, 3.55. These spectral data match those previously reported for this compound.[13c]

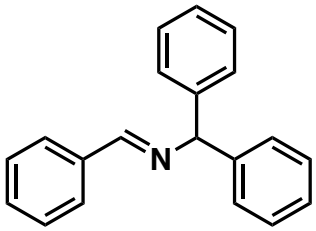

78a

***N*-benzylidene-1,1-diphenylmethanamine 78a:** Imine **78a** was prepared according to the procedure described above for imine **111a**. Crystallization (1:5 ethyl acetate/hexanes) and collection of the first crop afforded **78a** as white solid crystals (mp. 99-101 °C) in 80% isolated yield (1.09 g, 4 mmol).

Spectral data for **78a**: ^{1}H NMR ($CDCl_3$, 300 MHz) δ 5.64 (s, 1H), 7.20-7.90 (m, 15H), 8.46 (s, 1H); ^{13}C NMR ($CDCl_3$, 75 Hz) δ 77.62, 126.69, 127.40, 128.15, 128.19, 128.24, 130.47, 136.07, 143.64, 160.48. These spectral data match those previously reported for this compound.[13a]

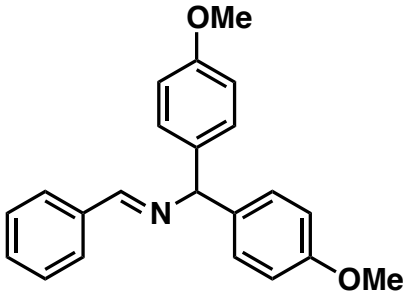

110a

***N*-benzylidene-bis(4-methoxyphenyl)methylamine 110a:** Imine **110a** was prepared according to the procedure described above for imine **111a**. Crystallization (1:25 CH_2Cl_2 / hexanes) and collection of the first crop afforded **110a** as white solid crystals (mp 60-61 ºC) in 91% isolated yield (1.51 g, 4.55 mmol).

Spectral data for **110a**: ^{1}H NMR ($CDCl_3$, 300 MHz) δ 3.76 (s, 6H), 5.51(s, 1H), 6.84 (d, 4H, J = 8.8 Hz), 7.25-7.27 (m, 4H), 7.37-7.40 (m, 3H), 7.79–7.82 (m, 2H), 8.37 (s, 1H); ^{13}C ($CDCl_3$, 75

MHz) δ 55.17, 76.55, 113.71, 128.35, 128.43, 128.61, 128.70, 130.60, 136.28, 158.43, 160.24. These spectral data match those previously reported for this compound.[19]

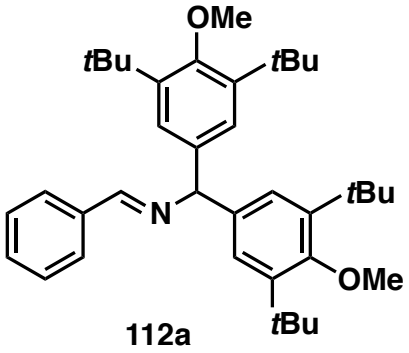

112a

***N*-benzylidene-1,1- bis(3,5-di-tert-butyl-4-methoxyphenyl) methanamine 112a:** Imine **112a** was prepared according to the procedure described above for imine **111a**. Crystallization (1:100 EtOAc/hexanes) and collection of the first crop afforded **112a** as white solid crystals (mp. 127-129 °C) in 90% isolated yield (2.5 g, 4.5 mmol).

Spectral data for **112a**: ^{1}H NMR ($CDCl_3$, 500 MHz) δ 1.429 (s, 18H), 1.433 (s, 18H), 3.70 (s, 3H), 3.70 (s, 3H), 5.51 (s, 1H), 7.27 (s, 4H), 7.42–7.44 (m, 3H), 7.86–7.89 (m, 2H), 8.52 (s, 1H); ^{13}C ($CDCl_3$, 75 MHz) δ 32.08, 35.77, 64.13, 78.20, 126.02, 128.40, 128.47, 130.50, 136.55, 137.42, 143.10, 158.29, 160.23. These spectral data match those previously reported for this compound.[13b]

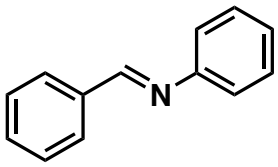

75a

***N*-benzylideneaniline 75a:** Imine **75a** was prepared according to the procedure described above for imine **111a**. Crystallization (1:5 EtOAc/hexanes) and collection of the first crop afforded **75a** as white solid crystals (mp. 48-50 °C) in 80% isolated yield (0.72 g, 4.0 mmol).

Spectral data for **75a**: ^{1}H NMR ($CDCl_3$, 500 MHz) δ 7.19-7.23 (m, 3H), 7.39 (t, 2H, J = 8 Hz), 7.46-7.48 (m, 3H), 7.88-7.91 (m, 2H), 8.45 (s, 1H); ^{13}C ($CDCl_3$, 125 MHz) δ 120.85, 125.91, 128.76, 128.80, 129.13, 131.36, 136.22, 152.09, 160.38. These spectral data match those previously reported for this compound.[35]

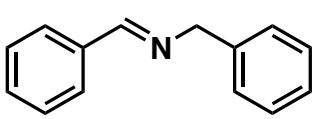

206a

***N*-benzylidene-1-phenylmethanamine 206a:** Imine **206a** was prepared according to the procedure described above for imine **111a**. Distillation afforded **206a** as colorless oil (bp 119-120 °C at 0.1 mm Hg) in 85% isolated yield (0.83 g, 4.25 mmol).

Spectral data for **206a**: ^{1}H NMR ($CDCl_3$, 300 MHz) δ 4.79 (s, 2H), 7.20-7.40 (m, 8H), 7.75-7.78 (m, 2H), 8.35 (s, 1H); ^{13}C ($CDCl_3$, 75 MHz) δ 64.94, 126.89, 127.88, 128.18, 128.40, 128.50, 130.67, 136.05, 139.20, 161.88. These spectral data match those previously reported for this compound.[36]

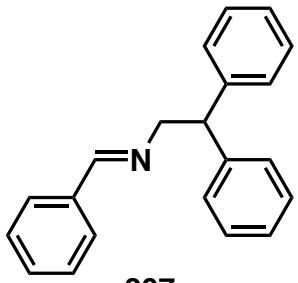

207a

***N*-benzylidene-1-phenylmethanamine 207a:** Imine **207a** was prepared according to the procedure described above for imine **111a**. Crystallization (1:9 EtOAc/hexanes) and collection of the first crop afforded **207a** as white solid crystals (mp. 92-94 °C) in 70% isolated yield (1.0 g, 3.5 mmol).

Spectral data for **207a**: ^{1}H NMR ($CDCl_3$, 600 MHz) δ 4.26 (dd, J = 7.2, 1.4 Hz, 2H), 4.46 (t, J = 7.2 Hz, 1H), 7.15 – 7.20 (m, 2H), 7.25 – 7.30 (m, 8H), 7.33 – 7.39 (m, 3H), 7.57 – 7.64 (m, 2H),

8.07 (t, J = 1.4 Hz, 1H); ^{13}C ($CDCl_3$, 150 MHz) δ 52.01, 66.29, 126.28, 128.00, 128.32, 128.42, 128.43, 130.47, 136.19, 143.08, 161.92; IR (thin film) 3061 m, 3026 m, 2841 m, 1645 s, 1493 s, 1451 s, 1309 m cm^{-1}; HRMS (ESI-TOF) *m/z* 286.1594 [(M+H$^+$); calcd. for $C_{21}H_{20}N$: 286.1596].

Synthesis of triphenoxyboroxine 191a:

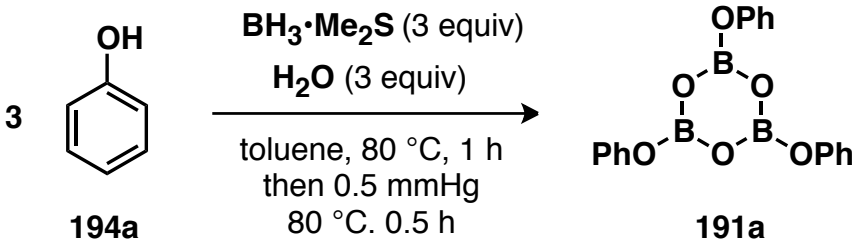

2,4,6-triphenoxy-1,3,5,2,4,6-trioxatriborinane 191a: To a 25 mL flame-dried home-made Schlenk flask (see Figure 2.26) equipped with a stir bar and flushed with argon was added phenol **194a** (28.2 mg, 0.3 mmol), BH_3•Me_2S (150 μL, 0.3 mmol, 2.0 M in toluene) and H_2O (5.4 μL, 0.3 mmol). Under an argon flow through the side-arm of the Schlenk flask, dry toluene (2 mL) was added. The flask was sealed by closing the Teflon valve, and then placed in an oil bath (80 ºC) for 1 h. After 1 h, a vacuum (0.5 mm Hg) was carefully applied by slightly opening the Teflon valve to remove the volatiles. After the volatiles are removed completely, a full vacuum is applied and is maintained for a period of 30 min at a temperature of 80 ºC (oil bath). The flask was then allowed to cool to room temperature yielding the boroxine **191a** as white solid. The boroxine prepared in this manner typically afforded boroxine **191a**: $B(OPh)_3$ **187a** = 12:1 as indicated by ^{13}C NMR.

Spectral data for boroxine **191a**: ^{1}H NMR ($CDCl_3$, 500 MHz) δ 7.07 (d, 6H, J = 7.5 Hz), 7.12 (t, 3H, J = 7.0 Hz), 7.30 (t, 6H, J = 7.5 Hz); ^{13}C NMR ($CDCl_3$, 125 MHz) δ 119.95, 123.95, 129.36, 152.00. These spectral data match those previously reported for this compound.[37]

Synthesis of Diazoacetamide 128b: See Chapter 8

2.6.3 Aziridination with different boron sources and pre-catalyst methods A-H (*Table 2.1*)

Pre-catalyst Method A:

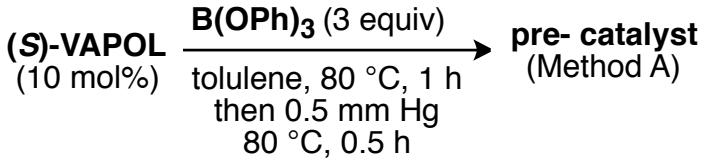

To a 25 mL flame-dried home-made Schlenk flask (see Figure 2.26) equipped with a stir bar and flushed with argon was added (*S)*-VAPOL (54 mg, 0.1 mmol) and commercial $B(OPh)_3$ (87 mg, 0.3 mmol). Under an argon flow through the side-arm of the Schlenk flask, dry toluene (2 mL) was added through the top of the Teflon valve to effect dissolution. The flask was sealed by closing the Teflon valve, and then placed in an 80 ºC oil bath for 1 h. After 1 h, a vacuum (0.5 mm Hg) was carefully applied by slightly opening the Teflon valve to remove the volatiles. After the volatiles were removed completely, a full vacuum was applied and maintained for a period of 30 min at a temperature of 80 ºC (oil bath). The flask was then allowed to cool to room temperature and opened to argon through the side-arm of the Schlenk flask.

Pre-catalyst Method B:

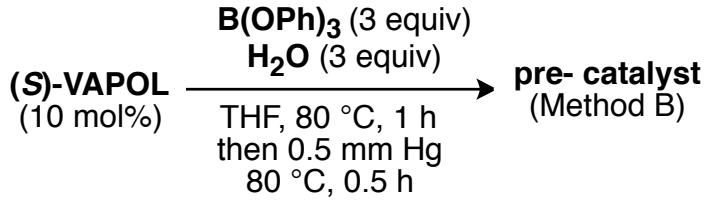

To a 25 mL flame-dried home-made Schlenk flask (see Figure 2.26) equipped with a stir bar and flushed with argon was added (*S)*-VAPOL (54 mg, 0.1 mmol) and commercial $B(OPh)_3$ (87 mg, 0.3 mmol) and water (5.4 μL, 0.3 mmol). Under an argon flow through the side-arm of the Schlenk flask, dry THF (2 mL) was added through the top of the Teflon valve to effect dissolution. The flask was sealed by closing the Teflon valve, and then placed in an 80 ºC oil bath for 1 h. After 1 h, a vacuum (0.5 mm Hg) was carefully applied by slightly opening the Teflon valve to remove the volatiles. After the volatiles were removed completely, a full vacuum was applied and maintained for a period of 30 min at a temperature of 80 ºC (oil bath). The flask was then allowed to cool to room temperature and opened to argon through the side-arm of the Schlenk flask.

Pre-catalyst Method C:

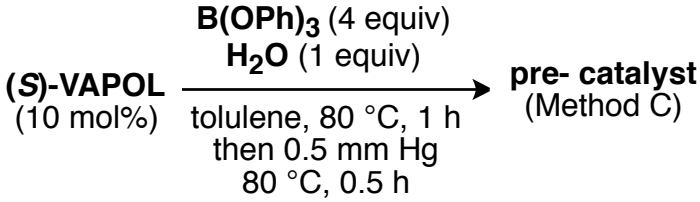

This method is similar to method A except that a combination of (*S)*-VAPOL (54 mg, 0.1 mmol) and commercial $B(OPh)_3$ (116 mg, 0.4 mmol) and water (1.8 μL, 0.1 mmol) was employed.

Pre-catalyst Method D:

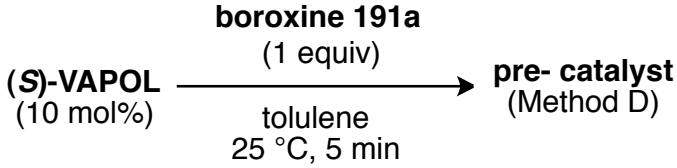

To a 25 mL flame-dried home-made Schlenk flask (see Figure 2.26) equipped with a stir bar and pre-made triphenoxyboroxine **191a** (0.1 mmol) was added (*S)*-VAPOL (54 mg, 0.1 mmol).

Pre-catalyst Method E:

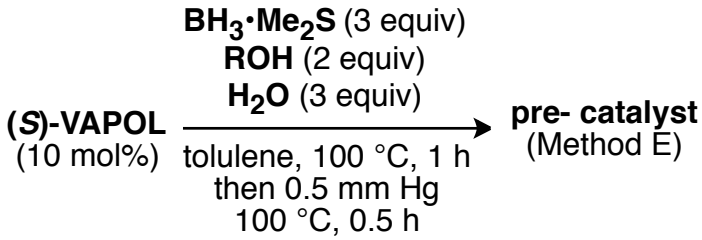

To a 25 mL flame-dried home-made Schlenk flask (see Figure 2.26) equipped with a stir bar and flushed with argon was added (*S)*-VAPOL (54 mg, 0.1 mmol) and BH_3•Me_2S (150 μL, 0.3 mmol, 2.0 M in toluene), PhOH (18.8, 0.2 mmol) and H_2O (5.4 μL, 0.3 mmol). Under an argon flow through the side-arm of the Schlenk flask, dry toluene (2 mL) was added through the top of the Teflon valve to effect dissolution. The flask was sealed by closing the Teflon valve, and then placed in an 100 ºC oil bath for 1 h. After 1 h, a vacuum (0.5 mm Hg) was carefully applied by slightly opening the Teflon valve to remove the volatiles. After the volatiles were removed completely, a full vacuum was applied and maintained for a period of 30 min at a temperature of 100 ºC (oil bath). The flask was then allowed to cool to room temperature and opened to argon through the side-arm of the Schlenk flask.

Pre-catalyst Method F:

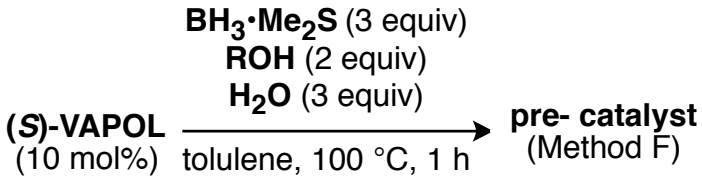

This method is similar to method E except that the removal of volatiles and a full vacuum for 30 min was excluded.

Pre-catalyst Method G:

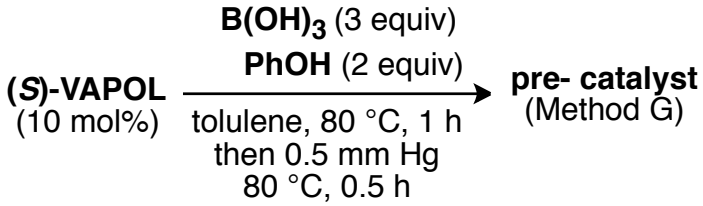

This method is similar to method A except that a combination of (*S)*-VAPOL (54 mg, 0.1 mmol) and $B(OH)_3$ (18.6 mg, 0.3 mmol) and PhOH (18.8, 0.2 mmol) was employed.

Pre-catalyst Method H:

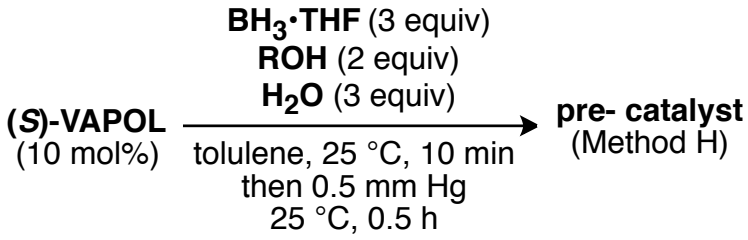

To a 25 mL flame-dried home-made Schlenk flask (see Figure 2.26) equipped with a stir bar and flushed with argon was added (*S)*-VAPOL (54 mg, 0.1 mmol) and BH_3•THF (300 μL, 0.3 mmol, 1.0 M in THF), PhOH (18.8, 0.2 mmol) and H_2O (5.4 μL, 0.3 mmol). Under an argon

flow through the side-arm of the Schlenk flask, dry toluene (2 mL) was added through the top of the Teflon valve to effect dissolution. The flask was sealed by closing the Teflon valve, and then stirred at 25 ºC for 10 min. After 10 min, a vacuum (0.5 mm Hg) was carefully applied by slightly opening the Teflon valve to remove the volatiles. After the volatiles were removed completely, a full vacuum was applied and maintained for a period of 30 min at 25 ºC. The flask was then opened to argon through the side-arm of the Schlenk flask.

***Aziridination with procedures I** (*pre-catalyst method A*), **III** (*pre-catalyst method B*), **IV** (*pre-catalyst method C*), **VI** (*pre-catalyst method E*), **VII** (*pre-catalyst method F*), **VIII** (*pre-catalyst method G*) **and IX** (*pre-catalyst method H*)**:**

General Procedure for performing aziridination – Illustrated for the synthesis of *(2R,3R)*-ethyl 1-benzhydryl-3-phenylaziridine-2-carboxylate 86a using pre-catalyst method A.

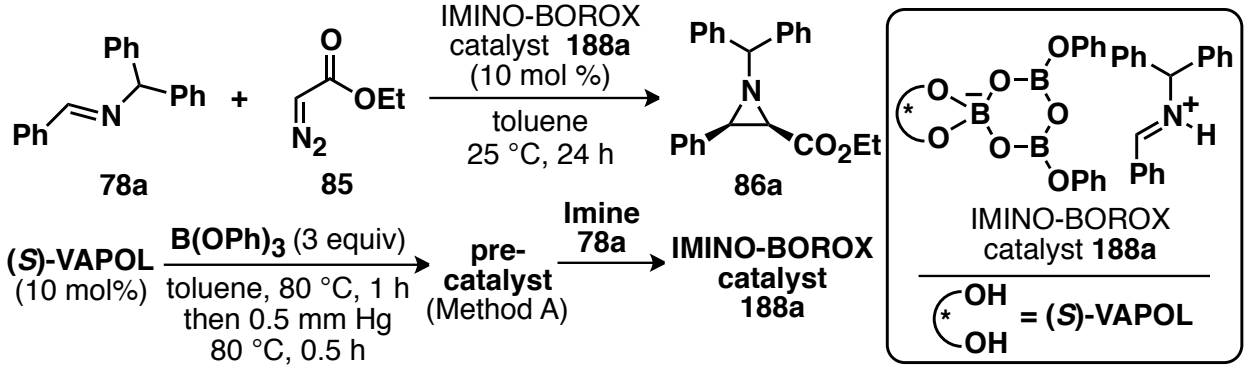

***(2R,3R)*- ethyl 1-benzhydryl-3-phenylaziridine-2-carboxylate 86a:** The pre-catalyst was made using method A employing 10 mol% of (*S*)-VAPOL. To the flask containing the pre-

catalyst (*made from method A*) was first added the aldimine **78a** (271 mg, 1 mmol) and then dry toluene (2 mL) under an argon flow through side-arm of the Schlenk flask. The reaction mixture was stirred for 5 min to give a light orange solution. To this solution was rapidly added ethyl diazoacetate (EDA) **85** (124 μL, 1.2 mmol) followed by closing the Teflon valve. The resulting mixture was stirred for 24 h at room temperature. Immediately upon addition of ethyl diazoacetate the reaction mixture became an intense yellow, which changed to light yellow towards the end of the reaction. The reaction was dilluted by addition of hexane (6 mL). The reaction mixture was then transferred to a 100 mL round bottom flask. The reaction flask was rinsed with dichloromethane (5 mL × 2) and the rinse was added to the 100 mL round bottom flask. The resulting solution was then concentrated *in vacuo* followed by exposure to high vacuum (0.05 mm Hg) for 1 h to afford the crude aziridine as an off-white solid.

A measure of the extent to which the reaction went to completion was estimated from the ^{1}H NMR spectrum of the crude reaction mixture by integration of the aziridine ring methine protons relative to either the imine methine proton or the proton on the imine carbon. The *cis/trans* ratio was determined by comparing the ^{1}H NMR integration of the ring methine protons for each aziridine in the crude reaction mixture. The *cis* (J = 7-8 Hz) and the *trans* (J = 2-3 Hz) coupling constants were used to differentiate the two isomers. The yields of the acyclic enamine side products **87a** and **88a** were determined by ^{1}H NMR analysis of the crude reaction mixture by integration of the *N*-H proton relative to the that of the *cis*-aziridine methine protons with the aid of the isolated yield of the *cis*-aziridine. Purification of the crude aziridine by silica gel chromatography (35 mm × 400 mm column, 19:1 hexanes/EtOAc as eluent, under gravity) afforded pure cis-aziridine **86a** as a white solid (mp. 127.5-128.5 °C on 92% ee material) in 83

% isolated yield (297 mg, 0.83 mmol); *cis/trans*: >50:1. Enamine side products: 8 % yield of **87a** and 4% yield of **88a.** The optical purity of **86a** was determined to be 91% *ee* by HPLC analysis ((CHIRALCEL OD-H column, 90:10 hexanes/*i*PrOH at 222 nm, flow-rate: 0.7 mL/min): retention times; R_t = 9.01 min (major enantiomer, **86a**) and R_t = 4.67 min (minor enantiomer, *ent*-**86a**).

Spectral data for **86a**: R_f = 0.3 (1:9 EtOAc/hexanes); ^{1}H NMR ($CDCl_3$, 500 MHz) δ 0.95 (t, 3H, J = 7.3 Hz), 2.64 (d, J = 6.8 Hz, 1H), 3.19 (d, J = 6.8 Hz, 1H), 3.91 (q, J = 7.1 Hz, 2H), 3.93 (s, 1H), 7.16-7.38 (m, 11H), 7.47 (d, J = 7.1 Hz, 2H), 7.58 (d, J = 7.6 Hz, 2H); ^{13}C NMR ($CDCl_3$, 75 Hz) δ 13.93, 46.36, 48.01, 60.57, 77.68, 127.18, 127.31, 127.39, 127.52, 127.76, 127.78, 128.48, 135.00, 142.37, 142.49, 167.75; $[\alpha]_D^{20}$ = + 33.4 (*c* 1.0, CH_2Cl_2) on 91.0% *ee* material (HPLC). These spectral data match those previously reported for this compound.[13a]

Aziridination with procedure II

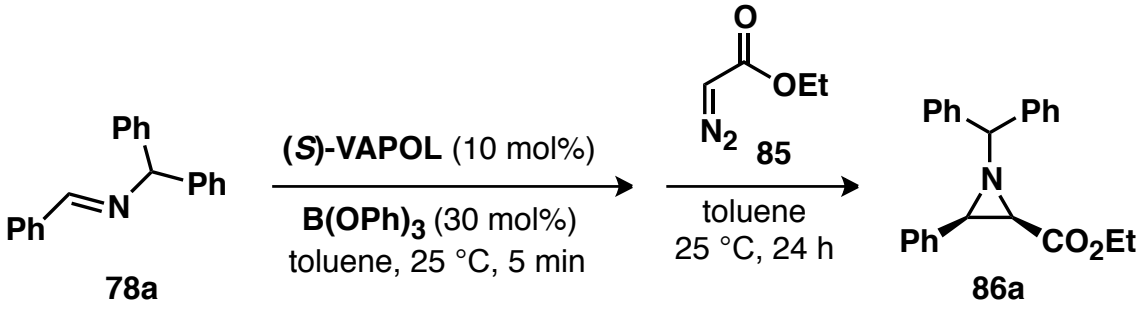

***(2R,3R)*- ethyl 1-benzhydryl-3-phenylaziridine-2-carboxylate 86a:** To a 25 mL flame-dried round bottom flask filled with argon was added (*S)*-VAPOL (54 mg, 0.1 mmol), commercial

$B(OPh)_3$ (87 mg, 0.3 mmol) and aldimine **78a** (271 mg, 1.00 mmol). The mixture was dissolved in toluene (1 mL) at room temperature. The reaction mixture was stirred for 5 min to give a light orange solution. To this solution was rapidly added EDA **85** (124 μL, 1.20 mmol) and the resulting mixture was stirred for 24 h at room temperature. The reaction was diluted by the addition of 6 mL hexane. The reaction mixture was then transferred to a 100 mL round bottom flask. The reaction flask was rinsed with dichloromethane (5 mL × 2) and the rinse was added to the 100 mL round bottom flask. The resulting solution was then concentrated *in vacuo* followed by exposure to high vacuum (0.05 mm Hg) for 1 h to afford the crude aziridine as an off-white solid. Purification of the crude aziridine by silica gel chromatography (as discussed above) afforded pure aziridine **86a** as a white solid in 80 % yield and 92 % ee.

Aziridination with procedures V

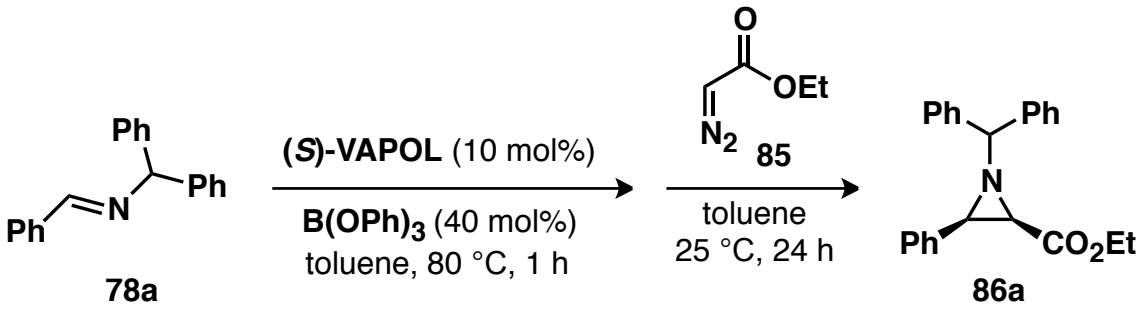

***(2R,3R)*- ethyl 1-benzhydryl-3-phenylaziridine-2-carboxylate 86a:** To a 25 mL flame-dried home-made Schlenk flask (see Figure 1) equipped with a stir bar and flushed with argon was added (*S)*-VAPOL (54 mg, 0.1 mmol) and commercial $B(OPh)_3$ (116 mg, 0.4 mmol) and aldimine **78a** (271 mg, 1 mmol). Under an argon flow through the side-arm of the Schlenk flask, dry toluene (2 mL) was added to dissolve the reagents. The flask was sealed by closing the Teflon valve, and then placed in an 80 ºC (oil bath) for 1 h. The catalyst mixture was then

allowed to cool to room temperature and open to argon through the side-arm of the Schlenk flask. To this solution was rapidly added ethyl diazoacetate (EDA) **85** (124 μL, 1.2 mmol) followed by closing the Teflon valve. The resulting mixture was stirred for 24 h at room temperature. Immediately upon addition of ethyl diazoacetate the reaction mixture became an intense yellow, which changed to light yellow towards the completion of the reaction. The reaction was diluted by addition of hexane (6 mL). The reaction mixture was then transferred to a 100 mL round bottom flask. The reaction flask was rinsed with dichloromethane (5 mL × 2) and the rinse was added to the 100 mL round bottom flask. The resulting solution was then concentrated *in vacuo* followed by exposure to high vacuum (0.05 mm Hg) for 1 h to afford the crude aziridine as an off-white solid. Purification of the crude aziridine by silica gel chromatography (as discussed above) afforded pure aziridine **86a** as a white solid in 80 % yield and 92 % ee.

2.6.4 Aziridination using different alcohols (*Table 2.3*) or ligands (*Table 2.4*) or imines (*Table 2.5*)

A) With different alcohols (*Table 2.3*): Aziridination was performed with procedure VII (pre-catalyst method F) described above using alcohols **194**.

B) With different ligands (*Table 2.4*): Aziridination was performed with procedure IV (pre-catalyst method C) described above using different ligands. See more details in Chapter 5.

C) With different imines (*Table 2.5*): Aziridination was performed with procedure IV (pre-catalyst method C) described above using different imines.

Synthesis of aziridine 113a using imine 110a:

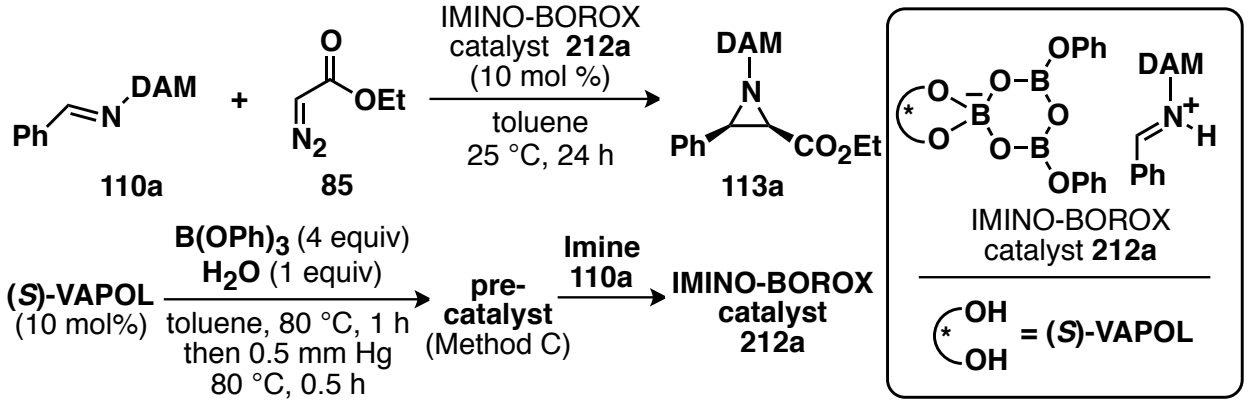

(2*R*,3*R*)-ethyl-1-(bis(4-methoxyphenyl)methyl)-3-phenylaziridine-2-carboxylate 113a: Imine **110a** (332 mg, 1 mmol) was reacted according to the general procedure IV (pre-catalyst method C) described above with (*S*)-VAPOL (10 mol%) as the ligand. Purification of the crude aziridine by silica gel chromatography (35 mm × 400 mm column, 9:1 hexanes/EtOAc as eluent, after elution of the first fraction, which contains EDA and / or enamine side products **116a** and **117a**, the eluent was changed to 5:1 hexanes / EtOAc) afforded pure cis-aziridine **113a** as a white solid (mp 89-90 ºC on 94% ee material) in 95 % isolated yield (396 mg, 0.95 mmol); *cis/trans*: 50:1. Enamine side products: 1% yield of **116a** and 1% yield of **117a**. The optical purity of **113a** was determined to be 92% *ee* by HPLC analysis (CHIRALPAK AD column, 90:10 hexane/2-propanol at 226nm, flow-rate: 1.0 mL/min): retention times; R_t = 8.80 min (major enantiomer, **113a**) and R_t = 15.70 min (minor enantiomer, *ent*-**113a**)

Spectral data for **113a**: R_f = 0.28 (1:5 EtOAc/hexanes). ^{1}H NMR ($CDCl_3$, 500 MHz) δ 0.93 (t, 3H, *J* = 7.1 Hz), 2.59 (d, 1H, *J* = 6.8 Hz), 3.13 (d, 1H, *J* = 6.8 Hz), 3.67 (s, 3H), 3.75 (s, 3H),

3.81 (s, 1H), 3.91-3.98 (m, 2H), 6.74 (d, 2H, J = 8.8 Hz), 6.82 (d, 2H, J = 8.8 Hz), 7.14-7.24 (m, 3H), 7.31-7.35 (m, 4H), 7.43 (d, 2H, J = 8.8 Hz); ^{13}C ($CDCl_3$, 75 MHz) δ 13.94, 46.39, 48.02, 55.15, 55.22, 60.54, 76.44, 113.80, 127.27, 127.75, 127.79, 128.16, 128.49, 134.93, 135.13, 135.16, 158.61, 158.71, 167.83 (one sp^2 carbon not located); $[\alpha]_D^{20}$ +36.5 (c 1.0, EtOAc) on 94% ee material (HPLC). These spectral data match those previously reported for this compound.[19]

Synthesis of aziridine 209a using imine 207a:

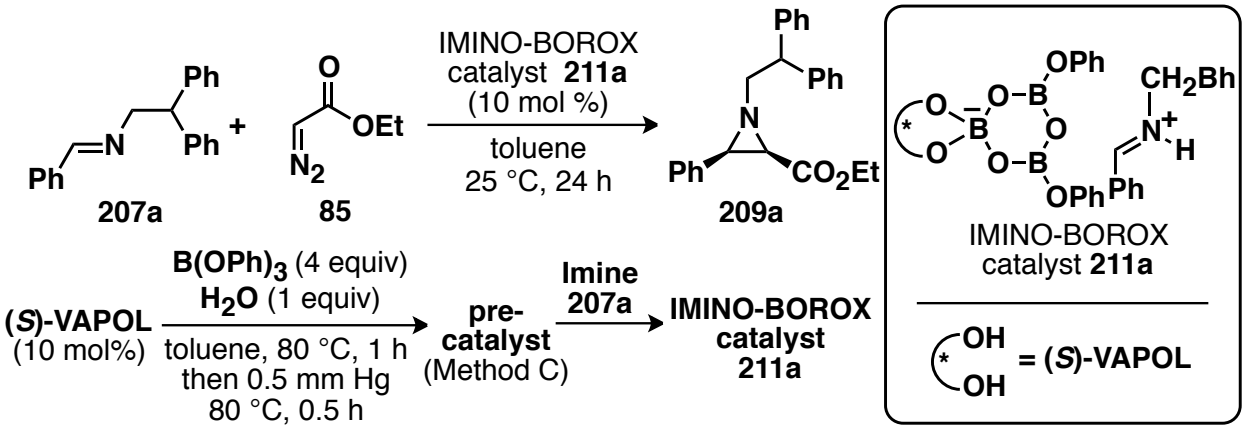

(2*R*,3*R*)-ethyl-1-(2,2-diphenylethyl)-3-phenylaziridine-2-carboxylate 209a: Imine **207a** (285 mg, 1 mmol) was reacted according to the general procedure IV (pre-catalyst method C) described above with (*S*)-VAPOL (10 mol%) as ligand except that the concentration of the reaction is 0.2 M i.e. 6 mL of toluene was used. A clear solution was obtained upon the addition imine and toluene. After 2-3 min, the clear solution turned to a yellow gel. A similar observation was made when CCl_4 was used as the solvent. However, no gel was observed in the case of CH_2Cl_2. Purification of the crude aziridine by silica gel chromatography (35 mm × 400

mm column, 15:1 hexanes/EtOAc as eluent, gravity) afforded pure cis-aziridine **209a** as a white solid (mp 99-101 ºC on 43% ee material) in 32 % isolated yield (119 mg, 0.32 mmol); *cis/trans*: >50:1. Enamine side products: <1% yield. The optical purity of **209a** was determined to be 52% *ee* by HPLC analysis (CHIRALCEL OD-H column, 99:1 hexane/2-propanol at 226nm, flow-rate: 0.7 mL/min): retention times; R_t = 74.06 min (major enantiomer, **209a**) and R_t = 21.4 min (minor enantiomer, *ent*-**209a**)

Spectral data for **209a**: R_f = 0.32 (1:9 EtOAc/hexanes). ^{1}H NMR ($CDCl_3$, 300 MHz) 0.98 (t, *J* = 7.1 Hz, 3H), 2.30 (d, *J* = 6.8 Hz, 1H), 2.79 (d, *J* = 6.8 Hz, 1H), 3.22 (dd, *J* = 11.6, 6.8 Hz, 1H), 3.33 (dd, *J* = 11.6, 7.6 Hz, 1H), 3.91 (qq, *J* = 10.8, 7.1 Hz, 2H), 4.47 (t, *J* = 7.1 Hz, 1H), 7.10 – 7.44 (m, 15H); ^{13}C ($CDCl_3$, 125 MHz) δ 13.90, 46.42, 47.82, 51.32, 60.45, 65.45, 126.41, 126.46, 127.17, 127.53, 127.78, 128.15, 128.27, 128.33, 128.40, 135.08, 142.82, 142.97, 167.95; IR (thin film, cm^{-1}) 3061 m, 3028 m, 2930 m, 1747 s, 1495 s, 1450 s, 1196 s; HRMS (ESI-TOF) *m/z* 372.1964 [($M+H^+$); calcd. for $C_{25}H_{26}NO_2$: 372.1964]; $[\alpha]_D^{20}$ +4.1 (*c* 1.0, CH_2Cl_2) on 43% ee material (HPLC).

2.6.5 NMR analysis of a mixture of VAPOL, various boron sources, and imine 111a at various conditions (*Figure 2.3, 2.4 and Table 2.2*)

As shown in Fig. 2.3, 2.4 and Table 2.2 of this chapter, a mixture of (*S*)-VAPOL **58** and $B(OPh)_3$ **187a** or triphenoxyboroxine **191a** or BH_3•Me_2S **192a** or $B(OH)_3$ **193** gives different yields of unreacted VAPOL **58**, mesoborate B1 **106** and pyroborate B2 **108** employing different

reaction conditions (pre-catalyst methods). The yields do not show any significant change after 24 h. Also, it was evident from the ^{1}H NMR and ^{11}B NMR that no boroxinate B3 **190a** was formed unless imine **111a** was added (characteristic peaks i.e. δ 10.2-10.4 and δ 5.5-5.7 were missing in ^{1}H NMR and ^{11}B NMR respectively). The amount of B3 **190a** differs with respect to different catalyst loading and different methods of preparation of the pre-catalyst. Unless otherwise noted, commercial $B(OPh)_3$ is used in all the experiments. Also, Ph_3CH is used as the internal standard.

Experimental:

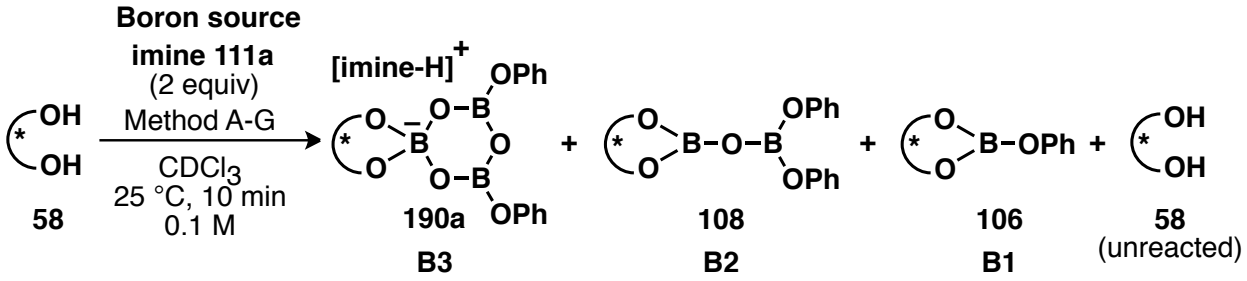

Entry 1, Figure 2.3 and Entry 1, Table 2.2: The pre-catalyst was made using method A employing (*S*)-VAPOL (54 mg, 0.1 mmol) and commercial $B(OPh)_3$ (87 mg, 0.3 mmol). To the flask containing the pre-catalyst was first added the Ph_3CH (12.22 mg, 0.05 mmol) and then $CDCl_3$ (1 mL) under an argon flow through side-arm of the Schlenk flask. The reaction mixture was then stirred for 10 min. The off-white colored solution was then directly transferred to a quartz NMR tube and was subjected to ^{1}H NMR and ^{11}B NMR analysis.

Entry 2, Figure 2.3 and Entry 2, Table 2.2:

The pre-catalyst was made using method A employing (*S*)-VAPOL (54 mg, 0.1 mmol) and commercial $B(OPh)_3$ (87 mg, 0.3 mmol). To the flask containing the pre-catalyst was first added the imine **111a** (78 mg, 0.2 mmol), Ph_3CH (12.22 mg, 0.05 mmol) and then $CDCl_3$ (1 mL) under an argon flow through side-arm of the Schlenk flask. The reaction mixture was then stirred for 10 min. The red colored solution was then directly transferred to a quartz NMR tube and was subjected to ^1H NMR and ^{11}B NMR analysis.

Entry 3, Figure 2.3 and Entry 6, Table 2.2: Same as entry 1 except that the pre-catalyst was made using method B.

Entry 4, Figure 2.3 and Entry 7, Table 2.2: Same as entry 2 except that the pre-catalyst was made using method B.

Entry 5, Figure 2.3 and Entry 9, Table 2.2: Same as entry 1 except that the pre-catalyst was made using method C.

Entry 6, Figure 2.3 and Entry 10, Table 2.2: Same as entry 2 except that the pre-catalyst was made using method C.

Entry 7, Figure 2.3 and Entry 11, Table 2.2: To a 10 mL flame-dried round bottom flask, equipped with a stir bar, filled with argon was added (*S*)-VAPOL **58** (54 mg, 0.1 mmol, 1 equiv), commercial $B(OPh)_3$ (87 mg, 0.3 mmol, 3 equiv), Ph_3CH (12.22 mg, 0.05 mmol) and $CDCl_3$(1 mL). The resultant mixture was stirred for 10 min at room temperature. The off-white colored solution was then directly transferred to a quartz NMR tube and was subjected to ^1H NMR and

^{11}B NMR analysis. A Teflon tape was wrapped on the cap of the NMR tube while storing the sample for 24h.

Entry 8, Figure 2.3 and Entry 12, Table 2.2: To a 10 mL flame-dried round bottom flask, equipped with a stir bar, filled with argon was added (*S*)-VAPOL **58** (54 mg, 0.1 mmol, 1 equiv), commercial $B(OPh)_3$ (87 mg, 0.3 mmol, 3 equiv), imine **111a** (78 mg, 0.2 mmol, 2 equiv), Ph_3CH (12.22 mg, 0.05 mmol) and $CDCl_3$(1 mL). The resultant mixture was stirred for 10 min at room temperature. The red colored solution was then directly transferred to a quartz NMR tube and was subjected to ^{1}H NMR and ^{11}B NMR analysis.

Entry 1, Figure 2.4 and Entry 14, Table 2.2: Same as entry 1 of Figure 2.3 except that the pre-catalyst was made using method D.

Entry 2, Figure 2.4 and Entry 15, Table 2.2: Same as entry 2 of Figure 2.3 except that the pre-catalyst was made using method D.

Entry 3, Figure 2.4 and Entry 16, Table 2.2: Same as entry 1 of Figure 2.3 except that the pre-catalyst was made using method E.

Entry 4, Figure 2.4 and Entry 17, Table 2.2: Same as entry 2 of Figure 2.3 except that the pre-catalyst was made using method E.

Entry 5, Figure 2.4 and Entry 19, Table 2.2: Same as entry 1 of Figure 2.3 except that the pre-catalyst was made using method G and CH_3CN used the solvent for catalyst preparation.

Entry 6, Figure 2.4 and Entry 20, Table 2.2: Same as entry 2 of Figure 2.3 except that the pre-catalyst was made using method G and CH_3CN used the solvent for catalyst preparation.

Temperature Studies of 190a:

The pre-catalyst was made using method B employing (*S*)-VAPOL (54 mg, 0.1 mmol) and $B(OPh)_3$ (87 mg, 0.3 mmol) and H_2O (5.4 μL, 0.3 mmol). To the flask containing the pre-catalyst was first added the imine **111a** (39 mg, 0.1 mmol), Ph_3CH (12.22 mg, 0.05 mmol) and then $CDCl_3$ (1 mL) under an argon flow through side-arm of the Schlenk flask. The reaction mixture was then stirred for 10 min. The red colored solution was then directly transferred to a quartz NMR tube and was subjected to ^1H NMR and ^{11}B NMR analysis at various temperatures.

2.6.6 NMR analysis of a mixture of VAPOL, $B(OPh)_3$ and bases 75a, 78a, 85, 111a, 126, 127, 128b, 206a, 207a, 216, 219, 221, 223, 225, 232 *(Figures 2.7, 2.9, 2.11, 2.12, 2.14, 2.15, 2.17-2.21 and Tables 2.7, 2.9-2.12)*

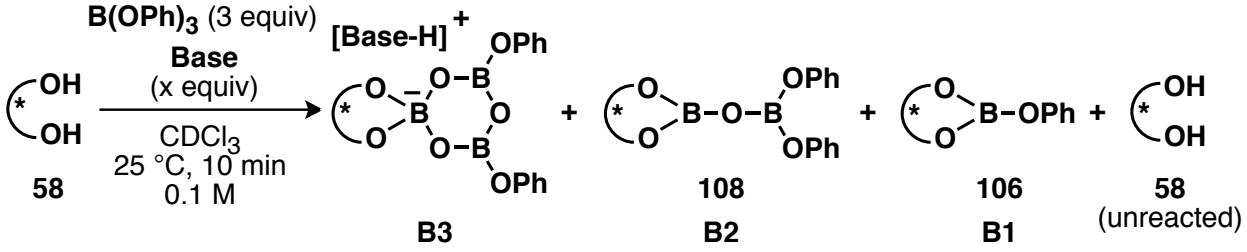

To a 10 mL flame-dried round bottom flask, equipped with a stir bar, filled with argon was added (*S*)-VAPOL **58** (54 mg, 0.1 mmol, 1 equiv.), $B(OPh)_3$ (87 mg, 0.3 mmol, 3 equiv.), base (x equiv.), Ph_3CH (12.22 mg, 0.05 mmol) and $CDCl_3$(1 mL). The resultant mixture was stirred for

10 min at room temperature. After 10 min, the mixture was then directly transferred to a quartz NMR tube and was subjected to ^{1}H NMR and ^{11}B NMR analysis.

In case of pyridine **216a**, a procedure same as entry 4 of Figure 2.3 and entry 7 of Table 2.2 with one equiv of the base.

2.6.7 Aziridination in the presence of SULFOX-BOROX catalyst 222a

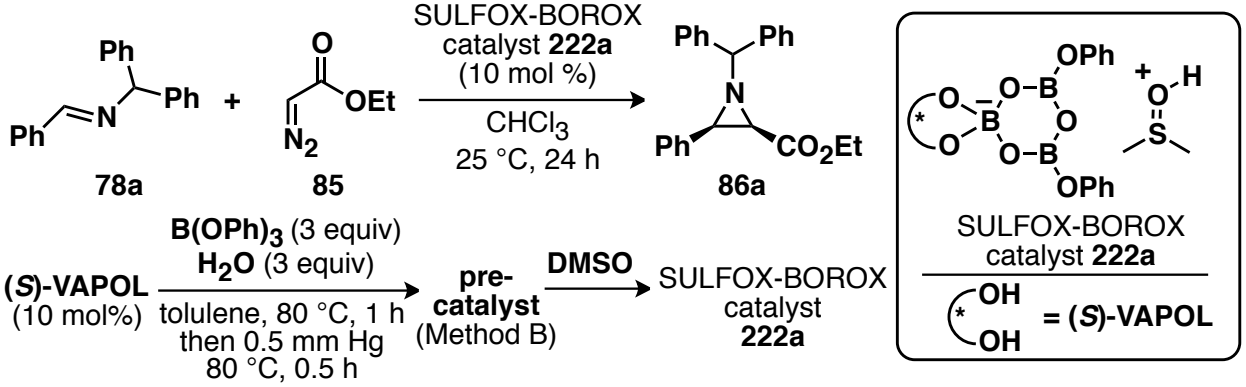

***(2R,3R)*- ethyl 1-benzhydryl-3-phenylaziridine-2-carboxylate 86a:** To The pre-catalyst was made using method B employing (*S*)-VAPOL (54 mg, 0.1 mmol), $B(OPh)_3$ (87 mg, 0.3 mmol) and H_2O (5.4 μL, 0.3 mmol). To the flask containing the pre-catalyst was first added the DMSO (7.1 μL, 0.1 mmol) under an argon flow through side-arm of the Schlenk flask. The reaction mixture was then stirred for 1 h. After 1 h, imine **78a** (271 mg, 1 mmol) was added to the flask containing the SULFOX-BOROX catalyst **222a** under an argon flow through side-arm of the Schlenk flask. To this solution was rapidly added ethyl diazoacetate (EDA) **85** (124 μL, 1.2 mmol) followed by closing the Teflon valve. The resulting mixture was stirred for 24 h at room temperature. Immediately upon addition of ethyl diazoacetate the reaction mixture became an

intense yellow, which changed to light yellow towards the end of the reaction. The reaction was dilluted by addition of hexane (6 mL). The reaction mixture was then transferred to a 100 mL round bottom flask. The reaction flask was rinsed with dichloromethane (5 mL × 2) and the rinse was added to the 100 mL round bottom flask. The resulting solution was then concentrated *in vacuo* followed by exposure to high vacuum (0.05 mm Hg) for 1 h to afford the crude aziridine as an off-white solid. Purification of the crude aziridine by silica gel chromatography (as discussed above) afforded pure aziridine **86a** as a white solid in 86 % yield and 90 % ee. The same reaction afforded aziridine 86a in 80% yield and 90% ee in the absence of catalyst **222a**.

2.6.8 NMR analysis of a mixture of VAPOL, $B(OPh)_3$ and base 234 and 126k (*Figure 2.23-2.24*)

A) with base 234:

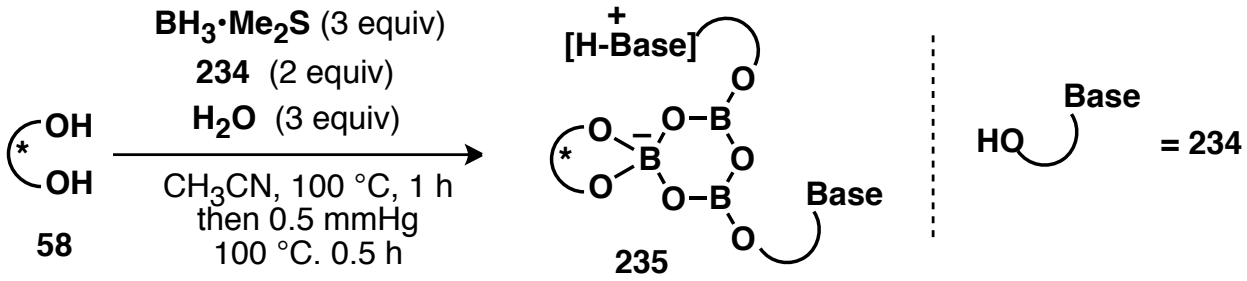

The catalyst **235** was made using the pre-catalyst method E employing (*S)*-VAPOL (54 mg, 0.1 mmol) and BH_3•Me_2S (150 μL, 0.3 mmol, 2.0 M in toluene), ROH **234** (18.8, 0.2 mmol) and H_2O (5.4 μL, 0.3 mmol). Acetonitrile was used as the solvent to make the catalyst. To the flask containing the catalyst was added Ph_3CH (12.22 mg, 0.05 mmol) and then $CDCl_3$ (1 mL) under an argon flow through side-arm of the Schlenk flask. The reaction mixture was then stirred for

10 min. The resulting solution was then directly transferred to a quartz NMR tube and was subjected to ^{1}H NMR and ^{11}B NMR analysis.

B) with base 126k:

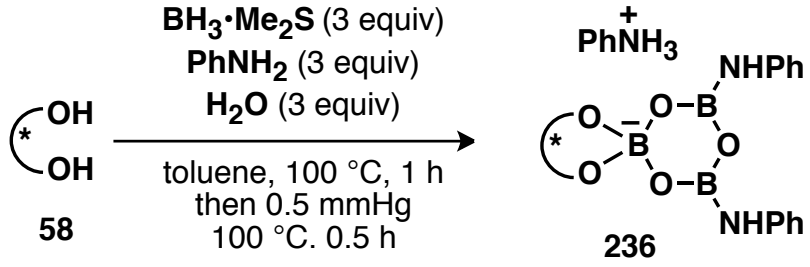

The catalyst **236** was made using the pre-catalyst method E employing (*S)*-VAPOL (54 mg, 0.1 mmol) and BH_3•Me_2S (150 μL, 0.3 mmol, 2.0 M in toluene), $PhNH_2$ **126k** (27.3 μL, 0.3 mmol) and H_2O (5.4 μL, 0.3 mmol). To the flask containing the catalyst was added $CDCl_3$ (1 mL) under an argon flow through side-arm of the Schlenk flask. The reaction mixture was then stirred for 10 min. The resulting solution was then directly transferred to a quartz NMR tube and was subjected to ^{1}H NMR and ^{11}B NMR analysis.

2.6.9 NMR analysis of a mixture of VAPOL, PhOH, H_2O and borane 192d (*Scheme 2.3*)

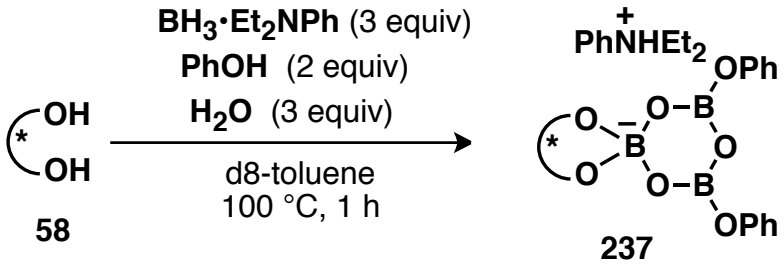

The catalyst **237** was made using the pre-catalyst method F employing (*S)*-VAPOL (54 mg, 0.1 mmol) and BH_3•Et_2NPh **192d** (53.3 μL, 0.3 mmol), PhOH (18.8, 0.2 mmol) and H_2O (5.4 μL,

0.3 mmol) in d_8-toluene. The resulting solution was then directly transferred to a quartz NMR tube and was subjected to ^{1}H NMR and ^{11}B NMR analysis. A peak at δ = 10.73 ppm (in ^{1}H NMR) and δ = 5.88 ppm (in ^{11}B NMR) supports the formation of the catalyst **237**.

2.6.10 NMR analysis of a mixture of VAPOL, BH_3•Me_2S (0.5 equiv) and imine 111a (0.5 equiv) (*Figure 2.25*)

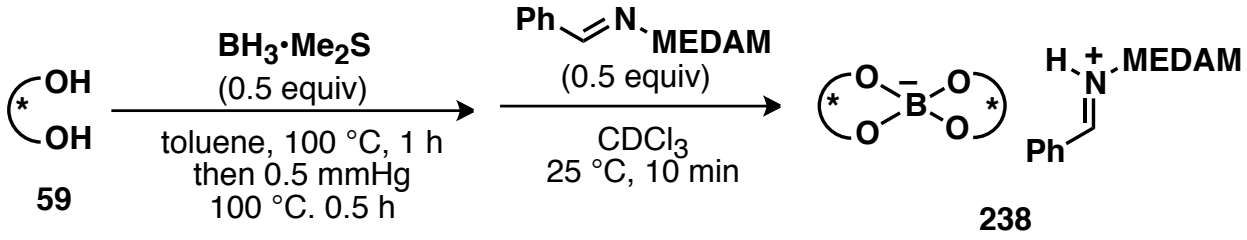

To a 25 mL flame-dried home-made Schlenk flask (see Figure 2.26) equipped with a stir bar and flushed with argon was added (*S)*-VANOL **59** (44 mg, 0.1 mmol) and BH_3•Me_2S (25 μL, 0.05 mmol, 2.0 M in toluene). Under an argon flow through the side-arm of the Schlenk flask, dry toluene (2 mL) was added through the top of the Teflon valve to effect dissolution. The flask was sealed by closing the Teflon valve, and then placed in an 100 ºC oil bath for 1 h. After 1 h, a vacuum (0.5 mm Hg) was carefully applied by slightly opening the Teflon valve to remove the volatiles. After the volatiles were removed completely, a full vacuum was applied and maintained for a period of 30 min at a temperature of 100 ºC (oil bath). The flask was then allowed to cool to room temperature and opened to argon through the side-arm of the Schlenk flask. To the flask containing the pre-catalyst was first added the imine **111a** (19 mg, 0.05 mmol) and then $CDCl_3$ (1 mL) under an argon flow through side-arm of the Schlenk flask. The

reaction mixture was then stirred for 10 min. The resulting solution was then directly transferred to a quartz NMR tube and was subjected to ^{1}H NMR and ^{11}B NMR analysis.

2.6.11 DFT Calculations of 190a, 215c, 222a, 222b, 217d, 222h, 222i, 228a and 233b (*Figure 2.8, 2.10, 2.16, 2.22*)

All quantum mechanical calculations were performed using the GAUSSIAN 03.[20] The B3LYP[38] and BHandHLYP[39] density functional were used along with 3-21G* and 6-31G* basis sets. There were no imaginary frequencies found in any calculations. The coordinates were provided to Prof. Wulff as a separate file.

NBO analysis on (*S*)-VAPOL-BOROX anion: NBO analysis was performed at the B3LYP/6-31G* level of theory as shown in Figure 2.27.

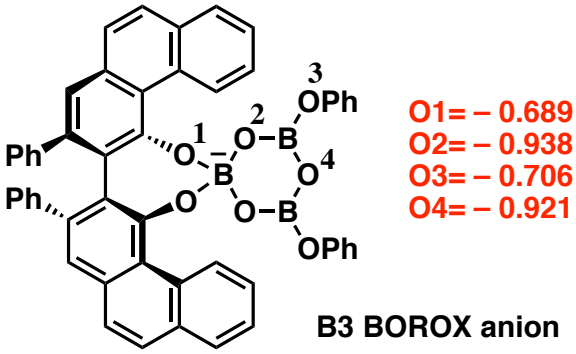

Figure 2.27 Natural charges on the oxygen atoms of the boroxinate anion

2.6.12 Crystallographic structure determination of BOROX complex 217b (*Figure 2.13*)

The crystallographic data of X-ray diffraction studies in this work were collected using a Bruker CCD (charge coupled device) based diffractometer equipped with an Oxford Cryostream low-temperature apparatus operating at 173 K. Data were measured using omega and phi scans of 0.5° per frame for 30 s. The total number of images was based on results from the program COSMO where redundancy was expected to be 4.0 and completeness to 0.83 Å to 100%. Cell

parameters were retrieved using APEX II software and refined using SAINT on all observed reflections. Data reduction was performed using the SAINT software, which corrects for Lp. Scaling and absorption corrections were applied using SADABS multi-scan technique, supplied by George Sheldrick. The structures are solved by the direct method using the SHELXS-97 program and refined by least squares method on F^2, SHELXL- 97, which are incorporated in SHELXTL-PC V 6.10. The structure was solved in the space group P2 (# 4). All non-hydrogen atoms are refined anisotropically. Hydrogens were calculated by geometrical methods and refined as a riding model except for those of the water molecules, which could not be found or refined. The Flack parameter is used to determine chirality of the crystal studied, the value should be near zero, a value of one is the other enantiomer and a value of 0.5 is racemic. The Flack parameter was refined to -0.02(18), confirming the absolute stereochemistry. Determination of absolute structure using Bayesian statistics on Bijvoet differences using the program within Platon report that we may have the correct enantiomer based on this comparison. All the drawings are done at 50% ellipsoids. The crystallographic data including hydrogen-bonds are summarized in Tables 2.13 and 2.14. The full structural parameters for **217b** have been submitted in Cambridge Crystallographic Data Center (Reference numbers CCDC).

Table 2.13 Crystal data and structure refinement for BOROX complex **217b**:

Empirical formula	C66 H66 B3 Cl3 N O11.25	
Formula weight	1191.98	
Temperature	173(2) K	
Wavelength	0.71073 Å	
Crystal system	Monoclinic	
Space group	P 21	
Unit cell dimensions	a = 9.7855(9) Å	α= 90°.
	b = 46.667(5) Å	β= 109.379(2)°.

Table 2.13 cont'd

	c = 13.9815(14) Å γ = 90°.
Volume	6023.0(10) $Å^3$
Z	4
Density (calculated)	1.315 Mg/m^3
Absorption coefficient	0.215 mm^{-1}

Table 2.13 cont'd

F(000)	2500
Crystal size	0.23 x 0.14 x 0.11 mm^3
Theta range for data collection	1.54 to 25.40°.
Index ranges	-9<=h<=11, -50<=k<=56, -16<=l<=16
Reflections collected	26222
Independent reflections	17859 [R(int) = 0.0788]
Completeness to theta = 25.40°	99.6 %
Absorption correction	Semi-empirical from equivalents
Max. and min. transmission	0.9776 and 0.9528
Refinement method	Full-matrix least-squares on F^2
Data / restraints / parameters	17859 / 1 / 1489
Goodness-of-fit on F^2	0.983
Final R indices [I>2sigma(I)]	R1 = 0.1101, wR2 = 0.2734
R indices (all data)	R1 = 0.2096, wR2 = 0.3440
Absolute structure parameter	-0.02(18)
Largest diff. peak and hole	1.075 and -0.388 $e.Å^{-3}$

Table 2.14 Hydrogen bonds [Å and °]

D-H...A	d(D-H)	d(H...A)	d(D...A)	∠(DHA)
O(1B)-H(1BA)...O(4B)	**0.84**	1.92	2.751(10)	168.2
N(1A)-H(1AA)...O(1A)	**0.88**	1.91	2.789(13)	175.6
O(1A)-H(1AB)...O(3A)	**0.84**	1.90	2.701(11)	157.8
N(1B)-H(1BB)...O(1B)	**0.88**	1.87	2.748(13)	174.1

REFERENCES

REFERENCES

(1) (a) Rueping, M.; Nachtsheim, B. J.; Ieawsuwan, W.; Atodiresei, I. *Angew. Chem., Int. Ed.* **2011**, *50*, 6706-6720. (b) Schenker, S.; Zamfir, A.; Freund, M.; Tsogoeva, S. B. *Eur. J. Org. Chem.* **2011**, 2209-2222. (c) Rueping, M.; Kuenkel, A.; Atodiresei, I. *Chem. Soc. Rev.* **2011**, *40*, 4539-4549. (d) List, B.; Kampen, D.; Reisinger, C. M. *Top Curr Chem* **2010**, *291*, 395-456. (e) Rueping, M.; Koenigs, R. M.; Atodiresei, I. *Chem.–Eur. J.* **2010**, *16*, 9350-9365. (f) Sohtome, Y.; Nagasawa, K. *Synlett* **2010**, 1-22. (g) Yamamoto, H.; Payette, J. N. In *Hydrogen Bonding in Organic Synthesis*; Wiley-VCH 2009, p 73-140. (h) Yu, X.; Wang, W. *Chem.–Asian. J.* **2008**, *3*, 516-532. (i) Doyle, A. G.; Jacobsen, E. N. *Chem. Rev.* **2007**, *107*, 5713-5743. (j) Akiyama, T. *Chem. Rev.* **2007**, *107*, 5744-5758. (k) Taylor, M. S. J., E. N. *Angew. Chem., Int. Ed.* **2006**, *45*, 1520-1543. (l) Akiyama, T.; Itoh, J.; Fuchibe, K. *Adv. Synth. Catal.* **2006**, *348*, 999-1010.

(2) (a) Terada, M. *Synthesis* **2010**, 1929-1982. (b) Terada, M. *Bull. Chem. Soc. Jpn.* **2010**, *83*, 101-119. (c) Zamfir, A.; Schenker, S.; Freund, M.; Tsogoeva, S. B. *Org. Biomol. Chem.* **2010**, *8*. (d) Terada, M. *Chem. Commun. (Cambridge, U. K.)* **2008**, 4097-4112. (e) Connon, S. J. *Angew. Chem., Int. Ed.* **2006**, *45*, 3909-3912.

(3) (a) Rueping, M.; Uria, U.; Lin, M.-Y.; Atodiresei, I. *J. Am. Chem. Soc.* **2011**, *133*, 3732-3735. (b) Hashimoto, T.; Nakatsu, H.; Yamamoto, K.; Maruoka, K. *J. Am. Chem. Soc.* **2011**, *133*, 9730-9733. (c) Rueping, M.; Nachtsheim, B. J.; Koenigs, R. M.; Ieawsuwan, W. *Chem.–Eur. J.* **2010**, *16*, 13116-13126. (d) Vellalath, S.; Coric, I.; List, B. *Angew. Chem., Int. Ed.* **2010**, *49*, 9749-9752. (e) Cheon, C. H.; Yamamoto, H. *J. Am. Chem. Soc.* **2008**, *130*, 9246-9247. (f) Rueping, M.; Ieawsuwan, W.; Antonchick, A. P.; Nachtsheim, B. J. *Angew. Chem., Int. Ed.* **2007**, *46*, 2097-2100. (g) Nakashima, D.; Yamamoto, H. *J. Am. Chem. Soc.* **2006**, *128*, 9626-9627.

(4) (a) Ratjen, L.; Garcìa-Garcìa, P.; Lay, F.; Beck, M. E.; List, B. *Angew. Chem., Int. Ed.* **2011**, *50*, 754-758. (b) Chen, L.-Y.; He, H.; Chan, W.-H.; Lee, A. W. M. *J. Org. Chem.* **2011**, *76*, 7141-7147. (c) He, H.; Chen, L.-Y.; Wong, W.-Y.; Chan, W.-H.; Lee, A. W. M. *Eur. J. Org. Chem.* **2010**, 4181-4184. (d) Treskow, M.; Neudoerfl, J.; Giernoth, R. *Eur. J. Org. Chem.* **2009**, 3693-3697.

(5) Berkessel, A.; Christ, P.; Leconte, N.; Neudörfl, J.-M.; Schäfer, M. *Eur. J. Org. Chem.* **2010**, 5165-5170.

(6) (a) Hashimoto, T.; Omote, M.; Maruoka, K. *Angew. Chem., Int. Ed.* **2011**, *50*, 3489-3492. (b) Hashimoto, T.; Omote, M.; Maruoka, K. *Angew. Chem., Int. Ed.* **2011**, *50*, 8952-8955. (c) Hashimoto, T.; Kimura, H.; Nakatsu, H.; Maruoka, K. *J. Org. Chem.* **2011**, *76*, 6030-6037. (d) Hashimoto, T.; Kimura, H.; Maruoka, K. *Angew. Chem., Int. Ed.* **2010**, *49*, 6844-6847. (e)

Hashimoto, T.; Uchiyama, N.; Maruoka, K. *J. Am. Chem. Soc.* **2008**, *130*, 14380-14381. (f) Hashimoto, T.; Maruoka, K. *J. Am. Chem. Soc.* **2007**, *129*, 10054-10055.

(7) (a) Hatano, M.; Sugiura, Y.; Akakura, M.; Ishihara, K. *Synlett* **2011**, 1247-1250. (b) Hatano, M.; Sugiura, Y.; Ishihara, K. *Tetrahedron: Asymmetry* **2010**, *21*, 1311-1314. (c) Hatano, M.; Maki, T.; Moriyama, K.; Arinobe, M.; Ishihara, K. *J. Am. Chem. Soc.* **2008**, *130*, 16858-16860.

(8) (a) Desai, A. A.; Wulff, W. D. *Synthesis* **2010**, 3670-3680. (b) Rowland, E. B.; Rowland, G. B.; Rivera-Otero, E.; Antilla, J. C. *J. Am. Chem. Soc.* **2007**, *129*, 12084-12085.

(9) (a) Senatore, M.; Lattanzi, A.; Santoro, S.; Santi, C.; Della, S. G. *Org. Biomol. Chem.* **2011**, *9*, 6205-6207. (b) Desai, A. A.; Huang, L.; Wulff, W. D.; Rowland, G. B.; Antilla, J. C. *Synthesis* **2010**, 2106-2109. (c) Larson, S. E.; Baso, J. C.; Li, G.; Antilla, J. C. *Org. Lett.* **2009**, *11*, 5186-5189. (d) Della, S. G.; Lattanzi, A. *Org. Lett.* **2009**, *11*, 3330-3333. (e) Rowland, G. B.; Rowland, E. B.; Liang, Y.; Perman, J. A.; Antilla, J. C. *Org. Lett.* **2007**, *9*, 2609-2611. (f) Liang, Y.; Rowland, E. B.; Rowland, G. B.; Perman, J. A.; Antilla, J. C. *Chem. Commun.* **2007**, 4477-4479. (g) Li, G.; Liang, Y.; Antilla, J. C. *J. Am. Chem. Soc.* **2007**, *129*, 5830-5831. (h) Rowland, G. B.; Zhang, H.; Rowland, E. B.; Chennamadhavuni, S.; Wang, Y.; Antilla, J. C. *J. Am. Chem. Soc.* **2005**, *127*, 15696-15697.

(10) (a) Xu, B.; Zhu, S.-F.; Xie, X.-L.; Shen, J.-J.; Zhou, Q.-L. *Angew. Chem., Int. Ed.* **2011**, *50*, 11483-11486. (b) Xing, C.-H.; Liao, Y.-X.; Ng, J.; Hu, Q.-S. *J. Org. Chem.* **2011**, *76*, 4125-4131. (c) Müller, S.; Webber, M. J.; List, B. *J. Am. Chem. Soc.* **2011**, *133*, 18534-18537. (d) Huang, D.; Xu, F.; Lin, X.; Wang, Y. Chiral spirocyclic phosphoric acid, its preparation method and application as catalyst CN102030780A Apr 27, 2011. (e) Xu, F.; Huang, D.; Han, C.; Shen, W.; Lin, X.; Wang, Y. *J. Org. Chem.* **2010**, *75*, 8677-8680. (f) Coric, I.; Mueller, S.; List, B. *J. Am. Chem. Soc.* **2010**, *132*, 17370-17373.

(11) (a) Akiyama, T. Preparation of cyclic erythritol phosphoric acid derivatives as catalysts for asymmetric synthesis WO2006092884A1 . (b) Voituriez, A.; Charette, A. B. *Adv. Synth. Catal.* **2006**, *348*, 2363-2370. (c) Akiyama, T.; Saitoh, Y.; Morita, H.; Fuchibe, K. *Adv. Synth. Catal.* **2005**, *347*, 1523-1526.

(12) (a) Ishihara, K.; Miyata, M.; Hattori, K.; Tada, T.; Yamamoto, H. *J. Am. Chem. Soc.* **1994**, *116*, 10520-10524. (b) Ishihara, K.; Kuroki, Y.; Yamamoto, H. *Synlett* **1995**, 41-42. (c) Kuroki, Y.; Ishihara, K.; Hanaki, N.; Ohara, S.; Yamamoto, H. *Bull. Chem. Soc. Jpn.* **1998**, *71*, 1221-1230. (d) Cros, J. P.; Pérez-Fuertes, Y.; Thatcher, M. J.; Arimori, S.; Bull, S. D.; James, T. D. *Tetrahedron: Asymmetry* **2003**, *14*, 1965-1968. (e) Kawate, T.; Yamada, H.; Matsumizu, M.; Nishida, A.; Nakagawa, M. *Synlett* **1997**, 761-762. (f) Yamada, H.; Kawate, T.; Matsumizu, M.; Nishida, A.; Yamaguchi, K.; Nakagawa, M. *J. Org. Chem.* **1998**, *63*, 6348-6354.

(13) (a) Zhang, Y.; Desai, A.; Lu, A.; Hu, G.; Ding, Z.; Wulff, W. D. *Chem. –Eur. J.* **2008**, *14*, 3785-3803. (b) Zhang, Y.; Lu, Z.; Desai, A.; Wulff, W. D. *Org. Lett.* **2008**, *10*, 5429-5432. (c) Mukherjee, M.; Gupta, A. K.; Lu, Z.; Zhang, Y.; Wulff, W. D. *J. Org. Chem.* **2010**, *75*, 5643-5660. (d) Ren, H.; Wulff, W. D. *Org. Lett.* **2010**, *12*, 4908-4911. (e) Hu, G.; Huang, L.; Huang, R. H.; Wulff, W. D. *J. Am. Chem. Soc.* **2009**, *131*, 15615-15617. (f) Hu, G.; Gupta, A. K.; Huang, R. H.; Mukherjee, M.; Wulff, W. D. *J. Am. Chem. Soc.* **2010**, *132*, 14669–14675. (g) Gupta, A. K.; Mukherjee, M.; Wulff, W. D. *Org. Lett.* **2011**, *13*, 5866-5869. (h) Newman, C. A.; Antilla, J. C.; Chen, P.; Predeus, A. V.; Fielding, L.; Wulff, W. D. *J. Am. Chem. Soc.* **2007**, *129*, 7216-7217. (i) Desai, A. A.; Wulff, W. D. *J. Am. Chem. Soc.* **2010**, *132*, 13100-13103. (j) Vetticatt, M. J.; Desai, A. A.; Wulff, W. D. *J. Am. Chem. Soc.* **2010**, *132*, 13104-13107. (k) Desai, A. A.; Morán-Ramallal, R.; Wulff, W. D. *Org. Synth.* **2011**, *88*, 224-237. (l) Ren, H.; Wulff, W. D. *J. Am. Chem. Soc.* **2011**, *133*, 5656-5659. (m) Desai, A. A.; Ren, H.; Mukherjee, M.; Wulff, W. D. *Org. Process Res. Dev.* **2011**, *15*, 1108-1115.

(14) Casarrubios, L.; Perez, J. A.; Brookhart, M.; Templeton, J. L. *J. Org. Chem.* **1996**, *61*, 8358-8359.

(15) (a) Antilla, J. C.; Wulff, W. D. *J. Am. Chem. Soc.* **1999**, *121*, 5099-5100. (b) Antilla, J. C.; Wulff, W. D. *Angew. Chem., Int. Ed.* **2000**, *39*, 4518-4521.

(16) Hattori, K.; Yamamoto, H. *J. Org. Chem.* **1992**, *57*, 3264-3265.

(17) Favrot, J.; Vocelle, D.; Sandorfy, C. *Photochem. Photobiol.* **1979**, *30*, 417-421.

(18) Ding, Z.; Osminski, W. E. G.; Ren, H.; Wulff, W. D. *Org. Process Res. Dev.* **2011**, *15*, 1089-1107 and references therein.

(19) Lu, Z.; Zhang, Y.; Wulff, W. D. *J. Am. Chem. Soc.* **2007**, *129*, 7185-7194.

(20) Gaussian 03, Revision D.01 M. J. Frisch, G. W. T., H. B. Schlegel, G. E. Scuseria, M. A. Robb, J. R. Cheeseman, J. A. Montgomery, Jr., T. Vreven, K. N. Kudin, J. C. Burant, J. M. Millam, S. S. Iyengar, J. Tomasi, V. Barone, B. Mennucci, M. Cossi, G. Scalmani, N. Rega, G. A. Petersson, H. Nakatsuji, M. Hada, M. Ehara, K. Toyota, R. Fukuda, J. Hasegawa, M. Ishida, T. Nakajima, Y. Honda, O. Kitao, H. Nakai, M. Klene, X. Li, J. E. Knox, H. P. Hratchian, J. B. Cross, V. Bakken, C. Adamo, J. Jaramillo, R. Gomperts, R. E. Stratmann, O. Yazyev, A. J. Austin, R. Cammi, C. Pomelli, J. W. Ochterski, P. Y. Ayala, K. Morokuma, G. A. Voth, P. Salvador, J. J. Dannenberg, V. G. Zakrzewski, S. Dapprich, A. D. Daniels, M. C. Strain, O. Farkas, D. K. Malick, A. D. Rabuck, K. Raghavachari, J. B. Foresman, J. V. Ortiz, Q. Cui, A. G. Baboul, S. Clifford, J. Cioslowski, B. B. Stefanov, G. Liu, A. Liashenko, P. Piskorz, I. Komaromi, R. L. Martin, D. J. Fox, T. Keith, M. A. Al-Laham, C. Y. Peng, A. Nanayakkara, M.

Challacombe, P. M. W. Gill, B. Johnson, W. Chen, M. W. Wong, C. Gonzalez, and J. A. Pople, Gaussian, Inc., Wallingford CT, 2004

(21) (a) Nishio, M. *Tetrahedron* **2005**, *61*, 6923-6950. (b) Nishio, M. H., M.; Umezawa, Y. *The CH/π Interaction: Evidence, Nature, and Consequences*; Wiley-VCH, 1998.

(22) Plevin, M. J.; Bryce, D. L.; Boisbouvier, J. *Nat Chem* **2010**, *2*, 466-471.

(23) Hall, H. K. *J. Am. Chem. Soc.* **1957**, *79*, 5441-5444.

(24) Braude, E. A.; Nachod, F. C.; Phillips, W. D.; Zuckerman, J. J. *Determination of Organic Structures by Physical Methods*; Academic Press: New York, 1955.

(25) Chiang, Y.; Whipple, E. B. *J. Am. Chem. Soc.* **1963**, *85*, 2763-2767.

(26) Desai, A.; Wulff, W. D., Unpublished results.

(27) Haake, P.; Cook, R. D.; Hurst, G. H. *J. Am. Chem. Soc.* **1967**, *89*, 2650-2654.

(28) Landini, D.; Modena, G.; Scorrano, G.; Taddei, F. *J. Am. Chem. Soc.* **1969**, *91*, 6703-6707.

(29) Hall, S. K.; Robinson, E. A. *Can. J. Chem.* **1964**, *42*, 1113-1122.

(30) Cook, A. G.; Mason, G. W. *J. Org. Chem.* **1972**, *37*, 3342-3345.

(31) Bell, R. P.; Higginson, W. C. E. *Proc. R. Soc. Lond. A* **1949**, *197*, 141-159.

(32) Jaffé, H. H.; Doak, G. O. *J. Am. Chem. Soc.* **1955**, *77*, 4441-4444.

(33) Kanbayashi, N.; Onitsuka, K. *Angew. Chem., Int. Ed.* **2011**, *50*, 5197-5199.

(34) Ghorbani-Choghamarani, A.; Sardari, S. *Chinese Journal of Catalysis* **2010**, *31*, 1347-1350.

(35) Luca, O. R.; Wang, T.; Konezny, S. J.; Batista, V. S.; Crabtree, R. H. *New J. Chem.* **2011**, *35*, 998-999.

(36) Hu, Z.; Kerton, F. M. *Org. Biomol. Chem.* **2012**, *10*, 1618-1624.

(37) Cole, T. E.; Quintanilla, R.; Rodewald, S. *Synth. React. Inorg. Met.-Org. Chem.* **1990**, *20*, 55-63.

(38) (a) Becke, A. D. *Phys. Rev. A* **1988**, *38*, 3098. (b) Lee, C. Y., W.; Parr, R. G. *Phys. Rev. B* **1988**, *37*, 785.

(39) (a) Becke, A. D. *J. Chem. Phys.* **1993**, *98*, 1372-1377. (b) Zhao, Y.; Truhlar, D. G. *J. Chem. Theory Comput.* **2005**, *1*, 415-432. (c) Yu, W.; Liang, L.; Lin, Z.; Ling, S.; Haranczyk, M.; Gutowski, M. *J. Comput. Chem.* **2009**, *30*, 589-600.

CHAPTER 3

MECHANISTIC STUDY OF THE CATALYTIC CYCLE OF A BRØNSTED ACID CATALYZED REACTION UTILIZING AZIRIDINATION AS THE TEMPLATE

I think you do not have enough work these days.

-William D. Wulff

3.1 Introduction

Generally, in a Brønsted acid catalyzed reaction (Scheme 3.1), substrate (S) binds to the catalyst (BA) giving S-BA complex that further reacts with nucleophile (Nu) resulting in a complex where product is bound to the catalyst (P-BA). This complex collapses to release the product (P) and the catalyst (BA). There is another associative pathway (Path II) where substrate directly replaces product from P-BA complex to give S-BA complex. To best of our knowledge, there is no example in literature, which provides evidence for the existence of such proposed complexes, especially the product bound to the catalyst in the case of the aziridination reaction. The aim of this work is to characterize and otherwise gain evidence for the existence of such complexes and other intermediates of the catalytic cycle. Another goal of this work is to explore the possibility of observing the depletion of P-BA complex in the presence of the substrate (S). The catalytic cycle of other systems have been studied using NMR spectroscopy,[1] mass spectrometry[2] and theoretical calculations.[3]

Scheme 3.1 Catalytic cycle of a Brønsted acid catalyzed reaction

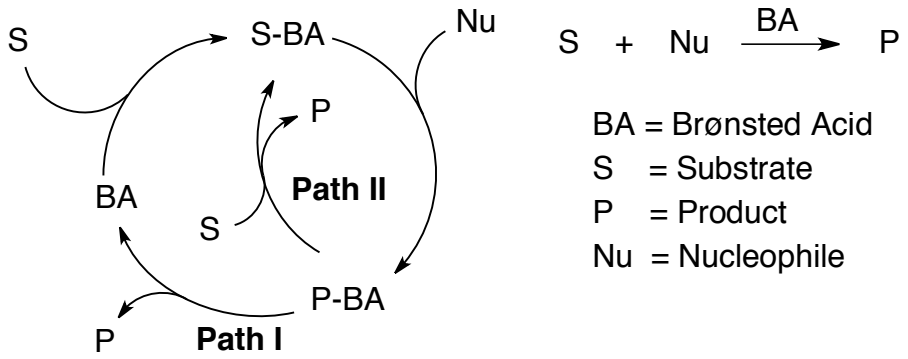

3.2 Characterization of the various stages of the catalytic cycle of a Brønsted Acid catalyzed aziridination reaction

In the field of organic synthesis, importance has always been given to efforts to provide tangible evidence to support the proposed mechanisms or reaction pathways. Most of the time, this helps to gain insight which can be the spark leading to new discoveries. With the aim of understanding the mechanistic aspect of our aziridination reaction, we decided to characterize the various proposed complexes and intermediates of the catalytic cycle. This, in turn, might support the existence of the proposed complexes in a general catalytic cycle of any Brønsted acid catalyzed reaction. Hence, our aziridination reaction might serve as the template for the catalytic cycle of a Brønsted acid catalyzed reaction. There is no such study reported in case of a Brønsted acid catalyzed reaction.[4] Over the last several years we have developed a general catalytic asymmetric aziridination that is based on the reaction of diazo compounds with imines mediated by asymmetric catalysts generated from the VANOL or VAPOL ligands and various boron compounds (Scheme 3.2).[5] As discussed in Chapter 2, the protocol for catalyst formation involves 3 equivalents of commercial $B(OPh)_3$ and 1 equivalent of ligand giving the mixture of

B1 **106**/**107** and B2 **108**/**109** (Scheme 3.2). Thereafter, the actual IMINO-BOROX catalyst is formed only upon the addition of the substrate i.e. imine. As mentioned earlier, the IMINO-BOROX catalyst **190** is comprised of a chiral borate anion containing a spiro-boroxinate ring and a protonated iminium ion (Scheme 3.2).[5f]

Scheme 3.2 Brønsted acid catalyzed aziridination reaction

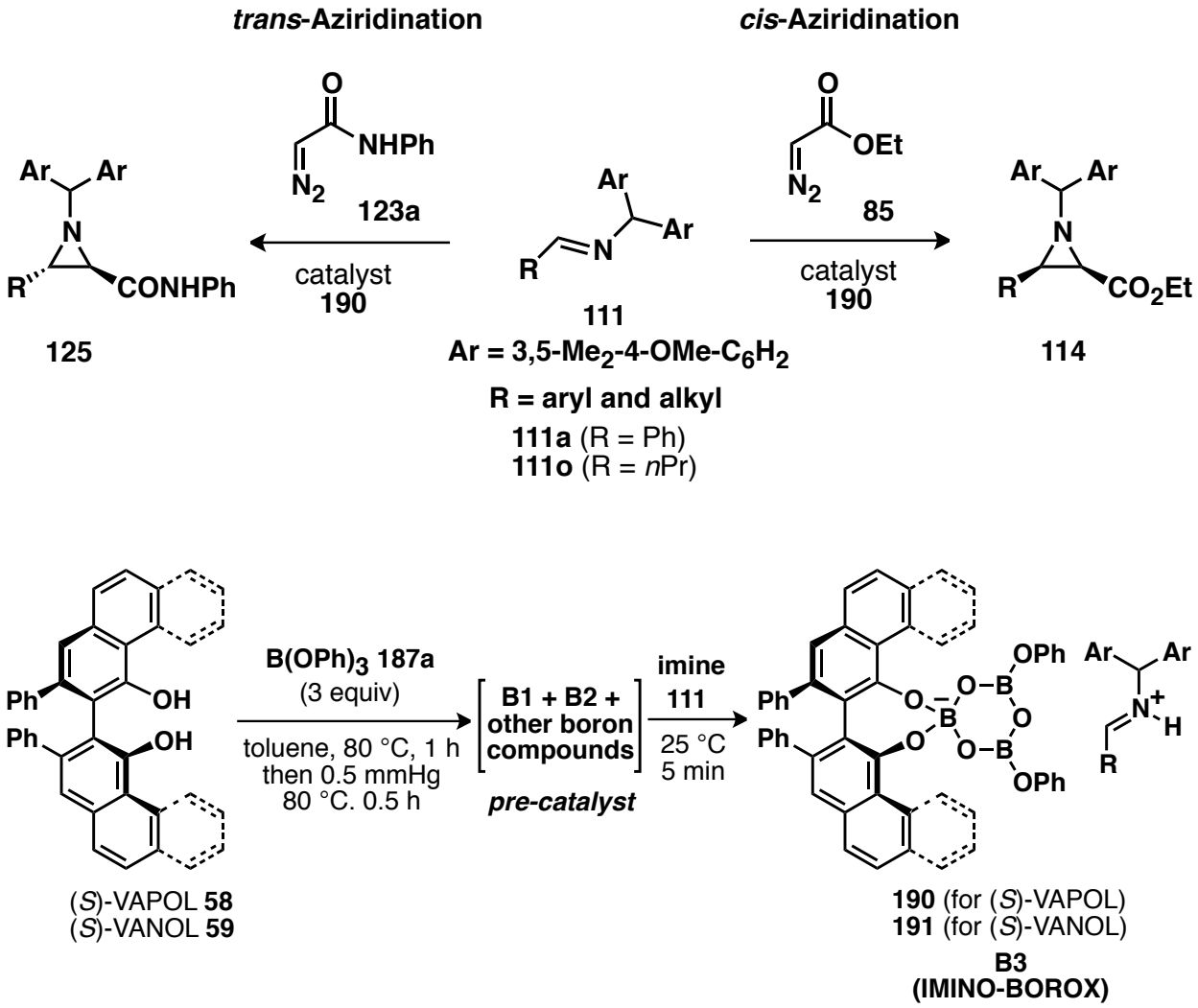

Scheme 3.2 cont'd

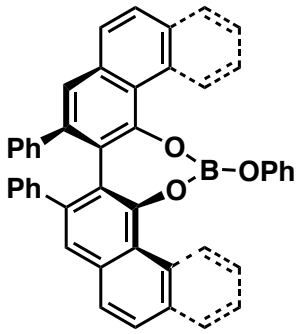

106 (for (*S*)-VAPOL)
107 (for (*S*)-VANOL)
B1

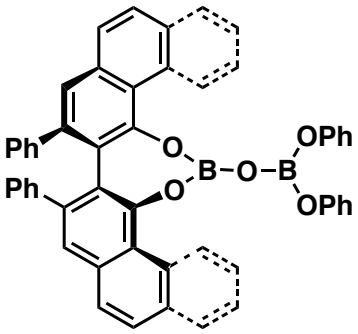

108 (for (*S*)-VAPOL)
109 (for (*S*)-VANOL)
B2

The catalytic cycle pertaining to the catalytic asymmetric aziridination reaction is shown in Scheme 3.3. As said earlier, addition of imine **111** to the pre-catalyst and other borates sources including commercial $B(OPh)_3$ and triphenoxyboroxine **191a** generates IMINO-BOROX catalyst **190**. Subsequent attack of diazoester **85** should form the proposed boroxinate-aziridine complex **239** (AZIRIDINO-BOROX) where aziridine is bound to the catalyst. Turnover then would lead to the loss of aziridine and then incorporation of another molecule of the imine **111** regenerating the IMINO-BOROX **190**. While we have not been able to obtain any direct evidence for the presence of the protonated boroxinate species **23**-H (Free BOROX), it is not clear if the overall conversion of the AZIRIDINO-BOROX **239** to the IMINO-BOROX **190** involves loss of aziridine to give the Brønsted acid **23**-H which then protonates the imine to give **190**, or if there is an associative reaction between **239** and the imine **111** which directly leads to the aziridine **114** and the IMINO-BOROX **190**. The fact that this reaction turns over is consistent with the assumption that aziridine is, most likely, significantly slower in inducing boroxinate formation than the imine.

Scheme 3.3 Catalytic cycle of a Brønsted acid catalyzed aziridination reaction

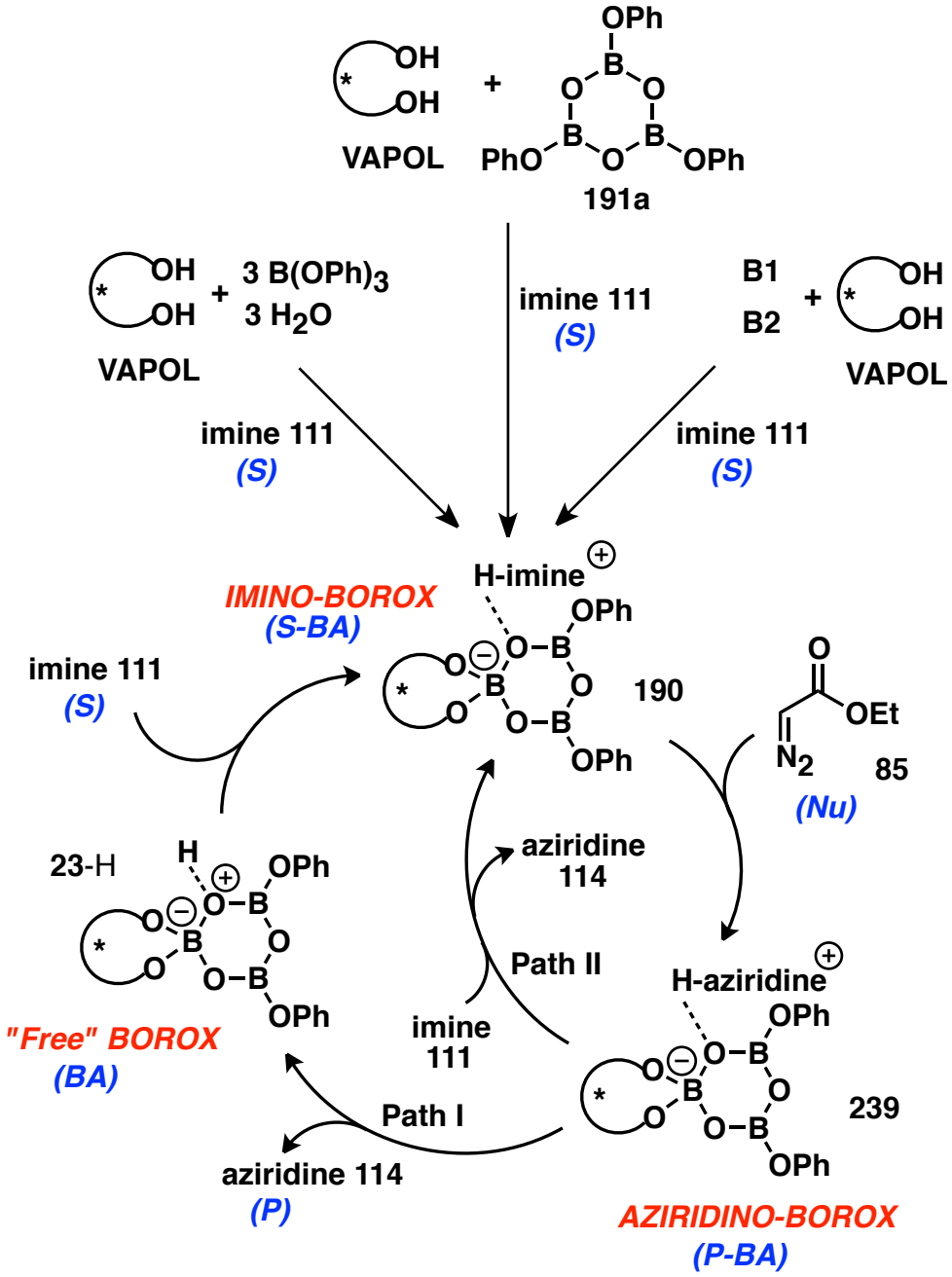

3.2.1 Evidence for IMINO-BOROX complex

In terms of the characterization of various stages of the catalytic cycle, we have already presented evidence for the structure and involvement of an IMINO-BOROX species as the

catalyst with the help of NMR spectroscopy and X-ray analysis.[5f] The identification of this species is facilitated by the fact that the bay protons (Hb) of VAPOL and its derivatives, which include IMINO-BOROX catalyst, are quite distinct (Figure 3.1). For VAPOL this doublet is at δ = 9.77 ppm ($CDCl_3$). The formation of the three B-O-B linkages in the boroxine ring in the BOROX catalyst **190** requires 3 equiv of water and the source of this most certainly results from partial hydrolysis of commercial $B(OPh)_3$. This is supported by the fact that no boroxinate occurs with extremely pure $B(OPh)_3$.[5f] Hence, we decided to study the effect of the addition of water on the generation of the IMINO-BOROX catalyst **190**.

Figure 3.1 Chemical shift of the bay proton of (*S*)-VAPOL **58** and its different derivatives

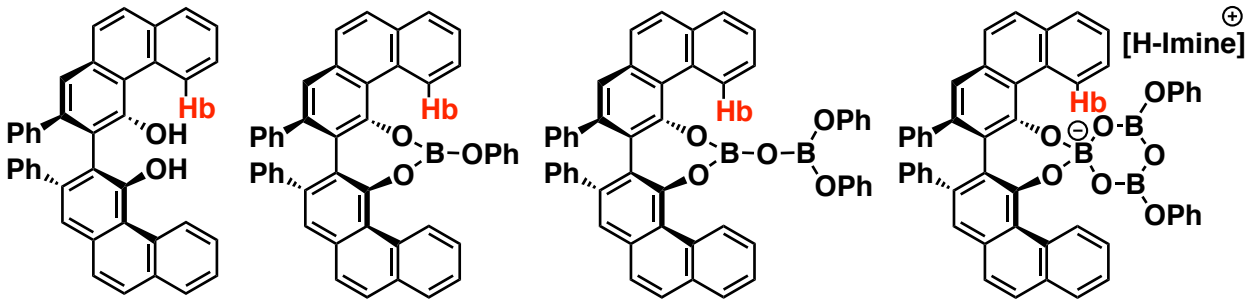

(*S*)-VAPOL **58**

δ = 9.77 ppm ($CDCl_3$)
δ = 9.91 ppm (d8-toluene)

mesoborate B1 **106**

δ = 9.55 ppm ($CDCl_3$)
δ = 9.77 ppm (d8-toluene)

pyroborate B2 **108**

δ = 9.22 ppm ($CDCl_3$)
δ = 9.55 ppm (d8-toluene)

IMINO-BOROX B3 **190** (imine = **111**)

δ ~ 10.3-10.4 ppm ($CDCl_3$)
δ ~ 10.5-10.6 ppm (d8-toluene)

As shown in Figure 3.2B, the traditional method for catalyst formation involves heating (*S*)-VAPOL with 3 equiv of commercial $B(OPh)_3$ at 80 °C generating the pre-catalyst (method A, Figure 3.2B, entry 1). Another procedure was also employed where 3 equiv of H_2O was

added to the mixture of ligand and commercial $B(OPh)_3$ (method B, Figure 3.2B, entry 3). With method A, the pyroborate **108** is formed in 53% yield (41% with H_2O, method B) along with a 6% yield (5% with H_2O, method B) of the mesoborate **106** and 20% (45% with H_2O, method B) of unreacted VAPOL **58** (Figure 3.2B, entries 1 and 3) as monitored by ^1H NMR spectroscopy. Treatment of either of these mixtures with 1 equiv of the imine **111a** (R = Ph) at room temperature resulted within a few minutes in the conversion of the colorless solution of **106** and **108** to a red solution of IMINO-BOROX catalyst **190a** in 90% yield (also 90% with H_2O, method B). There is not much change in terms of the yield of **190a** with respect to either method, however the amount of B2 **108** is higher in case of method A (entry 1 verses 3). The presence of the BOROX catalyst **190a** was indicated by the broadened doublet at δ =10.23 ppm (Figure 3.2B, entries 2 and 4). In order to confirm that other imines could induce catalyst formation, we utilized alkyl imines **111o** (R = *n*-propyl) and **112o′** (R = ethyl) to form the catalyst. Indeed, both imines generated the boroxinate catalysts **190o** and **213o′** in 49% yield (Figure 3.2B, entry 5) and 60% yield (Figure 3.2B, entry 6) respectively. Another tool utilized in this analysis is the ^{11}B NMR spectrum. Most, three coordinate aryl borate compounds have very broad absorptions at 16-18 ppm in the ^{11}B NMR spectrum. However, the increased spherical symmetry of four coordinate boron leads to sharp lines in the spectrum and the negative charge of the borate causes an up field shift. The IMINO-BOROX catalysts **190a**, **190o** and **213o′** have sharp absorptions at 5.38, 5.35 and 5.48 ppm respectively (Figure 3.2C, entries 2, 5 and 6). The X-ray structure of **190a** has been reported previously.[5f]

Figure 3.2 (**A**) Imine induced boroxinate catalyst formation. (**B**)[a] ^{1}H NMR spectra in $CDCl_3$ with Ph_3CH as internal standard with yields of boroxinate catalysts in parenthesis. (**C**) ^{11}B NMR spectra corresponding to the ^{1}H NMR spectra in Figure 3.2B.

A

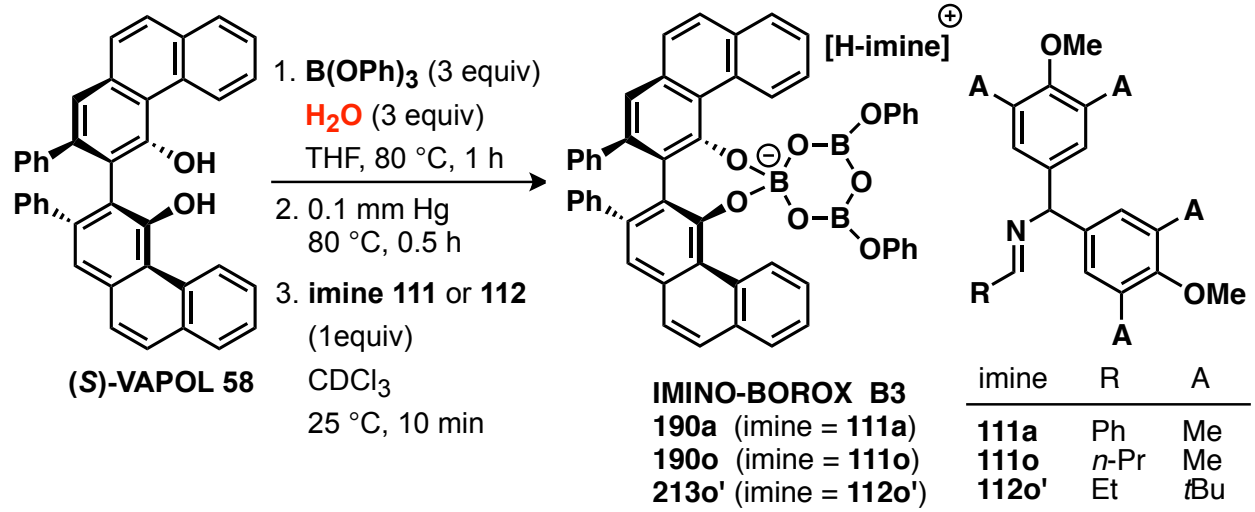

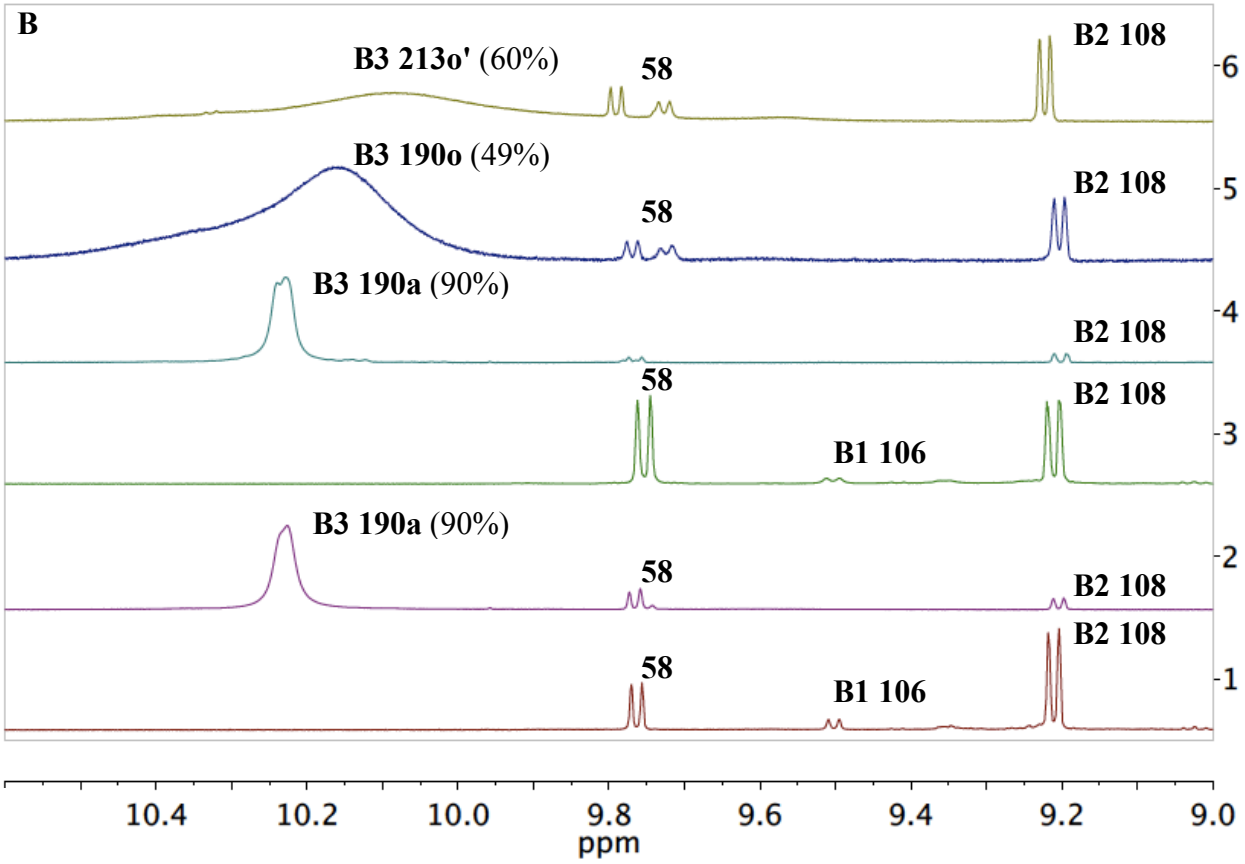

Figure 3.2 cont'd

C

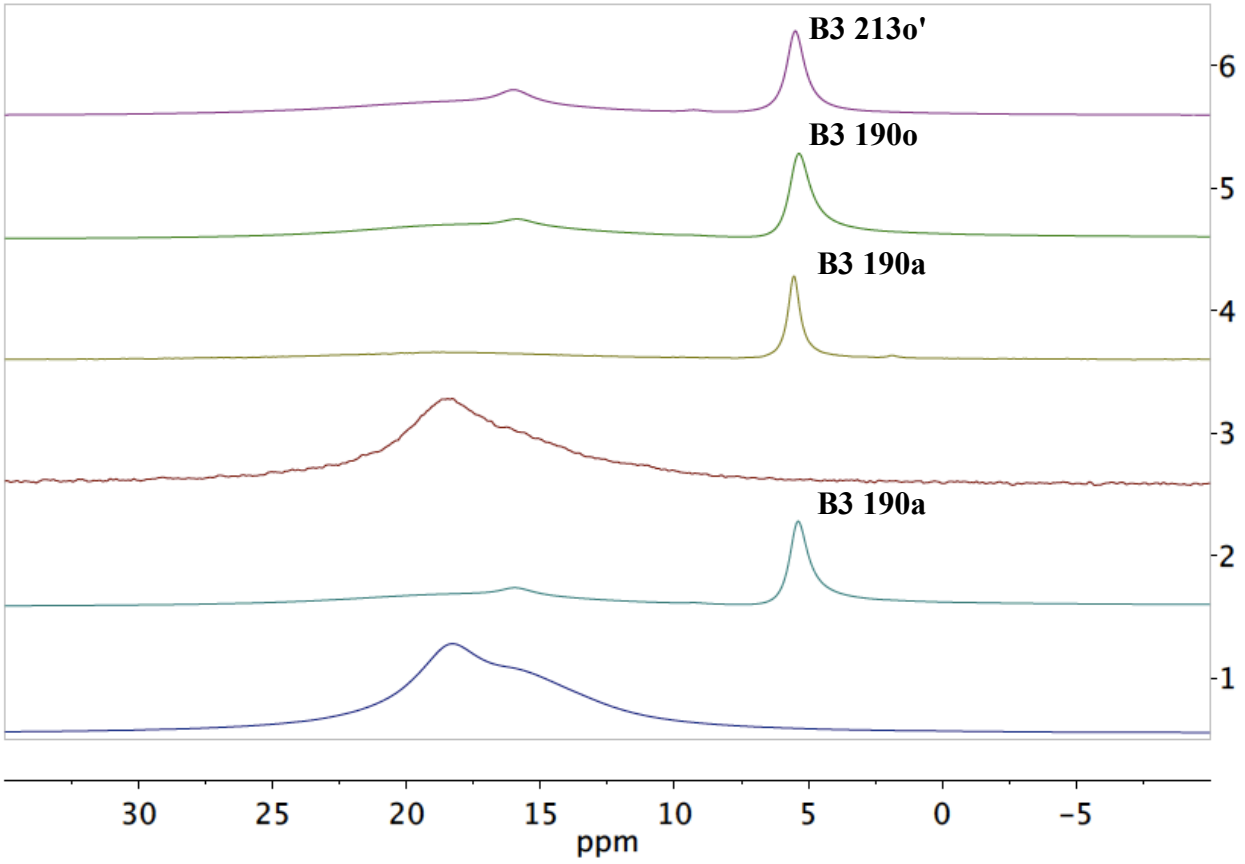

[a] Note for Figure 3.2B: Entry 1: (*S*)-VAPOL (0.1 mmol) plus 3 equiv of commercial $B(OPh)_3$ were heated at 80 °C in THF for 1 h followed by removal of volatiles under vacuum for 0.5 h (method A). Entry 2: 1.0 equiv of imine **111a** added to the solution in entry 1 for 10 min at 25 °C. Entry 3: Same as entry 1 except that 3 equiv of H_2O was also added to make the pre-catalyst (method B). Entry 4: 1.0 equiv of imine **111a** added to the solution in entry 3 for 10 min at 25 °C. Entry 5: 1.0 equiv of imine **111o** added to the solution in entry 3 for 10 min at 25 °C. Entry 6: 1.0 equiv of imine **112o′** added to the solution in entry 3 for 10 min at 25 °C.

3.2.2 Evidence for an AZIRIDINO-BOROX complex

Next, we moved on with the attempts to find evidence for the AZIRIDINO-BOROX specie **239**. In the past, there have been a lot of unsuccessful attempts in our group.

3.2.2.1 Monitoring the reaction by ^{1}H NMR Spectroscopy

One of the ways of observing AZIRIDINO-BOROX **239** is to follow the aziridination reaction by ^{1}H NMR spectroscopy. Presumably, that imine has higher binding affinity compared to the aziridine, which results in turnover. However, it was thought that the presence of **239** could perhaps be observable towards the end of the reaction when the amount of aziridine is much larger than the amount imine and this might help shift the equilibrium towards **239**. Hence we decided to follow the reaction using ^{1}H NMR spectroscopy. We employed three different procedures as shown in Scheme 3.4. The formation of aziridine and the alkylated VAPOL derivative **230** was observed in each case. The results are summarized in Table 3.1. A detailed discussion on the formation of **230** is given in section 3.2.4.

Scheme 3.4 Different procedures used to perform and monitor the aziridination reaction

Procedure i

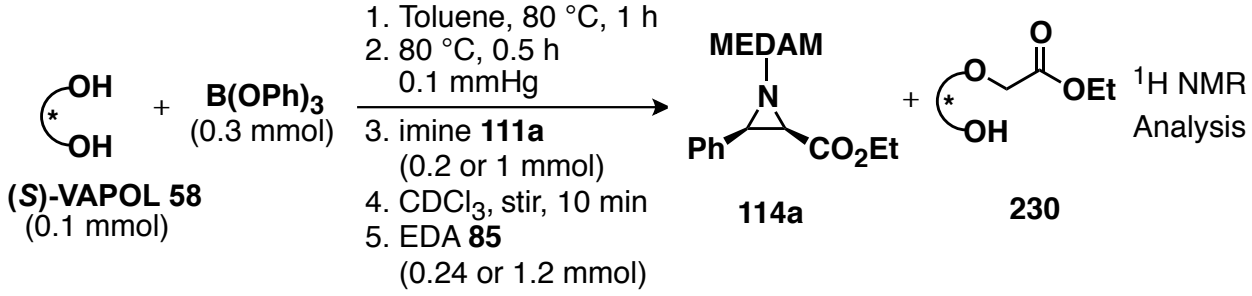

Procedure ii

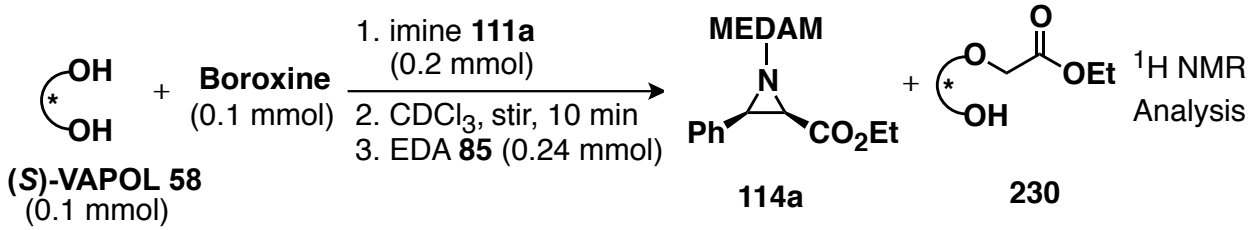

Scheme 3.4 cont'd

Procedure iii

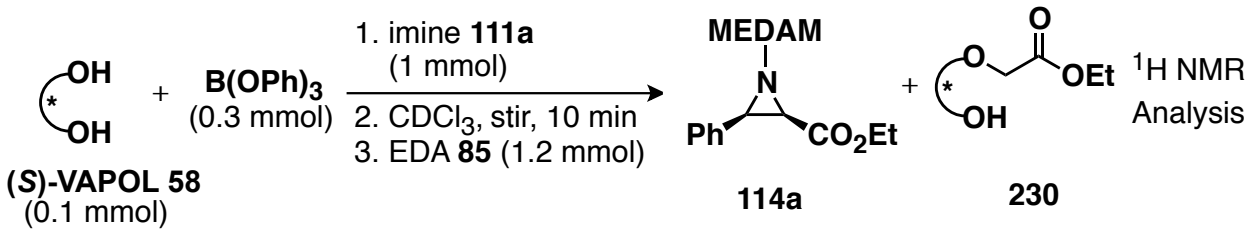

Table 3.1 Monitoring aziridination reaction by ^{1}H NMR spectroscopy [a]

	#	Proc [b]	Time (min)	(*S*)-VAPOL **58** [c,d]	**230**	B1 **106** [d]	B2 **108** [d]	B3 **190a** [d]	B3 **190a** [e]	**114a** [e]
B(OPh)3										
Before imine	X1	i	10	20	-	6	53	-	-	-
After imine (10 equiv)	X2	i	10	<1	-	<1	6	55	6	-
After EDA (12 equiv)	X3	i	10	<1	<1	<1	<1	62	6	31
	X4	i	30	14	38	8	20	20	2	96
	X5	i	80	18	37	<1	27	8	1	97
	X6	i	95	15	32	<1	25	<1	<1	99
B(OPh)3										
Before imine	Y1	i	10	20	-	6	53	-	-	-
After imine (2 equiv)	Y2	i	10	2	-	<1	13	81	41	-
After EDA (2.4 equiv)	Y3	i	10	2	<1	3	10	82	41	11
	Y4	i	15	<1	26	7	27	23	11	90
Boroxine										
Before imine	Y5	ii	-	69	-	4	23	-	-	-
After imine (2 equiv)	Y6	ii	10	19	-	<1	<1	55	28	-
After EDA (2.4 equiv)	Y7	ii	10	24	9	<1	1	66	33	65
	Y8	ii	15	12	38	<1	4	46	23	73
	Y9	ii	25	7	45	<1	4	38	19	78

Table 3.1 cont'd

	Y10	ii	75	4	52	<1	4	33	17	79
B(OPh)$_3$ Before imine	Z1	iii	10	85	-	<1	3	-		-
After imine (10 equiv)	Z2	iii	10	11	-	<1	<1	41	4	-
After EDA (12 equiv)	Z3	iii	15	10	<1	<1	<1	31	3	15
	Z4	iii	20	10	<1	<1	<1	31	3	17
	Z5	iii	25	11	<1	<1	<1	34	3	21
	Z6	iii	30	11	<1	<1	<1	34	3	22
	Z7	iii	60	12	<1	<1	<1	34	3	35
	Z8	iii	75	13	<1	<1	<1	34	3	65
	Z9	iii	90	14	<1	<1	<1	34	3	69
	Z10	iii	120	20	<1	<1	<1	47	5	82
	Z11	iii	160	26	9	<1	<1	45	5	86
	Z12	iii	170	27	11	<1	<1	30	3	88

[a] Unless otherwise specified, all NMR samples were prepared with (*S*)-VAPOL **58** (0.1 mmol), commercial $B(OPh)_3$ (0.3 mmol) or boroxine **191a** (0.1 mmol) and imine **111a** in $CDCl_3$ (1 mL) utilizing method i-iii. [b] For different methods; see scheme 3.4. [c] Unreacted (*S*)-VAPOL **58**. [d] NMR yield with Ph_3CH as internal standard with (*S*)-VAPOL **58** as the limiting reagent. [e] NMR yield with Ph_3CH as internal standard with imine **111a** as the limiting reagent.

Irrespective of various methods, there is no sign of AZIRIDINO-BOROX complex at any time interval. This was most evident in Figure 3.3A as there was no new significant peak in the bay region of the ^1H NMR spectrum of the ligand nor in the ^{11}B NMR spectrum.

Figure 3.3 (**A**) **A-01**: ^1H NMR spectra in $CDCl_3$ with Ph_3CH as internal standard (procedure i). Entry 1: (*S*)-VAPOL (0.1 mmol) plus 3 equiv commercial $B(OPh)_3$ were heated at 80 °C in toluene for 1 h followed by removal of volatiles under vacuum for 0.5 h. Entry 2: 10 equiv of imine **111a** added to the solution in entry 1 for 10 min at 25 °C. Entry 3: 12 equiv of EDA **85** added to the solution in entry 2 for 10 min at 25 °C. Entry 4: Same as entry 3 after 30 min.

Figure 3.3 cont'd

Entry 5: Same as entry 3 after 80 min. Entry 6: Same as entry 3 after 95 min. **A-02**: ^{1}H NMR spectra of the methoxy and methyl regions corresponding to the entries in Figure 3.3A-01. **A-03**: ^{11}B NMR spectra corresponding to the ^{1}H NMR spectra (entries 1, 2, 5 and 6) in Figure 3.3A-01. (**B**) ^{1}H NMR spectra in $CDCl_3$ with Ph_3CH as internal standard. The reaction is performed using procedures i and ii using 2 equiv of imine **111a** and 2.4 equiv of EDA **85**; see scheme 3.4 for procedures i and ii. (**C**) ^{1}H NMR spectra in $CDCl_3$ with Ph_3CH as internal standard. The reaction is performed using method iii using 10 equiv of imine **111a** and 12 equiv of EDA **85**; see scheme 3.4 for procedure iii.

A

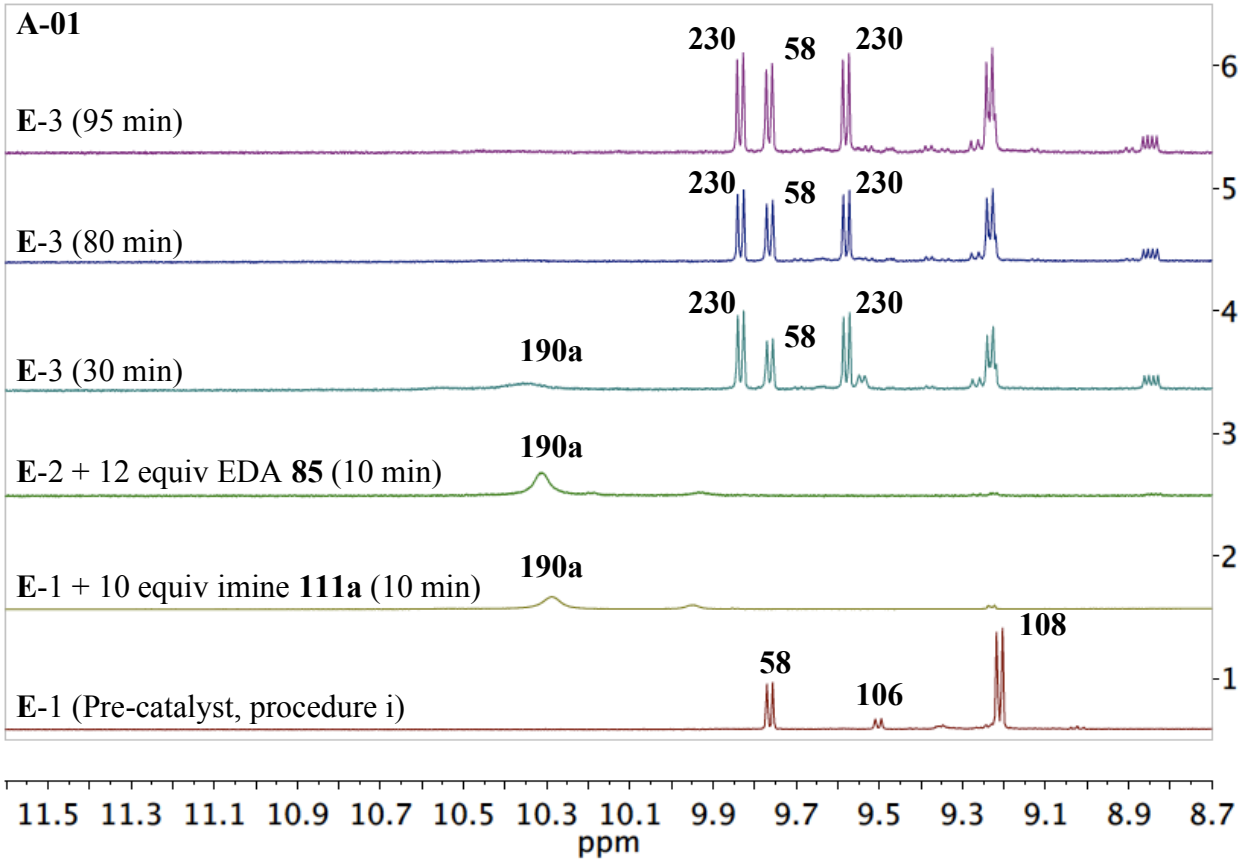

Figure 3.3 cont'd

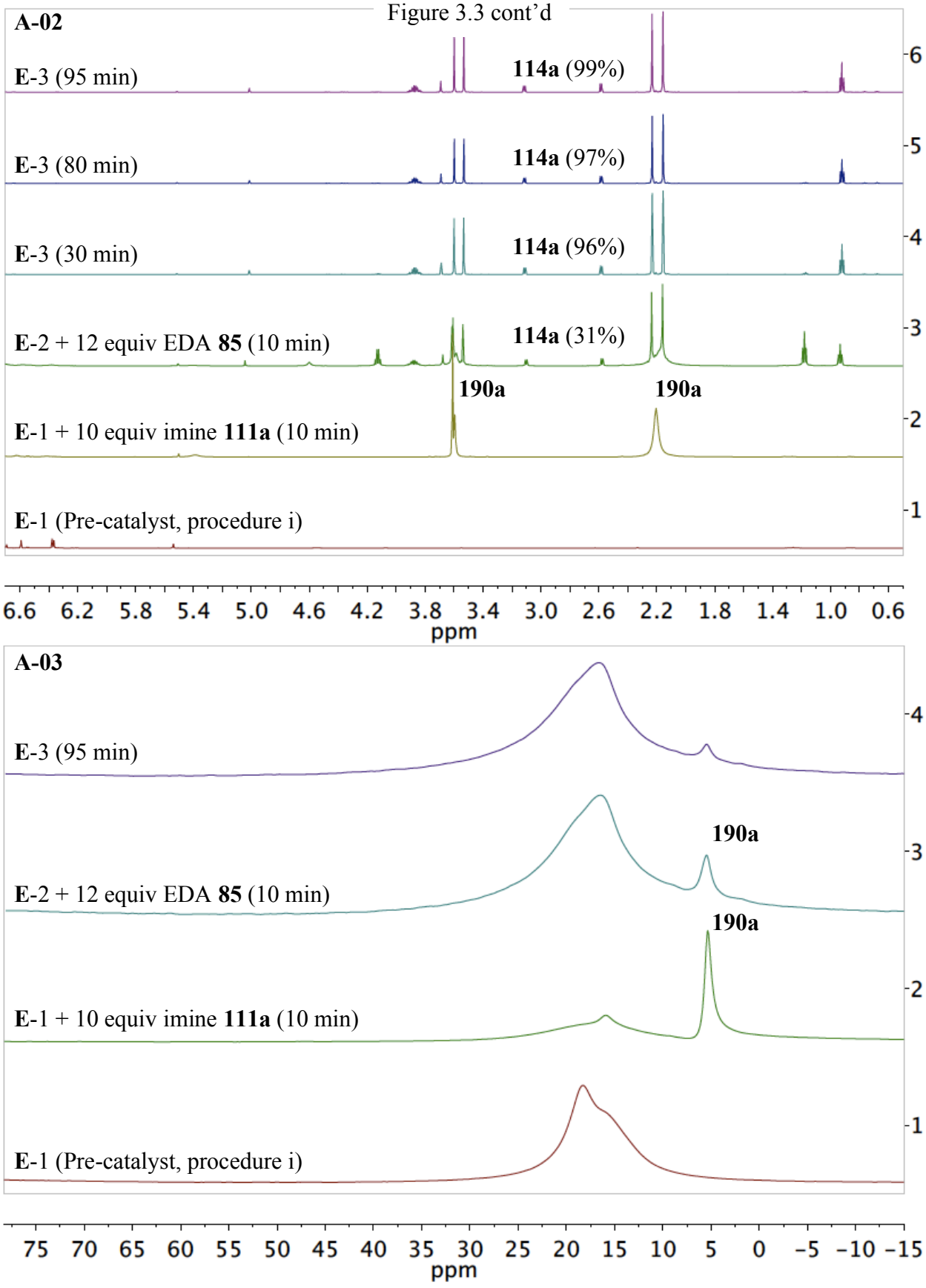

Figure 3.3 cont'd

B

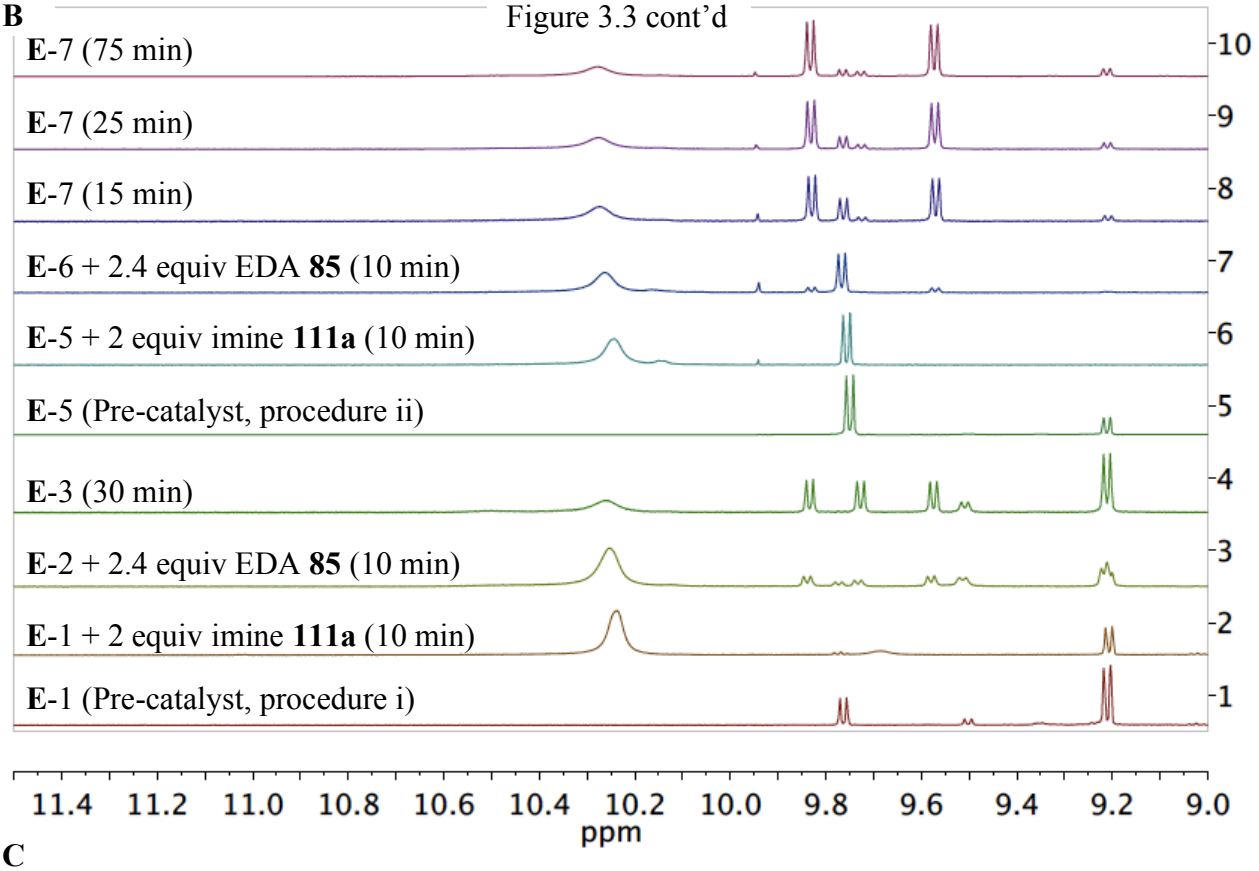

C

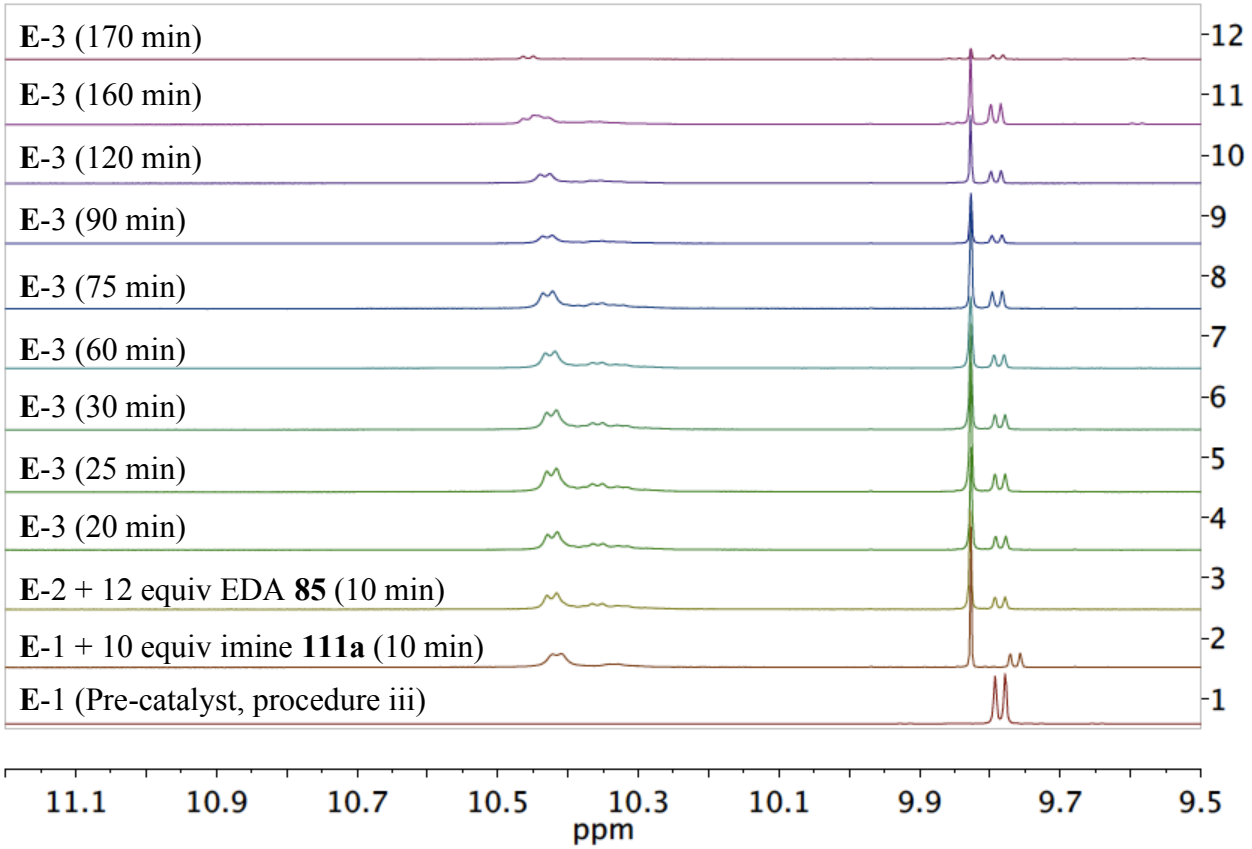

One of the interesting aspects of our catalytic aziridination reaction is that it is a substrate-induced catalytic system. Since imines are generally more basic than aziridines it should not be surprising that all of the NMR studies in Figure 3.3 and Table 3.1 failed to turn up any evidence for an aziridine-catalyst complex. However, this suggests that the second line of thought should be to employ aziridine **114** as a base to generate a boroxinate in the absence of an imine to avoid any competition for the catalyst. Presumably, the behavior of the species **239** should be similar to IMINO-BOROX catalyst **190**.

3.2.2.2 Initial attempts towards the generation of AZIRIDINO-BOROX complex using aziridine 114a

Initial attempts towards the generation of aziridine-boroxinate complex **239a** (with phenyl aziridine **114a**) by following the reaction were not that conclusive. We used aziridine **114a** to affect the desired result. At first instant, it seemed that the desired complex was formed. This inference was suggested by the ^{1}H NMR spectrum of the bay region and by the ^{11}B NMR spectrum. A very small peak at 5.95 ppm was seen in the ^{11}B NMR spectrum. With the help of NOESY1D and COSY, we were able to identify the peaks for the bay region protons at δ = 10.59 and δ = 11.12 ppm in d_8-toluene (δ = 10.5 and δ = 10.8 ppm in $CDCl_3$) at room temperature. Also, the proton attached to the N of aziridinium was found to be at δ = 10.89 ppm in d8-toluene (δ = 10.32 ppm in $CDCl_3$). A simple temperature study (–20 ºC to 80 ºC) revealed that aziridinium cation exchanges with increased rate on NMR time scale at higher temperature as both the bay protons come closer (Figure 3.4B). However, this complex was found to unstable at room temperature over a period of time. The evidence for the existence of complex **239a** was only indicative and not conclusive.

Figure 3.4 (**A**) Aziridine **114a** induced boroxinate catalyst formation. (**B**)[a] ^{1}H NMR spectra of the bay region in d_8-toluene.

A

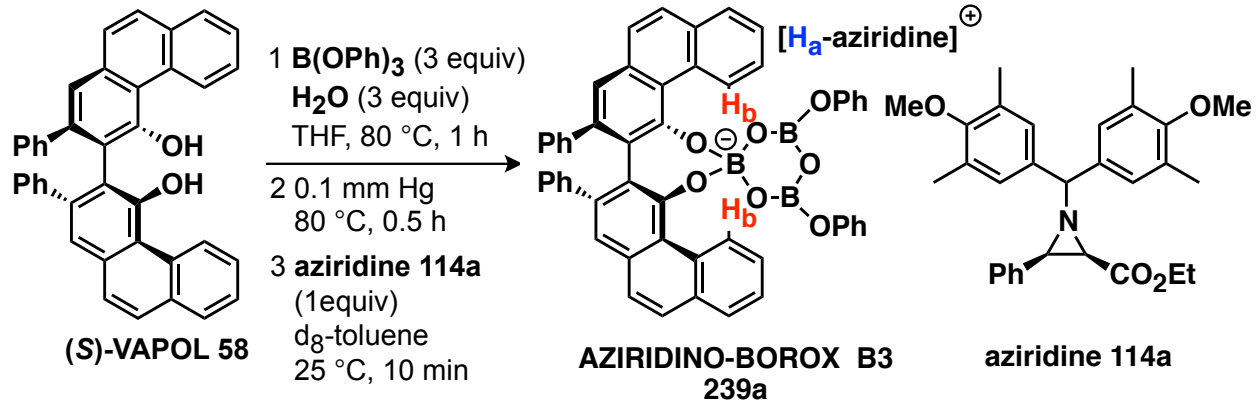

B

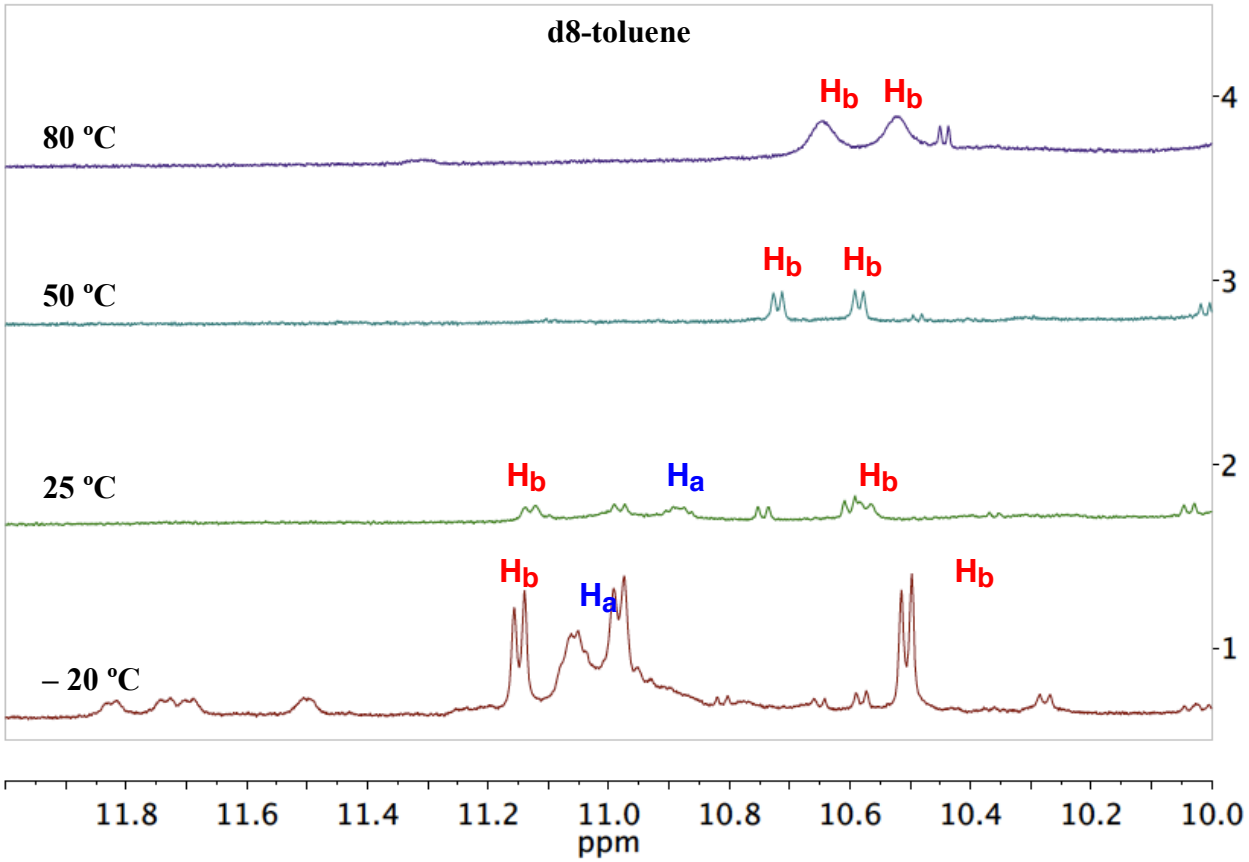

[a] Note for Figure 3.4B: Entry 1: (*S*)-VAPOL (0.1 mmol) plus 3 equiv commercial $B(OPh)_3$ and 3 equiv H_2O were heated at 80 °C in THF for 1 h followed by removal of volatiles under

vacuum for 0.5 h. Thereafter, 1.0 equiv of aziridine **114a** added to the pre-catalyst in d_8-toluene (1 mL) for 10 min at 25 °C. The NMR was taken at –20 °C. Entry 2: Same as entry 1 but the NMR was taken at 25 °C. Entry 3: Same as entry 1 but the NMR was taken at 50 °C. Entry 4: Same as entry 1 but the NMR was taken at 80 °C.

3.2.2.3 First glimpse of an AZIRIDINO-BOROX complex using aziridine 114o

Next, we examined aziridine **114o** as the substrate for the generation of a boroxinate-aziridine complex **239o**. To our delight, this provided the first conclusive evidence of an AZIRIDINO-BOROX **239o**. A characteristic peak at δ 5.36 ppm was observed in the ^{11}B NMR spectrum (Figure 3.5H). In fact, few peaks were observed at bay region of the ligand in ^{1}H NMR spectrum that is expected for a boroxinate species (Figure 3.5D and 3.5G). A bit of a more careful look revealed the presence of two bay protons of the ligand at δ = 10.2 ppm and δ = 10.6 ppm in $CDCl_3$ (Figure 3.5D). The presence of two bay protons peak is probably due the slow exchange of the aziridinium cation with the top and bottom face of the catalyst on the NMR time scale. The same peaks were observed at δ = 10.6 ppm and δ = 11.0 ppm in d8-toluene (Figure 3.5D). With the help of COSY and HMBC, we were able to identify the changes in the chemical shifts of key protons of aziridine **114o**. These observations are discussed below.

Figure 3.5 (**A**) Aziridine **114o** induced boroxinate catalyst formation. (**B**)[a] ^{1}H NMR spectra in $CDCl_3$. (**C**) Expanded view of ^{1}H NMR spectrum of neat aziridine **114o** (entry 2 in Figure 3.5B); (**D**) Expanded view of ^{1}H NMR spectrum of **B3 239o** (entry 1 in Figure 3.5B). (**E**) Expanded view of the superimposed ^{1}H NMR spectra of **B3 239o** and **114o** for the region

Figure 3.5 cont'd

between δ = 3 ppm to δ = 5.5 ppm. (**F**) Expanded view of the superimposed ^{1}H NMR spectra of **B3 239o** and **114o** for the region between δ = 0.1 ppm to δ = 2.5 ppm. (**G**) Same as entry 1 in Figure 3.5B except that the ^{1}H NMR spectrum was taken in d8-toluene. (**H**) ^{11}B NMR spectrum corresponding to the ^{1}H NMR spectrum of entry 1 in Figure 3.5B.

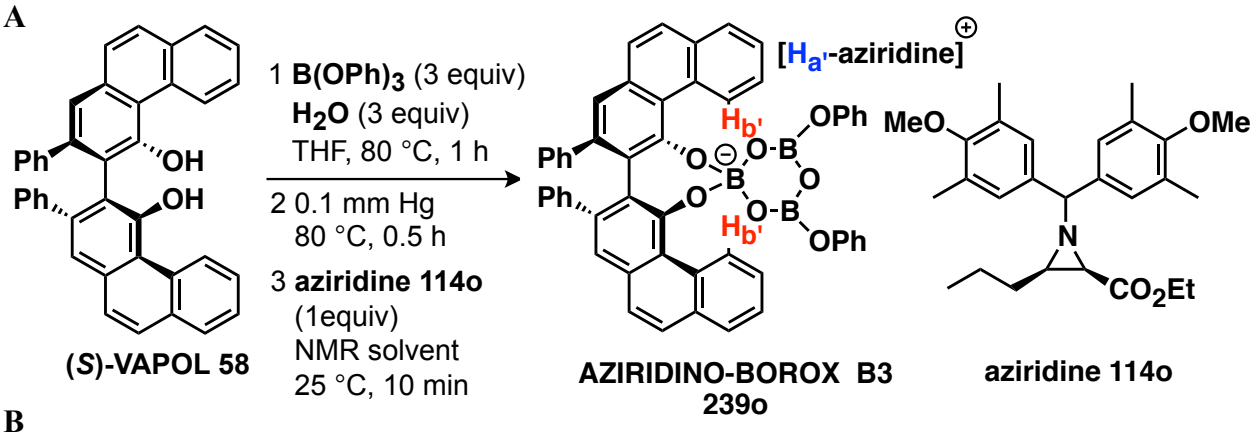

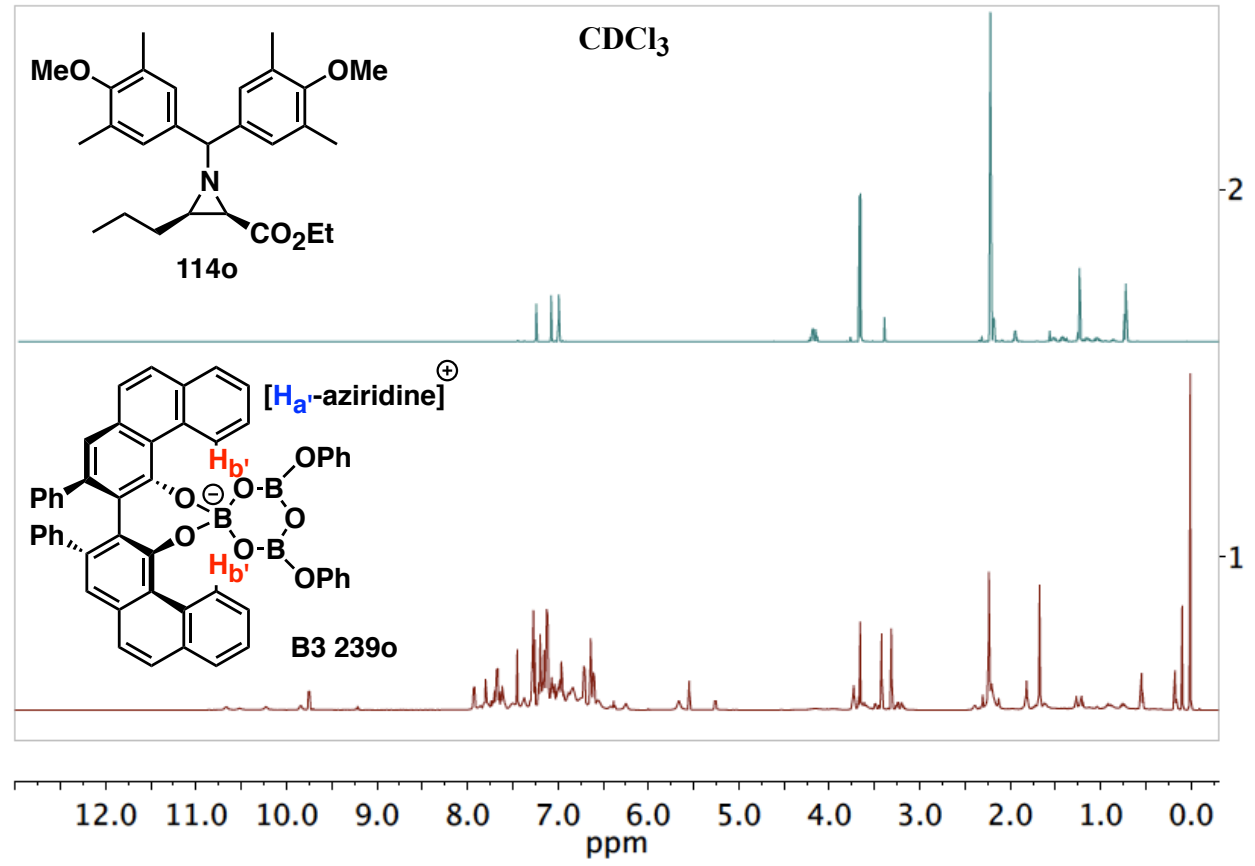

Figure 3.5 cont'd

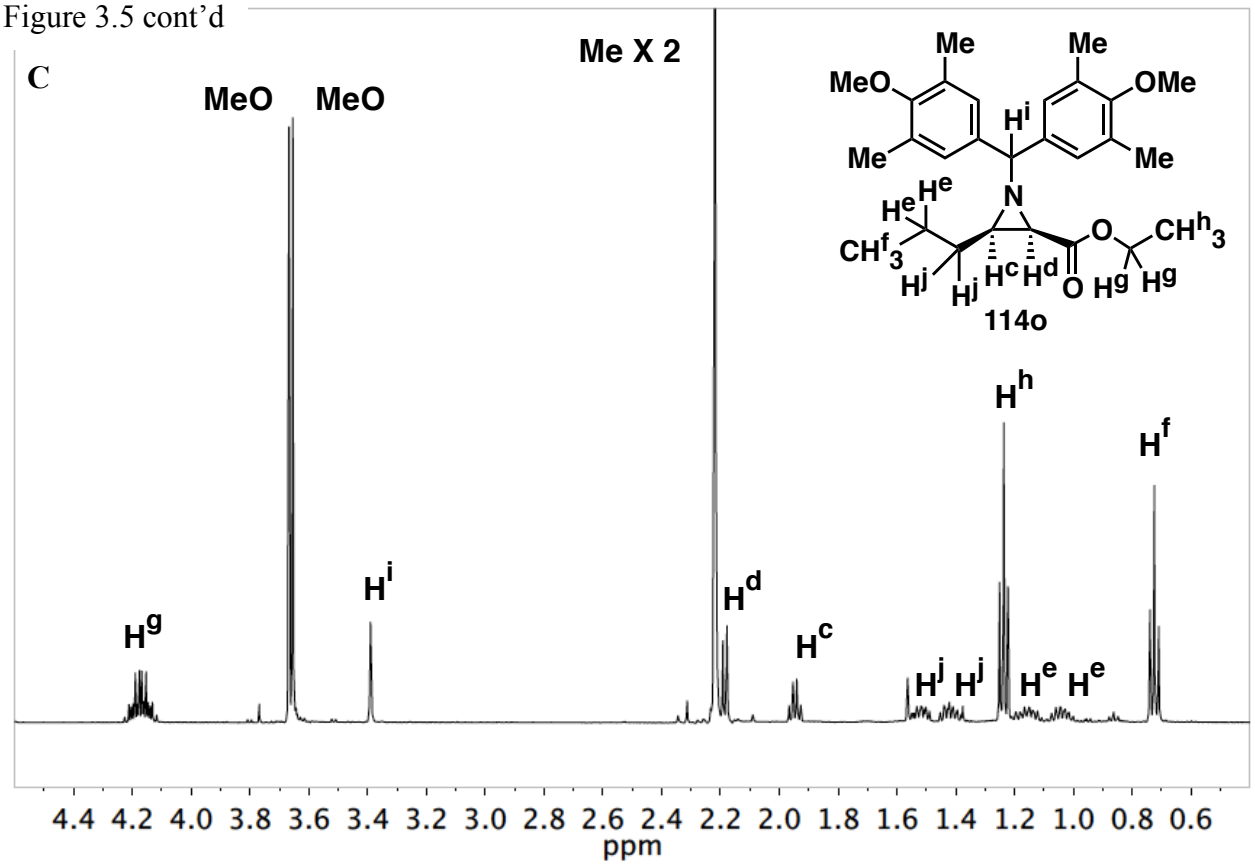

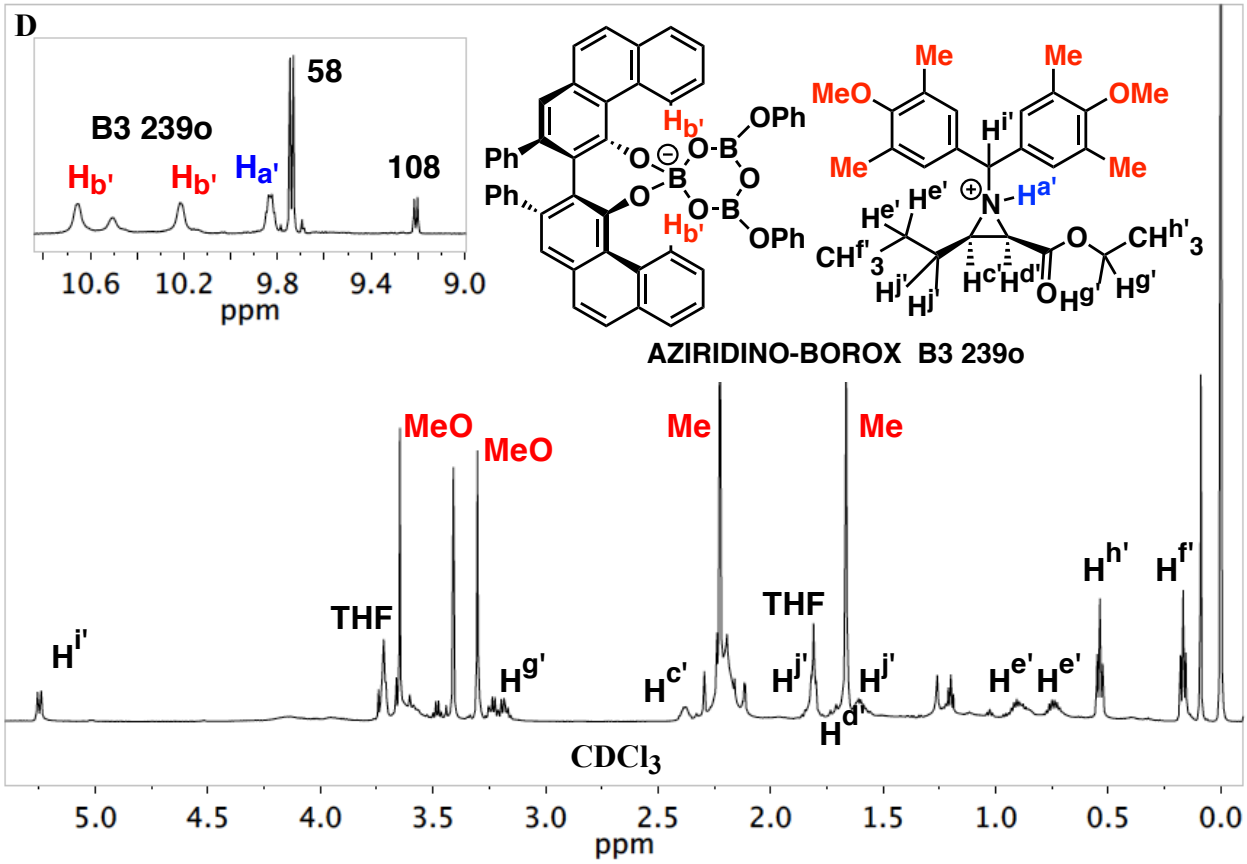

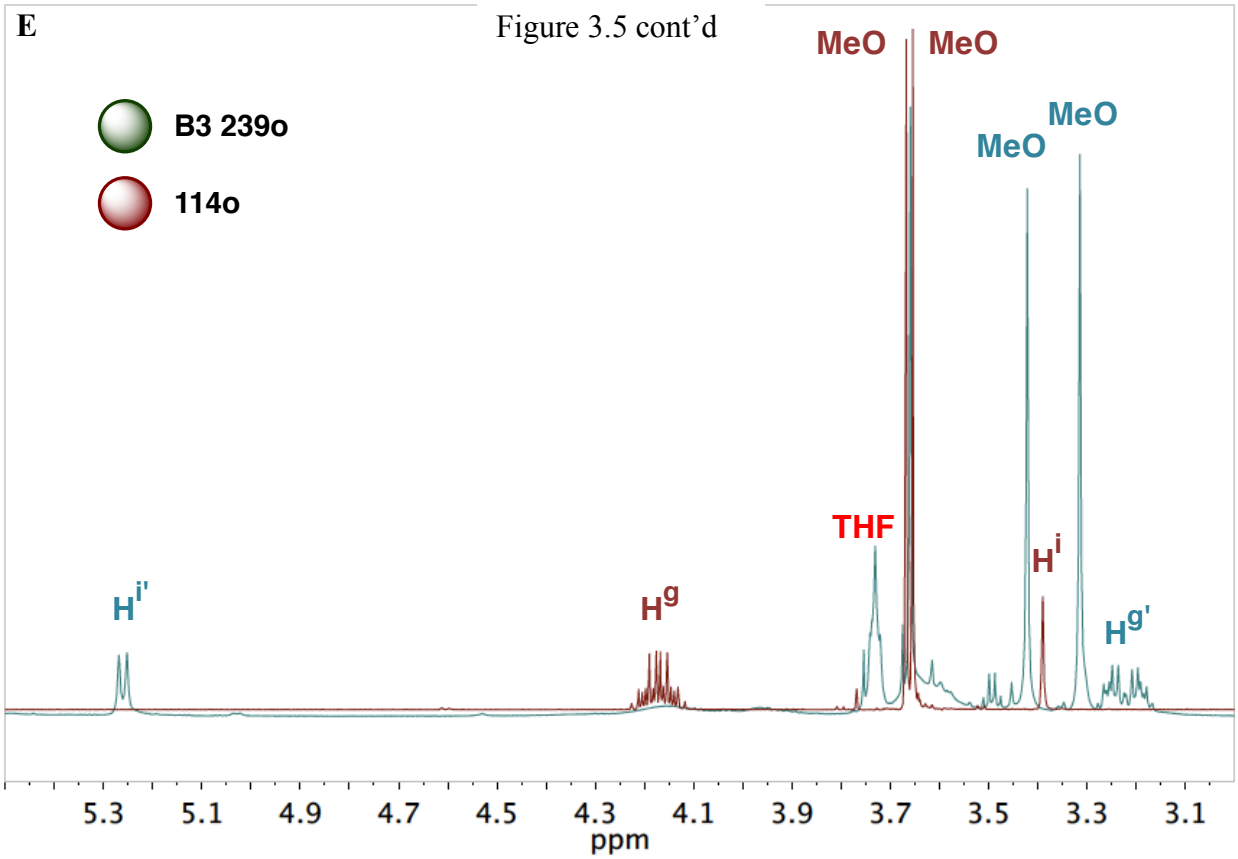

Figure 3.5 cont'd

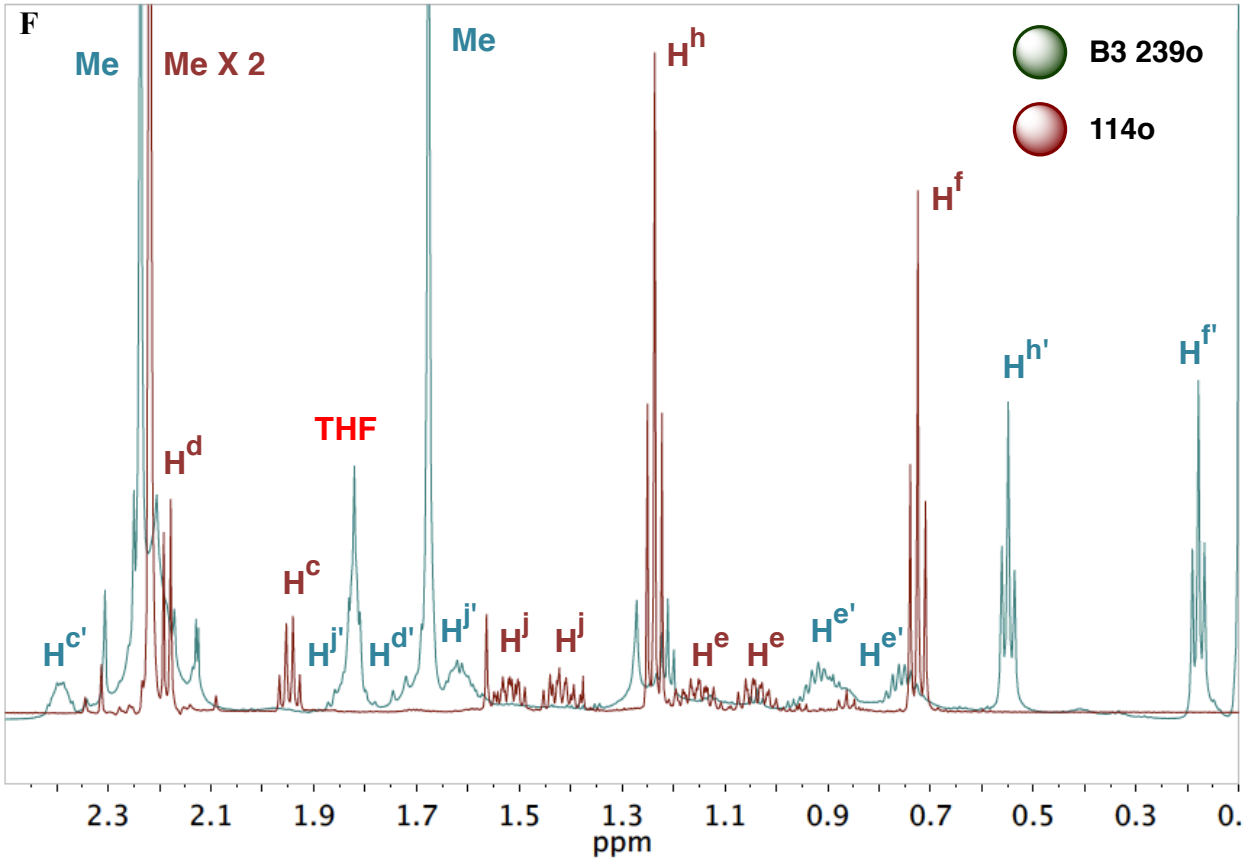

Figure 3.5 cont'd

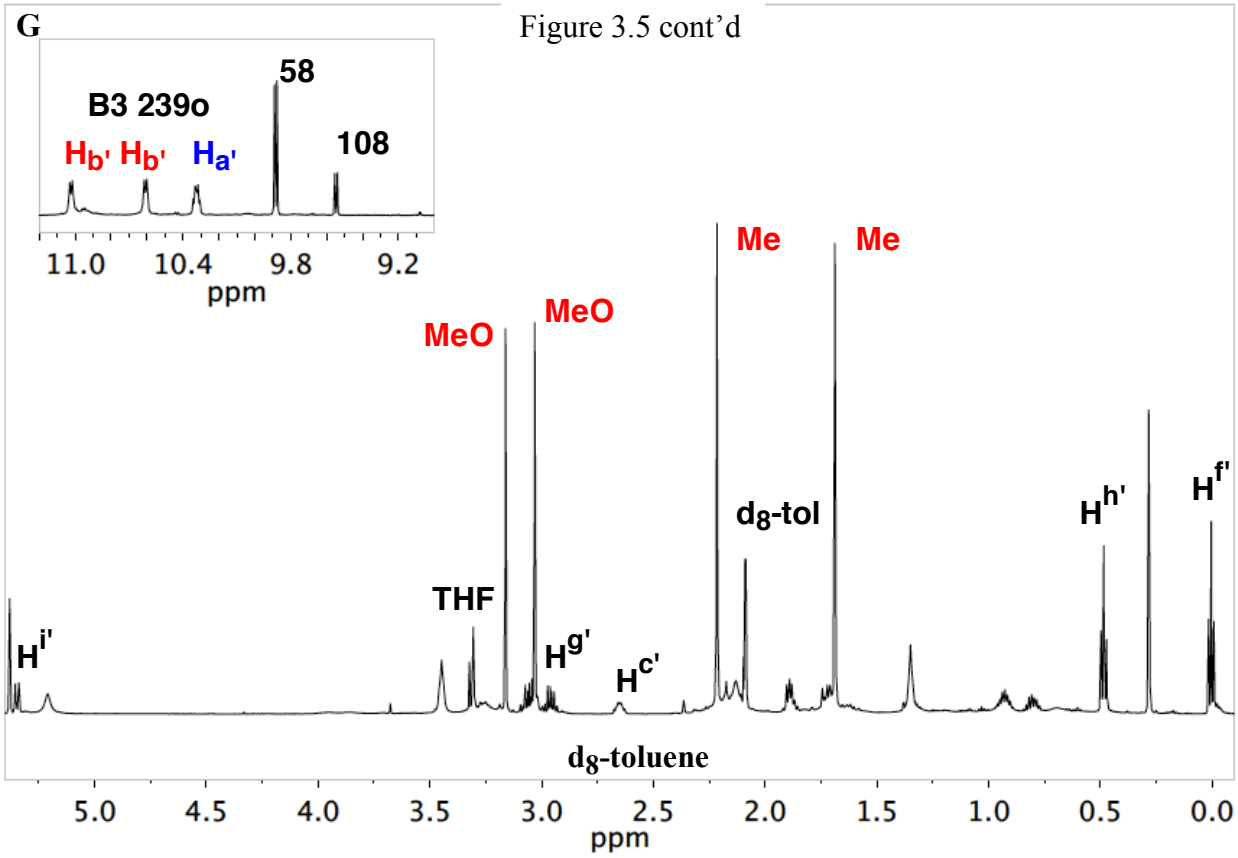

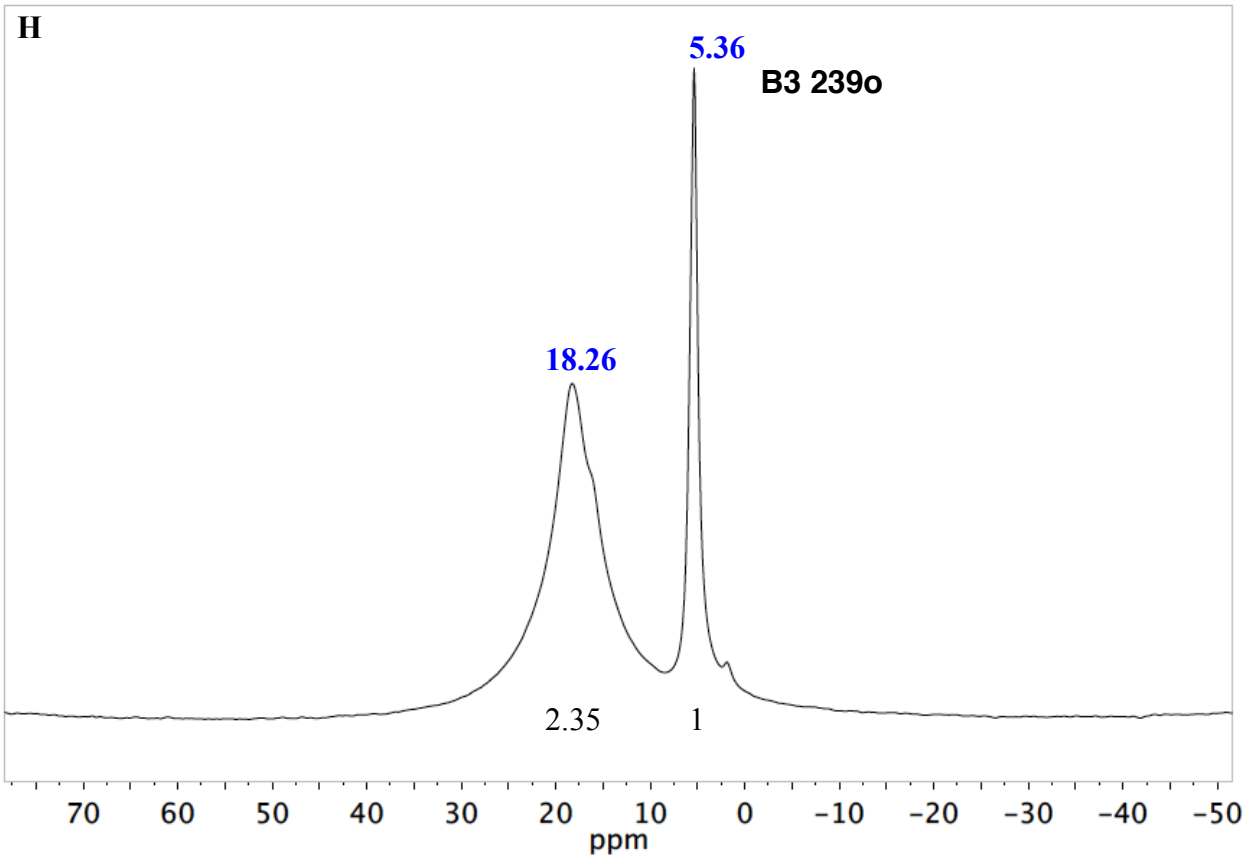

[a] Note for Figure 3.5B: Entry 1: (*S*)-VAPOL (0.1 mmol) plus 3 equiv commercial $B(OPh)_3$ and 3 equiv H_2O were heated at 80 °C in THF for 1 h followed by removal of volatiles under vacuum for 0.5 h. Thereafter, 1.0 equiv of aziridine **114o** was added to the pre-catalyst as a solution in $CDCl_3$ (1 mL) for 10 min at 25 °C. ^{1}H NMR spectrum was taken at 25 °C. Entry 2: ^{1}H NMR spectrum of the pure aziridine **114o**.

The chemzyme-product complex **239o** derived from the aziridine **114o** could not be induced to form crystals suitable for an X-ray diffraction study. It was then decided to explore the structure of **239o** by computational chemistry in order to compliment our observations by ^{1}H NMR spectroscopy. The possible AZIRIDNINO-BOROX complex **239o** was then computed by DFT calculations using Gaussian ′03 at B3LYP/6-31g* level of theory.[6] The calculated structure of **239o** not only supports the boroxinate ion pair motif, but also gives some insight as to how the aziridine might be docking with the boroxinate. The structural analysis further confirms the presence of an ion pair consisting of a protonated aziridinium ion and the boroxinate anion derived from a boroxine ring in which the tetra-coordinate boron is spiro-fused to the VAPOL ligand. This structure is consistent with the many non-covalent interactions observed between the boroxinate anion and the aziridinium observed by ^{1}H NMR spectroscopy. These interactions are summarized in Figure 3.6. As was seen in the case of iminiums,[5f] there is a hydrogen bond from the protonated aziridinium to the oxygen in the boroxinate ring that is attached to the four coordinate boron (O2). The H-O distance of 1.75 Å (Figure 3.6, d_1) suggests a strong to moderate hydrogen bond[4o] and the chemical shift of this proton is δ = 9.8 ppm in

$CDCl_3$ (δ = 10.3 ppm in d8-toluene) which is quite different from the proton associated with the nitrogen of the protonated imine in the IMINO-BOROX catalyst **190** (δ = 13-14 ppm).[5f]

Figure 3.6 Calculated structure of AZIRIDINO-BOROX complex **239o** using Gaussian ′03. (**A**) Calculated B3LYP/6-31g* structure visualized by the Mercury program (C, gray; O, red; N, blue; B, yellow; H, white). Hydrogen atoms are omitted from ligand for clarity (except that of aziridine and O2-H). Some secondary interactions are highlighted: d_1 = 1.75 Å (H-bonding), d_2 = 3.95 Å (CH-π), d_3 = 4.57 Å (CH-π), d_4 = 4.30 Å (CH-π), d_5 = 4.35 Å (CH-π), d_6 = 4.00 Å (CH-π) and d_7 = 2.71 Å (CH-O). (**B**) Space-filling rendition of **239o** with the same orientation and showing hydrogens. The boroxinate anion is given in green and the aziridinium is in traditional colors.

A

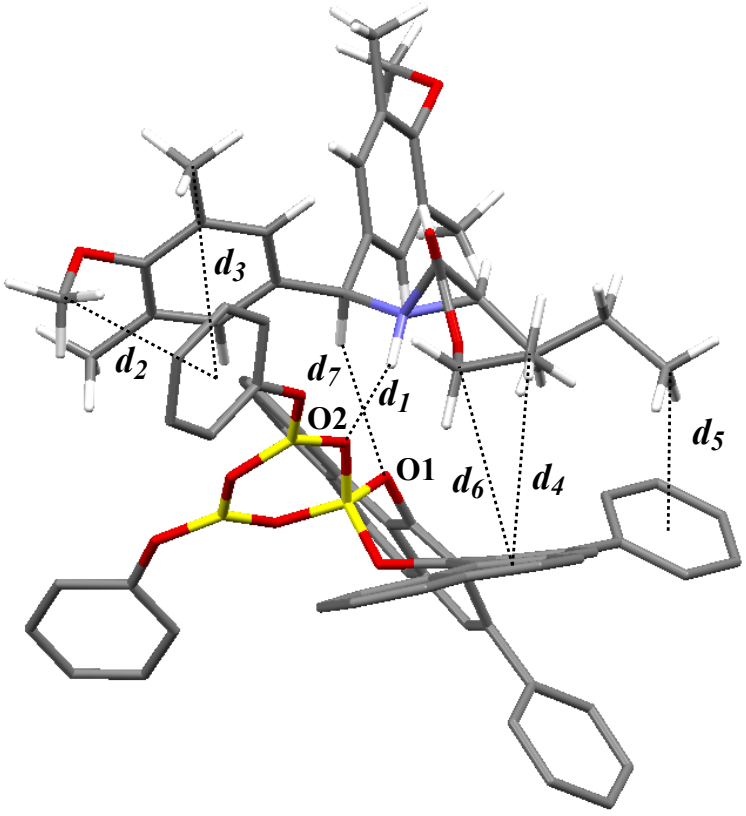

Figure 3.6 cont'd

B

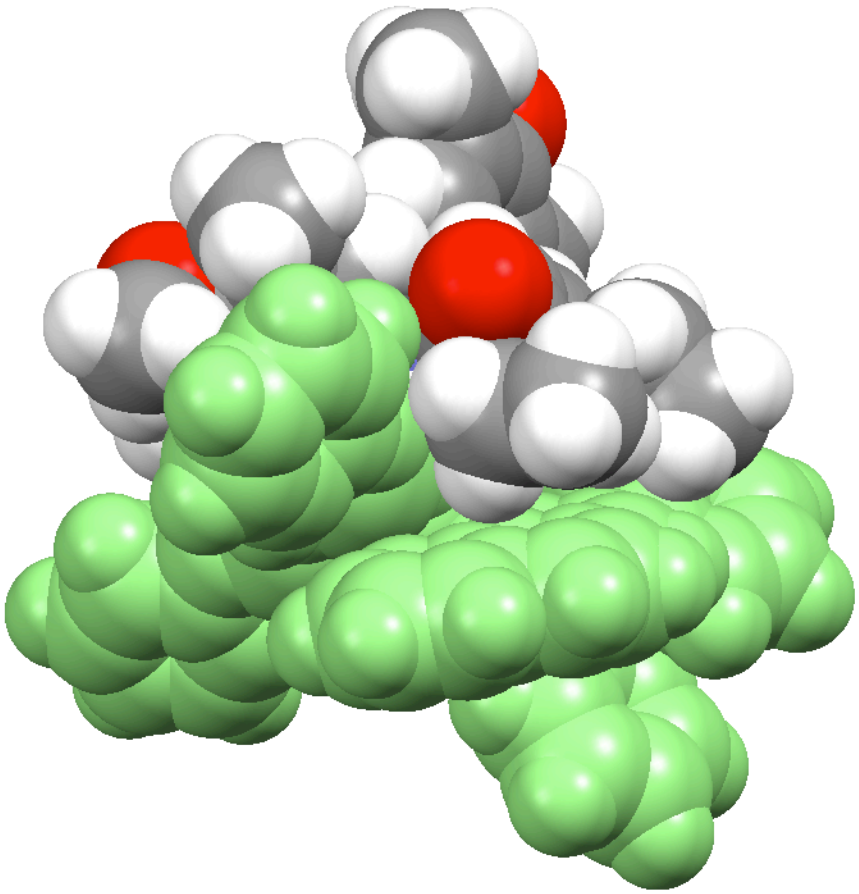

The calculated structure of **239o** provides insight to the up field shift observed for the key protons of the aziridine **114o** upon formation of the aziridine-boroxinate complex **239o**. There are several CH-π interactions.[7] One of the interesting interactions is between one of the MEDAM methoxy groups and the phenyl ring of the phenol component (Figure 3.6, d_2 = 3.95 Å). There are other CH-π interactions including one from a MEDAM methyl to the phenyl ring of the phenol component (Figure 3.6, d_3 = 4.57 Å). The observed dissymmetry (Figure 3.5E and 3.5F) in the case of methyl and methoxy groups of the MEDAM rings is consistent with these CH-π interactions. In fact, these interactions which place these methyl and methoxy groups in

the shielding region of various arene rings furthers confirms the observation in the ^{1}H NMR spectrum of complex **239o** (Figure 3.5E and 3.5F). The methoxy groups are observed as two singlets (δ = 3.42 ppm and δ = 3.31 ppm, 6H), which are shielded relative to the free aziridine **114o** (δ = 3.67 ppm and δ = 3.65 ppm, 6H) by 0.25 ppm and 0.34 ppm (Figure 3.5E). Similarly, the methyl groups are also observed as two singlets (δ = 2.23 ppm and δ = 1.68 ppm, 12H), which are shielded relative to the free aziridine **114o** (δ = 2.22 ppm, 12H) by 0.54 ppm (Figure 3.5F).

A similar upfield shift also occurs for the methyl groups in the propyl group and in the ester group of the aziridine **114o**. Both triplets were found to be shifted upfield by 0.53 and 0.65 ppm respectively (Figure 3.5F, H^{f} and H^{h} *vs.* $H^{f'}$ and $H^{h'}$). This upfield shift can be explained by the CH-π interactions between these groups and the phenyl ring of the phenol component (Figure 3.6, d_5 = 4.35 Å) and also with the arene rings of the phenanthrene ring of the VAPOL (Figure 3.6, d_4 = 4.30 Å). Similar upfield shifts and CH-π interactions were observed regarding the CH_2 units of propyl and ester groups of the aziridine **114o** (Figure 3.5F and Figure 3.6, H^{g} *vs.* $H^{g'}$, d_6 = 4.00 Å). One of the interesting observations was the downfield shift of the methine proton (Figure 3.5E, H^{i} vs. $H^{i'}$) by 1.87 ppm. The factors contributing to this high shift could be a) the adjacent protonated nitrogen behaves as an electron withdrawing group, b) the CH-O interaction between $H^{i'}$ and O1 (Figure 3.6, d_7 = 2.71 Å). A similar downfield shift (~1.37 ppm) was observed for the BOROX catalyst **190a** where the CH-O interaction (2.86 Å) was found to be present between the methine proton of imine and the O1 of the boroxinate anion (Chapter 2,

Figure 2.2B).[5f] To summarize, the first evidence for product binding to the catalyst in a Brønsted acid catalyzed aziridination reaction has been established by ^{1}H NMR spectroscopy,[8] and which is well supported by theoretical calculations.

3.2.2.4 Temperature studies of 239o and recovery of aziridine 114o

We then decided to carry out some additional experiments in order to confirm the presence of **239o**. The ^{1}H NMR spectrum of **239o** has two different bay proton absorptions (Figure 3.5D and 3.5G) and this was interpreted to mean that migration of the protonated aziridine from the top face of the catalyst to the bottom face is slow on the NMR time scale. To gain evidence for this interpretation a temperature study on the ^{1}H NMR spectrum of the complex **239o** was performed. On elevating the temperature from 25 ºC to 80 ºC, the two sets of bay protons ($H_{b'}$) in the aziridine-boroxinate complex **239o** begin to coalesce to give one single doublet (entry 3, Figure 3.7A). This reflects an increased exchange rate on NMR time scale at higher temperature. However, this complex seems to be unstable at higher temperature (80 ºC) as new peaks are observed in the ^{1}H NMR spectrum when the sample is brought back to room temperature (Figure 3.7A, entry 4). In order to study their exchange processes, NOE experiments were carried out at 50 ºC. Upon irradiation of one of the bay proton (δ = 11.06 ppm), the other bay proton appeared with the same sign (δ = 10.67 ppm). This observation further confirms that the aziridinium cation exchanges with the faces of the catalyst slowly on the NMR time scale.

Figure 3.7 (**A**) ^{1}H NMR spectra of the bay region of boroxinate **239o** in d_8-toluene. Entry 1: (*S*)-VAPOL (0.1 mmol) plus 3 equiv commercial $B(OPh)_3$ and 3 equiv H_2O were heated at 80 °C in THF for 1 h followed by removal of volatiles under vacuum for 0.5 h. Thereafter, 1.0 equiv of aziridine **114o** was added to the pre-catalyst as a solution in d_8-toluene (1 mL) for 10 min at 25 °C. The NMR was taken at 25 °C. Entry 2: Same as entry 1 but the NMR was taken at 50 °C. Entry 3: Same as entry 1 but the NMR was taken at 80 °C. Entry 4: entry 3 is cooled to 25 °C. (**B**) NOE (at 50 ºC) performed by irradiating one of the bay protons (δ = 11.06 ppm) in entry 2 of Figure 3.7A.

A

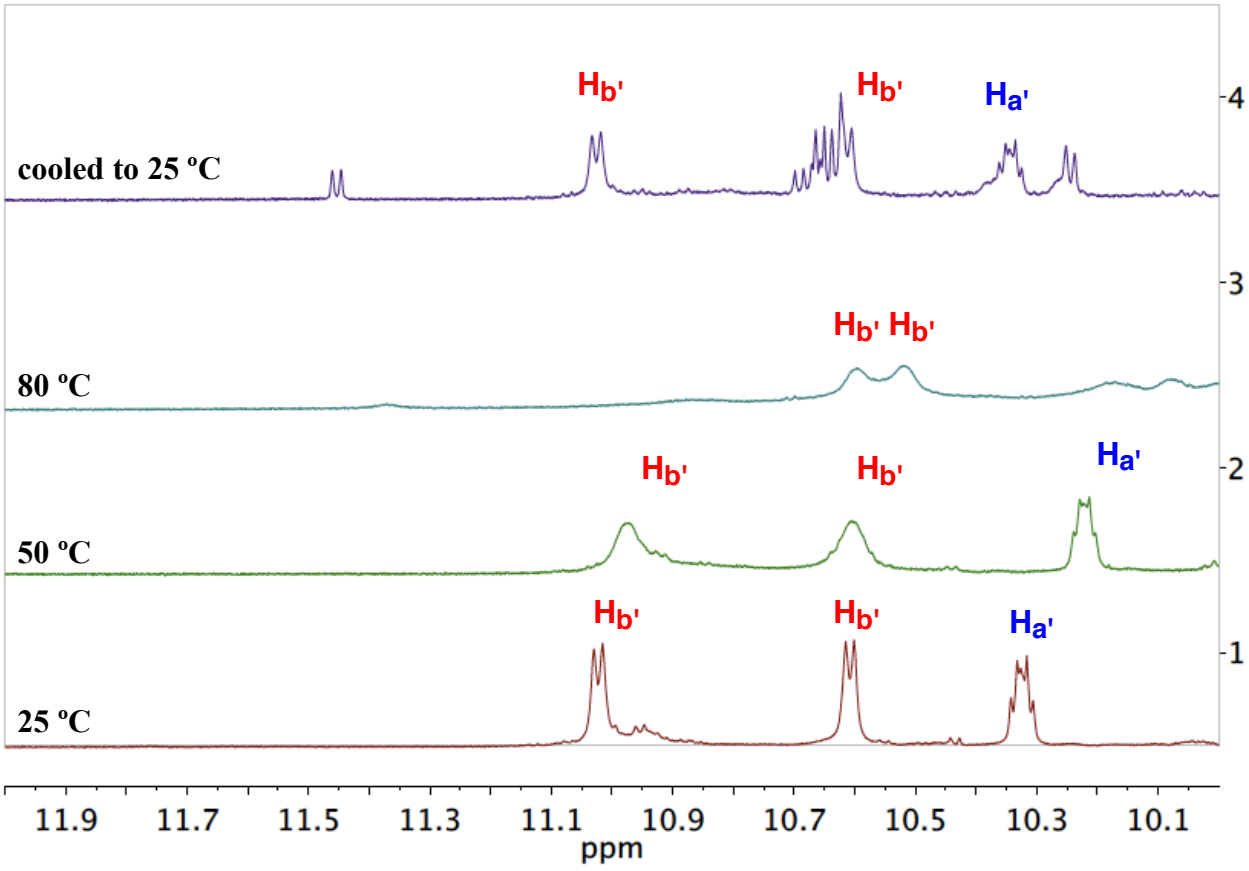

Figure 3.7 cont'd

B

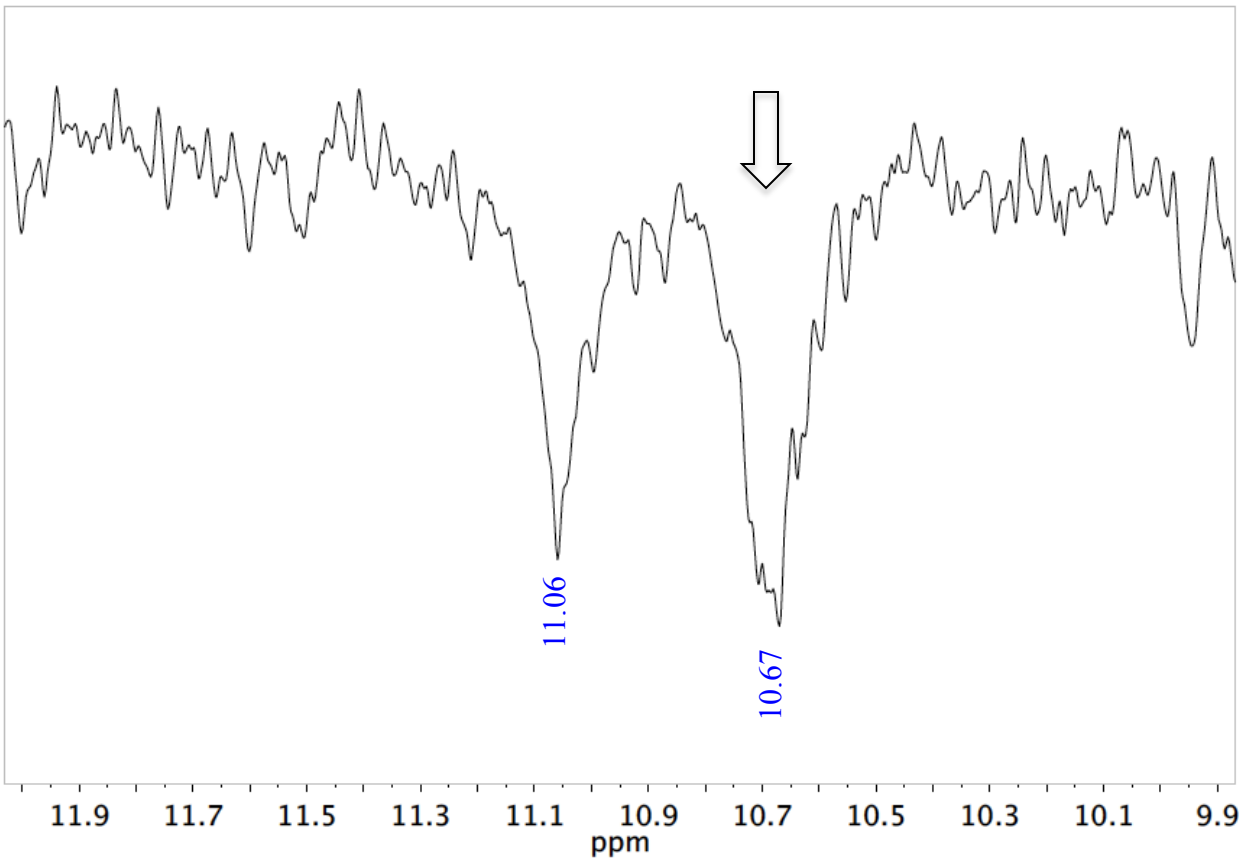

Additionally, it was thought that if the observed NMR behavior is due to the formation of AZIRIDINO-BOROX complex then it should be possible to recover aziridine upon the addition of water. In fact, aziridine release was observed when water was added in portions as shown in Figure 3.8. In fact, disappearance of the aziridine-boroxinate complex occurs concomitant with appearance of the free aziridine **114o** (Figure 3.8). The description of the protons labeled in Figure 3.8C has been given in the Figure 3.5. The aziridine **114o** was obtained with 85% recovery. The difference in amount of aziridine **114o** observed in the ^{1}H NMR spectrum (entry 4, after the addition of 0.4 mmol H_2O) and % recovery (70% *vs*. 85%) can be attributed to the

possibility that the aziridine **114o** can form complexes with other boron sources such as $B(OPh)_3$ or hydrolyzed derivatives.

Figure 3.8 (**A**) Treatment of **239o** with water. (**B**) ^{1}H NMR spectra of the bay region in $CDCl_3$ with Ph_3CH as internal standard. Entry 1: (*S*)-VAPOL (0.1 mmol) plus 3 equiv commercial $B(OPh)_3$ and 3 equiv H_2O were heated at 80 °C in THF for 1 h followed by removal of volatiles under vacuum for 0.5 h. Thereafter, 1.0 equiv of aziridine **114o** was added to the pre-catalyst as a solution in $CDCl_3$ (1 mL) for 10 min at 25 °C. The NMR was taken at 25 °C. Entry 2: 1 equiv H_2O added to entry 1. Entry 3: 2 equiv H_2O added to entry 1. Entry 4: 4 equiv H_2O added to entry 1. Entry 5: 10 equiv H_2O added to entry 1. (**C**) ^{1}H NMR spectra corresponding to the entries 1–4 in Figure 3.8B highlighting the methyl and methoxy regions. The description of the protons labeled in Figure 3.8C has been given in the Figure 3.5. Entry 5: aziridine **114o** isolated (purified by silica gel chromatography) after the addition of 1.0 mmol H_2O to entry 1. (**D**) ^{11}B NMR spectra corresponding to the ^{1}H NMR spectra of entries in Figure 3.8B

A

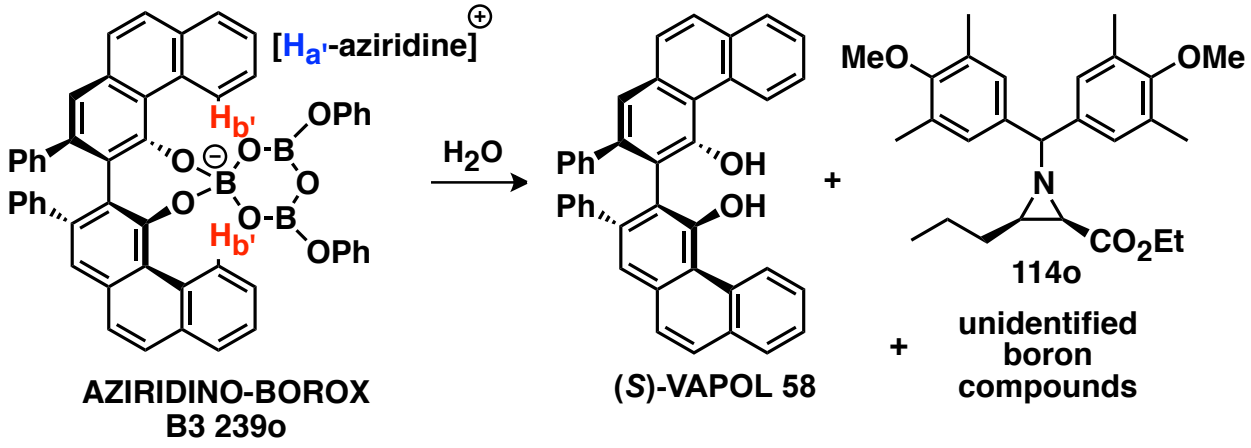

Figure 3.8 cont'd

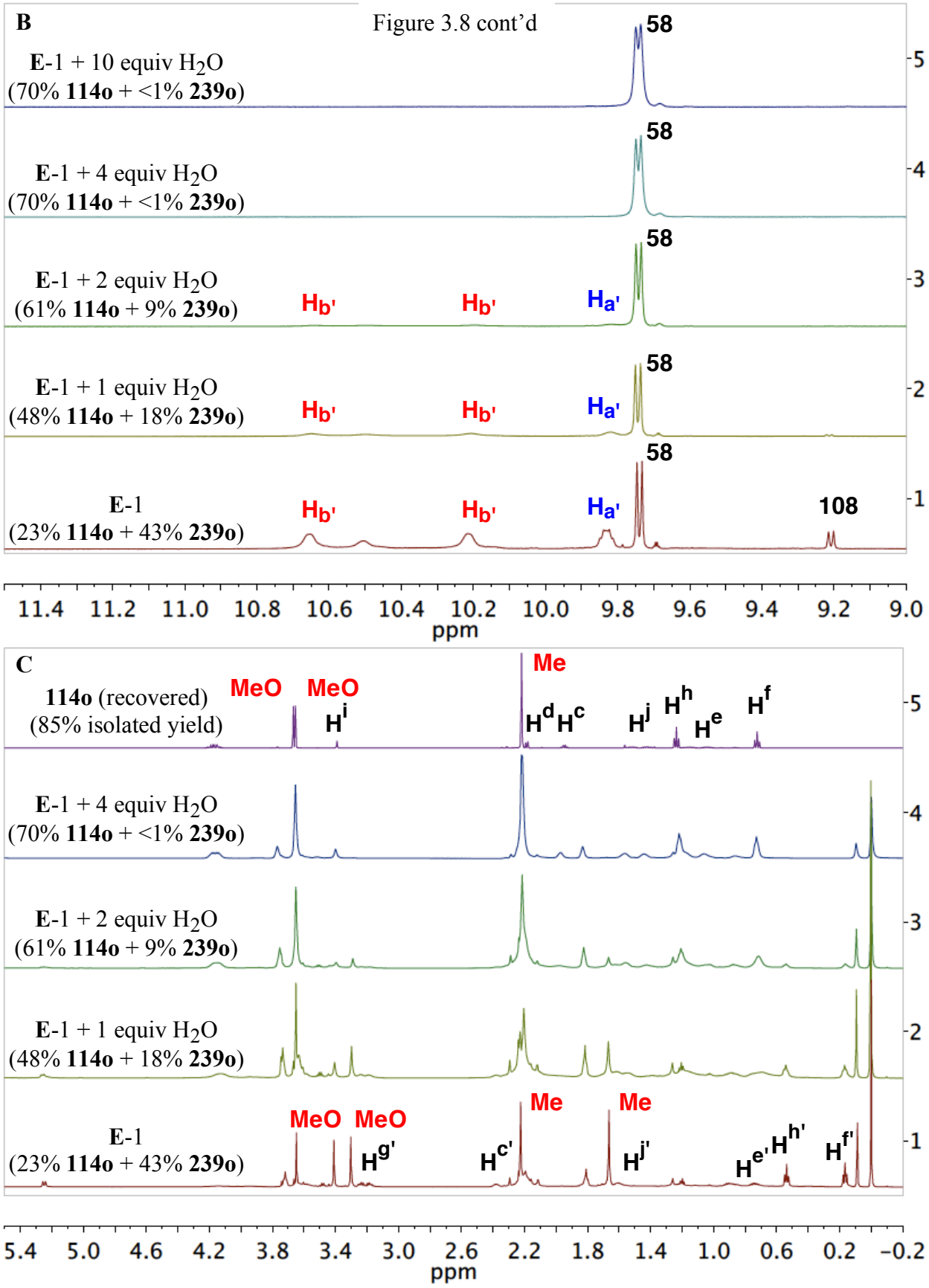

Figure 3.8 cont'd

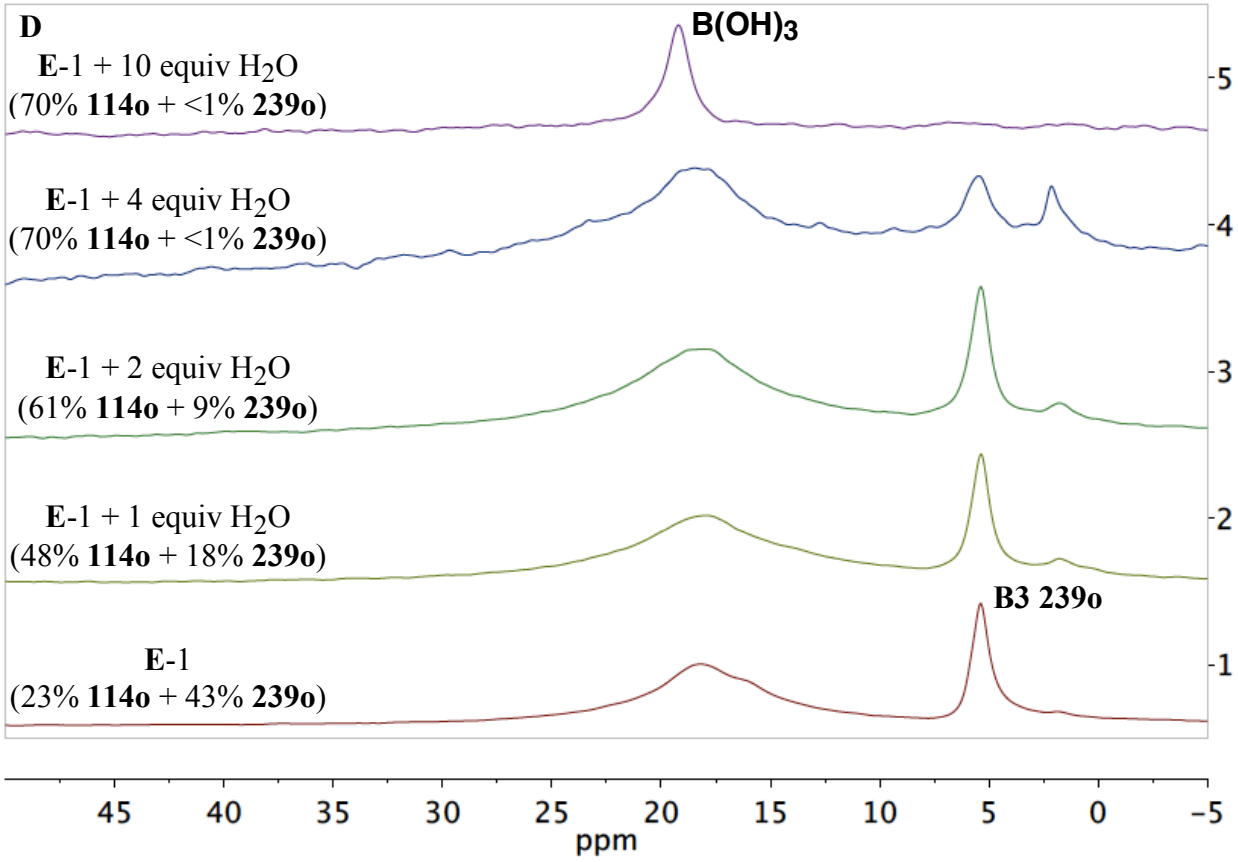

3.2.2.5 Dependence of the formation of AZIRIDINO-BOROX 239o on various protocols

After the confirmation of the presence of AZIRIDINO-BOROX complex, we became interested to find out whether the generation of the **239o** depends on the protocol used for pre-catalyst generation. As shown in Table 3.2, different yields were obtained for different protocols. Also, we found that this complex decomposes to some extent at elevated temperatures of as 80 °C and 50 °C (Table 3.2, entries 2 and 6). The complex is relatively stable to storage, however it decomposes slowly on being kept for long periods of time (Table 3.2, entry 7).

Table 3.2 Generation of AZIRIDINO-BOROX **239o** with different boron sources [a]

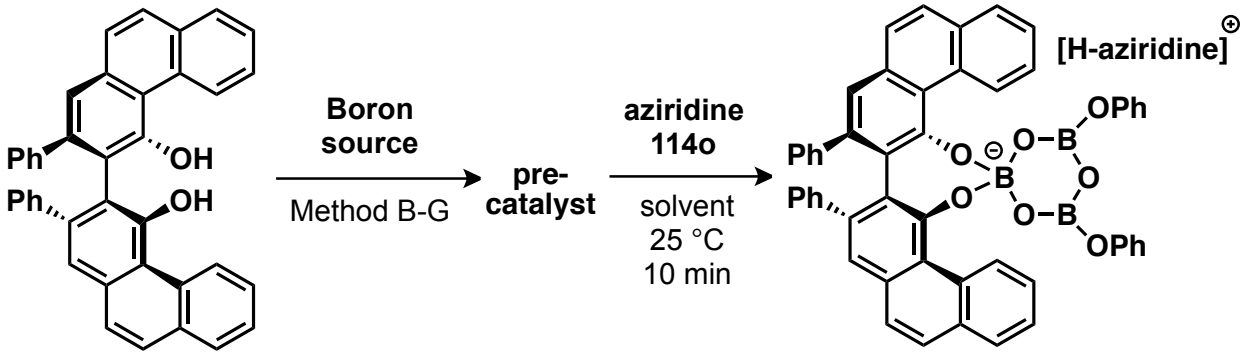

(*S*)-VAPOL 58 **AZIRIDINO-BOROX B3 239o**

#	Boron Source	Pre-catalyst (method) [b]	Solvent [c]	Yield **239o** (%) [d]
1	$B(OPh)_3$	B	d_8-toluene	47
2	$B(OPh)_3$	B	d_8-toluene	26 [e]
3	$B(OPh)_3$	B	$CDCl_3$	43
4	$B(OPh)_3$	C	$CDCl_3$	19
5	Boroxine	D	$CDCl_3$	30 (26) [g]
6	$BH_3.Me_2S$	E	$CDCl_3$	31
7	$BH_3.Me_2S$	E	$CDCl_3$	17 [f]

[a] Unless otherwise specified, all NMR samples were prepared with 0.1 mmol of aziridine **114o** in solvent (0.1 M in aziridine **114o**) with 1.0 equiv of (*S*)-VAPOL **58**. [b] Method B: The pre-catalyst was prepared by heating 1 equiv of (*S*)-VAPOL, 3 equiv of commercial $B(OPh)_3$ and 3 equiv of H_2O in THF at 80 °C for 1 h, followed by removing all volatiles under high vacuum (0.1 mm Hg) for 0.5 h at 80 °C. Method C: Same as Method B except 4 equiv of commercial $B(OPh)_3$ with 1 equiv of H_2O was used. Method D: By mixing 1 equiv of (*S*)-VAPOL and 1 equiv of triphenoxyboroxine **191a**. Triphenoxyboroxine **191a** was prepared by heating 3 equiv of $BH_3.Me_2S$, 2 equiv of PhOH and 3 equiv of H_2O in toluene at 100 °C for 1 h, followed by removing all volatiles under high vacuum (0.1 mm Hg) for 0.5 h at 100 °C. Method E: By heating 1 equiv of (*S*)-VAPOL, 3 equiv of $BH_3.Me_2S$, 2 equiv of PhOH and 3 equiv of H_2O in toluene at 100 °C for 1 h, followed by removing all volatiles under high vacuum (0.1 mm Hg) for 0.5 h at 100 °C. [c] NMR Solvent. [d] Determined by ^1H NMR using Ph_3CH as an internal standard. [e] In this case, the resulting mixture was heated at 80 °C for 0.5 h after the addition of aziridine **114o**. [f] In this case, the resulting mixture was heated at 50 °C for 1.0 h after the addition of aziridine **114o**. [g] Results in parenthesis are from NMR sample that was kept at 25 °C for 24 h prior to analysis.

3.2.2.6 Direct generation of AZIRIDINO-BOROX at room temperature

Recently, we have shown that IMINO-BOROX **190a** can be generated in 76% yield at room temperature by simple mixing the ligand, commercial $B(OPh)_3$ and imine **111a**.[5f] At this point, it became interesting to find out whether AZIRIDINO-BOROX **239o** can be directly generated at room temperature or not. It was delightful to observe **239o** in 15% yield when 2 equiv of aziridine **114o** was mixed with 1equiv of (*S*)-VAPOL and 3 equiv of commercial $B(OPh)_3$ (Figure 3.9, entry 5). The yield was determined by ^1H NMR using Ph_3CH as the internal standard. The low yield can be attributed to low binding affinity of aziridines to the catalyst as compared to imines. *However, it must be noted that the conversion of pre-catalyst to AZIRIDINO-BOROX **239o** is higher than direct generation from* commercial *$B(OPh)_3$ (43% yield vs 15% yield, Table 3.2 vs Figure 3.9).* The evidence for AZIRIDINO-BOROX **239a** is not observed on the NMR time scale possibly due to fast exchange processes (entry 4, Figure 3.9B). One observation to be noted was the presence of aldehydes due to partial hydrolysis of imines (entries 2 and 3, Figure 3.9B).

Figure 3.9 (**A**) Direct generation of aziridine-boroxinate complex at room temperature. (**B**)[a] ^1H NMR spectra of the bay region in $CDCl_3$ with Ph_3CH as internal standard. (**C**) ^{11}B NMR spectra corresponding to the ^1H NMR spectra in Figure 3.9A

Figure 3.9 cont'd

A

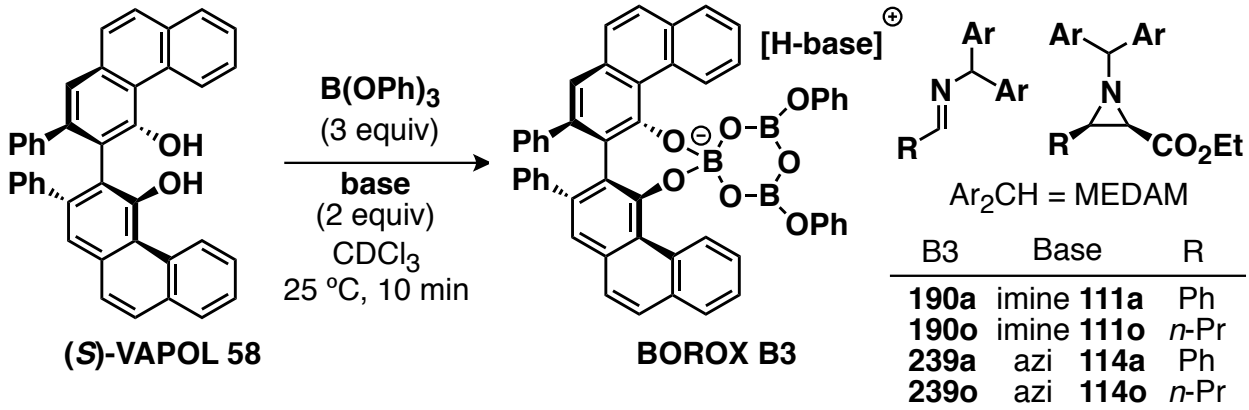

B3	Base	R
190a	imine **111a**	Ph
190o	imine **111o**	*n*-Pr
239a	azi **114a**	Ph
239o	azi **114o**	*n*-Pr

B

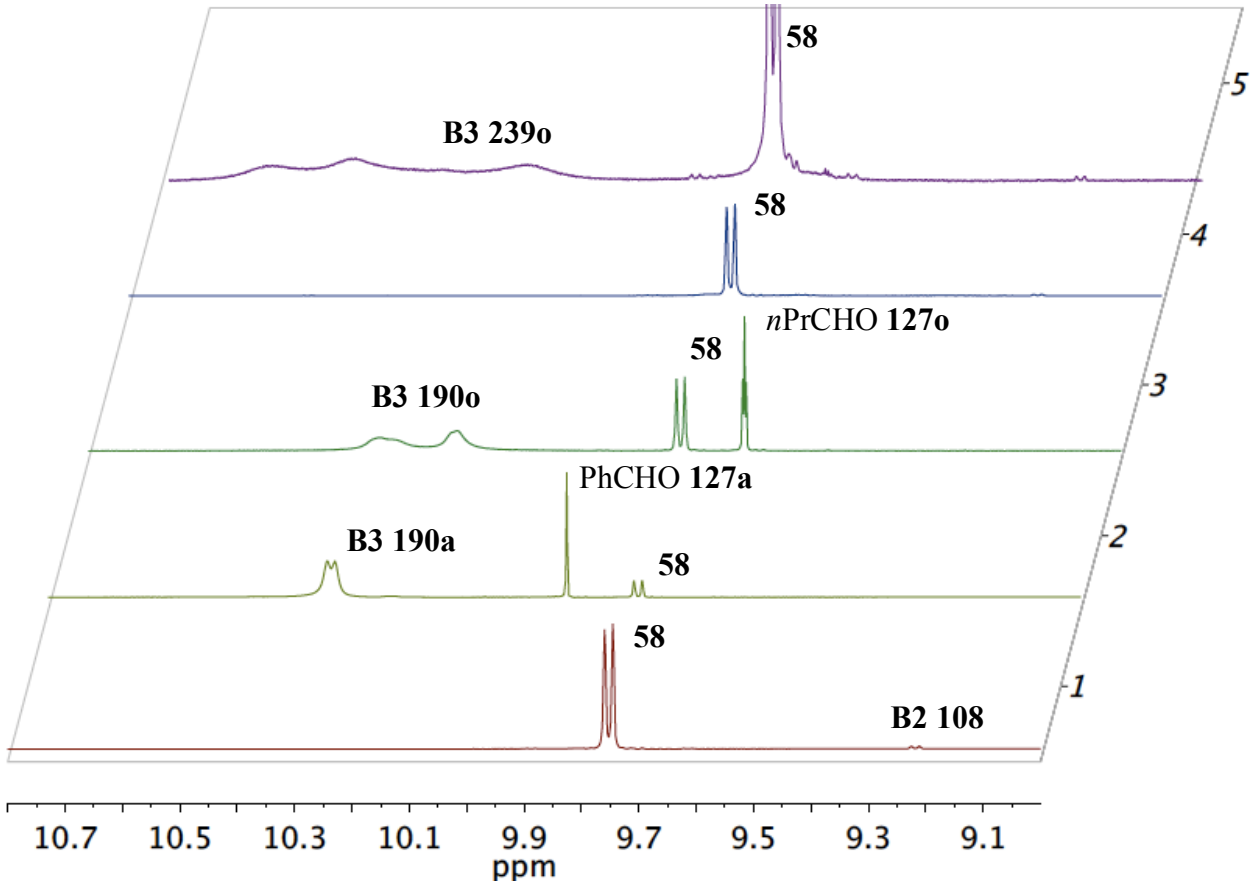

Figure 3.9 cont'd

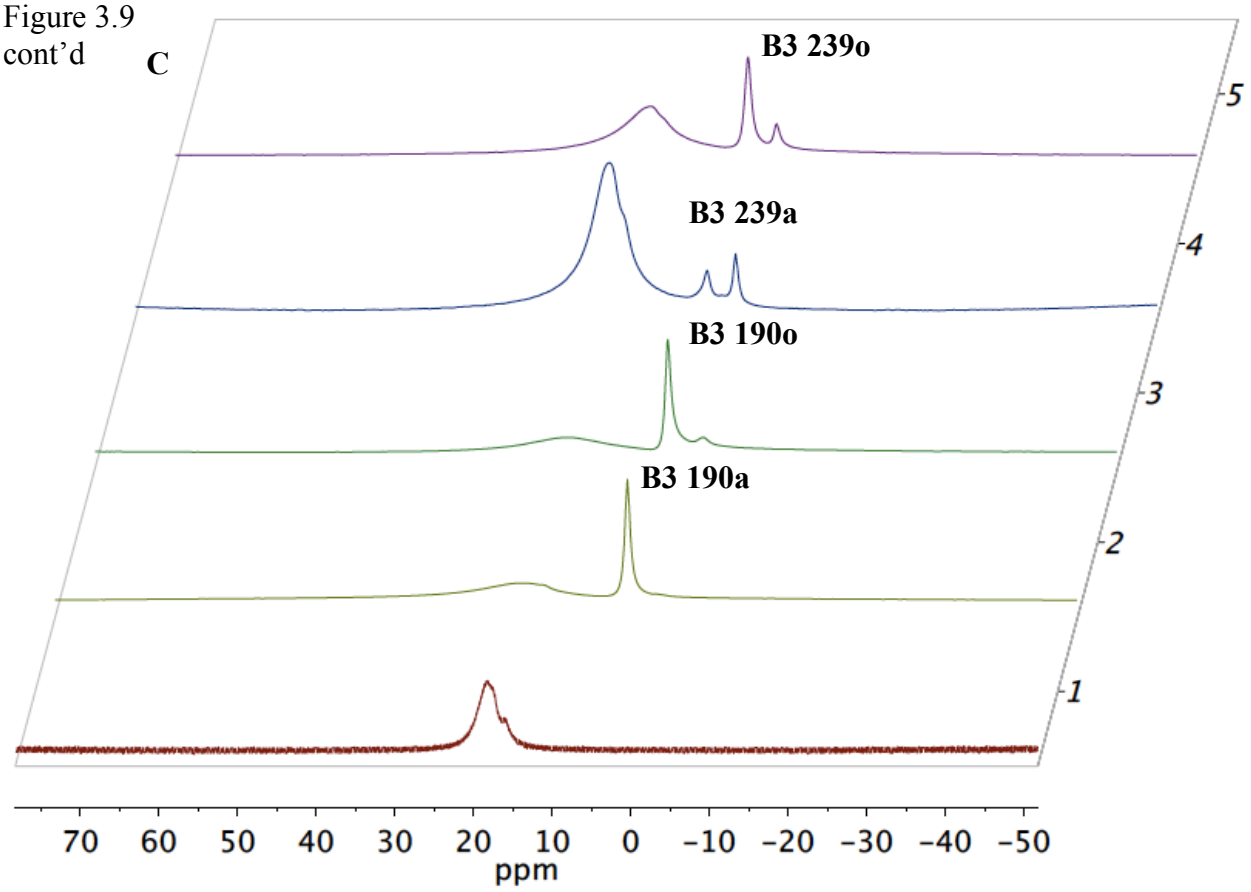

[a] Note for Figure 3.9B: Entry 1: (*S*)-VAPOL (0.1 mmol) plus 3 equiv commercial $B(OPh)_3$ at 25 °C for 10 min. Entry 2: (*S*)-VAPOL (0.1 mmol) plus 3 equiv commercial $B(OPh)_3$ and 2 equiv imine **111a** at 25 °C for 10 min. Entry 3: (*S*)-VAPOL (0.1 mmol) plus 3 equiv commercial $B(OPh)_3$ and 2 equiv imine **111o** at 25 °C for 10 min. Entry 4: (*S*)-VAPOL (0.1 mmol) plus 3 equiv commercial $B(OPh)_3$ and 2 equiv aziridine **114a** at 25 °C for 10 min. Entry 5: (*S*)-VAPOL (0.1 mmol) plus 3 equiv commercial $B(OPh)_3$ and 2 equiv aziridine **114o** at 25 °C for 10 min.

3.2.2.7 Generation of AZIRIDINO-BOROX complexes from other alkyl aziridines

Although the phenyl substituted aziridine **114a** failed to provide any conclusive evidence for an AZIRIDINO-BOROX complex, the *n*-propyl aziridine **114o** was able to assemble the boroxinate **239o** in 43% yield. This suggested that aziridines derived from aliphatic aldehydes are more prone to provide convincing evidence for boroxinate complexes formation. Hence, we decided to screen the ethyl, cyclohexyl and *tert*-butyl substituted aziridines **115o′**, **114v** and **114w**, respectively. Indeed, it was possible to observe the assembly of AZIRIDINO-BOROX **240o′** when aziridine **115o′** (protecting group = BUDAM) was reacted with the pre-catalyst. Interestingly, only one peak for bay protons of the boroxinate complex **240o′** was observed which indicates that the migration of the protonated aziridine from top face of the catalyst to the bottom face is fast on the NMR time scale in this case (Figure 3.10A, entry 1). It must be noted that aziridine **115o′** has the BUDAM group as the protecting group. When aziridine **114v** was used, two distinct bay protons were observed (Figure 3.10A, entry 3). In addition to the bay protons, an unknown peak around δ = 10.6 ppm was observed which increased along with the boroxinate species when excess aziridine **114v** was added (Figure 3.10A, entry 4). Interestingly, aziridine **114w** generated only a small amount of boroxinate **239w** as illustrated by the ^{11}B NMR spectrum (Figure 3.10B, entry 5).

Figure 3.10 (**A**) Examination of alkyl aziridines for boroxinate formation. (**B**)[a] ^{1}H NMR spectra of the bay region in $CDCl_3$ with Ph_3CH as internal stardard. (**C**) ^{11}B NMR spectra corresponding to the ^{1}H NMR spectra in Figure 3.10B

Figure 3.10 cont'd

A

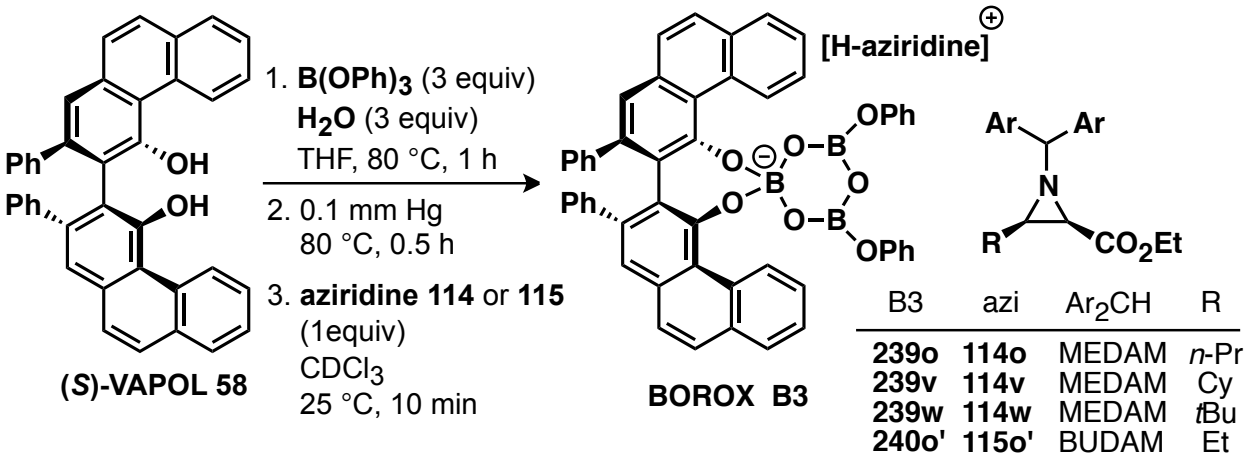

B3	azi	Ar_2CH	R
239o	**114o**	MEDAM	*n*-Pr
239v	**114v**	MEDAM	Cy
239w	**114w**	MEDAM	*t*Bu
240o'	**115o'**	BUDAM	Et

B

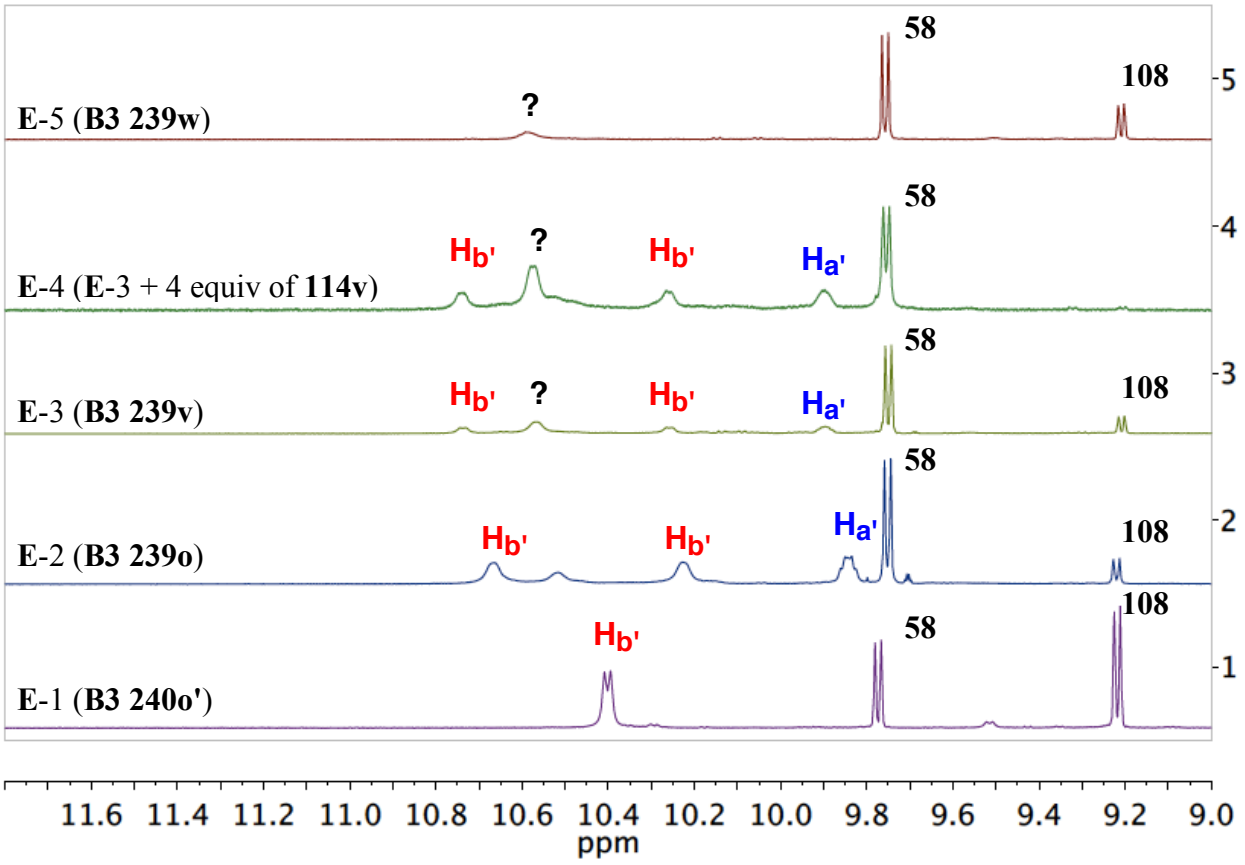

Figure 3.10 cont'd

C

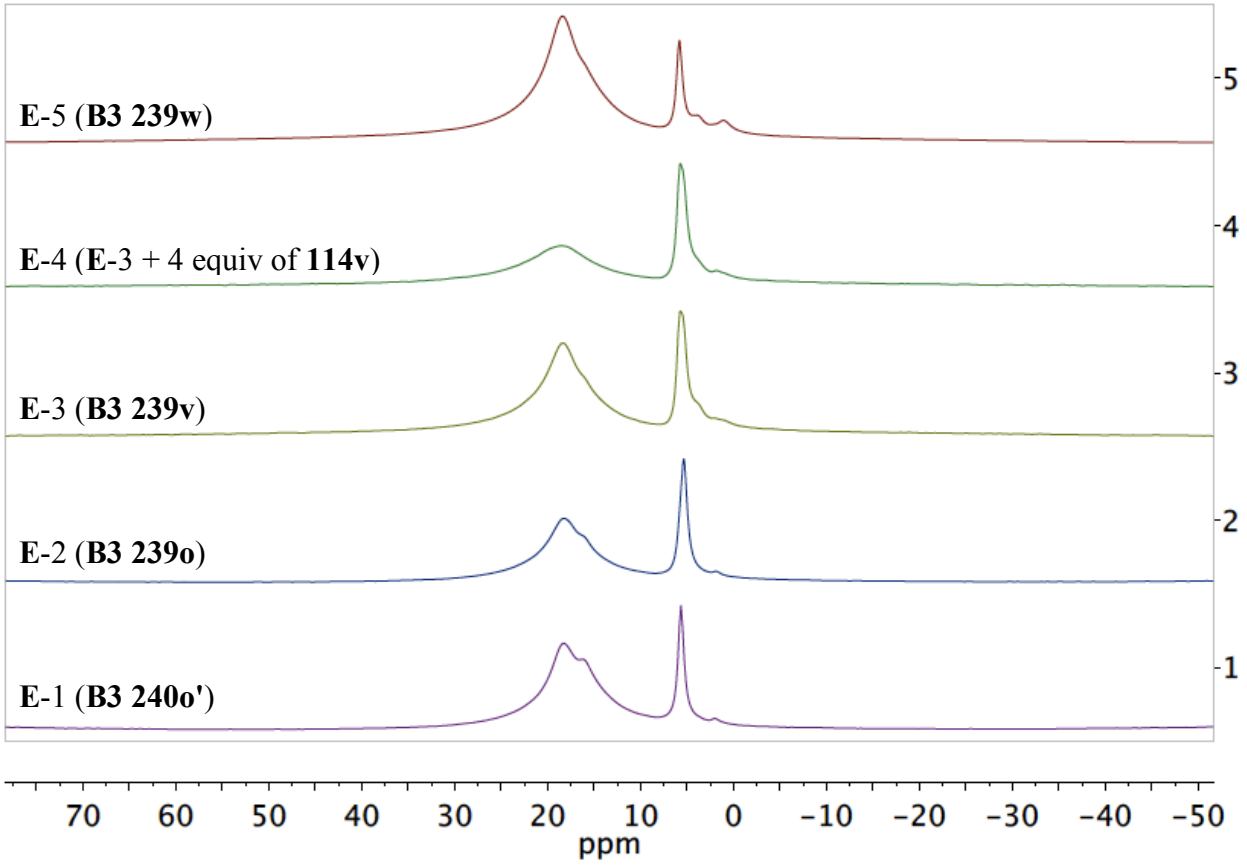

[a] Note for Figure 3.10B: Entry 1: (*S*)-VAPOL (0.1 mmol) plus 3 equiv commercial $B(OPh)_3$ and 3 equiv H_2O were heated at 80 °C in THF for 1 h followed by removal of volatiles under vacuum for 0.5 h. Thereafter, 1.0 equiv of aziridine **115o′** was added to the pre-catalyst as a solution in $CDCl_3$ (1 mL) for 10 min at 25 °C. Entry 2: Same as entry 1 except that aziridine **114o** was employed. Entry 3: Same as entry 1 except that aziridine **114v** was employed. Entry 4: 4 equiv of aziridine **114v** added to entry 1. Entry 5: Same as entry 1 except that aziridine **114w** was employed.

3.2.3 Equilibrium studies

After the establishment of conditions for the formation of a product-catalyst complex, it was important to know whether these species exist in equilibrium or not. It is a challenging task since it is not a simple case where the product binds to a pre-existing catalyst. In the present case, the equilibrium is in between the product and the catalyst and between all of the species from which the catalyst is assembled with the aid of substrate. However, we chose to carry out this study using the aziridine-catalyst complex rather than the imine-catalyst complex since the aziridine has a lower binding affinity (basicity) and it should be easier to observe equilibrium effects. We designed two sets of experiments. In the first, we started off with a concentrated mixture containing AZIRIDINO-BOROX complex and then diluted the mixture with the subsequent addition of solvent. As shown in Figure 3.11B, amount of the boroxinate **239o** decreases with the decrease in the concentration of the reaction mixture. A corresponding increase in the amount of (*S*)-VAPOL **58** was also observed. With further dilution, unbounded aziridine **114o** was also observed (entry 8, Figure 3.11B). This suggests that there is shift in the equilibrium towards free aziridine and ligand upon dilution.

Figure 3.11 (**A**) Aziridine induced boroxinate formation and its subsequent dilution studies. (**B**)[a] ^{1}H NMR spectra of the reaction mixture in d_8-toluene with Ph_3CH as internal standard. The numbers given in the spectra shows the NMR yield of respective species (red, **239o**; green, **58**; blue, **108**). The description of the protons labeled in Figure 3.11A has been given in the Figure 3.5. (**C**) ^{11}B NMR spectra corresponding to the ^{1}H NMR spectra in Figure 3.11B

Figure 3.11 cont'd

A

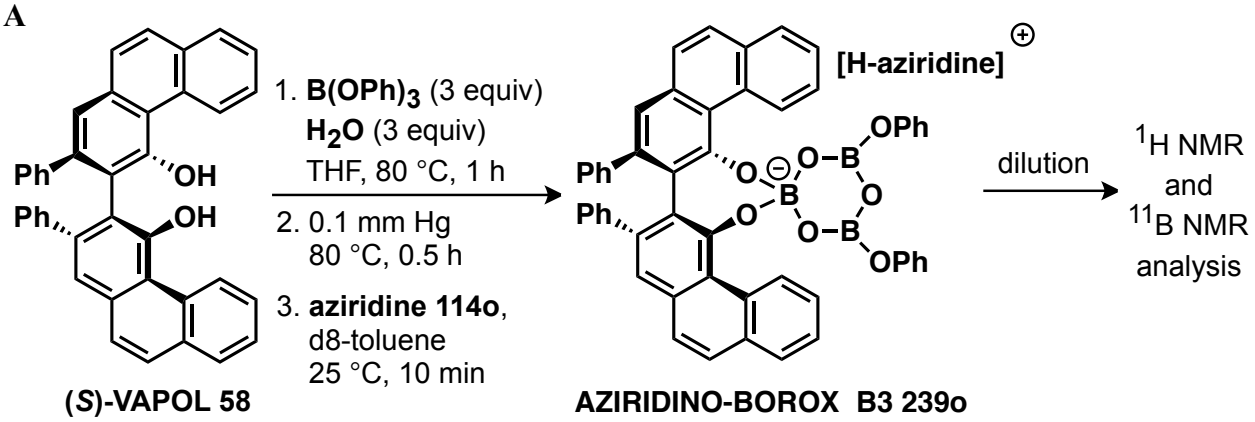

B

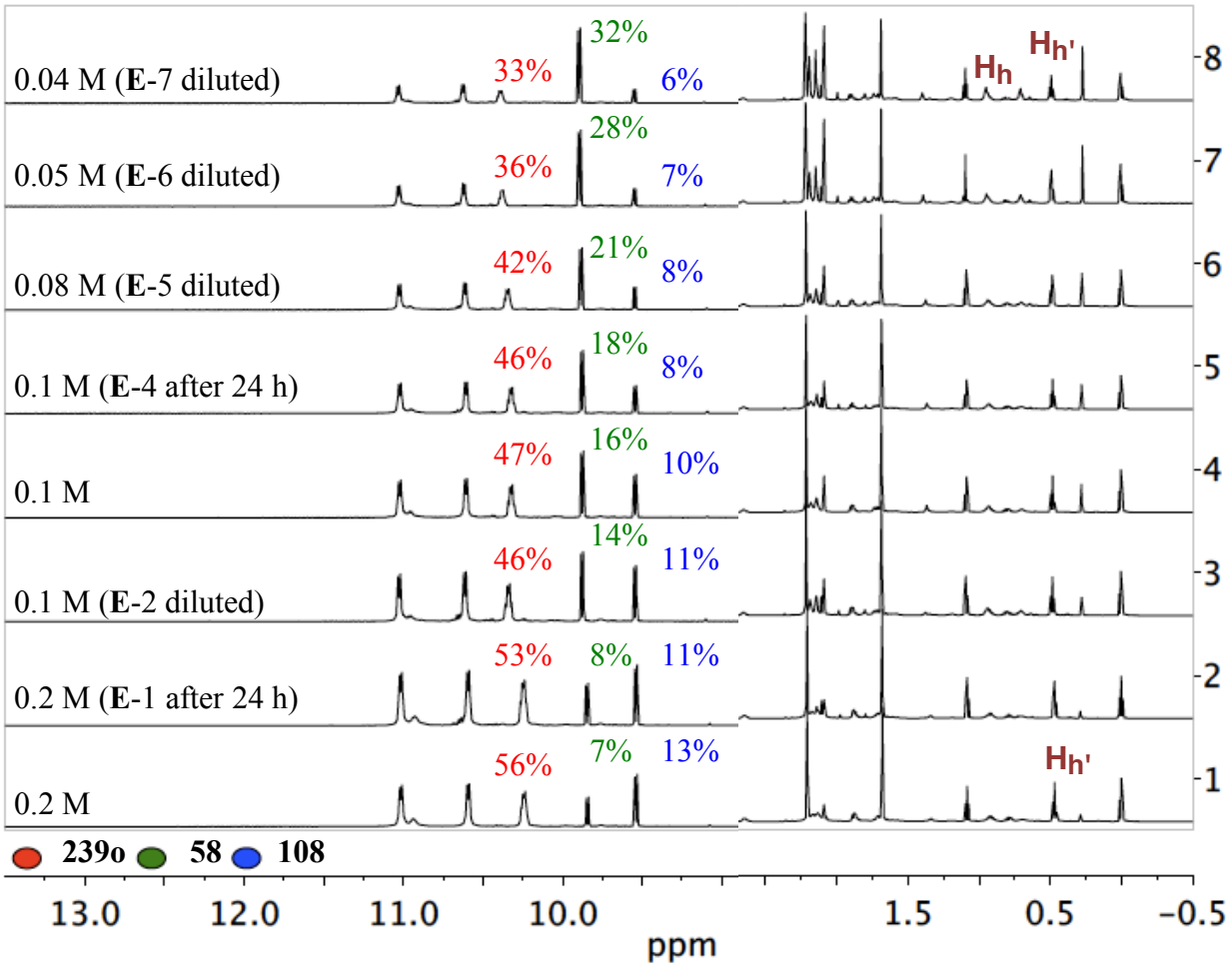

Figure 3.11 cont'd

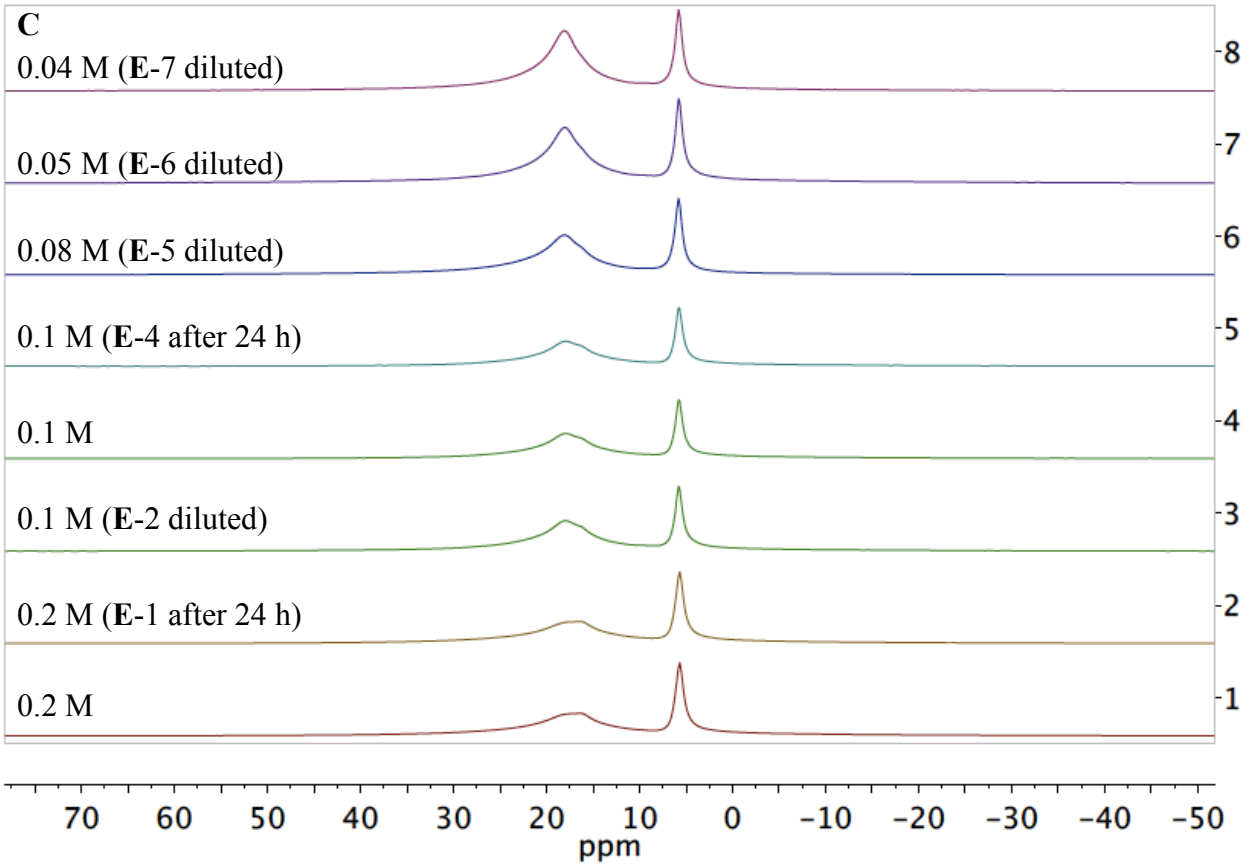

[a] Note for Figure 3.11B: Entry 1: (*S*)-VAPOL (0.2 mmol) plus 3 equiv commercial $B(OPh)_3$ and 3 equiv H_2O were heated at 80 °C in THF for 1 h followed by removal of volatiles under vacuum for 0.5 h. Thereafter, 1.0 equiv of aziridine **114o** was added to the pre-catalyst as a solution in d8-toluene (1 mL) for 10 min at 25 °C. Entry 2: Same as entry 1 after 24 h. Entry 3: An additional 1 mL of d8-toluene was added to entry 2 (0.1 M). Entry 4: (*S*)-VAPOL (0.1 mmol) plus 3 equiv commercial $B(OPh)_3$ and 3 equiv H_2O were heated at 80 °C in THF for 1 h followed by removal of volatiles under vacuum for 0.5 h. Thereafter, 1.0 equiv of aziridine **114o** was added to the pre-catalyst as a solution in d_8-toluene (1 mL) for 10 min at 25 °C. Entry 5:

Same as entry 4 after 24 h. Entry 6: An additional 0.25 mL of d_8-toluene was added to entry 4 (0.08 M). Entry 7: An additional 0.75 mL of d_8-toluene was added to entry 6 (0.05 M). Entry 8: An additional 0.50 mL of d_8-toluene was added to entry 7 (0.04 M).

The corresponding ^{11}B NMR spectra also show that there is an increase in the amount of tri-coordinate boron compounds as compared to tetra-coordinated boroxinate upon dilution. Hence these data suggest that these species are in equilibrium.

This equilibrium was further confirmed by another experiment where the concentration of aziridine **114o** was increased. An increase in AZIRIDINO-BOROX **239o** was observed with an increase in aziridine **114o** due to the shift in the equilibrium. This is presented in Figure 3.12 with the help of ^{1}H NMR and ^{11}B NMR spectroscopy.

Figure 3.12 (**A**) Aziridine induced boroxinate formation and its behavior with excess aziridine. (**B**)[a] ^{1}H NMR spectra of the reaction mixture in $CDCl_3$ with Ph_3CH as internal standard. The numbers given in the spectra shows the NMR yield of respective species. (**C**) ^{11}B NMR spectra corresponding to the ^{1}H NMR spectra in Figure 3.12B.

Figure 3.12 cont'd

A

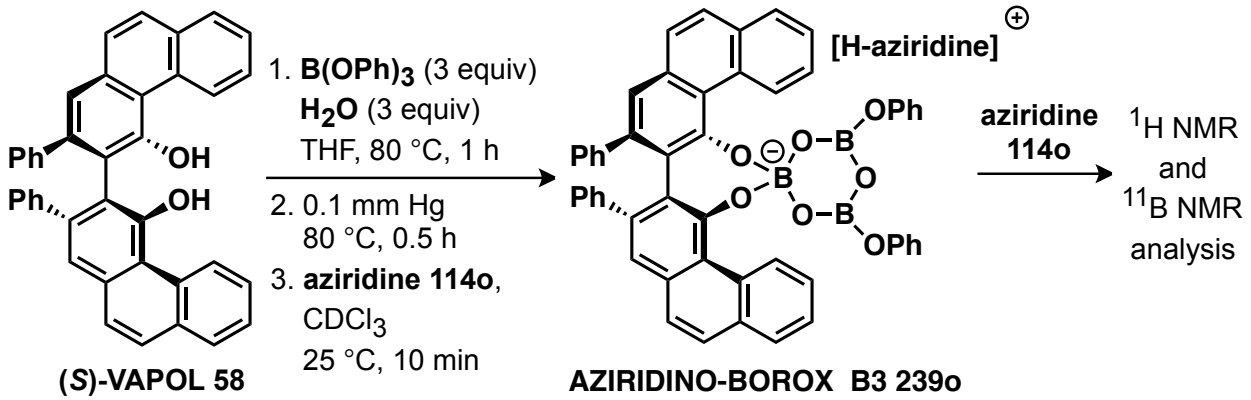

B

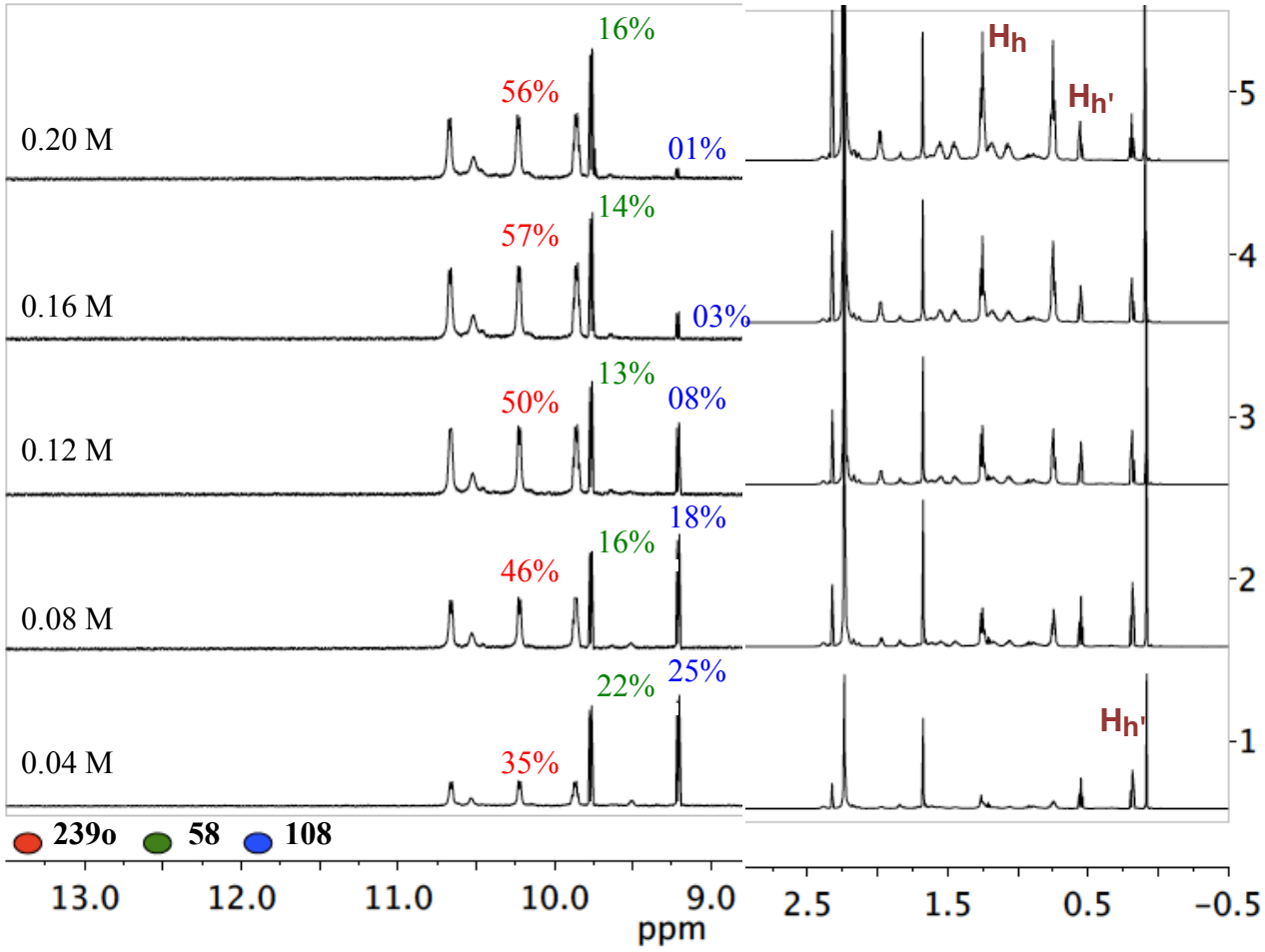

Figure 3.12 cont'd

C

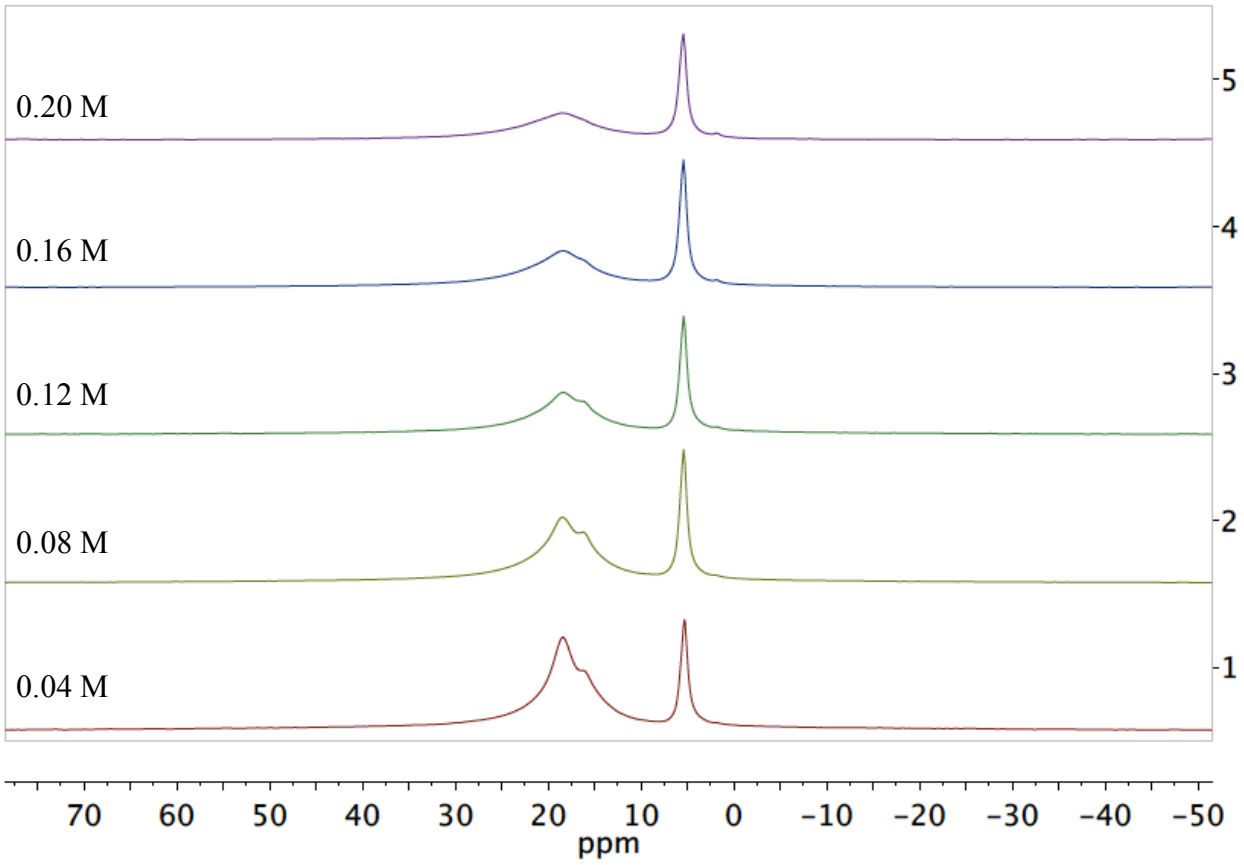

[a] Note for Figure 3.12B: Entry 1: (*S*)-VAPOL (0.4 mmol) plus 3 equiv commercial $B(OPh)_3$ and 3 equiv H_2O were heated at 80 °C in THF for 1 h followed by removal of volatiles under vacuum for 0.5 h. Thereafter, 1.0 equiv of aziridine **114o** was added to the pre-catalyst as a solution in $CDCl_3$ (10 mL) for 10 min at 25 °C. Further, an aliquot of 1mL of this resulting $CDCl_3$ solution was taken for NMR analysis (0.04 M). Entry 2: An additional 0.36 mmol aziridine **114o** was added to the remaining solution (9 mL). Thereafter, an aliquot of 1mL of the resulting $CDCl_3$ solution was taken for NMR analysis (0.08 M). Entry 3: An additional 0.32

mmol aziridine **114o** was added to the remaining solution (8 mL). Thereafter, an aliquot of 1mL of the resulting $CDCl_3$ solution was taken for NMR analysis (0.12 M). Entry 4: An additional 0.28 mmol aziridine **114o** was added to the remaining solution (7 mL). Thereafter, an aliquot of 1mL of the resulting $CDCl_3$ solution was taken for NMR analysis (0.16 M). Entry 5: An additional 0.24 mmol aziridine **114o** was added to the remaining solution (6 mL). Thereafter, an aliquot of 1mL of the resulting $CDCl_3$ solution was taken for NMR analysis (0.20 M).

The dilution experiments and the increase in concentration experiments provide enough support to conclude that there is an equilibrium operating between these species as the absorptions for the aziridine-catalyst complex increase with increasing concentration as the absorptions for the free ligand and the free aziridine decrease (Figure 3.13A). The reverse is true with decreasing concentration. The ^{11}B NMR spectrum also reveals an increase in the amount of 3-coordinate borate species as the amount of free ligand and free aziridine increases. The identity of these borate species can't be determined from these experiments but certainly could include commercial $B(OPh)_3$, B1 **106**, B2 **108** (Scheme 3.2) and triphenoxy boroxine **191a** (Scheme 3.3). The data in Figures 3.11 and 3.12 are plotted in Figure 3.13B and 3.13C, respectively. Note that in both experiments the same amount of AZIRIDINO-BOROX **239o** is observed at 0.2 M and at 0.04 M.

Figure 3.13 (**A**) Equilibrium between boroxinate **239o**, (*S*)-VAPOL **58**, aziridine **114o** and various borate species. (**B**) Plot corresponding to Figure 3.11 (**C**) Plot corresponding to Figure 3.12

Figure 3.13 cont'd

A

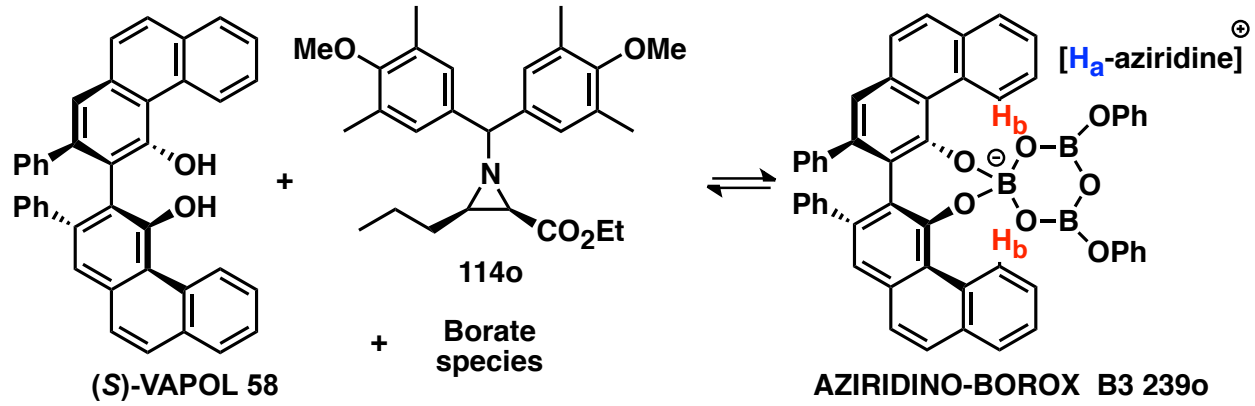

B

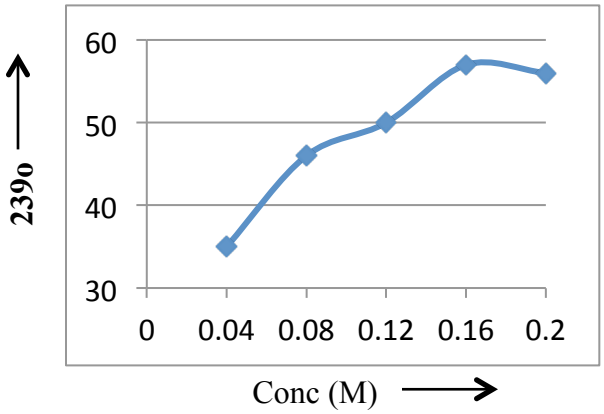

C

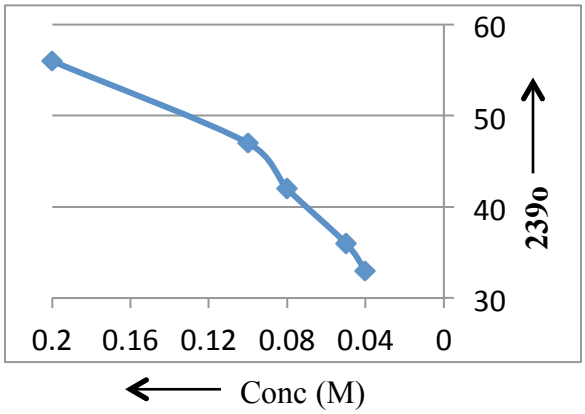

3.2.4 Probing path II of the catalytic cycle

At this point, it is unclear whether "free" BOROX catalyst **23**-H exists or not (path I, Scheme 3.3). Hence, we decided to probe path II of the catalytic cycle. In path II, the real question is whether we can observe the depletion of the aziridine-boroxinate complex in the presence of substrate i.e. imine. As shown in entry 1 of Figure 3.14, AZIRIDINO-BOROX complex **239o** is formed in 43% yield. To this mixture was then added one equivalent of imine **111o**. The bay region shows the complete replacement of the aziridine-boroxinate complex **239o**

by imine-boroxinate **190o** (Figure 3.14, entry 2). This further support the fact the imine (reactant) has a much higher binding affinity towards the catalyst as compared to the aziridine (product). These boroxinates **239o** and **190o** can also be easily followed by the methine protons H_{azi} and H_{imi} of aziridine and imine respectively (Figure 3.14C). The ratio of the **190o**:**239o** was found to be >100:1 for entry 2 based on the integration of the methine protons. The stability of the IMINO-BOROX catalyst **190o** was then examined and it was found that it slowly decomposes over a period of three days (Figure 3.14, entry 3). At this juncture, we decided to affect the generation of aziridine by the addition of the ethyl diazoacetate. The interesting part of this experiment is that we were able to observe the co-existence of both the complexes **190o** and **239o** (Figure 3.14, entry 4).

Figure 3.14 (**A**) Probing Path II of the catalytic cycle (part i). (**B**)[a] ^{1}H NMR spectra of the bay and methine region in $CDCl_3$ with Ph_3CH as internal standard. (**C**) The methine region in the ^{1}H NMR spectra of the **239o** and **190o** corresponding to ^{1}H NMR spectra in Figure 3.14B

A

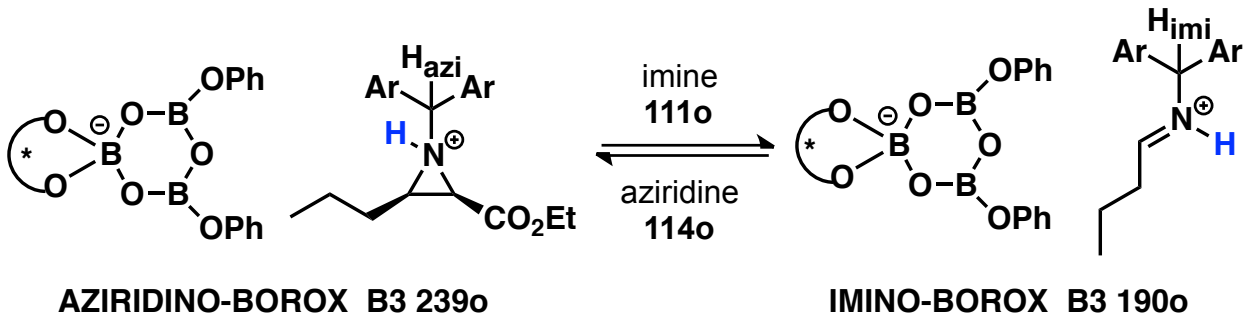

AZIRIDINO-BOROX B3 239o **IMINO-BOROX B3 190o**

Figure 3.14 cont'd

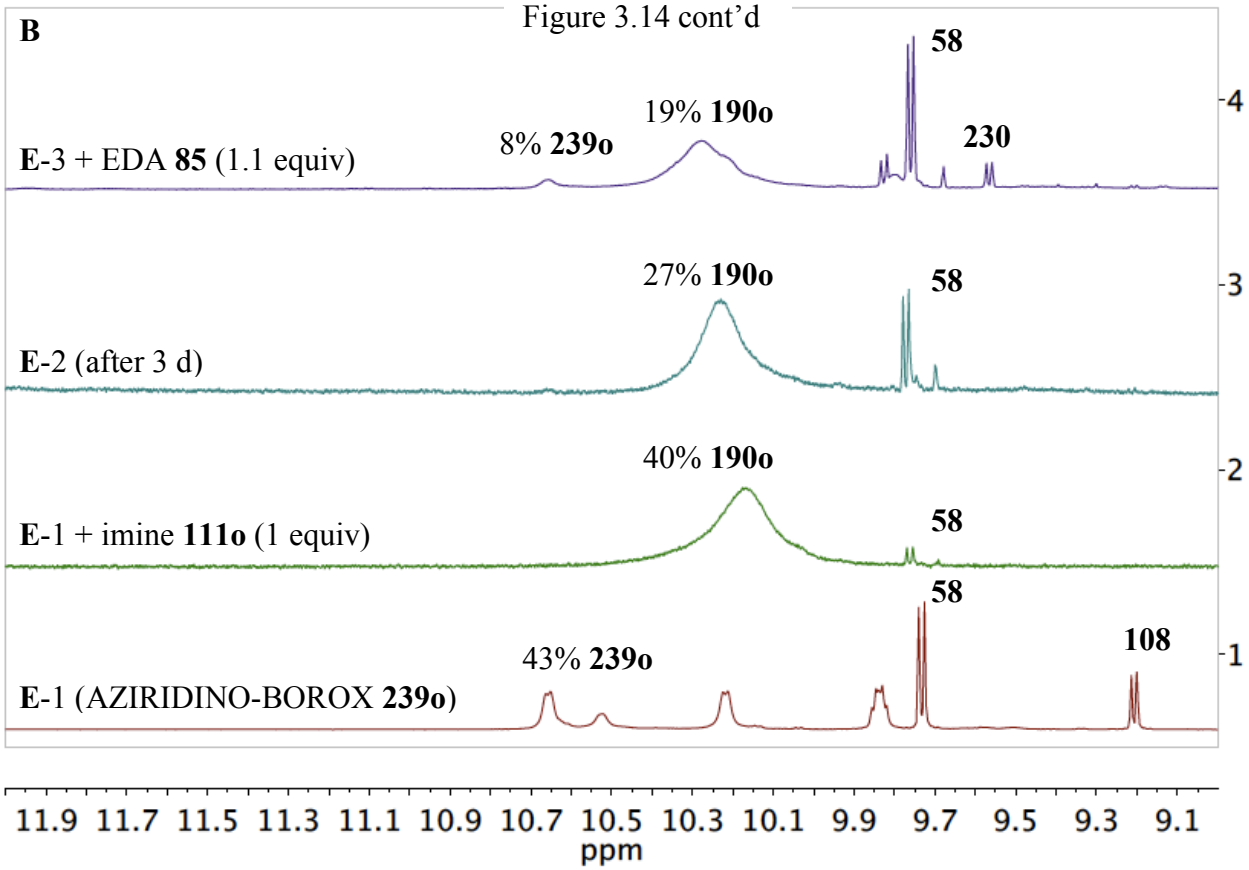

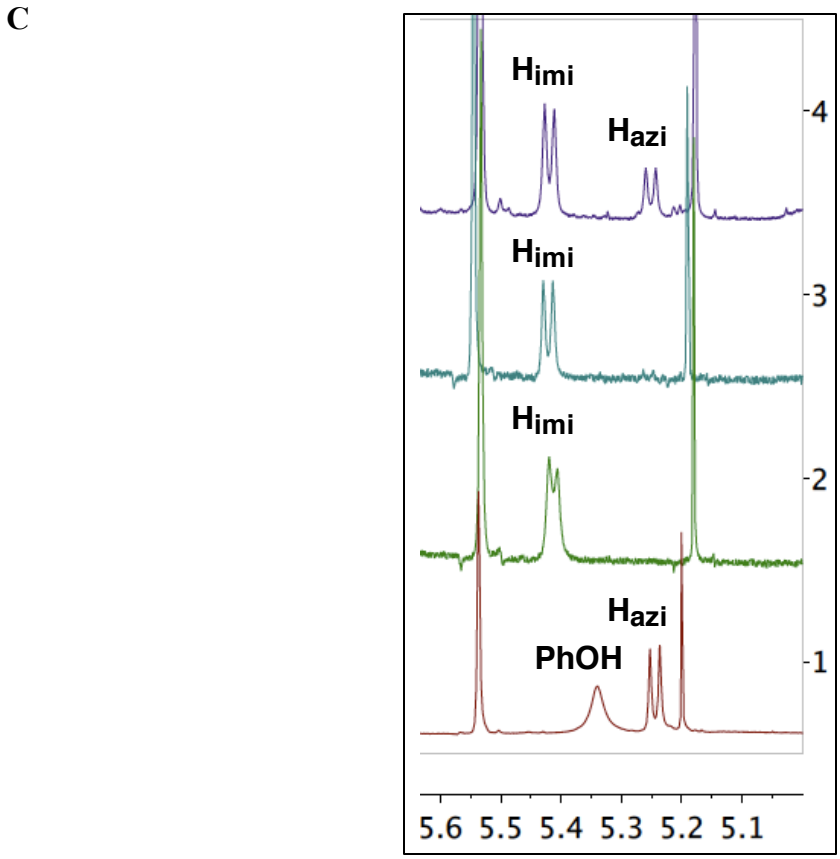

[a] Note for Figure 3.14B: Entry 1: (*S*)-VAPOL (0.1 mmol) plus 3 equiv commercial $B(OPh)_3$ and 3 equiv H_2O were heated at 80 °C in THF for 1 h followed by removal of volatiles under vacuum for 0.5 h. Thereafter, 1.0 equiv of aziridine **114o** was added to the pre-catalyst as a solution in $CDCl_3$ (1 mL) for 10 min at 25 °C. Entry 2: 1 equiv of imine **111o** was added to entry 1. Entry 3: entry 2 after 3 days. Entry 4: 1.1 equiv EDA **85** was added to entry 3.

An experiment was performed by the addition of 0.5 equivalent of imine **111o** to the aziridine-catalyst complex **239o** in order to observe the co-existence of **190o** and **239o** in a clean fashion. The results are shown in entry 2 of Figure 3.15. However at this point, it must be remembered that there is still a lot of unreacted VAPOL and some unreacted borate species in the mixture. Hence, after 1 h, the amount of imine-boroxinate increased from 34% to 53% showcasing higher binding affinity of imines (Figure 3.15, entries 2 and 3). Finally, the amount of imine complex **190o** started decreasing upon the addition of ethyl diazoacetate, possibly, due to the reaction between the imine **111o** and EDA (Figure 3.15, entry 4).

Figure 3.15 (**A**) Probing Path II of the catalytic cycle (part ii). (**B**)[a] ^{1}H NMR spectra of the bay and methine region in $CDCl_3$ with Ph_3CH as internal standard. (**C**) The methine region in the ^{1}H NMR spectra of the **239o** and **190o** corresponding to ^{1}H NMR spectra in Figure 3.15B

A

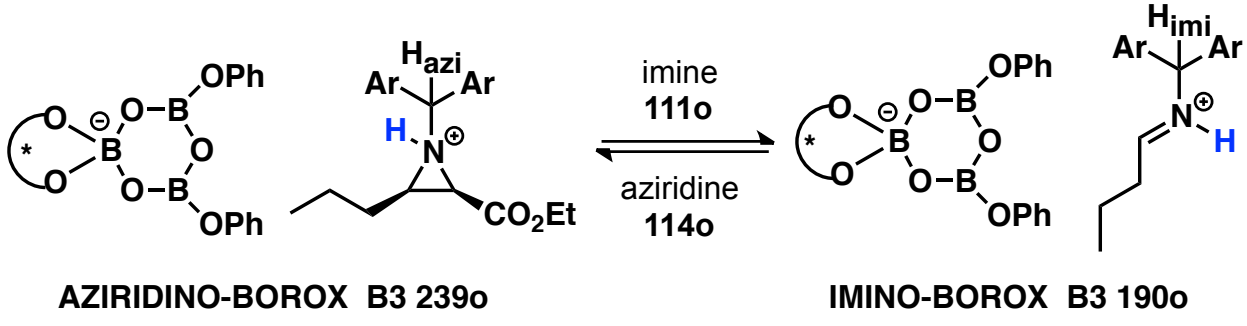

AZIRIDINO-BOROX B3 239o **IMINO-BOROX B3 190o**

Figure 3.15 cont'd

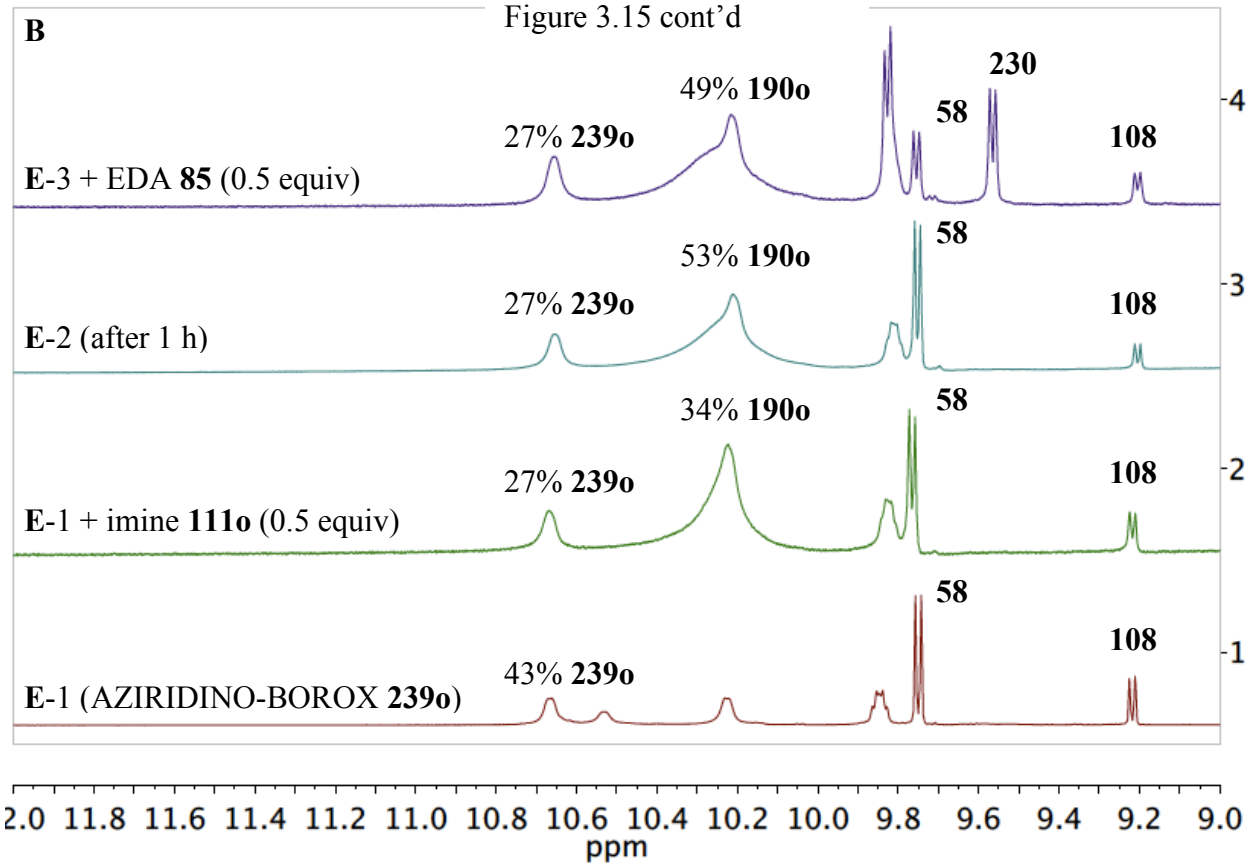

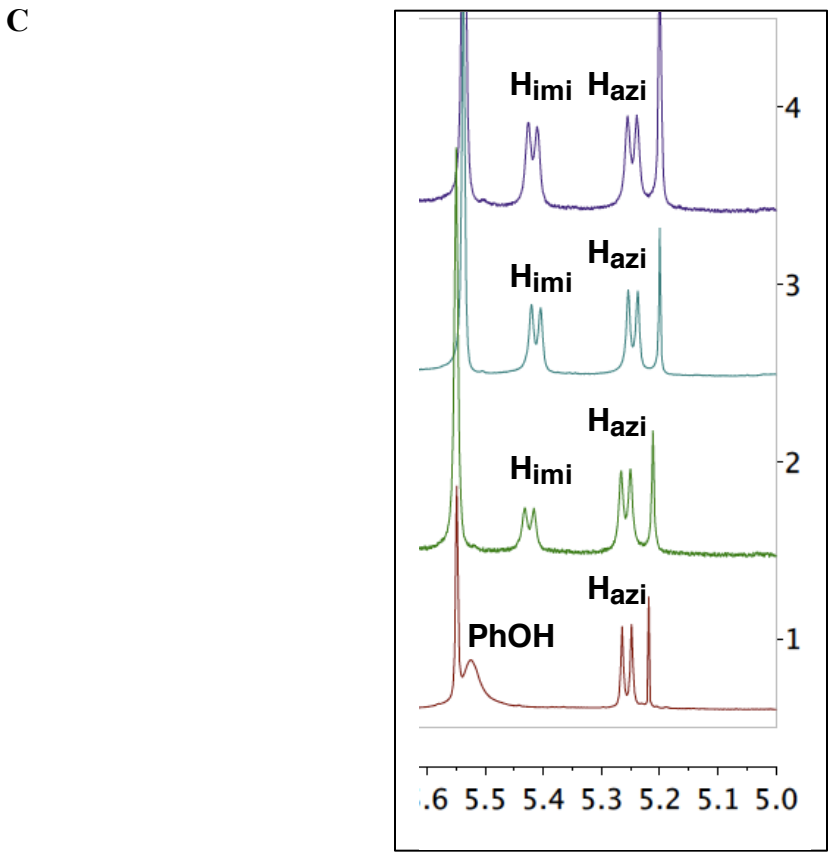

[a] Note for Figure 3.15B: Entry 1: (*S*)-VAPOL (0.1 mmol) plus 3 equiv commercial $B(OPh)_3$ and 3 equiv H_2O were heated at 80 °C in THF for 1 h followed by removal of volatiles under vacuum for 0.5 h. Thereafter, 1.0 equiv of aziridine **114o** was added to the pre-catalyst as a solution in $CDCl_3$ (1 mL) for 10 min at 25 °C. Entry 2: 0.5 equiv of imine **111o** was added to entry 1. Entry 3: entry 2 after 1 h. Entry 4: 0.5 equiv EDA **85** was added to entry 3.

3.2.5 Termination of the catalytic cycle of the aziridination reaction

When the reaction approaches completion; a mono-alkylated derivative of VAPOL i.e. **230** is often observed (Scheme 3.4 and 3.5).[5a] The alkylated VAPOL-derivative **230** has characteristic set of bay proton doublets at δ = 9.55 ppm and δ = 9.83 ppm in $CDCl_3$ (δ = 9.74 ppm and δ = 9.99 ppm in d8-toluene). The various components present in the mixture near the end of the reaction are as follows: AZIRIDINO-BOROX **239**, VAPOL **58**, aziridine **114**, unreacted ethyl diazoacetate **85** and a mixture of boron compounds (Scheme 3.5). There are two possible pathways that might lead to the formation of the VAPOL-derivatve **230**. These pathways could also be functioning in tandem. The alkylated ligand **230** is formed from the reaction of the AZIRIDINO-BOROX species **239o** with EDA perhaps mediated by an unspecified borate species. The second path Y involves the direct reaction between the free VAPOL ligand and EDA mediated by some borate species. Both pathways were considered and examined and are discussed below.

Scheme 3.5 Termination of the catalytic cycle and the aziridination reaction

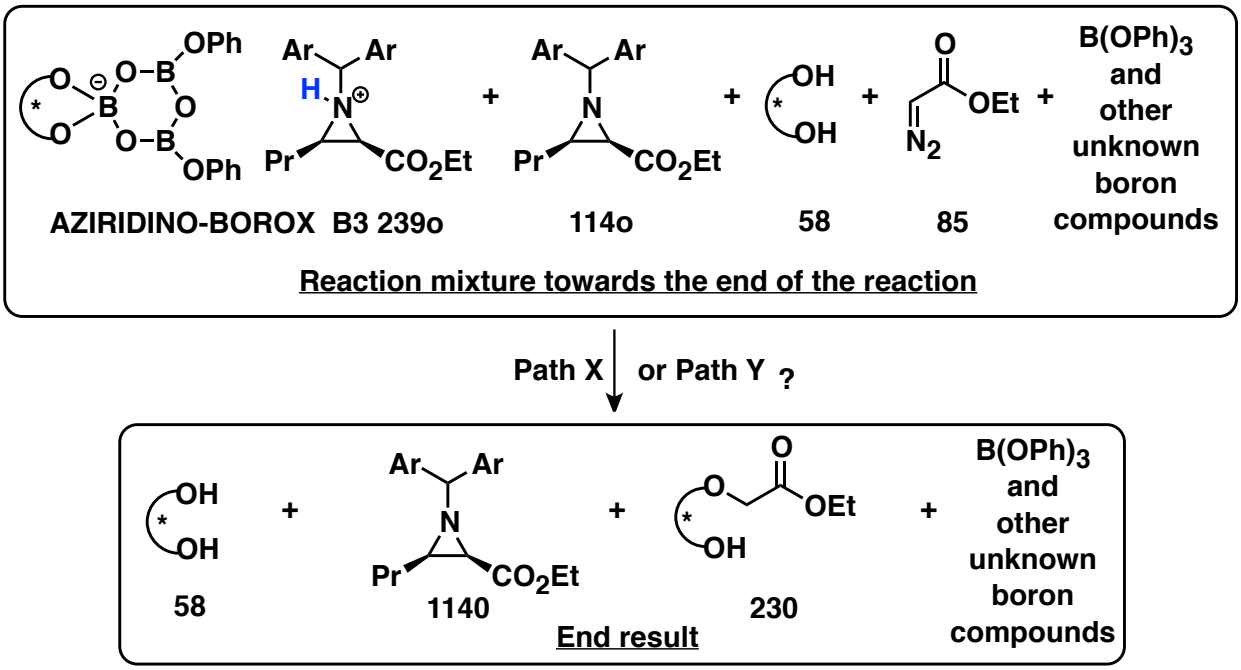

Path X

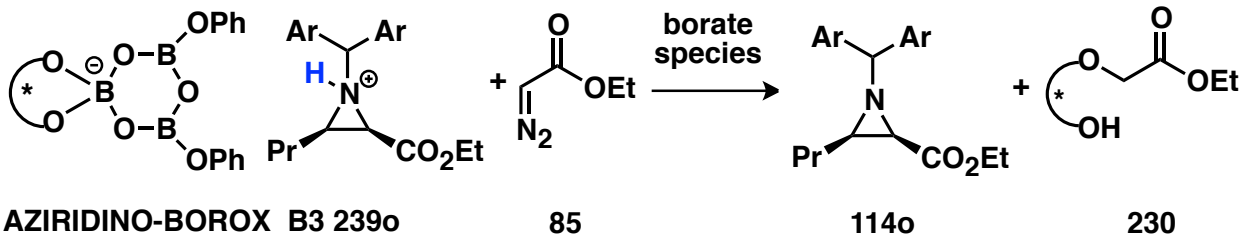

Path Y

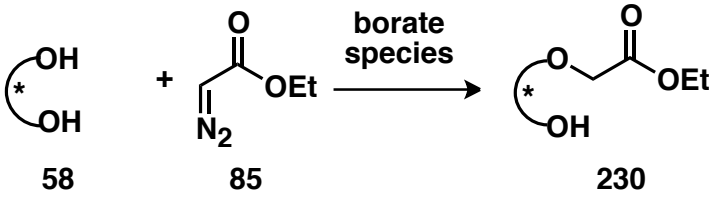

To probe path X, boroxinate **239o** was first generated from aziridine **114o** in 43% yield (Figure 3.16, entry 1). A decrease to 26% was observed when 0.5 equiv of EDA was added to

this AZIRIDINO-BOROX **239o** solution after 10 min (Figure 3.16, entry 2). This further decreased to 19% upon the addition of a second 0.5 equiv of EDA (Figure 3.16, entry 4). During this experiment, the spectra suggest that the direct alkylation of free VAPOL is faster than the decomposition of boroxinate **239o** (Figure 3.16, entries 1-4). In fact, both path X and Y appear to be operating at the same time. *It was strongly suspected that there is no decomposition of IMINO-BOROX **190** into alkylated adduct **230** in order to get the turnover.* In order to test this, a simple experiment was carried out. Aziridination with imine **111h** (R = 4-NMe_2-C_6H_4) was attempted. No aziridine was observed along with no signs of **230**.

Figure 3.16 Probing path X for the generation of the adduct **230**. (**A**) ^{1}H NMR spectra of the bay region in $CDCl_3$ with Ph_3CH as internal standard. Entry 1: (*S*)-VAPOL (0.1 mmol) plus 3 equiv commercial $B(OPh)_3$ and 3 equiv H_2O were heated at 80 °C in THF for 1 h followed by removal of volatiles under vacuum for 0.5 h. Thereafter, 1.0 equiv of aziridine **114o** was added to the pre-catalyst as a solution in $CDCl_3$ (1 mL) for 10 min at 25 °C. Entry 2: 0.5 equiv of EDA **85** was added to entry 1. Entry 3: entry 2 after 30 min. Entry 4: 0.5 equiv EDA **85** was added to entry 3. Entry 5: entry 3 after 90 min. Entry 6: entry 3 after 200 min. Entry 7: entry 3 after 3 days. (**B**) ^{1}H NMR spectra of the methyl and methoxy region corresponding to ^{1}H NMR spectra in Figure 3.16A.

Figure 3.16 cont'd

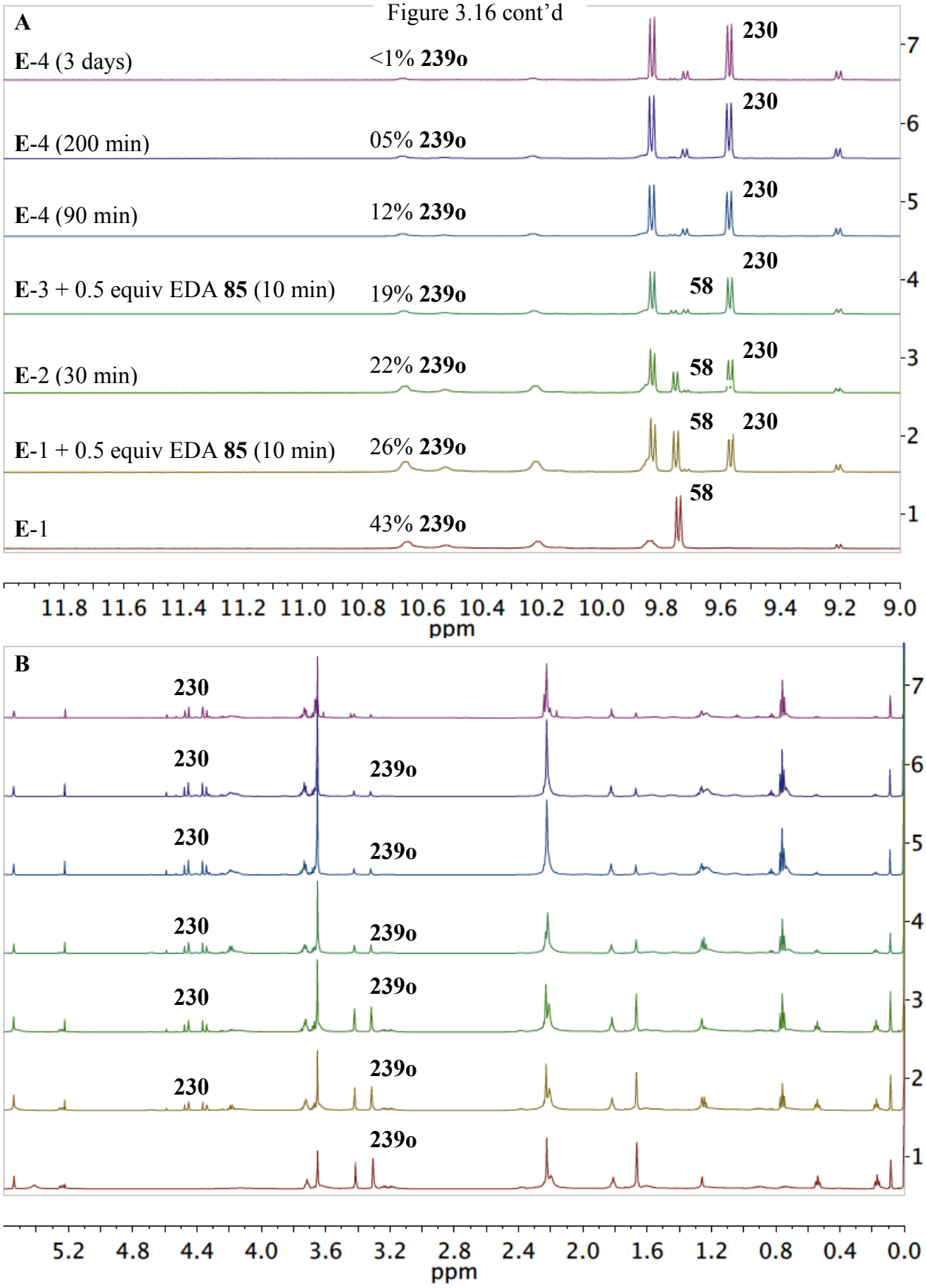

As of now, it is quite evident that path Y is also operating. So we decided to further examine this pathway in a separate experiment. First of all, it was found that (*S*)-VAPOL **58** and EDA **85** do not react in absence of boron compounds (Figure 3.17, entry 1). However, both of them react quickly in the presence of commercial $B(OPh)_3$ at room temperature by simple mixing all of them together in $CDCl_3$ to afford **230** in 80% yield within 10 minutes (Figure 3.17, entry 2). It was also found that if a mixture of (*S*)-VAPOL **58** and commercial $B(OPh)_3$ was heated prior to treating with EDA **85**, then the reaction is slow in generating only 18% of **230** in 10 minutes (Figure 3.17, entry 3). An unknown compound **241** with a peak at δ = 9.71 ppm ($CDCl_3$) is also observed in 8% yield. After 24 h, the unknown compound increases up to 20% yield where as **230** decreases to 5% yield (Figure 3.17, entry 4). Treatment of this mixture with one equiv of H_2O gave a 92% isolated yield of **230** (Figure 3.17, entry 5). As discussed earlier, an aziridination reaction between imine **111a** and 1.2 equiv of EDA **85** is also monitored (Figure 3.17, entry 6). After quenching, a 95% yield of **230** was isolated from the crude reaction mixture. It must be noted that (*S*)-VAPOL **58** can be easily recovered from **230** using SmI_2.[5a]

Figure 3.17 Probing path Y for the generation of **230**. ^{1}H NMR spectra of the bay region in $CDCl_3$ with Ph_3CH as internal standard and the yields of the respective species in the parenthesis. Entry 1: (*S*)-VAPOL (0.1 mmol) plus 2 equiv EDA **85** at 25 °C for 10 min. Entry 2: (*S*)-VAPOL (0.1 mmol) plus 3 equiv commercial $B(OPh)_3$ and 2 equiv EDA **85** at 25 °C for 10 min. Entry 3: (*S*)-VAPOL (0.1 mmol) plus 3 equiv commercial $B(OPh)_3$ were heated at 80 °C in toluene for 1 h followed by removal of volatiles under vacuum for 0.5 h. Thereafter, 2

Figure 3.17 cont'd

equiv of EDA **85** and $CDCl_3$ (1 mL) was added to the pre-catalyst at 25 °C for 10 min. Entry 4: entry 3 after 24 h. Entry 5: entry 4 plus 1 equiv of H_2O. Entry 6: (*S*)-VAPOL (0.1 mmol) plus 3 equiv commercial $B(OPh)_3$ were heated at 80 °C in toluene for 1 h followed by removal of volatiles under vacuum for 0.5 h. Thereafter, 10 equiv of imine **111a** and 12 equiv of EDA **85** were added to the pre-catalyst at 25 °C and kept for 95 min (Scheme 3.2). Entry 7: ^{1}H NMR spectrum of the bay region of the pure **230** in $CDCl_3$.

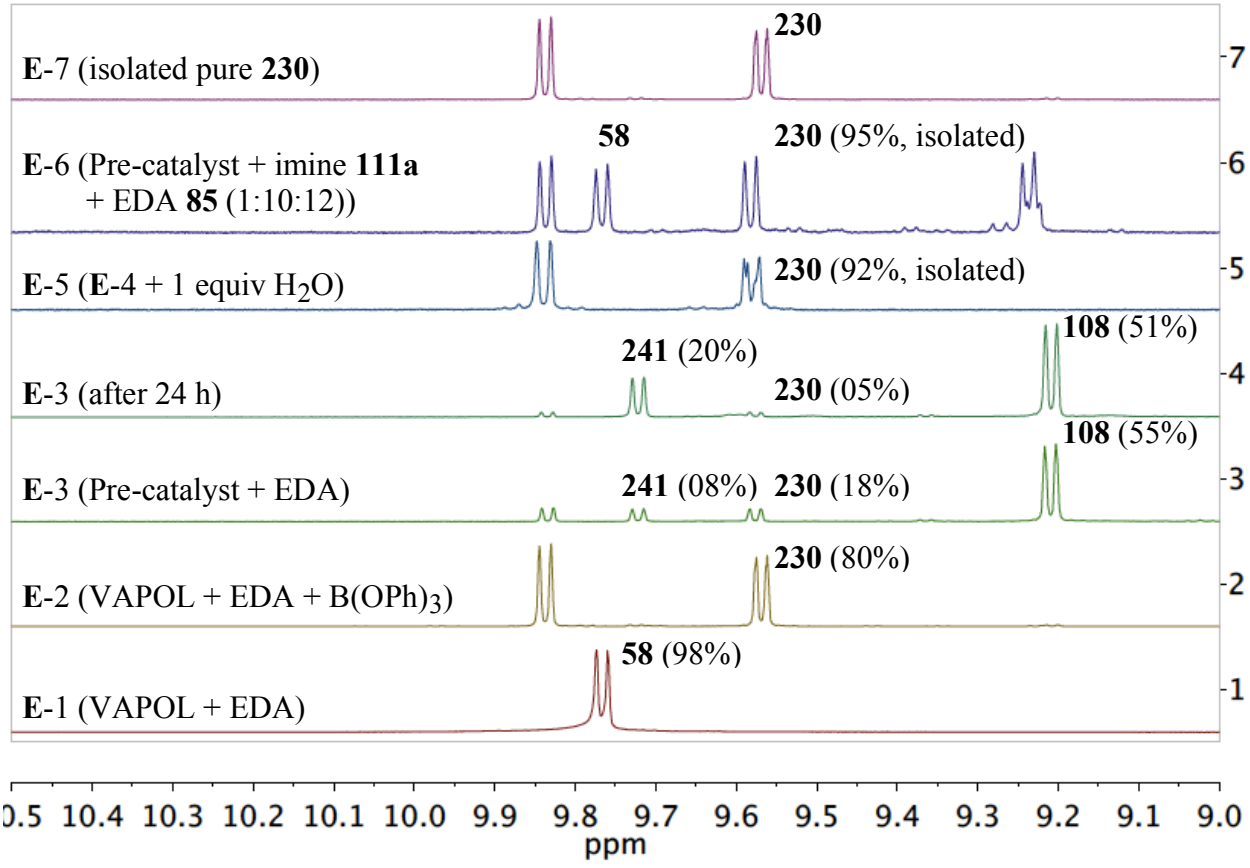

3.2.6 Possibility of 'free' BOROX complex **23**-H

Path I of the catalytic cycle involves the possibility of free BOROX **23**-H (Scheme 3.3). Hence, we were interested in finding the support for the existence of the free BOROX catalyst **23**-H. So far, there is no evidence for the existence of such kind of species either by NMR or X-ray crystallography. The help of computational chemistry was then sought. To begin, the energy minimized structure of the boroxinate anion **23** was computed by DFT calculations using Gaussian ′03[6] at B3LYP/6-31g* level of theory and the result is shown in Figure 3.18A. A free proton was then placed on either of the two oxygens O1 and O2 as they were found to posses the maximum electron densities. Interestingly, in both cases, the spiro-borate ring was no longer favorable and the tetra-coordinate boron transformed itself into a tri-coordinate boron (Figure 3.18B and 3.18C). This suggests that protonated form of **23** might not exist or they might have very short lifetimes. In both the cases, the distance (B-O1 or B-O2) between the O1/O2 and former tetra-coordinate boron was found to more than 2.5 Å (Figure 3.18B and 3.18C). Additionally, the former tetra-coordinate boron is found to be out of the plane by ~ <1–2.6º (Figure 3.18B and 3.18C). Out of both the structures **23**-H**a** is found to be more stable than **23**-H**b** by +8.6 kcal/mol. In the case of the boroxinate anion, the ∠oop and B-O2 was found to be 20.2º and 1.43 Å respectively (Figure 3.18A).

Figure 3.18 All calculations are performed using Gaussian ′03 at B3LYP/6-31g* level of theory. All structures are visualized by the Mercury program (C, gray; O, red; B, yellow; H, light blue). Hydrogens are omitted for clarity (except O-H). ∠oop = angle out of plane for the current/former tetra-coordinate boron, B-O2 = the distance between O-2 and the former tetra-

Figure 3.18 cont'd

coordinate boron. B-O1 = the distance between O-1 and the current/former tetra-coordinate boron. (**A**) Calculated structure of BOROX anion **23** (**B**) Calculated structure of the neutral BOROX catalyst **23**-H**a** resulting from protonation of **23** on O1. (**C**) Calculated structure of the neutral BOROX catalyst **23**-H**b** resulting from protonation of **23** on O2.

A

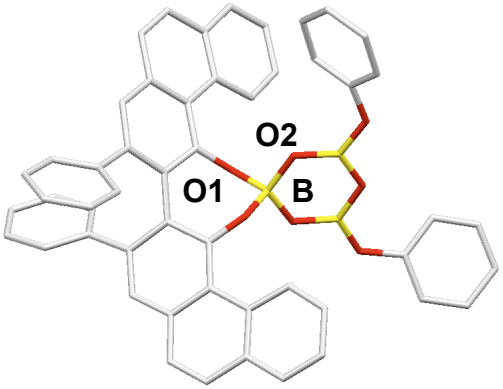

23
(∠oop = 20.2º, B-O1 = 1.50 Å, B-O2 = 1.43 Å)

B

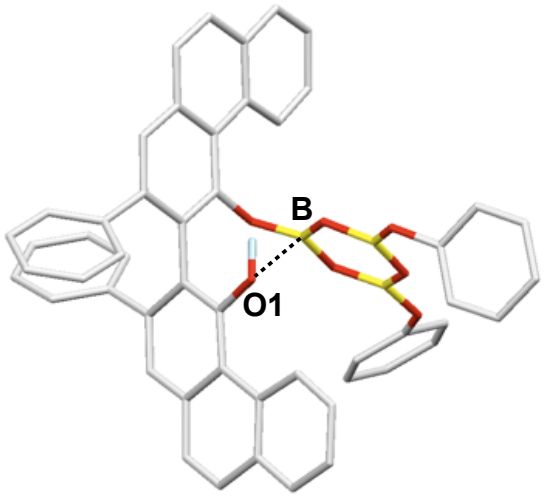

23-H**a**
(∠oop < 1º, B-O1 = 3.43 Å)
(ΔΔG = 0 Kcal/mol)

C

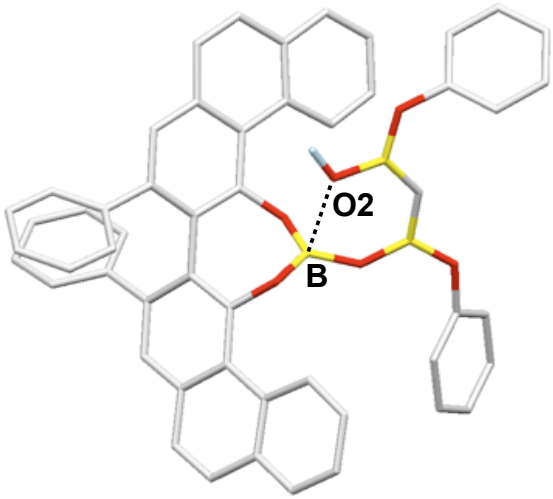

23-H**b**
(∠oop = 2.6º, B-O2 = 2.57 Å)
(ΔΔG = +8.6 Kcal/mol)

It was then undertaken to prepare the boroxinate anion in vitro followed by its protonation in order to observe **23**-H. Hence, the boroxinate anion core was prepared utilizing tetra-methyl ammonium acetate as the base to generate BOROX **242**.[5e] Several equivalents of TfOH were added to **242** (Figure 3.19B). Two new pair of doublets were observed at δ = 10.40 ppm and δ = 10.46 ppm in $CDCl_3$ (Figure 3.19B, entries 3 and 4). However, a free BOROX catalyst **23**-H would be expected to give a single doublet for a spiro structure due to the fast exchange of the free proton. Species **23a**-H and **23b**-H would be expected to exist as two doublets. Protonation of **242** does result in significant changes in the bay region of ^{1}H NMR spectrum but the structure of this protonated species is still uncertain. The next chapter has been devoted to address this issue.

Figure 3.19 (**A**) Design of the experiment to observe the free neutral BOROX **23**-H. (**B**)[a] ^{1}H NMR spectra of the bay region in $CDCl_3$. (**C**) ^{11}B NMR spectra corresponding to the ^{1}H NMR spectra in Figure 3.19B

A

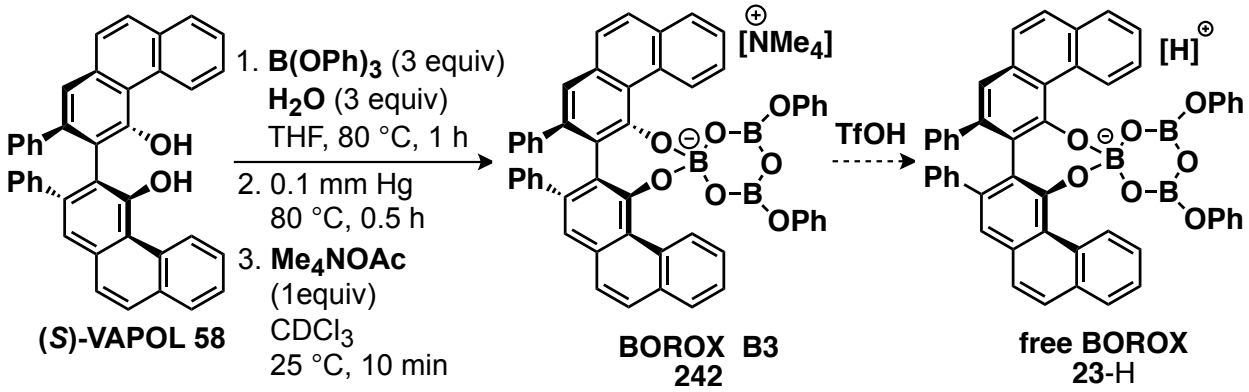

Figure 3.19 cont'd

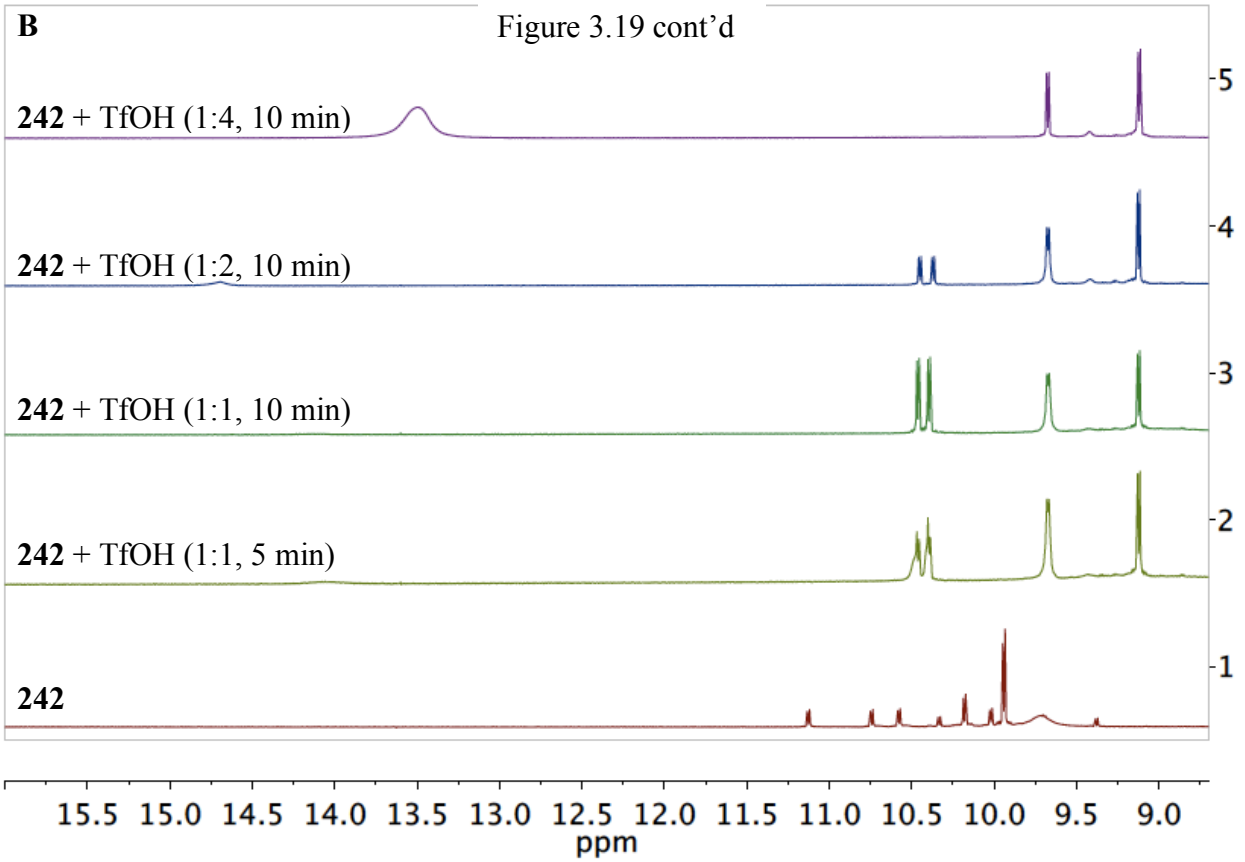

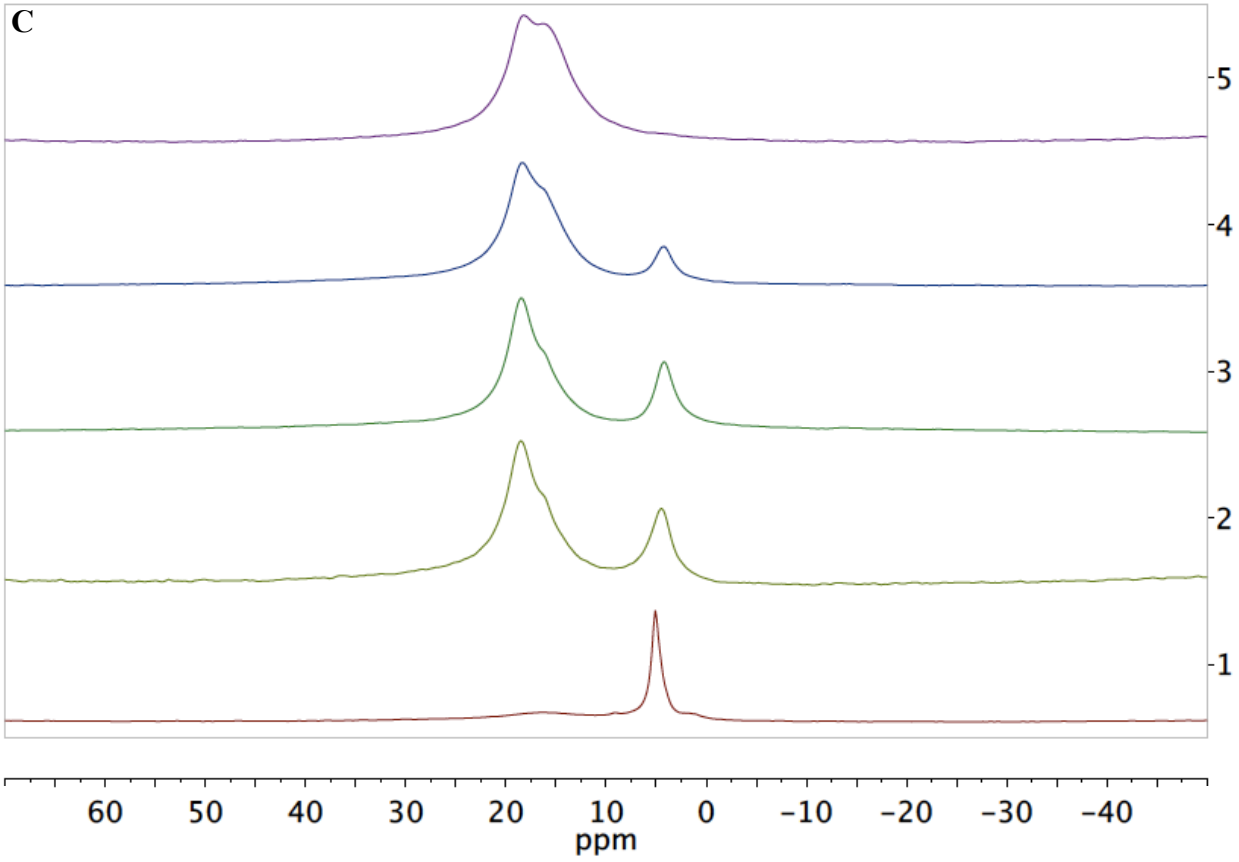

[a] Note for Figure 3.19B: Entry 1: (*S*)-VAPOL (0.1 mmol) plus 3 equiv commercial $B(OPh)_3$ and 3 equiv H_2O were heated at 80 °C in toluene for 1 h followed by removal of volatiles under vacuum for 0.5 h. Thereafter, 1 equiv of Me_4NOAc and $CDCl_3$ (1 mL) was added to the pre-catalyst at 25 °C for 10 min. Entry 2: 1 equiv of TfOH was added to entry 1 at 25 °C for 5 min. Entry 3: 1 equiv of TfOH was added to entry 1 at 25 °C for 10 min. Entry 4: 2 equiv of TfOH was added to entry 1 at 25 °C for 5 min. Entry 5: 4 equiv of TfOH was added to entry 1 at 25 °C for 5 min.

3.3 Conclusions

In this chapter, we have been able to characterize species in which a substrate is bound to the catalyst (S-BA) and in which a product is bound to the catalyst (P-BA) utilizing NMR spectroscopy. Also, their equilibrium was studied. Finally, it was possible to qualitatively and quantitatively analyze the process of depletion of the P-BA in presence of the substrate. The binding affinity of the substrate (imine) was found to be very high compared to that of the product (aziridine). All the above-mentioned observations have been achieved for the first time in case of a Brønsted acid catalyzed aziridination reaction.

Given the results from the present work, it should be possible to study the relative binding of various imines and of various aziridines as well as the relative binding between imines and aziridines and to probe the dynamics of their interchange.

APPENDIX

3.4 Experimental

3.4.1 General Information

Same as Chapter 2.

3.4.2 Synthesis of Imines **111a**, **111o, 111v, 111w** and **114o′ and triphenoxyboroxine 191a**

See Chapter 2 for the synthesis for the imine **111a** and triphenoxyboroxine **191a**. Imine **114o′** was prepared according to published procedure.[5b] All aldehydes were distilled prior to use.

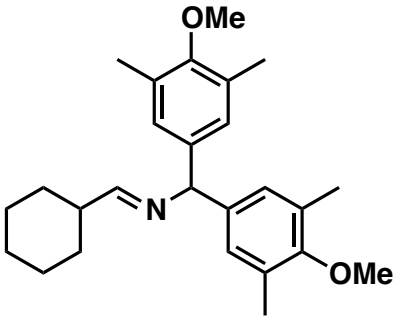

111v

***N*-Cyclohexylmethylidene-*bis*(3,5-dimethyl-4-methoxyphenyl)methylamine 111v:** Imine **111v** was prepared according to the procedure described in Chapter 2 for imine **111a**. Crystallization (1: 60 EtOAc/hexanes) and collection of the first crop afforded **111v** as white solid crystals (mp 108-109 ºC) in 71% isolated yield (1.40 g, 3.55 mmol).

Spectral data for **111v**: ^{1}H NMR ($CDCl_3$, 300 MHz) δ 1.17-1.34 (m, 5H), 1.64-1.84 (m, 5H), 2.19-2.35 (m, 1H), 2.23 (s, 12H), 3.67 (s, 6H), 5.05 (s, 1H), 6.91 (s, 4H), 7.59 (d, 1H, J = 5.1 Hz); ^{13}C NMR ($CDCl_3$, 75 MHz) δ 16.19, 25.42, 26.01, 29.79, 43.51, 59.59, 77.44, 127.74, 130.49, 139.39, 155.69, 168.59; IR (thin film): 2926s, 1665m, 1483s 1221s, 1142m, 1017s cm^{-1}; Mass spectrum *m/z* (% rel intensity) 393 M+ (0.22), 283 (100), 268 (15), 163 (54), 142 (24), 134 (15), 77 (11), 44 (10). These spectral data match those previously reported for this compound.[5c]

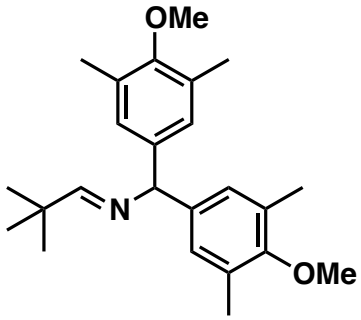

111w

***N*-(1,1′-dimethylethylidene)-bis(4-methoxy-3,5-dimethyl phenyl)methylamine 111w:** Imine **111w** was prepared according to the procedure described above for imine **111a**. Crystallization (1: 100 CH_2Cl_2/hexanes) and collection of the first crop afforded **111w** as white solid crystals (mp 90-91 ºC) in 85% isolated yield (1.56 g, 4.25 mmol).

Spectral data for **111w**: ^{1}H NMR ($CDCl_3$, 300 MHz) δ 1.09 (s, 9H), 2.23 (s, 12H), 3.68 (s, 6H), 5.08 (s, 1H), 6.91 (s, 4H), 7.61 (s, 1H); ^{13}C NMR ($CDCl_3$, 75 MHz) δ 16.22, 27.04, 36.33, 59.59, 76.75, 127.71, 130.41, 139.63, 155.62, 171.11; IR (thin film): 2955vs, 1663m, 1483s, 1221s, 1017s cm^{-1}; Mass spectrum *m/z* (% rel intensity) 367 M+(0.8), 283 (100), 268 (22), 253 (12), 210 (11), 195 (14), 178 (8), 141 (34), 133 (11), 118 (19), 41 (10). These spectral data match those previously reported for this compound.[5c]

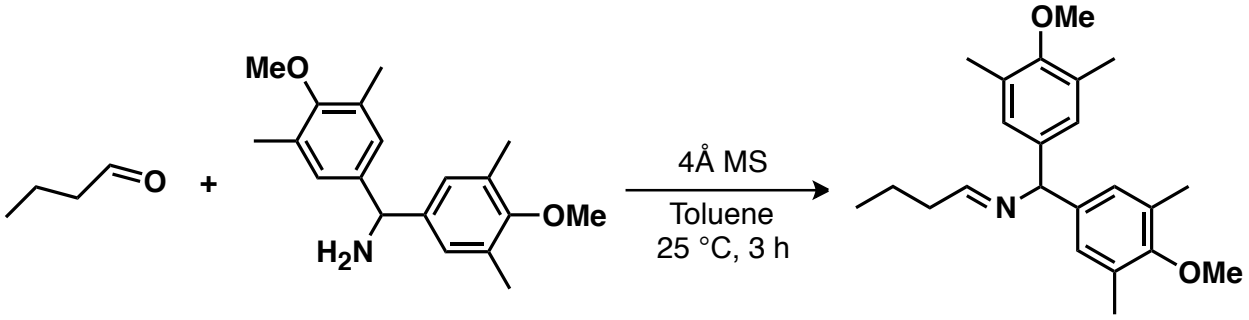

127o **126c** **111o**

(*E*)-*N*-butylidene-1,1-bis(4-methoxy-3,5-dimethylphenyl)methanamine 111o: To a 50 mL flame-dried round bottom flask filled with argon was added bis(2,6-di-methyl-4-methoxyphenyl)methylamine **126c** (1.49 g, 5.00 mmol), 4 Å Molecular Sieves (1.2 g, freshly dried) and dry toluene (5 mL). After stirring for 10 min, *n*-butanal **127o** (473 μL, 5.25 mmol, 1.05 equiv, freshly distilled) was added. The reaction mixture was stirred at room temperature for 3 h. The reaction mixture was filtered through Celite and the Celite bed was washed with

CH_2Cl_2 (10 mL × 3) and then the filtrate was concentrated by rotary evaporation to give the crude imine as an off-white solid. Crystallization (hexanes) and collection of the first crop afforded **111o** as white solid crystals (mp 102-103 ºC) in 80 % isolated yield (1.4 g, 4.0 mmol).

Spectral data for **111o**: ^{1}H NMR ($CDCl_3$, 500 MHz) δ 0.94 (t, 3H, J = 7.3 Hz), 1.58 (sextet, 2H, J = 7.3 Hz), 2.23 (s, 12H), 2.28-2.32 (m, 2H), 3.67 (s, 6H), 5.09 (s, 1H), 6.92 (s, 4H), 7.75 (t, 1H, J = 4.9 Hz); ^{13}C NMR (125 MHz, $CDCl_3$) δ 13.81, 16.17, 19.50, 37.84, 59.59, 77.71, 127.75, 130.55, 139.24, 155.73, 164.88; HRMS (ESI-TOF) *m/z* 354.2433 [($M+H^+$); calcd. for $C_{23}H_{32}NO_2$: 354.2433]. These spectral data match those previously reported for this compound.[5c]

3.4.3 Synthesis of aziridines 114a, 114o, 114v, 114w and 115o′

All aziridines but **115o′** have been prepared using procedure IV (pre-catalyst method C) of Table 2.1 in Chapter 2. The representative procedures for two aziridines **114a** and **114o** are given here and the details for the aziridines **114v** and **114w** can be found in reference 5c. Aziridine **115o′** have been prepared using procedure I (pre-catalyst method A) and is already reported.[5b]

Synthesis of aziridine 114a using imine 111a:

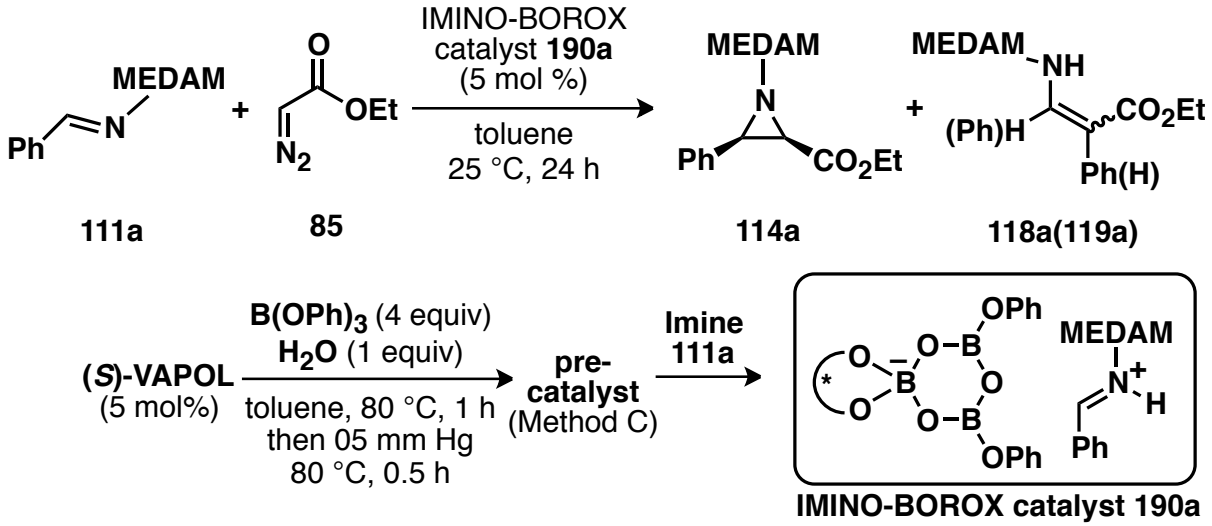

(2*R*,3*R*)-ethyl-1-(bis(4-methoxy-3,5-dimethylphenyl)methyl)-3-phenylaziridine-2-carboxylate 114a: Imine **111a** (387 mg, 1 mmol) was reacted according to the general procedure IV (pre-catalyst method C) described above (Chapter 2) with (*S*)-VAPOL (5 mol%) as the ligand. Purification of the crude aziridine by silica gel chromatography (30 mm × 300 mm column, 9:1 hexanes/EtOAc as eluent, gravity column) afforded pure *cis*-aziridine **114a** as a white solid (mp 107-108 ºC on 99.8% ee material) in 98 % isolated yield (464 mg, 0.980 mmol); *cis/trans*: >50:1. Enamine side products: 1 % yield of **118a** and 1 % yield of **119a**. The optical purity of **114a** was determined to be 99.8 % *ee* by HPLC analysis (CHIRALCEL OD-H column, 99:1 hexane/2-propanol at 226nm, flow-rate: 0.7 mL/min): retention times; R_t = 9.26 min (major enantiomer, **114a**) and R_t = 12.52 min (minor enantiomer, *ent*-**114a**).

Spectral data for **114a**: R_f = 0.42 (1:9 EtOAc/hexane); ^{1}H NMR ($CDCl_3$, 500 MHz) δ 0.98 (t, 3H, *J* = 7.1 Hz), 2.18 (s, 6H), 2.24 (s, 6H), 2.55 (d, 1H, *J* = 6.8 Hz), 3.10 (d, 1H, *J* = 6.6 Hz), 3.62 (s, 3H), 3.66 (s, 1H), 3.68 (s, 3H) 3.87-3.97 (m, 2H), 7.09 (s, 2H), 7.18 (s, 2H), 7.21-7.24

(m, 3H), 7.36 (d, 2H, J = 7.3 Hz); ^{13}C ($CDCl_3$, 125 MHz) δ 14.01, 16.16, 16.22, 46.26, 48.20, 59.52, 59.58, 60.47, 77.04, 127.21, 127.41, 127.70, 127.80,127.85, 130.59, 130.60, 135.33, 137.79, 137.96, 155.95, 156.10, 168.01; IR (thin film) 2961 vs, 1750 vs, 1414 vs, 1202 vs cm^{-1}; Mass spectrum: *m/z* (% rel intensity) 473 M+ (0.27), 284(78), 283 (100), 268 (34), 253 (20), 237 (11), 210(10), 117 (18), 89 (11); Anal calcd for $C_{30}H_{35}NO_4$: C, 76.08; H, 7.45; N, 2.96. Found: C, 76.31; H, 7.28; N, 2.82; $[\alpha]_D^{23}$ +41.3 (*c* 1.0, EtOAc) on 99% ee material (HPLC). These spectral data match those previously reported for this compound.[5c]

Synthesis of aziridine 114o using imine 111o:

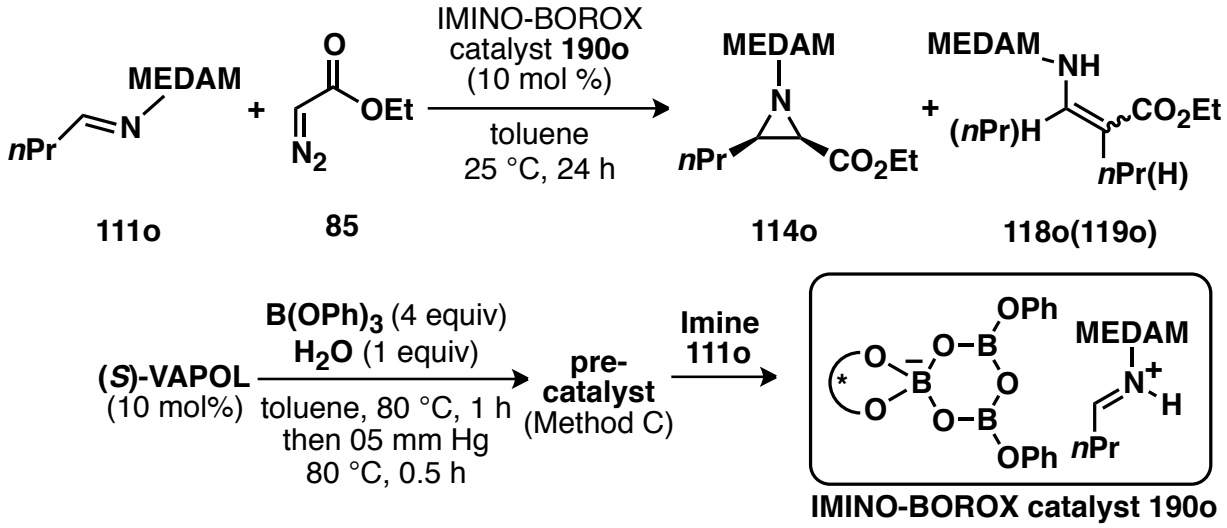

(2*R*,3*R*)-ethyl-1-(bis(4-methoxy-3,5-dimethylphenyl)methyl)-3-phenylaziridine-2-carboxylate 114o: Imine **111o** (353 mg, 1 mmol) was reacted according to the general procedure IV (pre-catalyst method C) described above (Chapter 2) with (*S*)-VAPOL (10 mol%) as the ligand. Purification of the crude aziridine by silica gel chromatography (20 mm × 250 mm

column, 4:2:0.1 hexanes/CH_2Cl_2/EtOAc, gravity column) afforded pure *cis*-aziridine **114o** as a yellow oil in 64 % isolated yield (281 mg, 0.640 mmol); *cis/trans*: not determined. Enamine side products: not observed. The optical purity of **114o** was determined to be 93% *ee* by HPLC analysis (CHIRALCEL OD-H column, 99:1 hexane/2-propanol at 226 nm, flow-rate: 0.7 mL/min): retention times; R_t = 4.73 min (major enantiomer, **114o**) and R_t = 5.68 min (minor enantiomer, *ent*-**114o**).

Spectral data for **114o**: R_f = 0.28 (4:2:0.1 hexanes/CH_2Cl_2/EtOAc); ^{1}H NMR ($CDCl_3$, 500 MHz) δ 0.72 (t, 3H, *J* = 7.6 Hz), 0.98-1.08 (m, 1H), 1.11-1.20 (m, 1H), 1.23 (t, 3H, *J* = 7.1 Hz), 1.38-1.45 (m, 1H), 1.49-1.55 (m, 1H), 1.95 (q, 1H, *J* = 6.6 Hz), 2.18 (d, 1H, *J* = 6.8 Hz) 2.22 (s, 12H), 3.39 (s, 1H), 3.65 (s, 3H), 3.67 (s, 3H), 4.12-4.23 (m, 2H), 6.99 (s, 2H), 7.07 (s, 2H); ^{13}C NMR ($CDCl_3$, 125 MHz) δ 13.57, 14.33, 16.09, 16.16, 20.33 29.93, 43.53, 46.76, 59.56, 59.60, 60.64, 77.32, 127.41, 128.07, 130.44, 130.47, 137.75, 138.18, 155.81, 156.12, 169.69; IR (thin film) 2957vs, 1744s, 1483s, 1221s, 1182vs cm^{-1}; HRMS (ESI-TOF) *m/z* 440.2817 [($M+H^+$); calcd. for $C_{27}H_{38}NO_4$: 440.2801]; $[\alpha]_D^{23}$ +95.3 (c 1.0, EtOAc) on 97 % ee material (HPLC). These spectral data match those previously reported for this compound.[5c]

3.4.4 NMR analysis of a mixture of VAPOL, commercial $B(OPh)_3$ and imines 111a, 111o and 114o′ with and without water (pre-catalyst methods A and B, *Figure 3.2*)

As shown in Figure 3.2 of this chapter, a mixture of (*S*)-VAPOL **58** and commercial $B(OPh)_3$ **187a** gives different yields of unreacted VAPOL **58**, mesoborate B1 **106** and pyroborate B2 **108** employing different reaction conditions (pre-catalyst methods A and B). Also, it was evident from the ^1H NMR and ^{11}B NMR that no boroxinate B3 **190a** was formed unless imine **111a** was added irrespective of the methods used. The characteristic peaks i.e. δ 10.2-10.4 and δ 5.5-5.7 were missing in ^1H NMR and ^{11}B NMR respectively. The same observation was made when alkyl imines **111o** and **114o′** were used. Unless otherwise noted, commercial $B(OPh)_3$ is used in all the experiments. Also, Ph_3CH is used as the internal standard.

Experimental:

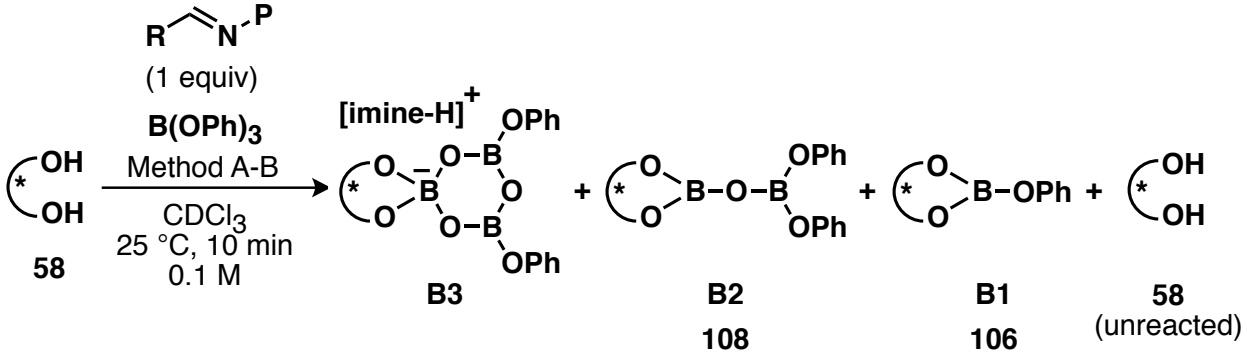

B3 = 190a (imine = 111a, R = Ph and P = MEDAM)
190o (imine = 111o, R = Pr and P = MEDAM)
213o' (imine = 112o', R = Et and P = BUDAM)

Entry 1, Figure 3.2: The pre-catalyst was made using method A (see Chapter 2) employing (*S*)-VAPOL (54 mg, 0.1 mmol) and commercial $B(OPh)_3$ (87 mg, 0.3 mmol). To the flask containing the pre-catalyst was first added the Ph_3CH (12.22 mg, 0.05 mmol) and then $CDCl_3$ (1

mL) under an argon flow through side-arm of the Schlenk flask. The reaction mixture was then stirred for 10 min. The off-white colored solution was then directly transferred to a quartz NMR tube and was subjected to ^{1}H NMR and ^{11}B NMR analysis.

Entry 2, Figure 3.2:

The pre-catalyst was made using method A (see Chapter 2) employing (*S*)-VAPOL (54 mg, 0.1 mmol) and commercial $B(OPh)_3$ (87 mg, 0.3 mmol). To the flask containing the pre-catalyst was first added the imine **111a** (39 mg, 0.1 mmol), Ph_3CH (12.22 mg, 0.05 mmol) and then $CDCl_3$ (1 mL) under an argon flow through side-arm of the Schlenk flask. The reaction mixture was then stirred for 10 min. The red colored solution was then directly transferred to a quartz NMR tube and was subjected to ^{1}H NMR and ^{11}B NMR analysis.

Entry 3, Figure 3.2: Same as entry 1 except that the pre-catalyst was made using method B (see Chapter 2) employing (*S*)-VAPOL (54 mg, 0.1 mmol), commercial $B(OPh)_3$ (87 mg, 0.3 mmol) and H_2O (5.4 μL, 0.3 mmol).

Entry 4, Figure 3.2: Same as entry 2 except that the pre-catalyst was made using method B (see Chapter 2) employing (*S*)-VAPOL (54 mg, 0.1 mmol), commercial $B(OPh)_3$ (87 mg, 0.3 mmol) and H_2O (5.4 μL, 0.3 mmol).

Entry 5, Figure 3.2: Same as entry 4 except that imine **111o** (1 equiv) was used.

Entry 6, Figure 3.2: Same as entry 4 except that imine **114o′** (1 equiv) was used.

3.4.5 Monitoring the aziridination reaction with imine 111a by NMR spectroscopy (*Table 3.1*)

Procedure (i)

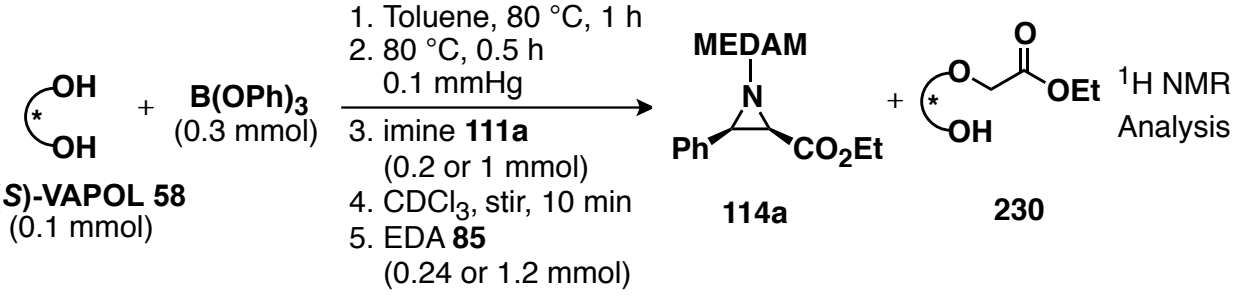

The pre-catalyst was made using method A (see Chapter 2) employing (*S*)-VAPOL (54 mg, 0.1 mmol) and commercial $B(OPh)_3$ (87 mg, 0.3 mmol). To the flask containing the pre-catalyst was first added the imine **111a** (78 mg, 0.2 mmol), Ph_3CH (12.22 mg, 0.05 mmol) and then $CDCl_3$ (1 mL) under an argon flow through side-arm of the Schlenk flask. The reaction mixture was then stirred for 10 min. The red colored solution was then directly transferred to a quartz NMR tube and was subjected to ^{1}H NMR and ^{11}B NMR analysis. After initial analysis, EDA **85** (25 μL, 0.24 mmol) was added to the NMR tube and the NMR tube was shaken for 1 min. Thereafter the NMR was taken at regular intervals. The reaction with 1.0 mmol was followed in the similar way. All details are given in Table 3.1 of the Chapter.

Procedure (ii)

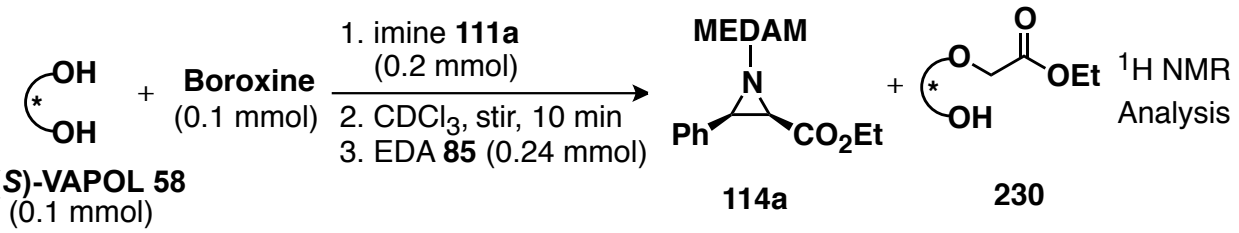

Same as procedure (i) except that the pre-catalyst was made using method D (see Chapter 2) employing (*S*)-VAPOL (54 mg, 0.1 mmol) and triphenoxyboroxine **191a** (360 mg, 0.1 mmol). All details are given in Table 3.1 of the Chapter.

Procedure (iii)

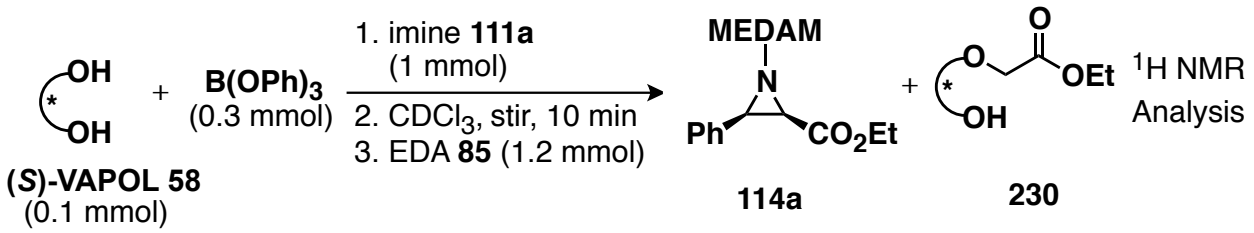

To a 10 mL flame-dried round bottom flask, equipped with a stir bar, filled with argon was added (*S*)-VAPOL **58** (54 mg, 0.1 mmol, 1 equiv.), commercial $B(OPh)_3$ (87 mg, 0.3 mmol, 3 equiv.), imine **111a** (387 mg, 1.00 mmol, 10 equiv.), Ph_3CH (12.22 mg, 0.05 mmol) and $CDCl_3$(1 mL). The resultant mixture was stirred for 10 min at room temperature. The red colored solution was then directly transferred to a quartz NMR tube and was subjected to ^{1}H NMR and ^{11}B NMR analysis. After initial analysis, EDA **85** (124 μL, 1.2 mmol) was added to the NMR tube and the NMR tube was shaken for 1 min. Thereafter the NMR was taken at regular intervals. All details are given in Table 3.1 of the Chapter.

3.4.6 NMR analysis of a mixture of VAPOL, commercial $B(OPh)_3$ and aziridines 114a, 114o, 114v, 114w and 115o′ (pre-catalyst method B, *Figure 3.5 and 3.10*)

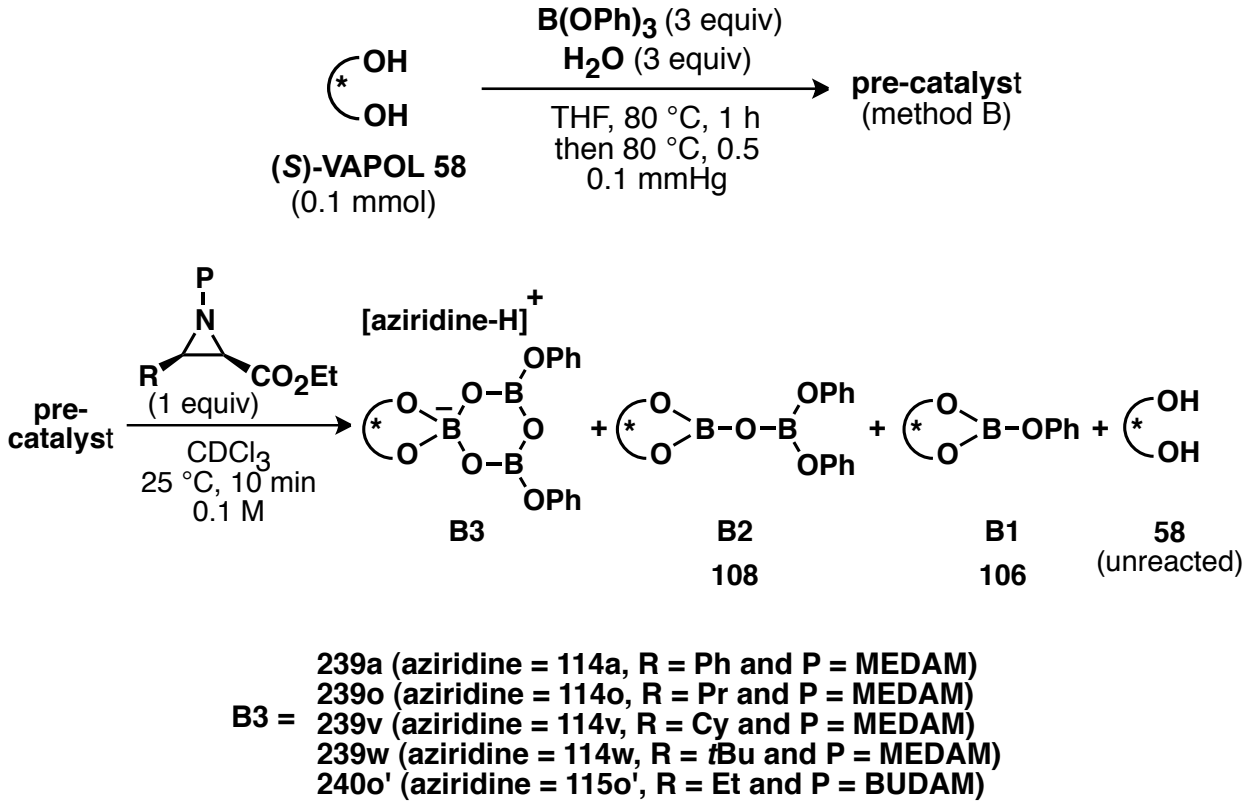

B3 =
239a (aziridine = 114a, R = Ph and P = MEDAM)
239o (aziridine = 114o, R = Pr and P = MEDAM)
239v (aziridine = 114v, R = Cy and P = MEDAM)
239w (aziridine = 114w, R = *t*Bu and P = MEDAM)
240o' (aziridine = 115o', R = Et and P = BUDAM)

The pre-catalyst was made using method B (see Chapter 2) employing (*S*)-VAPOL (54 mg, 0.1 mmol), commercial $B(OPh)_3$ (87 mg, 0.3 mmol) and H_2O (5.4 μL, 0.3 mmol). To the flask containing the pre-catalyst was first added the Ph_3CH (12.22 mg, 0.05 mmol) and then the aziridine **114o** (44 mg, 0.1 mmol) as a solution in $CDCl_3$ (1 mL) under an argon flow through side-arm of the Schlenk flask. The reaction mixture was then stirred for 10 min. The yellow colored solution was then directly transferred to a quartz NMR tube and was subjected to ^{1}H NMR and ^{11}B NMR analysis. A similar analysis was performed in d_8-toluene. Other aziridines (**114a, 114v, 114w** and **115o′**) were also examined following the same procedure.

3.4.7 NMR analysis of a mixture of VAPOL, different boron sources and aziridine 114o (pre-catalyst methods C, D and E, *Table 3.2*)

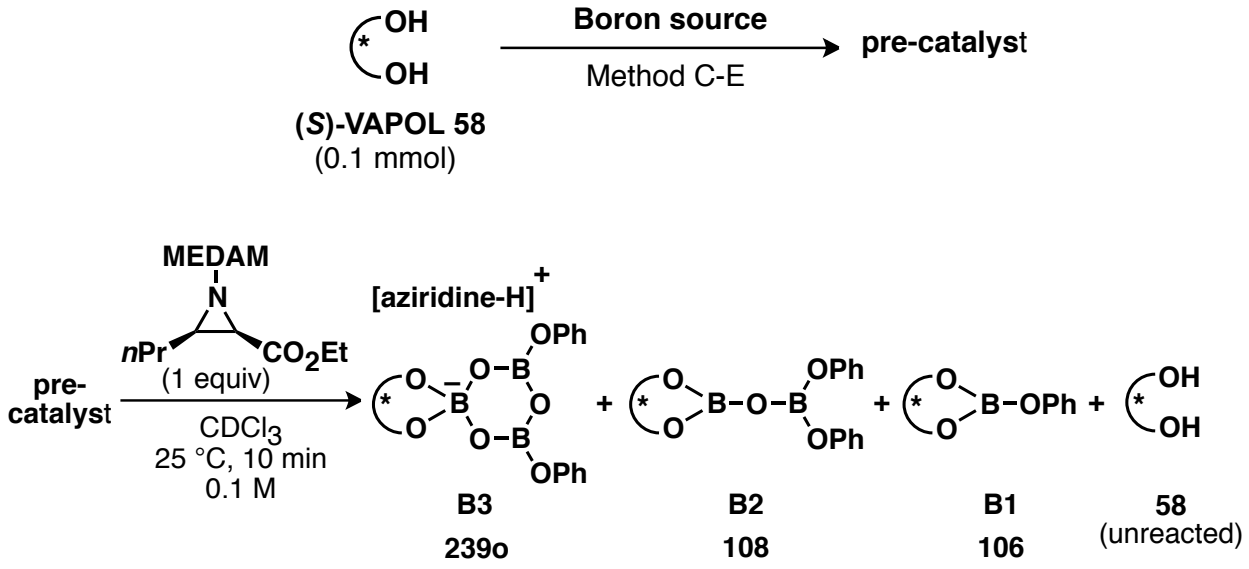

Entry 4, Table 3.2 (method C): The pre-catalyst was made using method C (see Chapter 2) employing (*S*)-VAPOL (54 mg, 0.1 mmol), commercial $B(OPh)_3$ (116 mg, 0.4 mmol) and H_2O (1.8 μL, 0.1 mmol). To the flask containing the pre-catalyst was first added the Ph_3CH (12.22 mg, 0.05 mmol) and then the aziridine **114o** (44 mg, 0.1 mmol) as a solution in $CDCl_3$ (1 mL) under an argon flow through side-arm of the Schlenk flask. The reaction mixture was then stirred for 10 min. The yellow colored solution was then directly transferred to a quartz NMR tube and was subjected to ^{1}H NMR and ^{11}B NMR analysis. All details are given in Table 3.2 of the Chapter.

Entry 5, Table 3.2 (method D): Same as entry 4 except that the pre-catalyst was made using method D (see Chapter 2) employing (*S*)-VAPOL (54 mg, 0.1 mmol), and triphenoxyboroxine **191a** (360 mg, 0.1 mmol). All details are given in Table 3.2 of the Chapter.

Entry 6, Table 3.2 (method E): Same as entry 4 except that the pre-catalyst was made using method E (see Chapter 2) employing (*S)*-VAPOL (54 mg, 0.1 mmol) and BH_3•Me_2S (150 μL, 0.3 mmol, 2.0 M in toluene), PhOH (18.8, 0.2 mmol) and H_2O (5.4 μL, 0.3 mmol). All details are given in Table 3.2 of the Chapter.

3.4.8 NMR analysis of a mixture of VAPOL, commercial $B(OPh)_3$ and a base (111a, 111o, 114a and 114o) by simple mixing at room temperature (*Figure 3.9*)

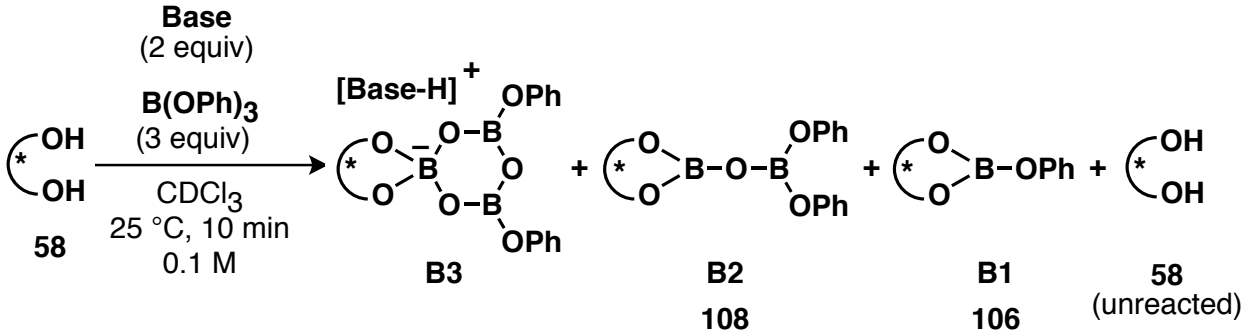

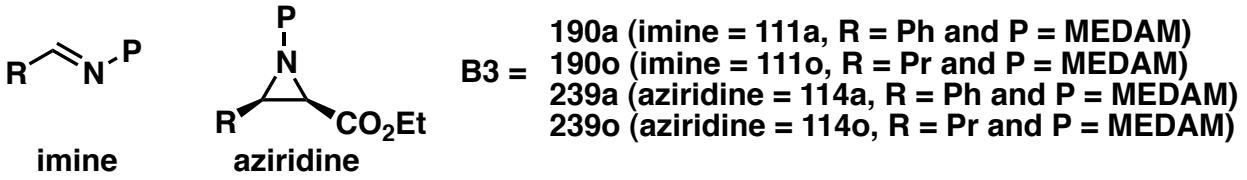

Entry 1, Figure 3.9: To a 10 mL flame-dried round bottom flask, equipped with a stir bar, filled with argon was added (*S*)-VAPOL **58** (54 mg, 0.1 mmol, 1 equiv.), commercial $B(OPh)_3$ (87 mg,

0.3 mmol, 3 equiv.), Ph_3CH (12.22 mg, 0.05 mmol) and $CDCl_3$(1 mL). The resultant mixture was stirred for 10 min at room temperature. The off-white colored solution was then directly transferred to a quartz NMR tube and was subjected to ^1H NMR and ^{11}B NMR analysis.

Entry 2, Figure 3.9: To a 10 mL flame-dried round bottom flask, equipped with a stir bar, filled with argon was added (*S*)-VAPOL **58** (54 mg, 0.1 mmol, 1 equiv.), commercial $B(OPh)_3$ (87 mg, 0.3 mmol, 3 equiv.), imine **111a** (78 mg, 0.2 mmol, 2 equiv.), Ph_3CH (12.22 mg, 0.05 mmol) and $CDCl_3$(1 mL). The resultant mixture was stirred for 10 min at room temperature. The red colored solution was then directly transferred to a quartz NMR tube and was subjected to ^1H NMR and ^{11}B NMR analysis.

Entry 3, Figure 3.9: Same as entry 2 with the imine **111o** (2 equiv).

Entry 4, Figure 3.9: Same as entry 2 with the aziridine **111a** (2 equiv).

Entry 5, Figure 3.9: Same as entry 2 with the aziridine **111o** (2 equiv). In this case, aziridine **114o** was added as solution in $CDCl_3$ (1mL).

3.4.9 Temperature studies of AZIRIDINO-BOROX 239a and 239o and the recovery of the aziridine 114o via hydrolysis of 239o (*Figure 3.4, 3.7 and 3.8*)

Temperature Studies:

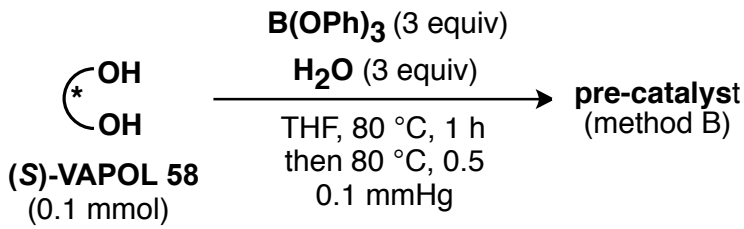

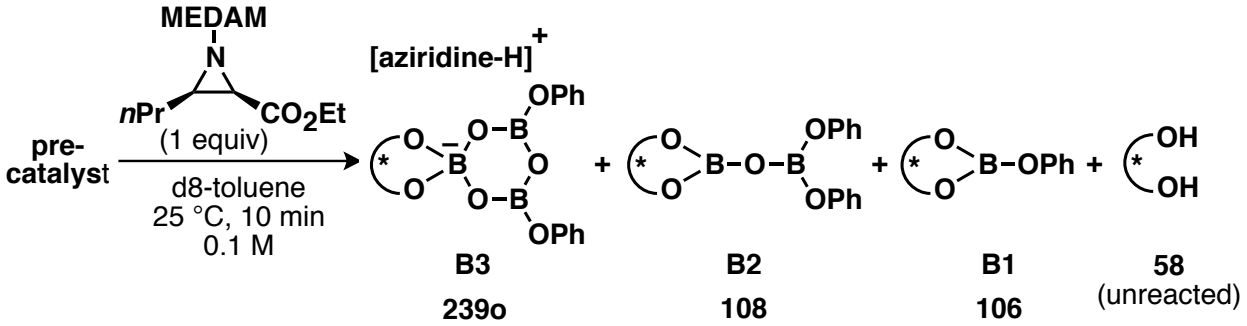

The pre-catalyst was made using method B (see Chapter 2) employing (*S*)-VAPOL (54 mg, 0.1 mmol), commercial $B(OPh)_3$ (87 mg, 0.3 mmol) and H_2O (5.4 μL, 0.3 mmol). To the flask containing the pre-catalyst was first added the Ph_3CH (12.22 mg, 0.05 mmol) and then the aziridine **114o** (44 mg, 0.1 mmol) as a solution in d_8-toluene (1 mL) under an argon flow through side-arm of the Schlenk flask. The reaction mixture was then stirred for 10 min. The yellow colored solution was then directly transferred to a quartz NMR tube and was subjected to ^1H NMR and ^{11}B NMR analysis at various temperatures. A similar analysis was performed for boroxinate **239a**.

Recovery of aziridine 114o via hydrolysis of 239o:

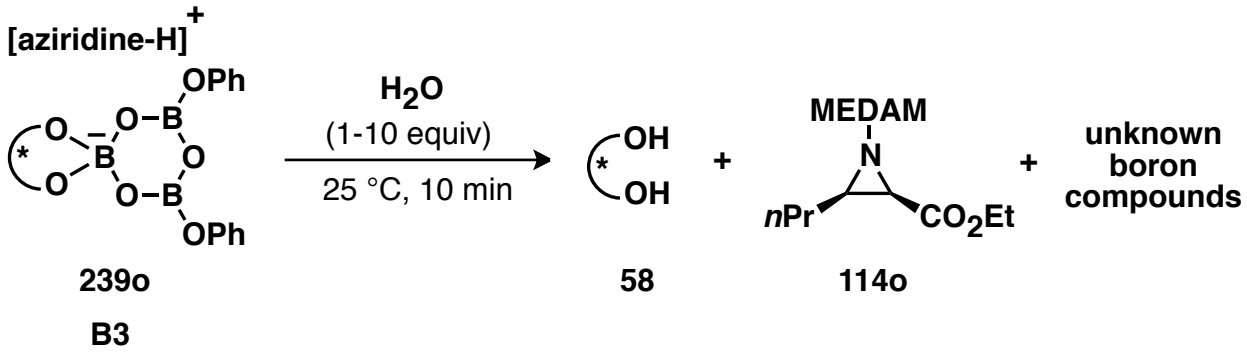

Entry 1, Figure 3.8: The boroxinate is formed in 43% yield in $CDCl_3$ using the protocol shown in section 3.4.6.

Entry 2-4, Figure 3.8: 1, 2 and 4 equiv of the H_2O is added to the NMR tube (entry 1) for entries 2, 3 and 3 respectively.

Entry 5, Figure 3.8: 10 equiv of the H_2O is added to the NMR tube and then the aziridine **114o** was recovered in 85% yield by silica gel chromatography.

3.4.10 Equilibrium studies of 239o, (*S*)-VAPOL 58 and boron compounds (*Figure 3.11 and 3.12*)

A) via dilution of 239o:

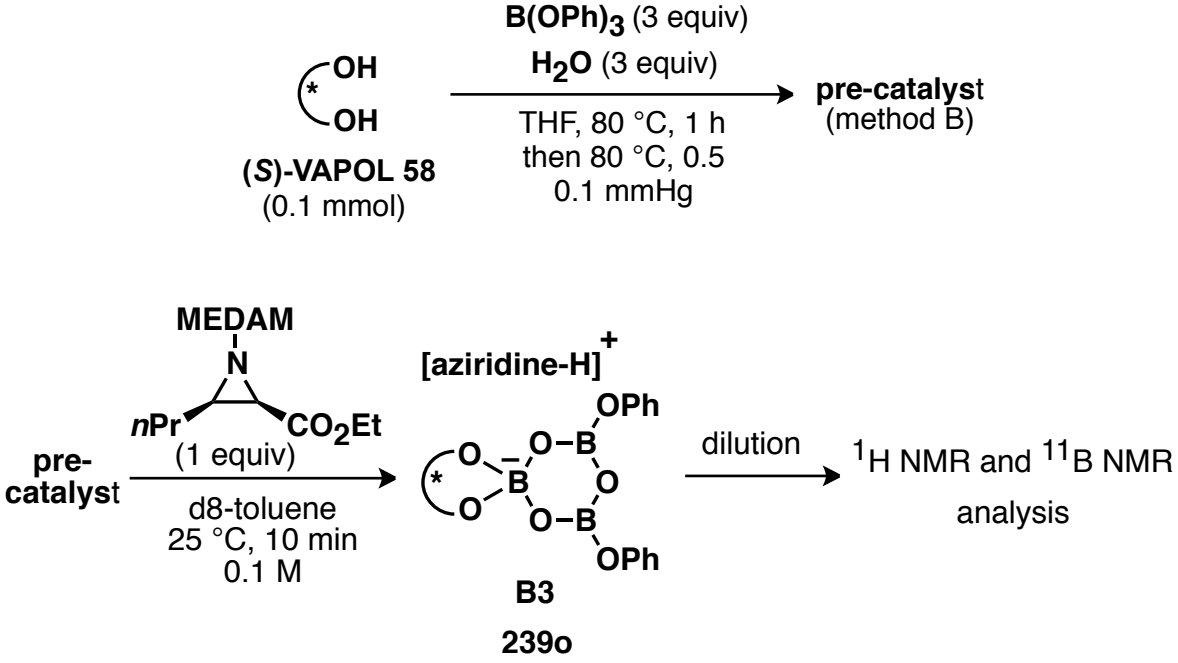

Entry 1, Figure 3.11: The boroxinate is formed in 56% yield in d_8-toluene using the protocol shown in section 3.4.6. The concentration of the solution is 0.2 M as 0.2 mmol of (*S*)-VAPOL **58** was used in 1 mL of d_8-toluene.

Entry 2, Figure 3.11: entry 1 after 24 h.

Entry 3, Figure 3.11: An additional 1 mL of d_8-toluene was added to entry 2 and the NMR was taken. The concentration is 0.1 M.

Entry 4, Figure 3.11: The boroxinate is formed in 47% yield in d_8-toluene using the protocol shown in section 3.4.6.

Entry 5, Figure 3.11: entry 4 after 24 h.

Entry 6-8, Figure 3.11: An additional 0.25 mL, 0.75 mL and 0.5 mL of d_8-toluene was added to entry 5, 6 and 7 respectively and then the NMR was taken. The concentration of the solution (with respect to the ligand **58**) is 0.08 M, 0.05 M and 0.04 M for entries 6,7 and 8 respectively.

B) via increase in the concentration of aziridine 114o:

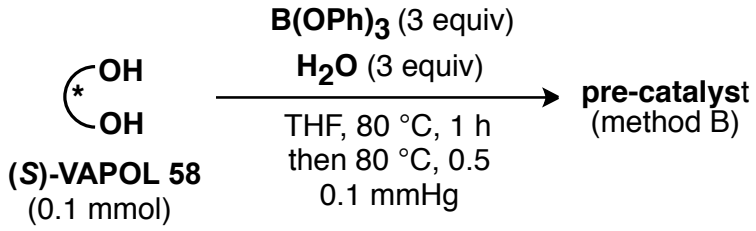

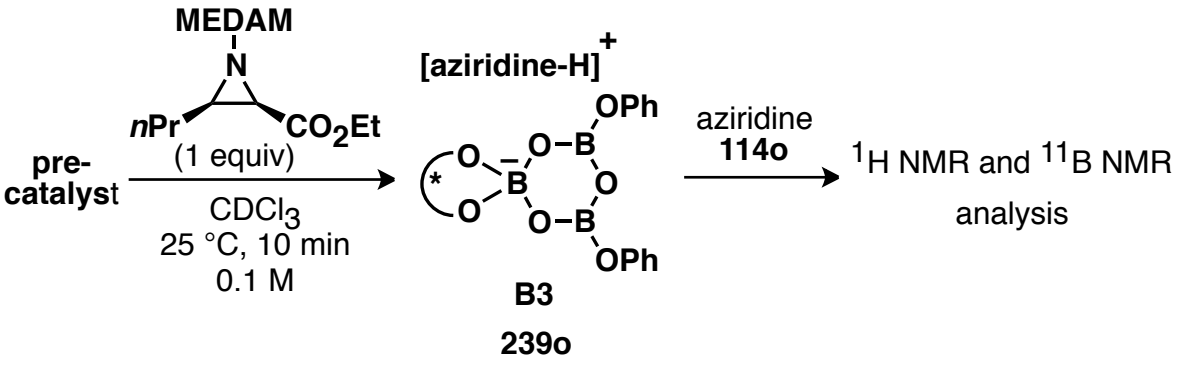

Entry 1, Figure 3.12: The boroxinate is formed in 35% yield in $CDCl_3$ using the protocol shown in section 3.4.6. The concentration of the solution is 0.4 M as 0.4 mmol of (*S*)-VAPOL **58** was used in 10 mL of $CDCl_3$. An aliquot of 1mL of this solution was withdrawn for NMR analysis.

Entry 2-5, Figure 3.12: An additional 0.36 mmol, 0.32 mmol, 0.28 mmol and 0.24 mmol of aziridine **114o** was added to the remaining solution in entries 1, 2, 3, and 4 respectively. After each addition, an aliquot of 1mL of the resulting $CDCl_3$ solution was withdrawn and subjected to NMR analysis. The concentration of the solution (with respect to aziridine **114o**) is 0.04 M, 0.08 M, 0.12 M, 0.16 M and 0.2 M for entries 1-5 respectively.

3.4.11 Probing the path II of the catalytic cycle i.e. the depletion of 239o in the presence of 111o (*Figure 3.14 and 3.15*)

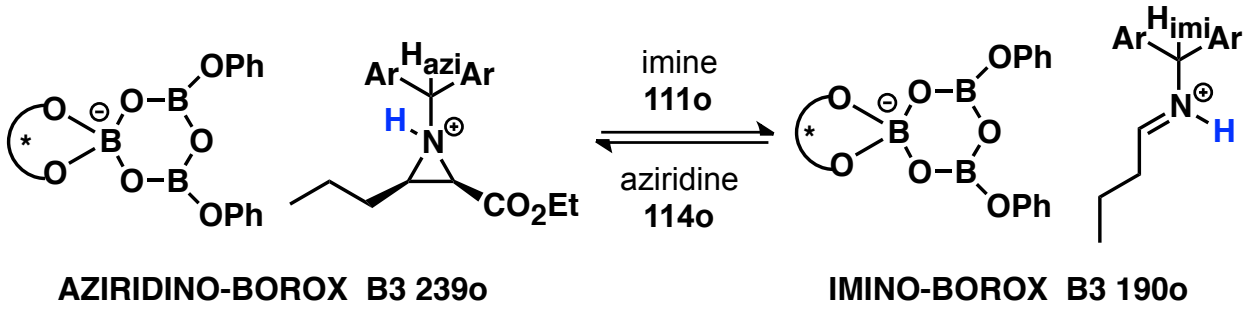

Entry 1, Figure 3.14 and Entry 1, Figure 3.15: The boroxinate **239o** is formed in 43% yield in $CDCl_3$ using the protocol shown in section 3.4.6.

Entry 2, Figure 3.14: 1 equiv of imine **111o** (36 mg, 0.1 mmol) was added to entry 1 of Figure 3.14.

Entry 2, Figure 3.15: 0.5 equiv of imine **111o** (18 mg, 0.1 mmol) was added to entry 1 of Figure 3.15.

Entry 4, Figure 3.14: 1.1 equiv of EDA **85** (12 μL, 0.1 mmol) was added to entry 2 of Figure 3.14, which was stored for 24 h (entry 3, Figure 3.14) prior to the addition.

Entry 4, Figure 3.15: 0.5 equiv of EDA **85** (5.2 μL, 0.05 mmol) was added to entry 2 of Figure 3.15, which was stored for 1 h (entry 3, Figure 3.15) prior to the addition.

3.4.12 Termination of the catalytic cycle i.e. Path X and path Y (*Figure 3.16 and 3.17*)

A) Path X: Treatment of AZIRIDINO-BOROX 239o with EDA 85:

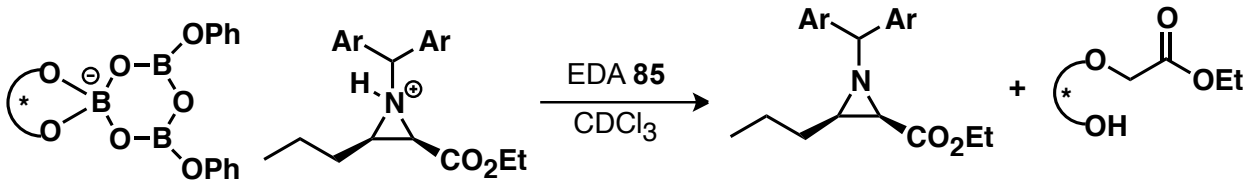

AZIRIDINO-BOROX B3 239o **114o** **230**

The boroxinate **239o** is formed in 43% yield in $CDCl_3$ using the protocol shown in section 3.4.6. Thereafter, 0.5 equiv of EDA **85** (5.2 μL, 0.05 mmol) was added after 10 min. Another 0.5 equiv of EDA **85** (5.2 μL, 0.05 mmol) was added after 30 min. The NMR spectra were recorded at regular time intervals. All details are given in Figure 3.16.

B) Path Y: Reaction between (*S*)-VAPOL 58 and EDA 85 under various conditions:

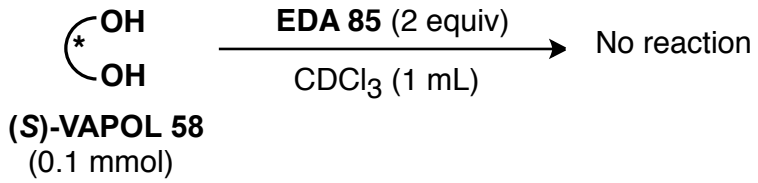

Entry 1, Figure 3.17: To a 10 mL flame-dried single-necked round bottom flask, equipped with a stir bar and a rubber septum and filled with argon was added (*S*)-VAPOL **58** (54 mg, 0.10 mmol, 1.0 equiv) and EDA **85** (21 μL, 0.20 mmol, 2.0 equiv), Ph_3CH (12.2 mg, 0.500 mmol) and $CDCl_3$ (1 mL). The resultant mixture was stirred for 10 min at room temperature. The resulting solution was then directly transferred to a quartz NMR tube (freshly flame-dried) and was subjected to NMR analysis.

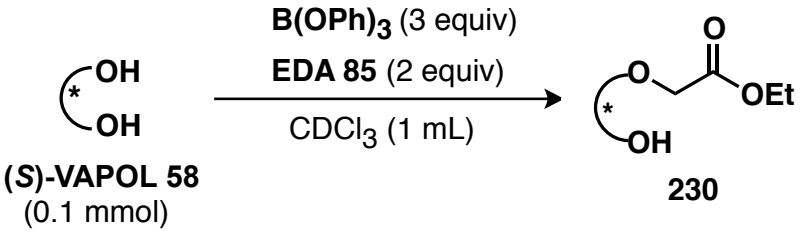

Entry 2, Figure 3.17: Same as entry 1 except that commercial $B(OPh)_3$ (87 mg, 0.30 mmol, 3.0 equiv) was aslo added.

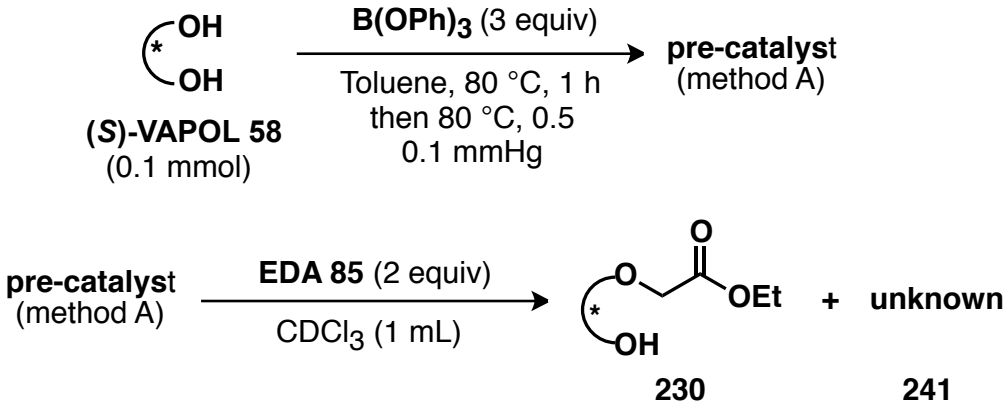

Entry 3, Figure 3.17: The precatalyst was made by method A (see Chapter 1) employing (*S*)-VAPOL **58** (54 mg, 0.10 mmol) and commercial $B(OPh)_3$ (87 mg, 0.30 mmol, 3.0 equiv). To the flask containing the pre-catalyst was first added the Ph_3CH (12.22 mg, 0.05 mmol) and then the $CDCl_3$ (1 mL) under an argon flow through side-arm of the Schlenk flask. The reaction mixture was then stirred for 10 min. The off-white colored solution was then directly transferred to a quartz NMR tube and was subjected to ^{1}H NMR and ^{11}B NMR analysis. After initial analysis, EDA **85** (21 μL, 0.20 mmol, 2.0 equiv) was added and the mixture was shaken for 5 min.

Entry 4, Figure 3.17: Entry 4 after 24 h.

Entry 5, Figure 3.17: 1 equiv of H_2O (1.8 μL, 0.1 mmol) was added to the NMR tube containing entry 4.

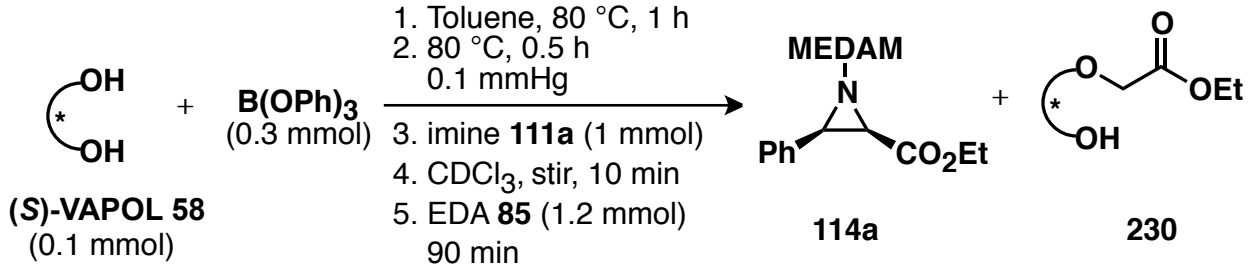

Entry 6, Figure 3.17: The pre-catalyst was made using method A (see Chapter 2) employing (*S*)-VAPOL (54 mg, 0.1 mmol) and commercial $B(OPh)_3$ (87 mg, 0.3 mmol). To the flask containing the pre-catalyst was first added the imine **111a** (387 mg, 1.00 mmol), Ph_3CH (12.22 mg, 0.05 mmol) and then $CDCl_3$ (1 mL) under an argon flow through side-arm of the Schlenk flask. The reaction mixture was then stirred for 10 min. The red colored solution was then directly transferred to a quartz NMR tube and was subjected to ^{1}H NMR and ^{11}B NMR analysis. After initial analysis, EDA **85** (124 μL, 1.20 mmol) was added to the NMR tube and the NMR tube was shaken for 2 min. Thereafter the NMR sample was kept for 90 min. The NMR sample was then poured into a 25 mL round bottom flask containing 6 mL of hexanes. The resulting solution was then concentrated *in vacuo* followed by exposure to high vacuum (0.05 mm Hg) for 1 h to afford the adduct as a white solid. Purification of the mono-alkylated adduct **230** by silica gel chromatography (35 mm × 400 mm column, 9:1 hexanes/EtOAc as eluent, under gravity) afforded pure **230** as a white solid (mp. 101-102 °C) in 95% isolated yield (59.3 mg, 0.095 mmol).

Spectral data for **230**: R_f = 0.25 (1:9 EtOAc/hexanes); ^{1}H NMR ($CDCl_3$, 300 MHz) δ 0.77 (t, 3H, *J* = 7.1Hz), 1.25 (brs, 1H), 2.74-3.68 (m, 2H), 4.40 (dd, 2H, *J* = 14.8, 37.6Hz), 6.70 (s, 1H), 6.79-6.85 (m, 4H), 6.93-7.12 (m, 6H), 7.44 (s, 1H), 7.56-7.82 (m, 8H), 7.88-7.94 (m, 2H), 9.55-9.58 (m, 1H), 9.83 (d, 1H, *J* = 8.5 Hz); ^{13}C NMR ($CDCl_3$, 75 Hz) δ 13.48, 60.91, 68.44, 120.48, 123.01, 123.19, 125.97, 126.35, 126.50, 126.67, 126.91, 126.96, 127.13, 127.48, 127.55, 127.64, 127.76, 128.19, 128.36, 128.66, 128.90, 129.08, 129.19, 129.33, 130.66, 132.79, 133.08, 134.41, 135.05, 139.37, 140.10, 140.62, 142.27, 152.26, 155.04, 167.66 (four sp^2 carbons not located). These spectral data match those previously reported for this compound.[5a,9]

3.4.13 NMR analysis of the addition of TfOH to boroxinate 242 (*Figure 3.19*)

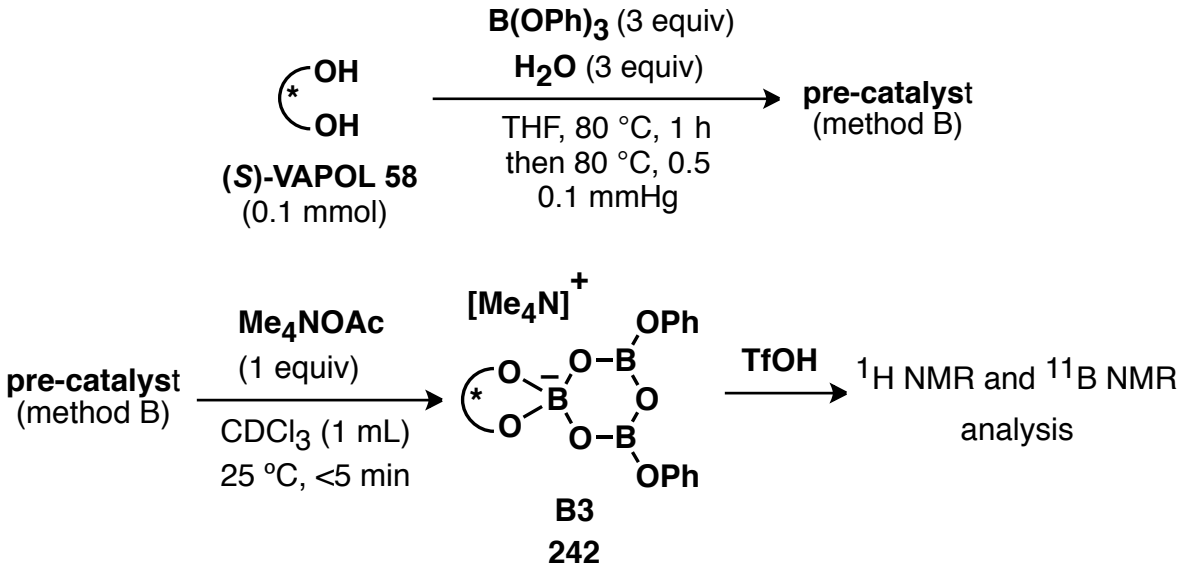

The pre-catalyst was made using method B (see Chapter 2) employing (*S*)-VAPOL (54 mg, 0.1 mmol) commercial $B(OPh)_3$ (87 mg, 0.3 mmol) and H_2O (5.4 μL, 0.3 mmol). To the flask containing the pre-catalyst was first added the Me_4NOAc (13.3 mg, 0.100 mmol), Ph_3CH (12.22

mg, 0.05 mmol) and then $CDCl_3$ (1 mL) under an argon flow through side-arm of the Schlenk flask. The reaction mixture was then stirred for 10 min. The red colored solution was then directly transferred to a quartz NMR tube and was subjected to ^{1}H NMR and ^{11}B NMR analysis. Thereafter, 1–4 equivalents of TfOH were added at regular intervals. All details are given in Figure 3.19.

3.4.14 DFT calculations:

All quantum mechanical calculations were performed using the GAUSSIAN 03.[6] The B3LYP[10] density functional was used along with 6-31G* basis sets.

3.4.14.1 Prediction of the structure of AZIRIDINO-BOROX complex 239o (*Figure 3.6*)

Coordinates of AZIRIDINO-BOROX complex 239o:

B3LYP/6-31G*

Energy = -4011.05566039 hartrees
Number of Imaginary frequencies = none

Zero-point correction=	1.348532 (Hartree/Particle)
Thermal correction to Energy=	1.432808
Thermal correction to Enthalpy=	1.433753
Thermal correction to Gibbs Free Energy=	1.218432
Sum of electronic and zero-point Energies=	-4009.707128
Sum of electronic and thermal Energies=	-4009.622852
Sum of electronic and thermal Enthalpies=	-4009.621908
Sum of electronic and thermal Free Energies=	-4009.837228

	E (Thermal) KCal/Mol	CV Cal/Mol-Kelvin	S Cal/Mol-Kelvin
Total	899.101	326.353	453.179

Standard orientation:

Center No.	Atomic No.	Atomic Type	Coordinates (Angstroms) X	Y	Z
1	6	0	-5.656871	-1.810910	1.301347
2	6	0	-5.779938	-0.423740	1.114612
3	6	0	-7.050565	0.097013	0.820102
4	6	0	-8.161181	-0.739691	0.711535
5	6	0	-8.023670	-2.116351	0.896119
6	6	0	-6.766367	-2.647549	1.192164
7	6	0	-4.614247	0.481173	1.322858
8	6	0	-3.321972	0.231947	0.775601
9	6	0	-2.213056	0.969017	1.227232
10	6	0	-2.370229	2.107515	2.086394
11	6	0	-3.708035	2.434593	2.472247
12	6	0	-4.779456	1.588010	2.135707
13	6	0	-3.983901	3.624281	3.223757
14	6	0	-2.995268	4.486392	3.567917
15	6	0	-1.629756	4.189433	3.254573
16	6	0	-1.293501	2.982118	2.558122
17	6	0	-3.151532	-0.777075	-0.313738
18	6	0	-2.257700	-1.839405	-0.104913
19	6	0	-2.207654	-2.974464	-0.972578
20	6	0	-2.994768	-2.897671	-2.161739
21	6	0	-3.804018	-1.773740	-2.412434
22	6	0	-3.915217	-0.719652	-1.515636
23	6	0	-1.438766	-4.194177	-0.719443
24	6	0	-1.414657	-5.215657	-1.724417
25	6	0	-2.165825	-5.052168	-2.935579
26	6	0	-2.937352	-3.952410	-3.133652
27	8	0	-1.471940	-1.778585	0.994567
28	5	0	-0.454976	-0.716368	1.080922
29	8	0	-0.982213	0.618355	0.747225
30	6	0	-4.772541	0.437364	-1.904912
31	6	0	-4.345129	1.767531	-1.745208
32	6	0	-5.123524	2.832578	-2.198237
33	6	0	-6.351519	2.595369	-2.819202
34	6	0	-6.794462	1.281257	-2.977725
35	6	0	-6.015134	0.217556	-2.524666
36	8	0	0.651373	-0.984195	0.094745
37	5	0	1.651458	-1.838704	0.462054
38	8	0	1.876094	-2.167880	1.776496

39	5	0	1.114217	-1.539989	2.762942
40	8	0	1.567557	-1.769810	4.043265
41	6	0	0.984483	-1.390519	5.231192
42	6	0	-0.380727	-1.120382	5.375559
43	6	0	-0.877616	-0.786924	6.636726
44	6	0	-0.036237	-0.723809	7.748638
45	6	0	1.323633	-1.000501	7.593445
46	6	0	1.834285	-1.334793	6.340547
47	8	0	2.457592	-2.320575	-0.555043
48	6	0	3.481020	-3.236516	-0.482465
49	6	0	4.428031	-3.189684	-1.513124
50	6	0	5.467170	-4.119743	-1.550014
51	6	0	5.574035	-5.099907	-0.560577
52	6	0	4.623921	-5.141156	0.461560
53	6	0	3.574999	-4.220661	0.508644
54	8	0	0.066312	-0.761212	2.445162
55	6	0	1.897877	0.677720	-3.157298
56	6	0	0.581119	1.357114	-2.933875
57	6	0	2.121507	-0.733296	-3.646884
58	8	0	3.120762	-1.022987	-4.271529
59	8	0	1.130044	-1.551183	-3.308054
60	6	0	1.267959	-2.969655	-3.637504
61	7	0	1.389023	0.890563	-1.775546
62	6	0	2.080216	1.819364	-0.762784
63	6	0	3.331440	1.156530	-0.206967
64	6	0	3.419637	0.999530	1.179900
65	6	0	4.543958	0.443028	1.799316
66	6	0	5.608069	0.031814	0.982906
67	6	0	5.563513	0.184567	-0.414052
68	6	0	4.417716	0.738549	-0.990487
69	6	0	4.597780	0.290213	3.299642
70	8	0	6.757613	-0.479140	1.550200
71	6	0	6.714002	-1.880713	1.845762
72	6	0	6.740879	-0.231652	-1.260898
73	6	0	2.228670	3.237816	-1.288713
74	6	0	3.350644	3.690653	-1.994588
75	6	0	3.435530	5.005144	-2.462746
76	6	0	2.368644	5.880031	-2.196259
77	6	0	1.225433	5.460833	-1.495534
78	6	0	1.179110	4.136158	-1.050910
79	6	0	4.636851	5.481831	-3.242860
80	8	0	2.433713	7.165858	-2.698240
81	6	0	2.911274	8.152883	-1.781839
82	6	0	0.078885	6.406563	-1.232452
83	1	0	2.724014	1.331274	-3.412184

84	1	0	4.336808	-2.425866	-2.278714
85	1	0	6.191017	-4.077927	-2.360026
86	1	0	6.381588	-5.826025	-0.590249
87	1	0	4.690375	-5.902861	1.234351
88	1	0	2.842105	-4.257675	1.303036
89	1	0	2.887333	-1.561104	6.202469
90	1	0	1.992070	-0.958736	8.449756
91	1	0	-0.435471	-0.462724	8.724812
92	1	0	-1.937987	-0.573601	6.744701
93	1	0	-1.034015	-1.156912	4.513182
94	1	0	-3.215883	5.401734	4.112042
95	1	0	-5.018020	3.828795	3.490054
96	1	0	-5.759389	1.804708	2.551771
97	1	0	-7.159946	1.164560	0.651763
98	1	0	-9.133697	-0.314777	0.475590
99	1	0	-8.888239	-2.769771	0.811574
100	1	0	-6.648507	-3.717026	1.346625
101	1	0	-4.687393	-2.229548	1.551979
102	1	0	-6.382308	-0.799215	-2.626283
103	1	0	-7.754692	1.081778	-3.446636
104	1	0	-6.958476	3.425849	-3.170177
105	1	0	-4.768016	3.851200	-2.064542
106	1	0	-3.396753	1.967352	-1.257374
107	1	0	-4.343907	-1.731812	-3.354066
108	1	0	-3.534712	-3.849105	-4.036656
109	1	0	-2.129681	-5.846463	-3.677836
110	1	0	1.332201	1.845827	0.030790
111	1	0	1.022148	0.042802	-1.267929
112	1	0	0.652943	2.436334	-3.040879
113	1	0	4.193967	3.028464	-2.160287
114	1	0	5.226206	6.212945	-2.675768
115	1	0	4.332749	5.974579	-4.171996
116	1	0	5.298128	4.646201	-3.490501
117	1	0	2.930150	9.096883	-2.330862
118	1	0	3.923774	7.916091	-1.430830
119	1	0	2.248766	8.252533	-0.913349
120	1	0	-0.855997	5.856095	-1.091362
121	1	0	-0.046901	7.110643	-2.059945
122	1	0	0.244274	6.994559	-0.320405
123	1	0	0.307364	3.800544	-0.493782
124	1	0	2.589210	1.309814	1.806834
125	1	0	5.630317	0.314437	3.657635
126	1	0	4.146732	-0.658615	3.616026
127	1	0	4.035921	1.089742	3.793170
128	1	0	7.682591	-2.126545	2.287327

129	1	0	6.561135	-2.476638	0.938853
130	1	0	5.917307	-2.114922	2.561158
131	1	0	6.867238	-1.320351	-1.261966
132	1	0	7.671519	0.198757	-0.877098
133	1	0	6.608766	0.088450	-2.299147
134	1	0	4.394266	0.818742	-2.072582
135	6	0	0.750667	-3.252143	-5.036825
136	1	0	2.317592	-3.242696	-3.524549
137	1	0	0.676383	-3.469507	-2.871362
138	1	0	0.818726	-4.327931	-5.233798
139	1	0	-0.298864	-2.957345	-5.132989
140	1	0	1.346173	-2.729013	-5.791144
141	6	0	-0.781836	0.783951	-3.244349
142	1	0	-0.846828	-0.266350	-2.955235
143	1	0	-1.525223	1.329267	-2.652983
144	6	0	-1.073287	0.953351	-4.747687
145	1	0	-0.957943	2.011241	-5.023776
146	1	0	-0.316217	0.402385	-5.322222
147	6	0	-2.470012	0.471412	-5.147777
148	1	0	-2.598160	-0.592062	-4.919789
149	1	0	-3.250276	1.020766	-4.610842
150	1	0	-2.633933	0.610762	-6.222097
151	6	0	-0.679315	-6.404617	-1.510788
152	1	0	-0.674836	-7.157182	-2.296485
153	6	0	-0.751162	-4.466972	0.491882
154	1	0	-0.798258	-3.741946	1.289630
155	6	0	-0.000675	-6.624847	-0.328926
156	1	0	0.555577	-7.545704	-0.176115
157	6	0	-0.054963	-5.649451	0.681123
158	1	0	0.447388	-5.822824	1.629240
159	6	0	0.087638	2.706430	2.398078
160	1	0	0.366416	1.760571	1.963908
161	6	0	-0.612605	5.077432	3.673579
162	1	0	-0.906136	5.988701	4.190223
163	6	0	1.065880	3.587989	2.829128
164	1	0	2.114005	3.337452	2.688351
165	6	0	0.720854	4.796101	3.456925
166	1	0	1.493018	5.484811	3.789402

REFERENCES

REFERENCES

(1) (a) Tokunaga, N.; Yoshida, K.; Hayashi, T. *Proc. Nat. Acad. Sci. U.S.A* **2004**, *101*, 5445-5449. (b) Uyeda, C.; Jacobsen, E. N. *J. Am. Chem. Soc.* **2011**, *133*, 5062-5075.

(2) (a) Amarante, G. W.; Benassi, M.; Milagre, H. M. S.; Braga, A. A. C.; Maseras, F.; Eberlin, M. N.; Coelho, F. *Chem.–Eur. J.* **2009**, *15*, 12460-12469. (b) Schrader, W.; Handayani, P. P.; Zhou, J.; List, B. *Angew. Chem., Int. Ed.* **2009**, *48*, 1463-1466.

(3) (a) Daniel, C.; Koga, N.; Han, J.; Fu, X. Y.; Morokuma, K. *J. Am. Chem. Soc.* **1988**, *110*, 3773-3787. (b) Kozuch, S.; Martin, J. M. L. *ACS Catal.* **2011**, *1*, 246-253. (c) Kozuch, S.; Martin, J. M. L. *Chem. Commun.* **2011**, *47*, 4935-4937.

(4) (a) Rueping, M.; Nachtsheim, B. J.; Ieawsuwan, W.; Atodiresei, I. *Angew. Chem., Int. Ed.* **2011**, *50*, 6706-6720. (b) Schenker, S.; Zamfir, A.; Freund, M.; Tsogoeva, S. B. *Eur. J. Org. Chem.* **2011**, 2209-2222. (c) Rueping, M.; Kuenkel, A.; Atodiresei, I. *Chem. Soc. Rev.* **2011**, *40*, 4539-4549. (d) List, B.; Kampen, D.; Reisinger, C. M. *Top Curr Chem* **2010**, *291*, 395-456. (e) Rueping, M.; Koenigs, R. M.; Atodiresei, I. *Chem.–Eur. J.* **2010**, *16*, 9350-9365. (f) Sohtome, Y.; Nagasawa, K. *Synlett* **2010**, 1-22. (g) Terada, M. *Synthesis* **2010**, 1929-1982. (h) Terada, M. *Bull. Chem. Soc. Jpn.* **2010**, *83*, 101-119. (i) Zamfir, A.; Schenker, S.; Freund, M.; Tsogoeva, S. B. *Org. Biomol. Chem.* **2010**, *8*. (j) Yamamoto, H.; Payette, J. N. In *Hydrogen Bonding in Organic Synthesis*; Wiley-VCH 2009, p 73-140. (k) Terada, M. *Chem. Commun. (Cambridge, U. K.)* **2008**, 4097-4112. (l) Yu, X.; Wang, W. *Chem.–Asian. J.* **2008**, *3*, 516-532. (m) Doyle, A. G.; Jacobsen, E. N. *Chem. Rev.* **2007**, *107*, 5713-5743. (n) Akiyama, T. *Chem. Rev.* **2007**, *107*, 5744-5758. (o) Taylor, M. S. J., E. N. *Angew. Chem., Int. Ed.* **2006**, *45*, 1520-1543. (p) Akiyama, T.; Itoh, J.; Fuchibe, K. *Adv. Synth. Catal.* **2006**, *348*, 999-1010. (q) Connon, S. J. *Angew. Chem., Int. Ed.* **2006**, *45*, 3909-3912.

(5) (a) Zhang, Y.; Desai, A.; Lu, A.; Hu, G.; Ding, Z.; Wulff, W. D. *Chem. –Eur. J.* **2008**, *14*, 3785-3803. (b) Zhang, Y.; Lu, Z.; Desai, A.; Wulff, W. D. *Org. Lett.* **2008**, *10*, 5429-5432. (c) Mukherjee, M.; Gupta, A. K.; Lu, Z.; Zhang, Y.; Wulff, W. D. *J. Org. Chem.* **2010**, *75*, 5643-5660. (d) Ren, H.; Wulff, W. D. *Org. Lett.* **2010**, *12*, 4908-4911. (e) Hu, G.; Huang, L.; Huang, R. H.; Wulff, W. D. *J. Am. Chem. Soc.* **2009**, *131*, 15615-15617. (f) Hu, G.; Gupta, A. K.; Huang, R. H.; Mukherjee, M.; Wulff, W. D. *J. Am. Chem. Soc.* **2010**, *132*, 14669–14675. (g) Gupta, A. K.; Mukherjee, M.; Wulff, W. D. *Org. Lett.* **2011**, *13*, 5866-5869. (h) Newman, C. A.; Antilla, J. C.; Chen, P.; Predeus, A. V.; Fielding, L.; Wulff, W. D. *J. Am. Chem. Soc.* **2007**, *129*, 7216-7217. (i) Desai, A. A.; Wulff, W. D. *J. Am. Chem. Soc.* **2010**, *132*, 13100-13103. (j) Vetticatt, M. J.; Desai, A. A.; Wulff, W. D. *J. Am. Chem. Soc.* **2010**, *132*, 13104-13107. (k) Desai, A. A.; Morán-Ramallal, R.; Wulff, W. D. *Org. Synth.* **2011**, *88*, 224-237. (l) Ren, H.; Wulff, W. D. *J. Am. Chem. Soc.* **2011**, *133*, 5656-5659. (m) Desai, A. A.; Ren, H.; Mukherjee, M.; Wulff, W. D. *Org. Process Res. Dev.* **2011**, *15*, 1108-1115.

(6) Gaussian 03, Revision D.01 M. J. Frisch, G. W. T., H. B. Schlegel, G. E. Scuseria, M. A. Robb, J. R. Cheeseman, J. A. Montgomery, Jr., T. Vreven, K. N. Kudin, J. C. Burant, J. M. Millam, S. S. Iyengar, J. Tomasi, V. Barone, B. Mennucci, M. Cossi, G. Scalmani, N. Rega, G. A. Petersson, H. Nakatsuji, M. Hada, M. Ehara, K. Toyota, R. Fukuda, J. Hasegawa, M. Ishida, T. Nakajima, Y. Honda, O. Kitao, H. Nakai, M. Klene, X. Li, J. E. Knox, H. P. Hratchian, J. B. Cross, V. Bakken, C. Adamo, J. Jaramillo, R. Gomperts, R. E. Stratmann, O. Yazyev, A. J. Austin, R. Cammi, C. Pomelli, J. W. Ochterski, P. Y. Ayala, K. Morokuma, G. A. Voth, P. Salvador, J. J. Dannenberg, V. G. Zakrzewski, S. Dapprich, A. D. Daniels, M. C. Strain, O. Farkas, D. K. Malick, A. D. Rabuck, K. Raghavachari, J. B. Foresman, J. V. Ortiz, Q. Cui, A. G. Baboul, S. Clifford, J. Cioslowski, B. B. Stefanov, G. Liu, A. Liashenko, P. Piskorz, I. Komaromi, R. L. Martin, D. J. Fox, T. Keith, M. A. Al-Laham, C. Y. Peng, A. Nanayakkara, M. Challacombe, P. M. W. Gill, B. Johnson, W. Chen, M. W. Wong, C. Gonzalez, and J. A. Pople, Gaussian, Inc., Wallingford CT, 2004

(7) (a) Nishio, M. *Tetrahedron* **2005**, *61*, 6923-6950. (b) Nishio, M. H., M.; Umezawa, Y. *The CH/π Interaction: Evidence, Nature, and Consequences*; Wiley-VCH, 1998. (c) Plevin, M. J.; Bryce, D. L.; Boisbouvier, J. *Nat Chem* **2010**, *2*, 466-471.

(8) This work was presented at the 241th American Chemical Society National Meeting, Anaheim (2011), ORGN 648.

(9) Lu, Z.; Zhang, Y.; Wulff, W. D. *J. Am. Chem. Soc.* **2007**, *129*, 7185-7194.

(10) (a) Becke, A. D. *Phys. Rev. A* **1988**, *38*, 3098. (b) Lee, C. Y., W.; Parr, R. G. *Phys. Rev. B* **1988**, *37*, 785.

CHAPTER 4

CAN "FREE" PROTON BE THE COUNTER CATION OF CHIRAL BORATE ANIONS IN THE ABSENCE OFA BASE IN NON-AQUEOUS MEDIA

If you think that this is wrong then you should give it a shot and nail it! I hate to publish anything, which is wrong even accidently!!!

-William D. Wulff

4.1 Introduction

In the preceding Chapter 3, various intermediates were characterized of the proposed catalytic cycle (Scheme 3.3, Chapter 3) of the Brønsted acid catalyzed aziridination reaction[1] between imines and stabilized diazo compounds. In the process, for the first time, the existence of the AZIRIDINO-BOROX complex **239** was demonstrated where product is bound to the catalyst (Scheme 3.3, Chapter 3). While discussing path II of the catalytic cycle, the possible existence of "free" Brønsted Acid **23**-H was proposed (Figure 4.1A). As discussed earlier (Chapter 3), there is no NMR or X-ray evidence in the support of the existence of **23**-H as of this time. Additionally, the calculated structure of **23**-H reveals that a species with a tri-coordinate boron is energetically more favorable than one with a tetra-coordinate boron (Figure 3.18, Chapter 3). It was then decided to revisit the literature to find if anything similar has ever been reported. This was extremely important, as it would help to find an optimum protocol for generating a species like **23**-H. Two such systems were identified which were reported from the field of asymmetric catalysis. One of such system includes the spiroborates (SB) **20**-H[2] and **21**-H[2e,2f] and the other is the fused-spiroborate (FSB) **22**-H[3] (Figure 4.1B). Both kinds of borates

were reported to posses a tetra-coordinate boron and a "free" proton as the counter cation. In search of an optimized protocol to generate **23**-H, the cases of **20**-H and **22**-H were examined in more detail. In order to examine these systems, techniques including computational chemistry, NMR spectroscopy and X-ray crystallography were used.

Figure 4.1 (**A**) Free BOROX **23**-H. (**B**) Spiroborates **20**-H and **21**-H and Fused-spiroborate **22**-H

A

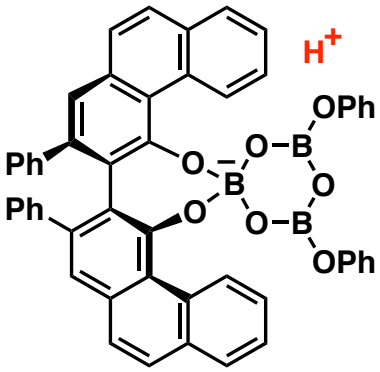

23-H

B

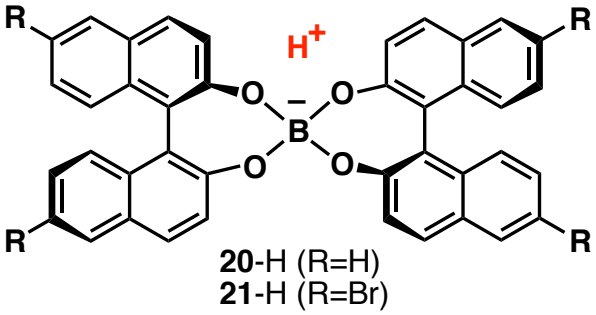

20-H (R=H)
21-H (R=Br)

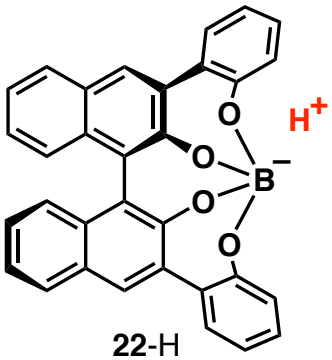

22-H

In the present work, ^{11}B NMR spectroscopy has been used as one of the most important tools to characterize borate intermediates. Out of all the borates shown in Figure 4.1, the only protonated neutral borate for which ^{11}B NMR spectrum is reported is for the fused-spiroborate

22-H.[3a] In the ^{11}B NMR analysis of borate anions, the chemical shift depends on the cation, concentration and the solvent. Hence, a list of ^{11}B NMR chemical shifts for some known achiral and chiral borate anions is given in Figure 4.2.[4] This provides us an idea of the general range of the chemical shift values for different types of borate anions and would help in the identification of the three systems listed in Figure 4.1. The detailed analysis of each system is described in subsequent sections.

Figure 4.2 ^{11}B NMR chemical shifts of $B(OPh)_3$ **187a**, triphenoxy boroxine **191a**, various achiral and chiral borate anions.

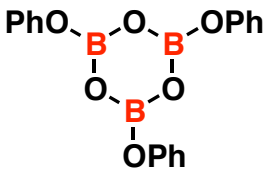

191a
δ = 18.5 ppm, br
$CDCl_3$
(Ref 4a)

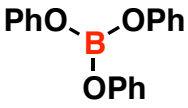

187a
δ = 16.2 ppm, br
$CDCl_3$
(Ref 4a)

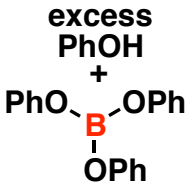

243
δ = 14.5 ppm, br
(Ref 3a)

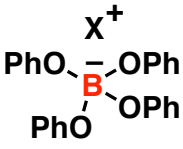

244a-d

X^+	δ, ppm	Solvent	Ref
Na^+	2.79	CD_3CN	4b
Li^+	2.00	$CDCl_3$	4c
$Me_2NH_2^+$	1.40	C_6D_6	4d
$C_5H_{11}NH_2$	2.60	THF-d_8	4e

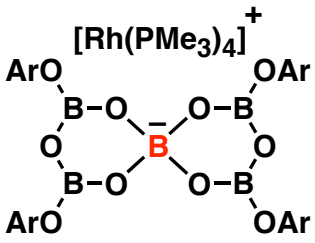

245 (Ar=4-MeO-C_6H_4)
δ = 4.76 ppm
acetone-d_6
(Ref 4f)

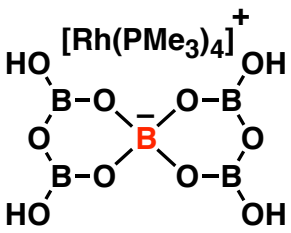

246
δ = 2.24 ppm, br
acetone-d_6
(Ref 4f)

Figure 4.2 cont'd

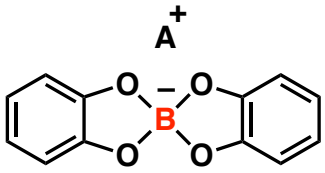

247a-c

A^+	δ, ppm	Solvent	Ref
Na^+	14.6	Diglyme	4g
Li^+	11.9	THF-d_8	4h
$Me_2NH_2^+$	14.0	C_6D_6	4i

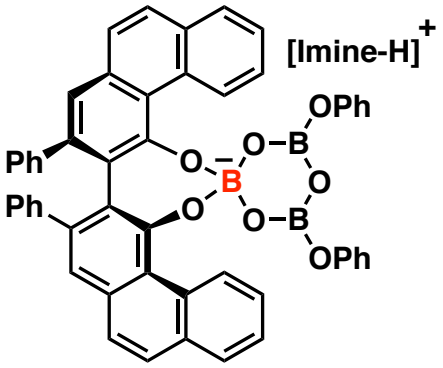

104a
δ = 5.5-5.7 ppm
$CDCl_3$
(Ref 1f)

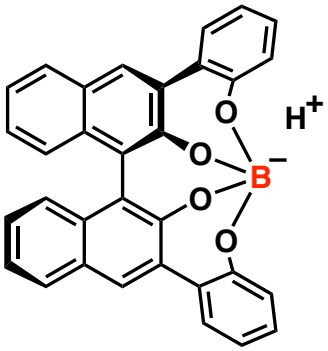

22-H
δ = 10 ppm, br
CD_2Cl_2
(Ref 3a)

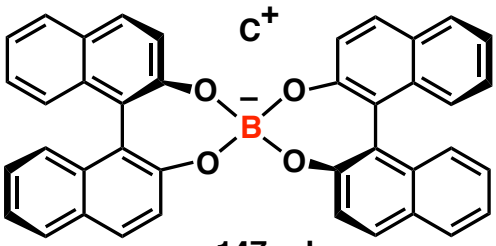

147a-d

C^+	δ, ppm	Solvent	Ref
Et_3NH^+	8.98	DMSO-d_6	4j
$Me_2NH_2^+$	8.96	DMSO-d_6	4j
(*R*)-Ph(Me)$CHNH_3^+$	9.01	DMSO-d_6	4j
Na^+	9.20	DMSO-d_6	4k

4.2 The case of the chiral spiroborates 20-H and 21-H

In 1994, Yamamoto and co-workers reported the preparation of the spiroborate **20**-H and its utilization for Mannich reactions[2a-2c] (Scheme 4.1A) and heteroatom Diels-Alder reactions of imines (Scheme 4.1B).[2a,2d] In the year 1997, the same catalyst was purported to effect an

asymmetric Pictet-Spengler reaction (Scheme 4.1C).[2e,2f] In all three reactions, excellent yields and enantioselectivities and diasteroselectivities were obtained, although stoichiometric amounts of the catalyst were required.

Scheme 4.1 Asymmetric reactions reported to be catalyzed by **20**-H

A Asymmetric imino-aldol reaction[2a-2c]

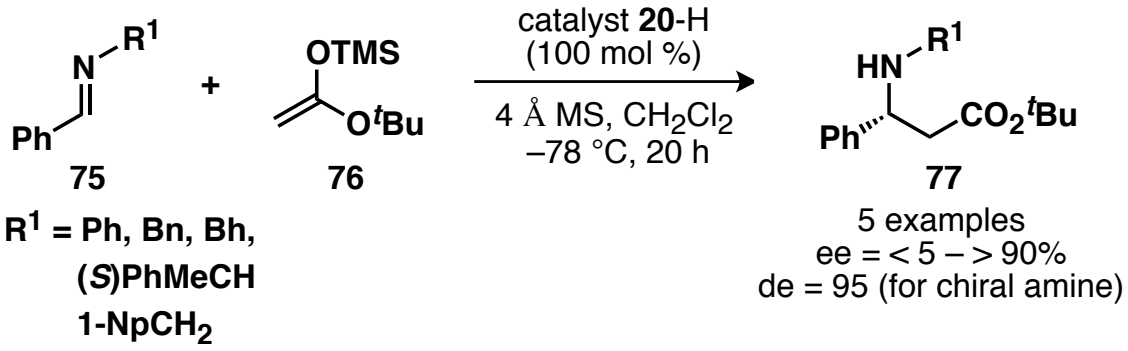

75 **76** **77**

R^1 = Ph, Bn, Bh, (*S*)PhMeCH, 1-NpCH_2

5 examples
ee = < 5 – > 90%
de = 95 (for chiral amine)

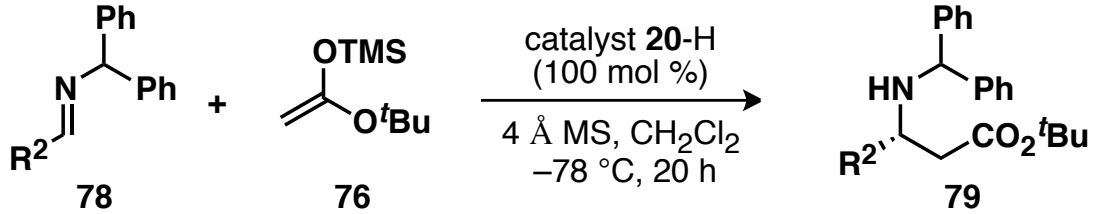

78 **76** **79**

R^2 = Ph, 2-naphthyl, *p*-Me-C_6H_4, *p*-Cl-C_6H_4, *p*-OAc-C_6H_4, 2,4-Cl_2-C_6H_4

6 examples
yield = 35 – 58%
ee = 95 – 98%

Scheme 4.1 cont'd

B Asymmetric heteroatom Diels-Alder reaction[2a,2d]

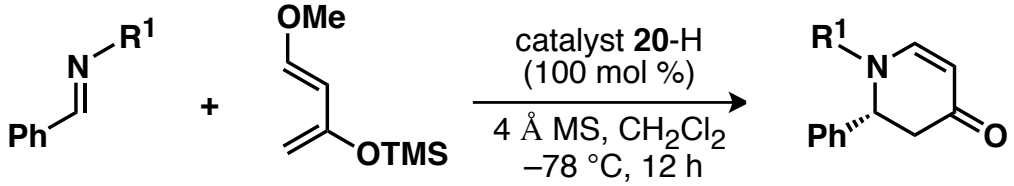

75 **80** **81**

R^1	y%	ee/de%
Bn	78	86
(*S*)PhMeCH	64	99
(*S*)PhMeCH (with *ent*-**20**-H)	49	83

C Asymmetric Pictet-Spengler reaction[2e,2f]

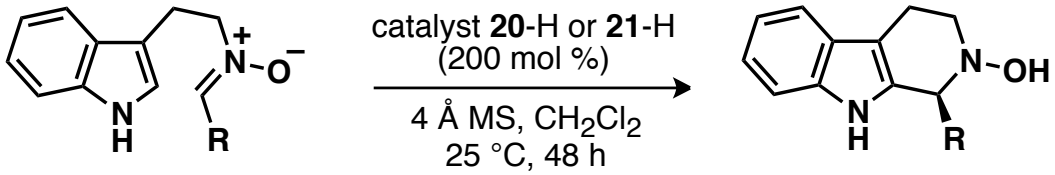

83

R = Ph, *p*-OMe-C_6H_4, *p*-NO_2-C_6H_4, Me, ^{i}Bu, 1-naphthyl,

84

6 examples
yield = 39 – 94%
ee = 15 – 94%

The reported structure represents the catalyst as a Brønsted acid **20**-H containing a tetra-coordinate boron atom (Scheme 4.2).[2a,2e] However, the mode of catalysis of **20**-H was proposed to be as a Brønsted acid assisted Lewis acid (BLA) catalysis. The catalytic function of **20**-H was proposed to be as a chiral Lewis acid where interaction with a Lewis base disrupts one of the boron-oxygen bonds to give the Lewis acid-Lewis base complex **71**/**71′** (Scheme 4.2).[2a,2e]

Scheme 4.2 Proposed catalytic activity of **20**-H

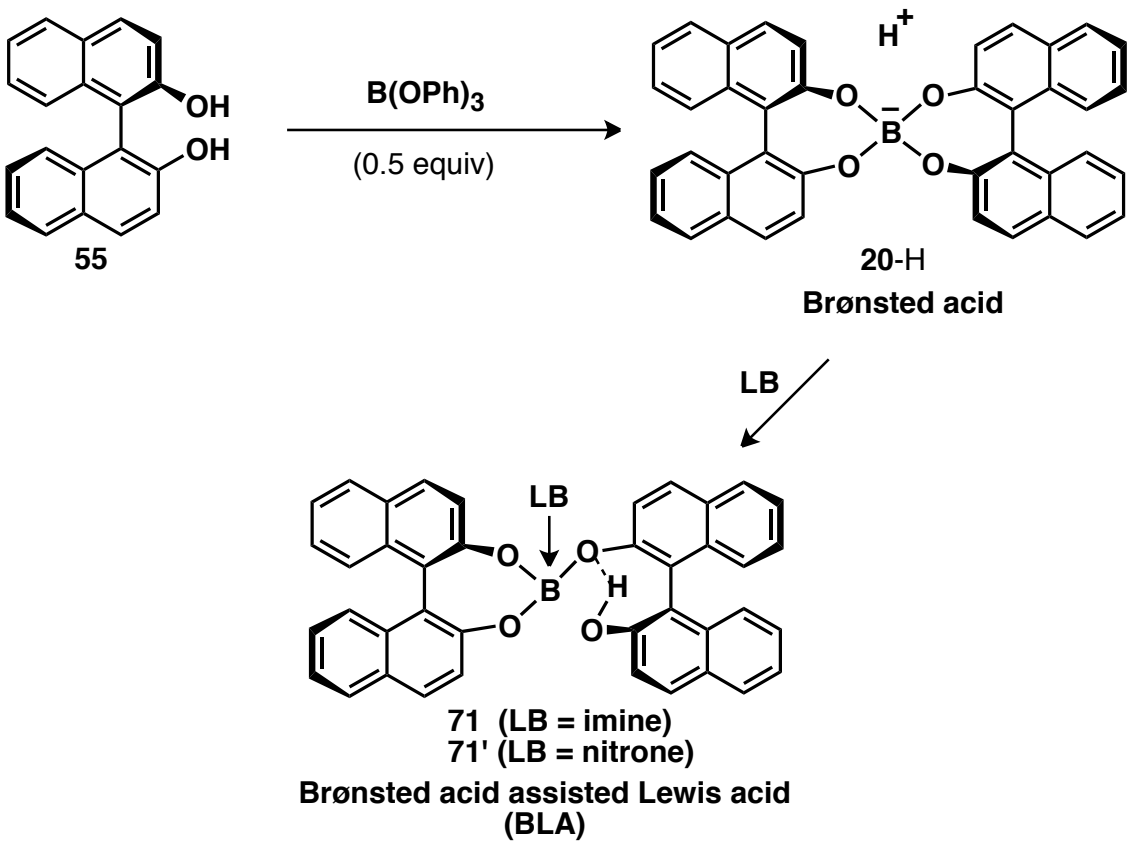

In the present work, the structure of **20**-H was then investigated with the help of computational chemistry. The proposed structure **20**-H was computed by DFT calculations using Gaussian ′03 at B3LYP/6-31g* level of theory.[5] First, the structure of spiroborate anion **20** was optimized (Figure 4.3A) which was then followed by optimization of **20**-H by putting a proton on each of the four oxygen atoms of the anion **20** (Figure 4.3B). Surprisingly, the calculations suggested the presence of a tri-coordinate boron atom instead of a tetra-coordinate boron atom as proposed in the original structure (Figure 4.3B *vs.* Figure 4.1B). Interestingly, the optimization converged to only one structure **72** (Figure 4.3B). In the calculated structure **72**, there is a hydrogen bonding (2.33 Å) between the O1-H of one of the BINOL units and an oxygen (O2) on the other BINOL unit (Figure 4.3B). As shown in Figure 4.3B, there is another

possibility **72′** (an isomer of **72**) where the H-bond is between the O1-H group on one of the BINOL units and an oxygen (O3) on that same BINOL unit. In this case, in order to obtain a geometry corresponding to the **72′**, calculation was initiated with the proton attached to O1 in proximity to O3, with the distance of the proton to O2 fixed at 3 Å. Starting from the optimized geometry **72′** (H-bond = 1.86 Å) from the fixed distance calculation and releasing the proton-O2 distance resulted in a new optimized geometry **72′′** where the H-bond (3.72 Å) is almost lost. The relative energy of each species either from complete minimization or fixed distance minimization is shown in Figure 4.3.

Figure 4.3 Calculated structures of **20**-H, **72** and **72′** obtained using Gaussian ′03 at B3LYP/6-31g* level of theory. All structures are visualized by the Mercury program (C, gray; O, red; B, yellow; H, light blue). Hydrogens are omitted for clarity (except O-H). All the bond distances are in Angstrom and energies in kcal/mol. ∠oop = angle out of plane for the current/former tetra-coordinate boron, B-On = the distance between O-n and the current/former tetra-coordinate boron where n = 1-4. (**A**) Calculated structure of Spiroborate anion **20**. (**B**) Calculated structures **72**, **72′** (from fixed distance calculation) and **72′′** obtained by putting a proton on any one of the four oxygen atoms.

A

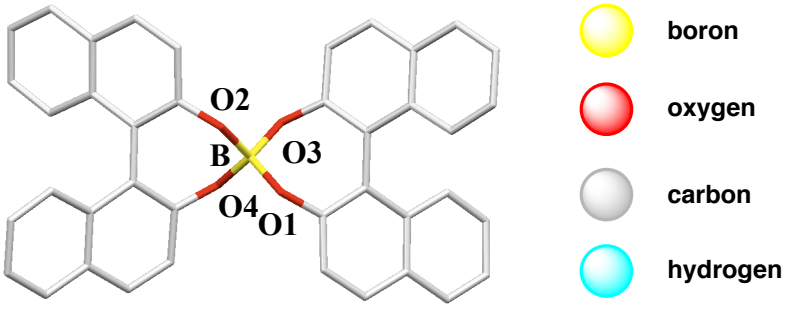

23

(∠oop = 19.4º, B-O1 = B-O2 = B-O3 = B-O4 = 1.47 Å)

Figure 4.3 cont'd

B

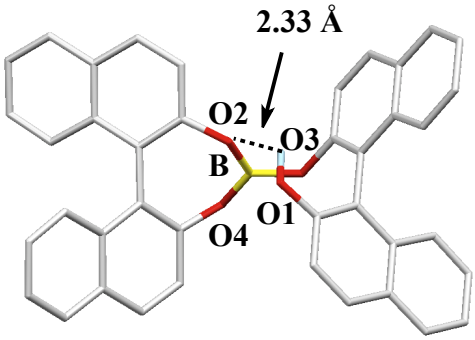

72
(∠oop < 1º, B-O1 = 3.51 Å,
B-O2 = 1.40 Å, B-O3 = 1.35 Å, B-O4 = 1.38 Å)
(ΔΔG = 0 Kcal/mol)

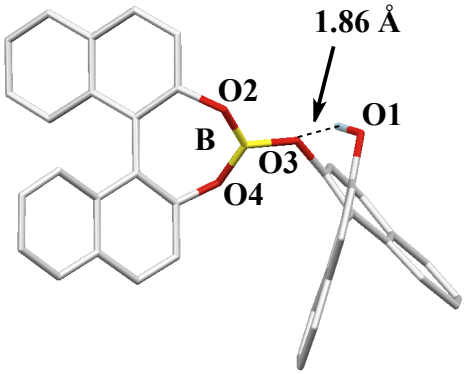

72′
(∠oop < 1º, B-O1 = 3.50 Å,
B-O2 = 1.37 Å, B-O3 = 1.37 Å, B-O4 = 1.37 Å)
(ΔΔG = +4.2 kcal/mol)
* fixed distance calculation (O2-H = 3Å)

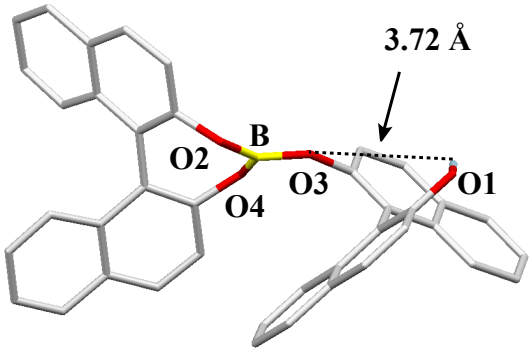

72′′
(∠oop < 1º, B-O1 = 5.41 Å,
B-O2 = 1.37 Å, B-O3 = 1.37 Å, B-O4 = 1.38 Å)
(ΔΔG = +1.6 kcal/mol)

Based on these computational results, the possibility of the existence of spiroborate **20**-H seems unlikely. It must be noted that various salts have been reported which contain the spiroborate anion **20** and these include those with protonated amines[4j,6] or metal cations[4k] in the

ion-pair (Figure 4.2). The ^{11}B NMR spectrum of these salts revealed the chemical shift of the tetra-coordinated boron atom to be ~ 9 ppm. Hence, it was thought that the ^{11}B NMR spectrum of the proposed structure would give a similar observation. At this point, it must be noted that Gang Hu, a former group member, performed the NMR studies presented in the first 5 entries in Figure 4.4. The entry 6 of Figure 4.4 is the part of this doctoral research. The reaction of $B(OPh)_3$ with two equivalents of BINOL was performed following Yamamoto's protocol[2a] for the preparation of the spiroborate **20**-H which involves stirring the two in CD_2Cl_2 over 4 Å molecular sieves for 1 h at room temperature. The solution was filtered and subjected to NMR analysis. The ^{1}H NMR and ^{11}B NMR spectra are shown in Figure 4.4B (entry 2) and Figure 4.4C (entry 1), respectively. The ^{1}H NMR spectrum reveals a complex mixture of species most of which have not been identified, but the ^{11}B NMR spectrum shows a broad absorption at 16.0 ppm that would be expected for any kind of three coordinate borate ester. Phenol should be present in the mixture as a result of exchange with BINOL. However, this should not be considered as indicative of the extent of exchange since it is our experience that most commercial $B(OPh)_3$ samples contains 20-30 percent phenol (see Figure 4.13, entry 5). In contrast, the reaction of VAPOL and $B(OPh)_3$ shows no reaction under the same conditions.[1f]

Our observations with the reactions of imines catalyzed by borate derivatives of VANOL and VAPOL are that the actual catalyst species is not formed until the imine is added. The *meso*-borate **106** (B1) and the *pyro*-borate **108** (B2) are pre-catalysts that are converted into the *poly*-

borate (BOROX) catalyst **188/189** by the imine **78** (Scheme 2.1, Chapter 2). Thus, it was decided to examine the effect of added imine on this mixture of BINOL and $B(OPh)_3$. When the mixture of 2 equivalents of BINOL and one equivalent of $B(OPh)_3$ is treated with one equivalent of the imine **78a**, the complex mixture of compounds is converted cleanly into a single compound within the time that it takes to load an NMR tube and take the ^{1}H NMR and ^{11}B NMR spectra (Figure 4.4B, entry 3 and Figure 4.4C, entry 2). This compound is assigned as the ion-pair **74a** comprised of a spiroborate anion **20** and the protonated form of imine **78a** (Figure 4.4A). The four coordinate anionic borate unit in **74a** displays a characteristic sharp absorption at δ = 8.9 ppm in the ^{11}B NMR spectrum (Figure 4.4C, entry 2) and reveals the complete disappearance of the broad three coordinate borate absorption at δ = 16 ppm, suggesting the formation of **74a** in near quantitative yield. Also, similar observations were made when (*S*)-**55** was used instead of (*R*)-**55** (not shown here). Further, the formation of ion-pair **74a**/**147f** was observed when different bases or NMR solvents were used (Figure 4.4B, entries 4-6).

Figure 4.4 (**A**) NMR Analysis of a mixture of (*R*)-**55** with $B(OPh)_3$ and imine **78a** or DMAP. (**B**)[a] ^{1}H NMR spectra (aromatic region) of the reaction mixture in CD_2Cl_2 or $CDCl_3$. (**C**) ^{11}B NMR spectra corresponding to the ^{1}H NMR spectra in Figure 4.4B starting from entry 2.

Figure 4.4 cont'd

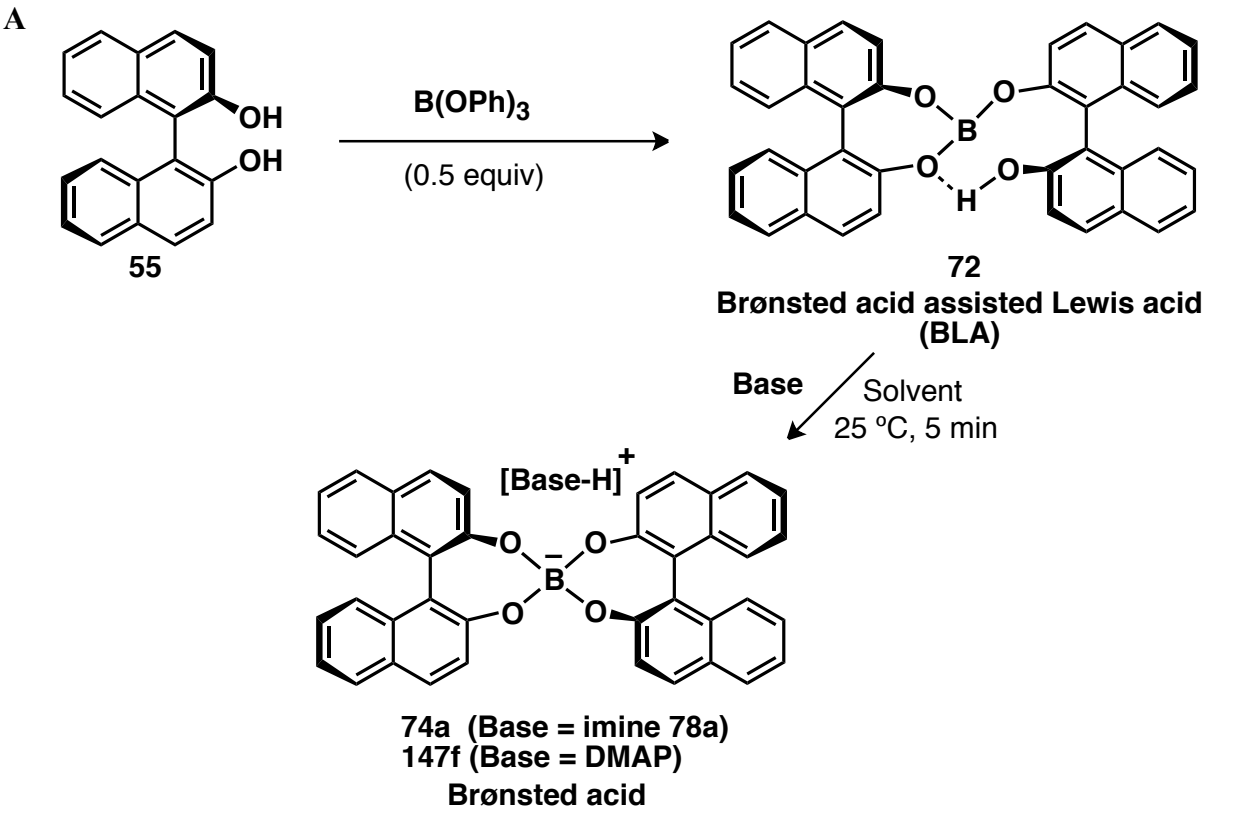

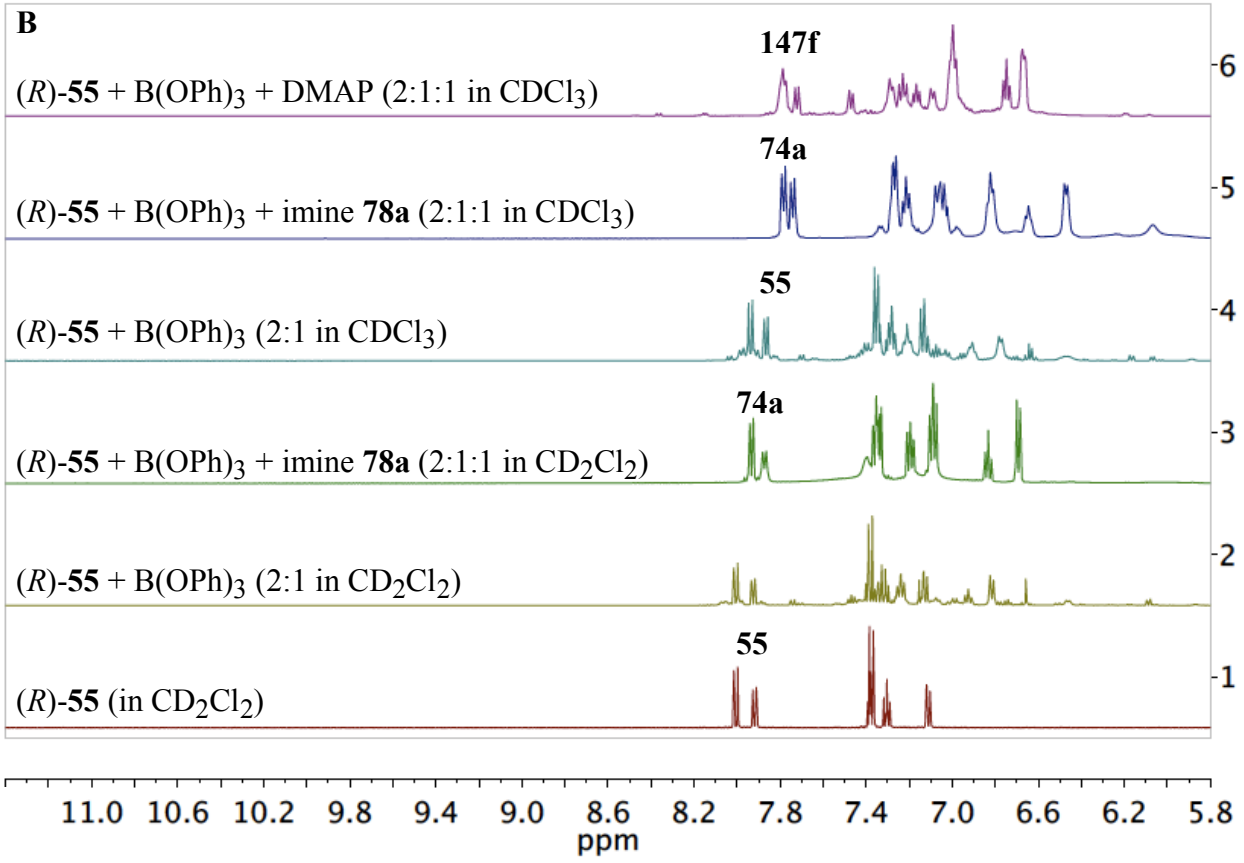

Figure 4.4 cont'd

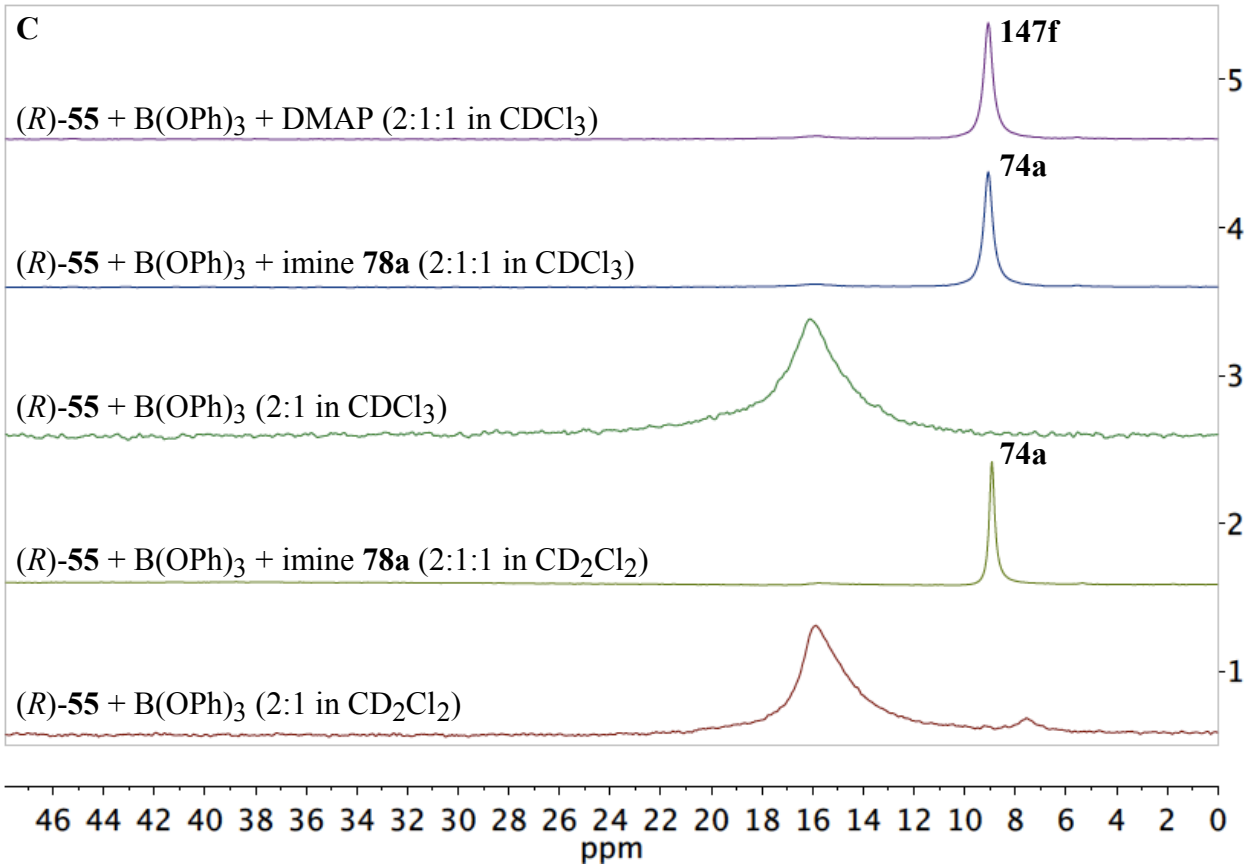

[a] Note for Figure 4.4B: Entry 1: pure BINOL (*R*)-**55** in CD_2Cl_2. Entry 2: (*R*)-**55** (0.1 mmol) plus 0.5 equiv $B(OPh)_3$ and powdered 4Å Molecular Sieves (150 mg) were stirred for 1 h in CD_2Cl_2 (3 mL) at 25 °C. Entry 3: 0.5 equiv imine **78a** was added to the entry 2 for 10 min at 25 °C. Entry 4: Same as entry 2 in $CDCl_3$. Entry 5: Same as entry 3 in $CDCl_3$. Entry 6: 0.5 equiv DMAP was added to the entry 4 for 10 min at 25 °C.

It is of course possible that the compound with the proposed structure **74a** could also have the structure **71a** or **73a** in which there is a Lewis acid-Lewis base complex which contains a tetra-coordinate boron atom (Figure 4.5). Support for the structure **74a** containing a

spiroborate anion and an iminium cation comes from the work of Yamamoto and coworkers who have previously studied heteroatom Diels-Alder and Mannich reactions of imines mediated by a stoichiometric amount of a catalyst prepared from two equivalents of BINOL and one equivalent of $B(OPh)_3$.[2a] In support of a spiroborate core in their catalyst they were able isolate and determine the X-ray structure of the complex **248** although no spectral data for **248** was presented (Figure 4.6).[2a] This complex consists of the spiroborate anion, a molecule of phenol and the protonated form of imine (*S*)-**139a** (Figure 4.6). There is no direct H-bonding between the protonated iminium and the spiroborate anion, but rather the protonated iminium is H-bonded to the phenol, which in turn is H-bonded to the spiroborate anion. This crystal was of the miss-

Figure 4.5 Bronsted acid **74a** and Brønsted acid assisted Lewis acid **71a** or **73a** (imine = **78a**)

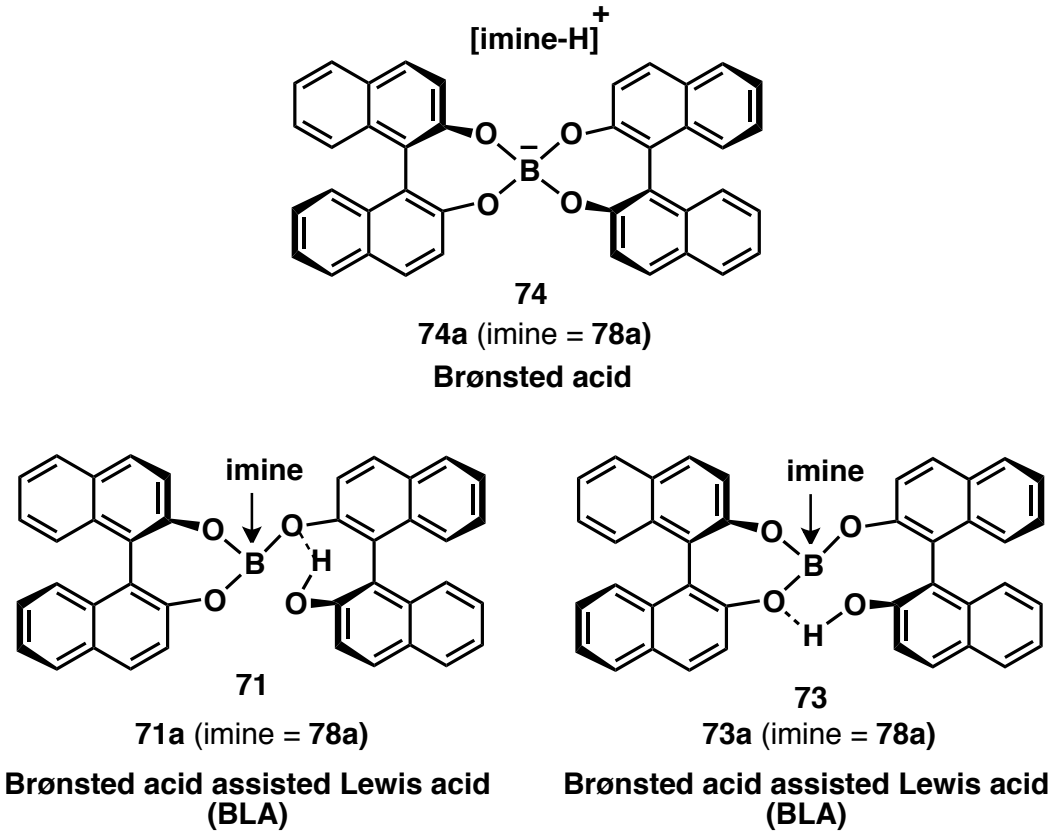

74

74a (imine = **78a**)

Brønsted acid

71

71a (imine = **78a**)

Brønsted acid assisted Lewis acid (BLA)

73

73a (imine = **78a**)

Brønsted acid assisted Lewis acid (BLA)

matched pair of (*S*)-BINOL **55** and (*S*)-**139a** and perhaps in the matched pair non-covalent contacts between the (*S*)-BINOL core and protonated (*R*)-**139a** would be more favorable. While studying the NMR spectra of the complex **74a** with (*S*)-BINOL **55**, Gang Hu observed that a few yellow crystals serendipitously formed in the NMR tube, which provided an opportunity to determine the crystal structure of the ion-pair **74a**. It was hoped that non-covalent interactions between the spiroborate core and the iminium could be found in **74a** since the imine **78a** from which it is derived is not chiral. The complex **74a** also crystallized with a molecule of phenol but an X-ray diffraction analysis of these crystals revealed that non-covalent interactions present in complex **249** are much different than in Yamamoto's complex **248** (Figure 4.6). The details about the crystal structure **249** can be found in Gang Hu's dissertation (Figure 4.6).[7] Also, the crystal structures of the other salts containing the spiroborate anion **20** and a) protonated amines, [6] b) metal ions[4k] are given in literature.

Figure 4.6 Schematic drawing of imine (*S*)-**139a**, Yamamoto's structure **248**[2a] and Gang Hu's structure **249**[7]

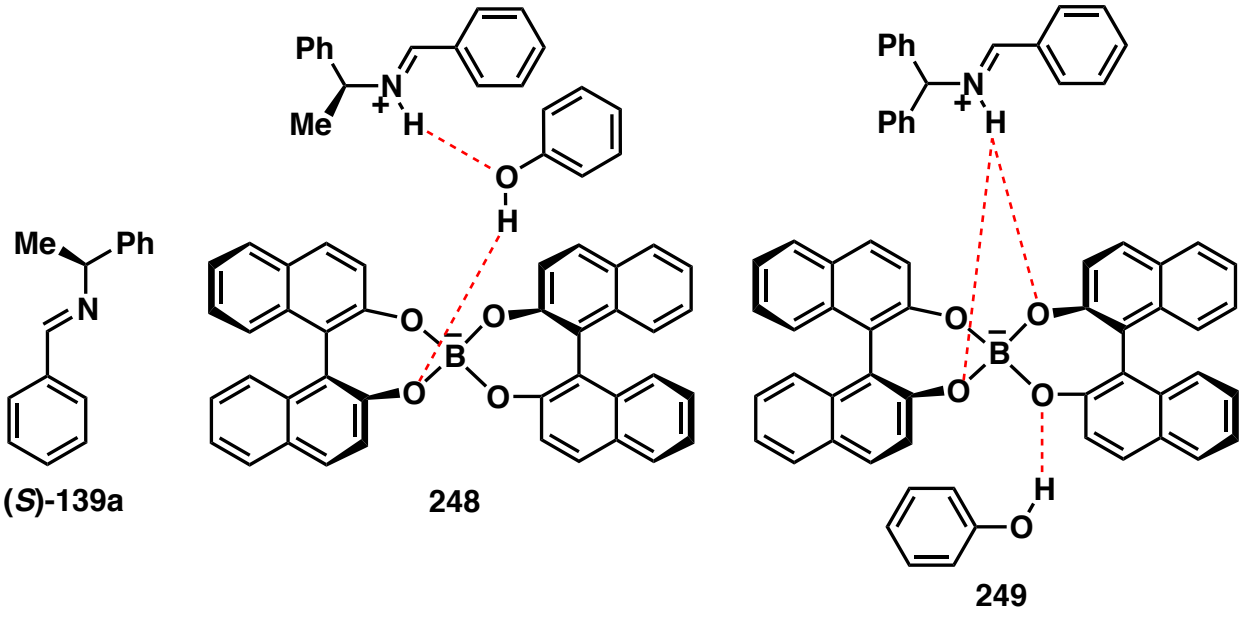

Based on the above discussion, it is quite clear that there is no spectroscopic evidence for the existence of spiroborate **20**-H. The data taken as a whole suggests that perhaps there is no tetra-coordinate boron species unless an imine is added to deprotonate the hydroxyl group in the BINOL **55**.

Although our interests are in chiral spiroborate species, an achiral spiroborate **251**-H similar to **20**-H has been reported as a protonated neutral species with a tetra-coordinate boron and was prepared from the reaction between boric acid and 2 equiv of catechol **250** (Scheme 4.3A).[8] However, there was no spectroscopic characterization provided for this compound. After almost a decade, Nöth and co-workers reported a different compound **252** for the same reaction and with the same conditions.[9] They characterized this compound by NMR spectroscopy and X-ray crystallography. As shown in Scheme 4.3A, there is no tetra-coordinate boron atom in **252** which is consistent with the chemical shift observed in the ^{11}B NMR spectrum (δ = 22.5 ppm, $CDCl_3$). This is in agreement with our observations for the spiroborate **20**-H.

Scheme 4.3 Common borate esters of catechol **250**

A

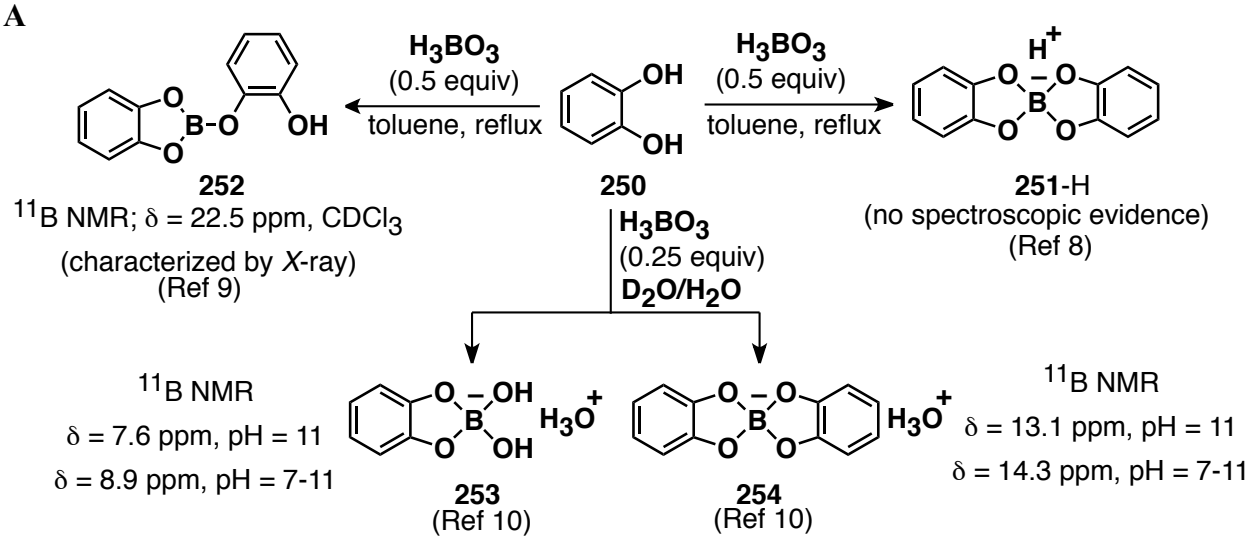

Scheme 4.3 cont'd

B

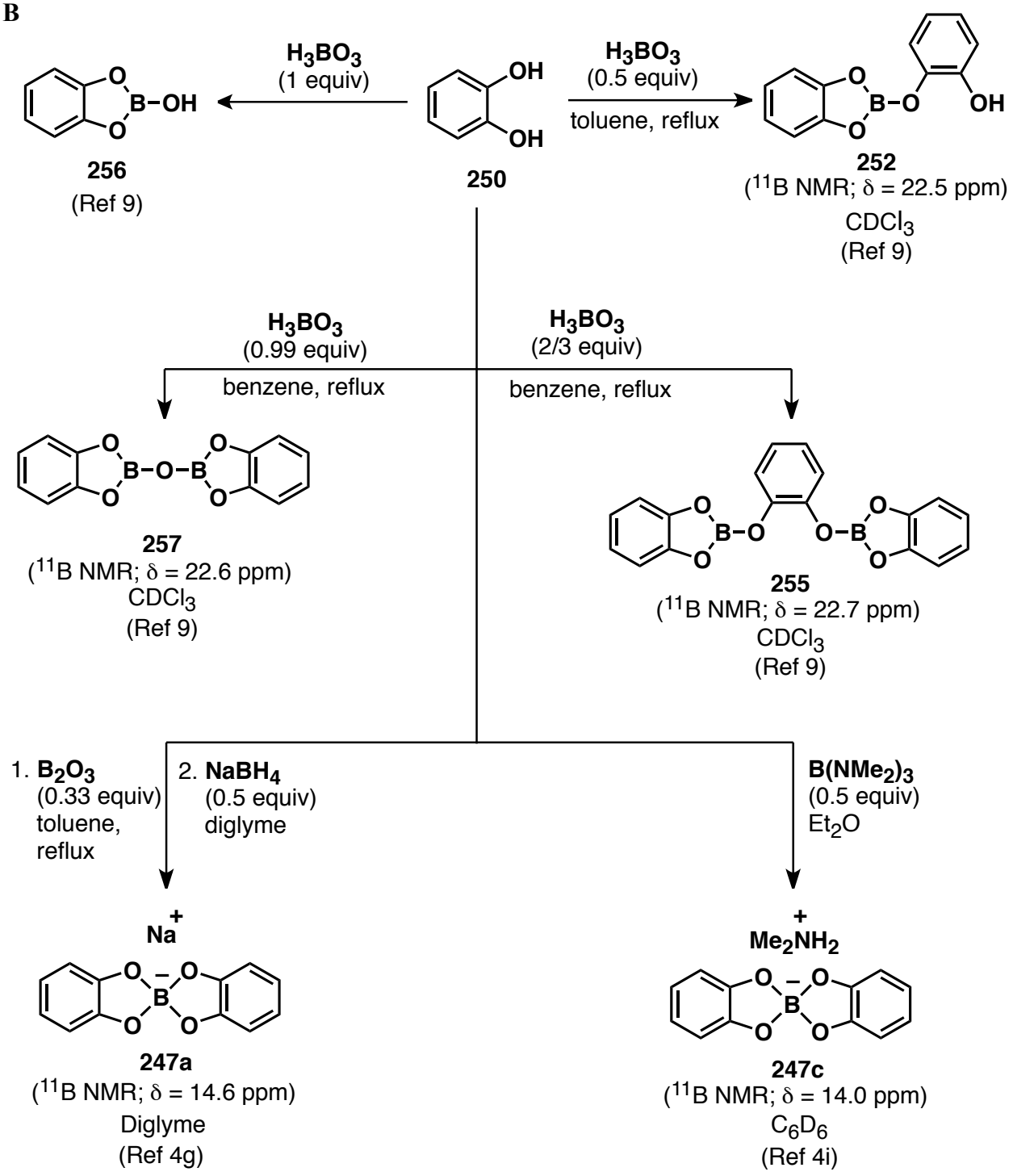

At this point, it was thought that the structure of **251**-H could be used to calibrate our computational method. Ideally, after the optimization of the proposed structure of **251**-H, the

finalized energy minimum structure should be close to that of the X-ray structure of **252**. This would validate our calculation method. In fact, the calculated structure was found to be essentially the same as the X-ray structure of **252** (Figure 4.7).

Figure 4.7 Calculated structures of **251** and **251**-H obtained using Gaussian ′03 at B3LYP/6-31g* level of theory. All structures are visualized by the Mercury program (C, gray; O, red; B, yellow; H, light blue). Hydrogens are omitted for clarity (except O-H). All the bond distances are in Angstroms and energies in kcal/mol. ∠oop = angle out of plane for the current/former tetra-coordinate boron, B-On = the distance between O-n and the current/former tetra-coordinate boron where n = 1-4. (**A**) Calculated structure of spiroborate anion **251** (**B**) Calculated structures of possible spiroborate **251**-H obtained by putting a proton on any one of the four oxygen atoms (**C**) X-ray structure of **252**.

A

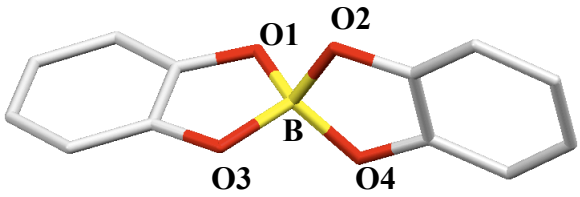

251
(∠oop = 19.4º, B-O1 = B-O2 = B-O3 = B-O4 = 1.49 Å)

B

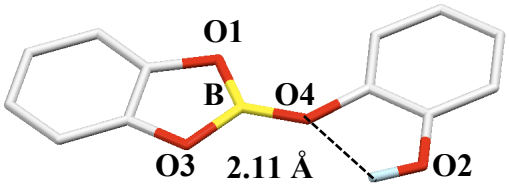

Calculated structure of **251**-H
(∠oop < 1º, B-O1 = 1.39 Å,
B-O2 = 3.99 Å, B-O3 = 1.39 Å, B-O4 = 1.35 Å)

C

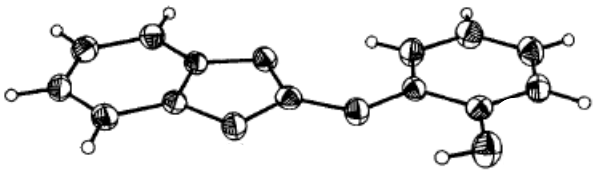

252

Importantly, two compounds **253** and **254** were reported when a mixture containing catechol and boric acid (0.5 equiv) was subjected to NMR analysis in aqueous solutions (Scheme 4.3A).[10] In the ^{11}B NMR spectrum, two peaks at δ = 7.6 ppm and δ = 13.1 ppm were reported for **253** and **254**, respectively, at pH = 11.[10a] This result was expected as the analysis was performed under aqueous conditions where water is acting as the base. Also, a variety of other products were reported that were a function of the different ratios of both the components (Scheme 4.3B).[9] Similar compounds have also been reported and observed for BINOL **55** (Scheme 5.4, Chapter 5). As shown in Scheme 4.3B, a salt **247c** derived from catechol **250**, $B(NMe_2)_3$ (0.5 equiv) is found to exhibit a peak at δ = 14.0 ppm (in C_6D_6) in the ^{11}B NMR spectrum.[4i] A number of similar spiroborates from different diols have been reported in the literature.[11]

In the end, the results suggest that the spiroborate **20**-H is unlikely to exist in the the absence of base. At the same time, ion-pair **74** can be generated as soon as imine is added. However, different ligands might behave differently. Hence, a second case was then examined involving the fused-spiroborate **22**-H (Figure 4.1B).

4.3 The case of the chiral fused-spiroborate 22-H

As discussed earlier, the fused-spiroborate (FSB) **22**-H is another example of a published neutral chiral borate containing a tetra-coordinate borate anion and a "free" proton as the counterion (Scheme 4.1). In 1994, Yamamoto and co-workers reported chiral catalyst **22**-H for the first time.[3a] They used this catalyst for the asymmetric Diels-Alder reaction between dienes

and enals/alkynals (Scheme 4.4A and 4.4B).[3a-3d] It must be noted that no spectroscopic data was provided for the catalyst **22**-H except a ^{11}B NMR spectrum (δ = 10 ppm).

Scheme 4.4 Asymmetric reactions reported to be catalyzed by **22**-H

A Asymmetric Diels-Alder reactions of dienes and enals[3a-3c]

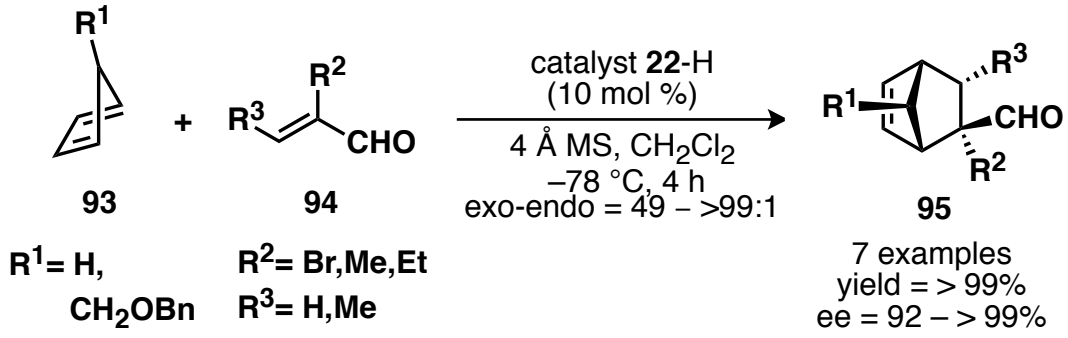

93 **94** **95**

R^1= H, CH_2OBn **R^2= Br,Me,Et** **R^3= H,Me**

7 examples
yield = > 99%
ee = 92 – > 99%

B Asymmetric Diels-Alder reactions of dienes and alkynals[3d]

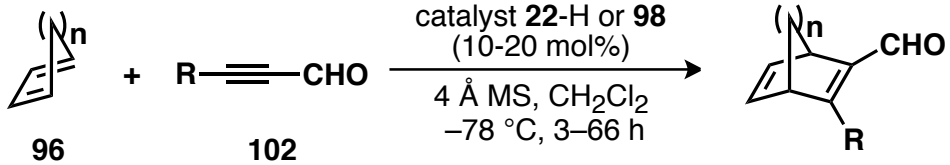

96 **102** **103**

n = 1,2 **R = I,Me,CO_2Et**

5 examples
yield = 28 – 98%
ee = 34 – 95%

C Formal [4+3] cycloaddition[3e]

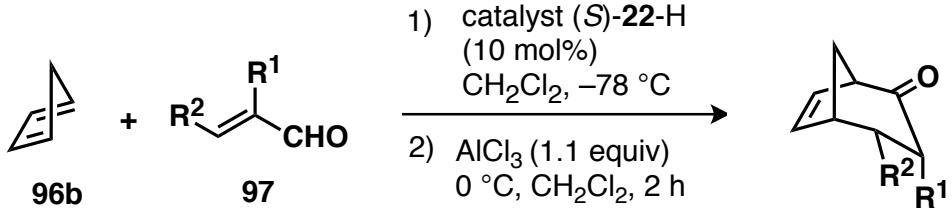

96b **97** **101**

R^1= Me,Et, Bn
R^2= -$(CH_2)_3$-

4 examples
yield = 72 – 85%
ee = 46 – 96%

In the year 2006, Davies and coworkers introduced a formal [4+3] cycloaddition by a tandem Diels Alder reaction/ring expansion using **22**-H as the catalyst (Scheme 4.4C).[3e]

The catalyst **22**-H was prepared by the reaction of the tetra-phenol **89** with 1 equiv of commercial $B(OPh)_3$ and its structure was proposed to contain a tetra-coordinate borate anion that was protonated at some unspecified location (Scheme 4.5).[3a-3d] Similar to the case of **20**-H, the mode of catalysis of **22**-H was proposed to be that of a Brønsted acid assisted Lewis acid (BLA) catalyst which means that it behaves as a chiral Lewis acid where interaction with a Lewis base disrupts one of the boron-oxygen bonds to give Lewis acid-Lewis base complex **90′** (Scheme 4.5). This case study is more likely to give **22**-H, perhaps, due to the presence of all four oxygens in the same molecule.

Scheme 4.5 Proposed catalytic activity of **22**-H

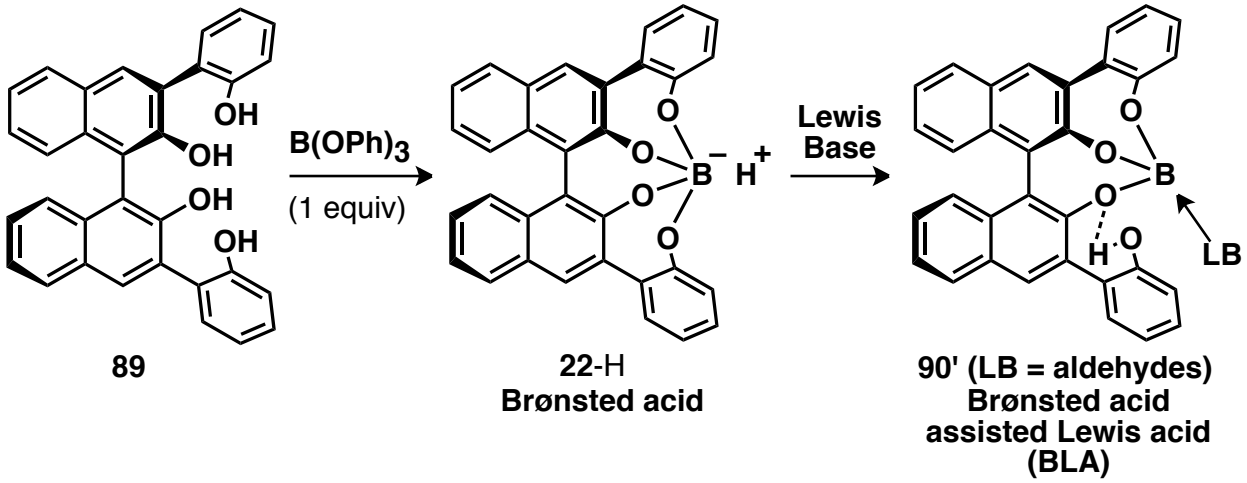

In the current work, the first step in characterization of the proposed structure **22**-H was the optimization by DFT calculations using Gaussian ′03 at B3LYP/6-31g* level of theory.[5] After the optimization of the fused-spiroborate anion **22**, energy minimization of **22**-H was performed

by putting a proton on each oxygens. The two structures **91** and **91′** were obtained where structure **91′** was found to be lying +4.3 kcal/mol higher in energy (Figure 4.8B). Additionally, structure **91** is stabilized by an extra hydrogen bond of the OH at O1 to one of the oxygen of the 3-coordinate borate ester. However, in both cases, the calculations revealed the presence of a tri-coordinate boron atom instead of a tetra-coordinate boron atom as proposed in the original structure of **22**-H. The observation is in agreement with that seen for the case of spiroborate **20**-H. However, this computational result is not consistent with the fact that a peak at δ = 10 ppm is reported for the ^{11}B NMR spectrum of **22**-H. This chemical shift lies in the range of a tetra-coordinate boron as was observed in the case of BINOL derivatives (Figure 4.2). The calculated value of the chemical shift of boron in **91** (Figure 4.8B) is found to be 19 ppm using Gaussian ′03. Hence, to address this discrepancy it was deemed important to experimentally reproduce Yamamoto's synthesis of **22**-H as it might lead us to a better understanding of finding a protocol towards the trapping of protonated form of VAPOL boroxinate i.e. **23**-H.

Figure 4.8 Calculated structures of **22**, **91** and **91′** obtained using Gaussian ′03 at B3LYP/6-31g* level of theory. All structures are visualized by the Mercury program (C, gray; O, red; B, yellow; H, light blue). Hydrogens are omitted for clarity (except O-H). ∠oop = angle out of plane for the current/former tetra-coordinate boron, B-On = the distance between O-n and the current/former tetra-coordinate boron where n = 1-4. (**A**) Calculated structure of fused-spiroborate anion **22** (**B**) Calculated structure **91** obtained by putting a proton on O1 (**C**) Calculated structure **91′** obtained by putting a proton on O3

Figure 4.8 cont'd

A

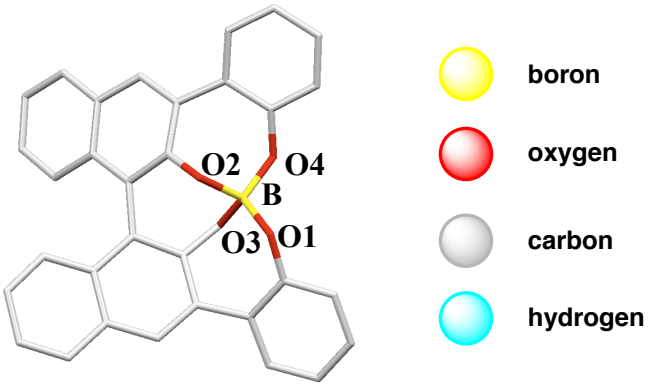

22
(∠oop = 18.1°–20.9°, B-O1 = B-O4 = 1.45 Å, B-O2 = B-O3 = 1.50 Å)

B

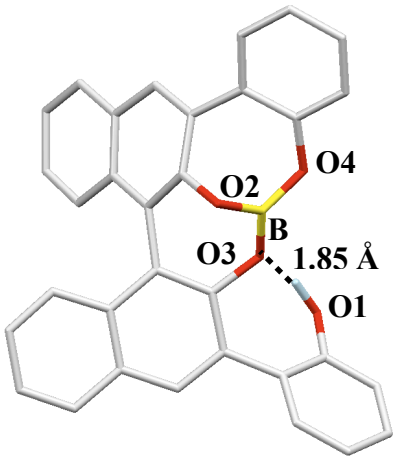

91
(∠oop < 1°, B-O1 = 3.94 Å,
B-O2 = 1.39 Å, B-O3 = 1.38 Å,
B-O4 = 1.37 Å)
(ΔΔG = 0 kcal/mol)

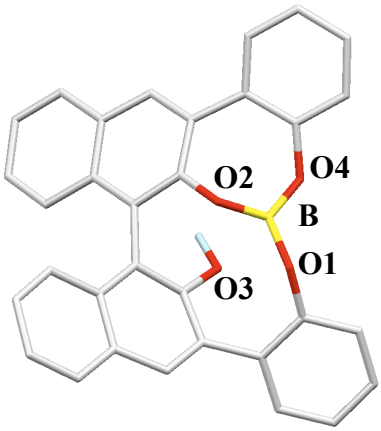

91′
(∠oop < 1°, B-O1 = 1.37 Å,
B-O2 = 1.39 Å, B-O3 = 2.50 Å,
B-O4 = 1.38 Å)
(ΔΔG = +4.2 kcal/mol)

The BINOL derivative (*R*)-**89** was prepared by Suzuki coupling of (*R*)-**259** with 2-methoxyphenylboronic acid **260** in the presence of $Pd(PPh_3)_4$ and subsequent demethylation (Scheme 4.6)

Scheme 4.6 Preparation of BINOL derivative **89**

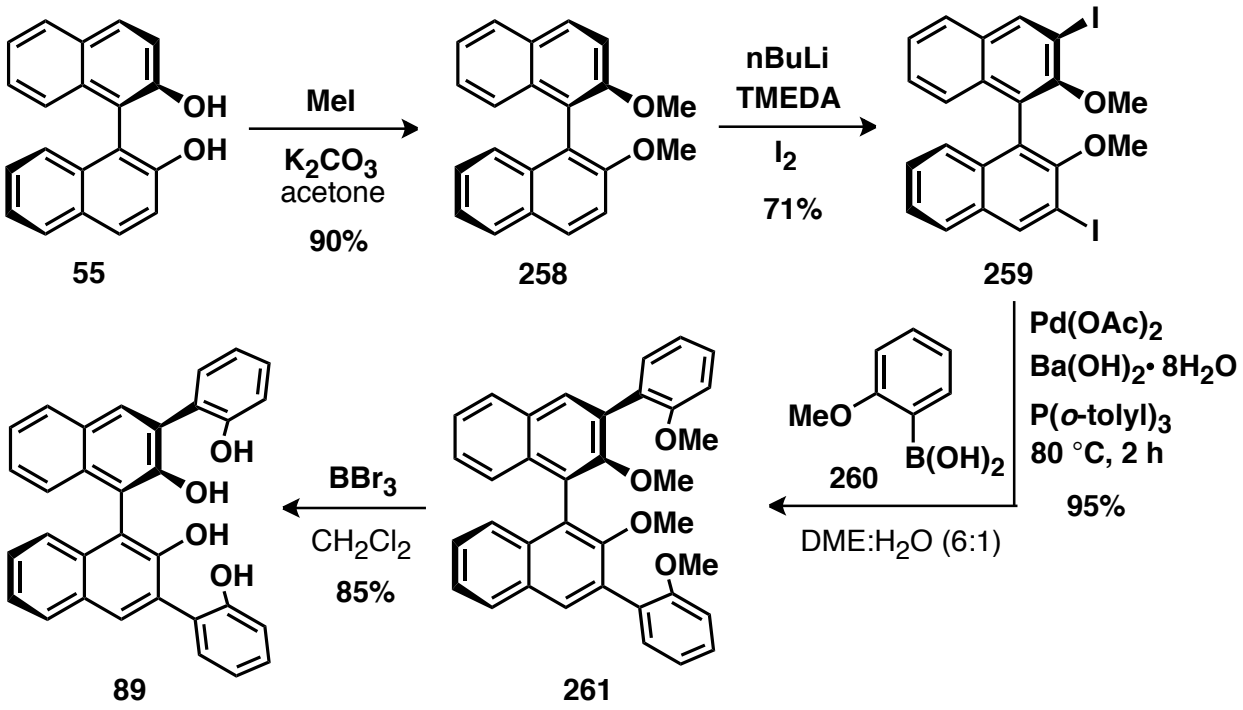

In order to independently characterize the structure **22**-H proposed by Yamamoto, the synthesis of **22**-H was performed following Yamamoto's protocol, which involves the reaction of the BINOL derivative (*R*)-**89** (0.05 mmol) with one equiv of $B(OMe)_3$. According to the procedure, both of the components were refluxed at 60 °C in CD_2Cl_2 (3 mL) for 2 h during which the methanol was removed using 4Å Molecular Sieves (pellets) in a Soxhlet thimble.[3a] A white precipitate was observed. Thereafter, it was then stirred vigorously for 0.5 h after the addition of extra CD_2Cl_2 (1.5 mL). Most of the white precipitate was dissolved and the resulting turbid solution was subjected to NMR analysis. The ^{1}H NMR spectrum reveals a complex mixture of species (Figure 4.9C, entry 2). Interestingly, no peak at δ = 10 ppm was observed in the ^{11}B NMR spectrum. In fact, the ^{11}B NMR spectrum shows a broad absorption

at 19.5 ppm that is very similar to that observed for **20**-H and which would be expected for a tri-coordinate borate species (Figure 4.9B, entry 2).

Figure 4.9 (**A**) NMR Analysis of a mixture of **89** with various boron sources and imine **78a**. (**B**)[a] ^{11}B NMR spectra of the reaction mixture in CD_2Cl_2. (**C**) ^{1}H NMR spectra (aromatic region) corresponding to the ^{11}B NMR spectra in Figure 4.9B.

A

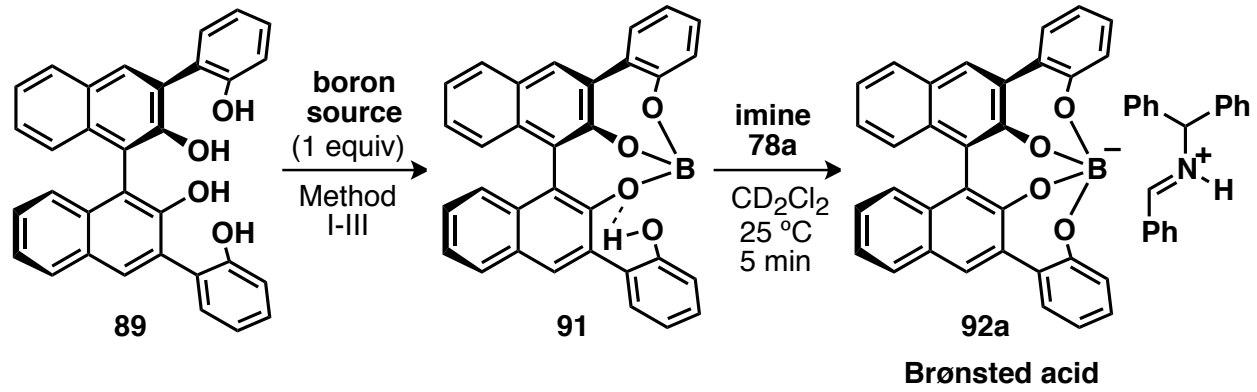

B

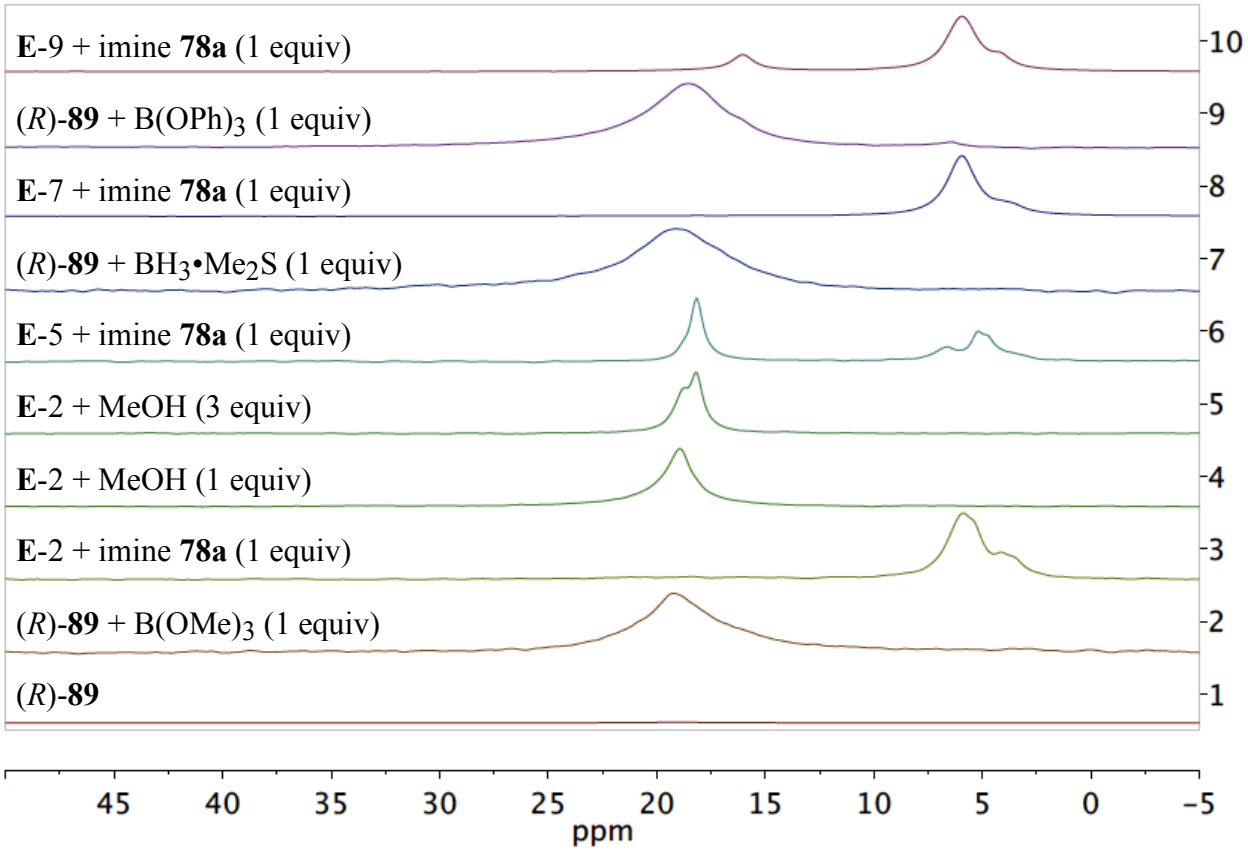

Figure 4.9 cont'd

C

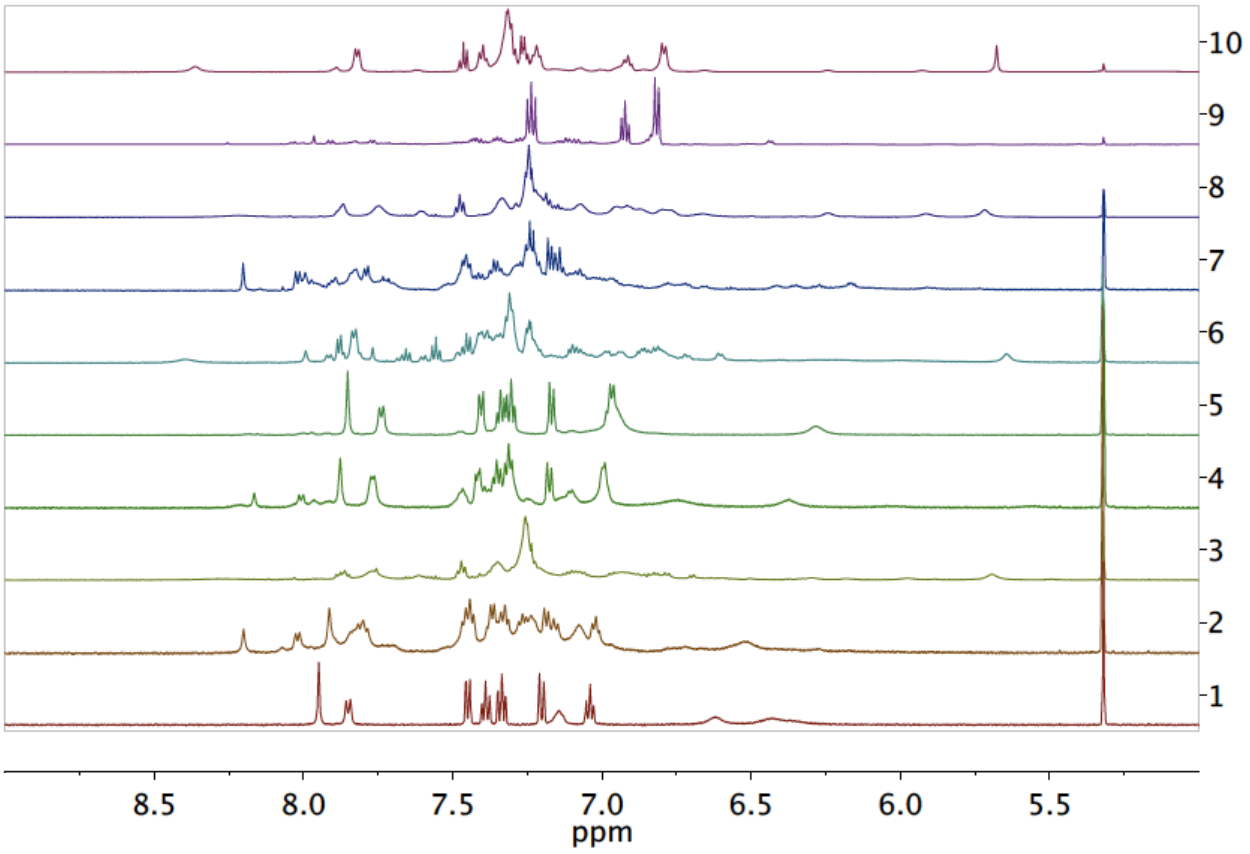

[a] Note for Figure 4.9B: Entry 1: pure BINOL derivative (*R*)-**89**. Entry 2: (*R*)-**89** (0.05 mmol) plus 1 equiv $B(OMe)_3$ were refluxed at 60 °C in CD_2Cl_2 (3 mL) for 2 h. The methanol was removed using 4Å Molecular Sieves (pellets) in a Soxhlet thimble. After cooling to 25 ºC, additional 1.5 mL of CD_2Cl_2 added and then stirred vigorously for 0.5 h and directly subjected to NMR analysis (**Method I**). Entry 3: 1.0 equiv imine **78a** was added to the entry 2 for 10 min at 25 °C. Entry 4: 1.0 equiv MeOH was added to the entry 2 for 10 min at 25 °C. Entry 5: 3.0 equiv MeOH was added to the entry 2 for 10 min at 25 °C. Entry 6: 1.0 equiv imine **78a** was

added to the entry 5 for 10 min at 25 °C. Entry 7: (*R*)-**89** (0.05 mmol) plus 1 equiv BH_3•Me_2S were heated at 80 °C in toluene for 1 h followed by removal of volatiles under vacuum for 0.5 h (**Method II**). Entry 8: 1.0 equiv imine **78a** was added to the entry 7 for 10 min at 25 °C. Entry 9: (*R*)-**89** (0.05 mmol) plus 1 equiv $B(OPh)_3$ and powdered 4Å Molecular Sieves (150 mg) were stirred for 1 h in CD_2Cl_2 (1.5 mL) at 25 °C (**Method III**). Entry 10: 1.0 equiv imine **78a** was added to the entry 9 for 10 min at 25 °C.

These results from the ^{11}B NMR spectrum suggests that a species like **22**-H, if formed at all, are highly unstable and can only be observed by NMR spectroscopy in the presence of a base. Although, the Diels-Alder reaction is performed with enals, which are weak bases, it was decided to use the imine **78a** as the base to generate the fused-spiroborate **92a**. In fact, a peak at $\delta = 5.93$ ppm in the ^{11}B NMR spectrum appeared when one equivalent of imine **78a** was added to the 1:1 mixture of ligand **89** and $B(OMe)_3$ (Figure 4.9B, entry 3). This compound is assigned as the ion-pair **92a** comprised of a fused-spiroborate anion **22** and the protonated form of imine **78a**. These observations further supports the hypothesis that a base is needed to induce the formation of these complexes under non-aqueous conditions. It is worth mentioning that methanol is reported to be involved in adduct formation with trimethylborate.[12] An explanation of the peak observed at $\delta = 10$ ppm in the ^{11}B NMR spectrum of the compound that Yamamoto assigned as **22**-H (Scheme 4.5) is that a residual amount of methanol might be functioning as a coordinating ligand in the original experiment reported by Yamamoto. To test this an additional

equivalent of the methanol was added to the mixture containing ligand **89** and $B(OMe)_3$. The increase in sharpness of the peak in the ^{11}B NMR spectrum revealed that the electrophilic boron centre might be experiencing a tetragonal environment (Figure 4.9B, entry 4). However, there was no change in the chemical shift and hence the possibility of the coordination of methanol was considered unlikely. In fact, when excess methanol (3 equiv) was added, the reaction furnished pure ligand (Figure 4.9B and 4.9C, entry 5). Addition of 1 equiv of imine **78a** to this mixture resulted in the generation of **92a** (Figure 4.9B and 4.9C, entry 6). Yamamoto and co-workers have also employed $B(OPh)_3$ and ligand **89** for catalyst formation in a Diels-Alder reaction. As shown by the ^{11}B NMR spectrum, no formation of a tetra-coordinate boron species occurs until a base (imine in this case) is added irrespective of the boron source being used (Figure 4.9B, entries 7 and 9 *vs*. 8 and 10). It must noted that a large amount of phenol was observed in the case of catalyst formation with $B(OPh)_3$ (Figures 4.9B and 4.9C, entry 9). This is thought to be due to the exchange of phenol in $B(OPh)_3$ by the ligand. The results from the analysis of **20**-H and **22**-H suggests that these species have similar structures. Although, no X-ray structure was obtained for **92a**, its structure was assigned as that shown in Figure 4.10 based on spectral similarities with **74a** and the X-ray structure of **74a** (Figure 4.5). However, a Lewis acid Lewis base complex of the type **90a** cannot be definitively ruled out (Figure 4.9). It must be noted that the original Diels-Alder reaction was performed with enals instead of imines. Hence, since an aldehyde is thought not be basic enough to form an ion-pair of the type **90**, it may very well be likely that a Lewis acid Lewis base complex of type **90** may be involved with reactions with enals.

Figure 4.10 Brønsted acid **92** and Brønsted acid assisted Lewis acid **90**

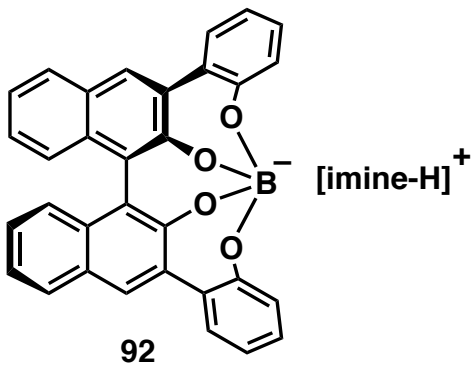

92

92a (imine = **78a**)

Brønsted acid

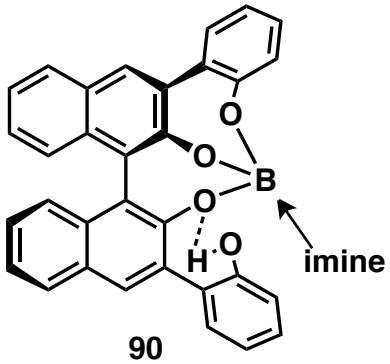

90

90a (imine = **78a**)

Brønsted acid assisted Lewis acid (BLA)

The results to this point indicate that the compounds **20**-H and **22**-H do not exist as protonated neutral species to any great extent. However, it is interesting to observe the common trend that theses complexes can be generated upon the addition of bases. Although this study is focused on chiral systems, it was decided to examine at least one achiral system. The structure of the tetraphenoxyborate **262**-H (Figure 4.11A) was examined and a discussion of the results is given below.

4.4 The case of the achiral tetraphenoxyborate 262-H

Although there is no literature precedent for **262**-H, various salts have been reported which have **262** as their anion (Figure 4.11C).[4b-4e] These salts usually have metal ions like Na^+, K^+, Li^+ and nitrogen bases as the counter cations (Figure 4.11C).

Figure 4.11 (**A**) tetraphenoxyborate anion **262** (**B**) proposed structure for **262**-H (**C**) common tetraphenoxyborates **244** (**D**) piperdine-$B(OPh)_3$ **244d′** (Lewis acid-Lewis base adduct) (**E**) proposed structure for $[imine\text{-}H]^+[B(OPh)_4]^-$ complex **263**/**264**

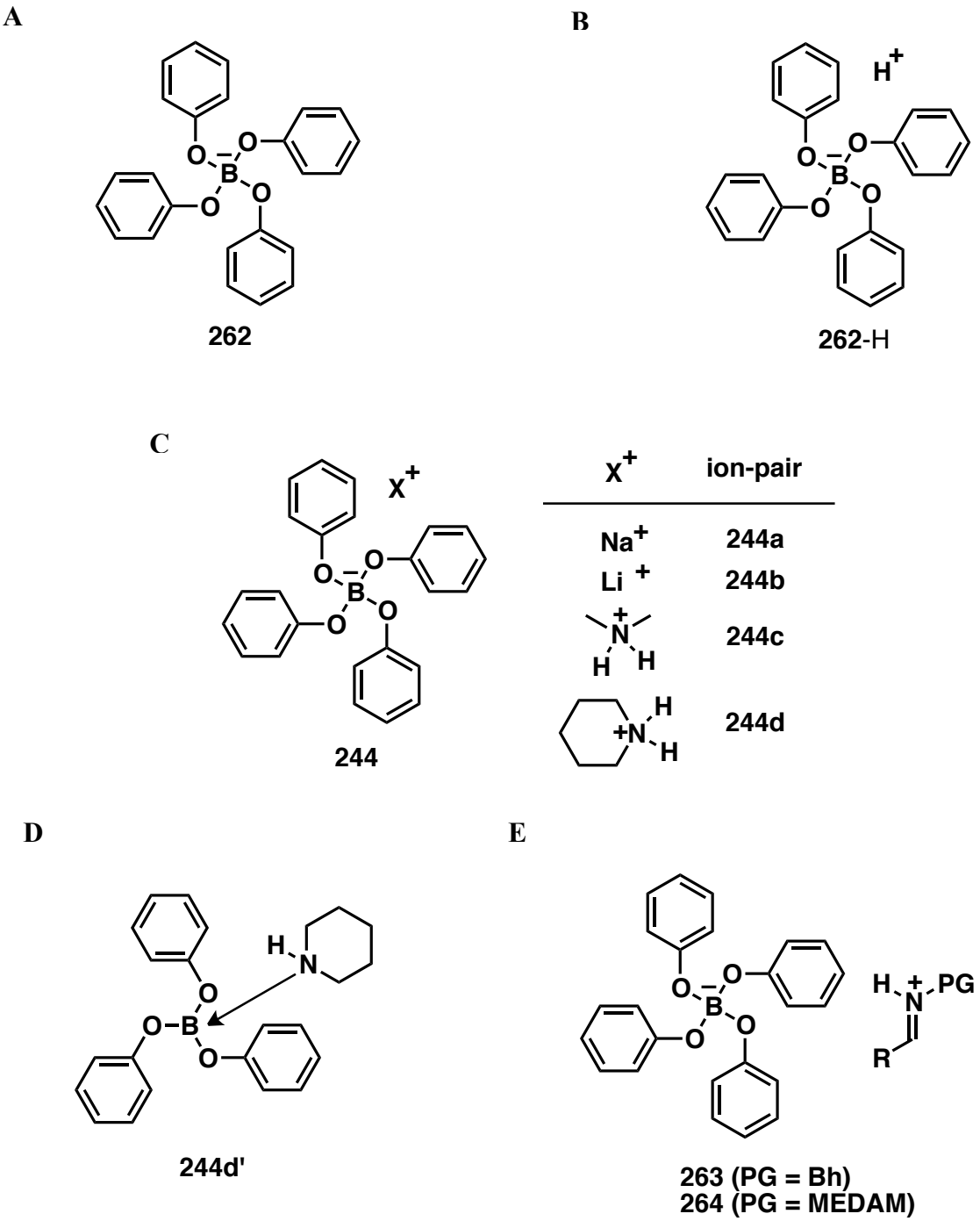

The proposed structure **262**-H was examined theoretically by computing the energy minimum for the anion **262** followed by a similar analysis of the protonated form **262**-H. Based on similar results with **20**-H and **22**-H it was not a surprise that **262**-H was found to be highly unstable and dissociated into $B(OPh)_3$ and phenol **182a** where phenol is held by hydrogen bonding to $B(OPh)_3$ (Figure 4.12B).

Figure 4.12 Calculated structures of **262** and **262**-H obtained using Gaussian ′03 at B3LYP/6-31g* level of theory. All structures are visualized by the Mercury program (C, gray; O, red; B, yellow; H, light blue). Hydrogens are omitted for clarity (except O-H). ∠oop = angle out of plane for the current/former tetra-coordinate boron, B-On = the distance between O-n and the current/former tetra-coordinate boron where n = 1-4. (**A**) Calculated structure of tetraphenoxyborate anion **262** (**B**) Calculated structure of **262**-H, the protonated tetraphenoxyborate anion **262**.

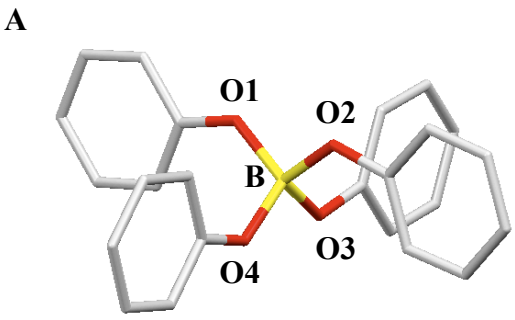

262
(∠oop = 19.4º, B-O1 = B-O2 = B-O3 = B-O4 = 1.47 Å)

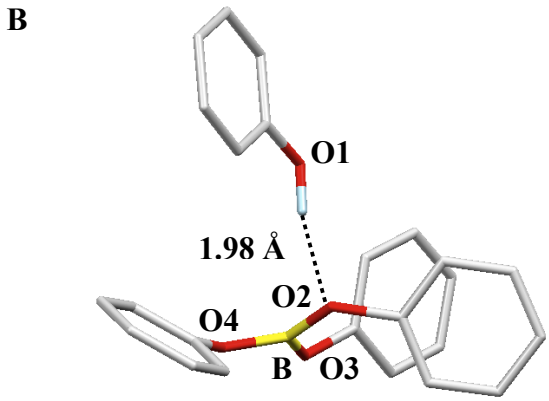

262-H
(∠oop <1º, B-O1 = 3.51 Å, B-O2 = 1.39 Å, B-O3 = 1.36 Å, B-O4 = 1.37 Å)

In order to further confirm that the presence of base is needed for the generation of tetraphenoxyborate anion **262**, a detailed study based on NMR experiments was performed. A fresh sample of $B(OPh)_3$ was prepared from BH_3•Me_2S and PhOH (see experimental). When one equiv of PhOH **194a** was added to freshly prepared $B(OPh)_3$, there is no significant change in the ^1H or the ^{11}B NMR spectra (Figure 4.13, entry 3). However, when one equivalent of DMAP was added to this mixture, ^1H NMR spectrum revealed the upfield shift in the doublet for the ortho hydrogens of the phenol component from 7.15 ppm to 7.03 ppm (Figure 4.13, entry 4). Additionally, appearance of a peak at δ = 2.24 ppm in the ^{11}B NMR spectrum is suggestive of the formation of **244e**. Similar observations were reported when piperidine was used as the base to form **244d** (δ = 2.6 ppm (THF-d_8), ^{11}B NMR) (Figure 4.11C).[4e] However, in the same work, it had been reported that a Lewis acid-base adduct (piperidine->$B(OPh)_3$) **241d′** (δ = 2.3 ppm (nitrobenzene), ^{11}B NMR) is generated from the reaction between piperidine and $B(OPh)_3$ in absence of phenol (Figure 4.11D).[4e] Hence, the ^{11}B NMR data is similar for the ion-pair **244d** and adduct **244d′**. Similar can be assumed for the complexes generated for the reaction between DMAP and freshly prepared $B(OPh)_3$. However, the presence of the ion-pair **244e** was supported by X-ray analysis described later. In the past, we have observed that commercial $B(OPh)_3$ always has some percentage of phenol in its composition (Figure 4.11, entry 2 *vs*. 3 and 5). An observation similar to entry 4 of Figure 4.13B and 4.13C was made when one equivalent of DMAP was added to commercial $B(OPh)_3$ (entry 6). In fact, a peak at δ ~ 2-3 ppm in the ^{11}B

NMR spectrum has been occasionally observed during the formation of an IMINO-BOROX catalyst from a mixture of a vaulted ligand, $B(OPh)_3$ and an imine. Hence, a similar ion-pair **263**/**264** can be assumed to be generated when commercial $B(OPh)_3$ and imines **78**/**111** interact with each other (Figure 4.11E). A racemic reaction between imine **78a** and EDA **85** mediated by commercial $B(OPh)_3$ results in 78% yield of aziridine **86a**. This is probably a racemic reaction catalyzed by the racemic Brønsted acid **264**.

Figure 4.13 (**A**) NMR Analysis of a mixture of PhOH **194a** with $B(OPh)_3$ **187a** and DMAP **216c**. (**B**)[a] ^{1}H NMR spectra of the reaction mixture in $CDCl_3$ (aromatic region). (**C**) ^{11}B NMR spectra corresponding to the ^{1}H NMR spectra in Figure 4.13B

A

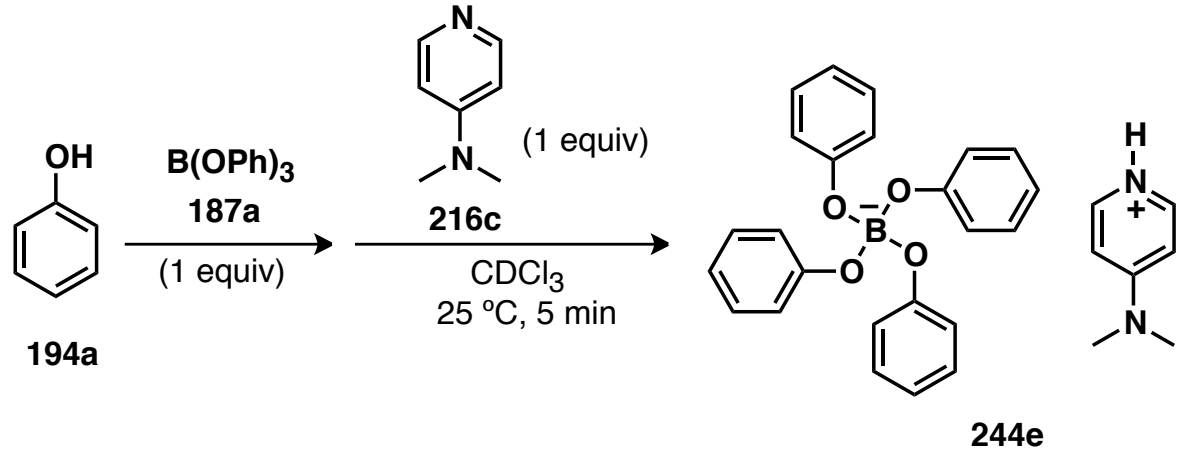

Figure 4.13 cont'd

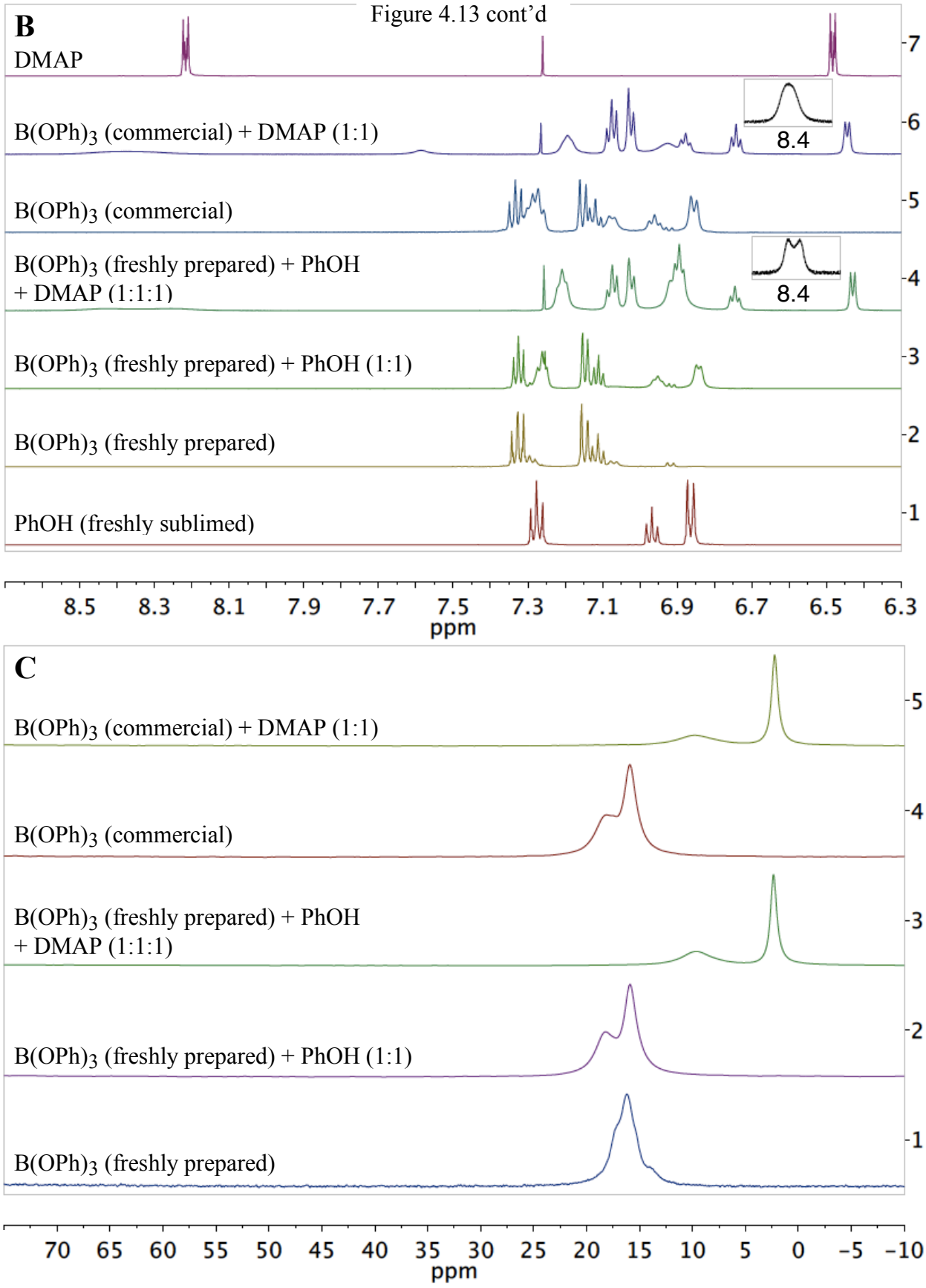

[a] Note for Figure 4.13B: Entry 1: freshly sublimed PhOH **194a**. Entry 2: freshly prepared $B(OPh)_3$; $BH_3 \bullet Me_2S$ (0.1 mmol) plus 3 equiv PhOH were heated at 80 °C in toluene for 1 h followed by removal of volatiles under vacuum for 0.5 h. Entry 3: 1.0 equiv PhOH **194a** was added to the entry 2 for 10 min at 25 °C. Entry 4: 1.0 equiv DMAP **216c** was added to the entry 3 for 10 min at 25 °C. Entry 5: commercial $B(OPh)_3$. Entry 6: 1.0 equiv DMAP **216c** was added to the entry 5 for 10 min at 25 °C. Entry 7: pure DMAP **216c**

A literature search revealed that there are several ion pairs comprised of the tetraphenoxyborate anion **262** and a protonated nitrogen base with ^{11}B NMR spectroscopic data given in some cases (Figure 4.2).[4e] Although, salts derived from **262** and metal ions have been characterized by X-ray crystallography, no X-ray analysis has been reported for ion-pairs generated from nitrogen bases. To our delight, a few colorless crystals of **244e** serendipitously formed in the NMR tube during the analysis of boroxinate complex **217c** (Chapter 2, Table 2.9) generated from a mixture of (*S*)-VAPOL **58**, $B(OPh)_3$ and DMAP (this work).[13] This provided an opportunity to confirm our proposed structure for the ion-pair **244e**. The X-ray structure of **244e** revealed the presence of protonated DMAP in two positions in 75% and 25% probabilities (Figure 4.14A). The key interaction is the hydrogen bond between the protonated nitrogen and one of the oxygens of the tetraphenoxyborate anion (d_1 = 1.99 Å, d_2 = 2.18 Å, Figure 4.14A). The complete proton transfer to nitrogen was further confirmed by the N-H bond of 0.81 Å. There also appears to be a π–π stacking interaction (d_5 = 3.23 Å) between one of the phenoxy

rings of the tetraphenoxyborate anion and the pyridinium ion of the protonated DMAP. In addition, there appears to be a CH–π interaction (d_3 = 3.64 Å) between an ortho hydrogen on the DMAP ring and a different phenoxy ring (Figure 4.14B). Another CH–π interaction (d_4 = 3.71 Å) is between one of the methyl groups on the protonated DMAP and a phenoxy ring.

Figure 4.14 (**A**) Solid state structure of the tetraphenoxyborate **244e** visualized by the Mercury program (C, gray; O, red; B, yellow; H, light blue). Calculated hydrogen atoms and solvent molecules were omitted for clarity. Hydrogen attached to nitrogen is shown to highlight the hydrogen bonding (d_1 = 1.99 Å and d_2 = 2.18 Å). ∠oop = angle out of plane for the current/former tetra-coordinate boron, B-On = the distance between O-n and the current/former tetra-coordinate boron where n = 1-4. (**B**) Some secondary interactions were proposed and highlighted: d_3 = 3.64 Å (CH–π); d_4 = 3.71 Å (CH–π) and d_5 = 3.23 Å (π–π stack). (**C**) Space-filling model of the complex **244e**. The color scheme is given in Figure 4.14A. (**D**) Drawing of the packing along the axis where the dotted lines represent potential hydrogen bonding.

A

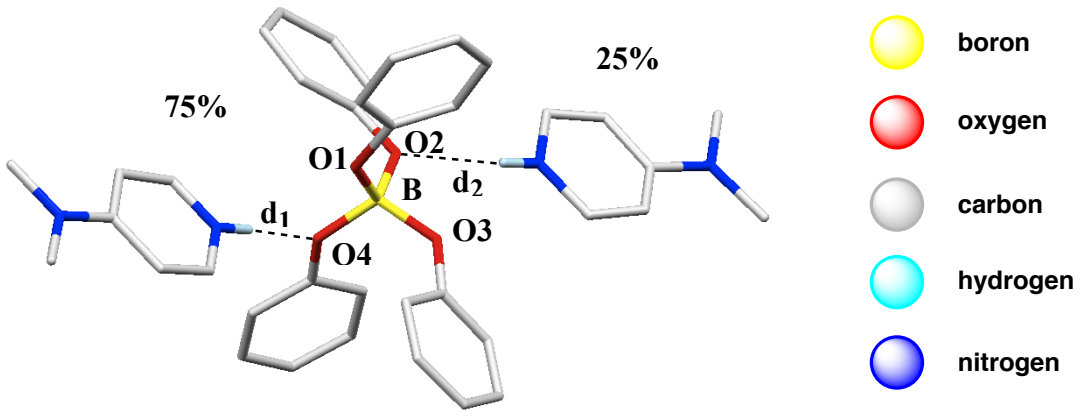

244e

(∠oop = 18.2º-19.7º, B-O1 = B-O3 = 1.46 Å, B-O2 = 1.48 Å, B-O4 = 1.47 Å)

B

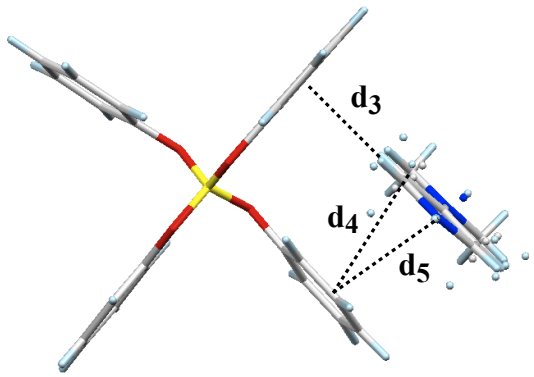

C

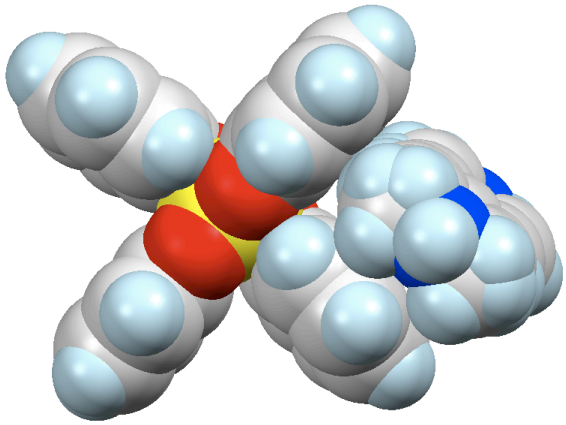

D

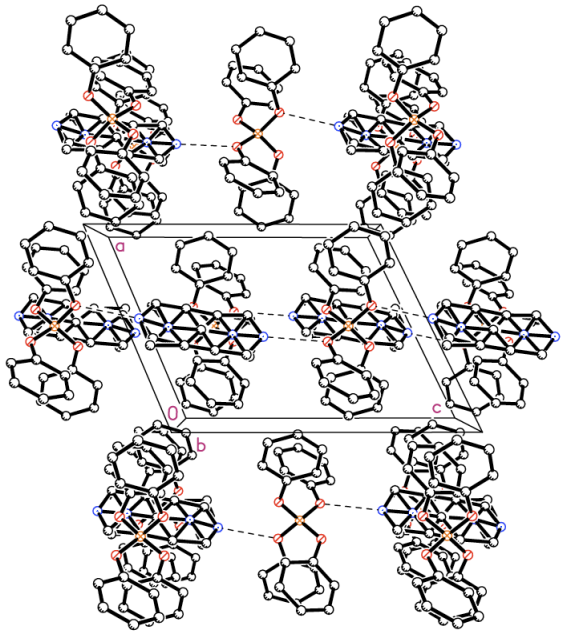

4.5 Mode of Catalysis: Lewis Acid Catalysis verses Brønsted Acid Catalysis

Based on the above ^{1}H NMR and computational analysis, it is quite clear that the protonated neutral spiroborates **20**-H, **21**-H and **22**-H are not favorable species. The data suggests that there is no tetra-coordinate boron species unless an imine is added to deprotonate the hydroxyl group in the BINOL **55** or BINOL derivative **89**. At this point, it became

interesting to explore the mode of catalysis for reactions that have been reported for these chiral catalysts.

4.5.1 Asymmetric Imino-aldol reaction and heteroatom Diels-Alder reactions catalyzed by **20**-H

As shown in Scheme 4.1, the catalyst **20**-H has been proposed to be the active catalyst in asymmetric imino-aldol reactions and in heteroatom Diels Alder reactions. In both cases, the mode of catalysis has been assumed to be as a Brønsted acid assisted Lewis acid (BLA) catalysis (Scheme 4.2). After we collected evidence that suggests that the catalyst is an ion-pair **74** consisting of a chiral borate anion and a protonated iminium ion (Figure 4.5), we became interested as to whether the mode of catalysis for these reactions involves a Brønsted acid (BA) or a Brønsted acid assisted Lewis acid (BLA) catalysis. Another current group member, namely Dr. Mathew Vetticat, initiated theoretical calculations to investigate the transition states for the asymmetric imino-aldol reaction. He found out that it indeed occurs *via* a Brønsted acid (BA) catalyzed reaction contrary to the proposed Brønsted acid assisted Lewis acid (BLA) mechanism.[14] The energy difference between the BA (TS-**263**) and BLA (TS-**264**) type transition states leading to the favored enantiomer was found to be +12 kcal/mol. Furthermore, it must be noted that a similar behavior has been assumed in case of heteroatom Diels-Alder reaction.

Figure 4.15 (**A**) Asymmetric imino-aldol reaction of imine **78a** catalyzed by **20**-H (**B**) Diagrammatic representation of TS-**263** and TS-**264** for BA and BLA type mechanism respectively.

A

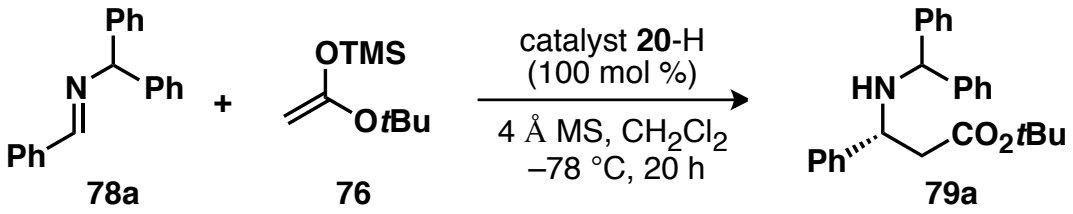

B

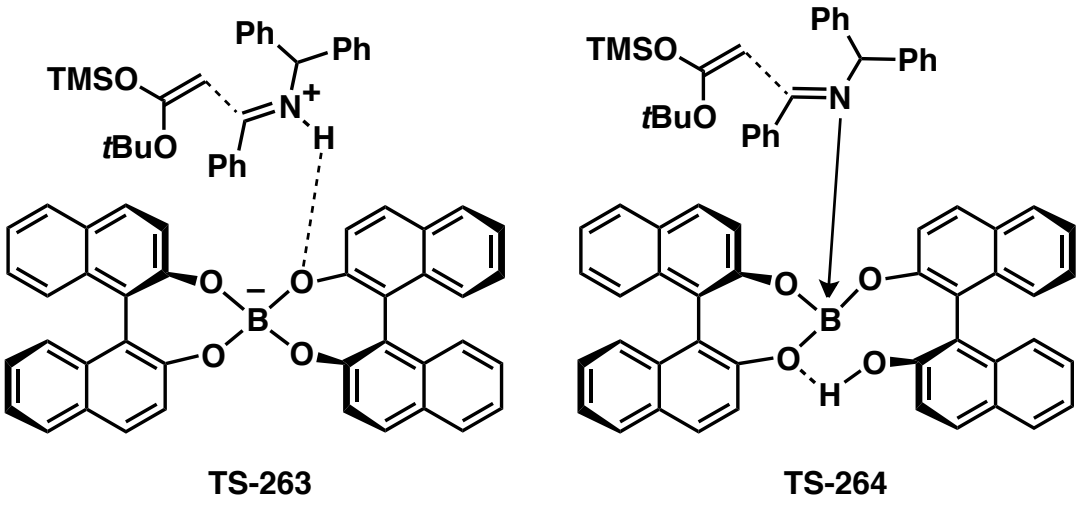

4.5.2 Asymmetric Pictet-Spengler reaction catalyzed by 20-H and 21-H.

The asymmetric Pictet-Spengler reaction is another reaction that has been reported with the catalyst **20**-H but requires the use of two equivalents of **20**-H.[2e,2f] This reaction was performed using nitrones instead of imines. Hence, the question arises of whether this reaction occurs *via* BA or BLA type catalysis. As a part of this doctoral research, the transition states for each mode of catalysis were located using Gaussian ′03 and are presented in Figure 4.16. In

order to reduce the computational cost, the hydrid DFT:Semi-emperical ONIOM method was implemented. The division of layers for the ONIOM calculations is illustrated by the given color scheme in Figure 4.7A. All the calculated distances are reported in angstroms and the reported energies are $\Delta\Delta G^{\ddagger}$ for fully optimized geometries from the ONIOM calculations.

Figure 4.16 (**A**) Asymmetric Pictet-Spengler reaction of nitrone **83a** catalyzed by **20**-H. (**B**) Division of layers for the ONIOM(B3LYP/6-31g**:AM1) level of calculations. (**C**) 3D structures and relative energies of TS-*S*-**265** and TS-*R*-**265** for BA type mechanism. The relative energies given in italics are the energies computed from the full DFT B3LYP/6-31g*. (**D**) 3D structures and relative energies of TS-*S*-**266** and TS-*R*-**266** for BLA type mechanism.

A

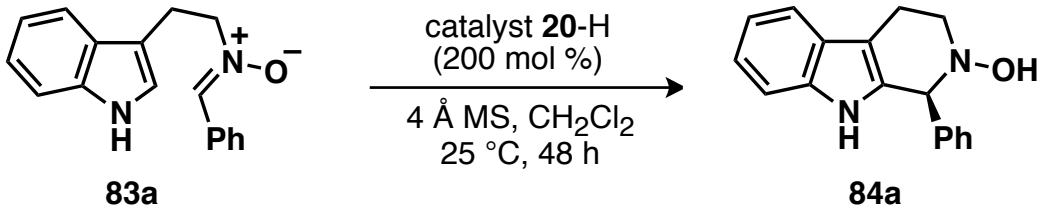

B

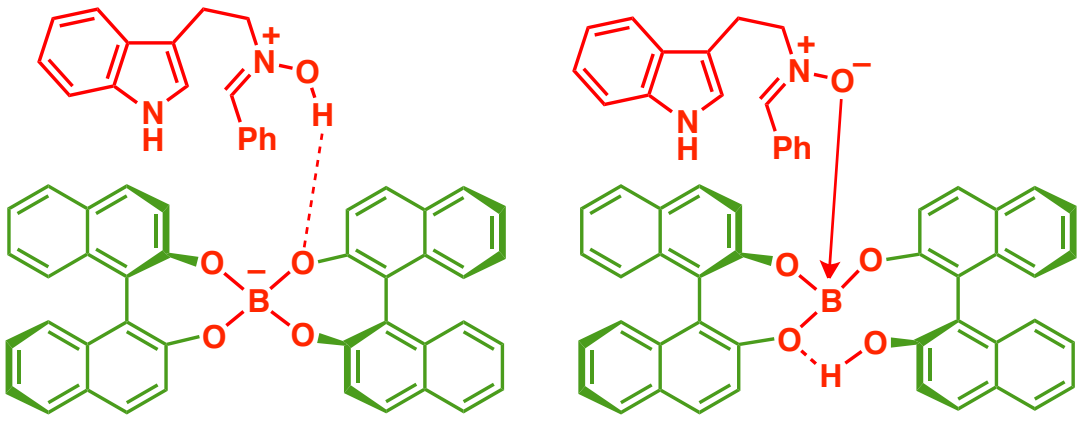

Red = B3LYP/6-31g**

Green = AM1

Figure 4.16 cont'd

C

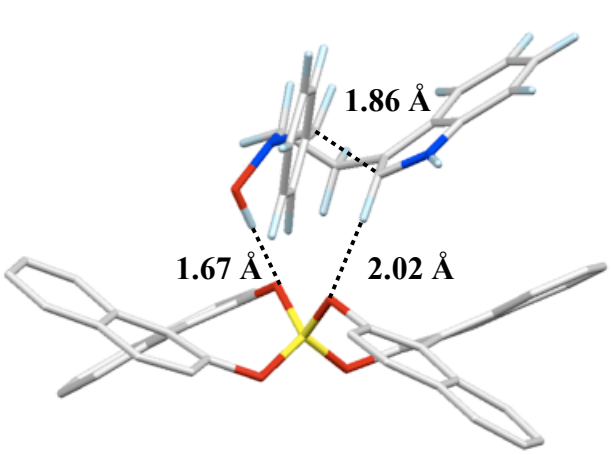

TS-*S*-265

($\Delta\Delta G^{\ddagger}$ = +1.0 kcal/mol)

($\Delta\Delta G^{\ddagger}$ = +1.4 kcal/mol)

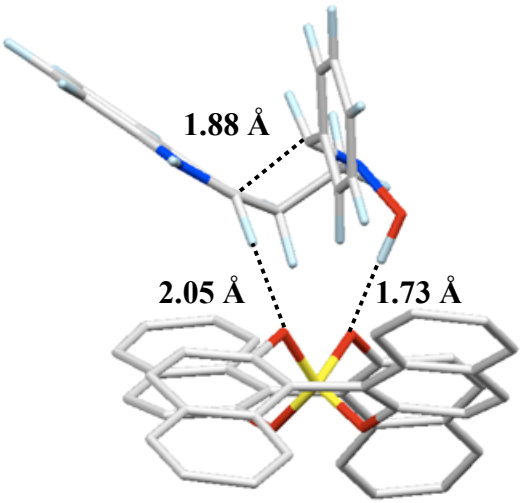

TS-*R*-265

($\Delta\Delta G^{\ddagger}$ = 0 kcal/mol)

($\Delta\Delta G^{\ddagger}$ = 0 kcal/mol)

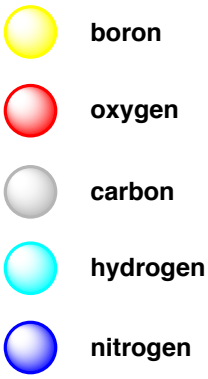

D

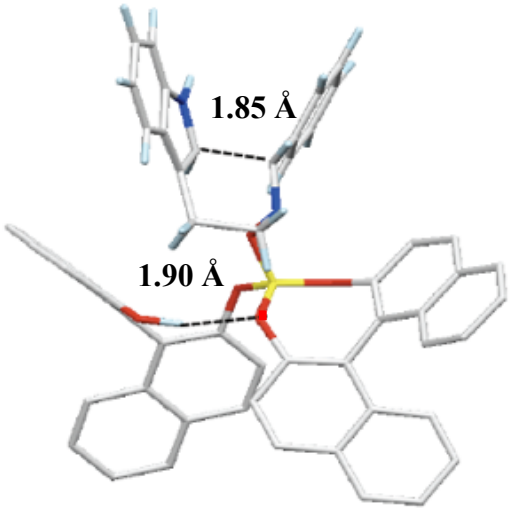

TS-*S*-266

($\Delta\Delta G^{\ddagger}$ = 0 kcal/mol)

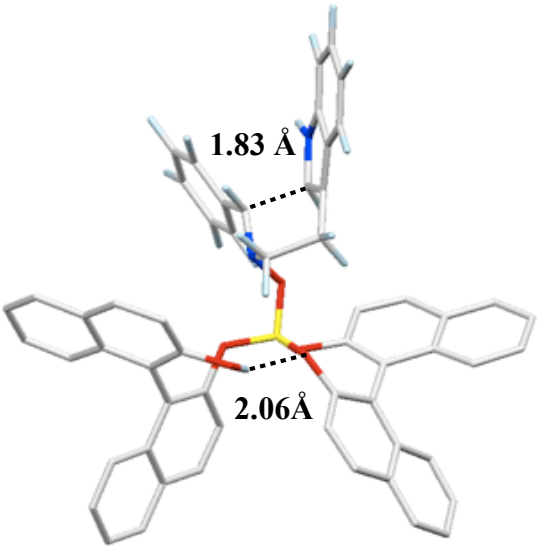

TS-*R*-266

($\Delta\Delta G^{\ddagger}$ = +0.6 kcal/mol)

In case of the BA type mechanism, the most stable transition state for the formation of both the *R* and *S* products from the (*S*, *S)*-catalyst were located and are given in Figure 4.16B. Other than the hydrogen bonding (1.67 Å, Figure 4.16B), there was one additional important interaction, a CH-O interaction between the hydrogen in the 2-position of the indole and oxygen of the spiroborate (2.02 Å, Figure 4.16B) in case of *S*-enantiomer formation. Unfortunately, these calculations do not match the experimental findings as the minor enantiomer (*R*) is found to be the one with lowest energy. Based of the ONIOM calculations, the major enantiomer (*S*) is found to be +1.0 kcal/mol higher in energy. In fact, calculations using full DFT (B3LYP/6-31g*) also predict a similar outcome with *S*-product formation favored by +1.4 kcal/mol. (Figure 4.16B).

It was found that transition state TS-*S*-**265** (*BA type mechanism*) leading to the favored enantiomer (*S*) was found to be +5.4 kcal/mol higher in energy than TS-*S*-**266** (*BLA type mechanism*) also leading to the *S*-enantiomer of the product (Figure 4.16B and 4.16C). Upon location of the two transition states **266** for the formation of both the *R* and *S* products *via* the BLA mechanism, it was found that the TS leading to the minor enantiomer (*R*) is 0.6 kcal/mol higher in energy than that for the major enantiomer (*S*). Single-point energies were then calculated and it was found that the disfavored enantiomer is +2 kcal/mol higher in energy. Hence, these computational studies suggest that a BLA mechanism is operational in case of nitrones for an asymmetric Pictet-Spengler reaction. Thus, a summary of the mode of catalysis for the reactions with **20**-H is presented in Scheme 4.7.

Scheme 4.7 Current understanding of the catalytic activity of **20**-H

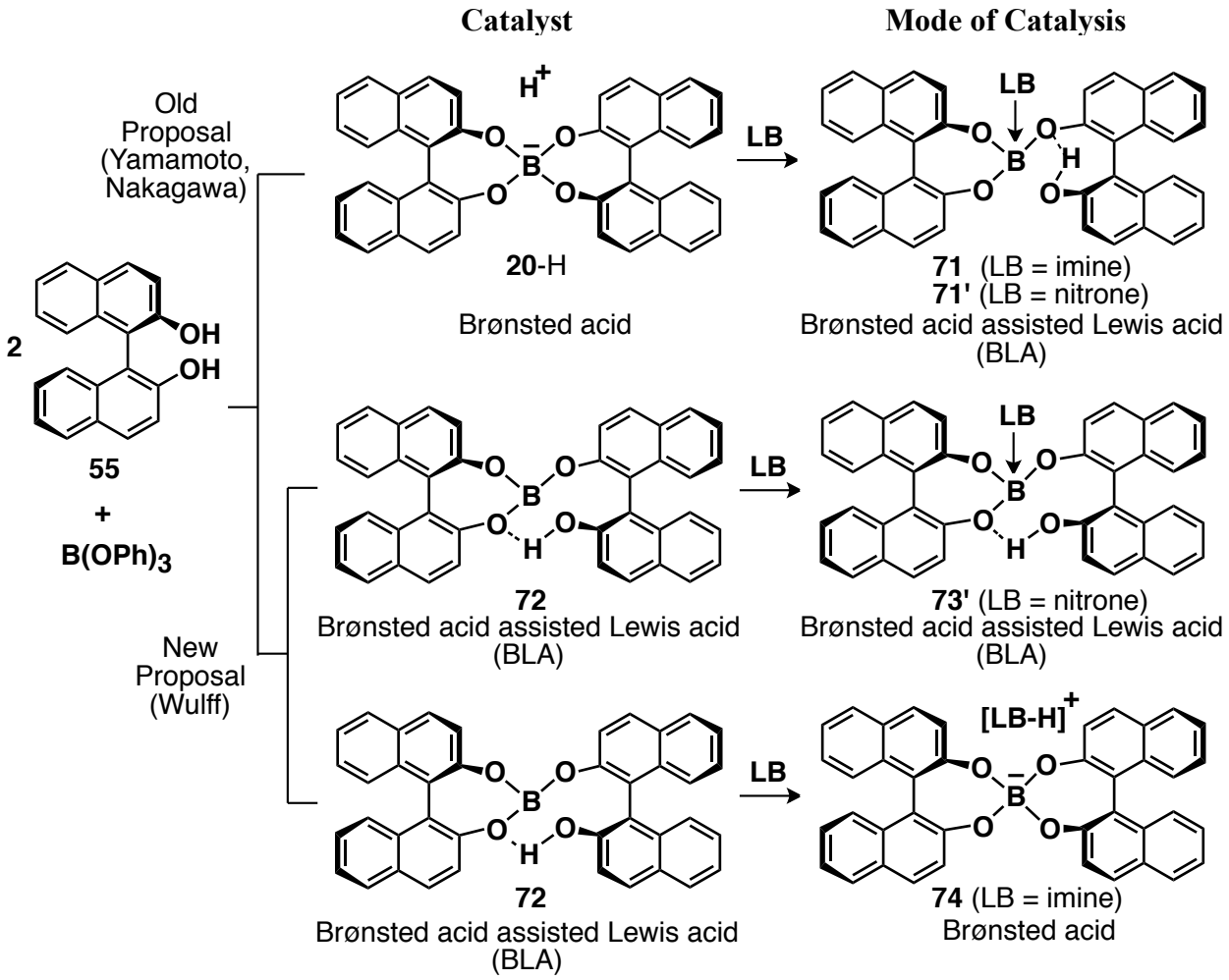

4.5.3 Asymmetric Diels-Alder reaction catalyzed by **22**-H.

Although no evidence could be gained for the existence of **22**-H by NMR spectroscopy, the mode of catalysis is thought to be more likely to be as a Brønsted acid assisted Lewis acid catalyst in the case of the Diels-Alder reaction between α-methylacrolein **94a** and cyclopentadiene **93a** (Figure 4.17A).[3a-3c] This is possibly due to high acidity of protonated aldehydes.

Figure 4.17 (**A**) Asymmetric Diels-alder reaction of **94a** catalyzed by **22**-H. (**B**) Diagrammatic representation of TS-**267** and TS-**268** for BA and BLA type mechanism respectively.

A

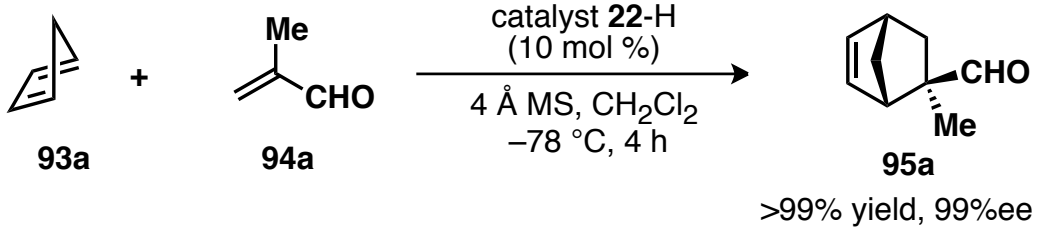

93a **94a** **95a**

>99% yield, 99%ee

B

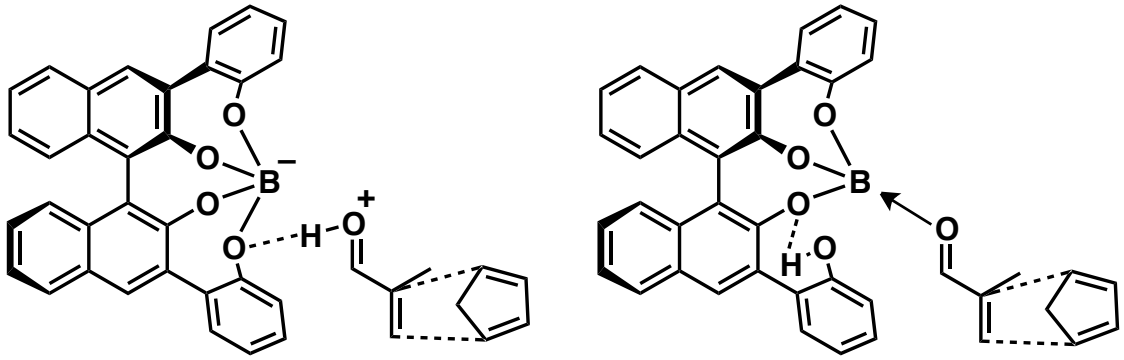

TS-267 **TS-268**

Dr. Mathew Vetticatt, a current group member, found from computational studies that indeed in this reaction between enals and dienes the catalyst appears to be operating as a Brønsted acid assisted Lewis acid (Figure 4.17B).[14] Hence, the current understanding of this reaction is presented in Scheme 4.8.

Scheme 4.8 Current understanding of the catalytic activity of **22**-H

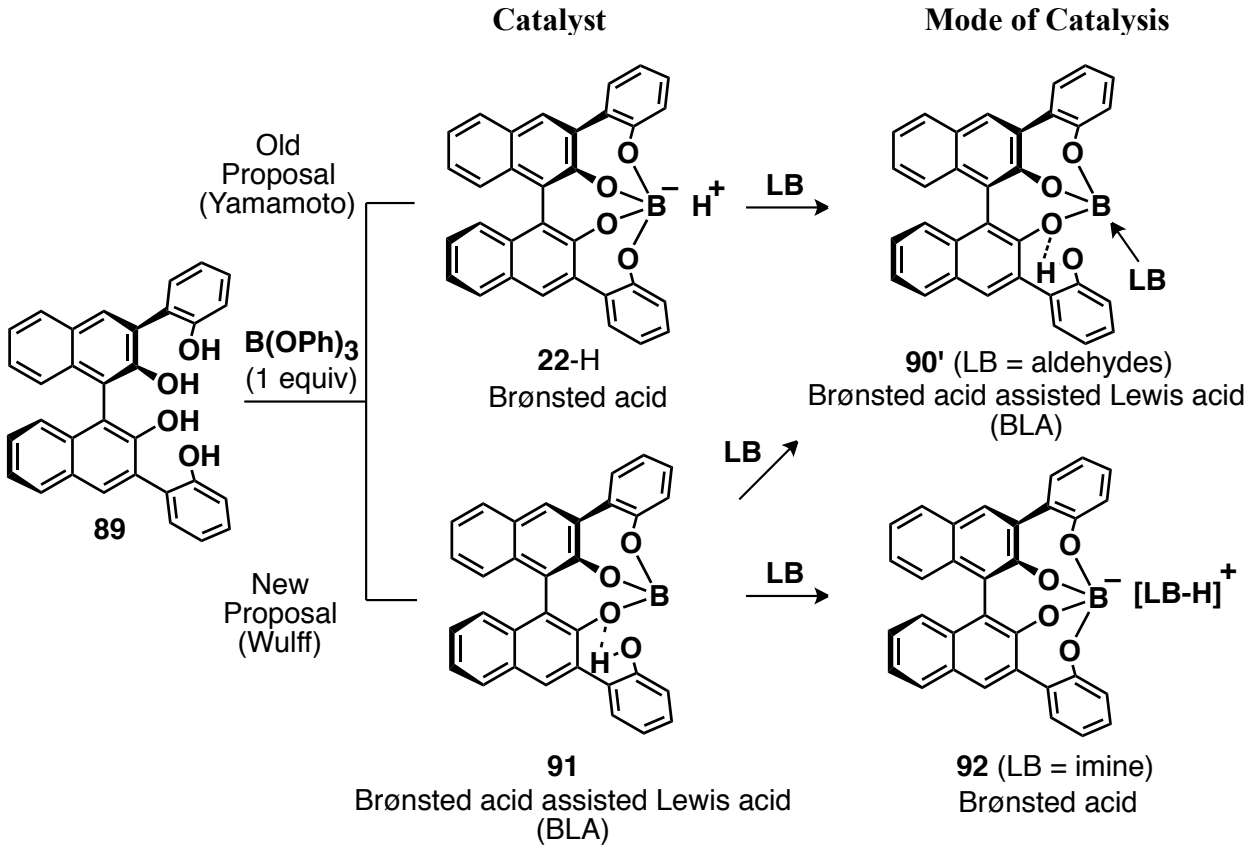

4.6 Conclusions

In the end, it is quite evident that ion-pairs **20**-H, **21**-H, **22**-H, and **262**-H, if they exist at all, are unfavorable with regard to alternative structures not containing a tetra-coordinate boron. In contrast, the ion-pairs **102a**, **74a**, **90a** and **244e** have been characterized by NMR spectroscopy and X-ray crystallography. As of now, there is no evidence for the protonated form of the VAPOL boroxinate **23**-H, but rather that like the case of **20**-H–**22**-H it appears to be unstable with respect to other structures. One of the biggest advantages of the above-discussed case studies is that it has provided a better understanding of the structure and function of variety of chiral Brønsted acids derived from chiral borate anions from both vaulted and linear biaryl ligands.

APPENDIX

4.7 Experimental

4.6.1 General information

The general information of this chapter is similar to that of Section 2.6.1 of Chapter 2. All reagents were purified by simple distillation or crystallization with simple solvents unless otherwise indicated. BINOL **55**, commercial $B(OPh)_3$ (stored in dessicators), and benzhydrylamine **126a** (distilled prior to use) obtained from Aldrich Chemical Co., Inc. and used as received.

4.6.2 Synthesis of Imine 78a, $B(OPh)_3$ 187a and (*R*)-3,3′-(2-OH-$C_6H_4)_2$-BINOL 89

a) Imine 78a: The synthesis of imine **78a** is given in section 2.6.2 of Chapter 2

b) $B(OPh)_3$ 187a:

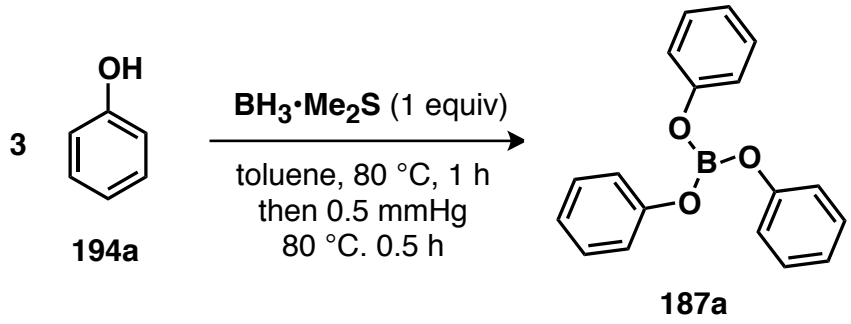

Triphenylborate 187a: To a flame dried home-made Schlenk flask equipped with a stir bar and flushed with argon was added PhOH **194a** (28.2 mg, 0.300 mmol) and BH_3•Me_2S (50 μL, 0.10 mmol, 2.0 M in toluene,). Under an argon flow through the side-arm of the Schlenk flask, dry toluene (2 mL) was added. The flask was sealed by closing the Teflon valve, and then placed in an oil bath (80 ºC) for 1 h. After 1 h, a vacuum (0.5 mm Hg) was carefully applied by slightly opening the Teflon valve to remove the volatiles. After the volatiles are removed completely, a

full vacuum is applied and is maintained for a period of 30 min at a temperature of 80 ºC (oil bath). The flask was then allowed to cool to room temperature yielding the $B(OPh)_3$ **187a** as white solid. The resulting freshly prepared $B(OPh)_3$ was directly used for NMR analysis.

Spectral data for $B(OPh)_3$ **187a**: ^{1}H NMR ($CDCl_3$, 500 MHz) δ 7.13 (t, 3H, *J* = 7.5 Hz), 7.16 (d, 6H, *J* = 9.0 Hz), 7.34 (t, 6H, *J* = 7.5 Hz). ^{13}C NMR ($CDCl_3$, 125 MHz) δ 120.21, 123.52, 129.26, 152.86. These spectral data match those previously reported for this compound.[4a]

c) (*R*)-3,3′-(2-OH-C_6H_4)$_2$-BINOL 89:

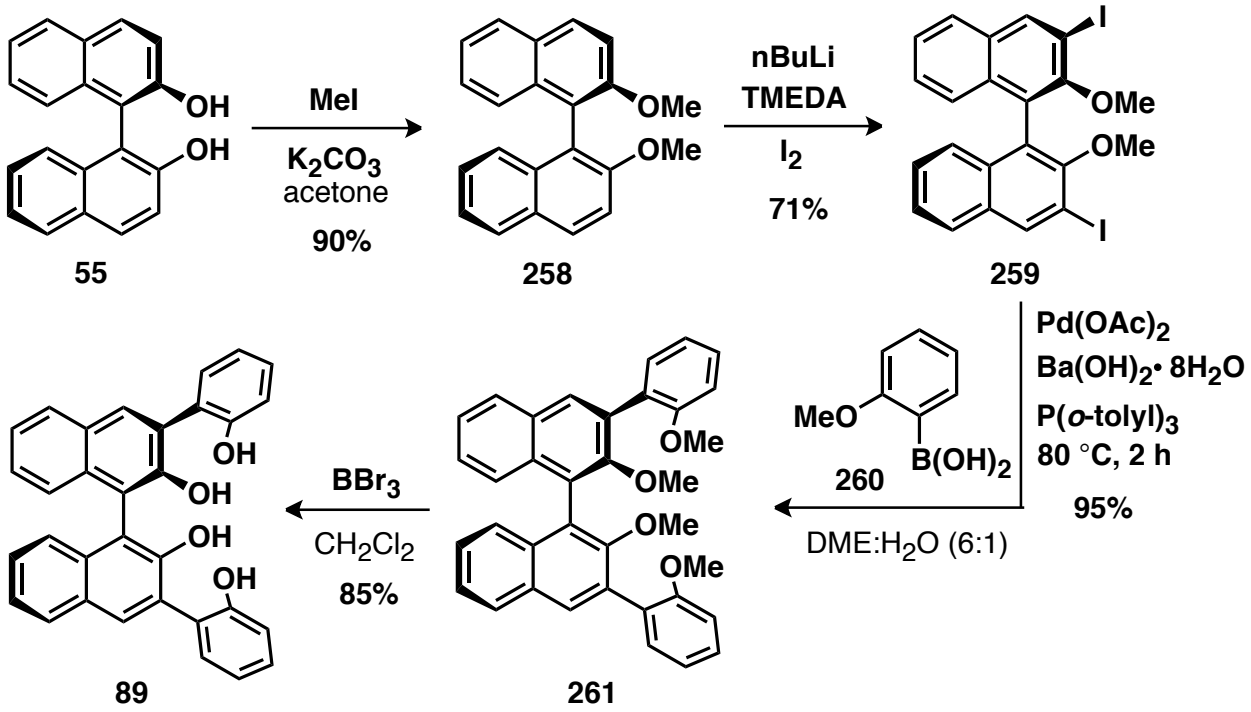

***(R)*-2,2'-Dimethoxy-1,1'-binaphthalene 258:** To 250 mL flame-dried round bottom flask was added (*R*)-**55** (2.5 g, 8.7 mmol) and acetone (80 mL). To this solution were added potassium

carbonate (4.0 g, 29 mmol) and methyl iodide (4.94 g, 2.17 mL, 35 mmol), and the mixture was set to reflux for 24 h. Additional methyl iodide (2.07 g, 0.910 mL, 14.6 mmol) was then added and reflux was continued for next 12 h. The solvent was then evaporated to leave a volume of 15 mL and treated with water (80 mL). The mixture was then stirred for 8 h, and the resulting solid was washed with water and dried under vacuum first at 25 °C and then at 95 °C (0.1 mm Hg, for 12 h) to afford (*R*)-**258** as white powder (mp. 225-226 °C) in 90% yield (2.25 g, 7.83 mmol).

Spectral data for (*R*)-**258:** ^{1}H NMR ($CDCl_3$, 300 MHz) δ 3.75 (s, 6H), 7.10 (d, *J* = 8.4 Hz, 2H), 7.17-7.24 (m, 2H), 7.28-7.33 (m, 2H), 7.45 (d, *J* = 9.0 Hz, 2H), 7.86 (d, *J* = 8.1 Hz, 2H), 7.97 (d, *J* = 9.0 Hz, 2H); ^{13}C NMR ($CDCl_3$, 75 MHz) δ 154.97, 134.00, 129.37, 129.21, 129.90, 126.28, 125.25, 123.48, 119.61, 114.25, 56.89; $[\alpha]_D^{25}$ +54.5 (*c* 1.0, $CHCl_3$). These spectral data match those previously reported for this compound.[15]

(*R*)-3,3'-diiodo-2,2'-dimethoxy-1,1'-binaphthalene (*R*)-**259:** In a 50 mL flame-dried three-necked round bottomed flask equipped with a N_2-inlet were placed dry Et_2O (15 mL) and TMEDA (349 mg, 0.450 mL, 3.00 mmol). To this solution was added ^{n}BuLi (1.2 mL, 3.0 mmol, 2.5 M in hexanes). The solution was stirred for 30 min at room temperature. To this solution was added solid (*R*)-**258** (314 mg, 1.00 mmol) in one portion and the reaction mixture was stirred for 12 h. The resulting suspension was cooled to –78 °C, and a solution of I_2 (1.7 g, 6.5 mmol) in THF (4 mL) was added *via* syringe over a period of 10 min. The solution was stirred for 1 h at

–78 °C and then allowed to warm to room temperature and was left stirring for 18 h. The reaction was quenched with saturated $Na_2S_2O_3$ solution (10 mL) and stirred for 30 min. The organic layer was separated, and the aqueous layer was extracted by CH_2Cl_2 (10 mL × 3). The combined organic solution was dried over anhydrous $MgSO_4$, filtered and concentrated *in vacuo* to afford crude product. Purification by silica gel column chromatography (35 mm × 350 mm column, 4:1 hexanes/CH_2Cl_2 as eluent, after elution of the first fraction, the eluent was changed to 1:1 hexanes/CH_2Cl_2) afforded (*R*)-**259** as yellow solid crystals (mp. 191-192 °C) in 71% yield (402 mg, 0.710 mmol).

Spectral data for (*R*)-**259**: R_f = 0.5 (4:1 hexanes/CH_2Cl_2); ^{1}H NMR ($CDCl_3$, 300 MHz) δ 3.39 (s, 6H), 7.05 (d, *J* = 8.5 Hz, 2H), 7.25 (dt, *J* = 1.2 Hz, 8.3 Hz, 2H), 7.39 (dt, *J* = 1.2 Hz, 8.3 Hz, 2H), 7.77 (d, *J* = 8.3 Hz, 2H), 8.51 (s, 2H); ^{13}C NMR ($CDCl_3$, 75 MHz) δ 61.10, 92.31, 125.39, 125.64, 125.79, 126.97, 127.07, 132.20, 133.89, 139.92, 154.54; $[\alpha]_D^{25}$ –30.0 (*c* 1.0, $CHCl_3$). These spectral data match those previously reported for this compound.[15c]

(*R*)-2,2'-dimethoxy-3,3'-bis(2-methoxyphenyl)-1,1'-binaphthalene (*R*)-**261:** To a 25 mL flame-dried home-made Schlenk flask (see Figure 2.26) equipped with a stir bar and flushed with argon was added (*R*)-3,3'-diiodo-2,2'-dimethoxy-1,1'-binaphthalene (*R*)-**259** (1.1 g, 2.0 mmol), 2-methoxyphenylboronic acid **260** (760 mg, 5 mmol), and barium hydroxide octahydrate (1.58 g, 5 mmol). Under an argon flow through the side-arm of the Schlenk flask, DME-H_2O (6:1, 21 mL) was added through the top of the Teflon valve to dissolve the two reagents. To this mixture was

added palladium(II) acetate (22.4 mg, 0.100 mmol) and tris-*o*-tolylphosphine (60.9 mg, 0.2 mmol). The resulting reaction mixture was degassed three times and charged with argon. The flask was sealed by closing the Teflon valve, and then placed in an 80 ºC oil bath for 2 h. The flask was then allowed to cool to room temperature and opened to argon through the side-arm of the Schlenk flask. Thereafter, the reaction mixture was filtered through a Celite pad and the filtrate was diluted with saturated NH4Cl (aq) and extracted twice with ether. The combined extracts were dried over $MgSO_4$, filtered, and concentrated *in vacuo*. Purification of the crude product by silica gel chromatography (35 mm × 400 mm column, 9:1 hexanes/EtOAc as eluent, under gravity) afforded pure (*R*)-**261** as a white solid (mp. 97-100 °C) in 95% isolated yield (1.0 g, 1.9 mmol).

Spectral data for (*R*)-**261**: R_f = 0.39 (9:1 hexanes/EtOAc); ^{1}H NMR ($CDCl_3$, 600 MHz) δ 3.19 (s, 6H), 3.76 (s, 6H), 6.99 (dd, *J* = 8.3, 1.0 Hz, 2H), 7.05 (td, *J* = 7.4, 1.0 Hz, 2H), 7.24-7.28 (m, 2H), 7.33 (d, *J* = 8.3 Hz, 2H), 7.34-7.39 (m, 4H), 7.46 (dd, *J* = 7.5, 1.8 Hz, 2H), 7.87 (d, 2H, *J* = 8.3 Hz), 7.89 (s, 2H); ^{13}C NMR ($CDCl_3$, 150 MHz) δ 55.71, 60.58, 111.01, 120.41, 124.53, 124.77, 125.85, 125.91, 127.88, 128.48, 128.81, 130.48, 130.81, 131.28, 132.53, 133.82, 154.94, 157.24; $[\alpha]_D^{20}$ +84.0 (*c* 1.0, CH_2Cl_2). These spectral data match those previously reported for this compound.[3e]

(*R*)-3,3'-bis(2-hydroxyphenyl)-[1,1'-binaphthalene]-2,2'-diol 89: To a 50 mL flame-dried round bottom flask was added (*R*)-**260** (790 mg, 1.5 mmol) and CH_2Cl_2 (10 mL). To this solution at –78 °C was added BBr_3 (12 mL, 1.0 M in CH_2Cl_2) drop-wise. The reaction was

allowed to warm to 0 °C. The reaction mixture was stirred for 0.5 h at 0 °C and then was allowed to warm to room temperature. After stirring at room temperature for 1 h, the reaction was quenched by the slow addition of the distilled water (15 mL). The aqueous layer was extracted with CH_2Cl_2 (10 mL × 3). The combined extracts were then washed with water, brine and then dried over $MgSO_4$, filtered, and concentrated *in vacuo*. Purification of the yellow colored crude product by silica gel chromatography (35 mm × 400 mm column, 3:1 hexanes/EtOAc as eluent, under gravity) afforded pure (*R*)-**89** as a white solid (mp. 144-145 °C) in 85 % isolated yield (600 g, 1.28 mmol).

Spectral data for (*R*)-**89**: R_f = 0.19 (4:1 hexanes/EtOAc); ^{1}H NMR ($CDCl_3$, 600 MHz) δ 6.03 (br s, 2H), 6.79 (br s, 2H), 6.90 (t, *J* = 7.7 Hz, 2H), 7.13-7.18 (m, 2H), 7.25-7.30 (m, 4H), 7.34 (dd, *J* = 7.7 Hz, 1.7 Hz, 2H), 7.64 (d, *J* = 7.8 Hz, 2H), 7.75 (s, 2H), (4 protons cannot be located); ^{13}C NMR ($CDCl_3$, 150 MHz) δ 114.37, 116.40, 121.10, 124.27, 124.39, 124.98, 127.11, 127.74, 128.43, 129.44, 129.83, 131.47, 132.18, 133.48, 149.66, 152.27; $[\alpha]_D^{25}$ –105 (*c* 1.0, $CHCl_3$). These spectral data match those previously reported for this compound.[3c,3e]

4.6.3 NMR analysis of a mixture of BINOL 55, commercial $B(OPh)_3$ and imine 78a or DMAP 216c

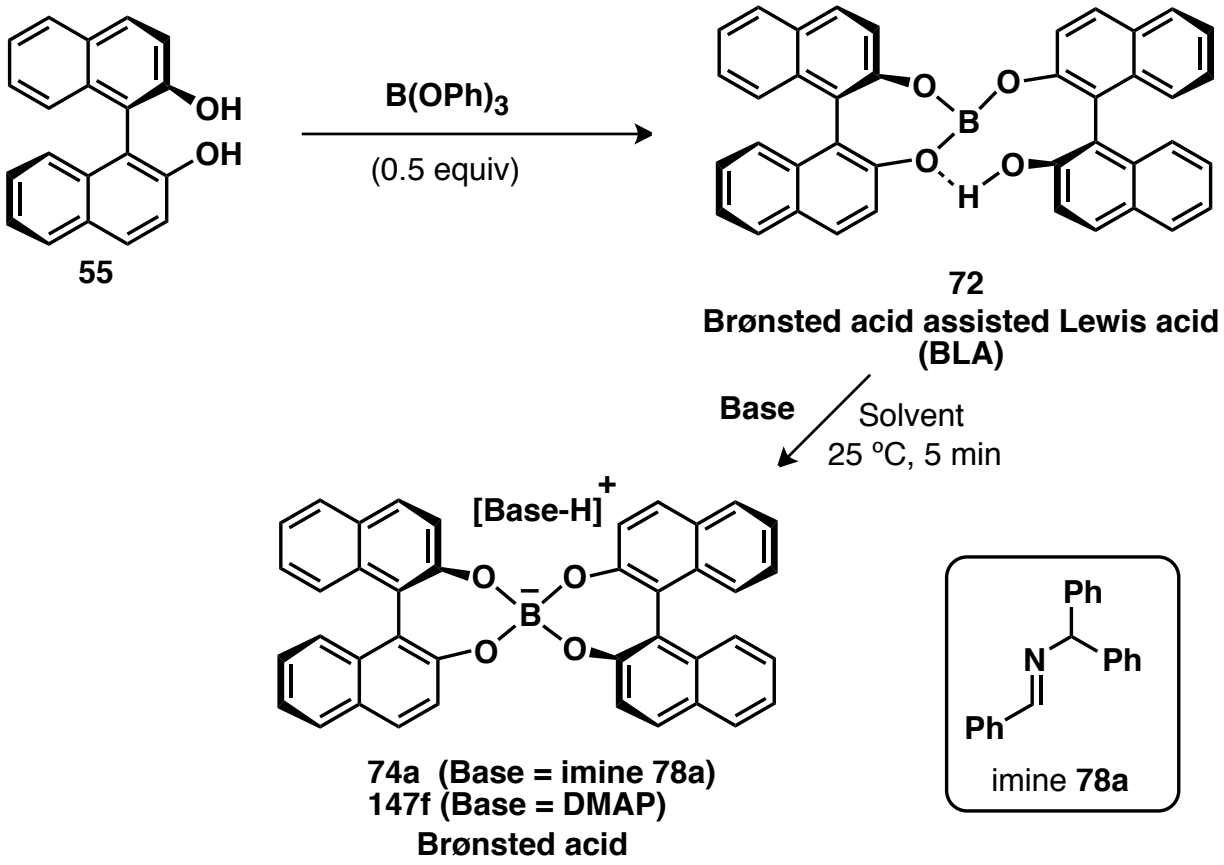

Entry 1, Figure 4.4: The NMR of pure BINOL **55** was taken in CD_2Cl_2.

Entry 2, Figure 4.4: To a flame dried 25 mL round bottom flask equipped with a stir bar and flushed with argon was added 4Å Molecular Sieves (150 mg). The sieves were then flame dried in the same flask. To the same flask was added BINOL **55** (28.6 mg, 0.100 mmol), $B(OPh)_3$ (14.5 mg, 0.050 mmol) and CD_2Cl_2 (3 mL). The resulting mixture was then stirred for 1 h. The sample was then filtered and transferred to a quartz NMR tube and was subjected to ^{1}H NMR and ^{11}B NMR analysis.

Entry 3, Figure 4.4: Imine **78a** (136 mg, 0.05 mmol, 0.5 equiv) was added to the NMR tube containing entry 2. The NMR tube was shaken for 2 min before the analysis.

Entry 4 and 5, Figure 4.4: Same as entry 2 and 3 respectively where $CDCl_3$ is used as the NMR solvent.

Entry 6, Figure 4.4: Same as entry 4 where DMAP **216c** is used as the base.

4.6.4 NMR analysis of a mixture of (*R*)-3,3′-(2-OH-C_6H_4)$_2$-BINOL 89, various boron sources and imine 78a

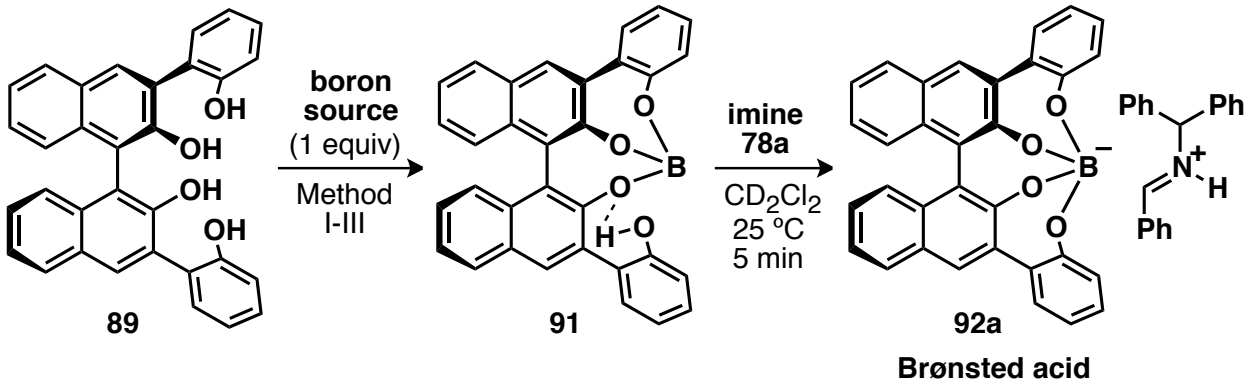

Entry 1, Figure 4.9: The NMR of pure BINOL derivative **89** was taken in CD_2Cl_2.

Entry 2, Figure 4.4: To a flame dried 25 mL round bottom flask equipped with a stir bar and a 10 mL pressure-equalized addition funnel (containing a cotton plug and ca. 4 g of 4Å Molecular Sieves (pellets) and functioning as a Soxhlet extractor) surmounted by a reflux condenser was added BINOL derivative **89** (23.5 mg, 0.050 mmol), $B(OMe)_3$ (0.5 mL, 0.1 M solution in

CD_2Cl_2, 0.050 mmol) and CD_2Cl_2 (3 mL). An argon atmosphere was secured and the solution was refluxed at 60 °C for 2 h. The reaction was cooled to room temperature and the addition funnel and condenser were quickly removed and replaced with septum. After cooling to 25 ºC, an additional 1.5 mL of CD_2Cl_2 was added and then stirred vigorously for 0.5 h. Most of the white precipitate was dissolved and the resulting turbid solution was directly transferred to a quartz NMR tube and was subjected to ^{1}H NMR and ^{11}B NMR analysis.

Entry 3, Figure 4.9: Imine **78a** (136 mg, 0.05 mmol, 1.0 equiv) was added to the NMR tube containing the sample from entry 2. The NMR tube was shaken for 2 min before the analysis. An appearance of yellow color was observed.

Entry 4 and 5, Figure 4.9: 1 and 3 equiv of methanol is added to the NMR tube (containing the sample from entry 2) for entries 4 and 5 respectively.

Entry 6, Figure 4.4: Same as entry 3 where imine **78a** (136 mg, 0.05 mmol, 1.0 equiv) is added to the entry 5.

Entry 7, Figure 4.9: To a flame dried 25 mL home made Schlenck flask (see Figure 2.26) equipped with a stir bar and flushed with argon was added BINOL derivative **89** (23.5 mg, 0.050 mmol) and toluene (1 mL). Under an argon flow through the side-arm of the Schlenk flask, BH_3•Me_2S (25 μL, 2.0 M solution in toluene, 0.05 mmol) was added through the top of the Teflon valve. The flask was sealed by closing the Teflon valve, and then placed in an 100 ºC oil bath for 1 h. After 1 h, a vacuum (0.5 mm Hg) was carefully applied by slightly opening the Teflon valve to remove the volatiles. After the volatiles were removed completely, a full

vacuum was applied and maintained for a period of 30 min at a temperature of 100 ºC (oil bath). The flask was then allowed to cool to room temperature and opened to argon through the side-arm of the Schlenk flask. The resulting solid was then dissolved in 1.5 mL of CD_2Cl_2. The sample was then filtered and transferred to a quartz NMR tube and was subjected to ^1H NMR and ^{11}B NMR analysis.

Entry 8, Figure 4.9: Imine **78a** (136 mg, 0.05 mmol, 1.0 equiv) was added to the NMR tube containing the sample from entry 7. The NMR tube was shaken for 2 min before the analysis. An appearance of yellow color was observed.

Entry 9, Figure 4.9: To a flame dried 25 mL round bottom flask equipped with a stir bar and flushed with argon was added 4Å Molecular Sieves (150 mg). The sieves were then flame dried in the same flask. To the same flask was added BINOL derivative **89** (23.5 mg, 0.050 mmol), $B(OPh)_3$ (14.5 mg, 0.050 mmol) and CD_2Cl_2 (1.5 mL). The resulting mixture was then stirred for 1 h. The sample was then filtered and transferred to a quartz NMR tube and was subjected to ^1H NMR and ^{11}B NMR analysis.

Entry 10, Figure 4.9: Imine **78a** (136 mg, 0.05 mmol, 1.0 equiv) was added to the NMR tube containing the sample from entry 9. The NMR tube was shaken for 2 min before the analysis. An appearance of yellow color was observed.

4.6.5 NMR analysis of a mixture of Phenol 194a, commercial and freshly prepared $B(OPh)_3$ and DMAP 216c

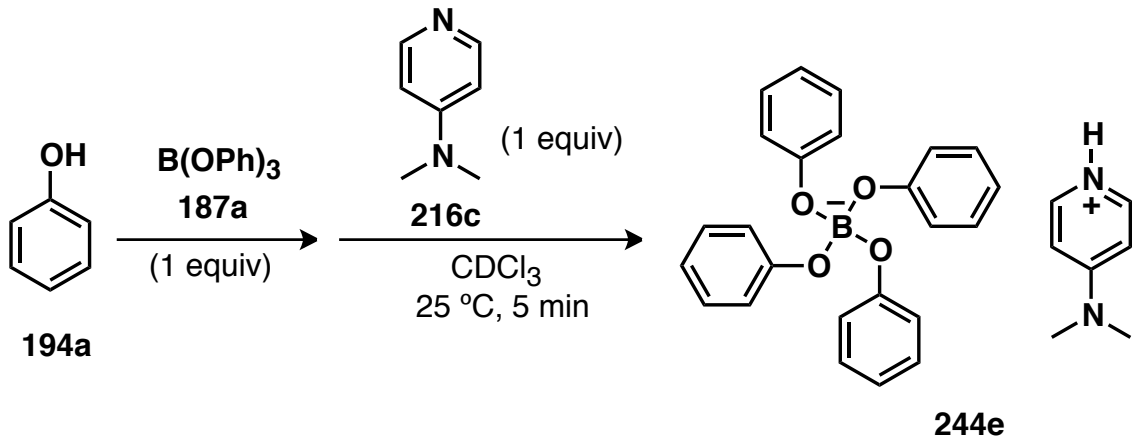

Entry 1, Figure 4.13: The NMR of freshly sublimed Phenol **194a** was taken in $CDCl_3$.

Entry 2, Figure 4.13: The NMR of freshly made $B(OPh)_3$ prepared using the procedure shown in section 4.6.2.

Entry 3, Figure 4.13: To the home-made Schlenck flask containing the freshly prepared $B(OPh)_3$ (entry 2) was added freshly sublimed PhOH **194a** (9.4 mg, 0.10 mmol, 1.0 equiv). The mixture was dissolved in $CDCl_3$ (1 mL) transferred to a quartz NMR tube and was subjected to ^{1}H NMR and ^{11}B NMR analysis.

Entry 4, Figure 4.13: DMAP **216c** (12.2 mg, 0.100 mmol, 1.00 equiv) was added to the NMR tube containing the sample from entry 3. The NMR tube was shaken for 2 min before the analysis. An appearance of yellow color was observed.

Entry 5 and 7, Figure 4.13: The NMR of commercial $B(OPh)_3$ and DMAP was taken in $CDCl_3$ respectively.

Entry 6, Figure 4.13: DMAP **216c** (12.2 mg, 0.100 mmol, 1.00 equiv) was added to the NMR tube containing the sample from entry 5. The NMR tube was shaken for 2 min before the analysis. An appearance of yellow color was observed.

4.6.6 DFT Calculations

All quantum mechanical calculations were performed using the Gaussian ′03.[5] The B3LYP[16] and BHandHLYP[17] density functional were used along with 6-31G* basis sets. The coordinates were provided to Prof. Wulff as a separate file.

REFERENCES

REFERENCES

(1) (a) Zhang, Y.; Desai, A.; Lu, A.; Hu, G.; Ding, Z.; Wulff, W. D. *Chem. –Eur. J.* **2008**, *14*, 3785-3803. (b) Zhang, Y.; Lu, Z.; Desai, A.; Wulff, W. D. *Org. Lett.* **2008**, *10*, 5429-5432. (c) Mukherjee, M.; Gupta, A. K.; Lu, Z.; Zhang, Y.; Wulff, W. D. *J. Org. Chem.* **2010**, *75*, 5643-5660. (d) Ren, H.; Wulff, W. D. *Org. Lett.* **2010**, *12*, 4908-4911. (e) Hu, G.; Huang, L.; Huang, R. H.; Wulff, W. D. *J. Am. Chem. Soc.* **2009**, *131*, 15615-15617. (f) Hu, G.; Gupta, A. K.; Huang, R. H.; Mukherjee, M.; Wulff, W. D. *J. Am. Chem. Soc.* **2010**, *132*, 14669–14675. (g) Gupta, A. K.; Mukherjee, M.; Wulff, W. D. *Org. Lett.* **2011**, *13*, 5866-5869. (h) Desai, A. A.; Wulff, W. D. *J. Am. Chem. Soc.* **2010**, *132*, 13100-13103. (i) Vetticatt, M. J.; Desai, A. A.; Wulff, W. D. *J. Am. Chem. Soc.* **2010**, *132*, 13104-13107. (j) Desai, A. A.; Morán-Ramallal, R.; Wulff, W. D. *Org. Synth.* **2011**, *88*, 224-237.

(2) (a) Ishihara, K.; Miyata, M.; Hattori, K.; Tada, T.; Yamamoto, H. *J. Am. Chem. Soc.* **1994**, *116*, 10520-10524. (b) Ishihara, K.; Kuroki, Y.; Yamamoto, H. *Synlett* **1995**, 41-42. (c) Kuroki, Y.; Ishihara, K.; Hanaki, N.; Ohara, S.; Yamamoto, H. *Bull. Chem. Soc. Jpn.* **1998**, *71*, 1221-1230. (d) Cros, J. P.; Pérez-Fuertes, Y.; Thatcher, M. J.; Arimori, S.; Bull, S. D.; James, T. D. *Tetrahedron: Asymmetry* **2003**, *14*, 1965-1968. (e) Kawate, T.; Yamada, H.; Matsumizu, M.; Nishida, A.; Nakagawa, M. *Synlett* **1997**, 761-762. (f) Yamada, H.; Kawate, T.; Matsumizu, M.; Nishida, A.; Yamaguchi, K.; Nakagawa, M. *J. Org. Chem.* **1998**, *63*, 6348-6354.

(3) (a) Ishihara, K.; Yamamoto, H. *J. Am. Chem. Soc.* **1994**, *116*, 1561-1562. (b) Ishihara, K.; Kurihara, H.; Yamamoto, H. *J. Am. Chem. Soc.* **1996**, *118*, 3049-3050. (c) Ishihara, K.; Kurihara, H.; Matsumoto, M.; Yamamoto, H. *J. Am. Chem. Soc.* **1998**, *120*, 6920-6930. (d) Ishihara, K.; Kondo, S.; Kurihara, H.; Yamamoto, H.; Ohashi, S.; Inagaki, S. *J. Org. Chem.* **1997**, *62*, 3026-3027. (e) Dai, X.; Davies, H. M. L. *Adv. Synth. Catal.* **2006**, *348*, 2449-2456.

(4) (a) Cole, T. E.; Quintanilla, R.; Rodewald, S. *Synth. React. Inorg. Met.-Org. Chem.* **1990**, *20*, 55-63. (b) Malkowsky, I. M.; Frohlich, R.; Griesbach, U.; Putter, H.; Waldvogel, S. R. *Eur. J. Inorg. Chem.* **2006**, 1690-1697. (c) Cole, T. E.; Bakshi, R. K.; Srebnik, M.; Singaram, B.; Brown, H. C. *Organometallics* **1986**, *5*, 2303-2307. (d) Linti, G.; Loderer, D.; Nöth, H.; Polborn, K.; Rattay, W. *Chem. Ber.* **1994**, *127*, 1909-1922. (e) Wilson, J. W. *J. Chem. Soc., Dalton Trans.* **1973**, 1628-1630. (f) Nishihara, Y.; Nara, K.; Osakada, K. *Inorg. Chem.* **2002**, *41*, 4090-4092. (g) Mannig, D.; Noth, H. *J. Chem. Soc., Dalton Trans.* **1985**, 1689-1692. (h) Knizek, J. r.; N√∂th, H. *J. Organomet. Chem.* **2000**, *614,Äì615*, 168-187. (i) Lawlor, F. J.; Norman, N. C.; Pickett, N. L.; Robins, E. G.; Nguyen, P.; Lesley, G.; Marder, T. B.; Ashmore, J. A.; Green, J. C. *Inorg. Chem.* **1998**, *37*, 5282-5288. (j) Carter, C.; Fletcher, S.; Nelson, A. *Tetrahedron: Asymmetry* **2003**, *14*, 1995-2004. (k) Raskatov, J. A.; Brown, J. M.; Thompson, A. L. *Crystengcomm* **2011**, *13*, 2923-2929.

(5) Gaussian 03, Revision D.01 M. J. Frisch, G. W. T., H. B. Schlegel, G. E. Scuseria, M. A. Robb, J. R. Cheeseman, J. A. Montgomery, Jr., T. Vreven, K. N. Kudin, J. C. Burant, J. M. Millam, S. S. Iyengar, J. Tomasi, V. Barone, B. Mennucci, M. Cossi, G. Scalmani, N. Rega, G. A. Petersson, H. Nakatsuji, M. Hada, M. Ehara, K. Toyota, R. Fukuda, J. Hasegawa, M. Ishida, T. Nakajima, Y. Honda, O. Kitao, H. Nakai, M. Klene, X. Li, J. E. Knox, H. P. Hratchian, J. B. Cross, V. Bakken, C. Adamo, J. Jaramillo, R. Gomperts, R. E. Stratmann, O. Yazyev, A. J. Austin, R. Cammi, C. Pomelli, J. W. Ochterski, P. Y. Ayala, K. Morokuma, G. A. Voth, P. Salvador, J. J. Dannenberg, V. G. Zakrzewski, S. Dapprich, A. D. Daniels, M. C. Strain, O. Farkas, D. K. Malick, A. D. Rabuck, K. Raghavachari, J. B. Foresman, J. V. Ortiz, Q. Cui, A. G. Baboul, S. Clifford, J. Cioslowski, B. B. Stefanov, G. Liu, A. Liashenko, P. Piskorz, I. Komaromi, R. L. Martin, D. J. Fox, T. Keith, M. A. Al-Laham, C. Y. Peng, A. Nanayakkara, M. Challacombe, P. M. W. Gill, B. Johnson, W. Chen, M. W. Wong, C. Gonzalez, and J. A. Pople, Gaussian, Inc., Wallingford CT, 2004

(6) Tu, T.; Maris, T.; Wuest, J. D. *Cryst. Growth Des.* **2008**, *8*, 1541-1546.

(7) Hu, G. PhD Dissertation, Michigan State University, 2007.

(8) Taube, R.; Weckmann, E.; Böhme, P.; Gehrke, J. P. *Z. Anorg. Allg. Chem.* **1989**, *577*, 245-254.

(9) Lang, A.; Knizek, J.; Nöth, H.; Schur, S.; Thomann, M. *Z. Anorg. Allg. Chem.* **1997**, *623*, 901-907.

(10) (a) Bishop, M.; Shahid, N.; Yang, J.; Barron, A. R. *Dalton Trans.* **2004**, 2621-2634. (b) Pasdeloup, M.; Brisson, C. *Org. Magn. Reson.* **1981**, *16*, 164-167.

(11) Steinberg, H. *Organoboron Chemistry*; Wiley Interscience: New York, N.Y., 1964; Vol. 1, ch. 15.

(12) Schlesinger, H. I.; Brown, H. C.; Mayfield, D. L.; Gilbreath, J. R. *J. Am. Chem. Soc.* **1953**, *75*, 213-215.

(13) Hu, G.; Huang, L.; Huang, R. H.; Wulff, W. D. *J. Am. Chem. Soc.* **2009**, *131*, 15615-15617.

(14) Vetticatt, M.; Wulff, W. D., Unpublished results.

(15) (a) Wipf, P.; Jung, J.-K. *J. Org. Chem.* **2000**, *65*, 6319-6337. (b) Lingenfelter, D. S.; Helgeson, R. C.; Cram, D. J. *J. Org. Chem.* **1981**, *46*, 393-406. (c) Gobbi, L.; Seiler, P.; Diederich, F.; Gramlich, V. *Helv. Chim. Acta* **2000**, *83*, 1711-1723.

(16) (a) Becke, A. D. *Phys. Rev. A* **1988**, *38*, 3098. (b) Lee, C. Y., W.; Parr, R. G. *Phys. Rev. B* **1988**, *37*, 785.

(17) (a) Becke, A. D. *J. Chem. Phys.* **1993**, *98*, 1372-1377. (b) Zhao, Y.; Truhlar, D. G. *J. Chem. Theory Comput.* **2005**, *1*, 415-432. (c) Yu, W.; Liang, L.; Lin, Z.; Ling, S.; Haranczyk, M.; Gutowski, M. *J. Comput. Chem.* **2009**, *30*, 589-600.

CHAPTER 5

AN EXAMINATION OF VARIOUS CHIRAL DIOLS AS LIGANDS FOR ASYMMETRIC AZIRIDINATION REACTION AND THEIR IMPACT ON THE STRUCTURE OF THE BOROX CATALYST

I think that we should pursue it a little more!

-William D. Wulff

5.1 Introduction

Over the past few years, the Wulff group has developed a universal catalytic asymmetric aziridination reaction of imines utilizing a catalyst derived from the vaulted ligands VAPOL **58** or VANOL **59** and commercial $B(OPh)_3$ (Chapter 1, Scheme 1.12).[1] The actual catalyst **190** is a complex consisting of a protonated imine and a chiral counteranion in the form of a boroxinate anion (Chapter 2 and Figure 5.1C). This boroxinate catalyst has been termed as the IMINO-BOROX catalyst **190**. As discussed in section 2.1.1.3 of chapter 2, these BOROX catalysts can be very diverse in nature. Diversity can be achieved by altering the *ligand*, the alcohol source and the *N*-substituent of the imine. Based on these variations, a large pool of catalysts can be generated. These catalysts could be very different in structure and reactivity for a given asymmetric reaction. The aim of the work in this chapter is to explore a novel family of catalysts by employing different ligands and to study the change in the mechanistic behavior of these catalysts. The vaulted biaryl ligand ISOVAPOL **197** and the linear biaryl ligand BINOL **55** and its derivatives of type **56** as well as TADDOL **61a** were examined for efficacy in the catalytic asymmetric aziridination reaction. In addition, in order to *investigate the structure of the catalyst*, NMR experiments were performed on these novel catalysts.

5.2 ISOVAPOL: a new entry to the family of vaulted biaryl ligands

In 1993, we introduced a new family of chiral diols in the form of the vaulted biaryl ligands. Two of the most studied and prominent members of this family of ligands are VAPOL **58** and VANOL **59** (Figure 5.1A). These vaulted biaryl ligands have been demonstrated to be useful in a variety of important asymmetric reactions including Diels-Alder reactions,[2] Mannich reactions,[3] Baeyer-Villiger reactions,[4] the Petasis reaction,[5] the hydroarylation of alkenes,[6] the hydrogenation of alkenes,[7] asymmetric chlorination and Michael reactions of oxindoles,[8] benzoyloxylation of aryloxindoles,[9] aza-Darzens reaction,[10] propargylation of ketones,[11] and hydroacylation of alkenes.[12] Specifically, the BOROX catalyst derived from VAPOL and VANOL ligands have been used in *cis*-aziridination of imines,[1a-1f,1j] *trans*-aziridination of imines,[1h,1i] multicomponent aziridination of aldehydes,[1g] heteroatom Diels-Alder reactions of imines,[13] aminoallylation of aldehydes,[14] [3+2] cycloaddition of imines,[15] and epoxidation of aldehydes.[15] More recently, chiral phosphoric acids **35** and **36** (Chapter 1) derived from these ligands have been used in the amidation[16] and imidation[17] of imines, the asymmetric reduction of imines,[18] pinacol rearrangement,[19] desymmetrization of aziridines[20] and reduction of aminals.[21]

In search of more diversity in the BOROX catalyst, in greater mechanistic understanding of its mode of catalysis and in an improvement in aziridination of benzhydryl imines **78**, we

envisioned the possibility of a new chiral ligand **197** as shown in Figure 5.2 (an isomer of VAPOL, hereafter abbreviated as ISOVAPOL).

5.2.1 Rational design of ISOVAPOL 197

In the past, a series of VAPOL and VANOL derivatives have been prepared[2d,22] and examined in the asymmetric aziridination reaction of imines.[22a] Some of these modified ligands were used as chiral Lewis acids in asymmetric Diels-Alder reaction,[2d] and Mannich reaction.[22b] However, these modifications were made, in most of cases, without any understanding of how the catalyst functions. Now, with the help of the information about the structure of the BOROX catalyst, rational design of new vaulted ligands is possible. One of the most puzzling aspects of the aziridination reaction is that the BOROX catalysts derived from both the VANOL and VAPOL ligands have a nearly identical profile of asymmetric induction over the same range of imine substrates.[1c] We were able to rationalize this observation with the help of the knowledge of the structure of the catalyst. The structure of the BOROX catalyst **190a** reveals that the π-π stacking interaction of the phenyl group of the imine is primarily over the central ring (B) of the phenanthrene unit of the VAPOL **58** (Figure 5.1C). This corresponds to the B ring of the VANOL boroxinate catalyst **191a** (Figure 5.1B). Although, an *X*-ray structure of the catalyst derived from VANOL has not yet been obtained, ^{1}H NMR studies suggest that the structure is analogous to the BOROX catalyst **190a** (Figure 5.1B). Thus, it appears that the extra benzene ring of VAPOL is not needed, at least in the catalyst for the aziridination reaction.

Figure 5.1 (**A**) Different chiral diols from vaulted biaryl ligands. (**B**) Different BOROX catalysts derived from VAPOL and VANOL. (**C**) Diagrammatic representation of X-ray structure of the BOROX catalyst **190a**.

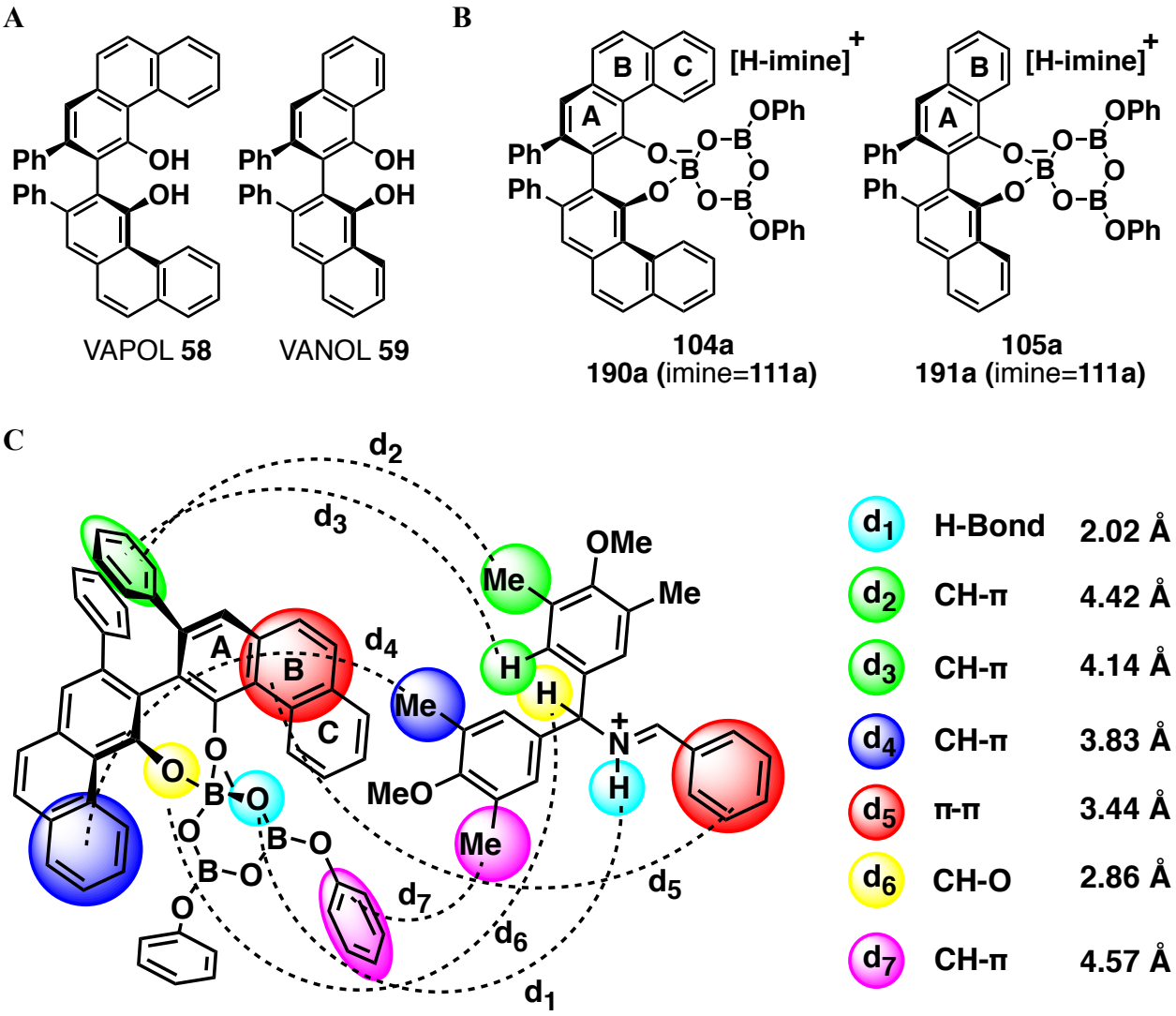

As evident from the structure of the catalyst-substrate complex **190a**, π-π stacking may be important for asymmetric induction in the case of aromatic aldehydes. However, the case of aliphatic aldehydes is interesting due to the absence of this π-π interaction. Also, as is revealed

in the structure of the catalyst; there are numerous CH-π interactions (Figure 5.1C). The mode of the docking of imines generated from aliphatic aldehydes to the catalyst is unknown. As there is no difference in the enantioinduction when either VAPOL or VANOL is used, the orientation of the alkyl group could be indifferent to the presence of ring C. However, it the alkyl group have been orienting in a way such that there are CH-π interactions with the imaginary ring C' (Figure 5.2A). If this were true, moving the C ring to the 9 and 10-positions of VAPOL (or adding another benzene ring at the 5 and 6-positions of VANOL) would lead to the rational design of our new chiral ligand ISOVAPOL **197** (Figure 5.2B). The aim of making ISOVAPOL is multi-faceted. One of the reasons to consider ISOVAPOL **197** is its potential lower cost to make than VAPOL. The starting material for the synthesis of ISOVAPOL, 1-naphthyl acetic acid **284** is 10 times cheaper (~$50/Kg) than 2-naphthyl acetic acid **269** (~$540/Kg), which is the starting material for the most convenient synthesis of VAPOL.[23] The former is manufactured on large scale as a plant growth regulator. Recently, we reported a new optimal method for VAPOL and hopefully, a direct application of this method towards the synthesis of ISOVAPOL can be undertaken.[23] Hence, in conjunction with our efforts to probe the mechanistic underpinning of the asymmetric induction observed for BOROX catalysts and to expand the members of the family of vaulted ligands, a project was initiated to synthesize and evaluate ISOVAPOL **197**.

Figure 5.2 (**A**) Possible orientation of the imine over the boroxinate core. (**B**) Rational design of the new vaulted ligand ISOVAPOL **197**

Figure 5.2 cont'd

A

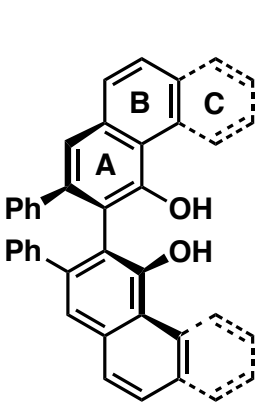

58 or **59**

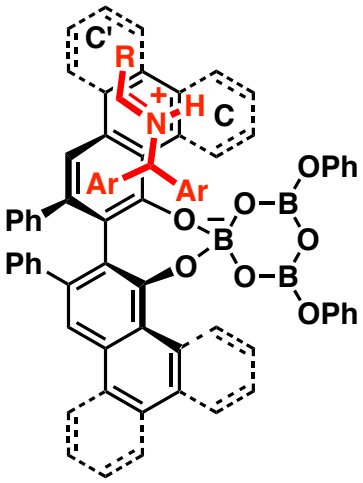

B

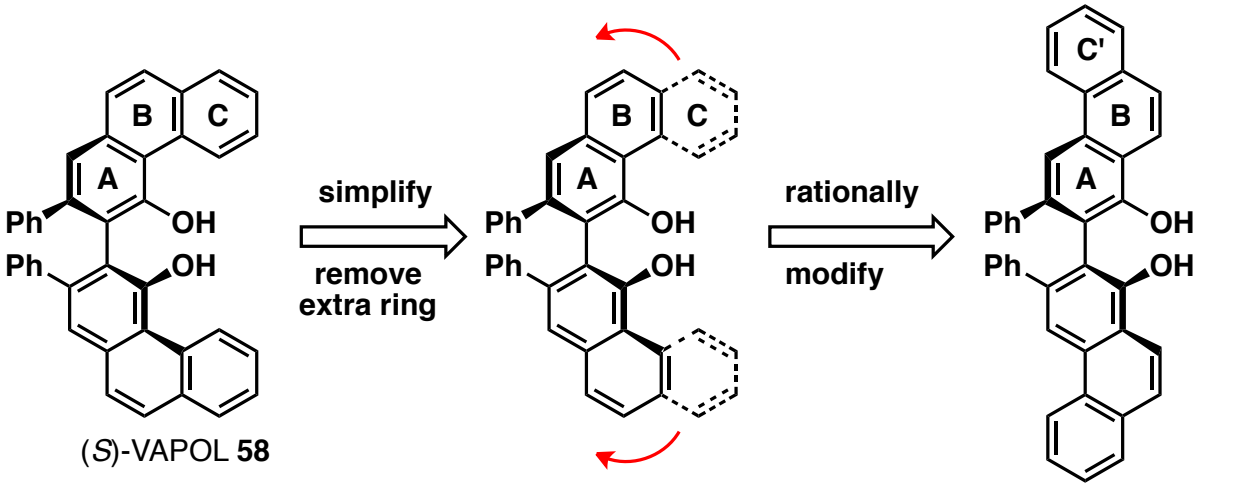

(*S*)-VAPOL **58**

(*S*)-ISOVAPOL **197**

5.2.2 Preparation of ISOVAPOL 197

Recently, we reported a very efficient and convenient large-scale synthesis of VAPOL **58**.[23] This synthesis of VAPOL involves the preparation of the monomer **263** followed by its oxidative coupling and resolution to get highly optically pure ligand. The key step in the

synthesis of the monomer **272** is a cycloaddition/electrocyclic ring-opening (CAEC)/electrocyclic ring- closure/tautomerization cascade (Scheme 5.1). Also, this cascade produces a byproduct that was identified as 2-(2-naphthyl)-3,5-diphenylphenol **273** obtained in <10% yield. The branch point between the two products is the ketene **277** and involves the competition between a [2 + 2] cycloaddition with phenylacetylene **270** giving **281** and an electrocyclic ring closure leading to the formation of **278** (Scheme 5.1B). The cyclobutenone **281** could be expected to begin its own electrocyclization cascade that is initiated with an electrocyclic ring opening to give the dienyl ketene **282** and then an electrocyclic ring closure to give the cyclohexadienone **283** and finally tautomerization to the byproduct **273** (Scheme 5.1B).

Scheme 5.1 (**A**) Preparation of the monomer **272** of VAPOL. (**B**) Proposed mechanism

A

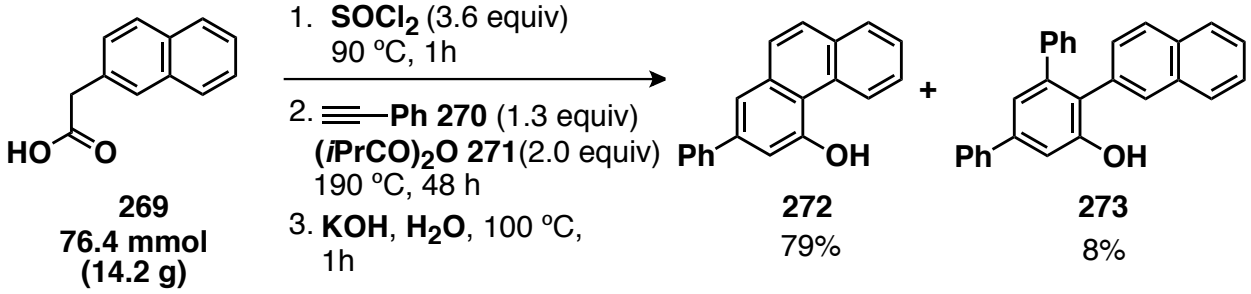

Scheme 5.1 cont'd

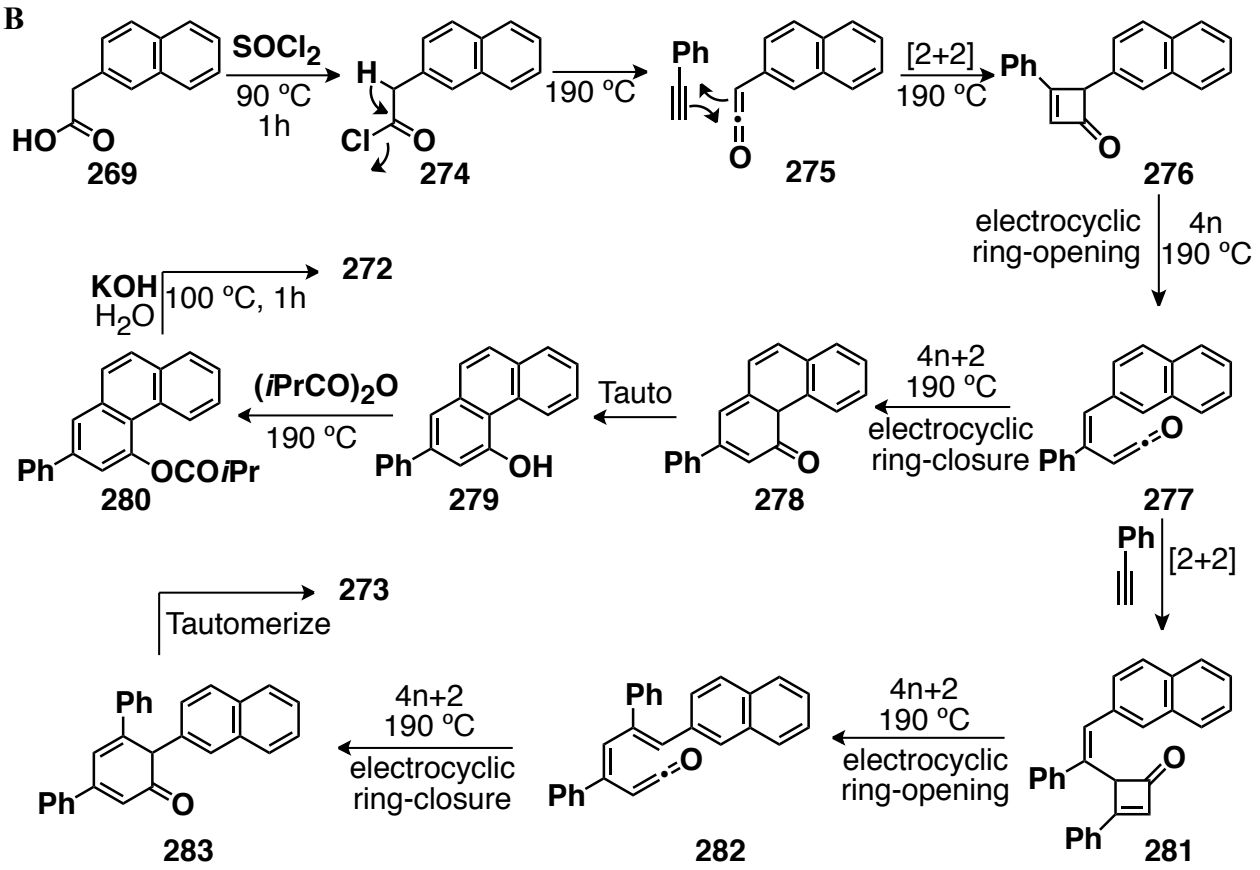

In the case of ISOVAPOL, the monomer **285** is expected to result from the acid chloride of **284** with phenyl acetylene in accord with the one-step protocol for the large scale synthesis of VAPOL **58** (Scheme 5.2).[23] First, 1-naphthyl acetyl chloride was prepared by reacting 1-naphthyl acetyl acid **284** with thionyl chloride at 90 °C for 1 h. Second, the procedure involves heating 1-naphthyl acetyl chloride (used without purification) in the presence of phenyl acetylene **270**. This initiates the [2+2] cycloaddition of an *in-situ* generated ketene and then electrocyclic ring opening of the resulting cyclobutenone and then finally, an electrocyclic ring closure of the vinyl ketene. The phenol product is trapped by the iso-butyric anhydride to give an ester. Hydrolysis gave the ISOVAPOL monomer **285** in 26–30% overall yield from acid **284** (Scheme 5.2). The low yield can be partially attributed to the formation of the by-product **286** that is

similar to the by-product **273** obtained in the synthesis of the monomer **272** for VAPOL (Scheme 5.2). Interestingly, another by-product **287** (structure not known) was also obtained.

Scheme 5.2 Preparation of the ISOVAPOL monomer **285**

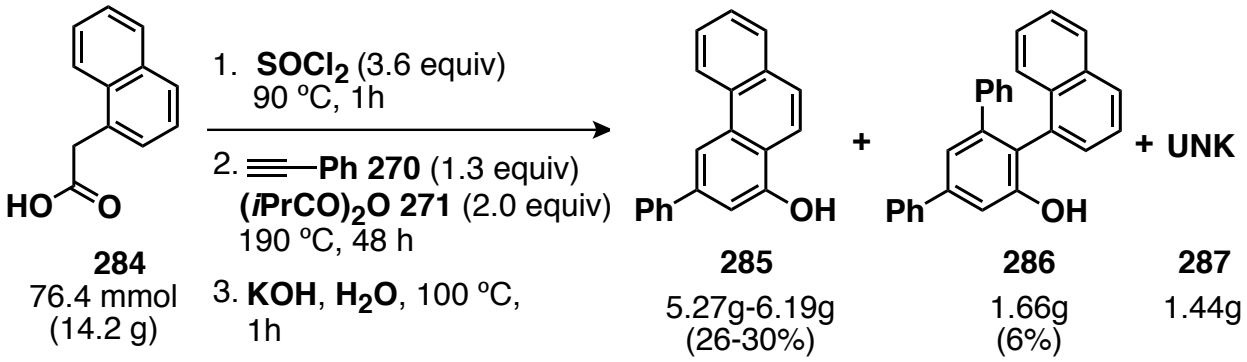

The synthesis of the *rac*-ISOVAPOL was carried out *via* oxidative coupling by stirring the monomer **285** in mineral oil at 190 °C in the presence of air (Scheme 5.3). This gave the dimer *rac*-ISOVAPOL in 70% yield. The optically pure ligand (*S*)-**197** was then readily obtained by the deracemization protocol[22c] developed in the group in 95% yield and > 99% *ee* (Scheme 5.3).

Scheme 5.3 Preparation of the *rac*-**197** and *(S)*-ISOVAPOL (*S*)-**197**

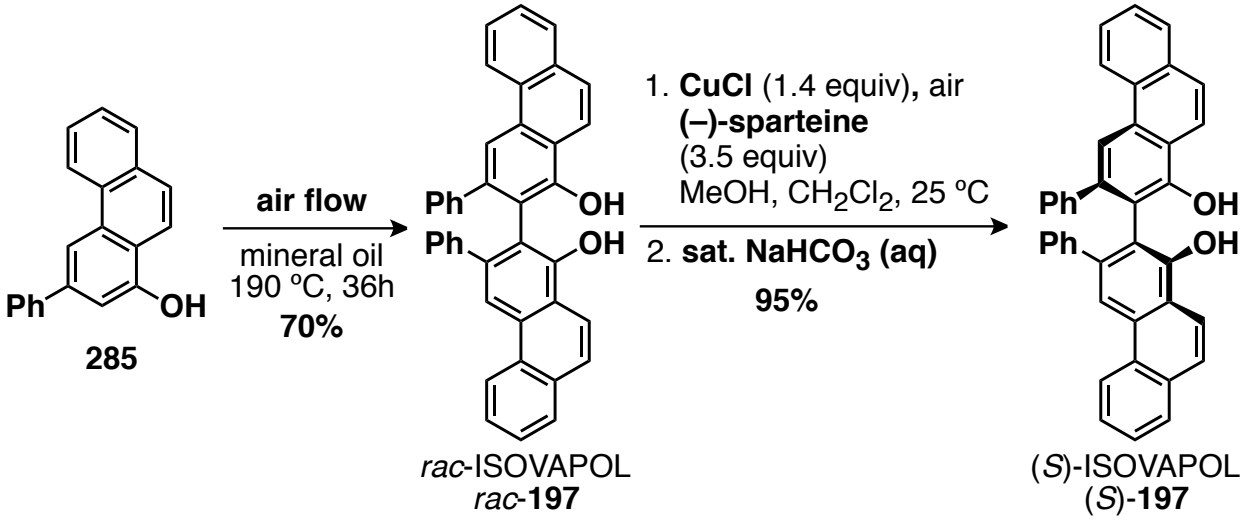

5.2.3 Asymmetric aziridination reaction catalyzed by BOROX catalyst derived from ISOVAPOL

After the development of a successful synthesis of ISOVAPOL, the stage was set for the examination of its effectiveness in the catalytic aziridination reaction. As a control, we decided to perform each reaction with ISOVAPOL and VANOL to have a better measure of the consequences of the structural differences. One of the first sets of experiments was the examination of ISOVAPOL derived catalyst with various *N*-protecting groups (Table 5.1) in the aziridination reaction. The new ligand **197** showed results very similar to *(R)*-VANOL for imines with the four different protecting groups. These results suggested that the binding of the imine with the catalyst prepared from the new ligand **197** might be similar to that from VAPOL or VANOL derived catalysts. Since the aziridination reaction is already well established with MEDAM protecting groups for aryl and alkyl substituents (up to 99% ee), it was decided to choose to the benzhydryl (Bh) protecting group for further study as the model system (lowest asymmetric induction among other *N*-protecting groups for aryl and alkyl substituents). It must be noted that the benzhydryl amine **126a** is commercially available whereas MEDAM amine **126c** is not.

Table 5.1 Screening of ISOVAPOL **197** with different *N*-protected imines[a]

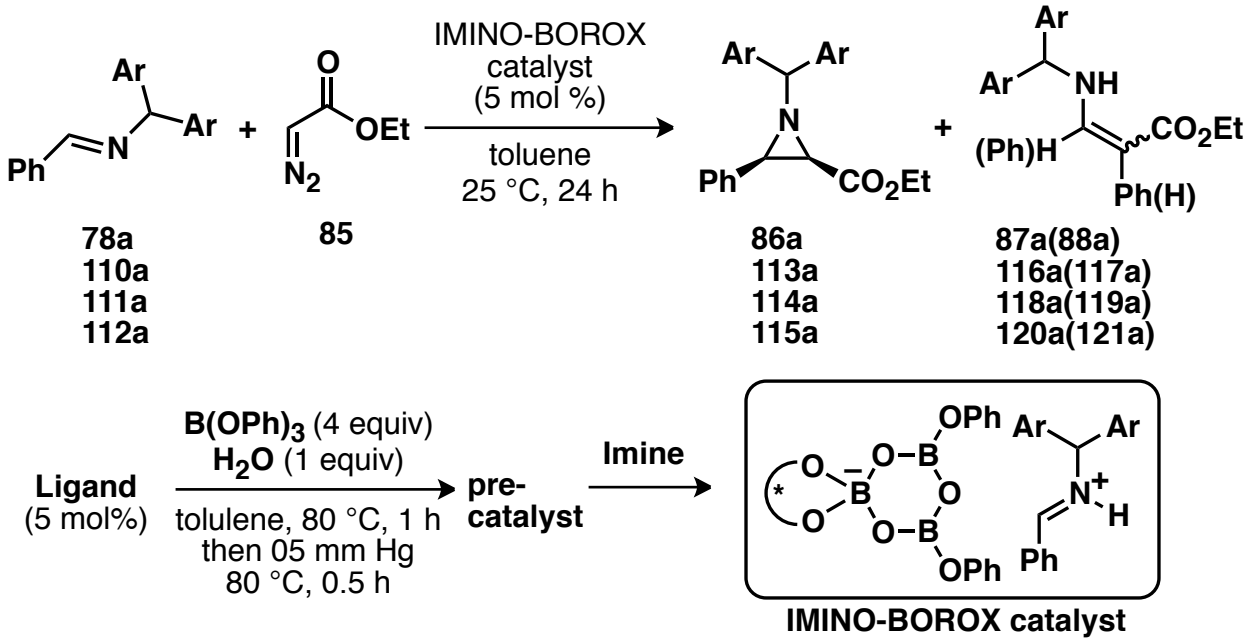

Table 5.1 cont'd

#	Cat	Ligand	Ar_2CH	azi	Yield azi (%) [b]	ee azi (%) [c]	c:t [d]	Yield enamine (%) [e]
1 [f]	**199a**	(*S*)-ISOVAPOL	Bh	**86a**	82	92	50:1	3/7
2	**189a**	(*R*)-VANOL	Bh		87	–89	>50:1	<1/<1
3 [f]	**288a**	(*S*)-ISOVAPOL	DAM	**113a**	91	96	50:1	6/<1
4	**289a**	(*R*)-VANOL	DAM		89	–92	>50:1	1/<1
5	**290a**	(*S*)-ISOVAPOL	MEDAM	**114a**	96	98	>50:1	2/1
6	**191a**	(*R*)-VANOL	MEDAM		98	–97	50:1	1/1
7	**291a**	(*S*)-ISOVAPOL	BUDAM	**115a**	97	96	>50:1	<1/<1
8	**292a**	(*R*)-VANOL	BUDAM		98	–96	50:1	<1/<1

[a] Unless otherwise specified, all reactions were performed with 1 mmol of imine in toluene (0.5 M in imine) with 1.2 equiv of **85** and 5 mol% of the catalyst at 25 °C. The pre-catalyst was prepared by heating 1 equiv of ligand with 4 equiv of commercial $B(OPh)_3$ and 1 equiv of H_2O in toluene at 80 °C for 1 h, followed by removing all volatiles under high vacuum (0.1 mm Hg) for 0.5 h at 80 °C. [b] Isolated Yield. [c] Determined by Chiral HPLC. [d] Ratio determined by integration of the methine protons of *cis*- and *trans*- aziridine in the ^{1}H NMR spectrum of the crude reaction mixture. [e] Determined by integration of the NH signals of enamines relative to the methine proton of *cis* aziridine in the ^{1}H NMR spectrum of the crude reaction mixture. [f] 94% and 96% conversion for entry 1 and 3 respectively. Percent conversion is determined by integration of the methine proton of *cis*-aziridine relative to the sp^2-CH proton of the unreacted imine in the ^{1}H NMR spectrum of the crude reaction mixture.

Prior to examining the substrate scope, it was thought to screen various solvents to observe any significant change in the yield or ee. While the reaction gave high asymmetric induction with halogenated solvents and with toluene, lower ees, in the range of 80, were obtained in case of oxygenated solvents like ether and EtOAc (Table 5.2). In the end, toluene was selected as the optimum solvent as it gave the highest enantioinduction and less toxic

compared to the other solvents. Also, the asymmetric induction was similar with benzhydryl imine **78a** for both ligands ISOVAPOL and VANOL in toluene (entries 1 and 2, Table 5.2).

Table 5.2 AZ reaction with imines **78** using *(S)*-ISOVAPOL and various solvents [a]

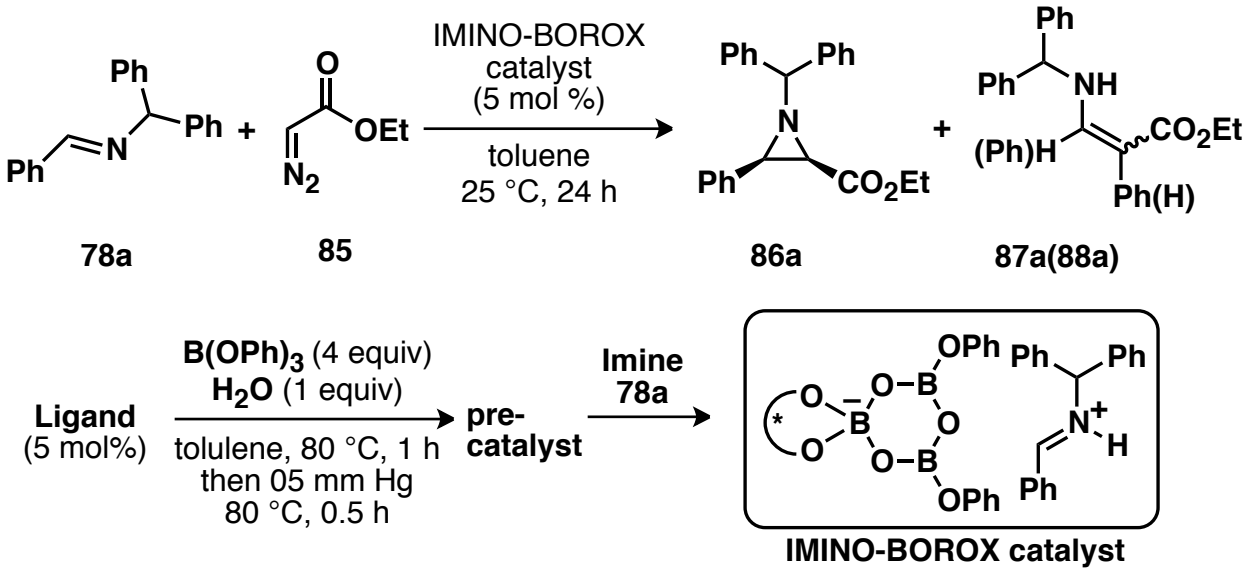

#	Cat	Ligand	Solvent	% conv [b]	Yield **86a** (%) [c]	ee **86a** (%) [d]	*c:t* [e]	Yield **87a/88a** (%) [f]
1	**199a**	(*S*)-ISOVAPOL	Toluene	94	82	92	50:1	3/7
2	**189a**	(*R*)-VANOL	Toluene	100	87	–89	>50:1	<1/<1
3	**199a**	(*S*)-ISOVAPOL	Ether	95	83	80	>50:1	5/6
4	**189a**	(*R*)-VANOL	Ether	96	83	–84	>50:1	4/5
5	**199a**	(*S*)-ISOVAPOL	Dichloromethane	94	79	91	25:1	4/9
6	**189a**	(*R*)-VANOL	Dichloromethane	100	83	–89	50:1	4/8
7	**199a**	(*S*)-ISOVAPOL	Dichloroethane	94	81	91	>50:1	4/8
8	**189a**	(*R*)-VANOL	Dichloroethane	100	83	–90	>50:1	4/8
9	**199a**	(*S*)-ISOVAPOL	EtOAc	45	36	81	20:1	5/4
10	**189a**	(*R*)-VANOL	EtOAc	55	43	–84	>50:1	7/4

[a] Unless otherwise specified, all reactions were performed with 1 mmol of imine **78a** in toluene (0.5 M in imine **78a**) with 1.2 equiv of **85** and 5 mol% of the catalyst at 25 °C. The pre-catalyst was prepared by heating 1 equiv of ligand with 4 equiv of commercial $B(OPh)_3$ and 1 equiv of H_2O in toluene at 80 °C for 1 h, followed by removing all volatiles under high vacuum (0.1 mm Hg) for 0.5 h at 80 °C. [b] Percent conversion is determined by integration

Table 5.2 cont'd

of the methine proton of *cis*-aziridine relative to the sp^2-CH proton of the unreacted imine in the ^{1}H NMR spectrum of the crude reaction mixture. [c] Isolated Yield. [d] Determined by HPLC. [e] Ratio determined by integration of the methine protons of *cis*- and *trans*-aziridine in the ^{1}H NMR spectrum of the crude reaction mixture. [f] Determined by integration of the NH signals of enamines relative to the methine proton of *cis*-aziridine in the ^{1}H NMR spectrum of the crude reaction mixture.

After the initial screening of the solvents, we moved on to examine the effect of *(S)*-ISOVAPOL **197** on the reactions of various aryl and alkyl imines **78**. Unfortunately, there was no improvement observed in the asymmetric inductions obtained using the ISOVAPOL catalyst for aryl imines as compared to the VANOL catalyst (Table 5.2). The results were quite similar and within the range of experimental error. In fact, both the ligands exhibited similar ees for the reactions of alkyl substituted imines as well (entries 9-12, Table 5.2).

Table 5.3 AZ reaction with imines **78** using *(S)*-ISOVAPOL AND *(R)*-VANOL[a]

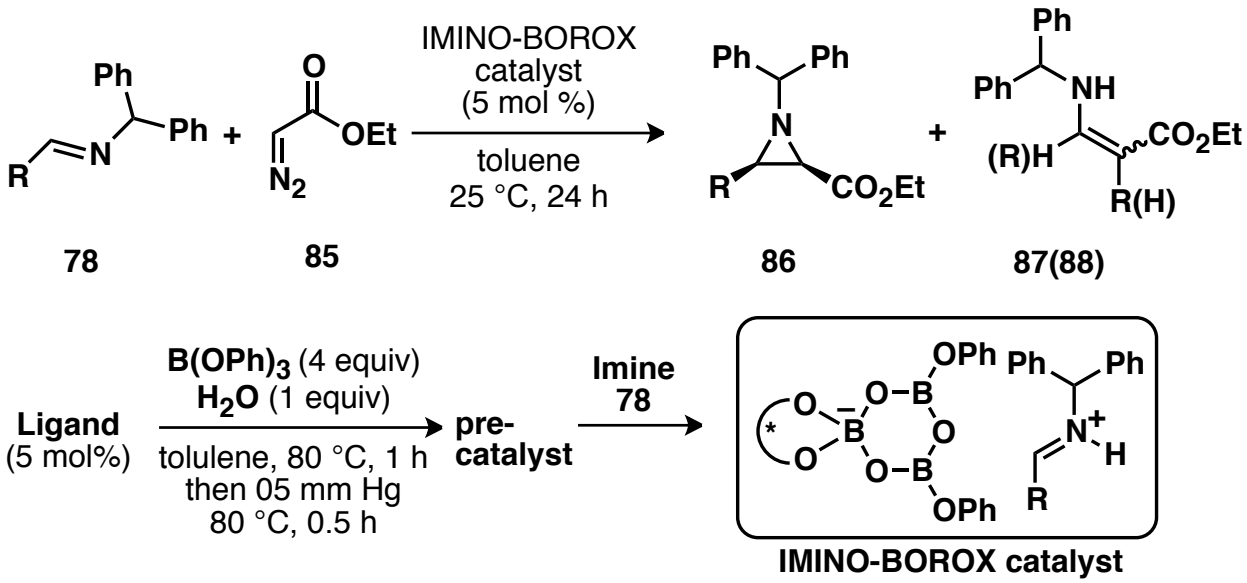

Table 5.3 cont'd

#	Cat	Ligand	R	% conv [b]	Yield **86** (%) [c]	ee **86** (%) [d]	*c:t* [e]	Yield **87(88)** (%) [f]
1	**199a**	(*S*)-ISOVAPOL	C_6H_5	94	82	92	50:1	3/7
2	**189a**	(*R*)-VANOL	C_6H_5	100	87	–89	>50:1	<1/<1
3	**199b**	(*S*)-ISOVAPOL	4-Me-C_6H_4	94	82	94	>50:1	3/7
4	**189b**	(*R*)-VANOL	4-Me-C_6H_4	100	79	–92	>50:1	3/6
5	**199c**	(*S*)-ISOVAPOL	4-MeO-C_6H_4	94	62	89	9:1	<1/6
6	**189c**	(*R*)-VANOL	4-MeO-C_6H_4	100	62	–91	10:1	<1/3
7	**199d**	(*S*)-ISOVAPOL	4-Br-C_6H_4	94	80	94	>50:1	2/6
8	**189d**	(*R*)-VANOL	4-Br-C_6H_4	100	83	–91	50:1	4/6
9	**199e**	(*S*)-ISOVAPOL	*t*-Bu	97	83	84	>50:1	6/<1
10	**189e**	(*R*)-VANOL	*t*-Bu	100	86	–84	>50:1	<1/8
11	**199f**	(*S*)-ISOVAPOL	Cy	100	72	79	>50:1	9/4
12	**189f**	(*R*)-VANOL	Cy	100	70	–77	>50:1	5/4

[a] Unless otherwise specified, all reactions were performed with 1 mmol of imine **78** in toluene (0.5 M in imine **78**) with 1.2 equiv of **85** and 5 mol% of the catalyst at 25 °C. The pre-catalyst was prepared by heating 1 equiv of ligand with 4 equiv of commercial $B(OPh)_3$ and 1 equiv of H_2O in toluene at 80 °C for 1 h, followed by removing all volatiles under high vacuum (0.1 mm Hg) for 0.5 h at 80 °C. [b] Percent conversion is determined by integration of the methine proton of *cis*-aziridine relative to the sp^2-CH proton of the unreacted imine **78** in the ^{1}H NMR spectrum of the crude reaction mixture. [c] Isolated Yield. [d] Determined by HPLC. [e] Ratio determined by integration of the methine protons of *cis*- and *trans*- aziridine in the ^{1}H NMR spectrum of the crude reaction mixture. [f] Determined by integration of the NH signals of enamines relative to the methine proton of *cis* aziridine in the ^{1}H NMR spectrum of the crude reaction mixture.

In conclusion, the new chiral ligand ISOVAPOL **197** was found to be equally good as VANOL and also is potentially less expensive than VAPOL or VANOL. Of course, it may very well behave differently from VAPOL or VANOL in asymmetric reactions other than aziridination. Finally, it adds to the library of the family of vaulted biaryl ligands in our group.

Incidentally, more recently, another group member namely Yong Guan was able to increase the stereoinduction (up to 98% ee) of aziridines from benzhydryl imines **78** by synthesizing a derivative of VANOL called to be 7,7′-*t*Bu$_2$-VANOL **198** (Chapter 2, Table 2.3).

5.2.4 NMR investigation of the BOROX catalysts 191a and 290a

In order to gain the evidence for the generation of the BOROX catalysts **191a** and **290a** from the VANOL and ISOVAPOL ligands, respectively, a series of NMR experiments were performed (Figure 5.3). Various species were identified based on the characteristic peaks i.e. Hx and Hy for VANOL **59** and ISOVAPOL **197** respectively (Figure 5.3A).

The study was started with VANOL **59**. The chemical shift of the proton Hx for VANOL **59** is at δ = 8.35 ppm (m, $CDCl_3$). The method for precatalyst formation involves heating (*S*)-VANOL with 4 equiv of commercial $B(OPh)_3$ and 1 equiv of H_2O of at 80 °C (pre-catalyst method C). This resulted in the generation of a mixture of pyroborate B2 **109** (δ Hx = 8.14 ppm, m, $CDCl_3$), meso-borate B1 **107** (δ Hx = 8.04 ppm, d, $CDCl_3$) and unreacted VANOL **59** in 2.9:1:<0.1 ratio (entry 2, Figure 5.3B). Treatment of this mixture with 1 equiv of the imine **111a** at room temperature within a few minutes results in the conversion of the colorless solution of **107** and **109** to a red solution of boroxinate **191a** (δ Hx = 8.55 ppm, d, J = 9.0 Hz, $CDCl_3$) (entry 3, Figure 5.3B). Also, the IMINO-BOROX catalyst **191a** has a sharp absorption at δ = 6.09 ppm in ^{11}B NMR (entry 2, Figure 5.3D). It must be noted that the ratio of B2 **109**: B1 **107**: unreacted VANOL **59** are 2.8:1:<0.1, 2.2:1:0.5 and 2.0:1:0.3 with pre-catalyst methods A (ligand:$B(OPh)_3$

= 1:3) , B (ligand:$B(OPh)_3$:H_2O = 1:3:3) and D (ligand:BH_3•Me_2S:PhOH:H_2O = 1:2:3:1) respectively (not shown here).

Figure 5.3 (**A**) Treatment of (*S*)-**59** and (*S*)-**197** with $B(OPh)_3$ and imine **111a**. (**B**)[a] ^1H NMR spectra of the reaction mixture in $CDCl_3$. (**C**) ^1H NMR spectra (methyl and methoxy region) corresponding to the entry 3 and 6 in ^1H NMR spectra in Figure 5.3B. (**D**) ^{11}B NMR spectra corresponding to entries 2,3,5 and 6 in the ^1H NMR spectra in Figure 5.3B.

A

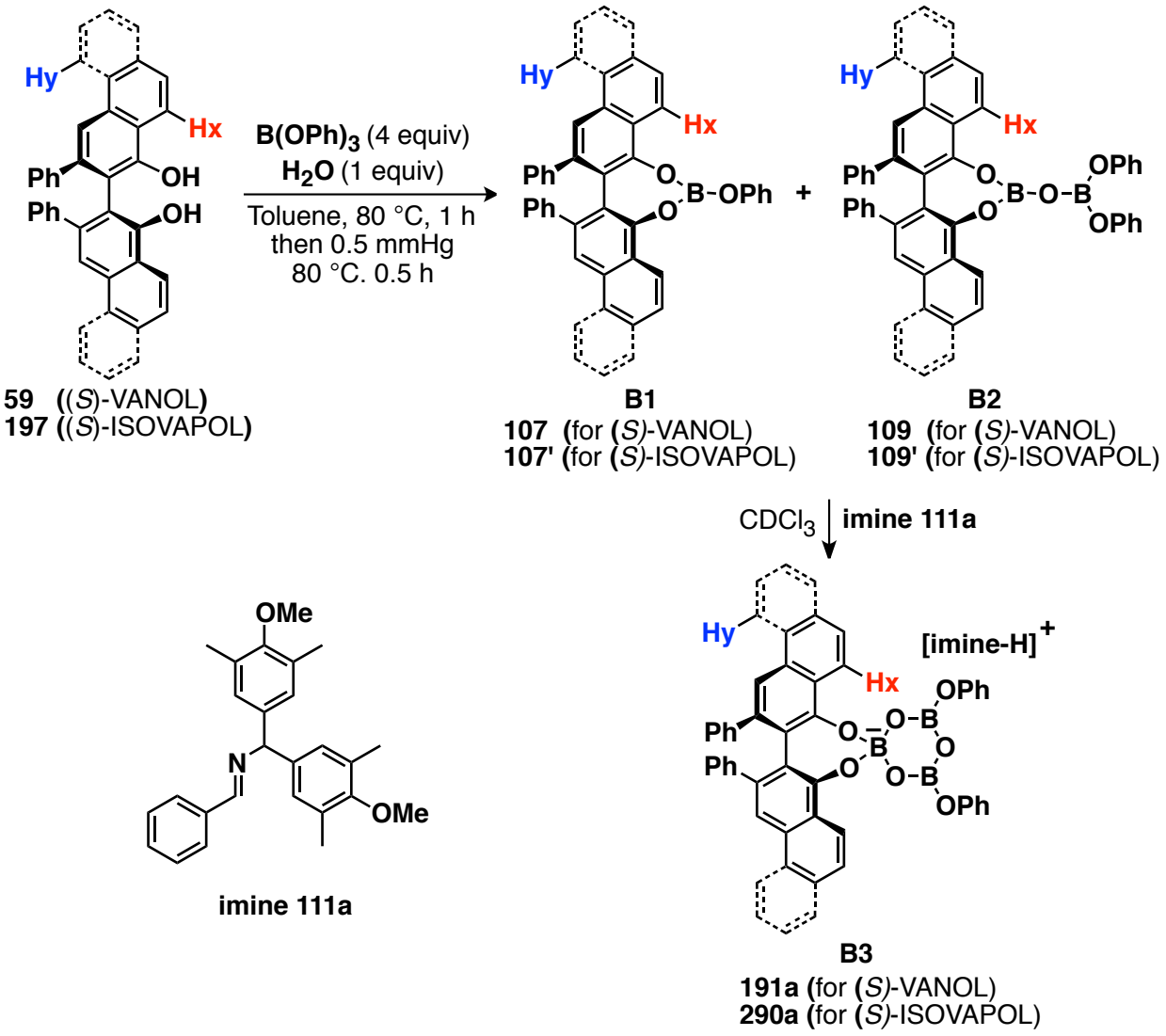

Figure 5.3 cont'd

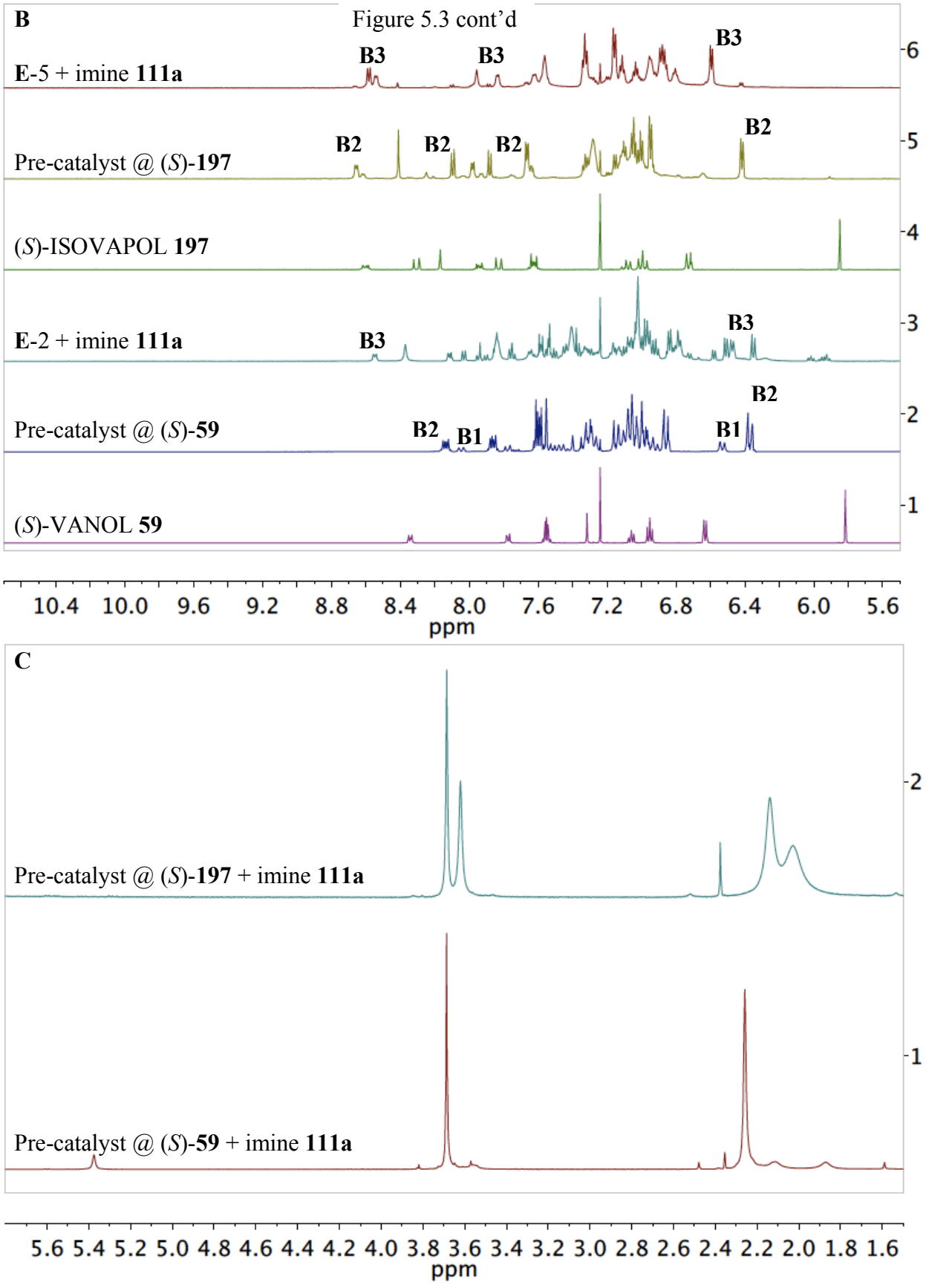

Figure 5.3 cont'd

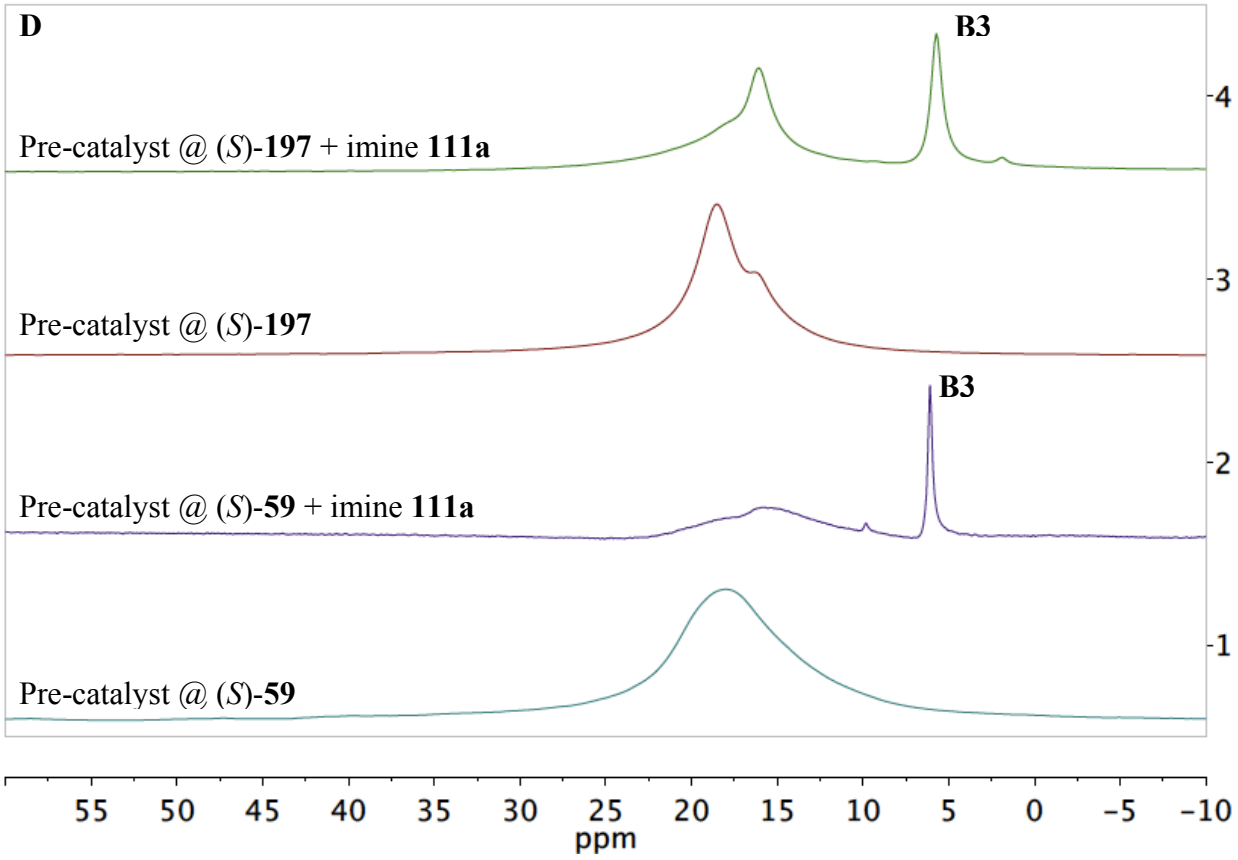

[a] Note for Figure 5.3B: Entry 1: pure (*S*)-**59**. Entry 2: (*S*)-**59** (0.1 mmol) plus 4 equiv $B(OPh)_3$ and 1 equiv H_2O were heated at 80 °C in toluene for 1 h followed by removal of volatiles under vacuum for 0.5 h. Entry 3: 1.0 equiv of imine **111a** was added to the entry 2 (pre-catalyst) for 10 min at 25 °C. Entry 4: pure (*S*)-**197**. Entry 5: (*S*)-**197** (0.1 mmol) plus 4 equiv $B(OPh)_3$ and 1 equiv H_2O were heated at 80 °C in toluene for 1 h followed by removal of volatiles under vacuum for 0.5 h. Entry 6: 1.0 equiv of imine **111a** was added to the entry 2 (pre-catalyst) for 10 min at 25 °C.

Similarly, we were able to identify pyroborate B2 **109′** (δ Hy = 8.65 ppm, $CDCl_3$) for ISOVAPOL **197** (entry 5, Figure 5.3B) using precatalyst method C (ligand:$B(OPh)_3$:H_2O = 1:4:1). A new doublet was observed at δ = 8.58 ppm (J = 8.8 Hz, $CDCl_3$) for proton Hy for the boroxinate **290a** when 1 equiv of imine **111a** was added (entry 6, Figure 5.3B). There are many other characteristic peaks in boroxinate **290a** and are shown in entry 6 of Figure 5.3B. Additionally, a peak at δ = 5.72 ppm in the ^{11}B NMR spectrum further supports the formation of **290a** (entry 4, Figure 5.3D). The presence of a single doublet in the both boroxinate complexes indicates that the exchange of the iminium ion from the top face of the catalyst to the bottom is fast on the NMR time scale. A striking difference between the two boroxinates **191a** and **290a** was that the splitting in the methyl and methoxy region of the MEDAM group was missing in the case of VANOL ligand derived catalyst **191a** (Figure 5.3C). The splitting of methyl and methoxy into two singlets has been observed for VAPOL derived catalysts (Chapter 2). The chemical shifts of the protons associated with the nitrogen of the protonated imines in the complexes **191a** and **290a** are δ = 13.74 ppm and δ = 13.67 ppm respectively.

5.2.5 Calculated structure of BOROX catalyst 290a derived from ISOVAPOL (*S*)-197

The structure of the IMINO-BOROX **290a** was explored using DFT calculations. Calculations were performed using Gaussian ′03 at B3LYP/6-31g* level of theory.[24] The predicted structure is shown in Figure 5.4. Several non-covalent interactions (CH-π and π–π) between imine and arene rings of the ISOVAPOL **197** are observed (Figure 5.4).

Figure 5.4 Calculated structure of IMINO-BOROX catalyst **290a** using Gaussian ′03. Calculated B3LYP/6-31g* structure visualized by the Mercury Program (C, gray; O, red; N, blue; B, pink). Hydrogen atoms omitted for clarity (except N-H). Some secondary interactions are highlighted: d_1 = 1.72 Å (H-bonding), d_2 = 4.02 Å (CH-π), d_3 = 4.10 Å (CH-π or π-π stack), d_4 = 4.54 Å (CH-π), d_5 = 4.02 Å (CH-π).

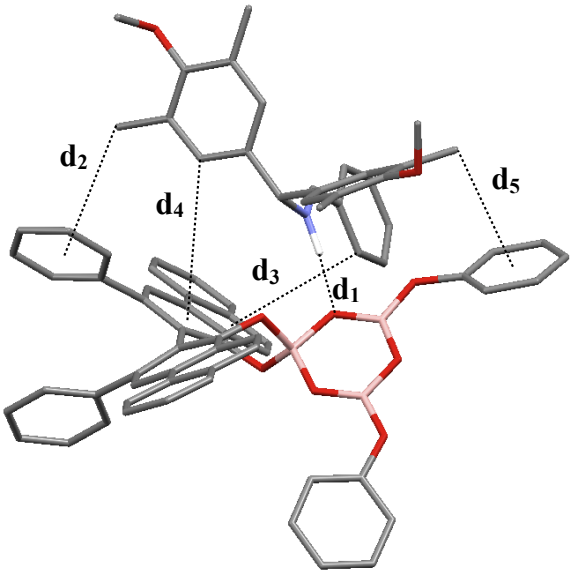

5.2.6 X-ray crystal structure of ISOVAPOL (*S*)-197 and VANOL (*R*)-59

Normally, ISOVAPOL is purified by silica gel chromatography rather than crystallization. In the process of purification of the ISOVAPOL, a few crystals were formed serendipitously. The crystals were then subjected to the X-ray diffraction analysis. The ORTEP diagram of the crystal structure of ISOVAPOL (*S*)-**197** is shown in Figure 5.5A. As was the case in the crystal structure of VAPOL (*S*)-**58**,[25] the solid state form of ISOVAPOL (*S*)-**197** lacks intermolecular hydrogen bonding that prevails for BINOL. The dihedral angle between the phenanthrene rings of the (*S*)-**197** is 70.6°. It varies from 80.1° to 88.5° in the case of VAPOL.[25] The dihedral angle is <90° corresponds to the cisoid conformation,[26,27] which alters

the preferred packing motif. Also, as in the case of VAPOL,[25] the hydroxyl groups are buried in the pocket created by the phenanthrene rings of the (*S*)-**197**. The steric repulsion of these phenanthrene groups inhibits possible hydrogen bonding. Similar observation was made with the X-ray crystal structure of VANOL (*R*)-**59**. Three conformations of the unit cell were observed with the dihedral angles 69.6°, 74.6°, 76.9° respectively (Figure 5.5B). This classifies VANOL (*R*)-**59** to be a cisoid conformation and also, like VAPOL and ISOVAPOL, it lacks inter molecular hydrogen bonding.

Figure 5.5 (**A**) ORTEP drawing of X-ray crystal structure of (*S*)-**197** and ORTEP drawing of crystal packing of (*S*)-**197** along b-axis. (**B**) ORTEP drawing of X-ray crystal structure of all three conformations (in the unit cell) of (*R*)-**59** and ORTEP drawing of crystal packing of (*R*)-**59** along b-axis.

A

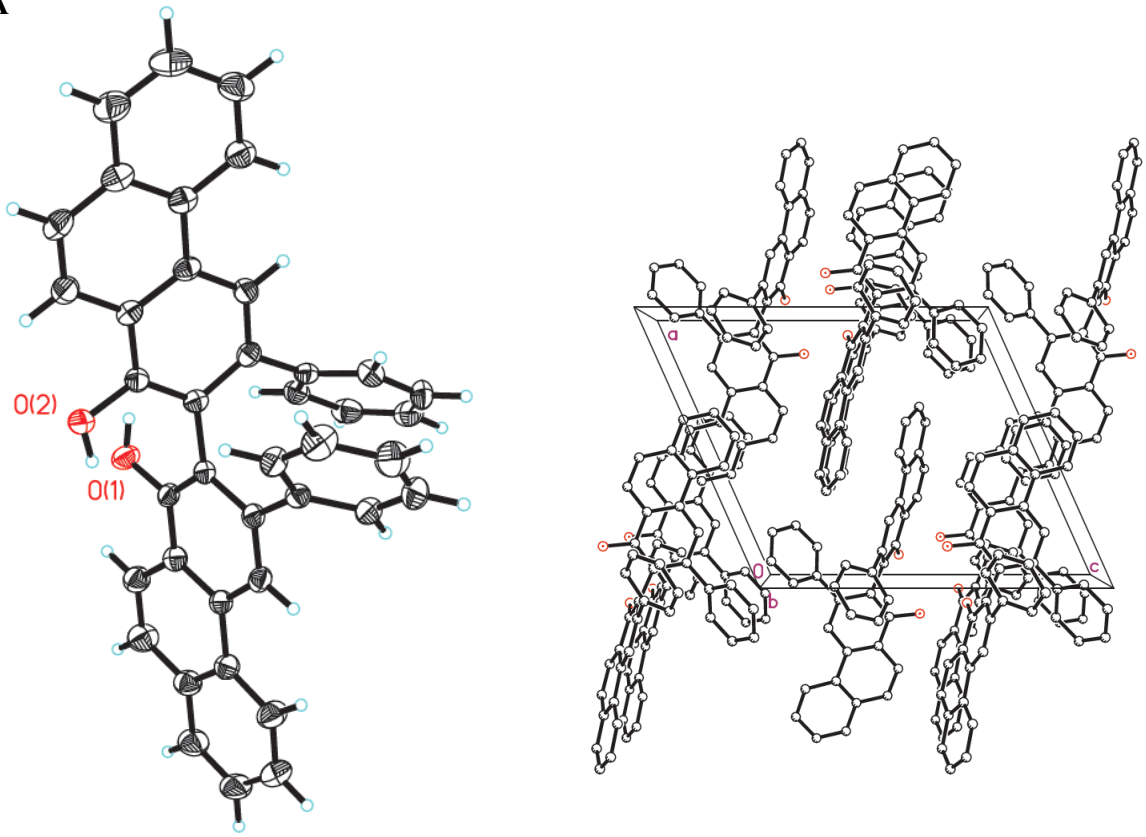

Figure 5.5 cont'd

B

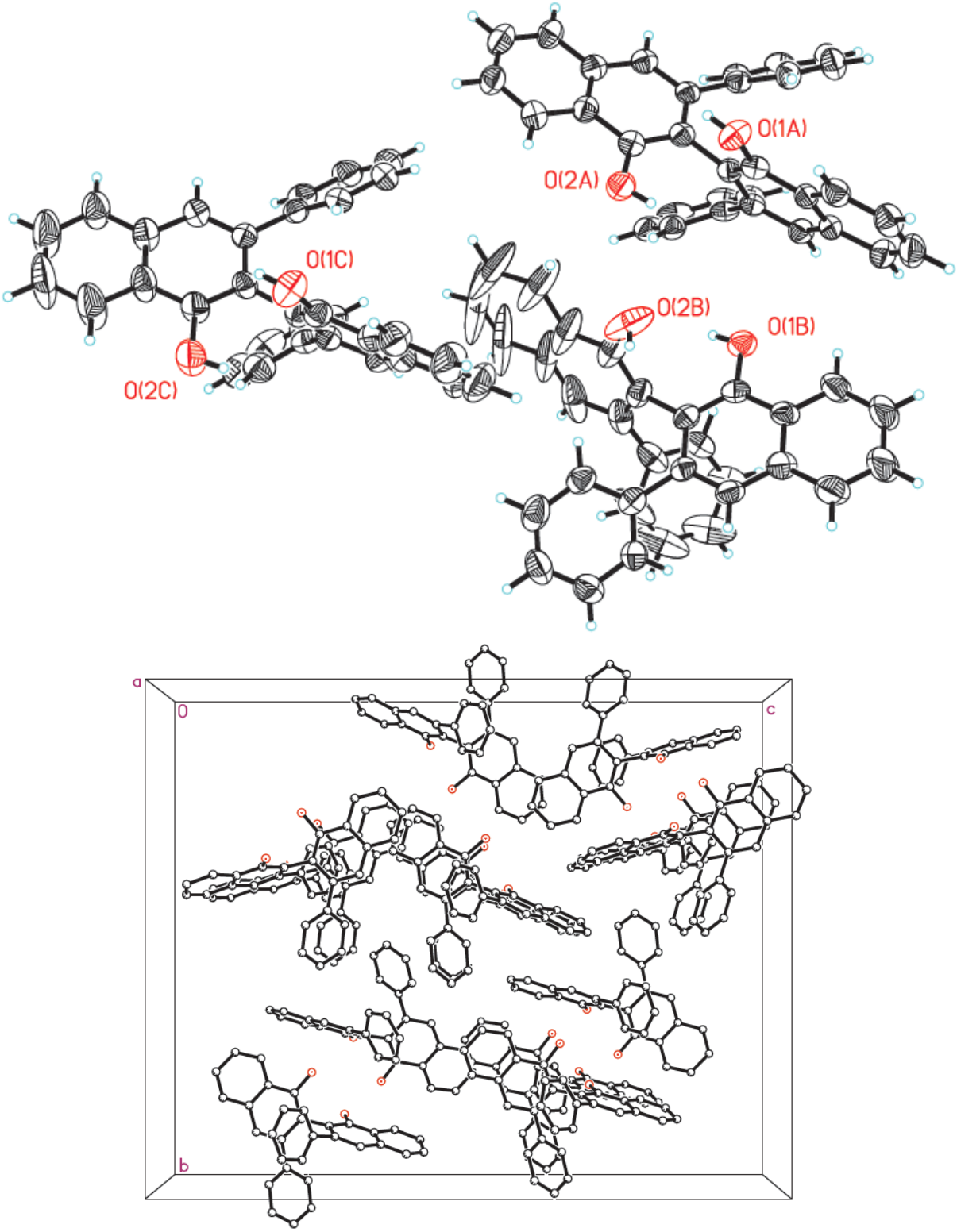

It must be remembered that in the case of BINOL, hydrogen bonding occurs in both the enantiopure and racemic crystal structures.[28] The dihedral angle between the naphthalenes of all known solid-state forms of BINOL is >90° which is referred to transoid conformation.[27]

5.3 BINOL and its derivatives

Up till now, our efforts have revealed the very important role that BOROX catalysts have in chemistry of vaulted biaryl ligands. Thereafter, it was deemed important to examine the role that linear biaryl ligands can play in BOROX catalysis. Prior to the evolution of vaulted biaryl ligands, BINOL **55**, a C2-symmetric linear biaryl ligand, has been widely used in a variety of asymmetric reactions.[29] However, one of the major reasons for the ineffectiveness of BINOL in inducing high asymmetric inductions in many reactions is the positioning of the major groove directly opposite to the active site containing the phenol functions (Figure 5.6C). This led us to design a new family of vaulted biaryl ligands where there is a substantially larger pocket around the active site due to the relocation of the major groove (Figure 5.6C). Previous solutions to this limitation of BINOL involved enhancing the chiral pocket around the active site. This approach involves the introduction of the substituents at 3- and 3′- positions of BINOL thereby generating the new BINOL derivatives **56** (Figure 5.6C).[30]

Figure 5.6 (**A**) Vaulted biaryl ligands (**B**) Linear biaryl ligands (**C**) Location of major and minor groove in vaulted and linear biaryl ligands.

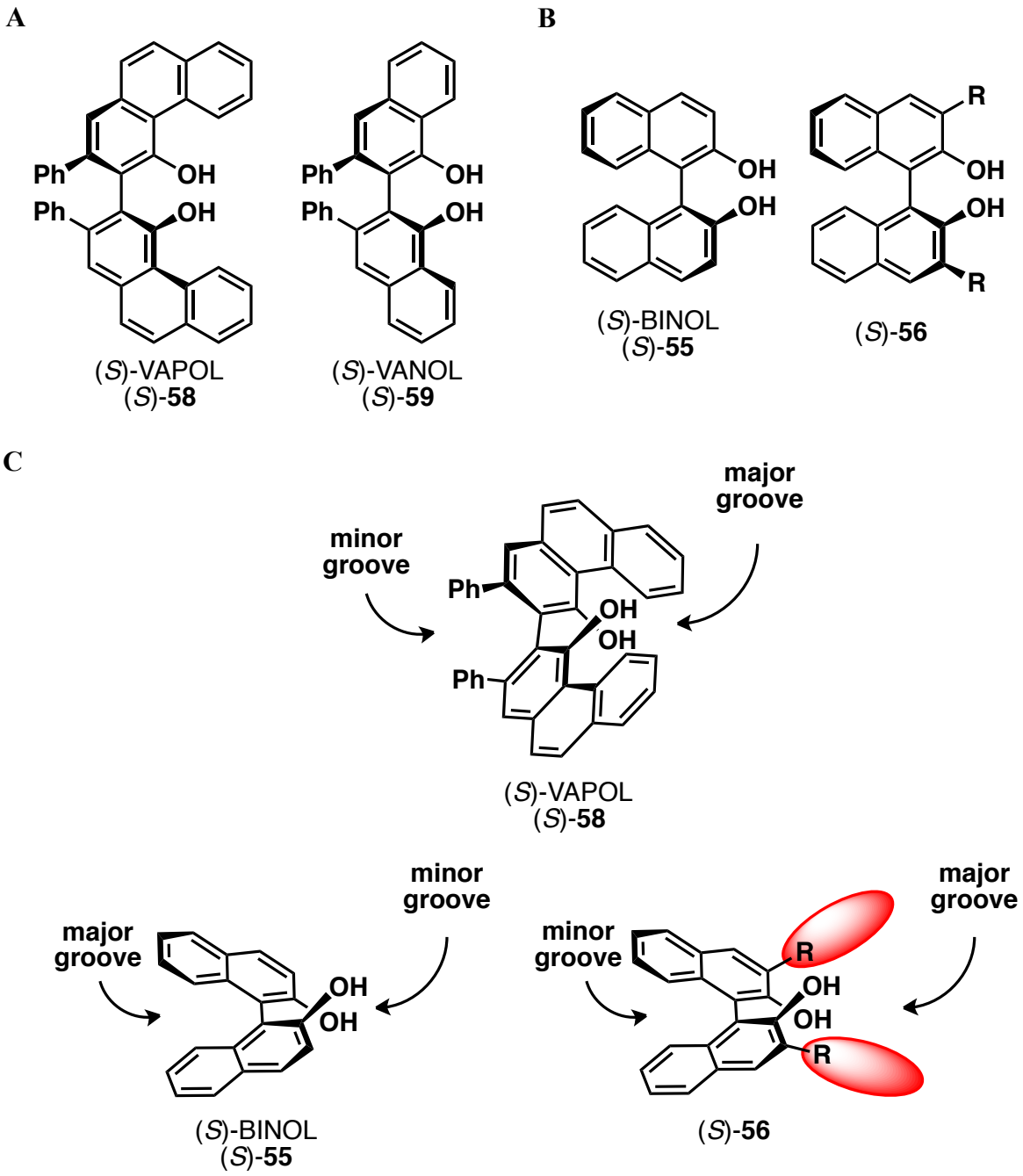

A few of the most common structural types reported for borate esters of BINOL and its derivatives are shown in Scheme 5.4. The reaction of BINOL with 1 equiv of $B(OPh)_3$ has been

reported to give a compound for which the most probable structure was suggested to be the mesoborate **293** but other possible structures could not be excluded (Scheme 5.4A).[31,32] This compound has been examined as a catalyst for Mannich and heteroatom Diels-Alder reactions of imines,[31,33] the heteroatom Diels-Alder reactions of aldehydes,[34] Diels-Alder reactions[35] and aldol reactions.[36] The reaction of BINOL with 0.5 equiv of $B(OPh)_3$ or $B(OMe)_3$ has been reported to give the spiroborate **20**-H (Scheme 5.4A). As discussed in Chapter 4, the structure **20**-H has been suggested to function as a chiral Lewis acid catalyst for a number of reactions including Mannich reactions,[33g,37] heteroatom Diels-Alder reactions of imines,[33g,38] and Pictet-Spengler reaction.[39] The catalytic function of **20**-H was proposed to be as a chiral Lewis acid where interaction with a Lewis base disrupts one of the boron-oxygen bonds to give the Lewis acid-Lewis base complex **71** (LB = imine) or **71′** (LB = nitrone).[33g,39a] It must be noted evidence was presented that this complex functions as a Brønsted acid catalyst in reactions with imines and as Lewis acid in reactions of nitrones (Chapter 4). There has been considerable interest in the chiral anion unit in **20**-H and the sources of interest include use as a vehicle for the resolution of BINOL,[40] as a structural unit in solution and in the solid state,[41] as a chiral shift reagent,[42] and also as a chiral counterion catalyst in aziridination reactions,[43] in cyclopropanation reactions,[43] in Friedel-Crafts reactions,[44] in hydrogenations,[45] and in ring-opening of meso aziridiniums.[44]

Scheme 5.4 Common borate esters of (**A**) BINOL **55** and (**B**) BINOL derivatives **55** and **89**

A

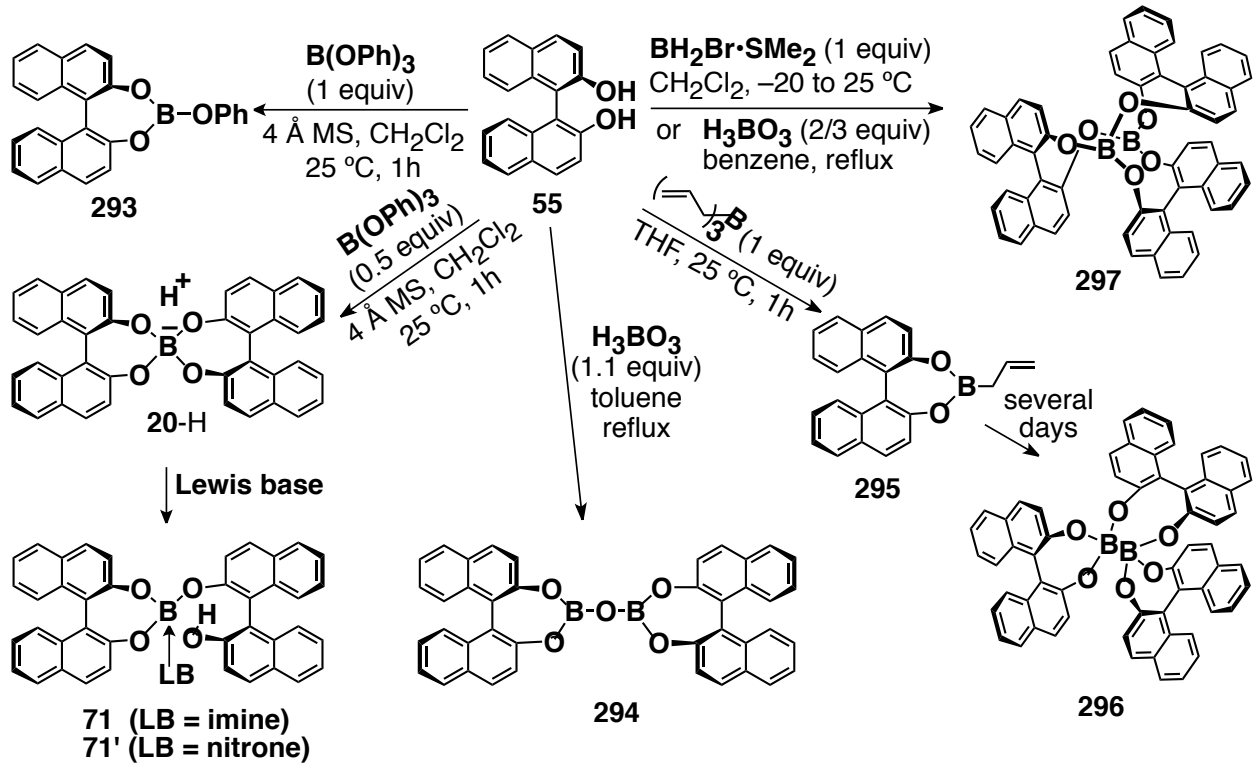

B

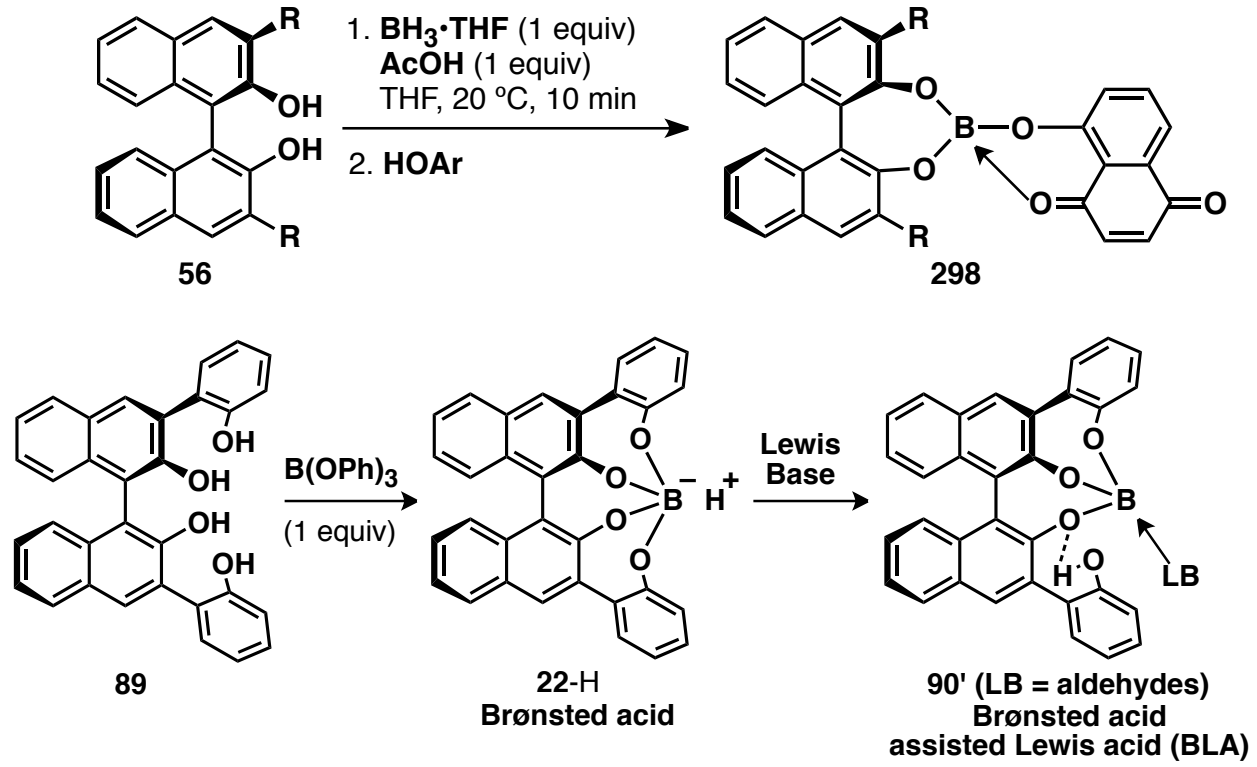

The intriguing propeller-like structure **297** was discovered by Kaufmann and Boese when they reacted BINOL with 1 equiv of $BH_2Br•SMe_2$ complex (Scheme 5.4A).[35] This bis-triaryl borate was isolated in nearly quantitative yield and contains a [6.6.6]-propellane unit composed of three units of BINOL and two borons and was characterized by X-ray diffraction. This complex has been shown to give high asymmetric inductions in Diels-Alder reactions as a chiral Lewis acid, however, as might be expected, the rates of reaction are quite slow.[35,46] A very similar structure **296** (an isomer of **297**) is reported by De-jun and coworkers (Scheme 5.4A).[47] This compound was also found to be composed of three units of BINOL and two borons and was characterized by NMR spectroscopy. It was reported to be formed due to the decomposition of the allyl-boronate **295** on being kept for several days. Another interesting structure that has been reported is the pyroborate **294,** which was reported to form upon refluxing BINOL with 1.1 equiv of boric acid in toluene (Scheme 5.4A).[48] The pyroborate **294** was characterized by combustion analysis and by IR spectroscopy and was used in the resolution of BINOL. The veracity of the structural assignment of **294** has been called into question as it has been reported that heating BINOL and 0.66 equiv of boric acid in benzene gives rise to the Kaufmann's propeller **297**.[40a] There are some examples of the borates derived from BINOL derivatives (Scheme 5.4B). In this case, perhaps the earliest and most widely used class of triaryl borates are those that have internal chelation of the boron to a quinone moiety. Kelly first prepared borates of the type **298** in 1986 for the purpose of effecting an asymmetric Diels-Alder reactions on naphthoquinones (Scheme 5.4B).[49] Also, the reaction between the BINOL derivative **89** and 1 equiv of $B(OPh)_3$ or $B(OMe)_3$ has been reported to give the fused-spiroborate **22**-H (Scheme

5.4B and Chapter 4).[50] Similar to **20**-H, the structure **22**-H has been suggested to function as a chiral Lewis acid catalyst for asymmetric Diels-Alder reaction between dienes and enals/alkynals.[50]

Gang Hu, one of the former group members, initiated the study of BINOL derived BOROX catalysts and this is summarized in Scheme 5.5B (method C).[51] Analogous to the reaction of the vaulted ligand VAPOL (Scheme 5.5A), he obtained the borate species B2 **299a**/**299b** in major quantities (Scheme 5.5B) when BINOL **55** was subjected to the conditions optimized for the generation of B2 borate of VAPOL (ligand:$B(OPh)_3$:H_2O = 1:4:1, method C, Chapter 2). Although a single species, NMR and mass spectroscopic analysis could not distinguish between the alternatives structures of **299a** and **299b**. A mixture of B3 BOROX catalyst **300** (imine = **78**) /**301** (imine = **111**) and spiroborate ion-pair **302** (imine = **78**) /**303** (imine = **111**) was obtained upon the addition of 1 equiv of imine **78**/**111** to the species B2. It was suggested that, the presence of more than one catalytic species explains the low asymmetric induction (13-20% ee) obtained in the case of the aziridination reaction with imine **78a** with BINOL as the ligand (Table 5.4, entries 1-2).[52] When the conditions optimized for B1 (ligand:$B(OPh)_3$ = 1:1 or ligand:BH_3•Me_2S:PhOH = 1:1:1) were applied, Gang Hu found that a complex mixture of B1 **293**, B2 **299a**/**299b** and Kaufmann's propeller **297** was formed. A clean generation of B2 **299a**/**299b** was obtained on employing B2 conditions (ligand:BH_3•Me_2S:PhOH:H_2O = 1:2:3:1). In the absence of PhOH (ligand:BH_3•Me_2S = 1:1 or 1:0.5 or 1:0.66**),** Kaufmann's propeller **297** is observed as the primary product. Up till this point,

all the observations were made by Gang Hu. As the boroxinate involves three boron atoms, we then thought to use 3 equivalents of BH_3•Me_2S. As a part of this doctoral research, it was found that employing conditions (ligand:BH_3•Me_2S:PhOH:H_2O = 1:3:2:3) optimal for B3 generation also resulted in the formation of B2 as the major species prior to the addition of imine **111a** (Figure 5.12A, entry 4). Also, as a part of this doctoral research, the structure of **263**/**264** was deduced based on the X-ray analysis of similar compound (Chapter 4).

Scheme 5.5 BOROX catalysts from (**A**) (*S*)-VAPOL **58** and (**B**) (*R*)-BINOL **55**

A

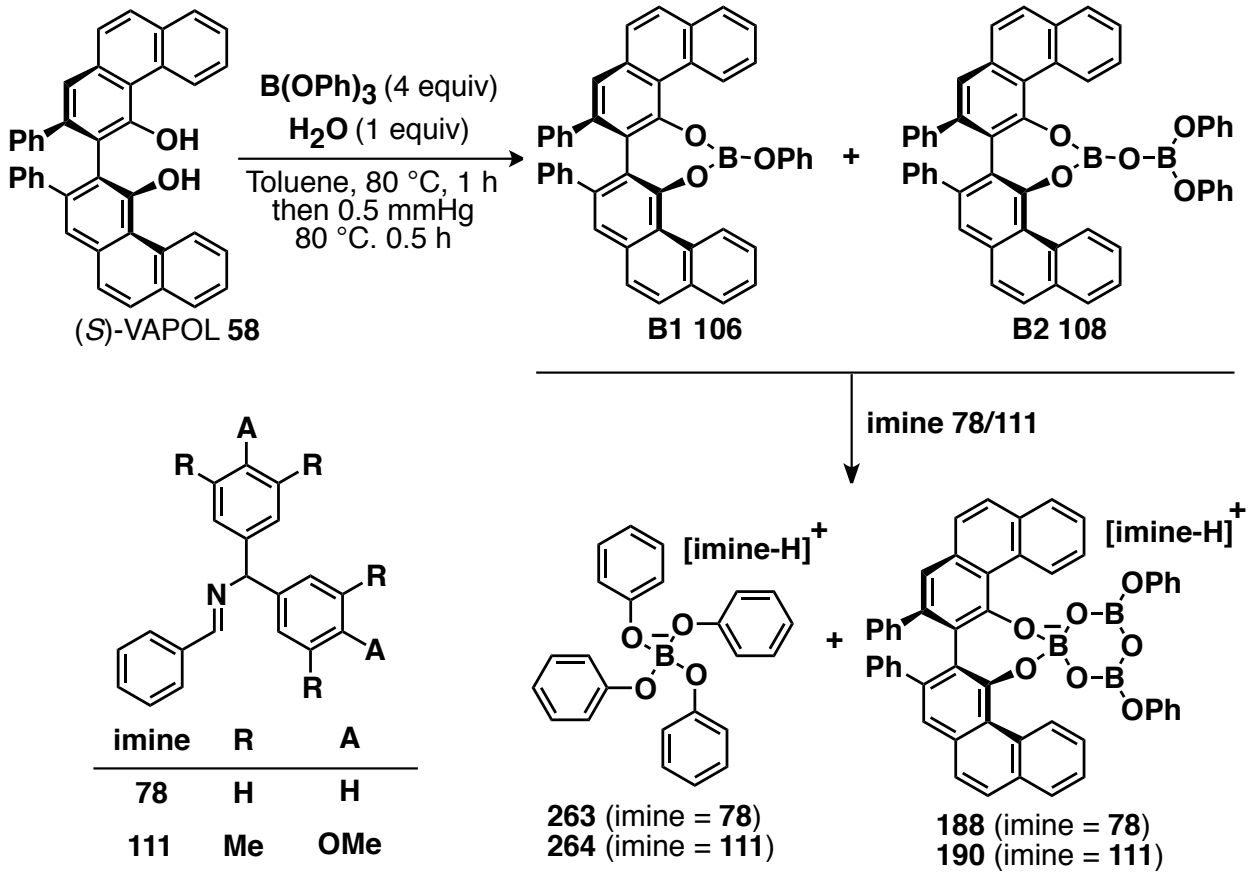

imine	R	A
78	H	H
111	Me	OMe

Scheme 5.5 cont'd

B

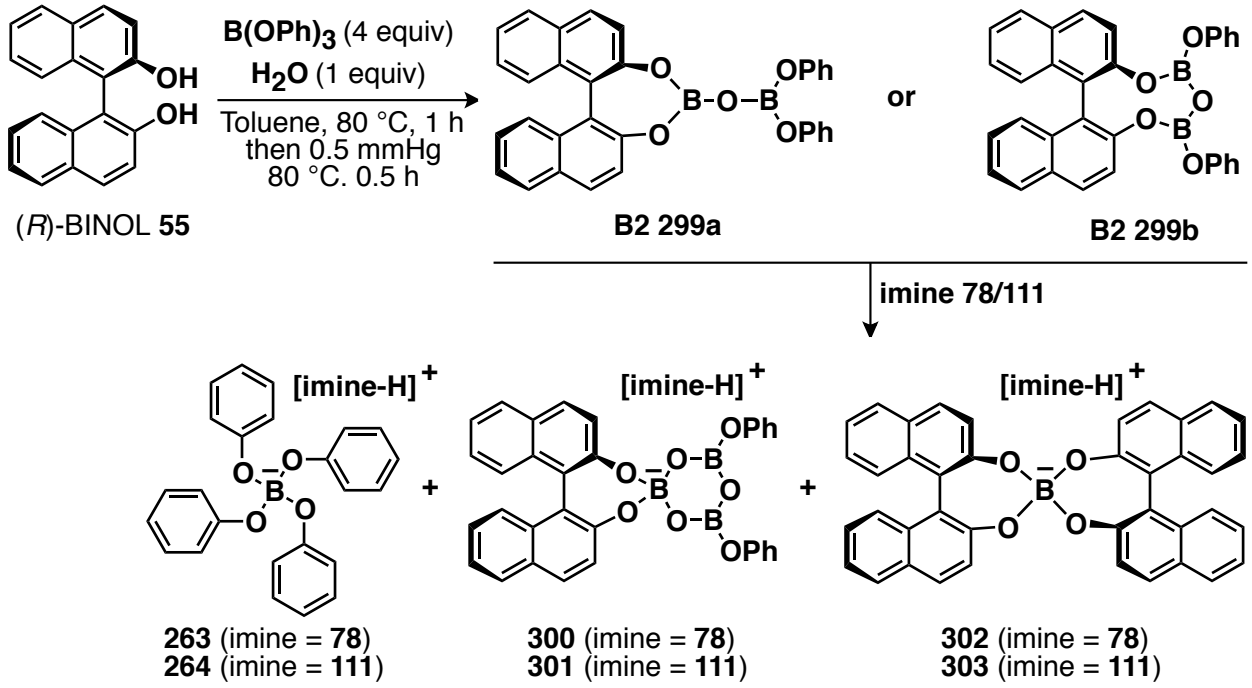

Later on, another former group member namely Li Huang, was able to obtain the BOROX catalyst in a clean fashion when employing 3,3′-Ph_2-BINOL derivative **56a** as the ligand.[53] Also, a significant increase in asymmetric induction (75-76% ee) was observed when **56a** was used as the ligand in asymmetric aziridination relative to unsubstituted BINOL **55** (Table 5.5, entries 3-4). However, in 2011, Chen and coworkers reported a huge drop in enantioinduction (34% ee) when they performed the Wulff asymmetric aziridination reaction between EDA and imine **78x** derived from *p*-(methylsulfonyl)benzaldehyde and benzhydryl amine **126a** using the BOROX catalyst derived from ligand **56a** (Table 5.4, entry 3).[54] In this case, it must be noted that the reaction was performed at –10 °C using $B(OH)_3$ as the boron source. In the search for more diversity in the BOROX catalyst, for increased mechanistic

understanding and for improvement in the aziridination with benzhydryl imines **78**, we decided to screen several BINOL derivatives of the type **56**. The synthesis of these ligands and their effect on the aziridination reaction is discussed below.

Table 5.4 AZ reaction with the catalysts derived from various ligands (Chen's work) [a]

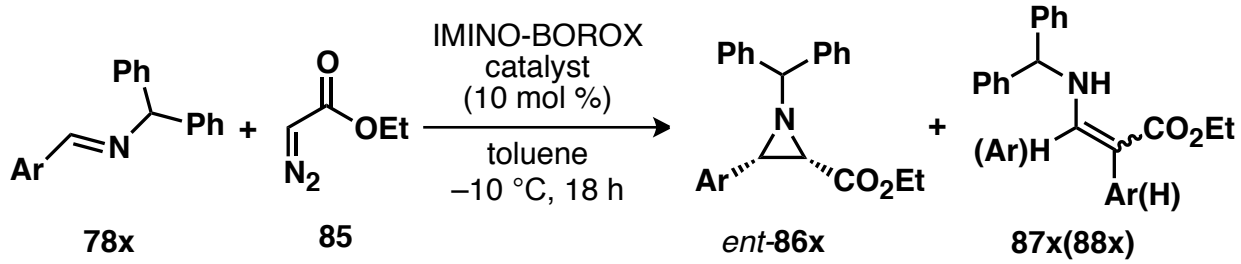

78x **85** *ent*-**86x** **87x(88x)**

Ar = 4-SO_2Me-C_6H_4

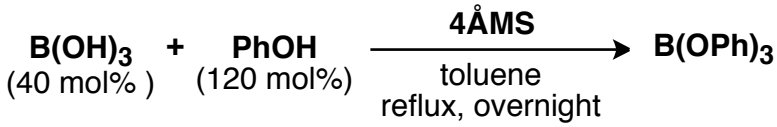

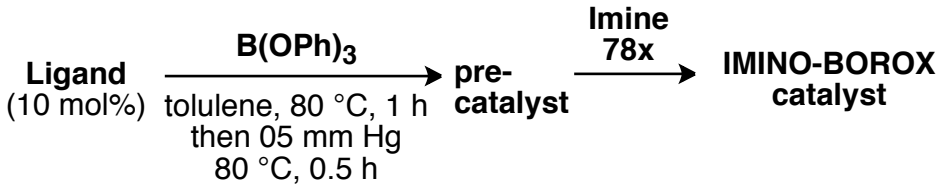

#	Ligand	Cat	Yield *ent*-**86x** (%) [b]	ee *ent*-**86x** (%) [c]	*cis:trans* [d]
1	(*R*)-VAPOL **58**	**188x**	92	84	>50:1
2	(*R*)-VANOL **59**	**189x**	93	85	>50:1
3	(*R*)-3,3′-Ph_2-BINOL **56a**	**304x**	85	34	>50:1
4	(*R*)- 3,3′-(9-anthracenyl)$_2$-BINOL **56i**	**305x**	86	0	>50:1
5 [e]	(*R*)- 3,3′-($SiPh_3$)$_2$-BINOL **56g**	**306x**	–	–	–
6 [e]	(*R,R*)- TADDOL **61a**	**307x**	–	–	–

[a] Unless otherwise specified, all reactions were performed with 1 mmol of imine **78x** in toluene (0.5 M in imine **78x**) with 1.1 equiv of **85** and 10 mol% of the catalyst at –10 °C. [c] Isolated yield. [d] Determined by HPLC. [e] Ratio determined by integration of the methine protons of *cis* aziridine in the ^{1}H NMR spectrum of the crude reaction mixture. [e] The reaction mixture was stirred at –10 ºC for 18 h and then at 25 ºC for another 18 h.

5.3.1 Preparation of BINOL derivatives

Based on both steric and electronic factors, we chose the five BINOL derivatives **56a**, **56d**, **56e**, **56f** and **56i** in our study (Scheme 5.7-5.9). Their syntheses all began with the protection of the hydroxyl units in BINOL by reaction with methyl iodide in the presence of a base.[49b,55] The resulting dimethoxy BINOL **258** was then treated with *n*BuLi to afford the bis-ortho-metalated intermediate, which was further reacted with I_2 or Br_2 to give **259**[56] or **308**[49b,55] in high yields. Thereafter, BINOL derivatives **56d**[57] (R = Br) and **56e**[58] (R = I) were easily obtained by subsequent demethylation using BBr_3 (Scheme 5.7).

Scheme 5.6 Preparation of dimethoxy-BINOL **258**

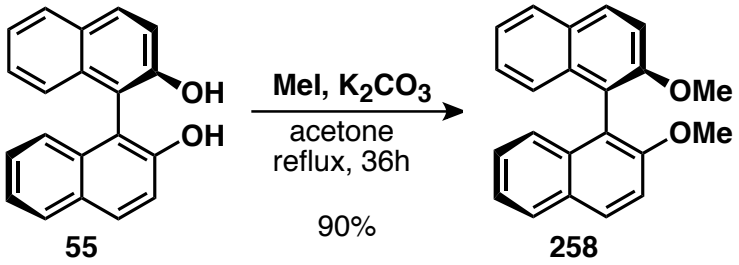

Scheme 5.7 Preparation of BINOL derivatives **56d** (R = Br) and **56e** (R = I)

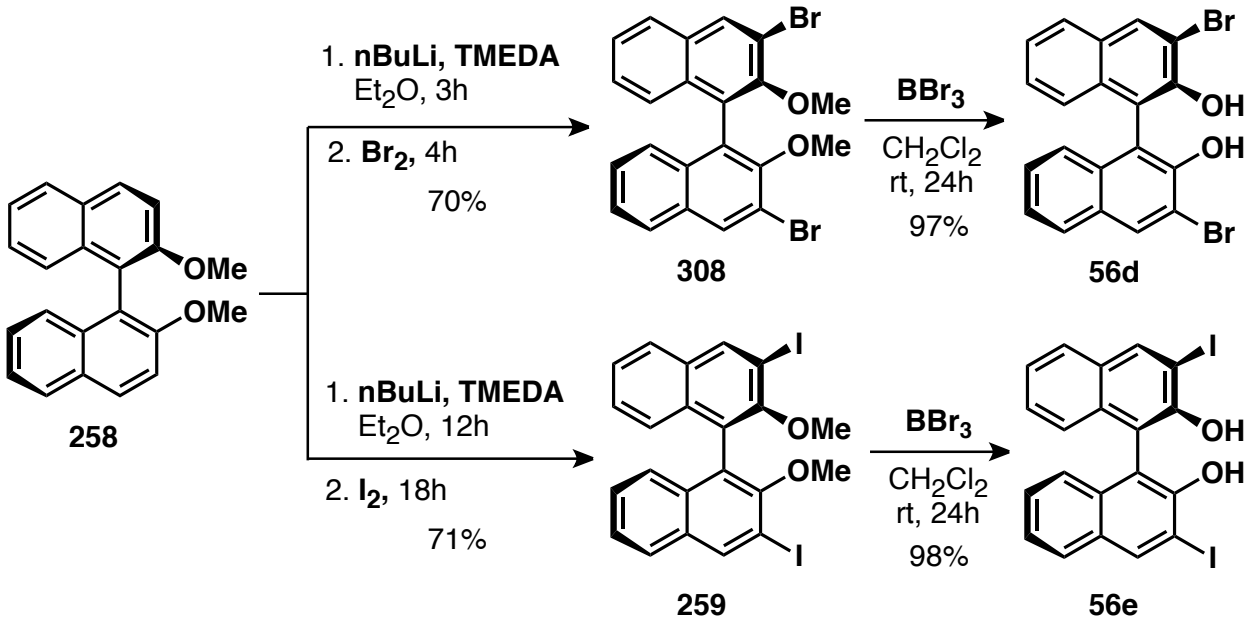

Utilizing Kumada's coupling in the presence of $Ni(PPh_3)_2Cl_2$, BINOL derivatives **56a**[49b,55] (R = Ph) and **56f**[59] (R = TRIP) were prepared in good yields after demethylation of the coupled products (Scheme 5.8).

Scheme 5.8 Preparation of BINOL derivative (**A**) **56a** (R = Ph) and (**B**) **56f** (R = TRIP)

A

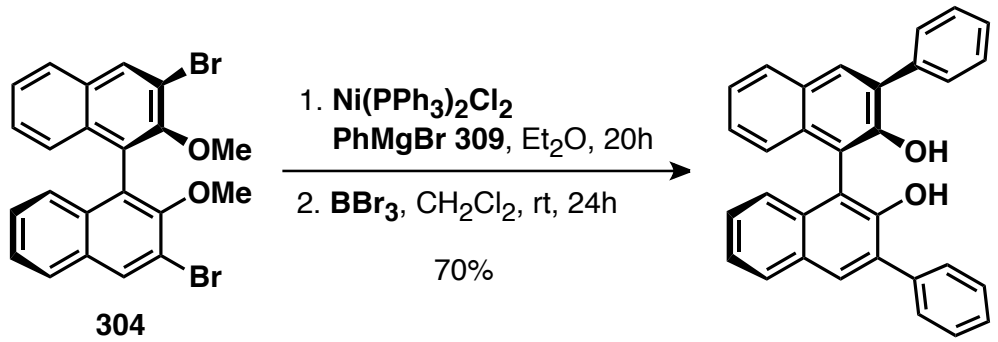

304 **56a**

B

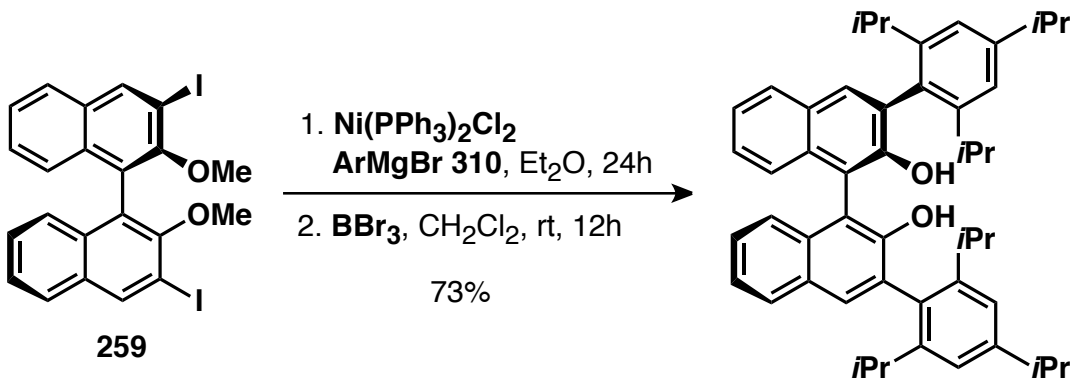

259 **56f**

Finally, BINOL derivative **56i** (R = 9-phenanthryl) was prepared in 71% yield by Suzuki coupling of **259** with 9-phenanthryl boronic acid **311** in the presence of $Pd(PPh_3)_4$ (Scheme 5.9). During the time of this doctoral research, there was no synthesis documented for **56i** despite being a well-used ligand. Hence, we used the procedure reported for the analogous ligand **56j** (R = 9-anthracenyl).[60] However, very recently, Gong and Hu reported the synthesis of **56i** using

the same strategy where they employed bis-MOM protected 3,3′-I_2-BINOL derivative instead of (*R*)-**259**.[61]

Scheme 5.9 Preparation of BINOL derivative **56i** (R = 9-phenanthryl)

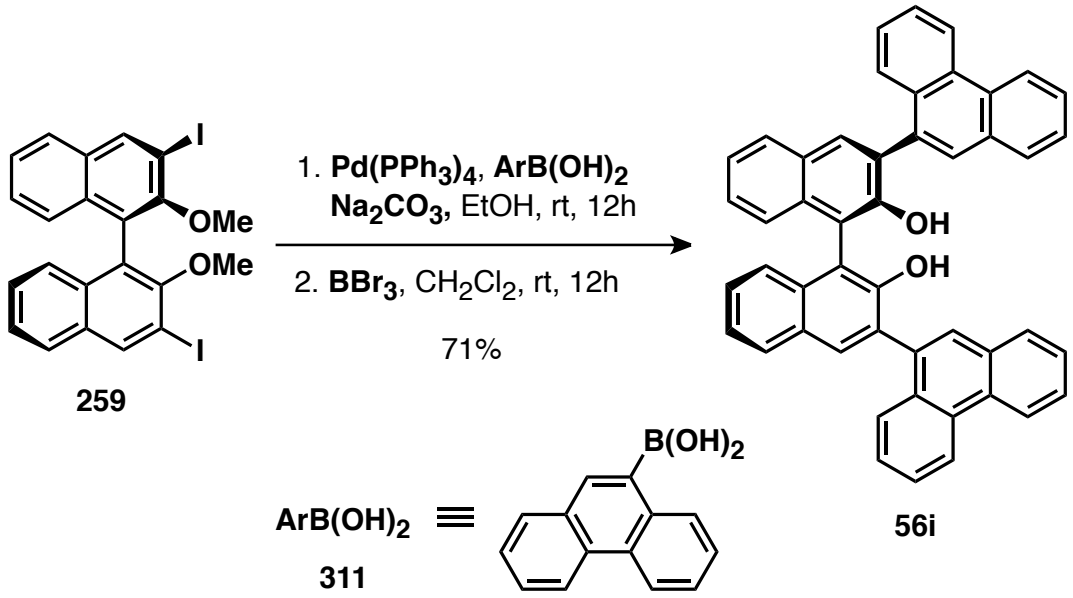

5.3.2 Screening of BINOL and its derivatives on aziridination reaction

The success of the BOROX catalyst derived from the 3,3′-Ph_2-BINOL derivative **56a** in the aziridination reaction (Table 5.5, entries 3-4) encouraged us to screen other substituted BINOL derivatives of type **56**. At the same period, Wipf and co-workers reported a screening of various 3,3′ di-substituted BINOL derivatives for the Wulff catalytic asymmetric aziridination reaction.[62] In their case, the optimized ligand was BINOL derivative **56b** (R = 4-β-Np-C_6H_4), which gave results (Table 5.5, entry 6) similar to the simple phenyl derivative **56a** shown in entries 3 and 4 of Table 5.5. Interestingly, Wipf and coworkers never screened ligand **56a** (R = Ph). Since this was a collaborative project, screening of ligands **56d**, **56g** and **56j** was carried out by Li Huang, a former group member. So, we decided to examine the effect of the electronic

and steric changes in the BINOL derivatives on the catalytic aziridination reaction. Ligands **56d** (R = Br) and **56e** (R = I) were used to probe the electronic effect. Both gave asymmetric inductions in the range of 50's (Table 5.4, entries 8 - 9).

Table 5.5 Asymmetric aziridination with the catalysts derived from various BINOL derivatives [a]

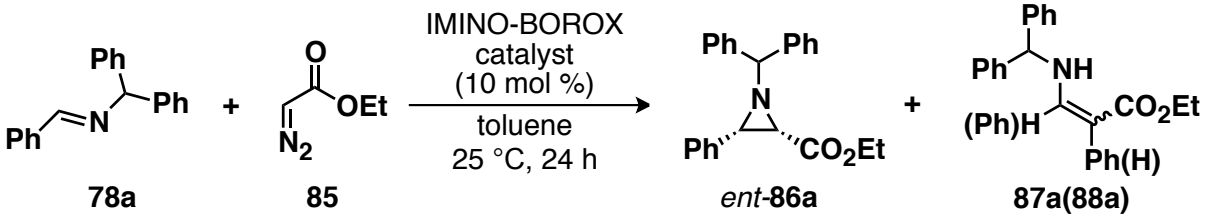

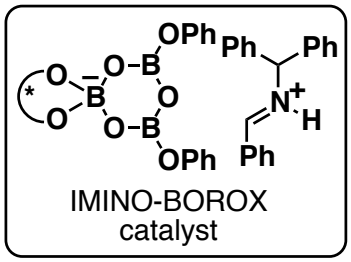

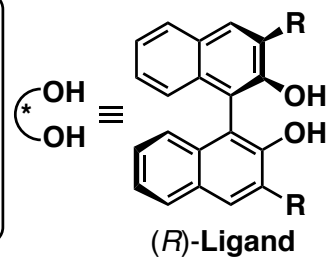

R	Ligand	R	Ligand
H	**55**	2,4,6-*i*Pr$_3$-C$_6$H$_3$	**56f**
Ph	**56a**	SiPh$_3$	**56g**
4-β–Np-C$_6$H$_4$	**56b**	2- naphthyl	**56h**
4-Ph-C$_6$H$_4$	**56c**	9-anthracenyl	**56i**
Br	**56d**	9-phenanthryl	**56j**
I	**56e**		

#	Ligand	R	Cat	Pre-cat. *(met)* [b]	Yield *ent*-**86** (%) [c]	ee *ent*-**86** (%) [d]	*c:t* [e]	Yield **87**/**88** (%) [f]	Reference
1 [g]	(*R*)-**55**	-H	**300a** + **302a**	A′	61	20	17:1	13/9	J. Antilla[52]
2				A	66	13	>50:1	10/7	L. Huang[53]
3	(*R*)-**56a**		**304a**	A	88	75	>50:1	5/4	L. Huang[53]
4				C	90	76	>50:1	4/6	This work
5 [g]	(*R*)-**56b**		**312a**	A′	67	64	>50:1	–	P. Wipf[62]
6				A′	76	78	>50:1	–	P. Wipf[62]

Table 5.5 cont'd

7	(*R*)-**56c**	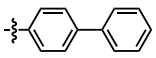	**313a**	A′	68	69	>50:1	–	P. Wipf[62]
8	(*R*)-**56d**		**314a**	C	89	55	>50:1	4/3	L. Huang[53]
9	(*R*)-**56e**		**315a**	C	80	51	>50:1	6/6	This work
10	(*R*)-**56f**	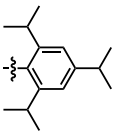	**316a**	A′	59	–1.3	>50:1	7/9	This work
11				C	78	–2.0	>50:1	5/9	This work
12				– [h]	55	–0.4	>50:1	8/10	This work
13	(*R*)-**56g**	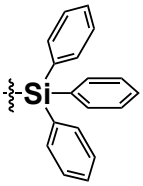	**306a**	C	80	1	>50:1	2/2	L. Huang[53]
14	(*R*)-**56h**	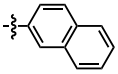	**317a**	A′	63	58	>50:1	–	P. Wipf[62]
15	(*R*)-**56i**	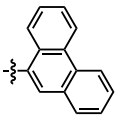	**305a**	C	50	13	15:1	10/11	This work
16	(*R*)-**56j**	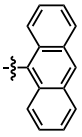	**318a**	C	75	3	25:1	13/10	L. Huang[53]

[a] Unless otherwise specified, all reactions were performed with 1 mmol of imine **78a** in toluene (0.5 M in imine **78a**) with 1.2 equiv of **85** and 10 mol% of the catalyst at 25 °C. [b] Method A: The pre-catalyst was prepared by heating 1 equiv of ligand with 3 equiv of commercial $B(OPh)_3$ in toluene at 80 °C for 1 h, followed by removing all volatiles under high vacuum (0.1 mm Hg) for 0.5 h at 80 °C. Method A′: The pre-catalyst was prepared by heating 1 equiv of ligand with 3 equiv of commercial $B(OPh)_3$ in CH_2Cl_2 at 55 °C for 1 h, followed by removing all volatiles under high vacuum (0.1 mm Hg) for 0.5 h at 55 °C. Method C: Same as Method A except 4 equiv of commercial $B(OPh)_3$ and 1 equiv of H_2O was used. [c] Isolated yield. [d] Determined by chiral HPLC. [e] Ratio determined by integration of the methine protons of *cis* aziridine in the ^1H NMR spectrum of the crude reaction

Table 5.5 cont'd
mixture. [f] Determined by integration of the NH signals of enamines relative to the methine proton of *cis*- and *trans*- aziridine in the ^{1}H NMR spectrum of the crude reaction mixture. [g] Reaction was performed in CH_2Cl_2. [h] In this case, catalyst is directly generated by heating a mixture of 1 equiv of ligand **56f** , 4 equiv of commercial $B(OPh)_3$ and 10 equiv of imine **78a** in toluene at 80 °C for 0.5 h.

An analysis of the ligands screened by Wipf and co-workers revealed that no ligand was examined bearing an ortho substituted aryl ring at the 3,3′ positions.[62] Therefore, we decided to screen ligand **56f** (R = TRIP). Unfortunately, it gave almost no induction irrespective of the method being used (Table 5.5, entries 10-12). This could be due to an inhibition of the formation of a boroxinate complex resulting for catalyst formation from steric hindrance from the ligand. This was further confirmed as a similar result was obtained when ligand **56g** (R = $SiPh_3$) was employed (Table 5.5, entry 13). Chen and coworkers reported no aziridine obtained in the case of the reaction between EDA and the imine **78x** derived from *p*-(methylsulfonyl)benzaldehyde and benzhydryl amine **126a** using the BOROX catalyst **306x** derived from ligand **56g** (Table 5.4, entry 5).[54]

Although no ligand with an ortho-substituted aryl ring at the 3,3′ positions was screened by Wipf and co-workers, they did screen ligand **56h** (R = 2-naphthyl) with meta-substitution that gave 58% ee (Table 5.5, entry 14).[62] In order to validate the observation that ortho substitution would have a detrimental effect on asymmetric induction, we decided to screen ligands **56i** (R = 9-phenanthryl) and **56j** (R = 9-anthracenyl) and as expected, they gave diminished results possibly due to lack of formation of a BOROX catalyst (Table 5.5, entries 15-16). Additionally,

Chen and coworkers reported aziridine **86x** (Table 5.4, entry 4) in 86% yield and 0% ee obtained from reaction between EDA and the imine derived from *p*-(methylsulfonyl)benzaldehyde and benzhydryl amine **126a** using the BOROX catalyst **305x** derived from ligand **56j** (R = 9-anthracenyl).[54]

As discussed earlier (Chapter 2), high asymmetric inductions were obtained in the case of the aziridination reaction mediated by the BOROX catalyst derived from vaulted ligands.[1] Over the years, our aziridination reaction has been further optimized by the fine-tuning of the *N*-protecting group of imines.[1a-1c,63] In the past, these protecting groups have been tested with BINOL as the ligand. With BINOL (*R*)-**55**, the maximum induction obtained was 67% with the BUDAM phenyl imine **112a** (Table 5.6, entry 3).[1b] An increase in asymmetric induction was obtained for the imines **78a**, **111a** and **112a** when ligand **56a** was used to make the catalyst (Table 5.6, entries 4-6). Surprisingly, an asymmetric induction up to 90% was obtained with the BUDAM phenyl imine **112a** when the boron source was switched from $B(OPh)_3$ to $BH_3 \bullet Me_2S$ (Table 5.6, entry 9). However, no significant change was observed for the imines **78a** and **111a**.

Table 5.6 Aziridination with different *N*-protected Imines using (*R*)-**55** and (*R*)-**56a** as ligands [a]

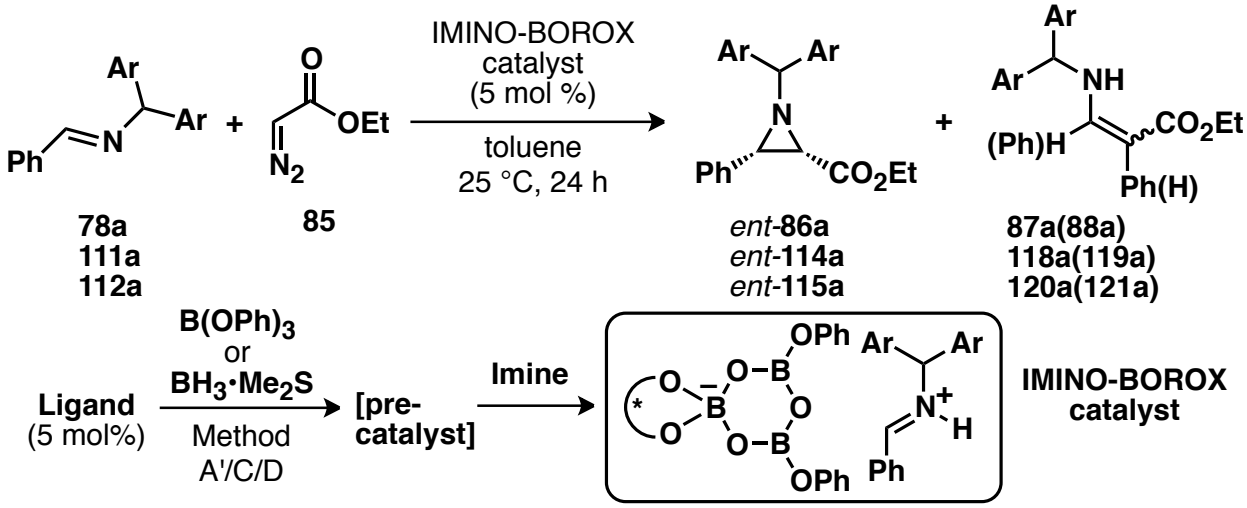

Table 5.6 cont'd

#	Cat	Ligand	Ar_2CH	Pre-cat. *(met)*[b]	Yield azi (%)[c]	ee azi (%)[d]	c:t[e]	Yield enamines (%)[f]
1[g]	**300a**	(*R*)-BINOL	Bh	A′	61	20	17:1	13/9
2[h]	**301a**		MEDAM	C[j]	72	38	17:1	14/10
3[i]	**319a**		BUDAM	A′	71	67	nd	nd
4	**304a**	(*R*)-3,3′Ph_2-BINOL	Bh	C	90	76	>50:1	4/6
5	**320a**		MEDAM	C	89	79	>50:1	2/6
6	**321a**		BUDAM	C	88	76	>50:1	4/8
7	**304a**	(*R*)-3,3′Ph_2-BINOL	Bh	D	89	76	50:1	4/7
8	**320a**		MEDAM	D	85	78	25:1	5/9
9	**321a**		BUDAM	D	90	90	>50:1	1/7

[a] Unless otherwise specified, all reactions were performed with 1 mmol of imine in toluene (0.5 M in imine) with 1.2 equiv of **85** and 5 mol% of the catalyst at 25 °C. [b] Method A′: The pre-catalyst was prepared by heating 1 equiv of ligand with 3 equiv of commercial $B(OPh)_3$ in CH_2Cl_2 at 55 °C for 1 h, followed by removing all volatiles under high vacuum (0.1 mm Hg) for 0.5 h at 55 °C. Method C: The pre-catalyst was prepared by heating 1 equiv of ligand with 4 equiv of commercial $B(OPh)_3$ and 1 equiv of H_2O in toluene at 80 °C for 1 h, followed by removing all volatiles under high vacuum (0.1 mm Hg) for 0.5 h at 80 °C. Method D: The pre-catalyst was prepared by heating 1 equiv of (*S*)-VAPOL, 3 equiv of BH_3•Me_2S, 2 equiv of PhOH and 3 equiv of H_2O in toluene at 100 °C for 1 h, followed by removing all volatiles under high vacuum (0.1 mm Hg) for 0.5 h at 100 °C. nd = not determined. [c] Isolated Yield. [d] Determined by HPLC. [e] Ratio determined by integration of the methine protons of *cis*- and *trans*- aziridine in the ^{1}H NMR spectrum of the crude reaction mixture. [f] Determined by integration of the NH signals of enamines relative to the methine proton of *cis* aziridine in the ^{1}H NMR spectrum of the crude reaction mixture. [g] Reference 52. [h] Reference 1c. [i] Reference 1b. [j] 5 mol% catalyst.

5.3.3 NMR studies on substrate induced BOROX catalyst formation from BINOL and BINOL derivatives by imine 209h

In order to gain an insight into the structures of various species, a detailed NMR study was carried out with imine **111h** (derived from *p*-dimethylamino-benzaldehyde and MEDAM amine **126c**). As discussed in Scheme 5.5, Gang Hu found that BINOL (*R*)-**55** formed a mixture of BOROX catalyst **301h** (imine = **111h**), spiroborate ion-pair **303h** (imine = **111h**) and an unidentified complex **264h** (imine = **111h**) following the same protocol, which is employed for our vaulted ligands i.e. VAPOL and VANOL (Figure 5.7B, entry 7). This possibly explains the low asymmetric induction obtained with (*R*)-**55** (Table 5.5, entries 1-3). As a part of this doctoral research, the structure of unidentified complex **264h** was found to be a imine-borate complex **264h** based on the X-ray analysis of a similar compound **244e** in which DMAP is used as the base (Figure 4.14, Chapter 4, δ (^{11}B NMR) = 1.5–2.5 ppm). Although the NMR experiments with BINOL (*R*)-**55** were performed by Gang Hu, the ^{1}H NMR spectra were neither reported nor analyzed in his dissertation. Hence, after obtaining the spectra from Gang Hu as a personal communication, a detailed critical analysis of these spectra was performed and is presented in Figure 5.7 (entries 1-7). It must be noted that B2 **299a/299b** is the major species in the presence of excess $B(OPh)_3$ prior to the addition of imine **111h** (Figure 5.7B and 5.7C, entry 6). Also, the presence of spiroborate **303h** was also identified during ^{1}H NMR analysis (Figure 5.7B and 5.7C, entry 5). Li Huang, a former group member has shown the clean generation of BOROX catalyst **323h** when ligand **56a** was used. Although the NMR experiments with ligand (*R*)-**56a** (Figure 5.7, entries 8-9) were performed by Li Huang, the ^{1}H NMR spectra were neither reported nor analyzed in her dissertation. Hence, after obtaining the spectra from Li Huang as a personal communication, a detailed critical analysis of these spectra was performed and is

presented in Figure 5.7 (entries 8-9). A careful ^{1}H NMR analysis reveal that the conversion of B2 **322a**/**322b** derived from **56a** to BOROX catalyst **323h** is small (Figure 5.7C, entries 8 and 9). This was further confirmed from the ^{11}B NMR where the ratio of tetra-coordinate boron: tri-coordinate boron is 1:6 instead of 1:2 (Figure 5.7B, entry 9). However, the chiral pocket of **323h** might be good enough to provide increased enantioselectivity compared to catalysts derived from other BINOL derivatives.

Figure 5.7 (**A**) Treatment of (*R*)-**55** and (*R*)-**56a** with commercial $B(OPh)_3$ and imine **111h**. (**B**)[a] ^{11}B NMR spectra of the reaction mixture in $CDCl_3$. (**C**) ^{1}H NMR spectra (aromatic region) corresponding to the ^{11}B NMR spectra in Figure 5.7B and entry 11 is pure (*R*)-**56a**. (**D**) ^{1}H NMR spectra (methyl and methoxy) corresponding to entries 2,5,7,9 and 10 in the ^{11}B NMR spectra in Figure 5.7B.

A

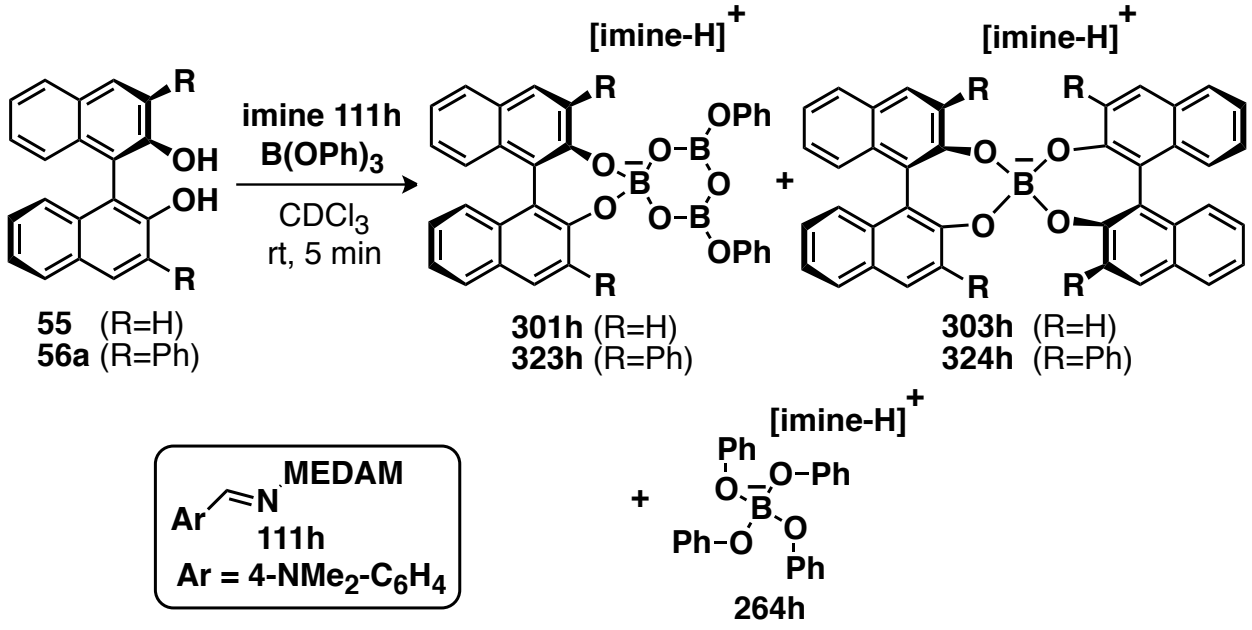

Figure 5.7 cont'd

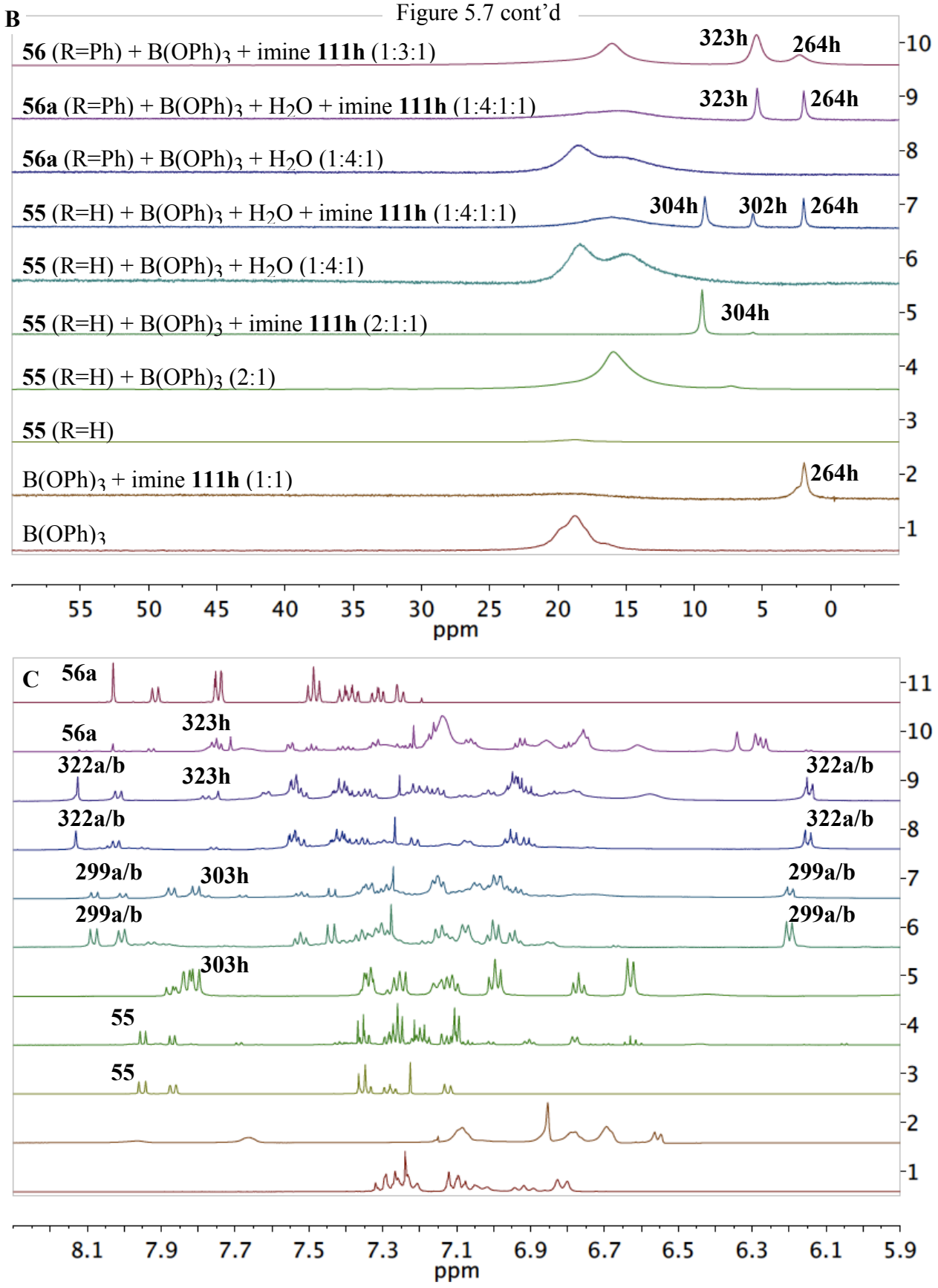

Figure 5.7 cont'd

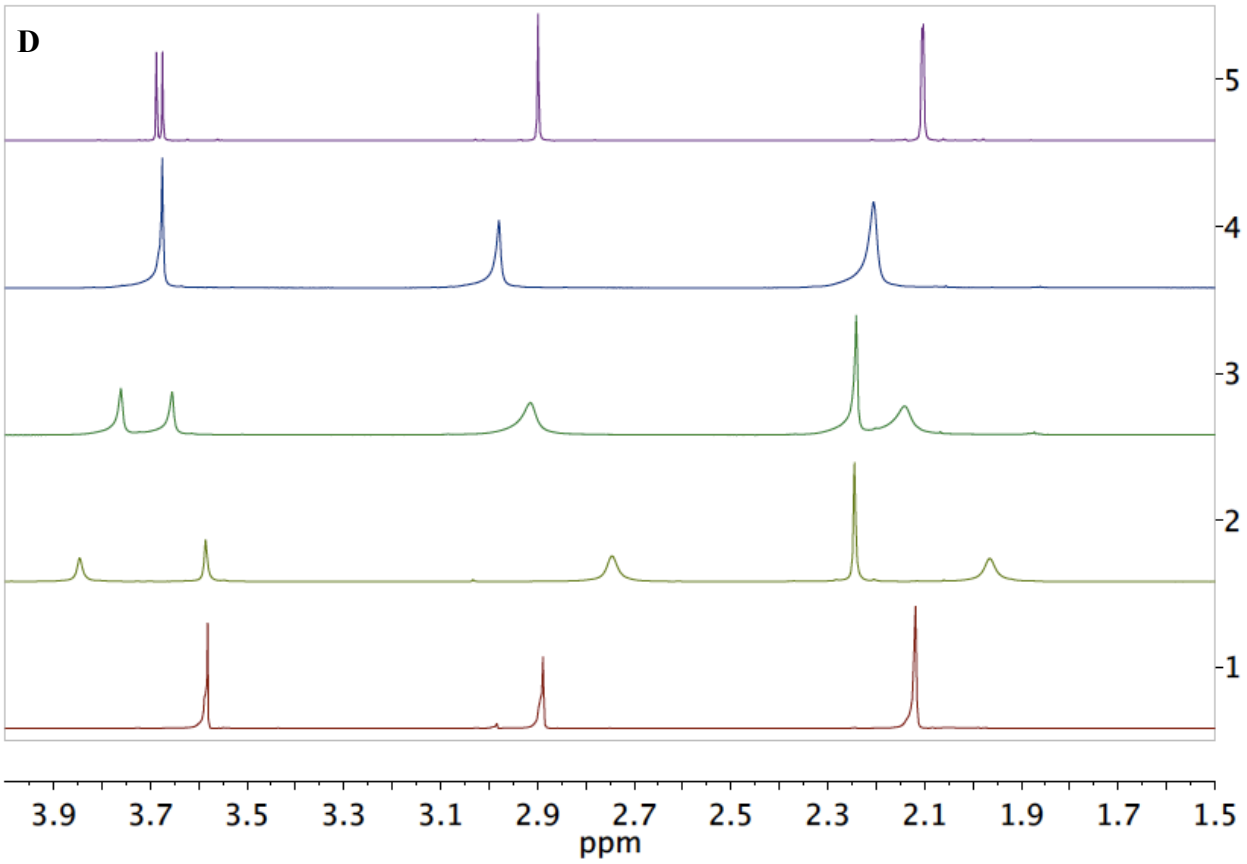

[a] Note for Figure 5.7B: Entry 1: neat $B(OPh)_3$. Entry 2: commercial $B(OPh)_3$ plus imine **111h** (1 equiv) for 5 min at 25 °C. Entry 3: pure BINOL (*R*)-**55**. Entry 4: (*R*)-**55** (0.2 mmol) plus 0.5 equiv commercial $B(OPh)_3$ for 5 min at 25 °C. Entry 5: (*R*)-**55** (0.2 mmol) plus 0.5 equiv commercial $B(OPh)_3$ plus imine **111h** (0.5 equiv) for 5 min at 25 °C. Entry 6: (*R*)-**55** (0.1 mmol) plus 4 equiv commercial $B(OPh)_3$ and 1 equiv H_2O were heated at 80 °C in toluene for 1 h followed by removal of volatiles under vacuum for 0.5 h. Entry 7: 1.0 equiv of imine **111h** was added to the entry 6 (pre-catalyst) for 10 min at 25 °C. Entry 8: same as entry 6 except (*R*)-**56a** is used instead of (*R*)-**55**. Entry 9: 1.0 equiv of imine **111h** was added to the entry 8 (pre-

catalyst) for 10 min at 25 °C. Entry 10: (*R*)-**56a** (0.1 mmol) plus 3 equiv commercial $B(OPh)_3$ plus imine **111h** (1 equiv) for 10 min at 25 °C.

As a result of work in this thesis (Chapter 2), it was envisioned that the direct generation of the boroxinate catalyst **323h** could be achieved without the generation of any pre-catalyst. Indeed, it was delightful to observe the generation of the boroxinate catalyst **323h** in greater amounts by simple mixing **56a**, commercial $B(OPh)_3$ and imine **111h** at room temperature (Figure 5.7B and 5.7C, entry10). The ^{1}H NMR spectrum shows that there is no formation of B2 **322a**/**322b** under these conditions similar to that observed for VAPOL. Additionally, the splitting in the methyl and methoxy regions (Figure 5.7D, entry10) is also observed similar to cases involving vaulted ligand, VAPOL (Chapter 2).[1f] Also, we have been able to perform the aziridination reaction with the BOROX catalyst **323h** generated by simple mixing of the components. The result is comparable to that obtained by employing the BOROX catalyst generated *via* pre-catalyst (75% ee, Scheme 5.10 *vs.* 76% ee, Table 5.6, entries 4 and 7). While good inductions were observed in the aziridination reaction of imine **78a** with the BOROX catalysts derived from the BINOL derivative **56a**, lower enantioselectivities were obtained when B1 catalysts of type **74a**[51] and **92a** (this work) were utilized (Scheme 5.10B).

Scheme 5.10 (**A**) One-pot aziridination with imine **78a** using (*R*)-**55** and (*R*)-**56a** as the ligands. (**B**) aziridination with **B1** catalysts.

A

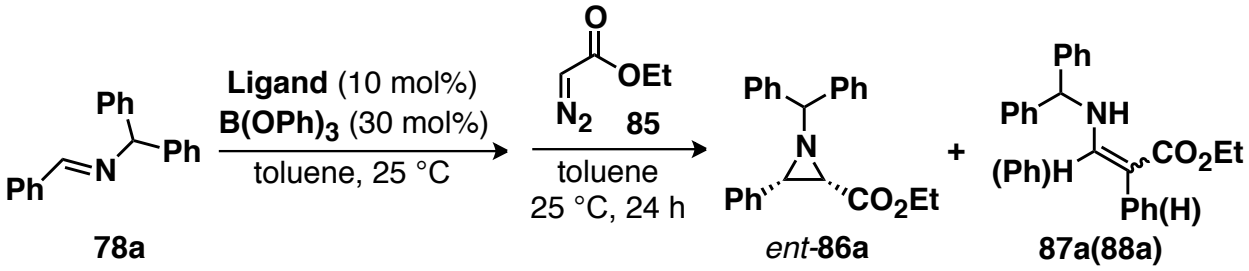

78a *ent*-**86a** **87a(88a)**

Ligand	Yield *ent*-**86a** (%)	ee *ent*-**86a** (%)	c:t	Yield **87a(88a)** (%)
(*R*)-**55**	63	13	18:1	3(4)
(*R*)-**56a**	84	75	50:1	7(8)

B

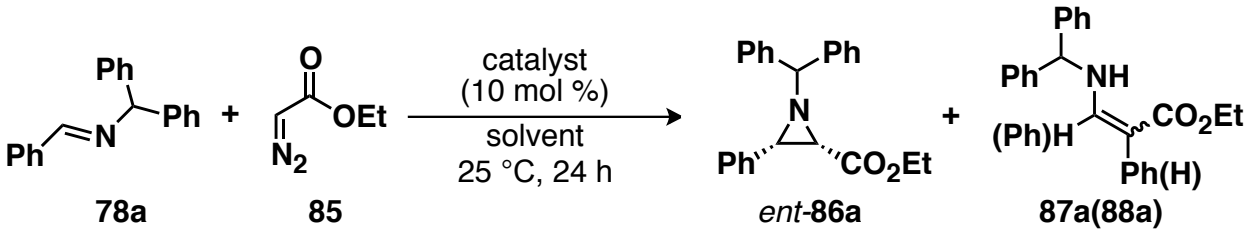

78a **85** *ent*-**86a** **87a(88a)**

Ligand	catalyst	solvent	Yield *ent*-**86a** (%)	ee *ent*-**86a** (%)	*cis:trans*	Yield **87a(88a)** (%)
(*S*)-**55**	(*S*,*S*)-**74a**	CH_2Cl_2	47	40	2:1	24(23)
(*R*)-**89**	(*R*)-**92a**	Toluene	80	48	>100:1	6(8)

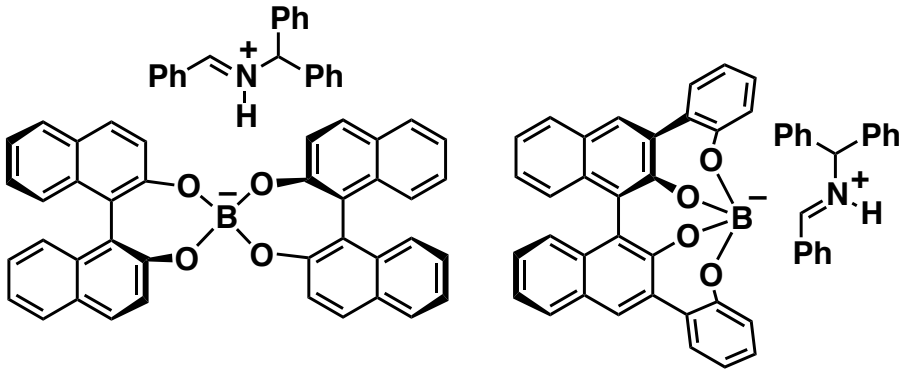

(*S*,*S*)-**74a** (*R*)-**92a**

B1 (SB) **B1 (FSB)**

The focus was then shifted towards NMR studies of BOROX catalysts from BINOL derivatives of type **56** other than **56a**. A detailed NMR study was carried out for ligands **56e**, **56f**, **56i** and **56j** (Scheme 5.11). The results with ligands **56e** and **56i** are presented in Figure 5.5.

Scheme 5.11 NMR study of the BOROX catalysts using (*R*)-**56** as the ligand

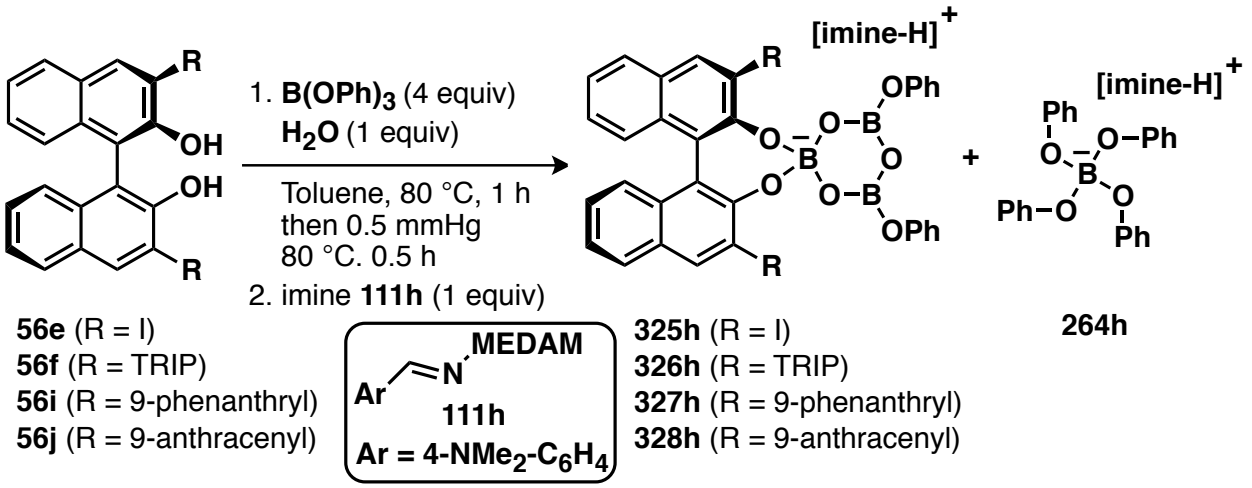

56e (R = I)
56f (R = TRIP)
56i (R = 9-phenanthryl)
56j (R = 9-anthracenyl)

325h (R = I)
326h (R = TRIP)
327h (R = 9-phenanthryl)
328h (R = 9-anthracenyl)

264h

A careful NMR study shows that the boroxinate catalyst **325h** was generated from ligand **56e** (R = I) (Figure 5.8, entries 1-3). A very interesting observation was made in the case of BINOL derivative **56i**. It must be remembered that only 13% ee was observed in the aziridination with a catalyst generated from **56i** (Table 5.4, entry 15). A small amount of BOROX catalyst **327h** was observed along with some amount of achiral borate imine complex **264h** (Figure 5.8, entry 4). It seems like the formation of the catalyst **327h** is slow as the absorption at δ (^{11}B NMR) ≅ 5 ppm increases with longer time periods (Figure 5.8, entries 4-7). Additionally, the splitting of the methyl and methoxy absorptions is also observed similar to observations involving vaulted ligands (Figure 5.8B). Further, the characteristic peak (δ, ^{1}H NMR = 8.75-8.83 ppm, multiplet) of the ligand **56i** was found to be shifted upfield to δ = 8.40 ppm, doublet (Figure 5.8C, entries 4-7). No spiroborate catalyst of the type **74a** was observed in

these cases due to the absence of an absorption at δ (^{11}B NMR) ≅ 10 ppm. In most cases, a peak at δ ≅ 11.7 ppm was observed for the proton attached to the nitrogen of the iminium ion (Figure 5.8C). All observations made for ligand **56i** were also made for ligand **56e**. In the case of ligand **56e**, the characteristic peak (δ, ^{1}H NMR = 8.52 ppm, singlet) of the ligand **56i** was found to be shifted upfield to δ = 8.12 ppm, singlet (Figure 5.8C, entries 1-3).

Figure 5.8 Treatment of (*R*)-**56e** and (*R*)-**56i** with commercial $B(OPh)_3$ and imine **111h**. (**A**)[a] ^{11}B NMR spectra of the reaction mixture in $CDCl_3$. (**B**) ^{1}H NMR spectra corresponding to the ^{11}B NMR spectra in Figure 5.8A. (**C**) ^{1}H NMR spectra showing the NH^{+} region corresponding to the ^{11}B NMR in Figure 5.8A.

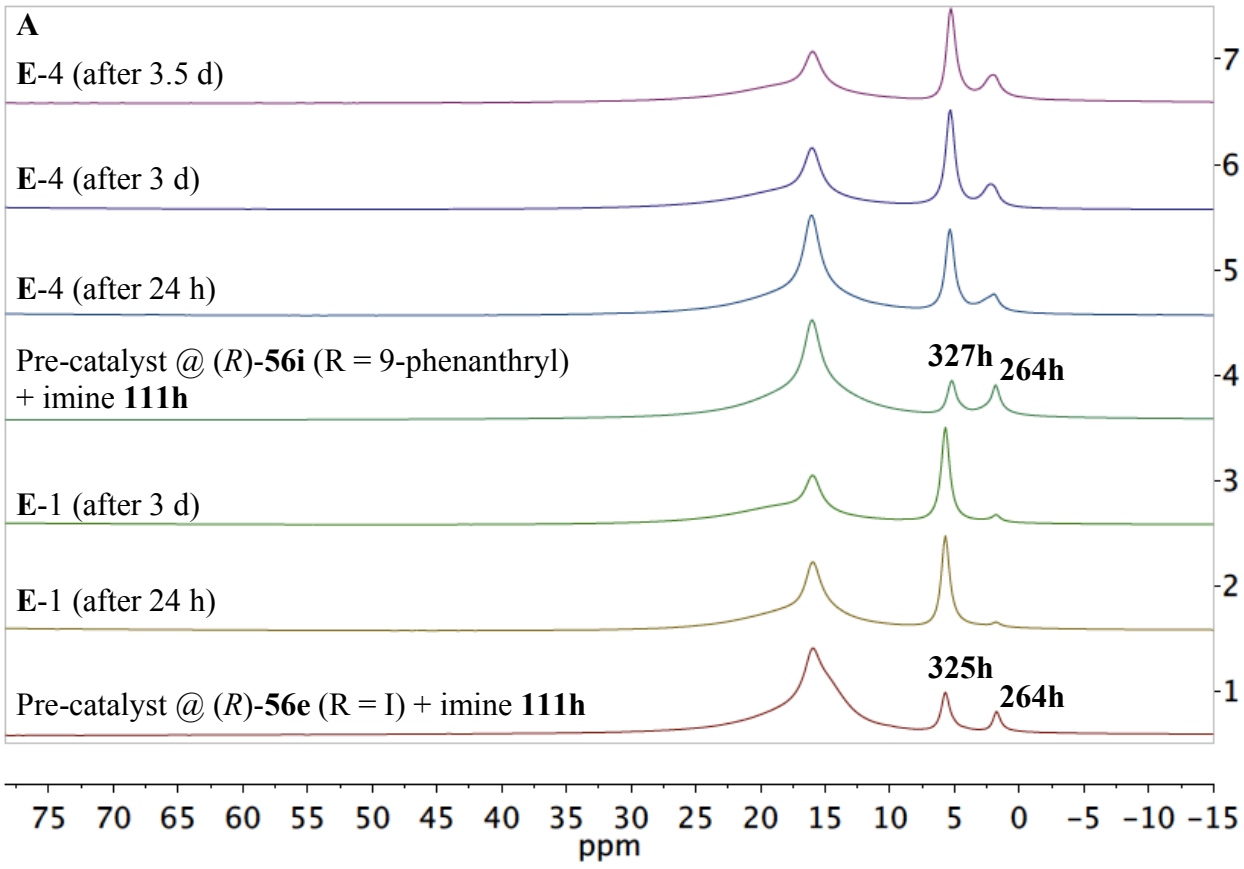

Figure 5.8 cont'd

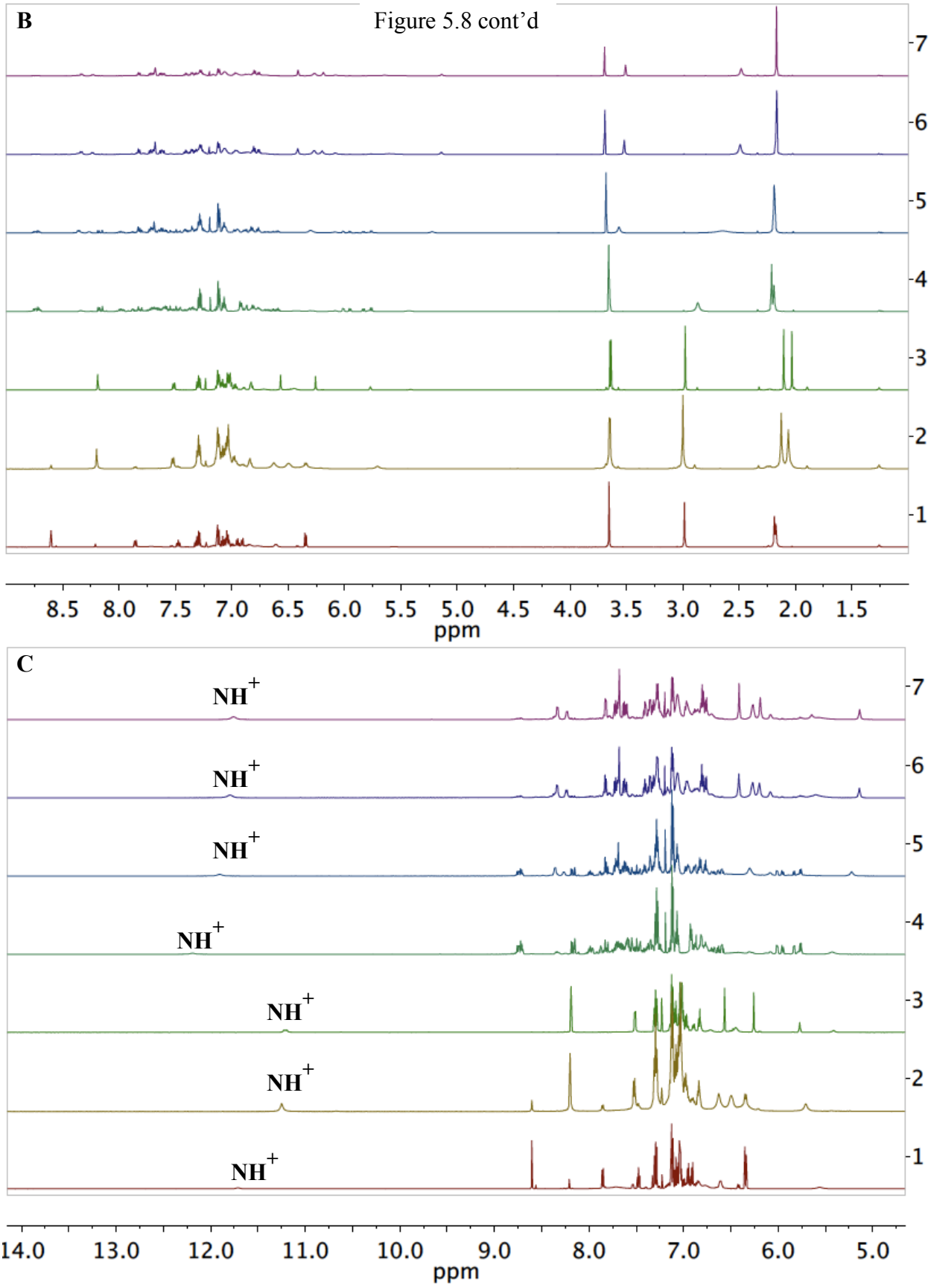

[a] Note for Figure 5.8A: Entry 1: (*R*)-**56e** (0.1 mmol) plus 4 equiv commercial $B(OPh)_3$ and 1 equiv H_2O were heated at 80 °C in toluene for 1 h followed by removal of volatiles under vacuum for 0.5 h. Thereafter, 1.0 equiv of imine **111h** was added at 25 °C. Entry 2 and 3: entry 1 after 24 h and 3 days respectively. Entry 4: (*R*)-**56i** (0.1 mmol) plus 4 equiv commercial $B(OPh)_3$ and 1 equiv H_2O were heated at 80 °C in toluene for 1 h followed by removal of volatiles under vacuum for 0.5 h. Thereafter, 1.0 equiv of imine **111h** was added at 25 °C. Entry 5: entry 4 after 24 h. Entry 6: entry 1 after 3 days. Entry 7: entry 1 after 3.5 days.

A small amount of BOROX catalyst **328h** and a large amount of the achiral borate-imine complex **264h** was observed when ligand **56j** (R = anthracenyl) was subjected to NMR analysis (Figure 5.9, entries 1-4). This could explain the low asymmetric induction in this case. In fact, a 78% yield of aziridine **86a** is obtained when imine **78a** is reacted with EDA in the presence of 40 mol% $B(OPh)_3$ only suggesting that the reaction is catalyzed by an achiral Brønsted acid of type **264a** $[\text{imine-H}]^+ [B(OPh)_4]^-$. In the case of ligand **56f** (R = TRIP), there was no sign of boroxinate catalyst. Instead, a lot of the achiral borate-imine complex **264h** was obtained which increased with time (Figure 5.9, entries 5-7). The NMR study of the boroxinate catalysts generated from BINOL derivatives **56** supports the results obtained in the Wulff catalytic asymmetric aziridination reaction (Figure 5.7-5.9 and Table 5.5).

Figure 5.9 Treatment of (*R*)-**56f** and (*R*)-**56j** with commercial $B(OPh)_3$ and imine **111h**. (**A**)[a] ^{11}B NMR spectra of the reaction mixture in $CDCl_3$. (**B**) ^{1}H NMR spectra corresponding to the ^{11}B NMR spectra in Figure 5.9A. (**C**) ^{1}H NMR spectra showing the NH^{+} region corresponding to the ^{11}B NMR spectra in Figure 5.9A.

A

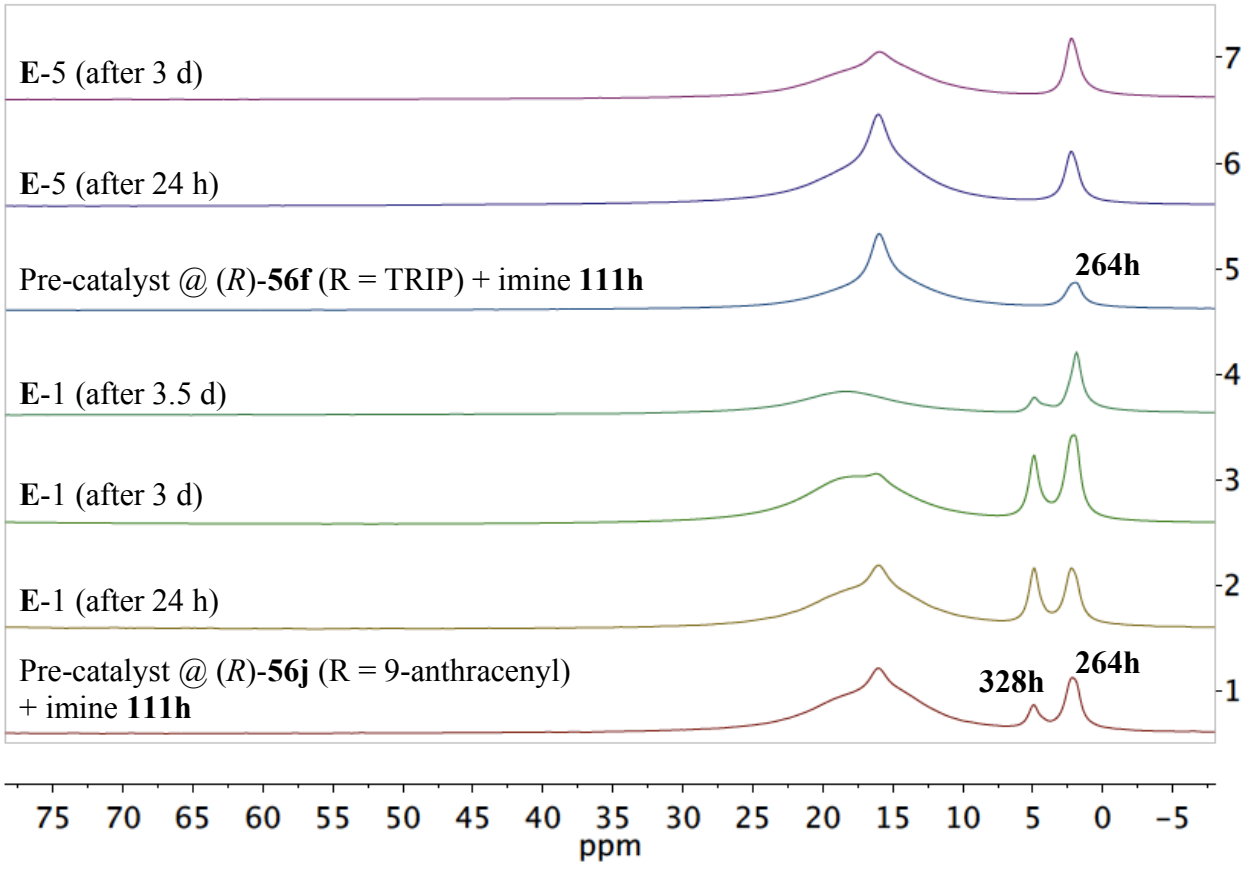

Figure 5.9 cont'd

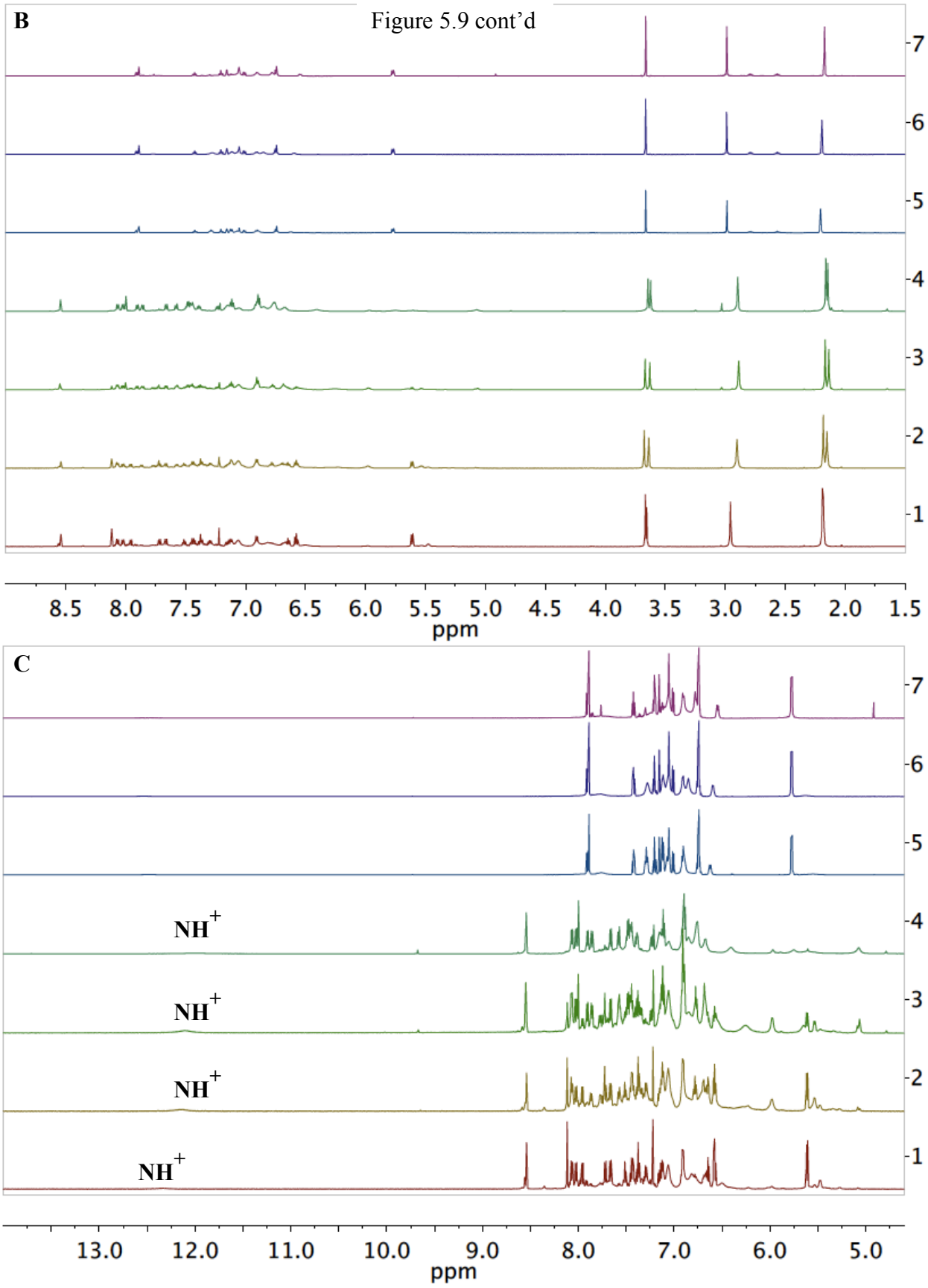

[a] Note for Figure 5.9A: Entry 1: (*R*)-**56j** (0.1 mmol) plus 4 equiv commercial $B(OPh)_3$ and 1 equiv H_2O were heated at 80 °C in toluene for 1 h followed by removal of volatiles under vacuum for 0.5 h. Thereafter, 1.0 equiv of imine **111h** was added at 25 °C. Entry 2: entry 1 after 24 h. Entry 3: entry 1 after 3 days. Entry 4: entry 1 after 3.5 days. Entry 5: (*R*)-**56f** (0.1 mmol) plus 4 equiv commercial $B(OPh)_3$ and 1 equiv H_2O were heated at 80 °C in toluene for 1 h followed by removal of volatiles under vacuum for 0.5 h. Thereafter, 1.0 equiv of imine **111h** was added at 25 °C. Entry 6: entry 4 after 24 h. Entry 7: entry 4 after 3 days.

We have observed that BINOL (*R*)-**55** formed a mixture of BOROX catalyst **301h**, spiroborate ion-par **303h**, and achiral imine-borate complex **264h** following the same protocol, which was employed for our vaulted ligands i.e. VAPOL and VANOL (Figure 5.7B, entry 7). The interesting question then arises as to whether H8-BINOL (*R*)-**53** would give clean formation of boroxinate or not? Unfortunately, only the achiral borate-imine complex **264h** was observed when the reaction of H8-BINOL (*R*)-**53** with $B(OPh)_3$ and imine **111h** was subjected to NMR analysis (Figure 5.10, entries 1-3). The achiral complex **264h** increased with time and a very small amount of boroxinate catalyst was observed in the ^{11}B NMR spectrum after 3 days (Figure 5.10A, entry 3). It is interesting to notice the completely different behavior of H8-BINOL (*R*)-**53** compared to BINOL (*R*)-**55**.

Figure 5.10 Treatment of (*R*)-**53** and commercial $B(OPh)_3$ and imine **111h**. (**A**) ^{11}B NMR spectra of the reaction mixture in $CDCl_3$. Entry 1: (*R*)-**53** (0.1 mmol) plus 4 equiv commercial $B(OPh)_3$ and 1 equiv H_2O were heated at 80 °C in toluene for 1 h followed by removal of volatiles under vacuum for 0.5 h. Thereafter, 1.0 equiv of imine **111h** was added at 25 °C. Entry 2: entry 1 after 24 h. Entry 3: entry 1 after 3 days. (**B**) ^{1}H NMR spectra corresponding to the ^{11}B NMR spectra in Figure 5.10A. (**C**) ^{1}H NMR spectra showing the methyl and methoxy region corresponding to the ^{11}B NMR spectra in Figure 5.10A.

A

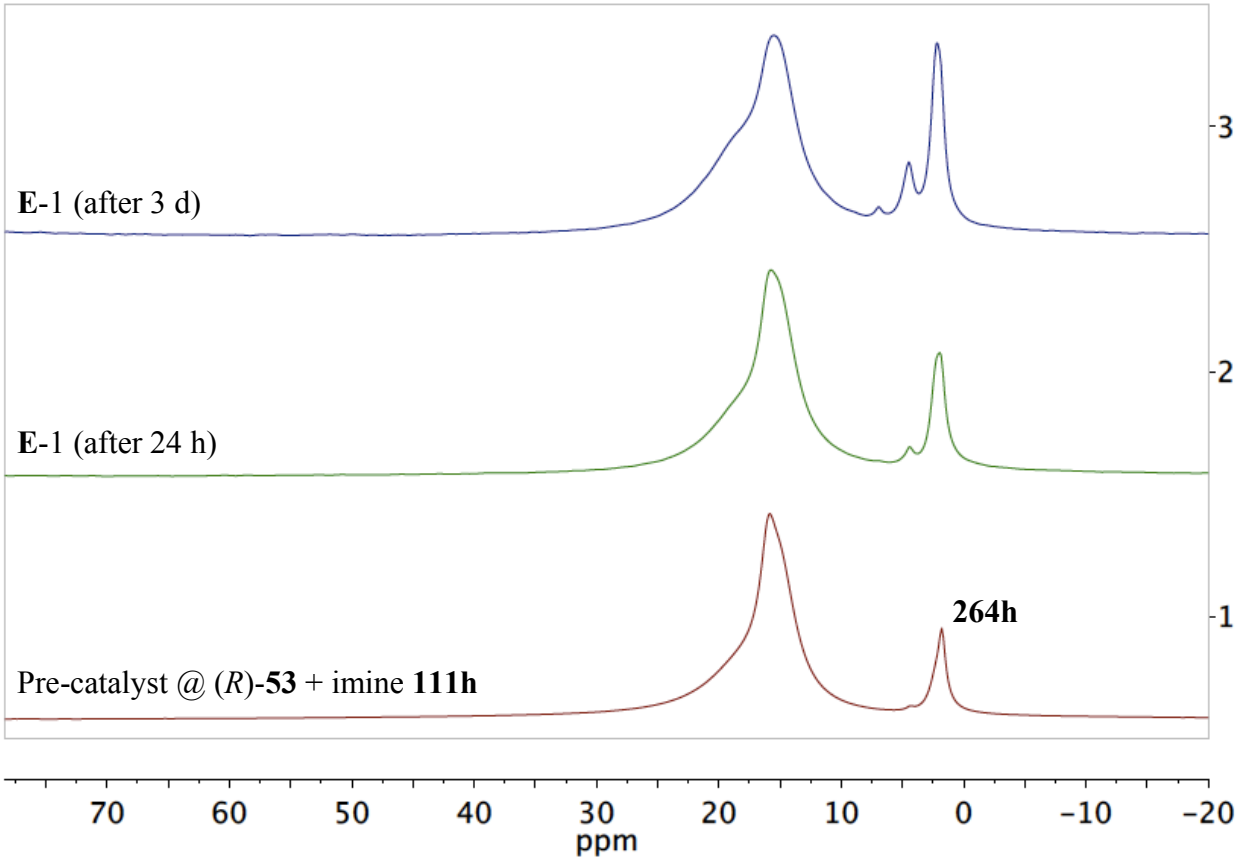

Figure 5.10 cont'd

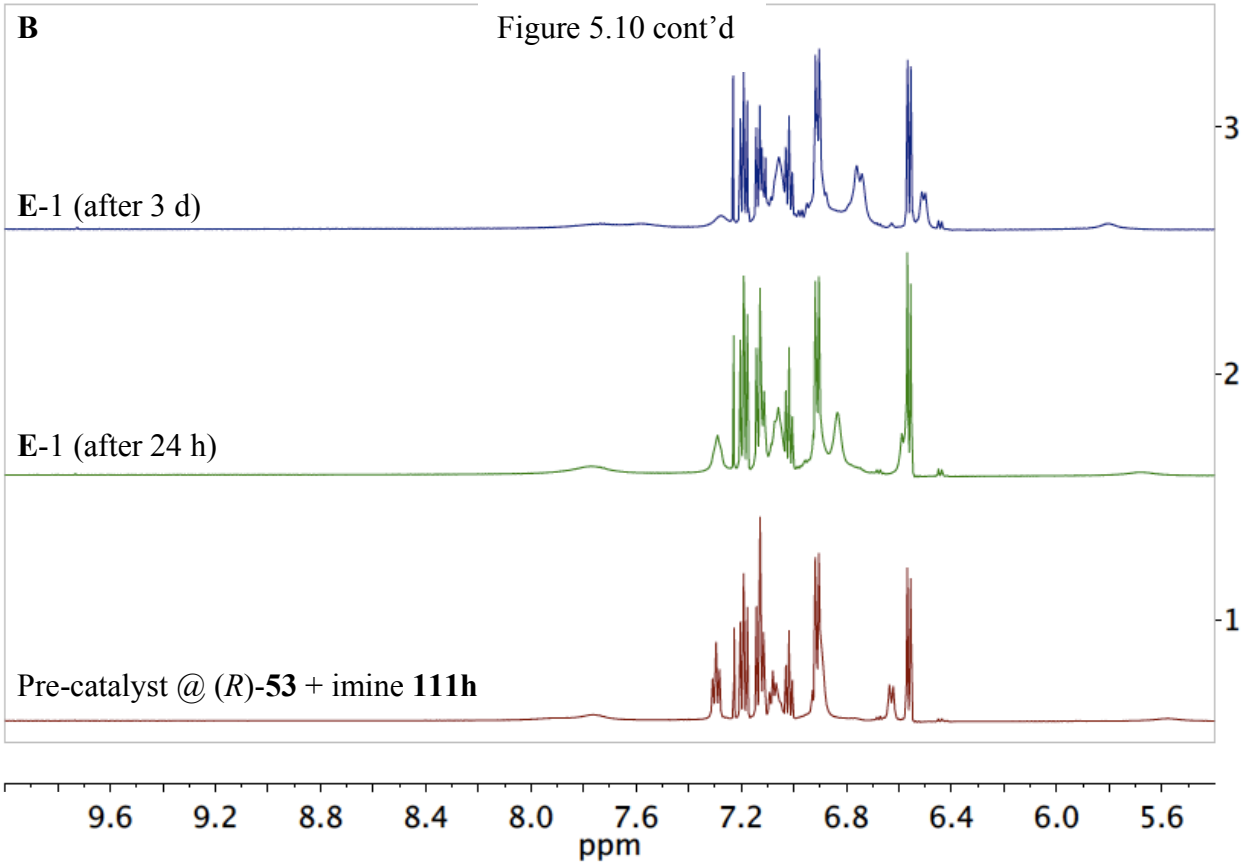

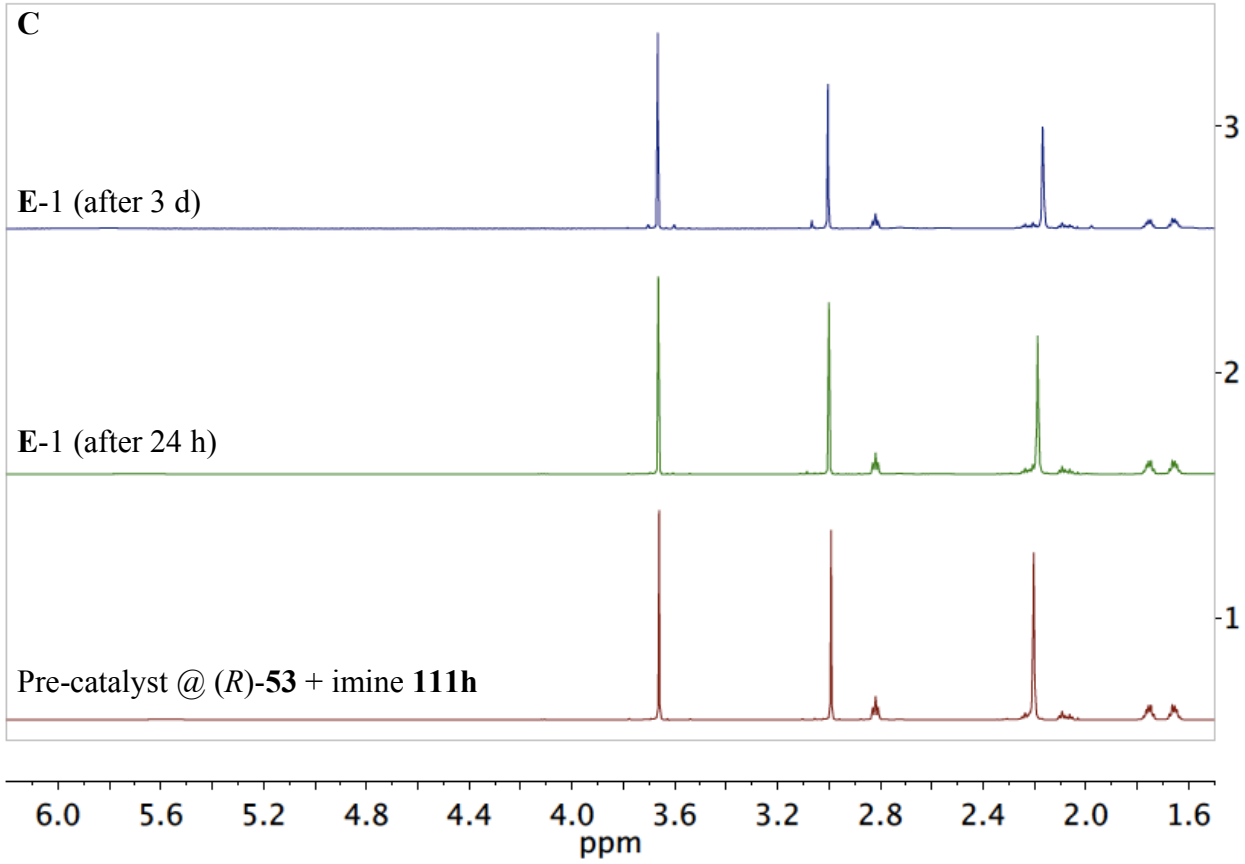

5.3.4 Calculated structure of BOROX catalyst 323a derived from 3,3′-Ph_2-BINOL 56a

We have observed many non-covalent interactions between the iminium ion and arene rings of the vaulted ligands with the aid of an X-ray crystal structure of the BOROX catalyst **190a** generated from (*S*)-VAPOL and imine **111a** (Figure 5.1C).[1f] We were not able to obtain single crystals of **323a** (imine = **111a** and ligand = (*S*)-**56a**) suitable for X-ray analysis. In an attempt to gain an insight into the nature of any non-covalent interactions in the IMINO-BOROX **323a**, computational methods were undertaken to explore its structure. Calculations were performed using Gaussian ′03 at B3LYP/6-31g* level of theory.[24] The calculated lowest energy structure is shown in Figure 5.11. Similar to the structure of **190a**, there are many non-covalent interactions suggested by the calculated structure of **323a**. In addition to the hydrogen bond (d_1 = 1.70 Å), there are several CH-π interactions: one is between one of the MEDAM methyl groups and one of the naphthalene rings (d_2 = 4.42 Å) and another is between a methyl group on the other MEDAM ring and a phenyl ring from the phenol component (d_4 = 4.30 Å). There are several other CH-π interactions including those between the ortho hydrogen on one aryl ring and the π-system of another aryl ring (d_3 = 4.28 Å, d_5 = 3.97 Å and d_6 = 4.58 Å). Another important interaction between the catalyst and the substrate is a π–π stacking interaction between the protonated iminium moiety and one of the phenyl rings at the 3,3′ positions of the ligand (d_7 = 3.75 Å). In addition, another π–π stacking interaction was found between one of the phenyl rings from the phenol component and the other phenyl ring at the 3,3′ positions of the ligand (d_8 = 4.44 Å). These possible interactions suggest that the iminium is tightly bound in the chiral

pocket and this might be responsible for higher asymmetric induction observed for the ligand 56a (Table 5.5). However, it must be remembered that this is only a prediction for the catalyst substrate complex and does not represent a transition state for the aziridination reaction since the diazo compound is not involved.

Figure 5.11 Calculated structure of IMINO-BOROX catalyst **323a** using Gaussian ′03. **(A)**[a] Calculated B3LYP/6-31g* structure visualized by the Mercury Program (C, gray; O, red; N, blue; B, yellow; H, white). Hydrogen atoms omitted for clarity (except N-H). (**B**) Space-filling rendition of **323a** with the same orientation and showing hydrogens. The boroxinate anion is given in green and the iminium cation is in traditional colors.

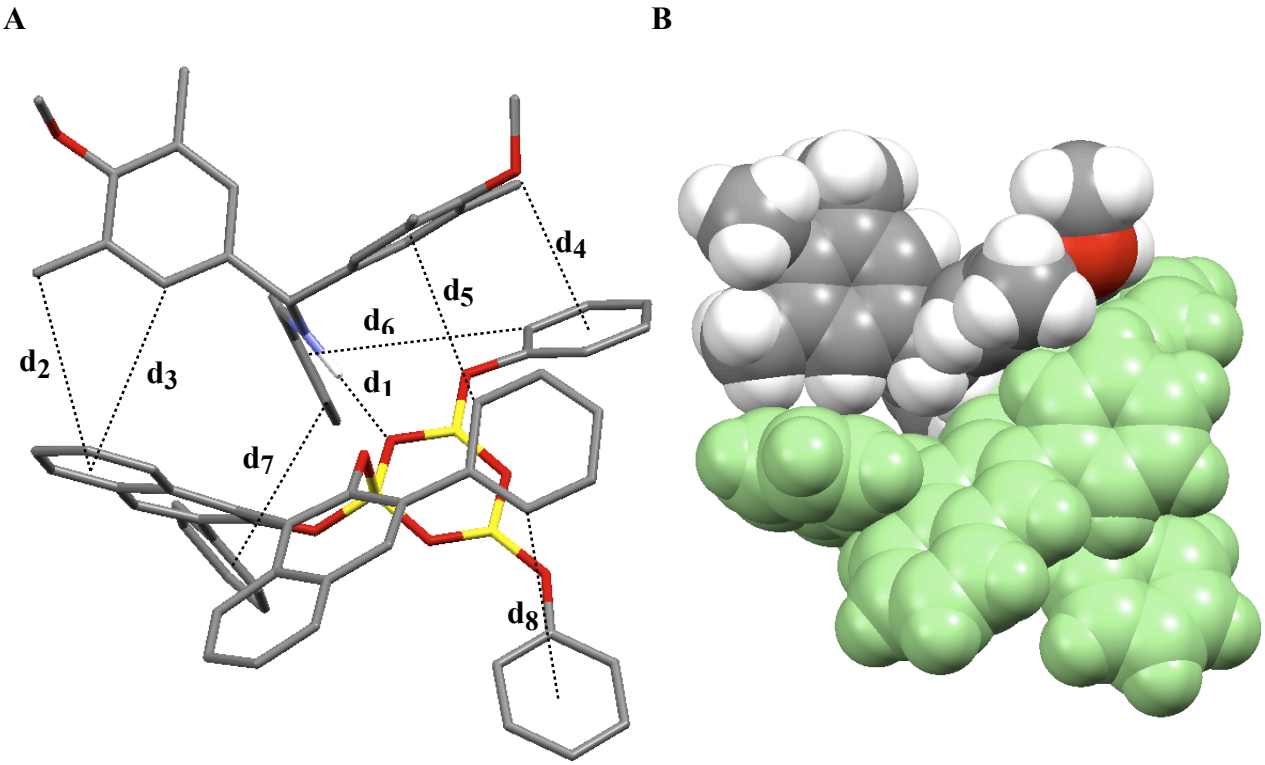

[a] Note for Figure 5.11A: Some secondary interactions are highlighted: d_1 = 1.70 Å (H-bonding), d_2 = 4.42 Å (CH-π), d_3 = 4.28 Å (CH-π), d_4 = 4.30 Å (CH-π), d_5 = 3.97 Å (CH-π), d_6 = 4.58 Å (CH-π), d_7 = 3.75 Å (CH-π or π-π stack), d_8 = 4.44 Å (CH-π or π-π stack).

5.4 Generation of BOROX catalyst 329 with BINOL 55 using DMSO as the base.

We have seen that DMSO is capable of generating the boroxinate catalyst in the case of vaulted ligands (Chapter 2). Hence, the thought was entertained as to whether or not DMSO would behave in a same manner with linear biaryl ligands. Meanwhile, another group member namely, Wynter Osminski found that a mixture of BINOL and commercial $B(OPh)_3$ in the ratio of 2:1 in d_6-DMSO would generate the spiroborate **330** (Figure 5.12, entry 2). As a part of this work, we mixed one equiv of BINOL **55** with 3 equiv of commercial $B(OPh)_3$ in d_6-DMSO. Surprisingly, boroxinate **329** was observed as the major species with only a small amount of the spiroborate **330** (Figure 5.12, entry 3). This is in stark contrast to the use of imine as the base, which gives a mixture of spiroborate and boroxinate catalyst (Figure 5.7). An appreciable amount of the achiral $[DMSOH]^+[B(OPh)_4]^-$ complex **244f** was also observed (Figure 5.12, entry 3). Thereafter, we performed these experiments in $CDCl_3$ with 1-5 equivalents of DMSO. This was done to quantify the amount needed to generate the boroxinate catalyst using DMSO. It seems that atleast 5 equivalents of DMSO is needed to drive the reaction in the forward direction towards the generation of boroxinate catalyst **329** (Figure 5.12, entries 5 and 6). It must be noted that spiroborate **330** appears not to have been formed due to the lack of an absorption at δ (^{11}B NMR) ≅ 10 ppm (Figure 5.12B, entry 6).

Figure 5.12 (**A**) Treatment of BINOL (*R*)-**55** and DMSO with different boron sources. (**B**)[a] ^{11}B NMR spectra of the reaction mixture. (**C**) ^{1}H NMR spectra corresponding to the ^{11}B NMR spectra in Figure 5.12B except that the entry 1 is pure (*R*)-**55** in d_6-DMSO.

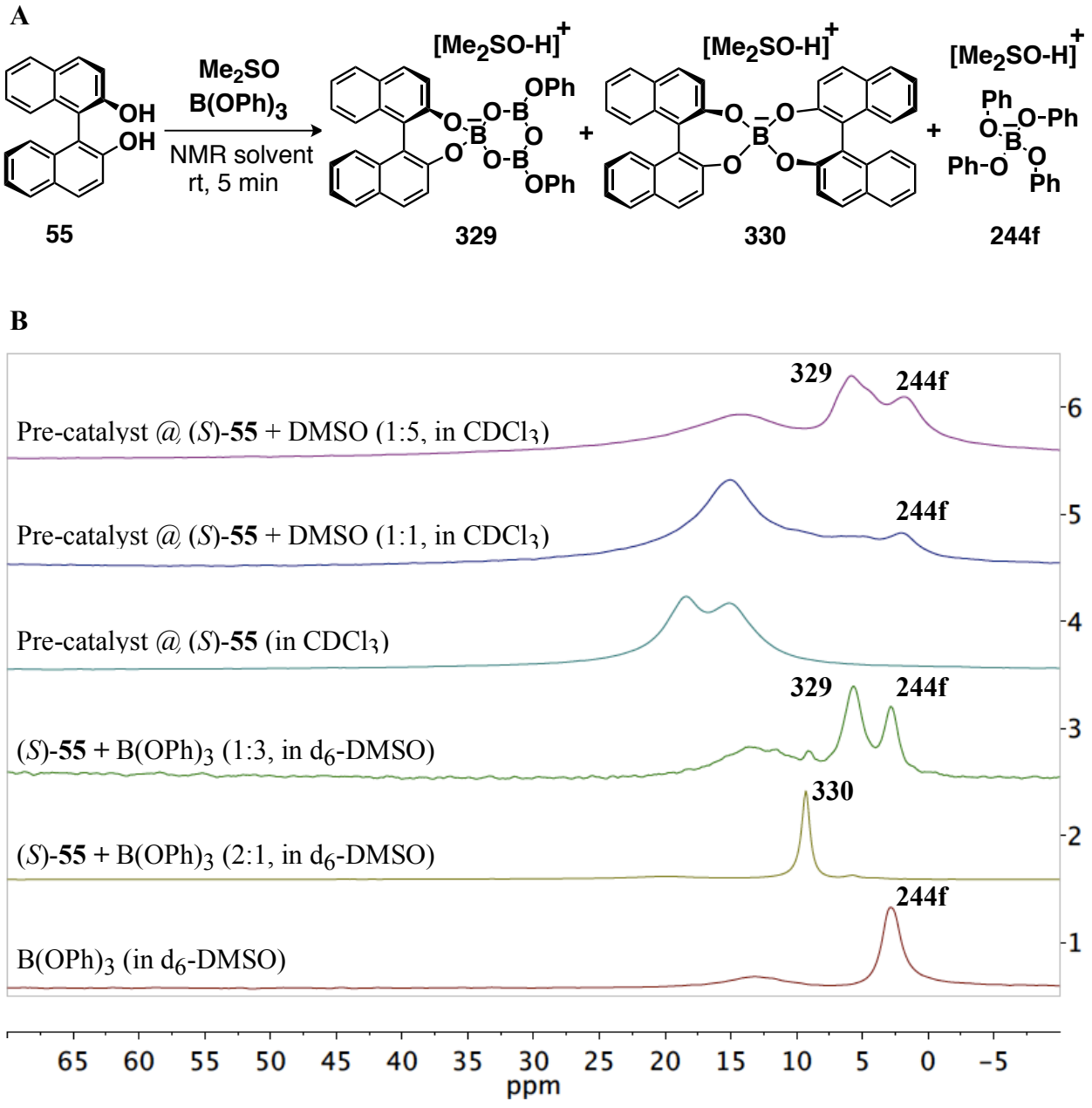

Figure 5.12 cont'd

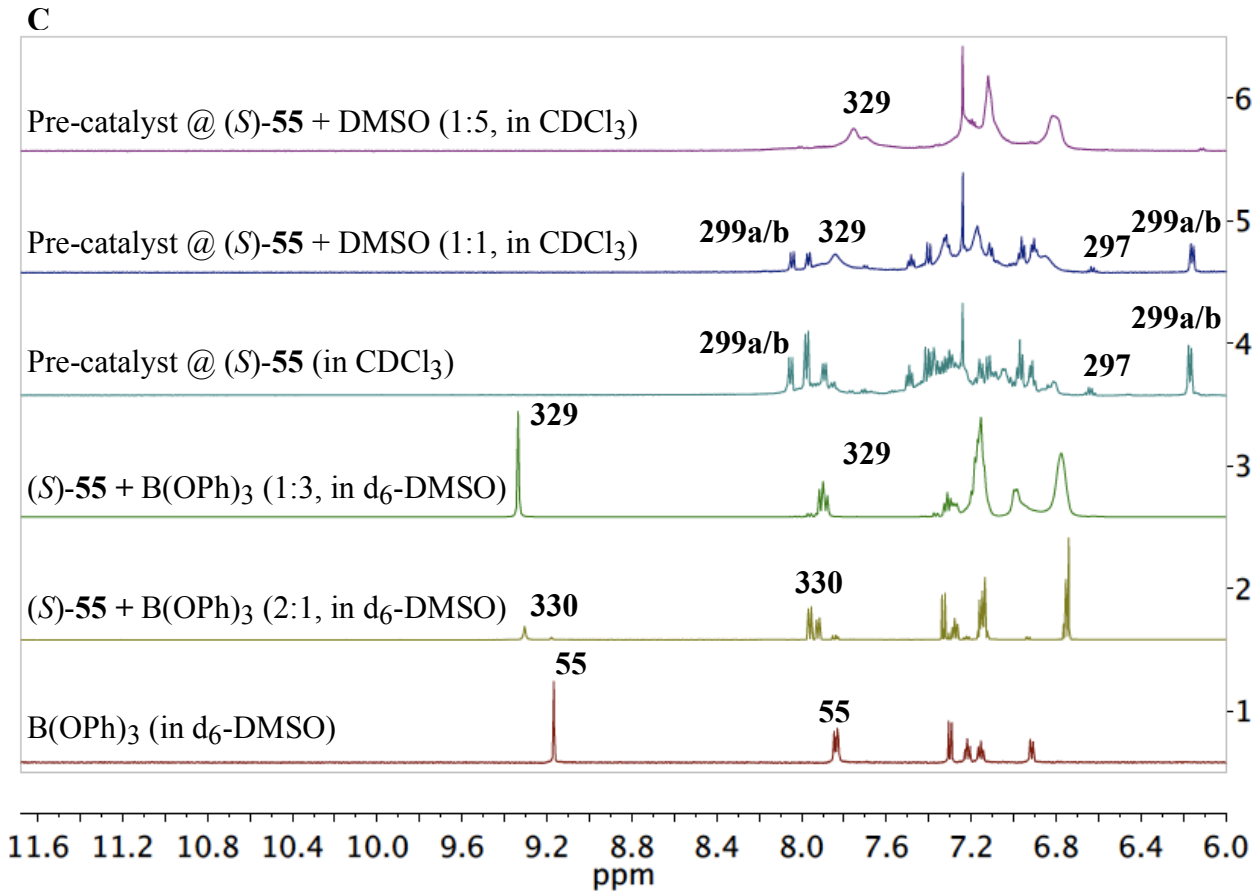

[a] Note for Figure 5.12B: Entry 1: commercial $B(OPh)_3$ in d_6-DMSO. Entry 2: (*R*)-**55** (0.1 mmol) plus 0.5 equiv commercial $B(OPh)_3$ stirred in d_6-DMSO (1 mL) for 1 h in presence of 150 mg 4Å Molecular Sieves. Entry 3: (*R*)-**55** (0.1 mmol) plus 3 equiv commercial $B(OPh)_3$ stirred in d_6-DMSO (1 mL) for 1 h. Entry 4: (*R*)-**55** (0.1 mmol) plus 3 equiv BH_3•Me_2S, 2 equiv of PhOH and 3 equiv H_2O were heated at 100 °C in toluene for 1 h followed by removal of volatiles under vacuum for 0.5 h. The NMR was taken in $CDCl_3$. Entry 5: 1.0 equiv of DMSO was added to entry 4 at 25 °C. Entry 5: 5.0 equiv of DMSO was added to entry 4 at 25 °C.

5.5 TADDOL and its effect on the Wulff catalytic asymmetric aziridination reaction

TADDOL is one of the most common chiral diols used in the field of asymmetric catalysis.[64] Hence, we decided to screen TADDOL (*R*,*R*)-**61a** as a ligand substitute for VANOL or VAPOL for our aziridination reaction. Unfortunately, while aziridine **86a** was obtained in 73% yield, no asymmetric induction was observed (Scheme 5.12).

Scheme 5.12 Aziridination with imine **78a** using (*R*,*R*)-**61a** as the ligand.

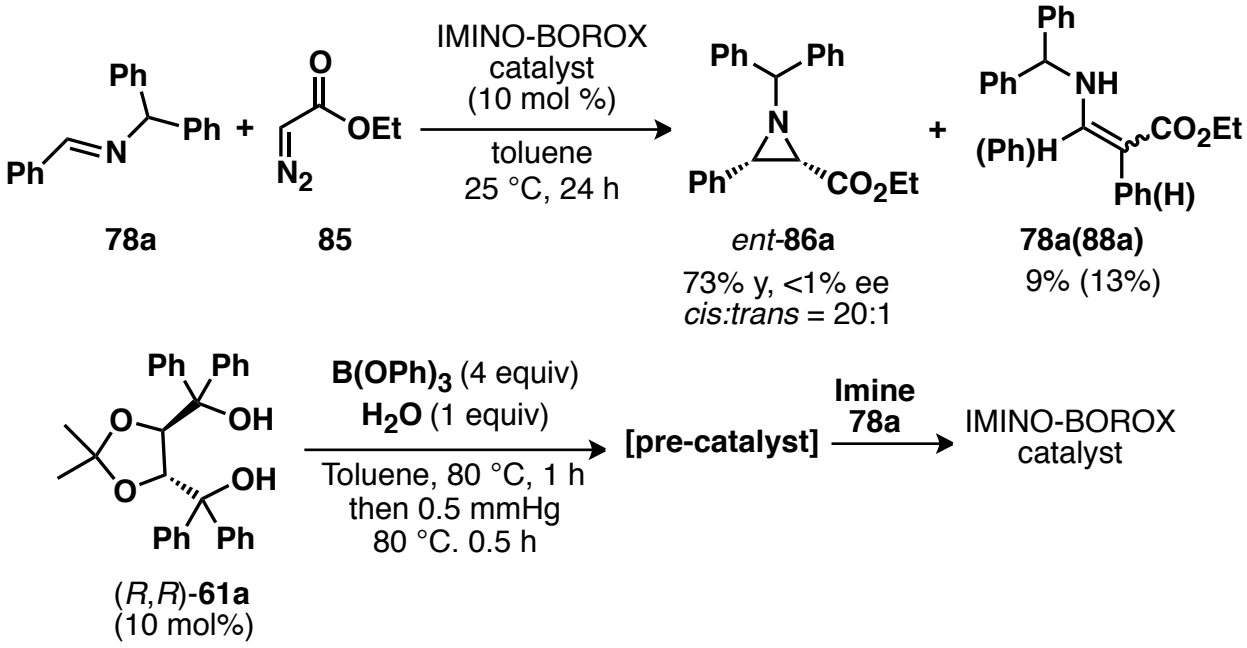

It is assumed that this result is due to the background reaction. A 78% yield of aziridine **86a** is obtained when imine **78a** is reacted with EDA in the presence of 40 mol% $B(OPh)_3$ only suggesting that the reaction is catalyzed by an achiral Brønsted acid of type **264a** $[\text{imine-H}]^+$ $[B(OPh)_4]^-$. The result with TADDOL (*R*,*R*)-**61a** was further supported by NMR analysis that failed to detect any boroxinate with TADDOL (*R*,*R*)-**61a** when imine **111h** was added (Figure

5.13, entry 3). No change was observed even after 12 h (Figure 5.13, entry 4). The only tetra-coordinate species observed is the achiral [imine-H]$^{+}$ [B(OPh)$_4$]$^{-}$ **264h**.

Figure 5.13 Treatment of (*R,R*)-**61a** and commercial B(OPh)$_3$ with imine **111h**. (**A**) ^{11}B NMR spectra of the reaction mixture in $CDCl_3$. Entry 1: pure B(OPh)$_3$. Entry 2: (*R,R*)-**61a** (0.1 mmol) plus 4 equiv commercial B(OPh)$_3$ and 1 equiv H_2O were heated at 80 °C in toluene for 1 h followed by removal of volatiles under vacuum for 0.5 h. Entry 3: 1.0 equiv of imine **111h** was added to the entry 3 (pre-catalyst) for 10 min at 25 °C. Entry 4: entry 3 after 12 h. (**B**) ^{1}H NMR spectra corresponding to the ^{11}B NMR spectra in Figure 5.13A expect that the entry 1 is pure (*R,R*)-**61a**.

A

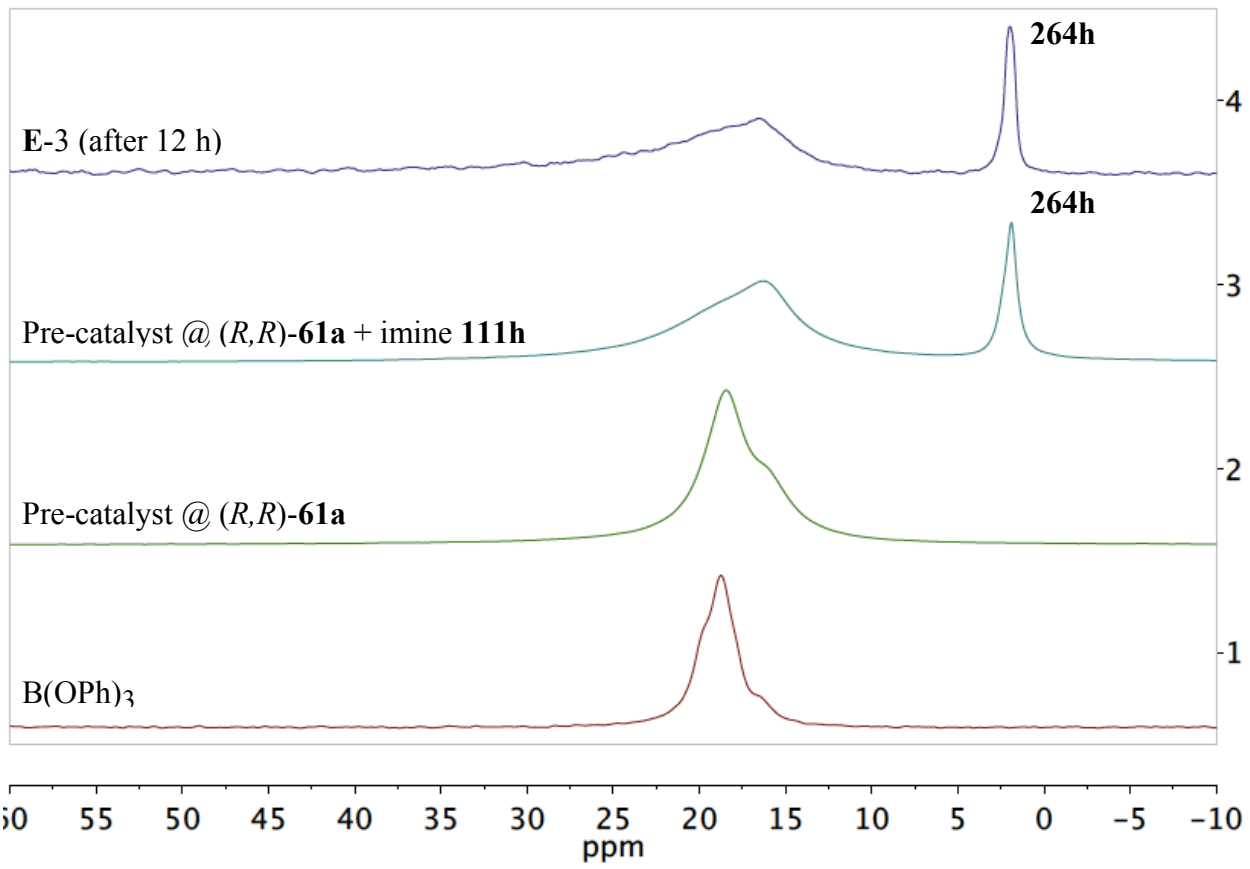

Figure 5.13 cont'd

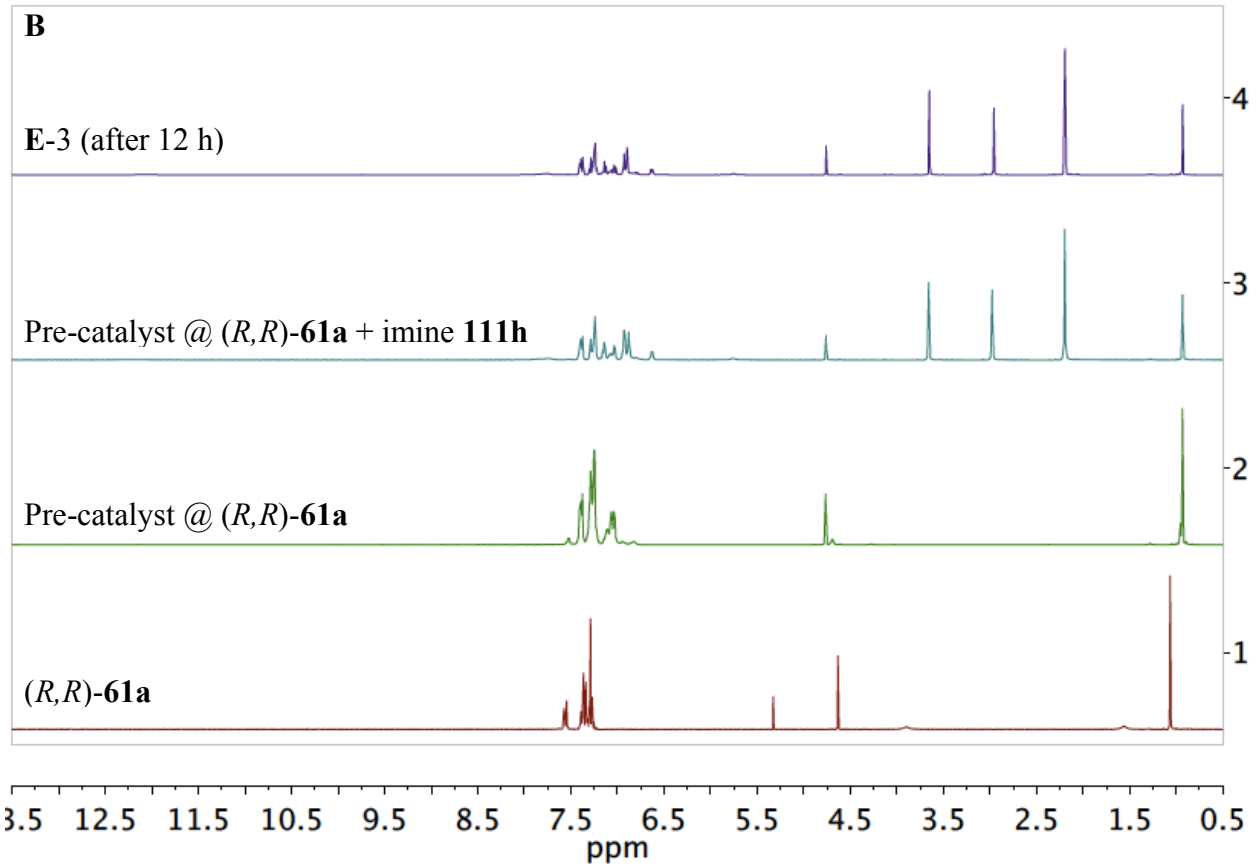

It must be noted that Chen and coworkers reported no aziridine **86x** (not shown) from reaction between EDA and imine derived from *p*-(methylsulfonyl)benzaldehyde and benzhydryl amine **126a** using the catalyst **307x** derived from TADDOL (*R*,*R*)-**61a**, $B(OH)_3$ and PhOH.[54] In this case, they performed the reaction at –10 °C (see Table 5.4, entry 6).

5.6 Conclusions

The diversity of the novel BOROX catalysts was explored by altering the chiral diol component in the boroxinate catalyst. In the process, a potentially inexpensive ligand ISOVAPOL **197** was developed and was found to be equally efficient as the other vaulted ligands that have been evaluated for the Wulff aziridination reaction. Also, linear biaryl ligands were screened for the first time. BINOL **55** and BINOL derivatives **56** generated boroxinate catalysts in various amounts depending on the sterics and electronics of the substituents at the 3,3′ positions. A detailed NMR study helped to reveal the favorable and unfavorable conditions for generation of the BOROX catalyst. Hopefully, the information gained from the experiments described in this chapter will help in designing new catalytic systems for other asymmetric reactions.

APPENDIX

5.7 Experimental

5.7.1 General Information

Same as Chapter 2.

5.7.2 Synthesis of imines 78, 110a, 111a, 111h and 112a

General Procedure for the synthesis of aldimines – Illustrated for the synthesis of *N*-benzylidene-1,1-diphenylmethanamine 78a.

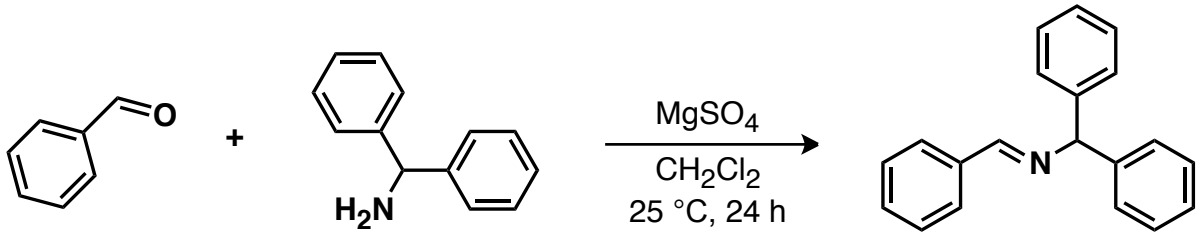

127a **126a** **78a**

***N*-benzylidene-1,1-diphenylmethanamine 78a:** To a 50 mL flame-dried round bottom flask filled with argon was added benzhydryl amine **126a** (0.92 g, 5.00 mmol), $MgSO_4$ (1.0 g, 8.4 mmol, freshly flame-dried) and dry CH_2Cl_2 (15 mL). After stirring for 10 min, benzaldehyde **127a** (0.54 g, 5.05 mmol, 1.01 equiv) was added. The reaction mixture was stirred at room temperature for 24 h. The reaction mixture was filtered through Celite and the Celite bed was washed with CH_2Cl_2 (10 mL × 3) and then the filtrate was concentrated by rotary evaporation to give the crude imine as an off-white solid. Crystallization (1:5 ethyl acetate/hexanes) and collection of the first crop afforded **78a** as white solid crystals (mp. 99-101 °C) in 80% isolated yield (1.09 g, 4 mmol).

Spectral data for **78a**: ^{1}H NMR ($CDCl_3$, 300 MHz) δ 5.64 (s, 1H), 7.20-7.90 (m, 15H), 8.46 (s, 1H); ^{13}C NMR ($CDCl_3$, 75 Hz) δ 77.62, 126.69, 127.40, 128.15, 128.19, 128.24, 130.47, 136.07, 143.64, 160.48. These spectral data match those previously reported for this compound.[1a]

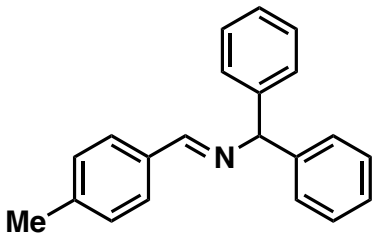

78d

***N*-(4-methylbenzylidene)-1,1-diphenylmethanamine 78d:** Imine **78d** was prepared according to the procedure described above for imine **78a**. Crystallization (1:5 ethyl acetate/hexanes) and collection of the first crop afforded **78d** as white solid crystals (mp. 73-74 °C) in 80% isolated yield (1.14 g, 4 mmol).

Spectral data for **78d**: ^{1}H NMR ($CDCl_3$, 300 MHz) δ 2.44 (s, 3H), 5.64 (s, 1H), 7.26-7.48 (m, 12H), 7.80 (d, J = 8 Hz, 2H), 8.45 (s, 1H); ^{13}C NMR ($CDCl_3$, 75 Hz) δ 21.50, 76.57, 126.89, 127.66, 128.38, 128.41, 129.21, 133.88, 141.01, 143.98, 160.67. These spectral data match those previously reported for this compound.[1a]

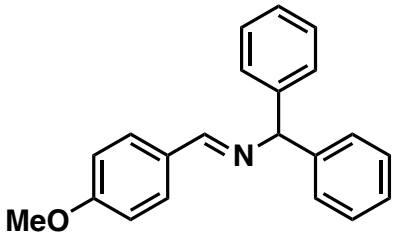

78e

***N*-(4-methoxybenzylidene)-1,1-diphenylmethanamine 78e:** Imine **78e** was prepared according to the procedure described above for imine **78a**. Crystallization (1:5 ethyl acetate/hexanes) and collection of the first crop afforded **78e** as white solid crystals (mp. 108-109 °C) in 80% isolated yield (1.21 g, 4 mmol).

Spectral data for **78e**: ^{1}H NMR ($CDCl_3$, 300 MHz) δ 3.82 (s, 3H), 5.55 (s, 1H), 6.91 (d, J = 8.8 Hz, 2H), 7.28-7.40 (m, 10H), 7.78 (d, J = 8.8 Hz, 2H), 8.34 (s, 1H); ^{13}C NMR ($CDCl_3$, 75 Hz) δ 55.32, 77.77, 113.88, 126.85, 127.67, 128.37, 129.99, 144.11, 160.01. These spectral data match those previously reported for this compound.[1a]

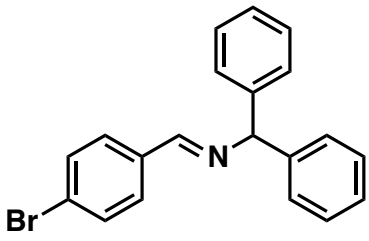

78g

***N*-(4-bromobenzylidene)-1,1-diphenylmethanamine 78g:** Imine **78g** was prepared according to the procedure described above for imine **78a**. Crystallization (1:5 ethyl acetate/hexanes) and collection of the first crop afforded **78g** as white solid crystals (mp. 96-97 °C) in 75% isolated yield (1.31 g, 3.75 mmol).

Spectral data for **78g**: ^{1}H NMR ($CDCl_3$, 300 MHz) δ 5.23 (s, 1H), 7.15-7.35 (m, 10H), 7.47 (d, J = 7 Hz, 2H), 7.64 (d, J = 7 Hz, 2H), 8.28 (s, 1H); ^{13}C NMR ($CDCl_3$, 75 Hz) δ 77.85, 127.05, 127.60, 128.46, 129.84, 131.75, 143.62, 159.51. These spectral data match those previously reported for this compound.[1a]

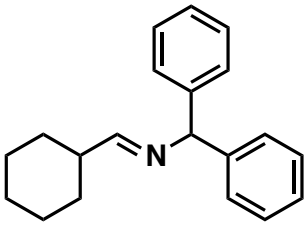

78v

***N*-(cyclohexylmethylene)-1,1-diphenylmethanamine 78v:** Imine **78v** was prepared according to the procedure described above for imine **78a**. Crystallization (1:5 ethyl acetate/hexanes) and collection of the first crop afforded **78v** as white solid crystals (mp. 49-51 °C) in 70% isolated yield (0.97 g, 3.5 mmol).

Spectral data for **78v**: ^{1}H NMR ($CDCl_3$, 300 MHz) δ 1.10-1.90 (m, 10H), 2.20 (bs, 1H), 5.21 (s, 1H), 7.00-7.60 (m, 10H), 7.59 (d, *J* = 5.5 Hz, 1H); ^{13}C NMR ($CDCl_3$, 75 Hz) δ 25.82, 26.41, 30.13, 43.91, 78.35, 127.20, 127.97, 128.73, 144.41, 169.51. These spectral data match those previously reported for this compound.[1a]

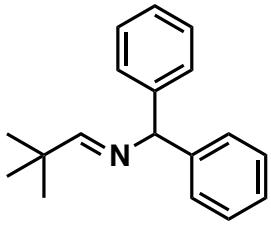

78w

***N*-(2,2-dimethylpropylidene)-1,1-diphenylmethanamine 78w:** Imine **78w** was prepared according to the procedure described above for imine **78a**. Crystallization (1:9 ethyl acetate/hexanes) and collection of the first crop afforded **78w** as white solid crystals (mp. 51-52 °C) in 50% isolated yield (0.63 g, 0.25 mmol).

Spectral data for **78w**: ^{1}H NMR ($CDCl_3$, 300 MHz) δ 1.27 (s, 9H), 5.50 (s, 1H), 7.34 (t, *J* = 7 Hz, 2H), 7.44 (t, *J* = 7 Hz, 4H), 7.49 (d, *J* = 7 Hz, 4H), 7.85 (s, 1H); ^{13}C NMR ($CDCl_3$, 75 Hz) δ 26.94, 36.38, 77.36, 126.68, 127.44, 128.25, 144.23, 171.48. These spectral data match those previously reported for this compound.[1a]

***N*-benzylidene-bis(4-methoxyphenyl)methylamine 110a:** See Chapter 2

***N*-phenylmethylidene-*bis*(4-methoxy-3,5-dimethylphenyl)methylamine 111a:** See Chapter 2

***N*-benzylidene-1,1-bis(3,5-di-tert-butyl-4-methoxyphenyl)methanamine 112a:** See Chapter 2

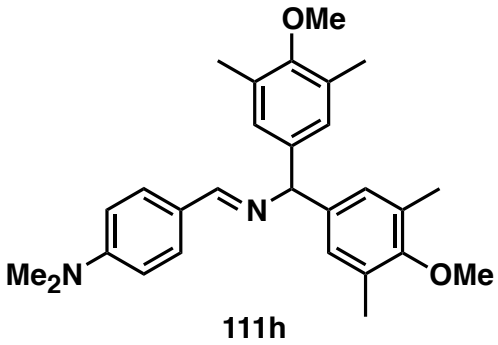

111h

***N*-(4-dimethylaminobenzylidene)-bis(4-methoxy-3,5-dimethylphenyl)methylamine 111h:** Imine **111h** was prepared according to the procedure described above for imine **78a** except following differences: (1) the scale of the reaction was 10 mmol; (2) 4 Å molecular sieves (6 g, freshly dried) were used instead of $MgSO_4$; (3) 1.03 equiv of aldehyde was used; (4) the reaction time was 1 week (the reaction was followed by ^{1}H NMR). Crystallization (1:3 EtOAc/hexanes) and collection of the first crop afforded **111h** as yellow solid crystals (mp 167-169 ºC) in 51% isolated yield (2.20 g, 5.10 mmol).

Spectral data for **111h:** ^{1}H NMR ($CDCl_3$, 300 MHz) δ 2.25 (s, 12H), 3.00 (s, 6H), 3.68 (s, 6H), 5.30 (s, 1H), 6.69 (d, J = 9.0 Hz, 2H), 7.00 (s, 4H), 7.70 (d, J = 9.0 Hz, 2H), 8.24 (s, 1H); ^{13}C NMR ($CDCl_3$, 75 MHz) δ 16.21, 40.26, 59.59, 77.30, 111.83, 125.37, 128.16, 129.93, 130.44, 134.00, 152.36, 155.96, 160.09; IR (thin film) 2926w, 2824w, 1636w, 1606s, 1526 m cm^{-1}; Mass spectrum (NPOE, +FAB): *m/z* (% rel intensity) 430 M^+ (52), 283 (100). Anal calcd for $C_{28}H_{34}N_2O_2$: C, 78.10; H, 7.96; N, 6.51; Found: C, 77.98; H, 8.17; N, 6.90. These spectral data match those previously reported for this compound.[1f]

5.7.3 Synthesis of ISOVAPOL (*S*)-197 (*Scheme 5.2 and 5.3*)

5.7.3.1 Preparation of ISOVAPOL monomer 285:

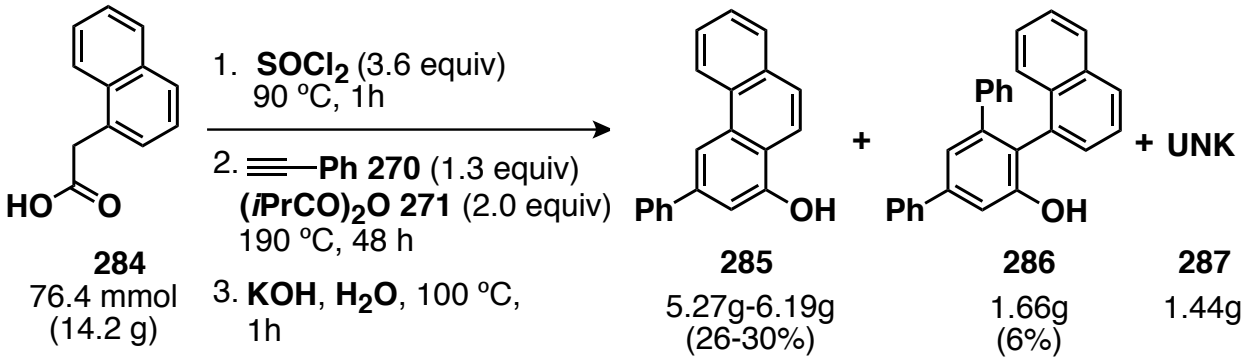

284 76.4 mmol (14.2 g)

285 5.27g-6.19g (26-30%)

286 1.66g (6%)

287 1.44g

3-phenylphenanthren-1-ol 284: To a 250 mL flame-dried round bottom flask equipped with a large stirrer bar and a condenser filled with argon was added 1-naphthylacetic acid **284** (14.23 g, 76.42 mmol) and thionyl chloride (20 mL, 274 mmol). The mixture was heated to reflux for 1 h (oil bath temperature: 90 °C), and then all of the volatiles were carefully removed by high vacuum (0.5 mmHg) with 2nd trap to protect the pump. To the flask containing the resulted brown oil was added phenylacetylene **270** (11.00 mL, 100.2 mmol) and isobutyric anhydride **271** (25.00 mL, 146.2 mmol) under argon, and the resulting mixture was heated and stirred at 190 °C for 48 h with gentle nitrogen flow across top of the condenser. The brown reaction mixture was cooled down to below 100 °C (about 80 °C, oil bath temperature), and then 4.5 N KOH (100 mL) was added. The reaction was then allowed to stir at 100 °C (oil bath temperature) for 15 h. The brown solution was then cooled to room temperature and ether (100 mL) was added and stirred for 10 min. The organic layer was separated. The aqueous layer was extracted twice with ether (100 mL × 2) and the combined organic layer was washed with brine (100 mL) and dried over $MgSO_4$, filtered. The dark-colored solution (crude product) was then combined with silica

gel (100 mL). A piece of cotton was inserted into the neck of the trap of the rotary evaporator before removing the solvents. Both the flask and trap was then put on high vacuum (0.5 mm Hg) for 30 min. A silica gel chromatography column (60 × 350 mm) was prepared by filling the column with hexanes followed by the addition of the silica gel slurry in hexanes. The dried silica gel with the pre-adsorbed crude product was then loaded onto the column carefully. The column was then eluted with a 1:2 mixture of CH_2Cl_2/hexanes under gravity for approximately 6 h. A void volume of about 700 mL was collected and discarded. A second fraction was collected containing the first byproduct **286** (1.66 g, R_f = 0.71 in 1:3 EtOAc: hexane, orange, mp. 82-84 °C) indicated by TLC. It was followed by second byproduct **287** (1.44 g, R_f=0.68 in 1:3 EtOAc: hexane, red, the structure is not known). When the byproducts had finished eluting, elution was continued under N_2 pressure (1:1 CH_2Cl_2/hexanes) to afford the pure monomer **285** as a yellow solid (mp. 177-178 °C) in 26-30 % yield (5.47-6.19 g, 19.9-22.9 mmol)

Spectral data for **285**: R_f = 0.65 (1:3 EtOAc/hexanes); ^{1}H NMR ($CDCl_3$, 300 MHz) δ 5.37 (s, 1 H), 7.2 (s, 1 H), 7.41-7.38 (m, 1 H), 7.49 (t, 2 H, J = 7.3 Hz), 7.66-7.58 (m, 2 H), 7.75-7.73 (m, 3 H), 7.89 (d, 1 H, J = 7.8 Hz), 8.13 (d, 1 H, J = 9.0 Hz), 8.72 (d, 1 H, J = 8.1 Hz). ^{13}C NMR ($CDCl_3$, 75 MHz) δ 110.12, 114.144, 119.76, 121.06, 123.15, 126.26, 126.62, 126.84, 127.49, 127.54, 128.70, 128.89, 130.20, 132.08, 132.48, 139.74, 141.32, 152.23; IR (KBr disc) 3521 s, 3059 w, 1619 w, 1601 m, 1569 w, 1405 w, 1277 w, 1227 w, 1152 w, 1138 m, 1076 m, 821 m, 749 s cm^{-1}; Mass spectrum *m/z* (% rel intensity) 270 (100) M^+, 241 (27), 165 (11), 135 (19), 120 (22), 77(10); Anal calcd for $C_{20}H_{14}O$: C, 88.86; H, 5.22; Found: C, 88.84; H, 5.21.

Spectral data for **286**: R_f = 0.71 in 1:3 EtOAc: hexane; ^{1}H NMR ($CDCl_3$, 600 MHz) δ 7.00-7.03 (m, 2H), 7.05-7.07 (m, 2H), 7.31 (dd, *J* = 7.0, 1.0 Hz, 1H), 7.36 (dd, *J* = 12.4, 1.8 Hz, 2H), 7.39-7.43 (m, 2H), 7.45 (td, *J* = 7.6, 1.3 Hz, 1H), 7.47-7.50 (m, 4H), 7.70-7.74 (m, 3H), 7.83 (d, *J* = 8.2 Hz, 1H), 7.86 (d, *J* = 7.8 Hz, 1H); ^{13}C NMR ($CDCl_3$, 151 MHz) δ 112.89, 121.32, 123.76, 125.54, 125.68, 126.30, 126.56, 126.87, 127.12, 127.53, 127.63, 128.50, 128.75, 128.83, 128.86, 129.86, 132.05, 132.36, 133.75, 140.47, 141.12, 142.26, 143.66, 153.88; IR (thin film) 3532 br, 3059 w, 1614 w, 1599 m, 1569 w, 1496 w, 1390 m, 1298 m, 1172 m cm^{-1}; HRMS (ESI-TOF) *m/z* 395.1405 [(M+Na$^+$); calcd. for $C_{28}H_{20}ONa$: 395.1412]

5.7.3.2 Preparation of racemic ISOVAPOL *rac*-197 and (*S*)-ISOVAPOL (*S*)-197:

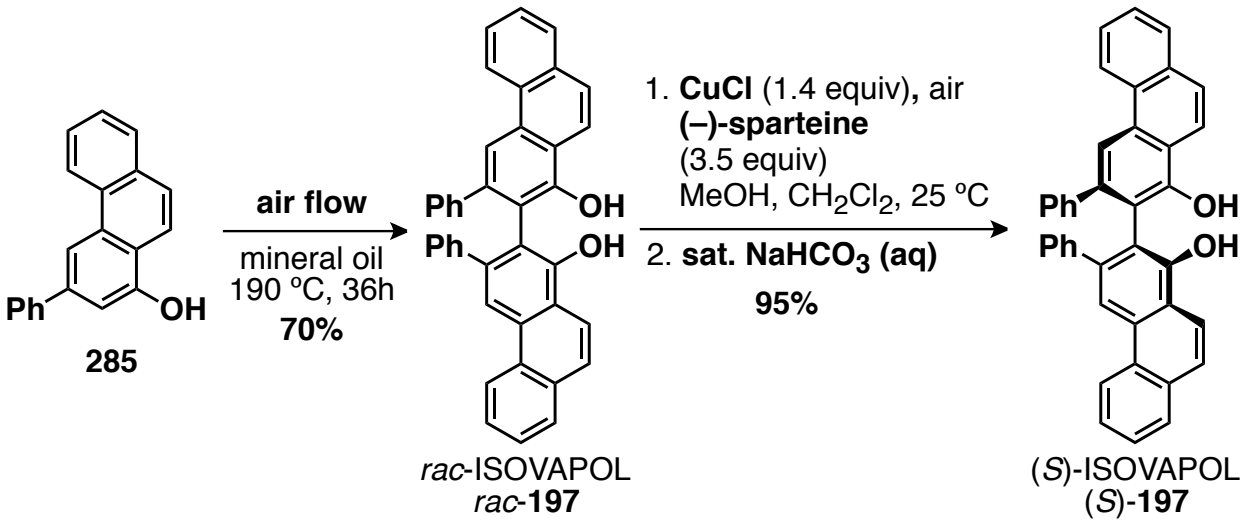

3,3'-diphenyl-2,2'-biphenanthrene-1,1'-diol *rac*-**197:** To a 500 mL three-neck round bottom flask equipped with a stir bar and a 400 mm Allihn water cooled condenser was added 3-phenylphenanthren-1-ol **285** (4.02 g, 14.9 mmol) and light mineral oil (25 mL). The flask was

transferred to oil bath at 190 °C. The stir bar in the oil bath was stopped before the flask was put into it to warm up for about 30 min till solid melted without any disturbance. A thick needle was introduced into the flask *via* the second neck to about 5 cm above the surface of reaction mixture and was used to provide a stream of house air, which was maintained at a flow rate of 0.15 – 0.20 L/min. The third neck was sealed with a rubber septum. Air flow was then introduced into the flask with a vigorous stirring of the reaction mixture. The reaction was kept at same temperature for 36 h. The flask was then cooled down to ambient temperature followed by the addition of hexanes (250 mL). The mixture was then stirred for 30 min. It was then kept at –20 °C for 12 h followed by suction filtration. It was then dried on high vacuum (0.5 mm Hg) for 2 h to afford the crude product as a yellow powder.

Purification by Crystallization: The crude product was then transferred to a 500 mL round bottom flask equipped with a condenser. The residue was rinsed with toluene (50 mL × 2) and transferred to the 500 mL round bottom flask. The resulted mixture was stirred and heated to boil while more toluene was added in 50 mL fraction till solid dissolved. The dark-brown solution was then cooled down to room temperature and kept at –20 °C overnight. The top solution was filtered without disturbing the precipitate over vacuum. A piece of new filter paper was then used to collect the brown crystal *via* suction filtration, washed by hexanes (20 mL × 2) and dried over vacuum to afford the first crop product *rac*-**197** as an off- white solid (mp. 312-313 °C) in 50% yield (2.00 g, 3.73 mmol). The mother liquor was dried and the residue was crystallized in toluene (150mL) and cooled down to room temperature for 12 h followed by –20 °C overnight to afford second crop product *rac*-**197** as an off-white solid (mp. 312-313 °C) in 20% yield (0.8 g, 1.49 mmol). The combined yield was 70% (2.80 g, 5.22 mmol).

Spectral data for *rac*-**197**: R_f = 0.33 (1:9 EtOAc/hexanes) ^{1}H NMR ($CDCl_3$, 300 MHz) δ 5.85 (s, 2 H), 6.73 (d, *J* = 7.1 Hz, 4H), 6.99 (t, *J* = 7.4 Hz, 4H), 7.06-7.11 (m, 2H), 7.59-7.65 (m, 4H), 7.83 (d, *J* = 9.1 Hz, 2H), 7.92-7.97 (m, 2H), 8.17 (s, 2H), 8.30 (d, *J* = 9.1 Hz, 2H), 8.58-8.62 (m, 2H); ^{13}C NMR (DMSO, 125 MHz) δ 114.98, 119.37, 121.15, 121.25, 123.15, 125.12, 126.16, 126.61, 126.64, 126.96, 128.31, 128.90, 129.63, 130.27, 131.70, 141.48, 141.68, 152.38; IR (KBr disc) 3521 vs, 3468 vs, 3059 w, 1616 w, 1594 m, 1566 w, 1509 w, 1482 w, 1393 m, 1362 m, 1253 m, 1224 s, 1195 w, 1141 m, 1076 w, 931 w, 866 w, 823 s, 752 s, 700 s cm^{-1} ; Mass spectrum *m/z* (% rel intensity) 538 (44) M^+, 537 (23), 370 (15), 269 (76), 241 (78), 231 (100), 215 (44), 77(2). Anal calcd for $C_{40}H_{26}O_2$: C, 89.19; H, 4.87; Found: C, 89.17; H, 4.89.

***(S)*-3,3'-diphenyl-2,2'-biphenanthrene-1,1'-diol (*S*)-197:** To a 50 mL round bottomed flask was added CuCl (155 mg, 1.60 mmol), (–)-sparteine (760 mg, 3.20 mmol) and MeOH (30 mL). The reaction mixture was open to air and sonicated in an ultrasonic water bath for 0.5 h to afford a deep green solution. The flask was then sealed with a rubber septum and deoxygenated by purging with argon for 1 h (30 min in the solution and 30 min above the solution). To another 500 mL round bottomed flask equipped with a stir bar was added *rac*-**197** (500 mg, 1.14 mmol) and CH_2Cl_2 (120 mL). The solution was purged with argon for 1 h as well (30 min in the solution and 30 min above the solution). The prepared Cu-sparteine complex solution was then transferred through a cannula to the solution of *rac*-**197**. The mixed solution was then sonicated for 10 min and the flask was then covered with aluminum foil and allowed to stir at room temperature under slow constant flow of argon for 3 h. To the reaction mixture was added saturated $NaHCO_3$ solution (10 mL) and the resulting mixture was stirred for 5 min. The

mixture was then poured into a 500 mL separatory funnel with water (50 mL). The aqueous layer was then extracted with CH_2Cl_2 (50 mL × 3). The combined organic layer was dried over anhydrous Na_2SO_4. The solution was then filtered through a short plug of dry silica gel (40 × 50 mm column) which was flushed with CH_2Cl_2 (100 mL) to give a light yellow solution with the Cu residue remaining on the top. The resulting solution was then concentrated *in vacuo* followed by exposure to high vacuum (0.05 mm Hg) for 30 min to afford the crude product as a dark yellow solid. Purification of the crude product by silica gel chromatography (40 mm × 300 mm column, 9:1 hexanes / EtOAc as eluent, dry loading) afforded pure *(S)*-ISOVAPOL **197** as an orange solid (mp. 315-316 ºC) in 95% yield (474 mg, 1.08 mmol). The optical purity of **197** was determined to be greater than 99% ee by HPLC analysis (Pirkle D-phenylglycine column, 75:25 hexane/*i*PrOH at 260nm, flow-rate: 2.0 mL/min). Retention times; R_t = 20.01 min ((*S*)-ISOVAPOL **197**) and R_t = 22.05 min ((*R*)-ISOVAPOL **197**).

Spectral data for (*S*)-**197**: R_f = 0.33 (1:9 EtOAc/hexanes) ^{1}H NMR ($CDCl_3$, 300 MHz) δ 5.85 (s, 2 H), 6.73 (d, *J* = 7.1 Hz, 4H), 6.99 (t, *J* = 7.4 Hz, 4H), 7.06-7.11 (m, 2H), 7.59-7.65 (m, 4H), 7.83 (d, *J* = 9.1 Hz, 2H), 7.92-7.97 (m, 2H), 8.17 (s, 2H), 8.30 (d, *J* = 9.1 Hz, 2H), 8.58-8.62 (m, 2H); ^{13}C NMR (DMSO, 125 MHz) δ 114.98, 119.37, 121.15, 121.25, 123.15, 125.12, 126.16, 126.61, 126.64, 126.96, 128.31, 128.90, 129.63, 130.27, 131.70, 141.48, 141.68, 152.38; IR (KBr disc) 3521 vs, 3468 vs, 3059 w, 1616 w, 1594 m, 1566 w, 1509 w, 1482 w, 1393 m, 1362 m, 1253 m, 1224 s, 1195 w, 1141 m, 1076 w, 931 w, 866 w, 823 s, 752 s, 700 s cm^{-1}; Mass spectrum *m/z* (% rel intensity) 538 (44) M^+, 537 (23), 370 (15), 269 (76), 241 (78), 231 (100),

215 (44), 77(2); Anal calcd for $C_{40}H_{26}O_2$: C, 89.19; H, 4.87; Found: C, 89.22; H, 4.86; $[\alpha]_D^{20}$ – 200.5 (*c* 1.0, EtOAc) on 99% ee material (HPLC).

5.7.4 Synthesis of aziridines 86, 113a, 114a and 115a using (*S*)-ISOVAPOL and (*R*)-VANOL (*Table 5.1, 5.2 and 5.3*)

General Procedure for performing aziridination – Illustrated for the synthesis of *(2R,3R)*-ethyl 1-benzhydryl-3-phenylaziridine-2-carboxylate 86a using pre-catalyst method C.

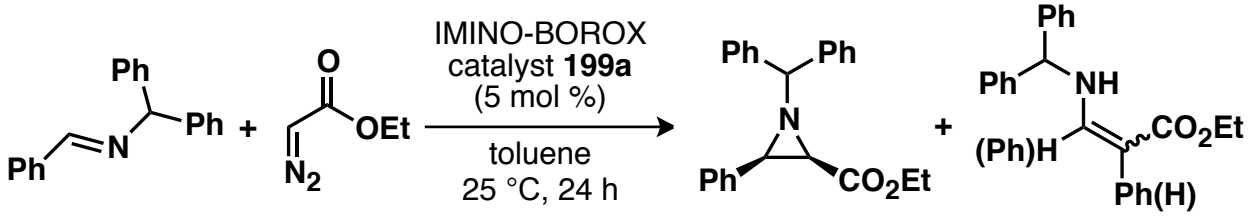

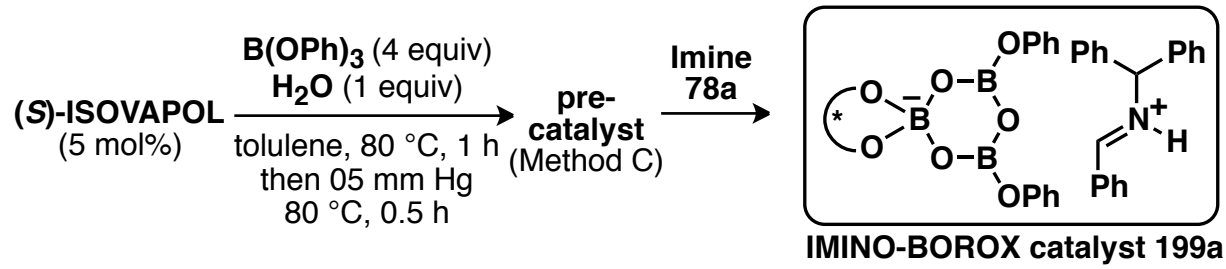

***(2R,3R)*- ethyl 1-benzhydryl-3-phenylaziridine-2-carboxylate 86a:** To a 25 mL flame-dried home-made Schlenk flask (see Figure 2.26) equipped with a stir bar and flushed with argon was added (*S)*-ISOVAPOL (27 mg, 0.05 mmol), commercial $B(OPh)_3$ (58 mg, 0.2 mmol) and water (0.9 μL, 0.05 mmol). Under an argon flow through the side-arm of the Schlenk flask, dry toluene (2 mL) was added through the top of the Teflon valve to dissolve the two reagents. The flask was sealed by closing the Teflon valve, and then placed in an 80 ºC oil bath for 1 h. After 1 h, a vacuum (0.5 mm Hg) was carefully applied by slightly opening the Teflon valve to remove

the volatiles. After the volatiles were removed completely, a full vacuum was applied and maintained for a period of 30 min at a temperature of 80 ºC (oil bath). The flask was then allowed to cool to room temperature and opened to argon through the side-arm of the Schlenk flask. To the flask containing the pre-catalyst (*made from method C*) was first added the aldimine **78a** (271 mg, 1 mmol) and then dry toluene (2 mL) under an argon flow through side-arm of the Schlenk flask. The reaction mixture was stirred for 5 min to give a light orange solution. To this solution was rapidly added ethyl diazoacetate (EDA) **85** (124 μL, 1.2 mmol) followed by closing the Teflon valve. The resulting mixture was stirred for 24 h at room temperature. Immediately upon addition of ethyl diazoacetate the reaction mixture became an intense yellow, which changed to light yellow towards the end of the reaction. The reaction was dilluted by addition of hexane (6 mL). The reaction mixture was then transferred to a 100 mL round bottom flask. The reaction flask was rinsed with dichloromethane (5 mL × 2) and the rinse was added to the 100 mL round bottom flask. The resulting solution was then concentrated *in vacuo* followed by exposure to high vacuum (0.05 mm Hg) for 1 h to afford the crude aziridine as an off-white solid.

A measure of the extent to which the reaction went to completion was estimated from the ^{1}H NMR spectrum of the crude reaction mixture by integration of the aziridine ring methine protons relative to either the imine methine proton or the proton on the imine carbon. The *cis/trans* ratio was determined by comparing the ^{1}H NMR integration of the ring methine protons for each aziridine in the crude reaction mixture. The *cis* (J = 7-8 Hz) and the *trans* (J = 2-3 Hz) coupling constants were used to differentiate the two isomers. The yields of the acyclic enamine side products **87a** and **88a** were determined by ^{1}H NMR analysis of the crude reaction mixture

by integration of the *N*-H proton relative to the that of the *cis*-aziridine methine protons with the aid of the isolated yield of the *cis*-aziridine. Purification of the crude aziridine by silica gel chromatography (35 mm × 400 mm column, 19:1 hexanes/EtOAc as eluent, under gravity) afforded pure cis-aziridine **86a** as a white solid (mp. 127.5-128.5 °C on 92% ee material) in 82% isolated yield (293 mg, 0.820 mmol); *cis/trans*: 50:1. Enamine side products: 3% yield of **87a** and 7% yield of **88a.** The optical purity of **86a** was determined to be 92% *ee* by HPLC analysis ((CHIRALCEL OD-H column, 90:10 hexanes/*i*PrOH at 222 nm, flow-rate: 0.7 mL/min): retention times; R_t = 9.01 min (major enantiomer, **86a**) and R_t = 4.67 min (minor enantiomer, *ent*-**86a**). The same reaction afforded aziridine **86a** in 87% yield and 89% ee using the (*R*)-VANOL boroxinate catalyst **189a**.

Spectral data for **86a**: R_f = 0.3 (1:9 EtOAc/hexanes); ^{1}H NMR ($CDCl_3$, 500 MHz) δ 0.95 (t, 3H, *J* = 7.3 Hz), 2.64 (d, *J* = 6.8 Hz, 1H), 3.19 (d, *J* = 6.8 Hz, 1H), 3.91 (q, *J* = 7.1 Hz, 2H), 3.93 (s, 1H), 7.16-7.38 (m, 11H), 7.47 (d, *J* = 7.1 Hz, 2H), 7.58 (d, *J* = 7.6 Hz, 2H); ^{13}C NMR ($CDCl_3$, 75 Hz) δ 13.93, 46.36, 48.01, 60.57, 77.68, 127.18, 127.31, 127.39, 127.52, 127.76, 127.78, 128.48, 135.00, 142.37, 142.49, 167.75; $[\alpha]_D^{20}$ + 33.4 (*c* 1.0, CH_2Cl_2) on 91% *ee* material (HPLC). These spectral data match those previously reported for this compound.[1a]

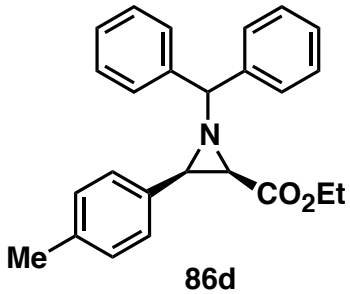

86d

(*2R,3R*)-ethyl 1-benzhydryl-3-p-tolylaziridine-2- carboxylate 86d: Imine **78d** (286 mg, 1.00 mmol) was reacted according to the general procedure described above with (*S*)-ISOVAPOL as the ligand. Purification of the crude aziridine by silica gel

chromatography (35 mm × 350 mm column, 9:1 hexanes / EtOAc as eluent) afforded pure aziridine **86d** as a white solid (mp. 148-149 °C) in 82% isolated yield (304 mg, 0.820 mmol). *cis/trans*: ≥ 50:1. Enamine side products: 3% yield of **87d** and 7% yield of **88d**. The optical purity of **86d** was determined to be 94% ee by HPLC analysis (CHIRALCEL OD-H column, 90:10 hexanes/*i*PrOH at 222 nm, flow-rate: 0.7 mL/min). Retention times, R_t = 8.54 min (major enaniomer, **86d**) and R_t = 4.46 min (minor enantiomer, *ent*-**86d**).

Spectral data for **86d:** R_f = 0.30 (1:9 EtOAc/hexanes). ^{1}H NMR ($CDCl_3$, 300 MHz) δ 0.99 (t, *J* = 7.3 Hz, 3H), 2.27 (s, 3H), 2.62 (d, *J* = 6.8 Hz, 1H), 3.16 (d, *J* = 6.6 Hz, 1H), 3.91 (s, 1H), 3.93 (q, *J* = 7.3 Hz, 2H), 7.03 (d, *J* = 8.0 Hz, 2H), 7.15-7.34 (m, 8H), 7.46 (d, *J* = 6.8 Hz, 2H), 7.57 (d, *J* = 6.8 Hz, 2H); ^{13}C NMR ($CDCl_3$, 75 Hz) δ 13.97, 21.12, 46.32, 48.00, 60.53, 77.72, 127.15, 127.20, 127.34, 127.51, 127.64, 128.45, 131.94, 136.88, 142.42, 142.53, 167.82; $[\alpha]_D^{20}$ +24.6 (*c* 1.0, CH_2Cl_2) on 94% *ee* material. These spectral data match those previously reported for this compound.[1a]

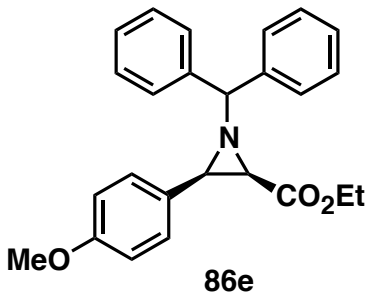

86e

(*2R,3R*)-ethyl 1-benzhydryl-3-(4-methoxyphenyl)aziridine-2-carboxylate 86e[2]: Imine **78e** (302 mg, 1.00 mmol) was reacted according to the general procedure described above with (*S*)-ISOVAPOL as ligand. The silica gel for column chromatography was pre-conditioned by preparing a slurry in a 1:9 mixture of Et_3N:CH_2Cl_2 which was loaded into a column (35 mm × 350 mm), the solvent was drained and then the silica gel was dried by flushing with nitrogen for one hour. The silica gel column was

then saturated with a 1:9 mixture of ethyl acetate:hexanes, the crude aziridine was loaded onto the column and then elution with the same solvent afforded pure aziridine **86e** as a white solid (mp. 136-137 °C) in 62% isolated yield (240 mg, 0.620 mmol). *cis/trans*: 9:1. Enamine side products: <1% yield of **87e** and 6% yield of **88e**. The optical purity of **86e** was determined to be 89 % ee by HPLC analysis (CHIRALCEL OD-H column, 95:5 hexanes/*i*PrOH at 222 nm, flow-rate: 0.7 mL/min). Retention times, R_t = 15.52 min (major enantiomer, **86e**) and R_t = 7.14 min (minor enantiomer, *ent*-**86e**).

Spectral data for **86e**: R_f = 0.2 (1:9 EtOAc/hexanes). ^{1}H NMR ($CDCl_3$, 300 MHz) δ 1.00 (t, J = 7.3 Hz, 3H), 2.60 (d, J = 6.8 Hz, 1H), 3.14 (d, J = 6.9 Hz, 1H), 3.74 (s, 3H), 3.91 (s, 1H), 3.93 (q, J = 7.1 Hz, 2H), 6.77 (d, J = 8.8 Hz, 2H), 7.14-7.32 (m, 8H), 7.45 (d, J = 6.9 Hz, 2H), 7.57 (d, J = 7.2 Hz, 2H); ^{13}C NMR ($CDCl_3$, 75 MHz) δ 13.99, 46.29, 47.70, 55.13, 60.52, 77.66, 113.18, 127.06, 127.15, 127.18, 127.34, 127.49, 128.44, 128.86, 142.39, 142.54, 158.85, 167.85; $[\alpha]_D^{20}$ +24.0 (*c* 1.0, CH_2Cl_2) on 89% *ee* material. These spectral data match those previously reported for this compound.[1a]

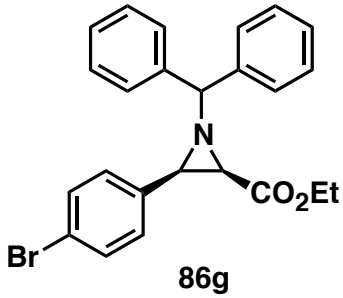

86g

(*2R,3R*)-ethyl 1-benzhydryl-3-(4-bromophenyl)aziridine-2-carboxylate 86g: Imine **78g** (350 mg, 1.00 mmol) was reacted according to the general procedure described above with (*S*)-ISOVAPOL as ligand. Purification of the crude aziridine by silica gel chromatography (35 mm × 350 mm column, 9:1 hexanes/EtOAc as eluent) afforded pure aziridine **86g** as a white solid (mp. 150-151 °C) in 80% isolated yield

(175 mg, 0.4 mmol). *cis/trans*: ≥ 50:1. Enamine side products: 2% yield of **87g** and 6% yield of **88g**. The optical purity of **86g** was determined to be 94% ee by HPLC analysis (CHIRALCEL OD-H column, 98:2 hexanes/*i*PrOH at 222 nm, flow-rate: 1.0 mL/min). Retention times, R_t = 14.31 min (major enaniomer, **86g**) and R_t = 5.56 min (minor enantiomer, *ent*-**86g**).

Spectral data for **86g**: R_f = 0.33 (1:9 EtOAc/hexanes). ^{1}H NMR ($CDCl_3$, 500 MHz) δ 1.00 (t, *J* = 7.1 Hz, 3H), 2.66 (d, *J* = 6.8 Hz, 1H), 3.12 (d, *J* = 6.6 Hz, 1H), 3.92 (s, 1H), 3.93 (q, *J* = 7.1 Hz, 2H), 7.16-7.37 (m, 10H), 7.43 (d, *J* = 6.8 Hz, 2H), 7.56 (d, *J* = 6.9 Hz, 2H); ^{13}C NMR ($CDCl_3$, 125 MHz) δ 13.98, 46.46, 47.33, 60.73, 77.58, 121.33, 127.12, 127.28, 127.41, 127.50, 128.52, 128.54, 129.54, 130.89, 134.03, 142.13, 142.30, 167.43; $[\alpha]_D^{20}$ +9.1 (*c* 1.0, CH_2Cl_2) on 94% *ee* material. These spectral data match those previously reported for this compound.[1a]

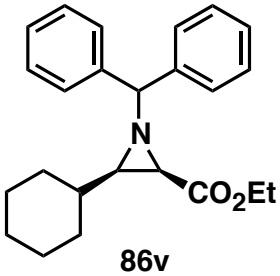

86v

(*2R,3R*)-ethyl 1-benzhydryl-3-cyclohexylaziridine-2-carboxylate 86v: Imine **78v** (278 mg, 1.00 mmol) was reacted according to the general procedure described above with (*S*)-ISOVAPOL as ligand. Purification of the crude aziridine by silica gel chromatography (35 mm × 350 mm column, 15:1 hexanes /EtOAc as eluent) afforded pure aziridine **86v** as a white solid (mp. 162.5-163 °C) in 72% isolated yield (262 mg, 0.72 mmol). *cis/trans*: ≥ 50:1. Enamine side products: 9% yield of **87v** and 4% yield of **88v**. The optical purity of **86v** was determined to be 79 % ee by HPLC analysis (CHIRALCEL OD-H column, 99:1 hexanes/*i*PrOH at 222 nm, flow-rate: 1.0 mL/min). Retention times, R_t = 6.88 min (major enaniomer, **86v**) and R_t = 3.41 min (minor enantiomer, *ent*-**86v**).

Spectral data for **86v**: R_f = 0.2 (1:15 EtOAc/hexanes). ^{1}H NMR ($CDCl_3$, 500 MHz) δ 0.49 (dq, *J* = 10 Hz, 3 Hz, 1H), 0.90-1.66 (m, 10H), 1.23 (t, *J* = 7.1 Hz, 3H), 1.78 (dd, *J* = 7.1 Hz, 3.0 Hz, 1H), 2.24 (d, *J* = 6.8 Hz, 1H), 3.59 (s, 1H), 4.13-4.26 (m, 2H), 7.18-7.34 (m, 8H), 7.47 (d, *J* = 7.5 Hz, 2H); ^{13}C NMR ($CDCl_3$, 75 MHz) δ 14.28, 25.35, 25.53,26.12, 30.10, 30.70, 36.26, 43.40, 52.12, 60.70, 78.17, 126.89, 127.05, 127.49, 128.27, 128.30, 128.36, 142.31, 142.71, 169.65; $[\alpha]_D^{20}$ +112.6 (*c* 1.0, CH_2Cl_2) on 79% *ee* material. These spectral data match those previously reported for this compound.[1a]

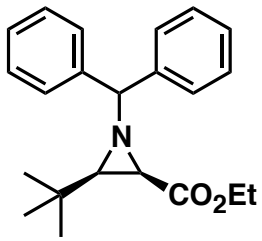

86w

(*2R,3R*)-ethyl 1-benzhydryl-3-tert-butylaziridine-2-carboxylate 86w: Imine **78w** (252 mg, 1.00 mmol) was reacted according to the general procedure described above with (*S*)-ISOVAPOL as ligand. Purification of the crude aziridine by silica gel chromatography (35 mm × 350 mm column, 9:1 hexanes / EtOAc as eluent) afforded pure aziridine **86w** as a white solid (mp. 149-150 °C) in 83% isolated yield (280 mg, 0.83 mmol). *cis/trans*: ≥ 50:1. Enamine side products: 6% yield of **87w** and <1% yield of **88w**. The optical purity of **86w** was determined to be 84 % ee by HPLC analysis (CHIRALCEL OD-H column, 99:1 hexanes/*i*PrOH at 222 nm, flow-rate: 1.0 mL/min). Retention times, R_t = 10.64 min (major enaniomer, **86w**) and R_t = 3.74 min (minor enantiomer, *ent*-**86w**).

Spectral data for **86w**: R_f = 0.33 (1:9 EtOAc/hexanes). ^{1}H NMR ($CDCl_3$, 300 MHz) δ 0.73 (s, 9H), 1.33 (t, *J* = 7.1 Hz, 3H), 1.79 (d, *J* = 7.3 Hz, 1H), 2.10 (d, *J* = 7.1 Hz, 1H), 3.63 (s, 1H), 4.07-4.18 (m, 1H), 4.22-4.33 (m, 1H), 7.21-7.37 (m, 6H), 7.43 (d, *J* = 6.8 Hz, 2H), 7.70 (d, *J* =

7.0 Hz, 2H); ^{13}C NMR ($CDCl_3$, 75 MHz) δ 14.09, 27.39, 31.60, 43.37, 56.05, 60.59, 79.19, 126.84, 127.24, 127.37, 128.17, 128.20, 128.27, 142.60, 143.44, 169.74; $[\alpha]_D^{20}$ +133.0 (*c* 1.0, CH_2Cl_2) on 84% *ee* material. These spectral data match those previously reported for this compound.[1a]

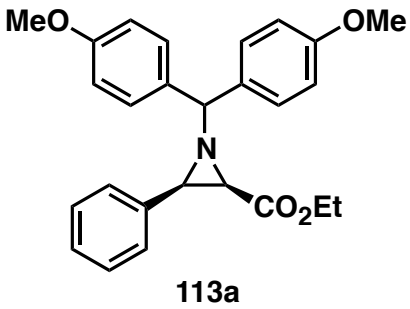

113a

(*2R,3R*)-*Cis*-1-(*N*-1-*bis*(4-methoxyphenyl)methyl) -2-carboxyethyl-3-phenylaziridine 113a. Imine **110a** (332 mg, 1.00 mmol) was reacted according to the general procedure described above with (*S*)-ISOVAPOL as ligand. Purification of the crude aziridine by silica gel chromatography (35 mm × 350 mm column, 9:1 hexanes / EtOAc as eluent, after elution of the first fraction, which contains EDA and / or enamine side products **116a** and **117a**, the eluent was changed to 5:1 hexanes / EtOAc) afforded pure aziridine **113a** as a white solid (mp 89.5-90.5 ºC) in 90% isolated yield (376 mg, 0.900 mmol); *cis/trans*: 50:1. Enamine side products: 6% yield of **116a** and <1% yield of **117a.** The optical purity of **113a** was determined to be 96% *ee* by HPLC analysis (CHIRALPAK AD column, 90:10 hexanes/*i*PrOH at 226nm, flow-rate: 1.0 mL/min): retention times; R_t = 8.78 min (major enantiomer, **113a**) and R_t = 15.49 min (minor enantiomer, *ent*-**113a**).

Spectral data for **113a**: See experimental of Chapter 2

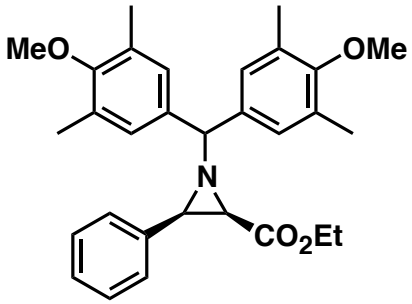

114a

***(2R,3R)-Cis*-1-(*N*-1-bis(4-methoxy-3,5-dimethylphenyl) methyl)-2-carboxyethyl-3-phenylaziridine 114a:** Imine **111a** (388 mg, 1.00 mmol) was reacted according to the general procedure described above with (*S*)-ISOVAPOL as ligand. Purification of the crude aziridine by silica gel chromatography (35 mm × 350 mm column, 9:1 hexanes / EtOAc as eluent, after elution of the first fraction, which contains EDA and / or enamine side products **118a** and **119a**, the eluent was changed to 5:1 hexanes / EtOAc) afforded pure aziridine **114a** as a white solid (mp 107-108 ºC) in 96 % isolated yield (454 mg, 0.96 mmol).; *cis/trans*: ≥ 50:1. Enamine side products: 2% yield of **118a** and 1% yield of **119a.** The optical purity of **114a** was determined to be 98% *ee* by HPLC (CHIRALCEL OD-H column, 99:1 hexanes/*i*PrOH at 226 nm, flow-rate: 0.7 mL/min). Retention times; R_t = 8.96 min (major enantiomer, **114a**) and R_t = 12.85 min (minor enantiomer, *ent*-**114a**).

Spectral data for **114a**: R_f = 0.42 (1:9 EtOAc/hexane). ^{1}H NMR ($CDCl_3$, 500 MHz) δ 0.98 (t, J = 7.1 Hz, 3H), 2.18 (s, 6H), 2.24 (s, 6H), 2.55 (d, J = 6.8 Hz, 1H), 3.10 (d, J = 6.6 Hz, 1H), 3.62 (s, 3H), 3.66 (s, 1H), 3.68 (s, 3H) 3.87-3.97 (m, 2H), 7.09 (s, 2H), 7.18 (s, 2H), 7.21 (d, J = 7.6 Hz, 2H), 7.35-7.37 (m, 3H); ^{13}C ($CDCl_3$, 125 MHz) δ 14.01, 16.16, 16.22, 46.26, 48.20, 59.52, 59.58, 60.47, 77.04, 127.21, 127.41, 127.70, 127.80,127.85, 130.59, 130.60, 135.33, 137.79, 137.96, 155.95, 156.10, 168.01. $[\alpha]_D^{20}$ +41.3 (*c* 1.0, EtOAc) on 99% ee material (HPLC). These spectral data match those previously reported for this compound.[1c]

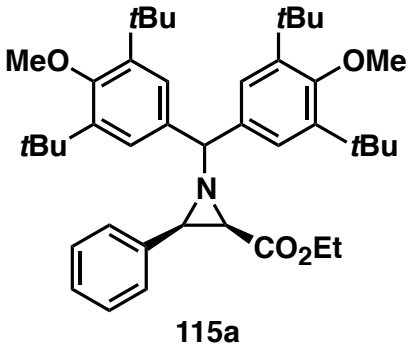

115a

(*2R,3R*)-ethyl-1-(bis(3,5-di-tert-butyl-4-methoxyphenyl) methyl)-3-phenylaziridine-2-carboxylate 115a: Imine **112a** (278 mg, 0.5 mmol) was reacted according to the general procedure described above with (*S*)-ISOVAPOL as ligand. Purification of the crude aziridine by silica gel chromatography (35 mm × 350 mm column, 20:1 hexanes/EtOAc as eluent) afforded pure aziridine **115a** as a white solid (mp. 156-158 ºC) in 97% isolated yield (652 mg, 0.97 mmol).; *cis/trans*: ≥ 50:1. Enamine side products: <1% yield of **120a** and <1% yield of **121a.** The optical purity of **115a** was determined to be 96% *ee* by HPLC (Pirkle covalent (R,R) Whelk-O 1 column, 99:1 hexanes/*i*PrOH at 225 nm, flow-rate: 1.0 mL/min). Retention times; R_t = 9.72 min (major enantiomer, **115a**) and R_t = 5.38 min (minor enantiomer, *ent*-**115a**).

Spectral data for **115a:** R_f = 0.26 (20:1 hexanes/EtOAc); ^{1}H NMR ($CDCl_3$, 300 MHz) δ = 0.97 (t, *J* = 7.1 Hz, 3H), 1.31 (s, 18H), 1.39 (s, 18H), 2.64 (d, *J* = 6.8 Hz, 1H), 3.15 (d, *J* = 6.8 Hz, 1H), 3.59 (s, 3H), 3.65 (s, 3H), 3.82 (s, 1H), 3.84-3.96 (m, 2H), 7.16-7.19 (m, 1H), 7.22-7.25 (m, 2H), 7.31 (s, 2H), 7.41 (s, 2H), 7.46 (d, *J* = 7.1 Hz, 2H); ^{13}C NMR ($CDCl_3$, 75 MHz) δ 13.95, 32.04, 32.13, 35.71, 35.78, 46.35, 48.78, 60.50, 63.93, 64.01, 125.37, 125.49, 127.23, 127.58, 128.15, 135.35, 136.69, 136.85, 143.00, 143.08, 158.23, 158.25, 168.27 (one sp^3 carbon not located). $[\alpha]_D^{20}$ +5.5 (*c* 1.0, EtOAc) on 96% ee material (HPLC). These spectral data match those previously reported for this compound.[1b]

5.7.5 NMR analysis of a mixture of VANOL, $B(OPh)_3$, and imine 111a (*Figure 5.3)*

As shown in Figure 5.3 of this chapter, a mixture of (*S*)-VANOL **59** and $B(OPh)_3$ **187a** results in mesoborate B1 **107** and pyroborate B2 **109** and unreacted VANOL **59** when subjected to the pre-catalyst method C. Also, it was evident from the ^1H NMR and ^{11}B NMR that no boroxinate B3 **191a** was formed unless imine **111a** was added (characteristic peaks i.e. δ 8.55-8.56 ppm and δ 5.5-5.7 were missing in ^1H NMR and ^{11}B NMR respectively). Unless otherwise noted, commercial $B(OPh)_3$ is used in all the experiments. Also, Ph_3CH is used as the internal standard.

Experimental:

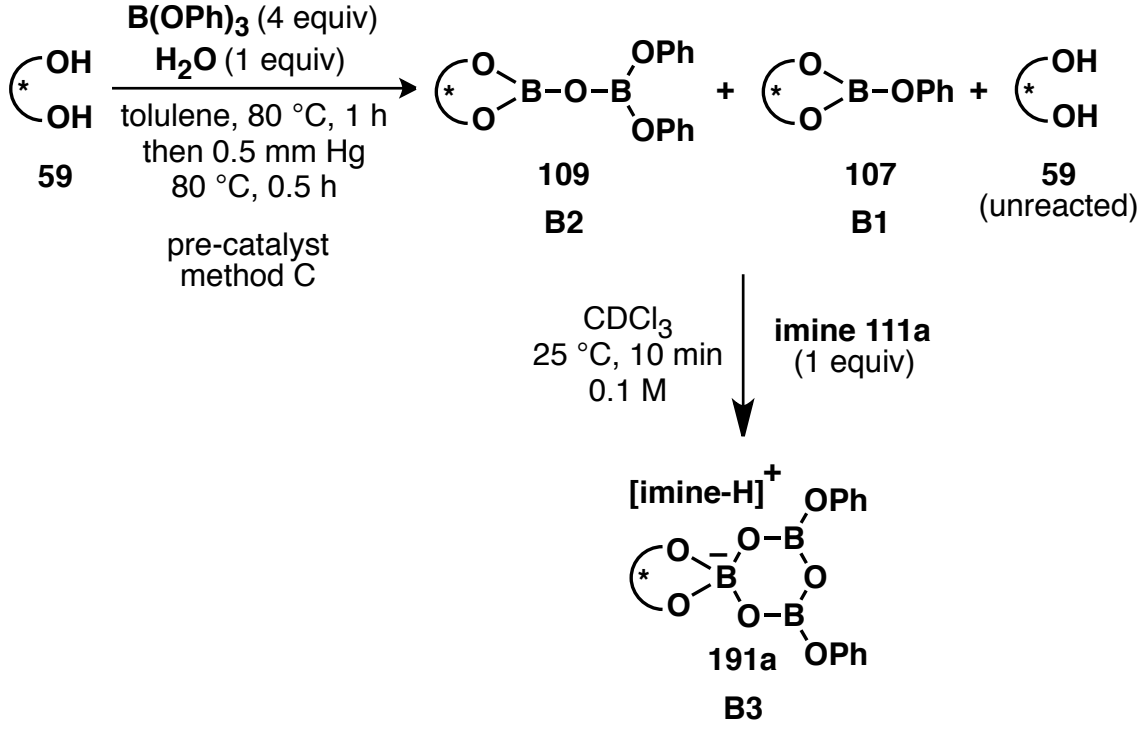

Entry 1, Figure 5.3: The ^1H NMR of pure (*S*)-VANOL taken in $CDCl_3$.

Entry 2, Figure 5.3: The pre-catalyst was made using method C employing (*S*)-VANOL (44 mg, 0.1 mmol), commercial $B(OPh)_3$ (116 mg, 0.4 mmol) water (1.8 μL, 0.1 mmol). To the flask containing the pre-catalyst was first added the Ph_3CH (12.22 mg, 0.05 mmol) and then $CDCl_3$ (1 mL) under an argon flow through side-arm of the Schlenk flask. The reaction mixture was then stirred for 10 min. The off-white colored solution was then directly transferred to a quartz NMR tube and was subjected to ^1H NMR and ^{11}B NMR analysis.

Entry 3, Figure 5.3:

The pre-catalyst was made using method C employing (*S*)-VANOL (44 mg, 0.1 mmol), commercial $B(OPh)_3$ (116 mg, 0.4 mmol) water (1.8 μL, 0.1 mmol). To the flask containing the pre-catalyst was first added the imine **111a** (39 mg, 0.1 mmol), Ph_3CH (12.22 mg, 0.05 mmol) and then $CDCl_3$ (1 mL) under an argon flow through side-arm of the Schlenk flask. The reaction mixture was then stirred for 10 min. The red colored solution was then directly transferred to a quartz NMR tube and was subjected to ^1H NMR and ^{11}B NMR analysis.

5.7.6 NMR analysis of a mixture of ISOVAPOL, $B(OPh)_3$, and imine 111a (*Figure 5.3)*

Same as section 5.7.5 using (*S*)-ISOVAPOL instead of (*S*)-VANOL.

5.7.7 Synthesis of BINOL derivatives 258, 259, 308, 56a, 56d, 56e, 56f and 56i (*Scheme 5.6-5.9)*

5.7.7.1 Synthesis of BINOL derivative 258: See experimental of Chapter 4

5.7.7.2 Synthesis of BINOL derivative 259: See experimental of Chapter 4

5.7.7.3 Synthesis of BINOL derivative 308:

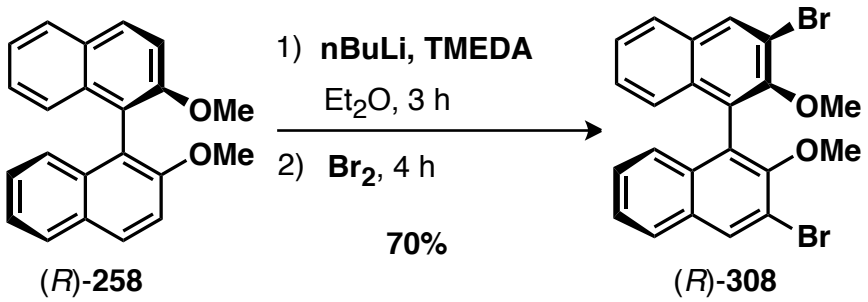

(*R*)-**258** (*R*)-**308**

(*R*)-3,3'-dibromo-2,2'-dimethoxy-1,1'-binaphthalene (*R*)-**308:** In a 50 mL flame-dried three-necked round bottomed flask equipped with a N_2-inlet were placed dry Et_2O (20 mL) and TMEDA (256 mg, 0.330 mL, 2.20 mmol). To this solution was added ^{n}BuLi (1.2 mL, 3.0 mmol, 2.5 M in hexanes). The solution was stirred for 30 min at room temperature. To this solution was added solid (*R*)-**258** (314 mg, 1.00 mmol) in one portion and the reaction mixture was stirred for 3 h. The resulting light brown suspension was cooled to –78 °C, and Br_2 (1.9 g, 0.62 mL, 12 mmol) was added *via* syringe over a period of 10 min. The solution was then allowed to warm to room temperature and was left stirring for 4 h. The reaction was quenched with saturated $Na_2S_2O_3$ solution (10 mL) and stirred for 30 min. The organic layer was separated, and the aqueous layer was extracted by CH_2Cl_2 (10 mL × 3). The combined organic solution was dried over anhydrous $MgSO_4$, filtered and concentrated *in vacuo* to afford crude product. Purification by silica gel column chromatography (35 mm × 350 mm column, 8:1 hexanes/EtOAc as eluent) afforded (*R*)-**308** as yellow solid (mp. 174-175 °C) in 70% yield (331 mg, 0.700 mmol).

Spectral data for (*R*)-**308**: R_f = 0.55 (4:1 hexanes/CH_2Cl_2); ^{1}H NMR ($CDCl_3$, 500 MHz) δ 3.51 (s, 6H), 7.09 (d, *J* = 8.5 Hz, 2H), 7.27 (ddd, *J* = 8.4, 6.9, 1.3 Hz, 2H), 7.41-7.44 (m, 2H), 7.82 (d, *J* = 8.2 Hz, 2H), 8.27 (s, 2H); ^{13}C NMR ($CDCl_3$, 125 MHz) δ 61.08, 117.48, 125.75, 125.84, 126.52, 126.83, 127.11, 131.43, 132.97, 133.07, 152.53; $[\alpha]_D^{20}$ +71.4 (*c* 1.4, THF). These spectral data match those previously reported for this compound.[49b,55]

5.7.7.4 Synthesis of BINOL derivative (*R*)-56a:

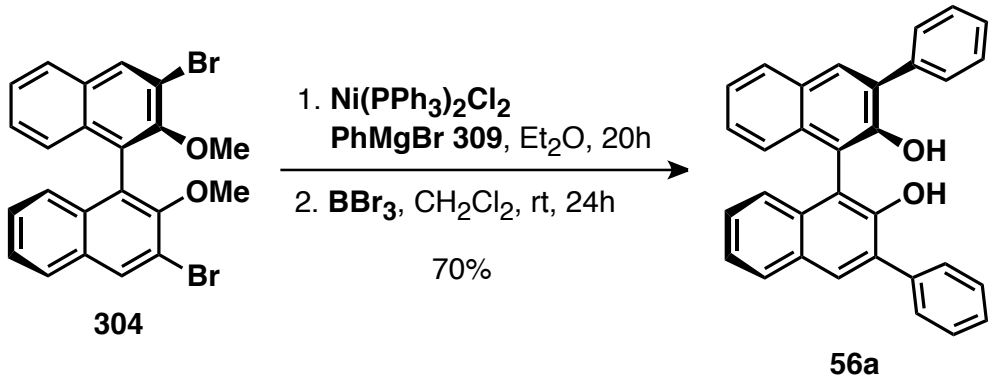

(*R*)-3,3'-diphenyl-[1,1'-binaphthalene]-2,2'-diol (*R*)-**56a:** In a 50 mL flame-dried round bottomed flask equipped with a N_2-inlet were placed (*R*)-**308** (236 mg, 0.500 mmol) and $Ni(PPh_3)_2Cl_2$ (26 mg, 0.04 mmol) and dry Et_2O (10 mL). To this suspension was added PhMgBr **309** (1.0 mL, 3.0 mmol, 3.0 M in ether) over a period of 10 min. The reaction mixture was heated at reflux for 20 h, cooled to 0 °C, and quenched with water (1 mL). After addition of 1 N HCl solution (20 mL), the mixture was stirred for 10 min and extracted with ether. The

ether layer was washed with brine, dried (Na_2SO_4), and concentrated *in vacuo*. Purification by silica gel column chromatography (35 mm × 350 mm column, 10:1 hexanes/EtOAc as eluent) afforded the coupling product as colorless solid in 75% yield (175 mg, 0.375 mmol). To a solution of this coupling product (175 mg, 0.375 mmol) in CH_2Cl_2 (10 mL) was added BBr_3 (1.5 mL, 1.5 mmol, 1.0 M in CH_2Cl_2) drop-wise at –78 °C. The reaction was allowed to warm to 0 °C. The reaction mixture was stirred for 0.5 h at 0 °C and then was allowed to warm to room temperature. After stirring at room temperature for 24 h, the reaction was quenched by the slow addition of the distilled water (1.5 mL) in an ice bath. The aqueous layer was extracted with CH_2Cl_2 (5 mL × 3). The combined extracts were then washed with water, brine and then dried over $MgSO_4$, filtered, and concentrated *in vacuo*. Purification of the yellow colored crude product by silica gel chromatography (20 mm × 200 mm column, 8:1 hexanes/EtOAc as eluent, under gravity) afforded pure (*R*)-**56a** as a white solid (mp. 202-203 °C) in 70% isolated yield (154 mg, 0.350 mmol, over two steps).

Spectral data for (*R*)-**56a**: R_f = 0.36 (8:1 hexanes/CH_2Cl_2); ^{1}H NMR ($CDCl_3$, 500 MHz) δ 5.30 (s, 2H), 7.16-7.54 (m, 12H), 7.82 (d, *J* = 7.5 Hz, 4H), 7.90 (d, *J* = 8.0 Hz, 2H), 8.00 (s, 2H); ^{13}C NMR ($CDCl_3$, 75 MHz) δ 112.30, 124.23, 124.30, 127.32, 127.74, 128.42, 128.46, 129.40, 129.57, 130.61, 131.38, 132.86, 137.40, 150.08; $[\alpha]_D^{20}$ +106.2 (*c* 1.0, THF). These spectral data match those previously reported for this compound.[49b,55]

5.7.7.5 Synthesis of BINOL derivative 56d:

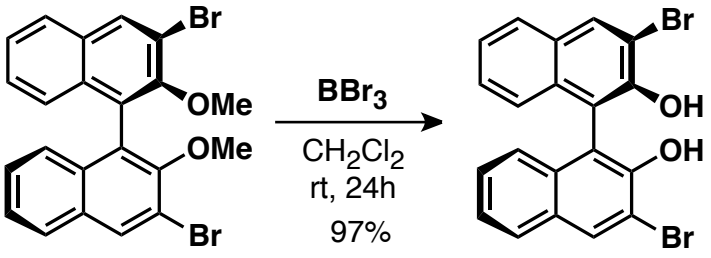

(R)-**308** *(R)*-**56d**

(*R*)-3,3'-dibromo-[1,1'-binaphthalene]-2,2'-diol (*R*)-56d: In a 50 mL flame-dried round bottomed flask equipped with a N_2-inlet were placed (*R*)-**308** (472 mg, 1.0 mmol) and dry CH_2Cl_2 (10 mL). To this solution was added BBr_3 (6.0 mL, 6.0 mmol, 1.0 M in CH_2Cl_2) drop-wise at 0 °C. The reaction was allowed to warm to room temperature. After stirring at room temperature for 12 h, the reaction was quenched by the slow addition of the distilled water (10 mL) in an ice bath. The aqueous layer was extracted with CH_2Cl_2 (10 mL × 3). The combined extracts were then washed with water, brine and then dried over $MgSO_4$, filtered, and concentrated *in vacuo*. Purification of the crude product by silica gel chromatography (35 mm × 400 mm column, 15:1 hexanes/EtOAc as eluent) afforded pure (*R*)-**56d** as a white solid (mp. 245-246 °C) in 97 % isolated yield (431 mg, 0.970 mmol).

Spectral data for (*R*)-**56d:** R_f = 0.31 (9:1 hexanes/ EtOAc); ^{1}H NMR ($CDCl_3$, 500 MHz) δ 5.54 (s, 2H), 7.12 (d, *J* = 8.5 Hz, 2H), 7.24-7.42 (m, 4H), 7.82 (d, *J* = 8.0 Hz, 6H), 8.25 (s, 2H); ^{13}C NMR ($CDCl_3$, 75 MHz) δ 112.22, 114.57, 124.60, 124.86, 127.39, 127.58, 129.70, 132.73,

132.75, 147.98; $[\alpha]_D^{20}$ + 98.6 (*c* 1.0, THF). These spectral data match those previously reported for this compound.[57]

5.7.7.6 Synthesis of BINOL derivative 56e:

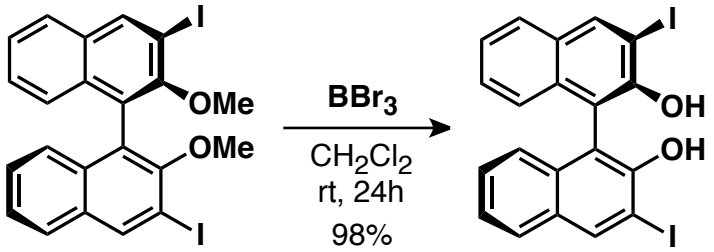

(R)-**259** *(R)*-**56e**

(*R*)-3,3'-diiodo-[1,1'-binaphthalene]-2,2'-diol (*R*)-56e: In a 50 mL flame-dried round bottomed flask equipped with a N_2-inlet were placed (*R*)-**259** (567 mg, 1.0 mmol) and dry CH_2Cl_2 (10 mL). To this solution was added BBr_3 (6.0 mL, 6.0 mmol, 1.0 M in CH_2Cl_2) drop-wise at 0 °C. The reaction was allowed to warm to room temperature. After stirring at room temperature for 12 h, the reaction was quenched by the slow addition of the distilled water (10 mL) in an ice bath. The aqueous layer was extracted with CH_2Cl_2 (10 mL × 3). The combined extracts were then washed with water, brine and then dried over $MgSO_4$, filtered, and concentrated *in vacuo*. Purification of the crude product by silica gel chromatography (35 mm × 400 mm column, 1:1 hexanes/CH_2Cl_2 as eluent) afforded pure (*R*)-**56e** as a yellow solid (mp. 312-315 °C) in 97 % isolated yield (527 mg, 0.980 mmol).

Spectral data for (*R*)-**56d:** R_f = 0.54 (1:1 hexanes/ CH_2Cl_2); ^{1}H NMR ($CDCl_3$, 300 MHz) δ 5.42

(brs, 2H), 7.07 (d, J = 8.2 Hz, 2H), 7.31 (ddd, J = 8.2, 6.9, 1.3 Hz, 2H), 7.38 (ddd, J = 8.2, 6.9, 1.3 Hz, 2H), 7.79 (d, J = 7.7 Hz, 2H), 8.52 (s, 2H); ^{13}C NMR ($CDCl_3$, 75 MHz) δ 86.51, 112.52, 124.34, 124.61, 127.11, 127.78, 130.63, 133.09, 140.20, 150.01; $[\alpha]_D^{20}$ +101.0 (*c* 1.0, THF). These spectral data match those previously reported for this compound.[58]

5.7.7.7 Synthesis of BINOL derivative 56f:

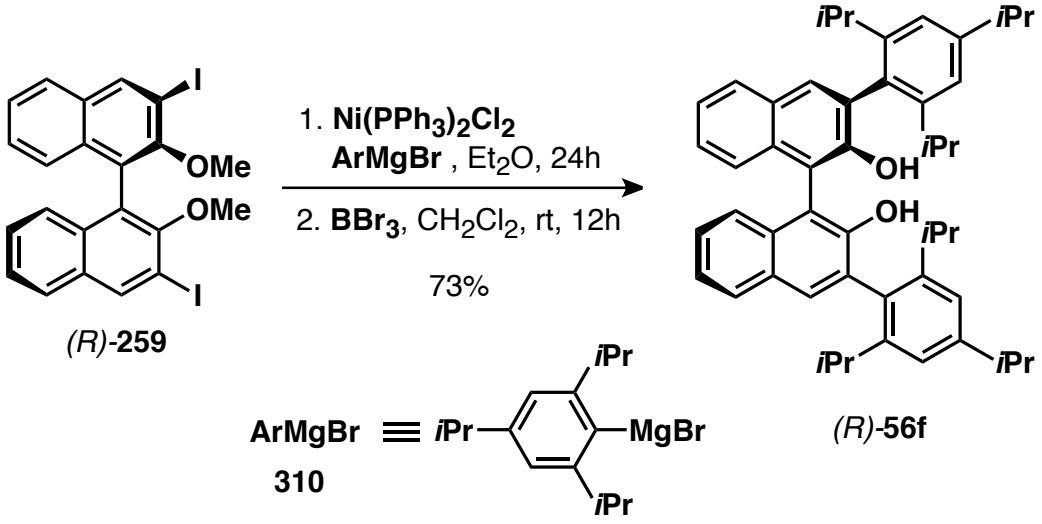

2-bromo-1,3,5-triisopropylbenzene 310′ : In a flame-dried 25 mL three-neck flask equipped with a condenser, was placed 1,3,5-triisopropylbenzene (3.07 g, 3.6 mL, 15 mmol), carbon tetrachloride (2 mL) and iron powder (0.12 g). The reaction vessel was cooled in an ice-salt bath and light was excluded by wrapping the flask in tin foil and covering it with a towel. Bromine (2.4 g, 0.77 mL, 15 mmol) in carbon tetrachloride (2 mL) was added dropwise over a 10-min period. Hydrogen Bromide evolved was led off through the condenser and absorbed in water. The reaction mixture was allowed to stand overnight. The mixture was then washed with water (10 mL × 2), 20% sodium hydroxide (5 mL × 2), and water (10 mL). The resulting solution was

then dried over anhydrous $CaC1_2$ and concentrated *in vacuo* to afford the crude product. Benzylic halide impurities in the product were destroyed by adding the crude concentrate to a solution obtained by dissolving sodium (0.5 g) in absolute ethanol (15 mL). The reaction mixture was then allowed to stand overnight followed by the dilution with water (50 mL). The organic layer was separated, and the aqueous layer was extracted with CCl_4 (10 mL × 3). The combined organic layers were washed with water (10 mL × 2), brine (10 mL) and then dried over anhydrous $CaCl_2$. It was then filtered and concentrated *in vacuo* to give crude product. Purification by distillation furnished **310′** (bp. 96 – 97 °C at 0.1 mm Hg) as a colorless oil in 70 % yield (2.97 g, 10.54 mmol).

Spectral data for **310′:** ^{1}H NMR ($CDCl_3$, 300 MHz) δ 1.29-1.32 (m, 18 H), 2.87 (sept, J = 6.8 Hz, 1H), 3.48 (sept, J = 6.8 Hz, 2H), 6.98 (s, 2H); ^{13}C NMR ($CDCl_3$, 75 MHz) δ 23.1, 24.03, 33.54, 34.05, 122.26, 147.36, 147.79.

(2,4,6-triisopropylphenyl)magnesium Bromide 310: A three-neck round-bottom flask containing Mg (301 mg, 12.4 mmol, 20 mesh) was equipped with a condenser and an addition funnel. A 1.0 mL portion of a 1.4 M solution of 2,4,6-triisopropylphenyl bromide **310′** (1.98 g in 5 mL of Et_2O, 7 mmol) was added to the flask through the addition funnel. After 5 min, 0.02 mL (0.0002 mmol) of 1,2-dibromoethane was added to the mixture. Once the solution began to reflux, the remaining 2,4,6-triisopropylphenyl-bromide solution was slowly added over 1 h. After the addition was complete, the reaction was allowed to reflux for 12 h. The resulting Grignard reagent was directly in the next step.

***(R)*-3,3'-Bis(2,4,6-triisopropylphenyl)-2,2'-dihydroxy-1,1'-dinaphthyl 56f:** In a 50 mL flame-

dried round bottomed flask equipped with a N_2-inlet were placed (*R*)-**259** (567 mg, 1.0 mmol) and $Ni(PPh_3)_2Cl_2$ (106 mg, 0.15 mmol) and dry Et_2O (12 mL). To this suspension was added freshly prepared Grignard reagent **310** (7.0 mmol) over a period of 10 min. The reaction mixture was stirred for 10 min at room temperature and then heated at reflux for 24 h. The reaction mixture was then cooled to 0 °C, and quenched slowly by the addition of HCl (6 mL, 1 M). After addition of 1 N HCl solution (6 mL), the mixture was stirred for 10 min and extracted with ether (10 mL × 3). The ether layer was washed with brine, dried (Na_2SO_4), and concentrated *in vacuo*. Purification by silica gel column chromatography (35 mm × 350 mm column, 9:1 hexanes/ CH_2Cl_2 as eluent) afforded the coupling product as colorless solid in 76% yield (547 mg, 0.76 mmol). To a solution of this coupling product (547 mg, 0.76 mmol) in CH_2Cl_2 (20 mL) was added BBr_3 (5.3 mL, 5.3 mmol, 1.0 M in CH_2Cl_2) drop-wise at 0 °C. The reaction was allowed to room temperature. After stirring at room temperature for 12 h, the reaction was quenched by the slow addition of the distilled water (7 mL) in an ice bath. The aqueous layer was extracted with CH_2Cl_2 (10 mL × 3). The combined extracts were then washed with water, brine and then dried over $MgSO_4$, filtered, and concentrated *in vacuo*. Purification of the brown colored crude product by silica gel chromatography (35 mm × 400 mm column, 5:1 hexanes/ CH_2Cl_2 as eluent) afforded pure (*R*)-**56f** as a white solid (mp. 134-135 °C) in 73% isolated yield (504 mg, 0.73 mmol, over two steps). Sometimes, (*R*)-**56f** has been obtained as yellow solid. In that case, it was washed with hexanes and white compound was obtained after the washings.

Spectral data for (*R*)-**56f:** R_f = 0.25 (5:1 hexanes/ CH_2Cl_2); ^{1}H NMR ($CDCl_3$, 300 MHz) δ 1.01(d, *J* = 6.8 Hz, 6H), 1.08 (t, *J* = 6.8 Hz, 12H), 1.17 (d, *J* = 6.8 Hz, 6H), 1.29 (d, *J* = 6.8 Hz, 12H), 2.66 (sept, *J* = 6.8 Hz, 2H), 2.82 (sept, *J* = 6.8 Hz, 2H), 2.94 (sept, *J* = 6.8 Hz, 2H), 4.90 (s, 2H), 7.10 (s, 2H), 7.12 (s, 2H), 7.25-7.38 (m, 6H), 7.74 (s, 2H), 7.84 (d, *J* = 7.6 Hz, 2H); ^{13}C NMR ($CDCl_3$, 75 MHz) δ 23.71, 23.91,23.96, 24.04, 24.27, 24.30, 30.85, 30.90, 34.34, 113.18, 121.17, 121.22, 123.75, 124.53, 126.53, 126.60, 128.23, 129.07, 129.14, 130.39, 130.65, 133.49, 147.77, 147.84, 149.15, 150.64; $[\alpha]_D^{20}$ + 79.0 (*c* 2.0, THF). These spectral data match those previously reported for this compound.[59]

5.7.7.8 Synthesis of BINOL derivative 56i:

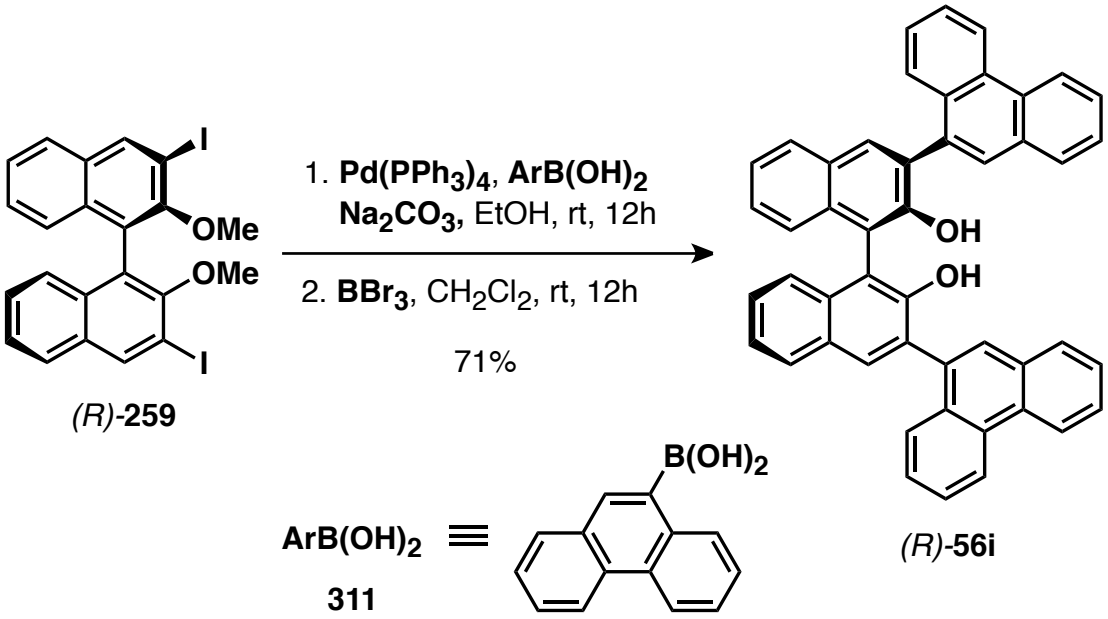

(*R*)-3,3'-di(phenanthren-9-yl)-[1,1'-binaphthalene]-2,2'-diol (*R*)-**56i:** In a 50 mL flame-dried home-made Schlenk (see Figure 2.26) flask equipped with a N_2-inlet were placed (*R*)-**259** (567 mg, 1.00 mmol) and 9-phenanthranylboronic acid **311** (922 mg, 4.15 mmol), dry toluene (8 mL),

ethanol (4 mL) and aqueous Na_2CO_3 (4 mL, 2M). The suspension was purged with nitrogen for 30 min. Under the flow of nitrogen, $Pd(PPh_3)_4$ (116 mg, 0.100 mmol) was added. The flask was sealed by closing the Teflon valve and then placed in an 90 ºC oil bath for 14 h. The reaction mixture was cooled to room temperature and was filtered followed by the addition of CH_2Cl_2 (10 mL) and water (5 mL). The aqueous layer was extracted with CH_2Cl_2 (10 mL × 3). The combined extracts were then washed with brine and then dried over $MgSO_4$, filtered, and concentrated *in vacuo*. The resulting crude coupling product was dissolved in CH_2Cl_2 (15 mL). To this solution was added BBr_3 (2.7 mL, 2.7 mmol, 1.0 M in CH_2Cl_2) drop-wise at 0 °C. The reaction was allowed to warm to room temperature. After stirring at room temperature for 12 h, the reaction was quenched by the slow addition of the distilled water (5 mL) in an ice bath. The aqueous layer was extracted with CH_2Cl_2 (5 mL × 3). The combined extracts were then washed with water, brine and then dried over $MgSO_4$, filtered, and concentrated *in vacuo*. Purification of the yellow colored crude product by silica gel chromatography (35 mm × 400 mm column, 4:1 hexanes/ CH_2Cl_2 as eluent, under gravity) afforded pure (*R*)-**56i** as a yellow solid (mp. 148-150 ºC, decomposition) in 71 % isolated yield (454 mg, 0.710 mmol, over two steps).

Spectral data for (*R*)-**56i**: R_f = 0.57 (4:1 hexanes/CH_2Cl_2); ^{1}H NMR ($CDCl_3$, 600 MHz) δ 5.22, 5.23, 5.28, 5.33, (4 singlets, combined integration: 2H), 7.42-7.80 (m, 15H), 7.88-7.92 (m, 2H), 7.95-8.00 (m, 5H), 8.10-8.12 (m, 2H), 8.75-8.83 (m, 4H); ^{13}C NMR ($CDCl_3$, 150 MHz) δ 113.07, 113.17, 113.48, 122.82, 122.85, 123.10, 123.14, 123.21, 123.24, 124.50, 124.53, 124.71,

124.74, 124.93, 125.00, 126.94, 127.01, 127.05, 127.13, 127.16, 127.22, 127.28, 127.53, 127.59, 128.60, 128.71, 129.01, 129.07, 129.19, 129.41, 129.52, 129.54, 129.66, 129.67, 129.77, 130.63, 130.66, 130.69, 130.76, 130.78, 130.81, 131.29, 131.34, 131.35, 131.39, 131.66, 131.68, 131.70, 131.71, 132.26, 132.32, 133.79, 133.82, 133.92, 133.94, 133.99, 134.20, 150.80, 150.85, 150.87; $[\alpha]_D^{20}$ +45.5.0 (*c* 1.0, $CHCl_3$). These spectral data match those previously reported for this compound.[61]

5.7.8 Asymmetric aziridination with BINOL 55, BINOL derivatives 56 and TADDOL 61a (*Table 5.4-5.5 and Scheme 5.12*)

General Procedure for performing aziridination – Illustrated for the synthesis of *(2S,3S)*-ethyl 1-benzhydryl-3-phenylaziridine-2-carboxylate 86a using pre-catalyst method C and 3,3′-Ph_2-BINOL (*R*)-56a as the ligand.

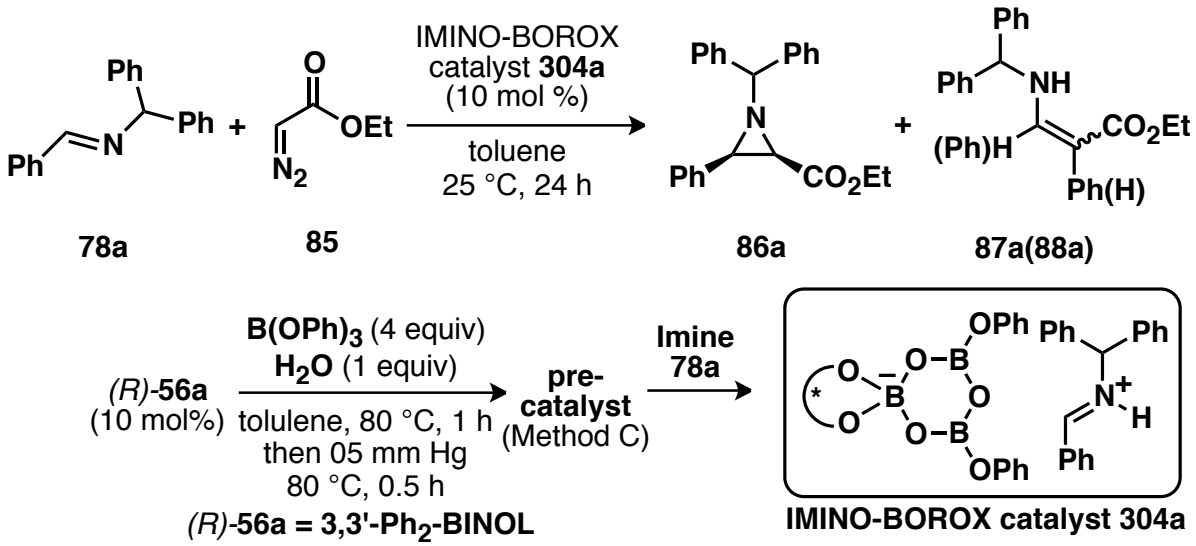

***(2S,3S)*- ethyl 1-benzhydryl-3-phenylaziridine-2-carboxylate *ent*-86a:** To a 25 mL flame-dried home-made Schlenk flask (see Figure 2.26) equipped with a stir bar and flushed with argon

was added (*R*)-**56a** (44 mg, 0.1 mmol), commercial $B(OPh)_3$ (116 mg, 0.4 mmol) and water (1.8 μL, 0.1 mmol). Under an argon flow through the side-arm of the Schlenk flask, dry toluene (2 mL) was added through the top of the Teflon valve to dissolve the two reagents. The flask was sealed by closing the Teflon valve, and then placed in an 80 ºC oil bath for 1 h. After 1 h, a vacuum (0.5 mm Hg) was carefully applied by slightly opening the Teflon valve to remove the volatiles. After the volatiles were removed completely, a full vacuum was applied and maintained for a period of 30 min at a temperature of 80 ºC (oil bath). The flask was then allowed to cool to room temperature and opened to argon through the side-arm of the Schlenk flask. To the flask containing the pre-catalyst (*made from method C*) was first added the aldimine **78a** (271 mg, 1 mmol) and then dry toluene (2 mL) under an argon flow through side-arm of the Schlenk flask. The reaction mixture was stirred for 5 min to give a light orange solution. To this solution was rapidly added ethyl diazoacetate (EDA) **85** (124 μL, 1.2 mmol) followed by closing the Teflon valve. The resulting mixture was stirred for 24 h at room temperature. Immediately upon addition of ethyl diazoacetate the reaction mixture became an intense yellow, which changed to light yellow towards the end of the reaction. The reaction was dilluted by addition of hexane (6 mL). The reaction mixture was then transferred to a 100 mL round bottom flask. The reaction flask was rinsed with dichloromethane (5 mL × 2) and the rinse was added to the 100 mL round bottom flask. The resulting solution was then concentrated *in vacuo* followed by exposure to high vacuum (0.05 mm Hg) for 1 h to afford the crude aziridine as an off-white solid.

A measure of the extent to which the reaction went to completion was estimated from the ^{1}H NMR spectrum of the crude reaction mixture by integration of the aziridine ring methine

protons relative to either the imine methine proton or the proton on the imine carbon. The *cis/trans* ratio was determined by comparing the ^{1}H NMR integration of the ring methine protons for each aziridine in the crude reaction mixture. The *cis* (J = 7-8 Hz) and the *trans* (J = 2-3 Hz) coupling constants were used to differentiate the two isomers. The yields of the acyclic enamine side products **87a** and **88a** were determined by ^{1}H NMR analysis of the crude reaction mixture by integration of the *N*-H proton relative to the that of the *cis*-aziridine methine protons with the aid of the isolated yield of the *cis*-aziridine. Purification of the crude aziridine by silica gel chromatography (35 mm × 400 mm column, 19:1 hexanes/EtOAc as eluent, under gravity) afforded pure cis-aziridine *ent*-**86a** as a white solid (mp. 127.5-128.5 °C) in 90% isolated yield (322 mg, 0.900 mmol); *cis/trans*: >50:1. Enamine side products: 4% yield of **87a** and 6% yield of **88a.** The optical purity of *ent*-**86a** was determined to be 76% *ee* by HPLC analysis ((CHIRALCEL OD-H column, 90:10 hexanes/*i*PrOH at 222 nm, flow-rate: 0.7 mL/min): retention times; R_t = 9.01 min (minor enantiomer, **86a**) and R_t = 4.67 min (major enantiomer, *ent*-**86a**).

Spectral data for *ent*-**86a**: R_f = 0.3 (1:9 EtOAc/hexanes); ^{1}H NMR ($CDCl_3$, 500 MHz) δ 0.95 (t, 3H, J = 7.3 Hz), 2.64 (d, J = 6.8 Hz, 1H), 3.19 (d, J = 6.8 Hz, 1H), 3.91 (q, J = 7.1 Hz, 2H), 3.93 (s, 1H), 7.16-7.38 (m, 11H), 7.47 (d, J = 7.1 Hz, 2H), 7.58 (d, J = 7.6 Hz, 2H); ^{13}C NMR ($CDCl_3$, 75 Hz) δ 13.93, 46.36, 48.01, 60.57, 77.68, 127.18, 127.31, 127.39, 127.52, 127.76, 127.78, 128.48, 135.00, 142.37, 142.49, 167.75; $[\alpha]_D^{20}$ –29.6 (*c* 1.0, CH_2Cl_2) on 76% *ee* material (HPLC). These spectral data match those previously reported for this compound.[1a]

The Wulff asymmetric aziridination reaction was performed following the above described procedure (precatalyst method C) using ligands (*R*)-**56a**, **56e**, **56f**, **56i and** (*R,R*)-**61a**. Also imines **111a** and **112a** were subjected to the asymmetric aziridination reaction using pre-catalyst methods C and D (see chapter 2 for details for pre-catalyst methods) and 10 mol% of liagand (*R*)-**56a**. The purification details and spectral data for resulting aziridines **114a** and **115a** has been described in section 5.7.4.

5.7.9 One-pot asymmetric aziridination with 3,3′-Ph_2-BINOL (*R*)-56a and aziridination with B1 catalyst (*R*)-92a (*Scheme 5.10*)

a) One-pot aziridination:

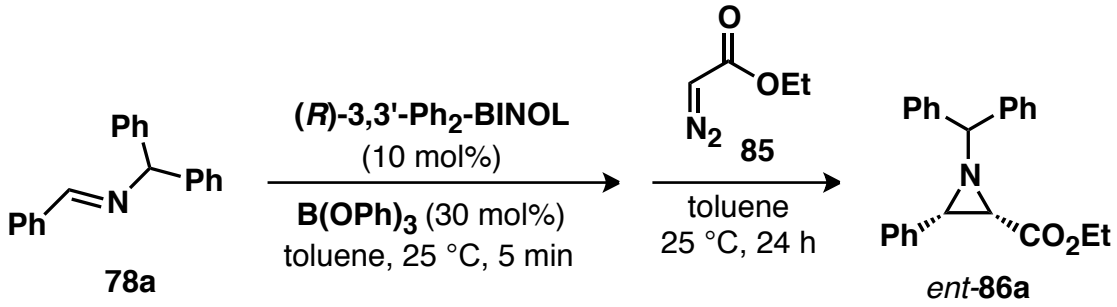

***(2S,3S)*- ethyl 1-benzhydryl-3-phenylaziridine-2-carboxylate** *ent*-**86a:** To a 25 mL flame-dried round bottom flask filled with argon was added (*R)*-**56a** (44 mg, 0.1 mmol), commercial $B(OPh)_3$ (87 mg, 0.3 mmol) and aldimine **78a** (271 mg, 1.00 mmol). The mixture was dissolved in toluene (1 mL) at room temperature. The reaction mixture was stirred for 5 min to give a light orange solution. To this solution was rapidly added EDA **85** (124 μL, 1.20 mmol) and the resulting mixture was stirred for 24 h at room temperature. The reaction was diluted by the addition of 6 mL hexane. The reaction mixture was then transferred to a 100 mL round bottom

flask. The reaction flask was rinsed with dichloromethane (5 mL × 2) and the rinse was added to the 100 mL round bottom flask. The resulting solution was then concentrated *in vacuo* followed by exposure to high vacuum (0.05 mm Hg) for 1 h to afford the crude aziridine as an off-white solid. Purification of the crude aziridine by silica gel chromatography (as discussed above) afforded pure aziridine **86a** as a white solid in 84% yield and 75% ee.

b) Aziridination with B1 catalyst (*R*)-92a:

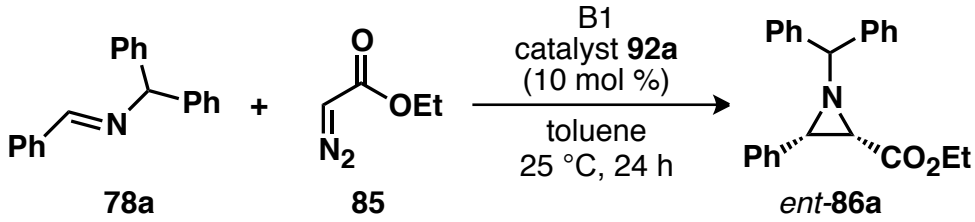

78a **85** *ent*-**86a**

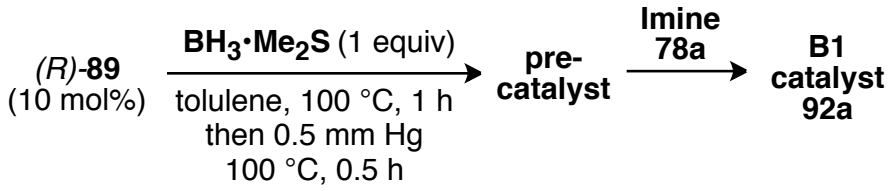

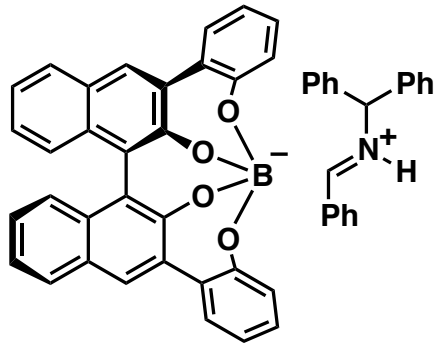

(*R*)-**92a**

B1 (FSB)

***(2S,3S)*- ethyl 1-benzhydryl-3-phenylaziridine-2-carboxylate** *ent*-**86a:** To a 25 mL flame-dried home-made Schlenk flask (see Figure 2.26) equipped with a stir bar and flushed with argon was added (*R*)-**89** (47 mg, 0.1 mmol) and BH_3•Me_2S (50 μL, 0.2 mmol, 2.0 M in toluene).

Under an argon flow through the side-arm of the Schlenk flask, dry toluene (2 mL) was added through the top of the Teflon valve to dissolve the two reagents. The flask was sealed by closing the Teflon valve, and then placed in an 100 ºC oil bath for 1 h. After 1 h, a vacuum (0.5 mm Hg) was carefully applied by slightly opening the Teflon valve to remove the volatiles. After the volatiles were removed completely, a full vacuum was applied and maintained for a period of 30 min at a temperature of 100 ºC (oil bath). The flask was then allowed to cool to room temperature and opened to argon through the side-arm of the Schlenk flask. To the flask containing the pre-catalyst was first added the aldimine **78a** (271 mg, 1 mmol) and then dry toluene (2 mL) under an argon flow through side-arm of the Schlenk flask. The reaction mixture was stirred for 5 min to give a light orange solution. To this solution was rapidly added ethyl diazoacetate (EDA) **85** (124 μL, 1.2 mmol) followed by closing the Teflon valve. The resulting mixture was stirred for 24 h at room temperature. The reaction was diluted by the addition of 6 mL hexane. The reaction mixture was then transferred to a 100 mL round bottom flask. The reaction flask was rinsed with dichloromethane (5 mL × 2) and the rinse was added to the 100 mL round bottom flask. The resulting solution was then concentrated *in vacuo* followed by exposure to high vacuum (0.05 mm Hg) for 1 h to afford the crude aziridine as an off-white solid. Purification of the crude aziridine by silica gel chromatography (as discussed above) afforded pure aziridine **86a** as a white solid in 80% yield and 48% ee.

5.7.10 NMR analysis of a mixture of $B(OPh)_3$, imine 111h and BINOL 56a (*Figure 5.7)*

The details for entries 1-9 of Figure 5.7 can be found in the theses of Gang Hu and Li Huang. The entry 10 of Figure 5.7 is part of this doctoral research and is described below.

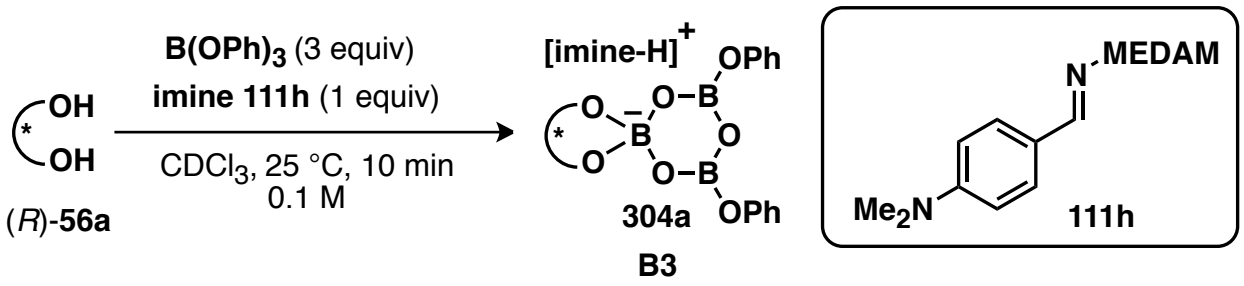

To a 10 mL flame-dried round bottom flask, equipped with a stir bar, filled with argon was added 3,3′-Ph_2-BINOL (*R*)-**56a** (44 mg, 0.1 mmol, 1 equiv.), commercial $B(OPh)_3$ (87 mg, 0.3 mmol, 3 equiv.), imine **111h** (43 mg, 0.1 mmol, 1 equiv.), Ph_3CH (12.22 mg, 0.05 mmol) and $CDCl_3$(1 mL). The resultant mixture was stirred for 10 min at room temperature. The red colored solution was then directly transferred to a quartz NMR tube and was subjected to ^1H NMR and ^{11}B NMR analysis.

5.7.11 NMR analysis of a mixture of $B(OPh)_3$, imine 111h with BINOL derivatives (*R*)-56 or H8-BINOL (*R*)-53 or TADDOL (*R,R*)-61a (*Figure 5.8-5.10 and 5.13)*

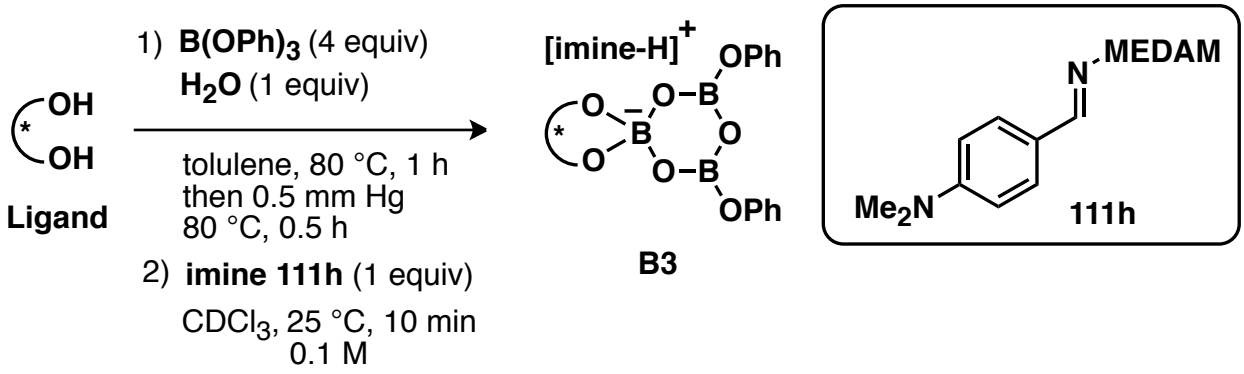

To a 25 mL flame-dried home-made Schlenk flask (see Figure 2.26) equipped with a stir bar and flushed with argon was added (*R*)-**56e** (54 mg, 0.1 mmol), commercial $B(OPh)_3$ (116 mg, 0.4 mmol) and water (1.8 μL, 0.1 mmol). Under an argon flow through the side-arm of the Schlenk flask, dry toluene (2 mL) was added through the top of the Teflon valve to dissolve the two reagents. The flask was sealed by closing the Teflon valve, and then placed in an 80 ºC oil bath for 1 h. After 1 h, a vacuum (0.5 mm Hg) was carefully applied by slightly opening the Teflon valve to remove the volatiles. After the volatiles were removed completely, a full vacuum was applied and maintained for a period of 30 min at a temperature of 80 ºC (oil bath). The flask was then allowed to cool to room temperature and opened to argon through the side-arm of the Schlenk flask. To the flask containing the pre-catalyst (*made from method C*) was first added the imine **111h** (43 mg, 0.1 mmol) and then and $CDCl_3$(1 mL) under an argon flow through side-arm of the Schlenk flask. The resultant mixture was stirred for 10 min at room temperature. The red colored solution was then directly transferred to a quartz NMR tube and was subjected to ^1H NMR and ^{11}B NMR analysis. The NMR tube was covered with aluminum foil and the cap was taped with Teflon for storage for longer time periods. Ligands **56f**, **56i**, **56j**, **53** and **61a** were subjected to NMR analysis following the above-described procedure.

5.7.12 NMR analysis of a mixture of $B(OPh)_3$, DMSO and BINOL (*R*)-55 (*Figure 5.12)*

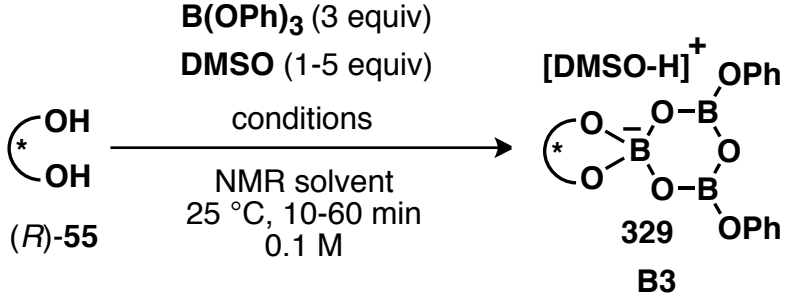

Entry 1, Figure 5.12: The ^{1}H NMR of commercial $B(OPh)_3$ has been taken in d_6-DMSO.

Entry 2, Figure 5.12: To a 10 mL flame-dried round bottom flask, equipped with a stir bar, filled with argon was added BINOL (*R*)-**55** (29 mg, 0.1 mmol, 1 equiv.), commercial $B(OPh)_3$ (14.5 mg, 0.050 mmol, 0.5 equiv), 4Å MS (150 mg, freshly flame dried) and d_6-DMSO (1 mL). The resultant mixture was stirred for 1 h at room temperature. The resulting solution was then filtered and then transferred to a quartz NMR tube and was subjected to ^{1}H NMR and ^{11}B NMR analysis.

Entry 3, Figure 5.12: To a 10 mL flame-dried round bottom flask, equipped with a stir bar, filled with argon was added BINOL (*R*)-**55** (29 mg, 0.1 mmol, 1 equiv), commercial $B(OPh)_3$ (87 mg, 0.3 mmol, 3 equiv) and d_6-DMSO (1 mL). The resultant mixture was stirred for 1 h at room temperature. The resulting solution was then directly transferred to a quartz NMR tube and was subjected to ^{1}H NMR and ^{11}B NMR analysis.

Entry 4, Figure 5.12: To a 25 mL flame-dried home-made Schlenk flask (see Figure 2.26) equipped with a stir bar and flushed with argon was added BINOL (*R*)-**55** (29 mg, 0.1 mmol, 1 equiv), and BH_3•Me_2S (150 µL, 0.3 mmol, 2.0 M in toluene), PhOH (18.8, 0.2 mmol) and H_2O (5.4 µL, 0.3 mmol). Under an argon flow through the side-arm of the Schlenk flask, dry toluene (2 mL) was added through the top of the Teflon valve to dissolve the two reagents. The flask was sealed by closing the Teflon valve, and then placed in an 100 ºC oil bath for 1 h. After 1 h, a vacuum (0.5 mm Hg) was carefully applied by slightly opening the Teflon valve to remove the

volatiles. After the volatiles were removed completely, a full vacuum was applied and maintained for a period of 30 min at a temperature of 100 ºC (oil bath). The flask was then allowed to cool to room temperature and opened to argon through the side-arm of the Schlenk flask. To the flask containing the pre-catalyst was added $CDCl_3$ (1 mL) under an argon flow through side-arm of the Schlenk flask. The reaction mixture was then stirred for 10 min. The off-white colored solution was then directly transferred to a quartz NMR tube and was subjected to ^{1}H NMR and ^{11}B NMR analysis.

Entry 5, Figure 5.12: Same as entry 4 except that DMSO (7 μL, 0.1 mmol, 1 equiv) was added prior to that analysis.

Entry 6, Figure 5.12: Same as entry 4 except that DMSO (35 μL, 0.5 mmol, 5 equiv) was added prior to that analysis.

5.7.13 DFT Calculations

All quantum mechanical calculations were performed using the Gaussian ′03.[24] The coordinates were provided to Prof. Wulff as a separate file.

REFERENCES

REFERENCES

(1) (a) Zhang, Y.; Desai, A.; Lu, A.; Hu, G.; Ding, Z.; Wulff, W. D. *Chem. –Eur. J.* **2008**, *14*, 3785-3803. (b) Zhang, Y.; Lu, Z.; Desai, A.; Wulff, W. D. *Org. Lett.* **2008**, *10*, 5429-5432. (c) Mukherjee, M.; Gupta, A. K.; Lu, Z.; Zhang, Y.; Wulff, W. D. *J. Org. Chem.* **2010**, *75*, 5643-5660. (d) Ren, H.; Wulff, W. D. *Org. Lett.* **2010**, *12*, 4908-4911. (e) Hu, G.; Huang, L.; Huang, R. H.; Wulff, W. D. *J. Am. Chem. Soc.* **2009**, *131*, 15615-15617. (f) Hu, G.; Gupta, A. K.; Huang, R. H.; Mukherjee, M.; Wulff, W. D. *J. Am. Chem. Soc.* **2010**, *132*, 14669–14675. (g) Gupta, A. K.; Mukherjee, M.; Wulff, W. D. *Org. Lett.* **2011**, *13*, 5866-5869. (h) Desai, A. A.; Wulff, W. D. *J. Am. Chem. Soc.* **2010**, *132*, 13100-13103. (i) Vetticatt, M. J.; Desai, A. A.; Wulff, W. D. *J. Am. Chem. Soc.* **2010**, *132*, 13104-13107. (j) Desai, A. A.; Morán-Ramallal, R.; Wulff, W. D. *Org. Synth.* **2011**, *88*, 224-237. (k) Desai, A. A.; Ren, H.; Mukherjee, M.; Wulff, W. D. *Org. Process Res. Dev.* **2011**, *15*, 1108-1115.

(2) (a) Bao, J. M.; Wulff, W. D.; Rheingold, A. L. *J. Am. Chem. Soc.* **1993**, *115*, 3814-3815. (b) Bao, J. M.; Wulff, W. D. *Tetrahedron Lett.* **1995**, *36*, 3321-3324. (c) Heller, D. P.; Goldberg, D. R.; Wulff, W. D. *J. Am. Chem. Soc.* **1997**, *119*, 10551-10552. (d) Heller, D. P.; Goldberg, D. R.; Wu, H. Q.; Wulff, W. D. *Can. J. Chem.* **2006**, *84*, 1487-1503.

(3) Xue, S.; Yu, S.; Deng, Y.; Wulff, W. D. *Angew. Chem., Int. Ed.* **2001**, *40*, 2271-2274.

(4) Bolm, C.; Frison, J. C.; Zhang, Y.; Wulff, W. D. *Synlett* **2004**, 1619-1621.

(5) Lou, S.; Schaus, S. E. *J. Am. Chem. Soc.* **2008**, *130*, 6922-6923.

(6) Harada, H.; Thalji, R. K.; Bergman, R. G.; Ellman, J. A. *J. Org. Chem.* **2008**, *73*, 6772-6779.

(7) van Leeuwen, P. W. N. M.; Rivillo, D.; Raynal, M.; Freixa, Z. *J. Am. Chem. Soc.* **2011**, *133*, 18562-18565.

(8) Zheng, W.; Zhang, Z.; Kaplan, M. J.; Antilla, J. C. *J. Am. Chem. Soc.* **2011**, *133*, 3339-3341.

(9) Zhang, Z.; Zheng, W.; Antilla, J. C. *Angew. Chem., Int. Ed.* **2011**, *50*, 1135-1138.

(10) Larson, S. E.; Li, G.; Rowland, G. B.; Junge, D.; Huang, R.; Woodcock, H. L.; Antilla, J. C. *Org. Lett.* **2011**, *13*, 2188-2191.

(11) Barnett, D. S.; Schaus, S. E. *Org. Lett.* **2011**, *13*, 4020-4023.

(12) Hoffman, T. J.; Carreira, E. M. *Angew. Chem., Int. Ed.* **2011**, *50*, 10670-10674.

(13) Newman, C. A.; Antilla, J. C.; Chen, P.; Predeus, A. V.; Fielding, L.; Wulff, W. D. *J. Am. Chem. Soc.* **2007**, *129*, 7216-7217.

(14) Ren, H.; Wulff, W. D. *J. Am. Chem. Soc.* **2011**, *133*, 5656-5659.

(15) Gupta, A. K.; Wulff, W. D., Unpublished results.

(16) Rowland, G. B.; Zhang, H.; Rowland, E. B.; Chennamadhavuni, S.; Wang, Y.; Antilla, J. C. *J. Am. Chem. Soc.* **2005**, *127*, 15696-15697.

(17) Liang, Y.; Rowland, E. B.; Rowland, G. B.; Perman, J. A.; Antilla, J. C. *Chem. Commun.* **2007**, 4477-4479.

(18) Li, G.; Liang, Y.; Antilla, J. C. *J. Am. Chem. Soc.* **2007**, *129*, 5830-5831.

(19) Snyder, S. A.; Thomas, S. B.; Mayer, A. C.; Breazzano, S. P. *Angew. Chem., Int. Ed.* **2012**, *51*, 4080-4084.

(20) (a) Rowland, E. B.; Rowland, G. B.; Rivera-Otero, E.; Antilla, J. C. *J. Am. Chem. Soc.* **2007**, *129*, 12084-12085. (b) Larson, S. E.; Baso, J. C.; Li, G. L.; Antilla, J. C. *Org. Lett.* **2009**, *11*, 5186-5189. (c) Della, S. G.; Lattanzi, A. *Org. Lett.* **2009**, *11*, 3330-3333.

(21) Chen, M.-W.; Chen, Q.-A.; Duan, Y.; Ye, Z.-S.; Zhou, Y.-G. *Chem. Commun.* **2012**, *48*, 1698-1700.

(22) (a) Loncaric, C.; Wulff, W. D. *Org. Lett.* **2001**, *3*, 3675-3678. (b) Rampalakos, K. PhD Thesis, Michigan State University, 2008. (c) Hu, G.; Holmes, D.; Gendhar, B. F.; Wulff, W. D. *J. Am. Chem. Soc.* **2009**, *131*, 14355-14364.

(23) Ding, Z.; Osminski, W. E. G.; Ren, H.; Wulff, W. D. *Org. Process Res. Dev.* **2011**, *15*, 1089-1107 and references therein.

(24) Gaussian 03, Revision D.01 M. J. Frisch, G. W. T., H. B. Schlegel, G. E. Scuseria, M. A. Robb, J. R. Cheeseman, J. A. Montgomery, Jr., T. Vreven, K. N. Kudin, J. C. Burant, J. M. Millam, S. S. Iyengar, J. Tomasi, V. Barone, B. Mennucci, M. Cossi, G. Scalmani, N. Rega, G. A. Petersson, H. Nakatsuji, M. Hada, M. Ehara, K. Toyota, R. Fukuda, J. Hasegawa, M. Ishida, T. Nakajima, Y. Honda, O. Kitao, H. Nakai, M. Klene, X. Li, J. E. Knox, H. P. Hratchian, J. B. Cross, V. Bakken, C. Adamo, J. Jaramillo, R. Gomperts, R. E. Stratmann, O. Yazyev, A. J. Austin, R. Cammi, C. Pomelli, J. W. Ochterski, P. Y. Ayala, K. Morokuma, G. A. Voth, P. Salvador, J. J. Dannenberg, V. G. Zakrzewski, S. Dapprich, A. D. Daniels, M. C. Strain, O. Farkas, D. K. Malick, A. D. Rabuck, K. Raghavachari, J. B. Foresman, J. V. Ortiz, Q. Cui, A. G. Baboul, S. Clifford, J. Cioslowski, B. B. Stefanov, G. Liu, A. Liashenko, P. Piskorz, I. Komaromi, R. L. Martin, D. J. Fox, T. Keith, M. A. Al-Laham, C. Y. Peng, A. Nanayakkara, M. Challacombe, P. M. W. Gill, B. Johnson, W. Chen, M. W. Wong, C. Gonzalez, and J. A. Pople, Gaussian, Inc., Wallingford CT, 2004

(25) Price, C. P.; Matzger, A. J. *J. Org. Chem.* **2005**, *70*, 1-6.

(26) The terms cisoid and transoid describe biaryl dihedral angles of <90° and >90°, respectively.

(27) (a) Kerr, K. A.; Robertso, J. M. *J Chem Soc B* **1969**, 1146-1149. (b) Kress, R. B.; Duesler, E. N.; Etter, M. C.; Paul, I. C.; Curtin, D. Y. *J. Am. Chem. Soc.* **1980**, *102*, 7709-7714.

(28) (a) Mori, K.; Masuda, Y.; Kashino, S. *Acta Crystallogr., Sect. C: Cryst. Struct. Commun.* **1993**, *49*, 1224-1227. (b) Toda, F.; Tanaka, K.; Miyamoto, H.; Koshima, H.; Miyahara, I.; Hirotsu, K. *J. Chem. Soc., Perkin Trans. 2* **1997**, 1877-1885.

(29) (a) Brunel, J. M. *Chem. Rev.* **2005**, *105*, 857-897. (b) Brunel, J. M. *Chem. Rev.* **2007**, *107*, PR1-PR45.

(30) Chen, Y.; Yekta, S.; Yudin, A. K. *Chem. Rev.* **2003**, *103*, 3155-3211.

(31) Hattori, K.; Yamamoto, H. *J. Org. Chem.* **1992**, *57*, 3264-3265.

(32) The preparation of **294** has been called into doubt due to failure at the preparation of related compounds, see: Chong, J. M.; Shen, L.; *J. Am. Chem. Soc.* **2009**, *131*, 12882-12883

(33) (a) Hattori, K.; Miyata, M.; Yamamoto, H. *J. Am. Chem. Soc.* **1993**, *115*, 1151-1152. (b) Hattori, K.; Yamamoto, H. *Tetrahedron* **1993**, *49*, 1749-1760. (c) Hattori, K.; Yamamoto, H.

Synlett **1993**, 129-130. (d) Hattori, K.; Yamamoto, H. *Synlett* **1993**, 239-240. (e) Hattori, K.; Yamamoto, H. *Bioorg. Med. Chem. Lett.* **1993**, *3*, 2337-2342. (f) Hattori, K.; Yamamoto, H. *Tetrahedron* **1994**, *50*, 2785-2792. (g) Ishihara, K.; Miyata, M.; Hattori, K.; Tada, T.; Yamamoto, H. *J. Am. Chem. Soc.* **1994**, *116*, 10520-10524. (h) Lock, R.; Waldmann, H. *Tetrahedron Lett.* **1996**, *37*, 2753-2756. (i) Lock, R.; Waldmann, H. *Chem.–Eur. J.* **1997**, *3*, 143-151. (j) Banerjee, A.; Schepmann, D.; Kohler, J.; Wurthwein, E. U.; Wunsch, B. *Bioorg. Med. Chem.* **2010**, *18*, 7855-7867.

(34) Momiyama, N.; Tabuse, H.; Terada, M. *J. Am. Chem. Soc.* **2009**, *131*, 12882-12883.

(35) Thormeier, S.; Carboni, B.; Kaufmann, D. E. *J. Organomet. Chem.* **2002**, *657*, 136-145.

(36) Zimmer, R.; Peritz, A.; Czerwonka, R.; Schefzig, L.; Reissig, H. U. *Eur. J. Org. Chem.* **2002**, 3419-3428.

(37) (a) Ishihara, K.; Kuroki, Y.; Yamamoto, H. *Synlett* **1995**, 41-42. (b) Kuroki, Y.; Ishihara, K.; Hanaki, N.; Ohara, S.; Yamamoto, H. *Bull. Chem. Soc. Jpn.* **1998**, *71*, 1221-1230.

(38) Cros, J. P.; Pérez-Fuertes, Y.; Thatcher, M. J.; Arimori, S.; Bull, S. D.; James, T. D. *Tetrahedron: Asymmetry* **2003**, *14*, 1965-1968.

(39) (a) Kawate, T.; Yamada, H.; Matsumizu, M.; Nishida, A.; Nakagawa, M. *Synlett* **1997**, 761-762. (b) Yamada, H.; Kawate, T.; Matsumizu, M.; Nishida, A.; Yamaguchi, K.; Nakagawa, M. *J. Org. Chem.* **1998**, *63*, 6348-6354.

(40) (a) Periasamy, M.; Venkatraman, L.; Sivakumar, S.; Sampathkumar, N.; Ramanathan, C. R. *J. Org. Chem.* **1999**, *64*, 7643-7645. (b) Periasamy, M.; Ramanathan, C. R.; Kumar, N. S. *Tetrahedron: Asymmetry* **1999**, *10*, 2307-2310. (c) Periasamy, M.; Kumar, N. S.; Sivakumar, S.; Rao, V. D.; Ramanathan, C. R.; Venkatraman, L. *J. Org. Chem.* **2001**, *66*, 3828-3833. (d) Liu, D.; Shan, Z.; Liu, F.; Xiao, C.; Lu, G.; Qin, J. *Helv. Chim. Acta* **2003**, *86*, 157-163.

(41) (a) Green, S.; Nelson, A.; Warriner, S.; Whittaker, B. *J. Chem. Soc., Perkin Trans. 1* **2000**, 4403-4408. (b) Tu, T.; Maris, T.; Wuest, J. D. *Cryst. Growth Des.* **2008**, *8*, 1541-1546. (c) Raskatov, J. A.; Brown, J. M.; Thompson, A. L. *Crystengcomm* **2011**, *13*, 2923-2929.

(42) Llewellyn, D. B.; Arndtsen, B. A. *Can. J. Chem.* **2003**, *81*, 1280-1284.

(43) Llewellyn, D. B.; Adamson, D.; Arndtsen, B. A. *Org. Lett.* **2000**, *2*, 4165-4168.

(44) Carter, C.; Fletcher, S.; Nelson, A. *Tetrahedron: Asymmetry* **2003**, *14*, 1995-2004.

(45) Chen, D.; Sundararaju, B.; Krause, R.; Klankermayer, J.; Dixneuf, P. H.; Leitner, W. *ChemCatChem* **2010**, *2*, 55-57.

(46) Kaufmann, D.; Boese, R. *Angew. Chem., Int. Ed.* **1990**, *29*, 545-546.

(47) De-jun, L.; Zi-xing, S.; Guo-ping, W.; Jin-gui, Q. *Wuhan University Journal of Natural Sciences* **2003**, *8*, 1138-1142.

(48) Shan, Z. X.; Xiong, Y.; Li, W. Z.; Zhao, D. J. *Tetrahedron: Asymmetry* **1998**, *9*, 3985-3989.

(49) (a) Kelly, T. R.; Whiting, A.; Chandrakumar, N. S. *J. Am. Chem. Soc.* **1986**, *108*, 3510-3512. (b) Wipf, P.; Jung, J.-K. *J. Org. Chem.* **2000**, *65*, 6319-6337. (c) Landells, J. S.; Larsen, D. S.; Simpson, J. *Tetrahedron Lett.* **2003**, *44*, 5193-5196. (d) Snyder, S. A.; Tang, Z. Y.; Gupta, R. *J. Am. Chem. Soc.* **2009**, *131*, 5744-5745.

(50) (a) Ishihara, K.; Yamamoto, H. *J. Am. Chem. Soc.* **1994**, *116*, 1561-1562. (b) Ishihara, K.; Kurihara, H.; Yamamoto, H. *J. Am. Chem. Soc.* **1996**, *118*, 3049-3050. (c) Ishihara, K.; Kurihara, H.; Matsumoto, M.; Yamamoto, H. *J. Am. Chem. Soc.* **1998**, *120*, 6920-6930. (d) Ishihara, K.; Kondo, S.; Kurihara, H.; Yamamoto, H.; Ohashi, S.; Inagaki, S. *J. Org. Chem.* **1997**, *62*, 3026-3027.

(51) Hu, G. PhD Dissertation, Michigan State University, 2007.

(52) Antilla, J. C.; Wulff, W. D. *Angew. Chem., Int. Ed.* **2000**, *39*, 4518-4521.

(53) Huang, L. PhD Dissertation, Michigan State University, 2011.

(54) Wang, Z. H.; Li, F.; Zhao, L.; He, Q. Q.; Chen, F. E.; Zheng, C. *Tetrahedron* **2011**, *67*, 9199-9203.

(55) Lingenfelter, D. S.; Helgeson, R. C.; Cram, D. J. *J. Org. Chem.* **1981**, *46*, 393-406.

(56) (a) Tsang, W. C. P.; Schrock, R. R.; Hoveyda, A. H. *Organometallics* **2001**, *20*, 5658-5669. (b) Gobbi, L.; Seiler, P.; Diederich, F.; Gramlich, V. *Helv. Chim. Acta* **2000**, *83*, 1711-1723.

(57) O'Dell, R.; McConville, D. H.; Hofmeister, G. E.; Schrock, R. R. *J. Am. Chem. Soc.* **1994**, *116*, 3414-3423.

(58) Kickova, A.; Donovalova, J.; Kasak, P.; Putala, M. *New J. Chem.* **2010**, *34*, 1109-1115.

(59) Zhu, S. S.; Cefalo, D. R.; La, D. S.; Jamieson, J. Y.; Davis, W. M.; Hoveyda, A. H.; Schrock, R. R. *J. Am. Chem. Soc.* **1999**, *121*, 8251-8259.

(60) Singh, R.; Czekelius, C.; Schrock, R. R.; Mueller, P.; Hoveyda, A. H. *Organometallics* **2007**, *26*, 2528-2539.

(61) Hu, W.; Zhou, J.; Xu, X.; Liu, W.; Gong, L. *Org. Synth.* **2011**, *88*, 406-417.

(62) Wipf, P.; Lyon, M. A. *ARKIVOC* **2007**, *xii*, 91-98.

(63) Lu, Z.; Zhang, Y.; Wulff, W. D. *J. Am. Chem. Soc.* **2007**, *129*, 7185-7194.

(64) (a) Pellissier, H. *Tetrahedron* **2008**, *64*, 10279-10317. (b) Seebach, D.; Beck, A. K.; Heckel, A. *Angew. Chem., Int. Ed.* **2001**, *40*, 92-138.

CHAPTER 6

DIRECT IMINO-BOROX CATALYSIS ASYMMETRIC AZIRIDINATION, [3+2] CYCLOADDITION, UGI REACTION AND KINETIC RESOLUTION OF IMINES

You should never ignore the crude weight and the crude NMR especially if the reaction fails to give the desired product.

-William D. Wulff

6.1 Catalytic asymmetric one-pot aziridination

In the present section of this chapter, the asymmetric catalytic aziridination reaction (AZ reaction) of imines derived from dianisylmethyl (DAM) amine was examined with the IMINO BOROX catalysts. As a result, a new one-pot procedure was developed for the aziridination reaction.

Apart from asymmetric aziridination reactions using chiral auxiliaries,[1] considerable advances have been made in the field of catalytic asymmetric aziridination over the past few years.[2] Primarily, there are two main approaches that have been taken towards catalytic asymmetric aziridination: a) addition of nitrogen to olefins *via* nitrene transfer with organometallic catalysts[3] or organocatalysis[4] b) addition of carbon to imines *via* metal-carbene transfer (carbene generated from diazo compound or sulfur ylides)[5] or the reaction of a diazo compound with an imine activated by either Lewis acid[6] or Brønsted acid.[7] It must noted that the asymmetric aziridination reaction between the imines and diazo compounds in the presence

of an acid catalyst must not be mistaken for Aza-Darzens reaction as both are mechanistically distinct.[2a] In fact, an asymmetric Aza-Darzens reaction has only been reported with chiral auxiliaries.[2a] As discussed in previous chapters, our aziridination protocol is a Brønsted acid catalyzed reaction.[8] Over the last several years we have developed a general method for the catalytic asymmetric synthesis of aziridines that is based on the reaction of diazo compounds with imines and which is mediated by asymmetric catalysts generated from the VANOL and VAPOL ligands and various boron compounds.[8-9] Early on it was determined that with imines derived from benzhydryl (Bh) amine **126a** and catalysts derived from triphenylborate, aziridines could be obtained in high yields and asymmetric inductions from the reaction of ethyl diazoacetate and other diazo compounds.[10] The reactions are also highly diastereoselective giving *cis*-2,3-disubstituted aziridines and in most cases only trace amounts of the *trans*-aziridine can be detected. The scope of the reaction is broad and includes imines derived from a variety of aldehydes including electron-rich and electron-poor aromatic aldehydes and 1°, 2° and 3° aliphatic aldehydes.[9a] The imines from aromatic aldehydes gave aziridines with 90-95% ee and imines from aliphatic aldehydes gave aziridines with 77-87% ee.[9a] Interestingly, both VANOL and VAPOL derived catalysts are equally effective and give nearly the same asymmetric inductions for each substrate across the entire range of 12 substrates examined.[9a]

During the studies directed toward mapping the active site of the chemzyme in this reaction, it was revealed that while the use of a diphenylmethyl group on the imine is essential to the success of this reaction, it does not represent the optimal substituent since it was found that

various diarylmethyl groups were far more effective.[9b] A collection of 14 different diarylmethyl substituents was screened for the reaction of imines derived from benzaldehyde and the optimal selectivity (99% ee) was found for the *tetra-t*-**bu**tyl**dia**nisyl**m**ethyl (BUDAM) group.[9b] With the identification of the BUDAM substituent as optimal for the imine from benzaldehyde, this substituent was in turn screened with imines prepared from BUDAM amine **126d** and eleven different aldehydes. The reactions of BUDAM imines from aromatic aldehydes were definitely superior to their benzhydryl analogs giving 98-99% ee for most substrates with VAPOL derived catalysts; however, the reactions of BUDAM imines from aliphatic aldehydes were not significantly different from their benzhydryl analogs giving ee's generally in the 80's. Thus, the goal of the present work is to identify the optimal diarylmethyl substituent that will provide universal access to optically pure aziridines from the AZ reaction irrespective of the substrate.

One of the great advantages of the BUDAM substituent is that it can be easily cleaved under acidic conditions without opening the aziridine ring when the aziridine is treated with 4 equivalents of triflic acid in anisole at room temperature.[9b] The corresponding benzhydryl aziridines leads to ring opening under all acidic conditions that were screened.[11] The facile cleavage of the BUDAM group under acidic conditions can be attributed to the fact that a significantly more stable diarylmethyl cation is formed during the cleavage. Thus, in seeking the ideal diarylmethyl substituent for the imine, one of the characteristics that would be most desired would be its ability to be removed from the aziridine without causing any deleterious effects to the aziridine. One of the other diarylmethyl groups that was identified in our previous work as superior to the unsubstituted diphenylmethyl (benzhydryl or Bh) group in the AZ reaction is the

dianisyl**m**ethyl (DAM) group.[11] The presence of the methoxyl substituents in the DAM group is sufficient to provide for the clean cleavage of the DAM group under acidic conditions.[11] We have previously examined the scope of the aziridination of DAM imines from a variety of aldehydes and found that these imines tend to give slightly improved yields and asymmetric inductions than the corresponding benzhydryl imines.[11] However, this survey was conducted with methylene chloride and carbon tetrachloride as solvent. Since we have subsequently found that toluene is in many respects superior to either methylene chloride and carbon tetrachloride for the AZ reaction,[9a] we decided to revisit the scope of the AZ reaction of DAM imines.

Meanwhile, a lot of mechanistic studies were carried out in our group regarding the identification of the active catalyst structures. Prior to these studies, it was believed that the active catalyst is B1 **106**/**107** (Scheme 2.1, Chapter 2) that was generated from VAPOL or VANOL when reacted with triphenyl borate. This proposed structure was based on studies by Yamamoto,[12] however no spectroscopic evidence existed for such catalyst structures. Further, Dr. Yu Zhang, one of the previous group members, found out that there are two boron species B2 **108**/**109** and B1 **106**/**107** on the basis of NMR and MS studies (Scheme 2.1, Chapter 2).[9a] Additionally, it was found that the catalyst enriched with B2 **108**/**109** gives higher asymmetric induction and higher rates in the aziridination reaction compared to a catalyst mixture enriched with B1 **106**/**107**.[9a] In the continuing effort to probe the mechanistic rationale for the asymmetric induction observed for catalysts generated from VAPOL and VANOL, a major breakthrough was the identification of the active boroxinate catalyst **188**/**189** (imine =

benzhydryl imines **78**) which contains three boron atoms (Scheme 2.1, Chapter 2).[8] Surprisingly, the catalyst proved to be a Brønsted acid catalysis in operation contrary to the common belief of that the aziridination reaction involved Lewis-acid catalysis. Furthermore, it was found that the boroxinate **188**/**189** is formed by the reaction of the pyroborate **108** with the imine **78**, with or without the presence of an additional equivalent of $B(OPh)_3$. Hence, the catalytic mixture obtained by mixing ligand (1 equiv), $B(OPh)_3$ (4 equiv) and H_2O (1 equiv) is actually a "pre-catalyst" (Method C, Table 2.1, entry 4, Chapter 2 and Scheme 6.2B). The protocol for the aziridination reaction using pre-catalyst made by method C is termed as procedure IV (Table 2.1, entry 4, Chapter 2 and Scheme 6.2B).

The shortcoming of the optimized protocol for the aziridination of imines include the need to generate a pre-catalyst (mixture of B1 **106/107** and B2 **108/109**) from the VAPOL or VANOL ligand and $B(OPh)_3$. In the pre-catalyst protocol, the exposure to high vacuum at 80 °C is not sufficient to remove the third equivalent of $B(OPh)_3$ after the pyroborate **108/109** is formed, although the phenol produced in the alkoxy exchange between the ligand and $B(OPh)_3$ is removed. However, the major difficulty of the protocol is the removal of the volatiles during the preparation of the pre-catalyst. Removing the solvent and other volatiles at 80 °C under high vacuum often occurs with splattering and loss of the pre-catalyst. Henceforth, the secondary aim of the work was to simplify the overall procedure, thus developing a one-pot aziridination reaction avoiding the generation of the pre-catalyst.

In the process of the optimization, a simplified procedure II (Table 2.1, entry 2, Chapter 2 and Scheme 6.1) was devised using benzhydryl phenyl imine **78a**. The procedure II involves the direct generation of the boroxinate catalyst **188a** by mixing 1 equiv of (*S*)-VAPOL, 3 equiv of

$B(OPh)_3$ and 20 equiv of imine **78a** in toluene at 25 °C for 5 min. Thereafter, EDA **85** (24 equiv) is added and the resulting mixture is stirred for 24 h at 25 °C. The reaction was performed open to air. It gave aziridine **86a** in 82% yield and 92% ee. A number of solvents (hexanes, dioxane, toluene, ether, DME etc.) were also examined.[8]

Scheme 6.1 Catalytic asymmetric aziridination of imine **78a** using procedure II

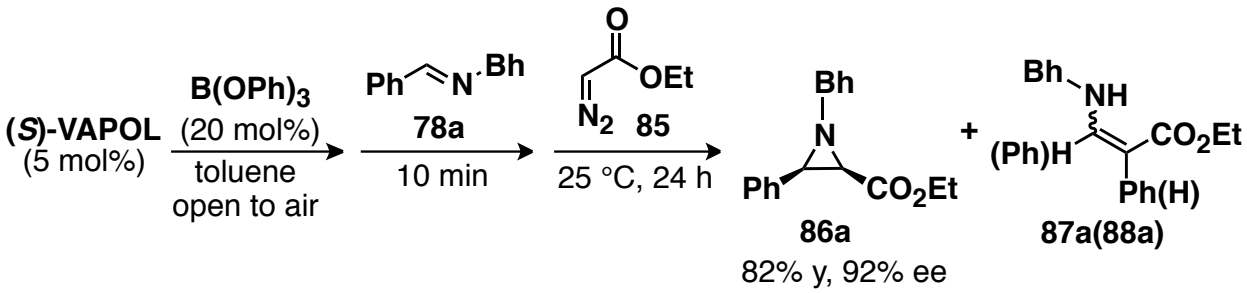

The application of procedure II to the reaction of *N*-DAM imines **110** was then tested (Table 6.1). Unfortunately, low conversions were observed when the reaction was performed open to air (Table 6.1, entries 1,3,5,7). It was then thought to carry out the reaction under argon atmosphere. Although a slight improvement was observed, the reactions were still far from complete (Table 6.1, entries 2,4,6,8). To our delight, high yield and high enantioselectivity were observed (Table 6.1, entry 7) on increasing the catalyst loading from 5 mol% to 10 mol% for imine **110g** (R = 4-Br-C_6H_4). This modified procedure seemed to be a much simplified procedure when compared to that which employs pre-catalyst preparation.

Table 6.1 One-pot aziridination reaction of *N*-DAM imines **110** using procedure II. [a]

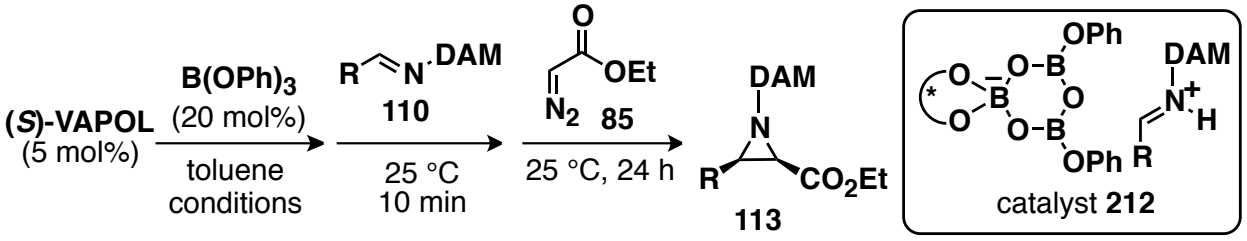

Table 6.1 cont'd

#	Series	Conditions	R	Conversion (%) [b]	Yield **113** (%) [c]	ee **113** (%) [d]
1	**a**	open to air	Ph	27	–	–
2	**a**	under argon	Ph	80	–	–
3	**d**	open to air	4-Me-C_6H_4	20	–	–
4	**d**	under argon	4-Me-C_6H_4	26	–	–
5	**f**	open to air	4-NO_2-C_6H_4	28	–	–
6	**f**	under argon	4-NO_2-C_6H_4	44	–	–
7	**g**	open to air	4-Br-C_6H_4	15	–	–
8	**g**	under argon	4-Br-C_6H_4	23	–	–
9 [e]	**g**	under argon	4-Br-C_6H_4	100	90	95

[a] Unless otherwise specified, all reactions were performed with 5 mol% of catalyst **212** with 0.50 mmol imine **110** (1.0 equiv, 0.5 M in toluene) and 0.6 mmol of EDA **85** (1.2 equiv) at room temperature. [b] Percent conversion is determined by integration of the methine proton of the *cis*-aziridine relative to the sp^2-CH proton of the unreacted imine **110** in the ^{1}H NMR spectrum of the crude reaction mixture. [c] Isolated Yield. [d] Determined by HPLC. [e] 10 mol% catalyst used.

Since one of the aims of the work was to utilize as of a low catalyst loading as possible, another procedure II′ was employed. The catalyst was generated by stirring a mixture of *(S)*-VAPOL (0.025 mmol), $B(OPh)_3$ (0.1 mmol) and imine **110g** (R = 4-Br-C_6H_4, 0.25 mmol) in toluene for 0.5 h. In this way, the catalyst loading was 10 mol% with respect to imine **110g** during the preparation of the catalyst. The actual catalyst loading was reduced to 5 mol% by adding imine **110g** (0.25 mmol) after 0.5 h. Unfortunately, this trick did not work and the reaction only went to 16 % conversion (Scheme 6.2A).

Scheme 6.2 Catalytic asymmetric aziridination of imine **110g** (R = 4-Br-C_6H_4) using (**A**) procedure II′ (**B**) procedure IV (**C**) procedure V′ (**D**) procedure V

A

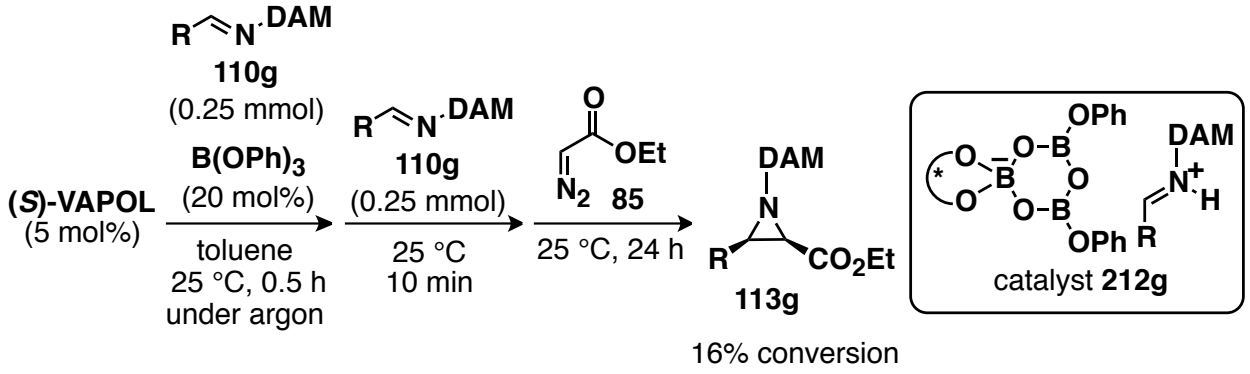

B

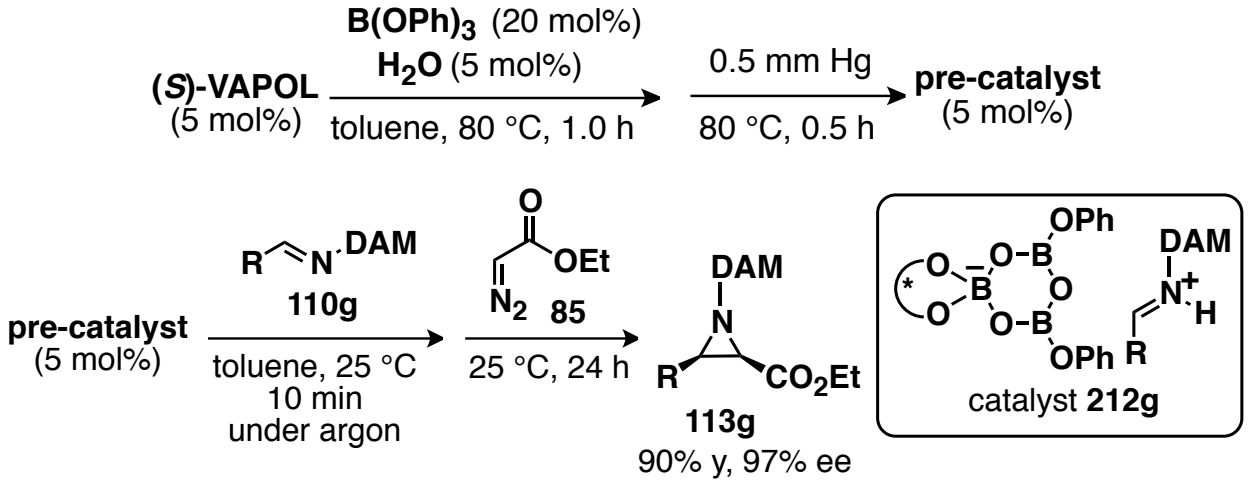

C

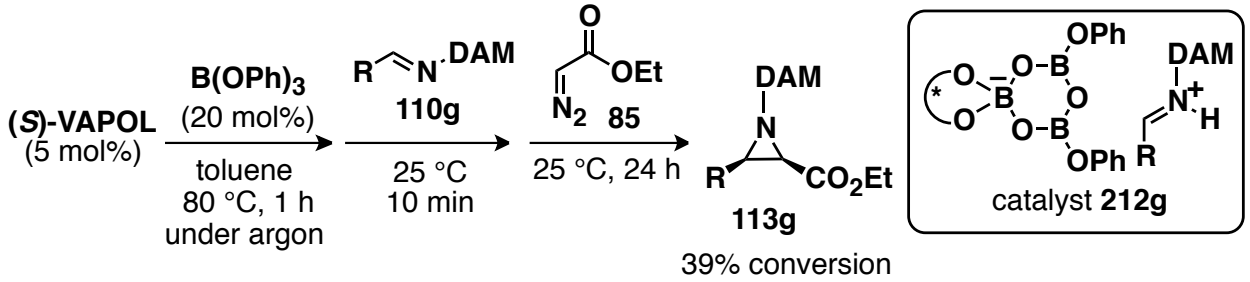

Scheme 6.2 cont'd

D

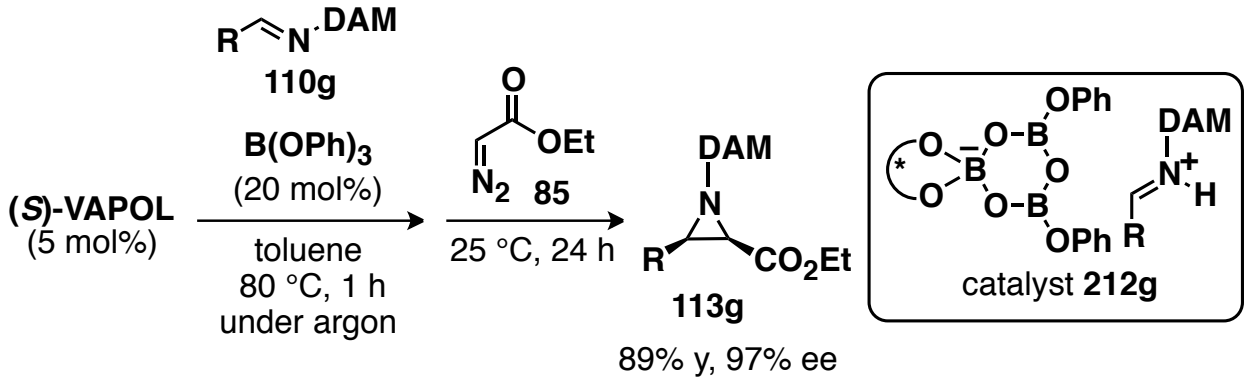

Furthermore, we thought of performing the reaction using procedure V′ where a pre-catalyst is made. The difference between the procedure IV and V′ was that there was no removal of the volatiles under reduced pressure (Scheme 6.2B vs 6.2C). An improved conversion of 39 % (compared to 16% conversion with procedure II′) was observed for imine **110g** using 5 mol% catalyst (Scheme 6.2C). This increase in conversion speaks to the necessity of the high temperature for generation of an effective catalyst system. Since it is known that the generation of the active catalyst occurs only after the addition of imine, it was thought to heat the ligand, borate and imine altogether (procedure V, Scheme 6.2D). Using procedure V, the reaction of imine **110g** with 5 mol% catalyst loading gave 100% conversion affording aziridine **113g** in 89% yield and 97% ee (Scheme 6.2D). The basic aspect of procedure V is that the ligand, $B(OPh)_3$ and all of imine for the reaction (Scheme 6.2D) are heated together in toluene at 80 °C for 1 h and then upon cooling to room temperature, the reaction is initiated by the addition of ethyl diazoacetate. Another significant incorporated into procedure V is that the step involving the removal of volatiles has been deleted and this did not have any adverse effect on the outcome of the reaction. This aids in the objective to simplify the system. Additionally, it was observed that

the presence of phenol does not significantly affect the outcome of the AZ reaction (Table 6.4). Finally, it should be noted that the water was left out of procedure V. Although the formation of a boroxinate does require three equivalents of water, studies on the efficiency of the formation of boroxinate by ^{1}H and ^{11}B NMR spectroscopy revealed that there is sufficient partial hydrolysis in commercial $B(OPh)_3$ to provide the equivalent of three molecules of water.[8] We have never encountered a bottle of commercial $B(OPh)_3$ that was pure. This fact, and the consistency of the impure nature of commercial $B(OPh)_3$ over the years has been responsible for the success and reproducibility of the AZ reaction. The reason that four equivalents of $B(OPh)_3$ is used in procedure IV and V is to compensate for the fact that $B(OPh)_3$ in not pure as supplied from commercial suppliers. In reality, we have not seen any significant difference in the catalyst prepared with either three or four equivalents of $B(OPh)_3$ either in reaction outcome or in its characterization by ^{1}H or ^{11}B NMR spectroscopy.[13] Even with two equivalents of $B(OPh)_3$ the reaction outcome is not significantly affected. All of this suggests that all of the boron that happens to be present is converted to the chiral boroxinate even if this leaves some of the ligand unreacted, and if any boron is left over, it not does interfere in terms of background reaction.[13]

The catalytic asymmetric aziridinations of the DAM imines **110** derived from aromatic aldehydes were screened in toluene following procedures IV and V and the results are presented in Table 6.2. All of the reactions were carried out for 24 h with 2-5 mol% catalyst but not all substrates required 24 h to go to completion. The reaction of the phenyl imine **110a** was complete in 2 h with 3 mol% catalyst (Table 6.2, entry 1). In all cases the reaction went to

completion except for entry 11 which went to 97% completion in 24 h with 2 mol% catalyst. The catalyst with VANOL was used for the *para*-methoxyl substrate **110e** since it had been found in our previous studies on DAM imines that this is the slowest substrate and that the VANOL catalyst is approximately twice as fast as the VAPOL catalyst.[11] One of the clear findings of this study is that, at least for DAM imines derived from aryl aldehydes, there is no difference in yields or asymmetric inductions between procedures IV and V for catalyst formation. This is an important observation since procedure V is experimentally much more simple as it does not involve the removal of solvent from the catalyst at high temperature under vacuum. Unfortunately, the asymmetric inductions in toluene do not represent a significant improvement over those previously observed with DAM imines from aryl aldehydes in carbon tetrachloride solvent.[11] This is not to ignore the fact that toluene is a much more desirable solvent than carbon tetrachloride for reasons of both safety and cost.

Table 6.2 Asymmetric Aziridination with Aryl DAM imines **110**. [a]

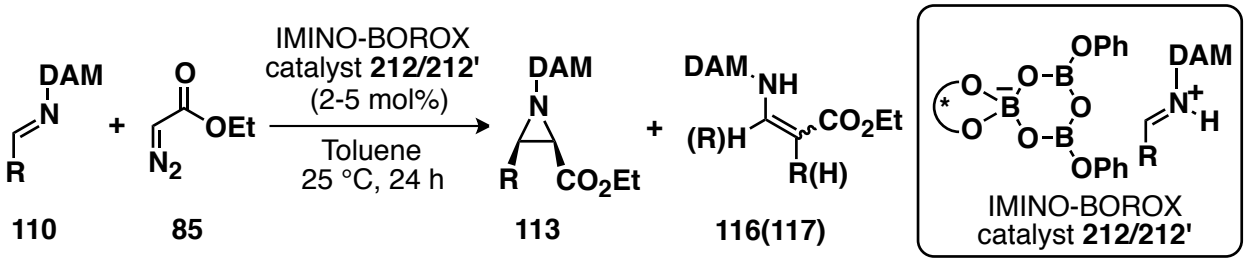

#	Series	R	Ligand	Cat. x mol%	Yield **113** (%) [b]	ee **113** (%) [c]	cis/trans [d]	Enamine (%) [e]
1 [f]	**a**	Ph	(*R*)-VAPOL	IV (5)	95	–92	50:1	1(1)
2 [g]	**a**	Ph	(*S*)-VAPOL	V (3)	90	94	>50:1	2.7(2.7)
3	**b**	1-napthyl	(*S*)-VAPOL	V (3)	80	98	>50:1	1.6(1.6)
4	**c**	2-Me-C_6H_4	(*S*)-VAPOL	V (3)	70	93	>50:1	1.4 (1.1)

Table 6.2 cont'd

5	**d**	4-Me-C_6H_4	(*S*)-VAPOL	IV (5)	90	94	>50:1	1(1)
6	**d**	4-Me-C_6H_4	(*S*)-VAPOL	V (3)	90	94	>50:1	1(1)
7	**e**	4-MeO-C_6H_4	(*R*)-VANOL	IV (5)	80	–93	>50:1	2(1)
8	**e**	4-MeO-C_6H_4	(*S*)-VANOL	V (3)	80	93	50:1	3.2(1.6)
9	**f**	4-NO_2-C_6H_4	(*S*)-VAPOL	IV (5)	85	94	33:1	1.6(1.6)
10	**f**	4-NO_2-C_6H_4	(*S*)-VAPOL	V (3)	85	95	50:1	<1(<1)
11	**g**	4-Br-C_6H_4	(*S*)-VAPOL	IV (5)	90	97	50:1	<1(<1)
12	**g**	4-Br-C_6H_4	(*S*)-VAPOL	IV (3)	90	97	50:1	<1(<1)
13[h]	**g**	4-Br-C_6H_4	(*S*)-VAPOL	IV (3)	94	97	50:1	<1(<1)
14[i]	**g**	4-Br-C_6H_4	(*S*)-VAPOL	IV (2)	87	97	50:1	1(1)
15	**g**	4-Br-C_6H_4	(*S*)-VAPOL	V (5)	89	97	33:1	4.5(2.7)

[a] Unless otherwise specified, all reactions were performed with x mol% of catalyst **212/212′** with 0.50 mmol imine **110** (1.0 equiv, 0.5 M in toluene) and 0.6 mmol of EDA **85** (1.2 equiv) at room temperature and went to completion. Procedure IV or V (Scheme 6.2B and 6.2D) were followed for the aziridination reaction. [b] Isolated Yield. [c] Determined by HPLC. [d] Ratio determined by integration of the methine protons of *cis*- and *trans*-aziridine in the ^{1}H NMR spectrum of the crude reaction mixture. [e] Determined by integration of the NH signals of enamines relative to the methine proton of *cis* aziridine in the ^{1}H NMR spectrum of the crude reaction mixture. [f] This reaction was complete in 2 h with 5 mol% catalyst. [g] This reaction was complete in 8 h. [h] Pre-catalyst made using Procedure IV except that water was excluded during the catalyst preparation. [i] 97% complete.

At this point we had not yet addressed the critical issue of whether the DAM imines would provide higher inductions for imines from aliphatic aldehydes since we had only screened the aryl imines shown in Table 6.2. The aziridinations of the aliphatic DAM imines **110** using procedure IV and V were carried out as indicated in Table 6.3 in toluene at room temperature for 24 h. Considering previous observations that alkyl substituted imines are generally slower, 5-10 mol% catalyst was used for imines **110o**, **110v** and **110w**. Unfortunately, the results from the

alkyl substituted DAM imines **110** do not represent an improvement in the asymmetric inductions over those of the corresponding benzhydryl imines **78** and in fact are slightly lower.[9a] In addition, the aziridination of the primary alkyl substituted imine **110o** essentially fails in the case of the DAM imine (Table 6.2, entries 1-4). This reaction produces a very complex mixture with both VANOL and VAPOL catalysts and at both room temperature and at 0 °C. A similar complex mixture was produced with DAM imine **110o** in carbon tetrachloride solvent with the VAPOL catalyst where the aziridine **113o** was isolated in 11% yield and in 63% ee.[11] This is to be compared to the corresponding reaction of the benzhydryl imine **78o** (R = *n*-Pr) prepared from *n*-butanal which gave the corresponding aziridine **86o** in 40% yield and 81% ee.[9a] The crude ^{1}H NMR spectrum of the reaction of imine **110o** in entries 1-4 in Table 6.3 reveals the presence of a small amount of aziridine **113o** (6-14%) and small amounts of the unreacted imine **110o** and of the non-cyclized enamine products **116o** and **117o**. The only other product that was prominent in the crude ^{1}H NMR was, identified after some effort, as the vinyl imine **333o** whose structure was confirmed by independent synthesis (see experimental). This compound presumably results from an aldol type condensation of two molecules of imine **110o** (*via* an enamine). In contrast, high yields of aziridines were obtained with the 2° and 3° aliphatic imines **110v** and **110w,** but unfortunately, the asymmetric inductions were not significantly different than those previously observed in carbon tetrachloride.[11] Thus our attempts to improve the asymmetric inductions with aliphatic imines by employing the dianisylmethyl (DAM) substituted imines were surceased. Later on, tetramethyldianisylmethyl (MEDAM) protecting was found to be optimum

for both aromatic and aliphatic imines.[9c] Nonetheless, a very simplified one-pot aziridination protocol was identified in these studies with DAM imines.

Table 6.3 Asymmetric Aziridination with Alkyl DAM imines **110**. [a]

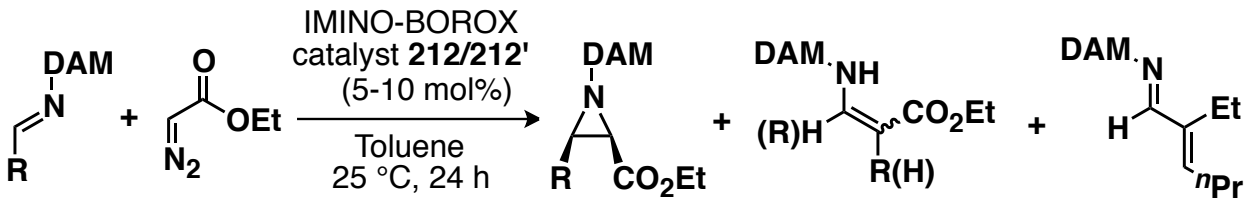

110 **85** **113** **116(117)** **333o**

#	Series	R	Ligand	Cat. x mol%	Yield **113** (%) [b]	ee **113** (%) [c]	cis/trans [d]	Enamine (%) [e]
1 [f]	**o**	*n*-propyl	(*R*)-VANOL	V (10)	nd	nd	nd	3(1)
2	**o**	*n*-propyl	(*R*)-VANOL	IV (10)	14	–52	nd	3(1)
3 [g]	**o**	*n*-propyl	(*S*)-VAPOL	IV (10)	11	73	nd	<1(2)
4 [g]	**o**	*n*-propyl	(*R*)-VANOL	IV (10)	10	–66	nd	2(1)
5	**v**	cyclohexyl	(*S*)-VANOL	V (5)	83	82	50:1	<1(<1)
6 [h]	**v**	cyclohexyl	(*R*)-VANOL	IV (5)	88	–80	50:1	<1(<1)
7 [i]	**w**	*t*-butyl	(*S*)-VANOL	V (10)	60	70	20:1	<1(<1)
8 [h]	**w**	*t*-butyl	(*R*)-VANOL	IV (10)	87	–83	50:1	<1(<1)

[a] Unless otherwise specified, all reactions were performed with x mol% of catalyst **212/212′** with 0.50 mmol imine **110** (1.0 equiv, 0.5 M in toluene) and 0.6 mmol of EDA **85** (1.2 equiv) at room temperature. Procedure IV or V (Scheme 6.2B and 6.2D) were followed for the aziridination reaction. The NMR yields of **332o** are 7, 4, 7, 8 for entries 1-4 respectively. The NMR yield for unreacted imine **110** are 4, 2, 10, 7, <1, <1, 25, <1 for entries 1-8 respectively. The NMR yield is determined from ^{1}H NMR spectrum of the crude reaction mixture with Ph_3CH as internal standard. [b] Isolated Yield. [c] Determined by HPLC. [d] Ratio determined by integration of the methine protons of *cis*- and *trans*- aziridine in the ^{1}H NMR spectrum of the crude reaction mixture. [e] Determined by integration of the NH signals of enamines relative to the methine proton of *cis* aziridine in the ^{1}H NMR spectrum of the crude reaction mixture. [f] The NMR yield of the aziridine **113o** is 6%. [g] This reaction was performed with at 0 °C for 48 h. [h] Reaction time = 48 h. [i] Reaction time = 55 h.

Following the procedure V (Scheme 6.2D), a study of the effect of various additives on the aziridination reaction was performed (Table 6.4). The additives (one equivalent with respect to the imine) were added prior to the addition of ethyl diazoacetate **85**. Low conversions were obtained when water and 4-pentylbicyclo [2.2.2]octane-1-carboxylic acid **334b** were used as additives (entries 1-2). A drop of 22% ee was observed when benzoic acid **334a** was added (entry 3). However, addition of phenol **194a** did not alter the result (entry 4).

Table 6.4 Effect of various additives on the aziridination reaction. [a]

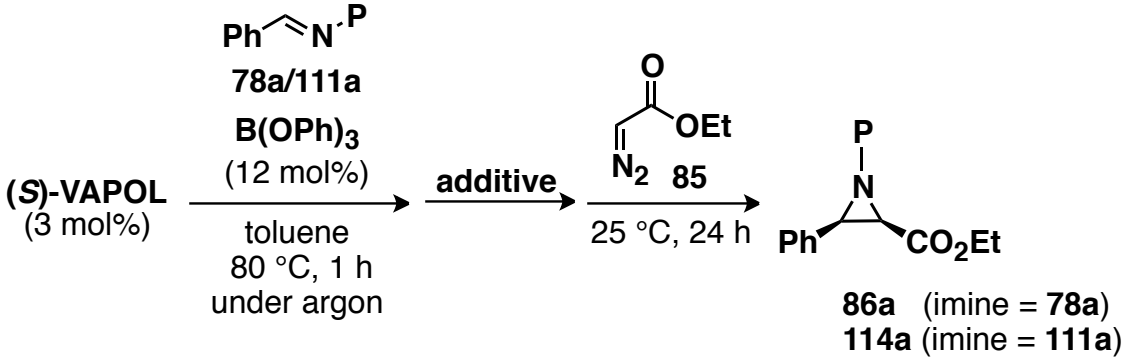

#	imine	P	Additive [b]	Conv (%) [c]	Yield azi (%) [d]	ee azi (%) [e]	cis/trans [f]	Enamine (%) [g]
1 [h]	**78a**	$CHPh_2$	H_2O	43	nd	nd	nd	nd
2	**111a**	MEDAM	H_2O	15	nd	nd	nd	nd
3	**111a**	MEDAM	4-pentylbicyclo [2.2.2]octane-1-carboxylic acid	22	nd	nd	nd	nd
4	**111a**	MEDAM	$PhCO_2H$	88	77	78	33:1	5(2)
5	**111a**	MEDAM	PhOH	100	98	96	50:1	4(5)

[a] Unless otherwise specified, all reactions were performed with 3 mol% of catalyst with 0.50 mmol imine **78a/111a** (1.0 equiv, 0.5 M in toluene) and 0.6 mmol of EDA **85** (1.2 equiv) at room temperature and went to completion. Procedure V (Scheme 6.2D) was followed for the aziridination reaction. [b] One equivalent of the additive was added with respect to the imine. [c] Percent conversion is determined by integration of the methine proton of the *cis*-aziridine relative to the sp^2-CH proton of the unreacted imine in the ^{1}H NMR spectrum of the crude reaction mixture. [d] Isolated Yield. [e] Determined by HPLC. [f] Ratio determined by integration

Table 6.4 cont'd

of the methine protons of *cis*- and *trans*- aziridine in the ^{1}H NMR spectrum of the crude reaction mixture. [g] Determined by integration of the NH signals of enamines relative to the methine proton of *cis* aziridine in the ^{1}H NMR spectrum of the crude reaction mixture. [h] Procedure IV (Scheme 6.2B) was followed for the aziridination reaction with 5 mol% catalyst.

6.2 Racemic Aziridination with various Lewis/Brønsted acids

During one of the studies, we found that the MEDAM group, which is the optimum for our aziridination reaction, is not as good as benzhydryl protecting group for a racemic aziridination with various Lewis or Brønsted acids (Table 6.5). We already know that the rate-limiting step in the case of the Wulff catalytic asymmetric aziridination reaction is the ring-closure step and carbon-carbon bond formation step for MEDAM imine **111a** and benzhydryl imine **78a** respectively. It would be interesting to find out the rate-limiting step in the case $Yb(OTf)_3$ catalyzed racemic aziridination reaction using benzhydryl imine **78a**. An experiment was performed (Table 6.5, entry 8) at a 10 mmol scale and the KIE studies were on progress at the time of writing of this dissertation.

Table 6.5 Racemic Aziridination with various Lewis/Brønsted acids. [a]

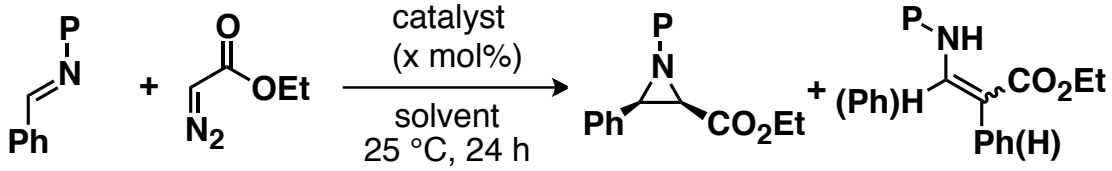

78a **111a** | **85** | **86a** **114a** | **87a(88a)** **118a(119a)**

Table 6.5 cont'd

#	imine	P	catalyst (x mol%)	Conc (M)	solvent	Yield azi (%) [b]	cis/trans [c]	Enamine (%) [d]
1 [e]	**111a**	MEDAM	BF_3•Et_2O (10)	0.055	toluene	5	3.8:1	3(1)
2 [e]	**111a**	MEDAM	BF_3•Et_2O (10)	0.4	toluene	6	6.3:1	<1(<1)
3 [e]	**111a**	MEDAM	BF_3•Et_2O (100)	0.4	toluene	24	9.9:1	2(<1)
4 [e]	**111a**	MEDAM	TfOH (25)	0.2	toluene	29	6.9:1	7(8)
5	**111a**	MEDAM	$Yb(OTf)_3$ (10)	0.1	hexanes	33	7.6:1	<1(<1)
6	**78a**	$CHPh_2$	$Yb(OTf)_3$ (10)	0.1	hexanes	63	16:1	<1(4)
7 [f]	**78a**	$CHPh_2$	$Yb(OTf)_3$ (20)	0.1	hexanes	68	20:1	5(6)
8	**78a**	$CHPh_2$	$Yb(OTf)_3$ (20)	0.1	hexanes	72	17:1	5(5)
9 [f]	**78a**	$CHPh_2$	$Yb(OTf)_3$ (10)	0.1	toluene	42	7.7:1	10(13)
10	**78a**	$CHPh_2$	$Yb(OTf)_3$ (10)	0.1	toluene	41	6.6:1	8(11)
11	**78a**	$CHPh_2$	$B(OPh)_3$ (40)	0.5	toluene	78	>50:1	8(2)

[a] Unless otherwise specified, all reactions were performed with x mol% of catalyst with 0.50 mmol imine **78a/111a** (1.0 equiv, C M in solvent) and 0.6 mmol of EDA **85** (2 equiv) at room temperature. The amount of unreacted imine **78a/111a** was 90%, 75%, 40%, 22%, 63%, 7%, <1%, <1%, 2%, 13% and <1% for entries 1-11 respectively. [b] Determined from ^{1}H NMR of crude reaction mixture with Ph_3CH as the internal standard. [c] Ratio determined by integration of the methine protons of *cis*- and *trans*-aziridine in the ^{1}H NMR spectrum of the crude reaction mixture. [d] Determined by integration of the NH signals of enamines relative to the methine proton of *cis*-aziridine in the ^{1}H NMR spectrum of the crude reaction mixture. [e] 1.2 equiv EDA used. [f] EDA added at 0 ºC.

6.3 Catalytic asymmetric [3+2] cycloaddition

Over the last several years we have developed a general method for the catalytic asymmetric synthesis of aziridines that is based on the reaction of stabilized diazo compounds with imines and which is mediated by asymmetric catalysts generated from the VANOL and

VAPOL ligands and various boron compounds.[8-9] The reactions are also highly diastereoselective giving *cis*- and *trans*-2,3-disubstituted aziridines depending upon the kind of diazo compounds used. The scope of the reaction is broad and includes imines derived from a variety of aldehydes including electron-rich and electron-poor aromatic aldehydes and 1°, 2° and 3° aliphatic aldehydes.[9a] It must be noted that while aziridines **114t**[14] and **124′a**[15] are obtained in high yields and ees from the reaction between imines **111t** (derived from dihydrocinnaldehyde **127t**) and **122′a** (derived from 3-phenyl-2-propynal **102a**) and EDA, imine **335a** (derived from cinnamaldehyde **336a**) failed to give any aziridine when reacted with EDA under aziridination reaction conditions (Scheme 6.3A). In this case, starting material i.e. imine was recovered. A similar trend was observed when diazoacetamide **123a** was utilized for aziridination reaction with imines **112z**[9f] and **122z**[15] and likewise, there was no reaction with the imine **335z** (derived from *trans*-crotonaldehyde **336c**) (Scheme 6.3B). The reason for the failure of the aziridination reaction with imines derived from α,β-unsaturated aldehydes has not been determined. However, there are six different products possible from the reaction between the imine **335** and ethyl diazoacetate **85** as shown in Scheme 6.3C. Apart from aziridines **337** and enamines **338-339**, the products include the diazo compound **340**, the pyrazoline **341** and the cyclopropane **342**.

Scheme 6.3 (**A**) Reaction between EDA and different imines (**B**) Reaction between diazoacetamide and different imines (**C**) Possible products from the reaction between EDA and conjugated imine **335**

Scheme 6.3 cont'd

A

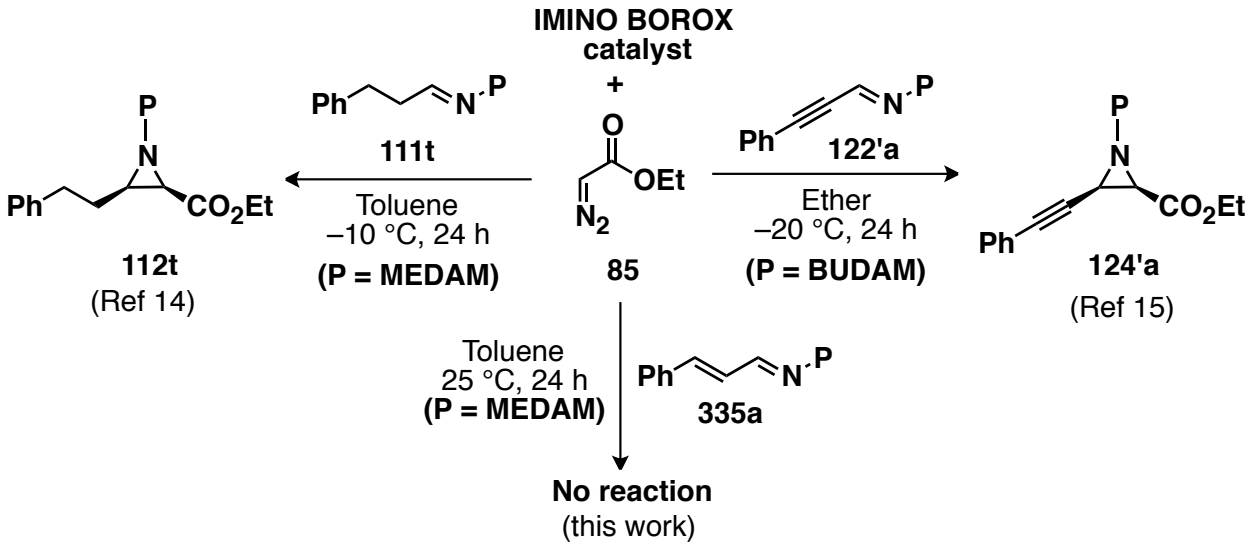

B

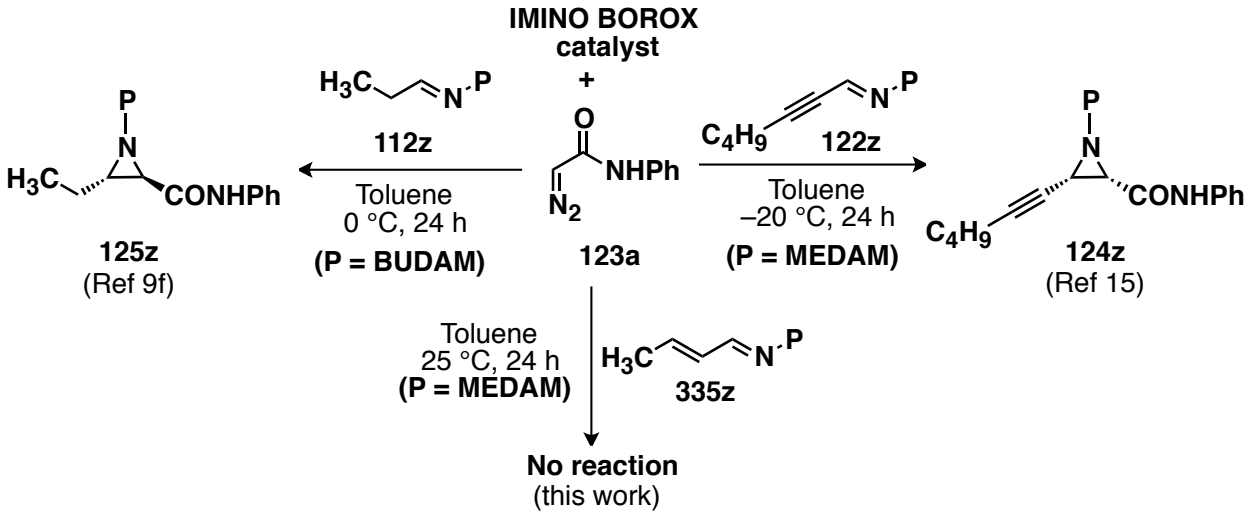

Scheme 6.3 cont'd

C

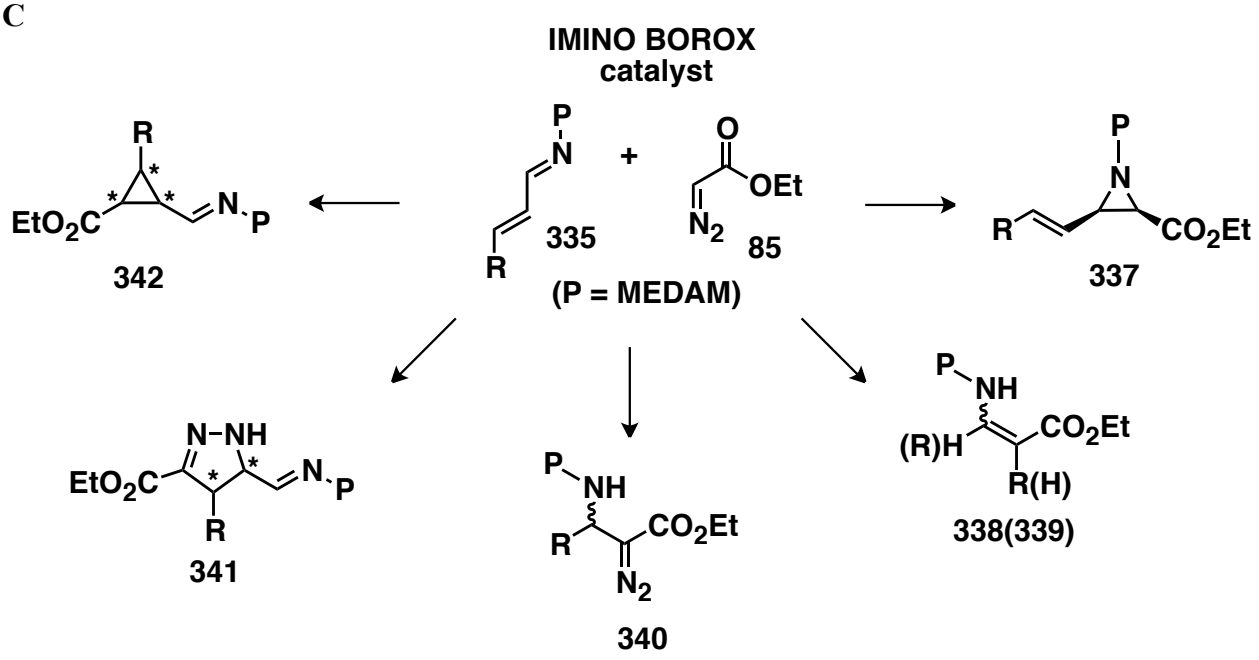

It must be pointed out that there is no prior report of a reaction between a diazo compound and imine derived from α,β-unsaturated aldehydes. However, pyrazolines and cyclopropanes have been observed from the reaction between α,β-unsaturated aldehydes and EDA with the outcome depending upon the substitution pattern of the aldehyde and the reaction conditions (Scheme 6.4 and 6.5). With no alpha substitution, it has been reported that [3+2] adduct is the major product which polymerizes very quickly (Scheme 6.4A and 6.4B).[16] However, in the year 2006, Hossain and coworkers showed that cyclopropanes can be obtained in high yields from these aldehydes if the reaction is performed in the presence of HBF_4 at –78 °C.[17] In 2006, Maruoka and coworkers reported the formation of a chiral all-carbon quaternary center *via* TfOH catalyzed insertion of aryldiazoacetates into an sp^2 carbon–CHO bond (Scheme 6.4C).[18] Nonetheless, based on the reported observations with aldehydes (Scheme 6.4), a similar outcome

can be assumed in the cases of the reaction between imine **335** derived from α,β-unsaturated aldehydes **336** and EDA. In other words, probably, a very small amount of the imine **335** undergoes [3+2] cycloaddition and the resulting adduct might bind to the catalyst thereby completely killing the reaction.

Scheme 6.4 (**A**) Reaction between EDA and unsubstituted acroleins[16-17] (**B**) Reaction between EDA and β-substituted acroleins[16-17] (**C**) Reaction between di-substituted aryldiazoacetate and β-disubstituted acroleins[18]

A

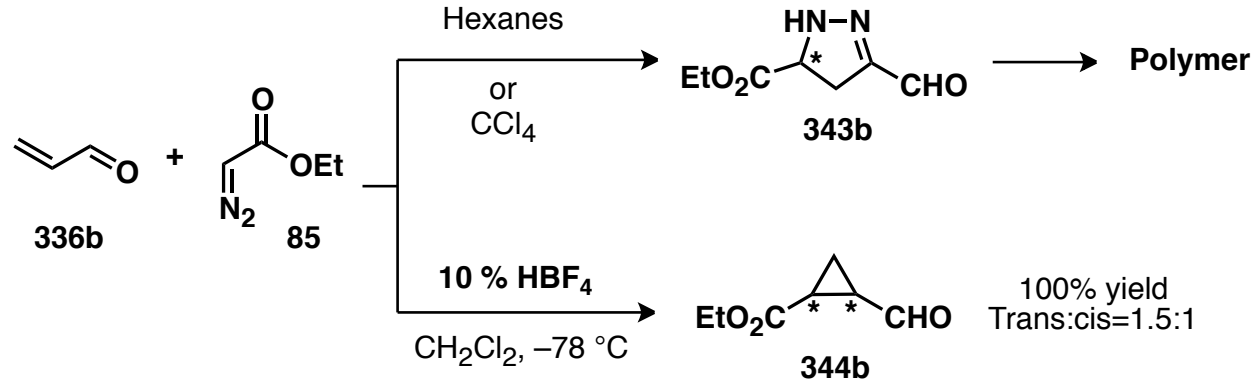

B

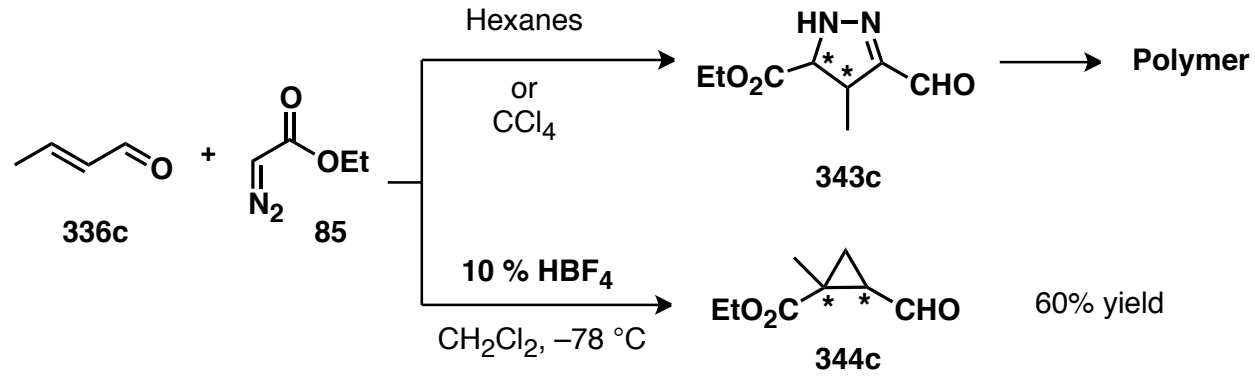

Scheme 6.4 cont'd

C

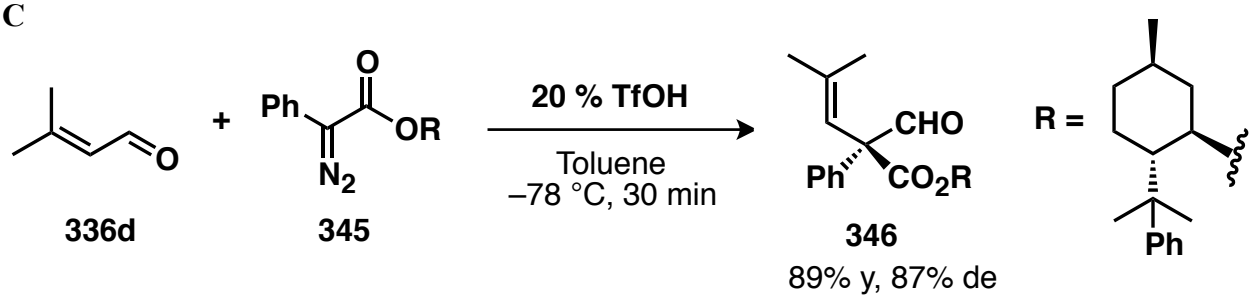

While [3+2] adducts[19] have been observed from the reaction of mono-substituted diazo compounds with α-substituted acroliens, di-substituted diazo compounds have been reported to form cyclopropanes[20] for the same reaction (Scheme 6.5). There are several other [3+2] cycloadditions reported using acroleins[21] and other carbonyl compounds.[22]

Scheme 6.5 (**A**) Reaction between **348** or EDA and α-substituted acroleins **347** (**B**) Reaction between EDA and α,β-substituted acroleins **352** (**C**) Reaction between di-substituted aryldiazoacetate and α-substituted acroleins **347**

A

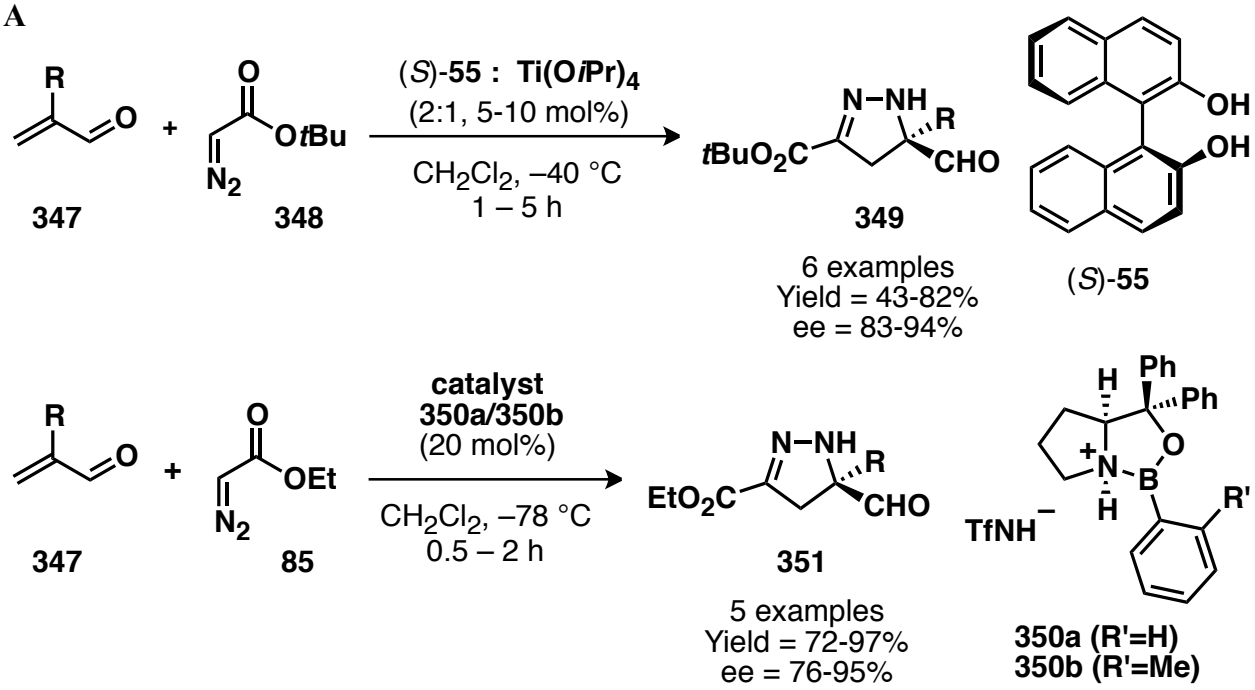

Scheme 6.5 cont'd

B

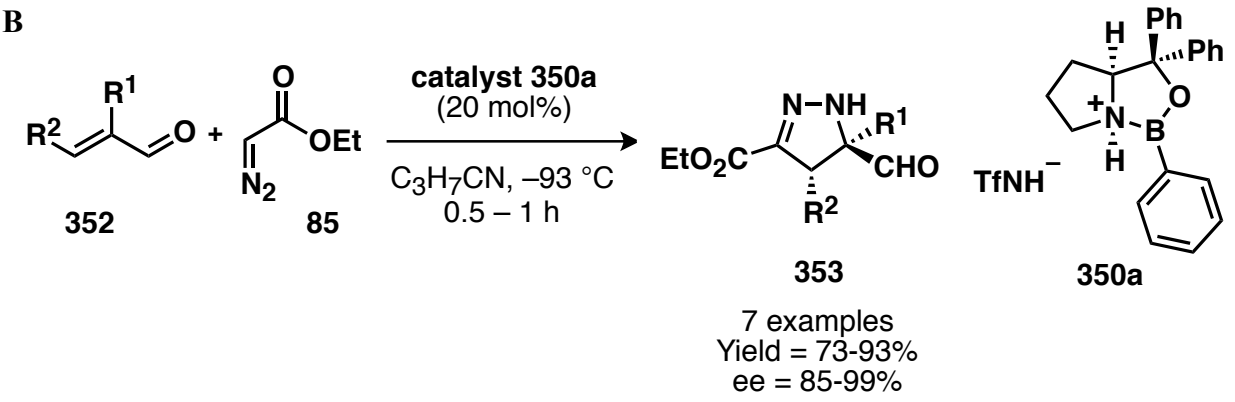

7 examples
Yield = 73-93%
ee = 85-99%

C

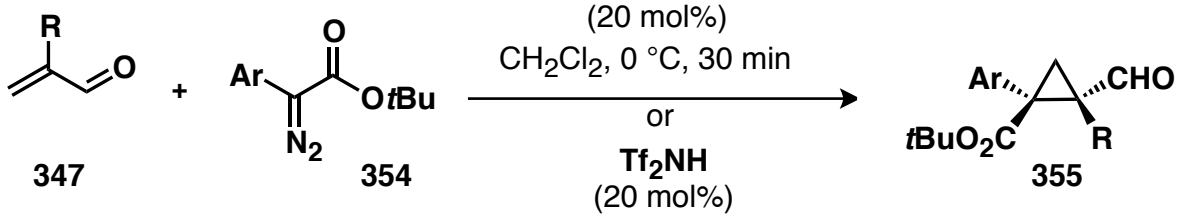

29 examples
Yield = 21-69%
trans:cis = > 20:1

Given the reported reactions of α,β-unsaturated aldehydes described above, the thought then arose to attempt the reaction of an imine generated from α-substituted acroleins with ethyl diazoacetate in the presence of IMINO-BOROX catalyst. At this point, it must be remembered that we did obtain a conjugated imine **333o** as the byproduct during the aziridination reaction of imine **110o** with EDA (Table 6.3, entry 1-4). This was found to be one of the reasons for the low yields obtained from the aziridination reaction with aliphatic imines. We then thought to react the imine **333o** with EDA, and surprisingly, we observed the [3+2] adduct **356o** in 41% yield in the presence of IMINO-BOROX catalyst **357o**. The asymmetric induction could not be measured. In HPLC analysis, multiple absorption peaks were observed, probably, due to the decomposition of the [3+2] adduct **356o**. There was no sign of any aziridine from NMR analysis

of the crude reaction mixture. This was unexpected and lead to the discovery of a novel and unprecedented [3+2] cycloaddition reaction catalyzed by our IMINO BOROX catalyst derived from vaulted ligands.

Scheme 6.6 [3+2] cycloaddition reaction between EDA and imine **328o**

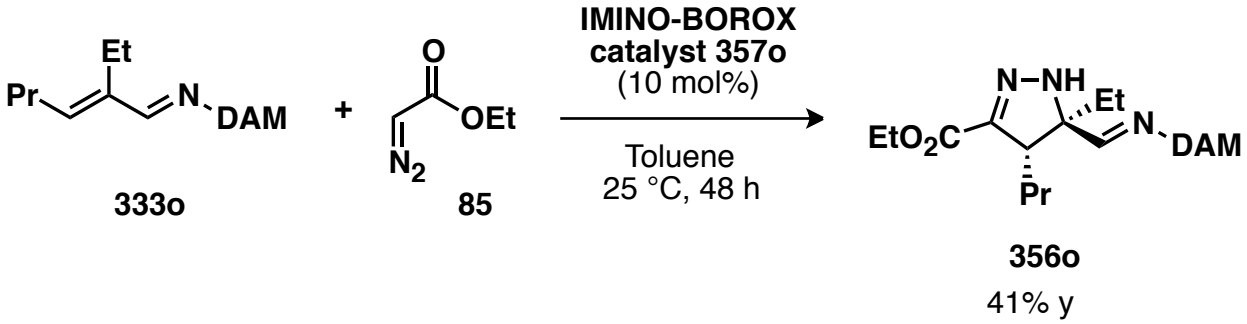

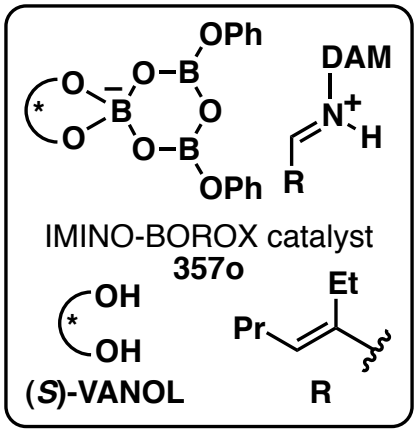

Thereafter, as a part of optimization, we subjected the reaction of the imine derived from *(E)*-2-methylbut-2-enal **352b** with ethyl diazoacetate **85** to different conditions (Table 6.6). Low yields were obtained with both VANOL and VAPOL catalysts when imine **359a**, derived from MEDAM amine **126c**, was employed (entries 1-2). However, imine **358a** derived from BUDAM amine **126d** gave the [3+2] adduct **360a** in 59% yield and 50% ee using the VAPOL catalyst (entry 4). The results in the table show that the reaction performed with the VAPOL catalyst

gives a higher yield than the reaction with the VANOL catalyst (entry 4 *vs.* 3). There was no reaction observed in the absence of catalyst or in the presence of only (*S*)-VAPOL as the catalyst (entries 5-6). Not much improvement was observed upon changing the solvent to dichloromethane and performing the reactions at –78 °C (entries 7-10). Even lowering the concentration to 0.1 M did not assist in any improvement of the yield (entry 10). A common observation in the reactions in dichloromethane is that there was an unknown side-product **366a** present in the reaction mixture. The structure of the unknown side-product is suspected to be cyclopropane, however, this was not confirmed.

Table 6.6 Initial optimization of the [3+2] cycloaddition reaction. [a]

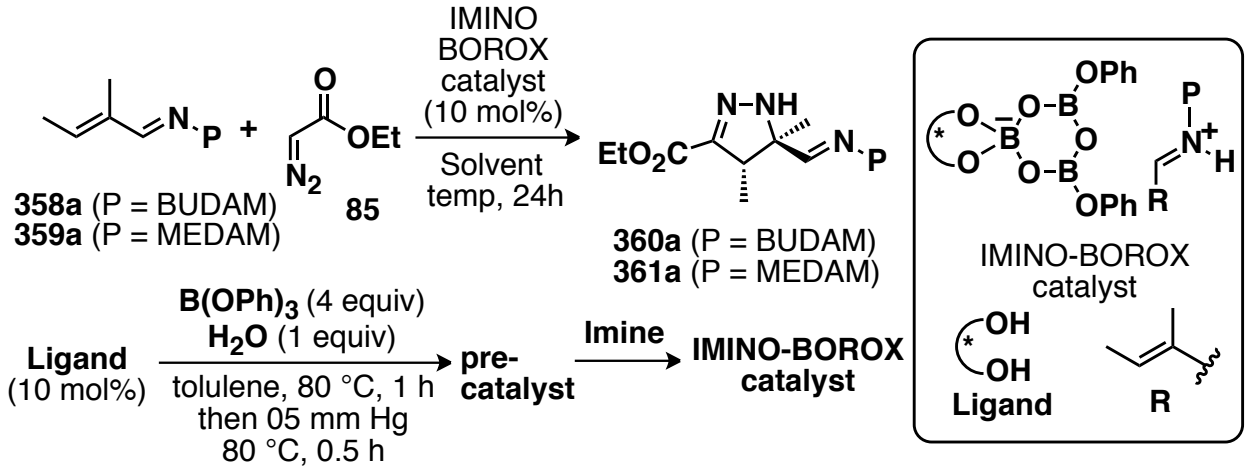

#	Cat.	Ligand	P	Temp (°C)	Solvent	Prod.	Yield (%) [b]	ee (%) [c]
1	**362a**	(*S*)-VANOL	MEDAM	25	toluene	**361a**	35	nd
2	**363a**	(*S*)-VAPOL	MEDAM	25	toluene	**361a**	33	nd
3	**364a**	(*S*)-VANOL	BUDAM	25	toluene	**360a**	34	52 [d]
4	**365a**	(*S*)-VAPOL	BUDAM	25	toluene	**360a**	59	50 [d]
5 [e]	**58**	(*S*)-VAPOL only	BUDAM	25	toluene	**360a**	<1	–
6 [f]	–	no catalyst	BUDAM	25	toluene	**360a**	<1	–
7 [g]	**365a**	(*S*)-VAPOL	BUDAM	–78	CH_2Cl_2	**360a**	50	50 [d]

Table 6.6 cont'd

8 [h]	**365a**	(*S*)-VAPOL	BUDAM	–78	CH_2Cl_2	**360a**	21	nd
9 [i]	**365a**	(*S*)-VAPOL	BUDAM	–78	CH_2Cl_2	**360a**	25	nd
10 [j]	**365a**	(*S*)-VAPOL	BUDAM	–78	CH_2Cl_2	**360a**	46	nd

[a] Unless otherwise specified, all reactions were performed with 10 mol% of catalyst with 0.20 mmol imine **358a/359a** (1.0 equiv, 0.4 M in toluene) and 0.4 mmol of EDA **85** (2 equiv) at room temperature. The pre-catalyst is made using method C (Chapter 2). [b] The NMR yield is determined by the ^{1}H NMR spectra of the crude reaction mixture with Ph_3CH as internal standard. [c] Determined by HPLC. [d] The sample was prepared by passing the crude product through a plug of neutral Al_2O_3 using 10:1 hexanes:EtOAc as the eluent. [e] The reaction was performed in presence of (*S*)-VAPOL only. [f] No catalyst was used for the reaction. [g] This reaction was allowed to warm to 25 ºC and then stirred for 15 min at 25 °C followed by dilution with hexanes. [h] Reaction time = 3 h. An unknown product **366a** (40%) was observed along with 18% of unreacted imine **358a**. [i] A small amount of unknown side product **366a** was observed. [j] The concentration of the reaction is 0.1 M. A small amount of unknown side product **366a** was also observed.

To our delight, the [3+2] cycloaddition reaction was also found to give comparable results when the reaction was performed in a multicomponent fashion (Scheme 6.7).

Scheme 6.7 Multicomponent [3+2] cycloaddition reaction.

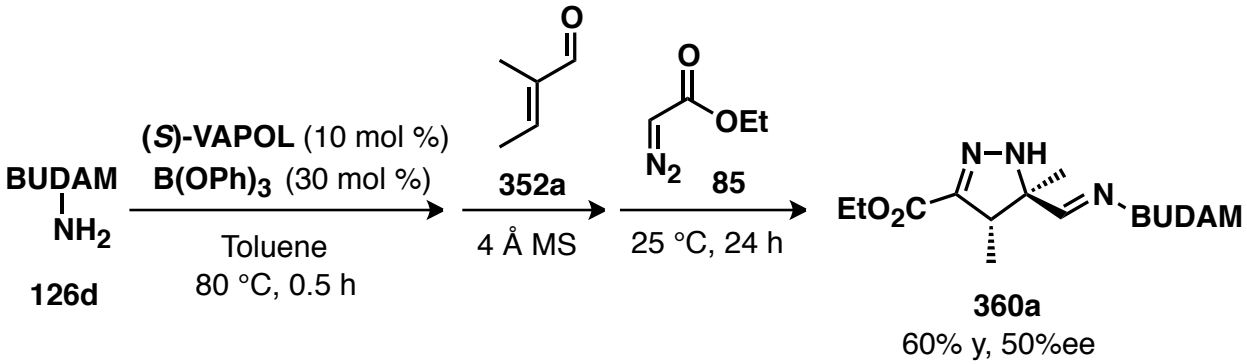

In an attempt to purify and isolate the product, we decided to either hydrolyze or reduce the resulting [3+2] adduct **360a** which itself is an imine. Several conditions were tried for

hydrolysis, however, a complex mixture of products was obtained along with the BUDAM amine **1126d** (Scheme 6.8A). Nonetheless, it was observed that the [3+2] adduct **360a** can be easily reduced to amine **367a** using $NaBH_4$ (Scheme 6.8B).

Scheme 6.8 Attempts towards the (**A**) hydrolysis of adduct **360a** (**B**) reduction of adduct **360a**.

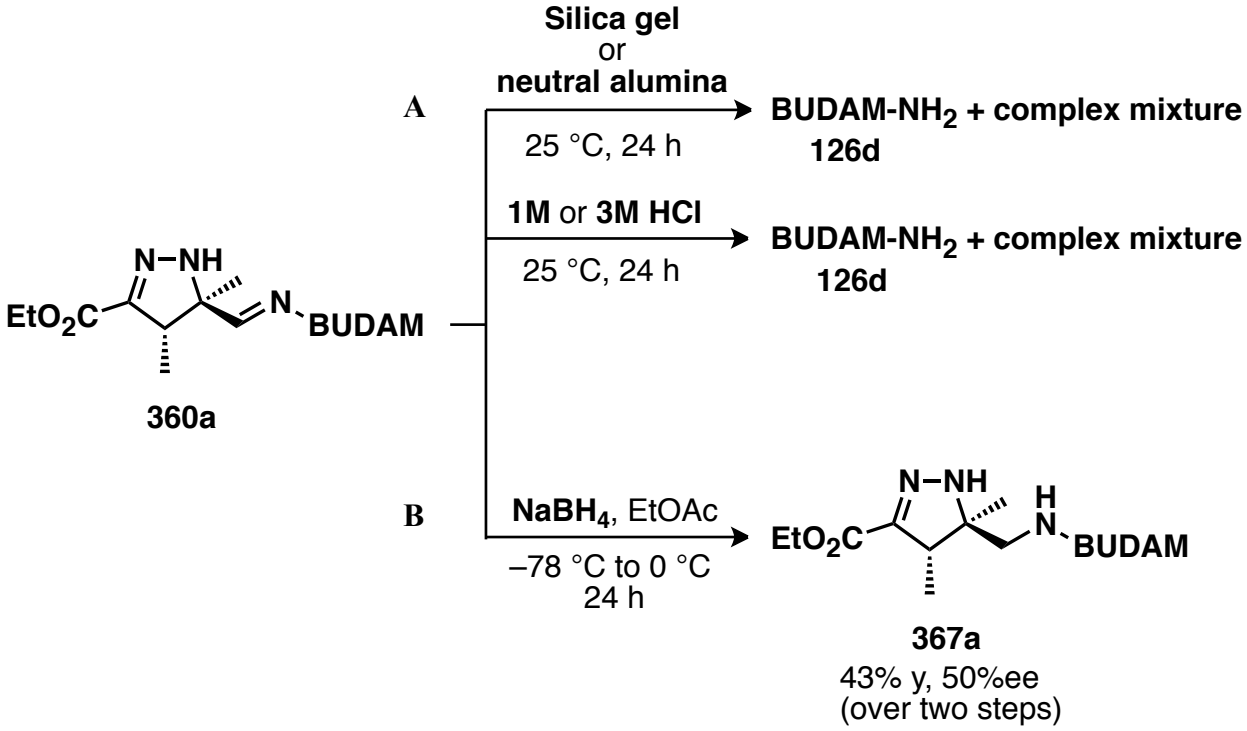

In the end, an unprecedented multicomponent [3+2] cycloaddition has been discovered and presented here. The project is still in an infant state and has the potential to broaden the scope of our BOROX catalysis. Hopefully, this methodology would provide an easy access to Manzacidins[19a] and the family of bromopyrrole alkaloids namely, Clathramides.[23] Also, it is worth mentioning that this work is a perfect example of why a crude NMR spectrum should never be ignored even if the reaction fails to give the desired product.

6.4 Attempts towards catalytic asymmetric Ugi 3CR, Ugi-type 2CR and Ugi-type 3CR.

In the process of the broadening the scope of our BOROX catalyst, we decided to explore the possible applications of the catalyst on other asymmetric reactions. One of such reactions is the Ugi four component coupling reaction (Ugi-4CR). The Ugi-4CR is one of the most widely used multicomponent reactions.[24] An enantioselective variant of this fundamental reaction is still unknown. The Ugi reaction, discovered by Ivar Ugi in 1959, is classified as an isocyanide-based multicomponent reaction.[25] It allows the formation of an *α*-*N*-acylamino amide **E** (peptide derivatives) by the coupling of isocyanides **D** with carbonyl compounds (usually an aldehyde of type **A**), primary amine **B** and carboxylic acid **C** (Scheme 6.9X). It introduces a high degree of diversity yielding compounds which can serve as scaffolds for the synthesis of natural products, therapeutic agents, and combinatorial libraries.

Mechanistically, the first step involves the condensation of aldehyde **A** and amine **B**, followed by the protonation of the imine **F** by acid **C** (Scheme 6.9Y). The next step involves the nucleophilic addition of isocyanide **D** to activated iminium **G**, followed by the trapping of the nitrilium species **H** by the carboxylate anion. The final irreversible acyl transfer (known as the Mumm rearrangement) results in the formation of the *α*-*N*-acylamino amide **E**.

Scheme 6.9 (**X**) Ugi-4CR reaction (**Y**) Proposed mechanism

X

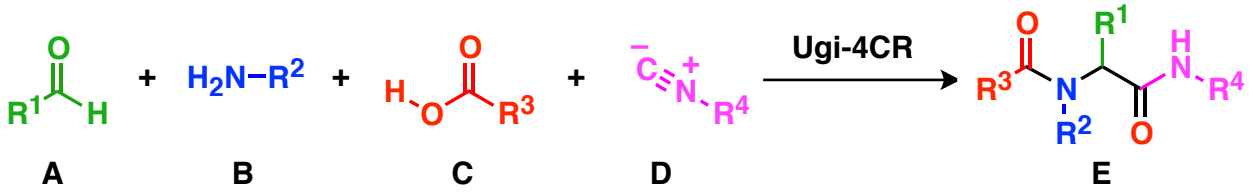

Scheme 6.9 cont'd

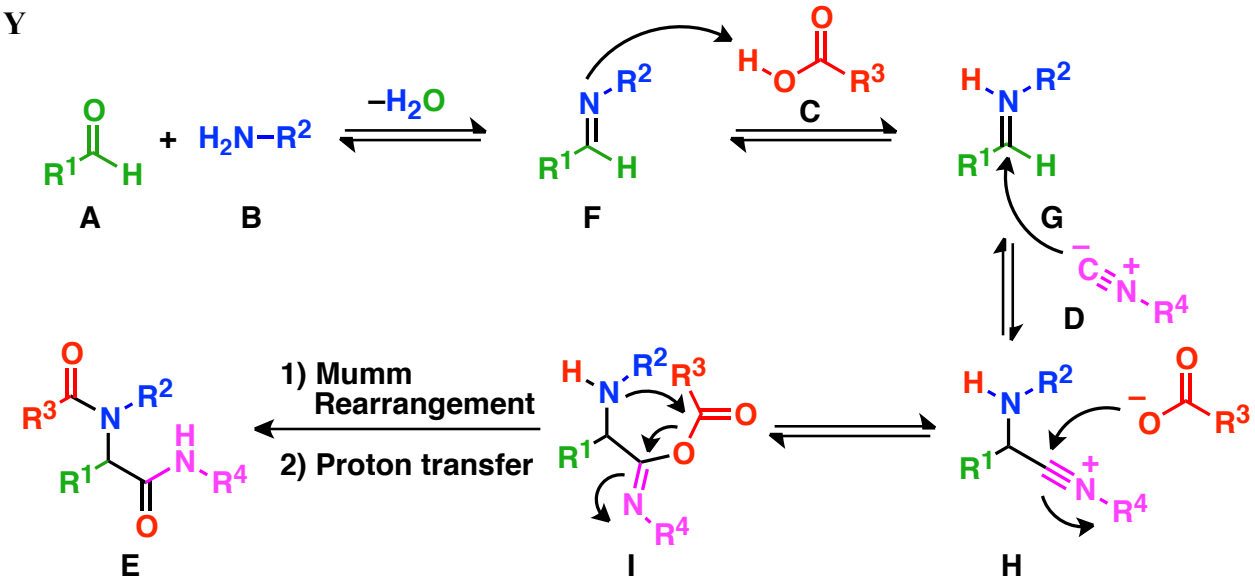

It was thus envisioned to examine the reaction using our IMINO-BOROX catalyst **104a** or chiral VAPOL phosphoric acid **35** (Scheme 6.10). The proposed Ugi reaction would involve the pre-formed imine **F** instead of an amine and aldehyde, thereby making it as a three component coupling (3CR) instead of four component coupling (4CR).

Scheme 6.10 Proposed Ugi-3CR

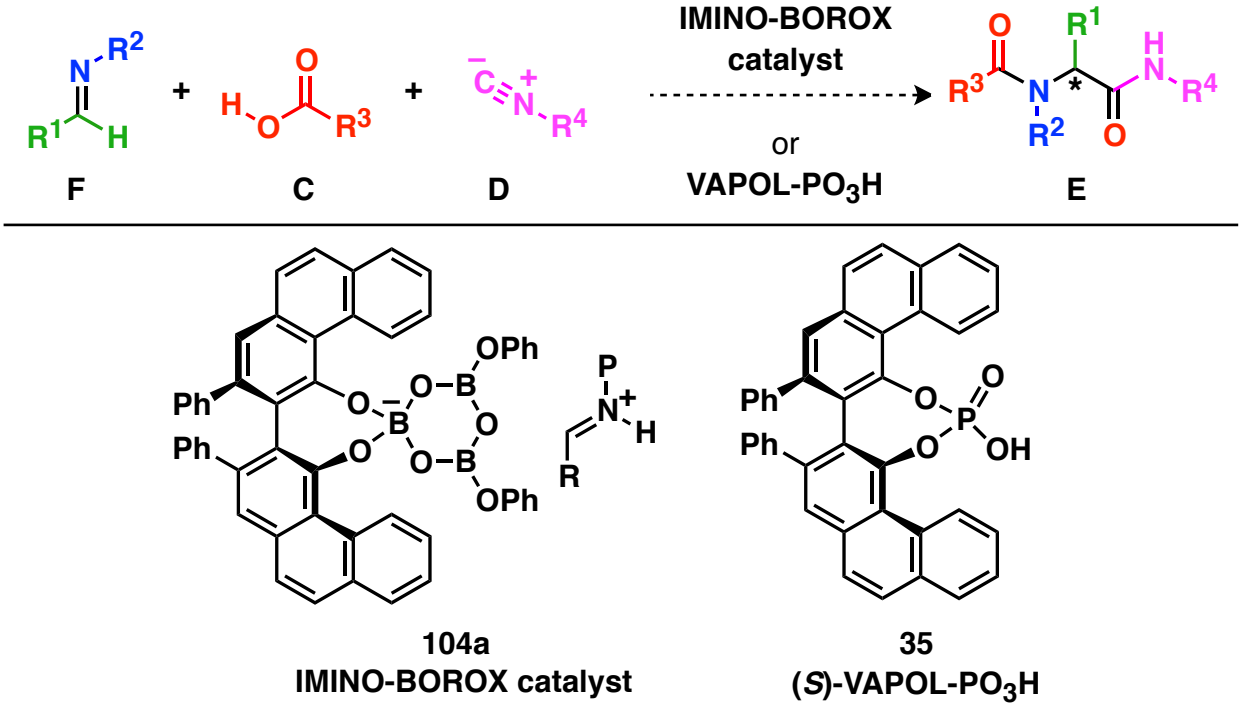

Finding a chiral inductor or catalyst for Ugi reaction would represent a major achievement not only for organic synthesis but also for the pharmaceutical industry. As stated by Ugi, "until today the problem of control of the newly formed stereocenter has not been solved conclusively".[24d] Thus, the aim of this project is to find a chiral variant of the Ugi reaction.

6.4.1 Attempts towards catalytic asymmetric Ugi -3CR

In the initial screening, the Ugi-3CR reaction was performed using benzoic acid **334a** and *t*-butyl isocyanide **368a**. The results are summarized in Table 6.7 (entries 1-5). A 20% yield of amide **369a** was obtained in the absence of any kind of catalyst (entry 1). The background reaction must have been facilitated by the benzoic acid as the promoter of the reaction. In the first experiment using 10 mol% IMINO-BOROX catalyst **190a**, an increase in the yield (40%) was observed at room temperature (entry 2). Unfortunately, no enantioselectivity was observed. As the carboxylic acid itself can catalyze the Ugi reaction, it was then thought that the uncatalyzed background reaction might be competing with the asymmetric reaction. In order to suppress the background reaction, if any, a stoichiometric amount of the catalyst was used. The ^{1}H NMR analysis of the crude reaction mixture shows no sign of the desired product (entry 3). Even the slow addition of the carboxylic acid **334a** over a period of 3 h did not bring any change in the outcome (entry 4). Meanwhile, an 8% yield of the racemic product **369a** was obtained when (*R*)-VAPOL phosphoric acid **35** was employed as the Brønsted acid catalyst (entry 5). It must be noted that compound **370a**, which could result from the reaction of imine **119a** and isocyanide **368a**, has not been observed in the first five entries of the Table 6.7.

Table 6.7 Preliminary results towards the Ugi-3CR reaction. [a]

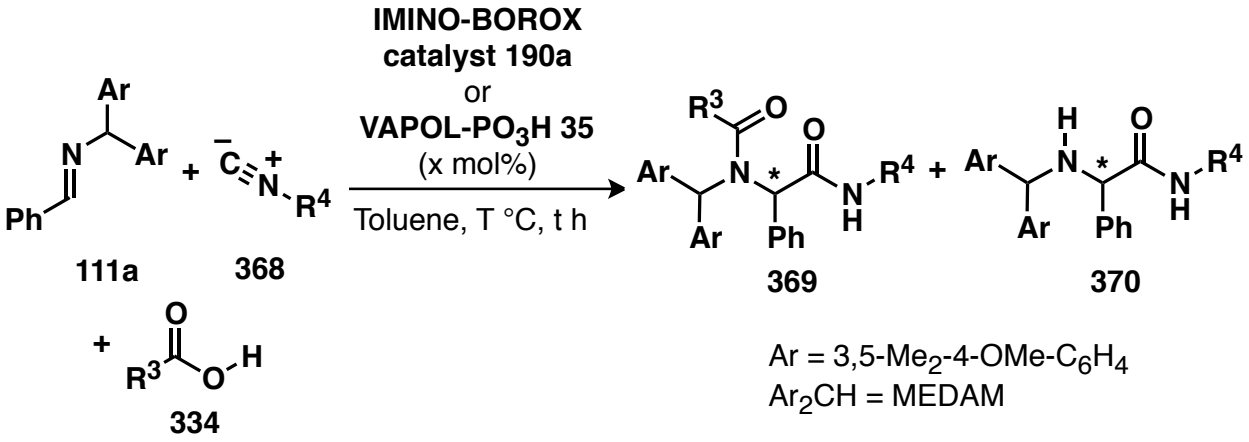

#	R^3	R^4	Temp	Cat. x mol%	Product	Yield **369** (%) [b]	ee **369** (%) [c]
1	Ph	*t*Bu	25	none	**369a**	20	–
2	Ph	*t*Bu	25	10	**369a**	40	<1
3	Ph	*t*Bu	25	100	**369a**	<1	–
4 [d]	Ph	*t*Bu	25	100	**369a**	<1	–
5 [e]	Ph	*t*Bu	25	20	**369a**	8	<1
6	4-pentylbicyclo [2.2.2]octyl	2-Naphthyl	25	none	**369b**	<1	–
7 [f]	4-pentylbicyclo [2.2.2]octyl	2-Naphthyl	25	10	**369b**	<1	–
8	4-pentylbicyclo [2.2.2]octyl	2-Naphthyl	25	20	**369b**	<1	–
9	4-pentylbicyclo [2.2.2]octyl	2-Naphthyl	40	20	**369b**	<1	–

[a] Unless otherwise specified, all reactions were performed with x mol% of catalyst **190a** with 0.50 mmol imine **111a** (1.0 equiv, 0.3 M in toluene), 0.5 mmol acid **334** (1.0 equiv) and 0.5 mmol of isocyanide **368** (1.0 equiv) at room temperature. The acid component **334** was added after 5 min of the addition of the isocyanide **368**. PhCOOH was sublimed prior to use. Ar_2CH = MEDAM. [b] Isolated Yield. [c] Determined by HPLC. [d] The acid component **334a** was added slowly over a period of 3 h *via* syringe pump. [e] (*R*)-VAPOL-PO_3H **35** was used as the catalyst. Reaction time = 48 h. [f] 26% yield of **370b** was isolated .

In order to suppress the background reaction, it was envisioned to utilize a weaker acid than benzoic acid. Hence, 4-pentylbicyclo[2.2.2]octane-1-carboxylic acid **334b** (pKa of bicyclo[2.2.2]octane-1-carboxylic acid = 6.75)[26] was examined. At the same time, the isocyanide component was switched to a weak and unreactive 2-napthyl isocyanide **368b**. As expected, there was no reaction observed in the absence of the catalyst (Table 6.7, entry 6). A complex mixture of six different compounds was obtained when the reaction was performed with 10 mol% IMINO-BOROX catalyst **190a** (entry 7). One of the fractions was isolated as an orange solid **370b** (72 mg, 26%). The ^{1}H NMR analysis of this compound revealed the absence of the acid component suggesting that this compound could be a product of imine **111a** and 2-naphthyl isocyanide **368b**. The compound was then completely characterized (see experimental). The asymmetric induction of **370b** was found to be 8% ee. The next two reactions were attempted with 20 mol % catalyst, one at room temperature and the other at 40°C (entries 8-9). The ^{1}H NMR spectrum of both the crude reaction mixtures were very much similar to that of the reaction with 10 mol% catalyst.

6.4.2 Attempts towards catalytic asymmetric Ugi-type 2CR and Ugi-type 3CR

We have seen that α–amino amide **370b** (Table 6.7, entry 7 and Table 6.8, entry 1) is formed, possibly, due to the reaction between imine **111a** and isocyanide **368b**. Based on this observation, we decided to examine an Ugi-type two-component reaction (Ugi-type-2CR) as shown in Scheme 6.11. Unfortunately, no α–amino amide **370** or **371** was observed when imine

111a or **78a** was reacted with isocyanides **368a** or **368b** using our IMINO-BOROX catalyst (Table 6.8, entries 2-4). The starting materials were recovered instead.

Scheme 6.11 Proposed Ugi-type 2CR

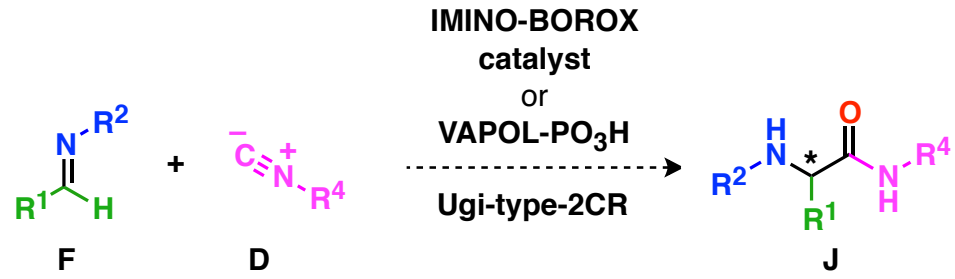

Table 6.8 Preliminary results towards the Ugi-2CR and Ugi-3CR. [a]

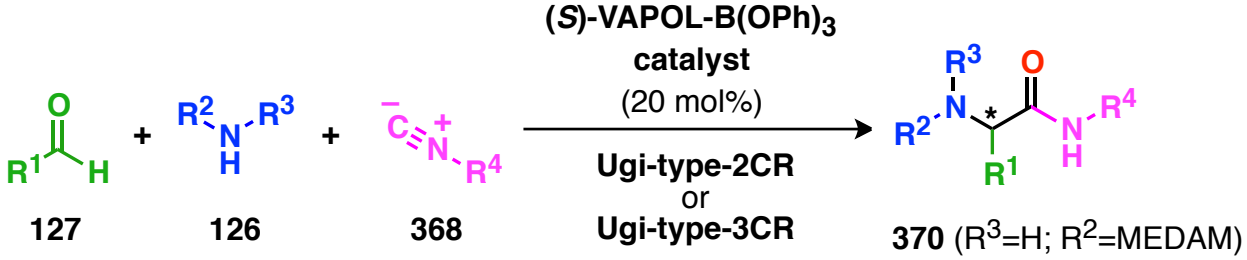

#	R^1	R^2	R^3	R^4	Product	Yield (%) [b]	ee (%) [c]
1 [d,e]	Ph	MEDAM	H	2-naphthyl	**370b**	26	8
2 [d]	Ph	MEDAM	H	2-naphthyl	**370b**	<1	–
3 [d]	Ph	MEDAM	H	*t*Bu	**370a**	<1	–
4 [d]	Ph	Ph_2CH	H	*t*Bu	**371a**	<1	–
5	Ph	Ph_2CH	H	*t*Bu	**371a**	<1 (<1) [g]	– (–) [g]
6 [f]	Ph	$PhCH_2$	$PhCH_2$	*t*Bu	**372a**	74 (44) [h]	17 (19) [h]
7 [f]	Ph	$PhCH_2$	$PhCH_2$	*t*Bu	**372a**	76 (72) [i]	18 (40) [i]

[a] Unless otherwise specified, all reactions were performed with 20 mol% of (*S*)-VAPOL-$B(OPh)_3$ catalyst with 0.50 mmol amine **126** (1.0 equiv, 0.1 M in toluene), 0.50 mmol aldehyde **127** (1.0 equiv) and 0.50 mmol of isocyanide **368** (1.0 equiv) at room temperature for 24 h. The (*S*)-VAPOL-$B(OPh)_3$ catalyst was prepared by heating 1 equiv of (*S*)-VAPOL, 4 equiv of $B(OPh)_3$ and 1 equiv of H_2O in toluene at 80 °C for 1 h, followed by removing all volatiles under high vacuum (0.1 mm Hg) for 0.5 h at 80 °C. [b] Isolated Yield. [c] Determined

Table 6.8 cont'd

by HPLC. [d] Reaction performed with pre-formed imines **78a** and **111a**. [d] 0.50 mmol of acid **334b** also added to the reaction mixture; same as entry 7 of Table 6.7. [g] Yield/ee in parenthesis is given for the reaction performed in presence of 4 Å MS. [f] Ratio of **126**:**127**:**368** = 2:1:1.5. Reactions were performed by Li Huang. [h] Yield/ee in parenthesis is given for the reaction performed in presence of 3 Å MS. [i] Yield/ee is given for the reaction where the catalyst was prepared by 1 equiv of (*S*)-VAPOL, 3 equiv of BH_3•Me_2S, 2 equiv of phenol and 3 equiv of H_2O in toluene at 100 °C for 1 h, followed by removing all volatiles under high vacuum (0.1 mm Hg) for 0.5 h at 100 °C. Yield/ee in parenthesis is given for the reaction where 2 equiv of 2,4,6-Me_3-C_6H_2OH is used for the catalyst preparation.

While the current work was in progress, List and co-workers reported an example of a catalytic achiral three-component Ugi-type reaction between an amine **126**, aldehyde **127** and isocyanide **368**.[27] Although *p*-methoxyaniline was their optimized amine, they did screen benzhydryl amine **126c** to afford **373b** in 36% yield when benzaldehyde **127a** and *tert*-butyl isocyanide **368a** were used as the other components (Scheme 6.12). However, they were able to obtain an asymmetric induction up to 18% only when they utilized 3,3′-TRIP-BINOL-PO_3H **376**.[27]

Scheme 6.12 Catalytic Ugi-type three-component reaction.[27]

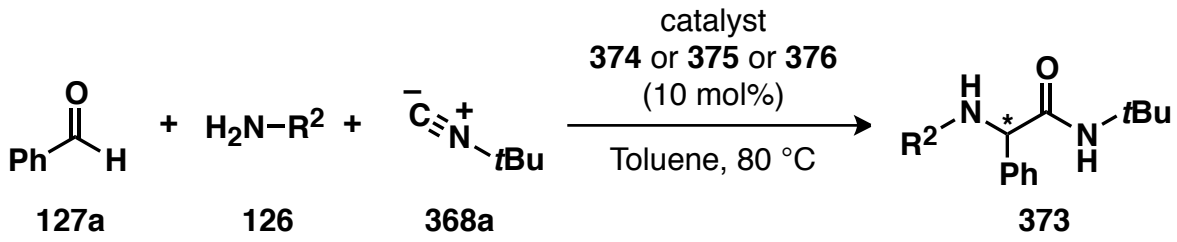

127a **126** **368a** **373**

Scheme 6.12 cont'd

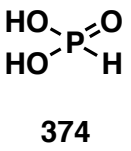

374

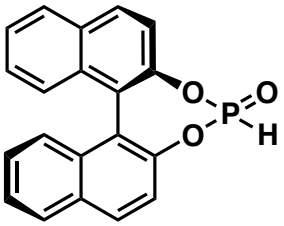

375

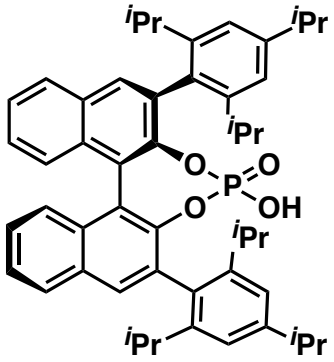

376

R^2	catalyst	% yield	% ee
$PhCH_2$	**374**	42	–
Ph_2CH	**374**	36	–
4-MeO-C_6H_4	**374**	91	–
4-MeO-C_6H_4	**375**	90	04
4-MeO-C_6H_4	**376**	15	18

The work reported by List and coworkers prompted us to screen our proposed Ugi-2CR reaction as a Ugi-3CR reaction starting from an amine and an aldehyde instead of an imine. This was important, as water is ostensibly needed as the nucleophile to attack the nitrilium ion. However, no desired product **371a** was obtained even when the reaction was done in a multicomponent fashion (Table 6.8, entry 5). To our surprise and delight, Li Huang, a former group member, was able to obtain the α-amino amide **372a** when a secondary amine **126h** was used instead of a primary amine (entries 6-7).[28] However, the asymmetric induction was found only to be 18%. After a lot of initial optimization, an improved result of 40% ee was obtained. Based on the failure of the reaction with a primary amine and success with secondary amine, a mechanism involving an aminal intermediate has been proposed. A detailed discussion can be found in Li Huang's dissertation.[29] It must be noted that there are some secondary amine related

Ugi-type three-component reactions in both racemic[30] and asymmetric[31] forms reported prior to List's work. Recently, Maruoka and coworkers reported a catalytic asymmetric Ugi-type reaction involving azomethine imines.[32]

6.5 Attempts towards catalytic asymmetric Passerini reaction

One of the early examples of a multicomponent reaction is the Passerini reaction.[33] It is a three-component reaction involving an aldehyde, acid and an isocyanide resulting in the formation of the acyloxycarboxamides (Scheme 6.13X). Apart from diastereoselective Passerini reactions, there have been few reports of asymmetric versions of this reaction.[34] A few of Passerini-type reactions have also been reported where the acid component has either been left out[35] or been replaced by acids other than carboxylic acids.[36] Prior to the work reported by Wang and and co-workers,[34c] all the reported examples needed an aldehyde with at least one chelating site. Hence, it was then thought to examine VAPOL phosphoric acids to find a general asymmetric Passerini reaction. The reaction involving benzaldehyde **127a**, benzoic acid **334a** and *tert*-butyl isocyanide **368a** afforded acyloxycarboxamide **377a** in 35% yield and 6% ee (Scheme 6.13Y). Due to time constraints, this reaction was not studied further.

Scheme 6.13 (**X**) Passerini reaction (**Y**) Attempts towards the asymmetric Passerini reaction.

X

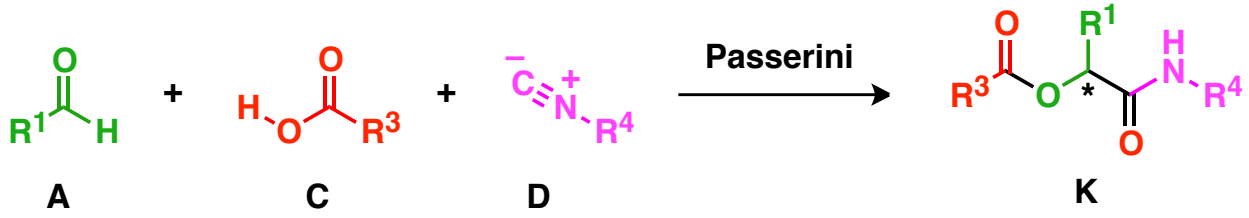

Scheme 6.12 cont'd

Y

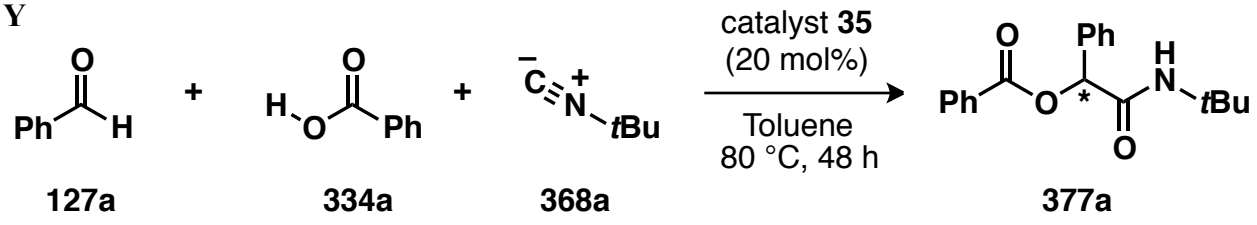

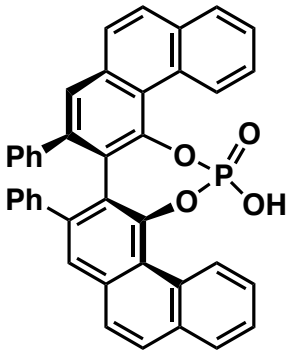

35
(*S*)-VAPOL-PO_3H

6.6 Attempts towards kinetic resolution of imines

Up to this point, we have performed the aziridination reaction between imines derived from achiral amines and EDA **85** using IMINO-BOROX catalysts. It would be interesting to see the effect of chiral imines on the catalytic asymmetric aziridination reaction. The reaction with chiral imines would present an opportunity for the matched and mismatched cases. Chiral imines can be prepared either by using chiral aldehydes with achiral amines or by using chiral amines and achiral aldehydes. The former case has been examined by a current group member namely Munmun Mukherjee and she found that the reaction is primarily a catalyst controlled reaction.[37] The latter study had been initiated by Dr. Yu Zhang, a former group member, and was studied in detail by another former group member, namely Li Huang.[38] During the studies of aziridination reaction performed with chiral imine (*S*)-**378**, Dr. Yu Zhang found a strong matched and mismatched case depending upon the ligand used (Table 6.9).[38] As shown in Table

6.9, the matched case is where the (*S*)-enantiomer of the imine is matched with the (*R*)-enantiomer of the ligand (R with S and S with R). Only a single diastereomer **380** was obtained in the matched case. For the mismatched case, the diastereomeric ratio was found to be 69:31 and 52:48 in the case of the VAPOL and VANOL catalysts, respectively. Nonetheless, the presence of such a strong matched case prompted us to examine this reaction in more detail as it might provide an access to chiral imines/amines *via* possible kinetic resolution of racemic imines/amines.

Table 6.9 Matched and mis-matched aziridinations of the phenylneopentyl imine (*S*)-**378**. [a]

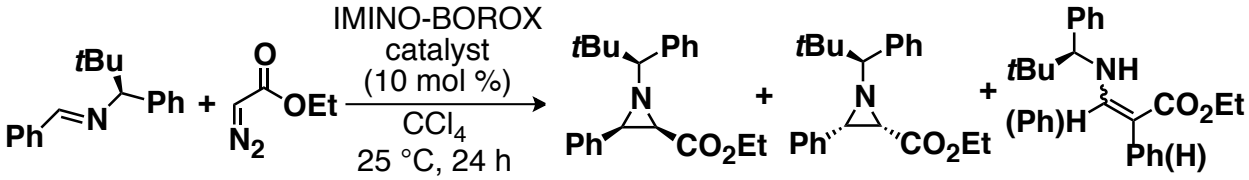

(S)-**378** **85** **379** **380** **381(382)**

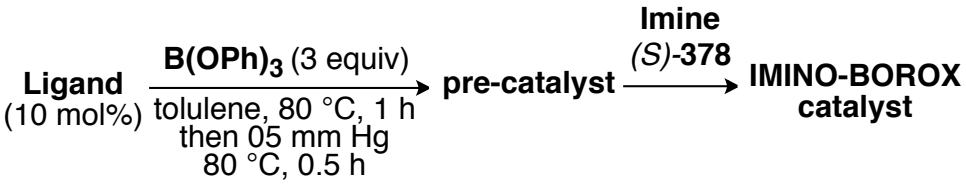

#	Ligand	**379** : **380** [b]	Yield **379** (%) [c]	Yield **380** (%) [d]	Enamines (%) [d]
1	(*S*)-VAPOL	69 : 31	56	25	nd
2	(*R*)-VAPOL	<2 : 98	<2 [d]	80 [c]	<2
3	(*S*)-VANOL	52 : 48	36	33	11/2
4	(*R*)-VAPOL	<2 : 98	<2 [d]	85 [c]	<2
5	$B(OPh)_3$ only	8 : 92	nd	nd	nd

[a] This set of data is taken from thesis of Dr. Yu Zhang. Unless otherwise specified, all reactions were performed with 10 mol% of IMINO-BOROX catalyst with 1 mmol imine (*S*)-**378** (1.0 equiv, 0.5 M in toluene) and 1.1 mmol of EDA **85** (1.1 equiv) at room temperature for 24 h. The pre-catalyst catalyst was prepared by heating 1 equiv of ligand and 3 equiv of $B(OPh)_3$ in toluene at 80 °C for 1 h, followed by removing all volatiles under high vacuum (0.1 mm Hg) for 0.5 h at 80 °C. nd = not determined. The *cis:trans* selectivity was >50:1 in all cases. [b] Determined from the ^{1}H NMR spectrum of the crude reaction mixture. [c] Isolated Yield. [d] Yield from ^{1}H NMR spectrum of the crude reaction mixture and based on the isolated yield of **379** or **380**.

There are not many methods available for kinetic resolution of amines. Most of the methods are based on the utilization of the enzymes.[39] In terms of asymmetric methods using catalysts other than enzymes, the normal practice is the selective derivatization of the amines, usually by an acetyl-transfer reagent.[40] Based on the results obtained from diastereoselective aziridination reaction, it was envisioned that a protocol for kinetic resolution of imines could possibly be developed. Hence it was then proposed that the reaction between racemic imine *rac*-**378** and a substoichiometric amount of EDA, in presence of catalyst derived from (*S*)-ligand, would lead to the chiral aziridine *ent*-**380** and chiral amine (*S*)-**384** after the hydrolysis of the unreacted imine (*S*)-**378** (Scheme 6.14A). Hence, the experiments related to the proposed kinetic resolution were performed and presented in Table 6.10 and 6.11. The *s*-factor was calculated based on the equation given in Scheme 6.14B. The *s*-factor is equal to the ratio of the rate of faster reacting enantiomer and the rate of slower reacting enantiomer.[41]

Scheme 6.14 (**A**) Proposed Kinetic resolution of imine *rac*-**378**. (**B**) Equation for the calculation of *s* factor.

A

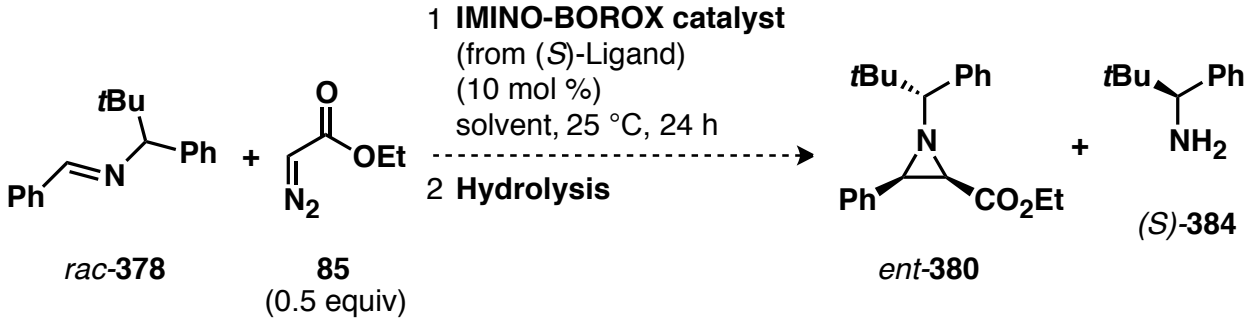

Scheme 6.14 cont'd

B

$$s = \frac{\ln [(1-C)(1- ee_{SM})]}{\ln [(1-C)(1+ ee_{SM})]}$$

$$C = ee_{SM} / ee_{SM} + ee_{P}$$

ee_{SM} = ee of the unreacted starting material

ee_{P} = ee of the product formed

In the first experiment, the reaction between *rac*-**378** and 0.5 equiv of EDA afforded the chiral aziridine *ent*-**380** in 33% yield and 94% ee (Table 6.10, entry 2). The diastereomeric ratio of *ent*-**380**:**379** was found to be 20:1. Subsequent hydrolysis of the unreacted imine (*S*)-**378** by dilute HCl resulted in chiral amine (*S*)-**384** in 34% yield and 66% ee (Table 6.10, entry 2). The *s*-factor calculated according to equation in Scheme 6.14B is 43 (C = Conv = 42). The observed ee of the amine (*S*)-**384** was moderate and was found to be directly proportional to the amount of the EDA used (Table 6.10, entries 1-3). However, the yield of (*S*)-**384** was substantially decreased as the equiv of EDA was increased. However, this survey was conducted with carbon tetrachloride as solvent. Since we have subsequently found that toluene is in many respects superior to carbon tetrachloride for the AZ reaction,[9a] we decided to re-examine the possibility of kinetic resolution where toluene as the solvent. Also, we decided to protect the resultant amine (*S*)-**384** with Boc_2O in order to avoid any loss in the yield during the isolation of the amine.[42]

Table 6.10 Kinetic resolution of phenylneopentyl imine *rac*-**378** furnishing amine *(S)*-**384**. [a]

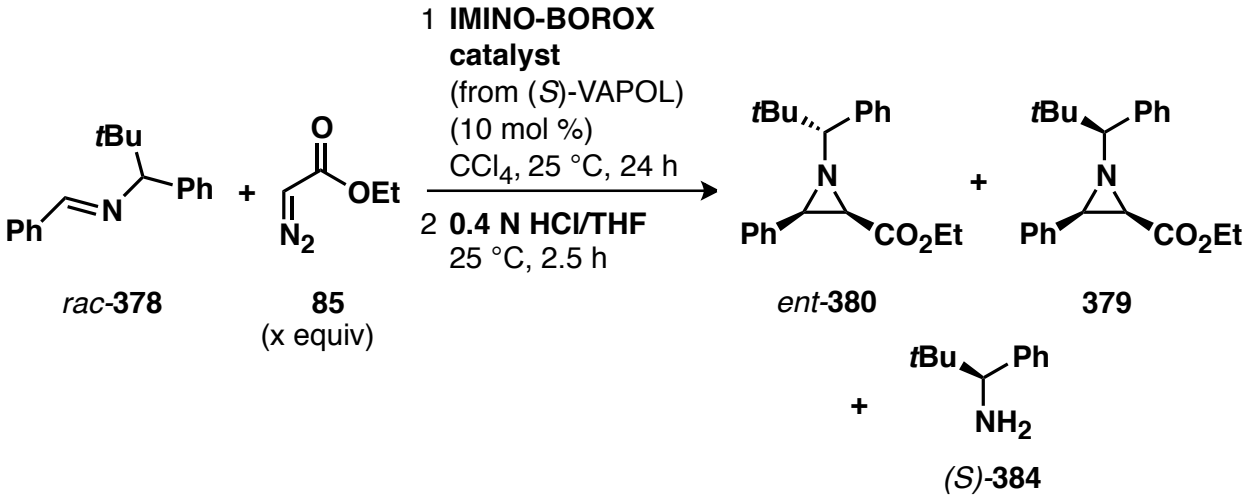

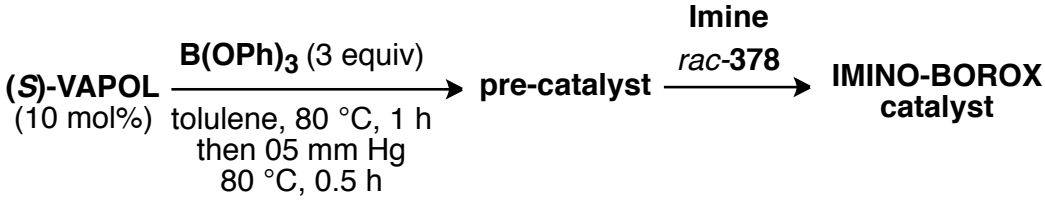

#	EDA (x equiv)	Conv [b]	Yield *ent*-**380** (%) [c]	ee *ent*-**380** (%) [d]	Yield **384** (%) [c]	ee **384** (%) [d]	*ent*-**380**:**379** [e]
1	0.4	32	30	94	38	48	50:1
2	0.5	50	33	94	34	66	20:1
3	0.6	51	41	94	26	80	13:1

[a] Unless otherwise specified, all reactions were performed with 10 mol% of IMINO-BOROX catalyst (derived from (*S*)-VAPOL) with 1 mmol imine *rac*-**378** (1.0 equiv, 0.5 M in toluene) and x mmol of EDA **85** (x equiv) at room temperature for 24 h. The pre-catalyst catalyst was prepared by heating 1 equiv of ligand and 3 equiv of $B(OPh)_3$ in toluene at 80 °C for 1 h, followed by removing all volatiles under high vacuum (0.1 mm Hg) for 0.5 h at 80 °C. [b] Percent conversion is determined by integration of the methine proton of *cis*-aziridine relative to the sp^2-CH proton of the unreacted imine *rac*-**378** in the ^{1}H NMR spectrum of the crude reaction mixture. [c] Isolated yield after chromatography on silica gel. [d] Determined by HPLC. [e] Determined from the ^{1}H NMR spectrum of the crude reaction mixture.

As discussed earlier, the AZ reaction was performed in toluene with 0.5 equiv of EDA and it resulted in chiral aziridine *ent*-**380** in 35% yield and 97% ee (Table 6.11, entry2). The diastereomeric ratio of *ent*-**380**:**379** was found to be 10:1 which is a little lower than in CCl_4 (Table 6.10). After hydrolysis of imine (*S*)-**378** and subsequent protection of the resulting amine, the Boc protected amine (*S*)-**385** was obtained in 44% yield and 54% ee (Table 6.11, entry 2). The *s*-factor calculated according to equation in Scheme 6.14B is 84 (C = Conv = 36). Although a high *s*-factor was observed in this case, the overall trend is similar to that in Table 6.10, i.e. the ee of the amine (*S*)-**385** was moderate and directly proportional to the amount of the EDA used (Table 6.11, entries 1-4). It must be pointed out that the isolation of amine after boc protection has greatly simplified the analysis and no column chromatography is needed, as the resulting amine is quite pure. Hence, this project needs a little more optimization in order to increase the enantioselectivity of the amine (*S*)-**385**.

Table 6.11 Kinetic resolution of phenylneopentyl imine *rac*-**378** furnishing amine *(S)*-**385**. [a]

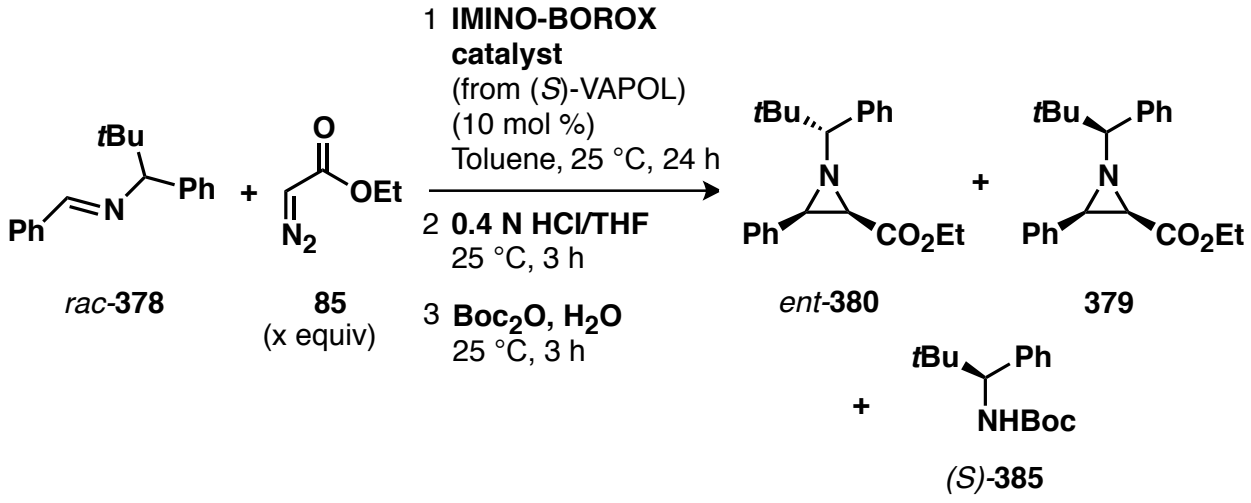

Table 6.11 cont'd

#	EDA (x equiv)	Conv [b]	Yield *ent*-**380** (%) [c]	ee *ent*-**380** (%) [d]	Yield **385** (%) [e]	ee **385** (%) [d]	*ent*-**380**:**377** [f]
1	0.4	36	28	97	54	43	10:1
2	0.5	44	35	97	44	54	10:1
3	0.6	54	45	96	34 (32)	77	10:1
4	0.7	61	50	97	26	89	8:1

[a] Unless otherwise specified, all reactions were performed with 10 mol% of IMINO-BOROX catalyst (derived from (*S*)-VAPOL) with 1 mmol imine *rac*-**378** (1.0 equiv, 0.5 M in toluene) and x mmol of EDA **85** (x equiv) at room temperature for 24 h. The pre-catalyst catalyst was prepared by heating 1 equiv of ligand and 4 equiv of $B(OPh)_3$ and 1 equiv of H_2O in toluene at 80 °C for 1 h, followed by removing all volatiles under high vacuum (0.1 mm Hg) for 0.5 h at 80 °C. [b] Percent conversion is determined by integration of the methine proton of *cis*-aziridine relative to the sp^2-CH proton of the unreacted imine *rac*-**378** in the ^{1}H NMR spectrum of the crude reaction mixture. [c] Isolated yield after chromatography on silica gel. [d] Determined by HPLC. [e] Isolated yield after purification by extraction. Yield in parenthesis is the isolated yield after purification by chromatography on silica gel. [f] Determined from the ^{1}H NMR spectrum of the crude reaction mixture.

6.7 Conclusions

The present chapter includes some failed and some successful catalytic asymmetric reactions. Nonetheless, this chapter serves as the stepping-stone towards the broadening of the scope of the unique BOROX catalysis developed in the Wulff group. Hopefully, reactions like [3+2] cycloadditions, Ugi-type reactions and kinetic resolution of imines will be developed in near future and thereby expanding the breath of our catalyst system. Additionally, two more reactions have been developed using the indirect IMINO-BOROX catalysis and SULFOX-BOROX catalysis respectively and these are the first true multicomponent aziridination reaction (Chapter 7) and the asymmetric epoxidation of aldehydes (Chapter 8)

APPENDIX

6.8 Experimental

6.8.1 General Information

Same as Chapter 2

6.8.2 Synthesis of amines 126b and *rac*-384 and imines 110a-w, 111a, 333o, 358a, 359a and *rac*-378

a) Synthesis of DAM amine 126b

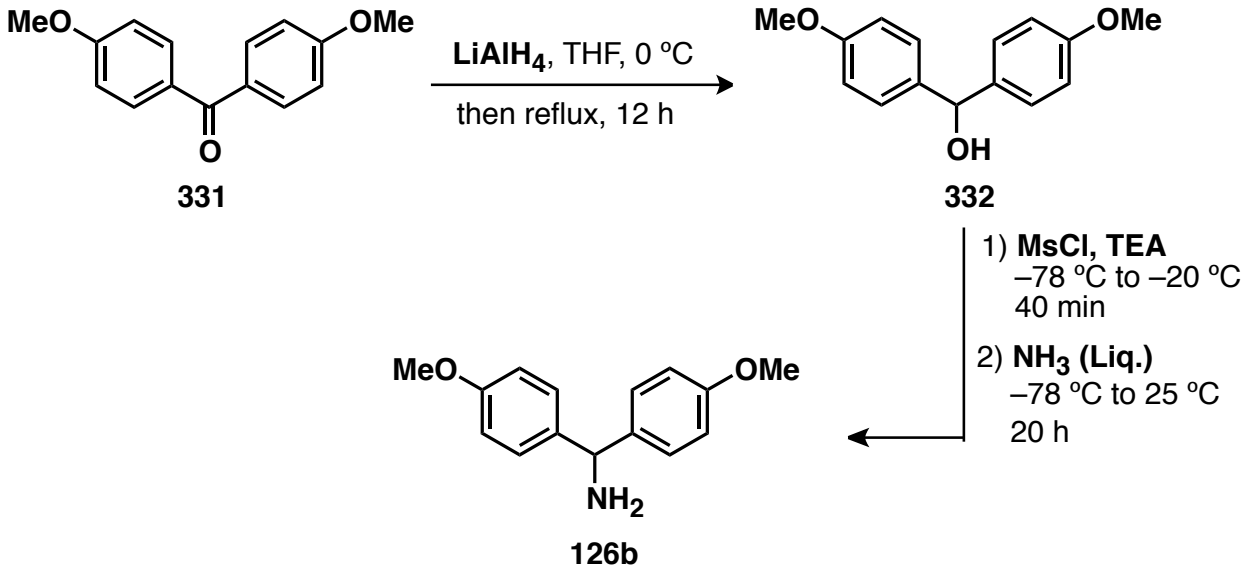

***Bis*(4-methoxyphenyl)methanol 332:** To a 500 mL flame-dried round bottom flask filled with argon was added $LiAlH_4$ (3.3 g, 88 mmol) and dried THF (250 mL) in an ice bath followed by stirring for 1 h. Simultaneously, 4,4'-dimethoxyl benzophenone **331** (19.4g, 80.0 mmol) and dried THF (350 mL) was added in a separate 1000 mL flame-dried round bottom flask filled with argon at 0 ºC. $LiAlH_4$ solution has been transferred to the ketone solution *via* cannula under the argon pressure. The flask containing $LiAlH_4$ solution was washed with dry THF (25 mL × 2). The reaction mixture was stirred at room temperature for 4 h followed by reflux for 12 h. The

reaction was cooled to room temperature and then to 0 ºC. To the reaction mixture was added dropwise H_2O (3.5 mL), 4 N NaOH (3.5 mL) and H_2O (8.8 mL). The reaction mixture was further diluted by adding Et_2O (300 mL). The reaction mixture was then filtered through Celite and the Celite bed was washed with CH_2Cl_2 (10 mL × 3). The filtrate was dried using anhydrous $MgSO_4$, filtered and concentrated *in vacuo* to afford the crude alcohol. Purification by silica gel chromatography (1:2 EtOAc/hexanes as eluent) afforded **332** as white solid (mp. 69-70 ºC) in 95% yield (18.6 g, 76.0 mmol).

Spectral data for **332:** R_f = 0.42 (1:3 EtOAc/hexanes); ^{1}H NMR ($CDCl_3$, 300 MHz) δ 2.08 (d, 1H, J = 2.3 Hz), 3.76 (s, 6H), 5.76 (d, 1H, J = 2.3 Hz), 6.84 (d, 4H, J = 9.0 Hz), 7.25 (d, 4H, J = 8.8 Hz); ^{13}C ($CDCl_3$, 75 MHz) δ 55.22, 75.30, 113.79, 127.76, 136.47, 158.91. These spectral data match those previously reported for this compound.[43]

***Bis*(4-methoxyphenyl)methylamine 126b:** To a 500 mL flame-dried three-neck round bottom flask equipped with a condenser filled with argon was added 4,4'-dimethoxybenzhydrol **332** (19.1 g, 78.2 mmol) and THF (250 mL). Et_3N (10.3 g, 101.7 mmol) was added dropwise at –78 °C followed by dropwise addition of mesylchloride (11.62 g, 101.7 mmol) *via* syringe with vigorous stirring. The mixture was warmed up to –20 ºC and stirred for 40 min at this temperature, then cooled to –78 ºC. Gaseous ammonia was introduced at a rate such that a dry-ice cooled condenser provided steady drop-wise addition of liquid NH_3 and this addition was continued for a period of 20 min. The reaction mixture was allowed to warm gradually to

ambient temperature after which it was stirred for an additional 20 h. The reaction was quenched by the addition of concentrated NH_4OH (200 mL) then extracted with EtOAc (100 mL × 3). The combined organic layer was dried over anhydrous $MgSO_4$ and concentrated *in vacuo* to afford crude amine as a white solid. The amine **126b** was purified by chromatography on a column (65 mm × 400 mm, with pre-neutralized (2% Et_3N) silica gel, 1:1 EtOAc/hexanes as eluent). An initial band containing a yellow impurity along with a small amount of alcohol **332** was discarded and elution continued to give the product **126b** as white solid (mp. 60-61ºC) in 79% yield (15 g, 62 mmol).

Spectral data for **126b:** R_f = 0.17 (1:1 hexanes/EtOAc). ^{1}H NMR ($CDCl_3$, 300 MHz) δ 1.78 (br s, 2H), 3.82 (s, 6H), 5.18 (s, 1H), 6.90 (d, 4H, J = 8.8 Hz), 7.33 (d, 4H, J = 8.5 Hz); ^{13}C ($CDCl_3$, 75 MHz) δ 55.14, 58.39, 113.67, 127.74, 138.11, 158.35. These spectral data match those previously reported for this compound.[11]

b) Synthesis of amine *rac*-384

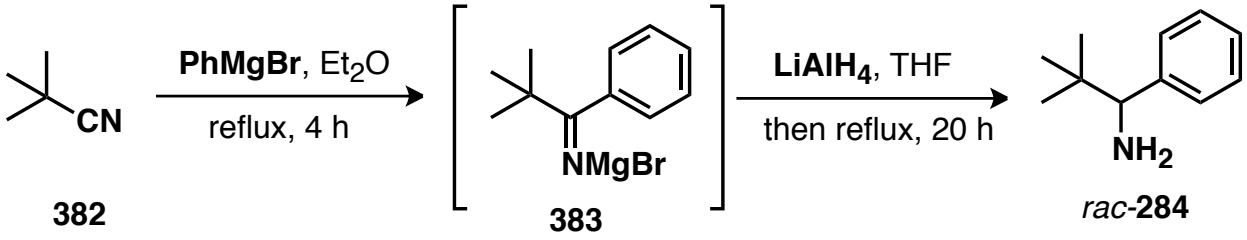

382 **383** ***rac*-284**

α-*tert*-butylbenzylamine *rac*-384: To a 250 mL flamed-dried three-neck round bottom flask filled with argon was added PhMgBr **309** (20 mL, 60 mmol, 3M in Et_2O) and dry Et_2O (40 mL) via syringe. Trimethyl acetonitrile **382** (4.24 g, 50.0 mmol) was added to the flask drop-wise via

syringe with the stirring of the Grignard reagent. The solution was the heated to reflux after addition was complete. After 4 h, a solution of $LiAlH_4$ (2.4 g, 60.0 mmol) in dry THF (40 mL) was transferred to the reaction flask via cannula. The solution was then heated and refluxed for another 20 h. After 20 h, the solution was allowed to cool to room temperature. To the flask was carefully added H_2O (2.5 mL), 20% NaOH solution (2.5 mL) and then H_2O (7.5 mL) in an ice bath. The white mud-like mixture was then filtered, the residue was washed with Et_2O until there was no presence of detectable amine in the filtered Et_2O (monitored by TLC spotting). The ether layer was dried over anhydrous Na_2SO_4. It was then filtered and concentrated *in vacuo* to give a light yellow liquid as the crude product. Purification by distillation furnished *rac*-**384** (bp. 47 – 48 °C at 0.15 mm Hg) as a colorless oil in 80% yield (6.53 g, 40 mmol).

Spectral data for *rac*-**384:** ^{1}H NMR ($CDCl_3$, 300 MHz) δ 10.89 (s, 9H), 1,42 (brs, 2H), 3.69 (s, 1H), 7.20-7.29 (m, 5H); ^{13}C NMR ($CDCl_3$, 75 MHz) δ 26.42, 34.89, 65.20, 126.60, 127.37, 128.13, 143.68. These spectral data match those previously reported for this compound.[44]

c) Synthesis of imines 110a-w, 111a, 333o, 358a, 359a and *rac*-378

All liquid aldehydes were distilled before use and the solid aldehydes were used as purchased from Aldrich.

General Procedure for the synthesis of aldimines – Illustrated for the synthesis of *N*-benzylidene-bis-(4-methoxyphenyl)methylamine 110a.

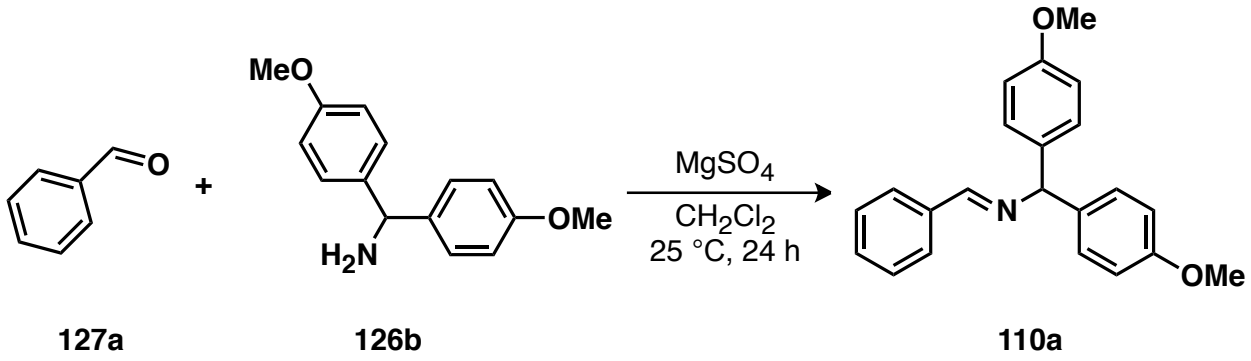

127a **126b** **110a**

***N*-benzylidene-bis-(4-methoxyphenyl)methylamine 110a:** To a 50 mL flame-dried round bottom flask filled with argon was added DAM amine **126b** (2.43 g, 10.00 mmol), $MgSO_4$ (2.0 g, 16.7 mmol, freshly flame-dried) and dry CH_2Cl_2 (30 mL). After stirring for 10 min, benzaldehyde **127a** (1.07 g, 10.1 mmol, 1.01 equiv) was added. The reaction mixture was stirred at room temperature for 24 h. The reaction mixture was filtered through Celite and the Celite bed was washed with CH_2Cl_2 (10 mL × 3) and then the filtrate was concentrated by rotary evaporation to give the crude imine as an off-white solid. Crystallization (1:25 CH_2Cl_2/hexanes) and collection of the first crop afforded **110a** as white solid crystals (mp. 60-61 °C) in 91% isolated yield (3.02 g, 9.1 mmol).

Spectral data for **110a**: ^{1}H NMR ($CDCl_3$, 300 MHz) δ 3.76 (s, 6H), 5.51(s, 1H), 6.84 (d, 4H, J = 8.8 Hz), 7.25-7.27 (m, 4H), 7.37-7.40 (m, 3H), 7.79–7.82 (m, 2H), 8.37 (s, 1H); ^{13}C ($CDCl_3$, 75

MHz) δ 55.17, 76.55, 113.71, 128.35, 128.43, 128.61, 128.70, 130.60, 136.28, 158.43, 160.24. These spectral data match those previously reported for this compound.[11]

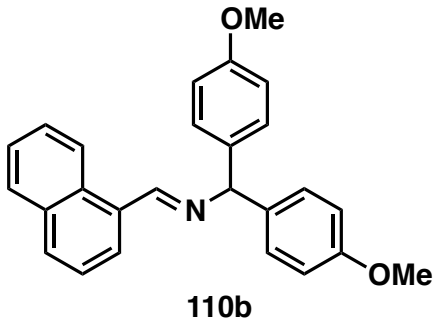

110b

***N*-(1-naphthylidene)-bis(4-methoxyphenyl)methylamine 110b:** Imine **110b** was prepared according to the procedure described above for imine **110a**. Crystallization (1:8 CH_2Cl_2/hexanes) and collection of the first crop afforded **110b** as white solid (mp. 92.5-93.5 ºC) in 82% isolated yield (3.12 g, 8.20 mmol).

Spectral data for **110b:** ^{1}H NMR ($CDCl_3$, 300 MHz) δ 3.77 (s, 6H), 5.60 (s, 1H), 6.86 (d, J = 8.8 Hz, 4H), 7.35 (d, J = 8.5 Hz, 4H), 7.47-7.58 (m, 3H), 7.85-7.95 (m, 3H), 9.02 (s, 1H), 9.09 (d, J = 8.5 Hz, 1H); ^{13}C ($CDCl_3$, 75 MHz) δ 55.20, 77.98, 113.79, 113.88, 124.68, 125.16, 125.98, 127.16, 128.56, 128.65, 128.74, 129.66, 131.10, 133.81, 136.48, 158.48, 160.35. These spectral data match those previously reported for this compound.[11]

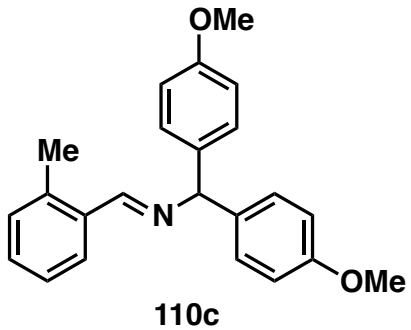

110c

***N*-(*o*-tolylbenzylidene)-bis(4-methoxyphenyl)methylamine 110c:** Imine **110c** was prepared according to the procedure described above for imine **110a**. Crystallization (1:8 CH_2Cl_2 / hexanes) and collection of the first crop afforded **110c** as white solid crystals (mp 64-65 ºC) in 80% isolated yield (2.76 g, 8.00 mmol).

Spectral data for **110c:** ^{1}H NMR ($CDCl_3$, 300 MHz) δ 2.55 (s, 3H), 3.78 (s, 6H), 5.53 (s, 1H), 6.88 (d, *J* = 8.8 Hz, 4H), 7.14-7.16 (m, 1H), 7.21-7.25 (m, 2H), 7.29 (d, *J* = 8.5 Hz, 4H), 7.95-7.98 (m, 1H), 8.72 (s, 1H); ^{13}C ($CDCl_3$, 75 MHz) δ 19.64, 55.21, 77.41, 113.73, 126.02, 128.28, 128.55, 130.15, 130.78, 134.22, 136.57, 137.79, 158.43, 159.09. These spectral data match those previously reported for this compound.[11]

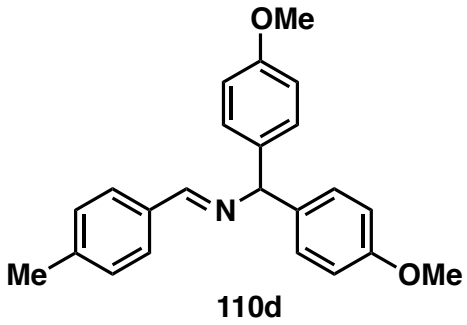

110d

***N*-(4-methylbenzylidene)-bis(4-methoxyphenyl) methyl amine 110d:** Imine **110d** was prepared according to the procedure described above for imine **110a**. Crystallization (1:5 CH_2Cl_2 / hexanes) and collection of the first crop afforded **110d** as white solid crystals (mp 110-111 ºC) in 94% isolated yield (3.24 g, 9.40 mmol).

Spectral data for **110d**: ^{1}H NMR ($CDCl_3$, 300 MHz) δ 2.36 (s, 3H), 3.76 (s, 6H), 5.50 (s, 1H), 6.84 (d, *J* = 8.8 Hz, 4H), 7.19 (d, *J* = 7.8 Hz, 2H), 7.28 (d, *J* = 8.3 Hz, 4H), 7.70 (d, *J* = 8.0 Hz, 2H), 8.34 (s, 1H); ^{13}C ($CDCl_3$, 75 MHz) δ 21.48, 55.24, 76.51, 113.76, 128.39, 128.69, 129.20, 133.85, 136.50, 140.89, 158.49, 160.19; IR (thin film, cm^{-1}) 2834 m, 1638 m, 1609 m, 1509 vs, 1246 vs, 1171 s, 1035 s, 815 w; Mass spectrum, *m/z* (% rel intensity) 345 M^+ (2), 227 (100), 212 (30), 169 (41), 141 (39), 115 (31). HRMS calcd for $C_{23}H_{24}NO_2$ (M+H) *m/z* 346.1807, mass 346.1816. These spectral data were not reported before.

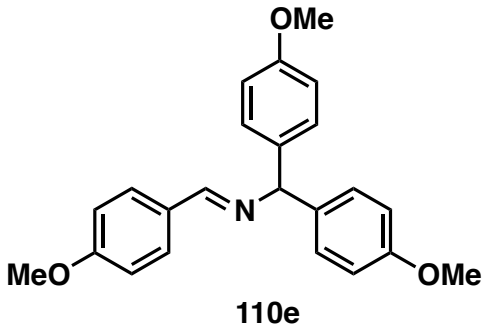

110e

***N*-(4-methoxybenzylidene)-bis(4-methoxyphenyl) methyl amine 110e:** Imine **110e** was prepared according to the procedure described above for imine **110a**. Crystallization (1:8 CH_2Cl_2/hexanes) and collection of the first crop afforded **110e** as white solid crystals (mp 129.5-130.5 ºC) in 92% isolated yield (3.32 g, 9.20 mmol).

Spectral data for **110e**: ^{1}H NMR ($CDCl_3$, 300 MHz) δ 3.76 (s, 6H), 3.81 (s, 3H), 5.47 (s, 1H), 6.83 (d, *J* = 8.8 Hz, 4H), 6.89 (d, *J* = 8.8 Hz, 2H), 7.25 (d, *J* = 8.5 Hz, 4H), 7.75 (d, *J* = 8.8 Hz, 2H), 8.29 (s, 1H); ^{13}C ($CDCl_3$, 75 MHz) δ 55.20, 55.29, 76.40, 113.68, 113.81, 128.47, 128.63, 129.92, 136.52, 158.37, 159.54, 161.30. These spectral data match those previously reported for this compound.[11]

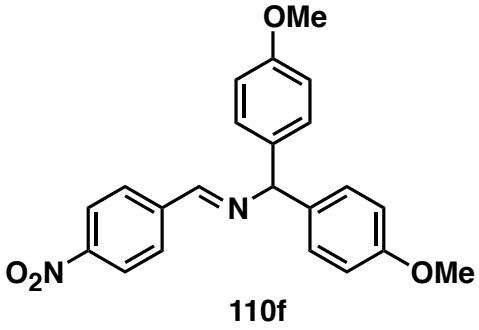

110f

***N*-(4-nitrobenzylidene)-bis(4-methoxyphenyl)methyl amine 110f**: Imine **110f** was prepared according to the procedure described above for imine **110a**. Crystallization (1:5 EtOAc/hexanes) and collection of the first crop afforded **110f** as a light yellow solid (mp 99-100 ºC) in 91% isolated yield (3.42 g, 9.10 mmol).

Spectral data for **110f:** ^{1}H NMR ($CDCl_3$, 300 MHz) δ 3.76 (s, 6H), 5.57 (s, 1H), 6.85 (d, *J* = 8.8 Hz, 4H), 7.26 (d, *J* = 8.8 Hz, 4H), 7.96 (d, *J* = 8.8 Hz, 2H), 8.24 (d, *J* = 8.8 Hz, 2H), 8.44 (s, 1H);

^{13}C ($CDCl_3$, 75 MHz) δ 55.19, 76.75, 113.84, 123.73, 128.55, 129.01, 135.52, 141.73, 148.95, 157.98, 158.65. These spectral data match those previously reported for this compound.[11]

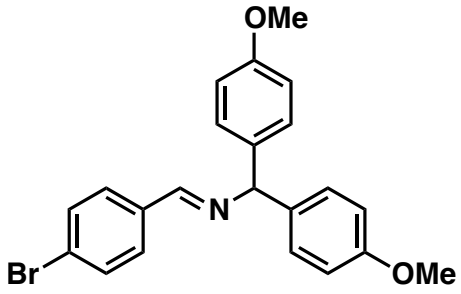

110g

***N*-(4-bromobenzylidene)-bis(4-methoxyphenyl)methyl amine 110g**: Imine **110g** was prepared according to the procedure described above for imine **110a**. Crystallization (1:10 CH_2Cl_2/ hexanes) and collection of the first crop afforded **110g** as white solid crystals (mp 125.5-126.5 ºC) in 85% isolated yield (3.49 g, 8.50 mmol).

Spectral data for **110g:** ^{1}H NMR ($CDCl_3$, 300 MHz) δ 3.76 (s, 6H), 5.51 (s, 1H), 6.85 (d, J = 8.8 Hz, 4H), 7.26 (d, J = 8.8 Hz, 4H), 7.52 (d, J = 8.3 Hz, 2H), 7.67 (d, J = 8.5 Hz, 2H), 8.31 (s, 1H); ^{13}C ($CDCl_3$, 75 MHz) δ 55.20, 76.56, 113.77, 125.02, 128.58, 129.78, 131.70, 135.20, 136.02, 158.51, 159.01. These spectral data match those previously reported for this compound.[11]

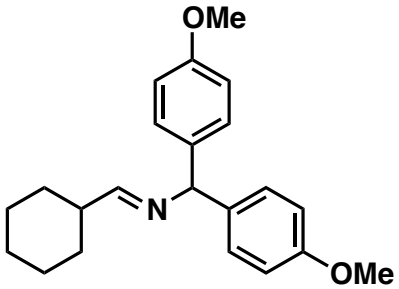

110v

***N*-cyclohexylmethylidene-bis(4-methoxyphenyl)methyl amine 110v:** Imine **110v** was prepared according to the procedure described above for imine **110a**. Crystallization (hexanes) and collection of the first crop afforded **110v** as white solid crystals (mp 77.5-78.5 ºC) in 84% isolated yield (2.83 g, 8.40 mmol).

Spectral data for **110v**: ^{1}H NMR ($CDCl_3$, 300 MHz) δ 1.25-1.37 (m, 6H), 1.68-1.90 (m, 4H), 2.31-2.33 (m, 1H), 3.82 (s, 6H), 5.27 (s, 1H), 6.87 (d, *J* = 8.8 Hz, 4H), 7.22 (d, *J* = 8.8 Hz, 4H), 7.68 (d, *J* = 5.1 Hz, 1H); ^{13}C ($CDCl_3$, 75 MHz) δ 25.34, 25.94, 29.67, 43.39, 55.09, 76.58, 113.58, 128.46, 136.39, 158.28, 168.48. These spectral data match those previously reported for this compound.[11]

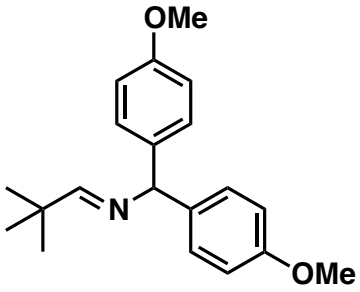

110w

***N-(*1,1-dimethylethylidene)-bis(4-methoxyphenyl)methylamine 110w:** Imine **110w** was prepared according to the procedure described above for imine **110a**. Crystallization (hexanes) and collection of the first crop afforded **110w** as white solid crystals (mp. 75.5-76.5 ºC) in 76% isolated yield (2.37 g, 7.60 mmol).

Spectral data for **110w**: ^{1}H NMR ($CDCl_3$, 300 MHz) δ 1.08 (s, 9H), 3.76 (s, 6H), 5.24 (s, 1H), 6.81 (d, *J* = 8.8 Hz, 4H), 7.18 (d, *J* = 8.8 Hz, 4H), 7.62 (s, 1H); ^{13}C ($CDCl_3$, 75 MHz) δ 26.94, 36.31, 55.16, 75.99, 113.59, 128.43, 136.70, 158.25, 171.09. These spectral data match those previously reported for this compound.[11]

Synthesis of imine 111a: See Chapter 2

Synthesis of imine 333o:

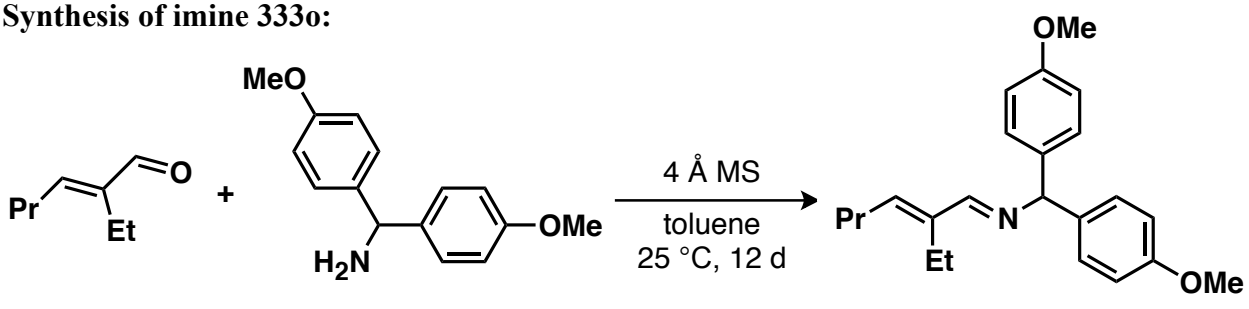

352b **126b** **333o**

(*E*)-*N*-((*E*)-2-ethylhex-2-en-1-ylidene)-1,1-bis(4-methoxyphenyl)methanamine 333o: To a 10 mL flame-dried round bottom flask filled with argon was added *bis*(4-methoxyphenyl)methylamine **126b** (243 mg, 1.00 mmol), 4Å MS (250 mg, freshly flame-dried) and dry toluene (1 mL). After stirring for 10 min, (*E*)-2-ethylhex-2-enal **352b** (126 mg, 1.05 mmol, purchased from Frinton Laboratories Inc.) was added. The reaction mixture was stirred at room temperature for 12 days. The resulting imine **333o** was used directly for the next step. A sample was isolated utilizing the filter syringe (Corning® syringe filters, Aldrich) in order to obtain spectral data.

Spectral data for **333o**: ^{1}H NMR ($CDCl_3$, 500 MHz) δ 0.92 (t, *J* = 7.0 Hz, 3H), 1.04 (t, *J* = 7.5 Hz, 3H), 1.43 (sextet, *J* = 7.0 Hz, 2H), 2.19 (q, *J* = 7.0 Hz, 2H), 2.45 (q, *J* = 7.0 Hz, 2H), 3.76 (s, 6H), 5.3 (s, 1H), 5.76 (t, *J* = 7.0 Hz, 3H), 6.82 (d, *J* = 7.5 Hz, 4H), 7.22 (d, *J* = 7.5 Hz, 2H), 7.82 (s, 1H); ^{13}C ($CDCl_3$, 125 MHz) δ 13.79, 13.86, 19.33, 22.45, 30.20, 55.14, 76.32, 113.63, 128.44, 137.08, 141.58, 142.34, 158.30, 163.79; HRMS (ESI-TOF) *m/z* 352.2273 [($M+H^+$); calcd. for $C_{23}H_{30}NO_2$: 352.2277]

Synthesis of imine 358a:

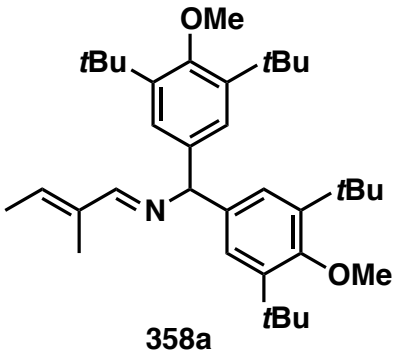

358a

(*E*)-1,1-bis(3,5-di-*tert*-butyl-4-methoxyphenyl)-*N*-((*E*)-2-methylbut-2-en-1-ylidene)methanamine 358a: Imine **358a** was prepared according to the procedure described above for imine **110a** except for the following differences: a) 1.5 equiv of

aldehyde **352a** used; b) the reaction was performed in benzene (40 mL). The reaction was monitored by ^{1}H NMR. Crystallization (hexanes) and collection of the first crop afforded **358a** as white solid crystals (mp. 131-132 ºC) in 80% isolated yield (4.27 g, 8.00 mmol).

Spectral data for **358a**: ^{1}H NMR ($CDCl_3$, 500 MHz) δ 1.39 (s, 36H), 1.85 (dd, *J* = 6.9, 1.0 Hz, 3H), 1.95 (t, *J* = 1.1 Hz, 3H), 3.67 (s, 6H), 5.28 (s, 1H), 5.96-6.00 (m, 1H), 7.17 (s, 4H), 7.99 (s, 1H); ^{13}C ($CDCl_3$, 125 MHz) δ 11.50, 14.20, 32.09, 35.76, 64.10, 77.55, 125.95, 135.96, 137.31, 138.02, 142.91, 158.11, 164.70; IR (thin film, cm^{-1}) 2961vs, 2870s, 1649m, 1628m, 1446m, 1412s, 1221s, 1115m; HRMS (ESI-TOF) *m/z* 534.4298 [($M+H^{+}$); calcd. for $C_{36}H_{56}NO_2$: 534.4311];

Synthesis of imine 359a:

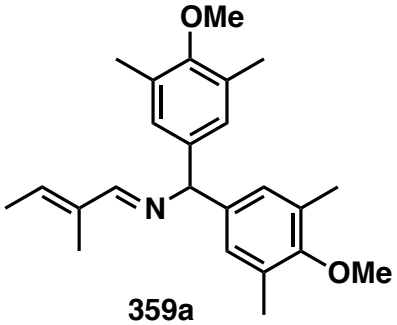

359a

(*E*)-1,1-bis(4-methoxy-3,5-dimethylphenyl)-*N*-((*E*)-2-methylbut-2-en-1-ylidene)methanamine 359a: Imine **359a** was prepared according to the procedure described above for imine **110a** except for the following differences: a) 1.5 equiv of aldehyde **352a** used; b) the reaction was performed in benzene (40 mL). The reaction was monitored by ^{1}H NMR. Crystallization (hexanes) and collection of the first crop afforded **359a** as white solid crystals (mp. 101-103 ºC) in 75% isolated yield (2.74 g, 7.50 mmol).

Spectral data for **359a**: ^{1}H NMR ($CDCl_3$, 500 MHz) δ 1.84 (dd, J = 6.9, 0.7 Hz, 3H), 1.96 (s, 3H), 2.27 (s, 12H), 3.70 (s, 6H), 5.20 (s, 1H), 5.93-5.97 (m, 1H), 6.98 (s, 4H), 7.91 (s, 1H); ^{13}C ($CDCl_3$, 125 MHz) δ 11.51, 14.15, 16.19, 59.56, (one sp^3 carbon not located), 127.76, 130.45, 136.22, 137.26, 139.72, 155.65, 164.68; IR (thin film, cm^{-1}) 2941vs, 2860s, 1645s, 1626vs, 1483vs, 1221s, 1144vs; HRMS (ESI-TOF) *m/z* 366.2439 [($M+H^+$); calcd. for $C_{24}H_{32}NO_2$: 366.2433];

Synthesis of imine *rac*-378:

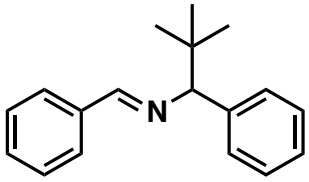

rac-**378**

***N*-benzylidene-2,2-dimethyl-1-phenylpropan-1-amine *rac*-378:** Imine *rac*-**378** was prepared according to the procedure described above for imine **110a**. Crystallization (hexanes) and collection of the first crop afforded *rac*-**378** as white solid crystals (mp. 69-70 ºC) in 80% isolated yield (2.01 g, 8.00 mmol).

Spectral data for *rac*-**378**: ^{1}H NMR ($CDCl_3$, 300 MHz) δ 0.94 (s, 9H), 3.93 (s, 1H), 7.18-7.43 (m, 8H), 7.75-7.78 (m, 2H), 8.23 (s, 1H); ^{13}C ($CDCl_3$, 75 MHz) δ 26.98, 35.73, 84.85, 126.58, 127.42, 128.21, 128.42, 128.87, 130.29, 136.68, 142.44, 159.27. These spectral data match those previously reported for the (*S*)-**378**.[38]

6.8.3 Different procedures for aziridination with imine 110g (*Table 6.1 and Scheme 6.2*)

Procedure II:

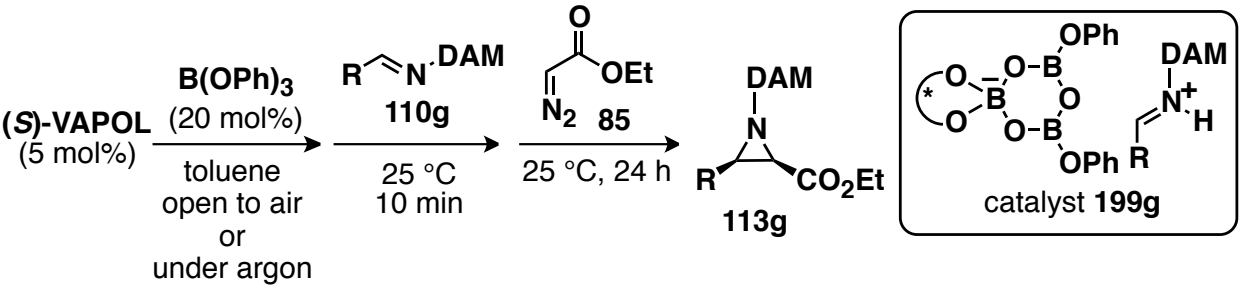

***(2R,3R)-Cis*-1-(*N*-1-bis(4-methoxyphenyl)methyl)-2-carboxyethyl-3-*p*-bromophenyl aziridine 113g:** To a 25 mL oven-dried round bottom flask was added (*S)*-VAPOL (13.5 mg, 0.025 mmol), $B(OPh)_3$ (29 mg, 0.1 mmol) and aldimine **110g** (205 mg, 0.5 mmol). The mixture was dissolved in toluene (1 mL) at room temperature. The reaction mixture was stirred for 5 min to give a light orange solution. To this solution was rapidly added EDA **85** (62 μL, 0.60 mmol) and the resulting mixture was stirred for 24 h at room temperature. The reaction was quenched by addition of 6 mL hexane. The reaction mixture was then transferred to a 100 mL round bottom flask. The reaction flask was rinsed twice with 5 mL of dichloromethane and the rinse was added to the 100 mL round bottom flask. The resulting solution was then concentrated *in vacuo* followed by exposure to high vacuum (0.05 mm Hg) for 5 min to afford the crude aziridine as an off-white solid. While the reaction gave 15% conversion with 5 mol% catalyst loading and open to air, 23% conversion was obtained when the reaction was performed under argon with 5 mol% catalyst loading. However, the reaction gave complete conversion using 10 mol% catalyst loading under argon.

The conversion was determined from the ^{1}H NMR spectrum of the crude reaction mixture by integration of the aziridine ring methine protons relative to either the imine methine proton or the proton on the imine carbon. The *cis/trans* ratio was determined by comparing the ^{1}H NMR integration of the ring methine protons for each aziridine in the crude reaction mixture. The *cis* (J = 7-8 Hz) and the *trans* (J = 2-3 Hz) coupling constants were used to differentiate the two isomers. The yields of the acyclic enamine side products **116g** and **117g** were determined by ^{1}H NMR analysis of the crude reaction mixture by integration of the *N*-H proton relative to the that of the *cis*-aziridine methine protons with the aid of the isolated yield of the *cis*-aziridine. Purification of the crude aziridine by silica gel chromatography (20 mm × 200 mm column, 9:1 hexanes/EtOAc as eluent, after elution of the first fraction, which contains EDA and / or enamine side products **116g** and **117g**, the eluent was changed to 5:1 hexanes / EtOAc) afforded pure aziridine **113g** as a white solid (mp. 49-50 ºC) in 90% isolated yield (223 mg, 0.45 mmol). *cis/trans*: 50:1. Enamine side products: <1 % yield of **116g** and < 1% yield of **117g**. The optical purity of **113g** was determined to be 97% ee by HPLC analysis (CHIRALPAK AD column, 90:10 hexane/*i*PrOH at 226nm, flow-rate: 1.0 mL/min). Retention times, R_t = 8.27 min (major enaniomer, **113g**) and R_t = 26.32 min (minor enantiomer, *ent*-**113g**).

Spectral data for **113g:** R_f = 0.25 (1:5 EtOAc/hexane); ^{1}H NMR ($CDCl_3$, 500 MHz) δ 1.00 (t, J = 7.1 Hz, 3H), 2.62 (d, J = 6.6 Hz, 1H), 3.07 (d, J = 6.6 Hz, 1H), 3.71 (s, 3H), 3.76 (s, 3H), 3.83 (s, 1H), 3.93 (q, J = 7.1 Hz, 2H), 6.76 (d, J = 8.3 Hz, 2H), 6.84 (d, J = 8.3 Hz, 2H), 7.25 (d, J = 8.8 Hz, 2H), 7.30 (d, J = 8.8 Hz, 2H), 7.35 (d, J = 8.3 Hz, 2H), 7.43 (d, J = 8.8 Hz, 2H); ^{13}C

($CDCl_3$, 75 MHz) δ 13.99, 46.46, 47.34, 55.12, 55.19, 60.68, 76.32, 113.82, 121.27, 128.08, 128.37, 129.54, 130.86, 134.16, 134.67, 134.88, 158.65, 158.75, 167.51 (one sp^2 carbon not located); $[\alpha]_D^{20}$ +15.0 (*c* 1.0, EtOAc) on 97% ee material (HPLC). These spectral data match those previously reported for this compound.[11]

Procedure II′:

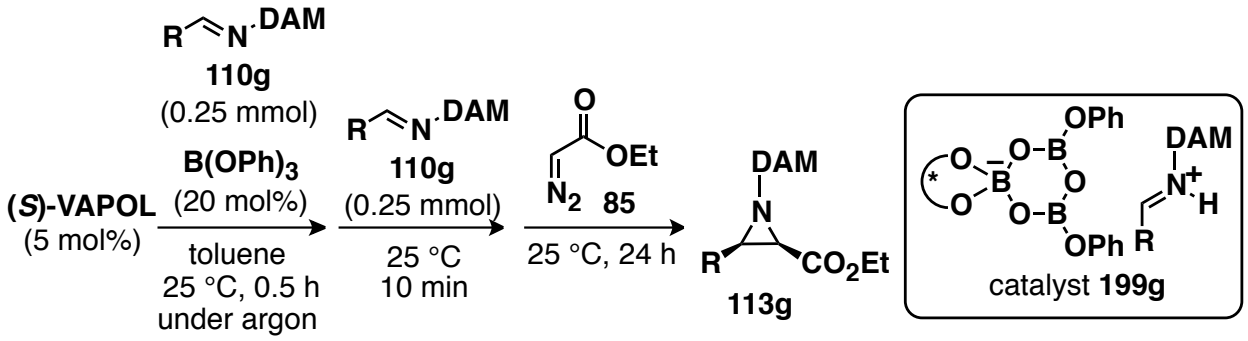

***(2R,3R)-Cis*-1-(*N*-1-bis(4-methoxyphenyl)methyl)-2-carboxyethyl-3-*p*-bromophenyl aziridine 113g:** To a 25 mL flame-dried Schlenk flask was added (*S*)-VAPOL (13.5mg, 0.025 mmol), $B(OPh)_3$ (29 mg, 0.1 mmol) and aldimine **110g** (102.5 mg, 0.25 mmol). The mixture was dissolved in dry toluene (0.5 mL) at room temperature. The reaction mixture was stirred for 0.5 h. To this solution was added aldimine **110g** (102.5 mg, 0.25 mmol) and dry toluene (0.5 mL) at room temperature. The reaction mixture was stirred for 5 min. To this solution was rapidly added EDA **85** (62 μL, 0.6 mmol) and the resulting mixture was stirred for 24 h at room temperature. The reaction was quenched by addition of 6 mL hexane. The reaction mixture was then transferred to a 100 mL round bottom flask. The reaction flask was rinsed twice with 5 mL of dichloromethane and the rinse was added to the 100 mL round bottom flask. The resulting

solution was then concentrated *in vacuo* followed by exposure to high vacuum (0.05 mm Hg) for 5 min to afford the crude aziridine as an off-white solid. The reaction gave 16 % conversion only.

Procedure IV:

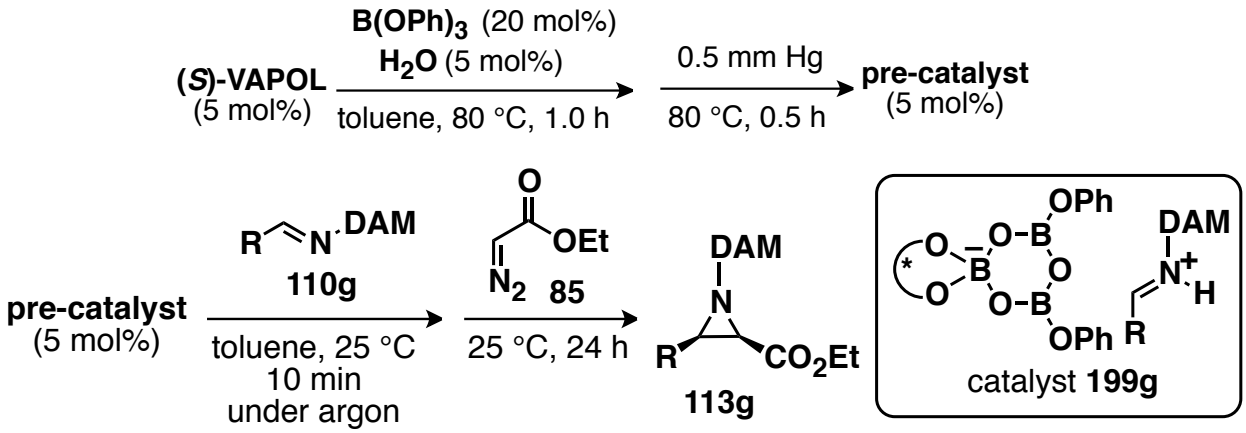

***(2R,3R)-Cis*-1-(*N*-1-bis(4-methoxyphenyl)methyl)-2-carboxyethyl-3-*p*-bromophenyl aziridine 113g:** To a 25 mL flame-dried Schlenk flask flushed with argon was added (*S*)-VAPOL (13.5 mg, 0.025 mmol) and $B(OPh)_3$ (29 mg, 0.1 mmol). Under an argon flow, dry toluene (2 mL) was added to dissolve the two reagents and this was followed by the addition of water (0.45 μL, 0.025 mmol). The flask was sealed, and then placed in an 80 ºC for 1 h. After 1 hour, a vacuum (0.5 mm Hg) was applied carefully to remove the volatiles. The vacuum is maintained for a period of 30 min at a temperature of 80 ºC. The flask was then filled with argon and the catalyst mixture was allowed to cool to room temperature.

To the flask containing the catalyst was first added the aldimine **110g** (205 mg, 0.50 mmol) and then dry toluene (1 mL). The reaction mixture was stirred for 5 min to give a light orange solution. To this solution was rapidly added EDA **85** (62 μL, 0.60 mmol) and the resulting mixture was stirred for 24 h at room temperature. Immediately upon addition of ethyl

diazoacetate the reaction mixture became an intense yellow and the formation bubbles from the release of nitrogen was noted. The reaction was quenched by addition of 6 mL hexane. The reaction mixture was then transferred to a 100 mL round bottom flask. The reaction flask was rinsed twice with 5 mL of dichloromethane and the rinse was added to the 100 mL round bottom flask. The resulting solution was then concentrated *in vacuo* followed by exposure to high vacuum (0.05 mm Hg) for 5 min to afford the crude aziridine as an off-white solid. The reaction resulted **113g** in 95% yield and 92% ee following the standard purification procedure.

Procedure V′:

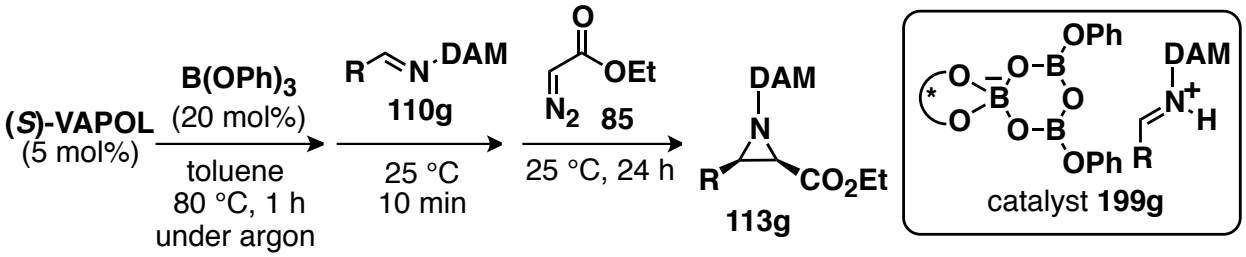

***(2R,3R)-Cis*-1-(*N*-1-bis(4-methoxyphenyl)methyl)-2-carboxyethyl-3-*p*-bromophenyl aziridine 113g:** To a 25 mL flame-dried Schlenk flask flushed with argon was added (*S*)-VAPOL (13.5 mg, 0.025 mmol) and $B(OPh)_3$ (29 mg, 0.1 mmol). Under an argon flow, dry toluene (0.5 mL) was added to dissolve the two reagents. The flask was sealed, and then placed in an 80 ºC for 1 h. The pre-catalyst mixture was then allowed to cool to room temperature and filled with argon. To the flask containing the pre-catalyst was first added the aldimine **110g** (205 mg, 0.5 mmol) and then dry toluene (0.5 mL). The reaction mixture was stirred for 5 min to give a light orange solution. To this solution was rapidly added EDA **85** (62 μL, 0.6 mmol) and the resulting mixture was stirred for 24 h at room temperature. The reaction was quenched by addition of 6 mL hexane. The reaction mixture was then transferred to a 100 mL round bottom

flask. The reaction flask was rinsed twice with 5 mL of dichloromethane and the rinse was added to the 100 mL round bottom flask. The resulting solution was then concentrated *in vacuo* followed by exposure to high vacuum (0.05 mm Hg) for 5 min to afford the crude aziridine as an off-white solid. The reaction gave 39 % conversion only.

Procedure V:

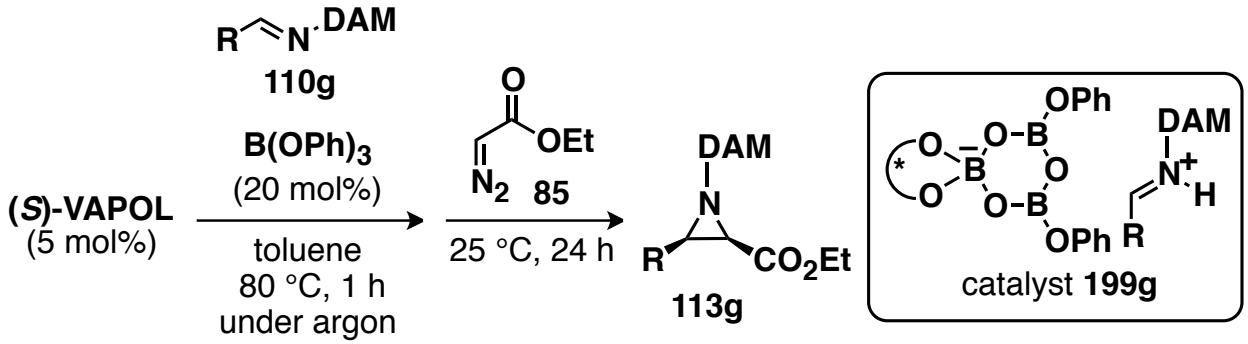

***(2R,3R)-Cis*-1-(*N*-1-bis(4-methoxyphenyl)methyl)-2-carboxyethyl-3-*p*-bromophenyl aziridine 113g**: To a 25 mL flame-dried Schlenk flask was added (*S)*-VAPOL (8 mg, 0.015 mmol), $B(OPh)_3$ (17.4 mg, 0.06 mmol) and aldimine **110g** (205 mg, 0.5 mmol). The mixture was dissolved in dry toluene (1 mL) at room temperature. The flask was sealed, and then placed in an 80 ºC for 1 h. The catalyst mixture was then allowed to cool to room temperature and filled with argon. To this solution was rapidly added EDA **85** (62 μL, 0.60 mmol) and the resulting mixture was stirred for 24 h at room temperature. The reaction was quenched by addition of 6 mL hexane. The reaction mixture was then transferred to a 100 mL round bottom flask. The reaction flask was rinsed twice with 5 mL of dichloromethane and the rinse was added to the 100 mL round bottom flask. The resulting solution was then concentrated *in vacuo* followed by exposure to high vacuum (0.05 mm Hg) for 5 min to afford the crude aziridine as an off-white

solid. The reaction resulted **113g** in 89% yield and 94% ee following the standard purification procedure.

6.8.4 Synthesis of aziridines 113g (*Table 6.2-6.3*)

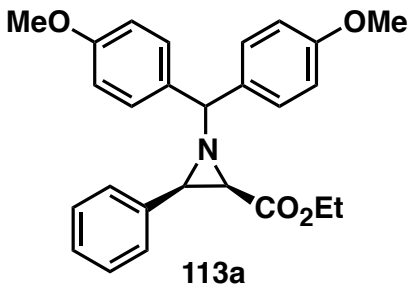

113a

***(2R,3R)-Cis*-1-(*N*-1-bis(4-methoxyphenyl)methyl)-2-carboxyethyl-3-phenylaziridine 113a**. Imine **110a** (166 mg, 0.500 mmol) was reacted according to the general procedure V described above with (*S*)-VAPOL as ligand. After purification, the product was afforded as white solid (mp 89-90 ºC) in 90% isolated yield (188 mg, 0.450 mmol) ; *cis/trans*: ≥ 50:1. Enamine side products: 2.7% yield of **116a** and 2.7% yield of **117a**. The optical purity of **113a** was determined to be 94% *ee* by HPLC analysis (CHIRALPAK AD column, 90:10 hexane/2-propanol at 226nm, flow-rate: 1.0 mL/min): retention times; R_t = 8.80 min (major enantiomer, **113a**) and R_t = 15.70 min (minor enantiomer, *ent*-**113a**)

Spectral data for **113a**: R_f = 0.28 (1:5 EtOAc/hexanes). ^{1}H NMR ($CDCl_3$, 500 MHz) δ 0.93 (t, 3H, *J* = 7.1 Hz), 2.59 (d, 1H, *J* = 6.8 Hz), 3.13 (d, 1H, *J* = 6.8 Hz), 3.67 (s, 3H), 3.75 (s, 3H), 3.81 (s, 1H), 3.91-3.98 (m, 2H), 6.74 (d, 2H, *J* = 8.8 Hz), 6.82 (d, 2H, *J* = 8.8 Hz), 7.14-7.24 (m, 3H), 7.31-7.35 (m, 4H), 7.43 (d, 2H, *J* = 8.8 Hz); ^{13}C ($CDCl_3$, 75 MHz) δ 13.94, 46.39, 48.02, 55.15, 55.22, 60.54, 76.44, 113.80, 127.27, 127.75, 127.79, 128.16, 128.49, 134.93, 135.13, 135.16, 158.61, 158.71, 167.83 (one sp^2 carbon not located); $[\alpha]_D^{20}$ +36.5 (*c* 1.0, EtOAc) on

94% ee material (HPLC). These spectral data match those previously reported for this compound.[11]

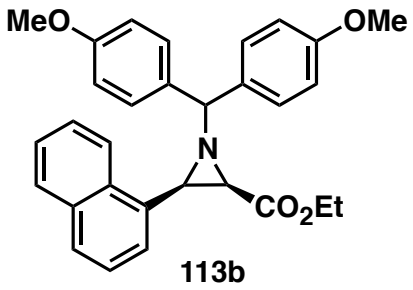

113b

***(2R,3R)-Cis*-1-(*N*-1-bis(4-methoxyphenyl)methyl)-2-carboxyethyl-3-1-naphthylaziridine 113b:** Imine **110b** (191 mg, 0.500 mmol) was reacted according to the general procedure V described above with (*S*)-VAPOL as ligand. After purification, the product was obtained as a white solid (mp. 154.5-155 ºC) in 80% isolated yield (187 mg, 0.4 mmol); *cis/trans*: ≥50:1. Enamine side products: 1.6% yield of **116b** and 1.6% yield of **117b**. The optical purity of **113b** was determined to be 98% ee by HPLC analysis (CHIRALPAK AD column, 90:10 hexane/*i*PrOH at 226nm, flow-rate: 1.0 mL/min); Retention times: R_t = 14.84 min (major enantiomer, **113b**) and R_t = 18.62 min (minor enantiomer, *ent*-**113b**).

Spectral data for **113b**: R_f = 0.22 (1:5 EtOAc/hexanes); ^{1}H NMR ($CDCl_3$, 300 MHz) δ 0.62 (t, 3H, *J* = 7.3 Hz), 2.88 (d, 1H, *J* = 6.8 Hz), 3.66 (d, 1H, *J* = 6.6 Hz), 3.72 (s, 3H), 3.70-3.74 (m, 2H), 3.78 (s, 3H), 3.99 (s, 1H), 6.81 (d, 2H, *J* = 8.5 Hz), 6.88 (d, 2H, *J* = 8.5 Hz), 7.35-7.47 (m, 5H), 7.53 (d, 2H, *J* = 8.8 Hz), 7.64-7.70 (m, 2H), 7.79 (d, 1H, *J* = 7.4 Hz), 8.09 (d, 1H, *J* = 7.7 Hz); ^{13}C ($CDCl_3$, 125 MHz) δ 13.57, 46.08, 46.40, 55.14, 55.21, 60.30, 76.72, 113.88, 113.91, 123.00, 125.33, 125.38, 125.79, 126.57, 127.54, 128.16, 128.49, 128.86, 130.71, 131.49, 133.09, 134.81, 135.17, 158.69, 158.94, 167.85; $[\alpha]_D^{20}$ +4.5 (*c* 1.0, EtOAc) on 98% ee material (HPLC). These spectral data match those previously reported for this compound.[11]

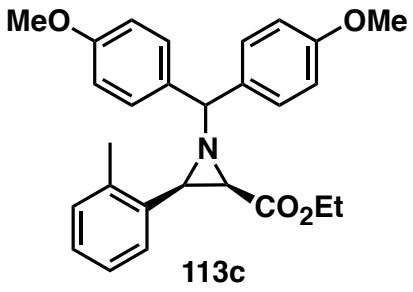

113c

***(2R,3R)-Cis*-1-(*N*-1-bis(4-methoxyphenyl)methyl)-2-carboxyethyl-3-*o*-tolylaziridine 113c:** Imine **110c** (173 mg, 0.500 mmol) was reacted according to the general procedure V described above with (*S*)-VAPOL as ligand. After purification, the product was obtained as a white solid (mp. 123-124 ºC) in 70% isolated yield (151 mg, 0.35 mmol). *cis/trans*: ≥ 50:1. Enamine side products: 1.4% yield of **116c** and 1.1% yield of **117c**. The optical purity of **113c** was determined to be 93% ee by HPLC analysis (CHIRALPAK AD column, 90:10 hexane/*i*PrOH at 226nm, flow-rate: 1.0 mL/min); retention times: R_t = 7.14 min (major enantiomer, **113c**) and R_t = 10.83 min (minor enantiomer, *ent*-**113c)**.

Spectral data for **113c**: R_f = 0.26 (1:5 EtOAc/hexane); ^{1}H NMR ($CDCl_3$, 500 MHz) δ 0.87 (t, 3H, *J* = 7.1 Hz), 2.27 (s, 3H), 2.67 (d, 1H, *J* = 6.8 Hz), 3.14 (d, 1H, *J* = 6.8 Hz), 3.72 (s, 3H), 3.77 (s, 3H), 3.84 (s, 1H), 3.87 (q, 2H, *J* = 7.1 Hz), 6.78 (d, 2H, *J* = 8.8 Hz), 6.84 (d, 2H, *J* = 8.5 Hz), 7.01-7.08 (m, 3H), 7.37 (d, 2H, *J* = 8.8 Hz), 7.47 (d, 3H, *J* = 9.0 Hz); ^{13}C ($CDCl_3$, 125 MHz) δ 13.83, 18.75, 45.72, 46.91, 55.17, 55.23, 60.38, 76.72, 113.86, 113.90, 125.34, 127.09, 128.14, 128.55, 128.69, 129.09, 133.29, 134.99, 135.25, 136.02, 158.67, 158.89, 168.03; $[\alpha]_D^{20}$ +38.6 (*c* 1.0, EtOAc) on 93% ee material (HPLC). These spectral data match those previously reported for this compound.[11]

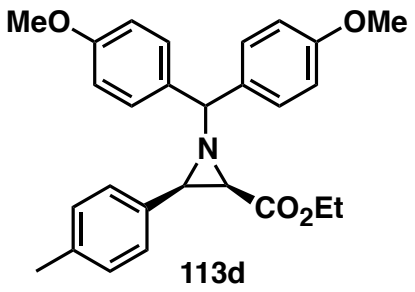

113d

***(2R,3R)-Cis*-1-(*N*-1-bis(4-methoxyphenyl)methyl)-2-carboxyethyl-3-*p*-tolylaziridine 113d:** Imine **17c** (173 mg, 0.500 mmol) was reacted according to the general procedure V described above with (*S*)-VAPOL as ligand. After purification, the product was obtained as a white solid in 90% isolated yield (194 mg, 0.450 mmol). *cis/trans*: ≥ 50:1. Enamine side products: 1% yield of **116d** and 1 % yield of **117d**. The optical purity **113d** was determined to be 94 % *ee* by HPLC analysis (CHIRALPAK AD column, 90:10 hexane/*i*PrOH at 226nm, flow-rate: 1.0 mL/min); retention times: R_t = 7.85 min (major enantiomer, **113d**) and R_t = 15.25 min (minor enantiomer, *ent*-**113d**).

Spectral data for **113d**: R_f = 0.34 (1:5 EtOAc/hexanes); ^{1}H NMR ($CDCl_3$, 300 MHz) δ 1.01 (t, 3H, *J* = 7.1 Hz), 2.29 (s, 3H), 2.63 (d, 1H, *J* = 6.8 Hz), 3.16 (d, 1H, *J* = 6.8 Hz), 3.71 (s, 3H), 3.77 (s, 3H), 3.86 (s, 1H), 3.95 (q, 2H, *J* = 7.1 Hz), 6.78 (d, 2H, *J* = 8.8 Hz), 6.87 (d, 2H, *J* = 8.8 Hz), 7.06 (d, 2H, *J* = 7.8 Hz), 7.29 (d, 2H, *J* = 8.0 Hz), 7.37 (d, 3H, *J* = 8.8 Hz), 7.49 (d, 3H, *J* = 8.5 Hz); ^{13}C ($CDCl_3$, 75 MHz) δ 13.93, 21.06, 46.33, 47.98, 55.04, 55.12, 60.42, 76.44, 113.73, 127.61, 128.14, 128.40, 128.42, 132.07, 134.96, 135.13, 136.77, 158.57, 158.65, 167.83 (one sp^2 carbon not located); IR (thin film, cm^{-1}) 2995 w, 1745 m, 1609 w, 1510 vs, 1301 w, 1247 s, 1175 s, 1035 m, 825 w; HRMS calcd for $C_{27}H_{29}NO_4Na$ *m/z* 454.1994, mass 454.1988; $[\alpha]_D^{20}$ +22.2 (*c* 1.0, EtOAc) on 94% ee material (HPLC).

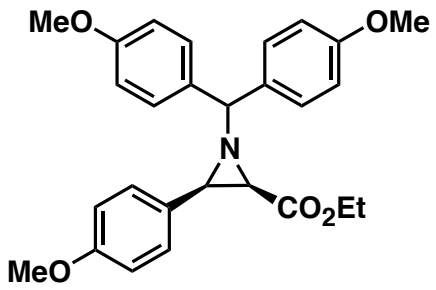

113e

***(2R,3R)-Cis*-1-(*N*-1-bis(4-methoxyphenyl)methyl)-2-carboxyethyl-3-*p*-methoxyphenyl aziridine 113e:** Imine **110e** (181 mg, 0.500 mmol) was reacted according to the general procedure V described above with (*R*)-VANOL as ligand. The silica gel for column chromatography was pre-conditioned by preparing a slurry in a 1:9 mixture of Et_3N:CH_2Cl_2 which was loaded into a column (35 mm × 350 mm), the solvent was drained and then the silica gel was dried by flushing with nitrogen for one hour. The silica gel column was then saturated with a 1:9 mixture of ethyl acetate:hexane, the crude aziridine was loaded onto the column and then elution with the same solvent mixture until the elution of the first fraction, which contains EDA and / or enamine side products **116e** and **117e**, the eluent was changed to 5:1 hexanes / EtOAc) afforded pure aziridine **113e** as a semi solid in 80% isolated yield (179 mg, 0.4 mmol); *cis/trans*: 50:1. Enamine side products: 3.2% yield of **116e** and 1.6% yield of **117e**. The optical purity of **113e** was determined to be 93% ee by HPLC analysis (CHIRALPAK AD column, 90:10 hexane/*i*PrOH at 226nm, flow-rate: 1.0 mL/min); retention times, R_t = 10.69 min (major enantiomer, **113e**) and R_t = 32.38 min (minor enantiomer, *ent*-**113e**).

Spectral data for **113e**: R_f = 0.2 (1:5 EtOAc/hexanes); ^{1}H NMR ($CDCl_3$, 300 MHz) δ 1.02 (t, 3H, *J* = 7.1 Hz), 2.61 (d, 1H, *J* = 6.6 Hz), 3.14 (d, 1H, *J* = 6.6 Hz), 3.70 (s, 3H), 3.74 (s, 3H), 3.76 (s, 3H), 3.85 (s, 1H), 3.95 (q, 2H, *J* = 7.1 Hz), 6.79 (dd, 4H, *J* = 8.8 Hz, 2.4 Hz), 6.86 (d, 2H, *J* = 8.8 Hz), 7.32 (d, 2H, *J* = 8.8 Hz); 7.36 (d, 2H, *J* = 8.5 Hz), 7.48 (d, 2H, *J* = 8.5 Hz) ; ^{13}C ($CDCl_3$, 75 MHz) δ 13.94, 46.26, 47.67, 55.01, 55.04, 55.08, 60.43, 76.34, 113.11, 113.68,

113.70, 127.14, 128.09, 128.38, 128.79, 134.89, 135.10, 158.51, 158.59, 158.76, 167.90; $[\alpha]_D^{20}$ +27.1 (*c* 2.0, EtOAc) on 95% ee material (HPLC). These spectral data match those previously reported for this compound.[11]

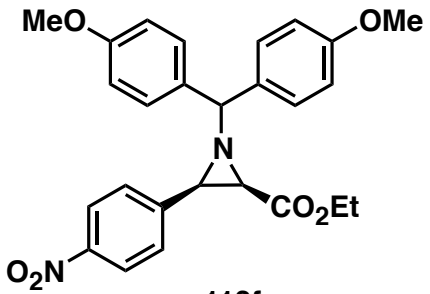

113f

***(2R,3R)-Cis*-1-(*N*-1-bis(4-methoxyphenyl)methyl)-2-carboxyethyl-3-*p*-nitrophenylaziridine 113f:** Imine **110f** (188 mg, 0.500 mmol) was reacted according to the general procedure V described above with (*S*)-VAPOL as ligand. After purification, the product was obtained as a yellow powder (mp. 56-57 ºC) in 85% isolated yield (197 mg, 0.430 mmol); *cis/trans*: 50:1. Enamine side products: <1% yield of **116f** and <1% yield of **117f**. The optical purity of **113f** was determined to be 95% ee by HPLC analysis (CHIRALPAK AD column, 90:10 hexane/*i*PrOH at 226nm, flow-rate: 1.0 mL/min), Retention times: R_t = 16.47 min (major enantiomer, **113f**) and R_t = 54.59 min (minor enantiomer, *ent*-**113f**).

Spectral data for **113f**: R_f = 0.15 (1:5 EtOAc/hexanes); ^{1}H NMR ($CDCl_3$, 300 MHz) δ 0.99 (t, 3H, *J* = 7.1 Hz), 2.74 (d, 1H, *J* = 6.6 Hz), 3.20 (d, 1H, *J* = 6.8 Hz), 3.70 (s, 3H), 3.77 (s, 3H), 3.88 (s, 1H), 3.92 (q, 2H, *J* = 7.3 Hz), 6.77 (d, 2H, *J* = 8.8 Hz), 6.85 (d, 2H, *J* = 8.8 Hz), 7.31 (d, 2H, *J* = 8.8 Hz), 7.44 (d, 2H, *J* = 8.5 Hz), 7.57 (d, 2H, *J* = 8.5 Hz), 8.09 (d, 2H, *J* = 8.8 Hz); ^{13}C ($CDCl_3$, 125 MHz) δ 14.01, 46.96, 47.09, 55.16, 55.24, 60.88, 76.37, 113.99, 123.04, 128.08, 128.38, 128.78, 134.37, 134.64, 142.68, 147.34, 158.87, 158.98, 167.05 (one sp^2 carbon not

located); $[\alpha]_D^{20}$ –1.4 (*c* 1.0, EtOAc) on 95% ee material (HPLC). These spectral data match those previously reported for this compound.[11]

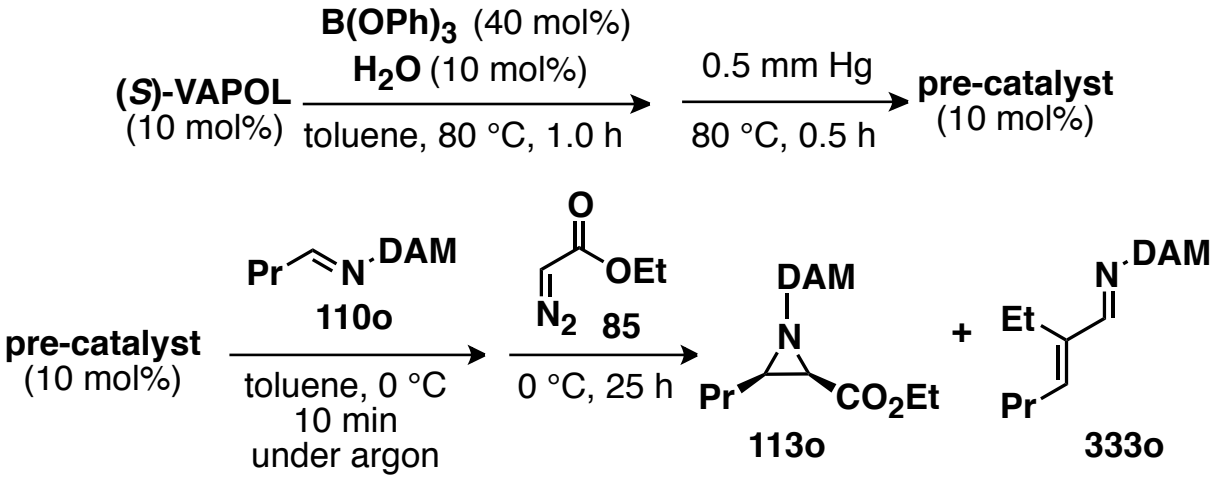

(*E*)-*N*-butylidene-1,1-bis(4-methoxyphenyl)methanamine 110o: To a 10 mL flame-dried round bottom flask filled with argon was added *bis*(4-methoxyphenyl)methylamine **126b** (243 mg, 1 mmol), 4Å MS (250 mg, freshly dried) and dry toluene (1.5 mL). After stirring for 10 min, butanal **127o** (78 mg, 1.05 mmol, freshly distilled) was added. The reaction mixture was stirred at room temperature for 6 h. The resulting imine **110o** was used without further purification.

Spectral data for **111o**: ^{1}H NMR ($CDCl_3$, 500 MHz) δ 0.95 (t, 3H, *J* = 7.5 Hz), 1.57 (sextet, 2H, *J* = 7.5 Hz), 2.26-2.33 (m, 2H), 3.75 (s, 6H), 5.25 (s, 1H), 6.80-6.83 (m, 4H), 7.16-7.19 (m, 4H), 7.83 (t, 1H, *J* = 5.0 Hz).

(2*R*,3*R*)-ethyl 1-(bis(4-methoxyphenyl)methyl)-3-propylaziridine-2-carboxylate 113o: To a 25 mL flame-dried home-made Schlenk flask (see Figure 2.26) equipped with a stir bar and flushed with argon was added (*S)*-VAPOL (54 mg, 0.1 mmol) and $B(OPh)_3$ (116 mg, 0.4 mmol).

Under an argon flow through the side-arm of the Schlenk flask, dry toluene (2 mL) was added to dissolve the two reagents and this was followed by the addition of water (1.8 μL, 0.1 mmol). The flask was sealed by closing the Teflon valve, and then placed in an 80 ºC (oil bath) for 1 h. After 1 h, a vacuum (0.5 mm Hg) was carefully applied by slightly opening the Teflon valve to remove the volatiles. After the volatiles are removed completely, a full vacuum is applied and is maintained for a period of 30 min at a temperature of 80 ºC (oil bath). The flask was then allowed to cool to room temperature and open to argon through side-arm of the Schlenk flask.

The toluene solution of imine **110o** (296 mg, 1 mmol, prepared as described above) was then directly transferred from the reaction flask in which it was prepared to the flask containing the catalyst (precooled at 0 ºC) utilizing a filter syringe (Corning® syringe filters, Aldrich) to remove the 4Å Molecular Sieves. The flask, which had imine **110o**, was then rinsed with toluene (0.5 mL) and the rinse was transferred to the flask containing the catalyst under argon flow through side-arm of the Schlenk flask. The reaction mixture was stirred for 5 min to give a light yellow solution. To this solution was rapidly added EDA **85** (124 μL, 1.2 mmol) at 0 ºC followed by closing the Teflon valve. The resulting mixture was stirred for 24 h at room temperature. The reaction was dilluted by addition of hexane (6 mL). The reaction mixture was then transferred to a 100 mL round bottom flask. The reaction flask was rinsed with dichloromethane (5 mL × 2) and the rinse was added to the 100 mL round bottom flask. The resulting solution was then concentrated *in vacuo* followed by exposure to high vacuum (0.05 mm Hg) for 1 h to afford the crude aziridine as a pale yellow semi solid. Purification of the crude aziridine by silica gel chromatography (35 mm × 400 mm column, 9:1 hexanes/EtOAc as eluent) afforded pure cis-aziridine **113o** as a white solid (mp 99-100 ºC on 66% ee material) in 11% isolated yield (42 mg,

0.11 mmol); *cis/trans*: not determined. Enamine side products: <1% yield of **116o** and 2% yield of **117o**. The amount of byproduct **333o** was determined to be 7% by integration of the ^{1}H NMR spectrum of the crude reaction mixture relative to the aziridine **116o** with aid of the authentic sample of **333o** prepared as described above. The optical purity of **113o** was determined to be 73% *ee* by HPLC analysis (CHIRALPAK AD column, 90:10 hexane/2-propanol at 226nm, flow-rate: 1.0 mL/min): retention times; R_t = 5.9 min (major enantiomer, **113o**) and R_t = 8.3 min (minor enantiomer, *ent*-**113o**).

Spectral data for **113o**: R_f = 0.28 (1:5 EtOAc/hexanes). ^{1}H NMR ($CDCl_3$, 500 MHz) δ 0.74 (t, 3H, J = 7.4 Hz), 1.02-1.16 (m, 2H), 1.23 (t, 3H, J = 7.1 Hz), 1.40-1.54 (m, 2H), 1.99 (q, 1H, J = 6.6 Hz), 2.23 (d, 1H, J = 6.9 Hz), 3.56 (s, 1H), 3.74 (s, 6H), 4.11-4.21 (m, 2H), 6.77-6.82 (m, 4H), 7.26 (d, 2H, J = 8.5 Hz), 7.34 (d, 2H, J = 8.8 Hz); ^{13}C ($CDCl_3$, 75 MHz) δ 13.65, 14.26, 20.35, 29.91, 43.35, 46.74, 55.16, 60.65, 76.70, 113.61, 113.67, 128.09, 128.81, 134.98, 135.46, 158.47, 158.73, 169.60 (one sp^3 carbon not located); $[\alpha]_D^{20}$ +70.7 (*c* 1.0, EtOAc) on 73% ee material (HPLC). These spectral data match those previously reported for this compound.[11]

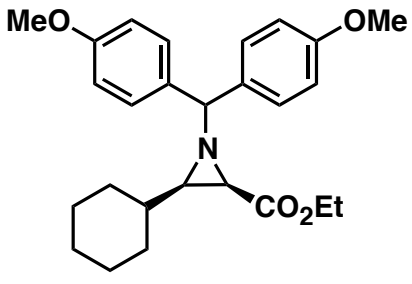

113v

***(2R,3R)-Cis*-1-(*N*-1-bis(4-methoxyphenyl)methyl)-2-carboxyethyl-3-cyclohexylaziridine 113v:** Imine **110v** (169 mg, 0.500 mmol) was reacted according to the general procedure V described above with (*S*)-VANOL as ligand. After purification, the product was obtained as a white solid

(mp. 119.5-121 ºC) in 83% isolated yield (176 mg, 0.42 mmol); *cis/trans*: 50:1. Enamine side products: < 1% yield of **116v** and < 1% yield of **117v**. The optical purity of **113v** was determined to be 82% ee by HPLC analysis (CHIRALPAK AD column, 98:2 hexane/*i*PrOH at 226nm, flow-rate: 1.0 mL/min); Retention times: R_t = 11.61 min (major enantiomer, **113v**) and R_t = 17.90 min (minor enantiomer, *ent*-**113v**).

Spectral data for **113v**: R_f = 0.3 (1:5 EtOAc/hexanes). ^{1}H NMR ($CDCl_3$, 300 MHz) δ 0.50-0.53 (m, 1H), 0.89-1.11 (m, 4H), 1.22 (t, 3H, *J* = 7.1 Hz), 1.22-1.24 (m, 2H), 1.31-1.66 (m, 4H), 1.75 (dd, 1H, *J* = 6.9, 9.0 Hz), 2.20 (d, 1H, *J* = 6.9 Hz), 3.50 (s, 1H), 3.74 (s, 6H), 4.12-4.24 (m, 2H), 6.78 (d, 2H, *J* = 8.8 Hz), 6.80 (d, 2H, *J* = 8.8 Hz), 7.21 (d, 2H, *J* = 8.5 Hz), 7.34 (d, 2H, *J* = 8.5 Hz); ^{13}C ($CDCl_3$, 75 MHz) δ 14.25, 25.35, 25.52, 26.11, 30.10, 30.80, 36.29, 43.35, 52.21, 55.17, 60.64, 76.99, 113.53, 113.62, 127.97, 129.26, 134.82, 135.41, 158.36, 158.78, 169.71; $[\alpha]_D^{20}$ +116.3 (*c* 1.0, EtOAc) on 99% ee material (HPLC). These spectral data match those previously reported for this compound.[11]

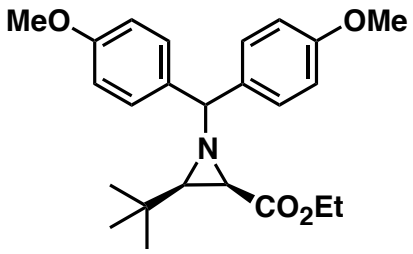

113w

***(2R,3R)-Cis*-1-(*N*-1-bis(4-methoxyphenyl)methyl)-2-carboxyethyl-3-1,1-dimethylethyl aziridine 113w:** Imine **110w** (156 mg, 0.500 mmol) was reacted according to the general procedure V described above with (*S*)-VANOL as ligand. After purification, the product was obtained as a white solid (mp. 81-83 ºC) in 60% isolated yield (119 mg, 0.3 mmol); *cis/trans*: 20:1. Enamine side products: <1% yield of **116w** and <1% yield of **117w**. The optical purity of **113w** was determined to be 70% ee by HPLC

analysis (CHIRALCEL OD-H column, 99:1 hexane/*i*PrOH at 226nm, flow-rate: 0.7 mL/min); Retention times: R_t = 14.21 min (major enantiomer, **113w**) and R_t = 11.54 min (minor enantiomer, *ent*-**113w**).

Spectral data for **113w**: R_f = 0.65 (1:5 EtOAc/hexanes); ^{1}H NMR ($CDCl_3$, 300 MHz) δ 0.75 (s, 9H), 1.33 (t, 3H, *J* = 7.1 Hz), 1.78 (d, 1H, *J* = 7.2 Hz), 2.18 (d, 1H, *J* = 7.2 Hz), 3.55 (s, 1H), 3.79 (s, 3H), 3.80 (s, 3H), 4.09-4.31 (m, 2H), 6.83-6.89 (m, 4H), 7.33 (d, 2H, *J* = 8.7 Hz), 7.60 (d, 2H, *J* = 8.7 Hz); ^{13}C ($CDCl_3$, 75 MHz) δ 14.15, 27.54, 31.71, 43.46, 55.22, 56.26, 60.65, 78.03, 113.64, 128.26, 129.13, 135.30, 136.25, 158.46, 158.84, 170.01 (one sp^2 carbon and one sp^3 carbon not located); $[\alpha]_D^{20}$ +142.4 (*c* 1.0, EtOAc) on 99% ee material (HPLC). These spectral data match those previously reported for this compound.[11]

6.8.5 [3+2] Cycloaddition of imine 333o, 358a and 359a (*Scheme 6.6 and Table 6.6*)

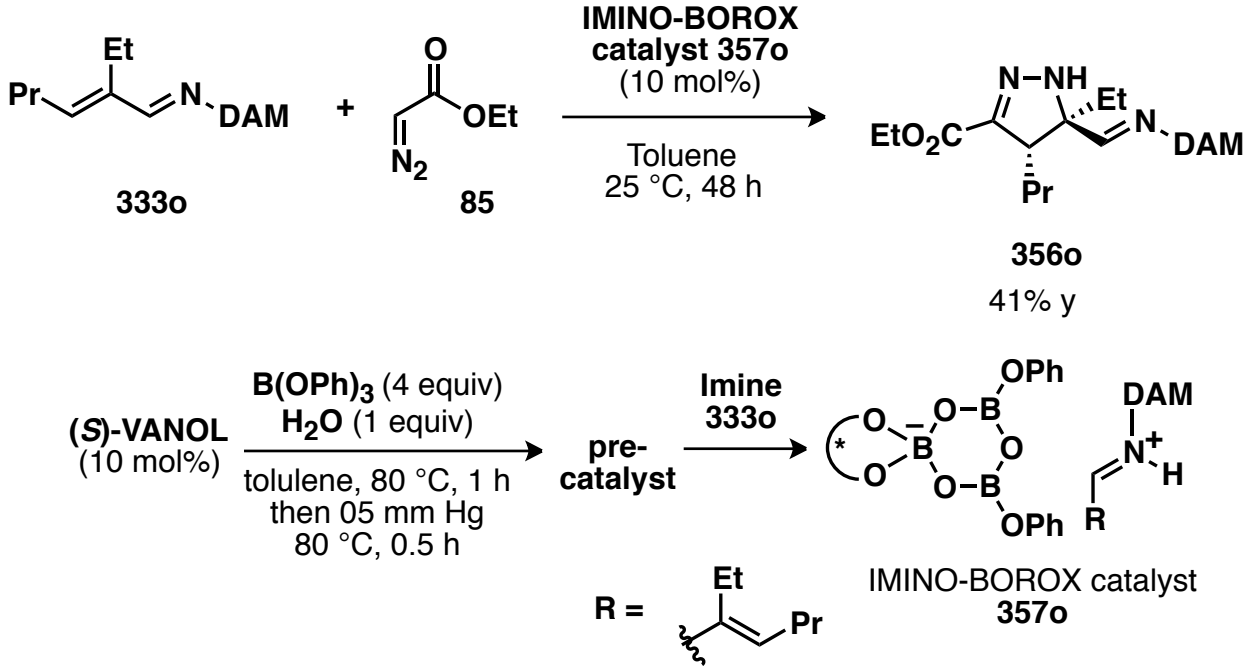

(4*S*,5*R*)-ethyl-5-((*E*)-((bis(4-methoxyphenyl)methyl)imino)methyl)-5-ethyl-4-propyl-4,5-dihydro-1*H*-pyrazole-3-carboxylate 356o: To a 25 mL flame-dried home-made Schlenk flask (see Figure 2.26) equipped with a stir bar and flushed with argon was added (*S*)-VANOL (44 mg, 0.1 mmol) and $B(OPh)_3$ (116 mg, 0.4 mmol). Under an argon flow through the side-arm of the Schlenk flask, dry toluene (2 mL) was added to dissolve the two reagents and this was followed by the addition of water (1.8 μL, 0.1 mmol). The flask was sealed by closing the Teflon valve, and then placed in an 80 ºC (oil bath) for 1 h. After 1 h, a vacuum (0.5 mm Hg) was carefully applied by slightly opening the Teflon valve to remove the volatiles. After the volatiles are removed completely, a full vacuum is applied and is maintained for a period of 30 min at a temperature of 80 ºC (oil bath). The flask was then allowed to cool to room temperature and open to argon through side-arm of the Schlenk flask.

The toluene solution of imine **333o** (352 mg, 1 mmol, prepared as described above) was then directly transferred from the reaction flask in which it was prepared to the flask containing the catalyst utilizing a filter syringe (Corning® syringe filters, Aldrich) to remove the 4Å Molecular Sieves. The flask, which had imine **330o**, was then rinsed with toluene (0.5 mL) and the rinse was transferred to the flask containing the catalyst under argon flow through side-arm of the Schlenk flask. The reaction mixture was stirred for 5 min to give a light yellow solution. However, the solution became turbid after 10 min. To this solution was rapidly added EDA **85** (124 μL, 1.2 mmol) followed by closing the Teflon valve. The resulting mixture was stirred for 48 h at room temperature. The color of solution became brown after 1 h. The reaction was dilluted by addition of hexane (6 mL). The reaction mixture was then transferred to a 100 mL round bottom flask. The reaction flask was rinsed with dichloromethane (5 mL × 2) and the

rinse was added to the 100 mL round bottom flask. The resulting solution was then concentrated *in vacuo* followed by exposure to high vacuum (0.05 mm Hg) for 1 h to afford the crude aziridine as a pale yellow semi solid. Purification of the crude [3+2] adduct by neutral alumina chromatography (20 mm × 200 mm column, 3:1 hexanes/EtOAc as eluent) afforded pure adduct **356o** as a yellow semi-solid in 41% isolated yield (191 mg, 0.41 mmol); *dr*: not determined. The optical purity of **356o** could not be determined due to messy HPLC signals.

Spectral data for **356o**: R_f = 0.29 (1:3 EtOAc/hexanes). ^{1}H NMR ($CDCl_3$, 500 MHz) δ 0.80 (t, *J* = 7.5 Hz, 3H), 0.89 (t, *J* = 7.3 Hz, 3H), 1.32-1.39 (m, 5H), 1.58-1.71 (m, 2H), 1.78-1.87 (m, 2H), 3.18 (t, *J* = 6.2 Hz, 1H), 3.76 (s, 3H), 3.77 (s, 3H), 4.25-4.30 (m, 2H), 5.39 (s, 1H), 6.78-6.84 (m, 5H), 7.13 (dd, *J* = 16.8, 8.6 Hz, 4H), 7.50 (s, 1H); ^{13}C ($CDCl_3$, 75 MHz) δ 8.87, 14.24, 14.31, 20.50, 23.21, 28.63, 48.41, 55.18, 60.96, 74.72, 74.99, (one sp^3 carbon not located), 113.66, 113.74, 113.81, 128.20, 128.53, 135.66, 135.80, 147.45, 158.52, 162.57, 164.36; IR (thin film, cm^{-1}) 3331 br, 2961m, 2836w, 1701m, 1608w, 1510vs, 1464w, 1246vs; HRMS (ESI-TOF) *m/z* 466.2703 [(M+H$^+$); calcd. for $C_{27}H_{36}N_3O_4$: 466.2706]

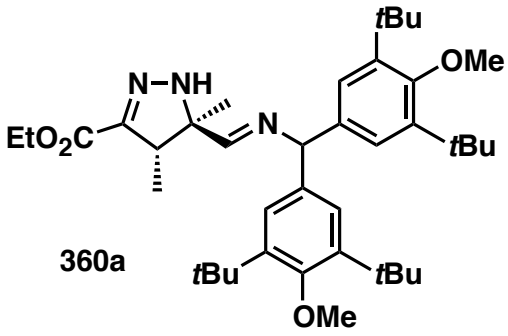

360a

(4*S*,5*R*)-ethyl-5-((*E*)-((bis(3,5-di-*tert*-butyl-4-methoxyphenyl)methyl)imino)methyl)-4,5-dimethyl-4,5-dihydro-1*H*-pyrazole-3-carboxylate 360a: Imine **358a** (107 mg, 0.200 mmol) was reacted according to the procedure described above for imine **333o** with (*S*)-VAPOL as ligand except with the following differences; a) the reaction is 0.4 M in imine **358a**,

b) 2 equiv of EDA used, c) purified imine **358a** was added in neat form. The reaction resulted adduct **360a** in 59% NMR yield which was determined by ^{1}H NMR spectra with Ph_3CH as the internal standard. The resulting crude [3+2] adduct **360a** could not be purified on either neutral alumina or silica gel chromatography. However, a sample was prepared by quickly passing the crude product through a plug of neutral alumina for HPLC analysis. The optical purity of **360a** was determined to be 50% *ee* by HPLC analysis (CHIRALCEL OD column, 99:01 hexane/*i*PrOH at 222nm, flow-rate: 0.7 mL/min). Retention times, R_t = 11.82 min (major enantiomer, **360a**) and R_t = 17.27 min (minor enantiomer, *ent*-**360a**).

Spectral data for **360a**: R_f = 0.29 (1:3 EtOAc/hexanes). ^{1}H NMR ($CDCl_3$, 500 MHz) δ 1.26 (d, *J* = 7.0 Hz, 3H), 1.35-1.42 (m, 42H), 3.36 (q, *J* = 7.2 Hz, 1H), 3.70 (s, 3H), 3.70 (s, 3H), 4.29 (q, *J* = 7.2 Hz, 2H), 5.34 (s, 1H), 6.72 (s, 1H), 7.06 (s, 2H), 7.08 (s, 2H), 7.75 (s, 1H). This compound was not characterized as it's being in crude form. However, it was further reduced to amine **367a** and thereafter the amine **367a** is completely characterized and given below.

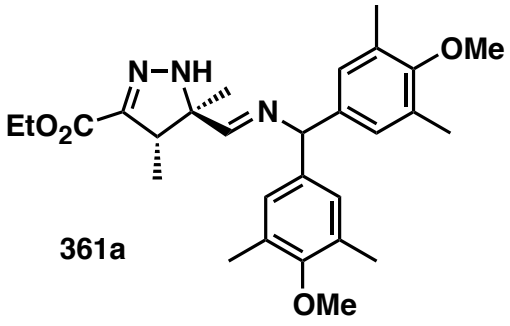

361a

((4*S*,5*R*)-ethyl-5-((*E*)-((bis(4-methoxy-3,5-dimethylphenyl)methyl)imino)methyl)-4,5-dimethyl-4,5-dihydro-1*H*-pyrazole-3-carboxylate 361a: Imine **359a** (73 mg, 0.200 mmol) was reacted according to the procedure described above for imine **333o** with (*S*)-VAPOL as ligand except with the following differences; a) the reaction is 0.4 M in imine **359a**, b) 2 equiv of EDA used, c) purified imine **359a** was added in neat form. The reaction resulted adduct **361a** in 33% NMR yield which was determined by ^{1}H NMR spectra with Ph_3CH as the

internal standard. The resulting crude [3+2] adduct **361a** could not be purified on either neutral alumina or silica gel chromatography. No further attempt was made to isolate or analyze adduct **361a**.

6.8.6 Multicomponent [3+2] Cycloaddition of aldehyde 352a (*Scheme 6.7*)

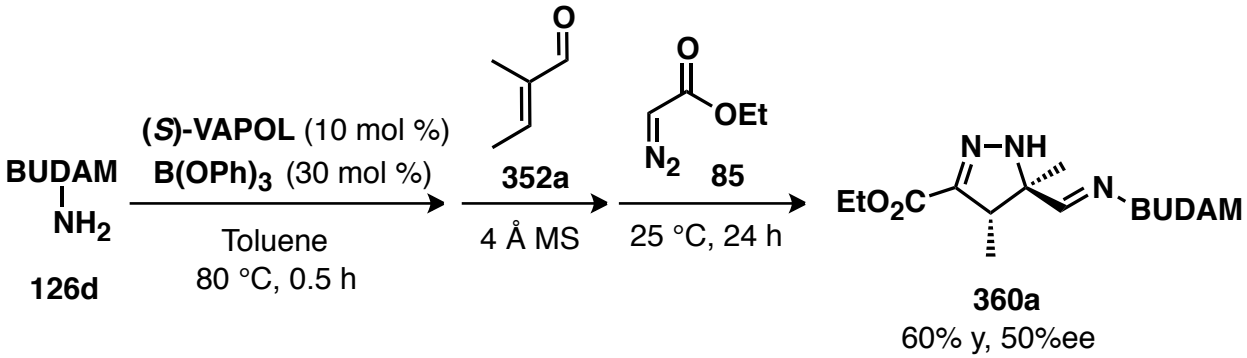

(4*S*,5*R*)-ethyl-5-((*E*)-((bis(3,5-di-*tert*-butyl-4-methoxyphenyl)methyl)imino)methyl)-4,5-dimethyl-4,5-dihydro-1*H*-pyrazole-3-carboxylate 360a: To a 25 mL flame-dried home-made Schlenk flask (see Figure 2.26) equipped with a stir bar and flushed with argon was added (*S*)-VAPOL **58** (11 mg, 0.02 mmol), commercial $B(OPh)_3$ (17.4 mg, 0.060 mmol) and amine **126d** (94 mg, 0.2 mmol) and toluene (0.5 mL). The flask was sealed by closing the Teflon valve, and then placed in an 80 ºC (oil bath) for 1 h. The flask was then allowed to cool to room temperature and open to argon through side-arm of the Schlenk flask. To this flask was then added 4Å MS (50 mg, freshly flame-dried) and aldehyde **352a** (19 mg, 0.22 mmol, 1.1 equiv). The resulting mixture was stirred for 5 min at room temperature. To this solution was rapidly added EDA **85** (42 μL, 0.4 mmol). The resulting mixture was stirred for 24 h at room temperature. The reaction was dilluted by addition of hexane (6 mL). The reaction mixture was then transferred to a 100 mL round bottom flask. The reaction flask was rinsed with

dichloromethane (5 mL × 2) and the rinse was added to the 100 mL round bottom flask. The resulting solution was then concentrated *in vacuo* followed by exposure to high vacuum (0.05 mm Hg) for 1 h to afford the crude aziridine as a pale yellow semi solid. The reaction resulted adduct **360a** in 60% NMR yield which was determined by ^{1}H NMR spectra with Ph_3CH as the internal standard. A sample was prepared by quickly passing the crude product through a plug of neutral alumina for HPLC analysis. The optical purity of **360a** was determined to be 50% *ee* by HPLC analysis (CHIRALCEL OD column, 99:01 hexane/*i*PrOH at 222nm, flow-rate: 0.7 mL/min). Retention times, R_t = 11.82 min (major enantiomer, **360a**) and R_t = 17.27 min (minor enantiomer, *ent*-**360a**).

6.8.7 Hydrolysis and reduction of [3+2] adduct 360a (*Scheme 6.8*)

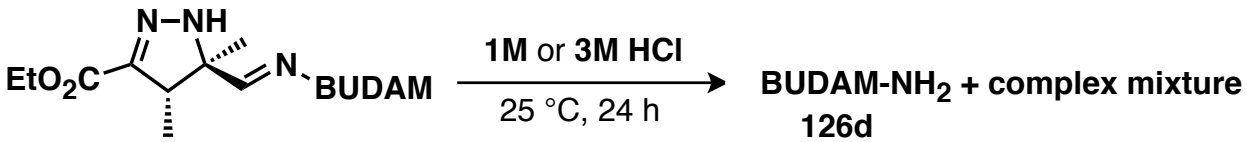

360a
crude from a 0.25 mmol scale reaction

a) *Hydrolysis:* To a 50 mL round bottom flask was taken the crude [3+2] adduct from the 0.25 mmol scale reaction and THF (1 mL). To this solution was added HCl (0.1 mL, 1 M) dropwise and the resulting mixture stirred for 24 h. A continuous stirring was maintained during the addition of the acid. After 24 h, the reaction mixture was extracted with ether (15 mL × 3) to get crude product. The combined organic layer was then washed with brine, dried over anhydrous $MgSO_4$, filtered and concentrated *in vacuo* to afford the crude reaction mixture. A complex

mixture of compounds along with BUDAM amine **126d** was observed based on the ^{1}H NMR analysis of crude reaction mixture.

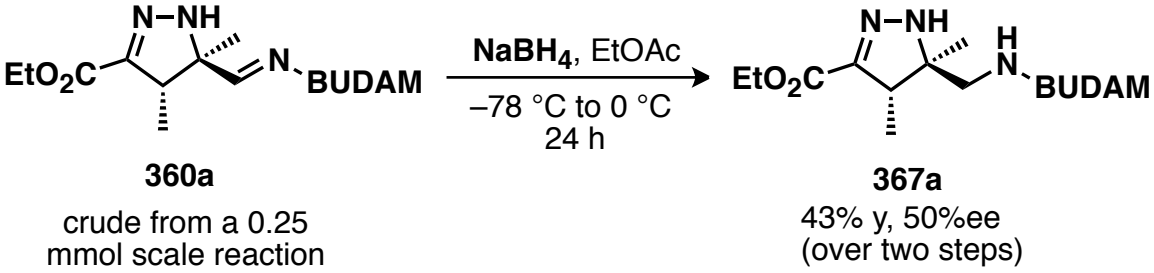

360a
crude from a 0.25 mmol scale reaction

367a
43% y, 50%ee (over two steps)

b) *Reduction:* To a 50 mL round bottom flask was taken the crude [3+2] adduct from the 0.25 mmol scale reaction and EtOAc (1 mL). To this solution was added $NaBH_4$ (11 mg, 0.28 mmol) at –78 ºC and the resulting mixture allowed to warm to 0 ºC over a period of 30 min. The reaction was stirred for 24 h at 0 ºC. After 24 h, the reaction was quenched by the addition of aqueous NH_4Cl (3 mL) and extracted with EtOAc (5 mL × 3). The combined organic layer was then washed with brine, dried over anhydrous $MgSO_4$, filtered and concentrated *in vacuo* to afford crude amine **367a**. Purification by silica gel chromatography (20 mm × 200 mm column, 8:1 hexanes/EtOAc as eluent) afforded pure amine **367a** as a white foamy solid in 43% isolated yield (70 mg, 0.11 mmol, over two steps). The optical purity of **367a** was determined to be 50% *ee* by HPLC analysis (CHIRALCEL OD column, 99:01 hexane/*i*PrOH at 222nm, flow-rate: 0.7 mL/min). Retention times, R_t = 6.66 min (major enantiomer, **367a**) and R_t = 12.04 min (minor enantiomer, *ent*-**367a**).

Spectral data for **367a**: R_f = 0.31 (1:8 EtOAc/Hexanes) ^{1}H NMR ($CDCl_3$, 500 MHz) δ 1.15 (d, J = 7.3 Hz, 3H), 1.17 (s, 3H), 1.35-1.37 (m, 39H), 2.51 (d, J = 12.1 Hz, 1H), 2.56 (d, J = 12.1

Hz, 1H), 3.13 (q, J = 7.3 Hz, 1H), 3.66 (s, 6H), 4.24-4.30 (m, 2H), 4.62 (s, 1H), 7.16 (s, 2H), 7.19 (s, 2H), 7.73 (s, 1H); ^{13}C NMR ($CDCl_3$, 125 MHz) δ 11.39, 14.25, 18.27, 31.99, 32.02, 32.04, 32.08, 32.10, 35.73, 35.93, 44.11, 55.04, 60.73, 64.04, 64.06, 64.36, 67.60, 69.42, (one sp^3 carbon not located), 125.45, 125.56, 129.00, 132.32, 143.19, 143.27, 158.30, 158.33, 162.81, 163.24. IR (thin film, cm^{-1}) 3332br, 2961m, 1701m, 1653w, 1559m, 1456s, 1412s, 1223vs; HRMS (ESI-TOF) *m/z* 650.4890 [($M+H^+$); calcd. for $C_{40}H_{64}N_3O_4$: 650.4897].

6.8.8 Attempts towards catalytic asymmetric Ugi 3CR, Ugi-type 2CR and Ugi-type 3CR and Passerini reaction (*Table 6.7-6.8 and Scheme 6.13*)

a) Ugi-3CR:

i) with isocyanide **368a** and acid **334a**

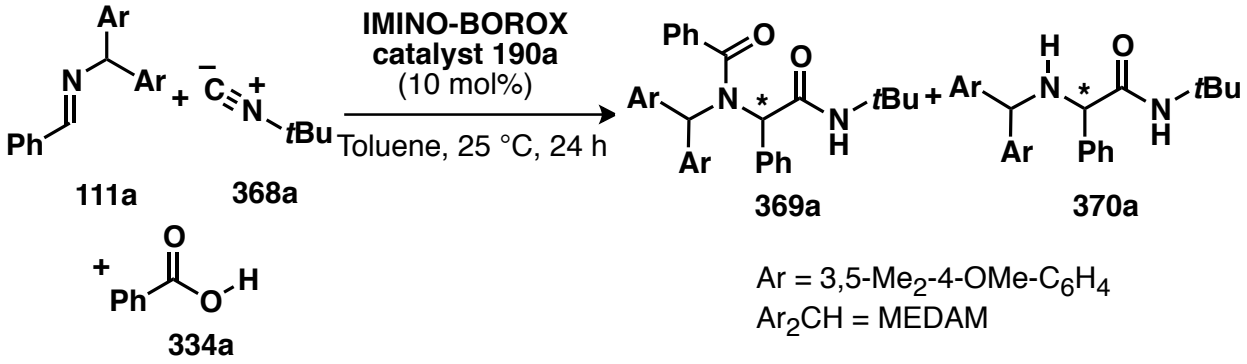

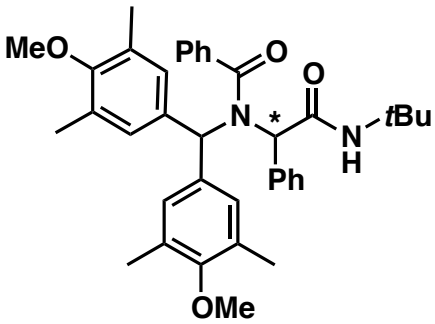

***N*-(bis(4-methoxy-3,5-dimethylphenyl)methyl)-*N*-(2-(tert-butylamino)-2-oxo-1-phenylethyl)benzamide 369a:** To a 25 mL flame-dried home-made Schlenk flask (see Figure 2.26) flushed with argon was added imine **111a** (194 mg, 0.500 mmol), (*S)*-VAPOL (27 mg, 0.05 mmol) and $B(OPh)_3$ (58 mg, 0.2 mmol) and toluene (1 mL). The stopcock was sealed, and the flask was

then placed in an 80 °C oil bath for 1 h. The flask was then cooled to room temperature. Isocyanide **368a** (57 μL, 0.50 mmol) was then added and the mixture was stirred for 5 min at room temperature. Benzoic acid **334a** (61 mg, 0.5 mmol) was then added in one portion followed by the addition of toluene (0.5 mL). The reaction mixture was then stirred for 24 h. After 24 h, the reaction was quenched by the addition of water (3 mL). The solution was diluted with EtOAc (2 mL). The organic layer was then separated, and the aqueous layer was extracted by EtOAc (5 mL × 3). The combined organic solution was then washed with brine, dried over anhydrous Na_2SO_4, filtered and concentrated *in vacuo* to afford crude product. Purification by silica gel chromatography (35 mm × 350 mm column, 5:1 hexanes/EtOAc as eluent) afforded pure amide **369a** (mp. 174-176 ºC) as a white solid in 40% isolated yield (119 mg, 0.20 mmol). The optical purity of **369a** was determined to be <1% *ee* by HPLC analysis (CHIRALCEL OD column, 99:01 hexane/*i*PrOH at 222nm, flow-rate: 0.7 mL/min). Retention times, R_t = 23.61 min (**369a**) and R_t = 31.49 min (*ent*-**369a**).

Spectral data for **369a**: R_f = 0.21 (1:5 EtOAc/Hexanes) ^{1}H NMR ($CDCl_3$, 500 MHz) δ 1.20 (s, 9H), 1.94 (s, 6H), 2.29 (s, 6H), 3.50 (s, 3H), 3.76 (s, 3H), 4.87 (s, 1H), 5.55 (s, 1H), 6.06 (s, 1H), 6.42 (s, 2H), 7.01 (s, 4H), 7.38-7.31 (m, 6 H), 7.48-7.45 (m, 2 H); ^{13}C NMR ($CDCl_3$, 125 MHz) δ 15.79,16.33, 28.44, 51.07, 59.36, 59.65, 65.87, 66.81, 126.5, 127.12, 127.68, 128.39, 128.61, 128.95, 129.67, 130.14, 130.52, 130.75, 134.05, 134.28, 136.81, 155.95, 156.24, 168.47, 172.72; IR (thin film, cm^{-1}) 3424m, 2928m, 1682s, 1637s, 1487s, 1419m, 1223s; Mass spectrum *m/z* (% rel intensity) 592.7 (100) M^+, 278.4, 260.4. Anal. calcd for $C_{38}H_{44}N_2O_4$: C, 77.00; H, 7.48; N, 4.73. Found: C, 76.04; H, 7.84; N, 4.26.

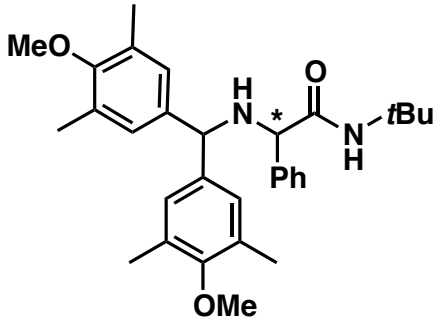

2-((bis(4-methoxy-3,5-dimethylphenyl)methyl)amino)-*N*-(*tert*-butyl)-2-phenylacetamide 370a: There was no sign of **370a** based on ^{1}H NMR analysis of crude reaction mixture.

ii) with isocyanide **368b** and acid **334b**

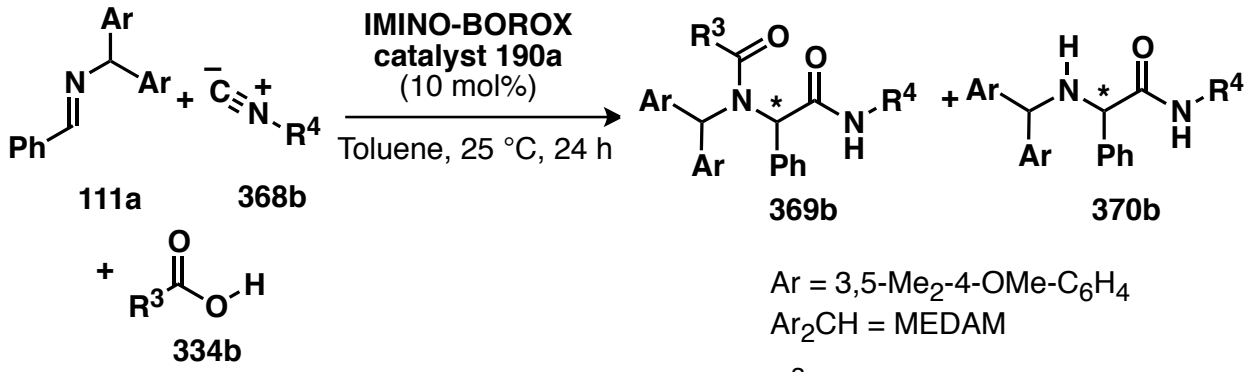

Ar = 3,5-Me_2-4-OMe-C_6H_4
Ar_2CH = MEDAM

R^3 = 4-pentylbicyclo[2.2.2]octyl
R^4 = 2-Naphthyl

The reaction was performed as described above with acid **334b** and isocyanide **368b**. A complex mixture of six different compounds was obtained. None of them was **369b**. One of the fractions obtained was amide **370b**.

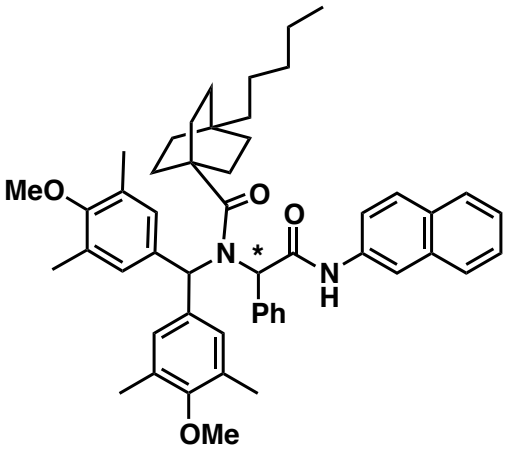

***N*-(bis(4-methoxy-3,5-dimethylphenyl)methyl)-*N*-(2-(naphthalene-2-ylamino)-2-oxo-1-phenyl ethyl)-4-pentyl bicyclo[2.2.2]octane-1-carboxamide 369b:** There was no sign of **360a** based on ^{1}H NMR analysis of crude reaction mixture.

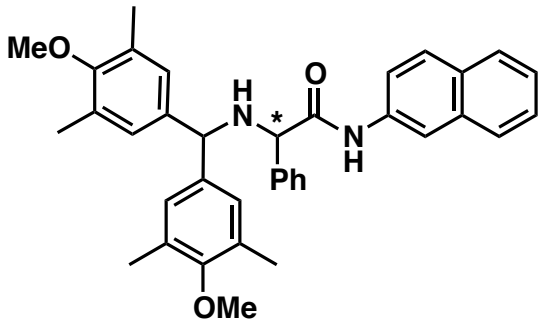

2-((bis(4-methoxy-3,5-dimethylphenyl)methyl) amino)-*N*-(naphthalen-2-yl)-2-phenyl acetamide 370b: Purification by silica gel chromatography (35 mm × 350 mm column, 5:1 hexanes/EtOAc as eluent) afforded pure amide **370b** (mp. 87-89 ºC) as a yellow solid in 26% isolated yield (72 mg, 0.13 mmol). The optical purity of **370b** was determined to be 8% *ee* by HPLC analysis (CHIRALCEL OD-H column, 99:01 hexane/*i*PrOH at 222nm, flow-rate: 0.7 mL/min). Retention times, R_t = 50.17 min (major enantiomer, **370b**) and R_t = 89.96 min (minor enantiomer, *ent*-**370b**).

Spectral data for **370b**: R_f = 0.55 (1:5 EtOAc/Hexanes) ^{1}H NMR ($CDCl_3$, 500 MHz) δ 2.28 (s, 6H), 2.29 (s, 6H), 3.65 (s, 3H), 3.73 (s, 3H), 4.37 (s, 1H), 4.74 (s, 1H), 6.97 (s, 2H), 7.04 (s, 2H), 7.33-7.42 (m, 7H), 7.45-7.48 (m, 1H), 7.49 (dd, *J* = 8.8, 2.1 Hz, 1H), 7.79 (t, *J* = 9.2 Hz, 3H), 8.26 (d, *J* = 1.6 Hz, 1H), 9.51 (s, 1H); ^{13}C NMR ($CDCl_3$, 125 MHz) δ 16.23, 16.27, 59.53, 59.64, 64.90, 66.11, 116.07, 119.46, 124.89, 126.47, 127.47, 127.49, 127.58, 127.71, 128.28, 128.68, 128.99, 130.58, 131.07, 131.08, 133.85, 135.05, 137.68, 137.96, 139.21, 156.19, 170.55 (two sp^2 carbon not located); IR (thin film, cm^{-1}) 3312br, 2926m, 1684s, 1632m, 1603m, 1529s, 1485s, 1221s; HRMS (ESI-TOF) *m/z* 559.2961 [(M+H$^+$); calcd. for $C_{37}H_{39}N_2O_3$: 559.2961]. $[\alpha]_D^{20}$ –0.8 (c 1.0, CH_2Cl_2) on 8% ee material.

b) Ugi-type-2CR:

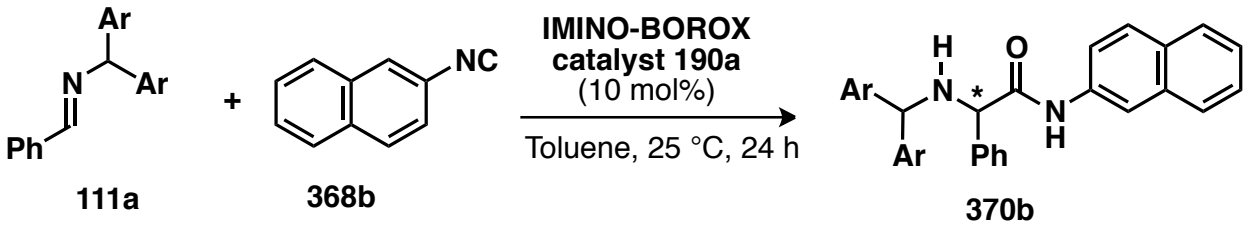

111a **368b** **370b**

Ar = 3,5-Me_2-4-OMe-C_6H_4
Ar_2CH = MEDAM

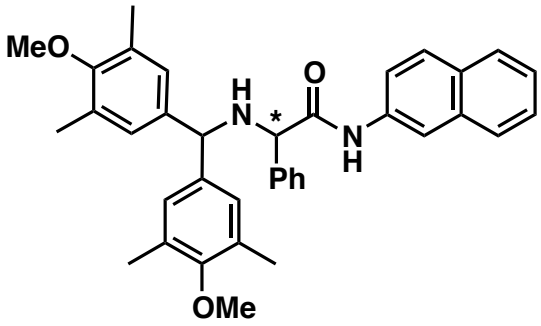

2-((bis(4-methoxy-3,5-dimethylphenyl)methyl) amino)-*N*-(naphthalen-2-yl)-2-phenyl acetamide 370b: To a 25 mL flame-dried home-made Schlenk flask (see Figure 2.26) flushed with argon was added imine **111a** (194 mg, 0.500 mmol), (*S)*-VAPOL (27 mg, 0.05 mmol) and $B(OPh)_3$ (58 mg, 0.2 mmol) and toluene (1 mL). The stopcock was sealed, and the flask was then placed in an 80 °C oil bath for 1 h. The flask was then cooled to room temperature. Isocyanide **368b** (77 mg, 0.5 mmol) was then added and the mixture was stirred for 5 min at room temperature. The reaction mixture was then stirred for 24 h. After 24 h, the reaction was quenched by the addition of water (3 mL). The solution was diluted with EtOAc (2 mL). The organic layer was then separated, and the aqueous layer was extracted by EtOAc (5 mL × 3). The combined organic solution was then washed with brine, dried over anhydrous Na_2SO_4, filtered and concentrated *in vacuo* to afford crude reaction mixture.

Unfortunately, no **370b** was observed based on the ^{1}H NMR analysis of the crude reaction mixture.

c) Ugi-type-3CR:

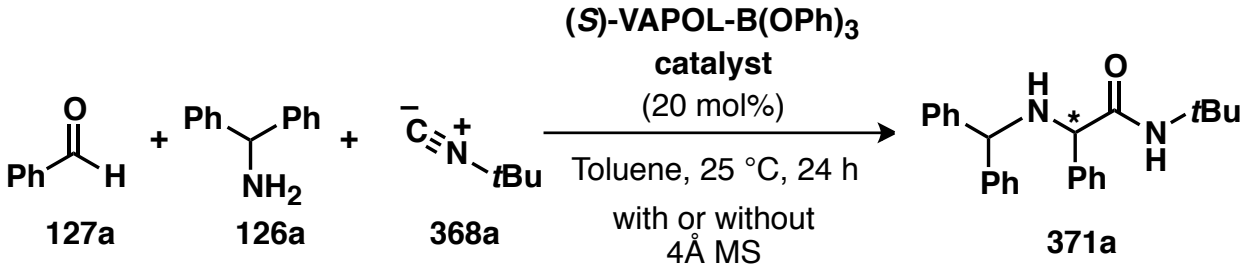

2-(benzhydrylamino)-*N*-(*tert*-butyl)-2-phenylacetamide: To a 25 mL flame-dried home-made Schlenk flask (see Figure 2.26) equipped with a stir bar and flushed with argon was added (*S*)-VAPOL (54 mg, 0.1 mmol) and commercial $B(OPh)_3$ (116 mg, 0.1 mmol) and water (1.8 μL, 0.1 mmol). Under an argon flow through the side-arm of the Schlenk flask, dry toluene (2 mL) was added through the top of the Teflon valve. The flask was sealed by closing the Teflon valve, and then placed in an 80 ºC oil bath for 1 h. After 1 h, a vacuum (0.5 mm Hg) was carefully applied by slightly opening the Teflon valve to remove the volatiles. After the volatiles were removed completely, a full vacuum was applied and maintained for a period of 30 min at a temperature of 80 ºC (oil bath). The flask was then allowed to cool to room temperature and opened to argon through the side-arm of the Schlenk flask. To the flask containing the pre-catalyst was added amine **127a** (92 mg, 0.50 mmol), benzaldehyde **126a** (51 μL, 0.50 mmol), isocyanide **368a** (57 μL, 0.50 mmol) and toluene (1 mL). The stopcock was sealed, and the reaction mixture was then stirred for 24 h. After 24 h, the reaction was quenched by the addition of water (3 mL). The solution was diluted with EtOAc (2 mL). The organic layer was then

separated, and the aqueous layer was extracted by EtOAc (5 mL × 3). The combined organic solution was then washed with brine, dried over anhydrous Na_2SO_4, filtered and concentrated *in vacuo* to afford crude reaction mixture. Unfortunately, no **371a** was observed based on the ^1H NMR analysis of the crude reaction mixture. The imine **78a** was observed.

d) Passerini reaction

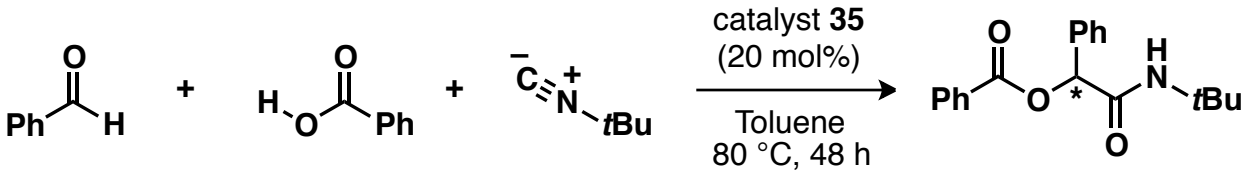

127a + **334a** + **368a** → **377a**

35% y, 6% ee

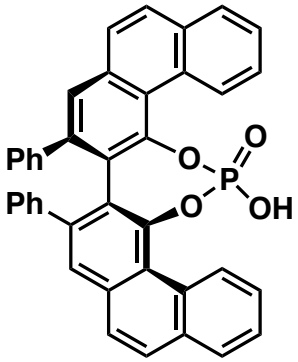

35
(*S*)-VAPOL-PO_3H

2-(*tert*-butylamino)-2-oxo-1-phenylethyl benzoate 377a: To a 25 mL flame-dried Schlenk flask flushed with argon was added (*S*)-VAPOL Phosphoric acid **35** (0.1 mmol) and toluene (1 mL). To the catalyst solution was added benzaldehyde **126a** (51 μL, 0.50 mmol), isocyanide **368a** (57 μL, 0.50 mmol) and the mixture was stirred for 5 min at room temperature. Benzoic acid **334a** (61 mg, 0.50 mmol) was then added in one portion followed by the addition of toluene (0.5 mL). The mixture was then stirred for 48 h. The reaction was quenched by the addition of

sat. $NaHCO_3$ (3 mL). The solution was diluted with EtOAc (2 mL). The organic layer was then separated, and the aqueous layer was extracted by EtOAc (5 mL × 3). The combined organic solution was then washed with brine, dried over anhydrous Na_2SO_4, filtered and concentrated *in vacuo* to afford crude product. Purification by silica gel chromatography (35 mm × 350 mm column, 9:1 hexanes/EtOAc as eluent) afforded product **377a** (mp. 149-150 ºC) as a white solid in 35% isolated yield (54.5 mg, 0.175 mmol). The optical purity of **377a** was determined to be 6% ee by HPLC analysis (CHIRALCEL OD column, 99:01 hexanes/*i*PrOH at 222 nm, flow-rate: 0.7 mL/min). Retention times, R_t = 42.42 min (major enaniomer, **377a**) and R_t = 52.24 min (minor enantiomer, *ent*-**377a**).

Spectral data for **377a**: R_f = 0.24 (1:9 EtOAc/Hexanes) ^{1}H NMR ($CDCl_3$, 300 MHz) δ 1.35 (s, 9 H), 5.98 (br s, 1H), 6.20 (s, 1H), 7.34-7.52 (m, 7H), 7.59 (t, 1H, *J* = 7.5 Hz), 8.07 (d, 2H, *J* = 7.2 Hz); ^{13}C ($CDCl_3$, 75 MHz) δ 28.69, 51.63, 76.09, 164.87, 167.30. These spectral data match those previously reported for this compound.[45]

6.8.9 Attempts towards kinetic resolution of imines (*Table 6.10-6.11*)

a) Kinetic resolution of phenylneopentyl imine *rac*-378 furnishing amine (*S*)-384

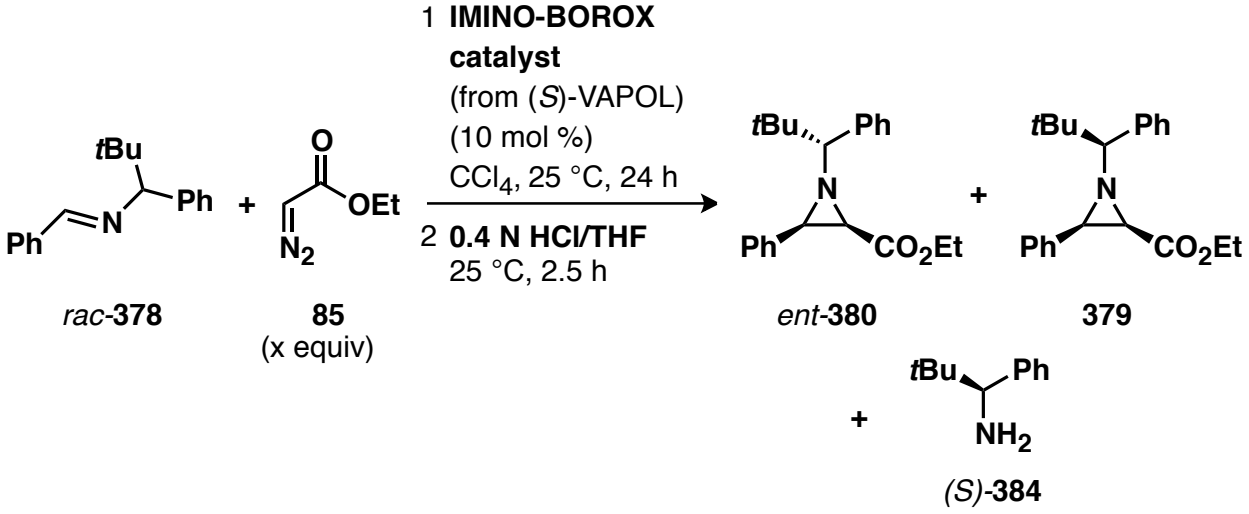

Aziridination: To a 25 mL flame-dried home-made Schlenk flask (see Figure 2.26) equipped with a stir bar and flushed with argon was added (*S)*-VAPOL (54 mg, 0.1 mmol) and $B(OPh)_3$ (87 mg, 0.3 mmol). Under an argon flow through the side-arm of the Schlenk flask, dry toluene (2 mL) was added to dissolve the two reagents. The flask was sealed by closing the Teflon valve, and then placed in an 80 ºC (oil bath) for 1 h. After 1 h, a vacuum (0.5 mm Hg) was carefully applied by slightly opening the Teflon valve to remove the volatiles. After the volatiles are removed completely, a full vacuum is applied and is maintained for a period of 30 min at a temperature of 80 ºC (oil bath). The flask was then allowed to cool to room temperature and open to argon through side-arm of the Schlenk flask. To the flask containing the pre-catalyst was added aldimine *rac*-**378** (mg, 1.00 mmol) and CCl_4 (2 mL) under argon flow through side-arm of the Schlenk flask. The reaction mixture was stirred for 5 min to give a light yellow solution. To this solution was rapidly added EDA **85** (52 μL, 0.5 mmol) followed by closing the Teflon valve. The resulting mixture was stirred for 24 h at room temperature. The reaction was dilluted by addition of hexane (6 mL). The reaction mixture was then transferred to a 100 mL round bottom flask. The reaction flask was rinsed with dichloromethane (5 mL × 2) and the rinse was added to the 100 mL round bottom flask. The resulting solution was then concentrated *in vacuo* followed by exposure to high vacuum (0.05 mm Hg) for 1 h to afford the crude mixture. The conversion was 50% of *rac*-**378** as determined by the ^{1}H NMR of the crude reaction mixture.

Hydrolysis: To a 50 mL round bottom flask was taken the crude reaction mixture and THF (10 mL). To this solution was added HCl (2 mL, 0.4 N) dropwise and the resulting mixture stirred

for 2.5 h. A continuous stirring was maintained during the addition of the acid. After 2.5 h, the reaction mixture was extracted with ether (15 mL × 3) to get crude aziridine *ent*-**380**. The aqueous layer was treated with saturated aqueous Na_2CO_3 to bring the solution up to pH = 9. The resulting aqueous layer was further extracted with ether (10 mL × 8). The combined organic layer was then washed with brine, dried over anhydrous $MgSO_4$, filtered and concentrated *in vacuo* to afford the crude amine (*S*)-**384**.

Purification:

a) aziridine *ent*-**380**: Purification of the crude aziridine by silica gel chromatography (20 mm × 200 mm column, 35:1 hexanes/EtOAc as eluent) afforded pure *cis*-aziridine *ent*-**380** as a white solid (mp 47-52 ºC) in 41% isolated yield (138 mg, 0.41 mmol); dr (*ent*-**380**:**379**) = 20:1. The optical purity of *ent*-**380** was determined to be 94% *ee* by HPLC analysis (CHIRALPAK AD column, 99.5:0.5 hexane/2-propanol at 225nm, flow-rate: 1.0 mL/min): retention times; R_t = 6.8 min (major enantiomer, *ent*-**380**) and R_t = 8.8 min (minor enantiomer, **380**).

Spectral data for *ent*-**380**: R_f = 0.12 (1:35 EtOAc/hexanes). ^{1}H NMR ($CDCl_3$, 300 MHz) δ 0.99 (t, *J* = 7.1 Hz, 3H), 1.03 (s, 9H), 2.60 (s, 1H), 2.68 (d, *J* = 6.6 Hz, 1H), 2.73 (d, *J* = 6.6 Hz, 1H), 3.95 (q, *J* = 7.1 Hz, 2H), 7.11-7.39 (m, 10H); ^{13}C ($CDCl_3$, 75 MHz) δ 13.94, 27.27, 36.45, 44.52, 51.73, 60.43, 83.47, 126.84, 126.93, 127.22, 127.48, 127.68, 129.22, 135.54, 140.12, 167.82; $[\alpha]_D^{20}$ +82.5 (*c* 1.0, $CHCl_3$ on 94% ee material (HPLC). These spectral data match those previously reported for this compound.[38]

b) amine (*S*)-**384**: Purification of the crude amine by silica gel chromatography (20 mm × 200 mm column, 4:1:0.1 hexanes/EtOAc/MeOH as eluent) afforded pure amine (*S*)-**384** as a colorless oil in 34% isolated yield (56 mg, 0.34 mmol). The optical purity of (*S*)-**384** was determined to be 66% *ee* by HPLC analysis (CHIRALCEL OD-H column, 99:1 hexane/2-propanol at 250nm, flow-rate: 1.0 mL/min): retention times; R_t = 7.9 min (major enantiomer, (*S*)-**384**) and R_t = 4.2 min (minor enantiomer, (*R*)-**384**).

Spectral data for (*S*)-**384:** R_f = 0.24 (4:1:0.1 hexanes/EtOAc/MeOH). ^{1}H NMR ($CDCl_3$, 300 MHz) δ 10.89 (s, 9H), 1,42 (brs, 2H), 3.69 (s, 1H), 7.20-7.29 (m, 5H); ^{13}C NMR ($CDCl_3$, 75 MHz) δ 26.42, 34.89, 65.20, 126.60, 127.37, 128.13, 143.68. These spectral data match those previously reported for this compound.[44]

b) Kinetic resolution of phenylneopentyl imine *rac*-**378** furnishing amine (*S*)-**385**

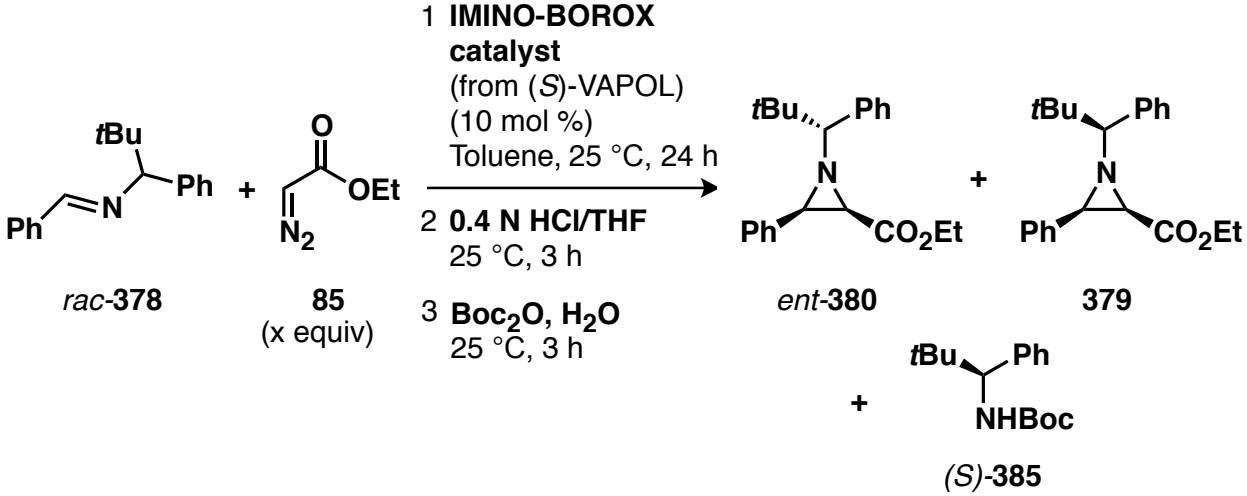

Aziridination: Same as above except that the pre-catalyst was made using (*S)*-VAPOL (54 mg, 0.1 mmol), $B(OPh)_3$ (116 mg, 0.4 mmol) and water (1.8 μL, 0.1 mmol). The reaction was

performed in toluene. The conversion was 44% of *rac*-**378** as determined by the ^{1}H NMR of the crude reaction mixture. dr (*ent*-**380**:**379**): 10:1.

Hydrolysis and Boc protection: To a 50 mL round bottom flask was taken the crude reaction mixture and THF (10 mL). To this solution was added HCl (4 mL, 0.4 N) dropwise and the resulting mixture stirred for 3 h. A continuous stirring was maintained during the addition of the acid. After 2.5 h, the reaction mixture was extracted with ether (15 mL × 3) to get crude aziridine *ent*-**380**. The aqueous layer was treated with saturated aqueous Na_2CO_3 to bring the solution up to pH = 9. The resulting aqueous layer was further extracted with ether (10 mL × 8). The combined organic layer was then washed with brine, dried over anhydrous $MgSO_4$, filtered and concentrated *in vacuo* to afford the crude amine (*S*)-**384**. To the flask containing crude amine was added H_2O (0.5 mL). The resulting mixture was stirred for 5 min at room temperature. To this mixture was added Boc_2O (126 μL, 0.55 mmol) at room temperature. Transparent droplets were formed and after stirring the reaction mixture, a white emulsion appeared on the surface of the walls of the flask with slow effervescence. A white solid settled down and indicated the completion of the reaction (time = 3 h). The resulting was extracted with EtOAc (5 mL × 3). The combined organic layer was then washed with brine, dried over anhydrous $MgSO_4$, filtered and concentrated *in vacuo* to afford the pure amine (*S*)-**385**.

Purification:

a) aziridine *ent*-**380**: Same as above

b) amine (*S*)-**385**: No purification was carried as the obtained amine was very pure. The reaction afforded pure amine (*S*)-**385** (mp. 111-112 ºC on 77% ee material) as a white solid in 44% isolated yield (116 mg, 0.44 mmol). The optical purity of (*S*)-**385** was determined to be 54% *ee* by HPLC analysis (PIRKLE COVALENT (R,R) WHELK-O 1 column, 99:1 hexane/2-propanol at 225nm, flow-rate: 1.0 mL/min): retention times; R_t = 9.83 min (major enantiomer, (*S*)-**385**) and R_t = 27.17 min (minor enantiomer, (*R*)-**385**).

Spectral data for (*S*)-**385:** R_f = 0.28 (1:9 EtOAc/hexanes). ^{1}H NMR (DMSO-d_6, 500 MHz) δ 0.83 (s, 9H), 1.37 (s, 9H), 4.39 (d, *J* = 10.1 Hz, 1H), 7.20 (t, *J* = 6.8 Hz, 2H), 7.26-7.30 (m, 3H), 7.37 (d, *J* = 10.0 Hz, 1H); ^{13}C (DMSO-d_6, 125 MHz) δ 26.57, 28.28, 34.84, 62.94, 77.57, 126.42, 127.24, 128.43, 140.97, 155.41.; IR (thin film, cm^{-1}) 3285br, 2972s, 1899vs, 1495m, 1366s, 1173s; HRMS (ESI-TOF) *m/z* 264.1960 [$(M+H^+)$; calcd. for $C_{16}H_{26}NO_2$: 264.1964]; $[\alpha]_D^{20}$ –21.3 (*c* 1.0, EtOAc) on 77% ee material (HPLC).

REFERENCES

REFERENCES

(1) Osborn, H. M. I.; Sweeney, J. *Tetrahedron: Asymmetry* **1997**, *8*, 1693-1715.

(2) (a) Pellissier, H. *Tetrahedron* **2010**, *66*, 1509-1555. (b) Müller, P.; Fruit, C. *Chem. Rev.* **2003**, *103*, 2905-2919.

(3) (a) Evans, D. A.; Faul, M. M.; Bilodeau, M. T.; Anderson, B. A.; Barnes, D. M. *J. Am. Chem. Soc.* **1993**, *115*, 5328-5329. (b) Li, Z.; Conser, K. R.; Jacobsen, E. N. *J. Am. Chem. Soc.* **1993**, *115*, 5326-5327. (c) Noda, K.; Hosoya, N.; Irie, R.; Ito, Y.; Katsuki, T. *Synlett* **1993**, 469-471. (d) Kawabata, H.; Omura, K.; Uchida, T.; Katsuki, T. *Chem.–Asian. J.* **2007**, *2*, 248-256. (e) Subbarayan, V.; Ruppel, J. V.; Zhu, S.; Perman, J. A.; Zhang, X. P. *Chem. Commun.* **2009**, 4266-4268.

(4) Deiana, L.; Dziedzic, P.; Zhao, G. L.; Vesely, J.; Ibrahem, I.; Rios, R.; Sun, J. L.; Cordova, A. *Chem.–Eur. J.* **2011**, *17*, 7904-7917.

(5) (a) Hansen, K. B.; Finney, N. S.; Jacobsen, E. N. *Angew. Chem., Int. Ed.* **1995**, *34*, 676-678. (b) Aggarwal, V. K.; Alonso, E.; Fang, G. Y.; Ferrara, M.; Hynd, G.; Porcelloni, M. *Angew. Chem., Int. Ed.* **2001**, *40*, 1433-1436. (c) Aggarwal, V. K.; Ferrara, M.; O'Brien, C. J.; Thompson, A.; Jones, R. V. H.; Fieldhouse, R. *J. Chem. Soc., Perkin Trans. 1* **2001**, 1635-1643. (d) Aggarwal, V. K.; Winn, C. L. *Acc. Chem. Res.* **2004**, *37*, 611-620.

(6) (a) Casarrubios, L.; Perez, J. A.; Brookhart, M.; Templeton, J. L. *J. Org. Chem.* **1996**, *61*, 8358-8359. (b) G. Rasmussen, K.; Anker Jorgensen, K. *J. Chem. Soc., Perkin Trans. 1* **1997**, 1287-1292. (c) Juhl, K.; G. Hazell, R.; Anker Jorgensen, K. *J. Chem. Soc., Perkin Trans. 1* **1999**, 2293-2297. (d) Mayer, M. F.; Hossain, M. M. *J. Organomet. Chem.* **2002**, *654*, 202-209. (e) Morales, D.; Pérez, J.; Riera, L.; Riera, V.; Corzo-Suárez, R.; García-Granda, S.; Miguel, D. *Organometallics* **2002**, *21*, 1540-1545. (f) Krumper, J. R.; Gerisch, M.; Suh, J. M.; Bergman, R. G.; Tilley, T. D. *J. Org. Chem.* **2003**, *68*, 9705-9710. (g) Redlich, M.; Hossain, M. M. *Tetrahedron Lett.* **2004**, *45*, 8987-8990.

(7) (a) Williams, A. L.; Johnston, J. N. *J. Am. Chem. Soc.* **2004**, *126*, 1612-1613. (b) Wipf, P.; Lyon, M. A. *ARKIVOC* **2007**, *xii*, 91-98. (c) Hashimoto, T.; Uchiyama, N.; Maruoka, K. *J. Am. Chem. Soc.* **2008**, *130*, 14380-14381. (d) Akiyama, T.; Suzuki, T.; Mori, K. *Org. Lett.* **2009**, *11*, 2445-2447. (e) Zeng, X.; Zeng, X.; Xu, Z.; Lu, M.; Zhong, G. *Org. Lett.* **2009**, *11*, 3036–3039. (f) Johnston, J. N.; Muchalski, H.; Troyer, T. L. *Angew. Chem., Int. Ed.* **2010**, *49*, 2290-2298.

(8) Hu, G.; Gupta, A. K.; Huang, R. H.; Mukherjee, M.; Wulff, W. D. *J. Am. Chem. Soc.* **2010**, *132*, 14669–14675.

(9) (a) Zhang, Y.; Desai, A.; Lu, A.; Hu, G.; Ding, Z.; Wulff, W. D. *Chem. –Eur. J.* **2008**, *14*, 3785-3803. (b) Zhang, Y.; Lu, Z.; Desai, A.; Wulff, W. D. *Org. Lett.* **2008**, *10*, 5429-5432. (c) Mukherjee, M.; Gupta, A. K.; Lu, Z.; Zhang, Y.; Wulff, W. D. *J. Org. Chem.* **2010**, *75*, 5643-5660. (d) Ren, H.; Wulff, W. D. *Org. Lett.* **2010**, *12*, 4908-4911. (e) Hu, G.; Huang, L.; Huang, R. H.; Wulff, W. D. *J. Am. Chem. Soc.* **2009**, *131*, 15615-15617. (f) Desai, A. A.; Wulff, W. D. *J. Am. Chem. Soc.* **2010**, *132*, 13100-13103. (g) Vetticatt, M. J.; Desai, A. A.; Wulff, W. D. *J. Am. Chem. Soc.* **2010**, *132*, 13104-13107. (h) Desai, A. A.; Morán-Ramallal, R.; Wulff, W. D. *Org. Synth.* **2011**, *88*, 224-237.

(10) (a) Antilla, J. C.; Wulff, W. D. *Angew. Chem., Int. Ed.* **2000**, *39*, 4518-4521. (b) Deng, Y. H.; Lee, Y. R.; Newman, C. A.; Wulff, W. D. *Eur. J. Org. Chem.* **2007**, 2068-2071.

(11) Lu, Z.; Zhang, Y.; Wulff, W. D. *J. Am. Chem. Soc.* **2007**, *129*, 7185-7194.

(12) Hattori, K.; Yamamoto, H. *J. Org. Chem.* **1992**, *57*, 3264-3265.

(13) Hu, G. PhD Dissertation, Michigan State University, 2007.

(14) Gupta, A. K.; Mukherjee, M.; Wulff, W. D. *Org. Lett.* **2011**, *13*, 5866-5869.

(15) Guan, Y.; Wulff, W. D., Unpublished results.

(16) Noels, A. F.; Braham, J. N.; Hubert, A. J.; Teyssie, P. *Tetrahedron* **1978**, *34*, 3495-3497.

(17) Branstetter, B.; Hossain, M. M. *Tetrahedron Lett.* **2006**, *47*, 221-223.

(18) Hashimoto, T.; Naganawa, Y.; Maruoka, K. *J. Am. Chem. Soc.* **2008**, *130*, 2434-2435.

(19) (a) Kano, T.; Hashimoto, T.; Maruoka, K. *J. Am. Chem. Soc.* **2006**, *128*, 2174-2175. (b) Gao, L.; Hwang, G. S.; Lee, M. Y.; Ryu, D. H. *Chem. Commun.* **2009**, 5460-5462.

(20) Hashimoto, T.; Naganawa, Y.; Kano, T.; Maruoka, K. *Chem. Commun.* **2007**, 5143-5145.

(21) (a) Kano, T.; Hashimoto, T.; Maruoka, K. *J. Am. Chem. Soc.* **2005**, *127*, 11926-11927. (b) Chen, W.; Yuan, X. H.; Li, R.; Du, W.; Wu, Y.; Ding, L. S.; Chen, Y. C. *Adv. Synth. Catal.* **2006**, *348*, 1818-1822.

(22) (a) Sibi, M. P.; Stanley, L. M.; Soeta, T. *Org. Lett.* **2007**, *9*, 1553-1556. (b) Sibi, M. P.; Stanley, L. M.; Soeta, T. *Adv. Synth. Catal.* **2006**, *348*, 2371-2375.

(23) (a) Cafieri, F.; Fattorusso, E.; Taglialatela-Scafati, O. *J Nat Prod* **1998**, *61*, 122-125. (b) Cafieri, F.; Fattorusso, E.; Mangoni, A.; TaglialatelaScafati, O. *Tetrahedron* **1996**, *52*, 13713-13720.

(24) (a) El Kaim, L.; Grimaud, L. *Tetrahedron* **2009**, *65*, 2153-2171. (b) Domling, A. *Chem. Rev.* **2006**, *106*, 17-89. (c) Zhu, J. *Eur. J. Org. Chem.* **2003**, *2003*, 1133-1144. (d) Domling, A.; Ugi, I. *Angew. Chem., Int. Ed.* **2000**, *39*, 3169-3210.

(25) Ugi, I. *Angew. Chem., Int. Ed.* **1962**, *1*, 8-21.

(26) Braude, E. A.; Nachod, F. C.; Phillips, W. D.; Zuckerman, J. J. *Determination of Organic Structures by Physical Methods*; Academic Press: New York, 1955.

(27) Pan, S. C.; List, B. *Angew. Chem., Int. Ed.* **2008**, *47*, 3622-3625.

(28) Huang, L.; Wulff, W. D., Unpublished results.

(29) Mukherjee, M. PhD Dissertation, Michigan State University, 2012.

(30) (a) McFarland, J. W. *J. Org. Chem.* **1963**, *28*, 2179-2181. (b) Keung, W.; Bakir, F.; Patron, A. P.; Rogers, D.; Priest, C. D.; Darmohusodo, V. *Tetrahedron Lett.* **2004**, *45*, 733-737. (c) Giovenzana, G. B.; Tron, G. C.; Paola, S. D.; Menegotto, I. G.; Pirali, T. *Angew. Chem., Int. Ed.* **2006**, *45*, 1099-1102. (d) Diorazio, L. J.; Motherwell, W. B.; Sheppard, T. D.; Waller, R. W. *Synlett* **2006**, *2006*, 2281,2283. (e) Tanaka, Y.; Hasui, T.; Suginome, M. *Org. Lett.* **2007**, *9*, 4407-4410. (f) Tanaka, Y.; Hidaka, K.; Hasui, T.; Suginome, M. *Eur. J. Org. Chem.* **2009**, 1148-1151.

(31) Yue, T.; Wang, M.-X.; Wang, D.-X.; Masson, G.; Zhu, J. *Angew. Chem., Int. Ed.* **2009**, *48*, 6717-6721.

(32) Hashimoto, T.; Kimura, H.; Kawamata, Y.; Maruoka, K. *Angew. Chem., Int. Ed.* **2012**, *ASAP*.

(33) Passerini, M. *Gazz. Chim. Ital.* **1921**, *51*, 126.

(34) (a) Kusebauch, U.; Beck, B.; Messer, K.; Herdtweck, E.; Dömling, A. *Org. Lett.* **2003**, *5*, 4021-4024. (b) Andreana, P. R.; Liu, C. C.; Schreiber, S. L. *Org. Lett.* **2004**, *6*, 4231-4233. (c) Wang, S. X.; Wang, M. X.; Wang, D. X.; Zhu, J. P. *Angew. Chem., Int. Ed.* **2008**, *47*, 388-391.

(35) (a) Yue, T.; Wang, M.-X.; Wang, D.-X.; Masson, G.; Zhu, J. *J. Org. Chem.* **2009**, *74*, 8396-8399. (b) Denmark, S. E.; Fan, Y. *J. Org. Chem.* **2005**, *70*, 9667-9676. (c) Denmark, S. E.; Fan, Y. *J. Am. Chem. Soc.* **2003**, *125*, 7825-7827.

(36) Yue, T.; Wang, M. X.; Wang, D. X.; Zhu, J. P. *Angew. Chem., Int. Ed.* **2008**, *47*, 9454-9457.

(37) Mukherjee, M.; Wulff, W. D., Unpublished results.

(38) Huang, L.; Zhang, Y.; Staples, R. J.; Huang, R. H.; Wulff, W. D. *Chem.–Eur. J.* **2012**, *18*, 5302-5313.

(39) (a) Lee, J. H.; Han, K.; Kim, M. J.; Park, J. *Eur. J. Org. Chem.* **2010**, 999. (b) Turner, N. J. *Nat. Chem. Biol.* **2009**, *5*, 567. (c) Höhne, M.; Bornscheuer, U. T. *ChemCatChem* **2009**, *1*, 42. (d) Gotor-Fernandez, V.; Gotor, V. *Curr. Opin. Drug Discovery Dev.* **2009**, *12*, 784.

(40) (a) Fu, G. C.; Arp, F. O. *J. Am. Chem. Soc* **2006**, *128*, 14264-14265. (b) Anstiss, M.; Nelson, A. *Org. Biomol. Chem.* **2006**, *4*, 4135. (c) Fu, G. C.; Arai, S.; Bellemin-Laponnaz, S. *Angew. Chem., Int. Ed.* **2001**, *40*, 234-236. (d) Yang, X.; Bumbu, V. D.; Birman, V. B. *Org. Lett.* **2011**, *13*, 4755. (e) Birman, V. B.; Jiang, H.; Li, X.; Guo, L.; Uffman, E. W. *J. Am. Chem. Soc* **2006**, *128*, 6536-6537. (f) Fowler, B. S.; Mikochik, P. J.; Miller, S. J. *J. Am. Chem. Soc.* **2010**, *132*, 2870. (g) Binanzer, M.; Hsieh, S. Y.; Bode, J. W. *J. Am. Chem. Soc.* **2011**, *133*, 19698. (h) Mioskowski, C.; Sabot, C.; Subhash, P. V.; Valleix, A.; Arseniyadis, S. *Synlett* **2008**, 268-272. (i) List, B.; Hoffmann, S.; Nicoletti, M. *J. Am. Chem. Soc* **2006**, *128*, 13074-13075. (j) Backvall, J. E.; Paetzold, J. *J Am Chem Soc* **2005**, *127*, 17620-17621. (k) Mioskowski, C.; Srseniyadis, S.; Valleix, A.; Wagner, A. *Angew. Chem., Int. Ed.* **2004**, *43*, 3314-3317. (l) Krasnov, V. P.; Levit, G. L.; Andreeva, I. N.; Grishakov, A. N.; Charushin, V. N.; Chupakhin, O. N. *Mendeleev Commun.* **2002**, *12*, 27-28. (m) Mittal, N.; Sun, D. X.; Seidel, D. *Org. Lett.* **2012**, *14 3084–3087*.

(41) Kagan, H. B.; Fiaud, J. C. *Top. Stereochem.* **1988**, *18*, 249.

(42) Chakraborti, A. K.; Chankeshwara, S. V. *Org. Lett.* **2006**, *8*, 3259-3262.

(43) Denegri, B.; Kronja, O. *J. Org. Chem.* **2007**, *72*, 8427-8433.

(44) Dalmolen, J.; Tiemersma-Wegman, T. D.; Nieuwenhuijzen, J. W.; van der Sluis, M.; van Echten, E.; Vries, T. R.; Kaptein, B.; Broxterman, Q. B.; Kellogg, R. M. *Chem.–Eur. J.* **2005**, *11*, 5619-5624.

(45) Lagiakos, H. R.; Aguilar, M.-I.; Perlmutter, P. *J. Org. Chem.* **2009**, *74*, 8001-8003.

CHAPTER 7

INDIRECT IMINO-BOROX CATALYSIS MULTICOMPONENT CATALYTIC ASYMMETRIC AZIRIDINATION (MCAZ)

I would like you to do one reaction for the grant!

-William D. Wulff

7.1 Introduction

In recent times, multicomponent reactions have been quite extensively studied and applied in the field of asymmetric catalysis.[1] An ideal multicomponent reaction is one which a) involves readily available starting materials and catalyst, b) is experimentally simple to perform, c) time and cost effective, d) atom-economical, e) is not effected by a diverse range of functionalities in the substrates.[1d] Other than the aforementioned criteria; the reaction also has to be regio- and chemoselective enough such that the compatibility of the several components is matched to the point that any formation of the side products resulting from unwanted reactions between various components is avoided.

Apart from asymmetric aziridinations using chiral auxiliaries,[2] considerable advances have been made in the field of catalytic asymmetric aziridination over the past few years.[3] Primarily, there are two main approaches towards catalytic asymmetric aziridination: a) addition of nitrogen to olefins *via* nitrene transfer with organometallic catalysts[4] or organocatalysis[5] b) addition of carbon to imines *via* metal-carbene transfer (carbene generated from diazo compound or sulfur ylides)[6] or the reaction of a diazo compound with an imine activated by either Lewis

acid[7] or Brønsted acid.[8] It must noted that the asymmetric aziridination reaction between the imines and diazo compounds in the presence of an acid catalyst must not be mistaken for Aza-Darzens reaction as both are mechanistically distinct.[3a] In fact, asymmetric Aza-Darzens reaction is reported with chiral auxiliaries.[3a] As discussed in previous chapters, our aziridination protocol is a Brønsted acid catalyzed reaction (Figure 7.1A).[9] However, to the best of our knowledge, no example of a multicomponent catalytic asymmetric aziridination has been reported.[1,10] Nishimura and coworkers have reported a stoichiometric asymmetric multicomponent aziridination of olefins.[11] A true multicomponent reaction involves the reaction of three or more reagents added simultaneously.[1] Multi-component reactions that involve reaction between two reagents and then interception of the resulting intermediate by the addition of a third reagent are sequential component reactions.[1,8d] Herein, we report the first multi-component catalytic asymmetric aziridination (MCAZ) which satisfies all the criteria discussed above and incorporates the most simplified protocol yet developed for our catalytic asymmetric aziridination reaction (Figure 7.1B).[12]

Figure 7.1 (**A**) Catalytic asymmetric aziridination of imines. (**B**) three-component catalytic asymmetric aziridination. (**C**) five-component catalyst assembly/catalytic asymmetric aziridination.

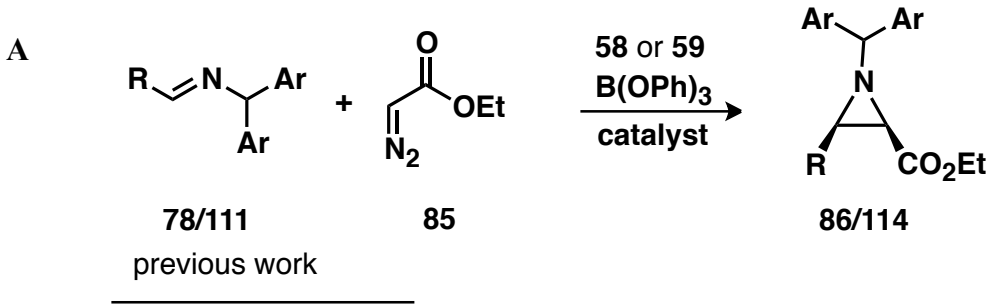

Figure 7.1 cont'd

B

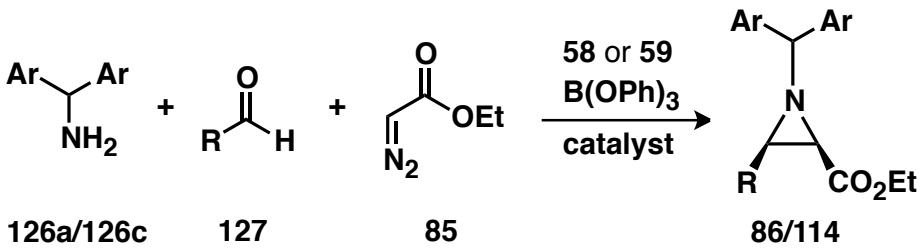

126a/126c **127** **85** **86/114**

unsolved challenge

C

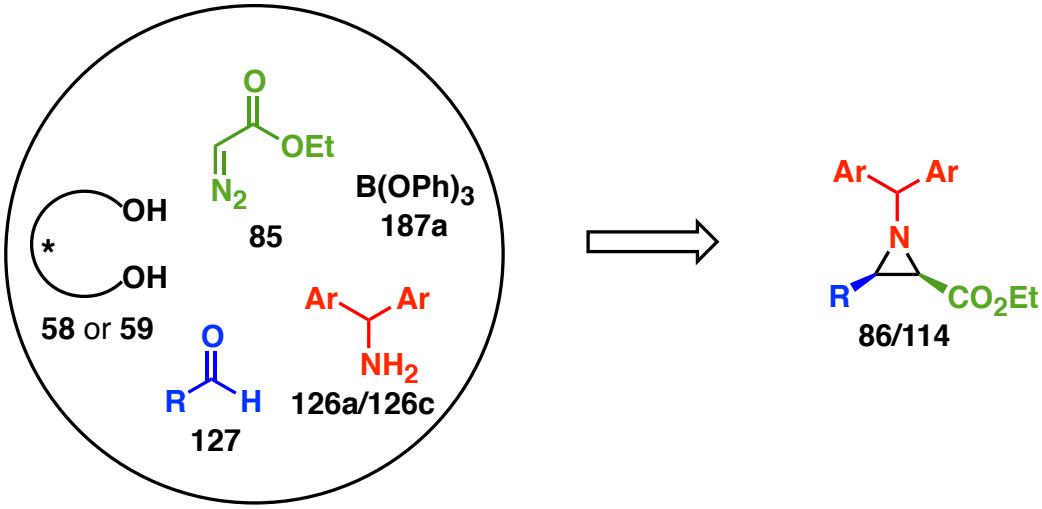

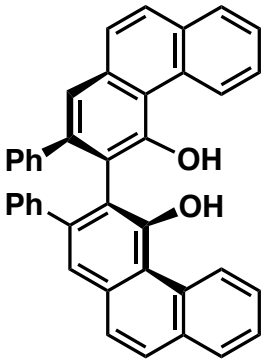

58

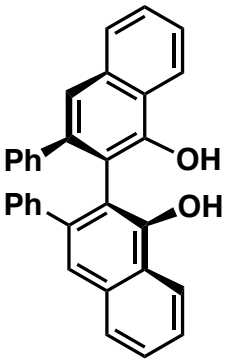

59

new finding

In the course of studying factors that affect catalyst formation and in investigating the processes involved in the three-component catalytic asymmetric aziridination, and in examining the relationship between these two processes, we have discovered that this reaction is actually a five-component process in which the catalyst is assembled by the amine from the ligand and $B(OPh)_3$ and then the catalyst causes imine formation and then finally, aziridine formation (Figure 7.1C).[13]

7.2 The real need for a true multicomponent aziridination reaction

Up to this point, all of the aziridination reactions we have reported have involved pre-formed imines.[9] A drawback to the use of imines of course is the requirement of an additional step. The difficulty in the purification of imines can vary from drawback to limitation. The method of choice for purification is crystallization since most imines tend to decompose on silica gel or upon distillation. For non-crystalline imines this usually necessitates the use of non-purified imines. This is especially true for imines from unbranched aliphatic aldehydes and, as a result, lower yields and inductions are often observed.[9a,9c] A more serious stricture is that for some unbranched alphatic imine substrates, no aziridines are observed at all.[14] After a rigorous analysis of the ^{1}H NMR spectra of the crude reaction mixtures from aziridination reactions performed in our lab over the last five years, we found that in the cases of imines derived unbranched alkyl aldehydes, the imines undergo self-condensation to give rise to a conjugated imine under the aziridination reaction conditions. For example, when imine **110o** was reacted with EDA **85**, the crude reaction mixture reveals the formation of the aziridine **113o** and vinyl imine **333o** whose structure was confirmed by independent synthesis (Scheme 7.1A and 7.1B).[9c] This mixture of species appears to kill the catalyst and this may very well be due to the amine **126b**, which is released in the formation of the condensation product **333o**. More importantly, in

some cases, the imine can't be generated in a clean fashion. For example, when aldehyde **127t** is treated with amine **126c**, long before complete formation of the imine **111t** can be realized, self-condensation of the imine begins to occur which gives rise to the conjugated imine **386t** along with release of amine **126c** (Scheme 7.1B and 7.1C). This imposes a serious limitation on the implementation of the AZ reaction in organic synthesis and the molecules in Figure 7.2 are illustrative of the point.[15]

Scheme 7.1 (**A**) Self-condensation of imine **110o** during aziridination. (**B**) Self condensation of imine **111t** during imine formation. (**C**) ^{1}H NMR spectra of the formation of imine **111t** at t = 4 h and 21 h

A

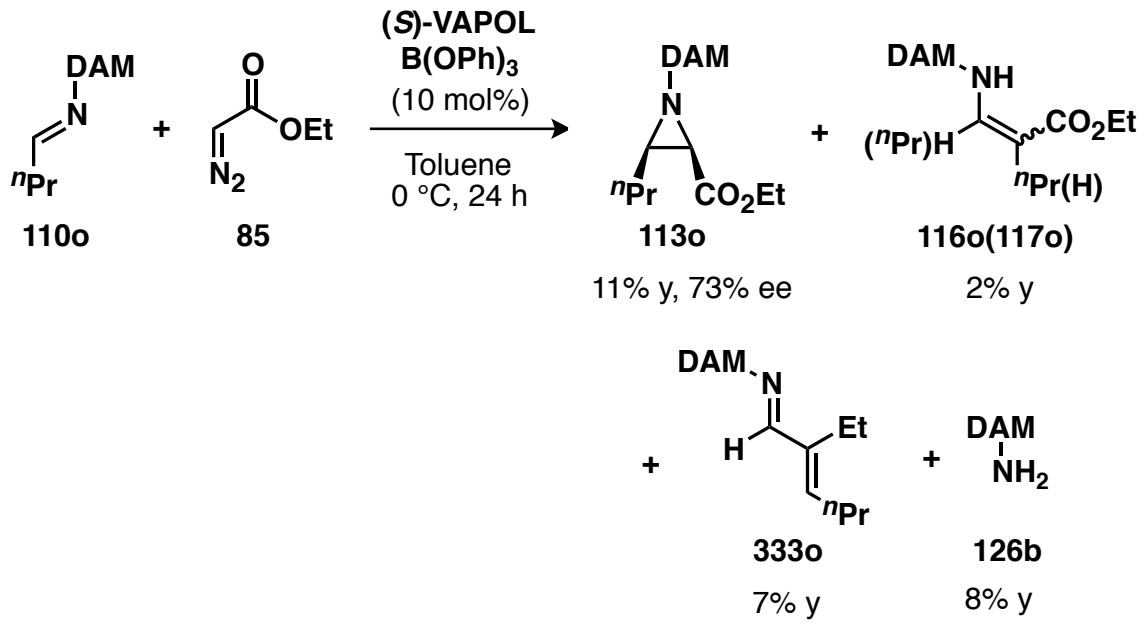

B

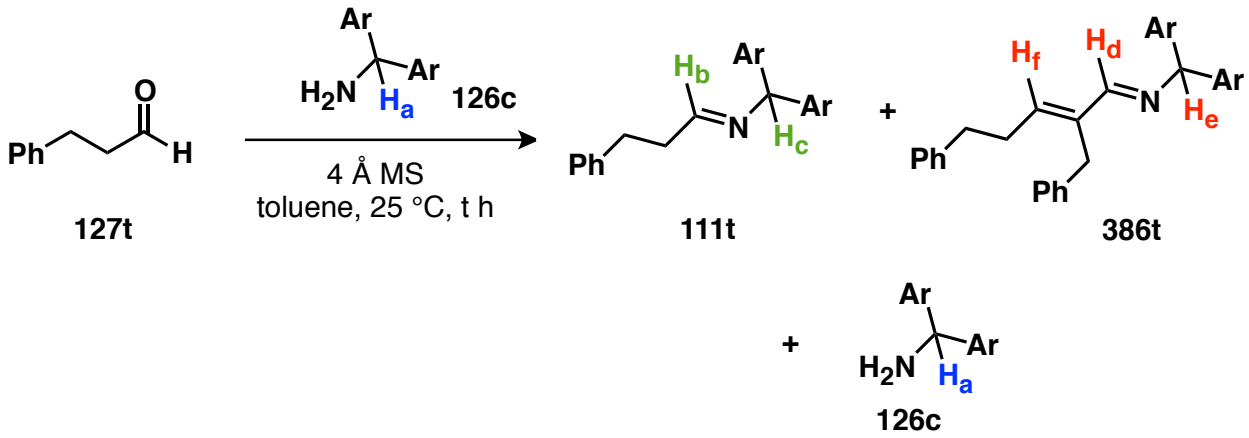

Scheme 7.1 cont'd

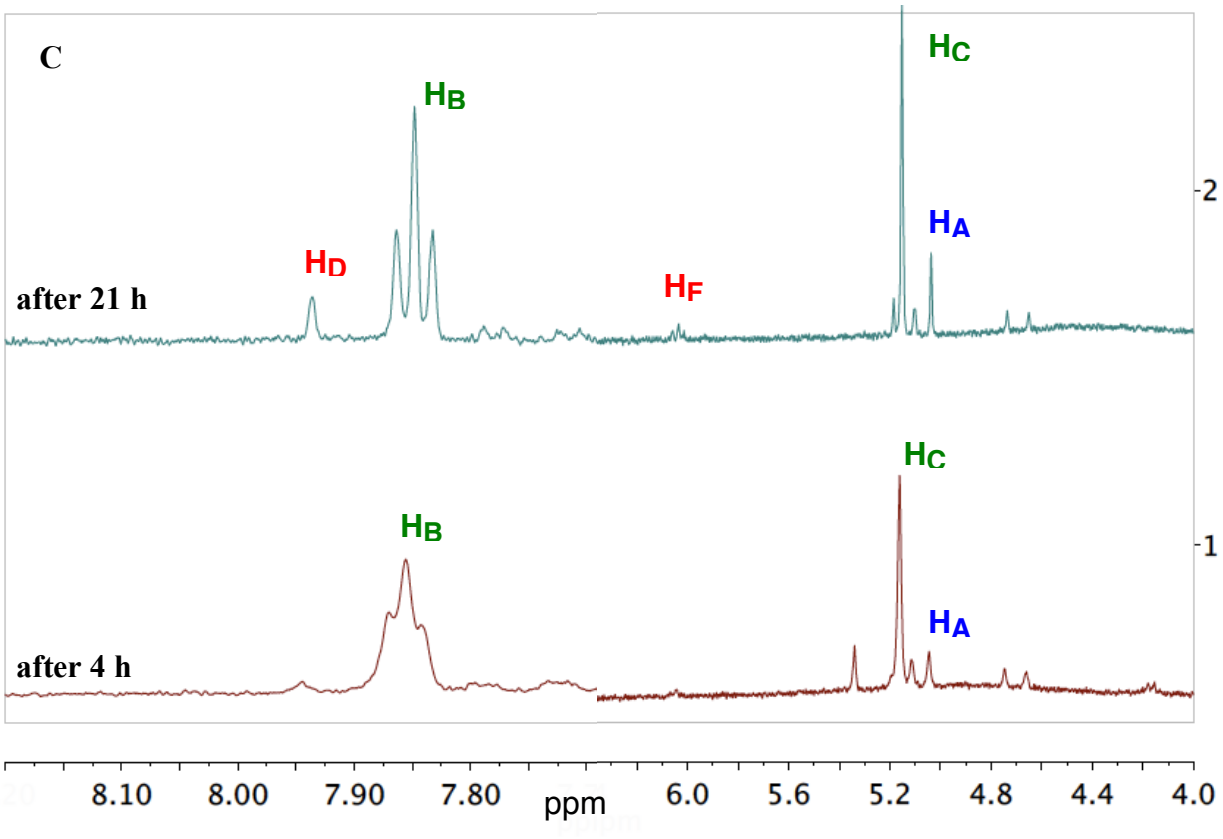

Figure 7.2 (**A**) Biologically important alkyl aziridines. **387**: antimicrobial activity against Gram-positive bacteria.[15b] **388** and **389**: cytotoxic and antimicrobial activity.[15c] **390**: inhibitor of arachidonate epoxygenase.[15d] (**B**) Sphinganine family (**391-394**) of biologically important compounds resulting from the ring-opening from alkyl aziridines.[15e]

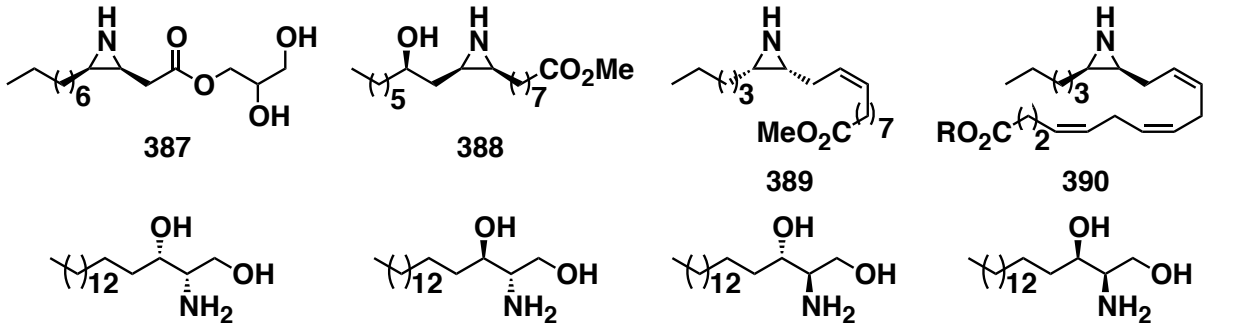

Additionally, an ideal multicomponent reaction is supposed to be experimentally simple to perform. The shortcoming of the optimized protocol for the catalytic asymmetric aziridination reaction include the need to generate a pre-catalyst (mixture of B1 **106/107** and B2 **108/109**, Scheme 7.2) from the VAPOL or VANOL ligand and $B(OPh)_3$. Henceforth, the secondary aim of the work was to simplify the overall procedure, thus developing a multicomponent aziridination reaction avoiding the generation of the pre-catalyst and thus validating its practical utility.

7.3 Can any or all the components of the proposed MCAZ reaction generate the boroxinate catalyst?

The VAPOL ligand and commercial $B(OPh)_3$ will react when heated to give a pre-catalyst which is a mixture of the mesoborate **106** (B1) and the pyroborate **108** (B2) with the latter typically predominating in ratios ranging from 4:1 to 20:1 depending on the exact protocol for catalyst formation (Scheme 7.2).[9a] Treatment of the mixture of **106** and **108** with imine **78a/111a** at room temperature leads to the formation of the chiral boroxinate **188a/190a** (B3).[9f,9h] Since this species has a boroxine ring as its core, we have decided to classify this family of catalysts as *BOROX* catalysts (Chapter 2). The BOROX species **188a/190a** is an ion pair consisting of a protonated base (imine) as the cation and a chiral borate as the anion in the form of a boroxinate: a boroxine in which one of the borons is four-coordinate. It has been shown that the active catalyst in the catalytic aziridination reaction[9f,9h] is an IMINO-BOROX catalyst **188a/190a**. This BOROX species is presumed to be the active catalyst in an aza-Diels-Alder reaction as well.[16] We have recently reported that the chiral boroxinate **188a/190a** (B3) can also be generated upon treatment of a mixture of the VAPOL ligand **58** and 3 equivalents of

$B(OPh)_3$ with the imine **78a/111a** at room temperature in a few minutes, conditions under which VAPOL and $B(OPh)_3$ do not react.[9f]

Scheme 7.2 Generation of IMINO-BOROX catalysts **190a** and **188a**

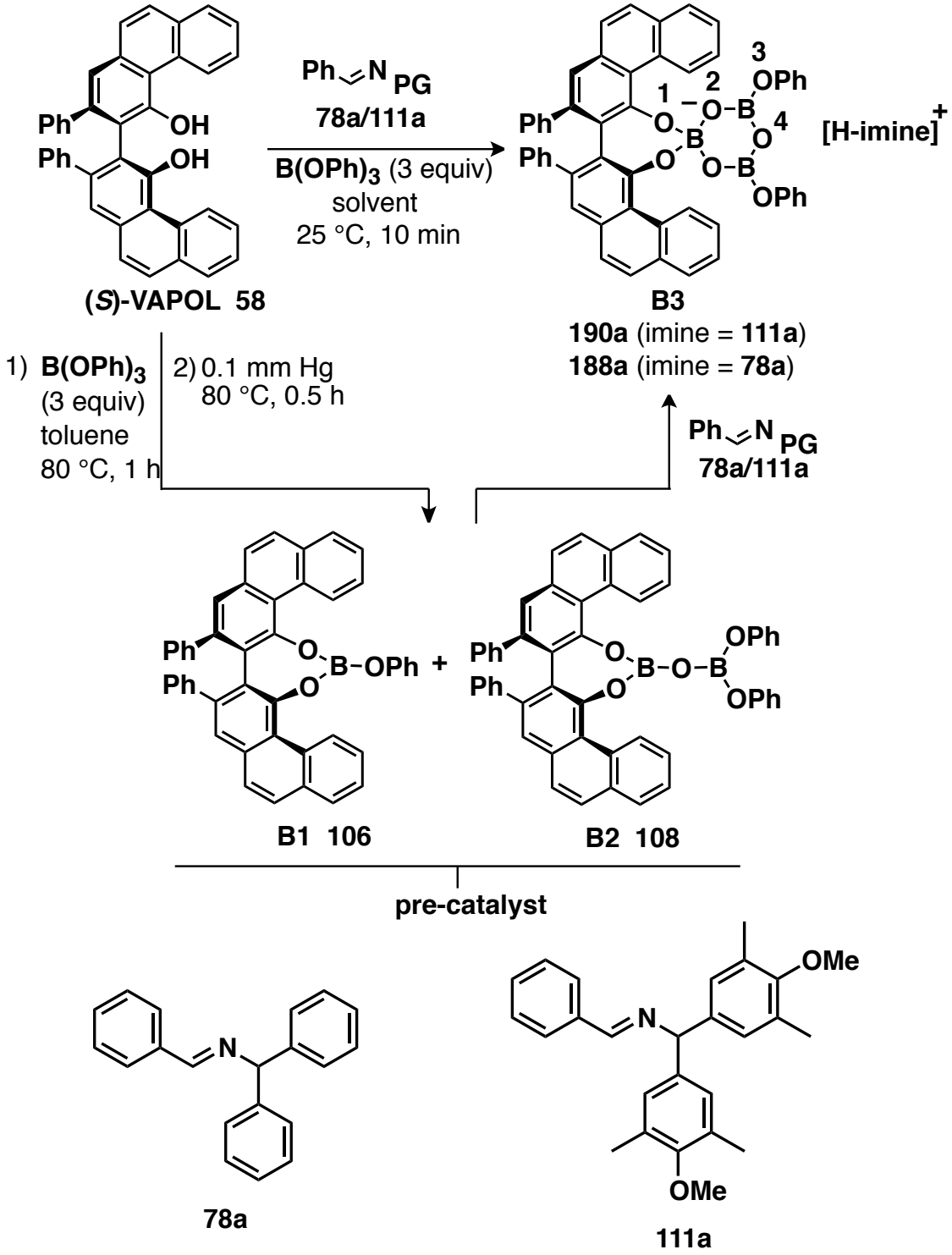

The proposed multicomponent aziridination reaction involves amine **126**, aldehyde **127** and EDA **85** (Figure 7.1B). The question then naturally arises: whether an amine would induce chiral boroxinate complex, and if yes, then whether other species like aldehyde **127** and EDA **85** would also generate a boroxinate which, in turn, could interfere the boroxinate formation from the amine? A series of NMR experiments were then carried out in search of the answers to these proposed questions. In the absence of a base, mixing (*S*)-VAPOL and $B(OPh)_3$ does not result in any detectable amount of a boroxinate (B3) species (Chapter 2). Given the greater basicity of an amine versus an imine, it was anticipated that the MEDAM amine **126c** could also generate the boroxinate catalyst **215b** (Scheme 7.3) from VAPOL and $B(OPh)_3$ in much the same way as does imine **111a** (Scheme 7.2) and indeed this was confirmed by NMR analysis (Table 2.7 and Figure 2.9, Chapter 2). In fact, primary, secondary and tertiary amines all induce the formation of an AMINO-BOROX catalyst of the type **215** (B3) which displays a characteristic bay region proton doublet at δ ~10.3 ppm in ^{1}H NMR and a sharp resonance in the ^{11}B NMR spectrum at δ ~ 5-6 ppm (Table 2.7 and Figure 2.9, Chapter 2).

Scheme 7.3 Generation of AMINO-BOROX catalysts **215a** and **215b**

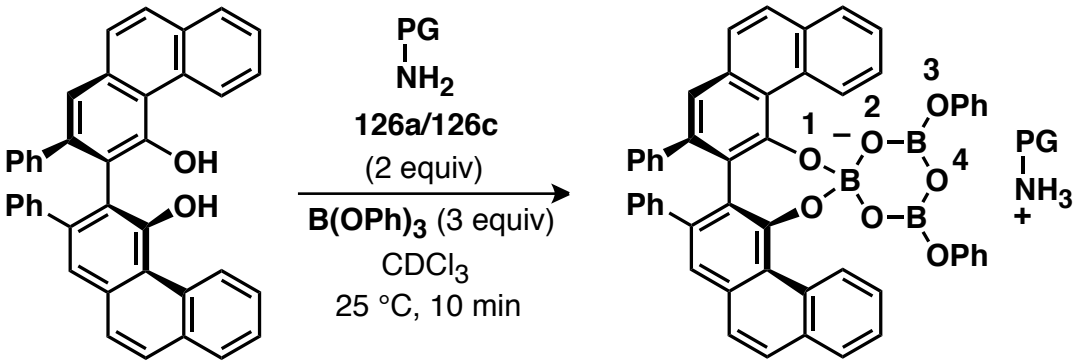

Aldehydes **127** are not strong enough bases to induce boroxinate formation (Figure 2.19, Chapter 2). Ethyl diazoacetate (EDA) does not induce the formation of a boroxinate, but, nonetheless there is a very rapid reaction (≤10 min) leading to the alkylation of one of the phenol functions of VAPOL via a formal insertion of a carbene into the O-H bond which results in the formation of the ester **230** in 80% yield (Scheme 7.4A). It seems like the initial analysis indicates the feasibility of the first multicomponent aziridination reaction. However, there are certain possible complications for the reaction and these are described below.

7.4 Possible complications for the five-component catalyst assembly/aziridination

As discussed above, the mono-alkylated VAPOL derivative **230** is formed upon treatment of VAPOL with EDA in the presence of $B(OPh)_3$ (Scheme 7.4A). However, there is no reaction between VAPOL and EDA in the absence of $B(OPh)_3$. Nonetheless, this presents at least one potential problem in a five-component catalyst assembly/aziridination of the type shown in Figure 7.1C. The VAPOL ligand could be disenabled by a $B(OPh)_3$ induced reaction with EDA before the amine can assemble the catalyst from the ligand and $B(OPh)_3$.

Scheme 7.4 (**A**) Alkylation of the VAPOL by EDA. (**B**) Common products obtained from the reaction between benzaldehyde and EDA.

A

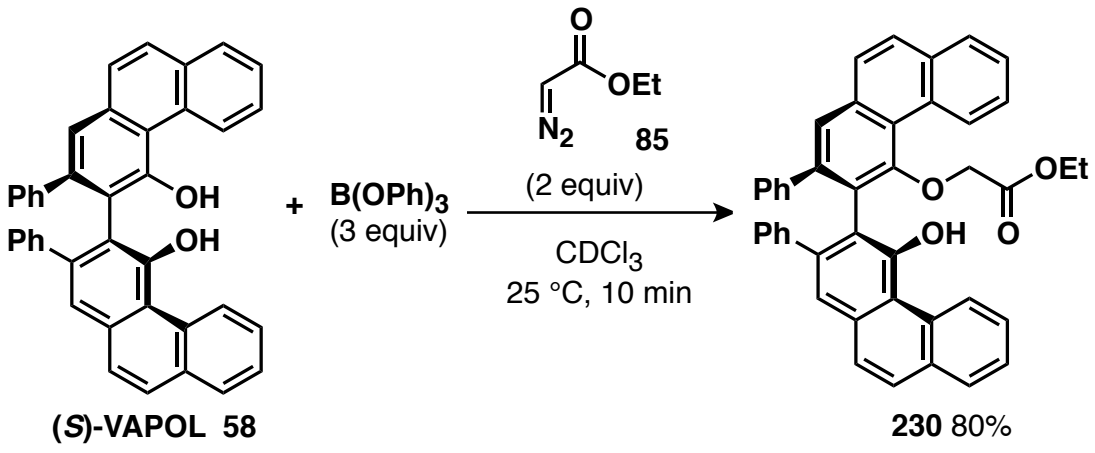

Scheme 7.4 cont'd

B

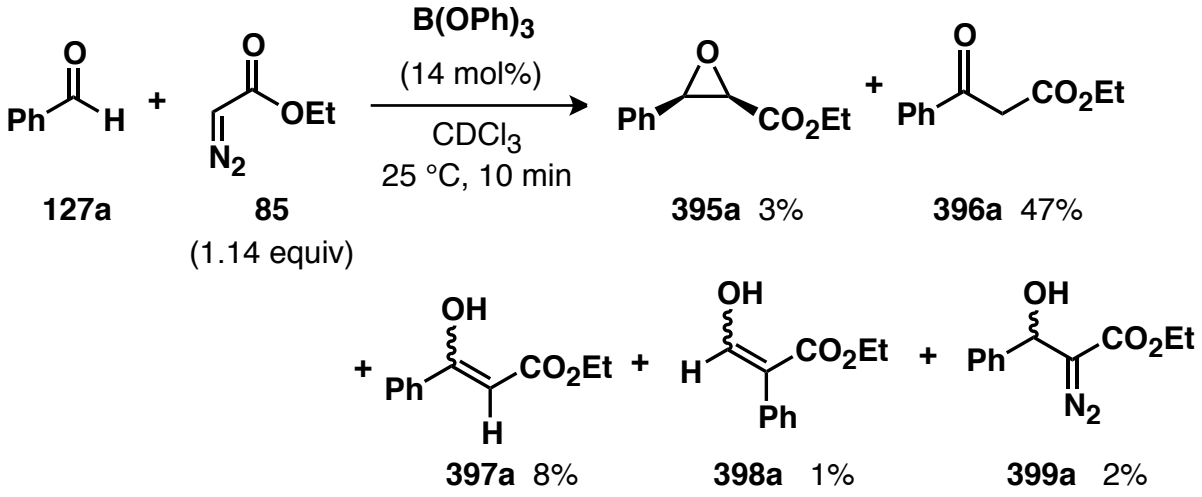

A second possible complication is an unwanted reaction between the aldehyde and EDA. In fact, several different products are known from the reaction of benzaldehyde and EDA mediated by Lewis or Brønsted acids.[17] Indeed, in a control experiment, the reaction of benzaldehyde and 1.14 equiv of ethyl diazoacetate mediated by 14 mol% $B(OPh)_3$ gave the five products shown in Scheme 7.4B with the major component as the β-keto ester **396a** and its tautomer **397a** in a total of 55% yield. In a separate control experiment it was found that there is no reaction between benzaldehyde and EDA in the presence of VAPOL. Nor is there any reaction between benzaldehyde and EDA in either the presence or absence of 4 Å molecular sieves at 25 °C after 24 h. Thus the possible reaction between the aldehyde and EDA mediated by $B(OPh)_3$ is a real concern for the success of the multi-component catalyst assembly/aziridination outlined in Figure 7.1C.

7.5 Optimization and substrate scope of aryl substrates in the MCAZ reaction

With the demonstration that an amine can induce catalyst assembly, the possibility of a multi-component aziridination (MCAZ) was then explored (Table 7.1). Given the problems with aliphatic aldehydes described above, the multi-component aziridination was first examined with aromatic substrates.

7.5.1 Different protocols for the multicomponent *cis*-aziridination (MCAZ)

During optimization, various protocols were examined for the MCAZ reaction. A few selected protocols are presented in Table 7.1. In the first experiment, the VAPOL ligand **A** (**58**) was mixed with 3 equiv of $B(OPh)_3$ **B** (**187a**) and 20 equiv of amine **C** (**126c)** and stirred in toluene at 80 °C for 0.5 h to ensure formation of the boroxinate catalyst and thus avoid any possibility of alkylation of VAPOL by the EDA. This was followed by the addition of the benzaldehyde **D** (**127a**) and 4 Å MS which was stirred for 2 h to ensure imine formation. Upon addition of EDA **E** (**85)** the mixture was stirred at 25 °C for 24 h to give the aziridine **114a** in 92% yield and 95% ee (procedure I).

A true multi-component reaction involves the reaction of three or more reagents added simultaneously.[1c,1d] Multi-component reactions that involve reaction between two reagents and then interception of the resulting intermediate by the addition of a third reagent are sequential component reactions.[1c,1d,8d,10-11] Hence, procedure I in Table 7.1 can be viewed as an example of a sequential component aziridination reaction as the addition of EDA was delayed for 2 h to ensure formation of the imine.[8d] However, when EDA was added immediately after the aldehyde, essentially the same results were obtained (procedures I vs IIA). This suggests that the

present work is an example of a true MCAZ. The data in Table 7.1 reveals that essentially the same results are obtained whether the pre-catalyst is first generated and employed in the multi-component aziridination or whether the boroxinate catalyst is directly generated by treating a mixture of VAPOL and $B(OPh)_3$ with the amine **C** (procedures IIA vs. IIB). It was also revealed that no advantage is to be gained by generating the AMINO-BOROX catalyst by heating to 80 °C rather than simply stirring at room temperature (procedures IIA vs. IIIA and IIB vs. IIIB). The use of the aldehyde **D** as the limiting reagent (0.6 equiv) leads to the complete shutdown of the reaction (procedure IIIC). This suggests that the amine **C** is a competitive inhibitor of the imine in binding to the boroxinate catalyst and this issue will be taken up in greater detail below (Tables 7.8 and 7.9). A comment is needed about the water added for catalyst generation in procedures IIB and IIIB in Table 7.1. Three equivalents of H_2O are required to create the three B-O-B linkages in the boroxinate **215b** from $B(OPh)_3$. The addition of three equivalents of H_2O is absolutely required if the $B(OPh)_3$ is pure but, commercial $B(OPh)_3$ contains sufficient water that the addition of additional water is typically not needed and indeed, our original procedure shown in Scheme 7.2 does not include the addition of H_2O.[9f] The addition of 3 equivalents of H_2O to commercial $B(OPh)_3$ in procedures IIB and IIIB was done to compensate for any variation in quality of commercial $B(OPh)_3$.

Table 7.1 Protocol dependence of the multicomponent aziridination [a]

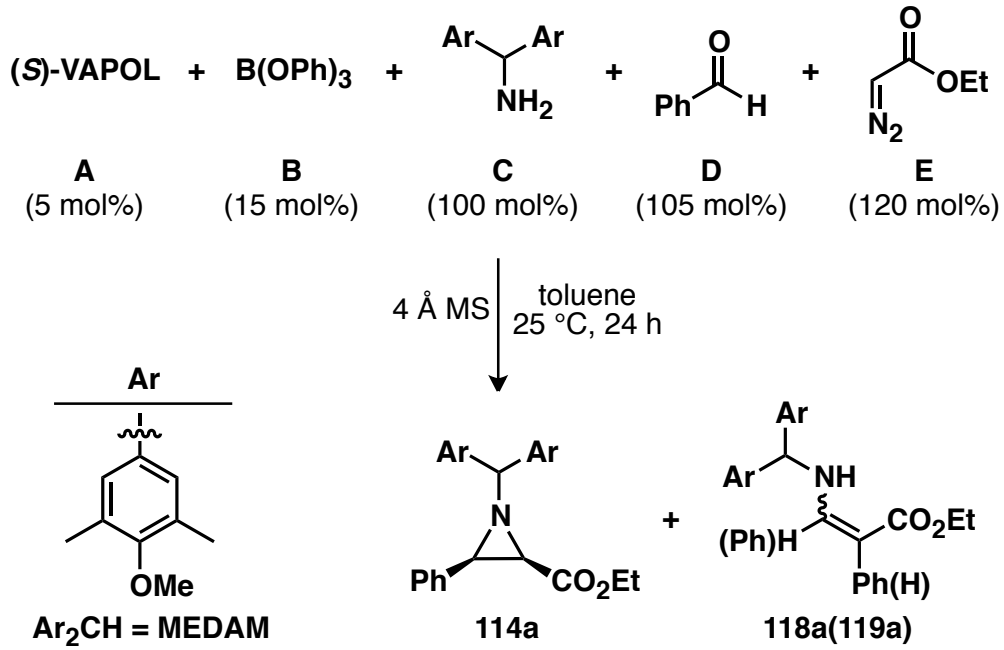

#	Proc	Reaction protocol	Yield **114a** (%) [b]	ee **114a** (%) [c]
1	**I**	**A+B+C** → 1) toluene, 80 °C, 0.5 h → 2) **D**, 4Å MS, 25 °C, 2 h → 3) **E**, 25 °C, 24 h	92	95
2	**IIA**	**A+B+C** → 1) toluene, 80 °C, 0.5 h → 2) **D**, 4Å MS, **E,** 25 °C, 24 h	97	98
3	**IIB**	**A+B** → 1) toluene, H_2O (15 mol%), 80 °C, 1 h, then 0.5 mm Hg, 80 °C, 0.5 h → 2) **C,** toluene, 80 °C, 0.5 h → 3) **D**, 4Å MS, **E,** 25 °C, 24 h	98	98
4	**IIIA**	**A+B+C** → 1) toluene, 25 °C, 1 h → 2) **D**, 4Å MS, **E,** 25 °C, 24 h	98	98

Table 7.1 cont'd

5	**IIIB**	**A**+**B**	1) toluene, H_2O (15 mol%), 80 °C, 1 h, then 0.5 mm Hg, 80 °C, 0.5 h → 3) **C,** toluene, 25 °C, 1 h → 3) **D**, 4Å MS, **E,** 25 °C, 24 h			94	98
6	**IIIC**	**A**+**B**+**C**	1) toluene, 80 °C, 0.5 h → 2) **D***, 4Å MS, **E,** 25 °C, 24 h, * 60 mol%			<1	–

[a] Unless otherwise specified, all reactions were performed with 0.025 mmol (*S*)-VAPOL **A** (5 mol%), 0.075 mmol $B(OPh)_3$ **B** (15 mol%), 0.50 mmol amine **C** (1.0 equiv), 0.525 mmol benzaldehyde **D** (1.05 equiv) and 0.60 mmol of EDA **E** (1.2 equiv) in 1.0 mL toluene (0.5 M in amine) at 25 °C for 24 h. In each case, 150 mg powdered 4Å MS was added immediately preceding benzaldehyde. [b] Isolated Yield. Analysis of the crude reaction mixture indicates >50:1 *cis:trans* selectivity for **114a.** In each case <1% **118a** and **119a** are formed. [c] Determined by HPLC.

7.5.2 Catalyst loading, *N*-substituent and ligand screening

The catalytic asymmetric synthesis of aziridines from imines and diazo compounds has been honed with both benzhydryl and bis-(3,5-dimethylanisyl)methyl (MEDAM) substituents on the imine nitrogen.[9] Thus, prior to the substrate scope, the multi-component aziridination was examined with both benzhydryl amine **126a** and the MEDAM amine **126c** and the results with benzaldehyde are shown in Table 7.2. In addition, the reactions of both amines were screened with both VANOL and VAPOL catalysts and the catalyst loading profile was explored as well. As was found for the reactions of the corresponding imines,[9c] the multi-component aziridination of benzaldehyde with MEDAM amine **126c** gives higher yields and asymmetric inductions than the benzhydryl amine **126a**. Nonetheless, the aziridines from benzhydryl amines can in most cases be crystallized to ≥ 99% ee which is important to note upon considering that benzhydryl

amine **126a** is commercially available while the MEDAM amine **126c** is not.[9a,9i] During this work, another current group member, namely Yong Guan, developed a new ligand (*S*)-*t*Bu-VANOL **198** which proved to be the optimal ligand for aziridination with benzhydryl imines **78**.[18] It was found that the multicomponent aziridination works well with this ligand giving results better than VAPOL and VANOL (Table 7.2, entry 8). However, as was observed with the corresponding imines, the multi-component aziridinations with VAPOL and VANOL catalysts are very similar with a slight edge in asymmetric induction to the VAPOL catalyst.[9a,9i] The optimal catalyst loading for the reaction with the MEDAM amine is 3-5 mol%. This reaction does not go to completion in 24 h with 1 mol% of either the VANOL or VAPOL catalyst but both go to completion with a 3 mol% catalyst loading. The reaction is severely impeded by the absence of molecular sieves and gives only a 35% yield of the aziridine **114a** along with a 52% yield of the unreacted imine **111a** generated from amine **126c** and benzaldehyde (entry 14). Finally, in the optimization studies it was noted that 4 Å molecular sieves was superior to 5 Å molecular sieves which gives more unknown side-products and a lower yield of the aziridine (entries 14 *vs.* 15).

Table 7.2 Catalyst Loading, *N*-substituent and Ligand Screening [a]

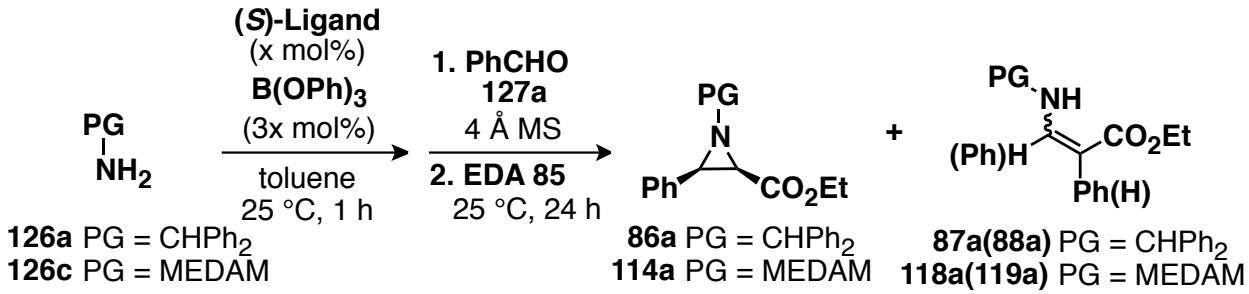

Table 7.2 cont'd

#	Ligand	PG	Cat. x mol%	Yield **86a**/**114a** (%) [b]	ee **86a**/**114a** (%) [c]	cis/trans [d]	Enamines (%) [e]
1	(*S*)-VAPOL	Bh	10 [f]	75	92	33:1	7
2	(*R*)-VANOL	Bh	10 [f]	78	–88	50:1	15
3	(*S*)-VAPOL	Bh	10	85	91	25:1	9
4	(*R*)-VANOL	Bh	10	77	–88	50:1	15
5	(*S*)-VAPOL	Bh	5	77	92	50:1	6
6	(*R*)-VANOL	Bh	5	72	91	50:1	7
7	(*S*)-VAPOL	Bh	5	77 [g]	86	50:1	7
8	(*S*)-*t*Bu-VANOL	Bh	5	80	97	> 50:1	6
9	(*S*)-VAPOL	MEDAM	10 [f]	90	98	> 50:1	<1
10	(*R*)-VANOL	MEDAM	10 [f]	93	–96	> 50:1	<1
11	(*S*)-VAPOL	MEDAM	5 [f]	97	98	> 50:1	<1
12	(*R*)-VANOL	MEDAM	5 [f]	90	–96	> 50:1	<1
13	(*S*)-VAPOL	MEDAM	5	98	98	> 50:1	<1
14	(*S*)-VAPOL	MEDAM	5	(35) [h,i]	–	> 50:1	<1
15	(*S*)-VAPOL	MEDAM	5	70 [j]	98	> 50:1	2
16	(*S*)-VANOL	MEDAM	5	95	95	> 50:1	<1
17	(*S*)-VAPOL	MEDAM	3	92	98	> 50:1	5
18	(*S*)-VANOL	MEDAM	3	94	97	> 50:1	6
19	(*S*)-VAPOL	MEDAM	1	(20)	–	> 50:1	<1
20	(*R*)-VANOL	MEDAM	1	(31)	–	> 50:1	<1
21	(*S*)-VAPOL	MEDAM	1	(48) [g]	–	> 50:1	4
22	(*R*)-VANOL	MEDAM	1	(29) [g]	–	> 50:1	<1

[a] Unless otherwise specified, all reactions were performed with procedure IIIA in Table 7.1 with 0.50 mmol amine **126a** or **126c** (1.0 equiv, 0.5 M), 0.525 mmol benzaldehyde **127a** (1.05 equiv) and 0.60 mmol of EDA **85** (1.2 equiv) and went to 100% completion. [b] Isolated Yield. Yield in parenthesis determined by ^{1}H NMR spectra with Ph_3CH as internal standard. [c] Determined by HPLC. [d] Ratio determined by integration of the methine protons of *cis*- and *trans*-aziridine in the ^{1}H NMR spectrum of the crude reaction mixture. [e] Determined by integration of the NH signals of enamines relative to the methine proton of *cis* aziridine in the ^{1}H NMR spectrum of the crude reaction mixture. [f] Reaction performed with procedure IIA in Table 7.1. [g] 8 equiv EDA used. [h] Reaction performed without 4 Å MS. [i] The ^{1}H NMR spectra of the crude reaction mixture indicates the presence of 52% unreacted imine **111a**. [j] Reaction performed with 5 Å MS.

7.5.3 Substrate scope for aromatic aldehydes

The general screen for the multi-component (MCAZ) was taken forward with the MEDAM amine **126c** since it gives aziridines with both higher yields and asymmetric inductions (Table 7.2) and a 12-fold increased rate over reactions with pre-formed imines.[9b] Likewise, the screen of the MCAZ reaction was pursued with VAPOL **58** since it gave small, but consistently higher inductions than VANOL **59** (Table 7.2). Excellent yields and asymmetric inductions were observed for a number of substituted benzaldehydes including those with both electron-withdrawing and electron-donating groups (Table 7.3). The reaction with benzaldehyde **127a** was complete in 1 h with 5 mol% catalyst as monitored by ^{1}H NMR but no attempt was made to determine minimum reaction times with the other substrates. Excellent inductions could also be obtained with hetero-aryl aldehydes giving aziridines **114i** – **114n** in 90 – 97% ee. The yields for the reactions of 2-thiophenyl and 2-furyl carboxaldehydes **127k** and **127l** were moderate but this could be substantially improved by employing excess EDA. There was no attempt made to optimize the amount of EDA. However, the corresponding pyrrole-2-carboxaldehyde **127m** did not give any aziridine (entry 20). It is interesting that pyridine-2-carboxaldehyde **127i** was an effective substrate,[8a] whereas, pyridine-3-carboxaldehyde **127j** failed to give any aziridine (entry 11). The results obtained from MCAZ were comparable to those obtained with imines.[9c]

Table 7.3 Multicomponent aziridination of aryl and hetero-aryl aldehydes [a]

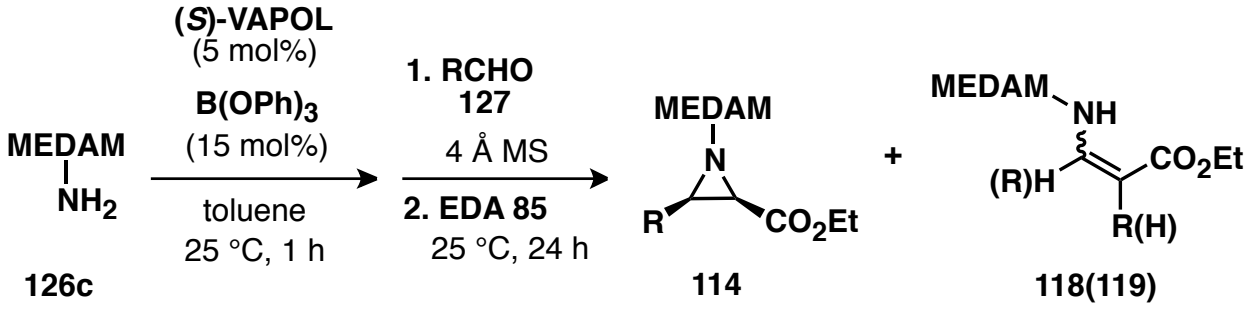

Table 7.3 cont'd

#	R	series	Yield **114** (%) [b]	ee **114** (%) [c]	cis/trans [d]	Enamines (%) [e]
1	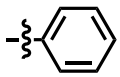	**a**	98	98	50:1	<1
2			97 [f]	98	50:1	<1
3	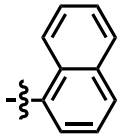	**b**	96	>99	50:1	3
4			94 [f]	99	50:1	4
5	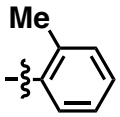	**c**	96	>99	50:1	3
6	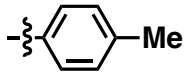	**d**	95	99	50:1	5
7	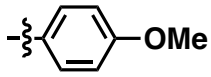	**e**	78	98	20:1	5
8	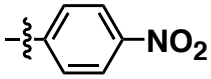	**f**	92	99	50:1	3
9	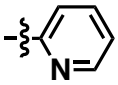	**i**	96	90	>50:1	<1
10			90 [f]	94	>50:1	<1
11	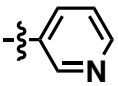	**j**	<1	–	–	–
11	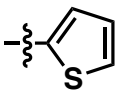	**k**	52	93	12.5:1	<1
12			88 [g]	97	25:1	<1
13			(62) [f]	–	9:1	<1
14			(19) [f,h]	–	50:1	<1
15	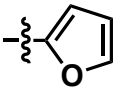	**l**	51 [i]	94	8.3:1	<1
16			65 [g, i]	95	8.5:1	<1
17			40 [f, g, h]	96	8.3:1	<1
18			57 [j]	89	9.3:1	1
19			55 [g, j]	95	7.0:1	3

Table 7.3 cont'd

20	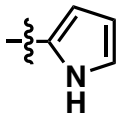	**m**	<1	–	–	–
21	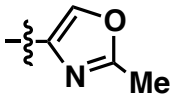	**n**	97 [g, k]	97	> 50:1	<1
22			98 [g, k]	96	> 50:1	<1

[a] Unless otherwise specified, all reactions were performed with procedure IIIA in Table 7.1 with 0.50 mmol amine **126c** (1.0 equiv, 0.5 M), 0.525 mmol aldehyde **127** (1.05 equiv) and 0.60 mmol of EDA **85** (1.2 equiv) and went to 100% completion. [b] Isolated Yield. Yield in parenthesis determined by ^{1}H NMR spectra with Ph_3CH as internal standard. [c] Determined by HPLC. [d] Ratio determined by integration of the methine protons of *cis*- and *trans*-aziridine in the ^{1}H NMR spectrum of the crude reaction mixture. [e] Determined by integration of the NH signals of enamines relative to the methine proton of *cis* aziridine in the ^{1}H NMR spectrum of the crude reaction mixture. [f] Reaction performed with procedure IIA in Table 7.1. [g] 8 equiv EDA used. [h] Reaction performed at –10 °C. [i] The aldehyde was added at –10 °C followed by the addition of EDA at –10 °C and the mixture was stirred at –10 °C for 2 h prior to warming to room temperature. [j] The pre-formed and purified imine **111l**, made from MEDAM-NH_2 **126c** and aldehyde **126l**, was used and EDA was added at –10 °C. The mixture was stirred at –10 °C for 2 h prior to warming to room temperature. Refer Scheme 7.5. [k] The aldehyde was added at –10 °C followed by the addition of EDA was carried out at –10 °C and the mixture was stirred at –10 °C for 15 min prior to warming to room temperature.

The efficacy of the multicomponent reaction is shown in Scheme 7.5. We have compared the preparation of aziridine **114l** by the MCAZ method described here with that of a two-step method involving the isolation of the imine from aldehyde **127l** and amine **126c**. Substantial material loss is encountered in the two-step method as a result of purification of the imine. Also, the asymmetric induction was found to drop by 6 percentage points (Table 7.3, entries 15 *vs*. 18 and Scheme 7.5).

Scheme 7.5 (**A**) Preparation of Imine **111l** (**B**) Synthesis of aziridine **114l** *via* two-step method

A

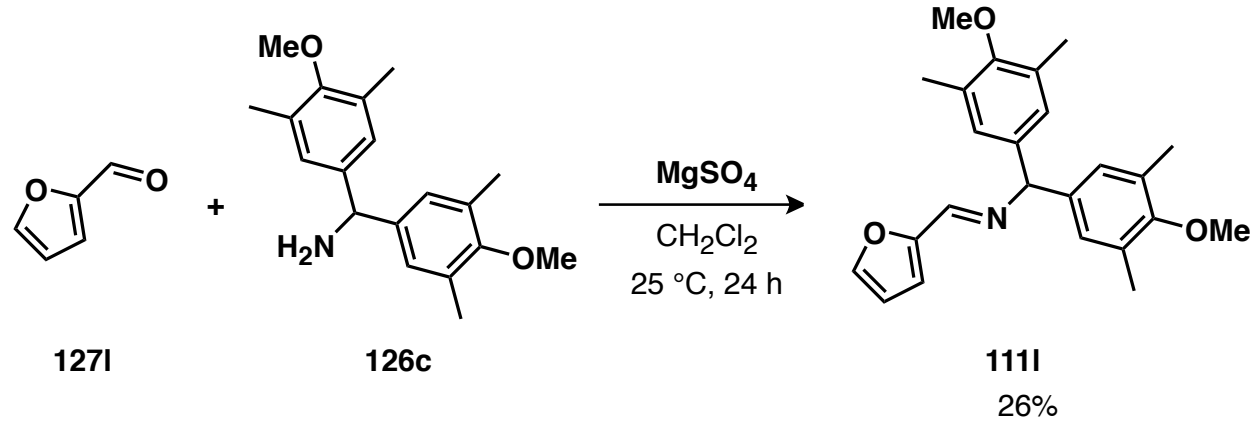

127l **126c** **111l**

26%

B

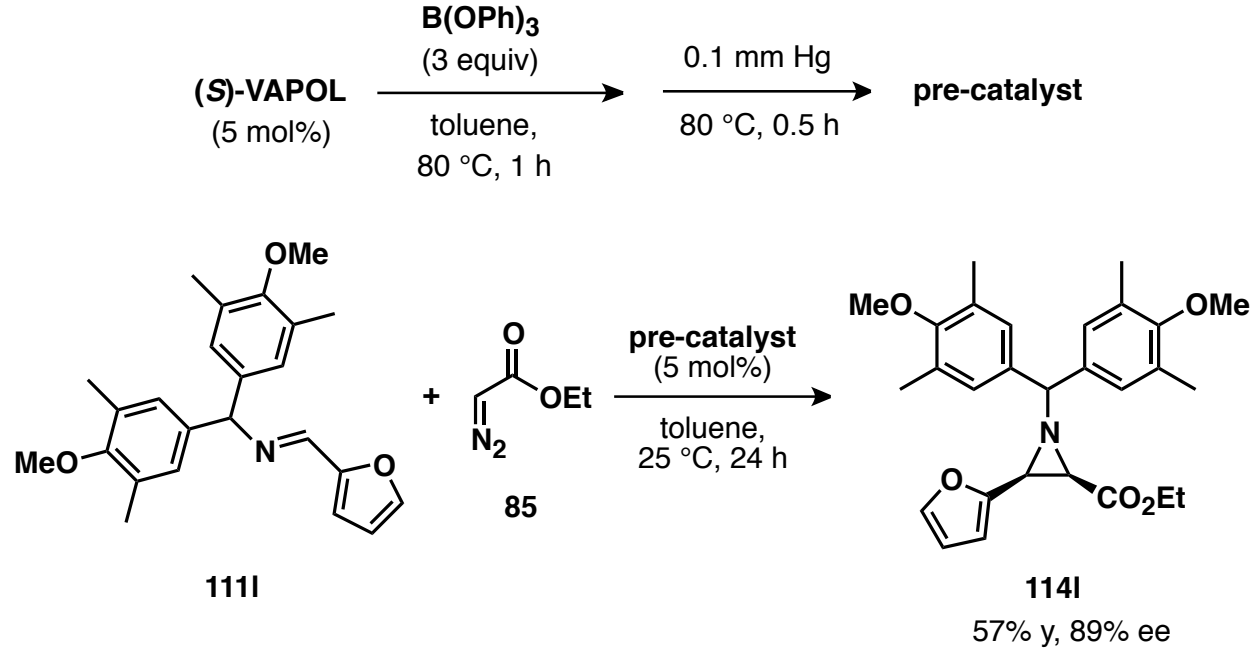

111l **85** **114l**

57% y, 89% ee

7.6 Optimization and substrate scope of alkyl substrates in the MCAZ reaction

Since the whole idea was envisioned to find a general solution for alkyl aziridination, we then decided to examine the MCAZ reaction with *n*-butanal **127o**. However, the procedure optimized for aromatic substrates was found to be non-applicable and further optimization was then carried out and is described below.

7.6.1 Initial optimization using *n*-butanal and *n*-hexadecanal

The problem of imine self-condensation was encountered in the MCAZ of *n*-butanal **127o**. The aziridination of *n*-butanal with MEDAM amine **126c** at room temperature with 5 mol% VANOL catalyst under the conditions in entry 1 of Table 7.4 gives only a 25% yield of aziridine **114o** along with a 20% yield of the condensation product **386o** as well as a 38% yield of the imine **111o** which was generated in-situ but did not undergo complete reaction. The formation of the side-product **386o** was found to be disfavored at lower temperatures. The same reaction with 5 mol% VANOL catalyst at 0 °C gives a 50% yield of **114o** with only a 6% yield of **386o** (Table 7.4, entry 2). The yield of the aziridine **114o** increases to 80% for reaction at –10 °C with 10 mol% VANOL catalyst (entry 4) but the reaction slows at –30 °C and only gives 45% yield under the same conditions and goes to only 61% completion in 24 h (entry 6). With VAPOL catalyst, the yield of the reaction can be increased to 94% (96% ee) and at the same time the catalyst loading can be lowered to 5 mol% catalyst if 8 equiv of EDA is used and in this case no detectable amount of **386o** was observed (Table 7.4, entry 9). Further optimization found that the reaction of *n*-butanal with only 3 mol% catalyst and 2 equiv of EDA can provide 2.4 g (6 mmol) of aziridine **114o** in 92% yield and 96% ee (entry 12).

Table 7.4 Optimization of the multicomponent aziridination reaction of *n*-butanal [a]

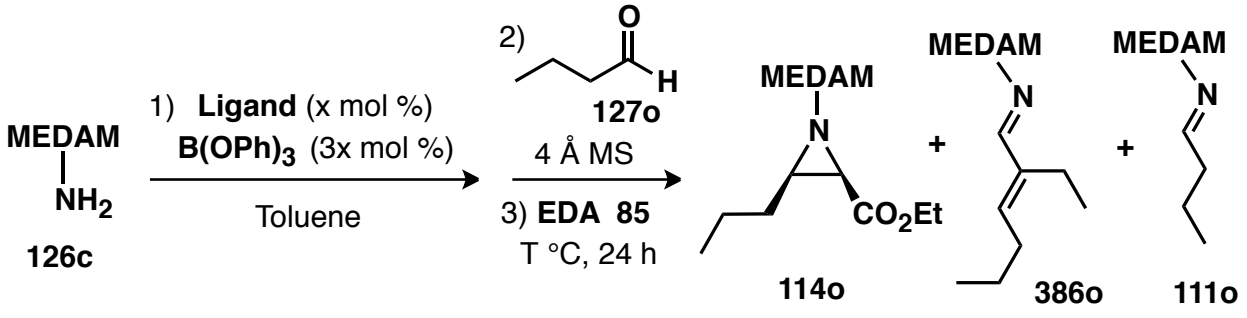

Table 7.4 cont'd

#	Ligand	Proc.	Cat. x mol%	T (°C)	Equiv **85**	Yield **114o** (%) [b]	ee **114o** (%) [c]	Yield **386o** (%) [d]	Yield **111o** (%) [e]
1	(*R*)-VANOL	**IIIA**	5	25	1.2	(25)	–	20	38
2	(*R*)-VANOL	**IIIA**	5	0	1.2	(50)	–	6	21
3	(*R*)-VANOL	**IIA**	5	0	1.2	(53)	–	6	17
4	(*R*)-VANOL	**IIA**	10	0	1.2	74	–95	2	<1
5	(*R*)-VANOL	**IIA**	10	–10	1.2	80	–96	<1	<1
6	(*R*)-VANOL	**IIA**	10	–30	1.2	45 [f]	–96	11	30
7	(*S*)-VAPOL	**IIA**	10	–10	1.2	82	98	<1	<1
8	(*S*)-VAPOL	**IIA**	5	–10	8	91	96	<1	<1
9	(*S*)-VAPOL	**IIIA**	5	–10	8	94	96	<1	<1
10	(*S*)-VAPOL	**IIIA**	5	–10	3	85	96	<1	<1
11	(*S*)-VAPOL	**IIIA**	4	–10	6	97 [g]	95	<1	<1
12	(*S*)-VAPOL	**IIIA**	3	–10	2	92 [h]	96	<2	<2

[a] Unless otherwise specified, all reactions were performed with procedure IIIA or IIA in Table 7.1 with 0.50 mmol amine **126c** (1.0 equiv, 0.5 M), 0.525 mmol *n*-butanal **127o** (1.05 equiv) and 0.60 mmol of EDA **85** (1.2 equiv) and went to 100% completion. [b] Isolated Yield. Yield in parenthesis determined by ^{1}H NMR spectra with Ph_3CH as internal standard. [c] Determined by HPLC. [d] Determined by integration of the γ-sp^2-CH signals of vinyl imine in ^{1}H NMR spectra with Ph_3CH as internal standard. [e] Determined by integration of the sp^2-CH signals of the imine in ^{1}H NMR spectra with Ph_3CH as internal standard. [f] Reaction went to 61% completion. [g] Reaction on 2.5 mmol scale. [h] Reaction on 6.0 mmol scale.

The real advantage of the MCAZ over two-step method aziridination is shown in Table 7.5. It must be noted that this study was performed by another current group member namely, Munmun Mukherjee (Entry 4 is part of this doctoral research work).[19] When the reaction was performed with pre-formed imine **111p** (derived from *n*-hexadecanal **127p**) using traditional

method of aziridination, low yields and asymmetric inductions were observed (Table 7.5, entries 1-2). However, a significant increase in yield and ee was observed when MCAZ protocol was utilized (Table 7.5, entries 3-4). Another group member, Yubai Zhou found that the reaction gave ee up to 98% using (*S*)-*t*Bu-VANOL **198** ligand (entry 8).[20]

Table 7.5 Optimization of the multicomponent aziridination reaction of *n*-hexadecanal **127p** [a]

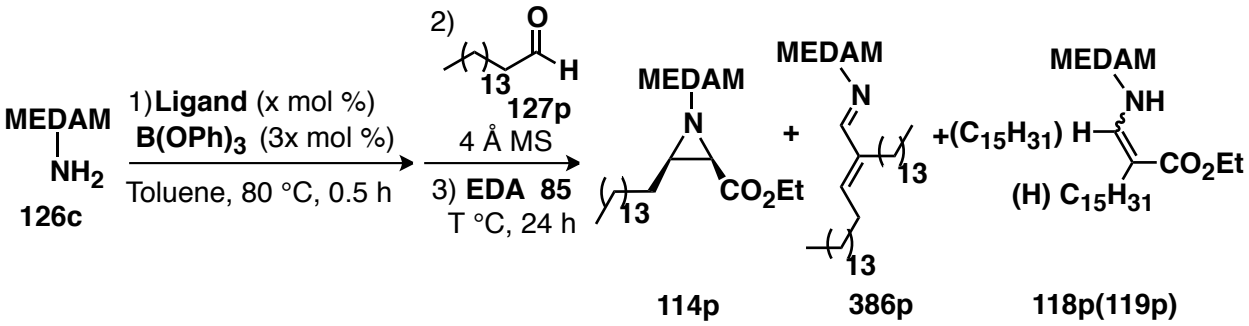

#	Ligand	Cat. x mol%	T (°C)	Equiv **85**	Yield **114p** (%) [b]	ee **114p** (%) [c]	Yield **386p** (%) [d]	Yield **118p+119p** (%) [e]
1 [f]	(*S*)-VAPOL	10	25	1.2	40	88	20	–
2 [g]	(*S*)-VAPOL	10	0	1.2	60	90	18	4
3	(*S*)-VAPOL	10	0	1.2	70	95	6	15
4 [h]	(*S*)-VAPOL	10	–10	1.2	82	96	<1	6
5 [i]	(*S*)-VAPOL	10	–10	2.0	85 [j]	95	<1	3
6 [i]	(*S*)-VAPOL	10	–10	2.0	90	95	<1	2
7 [i]	(*S*)-VANOL	10	–10	2.0	85	95	<1	2
8 [i,k]	(*S*)-*t*Bu-VANOL	10	–10	2.0	95	98	<1	<1

[a] Unless otherwise specified, all reactions were performed with procedure IIA in Table 7.1 with 0.50 mmol amine **126c** (1.0 equiv, 0.5 M), 0.525 mmol *n*-hexadecanal **127p** (1.05 equiv) and 0.60 mmol of EDA **85** (1.2 equiv) and went to 100% completion. [b] Isolated Yield. Yield in parenthesis determined by ^{1}H NMR spectra with Ph_3CH as internal standard. [c] Determined by Chiral HPLC. [d] Determined by integration of the γ-sp^2-CH signals of vinyl imine **386p** relative to the methine proton of *cis*-aziridine in the ^{1}H NMR spectra of the crude reaction mixture. [e] Determined by integration of the NH signals of the enamines relative to the methane proton of *cis*-aziridine in the ^{1}H NMR spectra of the crude reaction mixture.

Table 7.5 cont'd

[f] Reaction was performed with pre-formed imine **111p** (derived from *n*-hexadecanal **127p**). The imine was isolated and dried under high vacuum (~ 0.2 mmHg) for 0.5 h and the resulting oil was redissolved in toluene followed by its transfer to pre-catalyst (method C, Chapter 2). [g] Reaction was performed with pre-formed imine **111p** (derived from *n*-hexadecanal **127p**). The imine was not isolated and transferred directly to the pre-catalyst (method C, Chapter 2) using a filter syringe. [h] This work. [i] The concentration of the reaction = 0.2 M and aldehyde **127p** was added as a solution in toluene. [j] Reaction on 4.5 mmol scale. [k] Data provided by Yubai Zhou.

7.6.2 Substrate scope for aliphatic aldehydes

A series of nine aliphatic aldehydes were screened in the multi-component aziridination reaction (Table 7.6). Excellent asymmetric inductions were observed for the aziridination of a number of functionalized unbranched, α-branched and α,α-branched aliphatic aldehydes. These include a number of "problem" aldehydes that have failed to give aziridines *via in-situ* generated imines such as dihydrocinnamyl aldehyde **127t**, phenyl acetaldehyde **127u** and ethyl-5-oxopentanoate **127r** due to the problem pertaining to condensation product formation (Scheme 7.1).[14] Even with the optimized MCAZ protocol, the aziridination of aldehyde **127t** proceeds to give only a 24% yield of the aziridine **114t** (entry 10). The yield of aziridine **114t** can be increased to 96% if excess (8 equiv) of EDA is used and this is interpreted to mean that the imine undergoes aziridination before it can self condense (entry 11). A similar profile is noted with the phenyl acetaldehyde **127u** (entries 13-15). The "problem" aldehyde **127r** can be directly taken to the aziridine **114r** in 70% yield and with excess EDA the yield can be increased to 82% of material with 97% ee optical purity (entry 6, 7). However, in both cases, no attempt was made to optimize the amount of EDA. The MCAZ is also readily scalable as aziridines **114p** and **114o** are obtained with essentially the same induction and in slightly higher yield when the scale is increased ten-fold (Table 7.6, entries 3 vs 4) and twelve-fold (Table 7.4, entries 9 vs 12). The

side-reactions noted for α-unbranched aldehydes are not as severe for other types of aliphatic aldehydes and for this reason their reactions can be run at room temperature. The multi-component asymmetric catalytic aziridination of cyclohexane carboxaldehyde **127v** at room temperature gives the aziridine **114v** in 95% yield and 90% ee which is within experimental error of the results obtained from the aziridination of the cooresponding imine at either room temperature or at 0 °C.[9c] Likewise the MCAZ of the α,α-branched pivaldehyde **127w** gives the aziridine **114w** in 89% yield and 94% ee at room temperature which is to be compared with 95% yield and 94% ee from the aziridination of the pre-formed imine at the same temperature.[9c]

Table 7.6 Multicomponent aziridination of alkyl aldehydes [a]

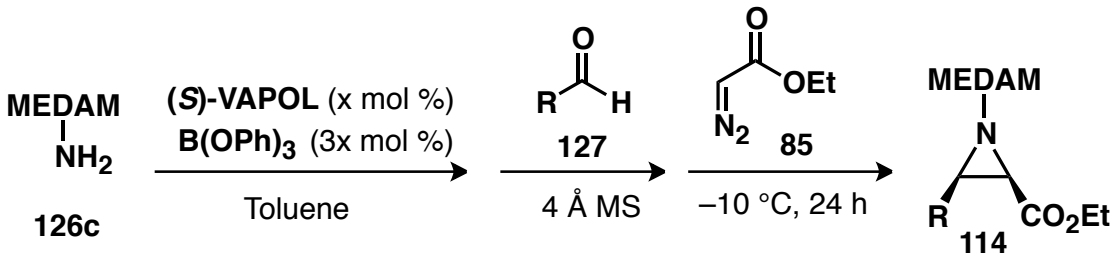

#	R	series	Proc	Cat. x mol%	Equiv **85**	Yield **114** (%) [b]	ee **114** (%) [c]
1	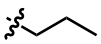	**o**	**IIA**	10	1.2	82	98
2			**IIIA**	5	8	94	96
3	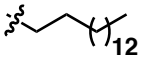	**p**	**IIA**	10	1.2	82	96
4			**IIA**	10	3	85	95 [d]
5	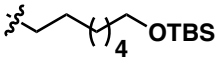	**q**	**IIA**	10	1.2	80	98
6	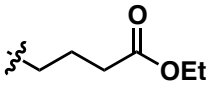	**r**	**IIA**	10	1.2	70	94
7			**IIIA**	5	8	82	97
8	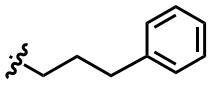	**s**	**IIA**	10	1.2	55	93
9			**IIIA**	5	8	50	90

Table 7.6 cont'd

10	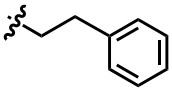	**t**	**IIA**	10	1.2	24 [e]	nd
11			**IIA**	10	8	96	97
12			**IIIA**	5	8	91	96
13	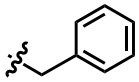	**u**	**IIA**	10	1.2	19 [e]	nd
14			**IIA**	10	8	94	98
15			**IIIA**	5	8	86	98
16 [f]	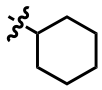	**v**	**IIIA**	5	1.2	95	90
17 [f]		**w**	**IIA**	10	1.2	89	94
18 [f]			**IIIA**	10	2	95	92
19 [f]			**IIIA**	10	8	97	90

[a] Unless otherwise specified, all reactions were performed with procedure IIA or IIIA in Table 7.1 with 0.50 mmol amine **126c** (1.0 equiv, 0.5 M), 0.525 mmol aldehyde **127** (1.05 equiv) and 0.60 mmol of EDA **85** (1.2 equiv) and went to 100% completion with a cis/trans ratio of >50:1 for aziridine **114**. Small amounts of enamine products were observed for some reactions (<1 to 6%). [b] Isolated Yield. [c] Determined by HPLC. [d] Reaction on 5.0 mmol scale. [e] Determined by ^{1}H NMR spectra with Ph_3CH as internal standard. nd = not determined. [f] Reaction performed at 25 °C.

7.7 Mechanistic study towards the five-component catalyst assembly/catalytic asymmetric aziridination

While studying the mechanistic aspects involving the order of the addition of the various components, we have discovered that this reaction is actually a five-component process in which the catalyst is assembled by the amine from the ligand and $B(OPh)_3$ and then the catalyst causes imine formation and then finally, aziridine formation (Figure 7.1C).[13] The possible combinations of all of the outcomes of all the different known reactions between the five species shown in Figure 7.1C would lead to a mixture of 10 different products (Figure 7.3) and yet a

solution of these five-species leads to the formation of the aziridine in very high yields and enantioselectivies. The purpose of the present work is to provide an insight to and support for the operation of this five-component catalyst assembly/catalytic asymmetric aziridination.

Figure 7.3 Chemoselectivity in the five-component catalyst assembly/catalytic asymmetric aziridination

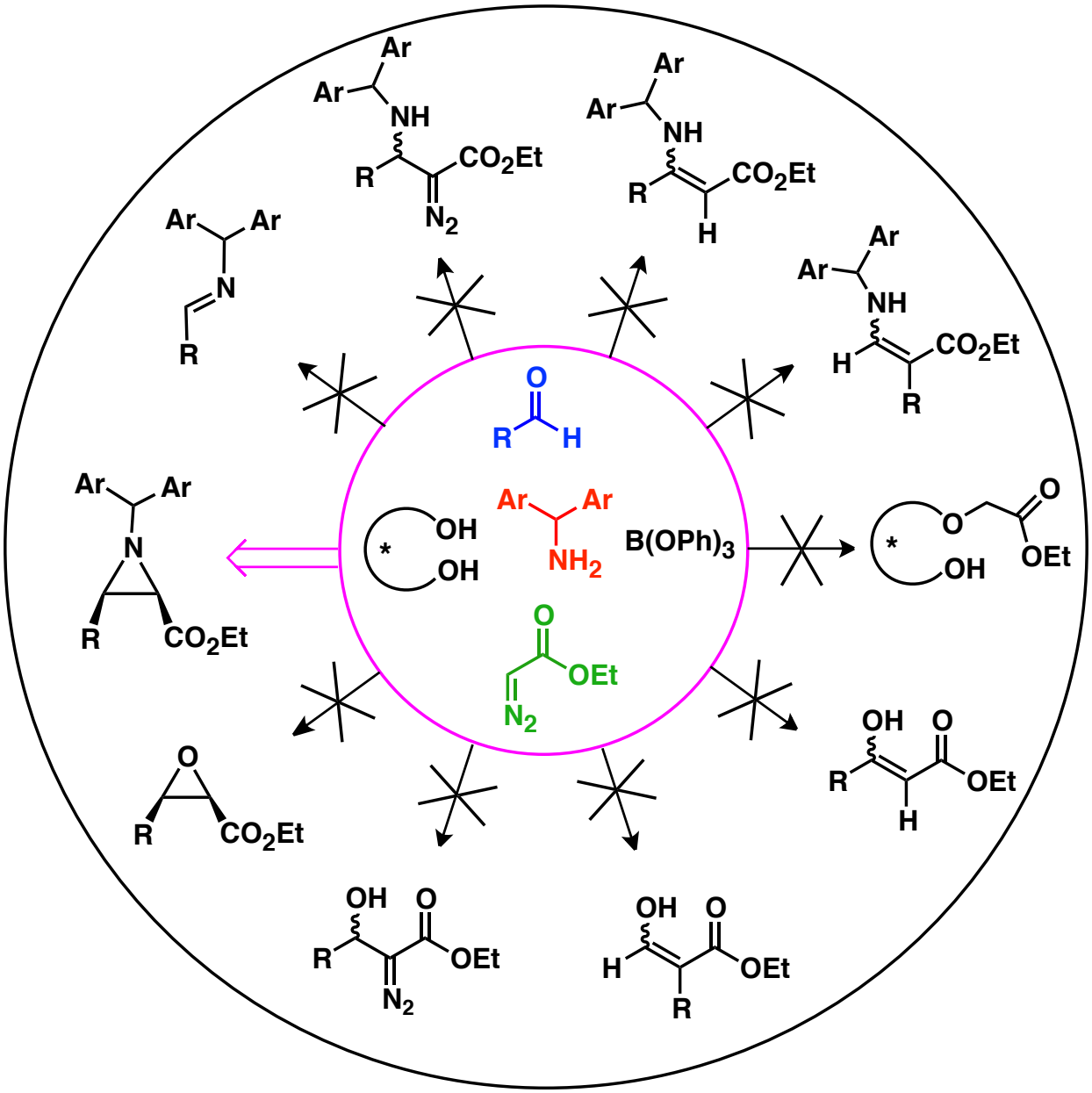

7.7.1 Effects of the order of addition on the multicomponent *cis*-aziridination

That the aziridination reaction of focus here is in fact a true multi-component reaction is indicated by the results shown by procedures V, VI and VII in Table 7.7. First of all, procedure IV reveals that all the components can be added followed by the addition of the solvent. Hence, 1 h of stirring is not required as in procedure IIIA. The successful aziridination from the reaction where the EDA (**E**) is added before the aldehyde (**D**) reveals that imine formation can occur in the presence of EDA (procedure V and VI). The VAPOL ligand is not alkylated by the EDA under these conditions (Table 7.7, procedures V and VI) as might have been expected from the results in Scheme 7.4A. This reveals that once the VAPOL boroxinate B3 catalyst **215b** is generated, the VAPOL ligand is protected from alkylation.

Table 7.7 Effect of order of addition on the multi-component aziridination reaction [a]

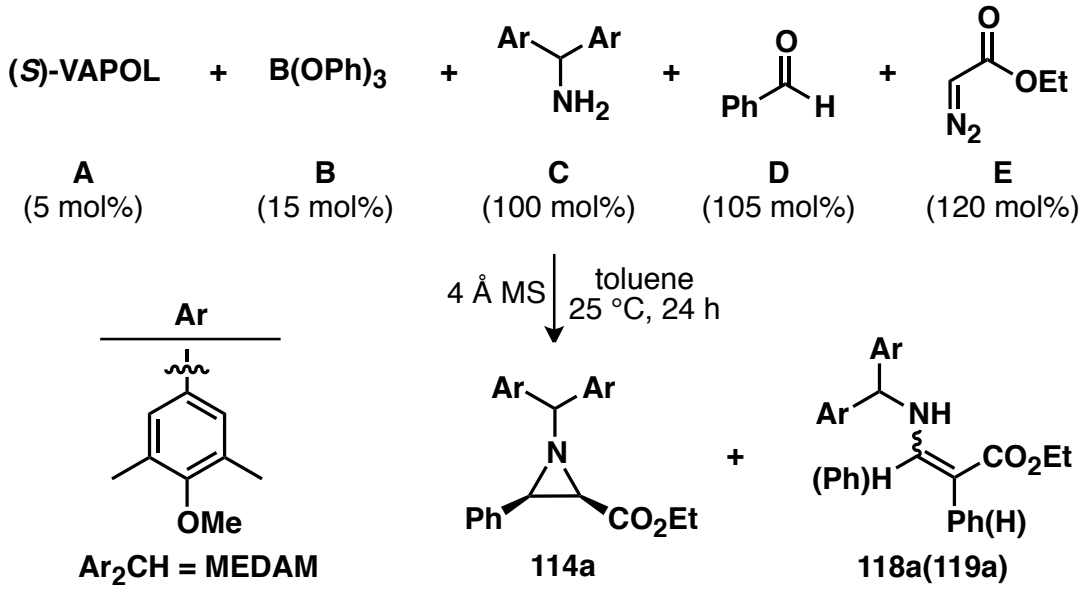

#	Procedure	Reaction protocol			Yield **114a** (%) [b]	ee **114a** (%) [c]
1	**IIIA** [d]	**A+B+C**	1) toluene, 25 °C, 1 h →	2) **D**, 4Å MS, **E**, 25 °C, 24 h →	98	95

Table 7.7 cont'd

2	**IV** [e]	**A+B+C**	**D**, 4Å MS →	1) **E**, toluene, 25 °C, 24 h →	88	98
3	**V** [f]	**A+B+C**	1) **E**, toluene, 25 °C, 1 h →	2) **D**, 4Å MS, 25 °C, 24 h →	94	98
4	**VI** [g]	**A+B+C**	**E**, toluene →	1) **D**, 4Å MS, 25 °C, 24 h →	94	98
5	**VII** [h]	**A+B**	**D**, 4Å MS, **E**, then **C** →	1) toluene, 25 °C, 24 h →	85 [i]	98
6	**VIII** [j]	**A+B**	1) **D**, 4Å MS, **E**, toluene, 2 min →	2) **C**, 25 °C, 24 h →	<1	–
7	**IX** [k]	**A+B**	**D**, 4Å MS →	1) **E**, toluene, 25 °C, 24 h →	–	–

[a] Unless otherwise specified, all reactions were performed with procedure **IIIA** or **IV-XI** with 0.025 mmol (*S*)-VAPOL **A** (**58**), 0.075 mmol $B(OPh)_3$ **B** (**187a**), 0.50 mmol amine **C** (**126c**) (1.0 equiv, 0.5 M), 0.525 mmol aldehyde **D** (**127**) (1.05 equiv) and 0.60 mmol of EDA **E** (**85**) (1.2 equiv) and went to 100% completion with a cis/trans ratio of >50:1 for aziridine **114**. In each case, 150 mg powdered 4Å MS was added immediately preceding benzaldehyde. [b] Isolated Yield. [c] Determined by HPLC. [d] See Table 7.1. [e] A mixture of **A**, **B**, **C**, 4 Å MS, **D**, and **E**, added in that order, was dissolved in toluene and the resulting solution allowed to stir for 24 h at 25 °C. [f] The diazo compound **E** is added to a mixture of **A**, **B** and **C** and then toluene is added and the mixture stirred at 25 °C for 1 h after which powdered 4 Å MS and **D** are added and the mixture stirred for 24 h at 25 °C. [g] A mixture of **A**, **B**, **C**, **E**, 4 Å MS, and **D**, added in that order, was dissolved in toluene and the resulting solution allowed to stir for 24 h at 25 °C. [h] A mixture of **A**, **B**, 4 Å MS, **D**, **E**, and **C**, added in that order, was dissolved in toluene and the resulting solution allowed to stir for 24 h at 25 °C. [i] A 3% yield of enamines **118a** and **119a** was observed. [j] A mixture of **A**, **B**, 4 Å MS, **D** and **E**, added in that order, was dissolved in toluene and the resulting solution allowed to stir for 2 min at 25 °C before **C** was added and the resulting solution stirred for 24 h at 25 °C. The products of this reaction are shown in Figure 7.4. [k] Same as procedure VIII except that **C** was not added. The products from this reaction are **395a** (5%), **396a** (38%), **397a** (11%), **398a** (5%), **399a** (<1%) and **230** (37%).

The results from procedure VII in Table 7.7 where the amine **C** is added last reveals that this is a five-component reaction where both the catalyst assembly and the aziridination reaction can be carried out simultaneously. Since the amine is added last, considerable concern arose from the results in Scheme 7.4A that suggest that the VAPOL ligand may be alkylated before the catalyst is generated. That is why in procedure VII all five of the components were added in the order shown without solvent, and at the end, solvent was added to effect dissolution. That this provides for a successful aziridination indicates that the amine, which is added last, can quickly assemble the catalyst such that the ligand is protected from alkylation by the EDA. The speed at which catalyst assembly occurs is indicated by procedure VIII in Table 7.7. When the first four components including EDA are dissolved in toluene and then 2 min later the amine is added, no aziridine formation is observed. A very complex reaction mixture is observed and the products are indicated in Figure 7.4 and include products from the reaction of EDA with both the aldehyde and the imine, however, no detectable amount of the aziridine **114a** could be observed. The major product is the imine **111a** (34%) and there is also a considerable amount of the unreacted amine **126c** (40%). Since the aldehyde is partially consumed in the formation of the *β*-keto ester **396a** (23%) and its tautomer **397a** (5%), the presence of the unreacted amine **126c** may lead to its selective binding to the catalyst thus preventing aziridination of the imine if indeed any boroxinate catalyst was formed at all in this reaction. As a control, the same reaction in which the amine is not added at all was also carried out (Table 7.7, procedure IX) and this gave a product mixture that was shown to have a very similar profile to the reaction of benzaldehyde **127a** and ethyl diazoacetate **85** promoted by $B(OPh)_3$ (Scheme 7.4B). The combined results from procedures VII and VIII in Table 7.7 make it clear that the assembly of the catalyst by the amine is *exceedingly fast*. The events that occur in the two minutes prior to

amine addition in procedure VIII are sufficient to completely thwart catalyst assembly and aziridination.

Figure 7.4 Products from the reaction with procedure VIII in Table 7.7

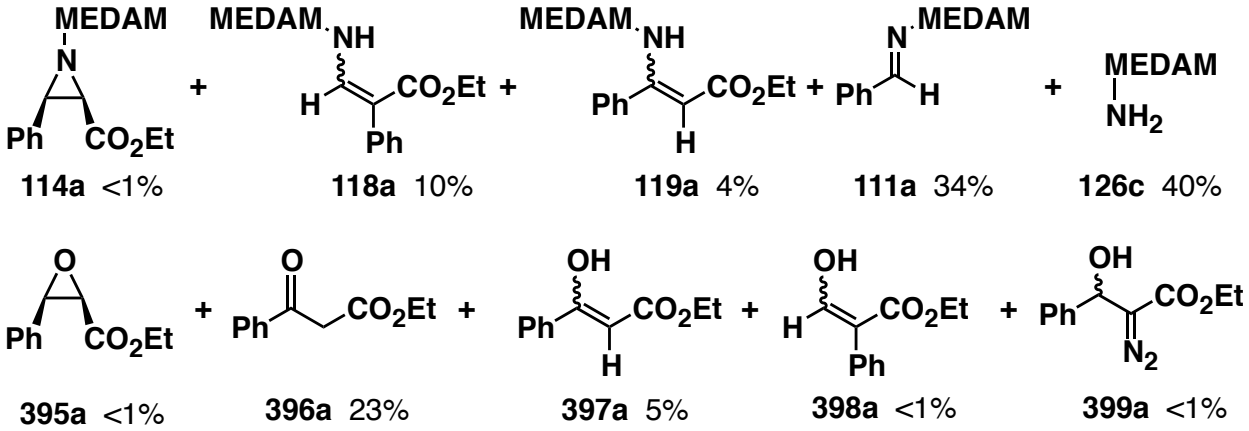

7.7.2 Mode of catalysis and sequence of the final steps in the five-component catalyst assembly/aziridination

The simultaneous presence of the five chemical species shown in Figure 7.5A together in the same solution could have lead to several possible outcomes. There could have been reaction between the VAPOL ligand **58** and the EDA **85** mediated by $B(OPh)_3$ to give the alkylated product **230** (Scheme 7.4A) or there could have been a reaction between the aldehyde **127** and EDA **85** mediated by $B(OPh)_3$ to give the series of products indicated in Scheme 7.4B. The data in Table 7.7 indicates that instead there is a very rapid assembly of a boroxinate species from the VAPOL ligand and $B(OPh)_3$ mediated by the amine **126a**/**126c** which gives rise to the AMINO-

BOROX species **215a**/**215b**. At this point the question arises as to the subsequent order of events. In one extreme, a small amount of imine **78**/**111** could be formed and then immediately converted to aziridine **86**/**114** before the rest of the imine is formed (Route I, C to E in Figure 7.5). This would suggest that the reaction is catalyzed by AMINO-BOROX species **215a**/**215b**, thereby resulting in AMINO-BOROX catalysis as the mode of the catalysis. In the other extreme, the process could first proceed to give complete conversion of the amine and aldehyde to the imine **78**/**111** and only then does the imine **78**/**111** react with EDA **85** under the ageis of the IMINO-BOROX catalyst **188**/**190** to give the aziridine **86**/**114** (Route II, D to E in Figure 7.5). The last entry in Table 7.1 suggests that it is the latter since the presence of excess amine over aldehyde (0.6 equiv) results in the complete suppression of aziridine formation. This issue was further probed with additional experiments and the results are presented in Tables 7.8 and 7.9.

Figure 7.5 Time course of events in the five-component catalyst assembly/aziridination reaction. (**A**) Time zero. (**B**) Assembly of AMINO-BOROX **215a**/**215b**. (**C**) Start of formation of imine **78**/**111** (**78a**/**111a** when R = Ph) in presence of AMINO-BOROX **215a**/**215b.** (**D**) Formation of IMINO-BOROX catalyst **188**/**190** (**188a**/**190a** when R = Ph). (**E**) Catalytic asymmetric aziridination.

Figure 7.5 cont'd

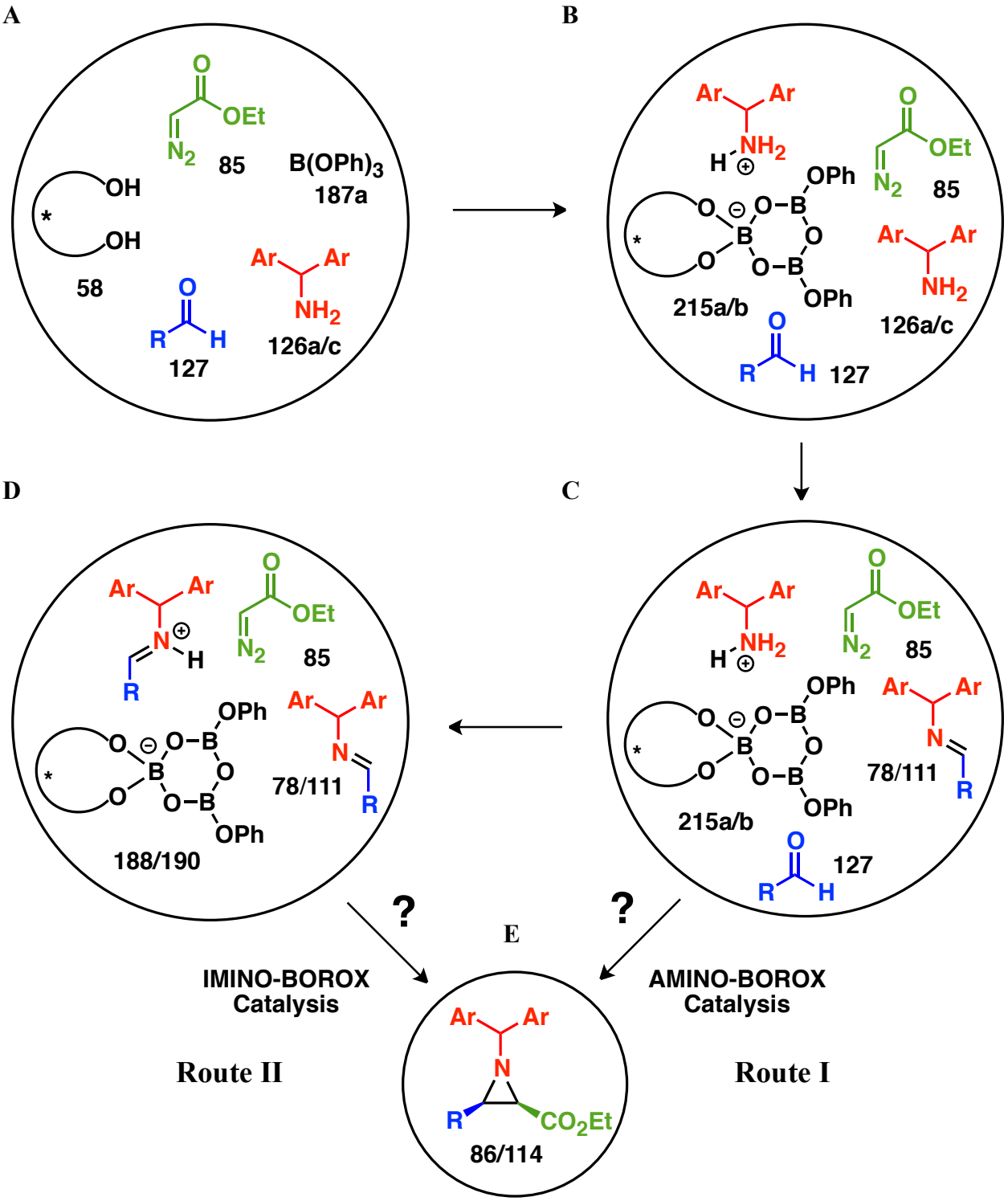

The multi-component aziridination of benzaldehyde **127a** with benzhydryl amine **126a** was examined with different amounts of benzaldehyde ranging from 0.6 to 1.0 equiv and the results are presented in Table 7.8. Just as with the reaction of the MEDAM amine **126c** with 0.6 equiv of benzaldehyde (Table 7.1, entry 6), the reaction of benzhydryl amine **126a** with 0.6 equiv of benzaldehyde results in essentially no formation of aziridine **86a** (1%) even though benzaldehyde is essentially completely transformed into the imine **78a** and 98% of this imine remains unreacted after 24 h (Table 7.8, entry 5). The amount of aziridine **86a** formed with 0.9 equiv of benzaldehyde (entry 2) is nearly the same as with 1.0 equiv (entry 1). However, it should be noted that with 0.9 equiv, 8% of the imine **78a** remains unreacted, whereas with 1.0 equiv of benzaldehyde, the imine **78a** is nearly completely consumed (1% unreacted). This suggests there is an equilibrium between the boroxinate **215a** containing a protonated amine and the boroxinate **188a** containing a protonated imine (Scheme 7.6). Given the fact that imines are ~ 10^3 times less basic than amines,[21] even when the amount of excess amine is equal to the amount of catalyst (0.9 equiv **127a** added, entry 2), there appears to be enough of the IMINO-BOROX catalytst **188a** present in solution containing the activated imine to allow the reaction to proceed in 24 h.

Table 7.8 Multicomponent aziridination with a deficiency of benzaldehyde [a]

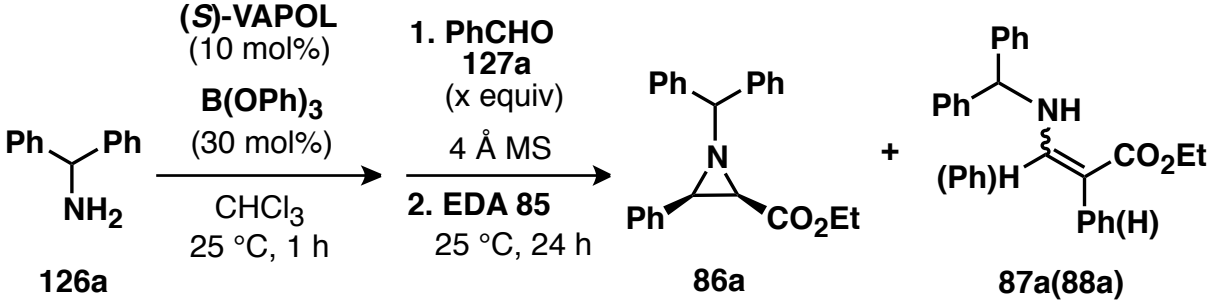

Table 7.8 cont'd

#	**127a** x equiv	Yield **86a** (%) [b,c]	ee **86a** (%) [d]	cis/trans [e]	Yield **87a+88a** (%) [f]	Unreacted **78a** (%) [b]
1	1.0	77 (78)	90	25:1	9	1
2	0.9	75 (73)	89	25:1	8	8
3	0.8	6	–	50:1	<1	94
4	0.7	4	–	> 50:1	<1	96
5	0.6	1	–	50:1	<1	98

[a] Unless otherwise specified, all reactions were performed with procedure IIIA in Table 7.1 with 0.50 mmol amine **126a** (1.0 equiv, 0.5 M), benzaldehyde **127a** (x equiv) and 0.60 mmol of EDA **85** (1.2 equiv) and went to 100% completion. [b] Determined by ^{1}H NMR spectra of crude reaction mixture with Ph_3CH as internal standard. [c] Yield in parentheses are after isolation by silica gel chromatography. [d] Determined by HPLC on purified aziridine. [e] Ratio determined by integration of the methine protons of *cis*- and *trans*-aziridine in the ^{1}H NMR spectrum of the crude reaction mixture. [f] Determined by integration of the NH signals of enamines relative to the methine proton of *cis* aziridine in the ^{1}H NMR spectrum of the crude reaction mixture.

It should be pointed out that factors other than basicity may affect the equilibrium of AMINO-BOROX and IMINO-BOROX species (see below, Table 7.9). Even if the equilibrium between **215a** and **188a** is facile (Figure 7.5 and Scheme 7.6), the reaction greatly slows when equal amounts of amine **126a** and imine **78a** are present since the amount of unreacted imine **78a** is 8% when the reaction with 10% excess amine **126a** is stopped after 24 h (Table 7.8, entry 2). This suggests that the greater base strength of the amine **126a** greatly favors the AMINO-BOROX species **215a** over that of the IMINO-BOROX **188a** when the concentrations of the amine and imine are similar. In the normal protocol for the multi-component catalytic asymmetric aziridination (Table 7.1), a slight excess of aldehyde (1.05 equiv) is typically used which assures

complete consumption of the amine and avoidance of a slow down during the end of the reaction.

Scheme 7.6 An equilibrium between (**A**) AMINO-BOROX catalyst **215a**/**b** and (**B**) IMINO-BOROX catalyst **188**/**190**

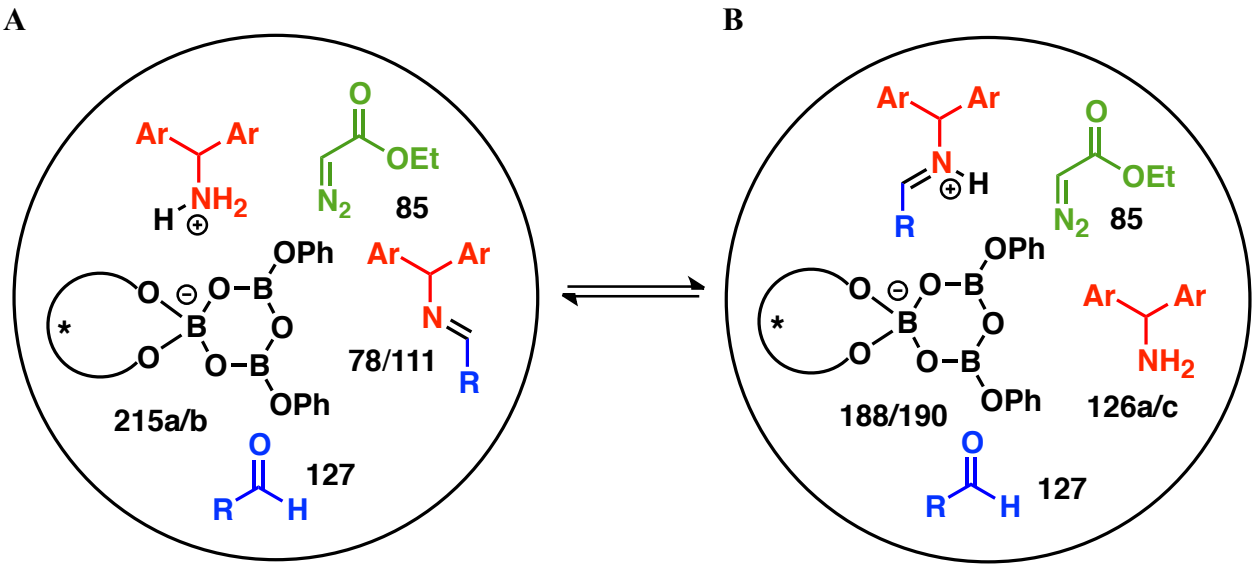

To futher examine the effect of the base strength of other species present in the reaction mixture, the aziridination of the pre-formed imine **78a** was carried out in the presence of varying amounts of four different nitrogen bases and the results are presented in Table 7.9. In the absence of any added base, the reaction gives aziridine **86a** in 85% isolated yield and 90% ee which is nearly the same as has been previously reported for this reaction in chloroform.[9a] In these reactions, a boroxinate species is assembled by treating VAPOL and 3 equiv of $B(OPh)_3$ with the base at room temperature for 1 h and then adding the imine **78a** and the EDA to consummate the reaction. These conditions directly generate the situation indicated in Figure 7.5D where only the imine and EDA substrates are present. The difference is that the reaction in

Table 7.9 begins with an AMINO-BOROX catalyst rather than an IMINO-BOROX catalyst. The reaction in the presence of 10 mol% of benzhydryl amine **126a** (Table 6, entry 5) gives nearly the same yield as the reaction without base, and this mirrors the result in entry 2 of Table 7.8. The only difference is that none of the imine **78a** remains unreacted at the end in case of the reaction with the pre-formed imine. However, the reaction with 20 mol% of benzhydryl amine **126a** slows the reaction dramatically and 86% of the imine **78a** remains after 24 h. Similar results are seen with 10 mol% Et_3N and 10 mol% benzhydryl amine **126a** (entries 2 vs 5), however, with 20 mol% Et_3N the reaction is completely stopped and no detectable amount of the aziridine is observed (entries 2 & 3). These results further suggest that an equilibrium is present between an AMINO-BOROX and an IMINO-BOROX species (Scheme 7.6). The fact that there is nearly complete reaction when 10 mol% Et_3N or 10 mol% Ph_2CHNH_2 are added, suggests that at the point when the ratio of amine to imine is 1:1, there is still enough of the IMINO-BOROX species present such that the reaction can still go forward.

Table 7.9 Aziridination reaction of pre-formed imine **78a** with added bases. [a]

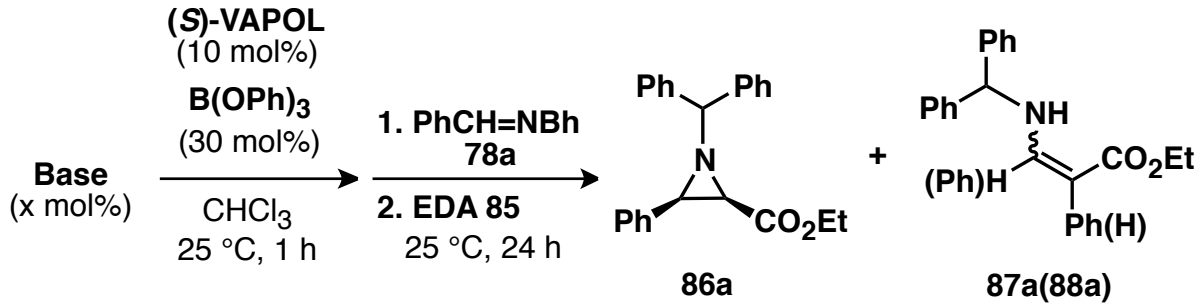

#	pKa	Base [b]	Base x mol%	Yield **86a** (%) [c,d]	ee **86a** (%) [e]	cis/trans [f]	Yield **87a+88a** (%) [g]	Unreacted **78a** (%) [c]
1	–	none	0	83 (85)	90	100:1	10	1

Table 7.9 cont'd

2			10	71 (77)	86	25:1	9	6
3	10.75	Et_3N	20	<1	–	–	–	89
4			40	<1	–	–	–	92
5	10.60	$BhNH_2$	10	77 (80)	89	27:1	10	<1
6			20	10	–	12:1	2	86
7	9.20	DMAP	10	<1	–	–	–	96
8			20	<1	–	–	–	80
9	4.60	$PhNH_2$	10	73 (78)	88	33:1	8	5
10			20	17 (20)	86	23:1	6	68

[a] Unless otherwise specified, the boroxinate catalyst **215** was prepared in $CHCl_3$ from 10 mol% (*S*)-VAPOL, 30 mol% $B(OPh)_3$ and x mol% of a base to induce the boroxinate formation. After 1 h at 25 °C, 100 mol% of imine **78a** and 120 mol% EDA **85** were added to the catalyst and the aziridination reaction carried out with 1.0 mmol of imine (0.5 M) for 24 h at 25 °C. [b] All bases were purified by distillation or sublimation. [c] Determined by ^{1}H NMR spectra of crude reaction mixture with Ph_3CH as internal standard. [d] Yield in parentheses are after isolation by silica gel chromatography. [e] Determined by HPLC on purified aziridine. [f] Ratio determined by integration of the methine protons of *cis*- and *trans*-aziridine in the ^{1}H NMR spectrum of the crude reaction mixture. [g] Determined by integration of the NH signals of enamines relative to the methine proton of *cis* aziridine in the ^{1}H NMR spectrum of the crude reaction mixture.

Aniline is a weaker base than aliphatic amines and this can be correlated with its decreased ability to slow the reaction since even with 20 mol% aniline there is 32% conversion of the imine giving a 20% isolated yield of aziridine **86a** (entry 10). The formation of aziridine in only 20% yield is surprising given the fact that aniline is a much weaker base than either the aliphatic amines or the imine **78a**. This suggests that equilibrium is shifted towards AMINO-BOROX species in spite of aniline being a weaker base. To this point, the reader's attention should be brought to the fact that although these reactions were performed with 10 mol%

catalyst, the aziridination reaction with benzhydryl imines **78** can be effected under these conditions with as little as 0.25 mol% catalyst.[9a]

The ability of the amine to inhibit the reaction does correlate to some degree with the basicity of the amine, but there are obviously other factors that must contribute to the magnitude of the equilbrium constant indicated in Scheme 7.6. This is most clear in the reaction with added DMAP. Although less basic than aliphatic amines, DMAP completely stops the reaction upon addition of just 10 mol% (Table 7.9, entry 7). In this case, any equilibrium between the AMINO-BOROX and IMINO-BOROX species may be determined by more than just the relative basicity of the amine and the imine. This equilibrium may be shifted to the AMINO-BOROX further than might be predicted from the basicity alone. The crystal structure of the AMINO-BOROX spieces containing DMAP reveals the presence of non-covalent interactions in addition to the H-bond between the protonated base and the boroxinate anion.[9e] Specifically, there is a π-π stacking interaction between the pyridinium cation and one of the phenanthrene rings of the VAPOL ligand and there is a CH-π interaction between one of the ortho-hydrogen of the pyridinium cation and one of the phenoxy groups of the boroxinate core.[9e] These results are consistent with the view that the catalytic cycle for the multi-component catalyst assembly/aziridination involves the complete (or nearly complete) formation of the imine before the aziridination reaction can commence (Route II, C to D then to E, Figure 7.5).

7.8 Multiplex diversity: evolution of a seven-component catalyst assembly/catalytic asymmetric aziridination

As discussed earlier, the diversity in BOROX catalyst can be achieved by replacing $B(OPh)_3$ with a combination of borane, water and different alcohols (Table 2.3, Chapter 2).

These variations would generate a large pool of catalyst and thereby provide new opportunities in asymmetric catalysis. Up to this point, we have only used these variations for aziridination reaction with imines. Hence, it was wondered that whether a seven-component catalyst assembly/catalytic asymmetric aziridination can be realized by using borane along with phenol and water. We have been able to achieve this goal by employing either BH_3•Me_2S or BH_3•THF as the boron source and the results are described below.

7.8.1 Using BH_3•Me_2S as the boron source

Considering the structure of the BOROX catalyst, the boroxinate catalyst can be assembled from a molecule of the ligand, three molecules of BH_3•Me_2S complex, three molecules of water and two molecules of a phenol or alcohol (Figure 2.5, Chapter 2). To start with, procedure I′ which is similar to procedure IIIA was used where a mixture of the ligand **A** (**58**/**59**), 2 equiv phenol **B** (**194a**), 20 equiv amine **C** (**126a**), 3 equiv BH_3•Me_2S **D** (**192a**), 3 equiv H_2O **E** was stirred in toluene at 25 °C for 1 h (Scheme 7.7). This was followed by the addition of the 4 Å MS, benzaldehyde **F** (**127a**) and EDA **G** (**85**) in the given order. The resulting mixture was stirred at 25 °C for 24 h. Unfortunately, no aziridine **86a** was observed (Table 7.10, entries 1-2). Procedure I was then examined which involved heating a mixture of **A**-**E** at 100 °C for 1 h (procedure I, Scheme 7.7) followed by the addition of 4Å MS, benzaldehyde **F** (**127a**) and EDA **G** (**85**) at 25 °C. The resulting mixture was stirred at 25 °C for 24 h to give aziridine **86a** in 82% yield and 95% ee (Table 7.10, entry 3). While the VAPOL catalyst gave complete conversion with procedure I leading to aziridine in high yields in 24 h, the VANOL catalyst gave incomplete conversion (70%) under the same conditions (entry 4).

This is the first time that there was any significant difference observed between these ligands in the aziridination reaction. Surprisingly, a similar but larger trend was observed in case of the MEDAM amine **126c** (Table 7.10, entries 5-6). Only a 17% conversion was observed in case of the reaction involving MEDAM amine **126c** and VANOL catalyst (entry 6). The reason for the failure of procedure I with the VANOL catalyst is not known yet. However, essentially optically pure aziridine **114a** was obtained with the VAPOL catalyst (entry 5).

Scheme 7.7 Various protocols for multicomponent aziridination reaction using BH_3•Me_2S.

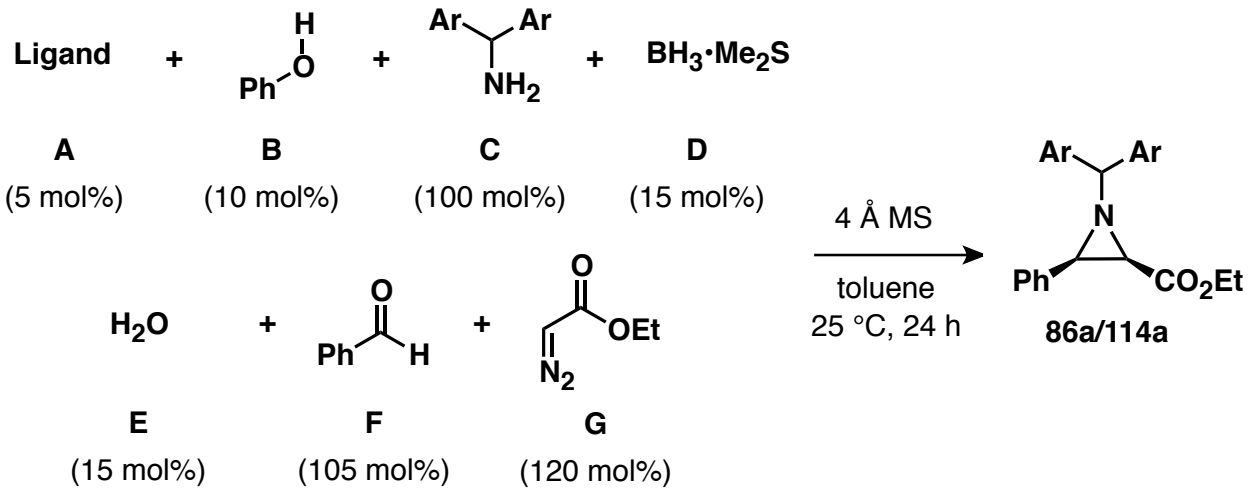

Procedure I′ **A+B+C** 1) toluene → 2) **D** + **E**, 25 °C, 1 h → 3) **F**, 4Å MS → **G,** 25 °C, 24 h

Procedure I **A+B+C** 1) toluene → 2) **D** + **E**, 100 °C, 1 h → 3) **F**, 4Å MS → **G,** 25 °C, 24 h

Procedure II **A+B** 1) toluene → 2) **D** + **E**, 100 °C, 1 h → 3) **C**, 25 °C, 1 h → 4) **F**, 4Å MS → **G,** 25 °C, 24 h

Procedure III **A+B** 1) toluene → 2) **D** + **E**, 100 °C, 1 h, 0.5 mm Hg, 100 °C, 0.5 h → 3) **C**, 25 °C, 1 h → 4) **F**, 4Å MS → **G,** 25 °C, 24 h

Table 7.10 Multicomponent aziridination using BH_3•Me_2S as the boron source [a]

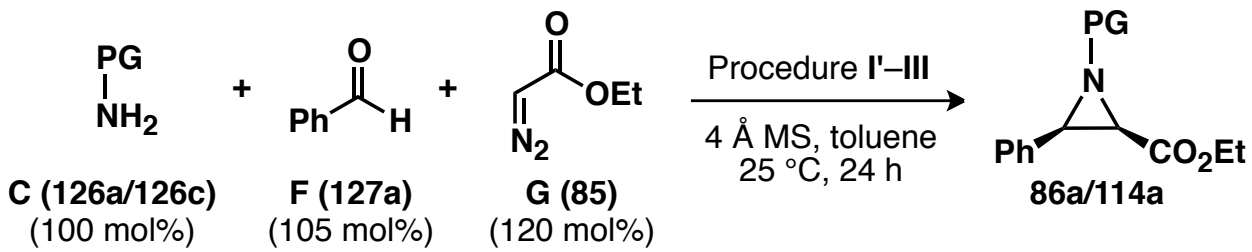

C (126a/126c) (100 mol%) **F (127a)** (105 mol%) **G (85)** (120 mol%) **86a/114a**

#	Procedure	catalyst x mol%	Ligand	PG	Yield azi (%) [b]	Ee azi (%) [c]
1	**I′**	10	(*S*)-VAPOL	Bh	<1	–
2	**I′**	10	(*S*)-VANOL	Bh	<1	–
3	**I**	10	(*S*)-VAPOL	Bh	82	95
4	**I**	10	(*S*)-VANOL	Bh	62 (70)	88
5	**I**	5	(*S*)-VAPOL	MEDAM	99	99.3
6	**I**	5	(*S*)-VANOL	MEDAM	– (17)	–
7	**II**	5	(*S*)-VAPOL	MEDAM	90	97
8	**II**	5	(*S*)-VANOL	MEDAM	85	95
9	**III**	5	(*S*)-VAPOL	MEDAM	89	97
10	**III**	5	(*S*)-VANOL	MEDAM	82	95

[a] Unless otherwise specified, all reactions were performed with procedures **I′-III** in Scheme 7.7 with 1 mmol of amine **126a/126c** in toluene (0.5 M in imine) with 1.05 equiv of aldehyde **127a** and 1.2 equiv of **85** and went to 100% completion and gave aziridine **86a**/**114a** with cis/trans ratio of >50:1. Small amount of enamine side-products were observed for some reactions (<1 to 9%). [b] Isolated Yield. Number in parenthesis is the percent conversion. Percent conversion is determined by integration of the methine proton of *cis*-aziridine relative to the sp^2-CH proton of the unreacted imine in the ^{1}H NMR spectrum of the crude reaction mixture. [c] Determined by HPLC.

In the process of further optimization, we tried to mimic the procedure that has been used for imines by replacing it with amine. Hence, the pre-catalyst was made by heating a mixture of

A, **B**, **D** and **E** at 100 °C for 1 h (procedure II, Scheme 7.7). This was followed by stirring the resulting mixture with amine **126c** for 1 h at 25 °C. Subsequent addition of 4Å MS, benzaldehyde **F** (**127a**) and EDA **G** (**85**) followed by stirring the reaction mixture for 24 h at 25 °C afforded aziridine **114a** in high yields and enantioselectivity (entries 7-8). Although a small drop in ee was encountered, the reaction seemed to have worked equally as well for the VANOL catalyst. In addition, no change in ee was observed when the pre-catalyst was kept under vacuum for 0.5 h at 100 °C prior to treatment with the amine **126c** (procedure III, Table 7.10, entries 9-10). The results in Table 7.10 establish the feasibility of a higher order seven-component catalyst assembly/catalytic asymmetric aziridination reaction. *Inspired by the procedure III of MCAZ, aza-Cope rearrangement was performed by Hong Ren, a current group member, using procedure III with a slight modification (heating of amine with the pre-catalyst instead of stirring at room temperature).*[22] It must be noted that the aza-Cope rearrangement was already optimized with imines prior to the evolution of the procedure III of MCAZ.

7.8.2 Using BH_3•THF as the boron source

With the demonstration that the reaction with seven components can be successfully realized with BH_3•Me_2S, the focus was then shifted to the further simplification by removing the heating unit operation in the procedure. It was thought that this could be possible with BH_3•THF **D** (**192b**) as it was reported earlier that it works very well with imines at room temperature (Table 2.1, entry 9 in Chapter 2). Procedure I was then employed where **A**-**E** were mixed and stirred for 1 h at 25 °C (Scheme 7.8). This was followed by the subsequent addition of 4Å MS,

benzaldehyde **F** (**127a**) and EDA **G** (**85**) and the resulting mixture was stirred for 24 h at 25 °C. Unexpectedly, both the VAPOL and VANOL catalysts gave incomplete conversions (78% for VAPOL and 46% for VANOL, Table 7.10, entries 1-2). In case of VAPOL, a 72% yield of aziridine **86a** was isolated with 92% ee. Another current group member, Wynter Osminski was able to obtain nearly complete conversion by adding $PhCO_2H$ to the mixture ($PhCO_2H$: ligand = 1 : 2) and using excess aldehyde (1.5 equiv) (entries 3-5).[23]

Scheme 7.8 Various protocols for multicomponent aziridination reaction using BH_3•THF

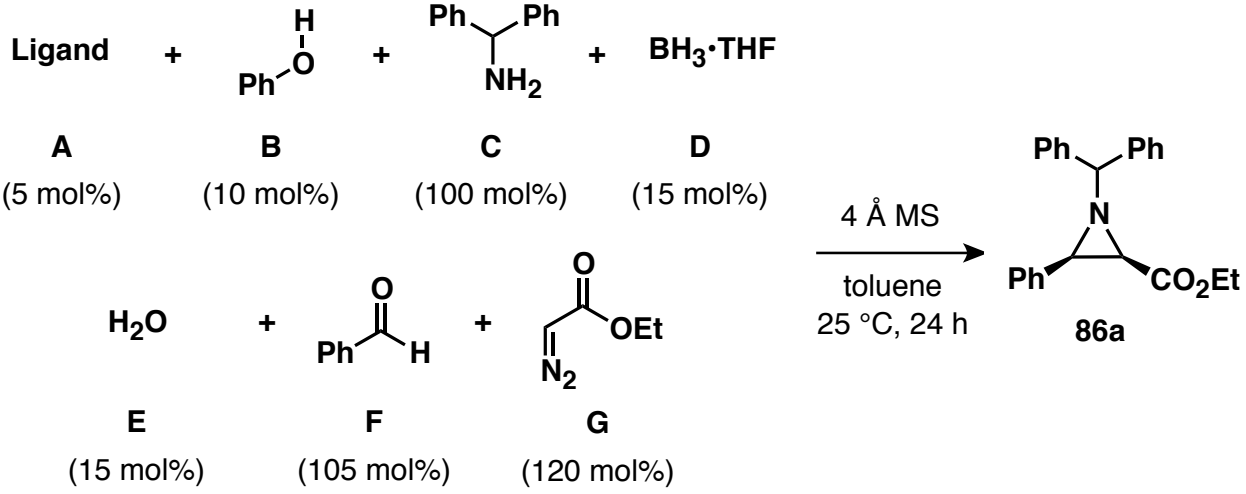

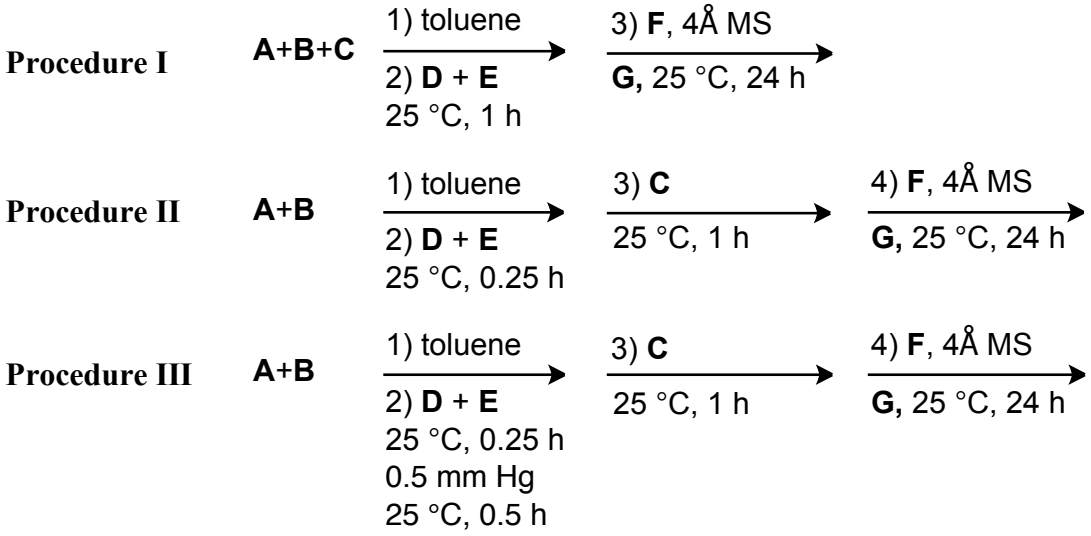

Procedure II in Scheme 7.8 is analogous to the procedure II in Scheme 7.7 except that the mixture of **A**, **B**, **D** and **E** are stirred at room temperature rather than at 100 °C. After stirring a mixture of **A**, **B**, **D** and **E** at 25 °C for 15 min the amine **C** (**126a**) is added and the resulting mixture was stirred for 1 h at 25 °C (procedure II, Scheme 7.8). Then 4Å MS, benzaldehyde **F** (**127a**) and EDA **G** (**85**) are added and the reaction mixture was stirred for 24h at 25 °C. The aziridine **86a** was obtained in 80% yield and 90% ee when VAPOL was used as the ligand (entry 6). Interestingly, complete conversion was also obtained with the VANOL catalyst using procedure II (entry 7). A slightly better result was obtained when the pre-catalyst was kept under vacuum for 0.5 h at 25 °C prior to treatment with the amine **126a** (procedure III, Table 7.11, entries 8-9).

Table 7.11 Multicomponent aziridination using BH_3•THF as the boron source [a]

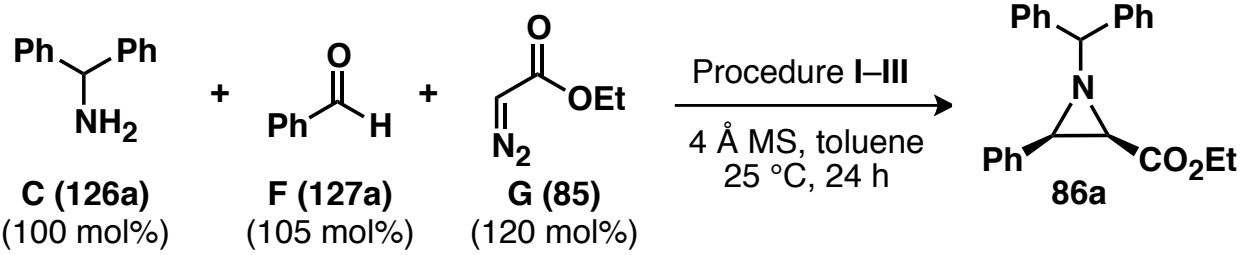

#	Procedure	Cat. loading	Ligand	Yield **86a** (%) [b]	ee **86a** (%) [c]
1	**I**	10	(*S*)-VAPOL	72 (78)	92
2	**I**	10	(*S*)-VANOL	– (46)	–
3	**I**	10	(*S*)-VAPOL	94 (98) [d]	95
4	**I**	10	(*S*)-VANOL	– (29) [d]	–
5	**I**	5	(*S*)-VAPOL	88 (90) [d]	96
6	**II**	10	(*S*)-VAPOL	80	90
7	**II**	10	(*S*)-VANOL	75	87
8	**III**	10	(*S*)-VAPOL	85	91
9	**III**	10	(*S*)-VANOL	82	89

Table 7.11 cont'd

[a] Unless otherwise specified, all reactions were performed with procedures I-III in Scheme 7.8 with 1 mmol of amine **126a** in toluene (0.5 M in imine) with 1.05 equiv of aldehyde **127a** and 1.2 equiv of **85** and went to 100% completion and gave aziridine **86a** with cis/trans ratio of >50:1. Small amount of enamine side-products were observed for some reactions (3 to 9%). All the reactions were performed with a new bottle of BH_3•THF. The data represents the average of two runs for each entry. [b] Isolated Yield. Number in parenthesis is the percent conversion. Percent conversion is determined by integration of the methine proton of *cis*-aziridine relative to the sp^2-CH proton of the unreacted imine **78a** in the ^{1}H NMR spectrum of the crude reaction mixture. [c] Determined by HPLC. [d] $PhCO_2H$ was used as an additive ($PhCO_2H$: ligand = 1:2) during the stirring of **A-E** for 1 h at 25 °C. Also, 1.5 equiv of aldehyde **127a** used. Data provided by Wynter Osminski.

The results presented in Table 7.11 are the average of two runs using a new bottle of BH_3•THF. However, it was found that the results did vary depending the quality of the BH_3•THF used in the reaction. The quality of BH_3•THF cannot be controlled as it decomposes over a period of time. Sometimes, the results were found to be unsatisfactory even if a new bottle of BH_3•THF was used.

7.9 Initial attempts towards a multicomponent *trans*-aziridination reaction

In the year 2010, our group reported the first examples of *trans*-aziridination using our IMINO-BOROX catalyst.[9g] The evolution of the *trans*-aziridination has been a step towards the universal aziridination as our protocol now provides easy access to both *cis*- and *trans*-aziridines from the same catalyst and the same imine. After successful completion of the project related to the first multicomponent *cis*-aziridination, it was thought to extend the methodology by expanding to include the first multicomponent *trans*-aziridination. This reaction was to found to be extremely substrate specific. The results are presented in Table 7.12.

Table 7.12 Multicomponent *trans*-aziridination of aldehydes [a]

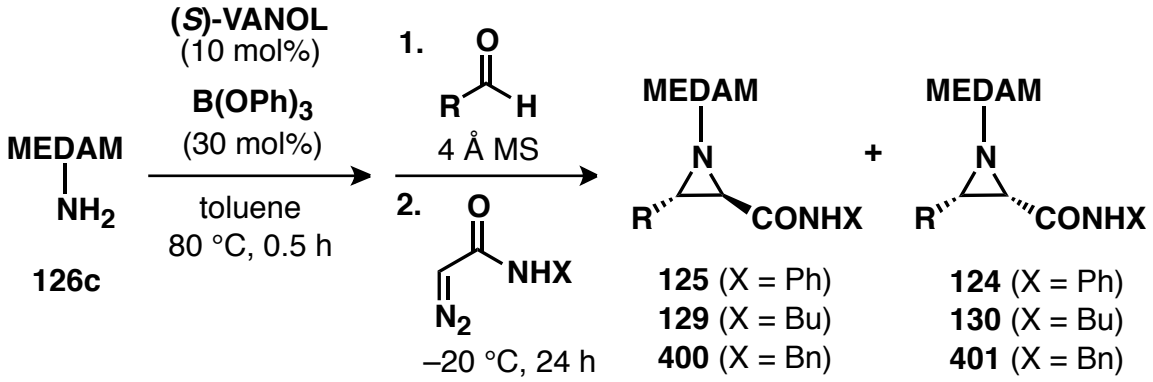

#	Aldehyde **127**	Diazo	Yield *trans*-azi (%) [b]	ee *trans*-azi (%) [c]	Yield *cis*-azi (%) [b]	ee *cis*-azi (%) [c]	t/c [d]
1		**128a** (X = Bu)	<1	–	–	–	–
2 [e]	Ph–CHO	**123a** (X = Ph)	(20) [f,g,h]	nd	(11) [j]	nd	1.8:1
3 [e]		**123a** (X = Ph)	(43) [f,i]	nd	(20) [j]	nd	2.2:1
4		**128a** (X = Bu)	65 [k,l]	92	<1	–	nd
5	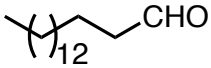	**128b** (X = Bn)	50 [k,m]	82	<1	–	nd
6		**123a** (X = Ph)	35 [k,m]	57	<1	–	nd
7	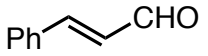	**128a** (X = Bu)	<1	–	<1	–	–
8	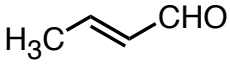	**128a** (X = Bu)	<1	–	<1	–	–
9		**128a** (X = Bu)	5	–	89	88	1:18
10	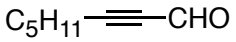	**128a** (X = Bu)	<1	–	70	88	nd
11		**128a** (X = Bu)	<1	–	93	88	1:50

[a] Unless otherwise specified, all reactions were performed with procedure IIA in Table 7.1 with 0.5 mmol of amine **126c** in toluene (0.2 M in imine) with 1.05 equiv of aldehyde **127** and 1.2 equiv of **123a** (X = Ph) or **128a** (X = Bu) or **128b** (X = Bn) and went to 100% completion. Small amount of enamine side-products were observed for some reactions (1 to 9%). [b] Isolated Yield. Yield in parentheses is determined by ^{1}H NMR spectra of crude reaction mixture with Ph_3CH as internal standard. [c] Determined by HPLC. [d] Ratio determined by integration of the methine protons of *cis*- and *trans*-aziridine in the ^{1}H NMR spectrum of the

Table 7.12 cont'd

crude reaction mixture. [e] The amount of epoxide **426a**, enamines and unreacted imine **111a** are 9%, 16%, 43% and 9%, 2%, 3% for entry 2 and 3 respectively. [f] The mixture of ligand , $B(OPh)_3$ and amine **126c** was stirred at 25 °C for 1 h. [g] Reaction temp = 0 °C. [h] 5 mol% catalyst loading and concentration = 0.3 M. [i] The mixture containing the AMINO-BOROX **215b**, aldehyde and 4Å MS was stirred for 1 h prior to the addition of diazoacetamide **123a**. [j] The opposite enantiomer of **124** was observed. [k] The AMINO-BOROX specie **215b** was prepared in 0.4 M. Aldehyde **127p** was added as a solution in toluene. [l] A 70% yield and 93% ee was obtained when the reaction was performed at –10 ºC. [m] Data provided by Munmun Mukherjee.

While the reaction between benzaldehyde **127a** and diazoacetamide **128a** (X = Bu) gave no aziridines, a 20% yield of *trans*-aziridine **125a** was obtained when diazoacetamide **123a** (X = Ph) was employed (Table 7.11, entries 1-2). Incomplete conversions and poor selectivities were obtained for the multicomponent *trans*-aziridination with benzaldehyde irrespective of the method used i.e. true multicomponent or sequential multicomponent reaction (entry 2 vs 3). Additionally, a small amount of epoxide **426a** (9%) resulting from the reaction between benzaldehyde and diazoacetamide **123a** was observed in both cases. To our delight and surprise, the same reaction between *n*-hexadecanal **127p** and diazoacetamide **128a** (X = Bu) yielded aziridine **129p** in 65% yield and 92% ee (entry 4). The same reaction gave an yield of 70% and an ee of 93% at –10 ºC. Later on, another group member, Munmun Mukherjee found that the reaction with *n*-hexadecanal **127p** is highly dependent on the kind of diazoacetamide used (entries 5-6). Since the reactions seemed to be highly dependent on the kind of substrate used, we decided to screen some alkenyl and alkynyl aldehydes. No reaction was obtained with cinnamaldehye or crotonaldehyde. It must be noted that it is also the case that no reaction was observed between the imines derived from these aldehydes and ethyl diazoacteate **85** (Chapter

6). Later, another current group member, Yong Guan, found that the aziridination reaction between imines derived from alkynyl aldehydes and diazoacetamide **123a** afforded *cis*-aziridines **124** in high yields and ees (Chapter 1).[18] More interestingly, the same reaction with the same enantiomer of the ligand afforded the opposite enantiomer of *cis*-aziridine **124** when ethyl diazoacetate **85** was employed (Chapter 1).[18] As a part of this doctoral research, we attempted theses reactions in a multicomponent fashion and we were able to obtain *cis*-aziridine **130** in high yields and ees when the reaction was performed with alkynyl aldehydes and diazoacetamide **128a** (entries 9-11). Although, the multicomponent *trans*-aziridination works well with aliphatic aldehydes, there is obviously still work needed to optimize the reaction with aromatic aldehydes.

7.10 Determination of absolute stereochemistry of *cis*- and *trans*-aziridines using circular dichroism

As a part of further understanding, we decided to determine the absolute chemistry of the *cis*-aziridines **124** and **130** and *trans*-aziridines **125**, **125′**, **129** and **400**. In this regard, the absolute configuration was established by the excellent method developed by Borhan and coworkers using circular dichroism.[24] This work was done in collaboration with Carmin Burrell, a current graduate student in Borhan group. The method was applied to a number of aziridines as listed in Figure 7.6A and 7.7A.

The absolute stereochemistry of the *cis*-aziridines was confirmed through evaluation by exciton coupled circular dichroism (ECCD). The sign of the observed ECCD curve is a reflection of the stereochemistry of the aziridines in that a pair of enantiomeric molecules will

exhibit ECCD signals with opposite sign. Each aziridine was titrated into a 1μM solution of the porphyrin tweezer, Zn-C_5-TPFP-Tz, in hexanes at 0 °C. Below is a summary of the ECCD data and the mnemonic to explain the signs of the observed ECCD signals.

Figure 7.6 Determination of absolute stereochemistry of *cis*-aziridines **124** and **130**. (**A**) Observed ECCD amplitudes for chiral *cis*-aziridines. All measurements were performed with 1μM tweezer in hexanes at 0 ºC. (**B**) Proposed mnemonic explaining the signs of the observed ECCD signals.

A

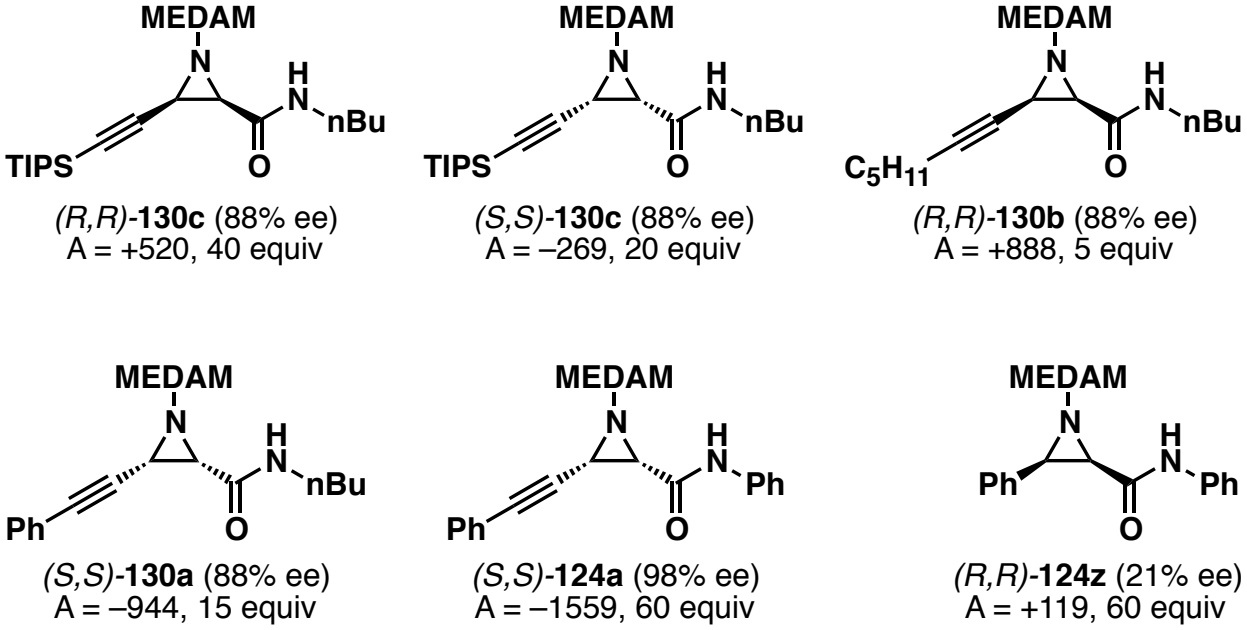

(R,R)-**130c** (88% ee)
A = +520, 40 equiv

(S,S)-**130c** (88% ee)
A = –269, 20 equiv

(R,R)-**130b** (88% ee)
A = +888, 5 equiv

(S,S)-**130a** (88% ee)
A = –944, 15 equiv

(S,S)-**124a** (98% ee)
A = –1559, 60 equiv

(R,R)-**124z** (21% ee)
A = +119, 60 equiv

Figure 7.6 cont'd

B

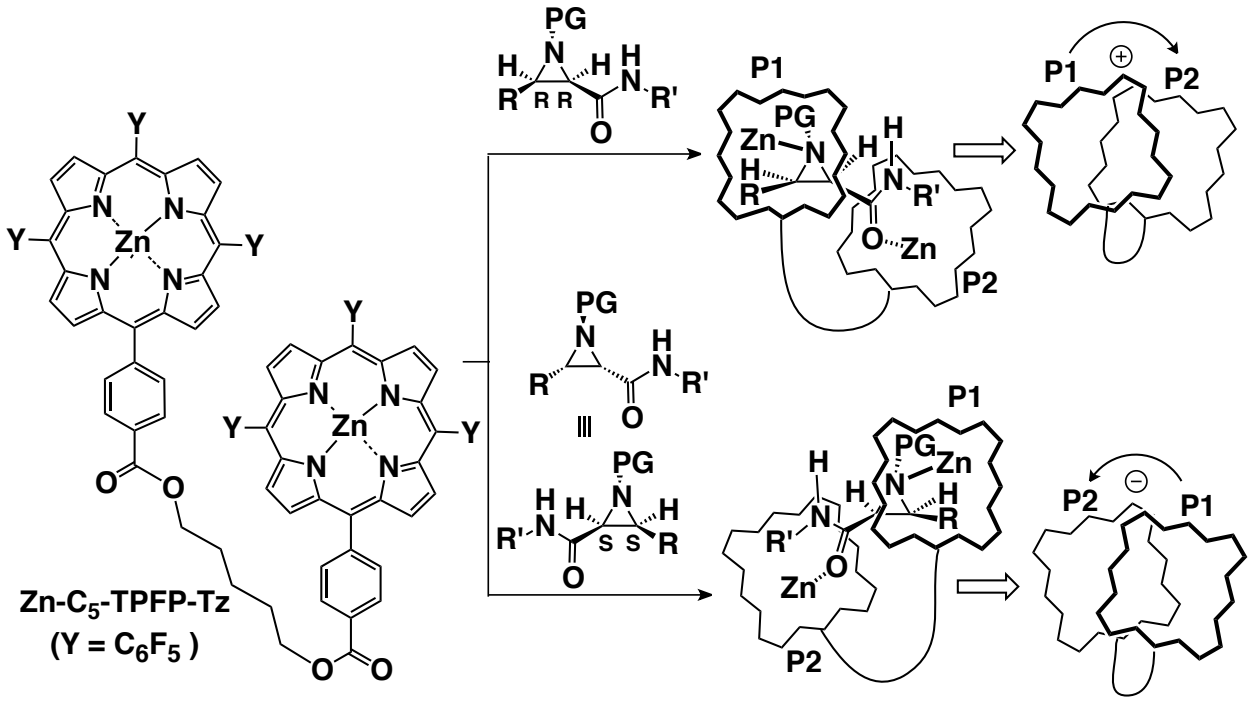

The host-guest, aziridine-tweezer, complex is formed by coordination of the nitrogen and the oxygen of the amide carbonyl to the zinc centers of the porphyrin tweezer. In the case of *cis*-aziridines, it is believed that the protecting group of the *cis*-aziridine nitrogen (PG) will reside opposite of the *cis*-aziridine substituents. Therefore, as shown in Figure 7.6B, the front porphyrin P1 binds to the *cis*-aziridine to the same face as the substituents and remains essentially static. The rear porphyrin P2 binds to the carbonyl of the amide and rotates away from the *cis*-aziridine. Hence, a positive ECCD signal is expected for the (*R,R*)-aziridines and a negative signal for the (*S,S*)-aziridines. It was delightful to observe the correct prediction of the absolute stereochemistry of *cis*-aziridines when compared to the already established absolute stereochemistry of (*S,S*)-**124a**[18] **and** (*R,R*)-**124z**[9g] via chemical derivatization.

In the case of *trans*-aziridines, the shown absolute configuration (Figure 7.7A) is based on a hypothetical mnemonic that will require conformation by other means. It is conjectured that for the *trans*-azridines, when bound to the porphyrin tweezer, the nitrogen is pyramidalized such that the lone pair electrons of the nitrogen are opposite to the amide functionality. As shown in Figure 7.7B, the rear porphyrin P2 binds to the nitrogen and rotates away from the R group. The front porphyrin P1 binds to the carbonyl of the amide and rotates toward the hydrogen. Therefore, substrates with an *(S,R)* configuration are expected to give a positive ECCD signal and a negative signal would be observed for the substrates with an *(S,R)* configuration.

Figure 7.7 Determination of absolute stereochemistry of *trans*-aziridines **125**, **125′**, **129** and **400**. (**A**) Observed ECCD amplitudes for chiral *trans*-aziridines. All measurements were performed with 1μM tweezer in hexanes at 0 ºC. (**B**) Proposed mnemonic explaining the signs of the observed ECCD signals.

A

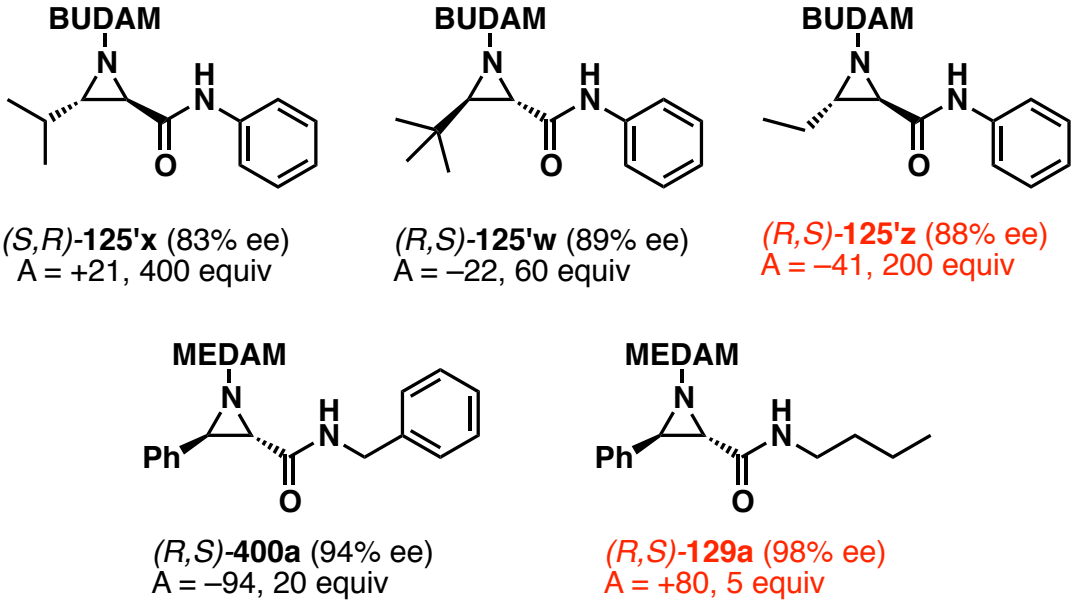

Figure 7.7 cont'd

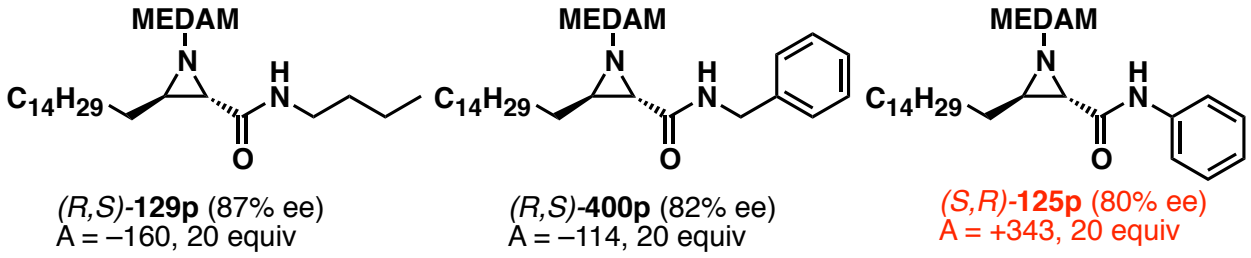

B

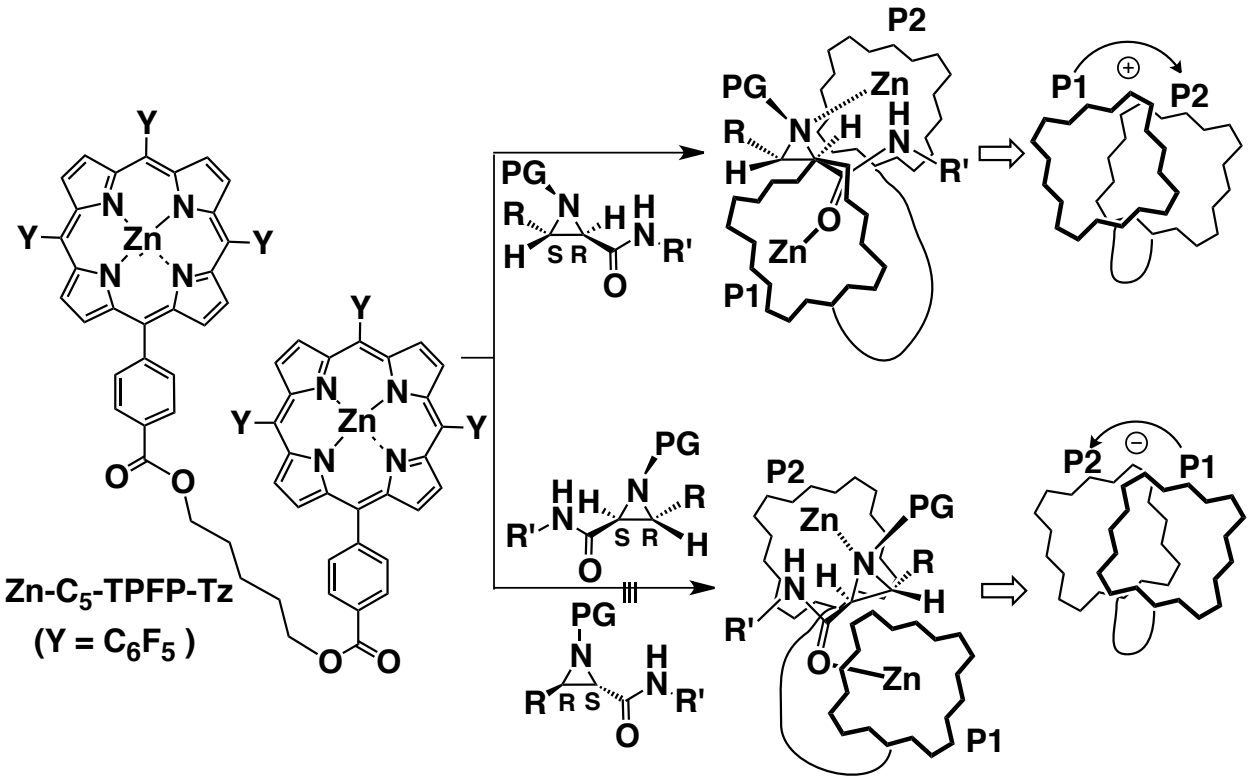

The absolute stereochemistry of *(S,R)*-**125a** (R = Ph, R′ = Ph, Figure 7.7B, aziridine not shown here) was established via chemical derivatization.[9g] The same stereochemistry has been assumed for other *trans*-aziridines prepared from same enantiomer of the ligand. It was delightful to observe the correct prediction of the absolute stereochemistry of *trans*-aziridines when compared to the already established absolute stereochemistry of *(S,R)*-**125a** (not shown

here). Unfortunately, the proposed mnemonic for the three aziridines *(R,S)*-**125′z**, *(R,S)*-**125p** and *(R,S)*-**129a** did not match to the experimental results (shown in red color in Figure 7.7A). It must be noted that the absolute stereochemistry of these substrates was not determined by any other means and the stereochemistry indicated in the Figure 7.7A is based on the expected configuration from the ligand employed for their synthesis. In these cases, the ECCD sign is opposite to what is predicted by proposed mnemonic. The result obtained from ECCD indicates either these three particular substrates behave differently with ligands or the substrate-tweezer complex favors a different conformation for these substrates, which is affecting the outcome of ECCD. Hence, to determine the cause of the incorrect ECCD sign, the stereochemistry of these substrates should be confirmed by other means and a screen of ECCD conditions should be conducted. Further probe is underway during the time of the writing of this dissertation.

7.11 Gram scale catalysis and large scale synthesis

The real application of any methodology lies in its easy adaption towards the large-scale synthesis. The multicomponent aziridination was easily applicable to gram scale without any detrimental effect on the yields or ee (Scheme 7.9).

Scheme 7.9 Gram scale asymmetric catalysis

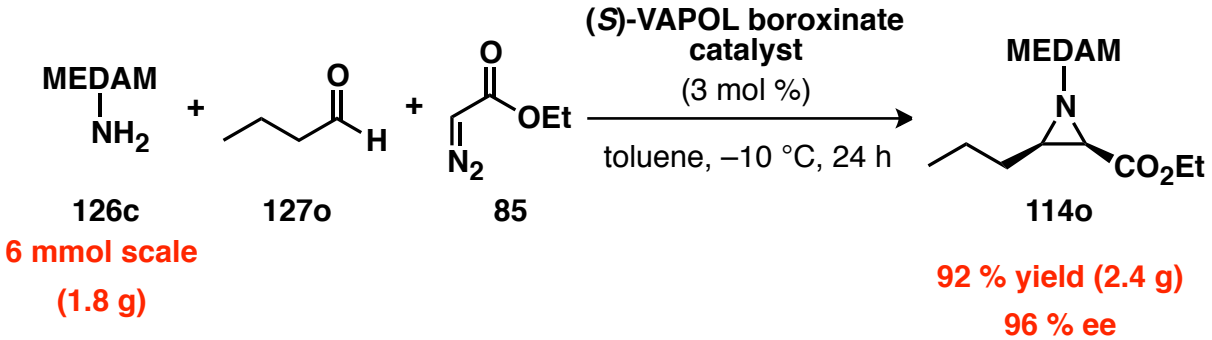

Scheme 7.9 cont'd

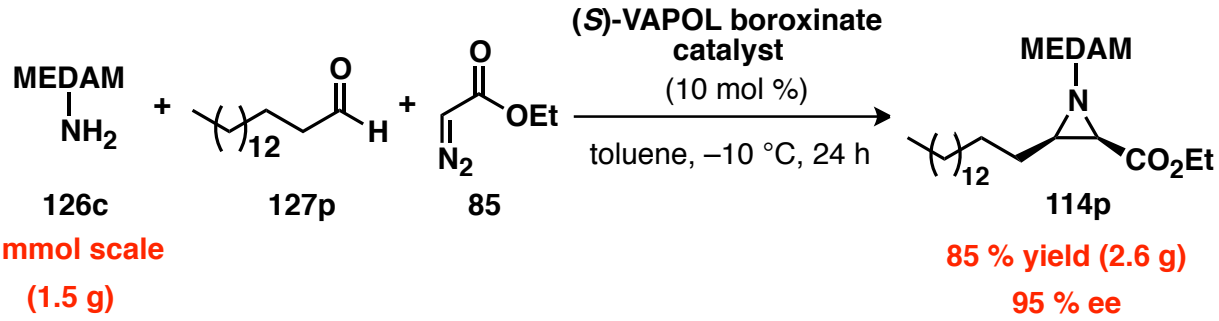

The tetra-methyldianisylmethyl (MEDAM) amine **126c** is the optimal protecting group in the case of the Wulff catalytic asymmetric *cis*-[9c] and *trans*-aziridination[9g] reaction. Unfortunately, the MEDAM amine **126c** is not commercially available. Hence, we decided to develop an easy and economic route to prepare amine **126c** from the commercially available starting materials. The synthesis of tetra-methyldianisylmethyl (MEDAM) amine **126c** shown in Scheme 7.10 follows that previously reported and was scaled up to 58 mmol on the commercially available bromide **403**.[9c] The nitrile **404** can be obtained from the bromide **403** by the Shechter modification of the Rosenmund-Van Braun reaction.[25] The key step in the synthesis of amine **126c** involves the reaction of the nitrile **404** with the *in-situ* generated Grignard reagent **405**. The subsequent *in-situ* reduction of the resulting imine intermediate **405′** provides the amine **126c** in 66% yield from the nitrile **404**. The entire process of preparation of MEDAM amine **126** was carried out efficiently without the use of any column chromatography purification. It must be noted that this project was initiated by Munmun Mukherjee. The modifications that were made in the reaction sequence are as follows: a) commercially available bromide **403** was used, b) the nitrle **404** was used in the Grignard reaction without any

purification and c) MEDAM amine•HCl salt was made using dry HCl gas instead of a 12 M HCl solution during the purification of final product **126c**.

Scheme 7.10 Large scale synthesis of MEDAM amine **126c**

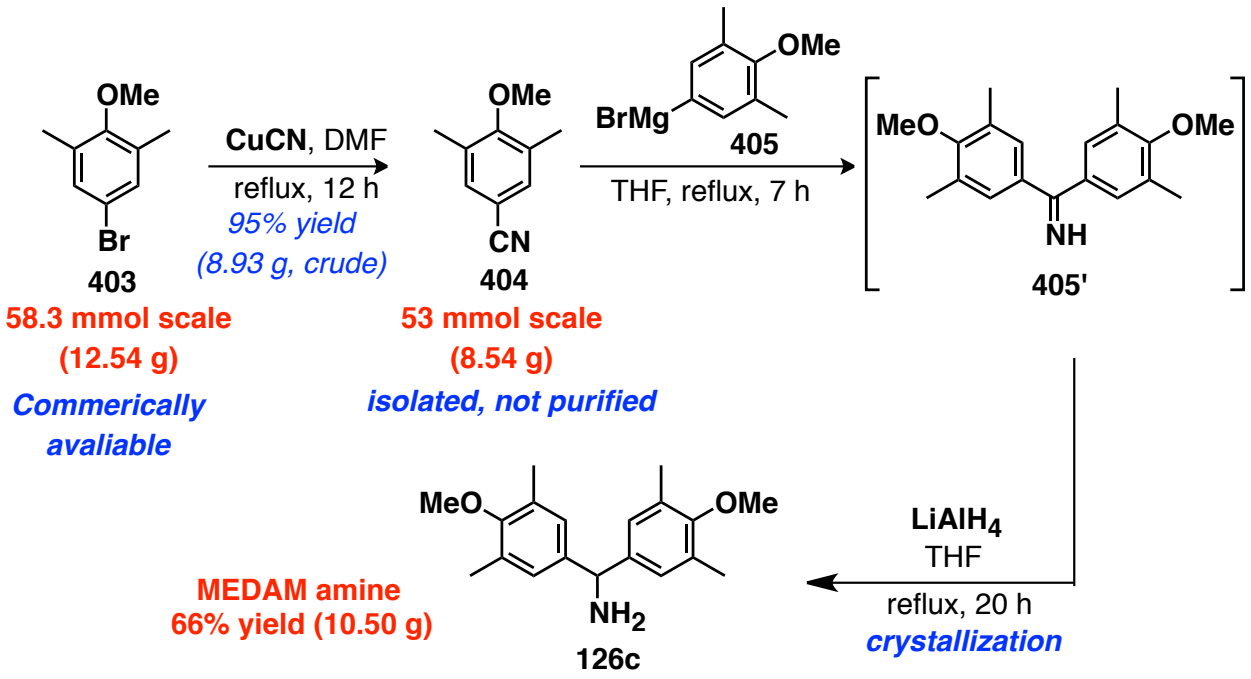

7.12 Application of multicomponent aziridination reaction in organic synthesis

The real advantage of any methodology lies in its practical application in the field of organic synthesis. Henceforth, we decided to apply the newly developed multicomponent aziridination reaction in organic synthesis. It must be pointed out that another current group member Munmun Mukherjee has done the following work shown in Scheme 7.11A-C. Following the MCAZ protocol, we have been able to accomplish the synthesis of all four diastereomers of sphinganines in good yield in four steps from amine **126c** (Scheme 7.11B).[19] Also, the MCAZ reaction has been found to be useful in the diastereoselective aziridination of chiral aldehydes (Scheme 7.11A).[26] Further, we have been able to perform a direct

transformation of benzaldehyde **127a** to β-hydroxy-α-amino ester **408** and α-amino ester **409** in a one-pot fashion (Scheme 7.11C).[12] Last, but not the least, a direct access to β-lactam **411** from aldehydes was possible in 58% overall yield as shown in Scheme 7.11D.[27]

Scheme 7.11 Application of MCAZ reaction in organic synthesis

A Studies towards enantioselective synthesis of phytosphingosines

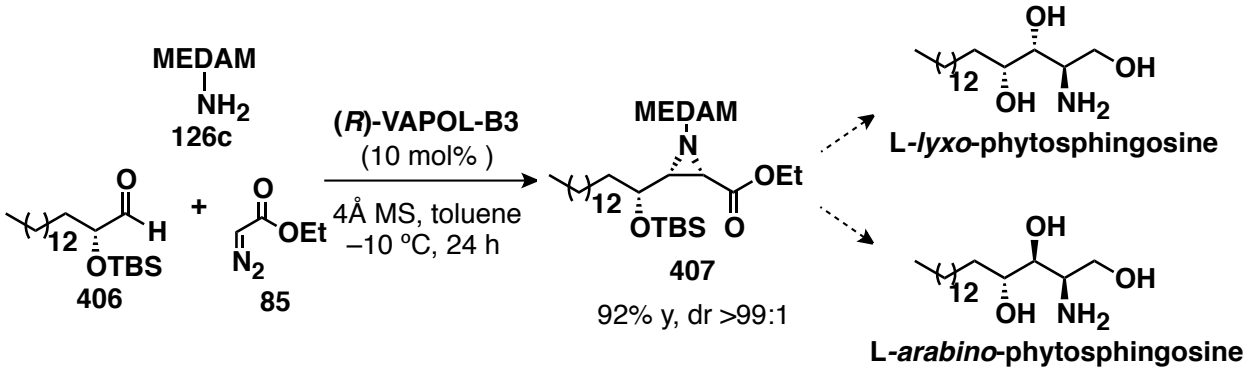

B Enantioselective synthesis of sphinganines

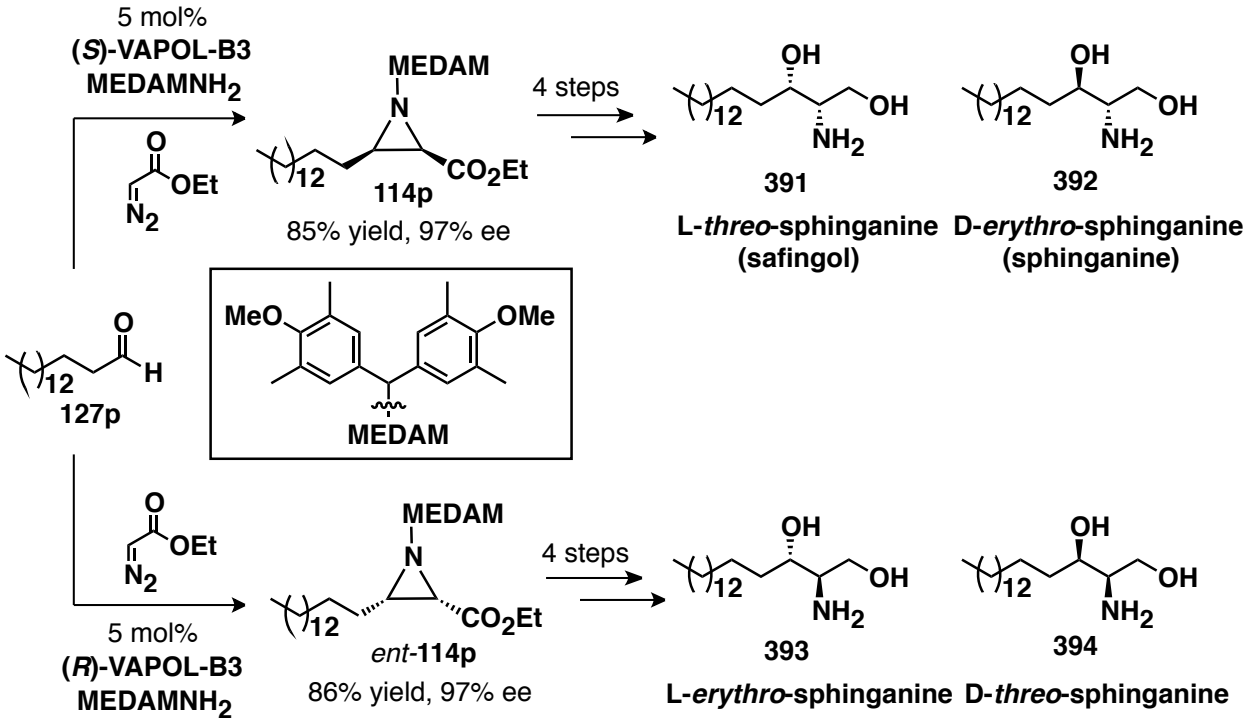

Scheme 7.11 cont'd

C One-pot synthesis of β-hydroxy-α-amino ester **408** and α-amino ester **409**

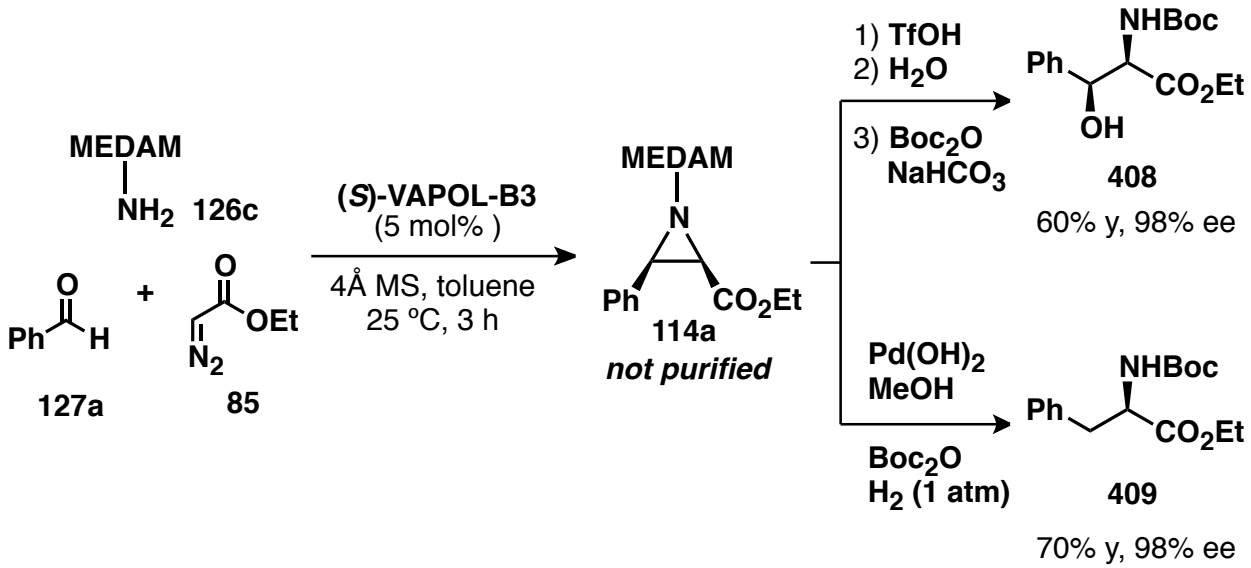

D One-pot synthesis of β-lactam **410**

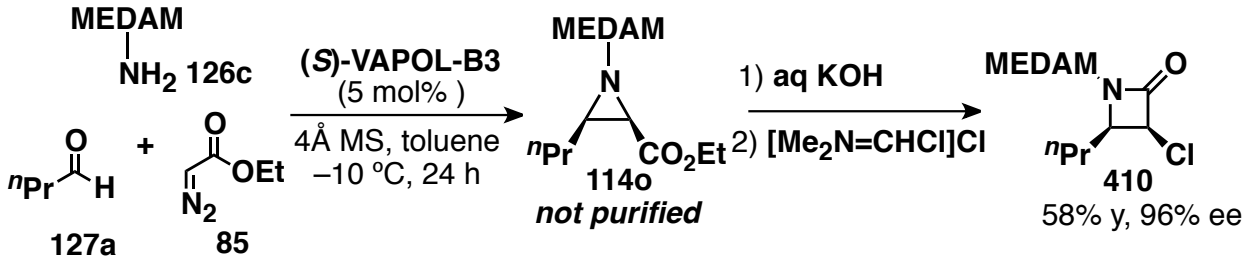

7.13 Future applications: multicomponent intra-molecular aziridination reaction

The Wulff group has been working on intra-molecular aziridination for quite a while. The initial idea is presented in Scheme 7.12A. However, the synthesis and stability of imine **411** was not known. Also, the possibility of self-condensation of the imine **411** under traditional aziridination conditions cannot be ruled out. The development of MCAZ protocol has taken the idea one step further. Hence, the stability of the imine and the possibility of aldol-adduct would not be a problem in the case of proposed multicomponent intra-molecular aziridination reaction (Scheme 7.12B). However, there is the daunting task of making the aldehyde **413**. It is an

unknown compound and might be highly unstable due to the presence of the diazo component. It was then envisioned that this problem could be solved by using compounds like **417** and **418** (Scheme 7.12B). The 2-(2-pyridyl)Propane-1,3-diol **416** is a mild protecting group and can be easily deprotected under mild basic conditions.[28] Although, we were able to make diol **416**, several attempts towards the generation of **417** and **418** were not successful and are not presented here. However, based on the information obtained from the multicomponent aziridination reaction described in this work, it is reasonable to expect that the intra-molecular aziridination reaction will be accomplished in the near future provided that the compounds **417** and **418** are available.

Scheme 7.12 Proposed intramolecular aziridination reaction via (**A**) Traditional aziridination (**B**) Multicomponent aziridination reaction.

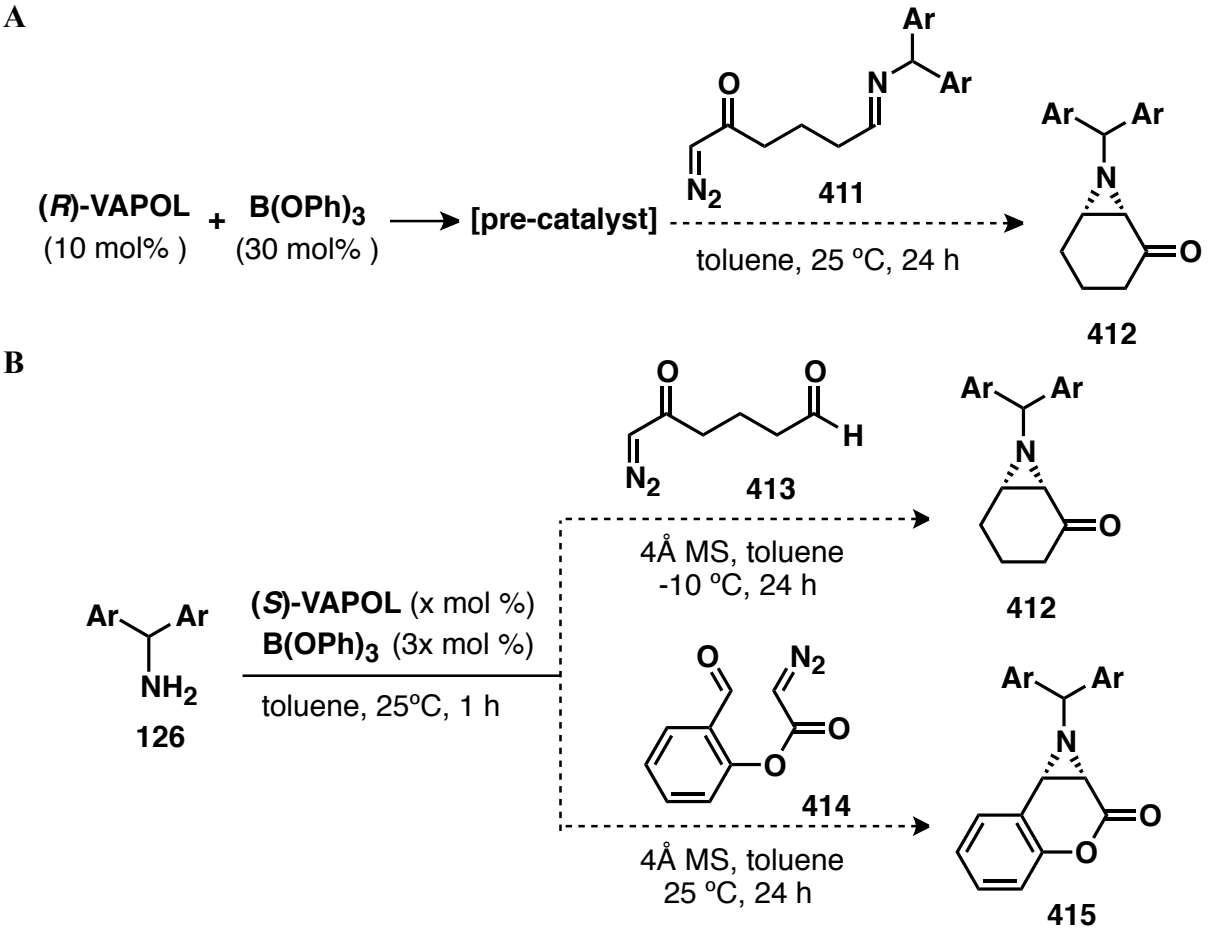

Scheme 7.12 cont'd

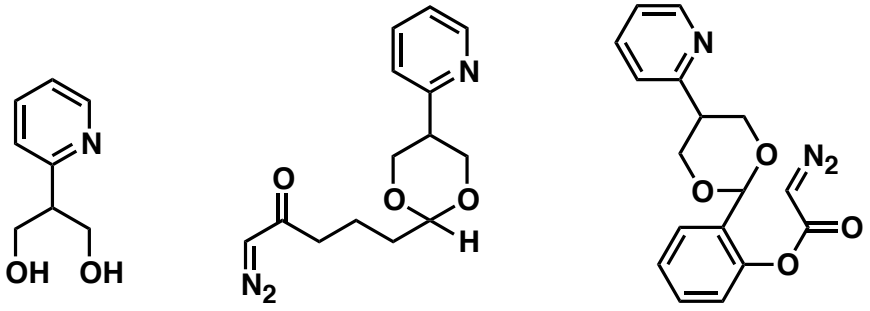

416 417 418

7.14 Conclusions

The practicing chemist now has at one's avail a multi-component asymmetric catalytic method for the preparation of aziridines directly from aldehydes, an amine and a diazo compound.[12] The chiral catalyst for this reaction has a boroxinate core comprised of a chiral polyborate that is assembled *in-situ* from a vaulted biaryl ligand (VANOL or VAPOL) and three equivalents of $B(OPh)_3$ by the amine substrate. The present work shows that this is actually a rather unique five-component process involving both catalyst assembly and a catalytic asymmetric aziridination reaction.[13] A solution of these five components has the potential to create a chaotic array of products and yet there is order since aziridines are formed in very high yields, diastereoselectivities and enantioselectivities. This order is imposed by the amine in causing an exceedingly fast assembly of the boroxinate catalyst from the ligand and $B(OPh)_3$. Once the catalyst is assembled, it is protected from alkylation by the diazo compound and since the $B(OPh)_3$ is consumed, the epoxidation reaction of the diazo compound and the aldehyde is thwarted. This then permits the formation of an imine from the aldehyde and amine and the

resulting imine binds in its protonated form to the boroxinate catalyst. This is followed by binding of the diazo compound to the chiral boroxinate catalyst in such proximity to the bound iminium that an aziridine is formed with high diastereo- and enantioselection.[9h] In addition, a seven-component catalyst assembly/catalytic asymmetric aziridination was also realized. Further, the methodology was used as the key step in the enantioselective synthesis of the sphinganine family of biologically important compounds.[19] In the synthesis of phytosphingosines, a diastereoselective aziridination was performed as the key step following the MCAZ protocol.[26] All in all, the MCAZ reaction incorporates a very simplified protocol and it provides an effective solution to the catalytic asymmetric syntheses of alkyl-substituted aziridines which have remained elusive until now. Also, it is quite general for a wide range of aldehydes bearing a variety of functional groups. More recently, the practical viability of this methodology has been highlighted in reputed magazines and journals.[29]

APPENDIX

7.15 Experimental

7.15.1 General Information

Same as Chapter 2

7.15.2 Synthesis of amine 126c, imines 78a, and diazoacetamides 123a, 128a and 128b

a) Large scale synthesis of MEDAM amine 126c

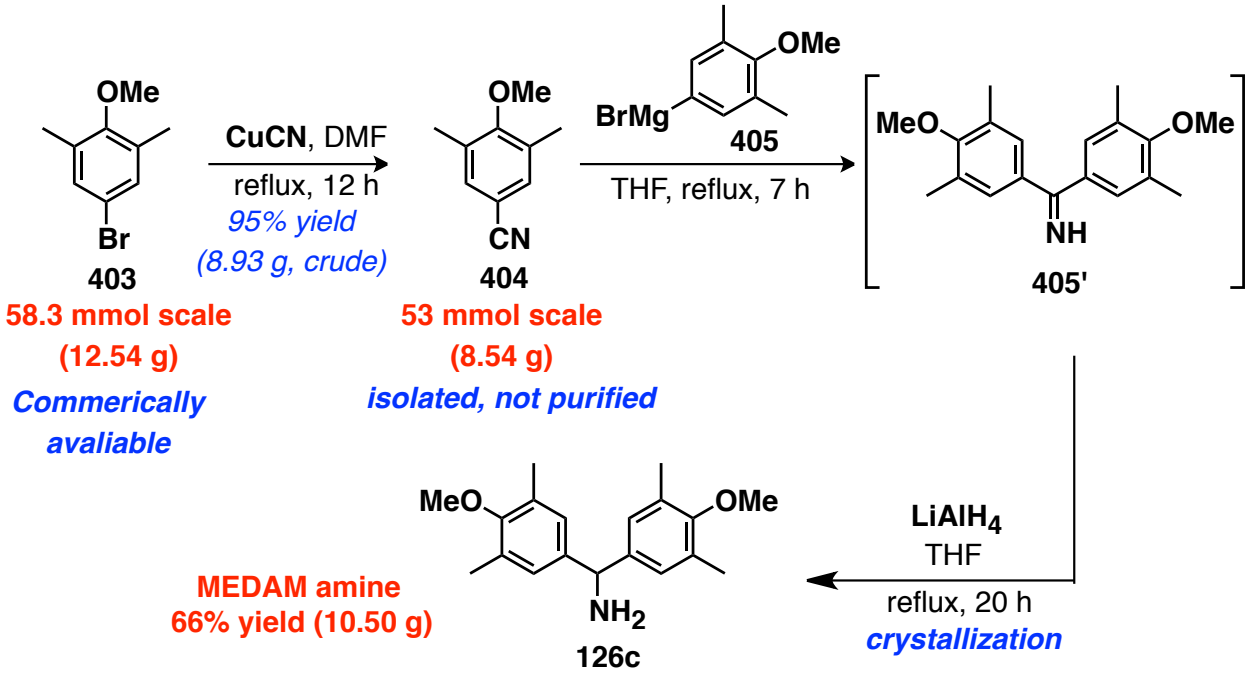

4-methoxy-3,5-dimethylbenzonitrile 404: A 500-mL three-necked round-bottomed flask, sealed with rubber septums at two necks and equipped with a big stir bar and a 24/40 vacuum adapter at the middle neck, was flame-dried and cooled under nitrogen. To this flask was added CuCN (6.27 g, 70 mmol, 1.2 equiv.) through one of the necks. During addition, a continuous flow of nitrogen was maintained at the middle neck *via* vacuum adapter along with an outlet of nitrogen (in the form of a bubbler) at the other neck. It was followed by the addition of 5-bromo-2-methoxy-1,3-dimethylbenzene **403** (9.3 mL, 12.54 g, 58.3 mmol) and anhydrous DMF (125 mL, freshly distilled and stored over 4Å MS) using 10 mL syringe and 60 mL syringe

respectively. The vacuum adapter, on the middle neck, was then replaced by a rubber septum with a nitrogen-filled balloon. Thereafter, the reaction mixture was purged with nitrogen under the surface of the solution for next 15 min via left neck of the flask utilizing the long metal needle attached directly to the nitrogen source. During purging, an outlet of nitrogen (in the form of a bubbler) was maintained through the other (right) neck. Immediately, an oven-dried Vigreux air condenser (25 mm × 350 mm) followed by an oven-dried water condenser (17 mm × 220 mm) was placed on the middle neck along with a Teflon sleeve at the joint. The source of nitrogen was then changed to a nitrogen-filled balloon on the top of the condenser through a rubber septum stopper. Thereafter, the rubber septums, at the other two necks, were replaced by teflon stoppers and all the necks were further sealed by Teflon tape. The mixture was then heated to reflux in an oil bath (178 ºC) for 12 h (the reaction was followed by TLC until the disappearance of the starting material). During the refluxing, the solid CuCN dissolved after approximately 15 min and a light green precipitate of CuBr was observed which further dissolves to give a brown colored solution in due course of time. The reaction mixture was then cooled gradually to room temperature and after cooling down, it was a dark green solution with little light green precipitate of copper salt at the bottom of the flask. Beyond this point, all the operations were carried out under the hood. The reaction mixture was then slowly poured into a 2 L Erlenmeyer flask containing an aqueous solution of ethylenediamine (25 mL ethylene diamine in 620 mL water) along with a big stir bar at 0 ºC (ice-bath). During addition, a continuous stirring was maintained. The three-neck round-bottomed flask was washed with 20 mL of an aqueous solution of ethylene diamine (25 mL ethylene diamine in 620 mL water). The resulting purple colored reaction mixture was then allowed to warm gradually to room temperature. It was then followed by the addition of benzene (200 mL) and the resulting mixture

was stirred vigorously at room temperature for 20 min and then transferred directly into a 2 L separatory funnel. The top organic layer (mud colored) was separated. The purple colored aqueous layer was then extracted with benzene (80 mL × 4). The combined organic layer was washed with 1.22 M NaCN solution (100 mL) and a change in color from mud to murky white was observed. The resulting solution was then washed with water (110 mL × 2), dried over $MgSO_4$ and filtered (washed with benzene (50 mL × 2)) to a 1 L round bottom flask. The yellow solution was then subjected to rotary evaporation (25 °C, 20 mmHg) to afford the crude product **2** as pale yellow oil, which became a murky white solid (8.93 g, 95% crude yield) on being kept under vacuum overnight. It was used in next step without any further purification.

Bis-(2,6-di-methyl-4-methoxyphenyl)methineamine 126c: A 500-mL three-necked round-bottomed flask, sealed with rubber septums at two necks and equipped with a big stir bar and a 24/40 vacuum adapter at the middle neck, was flame-dried and cooled under nitrogen. To this flask was added magnesium (3.6 g, 148.4 mmol, 2.8 equiv, 20 mesh) through one of the necks utilizing powder funnel. Next, anhydrous THF (125 mL, freshly distilled) and a few crystals of iodine (2 crystals, 92 mg) were added. During addition, a continuous flow of nitrogen was maintained at the middle neck *via* vacuum adapter. The vacuum adapter, on the middle neck, was then replaced by an oven-dried water condenser (33 mm × 470 mm) placed on the middle neck along with a Teflon sleeve at the joint and sealed with Teflon Tape. The source of nitrogen was then changed to a nitrogen-filled balloon on the top of the condenser through a rubber septum stopper. It was followed by the addition of 4-bromo-2,6-dimethylanisole **403** (9.3 mL, 12.54 g, 58.3 mmol, 1.1 equiv) using 10 mL syringe. During addition a continuous stirring was maintained Thereafter, the rubber septums, at the other two necks, were replaced by teflon stoppers and all the necks were further sealed by Teflon tape. The red color mixture was then

heated to reflux in an oil bath (78 ºC) for 4 h. The resulting clear grey solution was allowed to cool down to room temperature. One of the Teflon stoppers was then replaced by a rubber septum. Meanwhile, to a flame-dried 250 mL round-bottomed flask, filled with nitrogen, was added 4-methoxy-3,5-dimethylbenzonitrile **404** (8.54 g, 53 mmol, 1.0 equiv) and THF (100 mL, freshly distilled). This yellowish orange solution was then transferred (dropwise) *via* cannula to the 500 mL three-necked round-bottomed flask containing the freshly prepared Grignard reagent **405** over a period of 20 min at room temperature. The flask containing 4-methoxy-3,5-dimethylbenzonitrile **404** was then rinsed with THF (10 mL, freshly distilled) and the rinse was transferred to the flask containing Grignard reagent **405**. The resulting mixture was heated to reflux in an oil bath (78 ºC) for 7 h under nitrogen. A reddish brown colored solution was obtained and then allowed to cool down to room temperature, and then to 0 ºC (ice-bath). Meanwhile, a suspension of $LiAlH_4$ (2.2 g, 58.3 mmol, 1.1 equiv) in THF (55 mL, freshly distilled) was prepared in a flame-dried 1 L round-bottomed flask filled with nitrogen and pre-cooled at 0 ºC. Next, the *in-situ* generated imine **405′** was transferred to 1 L round-bottomed flask containing LAH suspension *via* cannula at 0 ºC. The flask containing *in-situ* generated imine **405′** was then rinsed with THF (10 mL, freshly distilled) and the rinse was transferred to the flask containing $LiAlH_4$ suspension. The ice bath was then removed and the same water condenser (along with the Teflon sleeve), utilized in the synthesis of Grignard reagent, was placed on the 1 L round-bottomed flask containing the reaction mixture. The joint was further sealed by Teflon tape. Thereafter, the resulting greenish yellow reaction mixture was heated to reflux in an oil bath (78 ºC) for 20 h under nitrogen. The reaction flask was cooled down to room temperature and then to 0 ºC, and carefully quenched (under hood) by the slow addition of water (2.2 mL), then 3.75 M NaOH solution (2.2 mL), and water (6.6 mL) over a period of 10 min. The

resulting green colored suspension was filtered through a Celite (503) pad into a 1 L round-bottomed flask and washed with ether (100 mL). The remaining filter cake was then transferred to a 1 L beaker along with a big stir bar. Thereafter, ether (150 mL) was added to it. The resulting suspension was stirred vigorously for 10 min. The top of the beaker was covered with aluminum foil during stirring. Meanwhile, the filtrate, after first washing, was concentrated using rotatory evaporation (25 °C, 20 mm Hg). The suspension, in 1 L beaker, was then filtered to 1 L round-bottomed flask containing the crude product. The beaker was then washed with ether (50 mL) and then filtered through the same Celite pad. The above process was repeated eight times using ether ((150 + 50) mL × 8). Subsequently, the filter cake was washed with ether (100 mL × 3) during the last filtration process. The color of the filter cake changed from grey to white. The filtrate was concentrated by rotary evaporation (25 °C, 20 mm Hg) to afford yellow solid (18.87 g, 119% crude yield) on being kept under vacuum overnight. The light yellow solid was then dissolved in EtOAc (100 mL) and stirred for 30 min. Further, the flask was cooled to 0 °C. A stream of *in-situ* generated dry HCl gas was gradually passed into the Erlenmeyer flask containing the amine until the pH ~ 2 (determined by pH paper) resulting in the appearance of yellowish white precipitate. It takes 20 min approximately. During the addition, a continuous stirring was maintained. After addition, the mixture was stirred for 10 min at room temperature. Thereafter, it was allowed to stand still for 1 h at room temperature. The flask was covered with aluminum foil during this period. The resulting yellow colored suspension was filtered through a Buchner Funnel into a 250 mL round-bottomed flask and washed with hexanes (50 mL × 2). The obtained filter cake (amine salt) was then transferred back to a 100 mL beaker with a big stir bar. To this beaker was added EtOAc (40 mL) and the resulting suspension was stirred for 10 min at 0 °C. The resulting yellow colored suspension was filtered through a Buchner Funnel into

the same 250 mL round-bottomed flask and washed with hexanes (50 mL). The above procedure was repeated once more. The resulting off-white cake (amine salt) was transferred to pre-weighed 500 mL round bottom flask and was dried overnight at 0.01 mmHg to provide amine salt as an off-white solid (14.67 g). The filtrate was subjected to rotary evaporation (30 °C, 20 mm Hg) to afford an orange solid (2.55 g) on being kept under vacuum overnight. Meanwhile, a stir bar was added to flask containing amine salt (14.67 g) followed by the addition of the ether (125 mL) and the resulting mixture was cooled to 0 °C. To this solution was added pre-cooled (0 ºC) 6 M NaOH (50 mL) was added portion-wise (~ 5 mL each time) till the pH (water layer) ~ 13. A continuous stirring should be maintained during the addition of the base. The flask was covered with aluminum foil before addtion of base. After pH ~ 13, the mixture was stirred under nitrogen for 0.5-1 h so as to dissolve the entire solid. The reaction mixture was then transferred to 250 mL separatory funnel. The flask was washed with ether (30 mL) and the washing was transferred to the separatory funnel. The organic layer was separated and aqueous layer was washed with ether (60 mL × 4), dried over $MgSO_4$, filtered (washed with ether (50 mL × 3) into a 1 L round-bottom flask. The resulting filtrate was reduced to approximately 100 mL by rotary evaporation (25 °C, 20 mm Hg). It was then transferred to a pre-weighed 250 mL round-bottom flask and concentrated to afford a pale yellow solid (12.71 g, 80.09 % crude yield) on being kept under vacuum overnight.

Purification: The crude amine **126c** was purified by crystallization. A sample of crude product (~ 5 mg) was saved to use as the seeding crystals later on. The 250 mL round-bottomed flask containing the crude solid (12.71 g) was then equipped with reflux condenser sealed with rubber septum having a nitrogen balloon at the top. The solid was then dissolved in hot hexanes (12 mL, 70 °C) and left to cool to room temperature. Thereafter, it was seeded by the sample of crude

product (~ 2 mg) and left overnight at room temperature under nitrogen. Thereafter, the mother liquor was decanted to another pre-weighed 100 mL round-bottomed flask using a 12 inch long pipette. The pipette was washed with hexanes (3 mL) directly into the same pre-weighed 100 mL round-bottomed flask. Now, to the flask containing the resulting pale yellow crystals was added ice-cold hexanes (2 mL × 2) and was decanted to the flask containing the mother liquor. The color of the crystals was changed to off-white. The crystals were dried overnight at 0.01 mmHg to provide **126c** as an off-white crystalline solid in 22.1 % yield (3.500 g, 11.66 mmol, first crop, mp. 60-61 ºC). The mother liquor along with the washings was then subjected to rotary evaporation (25 °C, 20 mmHg) to afford the crude product as a yellow solid (8.90 g). The resulting crude product was then subjected to re-crystallization using hot hexanes (8 mL, 70 °C) as discussed above. Likewise earlier, the mother liquor was decanted to another pre-weighed 100 mL round-bottomed flask using a 12 inch long pipette. The pipette was washed with hexanes (3 mL) directly into the same pre-weighed 100 mL round-bottomed flask. Now, to the flask containing the resulting pale yellow crystals was added ice-cold hexanes (3 mL × 1 and 2 mL × 2) and was decanted to the flask containing the mother liquor. The color of the crystals was changed to off-white. The crystals were dried overnight at 0.01 mmHg to provide **126c** as an off-white crystalline solid in 25.2 % yield (4.000 g, 13.36 mmol, second crop, mp. 59-60 ºC). The crude product (4.80 g) obtained after rotary evaporation (25 °C, 20 mmHg) was subjected to re-crystallization using hot hexanes (5 mL, 70 °C). Following the above discussed procedure, an 18.9 % yield (3.000 g, 10.02 mmol, third crop, mp. 59-61 ºC) of 126c was obtained after the washing with ice-cold hexanes (3 mL × 1 and 2 mL × 2). The resulting crude product (1.8 g, dark red) was not further purified. After three crystallizations, the combined yield of **126c** was 66.2% (10.50 g, 35.04 mmol).

Spectral Data for **126c**: R_f = 0.3 (5:1:0.2 EtOAc/Hexanes/MeOH). ^{1}H-NMR ($CDCl_3$, 300 MHz) δ 1.73 (s, 2H), 2.26 (s, 12H), 3.69 (s, 6H), 5.00 (s, 1H), 7.01 (s, 4H); ^{13}C-NMR ($CDCl_3$, 75 MHz) δ 16.10, 58.77, 59.50, 126.96, 130.56, 140.88, 155.65; IR (thin film) 3376m, 3306m, 2943vs, 1493s cm^{-1}; Mass spectrum: *m/z* (% rel intensity) 299 M$^+$ (35), 298 (54), 283 (47), 268 (94), 163 (100); Anal calcd for $C_{19}H_{25}NO_2$: C, 76.22; H, 8.42; N, 4.68. Found: C, 75.89; H, 8.54; N, 4.62. These spectral data match those previously reported for this compound.[9c]

b) Synthesis of imine 78a: see chapter 2 (experimental)

c) Synthesis of diazoacetamides 123a, 128a and 128b: see Chapter 8 (experimental)

7.15.3 Attempt to make imine 111t from aldehyde 127t *(Scheme 7.1)*

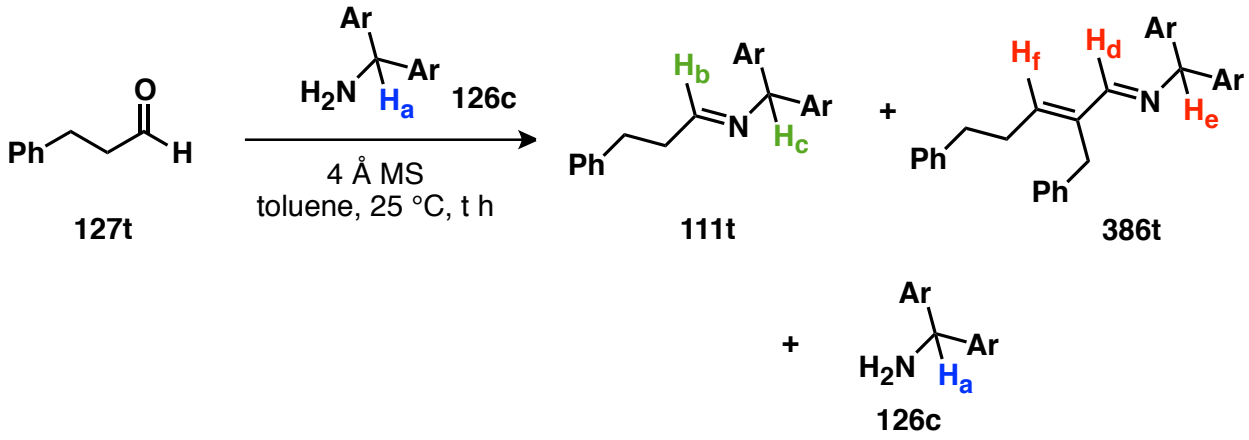

To a 5 mL flame-dried single-necked round bottom flask, equipped with a stir bar, filled with argon was added MEDAM amine **126c** (59.9 mg, 0.200 mmol), 4Å MS (50 mg, freshly dried) and dry toluene (1 mL). After stirring for 10 min, aldehyde **127t** (28.2 mg, 0.210 mmol, 1.05 equiv) was added. The reaction mixture was stirred at room temperature. The crude reaction

mixture was then monitored at different time intervals by ^{1}H NMR. The result is described in the chapter.

7.15.4 Possible complications for the five-component catalyst assembly/aziridination *(Scheme 7.4)*

A) Alkylation of the ligand:

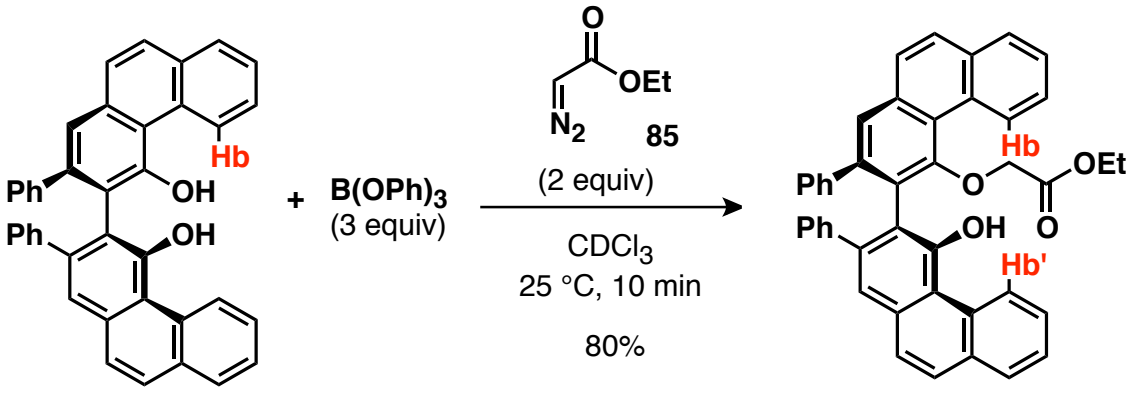

(*S*)-VAPOL 58
δ = 9.77 ppm
(Hb)

230
mono-alkylated (*S*)-VAPOL derivative
δ = 9.56 ppm and 9.83 ppm
(Hb and Hb')

To a 10 mL flame-dried round bottom flask, equipped with a stir bar and a rubber septum and filled with argon was added (*S*)-VAPOL **58** (54 mg, 0.10 mmol, 1.0 equiv), $B(OPh)_3$ (87 mg, 0.30 mmol, 3.0 equiv), ethyl diazoacetate **85** (0.20 mmol, 2.0 equiv.), Ph_3CH (12.2 mg, 0.500 mmol) and $CDCl_3$ (1 mL). The resultant mixture was stirred for 10 min at room temperature. The resulting solution was then directly transferred to a quartz NMR tube (freshly flame-dried) and was subjected to NMR analysis. The reaction furnished the mono-alkylated adduct **230** in

80% yield as determined by integration against an internal standard (Ph_3CH) and with the aid of the spectral data previously published for this compound.[9a,30]

B) NMR analysis of a mixture of PhCHO 127a and EDA 85 in different reaction conditions:

As discussed in the chapter, benzaldehyde and ethyl diazoacetate react with each other in presence of Lewis acids and Brønsted acids resulting in the formation of several products. It was thought to examine the possibility of these products under the reaction conditions of a possible **m**ulti**c**omponent **az**iridination (MCAZ).

(a) with $B(OPh)_3$:

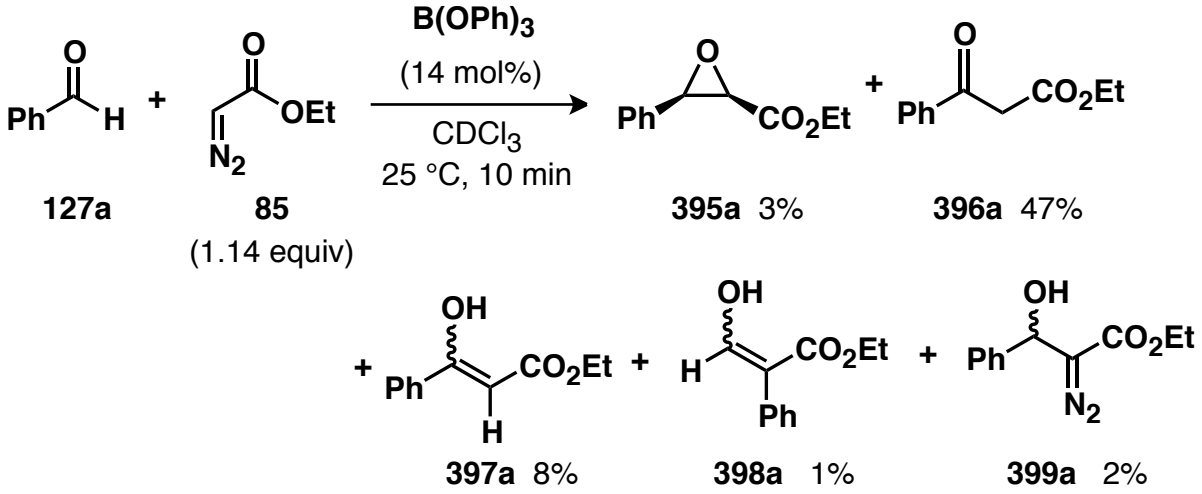

To a 10 mL flame-dried single-necked round bottom flask, equipped with a stir bar and a rubber septum and filled with argon was added $B(OPh)_3$ (22 mg, 0.075 mmol, 0.14 equiv), benzaldehyde **127a** (52.0 μL, 0.525 mmol, 1.00 equiv), ethyl diazoacetate **85** (62.0 μL, 0.600 mmoL, 1.14 equiv), Ph_3CH (12.2 mg, 0.500 mmol) and $CDCl_3$ (1 mL). The resultant mixture was stirred for 24 h at room temperature. The resulting solution was then directly transferred to a NMR tube and was then subjected to NMR analysis. Several products were observed as shown

in the reaction. The presence of each product was confirmed by characteristic peaks (δ 3.83 **395a**[31], δ 5.91 **399a**[17h], δ 12.20 **398a**[17j], δ 12.61 **397a**[32], δ 3.98 **396a**[17j]) in the ^{1}H NMR previously published for these compounds and the amount of each was quantified by integration against an internal standard (Ph_3CH). There was also 5% of unreacted benzaldehyde **127a**.

(b) with (*S*)-VAPOL:

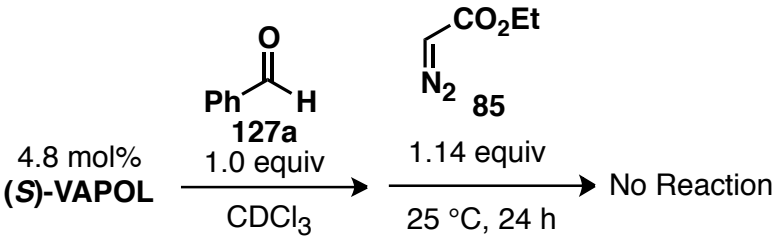

To a 10 mL flame-dried single-necked round bottom flask, equipped with a stir bar and a rubber septum and filled with argon was added (*S*)-VAPOL **58** (14 mg, 0.025 mmol, 0.048 equiv), benzaldehyde **127a** (52.0 μL, 0.525 mmol, 1.00 equiv), ethyl diazoacetate **85** (62.0 μL, 0.600 mmoL, 1.14 equiv), Ph_3CH (12.2 mg, 0.500 mmol) and $CDCl_3$ (1 mL). The resultant mixture was stirred for 24 h at room temperature. The resulting solution was then directly transferred to a NMR tube and was then subjected to NMR analysis. The crude NMR revealed the presence of unreacted starting materials.

(c) with 4 Å Molecular Seives :

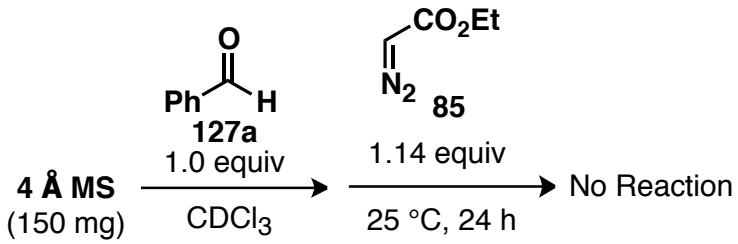

To a 10 mL flame-dried single-necked round bottom flask, equipped with a stir bar and a rubber septum and filled with argon was added 4Å Molecular Seives (150 mg, freshly flame-dried), benzaldehyde **127a** (52.0 μL, 0.525 mmol, 1.00 equiv.), ethyl diazoacetate **85** (62.0 μL, 0.600 mmoL, 1.14 equiv), Ph_3CH (12.2 mg, 0.500 mmol) and $CDCl_3$ (1 mL). The resultant mixture was stirred for 24 h at room temperature. The resulting solution was then directly transferred to a NMR tube utilizing a filter syringe (Corning® syringe filters, Aldrich) to remove the 4Å Molecular Sieves. It was then subjected to NMR analysis. The ^1H NMR of the crude reaction mixture revealed the presence of unreacted starting materials.

(d) without any catalyst/additive:

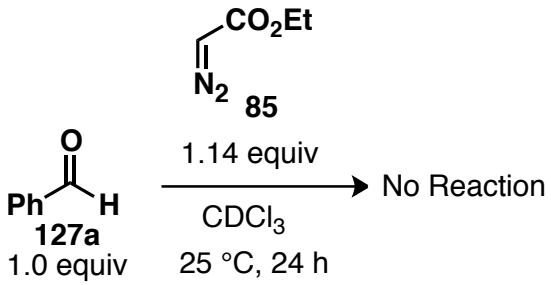

To a 10 mL flame-dried single-necked round bottom flask, equipped with a stir bar and a rubber septum and filled with argon was added benzaldehyde **127a** (52.0 μL, 0.525 mmol, 1.00 equiv.), ethyl diazoacetate **85** (62.0 μL, 0.600 mmoL, 1.14 equiv), Ph_3CH (12.2 mg, 0.500 mmol) and $CDCl_3$ (1 mL). The resultant mixture was stirred for 24 h at room temperature. The resulting solution was then directly transferred to a NMR tube and was then subjected to NMR analysis. The ^1H NMR of the crude reaction mixture revealed the presence of unreacted starting materials.

7.15.5 Different protocols for MCAZ: procedures (I, IIA-B, IIIA-C) (*Table 7.1*)

Procedure I: Catalyst @ 80 °C, 0.5 h and EDA 85 added after 2 h after the addition of aldehyde 127a.

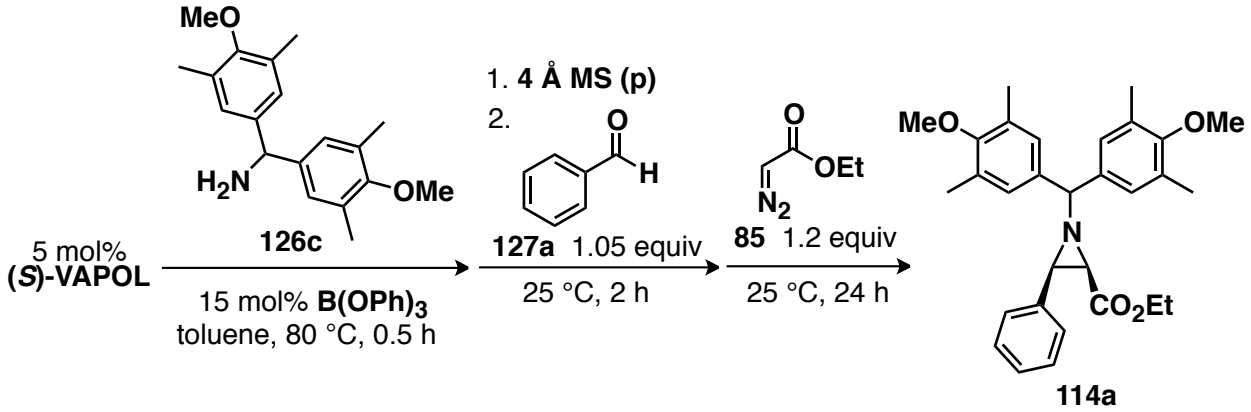

(2*R*,3*R*)-ethyl-1-(bis(4-methoxy-3,5-dimethylphenyl)methyl)-3-phenylaziridine-2-carboxylate 114a: To a 10 mL flame-dried home-made Schlenk flask, prepared from a single-necked 25 mL pear-shaped flask that had its 14/20 glass joint replaced with a high vacuum threaded Teflon valve, equipped with a stir bar and filled with argon was added (*S)*-VAPOL (14 mg, 0.025 mmol), $B(OPh)_3$ (22 mg, 0.075 mmol) and amine **126c** (149.7 mg, 0.5000 mmol). Under an argon flow through the side-arm of the Schlenk flask, dry toluene (2 mL) was added. The flask was sealed by closing the Teflon valve, and then placed in an oil bath (80 ºC) for 0.5 h. The flask was then allowed to cool to room temperature and open to argon through side-arm of the Schlenk flask. To the flask containing the catalyst was added the 4Å Molecular Sieves (150 mg, freshly flame-dried) and aldehyde **127a** (52.0 μL, 0.525 mmoL, 1.05 equiv). The resulting mixture was allowed to stir for 2 h at ambient temperature. Thereafter, ethyl diazoacetate (EDA) **85** (62 μL, 0.60 mmoL, 1.2 equiv) was added. The resulting mixture was stirred for 24 h at room temperature. The reaction was dilluted by addition of hexane (6 mL). The reaction mixture was

then filtered through a Celite pad to a 100 mL round bottom flask. The reaction flask was rinsed with EtOAc (3 mL × 3) and the rinse was filtered through the same Celite pad. The resulting solution was then concentrated *in vacuo* followed by exposure to high vacuum (0.05 mm Hg) for 1 h to afford the crude aziridine as an off-white solid.

The *cis/trans* ratio was determined by comparing the ^{1}H NMR integration of the ring methine protons for each aziridine in the crude reaction mixture. The *cis* (J = 7-8 Hz) and the *trans* (J = 2-3 Hz) coupling constants were used to differentiate the two isomers. The yields of the acyclic enamine side products **118a** and **119a** were determined by ^{1}H NMR analysis of the crude reaction mixture by integration of the *N*-H proton relative to the that of the *cis*-aziridine methine protons with the aid of the isolated yield of the *cis*-aziridine. Purification of the crude aziridine by silica gel chromatography (30 mm × 300 mm column, 9:1 hexanes/EtOAc as eluent, gravity column) afforded pure *cis*-aziridine **114a** as a white solid (mp 107-108 ºC on 99.8% ee material) in 92% isolated yield (218 mg, 0.460 mmol); *cis/trans*: >50:1. Enamine side products: <1 % yield of **118a** and <1% yield of **119a**. The optical purity of **114a** was determined to be 95% *ee* by HPLC analysis (CHIRALCEL OD-H column, 99:1 hexane/2-propanol at 226nm, flow-rate: 0.7 mL/min): retention times; R_t = 9.26 min (major enantiomer, **114a**) and R_t = 12.52 min (minor enantiomer, *ent*-**114a**).[9c]

Spectral data for **114a**: R_f = 0.42 (1:9 EtOAc/hexane); ^{1}H NMR ($CDCl_3$, 500 MHz) δ 0.98 (t, 3H, J = 7.1 Hz), 2.18 (s, 6H), 2.24 (s, 6H), 2.55 (d, 1H, J = 6.8 Hz), 3.10 (d, 1H, J = 6.6 Hz), 3.62 (s, 3H), 3.66 (s, 1H), 3.68 (s, 3H) 3.87-3.97 (m, 2H), 7.09 (s, 2H), 7.18 (s, 2H), 7.21-7.24 (m, 3H), 7.36 (d, 2H, J = 7.3 Hz); ^{13}C ($CDCl_3$, 125 MHz) δ 14.01, 16.16, 16.22, 46.26, 48.20,

59.52, 59.58, 60.47, 77.04, 127.21, 127.41, 127.70, 127.80,127.85, 130.59, 130.60, 135.33, 137.79, 137.96, 155.95, 156.10, 168.01; IR (thin film) 2961 vs, 1750 vs, 1414 vs, 1202 vs cm^{-1}; Mass spectrum: *m/z* (% rel intensity) 473 M+ (0.27), 284(78), 283 (100), 268 (34), 253 (20), 237 (11), 210(10), 117 (18), 89 (11); Anal calcd for $C_{30}H_{35}NO_4$: C, 76.08; H, 7.45; N, 2.96. Found: C, 76.31; H, 7.28; N, 2.82; $[\alpha]_D^{23}$ +41.3 (*c* 1.0, EtOAc) on 99% ee material (HPLC). These spectral data match those previously reported for this compound.

Procedure IIA: Catalyst @ 80 °C, 0.5 h and EDA 85 added immediately after the addition of the aldehyde 127a.

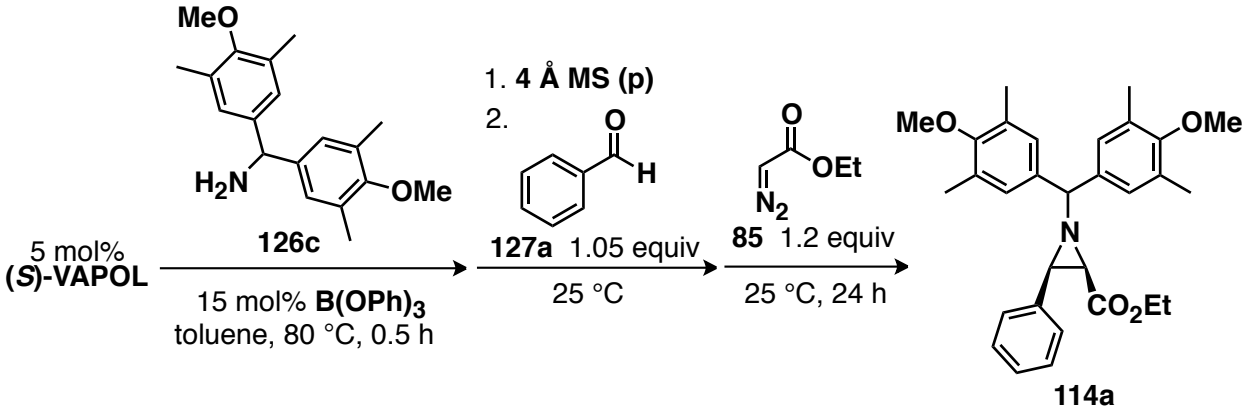

(2*R*,3*R*)-ethyl-1-(bis(4-methoxy-3,5-dimethylphenyl)methyl)-3-phenylaziridine-2-carboxylate 114a: To a 10 mL flame-dried home-made Schlenk flask, prepared from a single-necked 25 mL pear-shaped flask that had its 14/20 glass joint replaced with a high vacuum threaded Teflon valve, equipped with a stir bar and filled with argon was added (*S)*-VAPOL (14 mg, 0.025 mmol), $B(OPh)_3$ (22 mg, 0.075 mmol) and amine **126c** (149.7 mg, 0.5000 mmol). Under an argon flow through the side-arm of the Schlenk flask, dry toluene (2 mL) was added.

The flask was sealed by closing the Teflon valve, and then placed in an oil bath (80 ºC) for 0.5 h. The flask was then allowed to cool to room temperature and open to argon through side-arm of the Schlenk flask. To the flask containing the catalyst was added the 4Å Molecular Sieves (150 mg, freshly flame-dried) and aldehyde **127a** (52.0 μL, 0.525 mmoL, 1.05 equiv). To this solution was rapidly added ethyl diazoacetate (EDA) **85** (62 μL, 0.60 mmoL, 1.2 equiv). The resulting mixture was stirred for 24 h at room temperature. The reaction was dilluted by addition of hexane (6 mL). The reaction mixture was then filtered through a Celite pad to a 100 mL round bottom flask. The reaction flask was rinsed with EtOAc (3 mL × 3) and the rinse was filtered through the same Celite pad. The resulting solution was then concentrated *in vacuo* followed by exposure to high vacuum (0.05 mm Hg) for 1 h to afford the crude aziridine as an off-white solid. Purification of the crude aziridine by silica gel chromatography (30 mm × 300 mm column, 9:1 hexanes/EtOAc as eluent, gravity column) afforded pure *cis*-aziridine **114a** as a white solid (mp 107-108 ºC on 99.8% ee material) in 97% isolated yield (230 mg, 0.485 mmol); *cis/trans*: >50:1. Enamine side products: <1% yield of **118a** and <1% yield of **119a.** The optical purity of **114a** was determined to be 98% *ee* by HPLC analysis (CHIRALCEL OD-H column, 99:1 hexane/2-propanol at 226nm, flow-rate: 0.7 mL/min): retention times; R_t = 9.26 min (major enantiomer, **114a**) and R_t = 12.52 min (minor enantiomer, *ent*-**114a**).

Procedure IIB: Pre-catalyst followed by the addition of amine 6 and stirring @ 80 °C, 0.5 h and then EDA 2 added immediately after the addition of the aldehyde 7a.

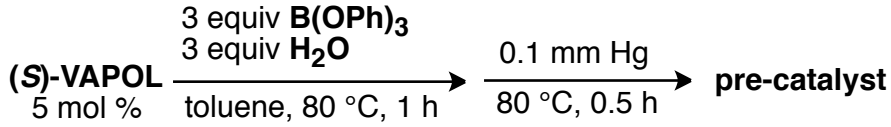

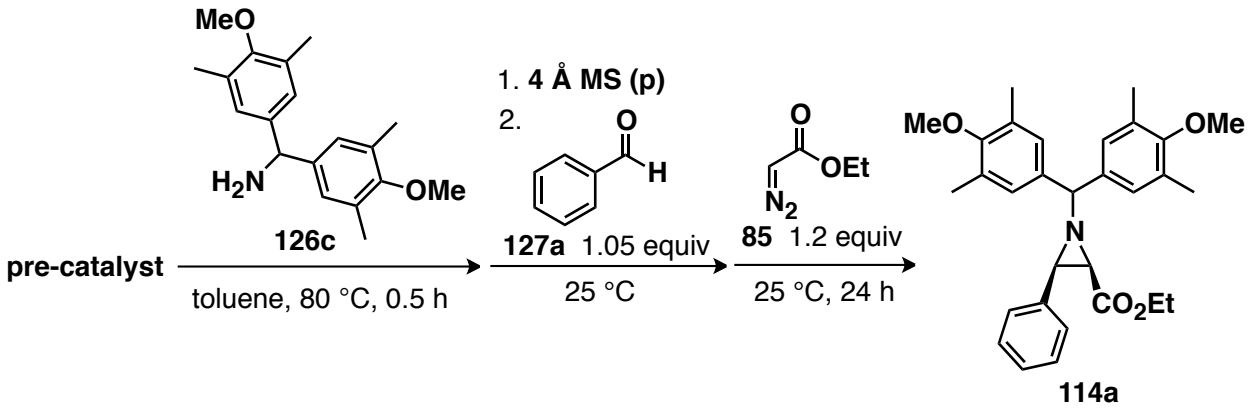

(2*R*,3*R*)-ethyl-1-(bis(4-methoxy-3,5-dimethylphenyl)methyl)-3-phenylaziridine-2-carboxylate 114a: To a 10 mL flame-dried home-made Schlenk flask, prepared from a single-necked 25 mL pear-shaped flask that had its 14/20 glass joint replaced with a high vacuum threaded Teflon valve, equipped with a stir bar and filled with argon was added (*S)*-VAPOL (14 mg, 0.025 mmol), $B(OPh)_3$ (22 mg, 0.075 mmol). Under an argon flow through the side-arm of the Schlenk flask, dry toluene (2 mL) was added through the top of the Teflon valve to dissolve the two reagents and this was followed by the addition of water (1.4 μL, 0.075 mmol). The flask was sealed by closing the Teflon valve, and then placed in an 80 ºC (oil bath) for 1 h. After 1 h, a vacuum (0.5 mm Hg) was carefully applied by slightly opening the Teflon valve to remove the volatiles. After the volatiles are removed completely, a full vacuum is applied and is maintained for a period of 30 min at a temperature of 80 ºC (oil bath). The flask was then allowed to cool to room temperature and opened to argon through the side-arm of the Schlenk flask. To the flask containing the pre-catalyst was added the amine **126c** (149.7 mg, 0.5000 mmol) and then dry toluene (1 mL) under an argon flow through side-arm of the Schlenk flask. The flask was sealed by closing the Teflon valve, and then placed in an oil bath (80 ºC) for 0.5 h. The flask was then allowed to cool to room temperature and open to argon through side-arm of the Schlenk flask. To

the flask containing the pre-catalyst was added the 4Å Molecular Sieves (150 mg, freshly flame-dried) and aldehyde **127a** (52.0 μL, 0.525 mmoL, 1.05 equiv). To this solution was rapidly added ethyl diazoacetate (EDA) **85** (62 μL, 0.60 mmoL, 1.2 equiv). The resulting mixture was stirred for 24 h at room temperature. The reaction was dilluted by addition of hexane (6 mL). The reaction mixture was then filtered through a Celite pad to a 100 mL round bottom flask. The reaction flask was rinsed with EtOAc (3 mL × 3) and the rinse was filtered through the same Celite pad. The resulting solution was then concentrated *in vacuo* followed by exposure to high vacuum (0.05 mm Hg) for 1 h to afford the crude aziridine as an off-white solid. Purification of the crude aziridine by silica gel chromatography (30 mm × 300 mm column, 9:1 hexanes/EtOAc as eluent, gravity column) afforded pure *cis*-aziridine **114a** as a white solid (mp 107-108 ºC on 99.8% ee material) in 98% isolated yield (232 mg, 0.490 mmol); *cis/trans*: >50:1. Enamine side products: <1% yield of **118a** and <1% yield of **119a**. The optical purity of **114a** was determined to be 98 % *ee* by HPLC analysis (CHIRALCEL OD-H column, 99:1 hexane/2-propanol at 226nm, flow-rate: 0.7 mL/min): retention times; R_t = 9.26 min (major enantiomer, **114a**) and R_t = 12.52 min (minor enantiomer, *ent*-**114a**).

Procedure IIIA: Catalyst @ 25 °C, 1 h and EDA 85 added immediately after the addition of the aldehyde 127a.

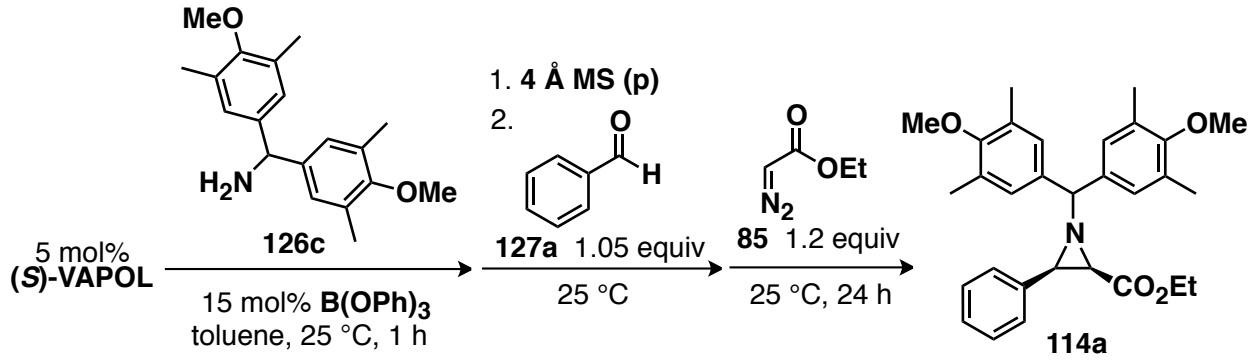

(2*R*,3*R*)-ethyl-1-(bis(4-methoxy-3,5-dimethylphenyl)methyl)-3-phenylaziridine-2-carboxylate 114a: To a 10 mL flame-dried single-necked round bottom flask equipped with a stir bar and filled with argon was added (*S)*-VAPOL (14 mg, 0.025 mmol), $B(OPh)_3$ (22 mg, 0.075 mmol) and amine **126c** (149.7 mg, 0.5000 mmol). Dry toluene (1 mL) was added under an argon atmosphere to dissolve the reagents. The flask was fitted with a rubber septum and a nitrogen balloon. The reaction mixture was stirred at room temperature for 1 h. Thereafter, 4Å Molecular Sieves (150 mg, freshly flame-dried) was added followed by the addition of the aldehyde **127a** (52.0 μL, 0.525 mmoL, 1.05 equiv). To this solution was rapidly added ethyl diazoacetate (EDA) **85** (62 μL, 0.60 mmoL, 1.2 equiv). The resulting mixture was stirred for 24 h at room temperature. The reaction was dilluted by addition of hexane (6 mL). The reaction mixture was then filtered through a Celite pad to a 100 mL round bottom flask. The reaction flask was rinsed with EtOAc (3 mL × 3) and the rinse was filtered through the same Celite pad. The resulting solution was then concentrated *in vacuo* followed by exposure to high vacuum (0.05 mm Hg) for 1 h to afford the crude aziridine as an off-white solid. Purification of the crude aziridine by silica gel chromatography (30 mm × 300 mm column, 9:1 hexanes/EtOAc as eluent, gravity column) afforded pure *cis*-aziridine **114a** as a white solid (mp 107-108 ºC on 99.8% ee material) in 97% isolated yield (230 mg, 0.490 mmol); *cis/trans*: >50:1. Enamine side products: <1% yield of **118a** and <1% yield of **119a**. The optical purity of **114a** was determined to be 98% *ee* by HPLC analysis (CHIRALCEL OD-H column, 99:1 hexane/2-propanol at 226nm, flow-rate: 0.7 mL/min): retention times; R_t = 9.26 min (major enantiomer, **114a**) and R_t = 12.52 min (minor enantiomer, *ent*-**114a**).

Procedure IIIB: Pre-catalyst followed by the addition of amine 126c and stirring @ 25 °C, 1 h and then EDA 85 added immediately after the addition of the aldehyde 127a.

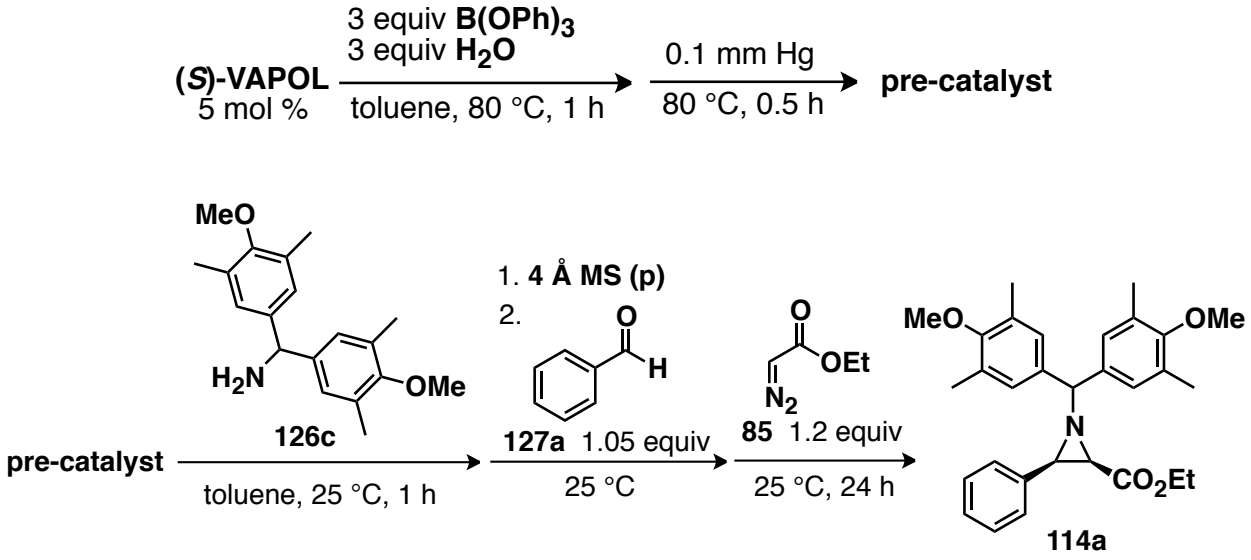

(2*R*,3*R*)-ethyl-1-(bis(4-methoxy-3,5-dimethylphenyl)methyl)-3-phenylaziridine-2-carboxylate 114a: To a 10 mL flame-dried home-made Schlenk flask, prepared from a single-necked 25 mL pear-shaped flask that had its 14/20 glass joint replaced with a high vacuum threaded Teflon valve, equipped with a stir bar and filled with argon was added (*S)*-VAPOL (14 mg, 0.025 mmol), $B(OPh)_3$ (22 mg, 0.075 mmol). Under an argon flow through the side-arm of the Schlenk flask, dry toluene (2 mL) was added through the top of the Teflon valve to dissolve the two reagents and this was followed by the addition of water (1.4 μL, 0.075 mmol). The flask was sealed by closing the Teflon valve, and then placed in an 80 ºC (oil bath) for 1 h. After 1 h, a vacuum (0.5 mm Hg) was carefully applied by slightly opening the Teflon valve to remove the volatiles. After the volatiles are removed completely, a full vacuum is applied and is maintained for a period of 30 min at a temperature of 80 ºC (oil bath). The flask was then allowed to cool to room temperature and opened to argon through the side-arm of the Schlenk flask. To the flask

containing the pre-catalyst was added the amine **126c** (149.7 mg, 0.5000 mmol) and then dry toluene (1 mL) under an argon flow through side-arm of the Schlenk flask. The flask was sealed by closing the Teflon valve, and then the resulting mixture was allowed to stir at room temperature for 1 h. The flask was then open to argon through side-arm of the Schlenk flask. To the flask containing the catalyst was added the 4Å Molecular Sieves (150 mg, freshly flame-dried) and aldehyde **127a** (52.0 μL, 0.525 mmoL, 1.05 equiv). To this solution was rapidly added ethyl diazoacetate (EDA) **85** (62 μL, 0.60 mmoL, 1.2 equiv). The resulting mixture was stirred for 24 h at room temperature. The reaction was dilluted by addition of hexane (6 mL). The reaction mixture was then filtered through a Celite pad to a 100 mL round bottom flask. The reaction flask was rinsed with EtOAc (3 mL × 3) and the rinse was filtered through the same Celite pad. The resulting solution was then concentrated *in vacuo* followed by exposure to high vacuum (0.05 mm Hg) for 1 h to afford the crude aziridine as an off-white solid. Purification of the crude aziridine by silica gel chromatography (30 mm × 300 mm column, 9:1 hexanes/EtOAc as eluent, gravity column) afforded pure cis-aziridine **114a** as a white solid (mp 107-108 ºC on 99.8% ee material) in 94% isolated yield (223 mg, 0.470 mmol); *cis/trans*: >50:1. Enamine side products: <1% yield of **118a** and <1% yield of **119a**. The optical purity of **114a** was determined to be 98% *ee* by HPLC analysis (CHIRALCEL OD-H column, 99:1 hexane/2-propanol at 226nm, flow-rate: 0.7 mL/min): retention times; R_t = 9.26 min (major enantiomer, **114a**) and R_t = 12.52 min (minor enantiomer, *ent*-**114a**).

Procedure IIIC: Catalyst @ 25 °C, 1 h and EDA 85 added immediately after the addition of the aldehyde 127a (0.6 equiv with respect to amine 126c).

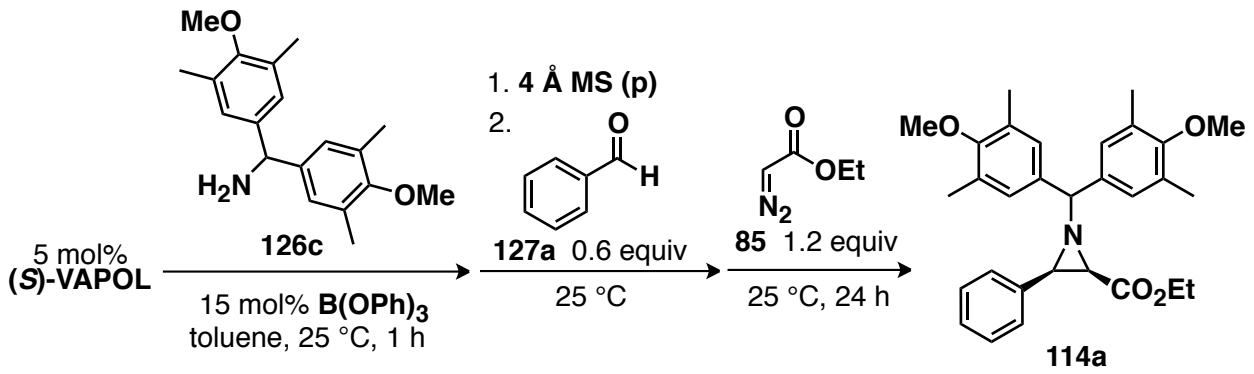

(2*R*,3*R*)-ethyl-1-(bis(4-methoxy-3,5-dimethylphenyl)methyl)-3-phenylaziridine-2-carboxylate 114a: The procedure is exactly similar to procedure IIIA except that 0.6 equiv of benzaldehyde **127a** was added. No aziridine **114a** was observed from the ^{1}H NMR analysis of crude reaction mixture.

7.15.6 Synthesis of aryl and heteroaryl MEDAM aziridines 114a-n (*via* Procedure IIIA, *Table 7.3*)

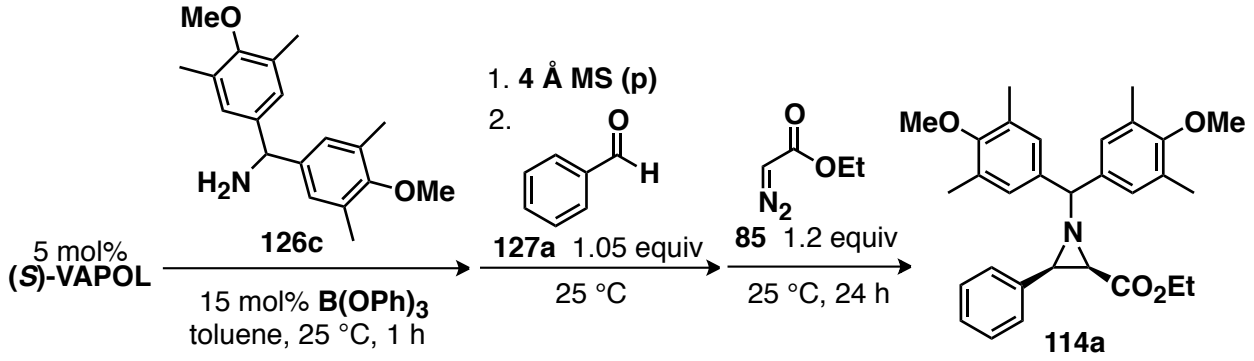

(2*R*,3*R*)-ethyl-1-(bis(4-methoxy-3,5-dimethylphenyl)methyl)-3-phenylaziridine-2-carboxylate 114a: Aldehyde **127a** (52.0 μL, 0.525 mmol) was reacted according to the general Procedure IIIA described above with (*S*)-VAPOL as ligand. Purification of the crude aziridine

by silica gel chromatography (30 mm × 300 mm column, 9:1 hexanes/EtOAc as eluent, gravity column) afforded pure *cis*-aziridine **114a** as a white solid (mp 107-108 ºC on 99.8% ee material) in 98% isolated yield (232 mg, 0.490 mmol); *cis/trans*: >50:1. Enamine side products: <1% yield of **118a** and <1 % yield of **119a**. The optical purity of **114a** was determined to be 98% *ee* by HPLC analysis (CHIRALCEL OD-H column, 99:1 hexane/2-propanol at 226nm, flow-rate: 0.7 mL/min): retention times; R_t = 9.26 min (major enantiomer, **114a**) and R_t = 12.52 min (minor enantiomer, *ent*-**114a**). This reaction was repeated and monitored by ^{1}H NMR Spectroscopy that revealed that the reaction had gone to completion in 1 h. Also, it gave 70 % yield of **114a** and 98% ee when the same reaction was carried out utilizing 5Å MS instead of 4Å MS.

Spectral data for **114a**: R_f = 0.42 (1:9 EtOAc/hexane); ^{1}H NMR ($CDCl_3$, 500 MHz) δ 0.98 (t, 3H, *J* = 7.1 Hz), 2.18 (s, 6H), 2.24 (s, 6H), 2.55 (d, 1H, *J* = 6.8 Hz), 3.10 (d, 1H, *J* = 6.6 Hz), 3.62 (s, 3H), 3.66 (s, 1H), 3.68 (s, 3H) 3.87-3.97 (m, 2H), 7.09 (s, 2H), 7.18 (s, 2H), 7.21-7.24 (m, 3H), 7.36 (d, 2H, *J* = 7.3 Hz); ^{13}C ($CDCl_3$, 125 MHz) δ 14.01, 16.16, 16.22, 46.26, 48.20, 59.52, 59.58, 60.47, 77.04, 127.21, 127.41, 127.70, 127.80,127.85, 130.59, 130.60, 135.33, 137.79, 137.96, 155.95, 156.10, 168.01; IR (thin film) 2961 vs, 1750 vs, 1414 vs, 1202 vs cm^{-1}; Mass spectrum: *m/z* (% rel intensity) 473 M+ (0.27), 284(78), 283 (100), 268 (34), 253 (20), 237 (11), 210(10), 117 (18), 89 (11); Anal calcd for $C_{30}H_{35}NO_4$: C, 76.08; H, 7.45; N, 2.96. Found: C, 76.31; H, 7.28; N, 2.82; $[\alpha]_D^{23}$ +41.3 (*c* 1.0, EtOAc) on 99% ee material (HPLC). These spectral data match those previously reported for this compound.[9c]

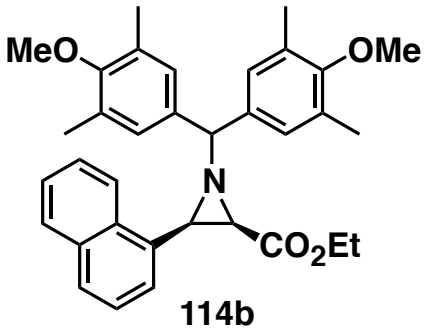

114b

(2*R*,3*R*)-ethyl-1-(bis(4-methoxy-3,5-dimethylphenyl) methyl)-3-(naphthalene-1-yl)aziridine-2-carboxylate 114b: Aldehyde **127b** (71.0 μL, 0.525 mmol) was reacted according to the general Procedure IIIA described above with (*S*)-VAPOL as ligand. Purification of the crude aziridine by silica gel chromatography (30 mm × 300 mm column, 9:1 hexanes/EtOAc) afforded pure *cis*-aziridine **114b** as a white solid (mp 79-80 ºC on 99% ee material) in 96% isolated yield (251 mg, 0.480 mmol); *cis/trans*: 50:1. Enamine side products: 2.9% yield of **118b** and <1% yield of **119b**. The optical purity of **114b** was determined to be 99.3% *ee* by HPLC analysis (CHIRALCEL OD-H column, 99:1 hexane/2-propanol at 226 nm, flow-rate: 0.7 mL/min): retention times; R_t = 8.15 min (major enantiomer, **114b**) and R_t = 16.15 min (minor enantiomer, *ent*-**114b**).

Spectral data for **114b**: R_f = 0.25 (9:1 hexanes/EtOAc); ^{1}H NMR ($CDCl_3$, 600 MHz) δ 0.65 (t, 3H, *J* = 7.1 Hz), 2.22 (s, 6H), 2.26 (s, 6H), 2.81 (d, 1H, *J* = 6.8 Hz), 3.58 (d, 1H, *J* = 6.8 Hz), 3.63 (s, 3H), 3.69 (s, 3H), 3.69-3.76 (m, 2H), 3.79 (s, 1H), 7.17 (s, 2H), 7.23 (s, 2H), 7.36 (dd, 1H, *J* = 7.8, 7.6 Hz), 7.40-7.46 (m, 2H), 7.67-7.69 (m, 2H), 7.78 (d, 1H, *J* = 7.8 Hz), 8.06 (d, 1H, *J* = 7.6 Hz); ^{13}C NMR ($CDCl_3$, 150 MHz) δ 13.67, 16.18, 16.24, 45.98, 46.63, 59.55, 59.62, 60.33, 77.47, 123.06, 125.31, 125.42, 125.83, 126.61, 127.36, 127.52, 128.12, 128.50, 130.68, 130.71, 130.85, 131.49, 133.08, 137.69, 137.95, 155.95, 156.26, 168.02; IR (thin film) 2942vs, 1748s, 1484s, 1221s, 1186s, 1017m cm^{-1}; HRMS (ESI-TOF) *m/z* 524.2807 [(M+H$^+$); calcd. for $C_{34}H_{38}NO_4$: 524.2801]; $[\alpha]_D^{20}$ –19.3 (c 1.0, EtOAc) on 99 % ee material (HPLC) of *ent*-**114b**.

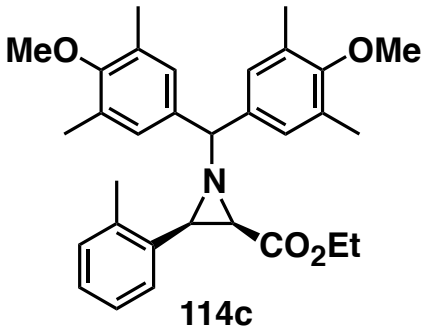

114c

(*2R,3R*)-ethyl-1-(bis(4-methoxy-3,5-dimethylphenyl) methyl)-3-(*o*-tolyl)aziridine-2-carboxylate 114c: Aldehyde **127c** (61.0 μL, 0.525 mmol) was reacted according to the general Procedure IIIA described above with (*S*)-VAPOL as ligand. Purification of the crude aziridine by silica gel chromatography (30 mm × 300 mm column, 9:1 hexanes/EtOAc as eluent, gravity column) afforded pure *cis*-aziridine **114c** as a white solid (mp 174-175 ºC on 99.7% ee material) in 96% isolated yield (234 mg, 0.480 mmol); *cis/trans*: 50:1. Enamine side products: 1.9% yield of **118c** and 1.0% yield of **119c**. The optical purity of **114c** was determined to be >99% *ee* by HPLC analysis (CHIRALCEL OD-H column, 99:1 hexane/2-propanol at 226 nm, flow-rate: 0.7 mL/min): retention times; R_t = 9.45 min (major enantiomer, **114c**) and R_t = 12.21 min (minor enantiomer, *ent*-**114c**).

Spectral data for **114c**: R_f = 0.38 (1:9 EtOAc/hexane); ^{1}H NMR ($CDCl_3$, 500 MHz) δ 0.89 (t, 3H, *J* = 7.1 Hz), 2.20 (s, 6H), 2.24 (s, 6H), 2.26 (s, 3H), 2.61 (d, 1H, *J* = 6.8 Hz), 3.08 (d, 1H, *J* = 6.6 Hz), 3.62 (s, 3H), 3.66 (s, 1H), 3.68 (s, 3H), 3.88 (q, 2H, *J* = 7.1 Hz), 7.01 (d, 1H, *J* = 6.6 Hz), 7.06-7.09 (m, 2H), 7.13 (s, 2H), 7.18 (s, 2H), 7.53 (d, 1H, *J* = 6.3 Hz); ^{13}C ($CDCl_3$, 125 MHz) δ 13.90, 16.16, 16.22, 18.76, 45.55, 47.15, 59.53, 59.59, 60.36, 77.34, 125.28, 127.05, 127.33, 127.95, 128.62, 129.08, 130.61, 130.63, 133.45, 136.03, 137.85, 138.01, 155.92, 156.18, 168.16; IR (thin film) 2937vs, 1749s, 1485s, 1221s, 1192vs cm^{-1};HRMS (ESI-TOF) *m/z* 488.2801 [(M+H$^+$); calcd. for $C_{31}H_{38}NO_4$: 488.2801]; $[\alpha]_D^{23}$ +46.4 (*c* 1.0, EtOAc) on 97% ee material (HPLC). These spectral data match those previously reported for this compound.[9c]

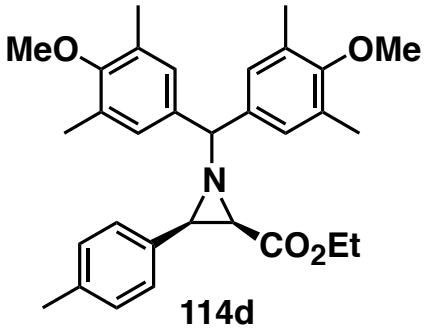

114d

(*2R,3R*)-ethyl-1-(bis(4-methoxy-3,5-dimethylphenyl) methyl)-3-(*p*-tolyl)aziridine-2-carboxylate 114d: Aldehyde **127d** (61.0 μL, 0.525 mmol) was reacted according to the general Procedure IIIA described above with (*S*)-VAPOL as ligand. Purification of the crude aziridine by silica gel chromatography (30 mm × 300 mm column, 9:1 hexanes/EtOAc as eluent, gravity column) afforded pure *cis*-aziridine **114d** as a white solid (mp 116-117 ºC on 99.5% ee material) in 95 % isolated yield (232 mg, 0.480 mmol); *cis/trans*: 50:1. Enamine side products: 3.8% yield of **118d** and 1.0% yield of **119d**. The optical purity of **114d** was determined to be >99% *ee* by HPLC analysis (CHIRALCEL OD-H column, 99:1 hexane/2-propanol at 226 nm, flow-rate: 0.7 mL/min): retention times; R_t = 9.22 min (major enantiomer, **114d**) and R_t = 11.62 min (minor enantiomer, *ent*-**114d**).

Spectral data for **114d**: R_f = 0.30 (1:9 EtOAc/hexanes); ^{1}H NMR ($CDCl_3$, 500 MHz) δ 1.01 (t, 3H, *J* = 7.1 Hz), 2.18 (s, 6H), 2.24 (s, 6H), 2.26 (s, 3H), 2.52 (d, 1H, *J* = 6.6 Hz), 3.07 (d, 1H, *J* = 6.8 Hz), 3.62 (s, 3H), 3.64 (s, 1H), 3.68 (s, 3H) 3.93 (dq, 2H, *J* = 3.2 Hz, 7.1 Hz), 7.02 (d, 2H, *J* = 7.8 Hz), 7.08 (s, 2H), 7.17 (s, 2H), 7.24 (d, 2H, *J* = 8.0 Hz); ^{13}C ($CDCl_3$, 125 MHz) δ 14.05, 16.16, 16.22, 21.11, 46.20, 48.21, 59.52, 59.58, 60.44, 77.11, 127.43, 127.72, 127.81, 128.41, 130.54, 130.57, 132.28, 136.78, 137.86, 138.00, 155.93, 156.08, 168.10; IR (thin film) 2978vs, 1748s, 1483s, 1221s, 1190vs cm^{-1}; HRMS (ESI-TOF) *m/z* 488.2806 [(M+H$^+$); calcd. for $C_{31}H_{38}NO_4$: 488.2801]; $[\alpha]_D^{23}$ +29.4 (*c* 1.0, EtOAc) on 99.8% ee material (HPLC). These spectral data match those previously reported for this compound.[9c]

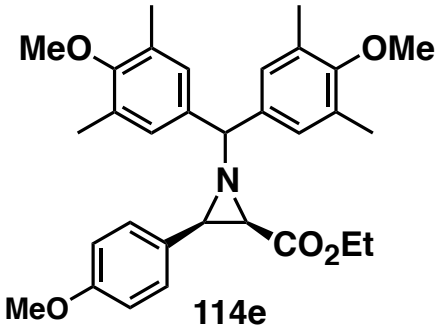

114e

(*2R,3R*)-ethyl-1-(bis(4-methoxy-3,5-dimethylphenyl) methyl)-3-(4-methoxyphenyl)aziridine-2-carboxylate 114e: Aldehyde **127e** (64.0 μL, 0.525 mmol) was reacted according to the general Procedure IIIA described above with (*S*)-VAPOL as ligand. Purification of the crude aziridine by silica gel chromatography (30 mm × 300 mm column, 9:1 hexanes/EtOAc with 1% Et_3N as eluent, gravity column; the column was set up by making a slurry of silica gel in hexanes with 2 % Et_3N) afforded pure *cis*-aziridine **114e** as a white solid (mp 56-57 ºC on 98% ee material) in 78% isolated yield (196 mg, 0.390 mmol); *cis/trans*: 20:1. Enamine side products: <1% yield of **118e** and 4.7% yield of **119e**. The optical purity of **114e** was determined to be 98% *ee* by HPLC analysis (CHIRALCEL OD-H column, 99:1 hexane/2-propanol at 226 nm, flow-rate: 0.7 mL/min): retention times; R_t = 12.07 min (major enantiomer, **114e**) and R_t = 19.20 min (minor enantiomer, *ent*-**114e**).

Spectral data for **114e**: R_f = 0.28 (1:9 EtOAc/hexane); ^{1}H NMR ($CDCl_3$, 500 MHz) δ 1.02 (t, 3H, *J* = 7.1 Hz), 2.19 (s, 6H), 2.24 (s, 6H), 2.51 (d, 1H, *J* = 6.8 Hz), 3.06 (d, 1H, *J* = 6.8 Hz), 3.63 (s, 3H), 3.65 (s, 1H), 3.68 (s, 3H), 3.74 (s, 3H), 3.89-3.99 (m, 2H), 6.77 (d, 2H, *J* = 9.5 Hz), 7.09 (s, 2H), 7.18 (s, 2H), 7.29 (d, 2H, *J* = 8.8 Hz); ^{13}C ($CDCl_3$, 125 MHz) δ 14.08, 16.16, 16.21, 46.20, 47.89, 55.19, 59.52, 59.57, 60.45, 77.05, 113.18, 127.43, 127.79, 128.93, 130.55, 130.57, 137.83, 138.01, 155.93, 156.07, 158.86, 168.14 (one sp^2 carbon not located); IR (thin film) 2942vs, 1743s, 1514s, 1250s, 1180vs cm^{-1}; HRMS (ESI-TOF) *m/z* 504.2744 [(M+H$^+$);

calcd. for $C_{31}H_{38}NO_5$: 504.2750]; $[\alpha]_D^{23}$ +25 (*c* 1.0, EtOAc) on 96% ee material (HPLC). These spectral data match those previously reported for this compound.[9c]

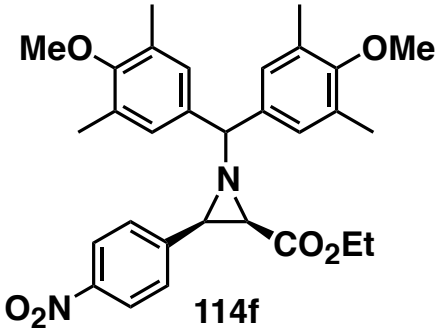

114f

(*2R,3R*)-ethyl-1-(bis(4-methoxy-3,5-dimethylphenyl) methyl)-3-(4-nitrophenyl)aziridine-2-carboxylate 114f: Aldehyde **127f** (79.3 mg, 0.525 mmol) was reacted according to the general Procedure IIIA described above with (*S*)-VAPOL as ligand. Purification of the crude aziridine by silica gel chromatography (30 mm × 300 mm column, 9:1 hexanes/EtOAc) afforded pure *cis*-aziridine **114f** as a white solid (mp 174-175 ºC on 99.7% ee material) in 92% isolated yield (239 mg, 0.460 mmol); *cis/trans*: 50:1. Enamine side products: <1% yield of **118o** and 2.8% yield of **119o**. The optical purity of **114f** was determined to be 99% *ee* by HPLC analysis (CHIRALCEL OD-H column, 99:1 hexane/2-propanol at 226 nm, flow-rate: 0.7 mL/min): retention times; R_t = 17.12 min (major enantiomer, **114f**) and R_t = 27.13 min (minor enantiomer, *ent*-**114f**).

Spectral data for **114f**: R_f = 0.30 (1:9 EtOAc/hexane); ^{1}H NMR ($CDCl_3$, 500 MHz) δ 1.02 (t, 3H, *J* = 7.1 Hz), 2.18 (s, 6H), 2.25 (s, 6H), 2.68 (d, 1H, *J* = 6.8 Hz), 3.15 (d, 1H, *J* = 6.8 Hz), 3.62 (s, 3H), 3.68 (s, 3H), 3.71 (s, 1H), 3.93 (dq, 2H, *J* = 2.2, 7.1 Hz), 7.06 (s, 2H), 7.16 (s, 2H), 7.57 (d, 2H, *J* = 8.8 Hz), 8.10 (d, 2H, *J* = 8.8 Hz); ^{13}C ($CDCl_3$, 125 MHz) δ 14.08, 16.19, 16.24, 46.81, 47.26, 59.55, 59.59, 60.85, 76.89, 122.98, 127.26, 127.59, 128.81, 130.81, 130.86, 137.25, 137.48, 142.82, 147.28, 156.13, 156.28, 167.20; IR (thin film) 2984 vs, 1745 vs, 1603 s, 1522 vs,

1221 vs cm^{-1}; HRMS (ESI-TOF) *m/z* 519.2505 [$(M+H^+)$; calcd. for $C_{30}H_{35}N_2O_6$: 519.2495]; $[\alpha]_D^{23}$ –4.8 (*c* 1.0, EtOAc) on 99.8% ee material (HPLC). These spectral data match those previously reported for this compound.[9c]

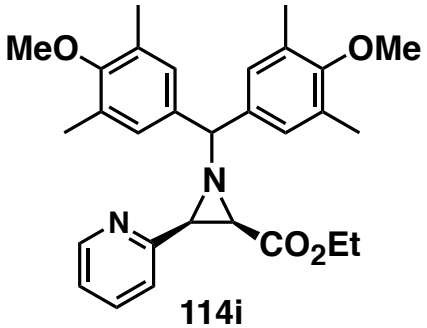

114i

(2*R*,3*S*)-ethyl-1-(bis(4-methoxy-3,5-dimethylphenyl) methyl)-3-(pyridin-2-yl)aziridine-2-carboxylate 114i: Aldehyde **127i** (50.0 μL, 0.525 mmol) was reacted according to the general Procedure IIIA described above with (*S*)-VAPOL as ligand. Purification of the crude aziridine by silica gel chromatography (30 mm × 300 mm column, 4:1 hexanes/EtOAc with 1% Et_3N followed by 2:1 hexanes/EtOAc with 1% Et_3N as eluent, gravity column; the column was set up by making a slurry of silica gel in hexanes with 2 % Et_3N) afforded pure *cis*-aziridine **114i** as a white solid (mp 60-61 ºC on 90.2% ee material) in 96% isolated yield (456 mg, 0.480 mmol); *cis/trans*: >50:1. Enamine side products: not observed. The optical purity of **114i** was determined to be 90% *ee* by HPLC analysis (CHIRALCEL OD-H column, 99:1 hexane/2-propanol at 226 nm, flow-rate: 0.7 mL/min): retention times; R_t = 16.90 min (major enantiomer, **114i**) and R_t = 31.83 min (minor enantiomer, *ent*-**114i**).

Spectral data for **114i**: R_f = 0.27 (2:1 hexanes/EtOAc); ^{1}H NMR ($CDCl_3$, 600 MHz) δ 1.01 (t, 3H, *J* = 7.1 Hz), 2.18 (s, 6H), 2.24 (s, 6H), 2.66 (d, 1H, *J* = 6.8 Hz), 3.27 (d, 1H, *J* = 6.8 Hz), 3.62 (s, 3H), 3.68 (s, 3H), 3.73 (s, 1H), 3.91-3.96 (m, 2H), 7.08 (s, 2H), 7.09-7.11 (m, 1H), 7.16

(s, 2H), 7.59-7.60 (m, 2H), 8.42 (td, 1H, J = 1.4, 4.6 Hz); ^{13}C NMR ($CDCl_3$, 150 MHz) δ 14.00, 16.16, 16.23, 45.91, 49.45, 59.54, 59.60, 60.63, 122.29, 122.83, 127.36, 127.79, 130.65, 130.68, 135.87, 137.56, 137.78, 148.57, 155.48, 155.99, 156.12, 167.75 (one sp^3 carbon not located); IR (thin film) 2984s, 1746s, 1591, 1482s, 1221s, 1184s, 1015m cm^{-1}; HRMS (ESI-TOF) *m/z* 475.2607 [(M+H$^+$); calcd. for $C_{29}H_{35}N_2O_4$: 475.2597]; $[\alpha]_D^{20}$ +40.2 (c 1.0, EtOAc) on 90% ee material (HPLC).

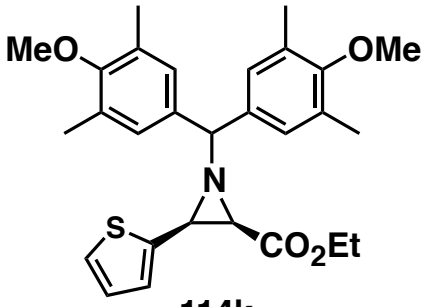

114k

(2*R*,3*S*)-ethyl-1-(bis(4-methoxy-3,5-dimethylphenyl) methyl)-3-(thiophen-2-yl)aziridine-2-carboxylate 114k: Aldehyde **127k** (48.0 μL, 0.525 mmol) was reacted according to the general Procedure IIIA described above with (*S*)-VAPOL as ligand except that an excess of EDA **85** (415 μL, 4.0 mmoL, 8 equiv) was used. Purification of the crude aziridine by silica gel chromatography (30 mm × 300 mm column, 9:1 hexanes/EtOAc with 1% Et_3N as eluent, gravity column; the column was set up by making a slurry of silica gel in hexanes with 2% Et_3N) afforded pure *cis*-aziridine **114k** as a white solid (mp 55-56 ºC on 97% ee material) in 88% isolated yield (211 mg, 0.440 mmol); *cis/trans*: 25:1. Enamine side products: not observed. The optical purity of **114k** was determined to be 97% *ee* by HPLC analysis (CHIRALCEL OD-H column, 99:1 hexane/2-propanol at 226 nm, flow-rate: 0.7 mL/min): retention times; R_t = 10.54 min (major enantiomer, **114k**) and R_t = 15.27 min (minor enantiomer, *ent*-**114k**).

Spectral data for **114k**: R_f = 0.21 (9:1 hexanes/EtOAc); ^{1}H NMR ($CDCl_3$, 600 MHz) δ 1.08 (t, 3H, *J* = 7.1 Hz), 2.21 (s, 6H), 2.24 (s, 6H), 2.58 (d, 1H, *J* = 6.6 Hz), 3.21 (d, 1H, *J* = 6.6 Hz), 3.64 (s, 3H), 3.66 (s, 1H), 3.67 (s, 3H), 3.96-4.06 (m, 2H), 6.86 (dd, 1H, *J* = 3.4, 4.9 Hz), 6.95-6.96 (m, 1H), 7.11 (dd, 1H, *J* = 1.2, 4.9 Hz), 7.14 (s, 2H), 7.16 (s, 2H); ^{13}C NMR ($CDCl_3$, 150 MHz) δ 14.00, 16.12, 16.17, 43.76, 46.65, 59.51, 59.53, 60.70, 76.93, 124.49, 125.74, 126.38, 127.34, 127.71, 130.59, 130.62, 137.50, 137.63, 139.00, 155.94, 156.07, 167.77; IR (thin film) 2942s, 1748s, 1484s, 1221s, 1190s, 1015m cm^{-1}; HRMS (ESI-TOF) *m/z* 480.2216 [(M+H$^+$); calcd. for $C_{28}H_{34}NO_4S$: 480.2209]; $[\alpha]_D^{20}$ +30.2 (c 1.0, EtOAc) on 97% ee material (HPLC).

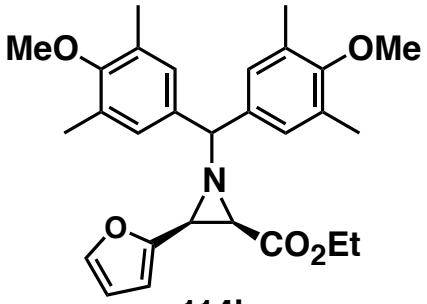

114l

(2*R*,3*S*)-ethyl-1-(bis(4-methoxy-3,5-dimethylphenyl) methyl)-3-(furan-2-yl)aziridine-2-carboxylate 114l: Aldehyde **127l** (44.0 μL, 0.525 mmol) was reacted according to the general Procedure IIIA described above with (*S*)-VAPOL as ligand except that the addition of aldehyde **127l** was carried out at –10 °C followed by the addition of EDA **85** (415 μL, 4.0 mmoL, 8 equiv) at the same temperature. The reaction was stirred for 2 h at –10 °C prior to warming it to room temperature. Purification of the crude aziridine by silica gel chromatography (30 mm × 300 mm column, 15:1 hexanes/EtOAc with 1% Et_3N as eluent, gravity column; the column was set up by making a slurry of silica gel in hexanes with 2% Et_3N) afforded pure *cis*-aziridine **114l** as a white solid (mp 45-46 ºC on 94% ee material) in 65% isolated yield (151 mg, 0.325 mmol); *cis/trans*: 8.3:1. Enamine side products: not observed. The optical purity of **114l** was

determined to be 95% *ee* by HPLC analysis (CHIRALCEL OD-H column, 99.5:0.5 hexane/2-propanol at 226 nm, flow-rate: 0.7 mL/min): retention times; R_t = 23.6 min (major enantiomer, **114l**) and R_t = 39.1 min (minor enantiomer, *ent*-**114l**).

Spectral data for **114l**: R_f = 0.21 (15:1 hexanes/EtOAc); ^{1}H NMR ($CDCl_3$, 600 MHz) δ 1.14 (t, 3H, *J* = 7.1 Hz), 2.21 (s, 6H), 2.24 (s, 6H), 2.60 (d, 1H, *J* = 6.6 Hz), 3.03 (d, 1H, *J* = 6.6 Hz), 3.65 (s, 3H), 3.67 (s, 1H), 3.68 (s, 3H), 4.03-4.13 (m, 2H), 6.28-6.29 (m, 1H), 6.29-6.30 (m, 1H), 7.09 (s, 2H), 7.14 (s, 2H), 7.26-7.27 (m, 1H); ^{13}C NMR ($CDCl_3$, 150 MHz) δ 14.05, 16.11, 16.15, 41.73, 45.27, 59.50, 59.52, 60.76, 76.84, 107.97, 110.32, 127.49, 127.64, 130.53, 130.61, 137.34, 137.44, 141.80, 149.77, 156.01, 156.04, 167.70; IR (thin film) 2940s, 1750s, 1485s, 1221s, 1179s, 1013m cm^{-1}; HRMS (ESI-TOF) *m/z* 464.2441 [(M+H$^+$); calcd. for $C_{28}H_{34}NO_5$: 464.2437]; $[\alpha]_D^{20}$ –8.2 (*c* 1.0, EtOAc) on 94% ee material (HPLC) of *ent*-**114l**.

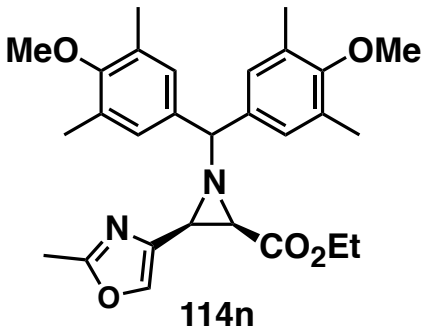

114n

(2*R*,3*S*)-ethyl-1-(bis(4-methoxy-3,5-dimethylphenyl) methyl)-3-(2-methyloxazol-4-yl)aziridine-2-carboxylate

114n: Aldehyde **127n** (59.0 mg, 0.525 mmol) was reacted according to the general Procedure IIIA described above with (*S*)-VAPOL as ligand except except that the addition of aldehyde **127n** was carried out at –10 °C followed by the addition of EDA **85** (415 μL, 4.0 mmoL, 8 equiv) at the same temperature. The reaction was stirred for 15 min at –10 °C prior to warming it to room temperature. Purification of the crude aziridine by silica gel chromatography

(30 mm × 300 mm column, 3:1 hexanes/EtOAc with 1% Et_3N as eluent, gravity column; the column was set up by making a slurry of silica gel in hexanes with 2% Et_3N) afforded pure *cis*-aziridine **114n** as a white solid (mp 58-59 ºC on 96% ee material) in 98% isolated yield (235 mg, 0.490 mmol); *cis/trans*: >50:1. Enamine side products: not observed. The optical purity of **114n** was determined to be 97% *ee* by HPLC analysis (CHIRALPAK AS column, 93:7 hexane/2-propanol at 226 nm, flow-rate: 0.7 mL/min): retention times; R_t = 7.7 min (major enantiomer, **114n**) and R_t = 10.55 min (minor enantiomer, *ent*-**114n**).

Spectral data for **114n**: R_f = 0.19 (3:1 hexanes/EtOAc); ^{1}H NMR ($CDCl_3$, 600 MHz) δ 1.13 (t, 3H, J = 7.2 Hz), 2.19 (s, 6H), 2.23 (s, 6H), 2.35 (s, 3H), 2.57 (d, 1H, J = 6.6 Hz), 2.94 (d, 1H, J = 6.0 Hz), 3.64 (s, 4H), 3.67 (s, 3H), 4.05 (q, 2H, J = 7.2 Hz), 7.03 (s, 2H), 7.09 (s, 2H), 7.49 (s, 1H); ^{13}C NMR ($CDCl_3$, 150 MHz) δ 13.85, 14.12, 16.18, 16.20, 41.75, 45.28, 59.55, 59.58, 60.69, 76.83, 127.40, 127.64, 130.57, 130.64, 135.90, 136.52, 137.44, 137.64, 155.99, 156.08, 160.79, 167.64; IR (thin film) 2936vs, 1746s, 1582s, 1484s, 1223s, 1194s, 1015m cm^{-1}; HRMS (ESI-TOF) *m/z* 479.2547 [(M+H$^+$); calcd. for $C_{28}H_{35}N_2O_5$: 479.2546]; $[\alpha]_D^{20}$ –33.3.0 (*c* 1.0, EtOAc) on 96% ee material (HPLC) of *ent*-**114n**.

7.15.7 Synthesis of alkyl MEDAM aziridines 114o-w (*via* Procedure IIIA, *Table 7.6*)

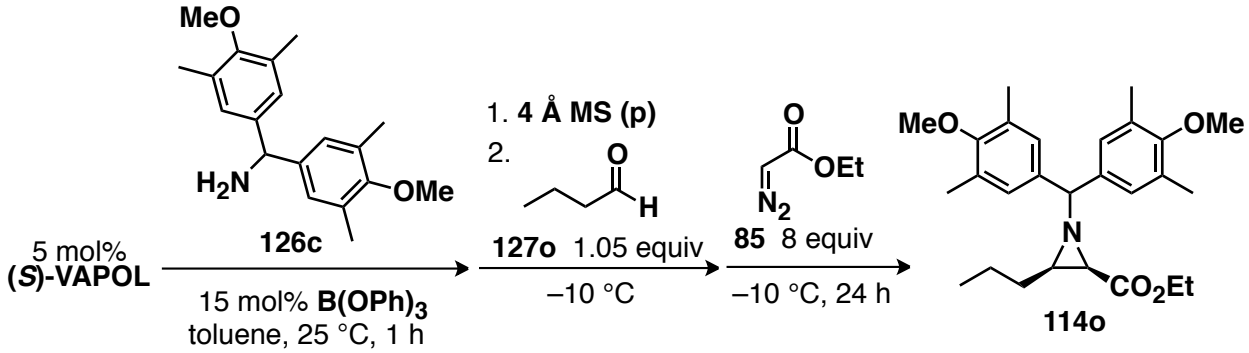

(2*R*,3*R*)-ethyl-1-(bis(4-methoxy-3,5-dimethylphenyl)methyl)-3-propylaziridine-2-carboxylate 114o: Aldehyde **127o** (46.0 μL, 38.0 mg, 0.525 mmol) was reacted according to the general Procedure IIIA described above with (*S*)-VAPOL as ligand except that the addition of aldehyde **127o** was carried out at –10 °C followed by the addition of EDA **85** (415 μL, 4.00 mmoL, 8.00 equiv) at the same temperature. The reaction was stirred at –10 °C for 24 h. Purification of the crude aziridine by silica gel chromatography (20 mm × 250 mm column, 4:2:0.1 hexanes/CH_2Cl_2/EtOAc, gravity column) afforded pure *cis*-aziridine **114o** as a yellow oil in 94% isolated yield (207 mg, 0.490 mmol); *cis/trans*: not determined. Enamine side products: not observed. The optical purity of **114o** was determined to be 96% *ee* by HPLC analysis (CHIRALCEL OD-H column, 99:1 hexane/2-propanol at 226 nm, flow-rate: 0.7 mL/min): retention times; R_t = 4.73 min (major enantiomer, **114o**) and R_t = 5.68 min (minor enantiomer, *ent*-**114o**).

Spectral data for **114o**: R_f = 0.28 (4:2:0.1 hexanes/CH_2Cl_2/EtOAc); ^{1}H NMR ($CDCl_3$, 500 MHz) δ 0.72 (t, 3H, *J* = 7.6 Hz), 0.98-1.08 (m, 1H), 1.11-1.20 (m, 1H), 1.23 (t, 3H, *J* = 7.1 Hz), 1.38-1.45 (m, 1H), 1.49-1.55 (m, 1H), 1.95 (q, 1H, *J* = 6.6 Hz), 2.18 (d, 1H, *J* = 6.8 Hz) 2.22 (s,

12H), 3.39 (s, 1H), 3.65 (s, 3H), 3.67 (s, 3H), 4.12-4.23 (m, 2H), 6.99 (s, 2H), 7.07 (s, 2H); ^{13}C NMR ($CDCl_3$, 125 MHz) δ 13.57, 14.33, 16.09, 16.16, 20.33 29.93, 43.53, 46.76, 59.56, 59.60, 60.64, 77.32, 127.41, 128.07, 130.44, 130.47, 137.75, 138.18, 155.81, 156.12, 169.69; IR (thin film) 2957vs, 1744s, 1483s, 1221s, 1182vs cm^{-1}; HRMS (ESI-TOF) *m/z* 440.2817 [(M+H$^+$); calcd. for $C_{27}H_{38}NO_4$: 440.2801]; $[\alpha]_D^{23}$ +95.3 (*c* 1.0, EtOAc) on 97% ee material (HPLC). These spectral data match those previously reported for this compound.[9c]

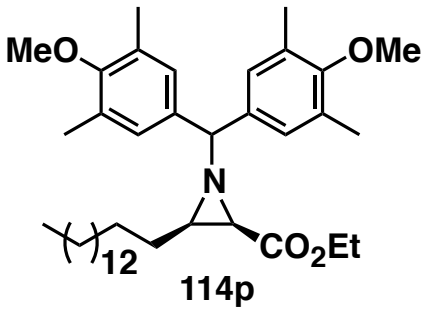

114p

(2*R*,3*R*)-ethyl-1-(bis(4-methoxy-3,5-dimethylphenyl) methyl)-3-pentadecylaziridine-2-carboxylate 114p: Aldehyde **127p** (126 mg, 0.525 mmol) was reacted according to the general Procedure IIA described above with (*S*)-VAPOL as ligand except the following differences : 1) the addition of aldehyde **127p** was carried out at –10 °C followed by the addition of EDA **85** (62 μL, 0.60 mmoL, 1.2 equiv) at the same temperature; 2) the catalyst loading was 10 mol%. The reaction was stirred at –10 °C for 24 h. Purification of the crude aziridine by neutral alumina chromatography (20 mm × 250 mm column, 2:1:0.1 hexanes/CH_2Cl_2/Et_2O, gravity column) afforded pure *cis*-aziridine **114p** as a white solid (mp 41-42 ºC on 95% ee material) in 80% isolated yield (243 mg, 0.400 mmol); *cis/trans*: not determined. Enamine side products: 6% yield of **118p** and 4% yield of **119p**. The optical purity of **114p** was determined to be 96% *ee* by HPLC analysis (PIRKLE COVALENT (R, R) WHELK-O 1 column, 99.5:0.5 hexane/2-propanol

at 226 nm, flow-rate: 0.7 mL/min): retention times; R_t = 18.26 min (major enantiomer, **114p**) and R_t = 33.43 min (minor enantiomer, *ent*-**114p**).

Spectral data for **114p**: R_f = 0.31 (2:1:0.2 hexanes/CH_2Cl_2/Et_2O); ^{1}H NMR ($CDCl_3$, 500 MHz) δ 0.86 (t, 3H, *J* = 7.0 Hz), 1.14-1.28 (m, 1H), 1.43-1.50 (m, 26H), 1.93 (q, 1H, *J* = 6.5 Hz), 2.18 (d, 1H, *J* = 6.5 Hz) 2.22 (s, 12H), 3.38 (s, 1H), 3.65 (s, 3H), 3.67 (s, 3H), 4.12-4.23 (m, 2H), 6.99 (s, 2H), 7.07 (s, 2H); ^{13}C NMR ($CDCl_3$, 125 MHz) δ 14.09, 14.34, 16.11, 16.16, 22.68, 27.24, 27.96, 29.18, 29.35, 29.51, 29.61, 29.62, 29.65, 29.68, 31.92, 43.56, 47.01, 59.57, 59.58, 60.64, 77.35, 127.41, 128.10, 130.42, 130.47, 137.78, 138.18, 155.81, 156.15, 169.69 (3 sp^3 carbon not located); IR (thin film) 2925vs, 1746s, 1484s, 1221s, 1183vs cm^{-1}; HRMS (ESI-TOF) *m/z* 608.4683 [(M+H$^+$); calcd. for $C_{39}H_{62}NO_4$: 608.4679]; $[\alpha]_D^{20}$ +57.9 (*c* 1.0, EtOAc) on 95% ee material (HPLC).

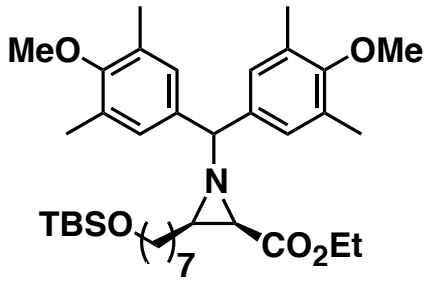

114q

(2*R*,3*R*)-ethyl-1-(bis(4-methoxy-3,5-dimethylphenyl) methyl)-3-(7- ((*tert*-butyldimethylsilyl) oxy)heptyl) aziridine-2-carboxylate 114q: Aldehyde **127q** (136 mg, 0.525 mmol) was reacted according to the general Procedure IIA described above with (*S*)-VAPOL as ligand except that the addition of aldehyde **127q** was carried out at –10 °C followed by the addition of EDA **85** (62 μL, 0.60 mmoL, 1.2 equiv) at the same temperature and the catalyst loading was 10 mol%. The

reaction was stirred at –10 °C for 24 h. Purification of the crude aziridine by silica gel chromatography (30 mm × 300 mm column, 1:15 EtOAc/hexanes, gravity column) afforded pure *cis*-aziridine **114q** as a yellow oil in 80% isolated yield (250 mg, 0.400 mmol); *cis/trans*: not determined. Enamine side products: <1% yield of **118q** and 2.8% yield of **119q**. The optical purity of **114q** was determined to be 98% *ee* by HPLC analysis (CHIRALCEL OD-H column, 99.5:0.5 hexane/2-propanol at 226 nm, flow-rate: 0.7 mL/min): retention times; R_t = 5.33 min (major enantiomer, **114q**) and R_t = 7.26 min (minor enantiomer, *ent*-**114q**).

Spectral data for **114q**: R_f = 0.28 (12:1 hexanes/EtOAc); ^{1}H NMR ($CDCl_3$, 500 MHz) δ 0.02 (s, 6H), 0.87 (s, 9H), 1.11-1.21 (m, 8H), 1.24 (t, 3H, *J* = 7.1 Hz), 1.40-1.50 (m, 4H), 1.94 (q, 1H, *J* = 6.6 Hz), 2.19 (d, 1H, *J* = 6.8 Hz) 2.22 (s, 12H), 3.39 (s, 1H), 3.55 (t, 2H, *J* = 6.8 Hz), 3.65 (s, 3H), 3.67 (s, 3H), 4.12-4.22 (m, 2H), 6.99 (s, 2H), 7.08 (s, 2H); ^{13}C NMR ($CDCl_3$, 125 MHz) δ -5.31, 14.31, 16.08, 16.12, 18.32, 25.62, 25.94, 27.17, 27.88, 29.12, 29.38, 32.80, 43.52, 46.92, 59.51, 59.52, 60.59, 63..22, 77.32, 127.37, 128.07, 130.38, 130.43, 137.74, 138.16, 155.79, 156.13, 169.63; IR (thin film) 2930s, 1746s, 1483s, 1221s, 1183vs cm^{-1}; HRMS (ESI-TOF) *m/z* 626.4243 [(M+H$^+$); calcd. for $C_{37}H_{60}NO_5Si$: 626.4241]; $[\alpha]_D^{20}$ +54.5 (*c* 1.0, EtOAc) on 98% ee material (HPLC).

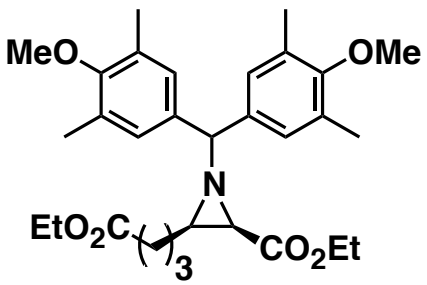

114r

(2*R*,3*R*)-ethyl-1-(bis(4-methoxy-3,5-dimethylphenyl) methyl)-3-(4-ethoxy-4-oxobutyl)aziridine-2-carboxylate 114r: Aldehyde **127r** (72.0 μL, 76.0 mg, 0.525 mmol) was reacted according to the general Procedure IIIA described

above with (*S*)-VAPOL as ligand except that the addition of aldehyde **127r** was carried out at –10 °C followed by the addition of EDA **85** (415 μL, 4.0 mmoL, 8 equiv) at the same temperature. The reaction was stirred at –10 °C for 24 h. Purification of the crude aziridine by silica gel chromatography (30 mm × 300 mm column, 1:40 Et_2O/CH_2Cl_2; 1:30 Et_2O/CH_2Cl_2; 1:20 Et_2O/CH_2Cl_2, gravity column) afforded pure *cis*-aziridine **114r** as a semi solid in 82% isolated yield (210 mg, 0.410 mmol); *cis/trans*: not determined. Enamine side products: not observed. The optical purity of **114r** was determined to be 97% *ee* by HPLC analysis (CHIRALCEL OD-H column, 99:1 hexane/2-propanol at 226 nm, flow-rate: 0.7 mL/min): retention times; R_t = 11.56 min (major enantiomer, **114r**) and R_t = 12.86 min (minor enantiomer, *ent*-**114r**).

Spectral data for **114r**: R_f = 0.31 (20:1 Et_2O/CH_2Cl_2); ^{1}H NMR ($CDCl_3$, 500 MHz) δ 1.19 (t, 3H, *J* = 7.1 Hz), 1.24 (t, 3H, *J* = 7.1 Hz), 1.31-1.38 (m, 1H), 1.40-1.48 (m, 1H), 1.48-1.56 (m, 2H), 1.95 (q, 1H, *J* = 6.1 Hz), 2.07 (t, 2H, *J* = 7.6 Hz), 2.20 (d, 1H, *J* = 6.8 Hz), 2.22 (s, 12H), 3.39 (s, 1H), 3.65 (s, 3H), 3.66 (s, 3H), 4.04 (q, 2H, *J* = 7.1 Hz), 4.12-4.21 (m, 2H), 6.98 (s, 2H), 7.07 (s, 2H); ^{13}C NMR ($CDCl_3$, 125 MHz) δ 14.16, 14.28, 16.08, 16.15, 22.51, 27.28, 33.53, 43.43, 46.22, 59.55, 60.12, 60.73, 77.26, 127.31, 128.02, 130.49, 130.57, 137.61, 138.01, 155.81, 156.21, 169.48, 173.21 (one sp^3 carbon not located) ; IR (thin film) 2940vs, 1738s, 1483s, 1221s, 1183vs cm^{-1}; HRMS (ESI-TOF) *m/z* 512.3015 [$(M+H^+)$; calcd. for $C_{30}H_{42}NO_6$: 512.3012]; $[\alpha]_D^{20}$ –68.5 (*c* 1.0, EtOAc) on 97% ee material (HPLC) of *ent*-**114r**.

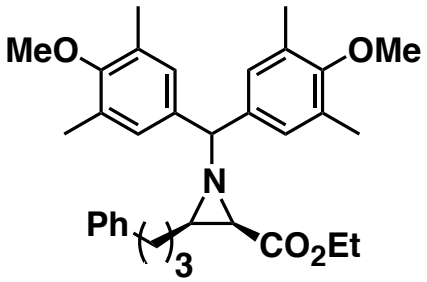

114s

(2*R*,3*R*)-ethyl-1-(bis(4-methoxy-3,5-dimethylphenyl) methyl)-3-(3-phenylpropyl)aziridine-2-carboxylate 114s: Aldehyde **127s** (75.0 μL, 78.0 mg, 0.525 mmol) was reacted according to the general Procedure IIIA described above with (*S*)-VAPOL as ligand except that the addition of aldehyde **127s** was carried out at –10 °C followed by the addition of EDA **85** (415 μL, 4.0 mmoL, 8 equiv) at the same temperature. The reaction was stirred at –10 °C for 24 h. Purification of the crude aziridine by silica gel chromatography (30 mm × 300 mm column, 1:9 EtOAc/hexanes, gravity column) afforded pure *cis*-aziridine **114s** as a yellow oil in 50% isolated yield (129 mg, 0.250 mmol); *cis/trans*: not determined. Enamine side products: not observed. The optical purity of **114s** was determined to be 90% *ee* by HPLC analysis (CHIRALCEL OD-H column, 99:1 hexane/2-propanol at 226 nm, flow-rate: 0.7 mL/min): retention times; R_t = 7.47 min (major enantiomer, **114s**) and R_t = 9.52 min (minor enantiomer, *ent*-**114s**).

Spectral data for **114s**: R_f = 0.30 (1:9 hexanes/EtOAc); ^{1}H NMR ($CDCl_3$, 500 MHz) δ 1.23 (t, 3H, *J* = 7.1 Hz), 1.27-1.35 (m, 1H), 1.40-1.48 (m, 1H), 1.50-1.61 (m, 2H), 1.97 (q, 1H, *J* = 7.1 Hz), 2.19 (s, 6H), 2.21 (d, 1H, *J* = 6.8 Hz) 2.23 (s, 6H), 2.42 (t, 2H, *J* = 8.1 Hz), 3.40 (s, 1H), 3.54 (s, 3H), 3.67 (s, 3H), 4.11-4.21 (m, 2H), 6.99-7.00 (m, 4H), 7.09 (s, 2H) 7.10-7.13 (m, 1H), 7.19-7.21 (m, 2H); ^{13}C NMR ($CDCl_3$, 125 MHz) δ 14.32, 16.08, 16.15, 27.69, 29.11, 35.38, 43.60, 46.61, 59.49, 59.56, 60.70, 77.36, 125.58, 127.33, 128.11, 128.16, 128.18, 130.49, 130.50, 137.67, 138.08, 142.30, 155.79, 156.24, 169.61; IR (thin film) 2930vs, 1744s, 1483s, 1221s,

1184vs cm^{-1}; HRMS (ESI-TOF) *m/z* 516.3115 [$(M+H^+)$; calcd. for $C_{33}H_{42}NO_4$: 516.3114]; $[\alpha]_D^{20}$ +61.7 (*c* 1.0, EtOAc) on 93% ee material (HPLC).

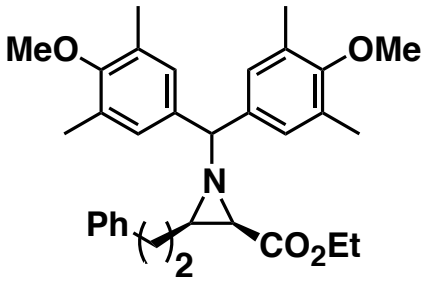

114t

(2*R*,3*R*)-ethyl-1-(bis(4-methoxy-3,5-dimethylphenyl) methyl)-3-phenethylaziridine-2-carboxylate 114t: Aldehyde **127t** (70.0 μL, 70.0 mg, 0.525 mmol) was reacted according to the general Procedure IIIA described above with (*S*)-VAPOL as ligand except that the addition of aldehyde **127t** was carried out at –10 °C followed by the addition of EDA **85** (415 μL, 4.0 mmoL, 8 equiv) at the same temperature. The reaction was stirred at –10 °C for 24 h. Purification of the crude aziridine by silica gel chromatography (30 mm × 300 mm column, 1:12 EtOAc/hexanes, gravity column) afforded pure *cis*-aziridine **114t** as a semi solid in 91% isolated yield (228 mg, 0.460 mmol); *cis/trans*: not determined. Enamine side products: <1% yield of **118t** and 1.8 % yield of **119t**. The optical purity of **114t** was determined to be 96% *ee* by HPLC analysis (CHIRALCEL OD-H column, 99:1 hexane/2-propanol at 226 nm, flow-rate: 0.5 mL/min): retention times; R_t = 11.33 min (major enantiomer, **114t**) and R_t = 12.80 min (minor enantiomer, *ent*-**114t**).

Spectral data for **114t**: R_f = 0.20 (12:1 hexanes/EtOAc); ^{1}H NMR ($CDCl_3$, 500 MHz) δ 1.24 (t, 3H, *J* = 7.1 Hz), 1.80-1.92 (m, 2H), 1.96 (q, 1H, *J* = 7.1 Hz), 2.21 (d, 1H, *J* = 6.8 Hz) 2.24 (s, 6H), 2.27 (s, 6H), 2.29-2.34 (m, 1H), 2.48-2.53 (m, 1H), 3.41 (s, 1H), 3.67 (s, 3H), 3.68 (s, 3H), 4.12-4.20 (m, 2H), 6.91 (d, 2H, *J* = 7.3 Hz), 7.01 (s, 2H), 7.10 (s, 2H), 7.13 (d, 1H, *J* = 7.3 Hz),

7.19 (t, 2H, J = 7.3 Hz); ^{13}C NMR ($CDCl_3$, 125 MHz) δ 14.29, 16.12, 16.15, 29.59, 33.25, 43.34, 46.13, 59.54, 59.60, 60.71, 77.22, 125.70, 127.26, 128.06, 128.15, 128.36, 130.50, 130.58, 137.77, 138.30, 141.35, 155.80, 156.22, 169.54; IR (thin film) 2934s, 1744s, 1484s, 1221s, 1182vs cm^{-1}; HRMS (ESI-TOF) *m/z* 502.2962 [$(M+H^+)$; calcd. for $C_{32}H_{40}NO_4$: 502.2957]; $[\alpha]_D^{20}$ –62.3 (*c* 1.0, EtOAc) on 96% ee material (HPLC) of *ent*-**114t**.

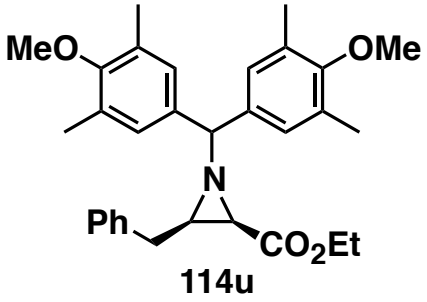

114u

(2*R*,3*R*)-ethyl-3-benzyl-1-(bis(4-methoxy-3,5-dimethyl phenyl)methyl)aziridine-2-carboxylate 114u: Aldehyde **127u** (59.0 μL, 63.0 mg, 0.525 mmol) was reacted according to the general Procedure IIIA described above with (*S*)-VAPOL as ligand except that the addition of aldehyde **127u** was carried out at –10 °C followed by the addition of EDA **85** (415 μL, 4.0 mmoL, 8 equiv) at the same temperature. The reaction was stirred at –10 °C for 24 h. Purification of the crude aziridine by silica gel chromatography (30 mm × 300 mm column, 1:12 EtOAc/hexanes, gravity column) afforded pure *cis*-aziridine **114u** as a semi solid in 86% isolated yield (209 mg, 0.430 mmol); *cis/trans*: not determined. Enamine side products: not observed. The optical purity of **114u** was determined to be 98% *ee* by HPLC analysis (PIRKLE COVALENT (R, R) WHELK-O 1 column, 95:5 hexane/2-propanol at 226 nm, flow-rate: 0.7 mL/min): retention times; R_t = 11.53 min (major enantiomer, **114u**) and R_t = 16.34 min (minor enantiomer, *ent*-**114u**).

Spectral data for **114u**: R_f = 0.30 (12:1 hexanes/EtOAc); ^{1}H NMR ($CDCl_3$, 500 MHz) δ 1.25 (t, 3H, *J* = 7.2 Hz), 2.20 (s, 6H), 2.24 (s, 6H), 2.25-2.28 (m, 2H), 2.85 (dd, 1H, J = 6.1, 14.7 Hz), 2.94 (dd, 1H, J = 5.6, 14.9 Hz), 3.45 (s, 1H), 3.68 (s, 3H), 3.69 (s, 3H), 4.16-4.25 (m, 2H), 6.96 (s, 2H), 6.98-6.99 (m, 2H), 7.09 (s, 2H), 7.10-7.15 (m, 3H); ^{13}C NMR ($CDCl_3$, 125 MHz) δ 14.26, 16.09, 16.13, 34.23, 43.04, 47.79, 59.49, 59.52, 60.78, 77.18, 126.01, 127.33, 127.95, 128.08, 128.53, 130.41, 130.49, 137.65, 137.86, 138.58, 155.80, 155.99, 169.59; IR (thin film) 2937s, 1742vs, 1484s, 1221s, 1182vs cm^{-1}; HRMS (ESI-TOF) *m/z* 440.2808 [(M+H$^+$); calcd. for $C_{31}H_{38}NO_4$: 488.2801]; $[\alpha]_D^{20}$ –54.2 (*c* 1.0, EtOAc) on 98% ee material (HPLC) of ***ent*-114u**.

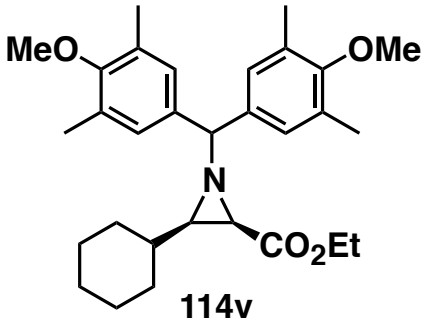

114v

(*2R,3R*)-ethyl-1-(bis(4-methoxy-3,5-dimethyl phenyl)methyl)-3-cyclohexylaziridine-2-carboxylate 114v: Aldehyde **127v** (63.0 μL, 59.0 mg, 0.525 mmol) was reacted according to the general Procedure IIIA described above with (*S*)-VAPOL as ligand. Purification of the crude aziridine by silica gel chromatography (30 mm × 300 mm column, 4:2:0.1 hexanes/CH_2Cl_2/Et_2O, gravity column) afforded pure *cis*-aziridine **114v** as a semi solid in 95% isolated yield (229 mg, 0.480 mmol); *cis/trans*: > 50:1. Enamine side products: <1% yield of **118v** and 1.9% yield of **119v**. The optical purity of **114v** was determined to be 90% *ee* by HPLC analysis (CHIRALCEL OD

column, 99:1 hexane/2-propanol at 223 nm, flow-rate: 0.7 mL/min): retention times; R_t = 10.06 min (major enantiomer, **114v**) and R_t = 12.37 min (minor enantiomer, *ent*-**114v**).

Spectral data for **114v**: R_f = 0.21 (2:1 hexane/CH_2Cl_2); ^{1}H NMR ($CDCl_3$, 300 MHz) δ 0.46-0.57 (m, 1H), 0.87-1.19 (m, 4H), 1.21 (t, 3H, J = 7.1 Hz), 1.22-1.32 (m, 2H), 1.40-1.60 (m, 4H), 1.71-1.76 (m, 1H), 2.16 (m, 1H), 2.19 (s, 6H), 2.20 (s, 6H), 3.35 (s, 1H), 3.60 (s, 3H), 3.63 (s, 3H), 4.10-4.25 (m, 2H), 6.95 (s, 2H), 7.10 (s, 2H); ^{13}C NMR ($CDCl_3$, 75 MHz) δ 13.85, 15.56, 15.67, 24.91, 25.09, 25.73, 29.65, 30.38, 35.88, 42.97, 51.76, 59.01, 59.07, 60.12, 77.01, 126.90, 128.10, 129.84, 129.95, 137.16, 137.71, 155.31, 155.83, 169.30; IR (thin film) 2928vs, 1744s, 1483s, 1221s, 1181s, 1017m cm^{-1}; Mass spectrum: *m/z* (% rel intensity) 479 M+ (0.7), 283 (100), 268 (25), 253 (12), 237 (7), 210 (7), 195 (9), 141 (8), 95 (10), 67 (16), 55 (10), 41 (16); $[\alpha]_D^{23}$ +107.9 (c 1.0, CH_2Cl_2) on 90% ee material (HPLC). These spectral data match those previously reported for this compound.[9c]

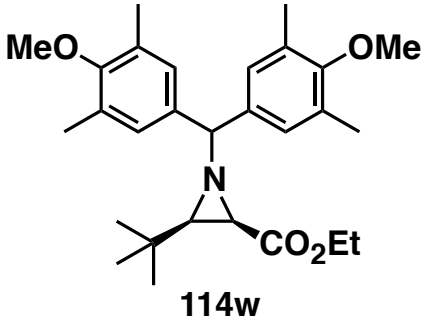

114w

(2*R*,3*R*)-ethyl-1-(bis(4-methoxy-3,5-dimethyl phenyl) methyl)-3-(*tert*-butyl)aziridine-2-carboxylate 114w: Aldehyde **127w** (58.0 μL, 45.0 mg, 0.525 mmol) was reacted according to the general Procedure IIIA described above with (*S*)-VAPOL as ligand except that 2 equiv of EDA **85** was used. Purification of the crude aziridine by silica gel chromatography (30 mm × 300 mm column, 4:2:0.1 hexanes/CH_2Cl_2/Et_2O and then 2:1:0.1 hexanes/CH_2Cl_2/Et_2O, gravity column)

afforded pure cis-aziridine **114w** as a semi solid in 95% isolated yield (216 mg, 0.480 mmol); *cis/trans*: >50:1. Enamine side products: <1% yield of **118w** and <1% yield of **119w**. The optical purity of **114w** was determined to be 92% *ee* by HPLC by HPLC analysis (CHIRALCEL OD column, 99:1 hexane/2-propanol at 226 nm, flow-rate: 1.0 mL/min): retention times; R_t = 6.8 min (major enantiomer, **114w**) and R_t = 10.55 min (minor enantiomer, *ent*-**114w**).

Spectral data for **114w**: R_f = 0.28 (1:2 hexane/CH_2Cl_2); ^{1}H NMR ($CDCl_3$, 300 MHz) δ 0.72 (s, 9H), 1.29 (t, 3H, *J* = 7.1 Hz), 1.70 (d, 1H, *J* = 7.3 Hz), 2.11 (d, 1H, *J* = 7.2 Hz), 2.24 (s, 6H), 2.26 (s, 6H), 3.38 (s, 1H), 3.63 (s, 3H), 3.66 (s, 3H), 4.05-4.26 (m, 2H), 7.04 (s, 2H), 7.30 (s, 2H); ^{13}C NMR ($CDCl_3$, 75 MHz) δ 13.92, 15.84, 15.96, 27.24, 31.39, 43.16, 55.94, 59.20, 59.27, 60.24, 78.20, 127.30, 128.18, 130.01, 137.77, 138.74, 155.51, 155.98, 169.66 (one sp^2 carbon not located); IR (thin film) 2953vs, 1747s, 1481s, 1221s, 1181s, 1017m cm^{-1}; Mass spectrum: *m/z* (% rel intensity) 453 M+ (1), 283 (100), 268 (45), 253 (26), 237 (17), 225 (11), 210 (13), 195 (17), 164 (9) 141 (26), 132 (11), 127 (12), 91 (11), 69 (18), 55 (37), 41 (55); $[\alpha]_D^{23}$ +110.0 (c 1.0, CH_2Cl_2) on 94% ee material (HPLC). These spectral data match those previously reported for this compound.[9c]

7.15.8 Synthesis of MEDAM imine 111l and aziridine 114l (aziridination with preformed imine, *Scheme 7.5*)

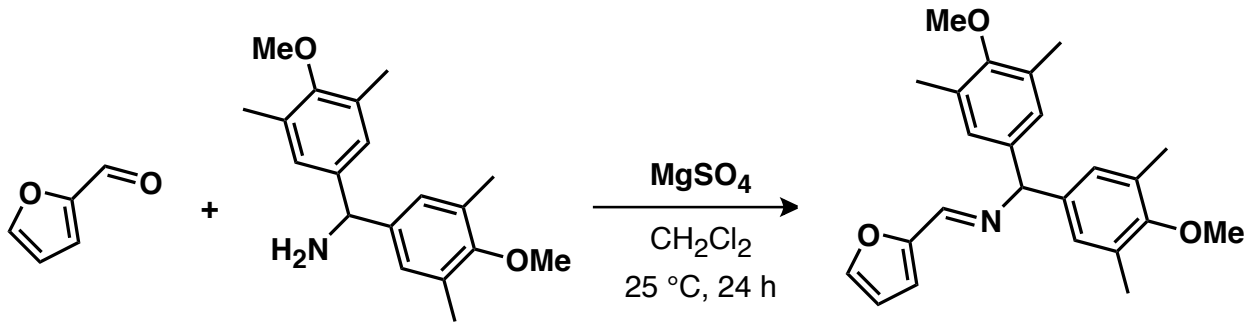

127l **126c** **111l** 26%

(*E*)-*N*-(furan-2-ylmethylene)-1,1-bis(4-methoxy-3,5-dimethylphenyl)methanamine 111l: To a 25 mL flame-dried round bottom flask, equipped with a stir bar, filled with argon was added MEDAM amine **126c** (598.8 g, 2.000 mmol), $MgSO_4$ (500 mg, freshly flame-dried) and dry CH_2Cl_2 (6 mL). After stirring for 10 min, aldehyde **127l** (174 μL, 2.10 mmol, 1.05 equiv) was added. The reaction mixture was stirred at room temperature for 24 h. The reaction mixture was filtered through Celite and the Celite bed was washed with CH_2Cl_2 (3 mL × 3) and then the filtrate was concentrated by rotary evaporation to give the crude imine as an off-white solid. Crystallization (1:25 CH_2Cl_2 / hexanes) and collection of the first crop afforded **111l** as a white solid (mp 116-117 ºC) in 26% isolated yield (200 mg, 0.520 mmol).

Spectral data for **111l**: ^{1}H NMR ($CDCl_3$, 600 MHz) δ 2.23 (s, 12H), 3.67 (s, 6H), 5.31 (s, 1H), 6.45 (dd, 1H, J = 1.7, 3.4 Hz), 6.77 (d, 1H, J = 3.4 Hz), 6.97 (s, 4H), 7.51 (d, 1H, J = 1.7 Hz), 8.13 (s, 1H); ^{13}C NMR ($CDCl_3$, 150 MHz) δ 16.16, 59.60, 77.71, 111.60, 114.46, 127.94,

130.66, 138.74, 144.77, 149.19, 151.73, 155.90; IR (thin film) 2944w, 1646s, 1484s, 1221 cm^{-1}; HRMS (ESI-TOF) *m/z* 378.2075 [$(M+H^+)$; calcd. for $C_{24}H_{28}NO_3$: 378.2069]

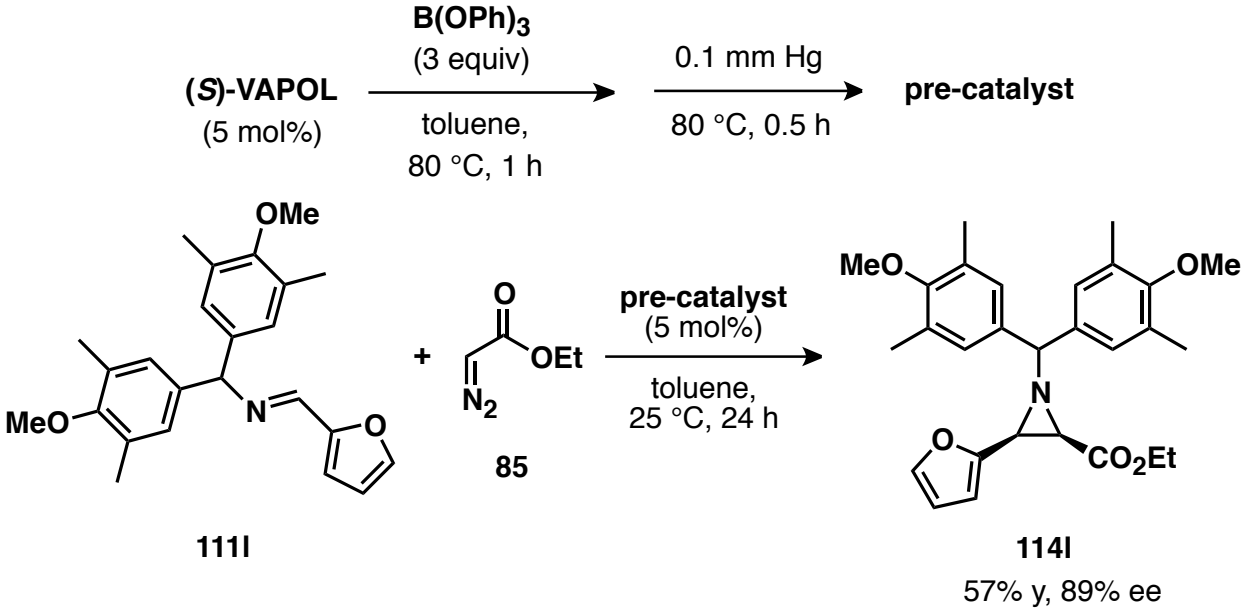

(2*R*,3*S*)-ethyl-1-(bis(4-methoxy-3,5-dimethylphenyl)methyl)-3-(furan-2-yl)aziridine-2-carboxylate 114l: To a 25 mL flame-dried home-made Schlenk flask , prepared from a single-necked 25 mL pear-shaped flask that had its 14/20 glass joint replaced with a high vacuum threaded Teflon valve, equipped with a stir bar and flushed with argon was added (*S)*-VAPOL (7.00 mg, 0.0125 mmol) and $B(OPh)_3$ (11.0 mg, 0.0375 mmol). Under an argon flow through the side-arm of the Schlenk flask, dry toluene (1 mL) was added through the top of the Teflon valve to dissolve the two reagents. The flask was sealed by closing the Teflon valve, and then placed in an 80 ºC oil bath for 1 h. After 1 h, a vacuum (0.5 mm Hg) was carefully applied by slightly opening the Teflon valve to remove the volatiles. After the volatiles were removed completely, a full vacuum was applied and maintained for a period of 30 min at a temperature of

80 ºC (oil bath). The flask was then allowed to cool to room temperature and opened to argon through the side-arm of the Schlenk flask.

To the flask containing the pre-catalyst was first added the aldimine **111l** (94.4 mg, 0.250 mmol) and then dry toluene (0.5 mL) under an argon flow through side-arm of the Schlenk flask. The reaction mixture was stirred for 5 min to give a light orange solution. The flask was then cooled to –10 °C. To this solution was rapidly added ethyl diazoacetate (EDA) **85** (31 μL, 0.30 mmol) followed by closing the Teflon valve. The resulting mixture was stirred for 2 h at –10 °C It was then warmed to room temperature and stirred for 24 h at room temperature. The reaction was dilluted by addition of hexane (6 mL). The reaction mixture was then transferred to a 50 mL round bottom flask. The reaction flask was rinsed with dichloromethane (3 mL × 2) and the rinse was added to the 50 mL round bottom flask. The resulting solution was then concentrated *in vacuo* followed by exposure to high vacuum (0.05 mm Hg) for 1 h to afford the crude aziridine as an off-white solid. Purification of the crude aziridine by silica gel chromatography (30 mm × 300 mm column, 15:1 hexanes/EtOAc with 1% Et_3N as eluent, gravity column; the column was set up by making a slurry of silica gel in hexanes with 2% Et_3N) afforded pure *cis*-aziridine **114l** as a white solid (mp 45-46 ºC on 94% ee material) in 57% isolated yield (66.0 mg, 0.143 mmol); *cis/trans*: 9.3:1. Enamine side products: 1.3% yield of **118l** and 1% yield of **119l**. The optical purity of **114l** was determined to be 89% *ee* by HPLC analysis (CHIRALCEL OD-H column, 99.5:0.5 hexane/2-propanol at 226 nm, flow-rate: 0.7 mL/min): retention times; R_t = 23.6 min (major enantiomer, **114l**) and R_t = 39.1 min (minor enantiomer, *ent*-**114l**). The spectral data of **114l** matched to those reported above.

7.15.9 Mechanistic study of MCAZ

(A) Different order of addition of reagents in MCAZ: Procedures (IV-IX)

Procedure IV: Catalyst + 4Å MS + 127a + EDA 85 @ 25 °C, 24 h

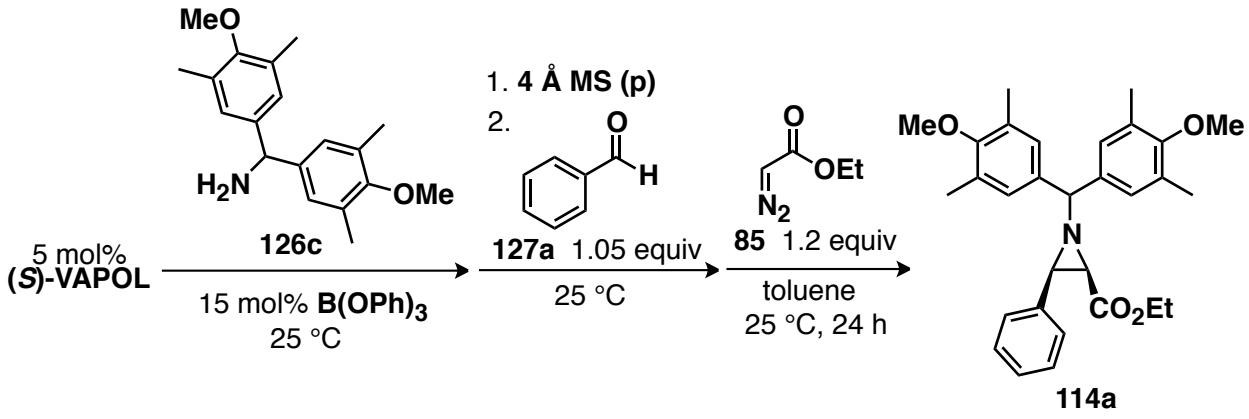

(2*R*,3*R*)-ethyl-1-(bis(4-methoxy-3,5-dimethylphenyl)methyl)-3-phenylaziridine-2-carboxylate 114a: To a 10 mL flame-dried single-necked round bottom flask equipped with a stir bar and filled with argon was added in the following order (*S)*-VAPOL (14 mg, 0.025 mmol), $B(OPh)_3$ (22 mg, 0.075 mmol), amine **126c** (149.7 mg, 0.5000 mmol), 4Å Molecular Sieves (150 mg, freshly flame-dried), aldehyde **127a** (52.0 μL, 0.525 mmoL, 1.05 equiv) and ethyl diazoacetate (EDA) **85** (62 μL, 0.60 mmoL, 1.2 equiv). Dry toluene (1 mL) was added under an argon atmosphere to dissolve the reagents. The flask was fitted with a rubber septum and a nitrogen balloon. The reaction mixture was stirred at room temperature for 24 h. The reaction was dilluted by addition of hexane (6 mL). The reaction mixture was then filtered through a Celite pad to a 100 mL round bottom flask. The reaction flask was rinsed with EtOAc (3 mL × 3) and the rinse was filtered through the same Celite pad. The resulting solution was then concentrated *in vacuo* followed by exposure to high vacuum (0.05 mm Hg) for 1 h to afford

the crude aziridine as an off-white solid. Purification of the crude aziridine by silica gel chromatography (30 mm × 300 mm column, 9:1 hexanes/EtOAc as eluent, gravity column) afforded pure cis-aziridine **114a** as a white solid (mp 107-108 ºC on 99.8% ee material) in 88% isolated yield (208 mg, 0.44 mmol); *cis/trans*: >50:1. Enamine side products: <1 % yield of **118a** and <1 % yield of **119a**. The optical purity of **114a** was determined to be 98% *ee* by HPLC analysis (CHIRALCEL OD-H column, 99:1 hexane/2-propanol at 226nm, flow-rate: 0.7 mL/min): retention times; R_t = 9.26 min (major enantiomer, **114a**) and R_t = 12.52 min (minor enantiomer, *ent*-**114a**).

Procedure V: Catalyst + EDA 85 @ 25 °C, 1 h and then addition of the aldehyde 127a.

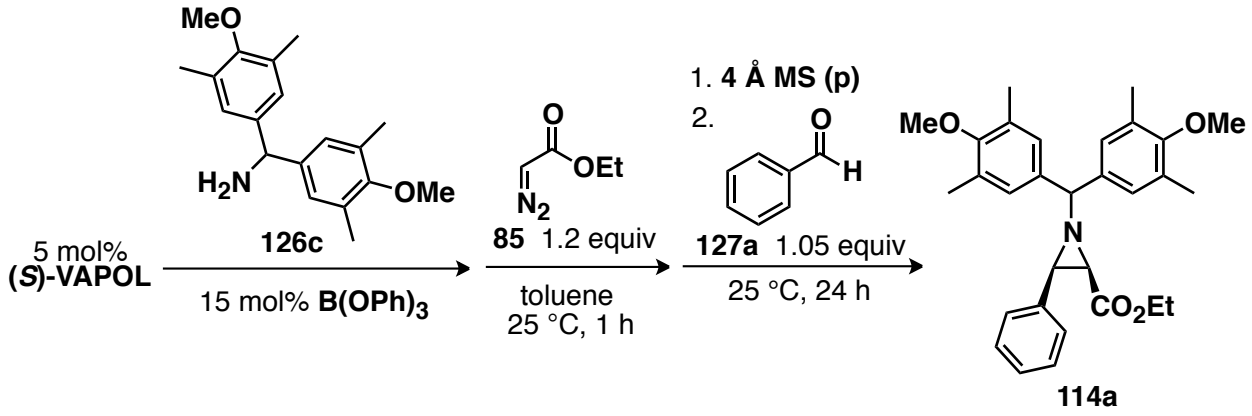

(2*R*,3*R*)-ethyl-1-(bis(4-methoxy-3,5-dimethylphenyl)methyl)-3-phenylaziridine-2-carboxylate 114a: To a 10 mL flame-dried single-necked round bottom flask equipped with a stir bar and filled with argon was added in the following order (*S)*-VAPOL (14 mg, 0.025 mmol), $B(OPh)_3$ (22 mg, 0.075 mmol), amine **126c** (149.7 mg, 0.5000 mmol) and ethyl diazoacetate (EDA) **85** (62 μL, 0.60 mmoL, 1.2 equiv). Dry toluene (1 mL) was added under an argon atmosphere to dissolve the reagents. The flask was fitted with a rubber septum and a

nitrogen balloon. The reaction mixture was stirred at room temperature for 1 h. Thereafter, 4Å Molecular Sieves (150 mg, freshly flame-dried) was added followed by the addition of the aldehyde **127a** (52.0 μL, 0.525 mmoL, 1.05 equiv). The resulting mixture was stirred for 24 h at room temperature. The reaction was diluted by addition of hexane (6 mL). The reaction mixture was then filtered through a Celite pad to a 100 mL round bottom flask. The reaction flask was rinsed with EtOAc (3 mL × 3) and the rinse was filtered through the same Celite pad. The resulting solution was then concentrated *in vacuo* followed by exposure to high vacuum (0.05 mm Hg) for 1 h to afford the crude aziridine as an off-white solid. Purification of the crude aziridine by silica gel chromatography (30 mm × 300 mm column, 9:1 hexanes/EtOAc as eluent, gravity column) afforded pure *cis*-aziridine **114a** as a white solid (mp 107-108 ºC on 99.8% ee material) in 94% isolated yield (223 mg, 0.47 mmol); *cis/trans*: >50:1. Enamine side products: <1% yield of **118a** and <1% yield of **119a**. The optical purity of **114a** was determined to be 98% *ee* by HPLC analysis (CHIRALCEL OD-H column, 99:1 hexane/2-propanol at 226nm, flow-rate: 0.7 mL/min): retention times; R_t = 9.26 min (major enantiomer, **114a**) and R_t = 12.52 min (minor enantiomer, *ent*-**114a**).

Procedure VI: Catalyst + EDA 85 + 4Å MS + 127a @ 25 °C, 24 h

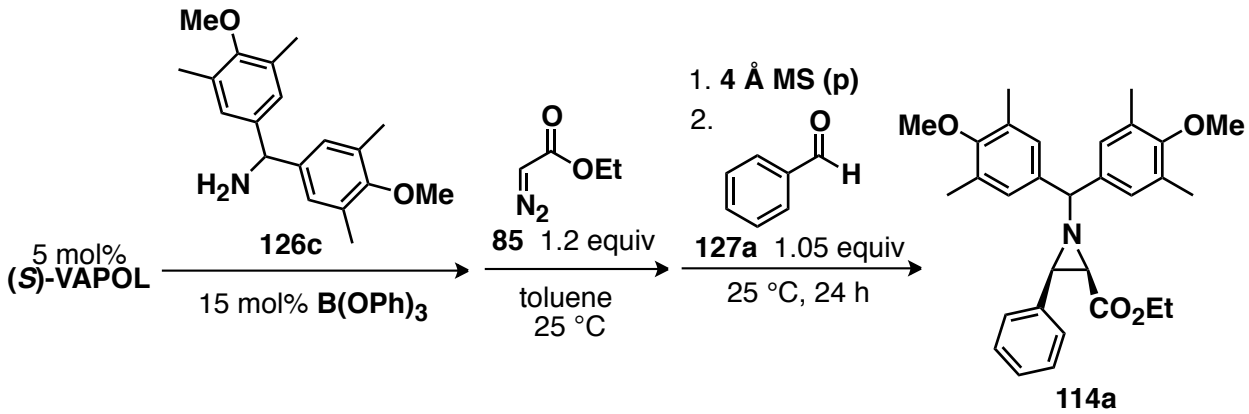

(2*R*,3*R*)-ethyl-1-(bis(4-methoxy-3,5-dimethylphenyl)methyl)-3-phenylaziridine-2-carboxylate 114a: To a 10 mL flame-dried single-necked round bottom flask equipped with a stir bar and filled with argon was added in the following order (*S)*-VAPOL (14 mg, 0.025 mmol), $B(OPh)_3$ (22 mg, 0.075 mmol), amine **126c** (149.7 mg, 0.5000 mmol) and ethyl diazoacetate (EDA) **85** (62 μL, 0.60 mmoL, 1.2 equiv). Dry toluene (1 mL) was added under an argon atmosphere to dissolve the reagents. The flask was fitted with a rubber septum and a nitrogen balloon. Thereafter, 4Å Molecular Sieves (150 mg, freshly flame-dried) was added followed by the addition of the aldehyde **127a** (52.0 μL, 0.525 mmoL, 1.05 equiv). The resulting mixture was stirred for 24 h at room temperature. The reaction was dilluted by addition of hexane (6 mL). The reaction mixture was then filtered through a Celite pad to a 100 mL round bottom flask. The reaction flask was rinsed with EtOAc (3 mL × 3) and the rinse was filtered through the same Celite pad. The resulting solution was then concentrated *in vacuo* followed by exposure to high vacuum (0.05 mm Hg) for 1 h to afford the crude aziridine as an off-white solid. Purification of the crude aziridine by silica gel chromatography (30 mm × 300 mm column, 9:1 hexanes/EtOAc as eluent, gravity column) afforded pure *cis*-aziridine **114a** as a white solid (mp 107-108 ºC on 99.8% ee material) in 94% isolated yield (223 mg, 0.47 mmol); *cis/trans*: >50:1. Enamine side products: <1% yield of **118a** and <1% yield of **119a**. The optical purity of **114a** was determined to be 98% *ee* by HPLC analysis (CHIRALCEL OD-H column, 99:1 hexane/2-propanol at 226nm, flow-rate: 0.7 mL/min): retention times; R_t = 9.26 min (major enantiomer, **114a**) and R_t = 12.52 min (minor enantiomer, *ent*-**114a**).

Procedure VII: Amine 126c added at the end prior to the addition of toluene.

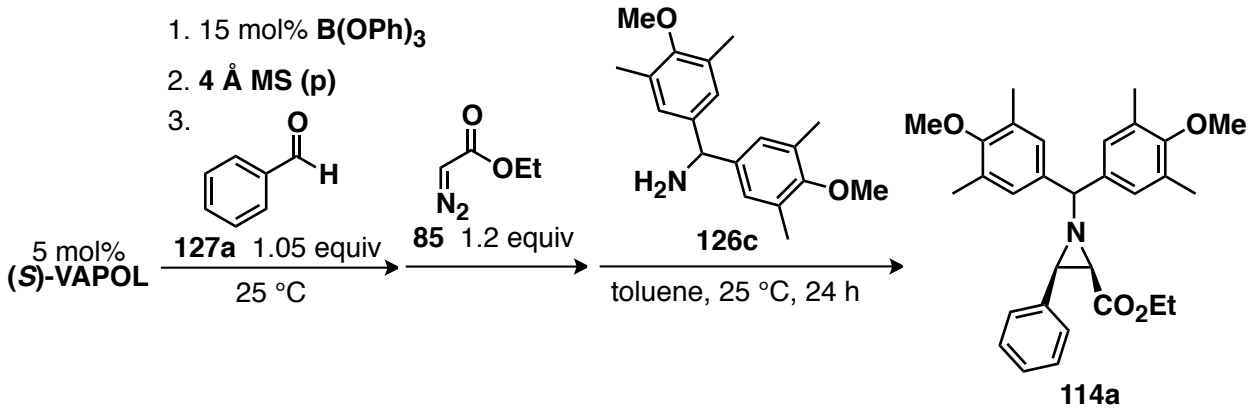

(2*R*,3*R*)-ethyl-1-(bis(4-methoxy-3,5-dimethylphenyl)methyl)-3-phenylaziridine-2-carboxylate 114a: To a 10 mL flame-dried single-necked round bottom flask equipped with a stir bar and filled with argon was added in following order (*S)*-VAPOL (14 mg, 0.025 mmol), $B(OPh)_3$ (22 mg, 0.075 mmol), 4Å Molecular Sieves (150 mg, freshly flame-dried), aldehyde **127a** (52.0 μL, 0.525 mmoL, 1.05 equiv), ethyl diazoacetate (EDA) **85** (62 μL, 0.60 mmoL, 1.2 equiv) and amine **126c** (149.7 mg, 0.5000 mmol). Dry toluene (1 mL) was added under an argon atmosphere to dissolve the reagents. The flask was fitted with a rubber septum and a nitrogen balloon. The reaction mixture was stirred for 24 h at room temperature. The reaction was dilluted by addition of hexane (6 mL). The reaction mixture was then filtered through a Celite pad to a 100 mL round bottom flask. The reaction flask was rinsed with EtOAc (3 mL × 3) and the rinse was filtered through the same Celite pad. The resulting solution was then concentrated *in vacuo* followed by exposure to high vacuum (0.05 mm Hg) for 1 h to afford the crude aziridine as an off-white solid. Purification of the crude aziridine by silica gel chromatography (30 mm × 300 mm column, 9:1 hexanes/EtOAc as eluent, gravity column) afforded pure *cis*-aziridine **114a** as a white solid (mp 107-108 ºC on 99.8% ee material) in 85% isolated yield (201 mg, 0.430 mmol); *cis/trans*: >50:1. Enamine side products: 2% yield of **118a** and 1% yield of

119a. The optical purity of **114a** was determined to be 98% *ee* by HPLC analysis (CHIRALCEL OD-H column, 99:1 hexane/2-propanol at 226nm, flow-rate: 0.7 mL/min): retention times; R_t = 9.26 min (major enantiomer, **114a**) and R_t = 12.52 min (minor enantiomer, *ent*-**114a**). A repeat of this reaction also gave **114a** in 85% yield. This is the ^{1}H NMR yield determined by integration against an internal standard (Ph_3CH).

Procedure VIII: Amine 126c added at the end after 2 min stirring of a mixture of VAPOL 58, $B(OPh)_3$, aldehyde 127a and EDA 85 in toluene.

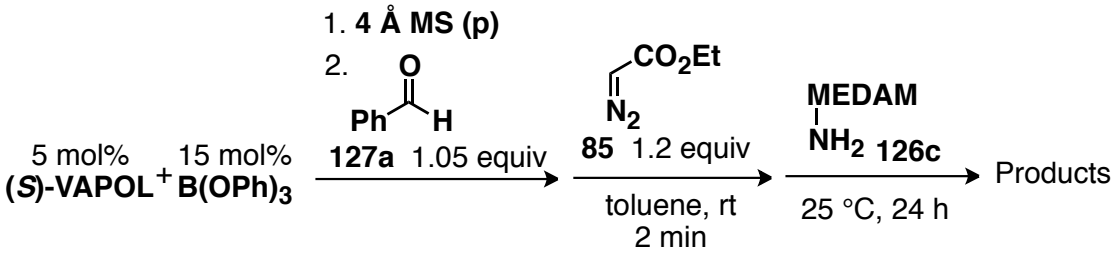

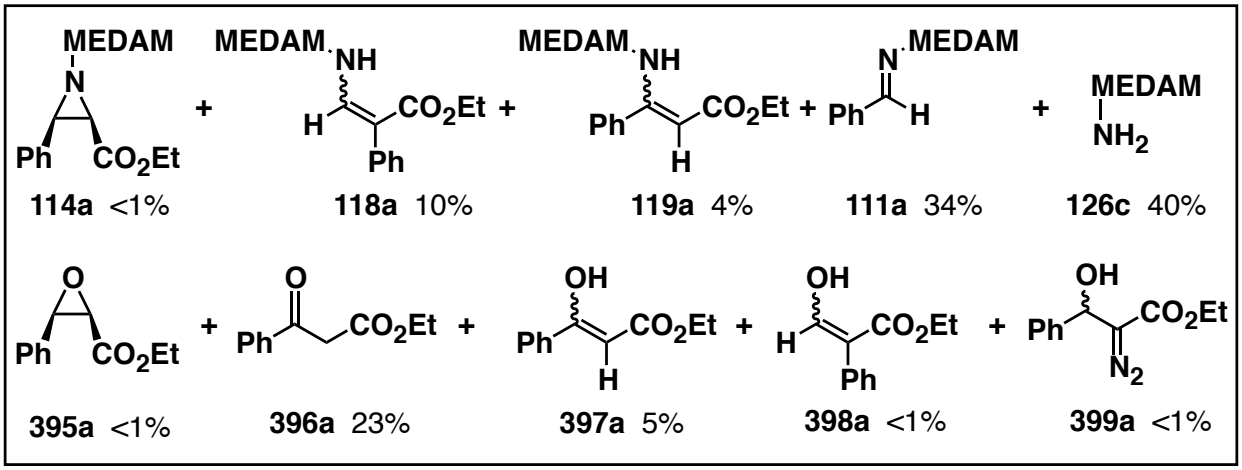

To a 10 mL flame-dried single-necked round bottom flask equipped with a stir bar and filled with argon was added in the following order (*S)*-VAPOL (14 mg, 0.025 mmol), $B(OPh)_3$ (22 mg, 0.075 mmol), 4Å Molecular Sieves (150 mg, freshly flame-dried), aldehyde **127a** (52.0 μL, 0.525 mmoL, 1.05 equiv), ethyl diazoacetate (EDA) **85** (62 μL, 0.60 mmoL, 1.2 equiv). Dry

toluene (1 mL) was added under an argon atmosphere to dissolve the reagents. The flask was fitted with a rubber septum and a nitrogen balloon. The mixture was stirred for 2 min followed by the addition of amine **126c** (149.7 mg, 0.5000 mmol). The reaction mixture was stirred for 24 h at room temperature. The reaction was dilluted by addition of hexane (6 mL). The reaction mixture was then filtered through a Celite pad to a 100 mL round bottom flask. The reaction flask was rinsed with EtOAc (3 mL × 3) and the rinse was filtered through the same Celite pad. The resulting solution was then concentrated *in vacuo* followed by exposure to high vacuum (0.05 mm Hg) for 1 h to afford the crude mixture. An internal standard Ph_3CH (12.2 mg, 0.500 mmol) was added and subjected to NMR analysis. The ^1H NMR of crude reaction mixture revealed the presence of several products as shown in the reaction scheme. The presence of each product was confirmed by characteristic peaks (as discussed earlier) in the ^1H NMR previously published for these compounds and the amount of each was quantified by integration against an internal standard (Ph_3CH).

Procedure IX: Same as Procedure VIII except that amine 126c is not added.

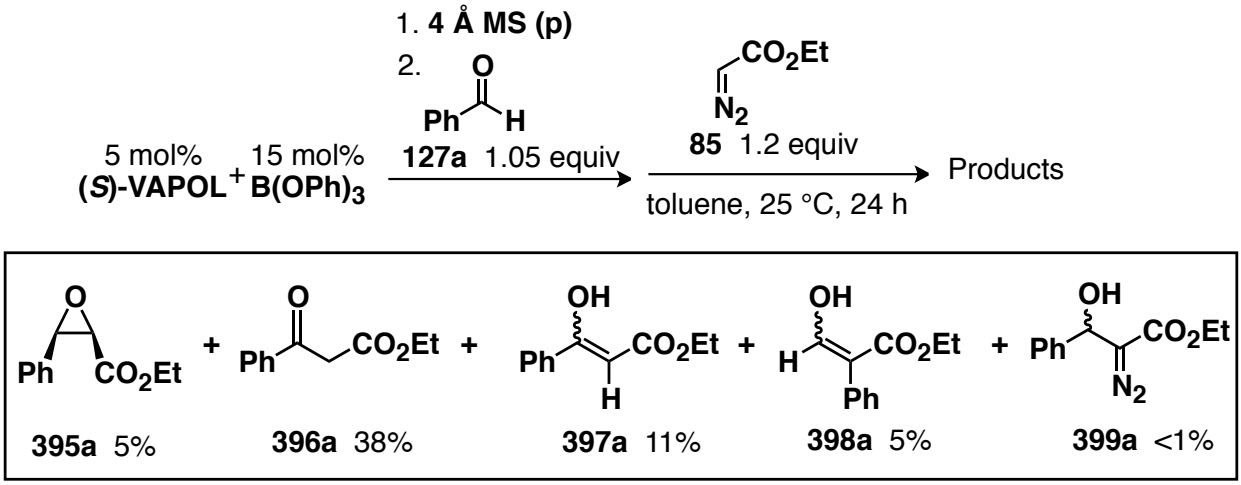

To a 10 mL flame-dried single-necked round bottom flask equipped with a stir bar and filled with argon was added in the following order (*S)*-VAPOL (14 mg, 0.025 mmol), $B(OPh)_3$ (22 mg, 0.075 mmol), 4Å Molecular Sieves (150 mg, freshly flame-dried), aldehyde **127a** (52.0 μL, 0.525 mmoL, 1.05 equiv), ethyl diazoacetate (EDA) **85** (62 μL, 0.60 mmoL, 1.2 equiv). Dry toluene (1 mL) was added under an argon atmosphere to dissolve the reagents. The flask was fitted with a rubber septum and a nitrogen balloon. The resulting mixture was stirred for 24 h at room temperature. The reaction was dilluted by addition of hexane (6 mL). The reaction mixture was then filtered through a Celite pad to a 100 mL round bottom flask. The reaction flask was rinsed with EtOAc (3 mL × 3) and the rinse was filtered through the same Celite pad. The resulting solution was then concentrated *in vacuo* followed by exposure to high vacuum (0.05 mm Hg) for 1 h to afford the crude mixture. An internal standard Ph_3CH (12.2 mg, 0.500 mmol) was added and subjected to NMR analysis. The ^1H NMR of the crude reaction mixture revealed the presence of several products as shown in the reaction scheme. The presence of each product was confirmed by characteristic peaks (as discussed earlier) in the ^1H NMR previously published for these compounds. There was also mono-alkylated (*S*)-VAPOL derivative **230** in 37% yield (with respect to (*S*)-VAPOL).

Procedure VIII in $CDCl_3$: Amine 126c added at the end after 2 min stirring of a mixture of VAPOL 58, $B(OPh)_3$, aldehyde 127a and EDA 2 in $CDCl_3$.

This reaction was run in $CDCl_3$ because the crude reaction mixture in toluene was stripped of volatiles before the ^1H NMR was taken and some of the products many have been lost**.**

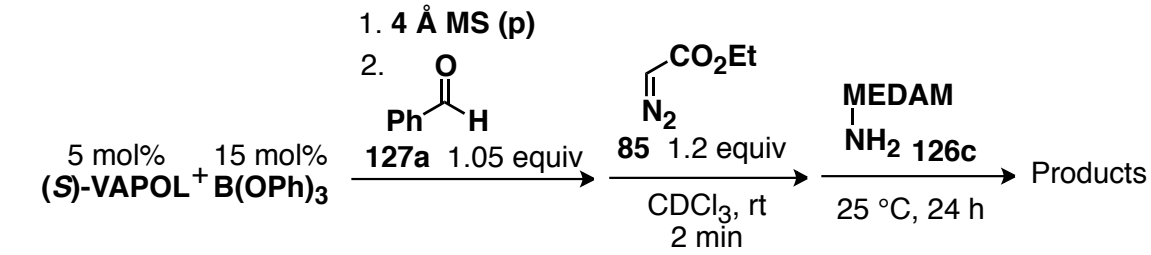

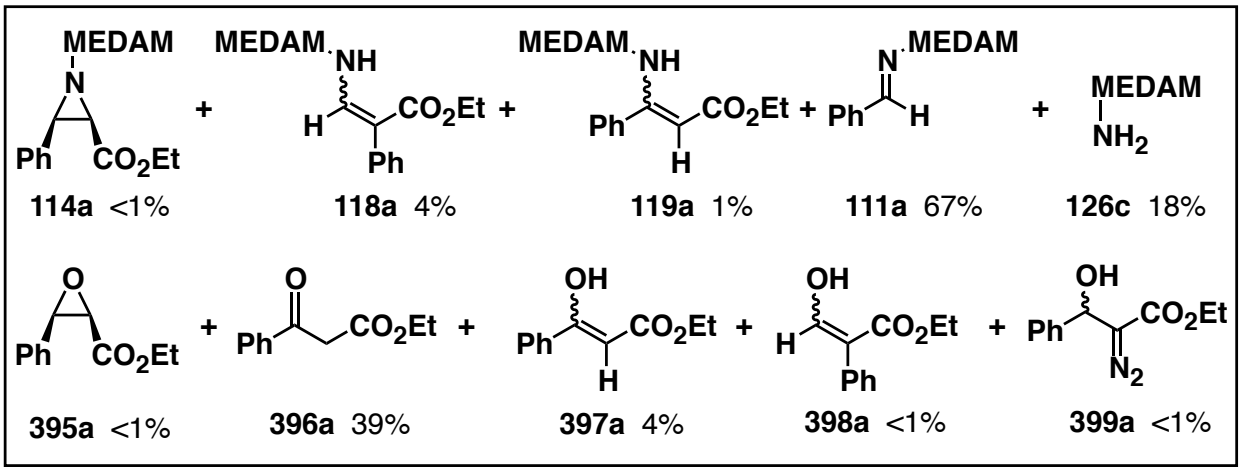

To a 10 mL flame-dried single-necked round bottom flask equipped with a stir bar and filled with argon was added (*S)*-VAPOL in the following order (14 mg, 0.025 mmol), $B(OPh)_3$ (22 mg, 0.075 mmol), 4Å Molecular Sieves (150 mg, freshly flame-dried), aldehyde **127a** (52.0 μL, 0.525 mmoL, 1.05 equiv), ethyl diazoacetate (EDA) **85** (62 μL, 0.60 mmoL, 1.2 equiv). Dry $CDCl_3$ (1 mL) was added under an argon atmosphere to dissolve the reagents. The flask was fitted with a rubber septum and a nitrogen balloon. The mixture was stirred for 2 min followed by the addition of amine **126c** (149.7 mg, 0.5000 mmol). The reaction mixture was stirred for 24 h at room temperature. After 24 h, an internal standard Ph_3CH (12.2 mg, 0.500 mmol) was added. The resulting solution was then directly transferred to a NMR tube utilizing a filter syringe (Corning® syringe filters, Aldrich) to remove the 4Å Molecular Sieves. It was then subjected to NMR analysis. The ^1H NMR of crude reaction mixture revealed the presence of

several products as shown in the reaction scheme. The presence of each product was confirmed by characteristic peaks (as discussed earlier) in the ^{1}H NMR previously published for these compounds. There was also mono-alkylated (*S*)-VAPOL derivative **230** in 28% yield (with respect to (*S*)-VAPOL).

Procedure IX in $CDCl_3$: Same as Procedure VIII except that amine 126c is not added (in $CDCl_3$).

This reaction was run in $CDCl_3$ because the crude reaction mixture in toluene was stripped of volatiles before the ^{1}H NMR was taken and some of the products many have been lost**.**

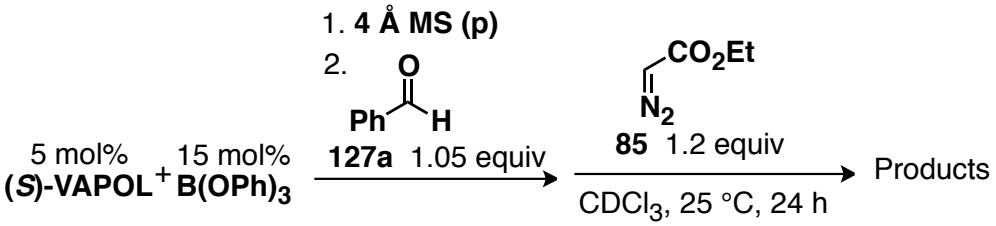

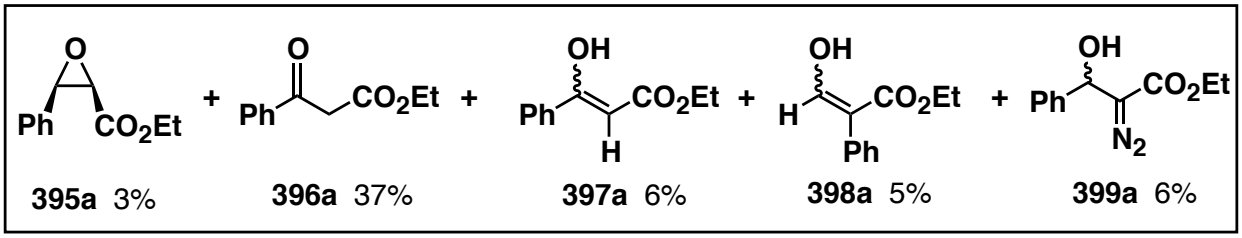

To a 10 mL flame-dried single-necked round bottom flask equipped with a stir bar and filled with argon was added in the following order (*S)*-VAPOL (14 mg, 0.025 mmol), $B(OPh)_3$ (22 mg, 0.075 mmol), 4Å Molecular Sieves (150 mg, freshly flame-dried), aldehyde **127a** (52.0 μL, 0.525 mmoL, 1.05 equiv), ethyl diazoacetate (EDA) **85** (62 μL, 0.60 mmoL, 1.2 equiv). Dry $CDCl_3$ (1 mL) was added under an argon atmosphere to dissolve the reagents. The flask was

fitted with a rubber septum and a nitrogen balloon. The resulting mixture was stirred for 24 h at room temperature. After 24 h, an internal standard Ph_3CH (12.2 mg, 0.5000 mmol) was added. The resulting solution was then directly transferred to a NMR tube utilizing a filter syringe (Corning® syringe filters, Aldrich) to remove the 4Å Molecular Sieves. It was then subjected to NMR analysis. The ^1H NMR of the crude reaction mixture revealed the presence of several products as shown in the reaction scheme. The presence of each product was confirmed by characteristic peaks (as discussed earlier) in the ^1H NMR previously published for these compounds. There was also 26% of unreacted benzaldehyde **127a**. There was also mono-alkylated (*S*)-VAPOL derivative **230** in 11% yield (with respect to (*S*)-VAPOL).

(B) MCAZ with 0.9 equivalents of benzaldehyde 127a and amine 126a (*Table 7.8*)

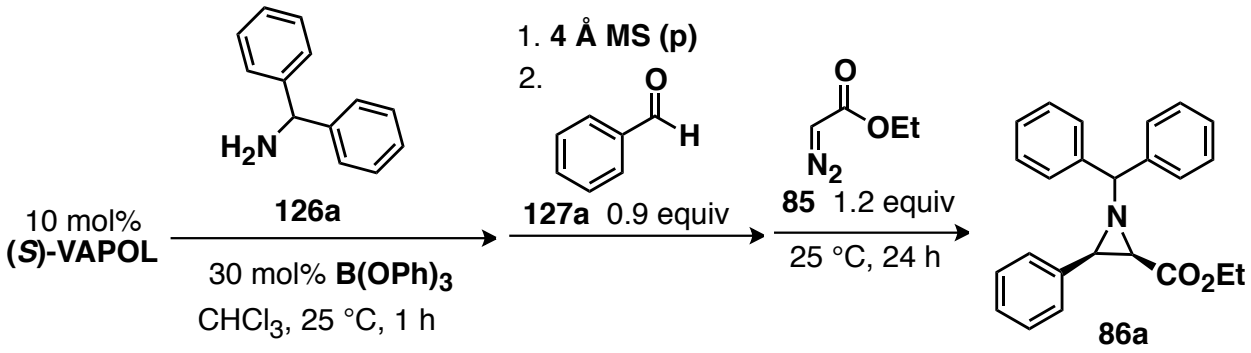

(2*R*,3*R*)-ethyl 1-benzhydryl-3-phenylaziridine-2-carboxylate 86a: Aldehyde **127a** (46.0 μL, 0.450 mmol, 0.900 equiv) was reacted according to the general Procedure IIIA described above with (*S*)-VAPOL as ligand. Purification of the crude aziridine by silica gel chromatography (30 mm × 300 mm column, 19:1 hexanes/EtOAc as eluent, gravity column) afforded pure *cis*-aziridine **86a** as a white solid (mp. 127.5-128.5 °C) in 73% isolated yield (117 mg, 0.323 mmol); *cis/trans*: 25:1. Enamine side products: 8% yield of enamines. The optical purity of **86a** was

determined to be 89% *ee* by HPLC analysis (CHIRALCEL OD-H column, 90:10 hexane/2-propanol at 226 nm, flow-rate: 0.7 mL/min): retention times; R_t = 9.01 min (major enantiomer, **86a**) and R_t = 4.67 min (minor enantiomer, *ent*-**86a**). There was 8% of unreacted imine **78a** was also observed. Same procedure was followed to do MCAZ for 0.6-1.0 equivalents of benzaldehyde **127a** and the results are presented in the chapter.

Spectral data for **86a**: R_f = 0.3 (1:9 EtOAc/hexanes); ^{1}H NMR ($CDCl_3$, 500 MHz) δ 0.95 (t, 3H, *J* = 7.3 Hz), 2.64 (d, 1H, *J* = 6.8 Hz), 3.19 (d, 1H, *J* = 6.8 Hz), 3.91 (q, 2H, *J* = 7.1 Hz), 3.93 (s, 1H), 7.16-7.38 (m, 11H), 7.47 (d, 2H, *J* = 7.1 Hz), 7.58 (d, 2H, *J* = 7.6 Hz); ^{13}C NMR ($CDCl_3$, 125 MHz) δ 13.93, 46.36, 48.01, 60.57, 77.68, 127.18, 127.31, 127.39, 127.52, 127.76, 127.78, 128.48, 135.00, 142.37, 142.49, 167.75 (one sp^2 carbon not located); $[\alpha]_D^{20}$ +33.4 (*c* 1.0, CH_2Cl_2) on 91% *ee* material (HPLC). These spectral data match those previously reported for this compound.

(C) Aziridination with preformed imine 78a with added bases illustrated by utilizing amine 126a as the base (*Table 7.9*)

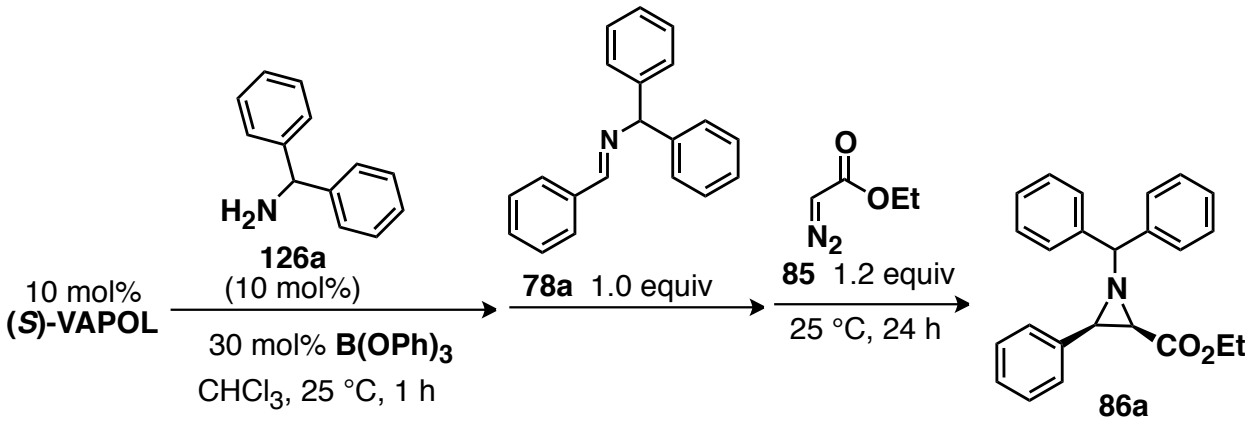

(2*R*,3*R*)-ethyl 1-benzhydryl-3-phenylaziridine-2-carboxylate 86a: To a 10 mL flame-dried single-necked round bottom flask equipped with a stir bar and filled with argon was added (*S)*-VAPOL (54 mg, 0.10 mmol), $B(OPh)_3$ (87 mg, 0.30 mmol) and amine **126a** (17.2 μL, 0.10 mmol). Dry toluene (2 mL) was added under an argon atmosphere to dissolve the reagents. The flask was fitted with a rubber septum and a nitrogen balloon. The reaction mixture was stirred at room temperature for 1 h. Thereafter, imine **78a** (271 mg, 1.00 mmoL) was added to the catalyst solution and stirred for 5 min. To this solution was rapidly added ethyl diazoacetate (EDA) **85** (124 μL, 1.20 mmoL, 1.2 equiv). The resulting mixture was stirred for 24 h at room temperature. The reaction was dilluted by addition of hexane (6 mL). The resulting solution was then concentrated *in vacuo* followed by exposure to high vacuum (0.05 mm Hg) for 1 h to afford the crude aziridine as an off-white solid. Purification of the crude aziridine by silica gel chromatography (30 mm × 300 mm column, 19:1 hexanes/EtOAc as eluent, gravity column) afforded pure *cis*-aziridine **86a** as a white solid (mp. 127.5-128.5 °C) in 80% isolated yield (286 mg, 0.800 mmol); *cis/trans*: 27:1. Enamine side products: 10% yield of enamines. The optical purity of **86a** was determined to be 89% *ee* by HPLC analysis (CHIRALCEL OD-H column, 90:10 hexane/2-propanol at 226 nm, flow-rate: 0.7 mL/min): retention times; R_t = 9.01 min (major enantiomer, **86a**) and R_t = 4.67 min (minor enantiomer, *ent*-**86a**). Same procedure was followed to do MCAZ for other bases.

7.15.10 MCAZ using BH_3•Me_2S as the boron source: Procedures (I′-III) (*Table 7.10*)

A) Procedure I′:

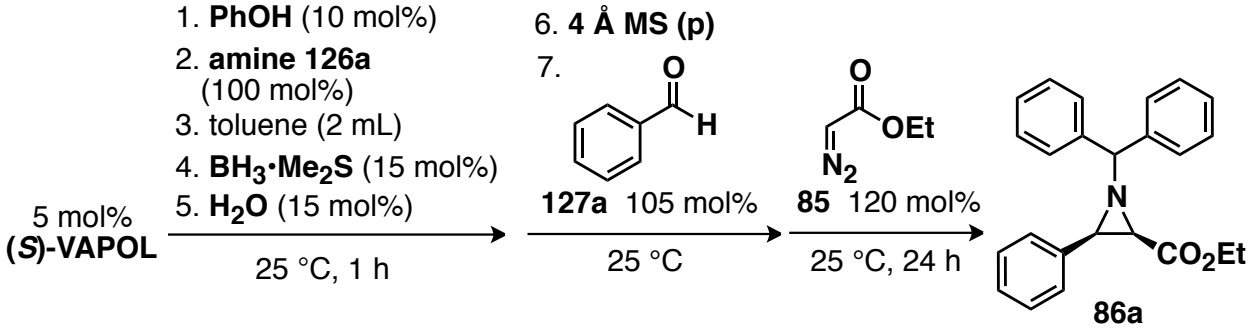

(2*R*,3*R*)-ethyl 1-benzhydryl-3-phenylaziridine-2-carboxylate 86a: To a 10 mL flame-dried single-necked round bottom flask equipped with a stir bar and filled with argon was added (*S*)-VAPOL (27 mg, 0.05 mmol), PhOH (9.4 mg, 0.10 mmol) and amine **126a** (183.3 mg, 1.00 mmol). Dry toluene (2 mL) was added under an argon atmosphere to dissolve the reagents. The flask was fitted with a rubber septum and a nitrogen balloon. To this mixture was added BH_3•Me_2S (75 μL, 0.15 mmol, 2.0 M in toluene) and H_2O (2.7 μL, 0.15 mmol). The reaction mixture was stirred at room temperature for 1 h. Thereafter, 4Å Molecular Sieves (300 mg, freshly flame-dried) was added followed by the addition of the aldehyde **127a** (104 μL, 1.05 mmoL, 1.05 equiv). To this solution was rapidly added ethyl diazoacetate (EDA) **85** (124 μL, 1.20 mmoL, 1.2 equiv). The resulting mixture was stirred for 24 h at room temperature. The reaction was dilluted by addition of hexane (6 mL). The reaction mixture was then filtered through a Celite pad to a 100 mL round bottom flask. The reaction flask was rinsed with EtOAc (3 mL × 3) and the rinse was filtered through the same Celite pad. The resulting solution was then concentrated *in vacuo* followed by exposure to high vacuum (0.05 mm Hg) for 1 h to afford the crude reaction mixture. The ^{1}H NMR analysis of crude reaction mixture revealed no presence of aziridine and only imine **78a** was observed.

B) Procedure I:

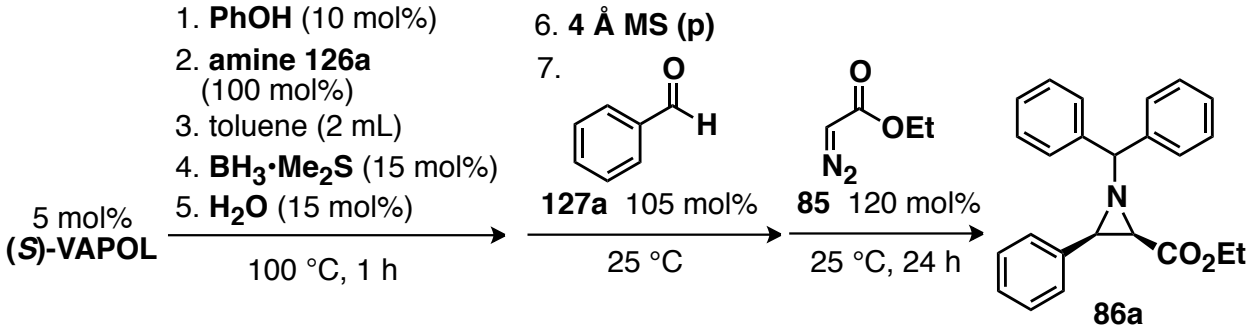

(2*R*,3*R*)-ethyl 1-benzhydryl-3-phenylaziridine-2-carboxylate 86a: Same as procedure I′ except that the temperature of the catalyst preparation was 100 ºC. Purification of the crude aziridine by silica gel chromatography (30 mm × 300 mm column, 19:1 hexanes/EtOAc as eluent, gravity column) afforded pure *cis*-aziridine **86a** as a white solid (mp. 127.5-128.5 °C) in 82% isolated yield (293 mg, 0.820 mmol); *cis/trans*: 50:1. Enamine side products: 7% yield of enamines. The optical purity of **86a** was determined to be 95% *ee* by HPLC analysis (CHIRALCEL OD-H column, 90:10 hexane/2-propanol at 226 nm, flow-rate: 0.7 mL/min): retention times; R_t = 9.01 min (major enantiomer, **86a**) and R_t = 4.67 min (minor enantiomer, *ent*-**86a**).

C) Procedure II:

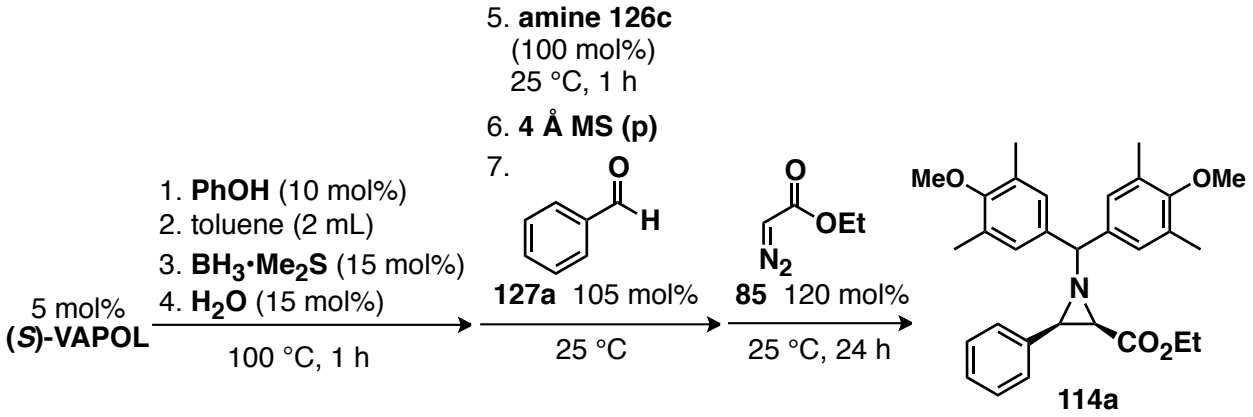

(2*R*,3*R*)-ethyl-1-(bis(4-methoxy-3,5-dimethylphenyl)methyl)-3-phenylaziridine-2-carboxylate 114a: To a 10 mL flame-dried home-made Schlenk flask, prepared from a single-necked 25 mL pear-shaped flask that had its 14/20 glass joint replaced with a high vacuum threaded Teflon valve, equipped with a stir bar and filled with argon was added (*S)*-VAPOL (27 mg, 0.05 mmol), PhOH (9.4 mg, 0.10 mmol). Under an argon flow through the side-arm of the Schlenk flask, dry toluene (2 mL) was added through the top of the Teflon valve to dissolve the reagents and this was followed by the addition of BH_3•Me_2S (75 μL, 0.15 mmol, 2.0 M in toluene) and H_2O (2.7 μL, 0.15 mmol). The flask was sealed by closing the Teflon valve, and then placed in an 100 ºC (oil bath) for 1 h. The flask was then allowed to cool to room temperature and opened to argon through the side-arm of the Schlenk flask. To the flask containing the pre-catalyst was added the amine **126c** (299.4 mg, 1.000 mmol) under an argon flow through side-arm of the Schlenk flask. The flask was sealed by closing the Teflon valve, and then the resulting mixture was allowed to stir at room temperature for 1 h. The flask was then open to argon through side-arm of the Schlenk flask. To the flask containing the pre-catalyst was added the 4Å Molecular Sieves (300 mg, freshly flame-dried) and aldehyde **127a** (104 μL, 1.05 mmoL, 1.05 equiv). To this solution was rapidly added ethyl diazoacetate (EDA) **85** (124 μL, 1.20 mmoL, 1.2 equiv). The resulting mixture was stirred for 24 h at room temperature. After 24 h, the reaction was diluted by addition of hexane (6 mL). The reaction mixture was then filtered through a Celite pad to a 100 mL round bottom flask. The reaction flask was rinsed with EtOAc (3 mL × 3) and the rinse was filtered through the same Celite pad. The resulting solution was then concentrated *in vacuo* followed by exposure to high vacuum (0.05 mm Hg) for 1 h to afford the crude aziridine as an off-white solid. Purification of the crude

aziridine by silica gel chromatography (30 mm × 300 mm column, 9:1 hexanes/EtOAc as eluent, gravity column) afforded pure cis-aziridine **114a** as a white solid (mp 107-108 ºC on 99.8% ee material) in 90% isolated yield (426 mg, 0.9 mmol); *cis/trans*: >50:1. Enamine side products: <1% yield of **118a** and <1% yield of **119a**. The optical purity of **114a** was determined to be 97% *ee* by HPLC analysis (CHIRALCEL OD-H column, 99:1 hexane/2-propanol at 226nm, flow-rate: 0.7 mL/min): retention times; R_t = 9.26 min (major enantiomer, **114a**) and R_t = 12.52 min (minor enantiomer, *ent*-**114a**).

D) Procedure III:

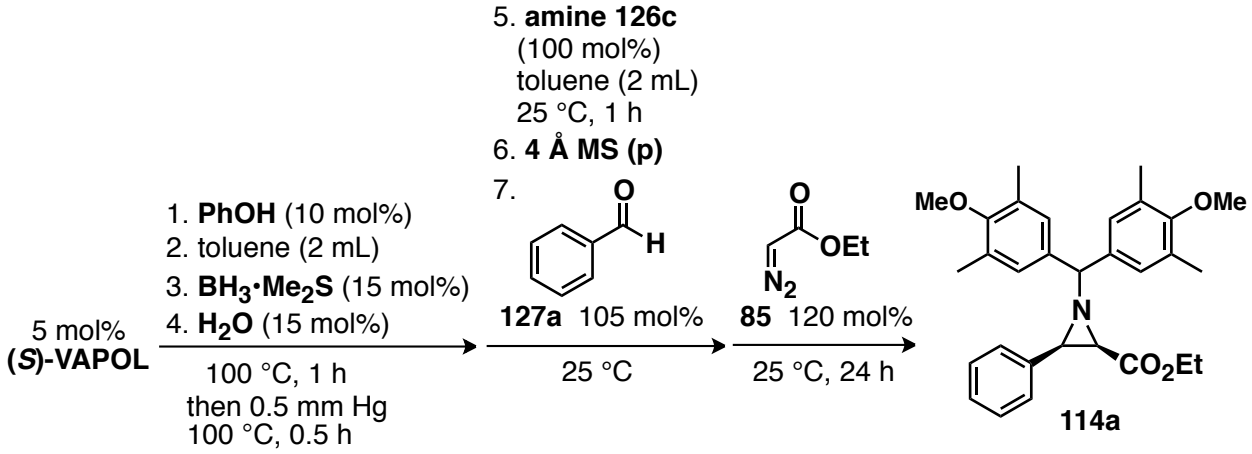

(2*R*,3*R*)-ethyl-1-(bis(4-methoxy-3,5-dimethylphenyl)methyl)-3-phenylaziridine-2-carboxylate 114a: Same as procedure II except that after 1 h of the stirring of the reaction mixture containing (*S)*-VAPOL (27 mg, 0.05 mmol), PhOH (9.4 mg, 0.10 mmol), BH_3•Me_2S (75 μL, 0.15 mmol, 2.0 M in toluene) and H_2O (2.7 μL, 0.15 mmol), a vacuum (0.5 mm Hg) was carefully applied by slightly opening the Teflon valve to remove the volatiles. After the volatiles are removed completely, a full vacuum is applied and is maintained for a period of 30 min at a temperature of 100 ºC (oil bath). The flask was then allowed to cool to room temperature and

opened to argon through the side-arm of the Schlenk flask. To the flask containing the pre-catalyst was added the amine **126c** (299.4 mg, 1.000 mmol) and toluene (1 mL) under an argon flow through side-arm of the Schlenk flask. The flask was sealed by closing the Teflon valve, and then the resulting mixture was allowed to stir at room temperature for 1 h. The procedure is similar to procedure to II from this point. Purification of the crude aziridine by silica gel chromatography (30 mm × 300 mm column, 9:1 hexanes/EtOAc as eluent, gravity column) afforded pure cis-aziridine **114a** as a white solid (mp 107-108 ºC on 99.8% ee material) in 89% isolated yield (422 mg, 0.89 mmol); *cis/trans*: >50:1. Enamine side products: <1% yield of **118a** and <1% yield of **119a**. The optical purity of **114a** was determined to be 97% *ee* by HPLC analysis (CHIRALCEL OD-H column, 99:1 hexane/2-propanol at 226nm, flow-rate: 0.7 mL/min): retention times; R_t = 9.26 min (major enantiomer, **114a**) and R_t = 12.52 min (minor enantiomer, *ent*-**114a**).

7.15.11 MCAZ using BH_3•THF as the boron source: Procedures (I-III) (*Table 7.11*)

A) Procedure I:

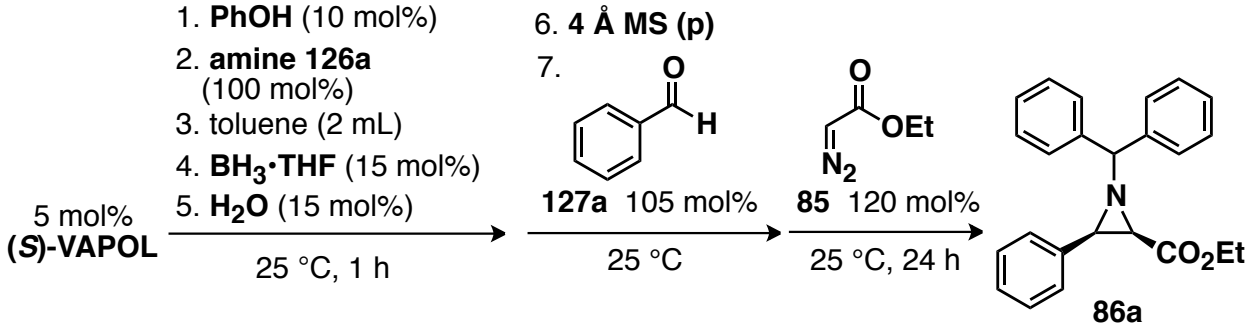

(2*R*,3*R*)-ethyl 1-benzhydryl-3-phenylaziridine-2-carboxylate 86a: Same as procedure I of 7.14.11 except that the temperature of the catalyst preparation was 25 ºC and BH_3•THF was used in place of BH_3•Me_2S.

B) Procedure II:

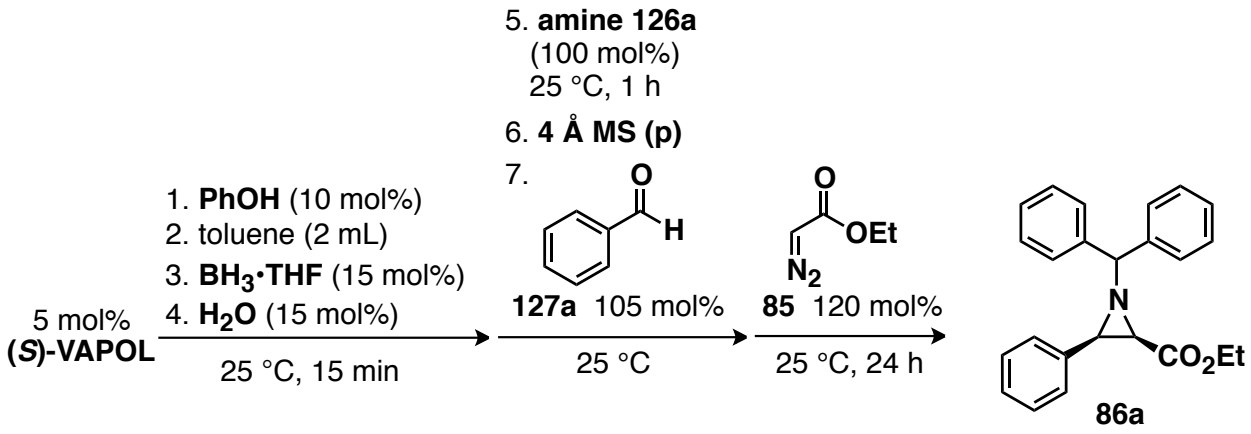

(2*R*,3*R*)-ethyl 1-benzhydryl-3-phenylaziridine-2-carboxylate 86a: Same as procedure II of 7.14.11 except that the temperature of the catalyst preparation was 25 ºC, time of stirring was 15 min, amine **126a** was used and BH_3•THF was used in place of BH_3•Me_2S.

C) Procedure III:

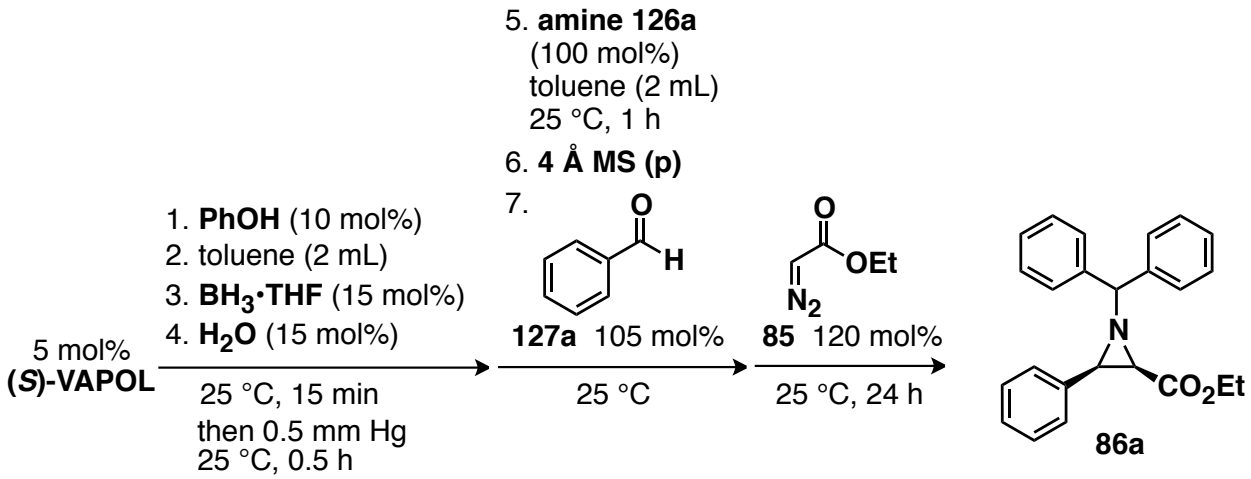

(2*R*,3*R*)-ethyl 1-benzhydryl-3-phenylaziridine-2-carboxylate 86a: Same as procedure III of 7.14.11 except that the temperature of the catalyst preparation was 25 ºC, time of stirring was 15 min, amine **126a** was used and BH_3•THF was used in place of BH_3•Me_2S.

7.15.12 Initial attempts towards multi-component *trans*-aziridination (*Table 7.12*)

A) Reaction with benzaldehyde 127a and diazoacetamide 123a:

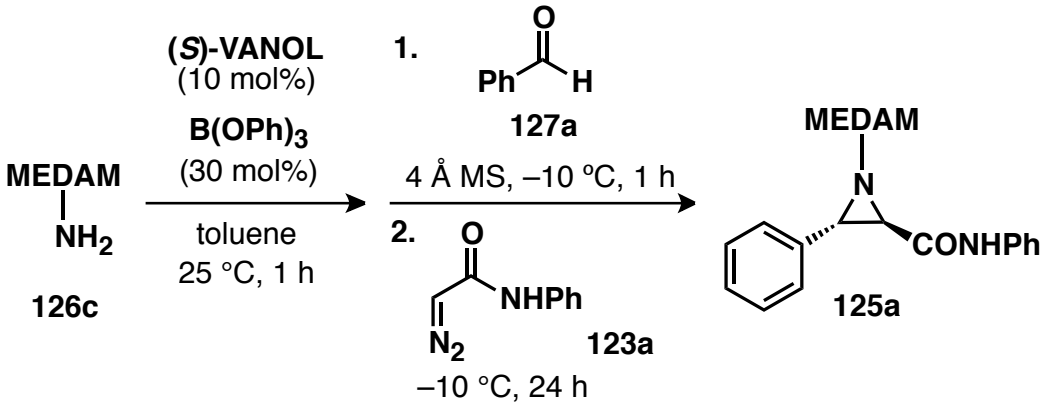

(2*R*,3*S*)-1-(bis(4-methoxy-3,5-dimethylphenyl)methyl)-*N*,3-diphenylaziridine-2-carboxamide: Aldehyde **127a** was reacted with diazoacetamide **123a** (85 mg, 0.6 mmol, 1.2 equiv) according to the general aziridination Procedure IIIA described above with (*S*)-VANOL (22 mg, 0.05 mmol, 10 mol%) as ligand at –20 ºC, to afford *trans*-aziridine **125a**. The mixture containing the catalyst, aldehyde and 4Å MS was stirred for 1 h prior to the addition of diazoacetamide. The ^{1}H NMR analysis of crude reaction mixture revealed the presence of trans-aziridine **125a** in 43% NMR yield using Ph_3CH as the internal standard. No further attempt was made to isolate the aziridine. The *trans:cis* ratio was found to be 2.2:1.

B) Reaction with *n*-hexadecanal 127p and diazoacetamide 128a:

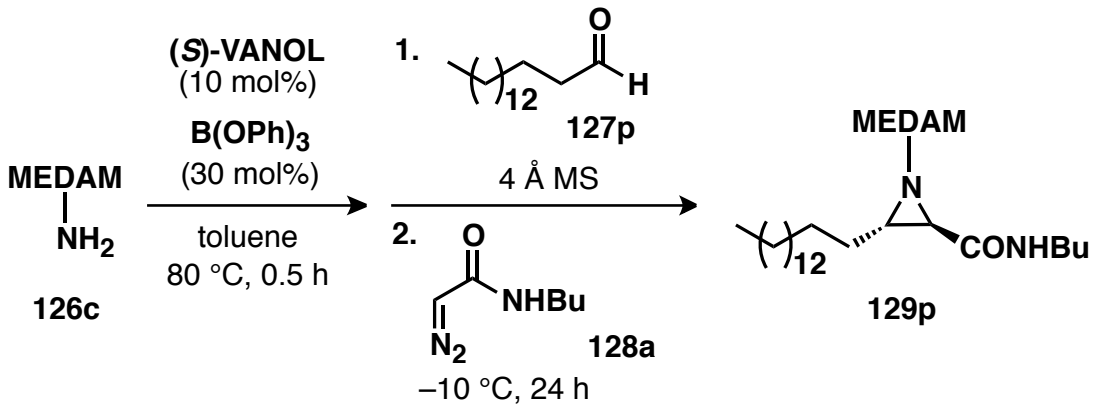

(2*R*,3*S*)-1-(bis(4-methoxy-3,5-dimethylphenyl)methyl)-*N*-butyl-3-pentadecylaziridine-2-carboxamide 129p: Aldehyde **127p** was reacted with *N*-butyl-2-diazoacetamide **128a** (85 mg, 0.6 mmol, 1.2 equiv) according to the general aziridination Procedure IIA described above with (*S*)-VANOL (22 mg, 0.05 mmol, 10 mol%) as ligand at –10 ºC, to afford *trans*-aziridine **129p**. The concentration of the reaction is 0.2 M in amine **126c**. Purification of the crude aziridine by silica gel chromatography (30 mm × 300 mm column, 5:1 hexanes/Et_2O as eluent, gravity column) afforded *trans*-aziridine **129p** as a colorless viscous liquid in 70% isolated yield (222 mg, 0.350 mmol). The optical purity of **129p** was determined to be 93% *ee* by HPLC analysis (CHIRALPAK AD column, 90:10 hexane/2-propanol at 222 nm, flow-rate: 0.7 mL/min): retention times; R_t = 5.11 min (major enantiomer, **129p**) and R_t = 8.93 min (minor enantiomer, *ent*-**129p**).

Spectral data for **129p:** R_f = 0.34 (1:1 Et_2O / hexanes). ^{1}H-NMR ($CDCl_3$, 500 MHz): δ 0.88 (t, *J* = 5.7 Hz, 3H), 0.90 (t, *J* = 6.0 Hz, 3H), 1.20-1.29 (m, 30H), 1.42 (dd, *J* = 14.5, 7.4 Hz, 2H), 1.48-1.53 (m, 1H), 2.04 (d, *J* = 2.9 Hz, 1H), 2.21 (s, 6H), 2.27 (s, 6H), 2.99 (dtd, *J* = 13.3, 6.8,

5.2 Hz, 1H), 3.34 (dq, J = 13.6, 6.9 Hz, 1H), 3.66 (s, 3H), 3.68 (s, 3H), 4.10 (s, 1H), 6.63 (dd, J = 7.1, 5.0 Hz, 1H), 6.94 (s, 2H), 7.07 (s, 2H); ^{13}C-NMR ($CDCl_3$, 126 MHz): δ 13.71, 14.04, 16.14, 16.22, 19.85, 22.62, 26.03, 28.06, 29.25, 29.29, 29.41, 29.44, 29.58, 29.59, 29.63, 31.81, 31.86, 38.23, 44.79, 47.29, 59.44, 59.52, 67.54, (3 sp^3 carbon not located), 126.88, 127.60, 130.45, 130.63, 138.53, 138.55, 155.76, 156.04, 170.45; IR (thin film) 3312br, 2926vs, 2855vs, 1647s, 1484s, 1221s, 1143s cm^{-1}; HRMS (ESI-TOF) *m/z* 635.5151 [(M+H$^+$); calcd. for $C_{41}H_{67}N_2O_3$: 635.5152]; $[\alpha]_D^{20}$ –22.0 (c 1.0, CH_2Cl_2) on 93% ee material.

C) Reaction with 3-phenylpropiolaldehyde 102a and diazoacetamide 128a:

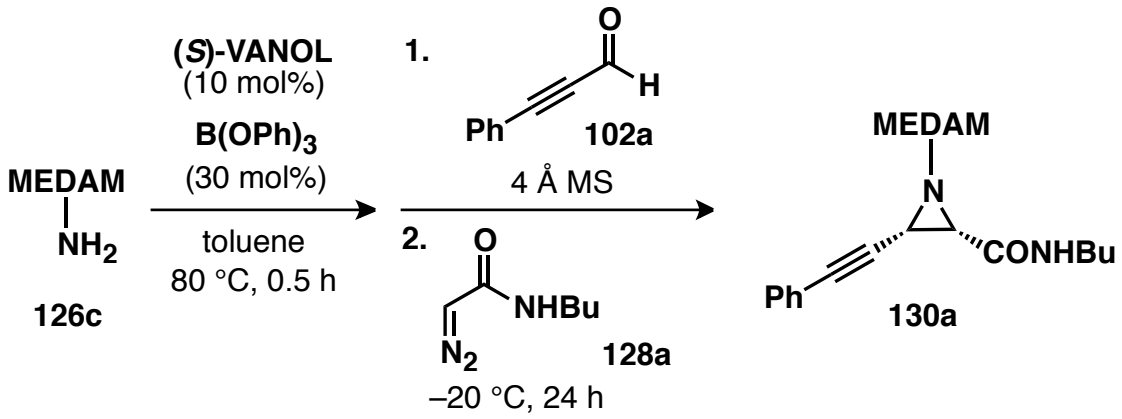

(2*S*,3*S*)-1-(bis(4-methoxy-3,5-dimethylphenyl)methyl)-*N*-butyl-3-(phenylethynyl)aziridine-2-carboxamide 130a: Aldehyde **102a** was reacted with *N*-butyl-2-diazoacetamide **128a** (85 mg, 0.6 mmol, 1.2 equiv) according to the general aziridination Procedure IIA described above with (*S*)-VANOL (22 mg, 0.05 mmol, 10 mol%) as ligand at –20 ºC, to afford *cis*-aziridine **130a**. The concentration of the reaction is 0.2 M in amine **126c**. Purification of the crude aziridine by silica gel chromatography (30 mm × 300 mm column, 2:1 to 1:1 hexanes/Et_2O as eluent) afforded *cis*-

aziridine **130a** (mp. 68-71 ºC on 88% ee material) as a yellow solid in 89% isolated yield (234 mg, 0.450 mmol). The optical purity of **130a** was determined to be 88% *ee* by HPLC analysis (CHIRALPAK AD column, 90:10 hexane/2-propanol at 222nm, flow-rate: 0.7 mL/min): retention times; R_t = 10.76 min (major enantiomer, **130a**) and R_t = 19.48 min (minor enantiomer, *ent*-**130a**).

Spectral data for **130a:** R_f = 0.07 (1:5 EtOAc / hexanes). ^{1}H-NMR ($CDCl_3$, 500 MHz): δ 0.80 (t, *J* = 7.3 Hz, 3H), 1.20-1.32 (m, 2H), 1.35-1.52(m, 2H), 2.25 (s, 6H), 2.29 (s, 6H), 2.58 (d, *J* = 6.6 Hz, 1H), 2.66 (d, *J* = 6.6 Hz, 1H), 3.25-3.18 (m, 1H), 3.27-3.33 (m, 1H), 3.68 (s, 1H), 3.70 (s, 3H), 3.72 (s, 3H), 6.71 (t, *J* = 6.1 Hz, 1H), 6.95 (s, 2H), 7.11 (s, 2H), 7.29-7.32 (m, 3H), 7.39 (dd, *J* = 7.4, 2.1 Hz, 2H); ^{13}C-NMR ($CDCl_3$, 125 MHz): δ 13.62, 16.15, 16.25, 19.90, 31.91, 35.38, 38.63, 46.08, 59.51, 59.57, 75.64, 82.62, 84.44, 122.44, 127.39, 127.78, 128.21, 128.43, 130.68, 130.87, 131.79, 136.74, 136.92, 156.06, 156.38, 167.11. These spectral data matched those previously reported for this compound.[18]

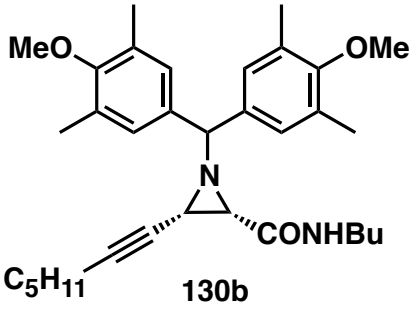

130b

(2*S*,3*S*)-1-(bis(4-methoxy-3,5-dimethylphenyl)methyl)-*N*-butyl-3-(hept-1-yn-1-yl)aziridine-2-carboxamide 130b: Aldehyde **102b** was reacted with *N*-butyl-2-diazoacetamide **128a** (85 mg, 0.6 mmol, 1.2 equiv) according to the general aziridination Procedure IIA described above with (*S*)-VANOL (22 mg, 0.05 mmol, 10 mol%) as ligand at –20 ºC, to afford *cis*-aziridine **130b**. The concentration of the reaction is 0.2 M in amine **126c**. Purification of the crude aziridine by silica

gel chromatography (30 mm × 300 mm column, 2:1 to 1:1 hexanes/Et_2O as eluent) afforded *cis*-aziridine **130b** (mp. 90-92 ºC on 88% ee material) as a yellow solid in 70% isolated yield (182 mg, 0.350 mmol). The optical purity of **130b** was determined to be 88% *ee* by HPLC analysis (CHIRALPAK AD column, 90:10 hexane/2-propanol at 222nm, flow-rate: 0.7 mL/min): retention times; R_t = 12.45 min (major enantiomer, **130b**) and R_t = 30.86 min (minor enantiomer, *ent*-**130b**).

Spectral data for **130b:** R_f = 0.17 (1:5 EtOAc / hexanes). ^{1}H-NMR ($CDCl_3$, 500 MHz): δ 0.90 (td, *J* = 7.2, 2.9 Hz, 6H), 1.25-1.38 (m, 8H), 1.42-1.50 (m, 4H), 2.16-2.13 (m, 2H), 2.23 (s, 6H), 2.27 (s, 6H), 3.15 (dq, *J* = 13.1, 6.6 Hz, 1H), 3.31 (dq, *J* = 13.7, 6.9 Hz, 1H), 3.57 (s, 1H), 3.68 (s, 3H), 3.70 (s, 3H), 6.62 (t, *J* = 6.1 Hz, 1H), 6.90 (s, 2H), 7.05 (s, 2H); ^{13}C-NMR ($CDCl_3$, 125 MHz): δ 13.76, 13.89, 16.15, 16.23, 18.69, 19.91, 22.14, 28.27, 30.91, 31.87, 35.41, 38.52, 45.61, 59.53, 59.58, 74.97, 75.65, 83.50, 127.37, 127.83, 130.58, 130.80, 136.93, 137.10, 155.98, 156.32, 167.42; IR (thin film) 3401br, 2957vs, 2932vs, 2241w, 1680s, 1485s, 1223s, 1147s cm^{-1}; HRMS (ESI-TOF) *m/z* 519.3597 [$(M+H^+)$; calcd. for $C_{33}H_{47}N_2O_3$: 519.3587]; $[\alpha]_D^{20}$ +23.0 (c 0.78, CH_2Cl_2) on 88% ee material.

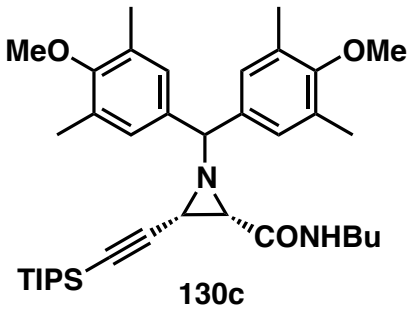

130c

(2*S*,3*S*)-1-(bis(4-methoxy-3,5-dimethylphenyl)methyl)-*N*-butyl-3-(triisopropylsilyl)ethynyl)aziridine-2-carboxamide 130c: Aldehyde **102c** was reacted with *N*-butyl-2-

diazoacetamide **128a** (85 mg, 0.6 mmol, 1.2 equiv) according to the general aziridination Procedure IIA described above with (*S*)-VANOL (22 mg, 0.05 mmol, 10 mol%) as ligand at –20 ºC, to afford *cis*-aziridine **130a**. The concentration of the reaction is 0.2 M in amine **126c**. Purification of the crude aziridine by silica gel chromatography (30 mm × 300 mm column, 6:1 hexanes/EtOAc as eluent) afforded *cis*-aziridine **130c** (mp. 62-64 ºC on 88% ee material) as a yellow solid in 93% isolated yield (281 mg, 0.465 mmol). The optical purity of **130c** was determined to be 88% *ee* by HPLC analysis (CHIRALPAK AD column, 90:10 hexane/2-propanol at 222nm, flow-rate: 0.7 mL/min): retention times; R_t = 9.59 min (major enantiomer, **130c**) and R_t = 6.20 min (minor enantiomer, *ent*-**130c**).

Spectral data for **130c:** R_f = 0.28 (1:5 EtOAc/ hexanes). ^{1}H-NMR ($CDCl_3$, 500 MHz): δ 0.89 (t, *J* = 7.3 Hz, 3H), 1.02-1.07 (m, 21H), 1.24-1.29 (m, 2H), 1.39-1.49 (m, 2H), 2.19-2.30 (m, 14H), 2.88-2.94 (m, 1H), 3.49 (dt, *J* = 13.7, 7.0 Hz, 1H), 3.59 (s, 1H), 3.68 (s, 3H), 3.70 (s, 3H), 6.62 (dd, *J* = 7.5, 4.1 Hz, 1H), 6.90 (s, 2H), 7.08 (s, 2H); ^{13}C-NMR ($CDCl_3$, 125 MHz): δ 11.07, 13.70, 16.11, 16.18, 18.52, 18.54, 19.86, 31.51, 35.77, 38.64, 45.85, 59.50, 59.57, 75.59, 84.13, 102.19, 127.16, 127.81, 130.64, 130.88, 136.81, 137.07, 155.97, 156.41, 166.97; IR (thin film) 3401br, 2943vs, 2866vs, 1680s, 1484s, 1223s, 1147s cm^{-1}; HRMS (ESI-TOF) *m/z* 605.4129 [$(M+H^+)$; calcd. for $C_{37}H_{57}N_2O_3$: 605.4138]; $[\alpha]_D^{20}$ +52.1 (c 1.0, CH_2Cl_2) on 88% ee material.

REFERENCES

REFERENCES

(1) (a) de Graaff, C.; Ruijter, E.; Orru, R. V. A. *Chem. Soc. Rev.* **2012**, *41*, 3969-4009. (b) Guillena, G.; Ramon, D. J.; Yus, M. *Tetrahedron: Asymmetry* **2007**, *18*, 693-700. (c) Ramon, D. J.; Yus, M. *Angew. Chem., Int. Ed.* **2005**, *44*, 1602-1634. (d) *Multicomponent Reactions*; Zhu, J.; Bienayme, H., Eds.; Wiley-VCH: Weinheim, 2005.

(2) Osborn, H. M. I.; Sweeney, J. *Tetrahedron: Asymmetry* **1997**, *8*, 1693-1715.

(3) (a) Pellissier, H. *Tetrahedron* **2010**, *66*, 1509-1555. (b) Müller, P.; Fruit, C. *Chem. Rev.* **2003**, *103*, 2905-2919.

(4) (a) Evans, D. A.; Faul, M. M.; Bilodeau, M. T.; Anderson, B. A.; Barnes, D. M. *J. Am. Chem. Soc.* **1993**, *115*, 5328-5329. (b) Li, Z.; Conser, K. R.; Jacobsen, E. N. *J. Am. Chem. Soc.* **1993**, *115*, 5326-5327. (c) Noda, K.; Hosoya, N.; Irie, R.; Ito, Y.; Katsuki, T. *Synlett* **1993**, 469-471. (d) Subbarayan, V.; Ruppel, J. V.; Zhu, S.; Perman, J. A.; Zhang, X. P. *Chem. Commun.* **2009**, 4266-4268. (e) Kawabata, H.; Omura, K.; Uchida, T.; Katsuki, T. *Chem.–Asian. J.* **2007**, *2*, 248-256.

(5) Deiana, L.; Dziedzic, P.; Zhao, G. L.; Vesely, J.; Ibrahem, I.; Rios, R.; Sun, J. L.; Cordova, A. *Chem.–Eur. J.* **2011**, *17*, 7904-7917.

(6) (a) Hansen, K. B.; Finney, N. S.; Jacobsen, E. N. *Angew. Chem., Int. Ed.* **1995**, *34*, 676-678. (b) Aggarwal, V. K.; Ferrara, M.; O'Brien, C. J.; Thompson, A.; Jones, R. V. H.; Fieldhouse, R. *J. Chem. Soc., Perkin Trans. 1* **2001**, 1635-1643. (c) Aggarwal, V. K.; Alonso, E.; Fang, G. Y.; Ferrara, M.; Hynd, G.; Porcelloni, M. *Angew. Chem., Int. Ed.* **2001**, *40*, 1433-1436. (d) Aggarwal, V. K.; Winn, C. L. *Acc. Chem. Res.* **2004**, *37*, 611-620.

(7) (a) Casarrubios, L.; Perez, J. A.; Brookhart, M.; Templeton, J. L. *J. Org. Chem.* **1996**, *61*, 8358-8359. (b) G. Rasmussen, K.; Anker Jorgensen, K. *J. Chem. Soc., Perkin Trans. 1* **1997**, 1287-1292. (c) Juhl, K.; G. Hazell, R.; Anker Jorgensen, K. *J. Chem. Soc., Perkin Trans. 1* **1999**, 2293-2297. (d) Mayer, M. F.; Hossain, M. M. *J. Organomet. Chem.* **2002**, *654*, 202-209. (e) Morales, D.; Pérez, J.; Riera, L.; Riera, V.; Corzo-Suárez, R.; García-Granda, S.; Miguel, D. *Organometallics* **2002**, *21*, 1540-1545. (f) Krumper, J. R.; Gerisch, M.; Suh, J. M.; Bergman, R. G.; Tilley, T. D. *J. Org. Chem.* **2003**, *68*, 9705-9710. (g) Redlich, M.; Hossain, M. M. *Tetrahedron Lett.* **2004**, *45*, 8987-8990.

(8) (a) Williams, A. L.; Johnston, J. N. *J. Am. Chem. Soc.* **2004**, *126*, 1612-1613. (b) Wipf, P.; Lyon, M. A. *ARKIVOC* **2007**, *xii*, 91-98. (c) Hashimoto, T.; Uchiyama, N.; Maruoka, K. *J. Am.*

Chem. Soc. **2008**, *130*, 14380-14381. (d) Akiyama, T.; Suzuki, T.; Mori, K. *Org. Lett.* **2009**, *11*, 2445-2447. (e) Zeng, X.; Zeng, X.; Xu, Z.; Lu, M.; Zhong, G. *Org. Lett.* **2009**, *11*, 3036–3039. (f) Johnston, J. N.; Muchalski, H.; Troyer, T. L. *Angew. Chem., Int. Ed.* **2010**, *49*, 2290-2298.

(9) (a) Zhang, Y.; Desai, A.; Lu, A.; Hu, G.; Ding, Z.; Wulff, W. D. *Chem. –Eur. J.* **2008**, *14*, 3785-3803. (b) Zhang, Y.; Lu, Z.; Desai, A.; Wulff, W. D. *Org. Lett.* **2008**, *10*, 5429-5432. (c) Mukherjee, M.; Gupta, A. K.; Lu, Z.; Zhang, Y.; Wulff, W. D. *J. Org. Chem.* **2010**, *75*, 5643-5660. (d) Ren, H.; Wulff, W. D. *Org. Lett.* **2010**, *12*, 4908-4911. (e) Hu, G.; Huang, L.; Huang, R. H.; Wulff, W. D. *J. Am. Chem. Soc.* **2009**, *131*, 15615-15617. (f) Hu, G.; Gupta, A. K.; Huang, R. H.; Mukherjee, M.; Wulff, W. D. *J. Am. Chem. Soc.* **2010**, *132*, 14669–14675. (g) Desai, A. A.; Wulff, W. D. *J. Am. Chem. Soc.* **2010**, *132*, 13100-13103. (h) Vetticatt, M. J.; Desai, A. A.; Wulff, W. D. *J. Am. Chem. Soc.* **2010**, *132*, 13104-13107. (i) Desai, A. A.; Morán-Ramallal, R.; Wulff, W. D. *Org. Synth.* **2011**, *88*, 224-237.

(10) (a) Nagayama, S.; Kobayashi, S. *Chem. Lett.* **1998**, 685-686. (b) Kubo, T.; Sakaguchi, S.; Ishii, Y. *Chem. Commun.* **2000**, 625-626. (c) Yadav, J. S.; Reddy, B. V. S.; Rao, M. S.; Reddy, P. N. *Tetrahedron Lett.* **2003**, *44*, 5275-5278. (d) Yadav, J. S.; Reddy, B. V. S.; Reddy, P. N.; Rao, M. S. *Synthesis* **2003**, 1387-1390. (e) Ishii, Y.; Sakaguchi, S. *Bull. Chem. Soc. Jpn.* **2004**, *77*, 909-920.

(11) (a) Minakata, S.; Ando, T.; Nishimura, M.; Ryu, I.; Komatsu, M. *Angew. Chem., Int. Ed.* **1998**, *37*, 3392-3394. (b) Nishimura, M.; Minakata, S.; Takahashi, T.; Oderaotoshi, Y.; Komatsu, M. *J. Org. Chem.* **2002**, *67*, 2101-2110.

(12) Gupta, A. K.; Mukherjee, M.; Wulff, W. D. *Org. Lett.* **2011**, *13*, 5866-5869.

(13) Gupta, A. K.; Mukherjee, M.; Hu, G.; Wulff, W. D. *J. Org. Chem.* **2012**, ASAP.

(14) Wulff, W. D.; Antilla, J. A.; Pulgam, V. R.; Zhang, Y.; Gilson-Osminksi, W., Unpublished results.

(15) (a) Ismail, F. M. D.; Levitsky, D. O.; Dembitsky, V. M. *Eur. J. Med. Chem.* **2009**, *44*, 3373-3387. (b) Kabara, J.; Vrable, R.; Lie Ken Jie, M. *Lipids* **1977**, *12*, 753-759. (c) Metzger, J. O.; Fürmeier, S. *Eur. J. Org. Chem.* **1999**, 661-664. (d) Falck, J. R.; Manna, S.; Viala, J.; Siddhanta, A. K.; Moustakis, C. A.; Capdevila, J. *Tetrahedron Lett.* **1985**, *26*, 2287-2290. (e) Howell, A. R.; So, R. C.; Richardson, S. K. *Tetrahedron* **2004**, *60*, 11327-11347.

(16) Newman, C. A.; Antilla, J. C.; Chen, P.; Predeus, A. V.; Fielding, L.; Wulff, W. D. *J. Am. Chem. Soc.* **2007**, *129*, 7216-7217.

(17) (a) Li, W.; Wang, J.; Hu, X.; Shen, K.; Wang, W.; Chu, Y.; Lin, L.; Liu, X.; Feng, X. *J. Am. Chem. Soc.* **2010**, *132*, 8532-8533. (b) Hashimoto, T.; Miyamoto, H.; Naganawa, Y.; Maruoka, K. *J. Am. Chem. Soc.* **2009**, *131*, 11280-11281. (c) Liu, W. J.; Lv, B. D.; Gong, L. Z. *Angew. Chem., Int. Ed.* **2009**, *48*, 6503-6506. (d) Trost, B. M.; Malhotra, S.; Fried, B. A. *J. Am. Chem. Soc.* **2009**, *131*, 1674-+. (e) Hashimoto, T.; Naganawa, Y.; Maruoka, K. *J. Am. Chem. Soc.* **2008**, *130*, 2434-2435. (f) Hasegawa, K.; Arai, S.; Nishida, A. *Tetrahedron* **2006**, *62*, 1390-1401. (g) Dudley, M. E.; Morshed, M. M.; Brennan, C. L.; Islam, M. S.; Ahmad, M. S.; Atuu, M.-R.; Branstetter, B.; Hossain, M. M. *J. Org. Chem.* **2004**, *69*, 7599-7608. (h) Yao, W.; Wang, J. *Org. Lett.* **2003**, *5*, 1527-1530. (i) Jiang, N.; Wang, J. B. *Tetrahedron Lett.* **2002**, *43*, 1285-1287. (j) Mahmood, S. J.; Hossain, M. M. *J. Org. Chem.* **1998**, *63*, 3333-3336. (k) Holmquist, C. R.; Roskamp, E. J. *J. Org. Chem.* **1989**, *54*, 3258-3260. (l) Zhu, Z.; Espenson, J. H. *J. Org. Chem.* **1995**, *60*, 7090-7091. (m) Curini, M.; Epifano, F.; Marcotullio, Maria C.; Rosati, O. *Eur. J. Org. Chem.* **2002**, 1562-1565. (n) Zhu, Z.; Espenson, J. H. *J. Am. Chem. Soc.* **1996**, *118*, 9901-9907.

(18) Guan, Y.; Wulff, W. D., Unpublished results.

(19) Mukherjee, M.; Gupta, A. K.; Wulff, W. D. *Org. Lett.* **2012**, *manuscript in preparation.*

(20) Zhou, Y.; Wulff, W. D., Unpublished results.

(21) Favrot, J.; Vocelle, D.; Sandorfy, C. *Photochem. Photobiol.* **1979**, *30*, 417-421.

(22) Ren, H.; Wulff, W. D. *J. Am. Chem. Soc.* **2011**, *133*, 5656-5659.

(23) Gilson-Osminksi, W.; Wulff, W. D., Unpublished results.

(24) Li, X.; Burrell, C. E.; Staples, R. J.; Borhan, B. *J. Am. Chem. Soc.* **2012**, *134*, 9026-9029.

(25) Friedman, L.; Shechter, H. *J. Org. Chem.* **1961**, *26*, 2522-2524.

(26) Mukherjee, M.; Wulff, W. D., Unpublished results.

(27) Zhao, W.; Wulff, W. D., Unpublished results.

(28) Katritzky, A. R.; Fan, W. Q.; Li, Q. L. *Tetrahedron Lett.* **1987**, *28*, 1195-1198.

(29) (a) *Chem. Eng. News.* **2011**, *89*, 25. (b) McLaughlin, M.; Widegren, M.; Ramirez, A.; Richardson, P.; Zlota, A.; Laird, T. *Org. Process Res. Dev.* **2012**, *16*, 3-10.

(30) Lu, Z.; Zhang, Y.; Wulff, W. D. *J. Am. Chem. Soc.* **2007**, *129*, 7185-7194.

(31) Deng, L.; Jacobsen, E. N. *J. Org. Chem.* **1992**, *57*, 4320-4323.

(32) Bolvig, S.; Hansen, P. E. *Magn. Reson. Chem.* **1996**, *34*, 467-478.

CHAPTER 8

SULFOX-BOROX CATALYSIS
CATALYTIC ASYMMETRIC EPOXIDATION OF ALDEHYDES

I think you can just a write a small chapter on this and someone else would take it further.

-William D. Wulff

8.1 Introduction

The field of asymmetric catalysis and organic synthesis has been enriched with many breakthrough developments in the last fifty years. One of those moments was the development of the Sharpless asymmetric epoxidation of allylic alcohols for the synthesis of the chiral epoxides.[1] When any modern day synthetic organic chemist ponders the construction of a typical organic molecule, that chemist's thought process will reflexively consider how a disconnection can be sought to a Sharpless asymmetric epoxidation. In addition, this thought process will also include a similar analysis for many of the more recent asymmetric epoxidations including the Jacobsen[2] and Katsuki[3] epoxidations, the Shi epoxidation[4] and many others.[5] It is now also instinctive for the synthetic organic chemist to analyze a retro-synthesis in terms any possible asymmetric catalytic kinetic resolution of epoxides due to the great applicability and reliability of the Jacobsen hydrolytic kinetic resolution process.[6] Clearly asymmetric catalysis has had a great impact on the way chemist think about using epoxides in making organic molecules. In all, chiral epoxides are highly versatile synthetic intermediates and for this reason a great deal of effort has been expended over the last three or four decades by both academic and

commercial laboratories to develop more catalytic asymmetric methods for the preparation of epoxides.[5] The following chapter describes a novel method for the catalytic asymmetric synthesis of epoxides from aldehydes using our new SULFOX-BOROX catalyst.

8.2 Previous approaches towards catalytic asymmetric synthesis of epoxides

With the advent of vast applications of epoxides, a new method for the catalytic asymmetric synthesis of epoxides surfaces at regular intervals. Likewise the case of aziridines, there are primarily two approaches: a) oxidation of olefins using i) metal catalysts[1-3,5a,5c,7] ii) organocatalysis[4,8]; oxidation of α,β-unsaturated carbonyl compounds using i) metal catalysts[9] ii) organocatalysis[10] b) addition of carbon to the aldehydes *via* i) α-halo enolate epoxidation (Darzens reaction)[11] ii) metal-carbene transfer (carbene generated from sulfur ylides)[12] iii) a reaction of a diazo compound with an aldehyde activated by Lewis acid (Scheme 8.1).[13] The former approach of oxidation of olefins has been benefitted from pioneering contributions from Sharpless,[1] Jacobsen[2,7e] and Katsuki[3,7e] epoxidation using metal catalysis and from Shi epoxidation[4] using organocatalysis. Yamamoto and coworkers have also reported epoxidation of allylic alcohols using various chiral Lewis acids.[7c,7d]

Scheme 8.1 Different approaches towards catalytic asymmetric epoxidation

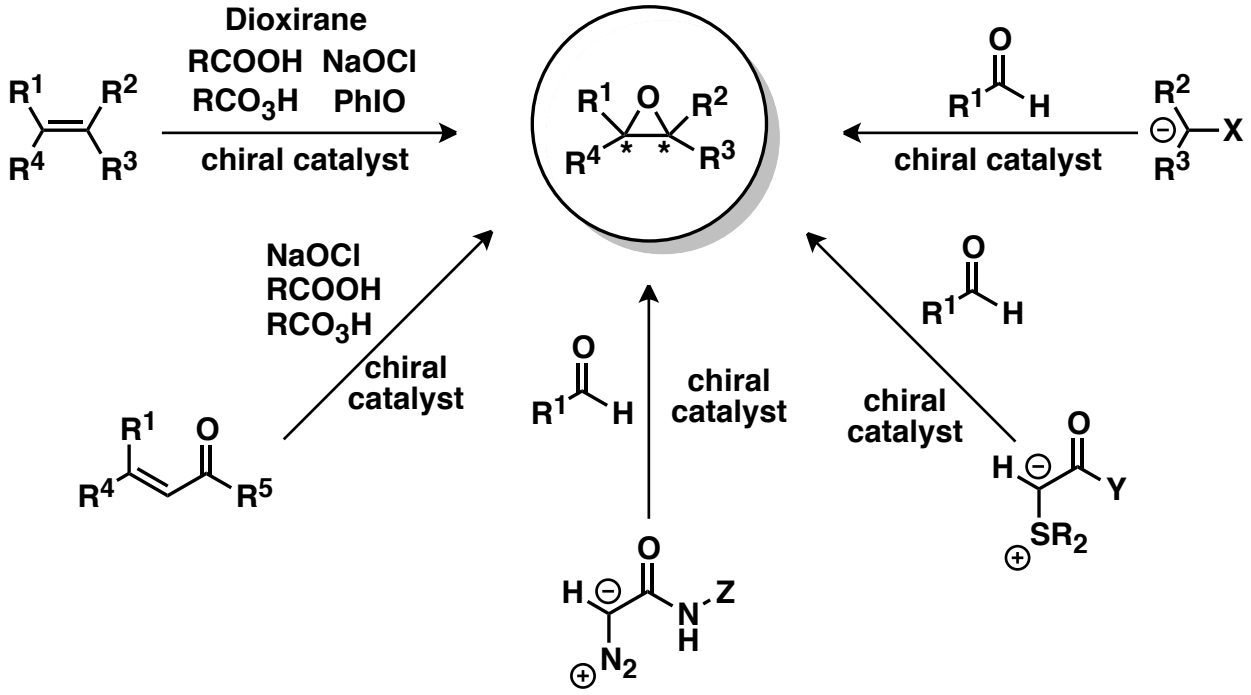

In terms of the addition of carbon to an aldehyde, one of the early approaches is the Darzens reaction, which involves an α-halo enolate. Very recently, Deng and co-workers reported the first example of a highly successful catalytic asymmetric Darzens reaction between α-chloro ketones and aldehydes using a phase transfer catalyst **421** (Scheme 8.2).[11a] It must be noted that they obtained *trans*- and tri-substituted epoxides. Prior to Deng's work, Arai and Shiroi have shown the use of cinchona alkaloid derived phase transfer catalyst to obtain only moderate enantioselectivity.[11c-11g] Also, in 2007, Jeong and coworkers obtained enantiomeric excess of over 90% for reactions between a highly limited range of aromatic aldehydes and a single nucleophile, α-chloromethyl phenyl sulfone using a phase transfer catalyst.[11b]

Scheme 8.2 Catalytic asymmetric Darzens reaction[11a]

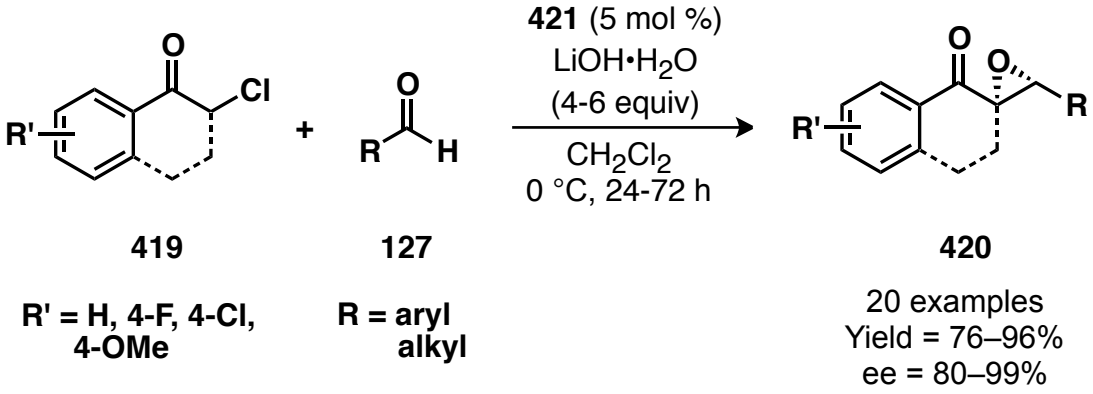

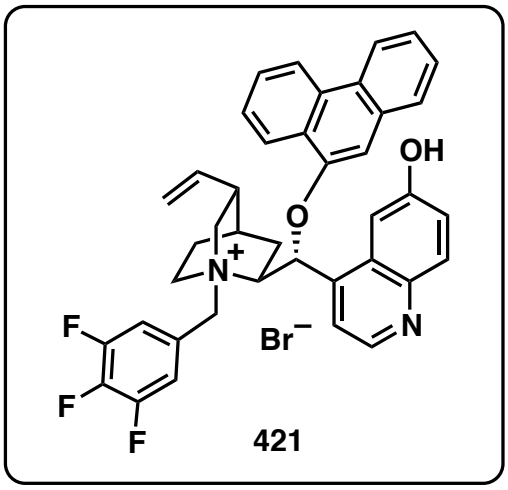

Aggarwal and coworkers reported asymmetric epoxidation using chiral sulfur ylides as the chiral auxiliaries. However, they did report one example of catalytic asymmetric epoxidation where they utilized chiral sulfide **424** to afford *trans*-epoxides **423** and **425** (Scheme 8.3).[12]

Scheme 8.3 Catalytic asymmetric epoxidation using sulfur ylides[12]

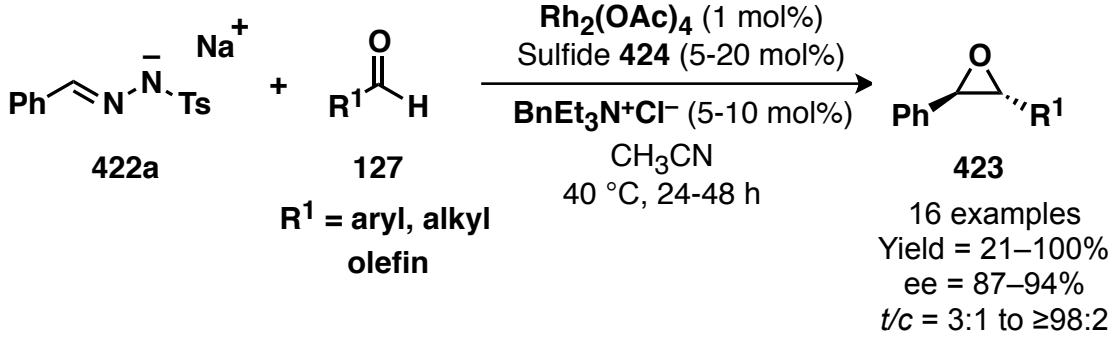

Scheme 8.3 cont'd

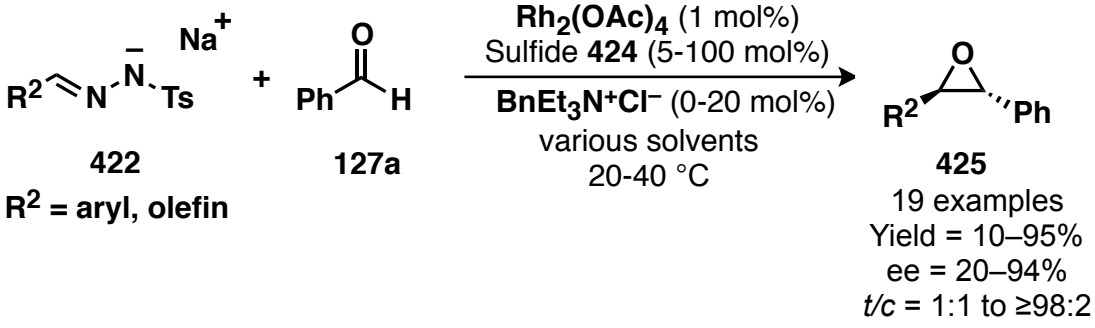

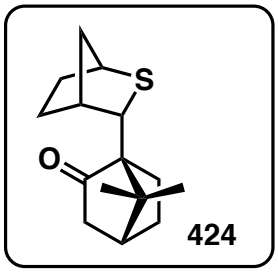

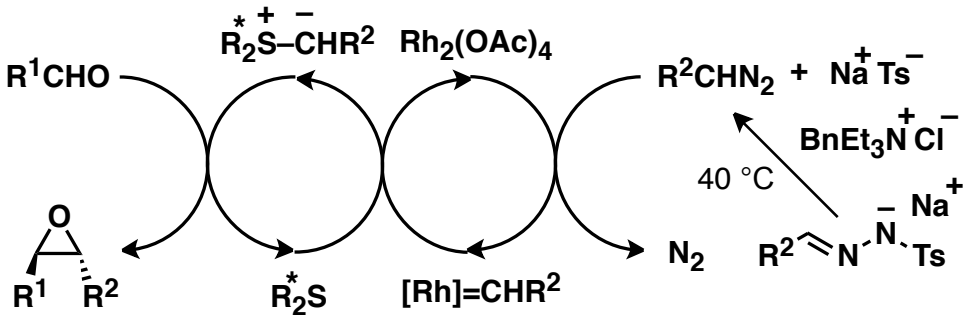

More recently, Gong and coworkers reported the first example of asymmetric epoxidation of aldehydes involving diazoacetamides as the nucleophile to afford *cis*-epoxides **426** in high yields and ees (Scheme 8.3).[13] They used chiral Lewis acids derived from either a combination of (*R*)-BINOL **55** and $Ti(O^{i}Pr)_4$ or (*R*)-3,3′-I_2-BINOL **56e** and $Zr(O^{n}Bu)_4$. Interestingly, they observed opposite enantiomers of **426** when they moved from one catalytic system to another using the same enantiomer of the ligands **55** and **56e**.

Scheme 8.4 Catalytic asymmetric epoxidation using diazoacetamides[13]

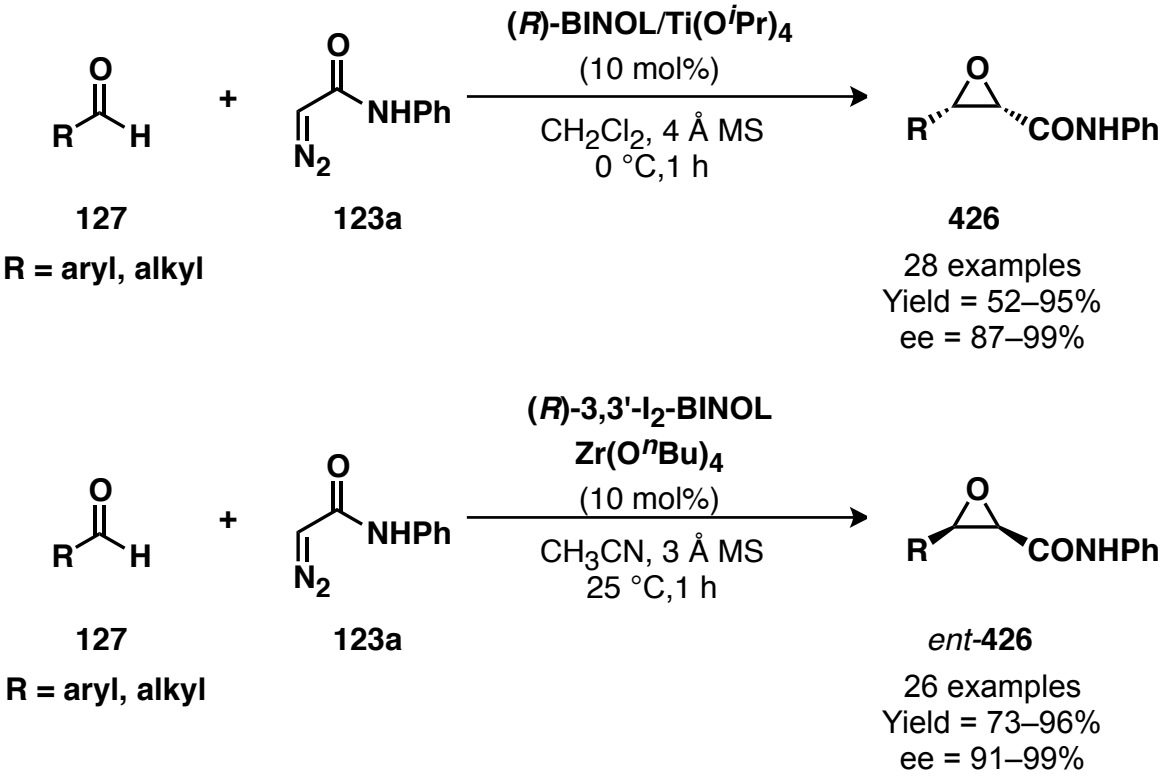

The reaction between aldehyde and diazoacetamide **123a** reported by Gong and co-workers is mediated by chiral Lewis acids. There are no examples of this reaction with a chiral Brønsted acid. This is probably due to the high acidity (pKa ~ –7) of protonated aldehydes. With the advent of a variety of BOROX catalysts developed during this doctoral research, we decided to examine novel BOROX catalysts in the case of the catalytic asymmetric epoxidation of the aldehydes. Prior to the screening of our catalyst, we decided to perform a background reaction in the presence of $B(OPh)_3$. It was interesting to observe that the epoxidation reaction is favored with diazoacetamide **123a** as compared to diazoester **85** when reacted with benzaldehyde **127a** (Scheme 8.5). The reaction of benzaldehyde and 1.14 equiv of ethyl diazoacetate **85** mediated by 14 mol% $B(OPh)_3$ gave the five products shown in Scheme 8.5A with the major

component as the β-keto ester **396a** and its tautomer **397a** in a total of 55% yield. A literature search revealed that several different products including the epoxide **395a** (*trans*-epoxide is major) are known from the reaction of benzaldehyde and EDA mediated by Lewis or Brønsted acids.[14] The same reaction afforded *cis*-epoxide **426a** and β-keto amide **427a** in 62% and 9% yield respectively when diazoacetamide **123a** was used in the place of diazo ester **85**. The *cis-trans* ratio was found to be 10:1. *It must be noted that there is no report for the racemic reaction between an aldehyde and the diazoacetamides.* Moreover, it was found there was no reaction in the presence of VAPOL or VANOL ligand and in the absence of any catalyst. Hence, the challenges in this case were the high background reaction and the formation of the byproduct in the form of the β-keto amide **427a**. These issues have been addressed and are discussed in the subsequent sections. Meanwhile, other diazoacetamides **128a** and **128c** were also tried for the racemic reaction (Scheme 8.5C).

Scheme 8.5 $B(OPh)_3$ catalyzed reaction between benzaldehyde and (**A**) diazoester **85** (**B**) diazoacetamide **123a** (**C**) diazoacetamides **128a** and **128c**

A

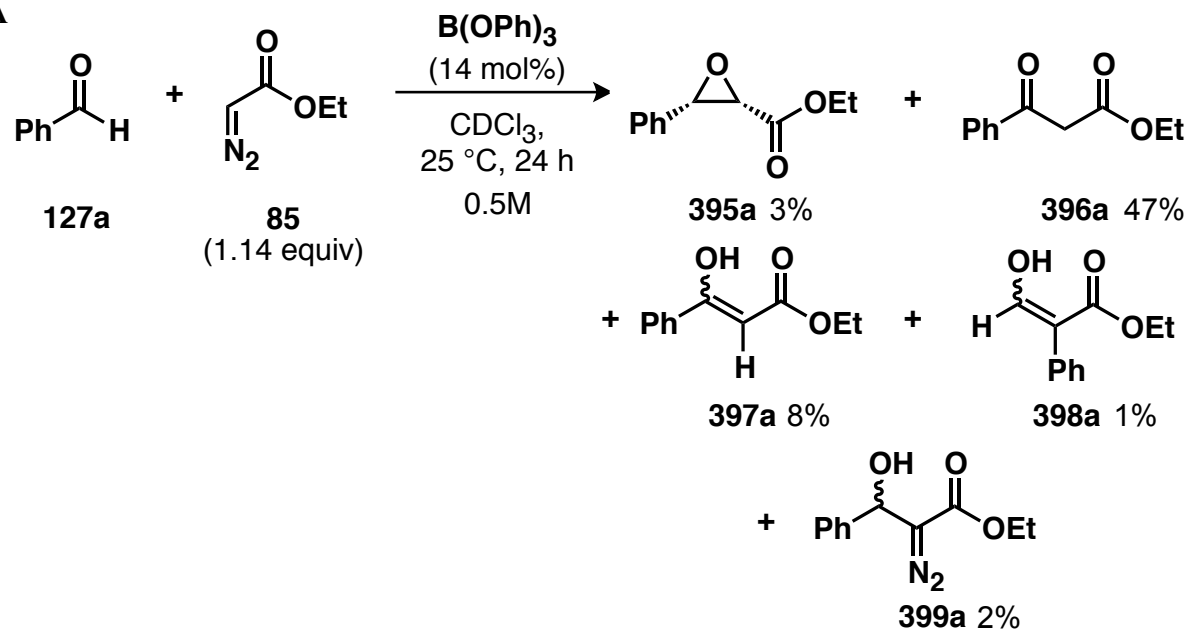

Scheme 8.5 cont'd

B

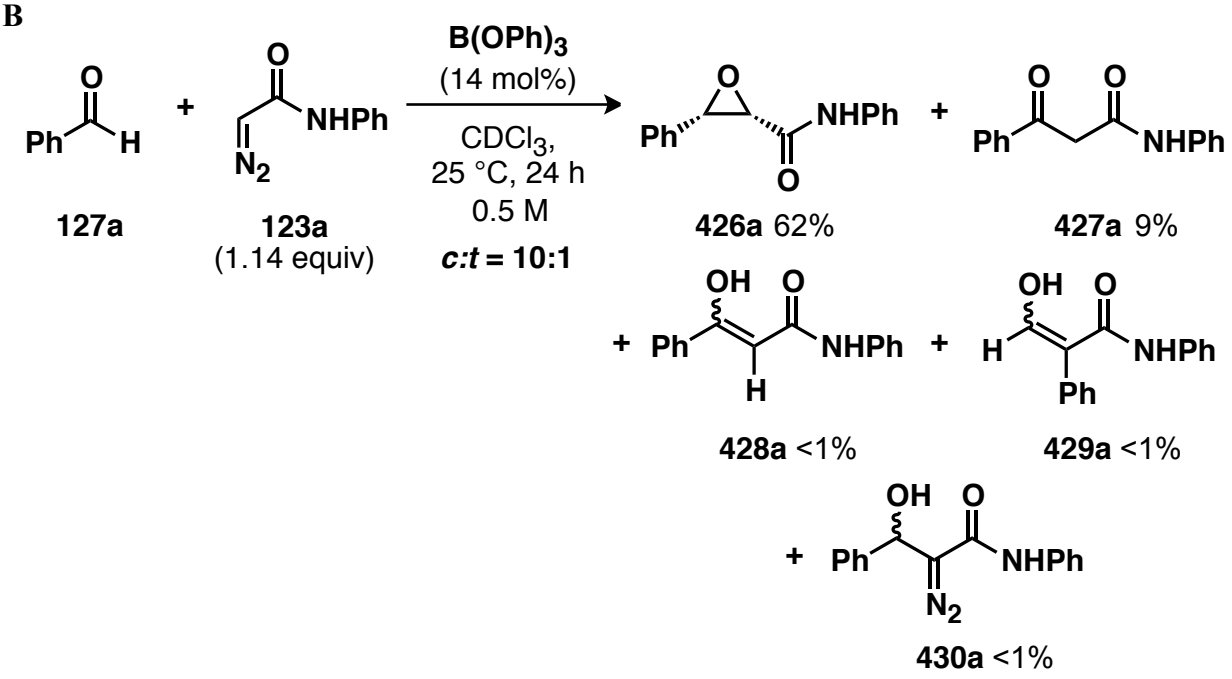

C

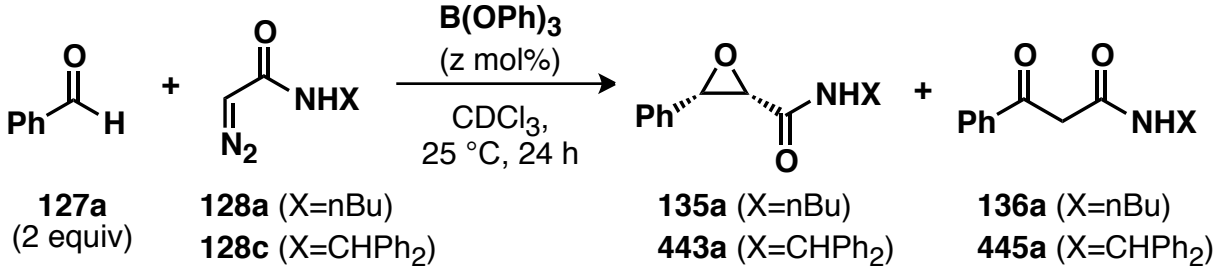

X	%z (cat)	Conc (M)	%y (epoxide)	*c:t*	%y (keto-amide)
nBu	20	0.2	50	3.3:1	6
$CHPh_2$	10	0.4	70	25:1	24

8.3 Initial optimization of catalytic asymmetric epoxidation of aldehydes

Given the result we got from the background reaction mediated by $B(OPh)_3$, we performed the reaction of diazocetamide **123a** with benzaldehyde in the presence of various BOROX catalysts (10 mol%) derived from the VAPOL ligand (Table 8.1, entries 1-4). Low yields and

ees were obtained employing the catalysts **215k**, **220** and **222a** derived from aniline **126k**, dimethylacetamide **219** and DMSO **221a**, respectively (Table 8.1, entries 2-4). In fact, racemic epoxide was obtained in the case of the catalyst **215k** derived from aniline. Interestingly, a slight increase in the asymmetric induction was observed when the SULFOX-BOROX catalyst **432** derived from VANOL was used (Table 8.1, entry 5 *vs.* 4). A huge jump in the enantioinduction was observed at –40 °C using the catalyst **432** derived from DMSO and the VANOL ligand (Table 8.1, entries 6). As a control, the reaction was also, performed without any base using both the ligands (Table 8.1, entries 1 and 9). An ee of 45% in the case of catalyst **434** derived from the VANOL ligand suggests that there is a possibility of the reaction catalyzed by a BOROX catalyst derived from diazoacetamide **123a**. Another viable possibility of its being a chiral Lewis acid catalyzed reaction cannot be excluded. Nonetheless, based on the results obtained from Table 8.1, it seems that the realization of an epoxidation reaction using a novel SULFOX-BOROX catalyst was quite possible.

Table 8.1 Initial screening of various BOROX catalysts for asymmetric epoxidation reaction [a]

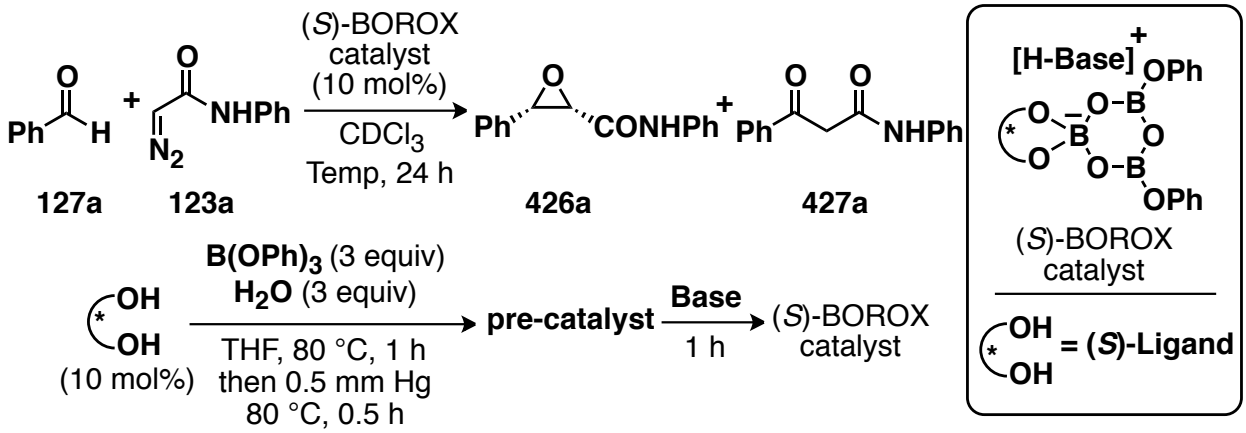

Table 8.1 cont'd

#	Ligand	Base	Cat.	Temp (°C)	**127a** :**123a**	Yield **426a** (%) [b]	ee **426a** (%) [c]	c/t [d]	Yield **427a** (%) [e]
1	(*S*)-VAPOL	none	**431**	25	1.2:1	20 (25)	13	9:1	5.1
2	(*S*)-VAPOL	$PhNH_2$	**215k**	25	1.2:1	35 (36)	<1	8:1	4.2
3	(*S*)-VAPOL	Me_2NCOMe	**220**	25	1.2:1	29 (31)	13	7:1	2.3
4	(*S*)-VAPOL	DMSO	**222a**	25	1.2:1	20 (27)	1	10:1	3.4
5	(*S*)-VANOL	DMSO	**432**	25	1.2:1	35 (41)	20	13:1	6.2
6	(*S*)-VANOL	DMSO	**432**	–40	1:1.25	50 (56)	63	50:1	15.3
7	(*S*)-VANOL	Me_2NCOMe	**433**	–40	1:1.25	57 (71)	35	50:1	5.3
8	(*S*)-VANOL	none	**434**	–40	1:1.25	40 (48)	45	21:1	8.6

[a] Unless otherwise specified, all reactions were performed with 10 mol% BOROX catalyst. Entries 1-5 were performed with 0.50 mmol diazoacetamide **123a** (1.0 equiv, 0.5 M), 0.6 mmol benzaldehyde **127a** (1.2 equiv) and entries 6-9 were performed with 0.50 mmol diazo **123a** (1.25 equiv), 0.4 mmol benzaldehyde **127a** (1.0 equiv, 0.4 M). The pre-catalyst was prepared by heating 1 equiv of (*S*)-ligand (10 mol%), 3 equiv of commercial $B(OPh)_3$ and and 3 equiv of H_2O in THF at 80 °C for 1 h, followed by removing all volatiles under high vacuum (0.1 mm Hg) for 0.5 h at 80 °C. Thereafter, the BOROX catalyst was prepared by stirring the pre-catalyst with 10 mol % base in $CDCl_3$ for 1 h at 25 °C. [b] Isolated Yield. Yield in parenthesis determined by ^1H NMR spectra with Ph_3CH as internal standard. [c] Determined by HPLC. [d] Ratio determined by integration of the methine protons of *cis*- and *trans*-epoxide in the ^1H NMR spectrum of the crude reaction mixture. [e] Determined by ^1H NMR spectra with Ph_3CH as internal standard.

After initial success, we then thought to do an initial screening of various diazoacetamides and the results are presented in Table 8.2. Almost similar ees were obtained irrespective of the diazoacetamide used with 10 mol% catalyst loading. We decided to choose diazoacetamide **123a** and **128a** for further screening. This was done for two reasons: a) one is aromatic and the other one is aliphatic b) diazoactamide **128a** is more soluble than other diazoacetamides.

Table 8.2 Initial screening of various diazoacetamides for asymmetric epoxidation. [a]

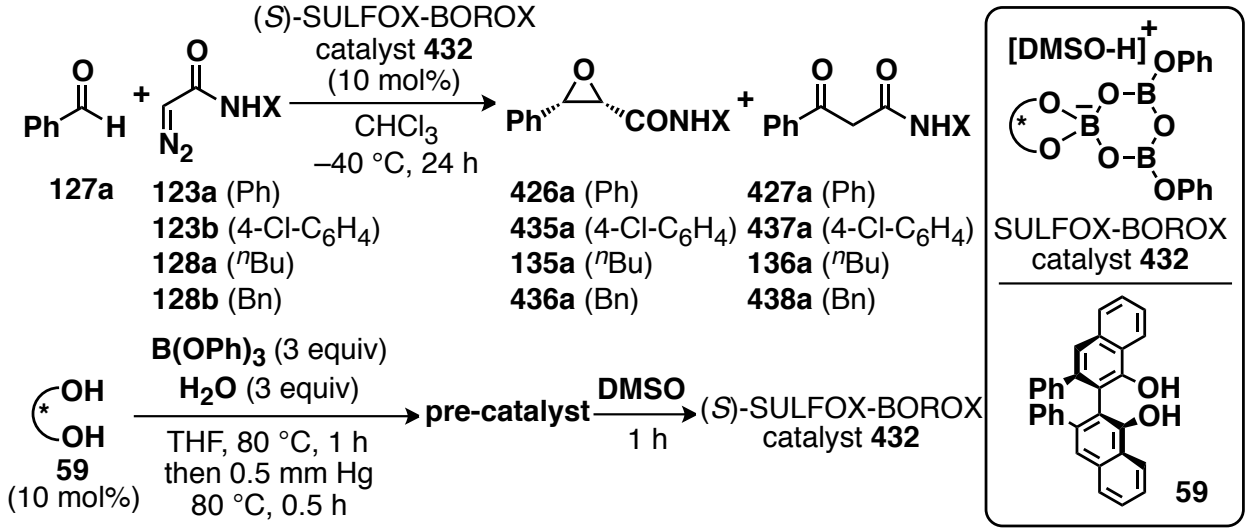

#	Diazo (X)	Yield epoxide (%) [b]	ee epoxide (%) [c]	*cis/trans* [d]	Yield *β*-keto amide (%) [e]
1	C_6H_5	68 (71)	62	40:1	13.6
2	4-Cl-C_6H_4	60 (66)	52	29:1	8.5
3	*n*-C_4H_9	50 (55)	62	16:1	13.7
4	$C_6H_5CH_2$	55 (59)	62	>50:1	15.5

[a] Unless otherwise specified, all reactions were performed with 10 mol % (*S*)-SULFOX-BOROX catalyst **432** and 0.50 mmol diazoacetamide (1.25 equiv), 0.4 mmol benzaldehyde **127a** (1.0 equiv, 0.4 M) at –40 °C in $CHCl_3$. The pre-catalyst was prepared by heating 1 equiv of (*S*)-VANOL (10 mol %), 3 equiv of commercial $B(OPh)_3$ and 3 equiv of H_2O in THF at 80 °C for 1 h, followed by removing all volatiles under high vacuum (0.1 mm Hg) for 0.5 h at 80 °C. Thereafter, the (*S*)-SULFOX-BOROX catalyst **432** was prepared by stirring the pre-catalyst with 10 mol % DMSO in $CHCl_3$ for 1 h at 25 °C. [b] Isolated Yield. Yield in parenthesis determined by ^{1}H NMR spectra with Ph_3CH as internal standard. [c] Determined by HPLC. [d] Ratio determined by integration of the methine protons of *cis*- and *trans*-epoxide in the ^{1}H NMR spectrum of the crude reaction mixture. [e] Determined by ^{1}H NMR spectra with Ph_3CH as internal standard.

We then examined variations in the temperature and concentration of the epoxidation reaction using the two diazoacetamides **123a** and **128a** and 10 mol% catalyst loading. The results are presented in Table 8.3. On decreasing the concentration from 0.4 M to 0.2 M, a marginal increase in asymmetric induction was observed in the cases of both diazoacetamides (Table 8.3, entries 1-2 verses 3-4). At this point, we decided to change the solvent from $CHCl_3$ to toluene and a huge increase in the ee up to 91% was observed in the case of diazoacetamide **128a** (Table 8.3, entries 4 verses 5). This, probably, can be explained by the assumption that the charged ion-pairs i.e. protonated DMSO (interacting with either of the reactants) and boroxinate anion are more stabilized and separated in a polar solvent ($CHCl_3$) than a non-polar solvent (toluene) due to solvation. However, similar increase in ee (90%) was observed in the case of $CHCl_3$ when the concentration of the reaction was further decreased to 0.1 M (Table 8.3, entry 6). It must be noted that the *cis:trans* ratio is also higher when toluene is used as the solvent as compared to $CHCl_3$. Nonetheless, we were able to obtain ee up to 97% when the reaction was performed in toluene at –60 °C and 0.1 M with diazoacetamide **128a** (Table 8.3, entry 7). It must be noted that the amount of *β*-keto amide **136a** was also minimized during this optimization. However, the major concern was the low yield of the epoxide in almost all the cases. Thereafter, further optimization was carried out using diazoacetamide **128a** keeping the temperature at –60 °C and concentration at 0.1 M.

Table 8.3 Screening of diazoacetamides at different concentrations, solvents and temperatures.[a]

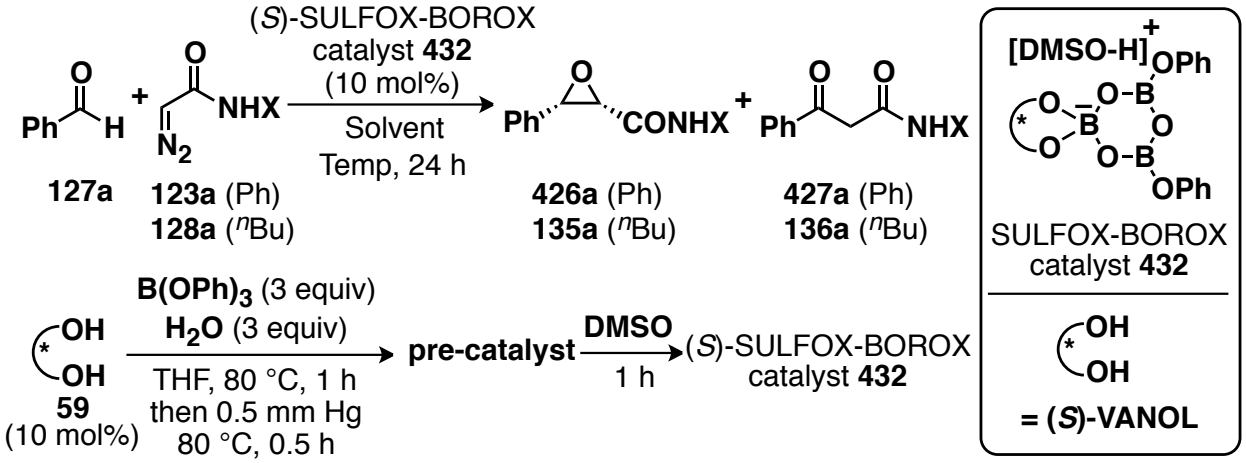

#	Diazo (X)	Solvent	Temp (°C)	Conc. (M)	Yield epoxide (%) [b]	ee epoxide (%) [c]	c/t [d]	Yield β-keto amide (%) [e]
1	Ph	$CHCl_3$	–40	0.4	68 (71)	62	40:1	13.6
2	^{n}Bu	$CHCl_3$	–40	0.4	50 (55)	62	16:1	13.7
3	Ph	$CHCl_3$	–40	0.2	44 (45)	70	24:1	20.0
4	^{n}Bu	$CHCl_3$	–40	0.2	55 (59)	73	31:1	9.8
5	^{n}Bu	$PhCH_3$	–40	0.2	46 (50)	91	90:1	7.0
6[f]	^{n}Bu	$CHCl_3$	–40	0.1	60 (64)	90	54:1	5.5
7	^{n}Bu	$PhCH_3$	–60	0.1	58 (62)	97	>100:1	7.0

[a] Unless otherwise specified, all reactions were performed with 10 mol % (*S*)-SULFOX-BOROX catalyst **432** and 0.50 mmol diazoacetamide (1.25 equiv), 0.4 mmol benzaldehyde **127a** (1.0 equiv, C M) at temp °C in the solvent. The pre-catalyst was prepared by heating 1 equiv of (*S*)-VANOL (10 mol %), 3 equiv of commercial $B(OPh)_3$ and 3 equiv of H_2O in THF at 80 °C for 1 h, followed by removing all volatiles under high vacuum (0.1 mm Hg) for 0.5 h at 80 °C. Thereafter, the (*S*)-SULFOX-BOROX catalyst **432** was prepared by stirring the pre-catalyst with 10 mol % DMSO in solvent for 1 h at 25 °C. [b] Isolated Yield. Yield in parenthesis determined by ^{1}H NMR spectra with Ph_3CH as internal standard. [c] Determined by HPLC. [d] Ratio determined by integration of the methine protons of *cis*- and *trans*-epoxide in the ^{1}H NMR spectrum of the crude reaction mixture. [e] Determined by ^{1}H NMR spectra with Ph_3CH as internal standard. [f] The ratio of **127a**:**128a** is 2:1.

In order to increase the yield of the epoxide **135a**, we then thought to vary the equivalents of both components i.e. diazoacetamide **128a** and benzaldehyde **127a** (Table 8.4, entries 1-7). A drop of 5% in ee along with increase of 10% in yield was observed when 3 equivalents of diazoacetamide **128a** was employed (Table 8.4, entry 2). To our delight, substantial increase in yield was observed when 3 or 5 equivalents of benzaldehyde **127a** were employed in asymmetric epoxidation reaction (Table 8.4, entries 4 and 6). Although, high yields were obtained, it is impractical to utilize such a high excess of one reagent. So we decided to utilize 2 equivalents of benzaldehyde, which resulted the epoxide **135a** in 65% yield and 98% ee. At this point, it worth mentioning that when the entry 4 of table 8.4 was repeated with the catalyst generated from 3 equivalents of DMSO, only 15% of epoxide was obtained (Table 8.4, entry 5). One of the variation was to utilize the purified $B(OPh)_3$ to prepare the catalyst. However, a substantial decrease in yield and ee were observed when freshly distilled $B(OPh)_3$ was employed (Table 8.4, entries 8-9). The reason for this dip is not known yet. At this point of time we decided to utilize BH_3•Me_2S as the boron source in place of $B(OPh)_3$. Not only this was expected to give better results, but also this would provide us a handle to screen different alcohols facilitating the screening of various boroxinate catalysts. Unfortunately, it resulted epoxide **135a** in 60% yield and 94% ee only (Table 8.4, entry 10). One of the important observations was that the diazoacetamide **128a** was added as solid which resulted in low solubility of the diazo compound at –60 °C. Hence, we decided to add the diazo as a solution in toluene. An appreciable increase in the yield up to 82% was observed (Table 8.4, entry 11). Thereafter, utilizing 1.1 equiv of benzaldehyde with 10 mol% catalyst **432**, we were able to obtain epoxide **135a** in 82% yield and 98% ee (Table 8.4, entry 12). To our delight, the reaction resulted in 98% ee with a slight drop

in yield (73%) when 5 mol% catalyst was employed (Table 8.4, entry 13). Last but not least, we tried another variation where diazoacetamide **128a** was added prior to the addition of the benzaldehyde **127a** (Table 8.4, entry 14). This was done to bring the large volume (diazo **128a** was added as a solution) of the toluene to –60 °C before the reaction starts. An improved result of 88% yield and 99.3% ee was obtained and thus this became the procedure of choice (Table 8.4, entry 14). In fact, high yield and ee was obtained with 5 mol% catalyst loading (Table 8.4, entry 15). It must be remembered that in order to screen various diazoaceatmides, which are insoluble in toluene, procedure used in entry 4 of Table 8.4 with either $B(OPh)_3$ or BH_3•Me_2S would be the procedure of choice.

Table 8.4 Varying the equivalents of aldehydes and boron sources and sequence of events.[a]

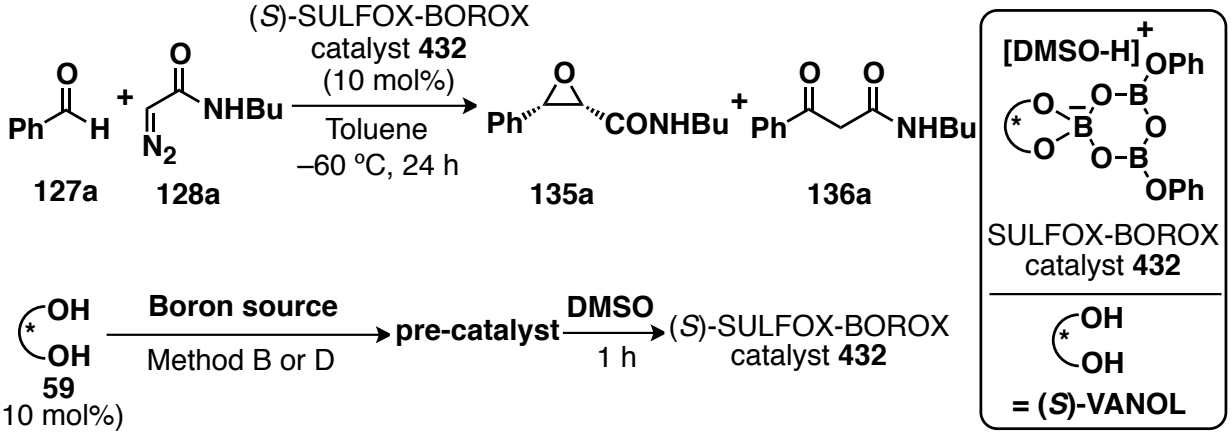

#	Boron source	Pre-catalyst (method)	Conc. (M)	**127a** (equiv)	**128a** (equiv)	Yield **135a** (%) [b]	ee **135a** (%) [c]	Yield **136a** (%) [d]
1	$B(OPh)_3$	B	0.1	1	1.25	58 (62)	97	7
2	$B(OPh)_3$	B	0.1	1	3	68 (72)	92	9
3	$B(OPh)_3$	B	0.1	1	1	60 (63)	98	6
4	$B(OPh)_3$	B	0.1	3	1	75 (80)	97	9
5	$B(OPh)_3$ [e]	B	0.1	3	1	– (15)	–	6
6	$B(OPh)_3$	B	0.1	5	1	80 (89)	99	8
7	$B(OPh)_3$	B	0.1	2	1	65 (72)	98	9

Table 8.4 cont'd

8	$B(OPh)_3$ [f]	B	0.1	2	1	50 (55)	73	10
9	$B(OPh)_3$ [f, g]	B	0.1	2	1	50 (59)	80	8
10	BH_3•Me_2S	E	0.1	2	1	60 (64)	94	17
11	BH_3•Me_2S [g,h]	E	0.05	2	1	82 (85)	95	6
12	BH_3•Me_2S [g,h]	E	0.05	1.1	1	82 (84)	98	1
13	BH_3•Me_2S [g,i]	E	0.05	1.1	1	73 (75)	98	2
14	BH_3•Me_2S [g,j]	E	0.05	1.1	1	88 (90)	99.3	<1
15	BH_3•Me_2S [g,i,j]	E	0.05	1.1	1	79 (80)	99	2

[a] Unless otherwise specified, all reactions were performed with 10 mol % SULFOX-BOROX catalyst **432** and 0.2 mmol diazo **128a** (1.0 equiv, C M), benzaldehyde **127a** (x equiv) at –60 °C in toluene. The pre-catalyst was prepared either by Method B or Method E. Method B: By heating 1 equiv of (*S*)-VANOL (10 mol %), 3 equiv of commercial $B(OPh)_3$ and 3 equiv of H_2O in THF at 80 °C for 1 h, followed by removing all volatiles under high vacuum (0.1 mm Hg) for 0.5 h at 80 °C. Method E: By heating 1 equiv of (*S*)-VANOL (10 mol %), 3 equiv of BH_3•Me_2S, 2 equiv of PhOH and 3 equiv of H_2O in toluene at 100 °C for 1 h, followed by removing all volatiles under high vacuum (0.1 mm Hg) for 0.5 h at 100 °C. Thereafter, the SULFOX-BOROX catalyst **432** was prepared by stirring the pre-catalyst (prepared by either method B or D) with 10 mol% DMSO in toluene for 1 h at 25 °C. All but entry 8 have shown the *cis:trans* ratio to be >100:1. The *cis:trans* ratio is 45:1 for entry 8. The *cis:trans* ratio is determined by integration of the methine protons of *cis*- and *trans*-epoxide in the ^1H NMR spectrum of the crude reaction mixture. [b] Isolated Yield. Yield in parenthesis determined by ^1H NMR spectra with Ph_3CH as internal standard. [c] Determined by HPLC. [d] Determined by ^1H NMR spectra with Ph_3CH as internal standard. [e] 3 equivalents of DMSO were added to make the catalyst. [f] Freshly distilled $B(OPh)_3$ used. [g] Diazoacetamide **128a** was added as a solution in toluene. [h] Reaction time = 1.5 h. [i] 5 mol% catalyst loading. [j] Diazoacetamide **128a** was added prior to the addition of benzaldehyde **127a**.

One of the last experiments undertaken was utilizing the BOROX catalyst generated by the simple mixing of the (*S*)-VANOL, 3 equiv $B(OPh)_3$ and 1 equiv DMSO. This would ideally simplify the procedure to a great deal and would lead to a one-pot procedure. Unfortunately, an

appreciable decrease in ee (~17%) and *cis:trans* ratio was observed in these cases (Table 8.5, entry 5 *vs.* 6). However, this method can be used for the large scale synthesis of epoxides as the purification can be done by crystallization, which in turn, increases the diastereoselectivity and enantioselectivity (discussed in later sections of this chapter).

Table 8.5 Screening of the one-pot procedure for asymmetric epoxidation.[a]

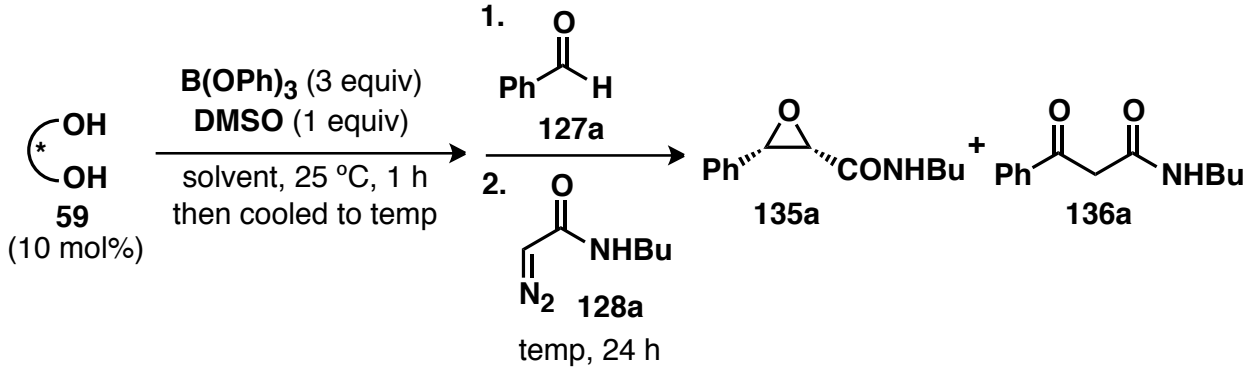

#	Solvent	Temp (°C)	Conc. (M)	Yield **135a** (%) [b]	ee **135a** (%) [c]	*c:t* [d]	Yield **136a** (%) [e]
1 [f,g]	$CHCl_3$	–40	0.2	55 (59)	73	31:1	9.8
2 [f]	$CHCl_3$	–40	0.2	66 (70)	69	11:1	2.0
3 [h]	$CHCl_3$	–60	0.1	65 (70)	60	11:1	3.0
4 [h,i]	$CHCl_3$	–60	0.1	60 (64)	70	11:1	4.0
5 [g]	$PhCH_3$	–60	0.1	75 (80)	97	>100:1	9.0
6	$PhCH_3$	–60	0.1	75 (79)	80	13:1	4.0
7	$PhCH_3$	–60	0.2	68 (75)	74	15:1	3.5
8	$PhCH_3$	–40	0.1	66 (71)	82	13:1	4.0

[a] Unless otherwise specified, all reactions were performed with 10 mol % (*S*)-SULFOX-BOROX catalyst **432** and 0.2 mmol diazoacetamide (1.0 equiv, C M), 0.6 mmol benzaldehyde **127a** (3.0 equiv) at temp °C in the solvent. The (*S*)-SULFOX-BOROX catalyst **432** was prepared directly by stirring a mixture of 1 equiv of (*S*)-VANOL (10 mol %), 3 equiv of commercial $B(OPh)_3$ and 10 mol % DMSO in solvent for 1 h at 25 °C. [b] Isolated Yield. Yield in parenthesis determined by ^1H NMR spectra with Ph_3CH as internal standard.

Table 8.5 cont'd

[c] Determined by HPLC. [d] Ratio determined by integration of the methine protons of *cis*- and *trans*-epoxide in the ^{1}H NMR spectrum of the crude reaction mixture. [e] Determined by ^{1}H NMR spectra with Ph_3CH as internal standard. [f] The ratio of **127a**:**128a** is 1:1.25. [g] The pre-catalyst was prepared by heating 1 equiv of (*S*)-VANOL (10 mol %), 3 equiv of commercial $B(OPh)_3$ and 3 equiv of H_2O in THF at 80 °C for 1 h, followed by removing all volatiles under high vacuum (0.1 mm Hg) for 0.5 h at 80 °C. Thereafter, the (*S*)-SULFOX-BOROX catalyst **432** was prepared by stirring the pre-catalyst with 10 mol % DMSO in solvent for 1 h at 25 °C. [h] The diazoacetamide **128a** was added as a solution in $CHCl_3$. [i] Tetramethylene sulfoxide (TMSO) is used as the base.

8.4 Substrate Scope

After we obtained the final optimized procedure, we then carried out a general screen for the catalytic asymmetric epoxidation reaction. The results of an examination of the scope of epoxidation reaction are presented in Table 8.5. Excellent yields and asymmetric inductions were observed for a number of substituted benzaldehydes (Table 8.5, entries 1, 4-12) and polyaromatic compounds (Table 8.5, entries 2-3). While the *p*-tolualdehyde gave high induction (entry 5), the *o*-tolualdehyde is slower and resulted the epoxide **135c** in 60% yield and 80% ee only (entry 4). Excellent result was obtained with *m*-anisaldehyde (entry 5). The reactions with electron-withdrawing groups at para-position gave high inductions (entries 7-8 and 11-12). These electron-withdrawing groups include nitro, bromide, cyanide and acetate. In fact, even *m*-bromobenzaldehyde gave excellent yield and asymmetric induction (entry 9). However, the reaction with 2-F,4-Br-C_6H_4CHO **127x** afforded the epoxide **135x** in 70% yield and 80% ee only (entry 10). Unfortunately, the reaction with 2-picolinaldehyde resulted the epoxide in 20% yield only (not shown here).

Table 8.6 Catalytic asymmetric epoxidation of aryl and alkyl aldehydes [a]

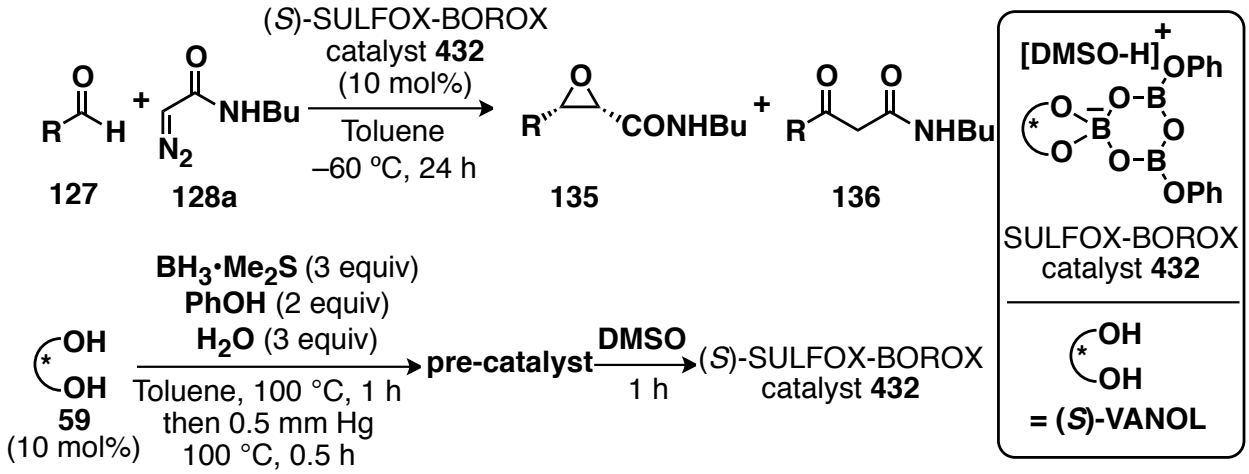

#	R	series	Yield **135** (%) [b]	ee **135** (%) [c]	cis/trans [d]	**136** (%) [e]
1	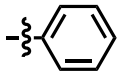	**a**	88	99	>100:1	<1
2	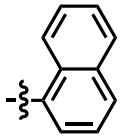	**b**	97	92	35:1	<1
3	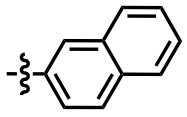	**b′**	92	98	>100:1	<1
4	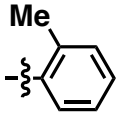	**c**	60	80	>100:1	<1
5	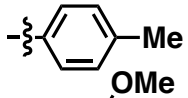	**d**	80	99	>100:1	<1
6	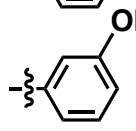	**e′**	80	90	31:1	6
7	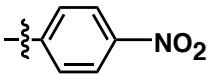	**f**	70	92	13:1	8

Table 8.6 cont'd

8	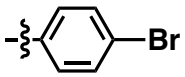	**g**	88	99	>100:1	<1
9	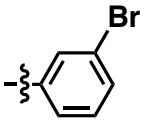	**g′**	88	96	>100:1	4
10	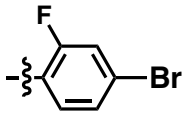	**x**	70	80	39:1	9
11	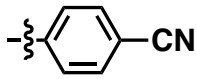	**y**	84	96	>100:1	<1
12	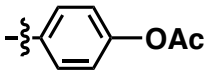	**z**	82	97	>100:1	4
13	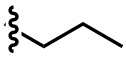	**o**	65	78	nd	9
14	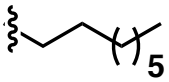	**p′**	84	90	nd	6

[a] Unless otherwise specified, all reactions were performed with 10 mol % (*S*)-SULFOX-BOROX catalyst **432** and 0.2 mmol diazo **128a** (1.0 equiv, 0.05 M), aldehyde **127** (1.1 equiv) at –60 °C in toluene. The pre-catalyst was prepared either by heating 1 equiv of (*S*)-VANOL (10 mol %), 3 equiv of BH_3•Me_2S, 2 equiv of PhOH and 3 equiv of H_2O in toluene at 100 °C for 1 h, followed by removing all volatiles under high vacuum (0.1 mm Hg) for 0.5 h at 100 °C. Thereafter, the (*S*)-SULFOX-BOROX catalyst **432** was prepared by stirring the pre-catalyst with 10 mol % DMSO in toluene for 1 h at 25 °C. In all cases, diazoacetamide **128a** was added a solution in toluene and prior to the addition of aldehyde. All liquid aldehydes are added in neat form whereas all solid aldehydes are added as a solution in toluene maintaining the concentration of the reaction to be 0.05 M in diazoaceatamide **128a**. [b] Isolated Yield. [c] Determined by HPLC. [d] The *cis:trans* ratio is determined by integration of the methine protons of *cis*- and *trans*-epoxide in the ^{1}H NMR spectrum of the crude reaction mixture. [e] Determined by ^{1}H NMR spectra with Ph_3CH as internal standard.

In terms of aliphatic substrates, while the *n*-nonanal gave high induction (entry 14), the *n*-butanal is slower and resulted the epoxide **135o** in 65% yield and 78% ee only (entry 13). Recently, our group reported the first example of catalytic asymmetric aziridination for the

synthesis of tri-substituted aziridines.[15] So we thought of employing the same protocol for tri-substituted epoxidation. Intial experiments suggested the formation of the tri-substituted epoxide using diazoacetamide **439a** as shown as in Scheme 8.6. The ^{1}H NMR analysis of the crude reaction mixture indicates that the ratio of the epoxide **440a** and *β*-keto amide **441a** is approximately 1:2. (Scheme 8.6A). In another experiment, same ratio (1:2) of epoxide **440b** and *β*-keto amide **441b** was obtained when diazoacetamide **439b** was utilized (Scheme 8.6B). The peak for Ha in $CDCl_3$ has been assumed to appear at δ = 4.25 ppm for **440a** and δ = 4.08 ppm for **440b** respectively.

Scheme 8.6 Tri-substitute epoxidation between PhCHO and (**A**) **439a** and (**B**) **439b**

A

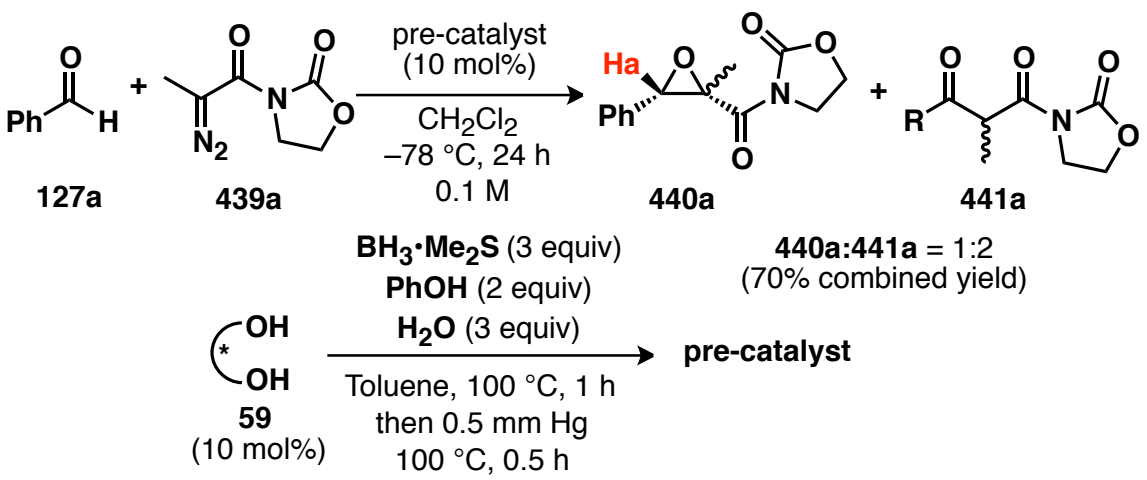

B

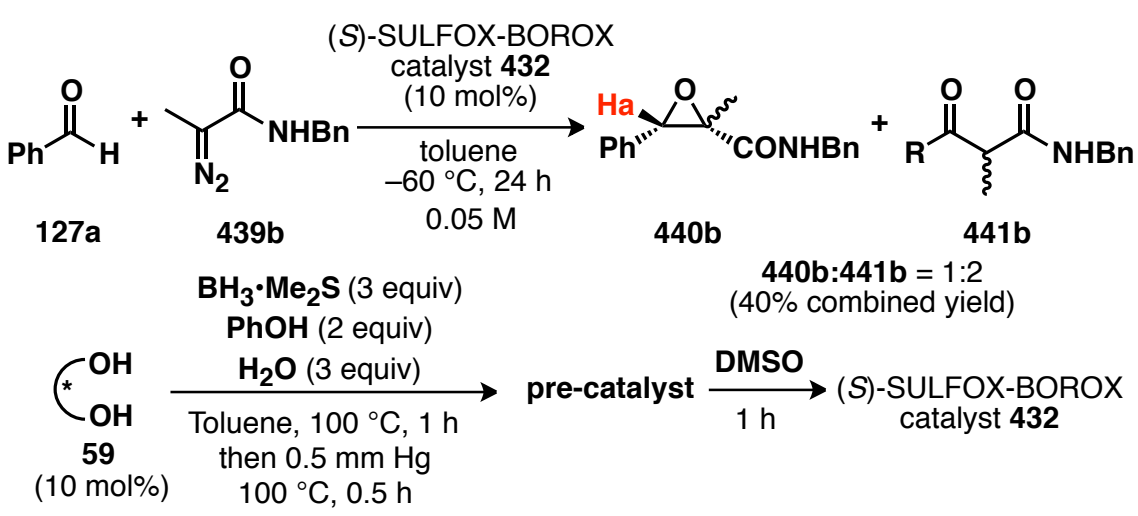

8.5 Determination of absolute stereochemistry of epoxides

The absolute configurations of the major diastereomer i.e. *cis*-epoxide **426a** and **135a** has been determined by three different ways.

8.5.1 *Via* optical rotation

The epoxide **426a** is a reported in literature;[13] hence we compared the optical rotation of the epoxide **426a** with 62% ee to the reported value for the known epoxide **426a** with 99% ee (Scheme 8.7). It was quite surprising to know that the *cis*-epoxide **426a** results from a *Re* face attack of the diazoacetamide **123a** on the aldehyde using the (*S*)-SULFOX-BOROX catalyst **432** derived from (*S*)-VANOL. Interestingly, this indicates that the facial selectivity of the *cis*-epoxidation with diazoacetamide is opposite for *cis*-aziridination with ethyldiazoacetate using the same enantiomer of the ligand because the *cis*-aziridine results from a *Si* face attack of the diazoacetate on the (*S*)-catalyst-imine complex. Similar kind of observation was made in the case of *trans*-aziridination when compared to *cis*-aziridination.[16]

Scheme 8.7 Comparison of the optical rotation values of epoxide (*S*,*S*)-**426a** obtained from the current work and from the literature

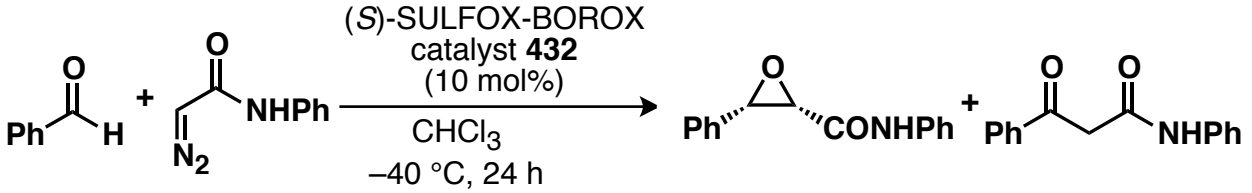

127a **123a** (*S*,*S*)-**426a** **427a**

68% yield, 62% ee **14% yield**

$[\alpha]_D^{20}$ = +14.7 (c=1.0, CH_2Cl_2, 62%ee) This work

$[\alpha]_D^{20}$ = +19.1 (c=0.9, CH_2Cl_2, 99%ee) Literature value (Reference 13)

8.5.2 *Via* X-ray structure

The absolute configuration of the epoxides obtained in our catalytic asymmetric epoxidation protocol was further confirmed by X-ray crystallography. To our delight, we were able to obtain X-ray diffraction analysis of epoxides **135g** and **435a**, which further confirms *cis*-epoxidation and the absolute configuration. It must be noted that epoxides **135g** and **435a** were obtained from (*S*)-SULFOX-BOROX catalyst **432** derived from (*S*)-VANOL ligand (Table 8.6, entry 8 and Table 8.2, entry 2). The ORTEP drawing of *cis*-epoxides (*S*,*S*)-**135g** and (*S*,*S*)-**435a** are shown in Figure 8.1.

Figure 8.1 ORTEP drawing of *cis*-epoxides (**A**) (*S*,*S*)-**135g** and (**B**) (*S*,*S*)-**435a**

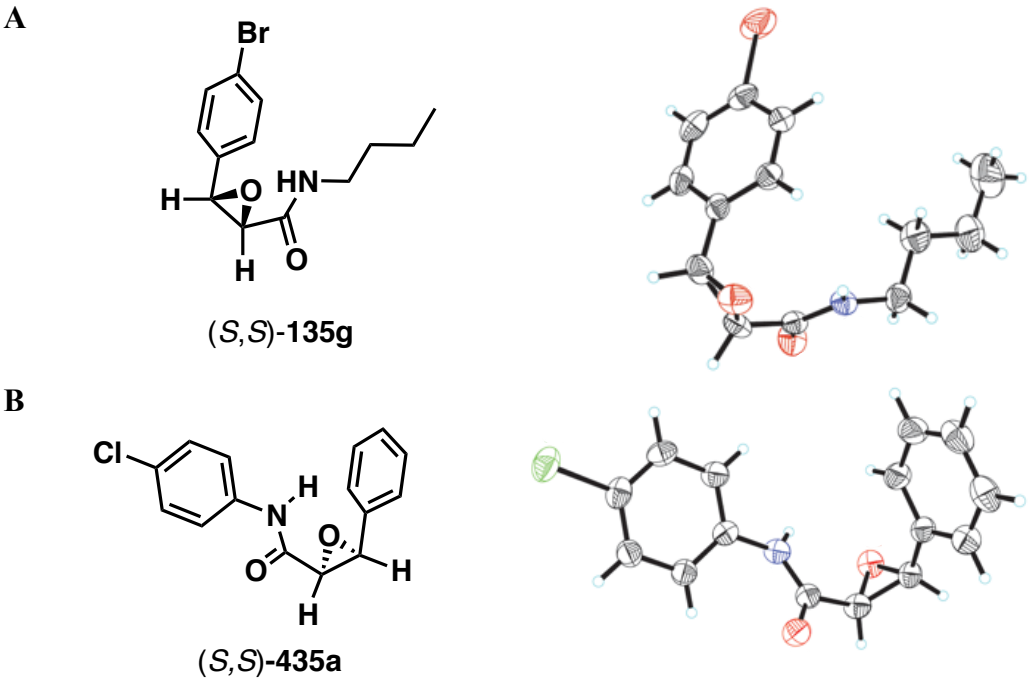

8.5.3 *Via* circular dichroism

Last but not the least, the absolute configuration of epoxides **135** was confirmed by the excellent method developed by Borhan and coworkers using circular dichroism.[17] This work

was done in collaboration with Carmin Burrell, a current graduate student in Borhan group. The method was applied to a number of epoxides as listed in Figure 8.2B.

The absolute stereochemistry of the *cis*-epoxides was confirmed through evaluation by exciton coupled circular dichroism (ECCD). The sign of the observed ECCD curve is a reflection of the stereochemistry of the epoxides in that a pair of enantiomeric molecules will exhibit ECCD signals with opposite sign. To develop a mnemonic for this class of substrates, initially an enantiomeric pair of epoxides was submitted to ECCD conditions. Each epoxide (40 equivalents, 0.04 μmol) was added to a 1μM solution of the porphyrin tweezer, Zn-C_5-TPFP-Tz, in hexanes at 0 °C. To our delight, under these conditions, the enantiomers did provide ECCD signal of opposite sign (Figure 8.2A).

Figure 8.2 Determination of absolute stereochemistry of *cis*-epoxides **135**, **426a** and **436a**. (**A**) CD spectra for the two enantiomers of *cis*-epoxide **135g** (**B**) Observed ECCD amplitudes for chiral *cis*-epoxides. All measurements were performed with 40 equivalents of the substrates (except 150 equiv used for (*S,S*)-**426a**) and 1μM tweezer in hexanes at 0 ºC. (**C**) Proposed mnemonic explaining the signs of the observed ECCD signals.

A

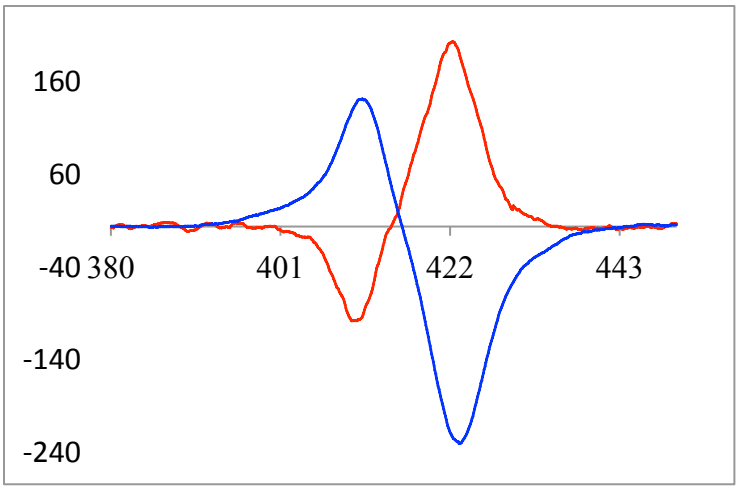

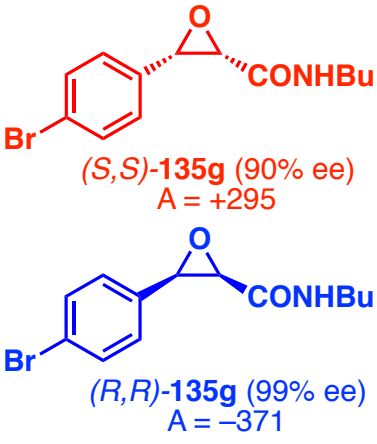

Figure 8.2 cont'd

B

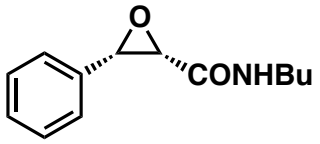

(S,S)-**135a** (99% ee)
A = +225

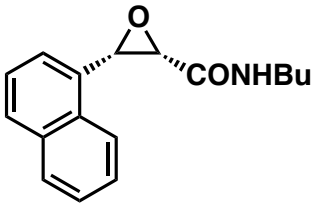

(S,S)-**135b** (92% ee)
A = +189

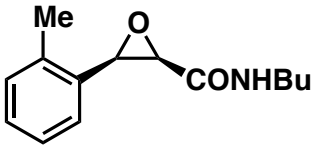

(R,R)-**135c** (80% ee)
A = –80

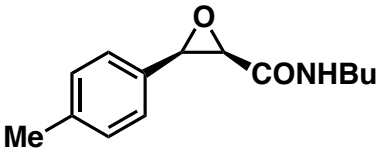

(R,R)-**135d** (99% ee)
A = –440

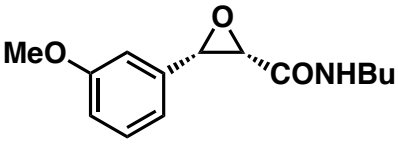

(S,S)-**135e'** (90% ee)
A = +432

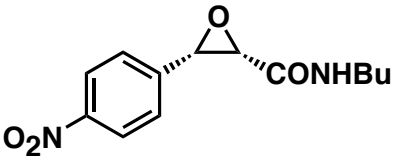

(S,S)-**135f** (92% ee)
A = +134

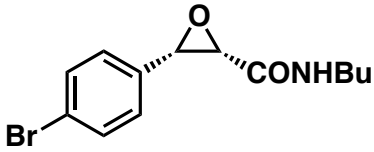

(S,S)-**135g** (90% ee)
A = +295

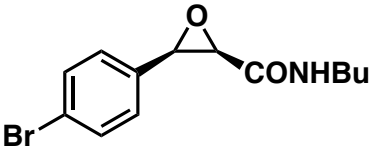

(R,R)-**135g** (99% ee)
A = –371

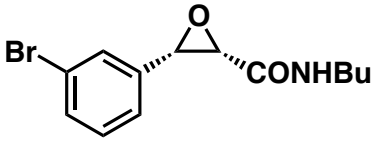

(S,S)-**135g'** (96% ee)
A = +233

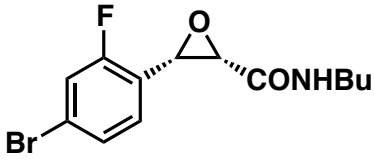

(S,S)-**135x** (80% ee)
A = +96

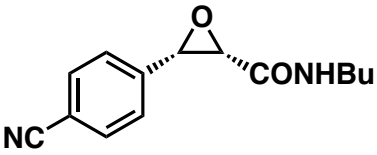

(S,S)-**135y** (96% ee)
A = +85

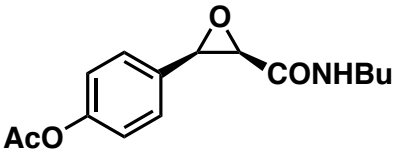

(R,R)-**135z** (97% ee)
A = –231

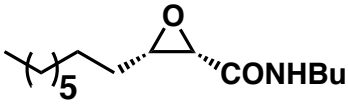

(S,S)-**135p'** (90% ee)
A = +1109

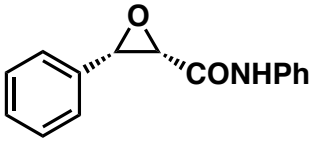

(S,S)-**426a** (55% ee)
A = +53

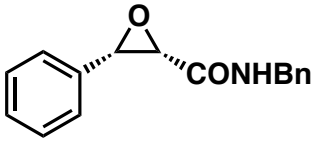

(S,S)-**436a** (62% ee)
A = +86

Figure 8.2 cont'd

C

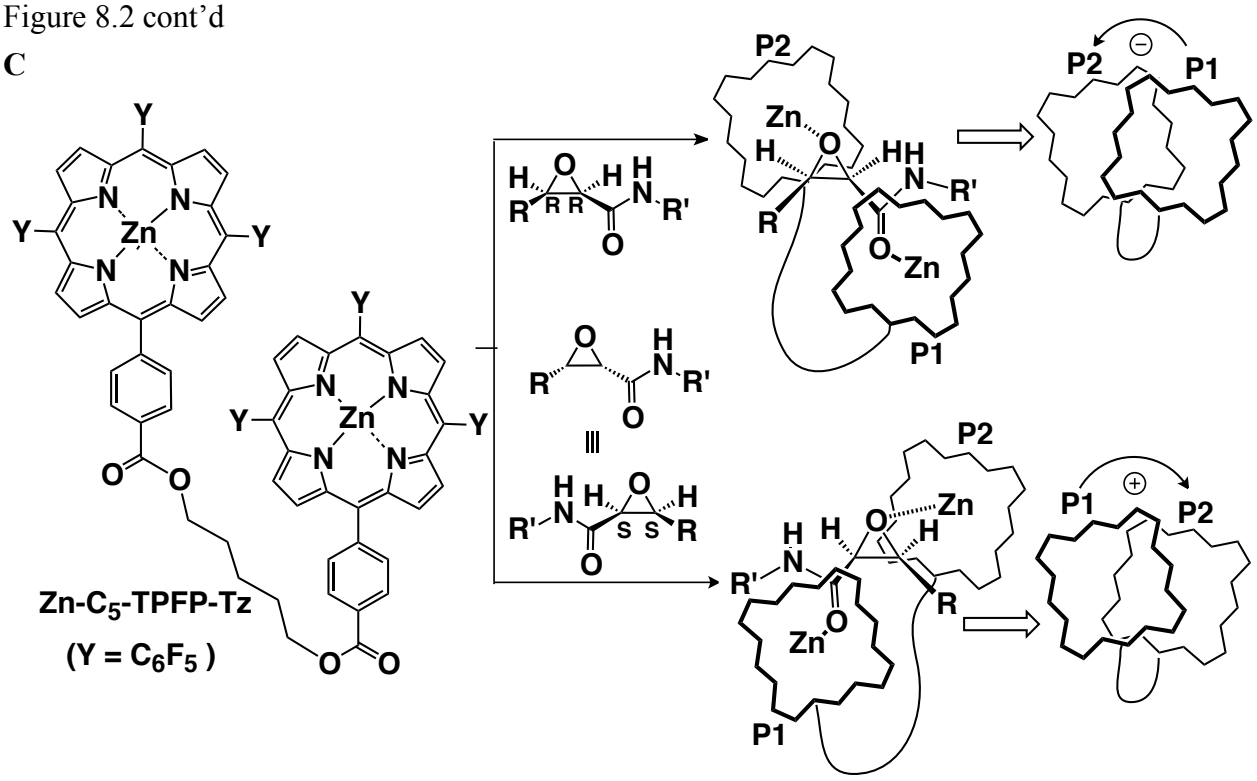

The host-guest, epoxide-tweezer, complex is formed by coordination of the epoxidic oxygen and the oxygen of the amide carbonyl to the zinc centers of the porphyrin tweezer. The sterics of the epoxide governs the overall rotation of the porphyrins relative to one another and the sign of the ECCD signal. As shown in Figure 8.2C, the rear porphyrin, P2, coordinates to rear face of the epoxide *via* the oxygen lone pair electrons. This rear face of the epoxide has two hydrogen substituents and so this porphyrin remains essentially static. The amide substituent is positioned to the front face of the epoxide; therefore, P1 approaches the molecule to the front face. Once bound, there is a steric interaction between the R group and the porphyrin forcing the porphyrin to rotate away from the R group. In the case of the (2*R*,3*R*) epoxides, P1 rotates clockwise and results in an overall counterclockwise orientation of P1 relative to P2 . Hence, for these epoxides, a negative ECCD signal is expected. For the enantiomeric (2*S*,3*S*) epoxides, an overall clockwise arrangement and a positive ECCD signal are expected. It was delightful to

observe the correct prediction of the absolute stereochemistry of *cis*-epoxide when compared to the already established absolute stereochemistry of (*S*,*S*)-**135g** *via* X-ray crystal structure. In fact, all the substrates do follow the proposed mnemonic.

In the case of *trans*-epoxide (minor product) obtained from the catalyst derived from the (*S*)-VANOL, the shown absolute configuration (Figure 8.3A) is based on a hypothetical mnemonic *that will require conformation by other means*. It is hypothesized that the rear porphyrin P2 binds to the epoxide to the rear face and rotates away from the R group. The front porphyrin binds to the carbonyl of the amide from the front face and rotates toward the hydrogen. This gives an overall clockwise helicity of the porphyrins and a positive sign is expected for *S,R* configured substrates and a negative signal for *R,S* substrates. Based on this hypothesis, the absolute configuration of the *trans*-epoxide is believed to be *R,S.*

Figure 8.3 Determination of absolute stereochemistry of *trans*-epoxide (*R*,*S*)-**135g**. (**A**) Observed ECCD amplitude for chiral *trans*-epoxide (*R*,*S*)-**135g**. All measurements were performed with 20 equivalents of the substrate and 1μM tweezer in hexanes at 0 ºC. (**C**) Proposed mnemonic explaining the signs of the observed ECCD signal.

A

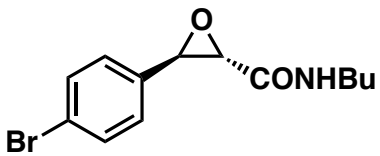

(R,S)-**135g** (20% ee)
A = –25

Figure 8.3 cont'd

B

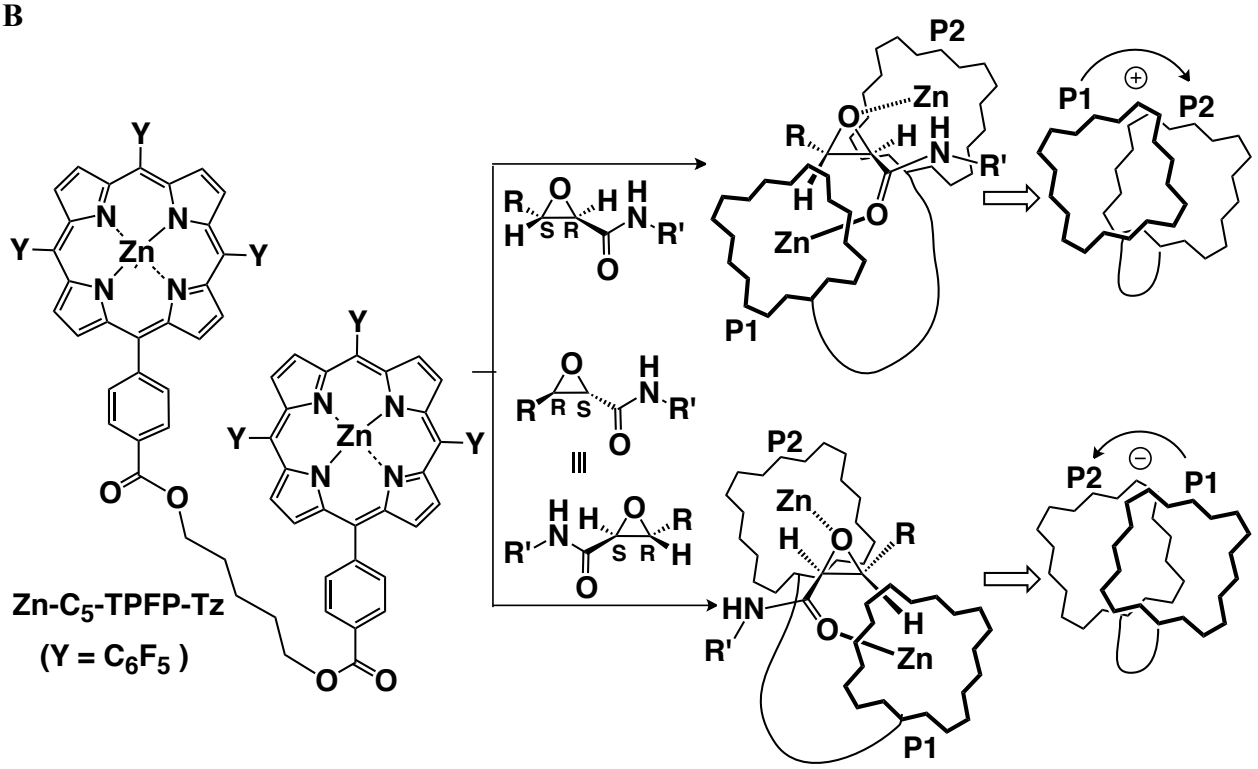

Finally, the absolute configuration of both the major (*cis*-epoxide) and minor (*trans*-epoxide) diastereomers have been determined using various techniques. Although, the absolute configuration of *trans*-epoxide needs to be confirmed by other means, it is quite surprising to observe opposite facial selectivity for *cis*- and *trans*-epoxide diastereomers using the catalyst derived from the same enantiomer of the ligand ((*S*)-VANOL in this case). To summarize, the *cis*-epoxide is obtained from a *Re* face attack of the diazoacetaamide on the aldehyde and the *trans*-epoxide is resulted from a *Si* face attack, when the catalyst derived from (*S*)-ligand is employed.

8.6 Mechanistic study towards the identification of the actual catalyst in the epoxidation reaction

A small amount of time of this doctoral research has been spent in the understanding of the

mechanism of the current catalytic asymmetric epoxidation reaction. A few of the experiments are described below.

8.6.1 Investigating non-covalent interactions

In the process of screening different diazo compunds, we found that the diazoacetamide **128c** derived from benzhydryl amine **126a** resulted the epoxide **443a** in 68% yield and 74%ee (Table 8.6, entry 1). This reflects an increase of 9% yield and 12% ee when compared to the epoxide **436a** (59% yield and 62%ee; Table 8.6, entry 2) obtained from the diazoacetamide **128b** derived from benzyl amine. This result indicates the possibility of certain non-covalent interactions (CH-π or π-π type) operating in the epoxidation reaction.

Up till now, we have used secondary diazoacetamide for the epoxidation reaction. In the case of aziridination reaction, it is observed that while diazoacetamides of the type **123/128** containing a secondary amide give *trans*-aziridines,[16] tertiary diazoacetamides lacking the N-H bond will react with a switch in the diastereoselectivity to give *cis*-aziridines.[16,18] The pertinent question thus becomes, will a tertiary diazoacetamide of type **442a** (Table 8.7) also reverse the diastereoselectivity to give the *trans*-epoxides? The answer is no. Surprisingly, *β*-keto amide **446a**[19] and its enol form were observed when the benzaldehyde **127a** was reacted with diazoacetamide **442a** (Table 8.6, entry 3). In fact, same was observed when a) the reaction was carried out with EDA **85**; b) the reaction was performed in the presence of commercial $B(OPh)_3$ only for all three cases. It suggests the importance of the secondary diazoacetamide for the successful realization of the catalytic asymmetric epoxidation reaction. Also, likewise the case of *trans*-aziridines,[20] it indicates the possibility of a potential hydrogen bonding interaction

between the catalyst and the N-H of the secondary diazoacetamide in the transition state of the reaction.

Table 8.7 N-H verses N-Me and O in the catalytic asymmetric epoxidation reaction

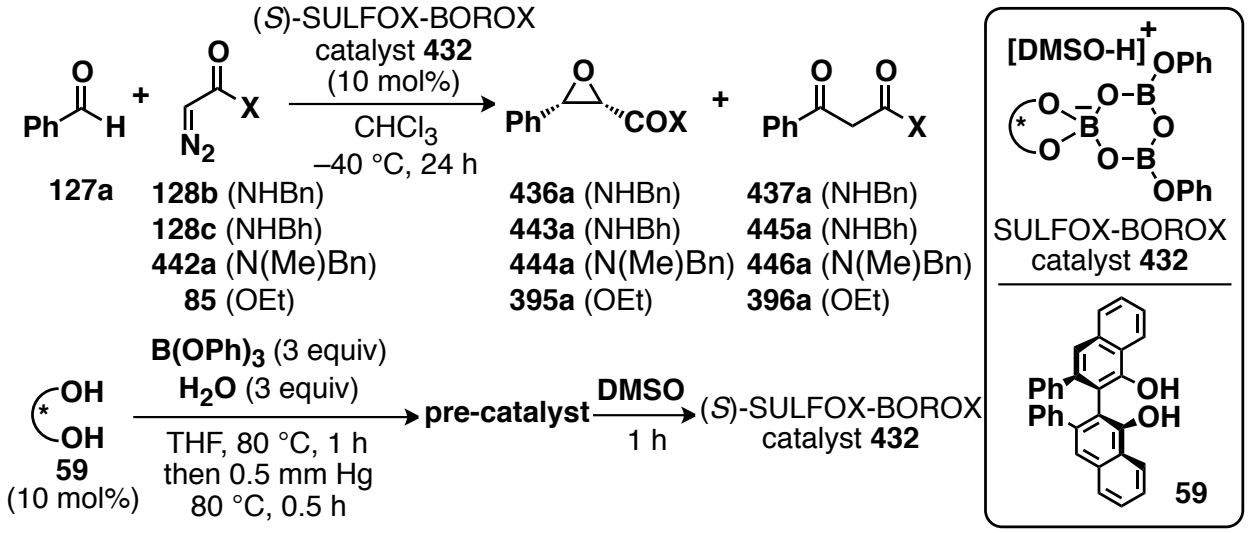

#	Diazo (X)	Yield epoxide (%) [b]	ee epoxide (%) [c]	*cis/trans* [d]	Yield *β*-keto amide (%) [e]
1	$NHCHPh_2$	65 (68)	74	>50:1	9.5
2	$NHCH_2Ph$	59 (55)	62	>50:1	15.5
3	$N(Me)CH_2Ph$	<1	–	–	25 [f]
4	OCH_2CH_3	<1	–	–	40

[a] Unless otherwise specified, all reactions were performed with 10 mol % SULFOX-BOROX catalyst **432** and 0.50 mmol diazoacetamide (1.25 equiv), 0.4 mmol benzaldehyde **127a** (1.0 equiv, 0.4 M) at –40 °C in $CHCl_3$. The pre-catalyst was prepared by heating 1 equiv of (*S*)-VANOL (10 mol %), 3 equiv of commercial $B(OPh)_3$ and 3 equiv of H_2O in THF at 80 °C for 1 h, followed by removing all volatiles under high vacuum (0.1 mm Hg) for 0.5 h at 80 °C. Thereafter, the SULFOX-BOROX catalyst **432** was prepared by stirring the pre-catalyst with 10 mol % DMSO in $CHCl_3$ for 1 h at 25 °C. [b] Determined by ^1H NMR spectra of the crude reaction mixture with Ph_3CH as internal standard. Yield in parenthesis is isolated yield. [c] Determined by HPLC. [d] Ratio determined by integration of the methine protons of *cis*- and *trans*-epoxide in the ^1H NMR spectrum of the crude reaction mixture. [e] Determined by ^1H NMR spectra of the crude reaction mixture with Ph_3CH as internal standard. [f] 50% yield of the enol form of **446a** was also observed.

8.6.2 Screening of a different catalytic system

We then decided to change the catalytic system in order to have a better understanding of the possible interactions of the substrate and the catalyst. One of the changes was the removal of the phenol component from the SULFOX-BOROX catalyst **432**. This would ideally result in a catalyst of type **447** (Scheme 8.8). Although the structure of the proposed catalyst is not confirmed, the epoxidation reaction resulted in epoxide **135g** in 85% yield and 90% ee with *cis:trans* = 55:1 using the catalyst **447**. Upon comparison to the reaction performed with catalyst **432**, a slight drop of 9% ee was observed in this case.

Scheme 8.8 Epoxidation reaction with catalyst **432** and **447**

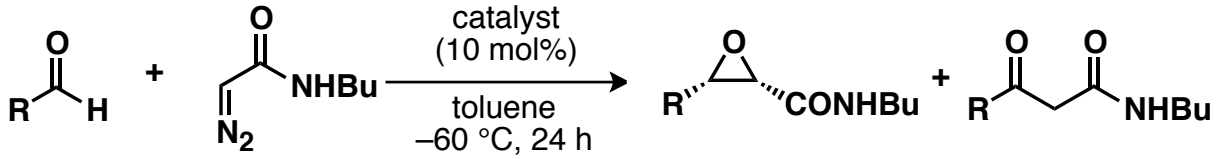

127g **128a** **135g** **136g**

R = 4-Br-C_6H_4

catalyst	%y	%ee	c:t	%y
432	88	99	>100:1	<1
447	85	90	55:1	1.4

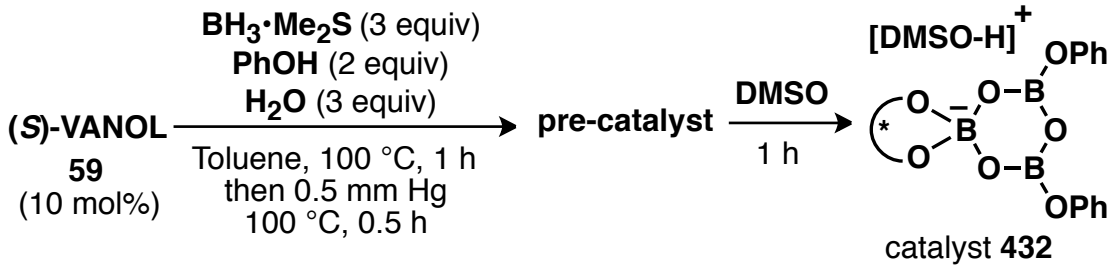

catalyst **432**

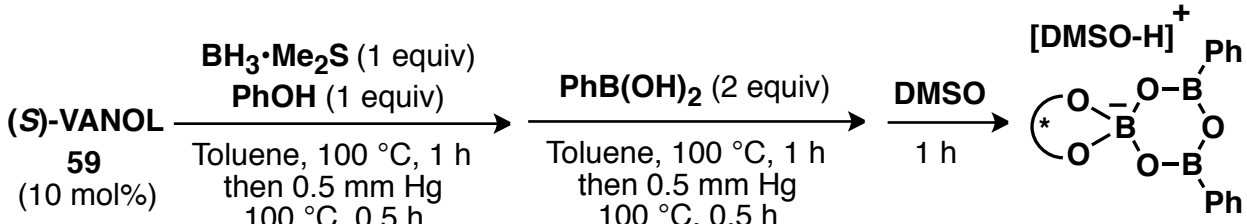

catalyst **447**

8.6.3 Catalytic asymmetric epoxidation reaction with and without DMSO

We have seen before that reaction also works in the absence of any base (Table 8.1, entry 1 and 8). The asymmetric induction observed in those cases was low as compared to the results obtained from SULFOX-BOROX catalyst **432** (Table 8.1, entry 6 *vs.* 9) respectively. At this point we became interested to employ newly optimized procedure and diazoacetamide **128a** for the epoxidation reaction where no base is used as an additive. Surprisingly, a drop of only 7% yield and 16% ee was noticed when the aldehyde was added prior to the addition of the diazoacetamide **128a** in the absence of DMSO (Table 8.8, entry 4 *vs.* 3). However, the difference was reduced to 8% when the order of the addition of the aldehyde and diazoacetamide was switched (Table 8.8, entry 6 *vs.* 5). Similar observation was made for *p*-bromobenzaldehyde **127g** (Table 8.8, entry 8 *vs.* 7). These intriguing results suggested the possibility of a different catalytic system where boroxinate of type **448a** is generated by the diazoacetamide **128a** itself, when there is no DMSO added. If this is true, then the epoxidation reaction would be similar to our aziridination reaction where the boroxinate catalyst is actual a substrate induced catalyst. However, a different mechanism along the idea of chiral Lewis acid type cannot be discarded.

Table 8.8 Catalytic asymmetric epoxidation with and without SULFOX-BOROX catalyst.[a]

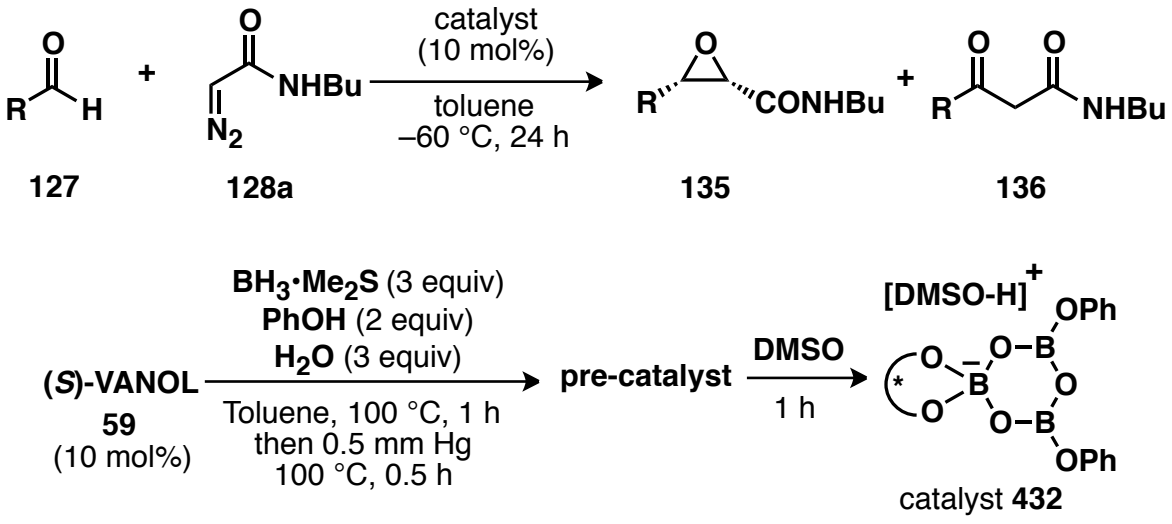

Table 8.8 cont'd

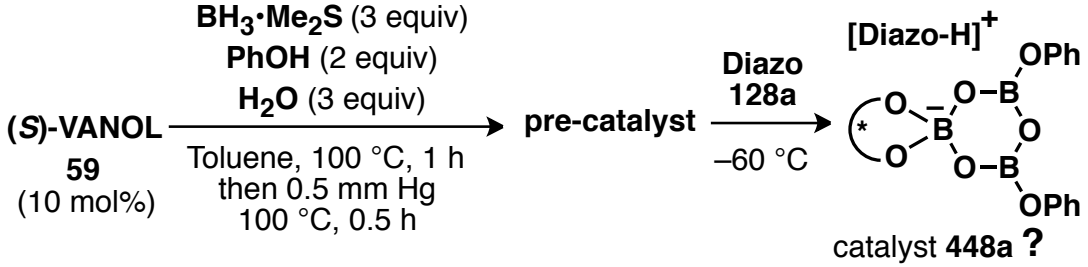

#	R	Base	Cat. (x mol%)	Yield **135** (%) [b]	ee **135** (%) [c]	c/t [d]	Yield **136** (%) [e]
1	C_6H_5	DMSO	**432** (5)	73 (75)	98	>100:1	2
2	C_6H_5	–	**448a** (5)	61 (60)	86	49:1	6
3	C_6H_5	DMSO	**432** (10)	82 (84)	98	>100:1	1
4	C_6H_5	–	**448a** (10)	75 (77)	82	49:1	9
5 [f]	C_6H_5	DMSO	**432** (10)	88 (90)	99.3	>100:1	<1
6 [f]	C_6H_5	–	**448a** (10)	78 (79)	90	55:1	5
7 [f]	4-Br-C_6H_4	DMSO	**432** (10)	88 (92)	99	>100:1	<1
8 [f]	4-Br-C_6H_4	–	**448a** (10)	86 (87)	91	56:1	2

[a] Unless otherwise specified, all reactions were performed with 10 mol % catalyst **432** or **448a** and 0.2 mmol diazo **128a** (1.0 equiv, 0.05 M), aldehyde **127** (1.1 equiv) at –60 °C in toluene. The pre-catalyst was prepared by by heating 1 equiv of (*S*)-VANOL (10 mol %), 3 equiv of BH_3•Me_2S, 2 equiv of PhOH and 3 equiv of H_2O in toluene at 100 °C for 1 h, followed by removing all volatiles under high vacuum (0.1 mm Hg) for 0.5 h at 100 °C. Thereafter, the catalyst **432** was prepared by stirring the pre-catalyst with 10 mol % DMSO in toluene for 1 h at 25 °C. And, the catalyst **448a** was prepared by stirring the pre-catalyst with 100 mol % diazoacetamide in toluene for 10 min at –60 °C. [b] Isolated Yield. Yield in parenthesis determined by ^{1}H NMR spectra with Ph_3CH as internal standard. [c] Determined by HPLC. [d] The *cis:trans* ratio is determined by integration of the methine protons of *cis*- and *trans*-epoxide in the ^{1}H NMR spectrum of the crude reaction mixture. [e] Determined by ^{1}H NMR spectra with Ph_3CH as internal standard. [f] Diazoacetamide added prior to the addition of aldehyde.

8.6.4 Temperature study

The role of the temperature in the asymmetric epoxidation was also examined and is presented in Table 8.9. This study was performed with 5 mol% catalyst loading. It is quite clear from the entries in Table 8.9 that the reaction slows down to a great extent at higher temperature. Only 31% yield of epoxide **135a** was obtained when the reaction was performed at room temperature (Table 8.9, entry 4). This corresponds to a difference of 44% yield compared to the reaction performed at – 60 ºC (Table 8.9, entry 1 *vs*. 4). Also, a decrease in *cis:trans* ratio was observed as the temperature of the reaction was increased.

Table 8.9 Screening of various temperatures for asymmetric epoxidation.[a]

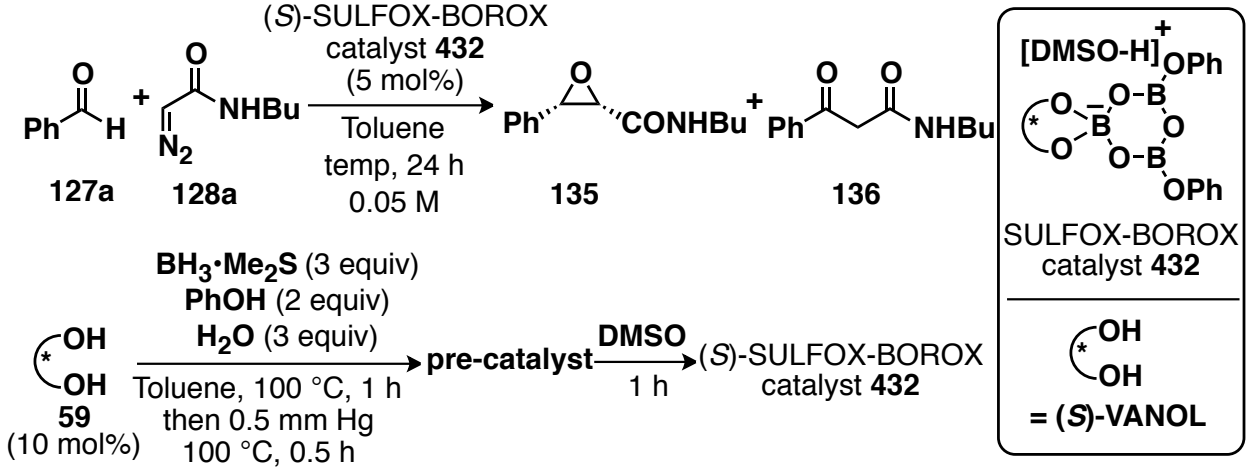

#	Temp (°C)	Yield **135a** (%) [b]	ee **135a** (%) [c]	*c:t* [d]	Yield **136a** (%) [e]	Yield **128a** (%) [e,f]
1	–60	75 (73)	98	>100:1	2.0	7
2	–40	51	–	81:1	7.0	24
3	–20	38	–	24:1	8.0	12
4	+25	31	–	16:1	6.0	19

[a] Unless otherwise specified, all reactions were performed with 5 mol % (*S*)-SULFOX-BOROX catalyst **432** and 0.2 mmol diazoacetamide (1.0 equiv, 0.05 M), 0.22 mmol benzaldehyde **127a** (1.1 equiv) at temp °C in the toluene. The (*S*)-SULFOX-BOROX catalyst **432** was prepared directly by stirring a mixture of 1 equiv of (*S*)-VANOL (10 mol %), 3 equiv of commercial $B(OPh)_3$ and 5 mol % DMSO in solvent for 1 h at 25 °C. The diazoacetamide

Table 8.9 cont'd

128a is added as a solution in toluene and added after the addition of benzaldehyde. [b] Yield is determined by ^{1}H NMR spectra with Ph_3CH as internal standard. Yield in parenthesis is isolated yield. [c] Determined by HPLC. [d] Ratio determined by integration of the methine protons of *cis*- and *trans*-epoxide in the ^{1}H NMR spectrum of the crude reaction mixture. [e] Determined by ^{1}H NMR spectra with Ph_3CH as internal standard. [f] unreacted diazoacetamide **128a**.

8.6.5 NMR Study

In order to have an understanding towards the identification of the catalytic system operational in the case where no base is employed, a detailed NMR study was performed. The aim of this study was to analyze the formation of the boroxinate using DMSO **221a** and diazoacetamide by locating the characteristic peaks for the boroxinate catalyst i.e. δ = ~ 5-6 ppm and ~ 8.5 ppm in ^{11}B NMR and ^{1}H NMR respectively (for VANOL derived catalyst). Using the procedure listed in Table 8.6, pre-catalyst was prepared and it was found to contain B1 **107**, B2 **109** and unreacted VANOL **59** in the ratio 1:1.5:0.2. A new doublet at δ = 8.66 ppm in the ^{1}H NMR spectrum was observed upon the addition of one equivalent of DMSO **221a** to the pre-catalyst at room temperature (Figure 8.4B, entry 3). Also, a peak at δ = 6.44 ppm in the ^{11}B NMR spectrum was observed (Figure 8.4C, entry 3). These observations suggest the formation of the SULFOX-BOROX catalyst **432**. There is also an up field shift (1.81 *vs*. 1.64) in the chemical shift of the methyl groups of DMSO **221a** possibly due to CH-π interaction (Figure 8.4D). No change in the ^{1}H NMR or ^{11}B NMR spectra was observed when one equiv of *p*-bromobenzaldehyde **127g** was added to the pre-catalyst (Figure 8.4B and 8.4C, entry 4). This result is supportive of the idea that aldehyde is not activated in the absence of DMSO **221a** or

diazoacetamide **128a**. When one equiv of diazoacetamide **128a** (solid or a solution in toluene) was treated with the pre-catalyst at room temperature, a tiny peak was observed at δ = 6.24 ppm in the ^{11}B NMR spectrum (Figure 8.4C, entries 6-7). However, a characteristic peak at δ = 5.91 ppm was observed when the same experiment was performed at –60 °C (Figure 8.4C, entry 8). Another interesting feature of the ^{11}B NMR was the shift in the tri-coordinate boron atoms (δ = 10.11 ppm) at –60 ºC in d_8-toluene (Figure 8.4C, entry 9). The same peak is observed at δ = 17.19 at room temperature (Figure 8.4C, entry 7). The corresponding ^{1}H NMR did show a broadening at ~ δ = 8.5 ppm, however, it was not conclusive. Nonetheless, initial experiments do suggest the possibility of the BOROX catalyst, perhaps, induced by the diazoacetamide itself.

Figure 8.4 (**A**) DMSO **221a** and diazoacetamide **128a** induced boroxinate formation. (**B**)[a] ^{1}H NMR spectra of the reaction mixture in d_8-toluene. (**C**) ^{11}B NMR spectra corresponding to entries in the ^{1}H NMR spectra in Figure 8.4B. (**D**) ^{1}H NMR spectra (methyl region); Entry 1. Pure DMSO **221a** in d_8-toluene. Entry 2: same as entry 3 in the ^{1}H NMR spectrum in Figure 8.4B.

A

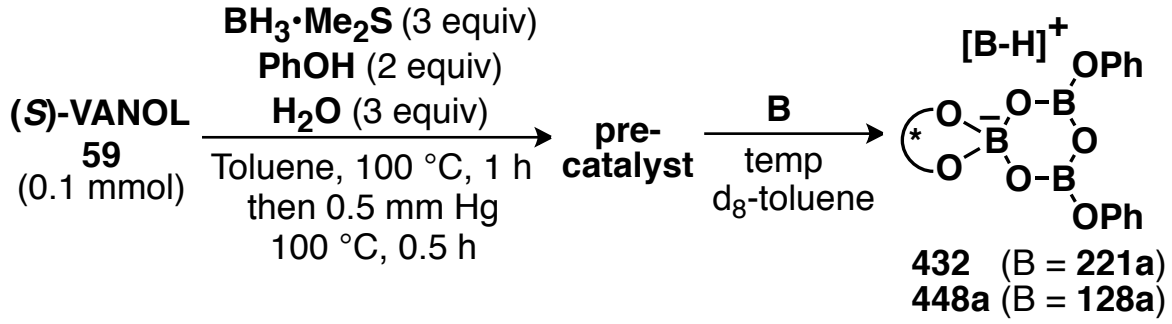

Figure 8.4 cont'd

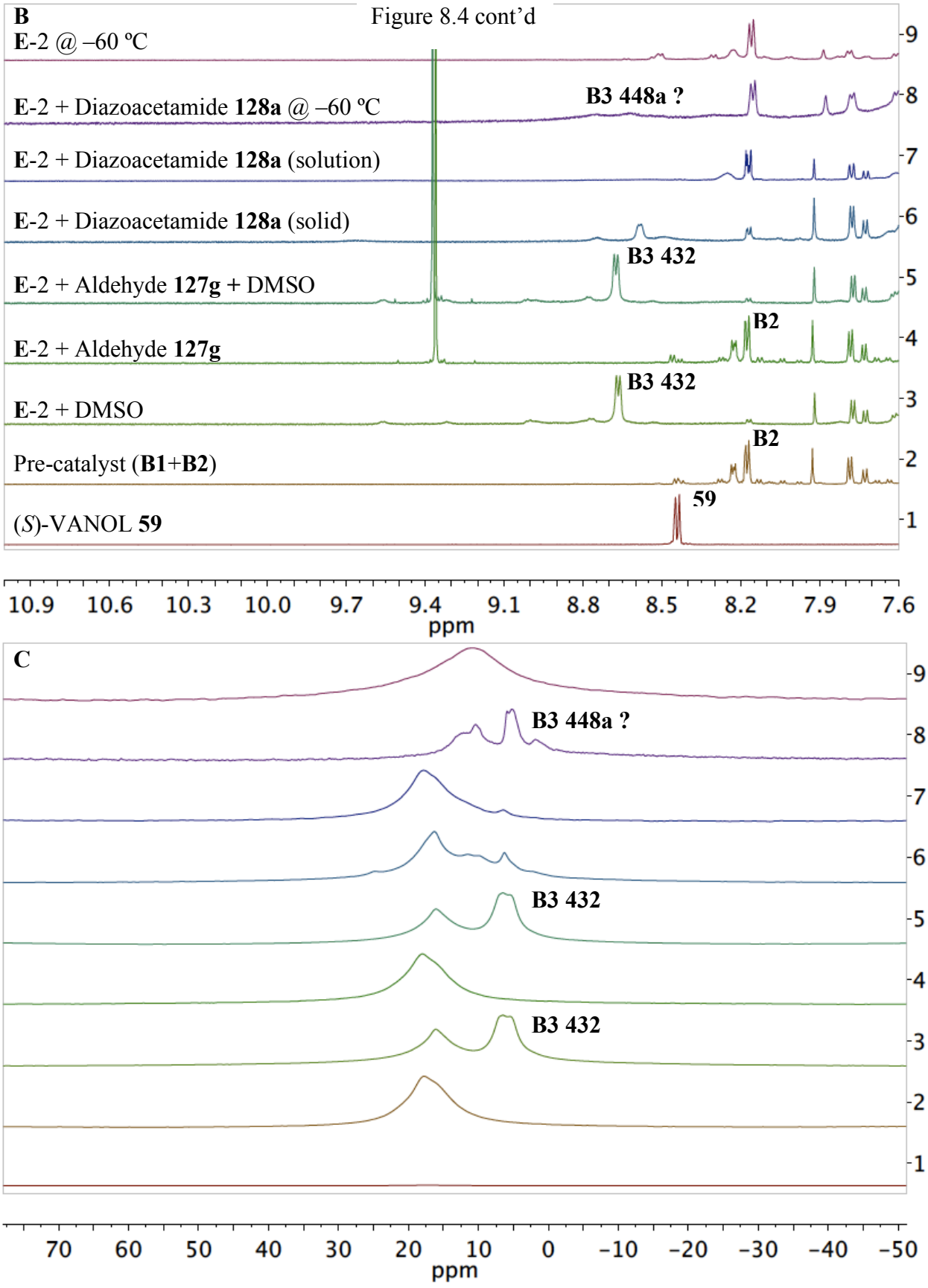

Figure 8.4 cont'd

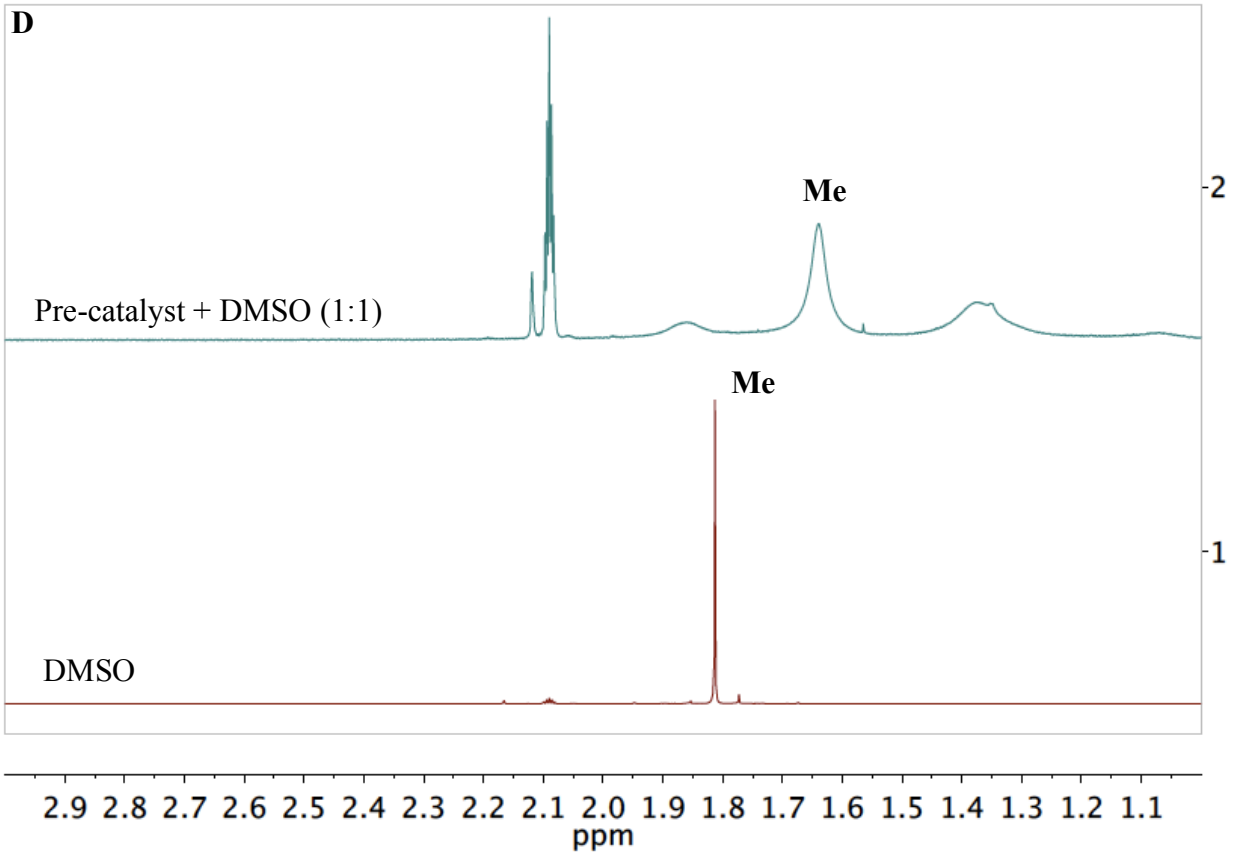

[a] Note for Figure 8.4B: Entry 1: pure (*S*)-**59**. Entry 2: (*S*)-**59** (0.1 mmol) plus 3 equiv BH_3•Me_2S **192a**, 2 equiv PhOH and 3 equiv H_2O were heated at 100 °C in toluene for 1 h followed by removal of volatiles under vacuum for 0.5 h. Entry 3: 1.0 equiv of DMSO **221a** and d_8-toluene (1 mL) was added to the entry 2 (pre-catalyst) for 10 min at 25 °C. Entry 4: 1.0 equiv of *p*-bromobenzaldehyde **127g** and d_8-toluene (1 mL) was added to the entry 2 (pre-catalyst) for 10 min at 25 °C. Entry 5: 1.0 equiv of DMSO **221a** was added to the entry 4 for 10 min at 25 °C. Entry 6: 1.0 equiv of diazoacetamide **128a** and d_8-toluene (1 mL) was added to the entry 2 (pre-catalyst) for 10 min at 25 °C. Entry 7: 1 mL of d_8-toluene was added to the pre-

catalyst followed by the addition of 1.0 equiv of diazoacetamide **128a** as a solution in d_8-toluene (1 mL) for 10 min at 25 °C. Entry 8: 1 mL of d_8-toluene was added to the pre-catalyst and the resulting solution was cooled to –60 ºC. Thereafter, a pre-cooled (–60 ºC) solution of 1.0 equiv of diazoacetamide **128a** in d_8-toluene (1 mL) was added and the NMR was taken at –60 ºC. Entry 9: 1 mL of d_8-toluene was added to the pre-catalyst and the resulting solution was cooled to –60 ºC. Thereafter, the NMR was taken at –60 ºC.

8.6.6 Calculated structures of boroxinate catalysts from DMSO and diazoacetamides

While looking for the possibility of the boroxinate generated by diazoacetamide **128a** and DMSO using the VANOL ligand, we decided to compute the probable structures of **432**, **448a** (Diazo = **128a**) and **448′a** (Diazo = **123a**). Calculations were preformed using Gaussian 03 at B3LYP/6-31g* level of theory.[21] The resulted structures are presented in Figure 8.5. Likewise the case of the calculated structure of the BOROX catalyst **222a** derived from DMSO and the VAPOL ligand, we observed two probable CH-π interactions between the methyl groups of DMSO and the naphthalene ring of the VANOL ligand (Figure 8.5A, d_2 = 3.89 Å and d_3 = 3.63 Å). The boroxinate **448a** and **448′a** from diazoacetamides **128a** and **123a** were also computed and presented in Figure 8.5C-F.

Figure 8.5[a] Calculated structure of SULFOX-BOROX catalyst **432**, DIAZO-BOROX catalyst **448a** and **448′a** using Gaussian ′03. They are visualized by the Mercury Program (C, gray; O, red; S, orange; B, yellow; H, white). Hydrogen atoms omitted for clarity (except protonated DMSO and diazoacetamides).

Figure 8.5 cont'd

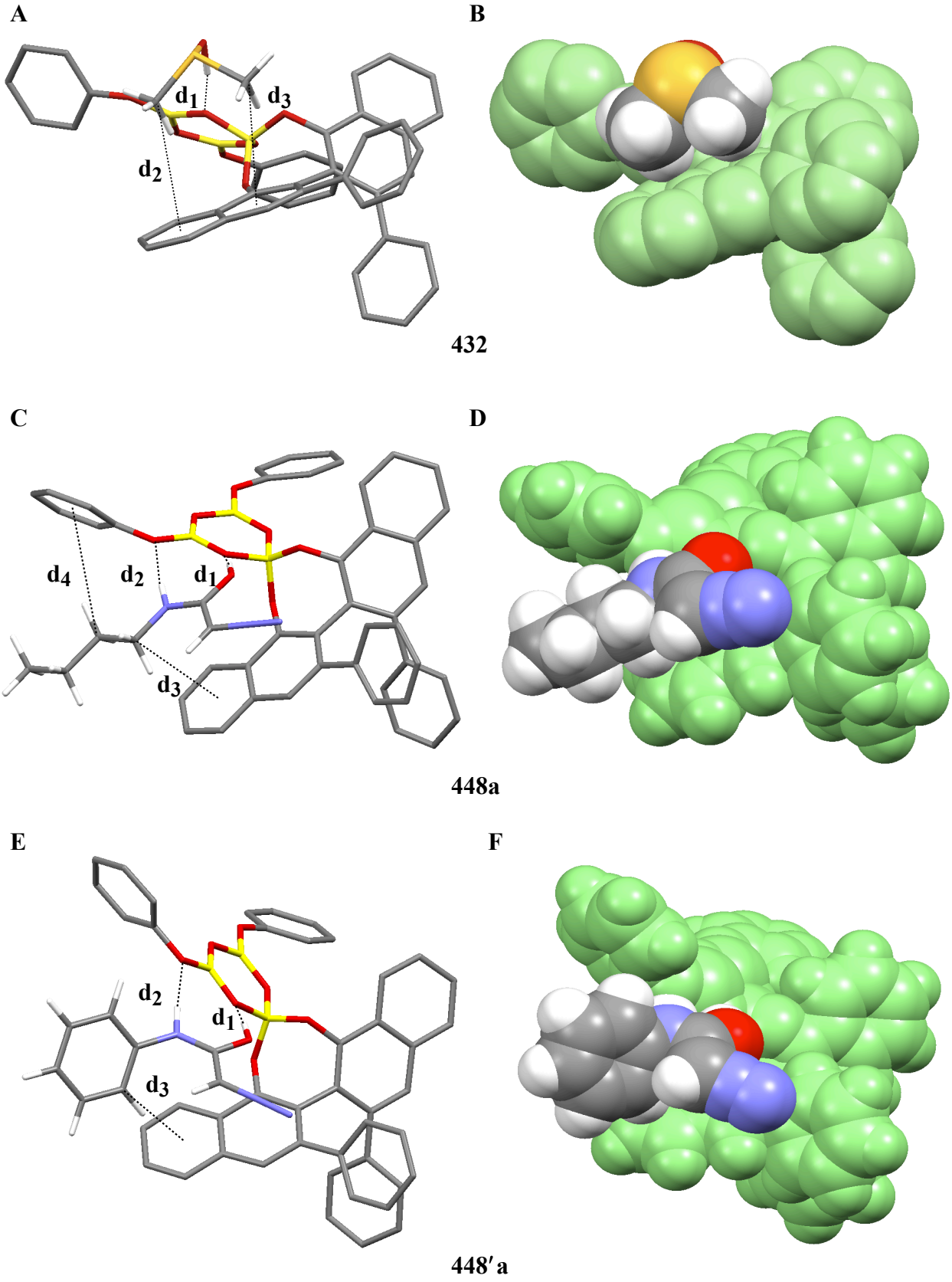

[a] Note for Figure 8.5**:** (**A**) Calculated B3LYP/6-31g* structure of **432**. Some secondary interactions are highlighted: d_1 = 1.44 Å (H-bonding), d_2 = 3.89 Å (CH-π), d_3 = 3.63 Å (CH-π). (**B**) Space-filling rendition of **432** with the same orientation and showing hydrogens. The boroxinate anion is given in green and the protonated DMSO is in traditional colors. (**C**) Calculated B3LYP/6-31g* structure of **448a**. Some secondary interactions are highlighted: d_1 = 1.50 Å (H-bonding), d_2 = 1.92 Å (H-bonding), d_3 = 3.95 Å (CH-π), d_4 = 4.51 Å (CH-π). (**D**) Space-filling rendition of **448a** with the same orientation and showing hydrogens. The boroxinate anion is given in green and the protonated **128a** is in traditional colors. (**E**) Calculated B3LYP/6-31g* structure of **448′a**. Some secondary interactions are highlighted: d_1 = 1.47 Å (H-bonding), d_2 = 1.85 Å (H-bonding), d_3 = 4.02 Å (CH-π). (**F**) Space-filling rendition of **448′a** with the same orientation and showing hydrogens. The boroxinate anion is given in green and the protonated **123a** is in traditional colors.

In the case of the possible boroxinate **448a** generated from diazoacetamide **128a**, two potential hydrogen bonding interactions were located (Figure 8.5C, d_1 = 1.50 Å and d_2 = 1.92 Å). Additionally, we observed two probable CH-π interactions between the methylene units of the diazo compound and the boroxinate ring (Figure 8.5C, d_3 = 3.95 Å and d_4 = 4.51 Å). Similarly, boroxinate **448′a** generated from diazoacetamide **123a** also revealed two potential hydrogen bonding interactions (Figure 8.5E, d_1 = 1.47 Å and d_2 = 1.85 Å) and one probable CH-π interaction (Figure 8.5E, d_3 = 4.02 Å).

8.6.7 Possible rationale for the observed stereochemical outcome of asymmetric epoxidation reaction

Although, we do not have any concrete evidence for the mechanism for the epoxidation reaction yet, there are some proposals based on the initial mechanistic findings during this doctoral research. These proposals are explained below.

8.6.7.1 With DMSO

When the reaction is performed with (*S*)-SULFOX-BOROX catalyst, two mechanisms can be proposed via; a) Brønsted acid catalysis (model I) b) Brønsted acid-assisted Lewis acid catalysis (model II). In both the models, hydrogen bonding interactions between the substrates and the catalyst have been assumed and point of interactions (oxygens (O1-O3) on the boroxinate anion) can be different from that shown in the Figure 8.6. The shift in the hydrogen bonding between DMSO and boroxinate anion from O2 to O1 has been proposed based on the similar studies reported on the aziridination reaction by our group.[20] In model I, both reactants are held by the hydrogen bonding and an extra hydrogen bonding stabilization comes from the secondary diazoacetamide. The third H-bond involving the diazoacetamide is crucial given the observation that there is no reaction when tertiary diazoacetamide is utilized. Also, the diazoacetamide is proposed to attack from the *Re* face of the aldehyde based on the absolute stereochemistry of the *cis*-epoxide. For *trans*-epoxide, the facial selectivity has been switched i.e. the *Si* face attack has been proposed to be favorable (Figure 8.6B). The proposed model suggests that the approach of diazoacetamide leading to the *cis*-epoxide in more favorable compared to *trans*-epoxide due to the dipolar interaction between the N_2^+ on the diazoacetamide and the carbonyl oxygen on the aldehyde. In the case of model II, the interactions were assumed

to be similar to model I except the interaction between the aldehyde and catalyst. The aldehyde is proposed to be coordinated to the sulfur of the DMSO as the Lewis acid-Lewis base complex.

Figure 8.6 Proposed models (I and II) for the mechanisms involving (*S*)-SULFOX-BOROX catalyst (derived from (*S*)-VANOL) leading to (**A**) *cis*-epoxide (**B**) *trans*-epoxide

A

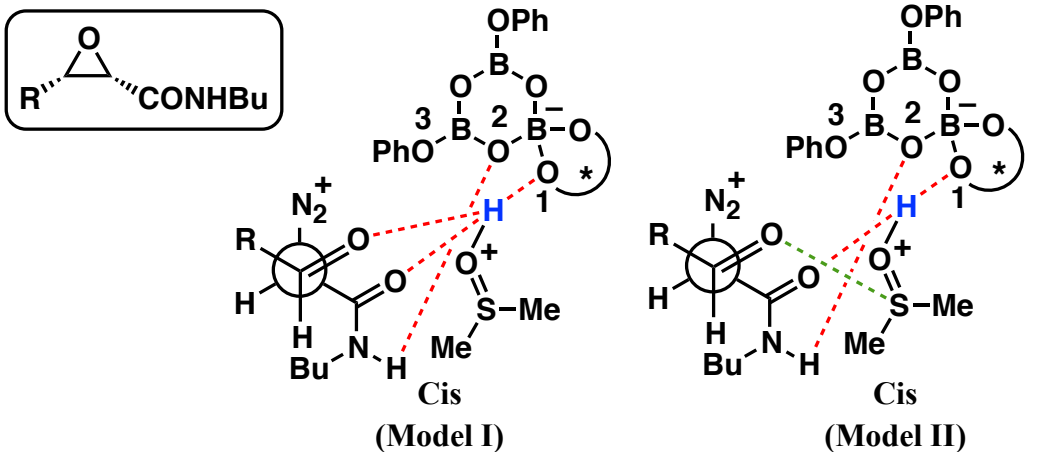

B

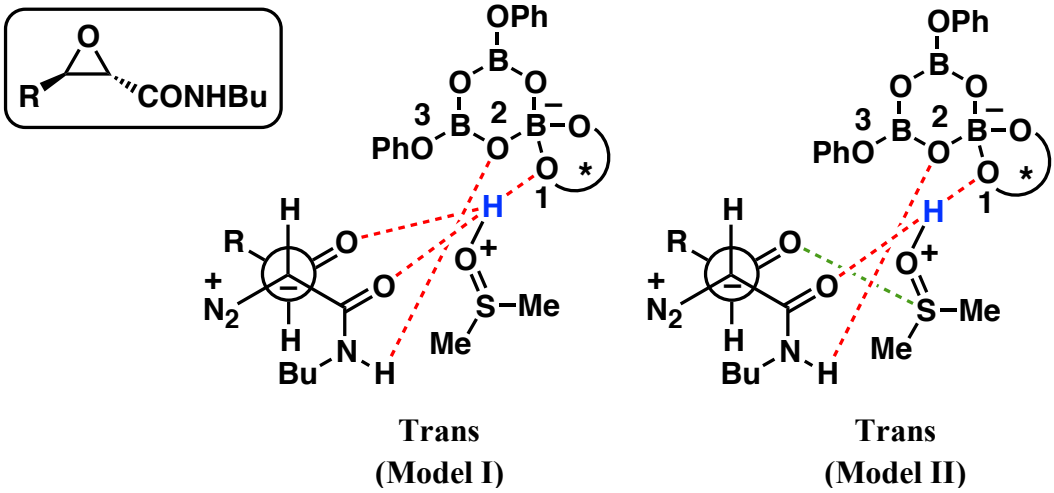

8.6.7.2 Without DMSO

As shown earlier, that the reaction works well even in the absence of SULFOX-BOROX catalyst. In those cases, preliminary NMR studies suggest the possibility of the DIAZO-BOROX

catalyst of type **448a** (Figure 8.5B). After initial assumption of the formation of **448a**, the working model III has been proposed and shown in Figure 8.7. In addition to **448a**, it has been proposed that the aldehyde is either hydrogen bonded to O1 (red in color) or O2 (green in color). As discussed earlier, an extra hydrogen bonding stabilization is proposed to be present due to the hydrogen bonding between the boroxinate core and the secondary diazoacetamide.

Figure 8.7 Proposed model III for the mechanism involving (*S*)-DIAZO-BOROX catalyst (derived from (*S*)-VANOL) leading to both *cis*-epoxide and *trans*-epoxide.

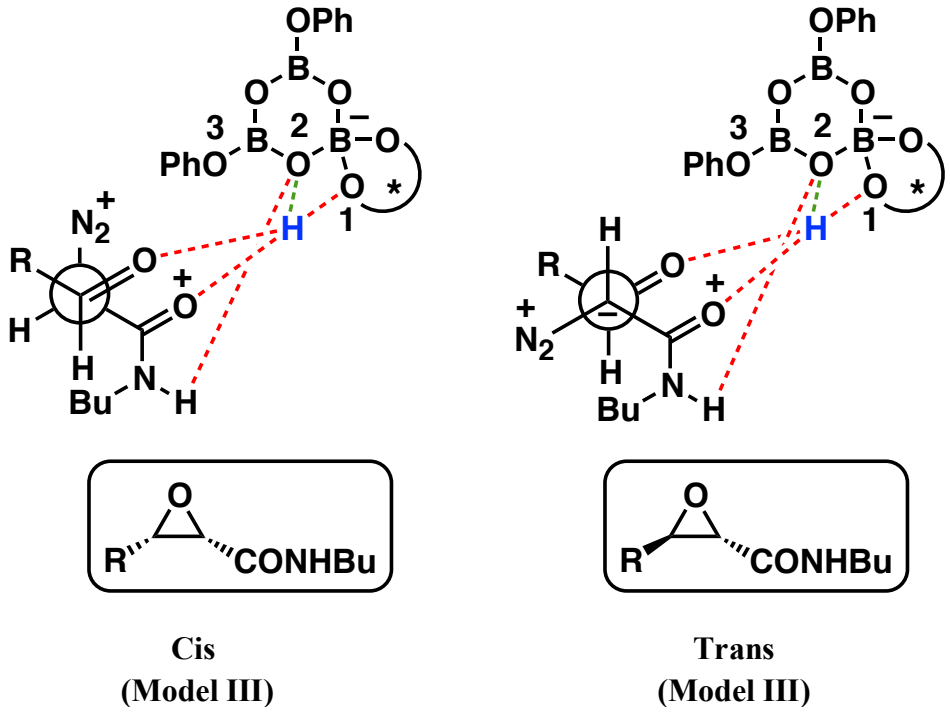

8.6.7.3 Lewis acid catalysis

Last but not the least, a completely different mechanism along the idea of chiral Lewis acid type cannot be discarded. In fact, as shown in Figure 8.8, a fourth model is proposed where a chiral Lewis acid in involved in the active site. As of now, the structure of the chiral Lewis cannot be predicted. It may or may not involve DMSO in the active site. However, it seems like

that there is a possibility of a hydrogen bonding site for the hydrogen bond with the secondary diazoacetamide.

Figure 8.8 Proposed model IV for the mechanism involving chiral Lewis catalyst (derived from (*S*)-VANOL) leading to both *cis*-epoxide and *trans*-epoxide.

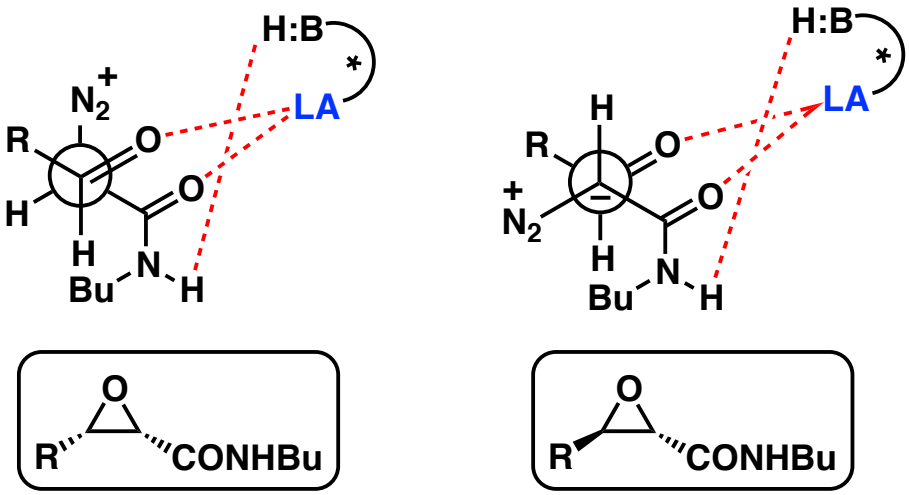

Cis
(Model IV)

Trans
(Model IV)

In all models proposed above, transoid transition structures have been assumed to be operating, however, there is no evidence to exclude cisoid transition structures. The mechanistic investigations regarding asymmetric epoxidation reaction discussed in this chapter is still in its infant state. Hopefully, future studies will reveal the actual catalyst involved in this case.

8.6.8 Kinetic Isotopic effect studies of asymmetric epoxidation reaction

In order to probe further the mechanism of the catalytic asymmetric epoxidation reaction, we decided to probe the transition state geometry of the rate-limiting step using ^{13}C kinetic

isotope effects (KIE) measured at natural abundance using the Singleton protocol.[22] As shown in Scheme 8.9A, the epoxidation reaction is generally assumed to go through a two step mechanism with addition of the diazoacetamide **128a** to the *p*-bromobenzaldehyde **127g** to form the diazonium ion intermediate (step I) followed by SN_2-like elimination (step II) of N_2 by the intramolecular nucleophile (the alkoxide). In the given mechanism, transoid transition structures have been assumed to be operating, however, there is no evidence to exclude cisoid transition structures (Scheme 8.9A). If the first step were rate-limiting, a significant KIE would be observed at the aldehyde carbon atom of *p*-bromobenzaldehyde **127g** while rate-limiting SN_2-like attack would result in a much smaller KIE on the aldehyde carbon. An additional benefit of such a high resolution picture of the transition state geometry is that differences in the transition state geometry with and without the DMSO additive can be probed effectively. With these goals in mind, we performed two experiments - one with and one without DMSO - where we took the starting *p*-bromobenzaldehyde to 80+/–2% conversion (Scheme 8.10). The unreacted *p*-bromobenzaldehyde **127g** was recovered and its isotopic composition was compared to that of *p*-bromobenzaldehyde **127g** from the same bottle, which was not subjected to the reaction conditions. From the relative ^{13}C content at each carbon atom for the two samples and the fractional conversion, the ^{13}C KIEs for each carbon of *p*-bromobenzaldehyde **127g** was computed using the equation given in Scheme 8.9B.

Scheme 8.9 (**A**) General mechanism of the epoxidation reaction of aldehydes and diazoacetamides catalyzed by our catalyst. (**B**) Equation used for the calculation of the ^{13}C KIE values.

A

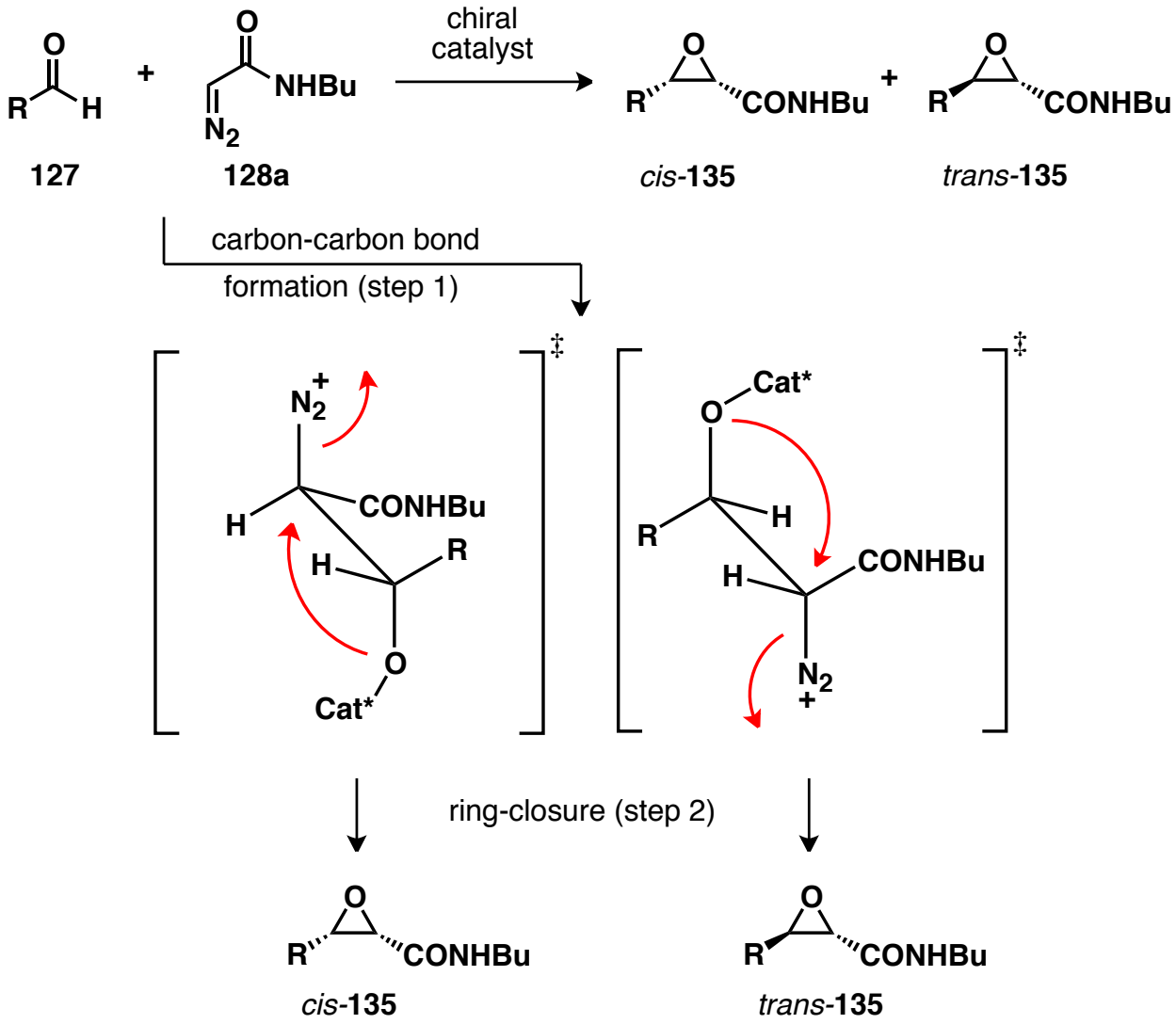

B

$$KIE = \frac{\ln(1-F)}{\ln[(1-F)(R/R_o)]}$$

F = fractional conversion

R/R_o = ratio of the ^{13}C in aldehyde prior to and after reaction as determined by quantitative ^{13}C NMR.

For the reaction with added DMSO, the aldehyde carbon exhibited a KIE of 1.025 (8) while for the reaction without DMSO, a KIE of 1.030 (6) was measured. The number in parenthesis is the uncertainty in the last digit of the measurement obtained with 95% confidence from 6 independent measurements. All other carbon atoms exhibited KIEs within error of unity. The qualitative interpretation of the KIEs is that the aldehyde carbon atom is involved in the rate-limiting transition state and assuming the above mentioned two-step mechanism, the carbon-carbon bond forming (step I) is the *rate-limiting step*. The quality of the NMR results was not sufficient to ascertain the slight difference between the experiments performed with and without DMSO but the different values suggest that the addition of DMSO slightly alters the transition state geometry (especially since the KIEs for the other carbon atoms are nearly identical). Further validation of these results can be obtained by calculation of the transition state and theoretical prediction of the ^{13}C KIEs.

8.7 Gram scale catalysis and large scale synthesis

The real application of any methodology lies in its easy adaption towards the large-scale synthesis. The catalytic asymmetric epoxidation was easily applicable to gram scale (Scheme 8.10). The large scale synthesis (4.8 mmol in diazoacetamide **128a**) was performed using the catalysts **432** (with DMSO) and **448a** (without DMSO). The same reaction was utilized in obtaining the sample of the unreacted *p*-bromobenzaldehyde **127g** for the KIE studies (section 8.6.8). The only downfall of the large scale reaction was the drop in the ee by ~9–11% in both the cases. However, the enantiomeric excess can easily be increased up to 99% ee by a single crystallization. It is advisable to reproduce this result so as to check whether the drop in ee is genuine or is actually an experimental error.

Scheme 8.10 Gram scale asymmetric catalysis

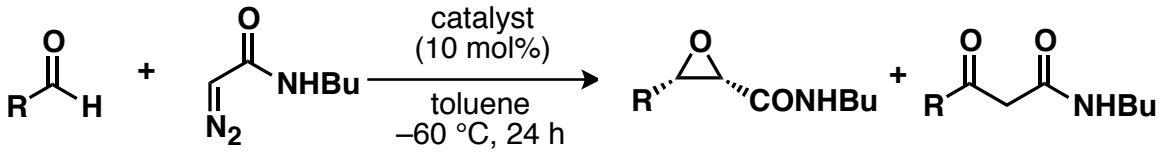

127g (6.0 mmol) **128a** (4.8 mmol) **135g** **136g**

R = 4-Br-C_6H_4

catalyst	%y **135g**	%ee before recryst **135g**	%ee 1st Crop **135g**	%yield 1st Crop **135g**	*c:t*	%y **136g**
432 (with DMSO)	78	90	99	65	30:1	5
448a (without DMSO)	70	79	97	60	15:1	13

In order to perform the large scale epoxidation reaction, we needed a large quantity of the diazoacetamide **128a**. Since, the same diazo compound has been the used in all the epoxidations we performed, we thought of devising an easy and economic route to prepare diazoacetamide **128a**. In doing so, we came across the large scale synthesis of the parent diazo compound i.e. succinimidyl diazoacetate **454**. This compound has been widely used in the synthesis of various diazo compounds.[23] The synthesis of this compound was reported via DCC coupling of the acid **451** and *N*-hydroxy succinimide **453**.[23] The reported procedure was often low yielding and irreproducible. In fact, the purification involved several column chromatographies and was too cumbersome. So, we decided to follow another reported procedure that involved the synthesis starting from acid chloride **452**.[24] We prepared the acid chloride **452** in large quantities (210 mmol scale) using a reported procedure.[25] Delightfully, the synthesis of **454** (50 mmol scale)

was found to be much cleaner using the second procedure where the reaction was started with acid chloride **452**. The crude succinimidyl diazoacetate **454** was purified by crystallization only. Thereafter, the diazoacetamide **128a** was prepared on a large scale (40 mmol) in 90–93% yield. The entire process of preparation of diazo compounds **454** and **128a** was carried out efficiently without the use of any column chromatography purification.

Scheme 8.11 Large scale synthesis of diazo compounds **454** and **128a**

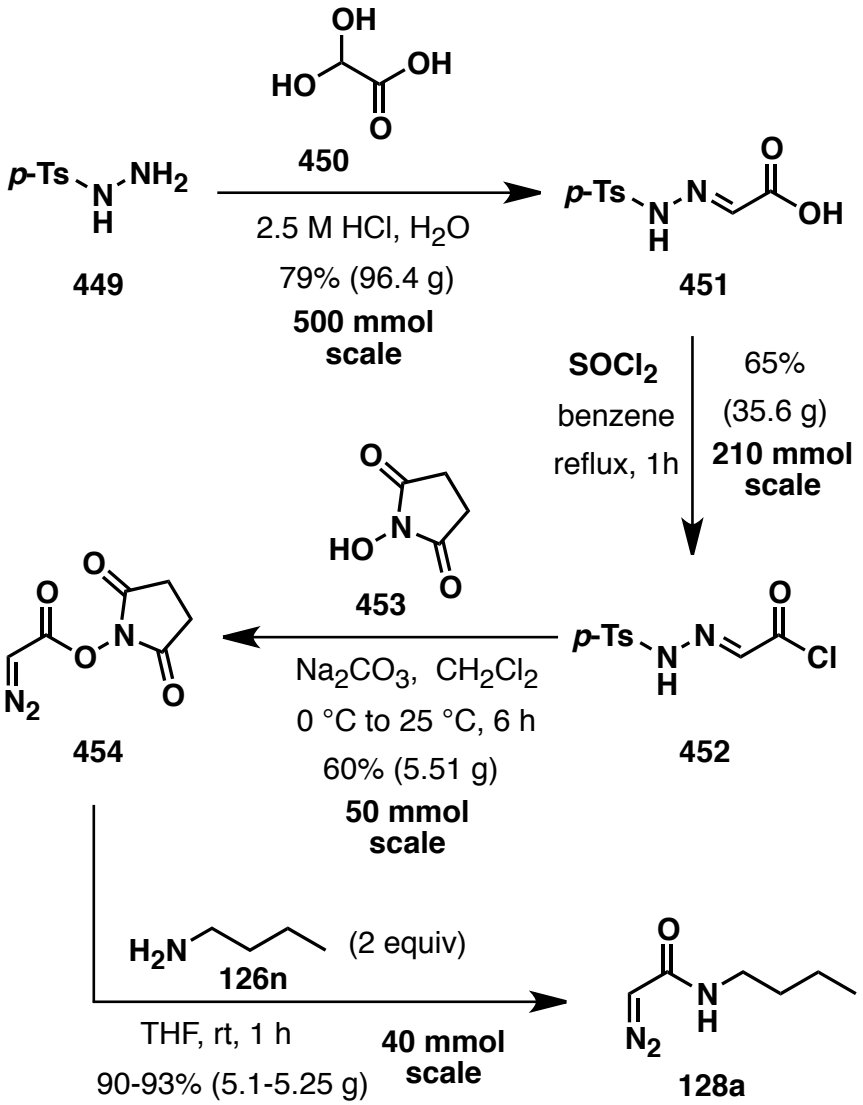

8.8 Conclusions

We have been able to successfully realize the catalytic asymmetric epoxidation of the aldehydes, probably, using either SULFOX-BOROX catalyst or DIAZO-BOROX catalyst. Although the mode of catalysis has not been completely determined, it seems that the reaction is potentially is a Brønsted acid catalyzed reaction based on the initial studies towards the mechanism of the reaction. Also, it is quite general for a wide range of aldehydes in terms of substrate group.

APPENDIX

8.9 Experimental

8.9.1 General Information

Same as Chapter 2.

8.9.2 Synthesis of diazoacetate 450, diazoacetamides 123a-b and 128a-f

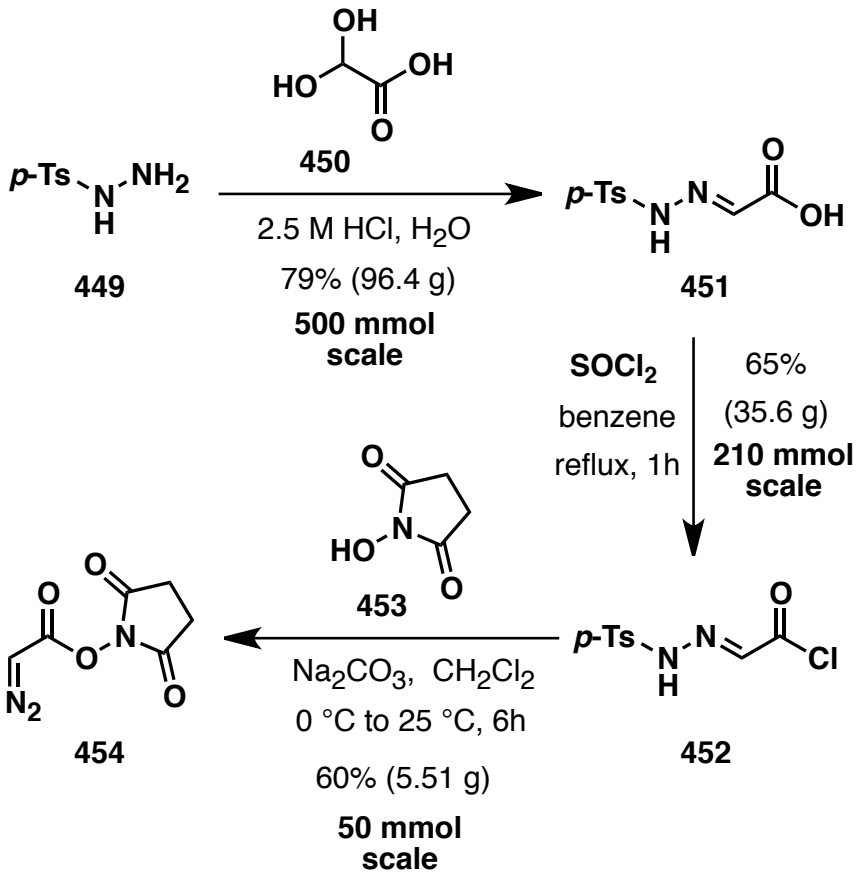

2-(2-tosylhydrazono)acetic acid 451: To a 1 L single-necked round bottom flask was added glyoxylic acid monohydrate **450** (46.3 g, 500 mmol) and water (500 mL). The mixture was stirred at 65 ºC (oil bath) until **450** dissolved completely. To this solution was then added a warm suspension (at approximately 65ºC) of *p*-toluenesulfonylhydrazide **449** (93.1 g, 500 mmol) in 2.5 M aqueous hydrochloric acid (300 mL). The reaction mixture was stirred at 65 ºC for 15 min, then allowed to cool to room temperature gradually until all of the oil solidified and then the flask was kept in a refrigerator overnight. The crude product was collected on filter paper using a Büchner funnel (8 cm diameter), washed with cold water (70 mL), and dried for 2 days in open

air followed by exposure to high vacuum overnight. To a 1 L single-necked round bottom flask containing acid **451** and equipped with a stir bar and with a condenser was added boiling EtOAc until the entire solid dissolved. Hexanes were added until the solution became cloudy. Thereafter, hot EtOAc was added until it just became clear again. The solution was then allowed to cool to room temperature and then allowed to set in a refrigerator overnight (–20 ºC). The solid was filtered and washed with ice-cold 1:2 EtOAc/hexanes to afford **451** as a white solid (mp 150-152 ºC) in 79% isolated yield (96.4 g, 400 mmol).

Spectral data for **451**: R_f = 0.45 (1:1, EtOAc/hexane); ^{1}H NMR ($CDCl_3$, 300 MHz) δ 2.39(s, 3H), 7.29 (s, 1H), 7.40 (d, 2H, J = 8.5Hz), 7.78 (d, 2H, J = 8.3Hz), 10.05 (brs, 1H), 11.00 (brs, 1H); ^{13}C NMR (CD_3COCD_3, 75 MHz) δ 21.37, 128.42, 130.57, 136.81, 137.28, 145.28, 163.72. These spectral data match those previously reported for this compound.[18]

2-(2-tosylhydrazono)acetyl chloride 452: To a suspension of acid **451** (50.2 g, 210 mmol) in benzene (250 mL) was added $SOCl_2$ (30 mL, 420 mmol, freshly distilled). The reaction mixture was heated to reflux (90 ºC oil bath) until vigorous gas evolution has ceased and most of the suspended solid has dissolved (~2 h). *The heating period is critical to the success of this reaction. After a heating period of 45-90 minutes the initially white suspension begins to turn yellow and the color gradually deepens as heating is continued. The correct heating period is normally reached about 10 minutes after vigorous gas evolution ceases; at this time the color of the reaction mixture is yellow-orange to orange. At this point the mixture is not clear, but relatively little suspended material separates when the stirrer is stopped for a short period. If heating is stopped too soon, a large amount of acid is lost during the filtration and the product is*

difficult to crystallize. If heating is continued too long, the product is contaminated with a brown colored impurity and is difficult to crystallize. The reaction mixture then was cooled under nitrogen and filtrated through a Celite pad on a sintered-glass funnel. After the filtrate has been concentrated to dryness under reduced pressure, the residual solid is mixed with anhydrous benzene (50 mL, warmed to ~40 to 50 ºC), and the solid mass was broken up to give a fine suspension. The suspension was cooled and filtered quickly using a Büchner funnel (8 cm diameter) and then the solid was washed quickly with cold benzene (30 mL × 2) to remove most of the residual colored impurities. The combined filtrates were stripped of solvent on the rotovapor and the residue was washed quickly with cold benzene (30 mL × 2) to give a second crop of the crude product. Purification by crystallization was achieved by dissolving the crude product in boiling benzene (~100 mL), followed by the addition of hexanes (~100 mL, bp. 60-90 ℃). The mixture was allowed to cool down to room temperature, and stand overnight. The acid chloride **452** was collected as a white solid (mp. 100-103℃) in 65% isolated yield (35.6g, 137 mmol).

Spectral data for **452**: ^{1}H NMR ($CDCl_3$, 500 MHz) δ 2.46 (s, 3H), 7.25 (d, 1H, J = 0.9 Hz), 7.38 (d, 2H, J = 8.0 Hz), 7.86 (d, 2H, J = 8.4 Hz), 9.38 (s, 1H); ^{13}C NMR ($CDCl_3$, 125 MHz) δ 21.70, 128.10, 130.14, 133.78, 136.05, 145.81, 165.01. These spectral data match those previously reported for this compound.[18]

2,5-dioxopyrrolidin-1-yl 2-diazoacetate 454: To a flame dried 500 mL single-necked round-bottom flask was added *N*-hydroxysuccinimide **453** (6.33 g, 55.0 mmol) and Na_2CO_3 (7.95 g,

75.0 mmol) and dry CH_2Cl_2 (75 mL). The flask was then brought to 0 °C using a chiller over a period of 30 min. Meanwhile, to another flame-dried 250 mL single-necked round-bottom flask was added acid chloride **452** (13.04 g, 50.00 mmol) and dry CH_2Cl_2 (100 mL). This solution was added to the suspension of succinimide at 0 °C over a period of 2 h utilizing a syringe pump. Two syringe pumps were used and two 60 mL plastic syringes, containing 50 mL of the CH_2Cl_2 solution of **452**, were employed. The resulting mixture was stirred for an additional hour at 0 ºC. After 1 h, the solution was warmed to room temperature and then stirred for 3 h at room temperature. The reaction mixture was then filtered using a Büchner funnel (8 cm diameter) with filter paper and the filtrate was collected in a 500 mL round-bottom flask. It must be noted that a direct passage of the reaction mixture through a short plug of silica plug results in the clogged plug, thereby a substantial loss of the material. The residue was then washed with EtOAc (200 mL × 2). A small amount of solid is observed in the filtrate. The solid impurities remaining in the filtrate were removed by passing through a short plug (35 mm × 60 mm) of silica gel. The filtrate was collected in a 500 mL round-bottom flask. The silica plug was then washed with EtOAc (150 mL × 2). The washing was monitored by TLC. The resulting solution was then concentrated under reduced pressure to provide crude succinimidyl diazoacetate as a light yellow solid (~6.36 g). The crude diazo compound was kept under vacuum for a period of 1 h. Recrystallization from CH_2Cl_2/ hexanes (55 mL, 4:1) gave diazo **454** (mp 113.5-115.0 °C) as light yellow solid crystals in 29% yield (2.68 g, 14.5 mmol, first crop). Successive crystallization yielded the diazo **454** a combined yield of 60% (29%, 2.68 g, mp 113.5-115.0 °C, first crop; 15%, 1.40 g, mp 115.0-118.0 °C, second crop; 16%, 1.43 g, mp 115.0-118.0 °C, third

crop). The amounts of solvent (CH_2Cl_2/ hexanes, 4:1) used for second and third crystallizations are 29 mL and 19 mL respectively. The amounts of the solid residue from the mother liquor after the first and second crystallizations are 3.57g and 2.15 g respectively. The second run of the reaction resulted in 56% yield of the diazoacetate **454**.

Spectral data for **454**: R_f = 0.13 (3:1 ether/hexanes); ^{1}H NMR ($CDCl_3$, 500 MHz) δ 2.81 (s, 4H), 5.10 (brs, 1H); ^{13}C NMR ($CDCl_3$, 125 MHz) δ 25.44, 45.11, 162.24, 169.36; IR (thin film) 3105w, 2135s, 1736vs, 1375s, 1206s, 1105s cm^{-1}; mass spectrum, *m/z* (% rel intensity) 183 M$^+$ (1), 155 (3), 69 (100), 56 (16), 42 (11). These spectral data match those previously reported for this compound.[18]

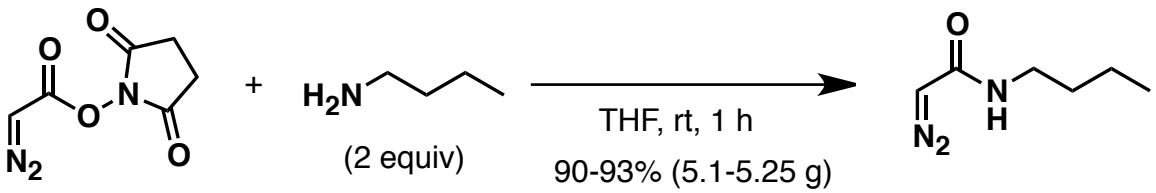

454 126n 128a

***N*-butyl-2-diazoacetamide 128a:** To a flame dried 100 mL single-necked round-bottom flask was added succinimidyl diazoacetate **454** (7.33 g, 40 mmol) and THF (400 mL). To the solution was added *n*-butylamine **126n** (8 mL, 80 mmol, freshly distilled) in one portion. Appearance of a yellow solid was observed after 1-2 min. The reaction mixture was stirred for 1 h at room temperature. The reaction was complete and the solvent was removed under reduced pressure. Purification of the crude diazo by silica gel chromatography (30 mm × 300 mm column, 1:3 hexanes/EtOAc) afforded pure diazo **128a** as a yellow solid (mp 75-76 ºC) in 90-93% isolated yield (5.10-5.25 g, 35-37.2 mmol). Alternatively, the crude product, after the evaporation of the

solvent, was directly passed through a short plug (35 mm × 60 mm) of silica gel. The silica plug was then washed with 1:3 hexanes/EtOAc (100 mL). The washing is continued until the yellow color has stopped coming down the plug. All yellow fractions can be collected in a flask and the solvent is evaporated to afford pure diazo **128a** as a yellow solid. No difference in the yield was observed when the purification was performed in this way compared to column chromatography.

Spectral data for **128a**: R_f = 0.33 (1:1 EtOAc:hexanes); ^{1}H NMR ($CDCl_3$, 500 MHz) δ 0.90 (t, 3H, J = 7.3 Hz), 1.29-1.36 (m, 2H), 1.44-1.50 (m, 2H), 3.26 (brs, 2H), 4.68 (brs, 1H), 5.10 (brs, 1H); ^{13}C NMR ($CDCl_3$,125 MHz) δ 13.42, 19.82, 31.90, 39.76, 46.82, 165.34. These spectral data match those previously reported for this compound.[16]

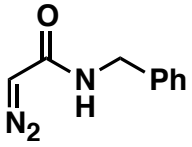

128b

***N*-benyl-2-diazoacetamide 128b:** Diazoacetamide **128b** was prepared according to the procedure described above for diazoacetamide **128a** except that the scale of the reaction was 4 mmol. Purification of the crude diazo by silica gel chromatography (30 mm × 300 mm column, 1:3 hexanes/EtOAc) afforded pure diazo **128b** as a yellow solid (mp 97-98 ºC) in 91% isolated yield (638 mg, 3.64 mmol).

Spectral data for **128b**: R_f = 0.33 (1:1 EtOAc:hexanes); ^{1}H NMR ($CDCl_3$, 500 MHz) δ 4.37 (d, 2H, J = 5.5 Hz), 4.82 (s, 1H), 6.22 (bs, 1H), 7.23-7.32 (m, 5H); ^{13}C NMR ($CDCl_3$,125 MHz) δ 43.74, 46.99, 127.34, 127.43, 128.56, 138.36, 165.51. These spectral data match those previously reported for this compound.[16]

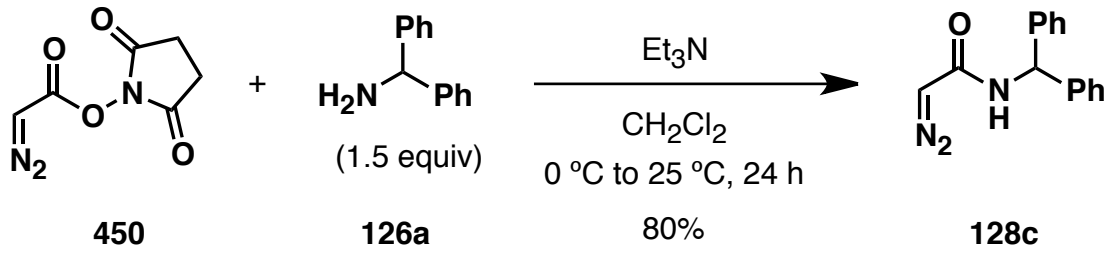

450 **126a** **128c**

***N*-benzhydryl-2-diazoacetamide 128c:** To a flame-dried 50 mL round bottom flask filled with argon was added benzhydrylamine **126a** (1.03 mL, 6.00 mmol) and CH_2Cl_2 (4 mL), followed by dry Et_3N (0.84 mL, 6.00 mmol) at 0 ºC. After stirring for 5 min, the solution of succinimidyl diazoacetate **454** (733 mg, 4.00 mmol) in CH_2Cl_2 (6 mL) was added slowly over a period of 10 min. The reaction mixture was stirred for 0.5 h at 0 ºC, then allowed to warm up to room temperature and stirred for another 24 h. The reaction was complete and the solvent was removed under reduced pressure, and the crude product was purified by silica gel chromatography (20 mm × 200 mm, 1:3 EtOAc/ hexanes as eluent) to afford diazoacetamide **128c** (mp 175-176 ºC) as a yellow solid in 80% yield (1.21 g, 3.20 mmol).

Spectral data for **128c**: R_f = 0.73 (1:1, EtOAc/hexanes). ^{1}H NMR ($CDCl_3$, 600 MHz) δ 4.76 (s, 1H), 5.56 (d, *J* = 6.6 Hz, 1H), 6.26 (brs, 1H), 7.23 (d, *J* = 7.3 Hz, 4H), 7.28 (d, *J* = 7.2 Hz, 2H), 7.33 (t, *J* = 7.3 Hz, 4H); ^{1}H NMR (DMSO-d_6, 500 MHz) δ 5.42 (s, 1H), 6.14 (d, *J* = 8.4 Hz, 1H), 7.25-7.35 (m, 10H), 8.52 (d, *J* = 8.3 Hz, 1H); ^{13}C (DMSO-d_6, 125 MHz) 46.37, 56.31, 126.94, 127.11, 128.37, 142.54, 164.28; IR (thin film) 3250br, 3090m, 2103vs, 1605s, 1543s,

1495w, 1371s cm^{-1}; HRMS (ESI-TOF) *m/z* 252.1140 [$(M+H^+)$; calcd. for $C_{15}H_{14}N_3O$: 252.1137].

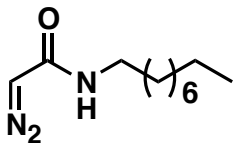

128d

2-diazo-*N*-nonylacetamide 128d: Diazoacetamide **128d** was prepared according to the procedure described above for diazoacetamide **128a** except that the scale of the reaction was 1 mmol and the reaction time was 3 h. Purification of the crude diazo by silica gel chromatography (30 mm × 300 mm column, 1:3 hexanes/EtOAc) afforded pure diazo **128d** as a yellow solid (mp 68-69 ºC) in 87% isolated yield (184 mg, 0.87 mmol).

Spectral data for **128d**: R_f = 0.62 (1:1 EtOAc:hexanes); ^{1}H NMR ($CDCl_3$, 500 MHz) δ 0.87 (t, *J* = 6.9 Hz, 3H), 1.25-1.29 (m, 12H), 1.47-1.51 (m, 2H), 3.25-3.28 (m, 2H), 4.69 (s, 1H), 5.07 (s, 1H); ^{13}C NMR ($CDCl_3$,125 MHz) δ 14.02, 22.59, 26.83, 29.19, 29.26, 29.45, 29.90, 31.80, 40.04, 46.88, 165.52. IR (thin film) 3297s, 3098w, 2922s, 2851m, 2108vs, 1603s, 1549s, 1474w, 1397m cm^{-1}; HRMS (ESI-TOF) *m/z* 212.1756 [$(M+H^+)$; calcd. for $C_{11}H_{22}N_3O$: 212.1763].

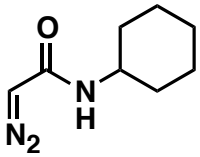

128e

***N*-cyclohexyl-2-diazoacetamide 128e:** Diazoacetamide **128e** was prepared according to the procedure described above for diazoacetamide **128a** except that the scale of the reaction was 1 mmol and the reaction time was 3 h.

Purification of the crude diazo by silica gel chromatography (30 mm × 300 mm column, 1:3 hexanes/EtOAc) afforded pure diazo **128e** as a yellow solid (mp 152-153 ºC) in 91% isolated yield (152 mg, 0.91 mmol).

Spectral data for **128e**: R_f = 0.50 (1:1 EtOAc:hexanes); ^{1}H NMR ($CDCl_3$, 500 MHz) δ 1.08-1.19 (m, 3H), 1.32-1.40 (m, 2H), 1.61 (dt, *J* = 13.0, 3.8 Hz, 1H), 1.67-1.72 (m, 2H), 1.91-1.94 (m, 2H), 3.79 (s, 1H), 4.68 (s, 1H), 5.01 (s, 1H); ^{13}C NMR ($CDCl_3$,125 MHz) δ 24.85, 25.47, 33.53, 47.00, 48.87, 164.48. IR (thin film) 3279s, 3100m, 2924s, 2853m, 2101vs, 1614s, 1562s, 1447w, 1387m cm^{-1}; HRMS (ESI-TOF) *m/z* 168.1138 [(M+H$^+$); calcd. for $C_8H_{14}N_3O$: 168.1137].

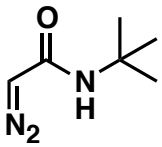

128f

***N*-(*tert*-butyl)-2-diazoacetamide 128f:** Diazoacetamide **128f** was prepared according to the procedure described above for diazoacetamide **128a** except that the scale of the reaction was 1 mmol, the reaction time was 36 h and 4 equivalents of *tert*-butyl amine was used. Purification of the crude diazo by silica gel chromatography (30 mm × 300 mm column, 1:3 hexanes/EtOAc) afforded pure diazo **128f** as a yellow solid (mp 141-142 ºC) in 81% isolated yield (114 mg, 0.81 mmol).

Spectral data for **128f**: R_f = 0.62 (1:1 EtOAc:hexanes); ^{1}H NMR ($CDCl_3$, 600 MHz) δ 1.37 (s, 9H), 4.61 (s, 1H), 4.86 (s, 1H); ^{13}C NMR ($CDCl_3$,125 MHz) δ 29.17, 47.45, 51.88, 164.75. IR (thin film) 3279s, 3098m, 2968m, 2091vs, 1616s, 1559s, 1456w, 1375s cm^{-1}; HRMS (ESI-TOF) *m/z* 142.0984 [(M+H$^+$); calcd. for $C_6H_{12}N_3O$: 142.0980].

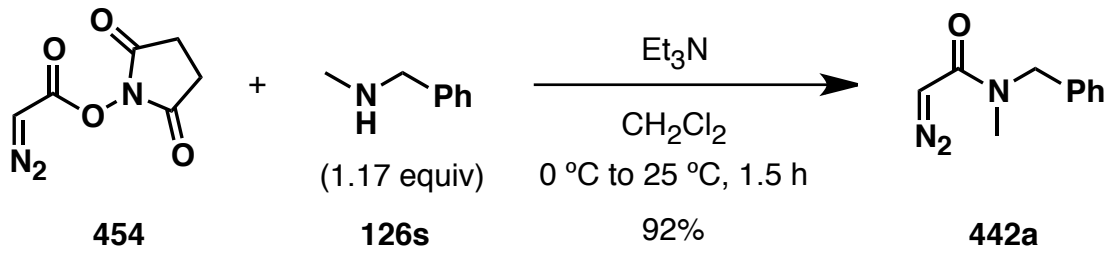

***N*-benzyl-2-diazo-*N*-methylacetamide 442a:** To a flame-dried 50 mL round bottom flask filled with argon was added amine **126s** (0.85 mL, 6.55 mmol) and CH_2Cl_2 (5 mL), followed by dry Et_3N (1.15 mL, 8.19 mmol) at 0 ºC. After stirring for 5 min, the solution of succinimidyl diazoacetate **454** (1.0 g, 5.6 mmol) in CH_2Cl_2 (10 mL) was added slowly over a period of 10 min. The reaction mixture was stirred for 0.5 h at 0 ºC, then allowed to warm up to room temperature and stirred for another 1 h. The reaction was complete and the solvent was removed under reduced pressure, and the crude product was purified by silica gel chromatography (25 mm × 450 mm, 1:1 EtOAc/ hexanes as eluent) to afford diazoacetamide **442a** as a yellow liquid in 92% yield (0.97 g, 5.10 mmol).

Spectral data for **442a**: R_f = 0.38 (1:1, EtOAc/hexanes). ^{1}H NMR ($CDCl_3$, 300 MHz) δ 2.84 (br s, 3H), 4.47 (br s, 2H), 4.96 (s, 1H), 7.19-7.34 (m, 5H); ^{13}C ($CDCl_3$, 75 MHz) δ 46.34, 51.72, 127.39, 128.62, 136.84, 166.00 (two sp^2 carbon not located); IR (thin film) 3065s, 2100vs, 1611vs, 1477s, 1408s cm^{-1}; mass spectrum, *m/z* (% rel intensity) 161 M^+–N_2 (2), 117 (45), 103 (97), 91 (100), 64 (24), 50 (17). These spectral data match those previously reported for this compound.[18]

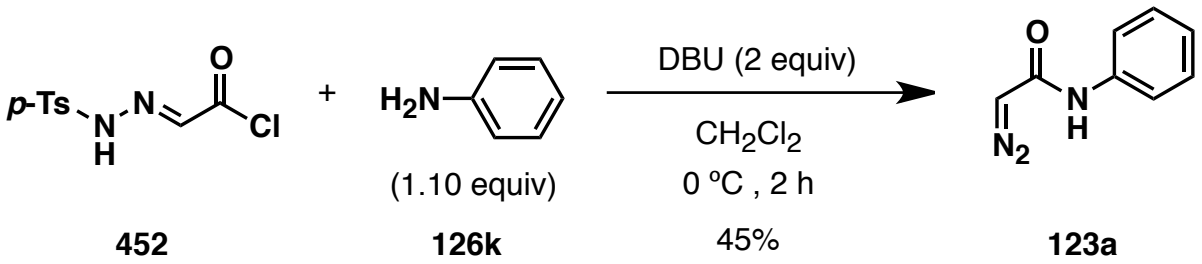

452 **126k** **123a**

2-diazo-*N*-phenylacetamide 123a: To a flame-dried 100 mL round bottom flask equipped with a magnetic stir bar and flushed with argon was added acid chloride **452** (3.60 g, 13.82 mmol, 1 equiv) and dry CH_2Cl_2 (30 mL). The flask was then fitted with a rubber septum and an Argon balloon and cooled to 0 °C in an ice-bath. The reaction mixture was stirred at 0 °C for 15 min. Aniline **126k** (1.40 mL, 15.2 mmol, 1.10 equiv) and DBU (4.20 mL, 27.6 mmol, 2.00 equiv) were then added sequentially to the reaction flask at 0 °C via plastic syringes. The reaction mixture was stirred at 0 °C for 2 h, and then warmed up to room temperature. It was then added to sat. NH_4Cl (~30 mL), and the layers separated. The aqueous layer was extracted with CH_2Cl_2 once, the organic layers combined, washed with brine once, dried over Na_2SO_4, and filtered. The product solution thereafter was transferred to a 250 mL round bottom flask and enough silica gel was added for subsequent column chromatography ("dry load"). This was then subjected to rotary evaporation till dryness, and directly loaded on a silica gel column (30 mm × 270 mm). An eluent mixture of 1:50 MeOH:CH_2Cl_2 was used for the flash chromatography, all yellow colored fractions were collected, and subjected to rotary evaporation till dryness and finally high vacuum to afford the impure product **123a** as a yellow solid. This was then washed with ether 1-4 times until a single spot was observed on TLC (1:29 MeOH:CH_2Cl_2), this

afforded pure diazoacetamide **123a** (mp. 147-149 ºC) as a bright yellow solid in 45% yield (1.0 g, 6.2 mmol).

Spectral data for **123a**: R_f = 0.18 (1:50 MeOH:CH_2Cl_2); ^{1}H NMR (d_6-DMSO, 500 MHz) δ 5.48 (s, 1H), 6.99 (t, *J* = 7.3 Hz, 1H), 7.26 (t, *J* = 8.5 Hz, 2H), 7.51 (d, *J* = 7.6 Hz, 2H), 9.69 (s, 1H); ^{13}C NMR (d_6-DMSO, 125 MHz) δ 48.01, 118.58, 122.66, 128.75, 139.52, 163.53. These spectral data match those previously reported for this compound.[16]

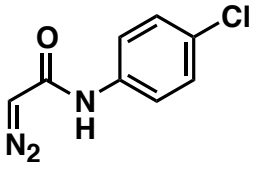

123b

***N*-(4-chlorophenyl)-2-diazoacetamide 123b:** Diazoacetamide **123b** was prepared according to the procedure described above for diazo **123a**. Purification of the crude diazo afforded pure diazo **123b** as a yellow solid (mp 145-146 ºC, decomposition) in 30% isolated yield (811 mg, 4.20 mmol).

Spectral data for **123b**: R_f = 0.32 (1:50 MeOH:CH_2Cl_2); ^{1}H NMR (d_6-DMSO, 500 MHz) δ 5.48 (s, 1H), 7.32 (d, 2H, *J* = 8.7 Hz), 7.54 (d, 2H, *J* = 8.7 Hz), 9.84 (s, 1H); ^{13}C NMR (d_6-DMSO, 125 MHz) δ 48.23, 120.08, 126.15, 128.64, 138.47, 163.68. These spectral data match those previously reported for this compound.[16]

8.9.3 Initial screening of various diazoacetamides *(Table 8.2)*

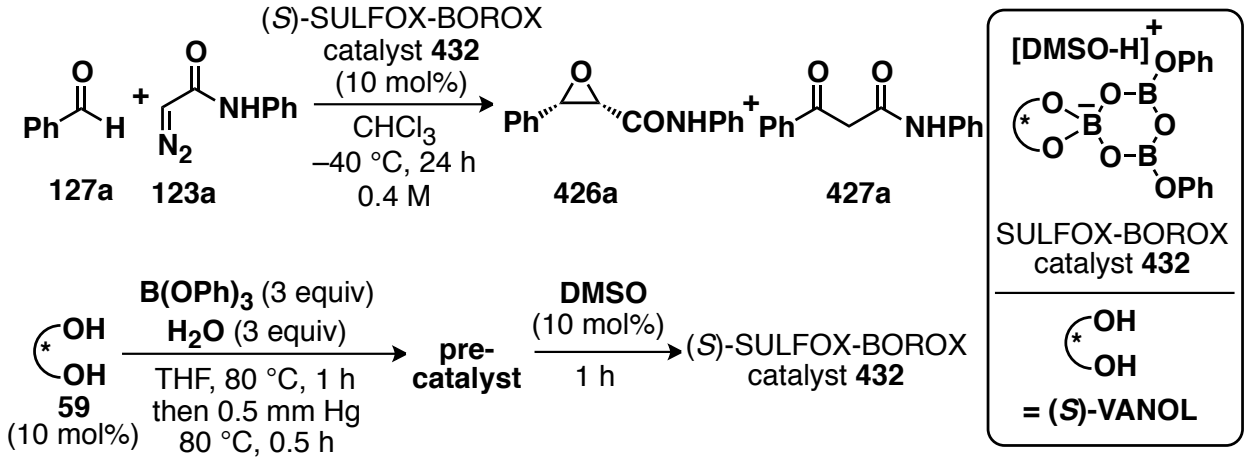

(2*S*,3*S*)-*N*,3-diphenyloxirane-2-carboxamide 426a: *Preparation of the pre-catalyst stock solution :* To a 25 mL flame-dried home-made Schlenk flask , prepared from a single-necked 25 mL pear-shaped flask that had its 14/20 glass joint replaced with a high vacuum threaded Teflon valve, equipped with a stir bar and flushed with argon was added (*S)*-VANOL (52.6 mg, 0.120 mmol) and commercial $B(OPh)_3$ (104.5 mg, 0.3600 mmol) and water (6.5 μL, 0.36 mmol). Under an argon flow through the side-arm of the Schlenk flask, dry THF (2 mL) was added through the top of the Teflon valve to effect dissolution. The flask was sealed by closing the Teflon valve, and then placed in a 80 ºC oil bath for 1 h. After 1 h, a vacuum (0.5 mm Hg) was carefully applied by slightly opening the Teflon valve to remove the volatiles. After the volatiles were removed completely, a full vacuum was applied and maintained for a period of 30 min at a temperature of 80 ºC (oil bath). The flask was then allowed to cool to room temperature and opened to argon through the side-arm of the Schlenk flask. This was then completely dissolved in dry $CHCl_3$ (3 mL) under an argon flow through side-arm of the Schlenk flask to afford the

stock solution of the pre-catalyst. An aliquot of 1mL of the pre-catalyst was then transferred to a 10 mL flame-dried home-made Schlenk flask equipped with a stir bar and flushed with argon.

Asymmetric epoxidation protocol: To the flask containing the pre-catalyst (1 mL aliquot from 0.04 M stock solution) was added the dimethyl sulfoxide **221a** (2.84 μL, 0.040 mmol) under an argon flow through side-arm of the Schlenk flask. The resulting mixture was stirred for 1 h at room temperature to give SULFOX-BOROX catalyst 432. After 1 h, the flask containing the catalyst was cooled to –40 °C for 10 min. To this solution was added benzaldehyde **127a** (40.4 μL, 0.400 mmol, freshly distilled). This was then followed by closing the Teflon valve and stirring the resulting mixture for 10 min at –40 °C. To this mixture was then added diazoacetamide **123a** (80.6 mg, 0.500 mmol, 1.25 equiv) and the resulting mixture was stirred for 24 h at –40 °C. The reaction was quenched by the addition of Et_3N (0.5 mL) and was then warmed to room temperature. The reaction mixture was then transferred to a 50 mL round bottom flask. The reaction flask was rinsed with EtOAc (3 mL × 2) and the rinse was added to the 50 mL round bottom flask. The resulting solution was then concentrated *in vacuo* followed by exposure to high vacuum (0.05 mm Hg) for 1 h to afford the crude epoxide as an off-white semi-solid.

The *cis/trans* ratio was determined by comparing the ^{1}H NMR integration of the ring methine protons for each epoxide in the crude reaction mixture. The yield of the acyclic *β*-ketoamide side product **427a** was determined by ^{1}H NMR analysis of the crude reaction mixture by integration of the methylene protons relative to the internal standard (Ph_3CH). Purification of the crude epoxide by neutral alumina chromatography (17 mm × 300 mm column, 10:1 to 1:1

hexanes/ CH_2Cl_2 as eluent) afforded pure *cis*-epoxide **426a** as a white solid (mp 101-103 ºC on 99% ee material) in 68% isolated yield (65.1 mg, 0.272 mmol); *cis/trans*: 40:1. *β*-ketoamide side product **427a**: 13.6% yield. The optical purity of **426a** was determined to be 62% *ee* by HPLC analysis (CHIRALCEL OD-H column, 90:10 hexane/2-propanol at 222 nm, flow-rate: 1 mL/min): retention times; R_t = 8.17 min (major enantiomer, **426a**) and R_t = 10.33 min (minor enantiomer, *ent*-**426a**). The melting point was taken after a single crystallization.

Spectral data for **426a**: R_f = 0.32 (1:3 EtOAc/hexanes); ^{1}H NMR ($CDCl_3$, 500 MHz) δ 3.94 (d, 1H, *J* = 4.6 Hz), 4.44 (d, 1H, *J* = 4.7 Hz), 7.07 (t, 1H, *J* = 7.1 Hz), 7.17-7.25 (m, 4H), 7.28-7.35 (m, 3H), 7.43 (d, 2H, *J* = 7.3 Hz), 7.55 (bs, 1H); ^{13}C ($CDCl_3$, 125 MHz) δ 56.51, 58.65, 120.21, 124.86, 126.39, 128.55, 128.69, 128.85, 132.78, 135.96, 164.40; IR (thin film) 3321w, 3061w, 2922w, 1672s, 1599m, 1529s, 1444s cm^{-1}; HRMS (ESI-TOF) *m/z* 240.1027 [(M+H$^+$); calcd. for $C_{15}H_{14}NO_2$: 240.1025]; $[\alpha]_D^{20}$ +14.7 (*c* 1.0, CH_2Cl_2) on 62% ee material (HPLC).

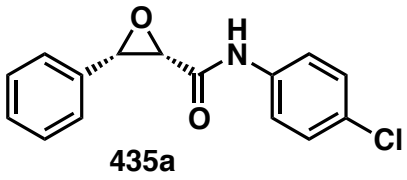

435a

(2*S*,3*S*)-*N*-(4-chlorophenyl)-3-phenyloxirane-2-carboxamide 435a: Aldehyde **127a** was reacted with diazoacetamide **123b** according to the method described above for epoxide **426a** with (*S*)-VANOL as ligand. Purification of the crude epoxide by neutral alumina chromatography (17 mm × 300 mm column, 10:1 to 1:1 hexanes/ CH_2Cl_2 as eluent) afforded pure *cis*-epoxide **435a** as a white solid (mp 113-114 ºC on 52% ee material) in 60% isolated yield (65.7 mg, 0.240 mmol); *cis/trans*: 29:1. *β*-ketoamide side product **437a**: 8.5%

yield. The optical purity of **435a** was determined to be 52% *ee* by HPLC analysis (PIRKLE COVALENT (R,R) WHELK-O 1 column, 93:7 hexane/2-propanol at 228 nm, flow-rate: 1 mL/min): retention times; R_t = 25.69 min (major enantiomer, **435a**) and R_t = 39.42 min (minor enantiomer, *ent*-**435a**).

Spectral data for **435a**: R_f = 0.48 (1:2 EtOAc/hexane); ^{1}H NMR ($CDCl_3$, 500 MHz): δ 3.91 (d, *J* = 4.8 Hz, 1H), 4.43 (d, *J* = 4.8 Hz, 1H), 7.10 (d, *J* = 8.9 Hz, 2H), 7.16 (d, *J* = 8.8 Hz, 2H), 7.28 (d, *J* = 7.1 Hz, 1H), 7.32 (t, *J* = 7.2 Hz, 2H), 7.39 (d, *J* = 7.2 Hz, 2H), 7.50 (s, 1H). ^{13}C ($CDCl_3$, 125 MHz) δ 56.35, 58.64, 121.34, 126.35, 128.58, 128.77, 128.92, 129.95, 132.69, 134.51, 164.49; IR (thin film) 3312 br, 3080 s, 1676 vs, 1589s, 1516vs, 1402 s cm^{-1}; HRMS (ESI-TOF) *m/z* 274.0641 [(M+H$^+$); calcd. for $C_{15}H_{13}ClNO_2$: 274.0635]; $[\alpha]_D^{20}$ +47.9 (*c* 1.0, EtOAc) on 52% ee material (HPLC).

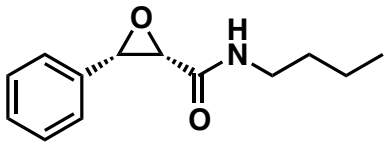

135a

(2*S*,3*S*)-*N*-butyl-3-phenyloxirane-2-carboxamide 135a: Aldehyde **127a** was reacted with diazoacetamide **128a** according to the method described above for epoxide **426a** with (*S*)-VANOL as ligand. Purification of the crude epoxide by neutral alumina chromatography (17 mm × 300 mm column, 3:1 hexanes/ EtOAc as eluent) afforded pure *cis*-epoxide **135a** as a white solid (52-53 ºC on 99.3 % ee material) in 50% isolated yield (43.9 mg, 0.200 mmol); *cis/trans*: 16:1. *β*-ketoamide side product **136a**: 13.7% yield. The optical purity of **135a** was determined to be 62% *ee* by HPLC analysis (PIRKLE COVALENT (R,R) WHELK-O 1 column, 93:7

hexane/2-propanol at 228 nm, flow-rate: 1 mL/min): retention times; R_t = 13.8 min (major enantiomer, **135a**) and R_t = 24.6 min (minor enantiomer, *ent*-**135a**).

Spectral data for **135a**: R_f = 0.61 (1:1 EtOAc/hexane); ^{1}H NMR ($CDCl_3$, 500 MHz) δ 0.72 (t, J = 7.2 Hz, 3H), 0.89-1.04 (m, 4H), 2.82-2.88 (m, 1H), 3.08 (dq, J = 13.6, 6.9 Hz, 1H), 3.77 (d, J = 4.8 Hz, 1H), 4.31 (d, J = 4.8 Hz, 1H), 5.84 (s, 1H), 7.35-7.28 (m, 5H); ^{13}C ($CDCl_3$, 125 MHz) δ 13.53, 19.62, 31.17, 38.21, 56.27, 58.08, 126.49, 128.31, 128.38, 133.19, 165.95; IR (thin film) 3316 br, 2959 vs, 2932 vs, 1651 vs, 1545 s, 1454 s cm^{-1}; HRMS (ESI-TOF) *m/z* 220.1334 [(M+H$^+$); calcd. for $C_{13}H_{18}NO_2$: 220.1338]; $[\alpha]_D^{20}$ +18.6 (*c* 1.0, EtOAc) on 99.3% ee material (HPLC).

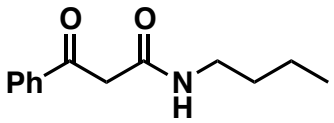

136a

***N*-butyl-3-oxo-3-phenylpropanamide 136a:** oil, isolated in 13% yield.

Spectral data for **136a**: R_f = 0.40 (1:3 EtOAc/hexane); ^{1}H NMR ($CDCl_3$, 500 MHz): δ 0.92 (t, J = 7.4 Hz, 3H), 1.33-1.39 (m, 2H), 1.49-1.55 (m, 2H), 3.30 (td, J = 7.1, 5.7 Hz, 2H), 3.94 (s, 2H), 7.07-7.15 (m, 1H), 7.47-7.51 (m, 2H), 7.61 (ddt, J = 8.4, 6.5, 1.6 Hz, 1H), 8.00 (dt, J = 8.4, 1.6 Hz, 2H); ^{13}C ($CDCl_3$, 125 MHz): δ 13.69, 20.04, 31.43, 39.40, 45.26, 128.56, 128.85, 134.04, 136.23, 165.55, 196.37. These spectral data match those previously reported for this compound.[26]

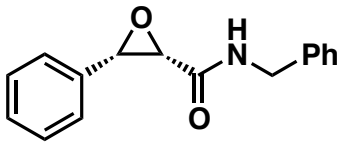

436a

(2*S*,3*S*)-*N*-benzyl-3-phenyloxirane-2-carboxamide 436a: Aldehyde **127a** was reacted with diazoacetamide **128b** according to the method described above for epoxide **426a** with (*S*)-VANOL as ligand. Purification of the crude epoxide by neutral alumina chromatography (17 mm × 300 mm column, 3:1 hexanes/ EtOAc as eluent) afforded pure *cis*-epoxide **436a** as a white solid (mp 108-110 ºC on 62% ee material) in 55% isolated yield (55.7 mg, 0.220 mmol); *cis/trans*: >50:1. *β*-ketoamide side product **438a**: 15.5% yield. The optical purity of **436a** was determined to be 62% *ee* by HPLC analysis (PIRKLE COVALENT (R,R) WHELK-O 1 column, 93:7 hexane/2-propanol at 228 nm, flow-rate: 1 mL/min): retention times; R_t = 32.55 min (major enantiomer, **436a**) and R_t = 18.91 min (minor enantiomer, *ent*-**436a**).

Spectral data for **436a**: R_f = 0.63 (1:1 EtOAc/hexane); ^{1}H NMR ($CDCl_3$, 500 MHz): δ 3.84 (d, *J* = 4.8 Hz, 1H), 4.06 (dd, *J* = 14.9, 5.0 Hz, 1H), 4.29 (dd, *J* = 14.9, 6.9 Hz, 1H), 4.34 (d, *J* = 4.8 Hz, 1H), 6.17 (s, 1H), 6.72 (d, *J* = 6.8 Hz, 2H), 7.14-7.20 (m, 3H), 7.28-7.35 (m, 5H); ^{13}C ($CDCl_3$, 125 MHz): δ 42.65, 56.31, 58.21, 126.51, 127.24, 127.37, 128.44, 128.47, 133.02, 137.00, 166.05 (one sp^2 carbon not located); IR (thin film) 3312 br, 3063 s, 3012 s, 1669 vs, 1535s, 1454s cm^{-1}; HRMS (ESI-TOF) *m/z* 254.1171 [(M+H$^+$); calcd. for $C_{16}H_{16}NO_2$: 254.1181]; $[\alpha]_D^{20}$ +23.2 (*c* 1.0, EtOAc) on 62% ee material (HPLC).

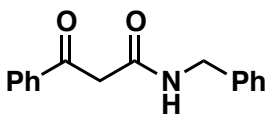

438a

***N*-benzyl-3-oxo-3-phenylpropanamide 438a:** Isolated in 15% yield (mp. 87-88 ºC).

Spectral data for **438a**: R_f = 0.34 (1:3 EtOAc/hexane); ^{1}H NMR ($CDCl_3$, 500 MHz): δ 4.01 (s, 2H), 4.51 (d, *J* = 5.7 Hz, 2H), 7.36-7.27 (m, 6H), 7.50 (t, *J* = 7.8 Hz, 2H), 7.62 (t, *J* = 7.4 Hz, 1H), 8.00 (d, *J* = 7.5 Hz, 2H); ^{13}C ($CDCl_3$, 125 MHz): δ 43.67, 45.26, 127.48, 127.68, 128.57, 128.70, 128.89, 134.11, 136.17, 137.88, 165.60, 196.05. These spectral data match those previously reported for this compound.[27]

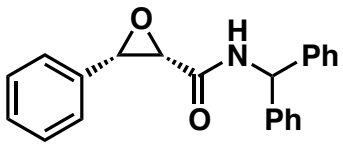

443a

(2*S*,3*S*)-*N*-benzhydryl-3-phenyloxirane-2-carboxamide 443a: Aldehyde **127a** was reacted with diazoacetamide **128c** according to the method described above for epoxide **426a** with (*S*)-VANOL as ligand. Purification of the crude epoxide by neutral alumina chromatography (17 mm × 300 mm column, 10:1 to 1:1 hexanes/ CH_2Cl_2 as eluent) afforded pure *cis*-epoxide **443a** as a white solid (mp 82-84 ºC on 74% ee material) in 65% isolated yield (85.6 mg, 0.260 mmol); *cis/trans*: >50:1. *β*-ketoamide side product **445a**: 9.5% yield. The optical purity of **443a** was determined to be 74% *ee* by HPLC analysis (CHIRALPAK AS column, 93:7 hexane/2-propanol at 228 nm, flow-rate: 1 mL/min): retention times; R_t = 22.36 min (major enantiomer, **443a**) and R_t = 12.94 min (minor enantiomer, *ent*-**443a**).

Spectral data for **443a**: R_f = 0.26 (0.1:1:1 EtOAc/CH_2Cl_2/hexane); ^{1}H NMR ($CDCl_3$, 500 MHz) δ 3.85 (s, 1H), 4.37 (d, *J* = 4.8 Hz, 1H), 5.95 (d, *J* = 8.0 Hz, 1H), 6.40 (d, *J* = 7.4 Hz, 2H), 6.43 (d, *J* = 7.7 Hz, 1H), 7.05 (t, *J* = 7.5 Hz, 2H), 7.13 (d, *J* = 7.2 Hz, 3H), 7.27 (d, *J* = 7.1 Hz, 1H), 7.31 (t, *J* = 7.2 Hz, 4H), 7.36 (d, *J* = 7.3 Hz, 3H); ^{13}C ($CDCl_3$, 125 MHz) δ 56.34, 56.53, 58.42,

126.66, 126.87, 126.97, 127.38, 127.60, 128.29, 128.55, 128.65, 128.68, 133.07, 140.34, 140.89, 165.35; IR (thin film) 3302 br, 3063 s, 3030 s, 1676 vs, 1518 vs, 1408 s cm^{-1}; HRMS (ESI-TOF) *m/z* 330.1499 [$(M+H^+)$; calcd. for $C_{22}H_{20}NO_2$: 330.1494]; $[\alpha]_D^{20}$ +22.0 (*c* 1.0, EtOAc) on 74% ee material (HPLC).

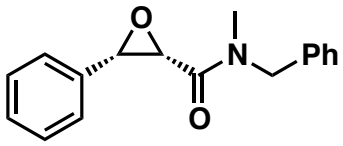

444a

(2*S*,3*S*)-*N*-benzyl-*N*-methyl-3-phenyloxirane-2-carboxamide 444a: Aldehyde **127a** was reacted with diazoacetamide **442a** according to the method described above for epoxide **426a** with (*S*)-VANOL as ligand. There was no epoxide observed based on the ^{1}H NMR analysis of the crude reaction mixture.

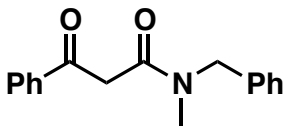

446a

***N*-benzyl-*N*-methyl-3-oxo-3-phenylpropanamide 446a:** The presence of **446a** was confirmed by the characteristic peak at δ = 4.13[19] ppm in the ^{1}H NMR previously published for this compound and the amount (25%) of the compound was quantified by integration against an internal standard (Ph_3CH). Additionally, 50% yield of the enol form of **446a** was also observed based on the characteristic peak at δ = 5.83[19] ppm in the ^{1}H NMR spectrum of crude reaction mixture.

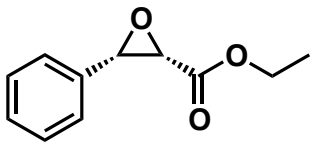

395a

(2*S*,3*S*)-ethyl-3-phenyloxirane-2-carboxylate 395a: Aldehyde **127a** was reacted with diazoacetate **85** according to the method described above for epoxide **426a** with (*S*)-VANOL as ligand. There was no epoxide observed based on the ^{1}H NMR analysis of the crude reaction mixture.

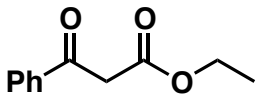

396a

ethyl-3-oxo-3-phenylpropanoate 396a: The presence of **396a** was confirmed by the characteristic peak at δ = 3.98[14i] ppm in the ^{1}H NMR previously published for this compound and the amount (40%) of the compound was quantified by integration against an internal standard (Ph_3CH).

8.9.4 Synthesis of epoxides 135a-g *(Table 8.6)*

Method A (for Liquid aldehydes)

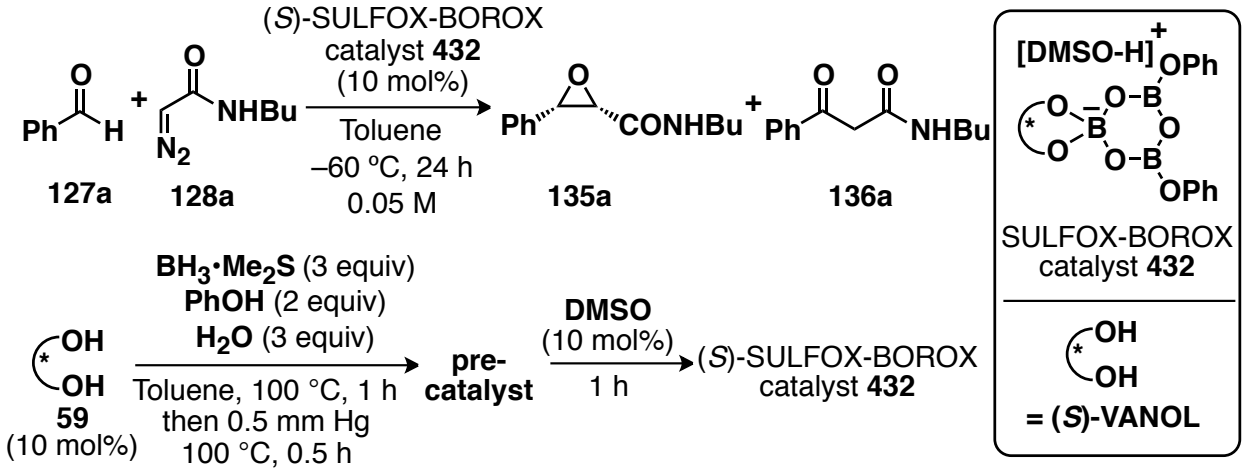

(2*S*,3*S*)-*N*-butyl-3-phenyloxirane-2-carboxamide 135a: *Preparation of the pre-catalyst stock solution :* To a 25 mL flame-dried home-made Schlenk flask , prepared from a single-necked 25 mL pear-shaped flask that had its 14/20 glass joint replaced with a high vacuum threaded Teflon valve, equipped with a stir bar and flushed with argon was added (*S)*-VANOL (26.3 mg, 0.06

mmol) and PhOH (11.3 mg, 0.120 mmol, freshly sublimed). Under an argon flow through the side-arm of the Schlenk flask, dry toluene (2 mL) was added through the top of the Teflon valve to effect dissolution. After the addition of the toluene, BH_3•Me_2S (90 μL, 0.18 mmol, 2 M in toluene) and water (3.24 μL, 0.180 mmol) was added. The flask was sealed by closing the Teflon valve, and then placed in a 100 ºC oil bath for 1 h. After 1 h, a vacuum (0.5 mm Hg) was carefully applied by slightly opening the Teflon valve to remove the volatiles. After the volatiles were removed completely, a full vacuum was applied and maintained for a period of 30 min at a temperature of 100 ºC (oil bath). The flask was then allowed to cool to room temperature and opened to argon through the side-arm of the Schlenk flask. This was then completely dissolved in dry toluene (3 mL) under an argon flow through side-arm of the Schlenk flask to afford the stock solution of the pre-catalyst. An aliquot of 1mL of the pre-catalyst was then transferred to a 10 mL flame-dried home-made Schlenk flask equipped with a stir bar and flushed with argon.

Asymmetric epoxidation protocol (method A): To the flask containing the pre-catalyst (1 mL aliquot from 0.02 M stock solution) was added the dimethyl sulfoxide **221a** (1.42 μL, 0.020 mmol) under an argon flow through side-arm of the Schlenk flask. The resulting mixture was stirred for 1 h at room temperature to give SULFOX-BOROX catalyst **432**. Meanwhile, to a separate 10 mL flame-dried round bottom flask was added diazoacetamide **128a** (28.23 mg, 0.2000 mmol) and dry toluene (2.5 mL). After 1 h, the flask containing the catalyst was cooled to –60 °C for 10 min. To this solution was added pre-made solution of diazoacetamide **128a**. The flask containing the diazoacetamide **128a** was then rinsed with toluene (0.5 mL) and the rinse was then transferred to the flask containing the catalyst at –60 °C. This was then followed by closing the Teflon valve and stirring the resulting mixture for 10 min at –60 °C. To this

mixture was then added benzaldehyde **127a** (22.2 μL, 0.220 mmol, freshly distilled) and the resulting mixture was stirred for 24 h at –60 °C. The reaction was quenched by the addition of Et_3N (0.5 mL) and was then warmed to room temperature. The reaction mixture was then transferred to a 50 mL round bottom flask. The reaction flask was rinsed with EtOAc (3 mL × 2) and the rinse was added to the 50 mL round bottom flask. The resulting solution was then concentrated *in vacuo* followed by exposure to high vacuum (0.05 mm Hg) for 1 h to afford the crude epoxide as an off-white semi-solid.

The *cis/trans* ratio was determined by comparing the ^{1}H NMR integration of the ring methine protons for each epoxide in the crude reaction mixture. The yield of the acyclic *β*-ketoamide side product **136a** was determined by ^{1}H NMR analysis of the crude reaction mixture by integration of the methylene protons relative to the internal standard (Ph_3CH). Purification of the crude epoxide by neutral alumina chromatography (17 mm × 300 mm column, 10:1 to 1:1 hexanes/ CH_2Cl_2 as eluent) afforded pure *cis*-epoxide **135a** as a white solid (52-53 ºC on 99.3 % ee material) in 88% isolated yield (38.6 mg, 0.176 mmol); *cis/trans*: >100:1. *β*-ketoamide side product **136a**: <1% yield. The optical purity of **135a** was determined to be 99.3% *ee* by HPLC analysis (PIRKLE COVALENT (R,R) WHELK-O 1 column, 93:7 hexane/2-propanol at 228 nm, flow-rate: 1 mL/min): retention times; R_t = 13.8 min (major enantiomer, **135a**) and R_t = 24.6 min (minor enantiomer, *ent*-**135a**).

Spectral data for **135a**: R_f = 0.61 (1:1 EtOAc/hexane); ^{1}H NMR ($CDCl_3$, 500 MHz) δ 0.72 (t, *J* = 7.2 Hz, 3H), 0.89-1.04 (m, 4H), 2.82-2.88 (m, 1H), 3.08 (dq, *J* = 13.6, 6.9 Hz, 1H), 3.77 (d, *J* =

4.8 Hz, 1H), 4.31 (d, J = 4.8 Hz, 1H), 5.84 (s, 1H), 7.35-7.28 (m, 5H); ^{13}C ($CDCl_3$, 125 MHz) δ 13.53, 19.62, 31.17, 38.21, 56.27, 58.08, 126.49, 128.31, 128.38, 133.19, 165.95; IR (thin film) 3316 br, 2959 vs, 2932 vs, 1651 vs, 1545 s, 1454 s cm^{-1}; HRMS (ESI-TOF) *m/z* 220.1334 [(M+H$^+$); calcd. for $C_{13}H_{18}NO_2$: 220.1338]; $[\alpha]_D^{20}$ +18.6 (*c* 1.0, EtOAc) on 99.3% ee material (HPLC).

Method B (for solid aldehydes)

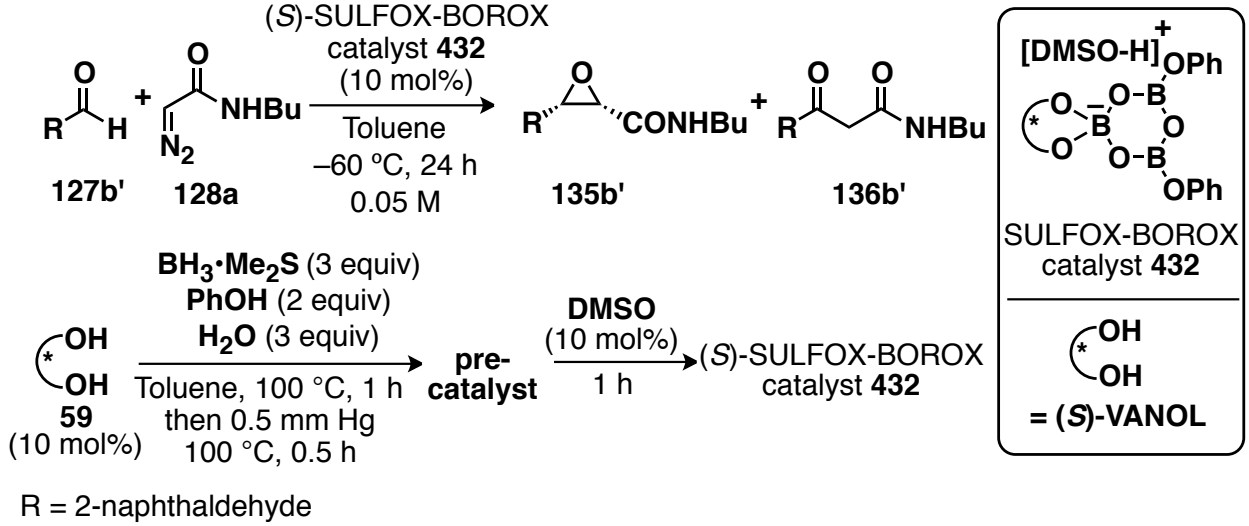

(2*S*,3*S*)-*N*-butyl-3-(naphthalen-2-yl)oxirane-2-carboxamide 135b': *Preparation of the pre-catalyst stock solution :* same as above.

Asymmetric epoxidation protocol (method B): To the flask containing the pre-catalyst (1 mL aliquot from 0.02 M stock solution) was added the dimethyl sulfoxide **221a** (1.42 μL, 0.020 mmol) under an argon flow through side-arm of the Schlenk flask. The resulting mixture was stirred for 1 h at room temperature to give SULFOX-BOROX catalyst **432**. Meanwhile, to a

separate 10 mL flame-dried round bottom flask was added diazoacetamide **128a** (28.23 mg, 0.2000 mmol) and dry toluene (1.5 mL). After 1 h, the flask containing the catalyst was cooled to –60 °C for 10 min. To this solution was added pre-made solution of diazoacetamide **128a**. The flask containing the diazoacetamide **128a** was then rinsed with toluene (0.5 mL) and the rinse was then transferred to the flask containing the catalyst at –60 °C. This was then followed by closing the Teflon valve and stirring the resulting mixture for 10 min at –60 °C. Meanwhile, to a separate 10 mL flame-dried round bottom flask was added aldehyde **127b'** (34.4 mg, 0.220 mmol, freshly purified) and dry toluene (1.0 mL). To the mixture containing diazoacetamide **128a** and catalyst was then added a pre-made solution of aldehyde **127b'** and the resulting mixture was stirred for 24 h at –60 °C. The reaction was quenched by the addition of Et_3N (0.5 mL) and was then warmed to room temperature. The reaction mixture was then transferred to a 50 mL round bottom flask. The reaction flask was rinsed with EtOAc (3 mL × 2) and the rinse was added to the 50 mL round bottom flask. The resulting solution was then concentrated *in vacuo* followed by exposure to high vacuum (0.05 mm Hg) for 1 h to afford the crude epoxide as an off-white semi-solid. Purification of the crude epoxide by neutral alumina chromatography (17 mm × 300 mm column, 10:1 to 1:1 hexanes/ CH_2Cl_2 as eluent) afforded pure *cis*-epoxide **135b'** as a white solid (105-106 ºC on 98% ee material) in 92% isolated yield (49.6 mg, 0.184 mmol); *cis/trans*: >100:1. *β*-ketoamide side product **136b'**: <1 % yield. The optical purity of **135b'** was determined to be 98% *ee* by HPLC analysis (PIRKLE COVALENT (R,R) WHELK-O 1 column, 93:7 hexane/2-propanol at 228 nm, flow-rate: 1 mL/min): retention times; R_t = 16.26 min (major enantiomer, **135b'**) and R_t = 19.95 min (minor enantiomer, *ent*-**135b'**).

Spectral data for **135b'**: R_f = 0.55 (1:1 EtOAc/hexane); ^{1}H NMR ($CDCl_3$, 500 MHz) δ 0.40 (t, *J* = 7.3 Hz, 3H), 0.65-0.72 (m, 2H), 0.80-0.86 (m, 2H), 2.75-2.81 (m, 1H), 3.05 (dq, *J* = 13.7, 6.9 Hz, 1H), 3.86 (d, *J* = 4.8 Hz, 1H), 4.47 (d, *J* = 4.8 Hz, 1H), 5.88 (s, 1H), 7.45-7.51 (m, 3H), 7.80-7.83 (m, 4H); ^{13}C ($CDCl_3$, 125 MHz) δ 13.19, 19.50, 31.22, 38.25, 56.49, 58.30, 124.02, 125.70, 126.41, 126.53, 127.77, 127.82, 128.32, 130.66, 132.85, 133.18, 165.96; IR (thin film) 3308 br, 2959 s, 2932 s, 1651 vs, 1545 s, 1437 s cm^{-1}; HRMS (ESI-TOF) *m/z* 270.1494 [(M+H$^+$); calcd. for $C_{17}H_{20}NO_2$: 270.1494]; $[\alpha]_D^{20}$ –50.6 (*c* 1.0, EtOAc) on 98% ee material (HPLC).

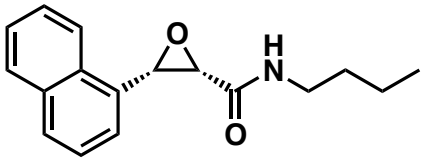

135b

(2*S*,3*S*)-*N*-butyl-3-(naphthalen-1-yl)oxirane-2-carboxamide 135b: Aldehyde **127b** was reacted according to the general method A described above with (*S*)-VANOL as ligand. Purification of the crude epoxide by neutral alumina chromatography (17 mm × 300 mm column, 10:1 to 1:1 hexanes/ CH_2Cl_2 as eluent) afforded pure *cis*-epoxide **135b** as a colorless viscous oil in 97% isolated yield (52.3 mg, 0.194 mmol); *cis/trans*: 35:1. *β*-ketoamide side product **136b**: <1 % yield. The optical purity of **135b** was determined to be 92% *ee* by HPLC analysis (PIRKLE COVALENT (R,R) WHELK-O 1 column, 93:7 hexane/2-propanol at 228 nm, flow-rate: 1 mL/min): retention times; R_t = 16.69 min (major enantiomer, **135b**) and R_t = 54.29 min (minor enantiomer, *ent*-**135b**).

Spectral data for **135b**: R_f = 0.56 (1:1 EtOAc/hexane); ^{1}H NMR ($CDCl_3$, 500 MHz) δ 0.57 (t, *J* = 7.1 Hz, 3H), 0.69 (dq, *J* = 14.7, 7.3 Hz, 2H), 0.74-0.81 (m, 2H), 2.73 (dq, *J* = 12.8, 6.4 Hz, 1H),

2.98 (dq, J = 13.7, 6.9 Hz, 1H), 4.02 (d, J = 4.7 Hz, 1H), 4.68 (d, J = 4.6 Hz, 1H), 5.73 (s, 1H), 7.42 (t, J = 7.6 Hz, 1H), 7.52 (d, J = 7.3 Hz, 2H), 7.57 (t, J = 7.6 Hz, 1H), 7.82 (d, J = 8.2 Hz, 1H), 7.85 (d, J = 8.1 Hz, 1H), 8.12 (d, J = 8.4 Hz, 1H); ^{13}C ($CDCl_3$, 125 MHz) δ 13.41, 19.41, 31.08, 38.12, 56.17, 57.41, 123.64, 124.47, 124.75, 126.33, 126.82, 128.47, 128.94, 129.48, 131.14, 133.28, 166.17; IR (thin film) 3323 br, 2959 vs, 2932 s, 1668 vs, 1539 s, 1464 s cm^{-1}; HRMS (ESI-TOF) *m/z* 270.1504 [$(M+H^+)$; calcd. for $C_{17}H_{20}NO_2$: 270.1494]; $[\alpha]_D^{20}$ +110.3 (*c* 1.0, EtOAc) on 92% ee material (HPLC).

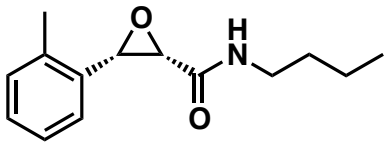

135c

(2*S*,3*S*)-*N*-butyl-3-(*o*-tolyl)oxirane-2-carboxamide 135c: Aldehyde **127c** was reacted according to the general method A described above with (*S*)-VANOL as ligand. Purification of the crude epoxide by neutral alumina chromatography (17 mm × 300 mm column, 10:1 to 1:1 hexanes/ CH_2Cl_2 as eluent) afforded pure *cis*-epoxide **135c** as a white solid (mp 41-43 ºC on 80% ee material) in 60% isolated yield (28 mg, 0.12 mmol); *cis/trans*: >100:1. *β*-ketoamide side product **136c**: <1% yield. The optical purity of **135c** was determined to be 80% *ee* by HPLC analysis (PIRKLE COVALENT (R,R) WHELK-O 1 column, 93:7 hexane/2-propanol at 228 nm, flow-rate: 1 mL/min): retention times; R_t = 17.11 min (major enantiomer, **135c**) and R_t = 20.61 min (minor enantiomer, *ent*-**135c**).

Spectral data for **135c**: R_f = 0.58 (1:1 EtOAc/hexane); ^{1}H NMR ($CDCl_3$, 500 MHz) δ 0.70 (t, J = 7.1 Hz, 3H), 0.87-0.96 (m, 4H), 2.36 (s, 3H), 2.78-2.83 (m, 1H), 3.07 (dq, J = 13.7, 6.9 Hz, 1H),

3.84 (d, J = 4.7 Hz, 1H), 4.25 (d, J = 4.7 Hz, 1H), 5.72 (s, 1H), 7.15 (dd, J = 11.6, 7.5 Hz, 2H), 7.21 (t, J = 7.2 Hz, 1H), 7.30 (d, J = 7.4 Hz, 1H); ^{13}C ($CDCl_3$, 125 MHz) δ 13.56, 18.69, 19.59, 31.20, 38.20, 56.13, 57.69, 125.46, 126.15, 128.31, 130.02, 131.77, 136.73, 166.11; IR (thin film) 3330 br, 2959 s, 2930 s, 1666 vs, 1539 vs, 1458 m cm^{-1}; HRMS (ESI-TOF) *m/z* 234.1503 [(M+H$^+$); calcd. for $C_{14}H_{20}NO_2$: 234.1494]; $[\alpha]_D^{20}$ +39.8 (*c* 1.0, EtOAc) on 80% ee material (HPLC).

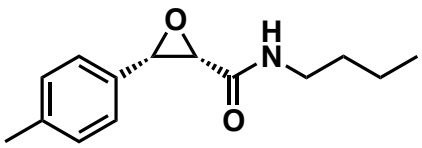

135d

(2*S*,3*S*)-*N*-butyl-3-(*p*-tolyl)oxirane-2-carboxamide 135d: Aldehyde **127d** was reacted according to the general method A described above with (*S*)-VANOL as ligand. Purification of the crude epoxide by neutral alumina chromatography (17 mm × 300 mm column, 10:1 to 1:1 hexanes/ CH_2Cl_2 as eluent) afforded pure *cis*-epoxide **135d** as a white solid (mp 58-59 ºC on 98% ee material) in 80% isolated yield (37.3 mg, 0.160 mmol); *cis/trans*: >100:1. *β*-ketoamide side product **136d**: <1% yield. The optical purity of **135d** was determined to be 98% *ee* by HPLC analysis (PIRKLE COVALENT (R,R) WHELK-O 1 column, 93:7 hexane/2-propanol at 228 nm, flow-rate: 1 mL/min): retention times; R_t = 23.76 min (major enantiomer, **135d**) and R_t = 35.09 min (minor enantiomer, *ent*-**135d**).

Spectral data for **135d**: R_f = 0.56 (1:1 EtOAc/hexane); ^{1}H NMR ($CDCl_3$, 500 MHz) δ 0.72 (t, J = 7.2 Hz, 3H), 0.88-0.96 (m, 2H), 1.00-1.06 (m, 2H), 2.32 (s, 3H), 2.83-2.89 (m, 1H), 3.11 (dq, J = 13.6, 6.9 Hz, 1H), 3.74 (d, J = 4.8 Hz, 1H), 4.27 (d, J = 4.7 Hz, 1H), 5.83 (s, 1H), 7.13 (d, J = 7.9 Hz, 2H), 7.23 (d, J = 8.0 Hz, 2H); ^{13}C ($CDCl_3$, 125 MHz) δ 13.58, 19.66, 21.15, 31.28,

38.26, 56.32, 58.09, 126.45, 128.99, 130.21, 138.21, 166.12; IR (thin film) 3310 br, 2961 s, 2932 s, 1653 vs, 1547 vs, 1433 s cm^{-1}; HRMS (ESI-TOF) *m/z* 234.1504 [$(M+H^+)$; calcd. for $C_{14}H_{20}NO_2$: 234.1494]; $[\alpha]_D^{20}$ +22.0 (*c* 1.0, EtOAc) on 98% ee material (HPLC).

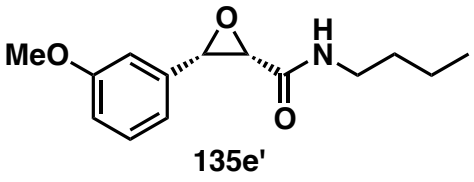

135e'

(2*S*,3*S*)-*N*-butyl-3-(3-methoxyphenyl)oxirane-2-carboxamide 135e': Aldehyde **127e'** was reacted according to the general method A described above with (*S*)-VANOL as ligand. Purification of the crude epoxide by neutral alumina chromatography (17 mm × 300 mm column, 10:1 to 1:1 hexanes/ CH_2Cl_2 as eluent) afforded pure *cis*-epoxide **135e'** as a white solid (mp 58-59 ºC on 90% ee material) in 80% isolated yield (40.0 mg, 0.160 mmol); *cis/trans*: 31:1. *β*-ketoamide side product **136e'**: 6% yield. The optical purity of **135e'** was determined to be 90% *ee* by HPLC analysis (PIRKLE COVALENT (R,R) WHELK-O 1 column, 93:7 hexane/2-propanol at 228 nm, flow-rate: 1 mL/min): retention times; R_t = 17.09 min (major enantiomer, **135e'**) and R_t = 38.66 min (minor enantiomer, *ent*-**135e'**).

Spectral data for **135e'**: R_f = 0.55 (1:1 EtOAc/hexane); ^{1}H NMR ($CDCl_3$, 500 MHz) δ 0.73 (t, *J* = 7.2 Hz, 3H), 0.95 (dq, *J* = 14.8, 7.3 Hz, 2H), 1.05 (dt, *J* = 14.6, 7.1 Hz, 2H), 2.87 (dq, *J* = 12.8, 6.4 Hz, 1H), 3.12 (dq, *J* = 13.6, 6.9 Hz, 1H), 3.76 (d, *J* = 4.8 Hz, 1H), 3.78 (s, 3H), 4.29 (d, *J* = 4.7 Hz, 1H), 5.84 (s, 1H), 6.83 (dd, *J* = 8.2, 2.0 Hz, 1H), 6.88 (s, 1H), 6.93 (d, *J* = 7.6 Hz, 1H), 7.24 (t, *J* = 7.9 Hz, 1H); ^{13}C ($CDCl_3$, 125 MHz) δ 13.57, 19.66, 31.29, 38.28, 55.23, 56.30, 58.05, 112.04, 114.07, 118.75, 129.54, 134.70, 159.61, 165.95; IR (thin film) 3312 br, 2959 s, 2934 s, 1663 vs, 1530 s, 1458 s cm^{-1}; HRMS (ESI-TOF) *m/z* 250.1443 [$(M+H^+)$; calcd. for

$C_{14}H_{20}NO_3$: 250.1443]; $[\alpha]_D^{20}$ +5.4 (*c* 0.5, EtOAc) on 90% ee material (HPLC).

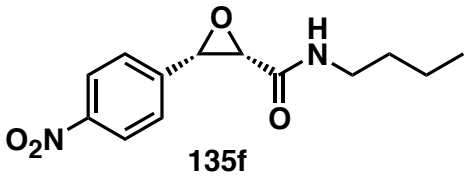

135f

(2*S*,3*S*)-*N*-butyl-3-(4-nitrophenyl)oxirane-2-carboxamide 135f: Aldehyde **127f** was reacted according to the general method B described above with (*S*)-VANOL as ligand. Purification of the crude epoxide by neutral alumina chromatography (17 mm × 300 mm column, 10:1 to 1:1 hexanes/ CH_2Cl_2 as eluent) afforded pure *cis*-epoxide **135f** as a white solid (mp 95-96 ºC on 92% ee material) in 70% isolated yield (37.0 mg, 0.140 mmol); *cis/trans*: 13:1. *β*-ketoamide side product **136f**: 8% yield. The optical purity of **135f** was determined to be 92% *ee* by HPLC analysis (PIRKLE COVALENT (R,R) WHELK-O 1 column, 93:7 hexane/2-propanol at 228 nm, flow-rate: 1 mL/min): retention times; R_t = 28.14 min (major enantiomer, **135f**) and R_t = 47.71 min (minor enantiomer, *ent*-**135f**).

Spectral data for **135f**: R_f = 0.55 (1:1 EtOAc/hexane); ^{1}H NMR ($CDCl_3$, 500 MHz) δ 0.73 (t, *J* = 7.3 Hz, 3H), 0.92-1.00 (m, 2H), 1.04-1.11 (m, 2H), 2.92 (dq, *J* = 13.0, 6.5 Hz, 1H), 3.08 (dq, *J* = 13.7, 6.9 Hz, 1H), 3.86 (d, *J* = 4.9 Hz, 1H), 4.36 (d, *J* = 4.9 Hz, 1H), 5.88 (s, 1H), 7.55 (d, *J* = 8.7 Hz, 2H), 8.21 (d, *J* = 8.7 Hz, 2H); ^{13}C ($CDCl_3$, 125 MHz) δ 13.45, 19.69, 31.35, 38.39, 56.50, 57.21, 123.57, 127.62, 140.29, 147.99, 164.97; IR (thin film) 3312 br, 2961 vs, 2934 s, 1655 vs, 1547 vs, 1518 vs, 1464 s, 1346 s cm^{-1}; HRMS (ESI-TOF) *m/z* 265.1179 [$(M+H^+)$; calcd. for $C_{13}H_{17}N_2O_4$: 265.1188]; $[\alpha]_D^{20}$ +42.2 (*c* 1.0, EtOAc) on 92% ee material (HPLC).

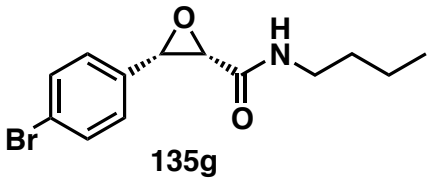

135g

(2*S*,3*S*)-*N*-butyl-3-(4-bromophenyl)oxirane-2-carboxamide 135g: Aldehyde **127g** was reacted according to the general method B described above with (*S*)-VANOL as ligand. Purification of the crude epoxide by neutral alumina chromatography (17 mm × 300 mm column, 10:1 to 1:1 hexanes/ CH_2Cl_2 as eluent) afforded pure *cis*-epoxide **135g** as a white solid (mp 109-110 ºC on 99% ee material) in 88% isolated yield (52.5 mg, 0.176 mmol); *cis/trans*: >100:1. *β*-ketoamide side product **136g**: <1% yield. The optical purity of **135g** was determined to be 99% *ee* by HPLC analysis (PIRKLE COVALENT (R,R) WHELK-O 1 column, 93:7 hexane/2-propanol at 228 nm, flow-rate: 1 mL/min): retention times; R_t = 15.09 min (major enantiomer, **135g**) and R_t = 27.43 min (minor enantiomer, *ent*-**135g**).

Spectral data for **135g**: R_f = 0.50 (1:1 EtOAc/hexane); ^{1}H NMR ($CDCl_3$, 500 MHz) δ 0.77 (t, *J* = 7.2 Hz, 3H), 0.92-0.99 (m, 2H), 1.04-1.10 (m, 2H), 2.86-2.92 (m, 1H), 3.13 (dq, *J* = 13.7, 6.9 Hz, 1H), 3.78 (d, *J* = 4.8 Hz, 1H), 4.25 (d, *J* = 4.8 Hz, 1H), 7.24 (d, *J* = 8.3 Hz, 2H), 7.47 (d, *J* = 8.4 Hz, 2H); ^{13}C ($CDCl_3$, 151 MHz) δ 13.67, 19.77, 31.39, 38.39, 56.29, 57.57, 122.66, 128.33, 131.61, 132.33, 165.69; IR (thin film) 3300 br, 2957 s, 2928 s, 1653 vs, 1545 s, 1435 s, 1286 s cm^{-1}; HRMS (ESI-TOF) *m/z* 298.0449 [$(M+H^+)$; calcd. for $C_{13}H_{17}BrNO_2$: 298.0443]; $[\alpha]_D^{20}$ +20.7 (*c* 1.0, EtOAc) on 99% ee material (HPLC).

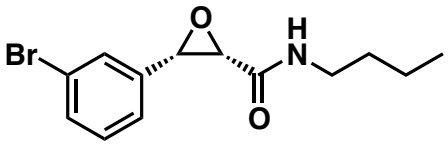

135g'

(2*S*,3*S*)-*N*-butyl-3-(3-bromophenyl)oxirane-2-carboxamide 135g': Aldehyde **127g'** was reacted according to the general method A described above with (*S*)-VANOL as ligand. Purification of the crude epoxide by neutral alumina chromatography (17 mm × 300 mm column, 10:1 to 1:1 hexanes/ CH_2Cl_2 as eluent) afforded pure *cis*-epoxide **135g'** as a white solid (mp 74-75 ºC on 96% ee material) in 88% isolated yield (52.5 mg, 0.176 mmol); *cis/trans*: >100:1. *β*-ketoamide side product **136g'**: 4% yield. The optical purity of **135g'** was determined to be 96% *ee* by HPLC analysis (PIRKLE COVALENT (R,R) WHELK-O 1 column, 93:7 hexane/2-propanol at 228 nm, flow-rate: 1 mL/min): retention times; R_t = 14.31 min (major enantiomer, **135g'**) and R_t = 27.29 min (minor enantiomer, *ent*-**135g'**).

Spectral data for **135g'**: R_f = 0.55 (1:1 EtOAc/hexane); ^{1}H NMR ($CDCl_3$, 500 MHz) δ 0.76 (t, *J* = 7.2 Hz, 3H), 0.97 (dqd, *J* = 14.9, 7.4, 2.9 Hz, 2H), 1.06-1.12 (m, 2H), 2.84-2.90 (m, 1H), 3.16 (dq, *J* = 13.7, 6.9 Hz, 1H), 3.77 (d, *J* = 4.8 Hz, 1H), 4.27 (d, *J* = 4.8 Hz, 1H), 5.88 (s, 1H), 7.20 (t, *J* = 7.8 Hz, 1H), 7.28 (d, *J* = 7.7 Hz, 1H), 7.44 (d, *J* = 8.0 Hz, 1H), 7.50 (s, 1H); ^{13}C ($CDCl_3$, 125 MHz) δ 13.60, 19.71, 31.36, 38.34, 56.38, 57.28, 122.49, 125.28, 129.50, 129.95, 131.59, 135.46, 165.42; IR (thin film) 3304 br, 2959 vs, 2932 vs, 1658 vs, 1568 vs, 1541 vs, 1435 s, 1284 s cm^{-1}; HRMS (ESI-TOF) *m/z* 298.0442 [(M+H$^+$); calcd. for $C_{13}H_{17}BrNO_2$: 298.0443]; $[\alpha]_D^{20}$ –17.8 (*c* 1.0, EtOAc) on 96% ee material (HPLC).

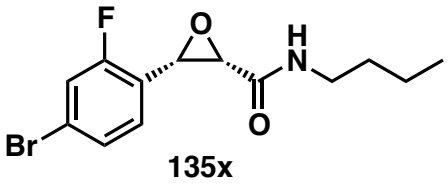

135x

(2*S*,3*S*)-*N*-butyl-3-(4-bromo-2fluorophenyl)oxirane-2-carboxamide 135x: Aldehyde **127x** was reacted according to the general method B described above with (*S*)-VANOL as ligand. Purification of the crude epoxide by neutral alumina chromatography (17 mm × 300 mm column, 10:1 to 1:1 hexanes/ CH_2Cl_2 as eluent) afforded pure *cis*-epoxide **135x** as a white solid (mp 86-87 ºC on 80% ee material) in 70% isolated yield (44.3 mg, 0.140 mmol); *cis/trans*: 39:1. *β*-ketoamide side product **136x**: 9% yield. The optical purity of **135x** was determined to be 80% *ee* by HPLC analysis (PIRKLE COVALENT (R,R) WHELK-O 1 column, 93:7 hexane/2-propanol at 228 nm, flow-rate: 1 mL/min): retention times; R_t = 15.61 min (major enantiomer, **135x**) and R_t = 23.23 min (minor enantiomer, *ent*-**135x**).

Spectral data for **135x**: R_f = 0.68 (1:1 EtOAc/hexane); ^{1}H NMR ($CDCl_3$, 500 MHz) δ 0.83 (t, *J* = 7.3 Hz, 3H), 1.01-1.08 (m, 2H), 1.16 (dt, *J* = 14.8, 7.3 Hz, 2H), 2.98 (dq, *J* = 12.9, 6.4 Hz, 1H), 3.20 (dq, *J* = 13.7, 6.9 Hz, 1H), 3.87 (d, *J* = 4.7 Hz, 1H), 4.32 (d, *J* = 4.7 Hz, 1H), 5.91 (s, 1H), 7.24 (t, *J* = 8.0 Hz, 1H), 7.29-7.32 (m, 2H); ^{13}C ($CDCl_3$, 125 MHz) δ 13.58, 19.74, 31.38, 38.40, 53.83, 53.86, 55.76, 119.24, 119.43, 120.09, 120.20, 122.87, 122.94, 127.16, 127.19, 129.17, 129.20, 160.06, 162.08, 165.29; IR (thin film) 3300 br, 2959 s, 2932 s, 1653 vs, 1547 vs, 1406 s cm^{-1}; HRMS (ESI-TOF) *m/z* 316.0364 [($M+H^+$); calcd. for $C_{13}H_{16}BrFNO_2$: 317.0348]; $[\alpha]_D^{20}$ +12.7 (*c* 1.0, EtOAc) on 80% ee material (HPLC).

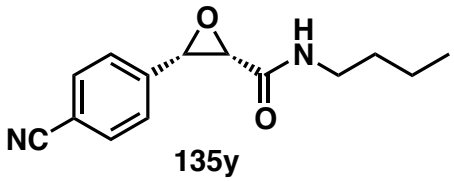

135y

(2*S*,3*S*)-*N*-butyl-3-(4-cyanophenyl)oxirane-2-carboxamide 135y: Aldehyde **127y** was reacted according to the general method B described above with (*S*)-VANOL as ligand. Purification of the crude epoxide by neutral alumina chromatography (17 mm × 300 mm column, 10:1 to 1:1 hexanes/ CH_2Cl_2 as eluent) afforded pure *cis*-epoxide **135y** as a white solid (mp 72-73 ºC on 96% ee material) in 84% isolated yield (41.0 mg, 0.168 mmol); *cis/trans*: >100:1. *β*-ketoamide side product **136y**: <1% yield. The optical purity of **135y** was determined to be 96% *ee* by HPLC analysis (PIRKLE COVALENT (R,R) WHELK-O 1 column, 93:7 hexane/2-propanol at 228 nm, flow-rate: 1 mL/min): retention times; R_t = 38.97 min (major enantiomer, **135y**) and R_t = 63.98 min (minor enantiomer, *ent*-**135y**).

Spectral data for **135y**: R_f = 0.23 (1:1 EtOAc/hexane); ^{1}H NMR ($CDCl_3$, 600 MHz) δ 0.76 (t, *J* = 7.3 Hz, 3H), 0.93-0.99 (m, 2H), 1.04-1.09 (m, 2H), 2.87-2.93 (m, 1H), 3.08 (dq, *J* = 13.7, 6.9 Hz, 1H), 3.83 (d, *J* = 4.9 Hz, 1H), 4.32 (d, *J* = 4.9 Hz, 1H), 5.86 (s, 1H), 7.48 (d, *J* = 8.0 Hz, 2H), 7.64 (d, *J* = 8.2 Hz, 2H); ^{13}C ($CDCl_3$, 125 MHz) δ 13.54, 19.67, 31.30, 38.33, 56.40, 57.29, 112.49, 118.17, 127.39, 132.10, 138.41, 165.06; IR (thin film) 3312 br, 2959 s, 2934 s, 2229 s, 1664 vs, 1541 s, 1437 s cm^{-1}; HRMS (ESI-TOF) *m/z* 245.1283 [$(M+H^+)$; calcd. for $C_{14}H_{17}N_2O_2$: 245.1290]; $[\alpha]_D^{20}$ +41.0 (*c* 1.0, EtOAc) on 96% ee material (HPLC).

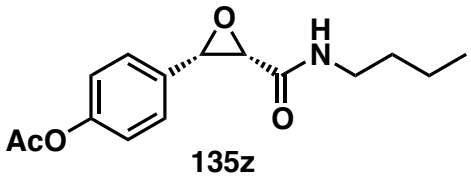

135z

4-((2*S*,3*S*)-3-(butylcarbamoyl)oxiran-2-yl)phenyl acetate 135z: Aldehyde **127z** was reacted according to the general method B described above with (*S*)-VANOL as ligand. Purification of the crude epoxide by neutral alumina chromatography (17 mm × 300 mm column, 10:1 to 1:1 hexanes/ CH_2Cl_2 as eluent) afforded pure *cis*-epoxide **135z** as a white solid (mp 113-114 ºC on 97% ee material) in 82% isolated yield (45.5 mg, 0.164 mmol); *cis/trans*: >100:1. *β*-ketoamide side product **136z**: 4% yield. The optical purity of **135z** was determined to be 97% *ee* by HPLC analysis (PIRKLE COVALENT (R,R) WHELK-O 1 column, 80:20 hexane/2-propanol at 228 nm, flow-rate: 1 mL/min): retention times; R_t = 26.76 min (major enantiomer, **135z**) and R_t = 46.04 min (minor enantiomer, *ent*-**135z**).

Spectral data for **135z**: R_f = 0.34 (1:1 EtOAc/hexane); ^{1}H NMR ($CDCl_3$, 600 MHz) δ 0.76 (t, *J* = 7.2 Hz, 3H), 1.00 (dq, *J* = 14.7, 7.3 Hz, 2H), 1.07 (dtd, *J* = 14.5, 7.2, 2.7 Hz, 2H), 2.28 (s, 3H), 2.90 (dq, *J* = 12.9, 6.4 Hz, 1H), 3.09 (dq, *J* = 13.7, 6.9 Hz, 1H), 3.77 (d, *J* = 4.7 Hz, 1H), 4.29 (d, *J* = 4.7 Hz, 1H), 5.82 (s, 1H), 7.07 (d, *J* = 8.6 Hz, 2H), 7.37 (d, *J* = 8.3 Hz, 2H); ^{13}C ($CDCl_3$, 125 MHz) δ 13.48, 19.70, 21.08, 31.19, 38.28, 56.27, 57.66, 121.64, 127.76, 130.74, 150.75, 165.83, 169.06; IR (thin film) 3310 br, 2957 s, 2930 s, 1757 vs, 1653 vs, 1545 vs, 1369 s, 1223 s cm^{-1}; HRMS (ESI-TOF) *m/z* 278.1395 [($M+H^+$); calcd. for $C_{15}H_{20}NO_4$: 278.1392]; $[\alpha]_D^{20}$ +14.5 (*c* 1.0, EtOAc) on 97% ee material (HPLC).

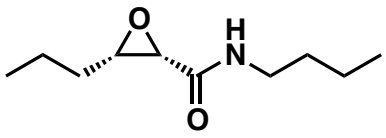

135o

(2*S*,3*S*)-*N*-butyl-3propyloxirane-2-carboxamide 135o: Aldehyde **127o** was reacted according to the general method A described above with (*S*)-VANOL as ligand. Purification of the crude epoxide by neutral alumina chromatography (17 mm × 300 mm column, 10:1 to 1:1 hexanes/ CH_2Cl_2 as eluent) afforded pure *cis*-epoxide **135o** as a white semi-solid in 65% isolated yield (24.1 mg, 0.130 mmol); *cis/trans*: nd. *β*-ketoamide side product **136o**: 9% yield. The optical purity of **135o** was determined to be 78% *ee* by HPLC analysis (PIRKLE COVALENT (R,R) WHELK-O 1 column, 97:3 hexane/2-propanol at 228 nm, flow-rate: 1 mL/min): retention times; R_t = 30.34 min (major enantiomer, **135o**) and R_t = 37.02 min (minor enantiomer, *ent*-**135o**).

Spectral data for **135o**: R_f = 0.44 (1:1 EtOAc/hexane); ^{1}H NMR ($CDCl_3$, 600 MHz) δ 0.92 (t, *J* = 7.4 Hz, 3H), 0.95-0.97 (m, 3H), 1.34 (dq, *J* = 15.0, 7.5 Hz, 2H), 1.46-1.55 (m, 6H), 3.15-3.17 (m, 1H), 3.24 (dq, *J* = 13.3, 6.6 Hz, 1H), 3.32 (dq, *J* = 13.5, 6.7 Hz, 1H), 3.48 (d, *J* = 4.8 Hz, 1H), 6.13 (s, 1H); ^{13}C ($CDCl_3$, 125 MHz) δ 13.63, 13.84, 19.41, 20.04, 29.64, 31.62, 38.55, 55.29, 58.39, 167.27; IR (thin film) 3306 br, 2961 s, 2934 s, 1653 vs, 1539 s, 1458 m cm^{-1}; HRMS (ESI-TOF) *m/z* 186.1500 [$(M+H^+)$; calcd. for $C_{10}H_{20}NO_2$: 186.1494]; $[\alpha]_D^{20}$ –1.9 (*c* 1.0, EtOAc) on 78% ee material (HPLC).

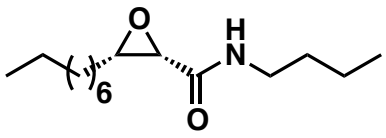

135p'

(2*S*,3*S*)-*N*-butyl-3octyloxirane-2-carboxamide 135p′: Aldehyde **127p′** was reacted according to the general method A described above with (*S*)-VANOL as ligand. Purification of the crude epoxide by neutral alumina chromatography (17 mm × 300 mm column, 10:1 to 1:1 hexanes/ CH_2Cl_2 as eluent) afforded pure *cis*-epoxide **135p′** as a white semi-solid in 84% isolated yield (42.9 mg, 0.168 mmol); *cis/trans*: nd. *β*-ketoamide side product **136p′**: 6% yield. The optical purity of **135p′** was determined to be 90% *ee* by HPLC analysis (PIRKLE COVALENT (R,R) WHELK-O 1 column, 97:3 hexane/2-propanol at 228 nm, flow-rate: 1 mL/min): retention times; R_t = 22.64 min (major enantiomer, **135p′**) and R_t = 27.43 min (minor enantiomer, *ent*-**135p′**).

Spectral data for **135p′**: R_f = 0.32 (1:2 EtOAc/hexane); ^{1}H NMR ($CDCl_3$, 600 MHz) δ 0.85 (t, *J* = 7.1 Hz, 3H), 0.90 (t, *J* = 7.4 Hz, 3H), 1.21-1.27 (m, 8H), 1.28-1.35 (m, 4H), 1.40-1.53 (m, 6H), 3.11-3.14 (m, 1H), 3.21 (dq, *J* = 13.2, 6.6 Hz, 1H), 3.30 (dq, *J* = 13.5, 6.7 Hz, 1H), 3.46 (d, *J* = 4.8 Hz, 1H), 6.11 (s, 1H); ^{13}C ($CDCl_3$, 125 MHz) δ 13.63, 14.04, 20.05, 22.61, 26.01, 27.64, 29.12, 29.30, 29.33, 31.63, 31.80, 38.55, 55.36, 58.57, 167.26; IR (thin film) 3312 br, 2957 s, 2938 s, 2857 m, 1661 vs, 1539 vs, 1458 m, cm^{-1}; HRMS (ESI-TOF) *m/z* 256.2271 [$(M+H^+)$; calcd. for $C_{15}H_{30}NO_2$: 256.2277]; $[\alpha]_D^{20}$ +2.9 (*c* 1.0, EtOAc) on 90% ee material (HPLC).

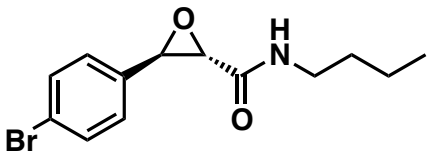

(2R,3S)-**135g**

(2*R*,3*S*)-*N*-butyl-3-(4-bromophenyl)oxirane-2-carboxamide 135g: A sample of *trans*-epoxide **135g** was obtained when aldehyde **127g** was subjected to the reaction conditions given in the entry 4 of Table 8.3 in $CHCl_3$. The optical purity of (2*R*,3*S*)-**135g** was determined to be 20% *ee* by HPLC analysis (PIRKLE COVALENT (R,R) WHELK-O 1 column, 93:7 hexane/2-propanol at 228 nm, flow-rate: 1 mL/min): retention times; R_t = 60.20 min (major enantiomer, (2*R*,3*S*)-**135g**) and R_t = 39.34 min (minor enantiomer, (2*S*,3*R*)-**135g**).

Spectral data for (2*R*,3*S*)-**135g**: R_f = 0.63 (1:1 EtOAc/hexane); ^{1}H NMR ($CDCl_3$, 500 MHz) δ 0.94 (t, *J* = 7.3 Hz, 3H), 1.37 (dq, *J* = 15.0, 7.5 Hz, 2H), 1.49-1.55 (m, 2H), 3.29 (qq, *J* = 13.2, 6.6 Hz, 2H), 3.47 (d, *J* = 2.0 Hz, 1H), 3.83 (d, *J* = 1.9 Hz, 1H), 6.19 (s, 1H), 7.14 (d, *J* = 8.6 Hz, 2H), 7.49 (d, *J* = 8.6 Hz, 2H); ^{13}C ($CDCl_3$, 151 MHz) δ 13.69, 20.00, 31.56, 38.67, 58.54, 58.99, 123.06, 127.39, 131.85, 134.06, 166.94; IR (thin film) 3275 br, 2859 m, 2932 m, 1655 vs, 1564 m, 1439 w cm^{-1}; HRMS (ESI-TOF) *m/z* 298.0444 [$(M+H^+)$; calcd. for $C_{13}H_{17}BrNO_2$: 298.0443].

8.9.5 One pot procedure for epoxidation reaction *(Table 8.5)*

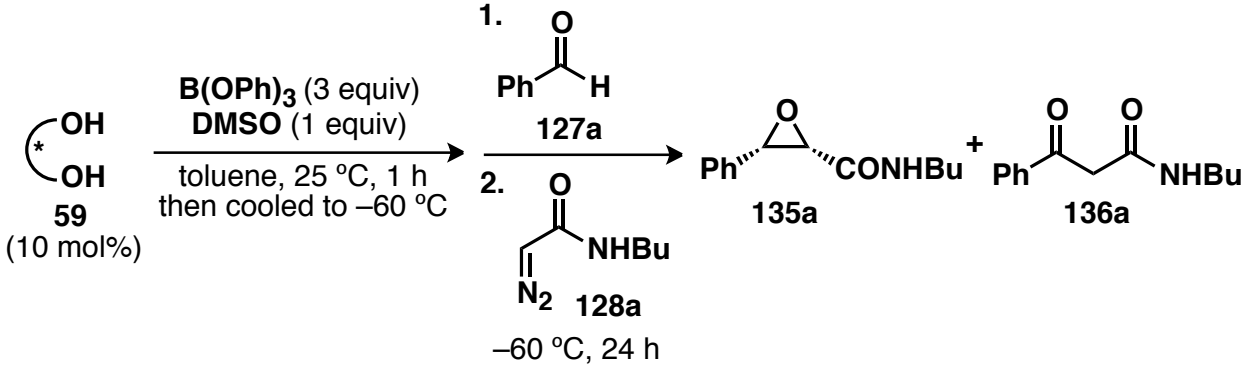

(2*S*,3*S*)-*N*-butyl-3-phenyloxirane-2-carboxamide 135a: To a flame-dried 10 mL round bottom flask filled with argon was added was added (*S)*-VANOL (9.0 mg, 0.02 mmol) and commercial $B(OPh)_3$ (17.4 mg, 0.060 mmol), dimethyl sulfoxide **221a** (1.42 μL, 0.020 mmol) and toluene (2 mL). The resulting mixture was stirred for 1 h at room temperature to give SULFOX-BOROX catalyst **432**. After 1 h, the flask containing the catalyst was cooled to –60 °C for 10 min. To this solution was added benzaldehyde **127a** (61 μL, 0.60 mmol, 3 equiv, freshly distilled). The resulting mixture was then stirred for 10 min at –60 °C. To this mixture was then added diazoacetamide **128a** (28.3 mg, 0.200 mmol) and the resulting mixture was stirred for 24 h at –60 °C. The reaction was quenched by the addition of Et_3N (0.5 mL) and was then warmed to room temperature. The reaction mixture was then transferred to a 50 mL round bottom flask. The reaction flask was rinsed with EtOAc (3 mL × 2) and the rinse was added to the 50 mL round bottom flask. The resulting solution was then concentrated *in vacuo* followed by exposure to high vacuum (0.05 mm Hg) for 1 h to afford the crude epoxide as an off-white semi-solid. Purification of the crude epoxide by neutral alumina chromatography (17 mm × 300 mm column, 10:1 to 1:1 hexanes/ CH_2Cl_2 as eluent) afforded pure *cis*-epoxide **135a** as a white solid in 75% isolated yield and 80% ee; *cis/trans*: 13:1. *β*-ketoamide side product **136a**: 4% yield.

8.9.6 Epoxidation using catalyst 447 *(Scheme 8.8)*

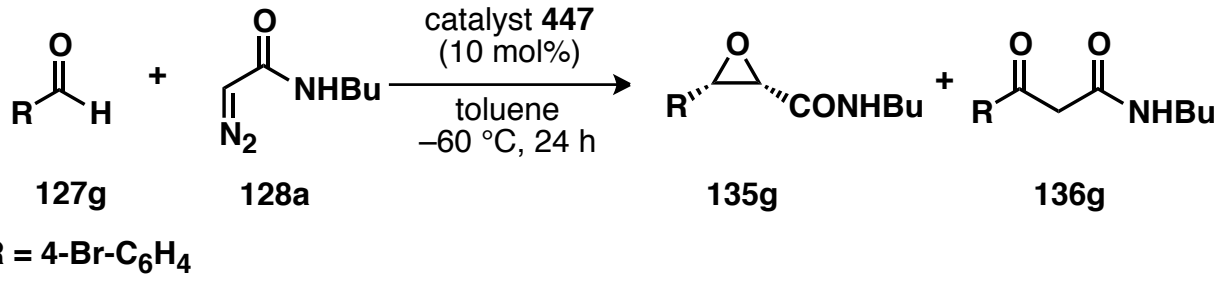

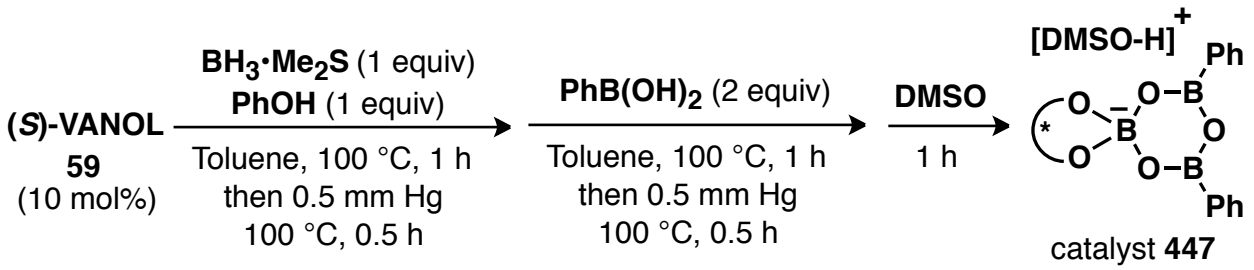

(2*S*,3*S*)-*N*-butyl-3-(4-bromophenyl)oxirane-2-carboxamide 135g: *Preparation of the pre-catalyst stock solution :* To a 25 mL flame-dried home-made Schlenk flask , prepared from a single-necked 25 mL pear-shaped flask that had its 14/20 glass joint replaced with a high vacuum threaded Teflon valve, equipped with a stir bar and flushed with argon was added (*S)*-VANOL (26.3 mg, 0.06 mmol) and PhOH (5.7 mg, 0.06 mmol, freshly sublimed). Under an argon flow through the side-arm of the Schlenk flask, dry toluene (2 mL) was added through the top of the Teflon valve to effect dissolution. After the addition of the toluene, BH_3•Me_2S (30 μL, 0.06 mmol, 2 M in toluene) was added. The flask was sealed by closing the Teflon valve, and then placed in a 100 ºC oil bath for 1 h. After 1 h, a vacuum (0.5 mm Hg) was carefully applied by slightly opening the Teflon valve to remove the volatiles. After the volatiles were removed completely, a full vacuum was applied and maintained for a period of 30 min at a temperature of 100 ºC (oil bath). The flask was then allowed to cool to room temperature and opened to argon through the side-arm of the Schlenk flask. To this flask was added $PhB(OH)_2$ (14.6 mg, 0.120 mmol) and toluene (2 mL). The flask was sealed by closing the Teflon valve, and then placed in a 100 ºC oil bath for 1 h. After 1 h, a vacuum (0.5 mm Hg) was carefully applied by slightly opening the Teflon valve to remove the volatiles. After the volatiles were removed completely, a full vacuum was applied and maintained for a period of 30 min at a temperature of 100 ºC (oil bath). The flask was then allowed to cool to room temperature and

opened to argon through the side-arm of the Schlenk flask. This was then completely dissolved in dry toluene (3 mL) under an argon flow through side-arm of the Schlenk flask to afford the stock solution of the pre-catalyst. An aliquot of 1mL of the pre-catalyst was then transferred to a 10 mL flame-dried home-made Schlenk flask equipped with a stir bar and flushed with argon.

Asymmetric epoxidation protocol: To the flask containing the pre-catalyst (1 mL aliquot from 0.02 M stock solution) was added the dimethyl sulfoxide **221a** (1.42 μL, 0.020 mmol) under an argon flow through side-arm of the Schlenk flask. The resulting mixture was stirred for 1 h at room temperature to give the catalyst **447**. The rest of the procedure was similar to method B (for solid aldehydes) discussed earlier. Purification of the crude epoxide by neutral alumina chromatography (17 mm × 300 mm column, 10:1 to 1:1 hexanes/ CH_2Cl_2 as eluent) afforded pure *cis*-epoxide **135g** in 85% isolated yield and 90% ee; *cis/trans*: 55:1. *β*-ketoamide side product **136g**: 1.4% yield.

8.9.7 Epoxidation using the DIAZO-BOROX catalyst 448a *(Table 8.8)*

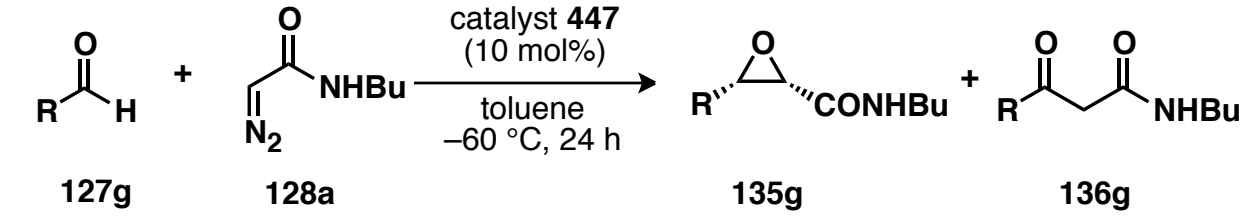

127g **128a** **135g** **136g**

R = 4-Br-C_6H_4

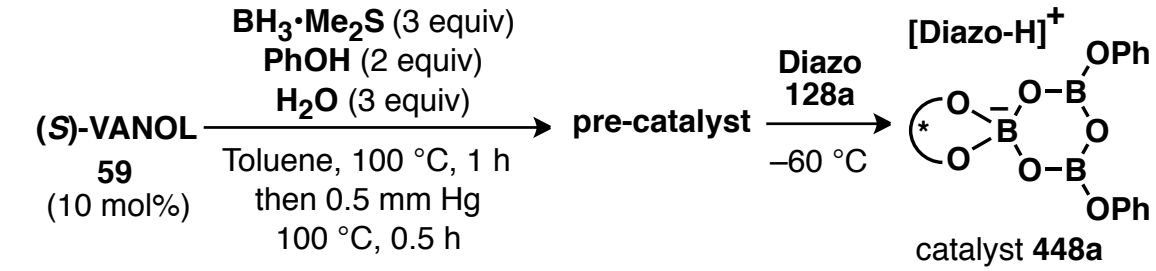

catalyst **448a**

(2*S*,3*S*)-*N*-butyl-3-(4-bromophenyl)oxirane-2-carboxamide 135g: *Preparation of the pre-catalyst stock solution :* same as discussed earlier for method A or method B.

Asymmetric epoxidation protocol: The flask containing the pre-catalyst was cooled to –60 °C for 10 min. Meanwhile, to a separate 10 mL flame-dried round bottom flask was added diazoacetamide **128a** (28.23 mg, 0.2000 mmol) and dry toluene (1.5 mL). To the falsk containing the pre-catalyst was added pre-made solution of diazoacetamide **128a**. The flask containing the diazoacetamide **128a** was then rinsed with toluene (0.5 mL) and the rinse was then transferred to the flask containing the catalyst at –60 °C. This was then followed by closing the Teflon valve and stirring the resulting mixture for 10 min at –60 °C. The rest of the procedure was similar to method B (for solid aldehydes) discussed earlier. Purification of the crude epoxide by neutral alumina chromatography (17 mm × 300 mm column, 10:1 to 1:1 hexanes/ CH_2Cl_2 as eluent) afforded pure *cis*-epoxide **135g** in 86% isolated yield and 91% ee; *cis/trans*: 56:1. *β*-ketoamide side product **136g**: 2% yield.

8.9.8 NMR analysis of boroxinate catalysts 432 and 448a *(Figure 8.4)*

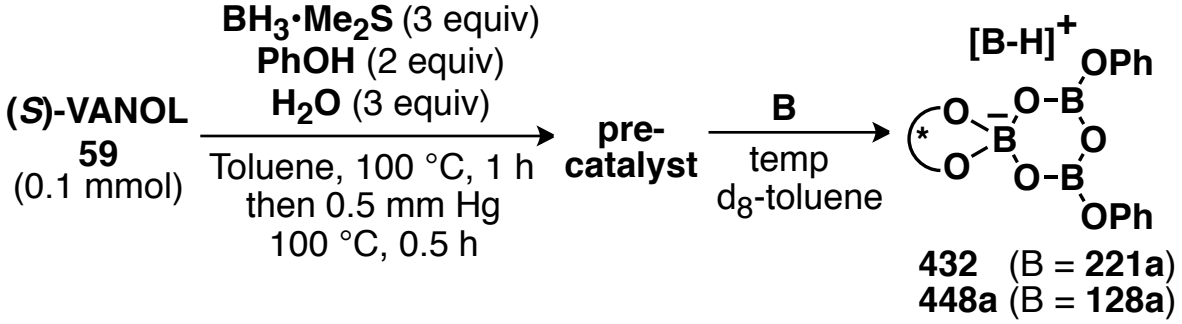

Entry 1, Figure 8.4A: ^{1}H NMR of pure VANOL (*S*)-**59** in d_8-toluene

Entry 2, Figure 8.4A: To a 25 mL flame-dried home-made Schlenk flask (see Figure 2.26) equipped with a stir bar and flushed with argon was added (*S)*-VANOL (44 mg, 0.1 mmol) and BH_3•Me_2S (150 μL, 0.3 mmol, 2.0 M in toluene), PhOH (18.8, 0.2 mmol) and H_2O (5.4 μL, 0.3 mmol). Under an argon flow through the side-arm of the Schlenk flask, dry toluene (2 mL) was added through the top of the Teflon valve to effect dissolution. The flask was sealed by closing the Teflon valve, and then placed in an 100 ºC oil bath for 1 h. After 1 h, a vacuum (0.5 mm Hg) was carefully applied by slightly opening the Teflon valve to remove the volatiles. After the volatiles were removed completely, a full vacuum was applied and maintained for a period of 30 min at a temperature of 100 ºC (oil bath). The flask was then allowed to cool to room temperature and opened to argon through the side-arm of the Schlenk flask. To the flask containing the pre-catalyst was d_8-toluene (1 mL) under an argon flow through side-arm of the Schlenk flask. The reaction mixture was then stirred for 10 min. The resulting solution was then directly transferred to a quartz NMR tube and was subjected to ^{1}H NMR and ^{11}B NMR analysis.

Entry 3, Figure 8.4A: 1.0 equiv of DMSO **221a** and d_8-toluene (1 mL) was added to the pre-catalyst (as shown in entry 2) for 10 min at 25 °C.

Entry 4, Figure 8.4A: same as entry 3 except *p*-bromobenzaldehyde **127g** used in place of DMSO.

Entry 5, Figure 8.4A: 1.0 equiv of DMSO **221a** was added to the entry 4 for 10 min at 25 °C.

Entry 6, Figure 8.4A: same as entry 3 except diazoacetamide **128a** used in place of DMSO.

Entry 7, Figure 8.4A: 1 mL of d_8-toluene was added to the pre-catalyst followed by the addition of 1.0 equiv of diazoacetamide **128a** as a solution in d_8-toluene (1 mL) for 10 min at 25

°C.

Entry 8, Figure 8.4A: 1 mL of d_8-toluene was added to the pre-catalyst and the resulting solution was cooled to –60 ºC. Thereafter, a pre-cooled (–60 ºC) solution of 1.0 equiv of diazoacetamide **128a** in d_8-toluene (1 mL) was added and the NMR was taken at –60 ºC.

Entry 9, Figure 8.4A: 1 mL of d_8-toluene was added to the pre-catalyst and the resulting solution was cooled to –60 ºC. Thereafter, the NMR was taken at –60 ºC.

8.9.9 Gram scale asymmetric catalysis and KIE studies *(Scheme 8.9-8.11)*

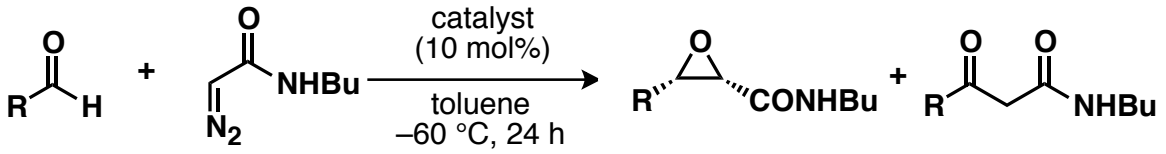

127g (6.0 mmol) **128a** (4.8 mmol) **135g** **136g**

R = 4-Br-C_6H_4

catalyst	%y **135g**	%ee before recryst **135g**	%ee 1st Crop **135g**	%yield 1st Crop **135g**	*c:t*	%y **136g**
432 (with DMSO)	78	90	99	65	30:1	5
448a (without DMSO)	70	79	97	60	15:1	13

(2*S*,3*S*)-*N*-butyl-3-(4-bromophenyl)oxirane-2-carboxamide 135g: *Preparation of the pre-catalyst stock solution :* To a 100 mL flame-dried home-made Schlenk flask , prepared from a single-necked 100 mL pear-shaped flask that had its 14/20 glass joint replaced with a high vacuum threaded Teflon valve, equipped with a stir bar and flushed with argon was added (*S)*-VANOL (632 mg, 1.44 mmol) and PhOH (271 mg, 2.18 mmol, freshly sublimed). Under an argon flow through the side-arm of the Schlenk flask, dry toluene (16 mL) was added through

the top of the Teflon valve to effect dissolution. After the addition of the toluene, BH_3•Me_2S (2.16 mL, 4.32 mmol, 2 M in toluene) and water (78.0 μL, 4.32 mmol) was added. The flask was sealed by closing the Teflon valve, and then placed in a 100 ºC oil bath for 1 h. After 1 h, a vacuum (0.5 mm Hg) was carefully applied by slightly opening the Teflon valve to remove the volatiles. After the volatiles were removed completely, a full vacuum was applied and maintained for a period of 30 min at a temperature of 100 ºC (oil bath). The flask was then allowed to cool to room temperature and opened to argon through the side-arm of the Schlenk flask. This was then completely dissolved in dry toluene (72 mL) under an argon flow through side-arm of the Schlenk flask to afford the stock solution of the pre-catalyst. An aliquot of 24 mL of the pre-catalyst was then transferred to a 250 mL flame-dried round bottom flask equipped with a stir bar and flushed with argon.

Asymmetric epoxidation protocol (with DMSO): To the flask containing the pre-catalyst (24 mL aliquot from 0.02 M stock solution) was added the dimethyl sulfoxide **221a** (37.5 μL, 0.48 mmol). The resulting mixture was stirred for 1 h at room temperature to give SULFOX-BOROX catalyst **432**. Meanwhile, to a separate 100 mL flame-dried round bottom flask was added diazoacetamide **128a** (677.6 mg, 4.800 mmol) and dry toluene (36 mL). After 1 h, the flask containing the catalyst was cooled to –60 °C for 10 min. To this solution was added pre-made solution of diazoacetamide **128a**. The flask containing the diazoacetamide **128a** was then rinsed with toluene (12 mL) and the rinse was then transferred to the flask containing the catalyst at –60 °C. This was then followed by the stirring of the resulting mixture for 10 min at –60 °C. Meanwhile, to a separate 50 mL flame-dried round bottom flask was added aldehyde **127g** (1.11 g, 6.00 mmol, 1.2 equiv, freshly purified) and dry toluene (24 mL). To the mixture containing

diazoacetamide **128a** and catalyst was then added a pre-made solution of aldehyde **127g** and the resulting mixture was stirred for 24 h at –60 °C. The reaction was quenched by the addition of Et_3N (4 mL) and was then warmed to room temperature. The reaction mixture was then transferred to a 500 mL round bottom flask. The reaction flask was rinsed with EtOAc (50 mL × 2) and the rinse was added to the 500 mL round bottom flask. The resulting solution was then concentrated *in vacuo* followed by exposure to high vacuum (0.05 mm Hg) for 1 h to afford the crude epoxide as an off-white semi-solid. The unreacted *p*-bromobenzaldehyde **127g** (148 mg, 0.8 mmol) was recovered by flash silica gel column chromatography followed by the sublimation. The sample of the aldehyde was further subjected to the KIE studies. The remaining crude epoxide was flushed through column using EtOAc. Purification of the crude epoxide by neutral alumina chromatography (30 mm × 300 mm column, 10:1 to 1:1 hexanes/ CH_2Cl_2 as eluent) afforded pure *cis*-epoxide **135g** as a white solid (mp 109-110 ºC on 99% ee material) in 78% isolated yield (1.12 g, 3.74 mmol) and 90% ee; *cis/trans*: 30:1. *β*-ketoamide side product **136g**: 5% yield. The ee of the epoxide was increased to 99% ee with a single recrystallization (1:9 EtOAc/hexanes). The yield of the 1st crop was 65%.

Asymmetric epoxidation protocol (without DMSO): The same reaction in the absence of the DMSO resulted *cis*-epoxide **135g** as a white solid (mp 109-110 ºC on 99% ee material) in 70% isolated yield (1.00 g, 3.36 mmol) and 79% ee; *cis/trans*: 15:1. *β*-ketoamide side product **136g**: 13% yield. The ee of the epoxide was increased to 97% ee with a single recrystallization (1:9 EtOAc/hexanes). The yield of the 1st crop was 60%.

REFERENCES

REFERENCES

(1) Katsuki, T.; Sharpless, K. B. *J. Am. Chem. Soc.* **1980**, *102*, 5974-5976.

(2) Zhang, W.; Loebach, J. L.; Wilson, S. R.; Jacobsen, E. N. *J. Am. Chem. Soc.* **1990**, *112*, 2801-2803.

(3) Irie, R.; Noda, K.; Ito, Y.; Katsuki, T. *Tetrahedron Lett.* **1991**, *32*, 1055-1058.

(4) Tu, Y.; Wang, Z.-X.; Shi, Y. *J. Am. Chem. Soc.* **1996**, *118*, 9806-9807.

(5) (a) Matsumoto, K.; Katsuki, T. In *Catalytic Asymmetric Synthesis, 3rd Ed.*; Ojima, I., Ed.; Wiley-VCH: New York, 2010, p 839. (b) Wong, O. A.; Shi, Y. *Chem. Rev.* **2008**, *108*, 3958-3987. (c) Matsumoto, K.; Sawada, Y.; Katsuki, T. *Pure Appl. Chem.* **2008**, *80*, 1071-1077. (d) *Aziridines and Epoxides in Organic Synthesis*; Yudin, A. K., Ed.; Wiley-VCH: Weinheim, 2006.

(6) Tokunaga, M.; Larrow, J. F.; Kakiuchi, F.; Jacobsen, E. N. *Science* **1997**, *277*, 936-938.

(7) (a) Katsuki, T. In *Comprehensive Asymmetric Catalysis, 1st Ed.*; Jacobsen, E. N., Pfaltz, A., Yamamoto, H., Eds.; Springer: New York, 1999. (b) Johnson, R. A.; Sharpless, K. B. In *Catalytic Asymmetric Synthesis, 2nd Ed.*; Ojima, I., Ed.; Wiley-VCH: New York, 2000. (c) Li, Z.; Yamamoto, H. *J. Am. Chem. Soc.* **2010**, *132*, 7878-+. (d) Zhang, W.; Yamamoto, H. *J. Am. Chem. Soc.* **2007**, *129*, 286-287. (e) Jacobsen, E. N.; Wu, M. H. E. In *Comprehensive Asymmetric Catalysis, 2nd Ed.*; Jacobsen, E. N., Pfaltz, A., Yamamoto, H., Eds.; Springer: New York, 1999, Vol. Vol 2, p 649-677.

(8) (a) Aggarwal, V. K.; Wang, M. F. *Chem. Commun.* **1996**, 191-192. (b) Yang, D.; Wong, M.-K.; Yip, Y.-C.; Wang, X.-C.; Tang, M.-W.; Zheng, J.-H.; Cheung, K.-K. *J. Am. Chem. Soc.* **1998**, *120*, 5943-5952. (c) Denmark, S. E.; Matsuhashi, H. *J. Org. Chem.* **2002**, *67*, 3479-3486. (d) Page, P. C. B.; Buckley, B. R.; Heaney, H.; Blacker, A. J. *Org. Lett.* **2005**, *7*, 375-377.

(9) (a) Nishikawa, Y.; Yamamoto, H. *J. Am. Chem. Soc.* **2011**, *133*, 8432-8435. (b) Shibasaki, M.; Kanai, M.; Matsunaga, S. *Aldrichimica Acta* **2006**, *39*, 31–39.

(10) (a) Juliá, S.; Masana, J.; Vega, J. C. *Angew. Chem., Int. Ed.* **1980**, *19*, 929-931. (b) Ooi, T.; Ohara, D.; Tamura, M.; Maruoka, K. *J. Am. Chem. Soc.* **2004**, *126*, 6844-6845. (c) Lattanzi, A. *Org. Lett.* **2005**, *7*, 2579-2582. (d) Marigo, M.; Franzén, J.; Poulsen, T. B.; Zhuang, W.;

Jørgensen, K. A. *J. Am. Chem. Soc.* **2005**, *127*, 6964-6965. (e) Lee, S.; MacMillan, D. W. C. *Tetrahedron* **2006**, *62*, 11413-11424.

(11) (a) Liu, Y.; Provencher, B. A.; Bartelson, K. J.; Deng, L. *Chem. Sci.* **2011**, *2*, 1301-1304. (b) Ku, J.-M.; Yoo, M.-S.; Park, H.-g.; Jew, S.-s.; Jeong, B.-S. *Tetrahedron* **2007**, *63*, 8099-8103. (c) Arai, S.; Shioiri, T. *Tetrahedron* **2002**, *58*, 1407-1413. (d) Arai, S.; Shirai, Y.; Ishida, T.; Shioiri, T. *Tetrahedron* **1999**, *55*, 6375-6386. (e) Arai, S.; Shirai, Y.; Shioiri, T.; Ishida, T. *Chem. Commun.* **1999**, 49-50. (f) Arai, S.; Shioiri, T. *Tetrahedron Lett.* **1998**, *39*, 2145-2148. (g) Arai, S.; Ishida, T.; Shioiri, T. *Tetrahedron Lett.* **1998**, *39*, 8299-8302.

(12) (a) Aggarwal, V. K.; Alonso, E.; Hynd, G.; Lydon, K. M.; Palmer, M. J.; Porcelloni, M.; Studley, J. R. *Angew. Chem., Int. Ed.* **2001**, *40*, 1430-1433. (b) Aggarwal, V. K.; Alonso, E.; Bae, I.; Hynd, G.; Lydon, K. M.; Palmer, M. J.; Patel, M.; Porcelloni, M.; Richardson, J.; Stenson, R. A.; Studley, J. R.; Vasse, J.-L.; Winn, C. L. *J. Am. Chem. Soc.* **2003**, *125*, 10926-10940. (c) Aggarwal, V. K.; Winn, C. L. *Acc. Chem. Res.* **2004**, *37*, 611-620.

(13) (a) He, L.; Liu, W.-J.; Ren, L.; Lei, T.; Gong, L.-Z. *Adv. Synth. Catal.* **2010**, *352*, 1123-1127. (b) Liu, W. J.; Lv, B. D.; Gong, L. Z. *Angew. Chem., Int. Ed.* **2009**, *48*, 6503-6506.

(14) (a) Li, W.; Wang, J.; Hu, X.; Shen, K.; Wang, W.; Chu, Y.; Lin, L.; Liu, X.; Feng, X. *J. Am. Chem. Soc.* **2010**, *132*, 8532-8533. (b) Hashimoto, T.; Miyamoto, H.; Naganawa, Y.; Maruoka, K. *J. Am. Chem. Soc.* **2009**, *131*, 11280-11281. (c) Trost, B. M.; Malhotra, S.; Fried, B. A. *J. Am. Chem. Soc.* **2009**, *131*, 1674-+. (d) Hashimoto, T.; Naganawa, Y.; Maruoka, K. *J. Am. Chem. Soc.* **2008**, *130*, 2434-2435. (e) Hasegawa, K.; Arai, S.; Nishida, A. *Tetrahedron* **2006**, *62*, 1390-1401. (f) Dudley, M. E.; Morshed, M. M.; Brennan, C. L.; Islam, M. S.; Ahmad, M. S.; Atuu, M.-R.; Branstetter, B.; Hossain, M. M. *J. Org. Chem.* **2004**, *69*, 7599-7608. (g) Yao, W.; Wang, J. *Org. Lett.* **2003**, *5*, 1527-1530. (h) Jiang, N.; Wang, J. B. *Tetrahedron Lett.* **2002**, *43*, 1285-1287. (i) Mahmood, S. J.; Hossain, M. M. *J. Org. Chem.* **1998**, *63*, 3333-3336. (j) Holmquist, C. R.; Roskamp, E. J. *J. Org. Chem.* **1989**, *54*, 3258-3260. (k) Zhu, Z.; Espenson, J. H. *J. Am. Chem. Soc.* **1996**, *118*, 9901-9907. (l) Zhu, Z.; Espenson, J. H. *J. Org. Chem.* **1995**, *60*, 7090-7091. (m) Curini, M.; Epifano, F.; Marcotullio, Maria C.; Rosati, O. *Eur. J. Org. Chem.* **2002**, 1562-1565.

(15) Huang, L.; Wulff, W. D. *J. Am. Chem. Soc.* **2011**, *133*, 8892-8895.

(16) Desai, A. A.; Wulff, W. D. *J. Am. Chem. Soc.* **2010**, *132*, 13100-13103.

(17) Li, X.; Burrell, C. E.; Staples, R. J.; Borhan, B. *J. Am. Chem. Soc.* **2012**, *134*, 9026-9029.

(18) Mukherjee, M.; Gupta, A. K.; Lu, Z.; Zhang, Y.; Wulff, W. D. *J. Org. Chem.* **2010**, *75*, 5643-5660.

(19) Hasegawa, T.; Aoyama, H.; Omote, Y. *J. Chem. Soc., Perkin Trans. 1* **1979**, 963-969.

(20) Vetticatt, M. J.; Desai, A. A.; Wulff, W. D. *J. Am. Chem. Soc.* **2010**, *132*, 13104-13107.

(21) Gaussian 03, Revision D.01 M. J. Frisch, G. W. T., H. B. Schlegel, G. E. Scuseria, M. A. Robb, J. R. Cheeseman, J. A. Montgomery, Jr., T. Vreven, K. N. Kudin, J. C. Burant, J. M. Millam, S. S. Iyengar, J. Tomasi, V. Barone, B. Mennucci, M. Cossi, G. Scalmani, N. Rega, G. A. Petersson, H. Nakatsuji, M. Hada, M. Ehara, K. Toyota, R. Fukuda, J. Hasegawa, M. Ishida, T. Nakajima, Y. Honda, O. Kitao, H. Nakai, M. Klene, X. Li, J. E. Knox, H. P. Hratchian, J. B. Cross, V. Bakken, C. Adamo, J. Jaramillo, R. Gomperts, R. E. Stratmann, O. Yazyev, A. J. Austin, R. Cammi, C. Pomelli, J. W. Ochterski, P. Y. Ayala, K. Morokuma, G. A. Voth, P. Salvador, J. J. Dannenberg, V. G. Zakrzewski, S. Dapprich, A. D. Daniels, M. C. Strain, O. Farkas, D. K. Malick, A. D. Rabuck, K. Raghavachari, J. B. Foresman, J. V. Ortiz, Q. Cui, A. G. Baboul, S. Clifford, J. Cioslowski, B. B. Stefanov, G. Liu, A. Liashenko, P. Piskorz, I. Komaromi, R. L. Martin, D. J. Fox, T. Keith, M. A. Al-Laham, C. Y. Peng, A. Nanayakkara, M. Challacombe, P. M. W. Gill, B. Johnson, W. Chen, M. W. Wong, C. Gonzalez, and J. A. Pople, Gaussian, Inc., Wallingford CT, 2004

(22) Singleton, D. A.; Thomas, A. A. *J. Am. Chem. Soc.* **1995**, *117*, 9357-9358.

(23) Ouihia, A.; Rene, L.; Guilhem, J.; Pascard, C.; Badet, B. *J. Org. Chem.* **1993**, *58*, 1641-1642.

(24) Doyle, M. P.; Kalinin, A. V. *J. Org. Chem.* **1996**, *61*, 2179-2184.

(25) Blankley, C. J.; Sauter, F. J.; House, H. O. *Org. Synth.* **1969**, *49*, 22.

(26) García, M. J.; Rebolledo, F.; Gotor, V. *Tetrahedron* **1994**, *50*, 6935-6940.

(27) Neo, A. G.; Delgado, J.; Polo, C.; Marcaccini, S.; Marcos, C. F. *Tetrahedron Lett.* **2005**, *46*, 23-26.

CHAPTER 9

IS IT REALLY A LEWIS ACID CATALYED ASYMMETRIC IMINO-ALDOL REACTION? - PROBING THE NATURE OF THE ACTIVE SITE VIA NMR SPECTROSCOPY, COMPUTATIONAL STUDIES AND SUBSTRATE AND CATALYST MODIFICATIONS

Another year; another reaction. I think that we should pursue it a little more!

-William D. Wulff

9.1 Introduction

Out of all catalytic asymmetric reactions, the Mannich reaction[1] and Mannich-type reactions are some of the most important and useful reactions.[2] One of the Mannich-type reactions is the reaction of an enolate or enolate equivalent with an aldimine. This reaction provides an easy access to the optically active β-amino esters or ketones, which can easily be transformed into β-amino acids, β-amino-alcohols, β-lactams etc.[3] In the 90's, several examples of enantioselective Mannich-type reactions using a stoichiometric amount of an activator for the imines were reported.[4] However, in last decade or so, various kinds of asymmetric catalysis have been utilized for the realization of this reaction. This includes a variety of chiral Lewis acid[2a,2e] and Brønsted acid[5] mediated asymmetric reactions. Specifically, one of the early examples involving chiral Lewis acids was reported by Kobayashi and co-workers in 1997.[6] They reported the first asymmetric Mannich type reaction between imine **458** and ketene silyl acetal **460** using a catalyst derived from $Zr(OtBu)_4$ **463b**, NMI **464** and (*R*)-6,6′-Br_2-BINOL **459**.

In due course of time, they reported several modifications of this catalytic system for the same reaction.[2a] Within four years of the first example, the Wulff group reported an unusually robust and temperature independent catalytic system which provided higher selectivities by employing vaulted biaryl ligand (*S*)-VAPOL **59** rather than the linear biaryl ligands **55** and **459**.[7] A list of various ligands and imines screened for imino-aldol reaction are presented in Figure 9.1.

Figure 9.1 Ligands and imines used in the imino-aldol reaction.

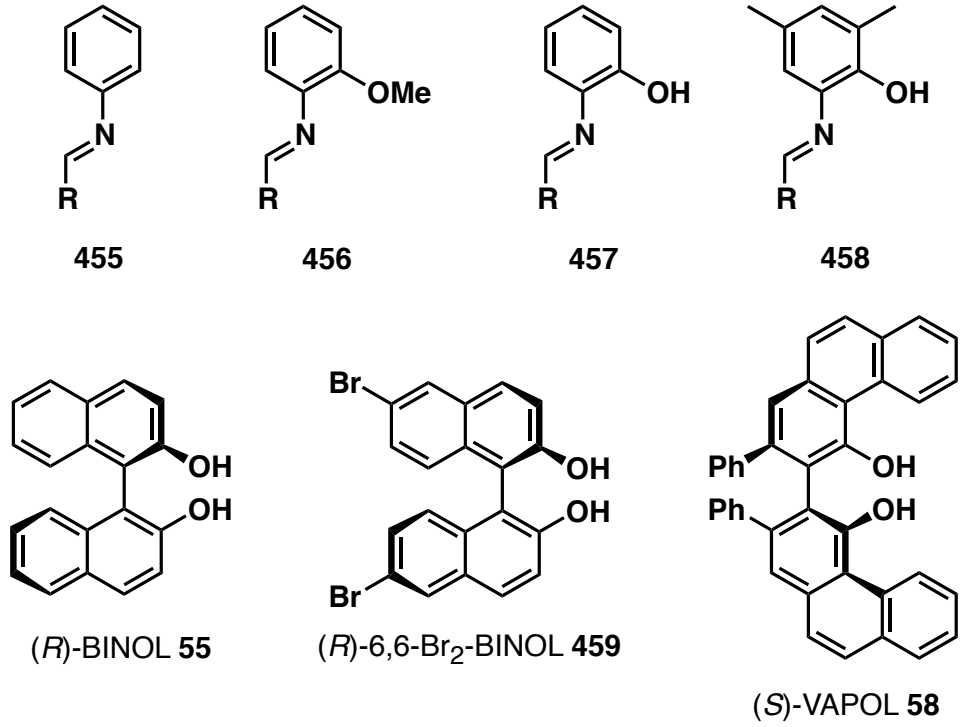

Based on the initial CPK models, Wulff and cowerkers installed two methyl groups at the 3 and 5 positions of the phenyl ring of the imine **457**, thereby, transforming it to the imine **458** (Figure 9.1). Excellent results were obtained utilizing imine **458** and also, it was found to be independent of the temperature (Table 9.1).[7] More importantly, they were able to employ a

catalyst loading as low as up to 2 mol% (Table 9.1, entries 7 and 9). The only data from Table 9.1 that comes from the present dissertation is entry 6 (solvent = CH_2Cl_2).

Table 9.1 Imino-aldol reaction between imine **457/458** with ketene acetal **460** using various ligands.

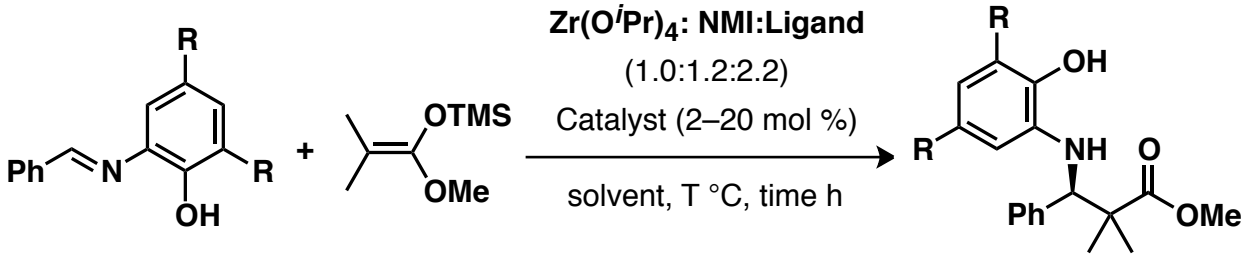

457a (R=H)
458a (R=Me)

460

461a (R=H)
462a (R=Me)

#	Imine	L	Cat (mol%)	T (°C)	Ester	Solvent					
						CH_2Cl_2			Toluene		
						Yield (%)[b]	ee (%)[c]	Time (h)	Yield (%)[b]	ee (%)[c]	Time (h)
1	**457a**	**55**	20	–45	**461a**	80	36	19	–	–	–
2[d]	**457a**	**55**	10	–45	**461a**	87	86	19	–	–	–
3	**457a**	**58**	20	–45	**461a**	50	80	10	92	91	20
4	**457a**	**55**	20	25	**461a**	100	28	4	–	–	–
5[d]	**457a**	**459**	10	25	**461a**	87	48	4	95	62	18
6	**457a**	**58**	20	25	**461a**	78	84[e]	18	94	89[f,g]	15
7	**457a**	**58**	2	40	**461a**	–	–	–	100	86[g,h]	6
8[d]	**458a**	**459**	10	25	**462a**	–	–	–	93	47	18
9	**458a**	**58**	20	25	**462a**	–	–	–	100	98	15
10	**458a**	**58**	2	100	**462a**	–	–	–	95	98.5	5

[a] Unless otherwise specified, all reactions were performed with 0.25 mmol of imine **457**/**458** in toluene (0.125 M in imine) with 1.2 equiv of **460** and 10, 20 or 2 mol% of the catalyst at T °C. The catalyst was prepared from Zr(O^{i}Pr)$_4$/^{i}PrOH **463a**, ligand **55/58/459** (2.2 equiv) and NMI **464** (1.2 equiv) in CH_2Cl_2 (entries 1, 2, 4, 5 and 8) or toluene (entries 3, 6, 7, 9 and 10) at 25 °C for 1h. L = Ligand. [b] Isolated Yield. [c] Determined by HPLC. [d] Zr(O^{t}Bu)$_4$ **463b** used. [e] 15:1 CH_2Cl_2: toluene. [f] 0.5 M in imine. [g] 15:1 toluene:CH_2Cl_2. [h] 1.0 M in imine.

Our catalyst was prepared by the reaction of 2.2 equivalents of (*S*)-VAPOL **58** with 1 equiv of $Zr(iPrO)_4$ **463a** and 1.2 equiv of *N*-methylimidazole (NMI) **464** at room temperature for 1 h. In dichloromethane, it was found that (*S*)-VAPOL **58** and (*R*)-6,6′-Br_2-BINOL **459** were superior to (*R*)-BINOL **55** at –45 °C (Table 9.1, entries 1-3). At 25 °C, while asymmetric induction in the case of VAPOL remains almost unchanged (84% ee, Table 9.1, entry 6), it decreased quite sharply in the case of (*R*)-6,6′-Br_2-BINOL **459** (48% ee, Table 9.1, entry 5). When the solvent is changed to toluene, the induction increases in both cases at room temperature. However, (*S*)-VAPOL **58** proved still to be the best ligand for this reaction in toluene at room temperature (89% ee vs 62% ee, Table 9.1 entries 6 *vs*. 5). In fact, quantitative yield was obtained with only a small drop-off in the asymmetric induction (86% ee), when the reaction was performed at 40 °C with 2 mol% catalyst loading. Additionally, almost optically pure *β*-amino ester was obtained employing imine **458a** independent of temperature (entries 9-10). However, only 47% ee was observed when (*R*)-6,6′-Br_2-BINOL **459** was used as the ligand in the case of the imine **458a** (entry 8). Thus, the catalyst generated from VAPOL is far more efficient than the catalyst generated from (*R*)-BINOL **55** or its derivative **459** as low temperature is not necessary for attaining high asymmetric inductions.

9.2 Proposed catalytic cycle of imino-aldol reaction

In the year 2001, Wulff proposed a mechanism for the imino-aldol reaction and this is presented in Scheme 9.1. Initially, the proposed catalytic cycle I involved a catalyst bearing two VAPOL ligands on one zirconium and *o*-hydroxyphenylimine **457** is coordinated to the

zirconium. Based on the initial space-filling CPK models, we found that the binding of the two VAPOL units to one zirconium atom is possible only with a facial arrangement of the four oxygen atoms as illustrated by structure **465** in Scheme 9.1. Also, two NMIs are proposed to be coordinating at the axial positions. Thereafter, the imine is proposed to replace one of the NMI at one of the apical position. This would lead to imine-catalyst complex **466** where a phenol exchange has occurred. Subsequent attack of ketene acetal **460** would give **467** first, and then **468**, whose trimethylsilylated oxygen atom attacks the Zr center to afford the product **469**. Subsequent hydrolysis would furnish the β-amino ester **461**.

Scheme 9.1 Proposed catalytic cycles of imino-aldol reaction using (*S*)-VAPOL **58** (A, B, C) and (*R*)-6,6′-Br_2-BINOL **459** (D) as the ligands. (**A**) Catalytic cycle I (**B**) Catalytic cycle II (**C**) Catalytic cycle III (**D**) Catalytic cycle III′

A

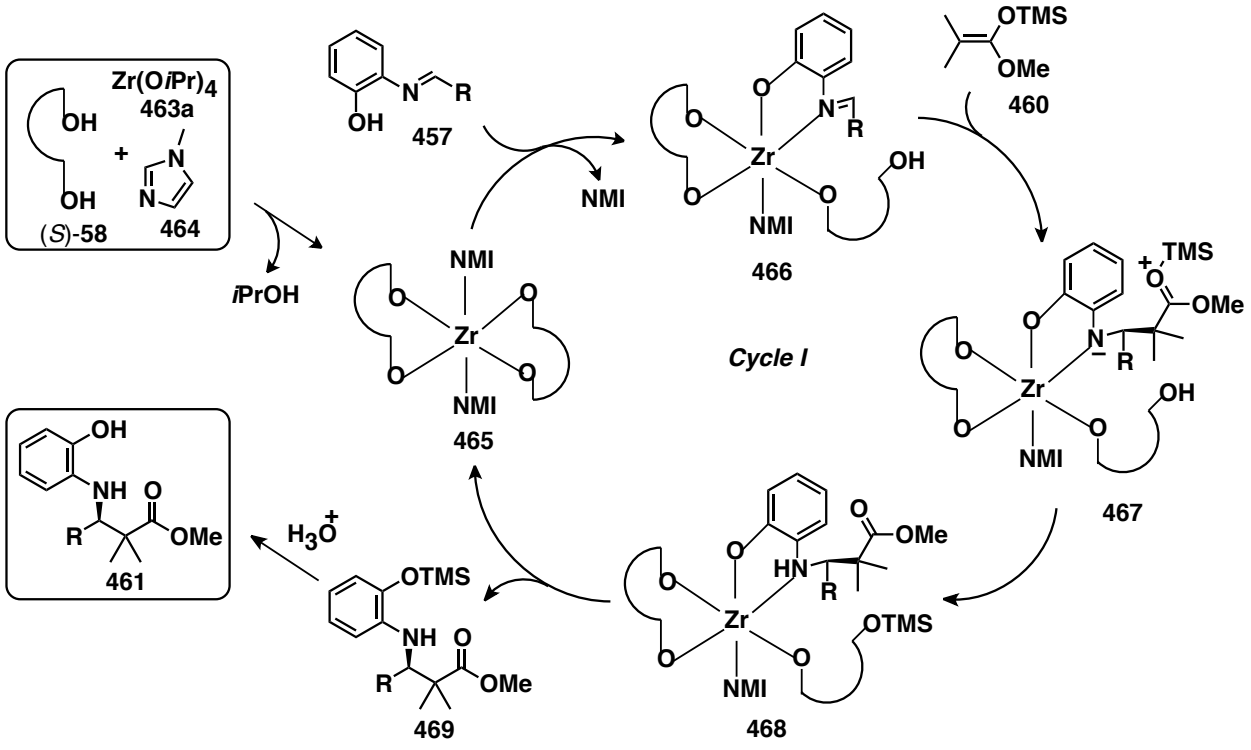

Scheme 9.1 cont'd

B

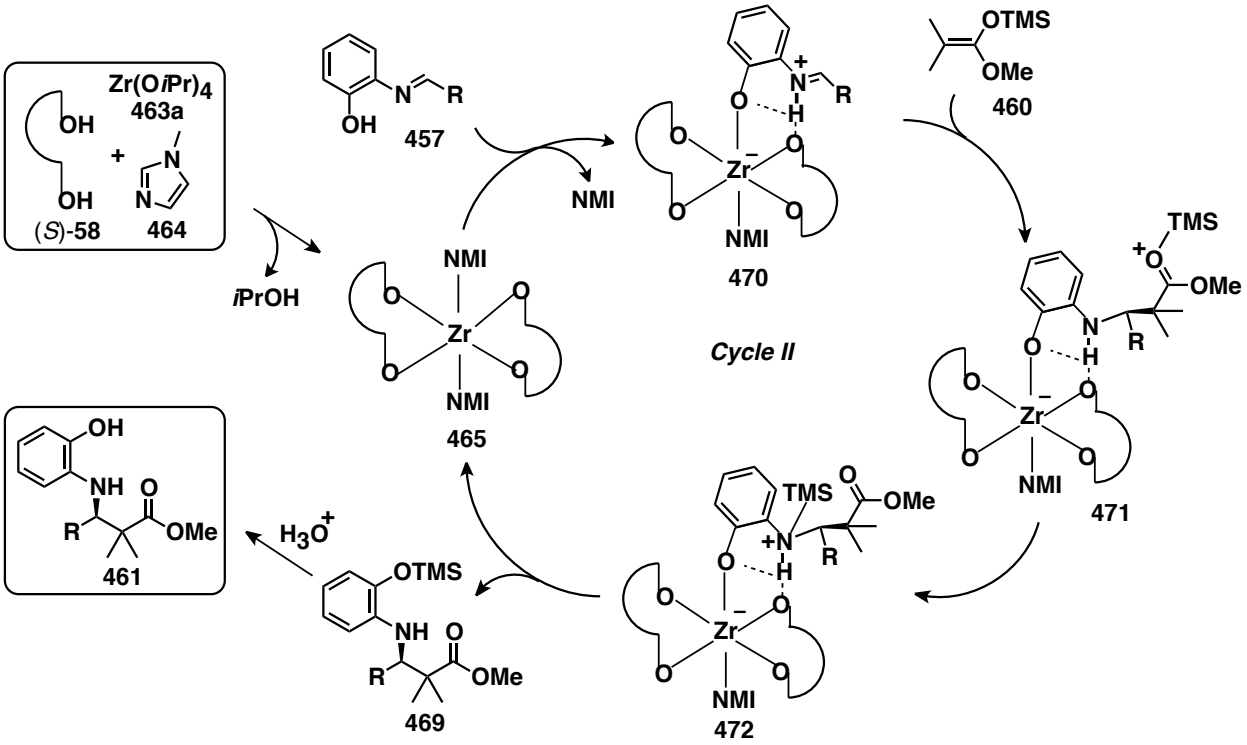

C

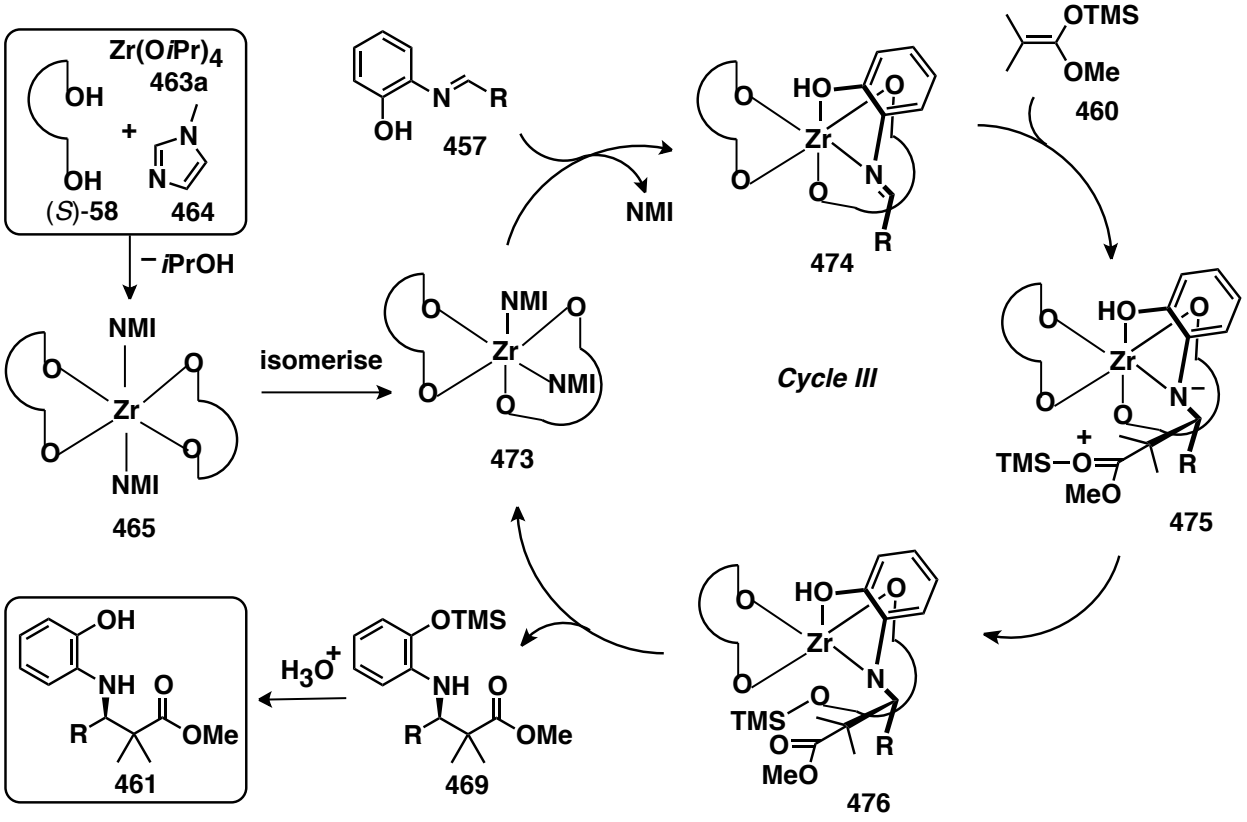

Scheme 9.1 cont'd

D

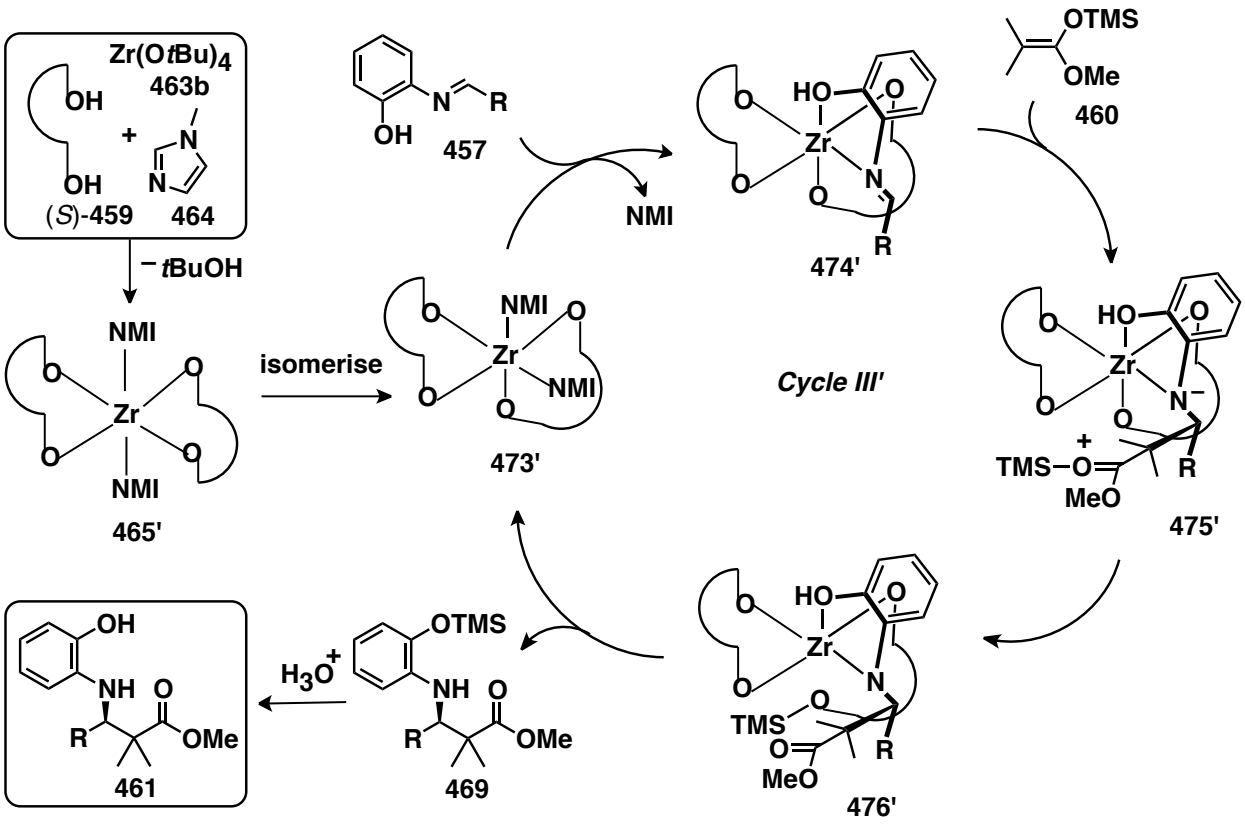

During recent mechanistic investigations, we envisioned another catalytic cycle with a different mode of activation of the imine (Scheme 9.1B). This involves the presence of the imine–catalyst complex **470** where the imine is protonated and is hydrogen bonded to the oxygen of the ligand **58**. As the imine is covalently bonded to zirconium after phenol exchange, this type of interaction would fall in the category of Lewis acid assisted Brønsted acid catalysis. Another plausible mechanism was proposed by Kobayashi and coworkers and involves (*R*)-6,6′-Br_2-BINOL **459** as the ligand. It excludes the presence of NMI in the transition states (Catalytic cycle III′, Scheme 9.1D and Scheme 9.2B). The catalyst is generated from a mixture of $Zr(OtBu)_4$ **463b**, NMI **464** and (*R*)-6,6′-Br_2-BINOL **459**. In this mechanism, it has been

assumed that step one involves the isomerization of complex **465'**, where there are two NMI groups that are trans to each other (Catalytic cycle III, Scheme 9.2B), to **473'** where the NMI groups are cis to each other. The second step involves the exchange of the NMI groups by the imine **457** leading to the formation of the imine-catalyst complex **474'**. The coordination of the hydroxyl group to the zirconium atom indicates the importance of the hydroxyl group. Subsequent attack of ketene acetal **460** would give **475'** then **476'**, which is followed by the final release of the product **461**. A similar kind of mechanism can also be assumed for the reaction involving (*S*)-VAPOL **58** as the ligand (Catalytic cycle III, Scheme 9.1C). Various techniques such as NMR studies and theoretical calculations were then used to determine the most probable catalytic cycle and to support the proposed intermediates of the corresponding catalytic cycle. The details are discussed below.

9.3 NMR experiments:

In support of the intermediate **465**, a clean spectrum was observed when a catalyst derived from Zr(*i*PrO)$_4$, 2 equiv of (*S*)-VAPOL **58** and 2 equiv of *N*-methyl imidazole **464** was subjected to ^{1}H NMR analysis. The observed ^{1}H NMR spectrum with a single bay proton doublet at δ = 11.33 ppm clearly indicates the presence of a C_2-symmetric species **465** bearing two mutually trans NMI ligands bound to zirconium. Thereafter, another NMR experiment was performed to gain an insight into the interaction of the imine with the catalyst. This provides some information about the phenol exchange. An excess amount of imine **457a** (2 equiv) was added to the catalyst that was generated from 1 equiv of Zr(*i*PrO)$_4$ **463a**, 2 equiv of VAPOL **58** and 2

equiv of *N*-methyl imidazole **464** in d8-toluene. Non-equivalent phenanthrene units were observed in the ^{1}H NMR spectrum. In fact, the appearance of new bay protons at δ = 11.4 and δ = 11.8 ppm indicated the loss of C_2 symmetry and supported the proposal of phenol exchange resulting from the addition of the imine to the catalyst. Another piece of evidence comes from the fact that the reaction of imine **456a** (R = Ph) gave the racemic product in 5% yield only (Figure 9.1).[7] Also, a similar observation has been made for the catalyst derived from (*R*)-6,6′-Br_2-BINOL **459** where the imines **455a** (R = Ph) and **456a** (R = Ph) gave good yields but only in 5% ee.[6]

9.4 DFT calculations

Intrigued by the observations from the NMR experiments on the catalyst for the imino-aldol reaction, we decided to investigate the catalyst and catalytic cycle further using computational chemistry. Specifically, the nature of the active site and subsequent transition state of the imino-aldol reaction were point of interests in these theoretical calculations. The possibility of hydrogen bonding in **470** (Scheme 9.1) motivated us to study the mechanism of the reaction in detail. The catalytic asymmetric imino-aldol reaction is a challenging system to examine computationally due to the size of the system which includes two VAPOL units and the zirconium atom (with d-orbitals). The number of atoms is more than 125 in each of the reactions studied computationally. Hence, in order to reduce the computational cost, the hybrid DFT:HF ONIOM method was employed to obtain quality results. It must be noted that it is not reasonable to expect quantitative matches of experimental and theoretical $\Delta\Delta G^{\ddagger}$ given the size of the experimental system and the errors associated with each of the methods. The

'extrapolated energy' from the ONIOM calculation gives an initial measure of the relative energy of the transition state structures. Thereafter, following the common approach, one can then perform a single point energy calculation on the ONIOM optimized geometries using the DFT method with a larger basis set for the whole system. All calculations were performed with the Gaussian ′03.[8] Geometries and transition states were fully optimized and characterized by frequency using B3LYP or hybrid density functional theory (BHandHLYP) with the LanL2DZ or DGDZVP basis sets for the high level and HF with STO-3G basis set for the low level in ONIOM calculations. Free energies (298.15 K, 1 atm) and natural charges from the natural population analysis were also computed for the gas phase. As the reaction was performed in toluene, one does not expect much stabilization from toluene for the charged intermediates/transition states along the reaction coordinate. In the continuum solvation model, the single-point energy calculations with the self-consistent reaction field (SCRF) calculation based on the polarizable continuum model (PCM, $\varepsilon = 2.379$ for toluene) were carried out at the high level for the one used for geometry optimization in ONIOM calculations.

9.4.1 Catalytic cycle I verses catalytic cycle II

As stated earlier, there are two possible kinds of imine-catalyst complexes and these are **466a** and **470a**. These two complexes **466a** and **470a** were computed using ONIOM (B3LYP/LanL2DZ:HF/STO-3G) calculations. The division of layers for the ONIOM calculations is illustrated by the color scheme given in Figure 9.2. The choice of the basis sets for the higher level calculations were made after carefully considering the available options for the zirconium atom in Gaussian ′03. All distances in the fully optimized structures are reported in angstroms. The reported energies are the free energies ($\Delta\Delta G$) of fully optimized geometries from the ONIOM calculations.

Figure 9.2 Division of layers for the ONIOM calculations ONIOM(B3LYP/LanL2DZ:HF/ STO-3G) and ONIOM(BHandHLYP/DGDZVP:HF/STO-3G) level.

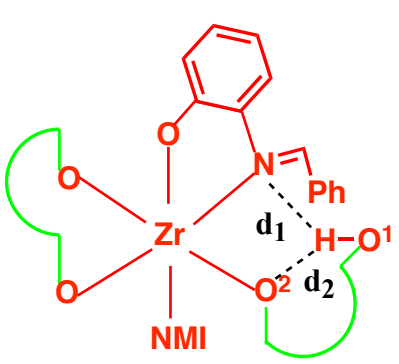

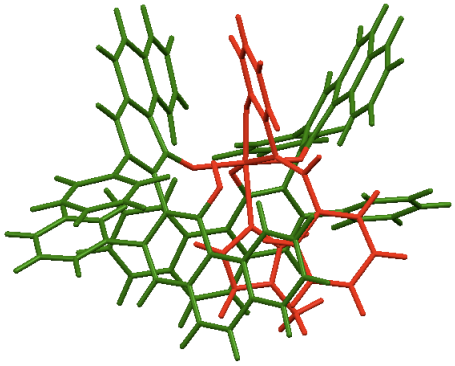

466a

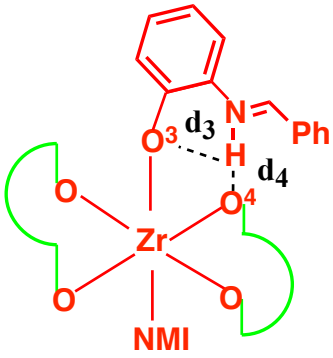

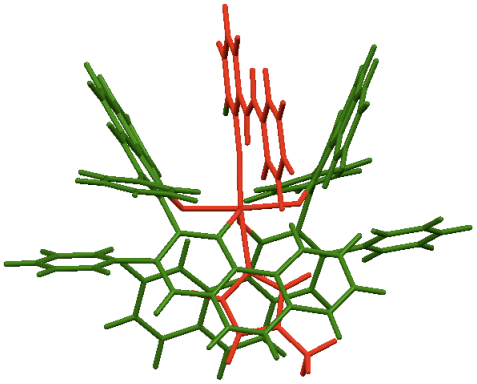

470a

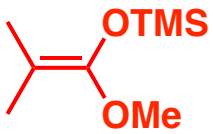

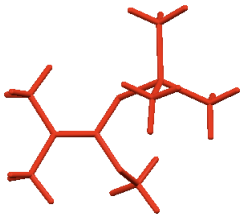

460

Red = B3LYP/LanL2DZ

or BHandHLYP/DGDZVP

Green = HF/STO-3G

Interestingly, the imine-catalyst complex **470a** was found to be the preferred complex as the other complex **466a** was found to be +38.0 Kcal/mol higher in energy (Figure 9.3). The huge difference in energy suggests that the complex **466a** is highly unfavorable. In complex **466a**, the proposed hydrogen bonding (d_1 = 2.87 Å, Figure 9.3) between nitrogen of imine and the proton attached to O1 is found to be a very weak interaction and in fact the bond angle (98º) is far away

from linear. The preference for the imine-catalyst complex **470a** suggests that a Lewis acid assisted Brønsted acid catalysis might be a plausible mechanism in this case. There is a probability of a weak hydrogen bonding (d_4) existing in the case of complex **470a** with a calculated bond distance of 2.53 Å (d_4, O^4-H, Figure 9.3) and bond angle of 169.6º ($\angle O^4HN$, Figure 9.3). In order to refine the analysis, we subjected the both complexes to geometry optimization using hybrid density functional (BHandHLYP) with DGDZVP basis set. BHandHLYP is considered to be a better method than B3LYP for the case of hydrogen bonding and other non-covalent interactions.[9] In this case, the bond distance (d_4) and bond angle were determined to be 2.32 Å (d_4, O^4-H, Figure 9.3) and 179.6º ($\angle O^4HN$, Figure 9.3) respectively. This indicated the presence of a hydrogen bond of moderate strength. Another weak interaction was found to be operating between O^3 and the H attached to nitrogen of imine (d_3 = 2.31 Å, Figure 9.3). It must be noted that complex **466a** is +29 Kcal/mol higher in energy as compared to complex **470a** even at the higher level of calculations (ONIOM(BHandHLYP/DGDZVP:HF/STO-3G), Figure 9.3).

Figure 9.3 Calculated 3D structures and relative energies of the imine-catalyst complexes **466a** and **470a** at ONIOM(B3LYP/LanL2DZ:HF/STO-3G) level and ONIOM(BHandHLYP/DGDZVP:HF/STO-3G) level. The structures are visualized by the Mercury program (C, gray; O, red; N, blue; Zr, yellow; H, white). Hydrogen atoms are omitted (except N-H) and the ligand is given in green color for clarity. Free energies and bond lengths are in Kcal/mol and Å respectively. Some interactions are highlighted: d_1 = 2.87 Å, d_2 = 3.02

Figure 9.3 cont'd

Å, d_3 = 2.21 Å and d_4 = 2.53 Å with ONIOM(B3LYP/LanL2DZ:HF/STO-3G) and d_1 = 2.95 Å, d_2 = 2.97 Å, d_3 = 2.31 Å and d_4 = 2.32 Å with ONIOM(B3LYP/LanL2DZ:HF/STO-3G)

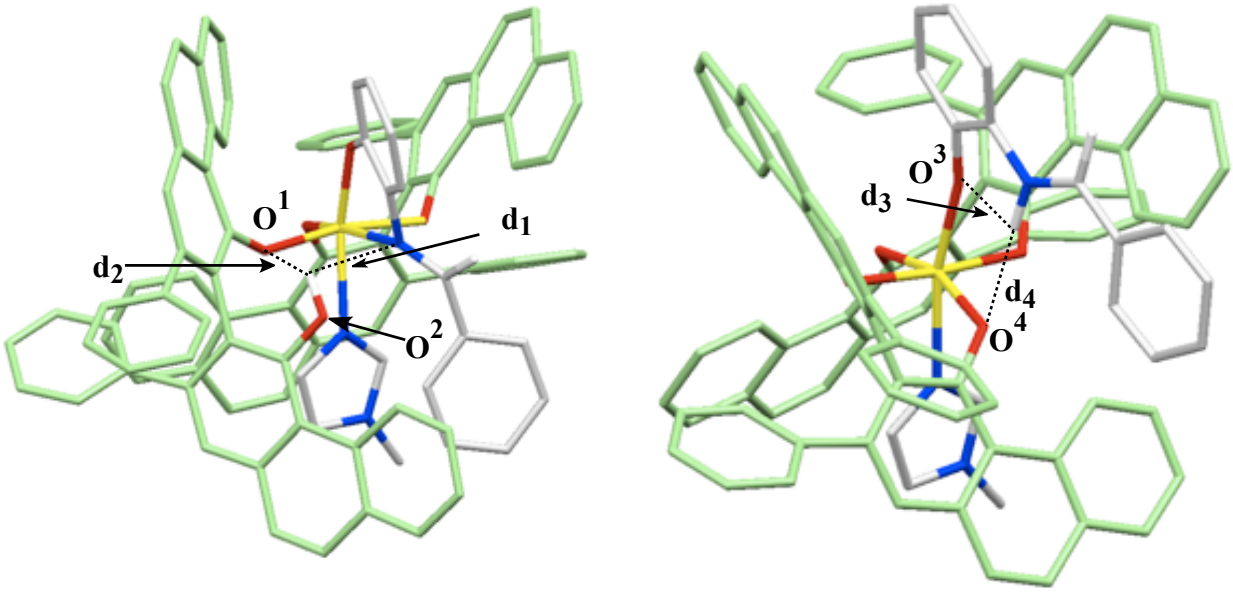

466a
ΔΔG = +38

470a
ΔΔG = 0

Although the imine-catalyst complex **466a** is highly unlikely to be a viable intermediate, we decided to compute the transition states for the reaction of ketene acetal **460** with both complexes **466a** and **470a**. More unstable intermediates tend to be also much more reactive and therefore, it is important to explore reactivity and compare the activation barriers for reaction of both complexes. Transition states for the key carbon-carbon bond-forming step of the reactions between **466a** and **460** and **470a** and **460** were located by scanning the coordinates at the ONIOM(B3LYP/LanL2DZ:HF/STO-3G) level. All distances are reported in angstroms, and all reported energies are $\Delta\Delta G^{\ddagger}$ of fully optimized geometries from the ONIOM calculations. Also,

it must be noted that the ketene acetal **460** was calculated at B3LYP/LanL2DZ level of theory.

Figure 9.4 Free Energy diagram for the transition states TS0-**477**-*Si* and TS1-**478**-*Si* at ONIOM(B3LYP/LanL2DZ:HF/STO-3G) level. Energy in parenthesis is enthalpy.

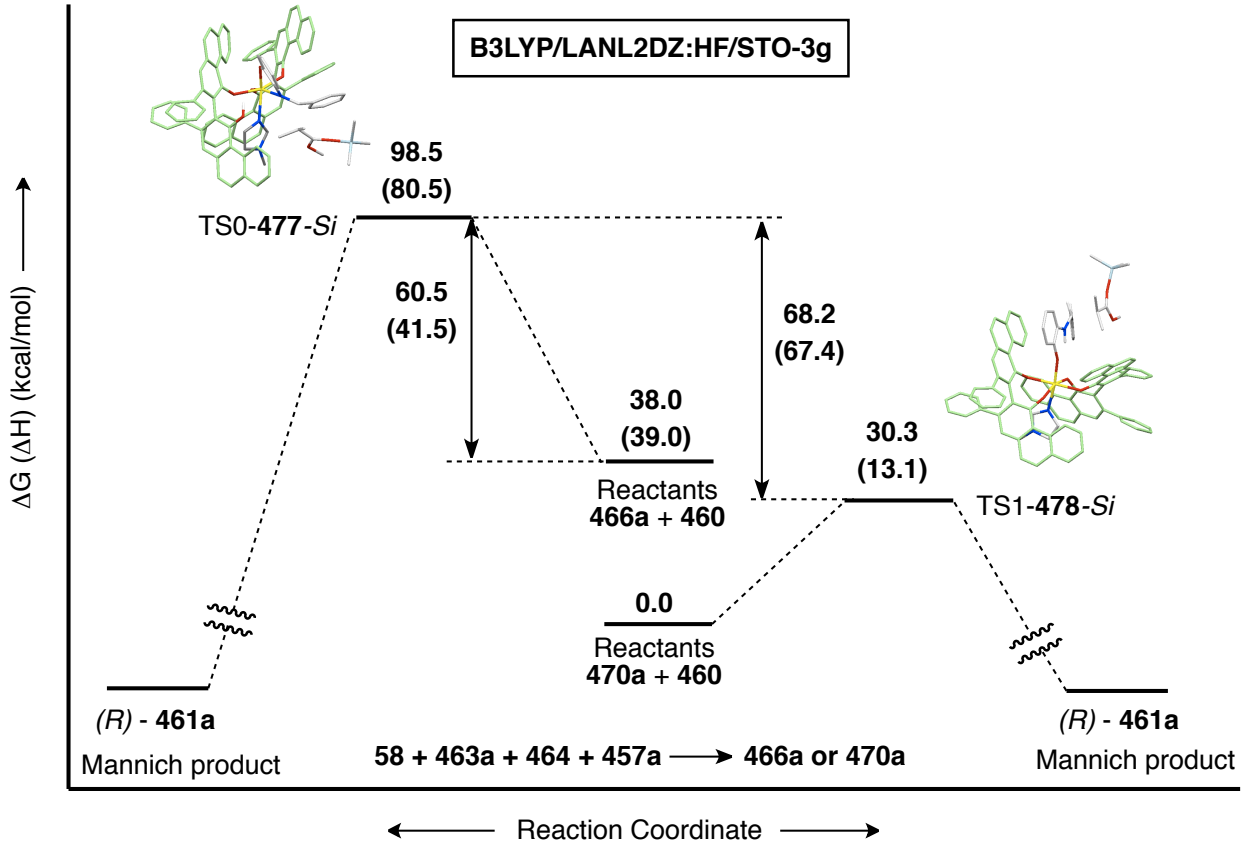

The DFT calculations at B3LYP/LanL2DZ level of theory revealed that a direct coordination of N of imine to the zirconium atom in complex **466** is highly unfavorable as a high energy barrier of +60.5 kcal/mol was found in the case of the corresponding transition state (TS0 **477**-*Si*, Figure 9.4 and 9.5) leading to favored enantiomer (*R*). The fact that the calculated barrier for TS1-**478**-*Si* (**470→471**) is approximately three times lower than the barrier for TS0-**477**-*Si* (**466→467**) strongly supports the catalytic cycle II (Figure 9.4 and 9.5).

Figure 9.5 Calculated 3D structures of the TS0-**477**-*Si* and TS1-**478**-*Si* at ONIOM(B3LYP/LanL2DZ:HF/STO-3G) level. The structures are visualized by the Mercury program (C, gray; O, red; N, blue; Zr, yellow; Si = light blue). Hydrogen atoms are omitted (except N-H) and the ligand is given in green color for clarity. Bond lengths are in Å. Some interactions are highlighted: d_1 = 3.55 Å, d_2 = 3.07 Å, d_5 = 1.95 Å, d_3 = 2.17 Å, d_4 = 2.97 Å and d_6 = 2.08 Å.

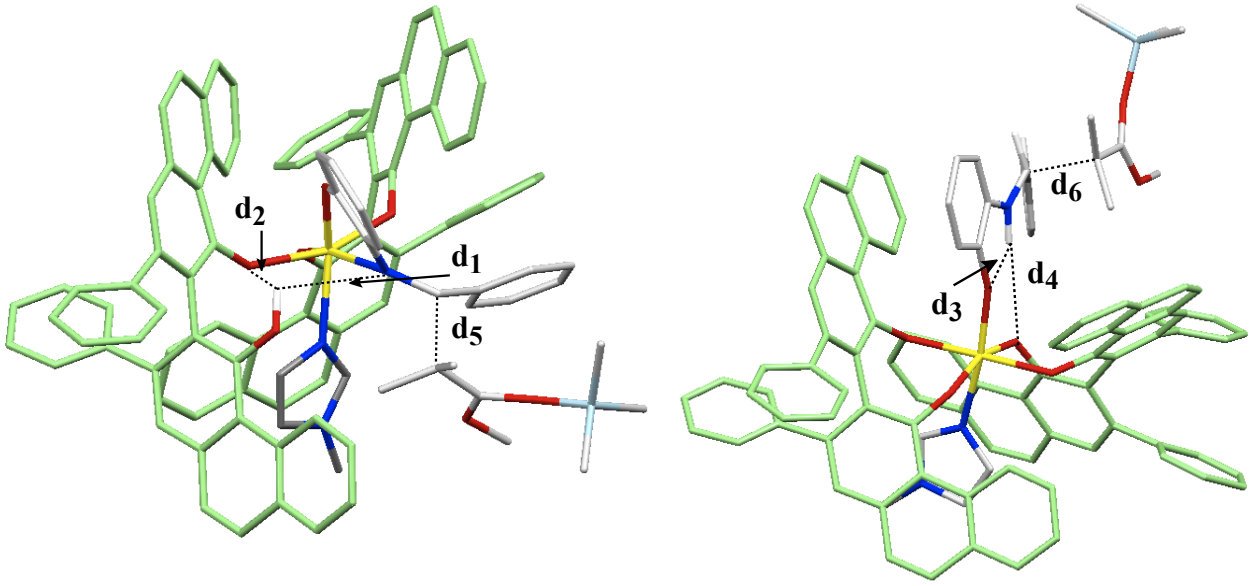

TS0-**477**-*Si* TS1-**478**-*Si*

The computations discussed above were performed with four different orientations of attack by the ketene acetal and the data presented above was for the lowest energy orientation of the four. The discussion of the other possible transition states is given below.

9.4.2 Various transition states for catalytic cycle II

As discussed above, four transition states (including TS1-**478**-*Si*) were located for one particular enantiomer by employing the different orientations and conformations of silyl ketene

acetal **460** (Figure 9.6A). The lowest energy transition state leading to the favored enantiomer (*R*) was found to be TS1-**478**-*Si* when it was subjected to ONIOM(BHandHLYP/DGDZVP:HF/STO-3G) level of calculations. The key observation in the favored structure is that the hydrogen bonding (d_4) is further weakened due to increase in the bond distance from 2.3 to 2.9 Å (Figure 9.6). Nonetheless, a weak interaction is still operational providing the R enantiomer as the major product. Also, it must be noted that the *Re* face of the imine **457a** is completely shielded by the (*S*)-VAPOL **58**. The carbon-carbon bond distance for transition state TS1-**478**-*Si* is 2.08 Å (Figure 9.5). Interestingly, TS3-**480**-*Re* which leads to lowest energy structure for minor enantiomer was found to have no hydrogen bonding as the O-H distance was ~ 4 Å. The energy difference between favored transition state TS1-**479**-*Si* and disfavored transition state TS3-**480**-*Re* was determined to be **+1.8** Kcal/mol (Figure 9.6). The absence of the hydrogen bonding is probably due to the steric hindrance between the methyl groups of ketene acetal **460** and the phenanthrene ring of the (*S*)-VAPOL **58**.

Figure 9.6 (**A**) Different conformations and orientations of silyl ketene acetal **460** used for calculations. (**B**) Calculated 3D structures and relative free energies of TS1-**478** to TS4-**481** at ONIOM(BHandHLYP/DGDZVP:HF/STO-3G) level. The structures are visualized by the Mercury program (C, gray; O, red; N, blue; Zr, yellow; Si = light blue). Hydrogen atoms are omitted (except N-H) and the ligand is given in green color for clarity. Free energies and bond lengths are in kcal/mol and Å respectively. Some interactions are highlighted: d_3 (O^3–H), d_4 (O^4–H) and d_6 (C–C). (**C**) Space-filling rendition of TS1-**478**-*Si* and TS3-**480**-*Re* with top and side-view with hydrogens showing.

Figure 9.6 cont'd

A

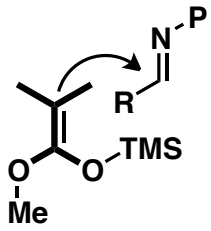

(For TS1-**478**)

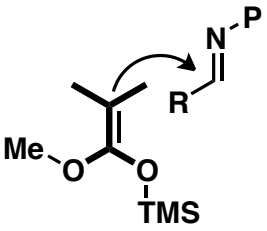

(For TS2-**479**)

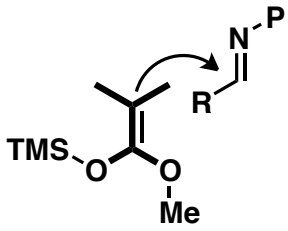

(For TS3-**480**)

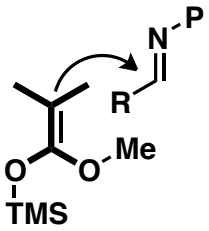

(For TS4-**481**)

B

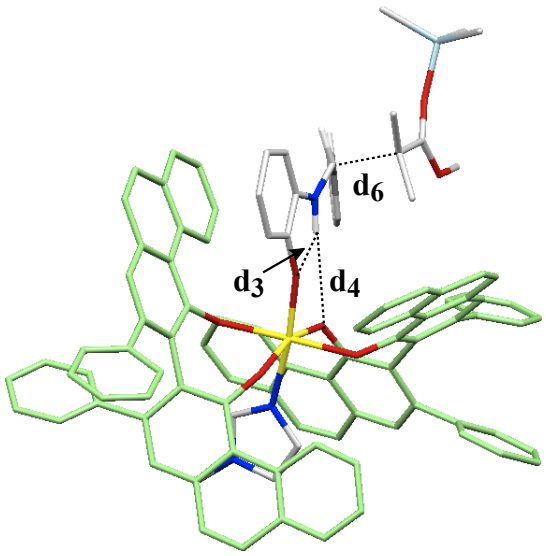

TS1-**478**-*Si*

$\Delta\Delta G^{\ddagger}$ = +0.0

d_3 = 2.16 Å, d_4 = 2.99 Å and d_6 = 2.09 Å

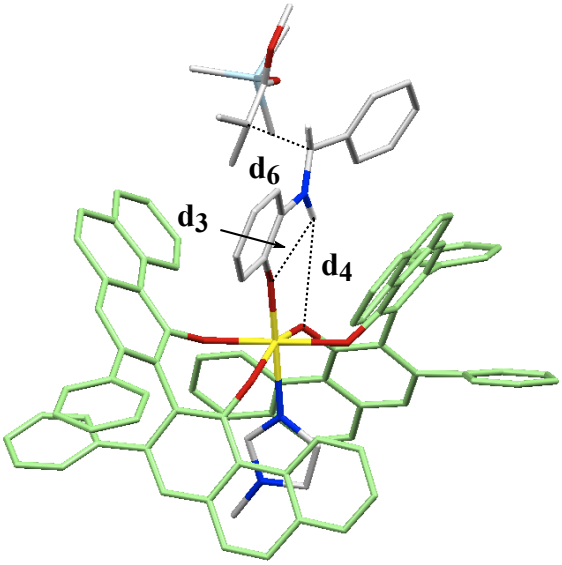

TS1-**478**-*Re*

$\Delta\Delta G^{\ddagger}$ = +2.2

d_3 = 2.24 Å, d_4 = 3.98 Å and d_6 = 2.09 Å

Figure 9.6 cont'd

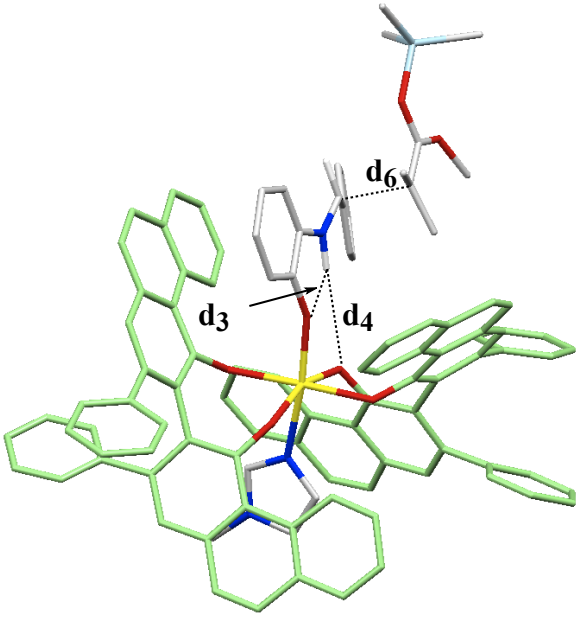

TS2-**479**-*Si*

$\Delta\Delta G^{\ddagger}$ = +1.9

d_3 = 2.15 Å, d_4 = 2.99 Å and d_6 = 2.09 Å

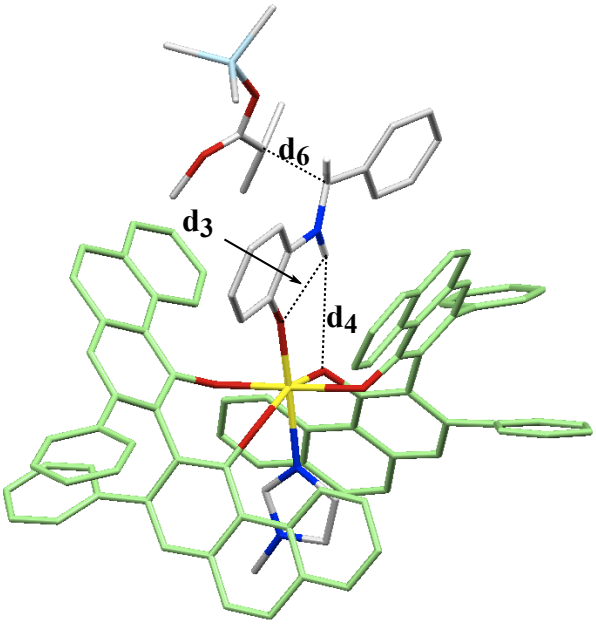

TS2-**479**-*Re*

$\Delta\Delta G^{\ddagger}$ = +2.8

d_3 = 2.21 Å, d_4 = 3.94 Å and d_6 = 2.15 Å

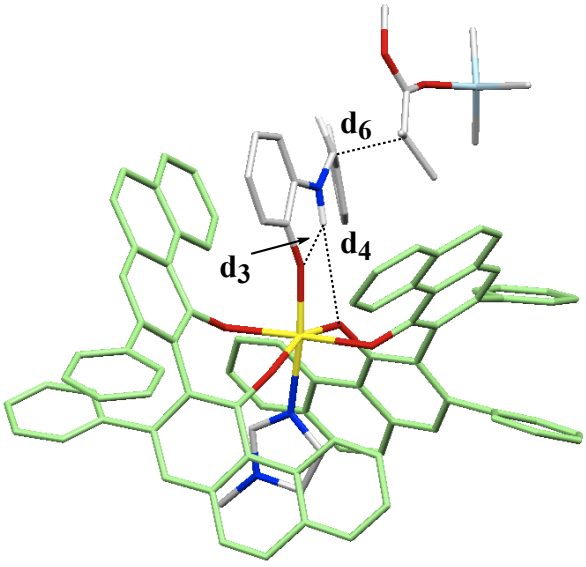

TS3-**480**-*Si*

$\Delta\Delta G^{\ddagger}$ = +0.1

d_3 = 2.17 Å, d_4 = 2.93 Å and d_6 = 2.09 Å

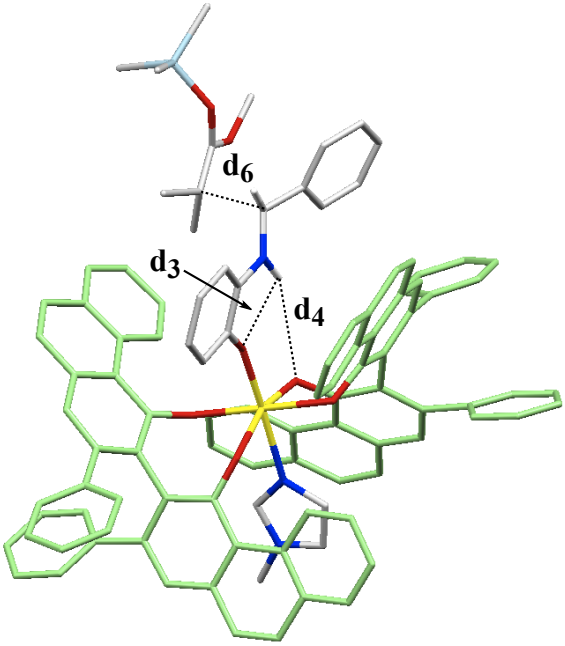

TS3-**480**-*Re*

$\Delta\Delta G^{\ddagger}$ = +1.8

d_3 = 2.24 Å, d_4 = 3.96 Å and d_6 = 2.08 Å

Figure 9.6 cont'd

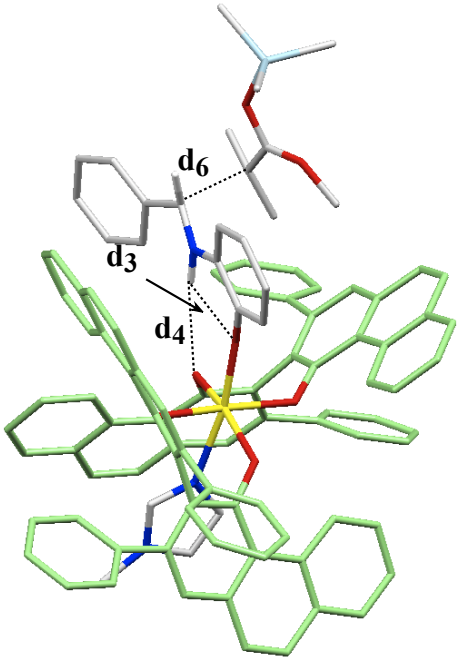

TS4-**481**-*Si*

$\Delta\Delta G^{\ddagger}$ = +0.5

d_3 = 2.18 Å, d_4 = 3.09 Å and d_6 = 2.15 Å

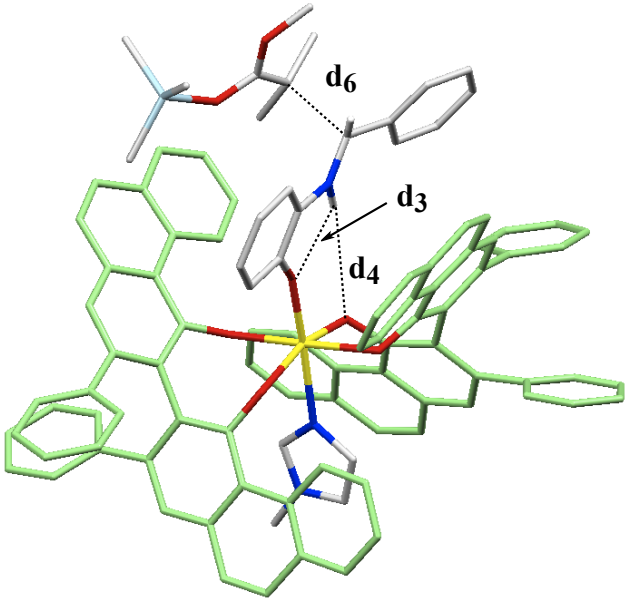

TS4-**481**-*Re*

$\Delta\Delta G^{\ddagger}$ = +7.1

d_3 = 2.16 Å, d_4 = 3.89 Å and d_6 = 2.16 Å

C

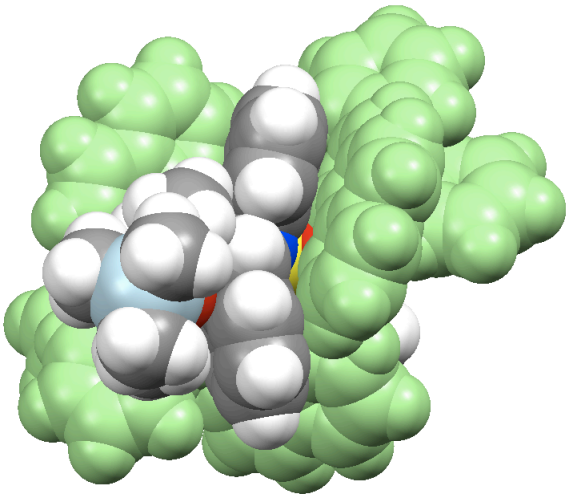

Top view

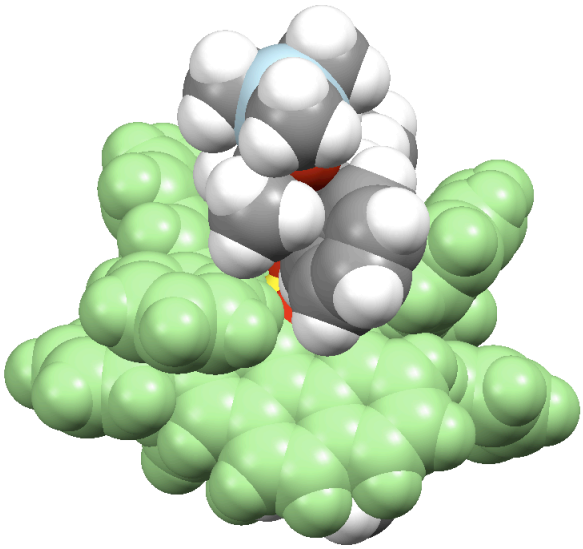

Side view

TS1-**478**-*Si*

$\Delta\Delta G^{\ddagger}$ = +0.0

Figure 9.6 cont'd

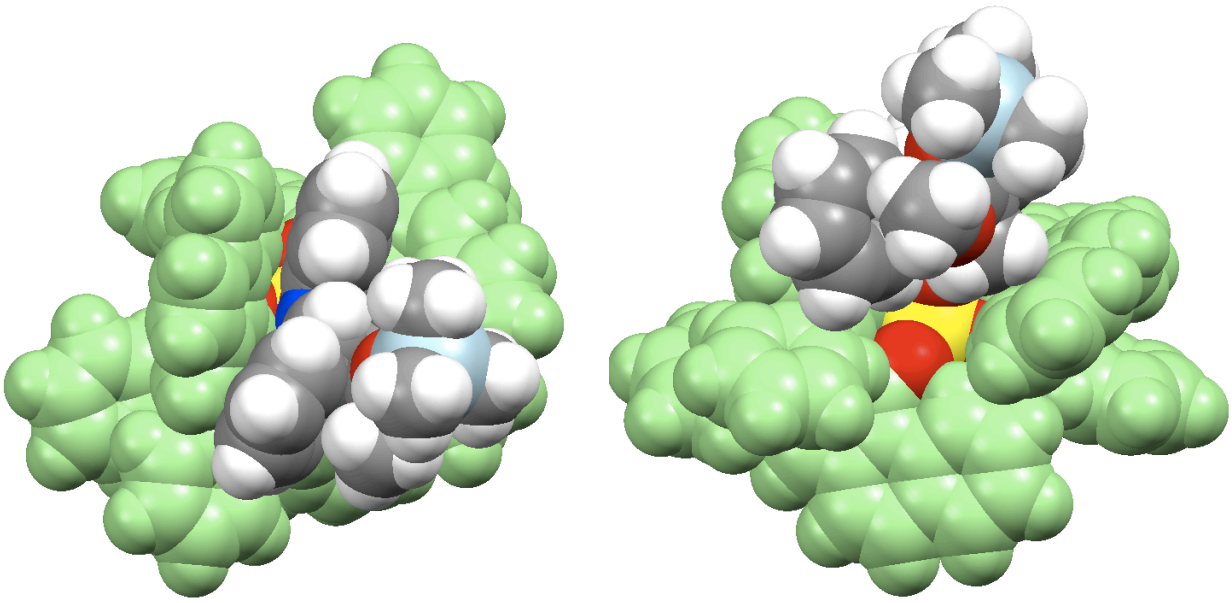

Top view TS3-**480**-*Re* **Side view**

$\Delta\Delta G^{\ddagger} = +1.8$

Further, the single point energies with the self-consistent field (SCRF) calculation based on the polarizable continuum model (PCM, ε = 2.379 for toluene) were calculated at BHandHLYP/DGDZVP level of theory and the TS3-**480**-*Re* was found to be **+1.1** kcal/mol ($\Delta\Delta G_{sol}^{\ddagger}$) higher in energy as compared to TS1-**478**-*Si*.

9.5 Catalyst modifications

After location of the transition states for the zirconium mediated imino-aldol reaction, it was decided to experimentally test them via some modified catalytic systems. According to the calculated transition states, the third ring C in (*S*)-VAPOL **58** is extremely important. Hence, it would be interesting to screen the reaction in the absence of the ring C. Subsequently, we examined some ligands like (*S*)-VANOL **59** and (*S*)-ISOVAPOL **197** where either the third ring

is removed or shifted (Figure 9.7). As predicted, a sharp decrease in ee was observed in both cases as compared to (*S*)-VAPOL **58** (entries 2 and 3, Table 9.2).

Figure 9.7 Various ligands used for imino-aldol reaction.

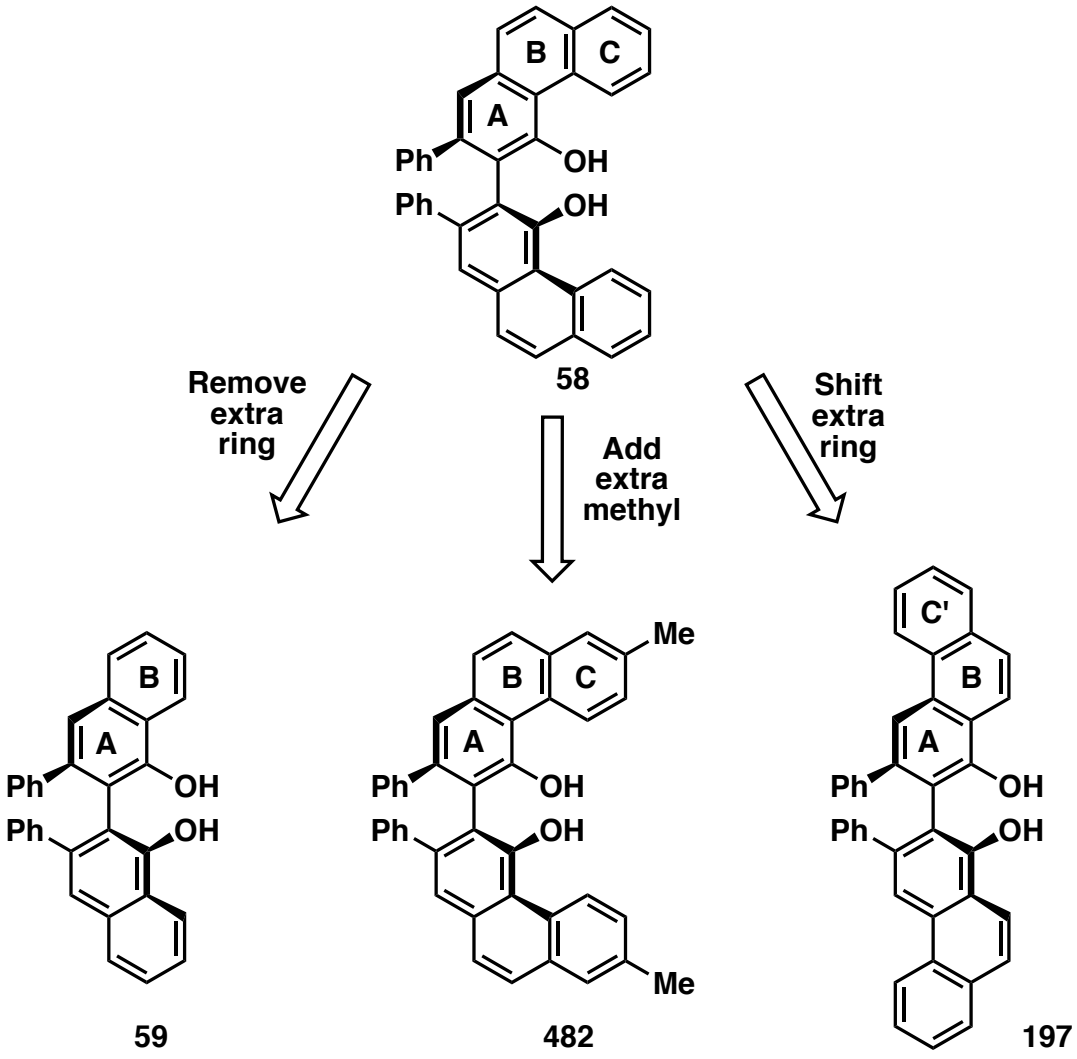

In an attempt to increase the asymmetric induction based on the computational findings and initial CPK model study, Kostas Rampalokos, a former group member, prepared (*S*)-8,8′-Me_2-VAPOL **482**. Although it did not improve the asymmetric induction, it did give essentially the same results as (*S*)-VAPOL **58**. Hence the results obtained further supports the proposed

mechanism. The details of the screening of the ligands at various temperatures are given in Table 9.2.

Table 9.2 Imino-aldol reaction between imine **457a** with keten acetal **460** using various ligands.

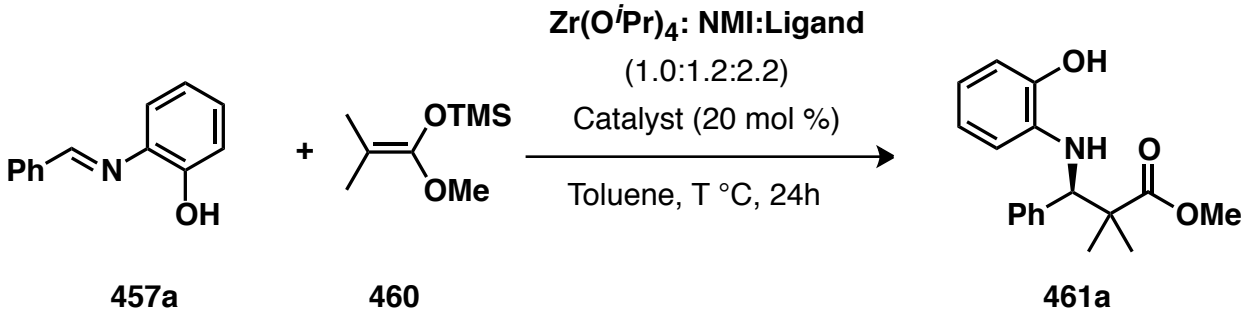

457a **460** **461a**

#	Ligand	Temperature			
		–45 °C		25 °C	
		Yield (%) [b]	ee (%) [c]	Yield (%) [b]	ee (%) [c]
1	(*S*)-VAPOL **58**	92	91	95	89
2	(*S*)-8,8′-Me$_2$-VAPOL **482**	90	91	97	86
3	(*S*)-ISOVAPOL **197**	58	06	63	71
4	(*S*)-VANOL **59**	53	–18	71	51

[a] Unless otherwise specified, all reactions were run with 0.25 mmol of imine **457a** in toluene (0.125 M in imine) with 1.2 equiv of **460** and 20 mol% of the catalyst at T °C. The catalyst was prepared from Zr(O*i*Pr)$_4$/iPrOH, ligand (1.2 equiv) and NMI (1.2 equiv) in toluene at 25 °C for 1 h. [b] Isolated Yield. [c] Determined by HPLC.

9.6 Imine modifications

Based on initial studies with CPK models, there were some modifications done in the structure of the imine **457**. A new imine **458** was prepared by installing two methyl groups at 3 and 5 position of the phenyl ring of the imine **457** (Figure 9.1). Excellent results were obtained with imine **458a** (Table 9.1, entries 8-10) and also the asymmetric inductions were found to be independent of temperature. Hence, we decided to locate and analyze the transition states where

the imine **458a** was used in the reaction. The calculated transition structures are shown in Figure 9.8.

Figure 9.8 Calculated 3D structures and relative free energies of (**A**) TS-**483**-*Si* and (**B**) TS-**483**-*Re* at ONIOM(BHandHLYP/DGDZVP:HF/STO-3G) level. The structures are visualized by the Mercury program (C, gray; O, red; N, blue; Zr, yellow; Si, light blue; H, white). Hydrogen atoms are omitted (except N-H) and the ligand is given in green color for clarity. Free energies and bond lengths are in kcal/mol and Å respectively. Some interactions are highlighted: d_3 (O^3–H), d_4 (O^4–H) and d_6 (C–C). Space-filling rendition of TS-**483**-*Si* and TS-**483**-*Re* with top and side-view with hydrogens showing. The ortho methyl group is shown in magenta color in the space filling models.

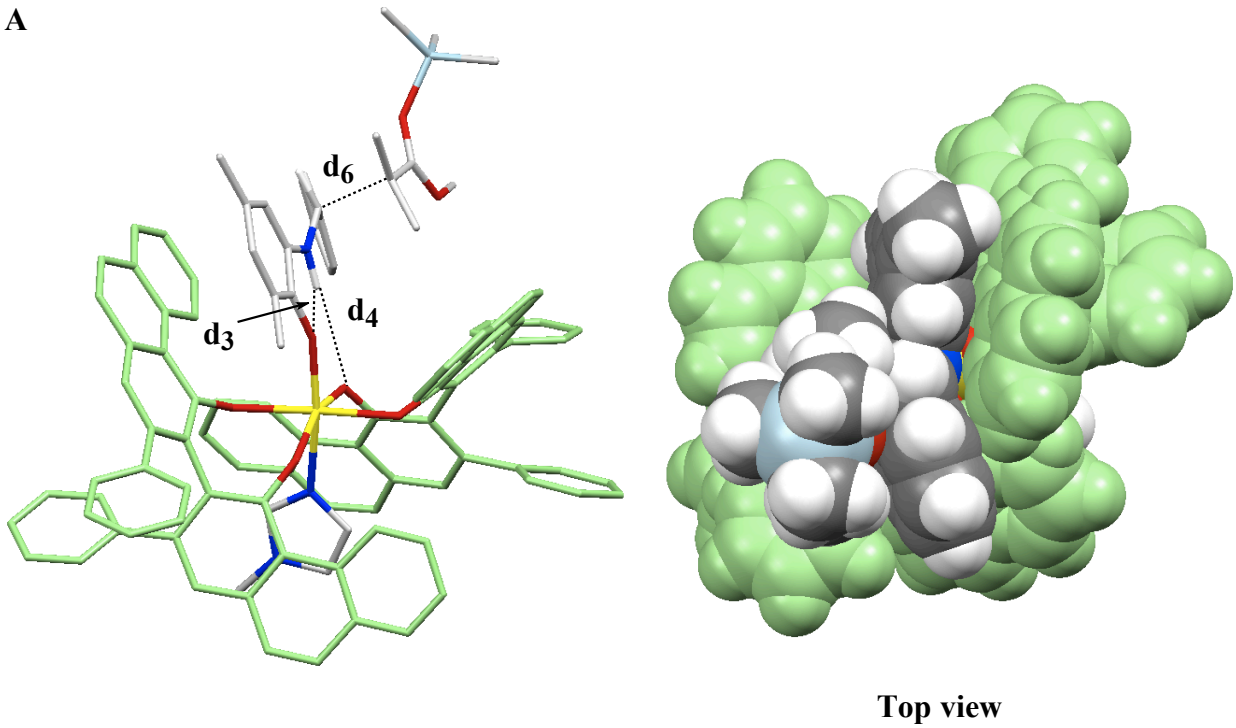

Figure 9.8 cont'd

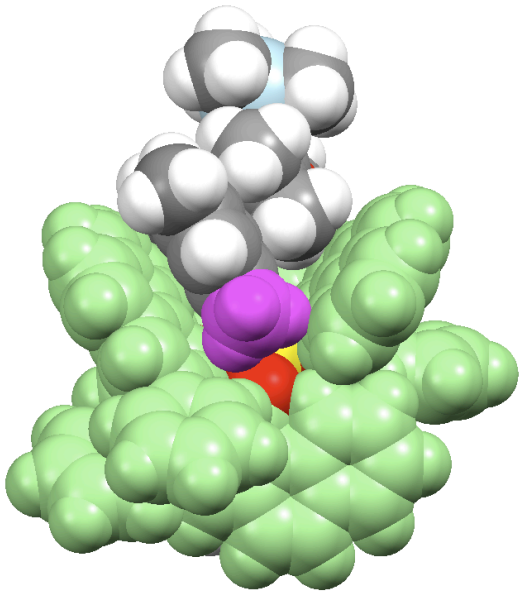

Side view-A

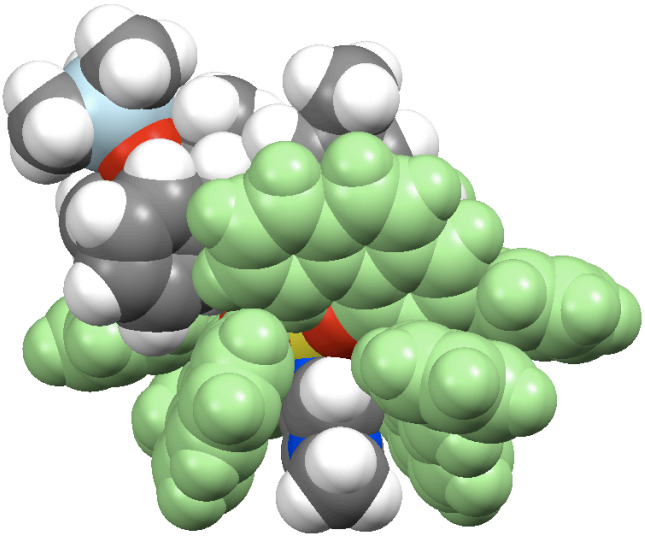

Side view-B

TS-**483**-*Si*

$\Delta\Delta G^{\ddagger} = +0.0$

$d_3 = 2.23$ Å, $d_4 = 2.84$ Å and $d_6 = 2.09$ Å

B

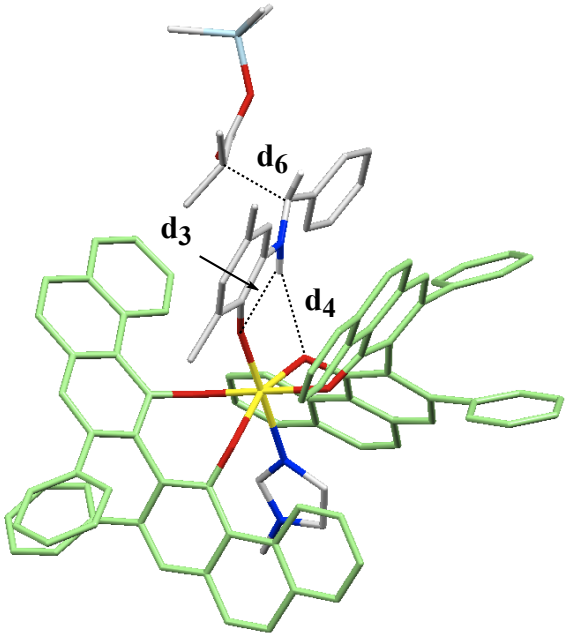

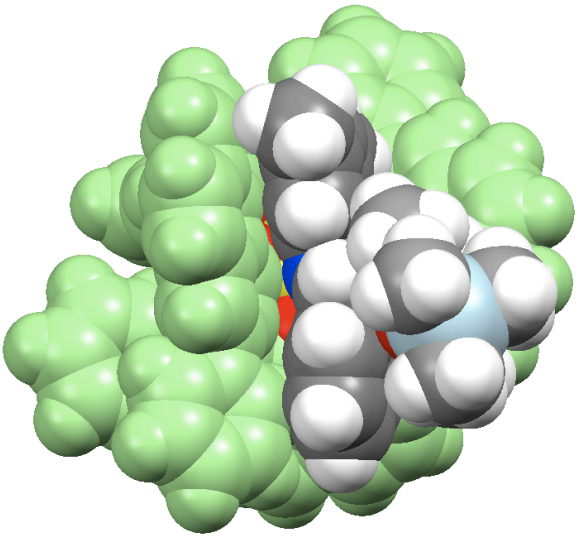

Top view

Figure 9.8 cont'd

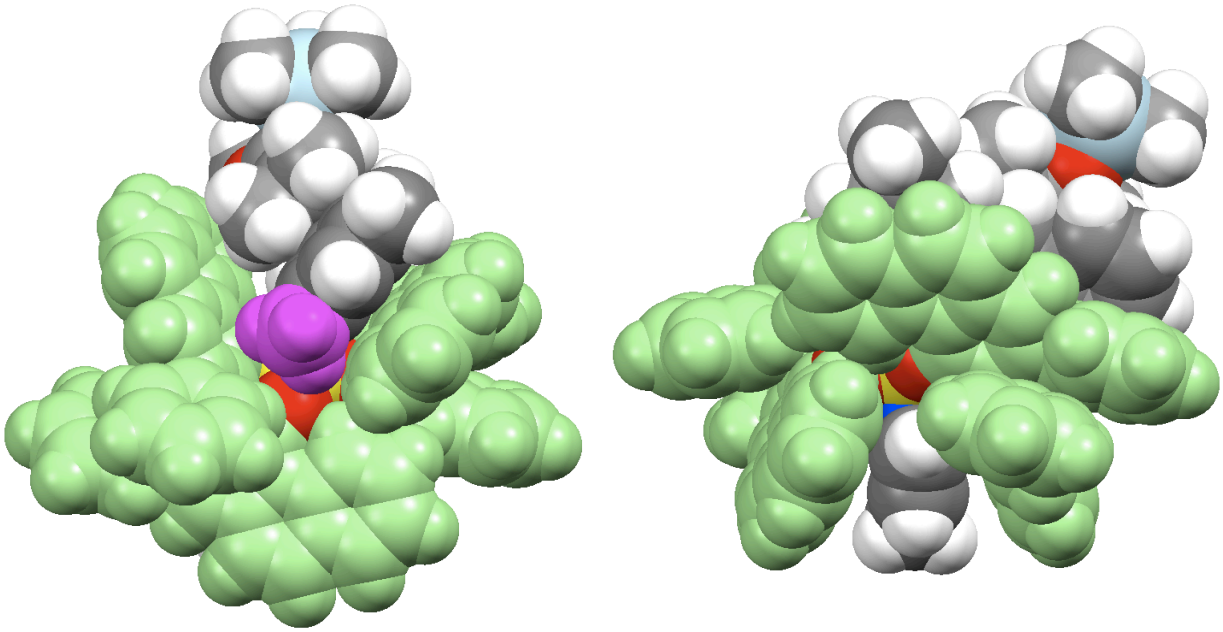

Side view-A **Side view-B**

TS-**483**-*Re*

$\Delta\Delta G^{\ddagger} = +4.4$

$d_3 = 2.23$ Å, $d_4 = 2.92$ Å and $d_6 = 2.05$ Å

As stated earlier, based on initial CPK models, it was predicted that rocking the imine down into the cleft should provide a conformation that provides a greater facial selectivity of attack on the imine since it should provide greater shielding of the *Re*-face by the phenanthrene unit on the right side of the molecule. The methyl group at the ortho position should be sufficient to push the imine down into the cleft, thus increasing the selectivity of the reaction. This was indeed observed in the calculated transition states (Figure 9.8). The ortho methyl group is given in the magenta color in the side-view-A of both transition states (TS-**483**-*Si* and TS-**483**-*Re*). As shown in Figure 9.8, this methyl group makes close contacts with the floor of the cleft even when the imine is rotated down into the cleft and results in greatly restricted movement

about the Zr–O–C unit to the imine moiety. Another important interaction is π-π stacking between the phenanthrene unit of the ligand and the phenyl ring of the imine **458a** (Figure 9.8). Last but not least, the TS for favored enantiomer is found to be +4.4 kcal/mol lower than the disfavored TS. In all, the calculated transition states also support the concept of the modified imines **458**.

Figure 9.9 Free Energy diagram of transition states for imines **457a** and **458a** at ONIOM(BHandHLYP/DGDZVP:HF/STO-3G) level for catalytic cycle II. Energy in parenthesis is enthalpy.

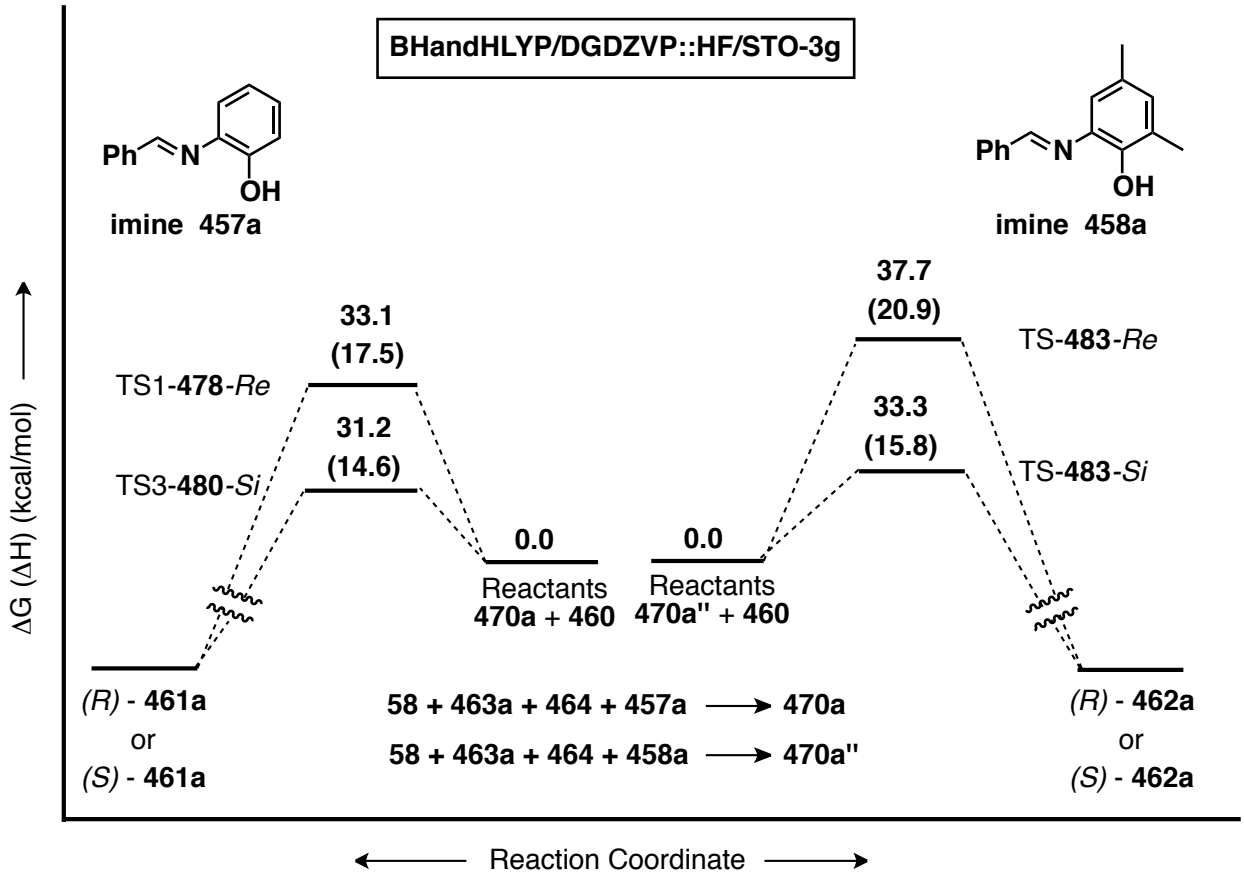

An energy diagram showing the energy barriers in the reactions of the imines **457a** and **458a** for the final optimized transition states for the carbon-carbon bond forming step is presented in Figure 9.9. Finally, a new mechanism has been established with the aid of NMR spectroscopy, computational studies and substrate and catalyst modifications. The observed mechanism is unprecedented and hopefully will lead to new applications to the field of asymmetric catalysis.

9.7 Examination of the catalytic cycle III for (*S*)-VAPOL 58

At this point, we were curious as to whether the proposed catalytic cycle III holds true for the imino-aldol reaction using (*S*)-VAPOL **58** (Scheme 9.1C). Hence, we located two transition states for the carbon-carbon bond forming step in catalytic cycle III (**474→475**) using ONIOM(BHandHLYP/DGDZVP:HF/STO-3G) level of theory. The new optimized transition states (TS-**484**-*Si* and TS-**484**-*Re*) are presented in Figure 9.10. Interestingly, the calculated results are not consistent with the experimental results. Hence, it is likely that the proposed catalytic cycle III is not favored in the case of (*S*)-VAPOL **58**. An important feature to be noted is the elongated bond distance between Zr and N of the imine (d_8 = 2.43–2.39 Å). This probably is due to steric compulsions and leads to a weak coordination.

Figure 9.10 Calculated 3D structures and relative free energies of TS-**484**-*Si* and TS-**484**-*Re* at ONIOM(BHandHLYP/DGDZVP:HF/STO-3G) level. The structures are visualized by the Mercury program (C, gray; O, red; N, blue; Zr, yellow; Si, light blue; H, white). Hydrogen atoms are omitted (except O-H and sp^2-C-H of imine) and the ligand is given in green color for clarity. Free energies and bond lengths are in kcal/mol and Å respectively. Some bond distances

Figure 9.10 cont'd

are highlighted: d_7 (Zr–O), d_8 (Zr–N) and d_9 (C–C).

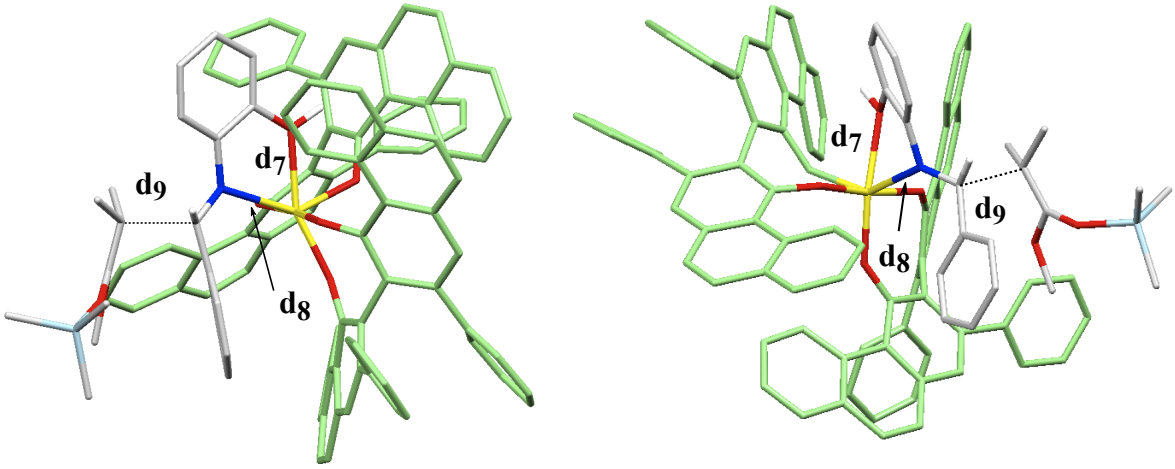

TS-**484**-*Si*

$\Delta\Delta G^{\ddagger} = +10.0$

$d_7 = 2.28$ Å, $d_8 = 2.43$ Å and $d_9 = 2.02$ Å

TS-**484**-*Re*

$\Delta\Delta G^{\ddagger} = +0.0$

$d_7 = 2.31$ Å, $d_8 = 2.39$ Å and $d_9 = 2.04$ Å

9.8 Case of BINOL derivative 459

In the preceding sections, we found evidence for a new mechanism for the imino-aldol reaction catalyzed by a zirconium compound incorporating the using the (*S*)-VAPOL ligand **58** (Catalytic cycle II, Scheme 9.1B). This reaction was originally reported by Kobayashi and coworkers where they used (*R*)-6,6′-Br_2-BINOL **459** as the ligand.[6] As stated earlier (Catalytic cycle III', Scheme 9.1D), Kobayashi and coworkers proposed another plausible mechanism, which excludes the presence of NMI in the transition states (Catalytic cycle III', Scheme 9.1D and 9.2B). The catalyst was generated from a mixture of Zr(O*t*Bu)$_4$ **463b**, NMI **464** and (*R*)-6,6′-Br_2-BINOL **459**. In this mechanism, it has been assumed that step one involves an isomerization of complex **465'** in which there are two NMI groups trans to each other (Catalytic

cycle III', Scheme 9.2B). Complex **465'** isomerizes to **473'** in which the two NMI groups are cis to each other. The second step involves the exchange of the NMI groups by the imine **457** leading to the formation of the imine-catalyst complex **474'**. The coordination of the hydroxyl group to the zirconium atom indicates the importance of the hydroxyl group. Subsequent attack of ketene acetal **460** would give **475'** then **476'**, which is followed by the final release of the product **461** in the form of its silylated derivative **469**. The obvious question then arises as to whether the mechanism of the reaction can change depending on the ligand used (Catalytic cycle II' vs III', Scheme 9.2). Hence, we decided to gather more information about the transition states for the reaction involving catalysts derived from for BINOL derivative **459** by examining both catalytic cycles II' and III'.

Scheme 9.2 Proposed catalytic cycles of imino-aldol reaction using (*R*)-6,6′-Br_2-BINOL **459** as the ligand. (**A**) Catalytic cycle II' (**B**) Catalytic Cycle III'

A

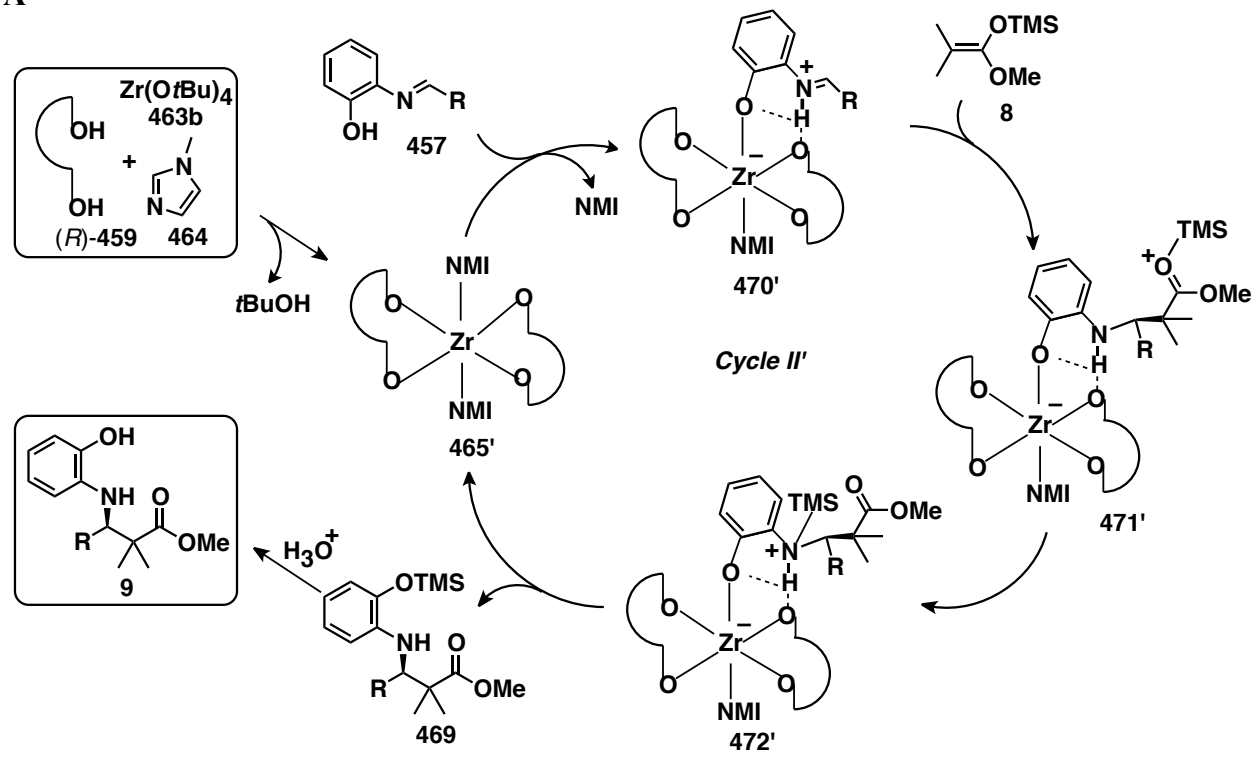

Scheme 9.2 cont'd

B

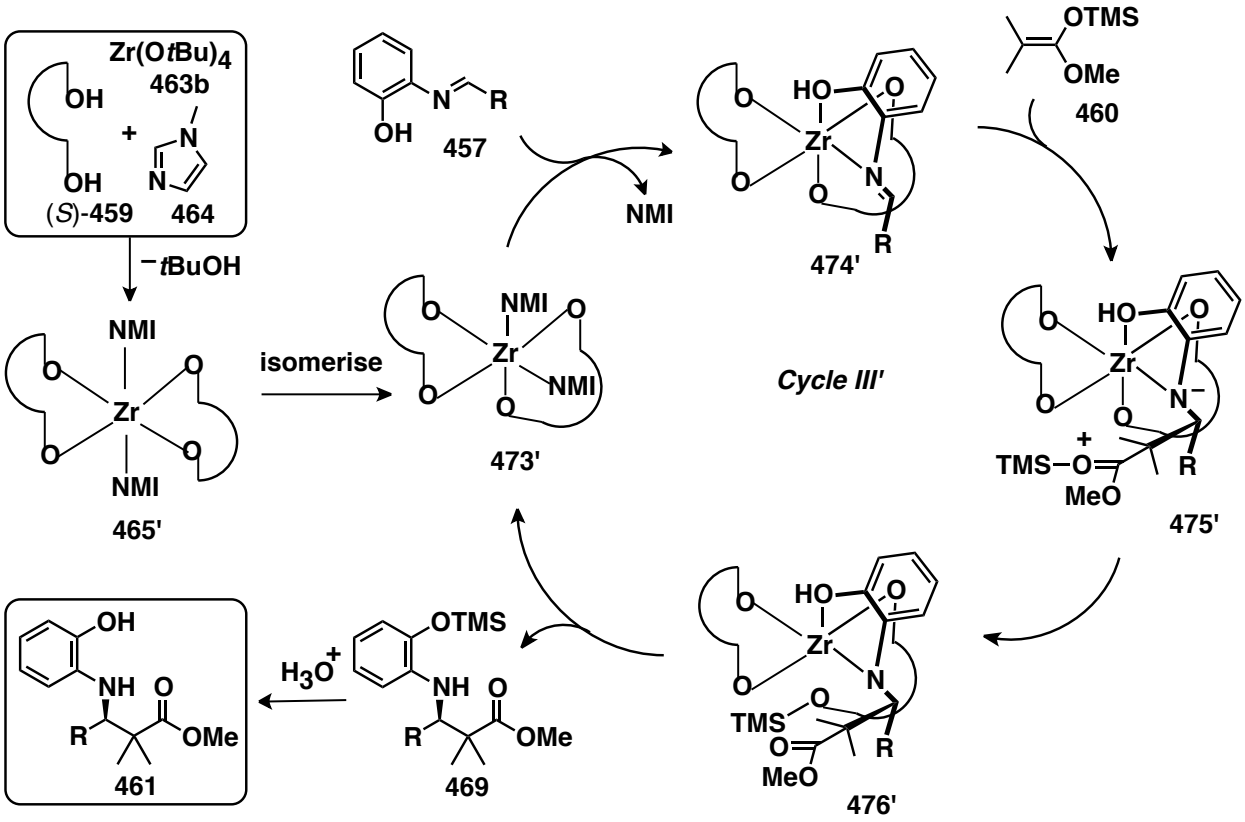

In this case, the division of layers for ONIOM calculations is shown in Figure 9.11.

Figure 9.11 Division of layers for the ONIOM calculations ONIOM(B3LYP/LanL2DZ:HF/ STO-3G) and ONIOM(B3LYP/DGDZVP:B3LYP/LanL2MB) level.

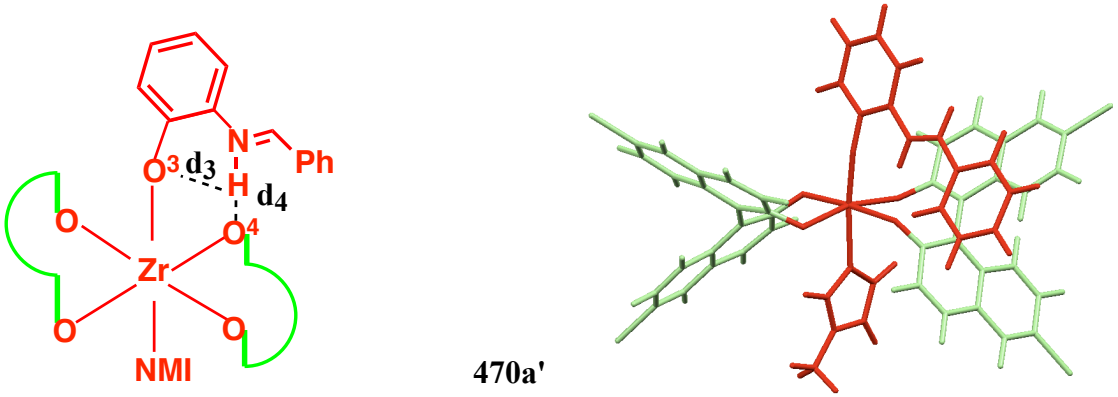

Figure 9.11 cont'd

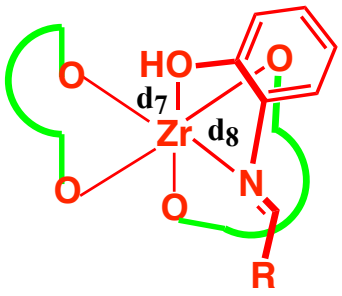

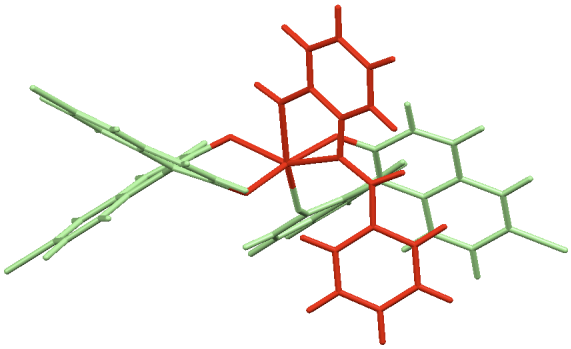

474a'

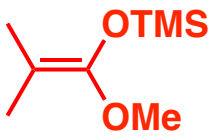

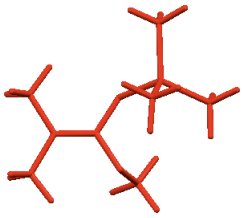

460

Red = B3LYP/LanL2DZ or B3LYP/DGDZVP

Green = HF/STO-3G or B3LYP/LanL2MB

Four different orientations of the ketene acetals were taken into consideration. Subsequently, four transition states (TS1-**485** to TS4-**488**) were located for one particular enantiomer depending upon the different orientations and conformations of silyl ketene acetal **460** (Figure 9.12). The method used for above calculations is ONIOM(B3LYP/LanL2DZ:HF/STO-3G). The lowest energy transition states for S and R enantiomers were then carefully examined (TS1-**485**-*Re* and TS3-**487**-*Si*, Figure 9.12). Interestingly, the observed theoretical results were not consistent with the experimental observations. The lowest energy transition state (TS3-**487**-*Si*) leading to the favored enantiomer was found to be higher in energy by +0.5 kcal/mol than the lowest energy transition state (TS1-**485**-*Re*) leading to the disfavored enantiomer (Figure 9.12).

Figure 9.12 (**A**) Different conformations and orientations of silyl ketene acetal **460** used for calculations. (**B**) Calculated 3D structures and relative free energies of TS1-**485** to TS4-**488** at ONIOM(B3LYP/LanL2DZ:HF/STO-3G) level. The structures are visualized by the Mercury program (C, gray; O, red; N, blue; Zr, yellow; Si, light blue; Br, magenta; H, white). Hydrogen atoms are omitted (except N-H) and the ligand is given in green color for clarity. Free energies and bond lengths are in kcal/mol and Å respectively. Some interactions are highlighted: d_3 (O^3–H), d_4 (O^4–H) and d_6 (C–C).

A

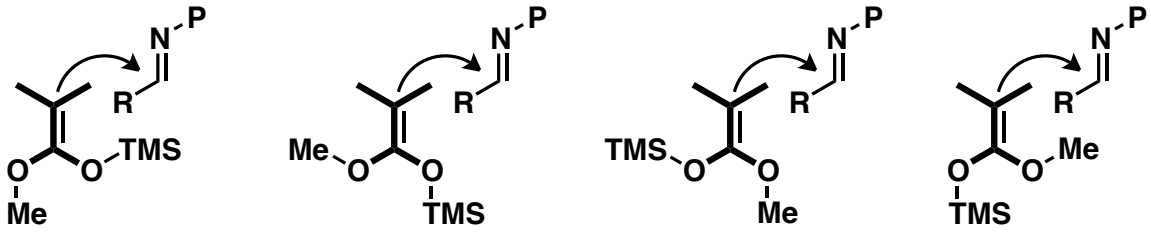

(For TS1-**485**) (For TS2-**486**) (For TS3-**487**) (For TS4-**488**)

B

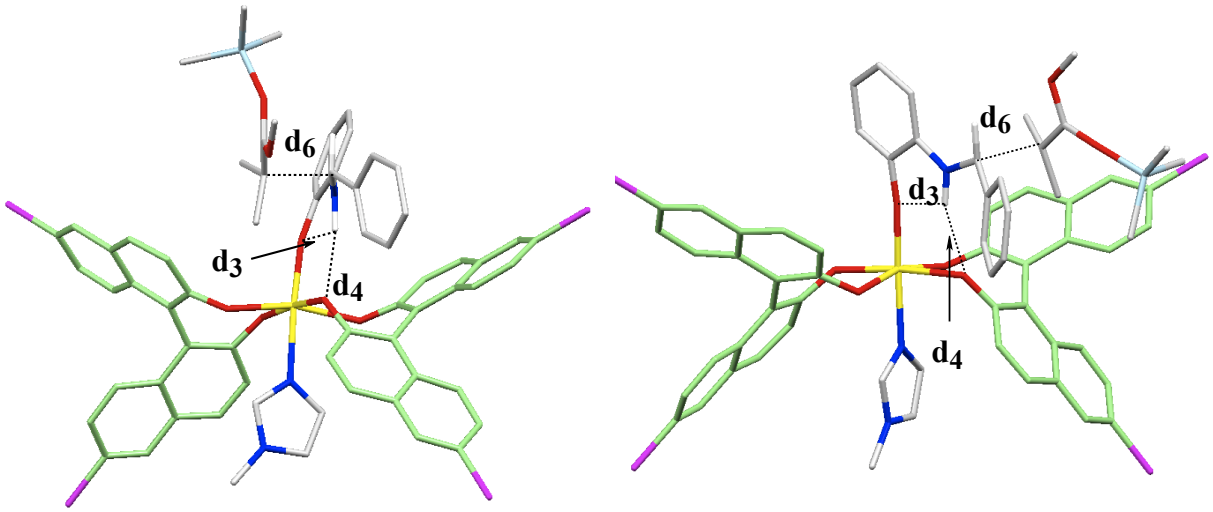

TS1-**485**-*Si*

$\Delta\Delta G^{\ddagger}$ = +0.9

d_3 = 2.42 Å, d_4 = 2.17 Å and d_6 = 2.09 Å

TS1-**485**-*Re*

$\Delta\Delta G^{\ddagger}$ = +0.0

d_3 = 2.21 Å, d_4 = 2.46 Å and d_6 = 2.18 Å

Figure 9.12 cont'd

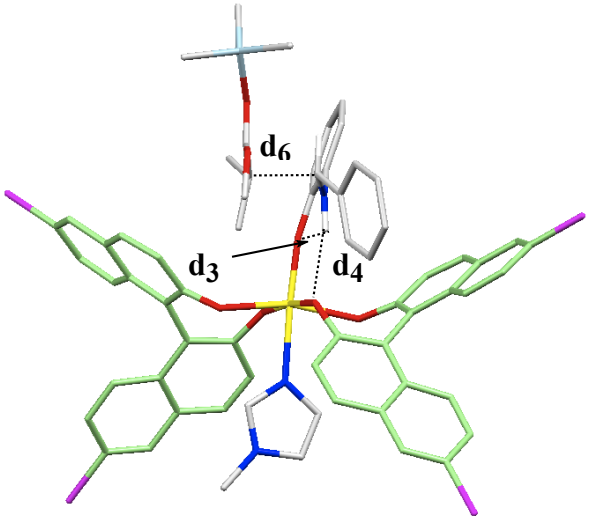

TS2-**486**-*Si*

$\Delta\Delta G^{\ddagger}$ = +2.1

d_3 = 2.40 Å, d_4 = 2.21 Å and d_6 = 2.06 Å

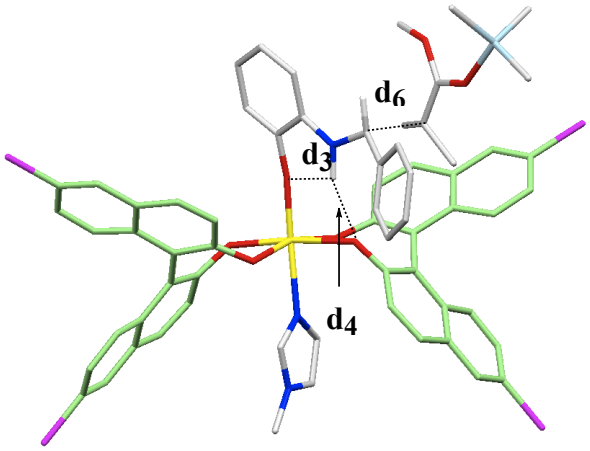

TS2-**486**-*Re*

$\Delta\Delta G^{\ddagger}$ = +2.9

d_3 = 2.26 Å, d_4 = 2.35 Å and d_6 = 2.11 Å

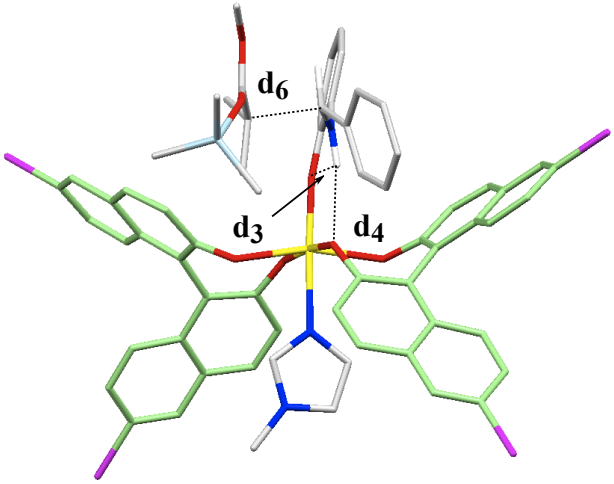

TS3-**487**-*Si*

$\Delta\Delta G^{\ddagger}$ = +0.5

d_3 = 2.40 Å, d_4 = 2.23 Å and d_6 = 2.09 Å

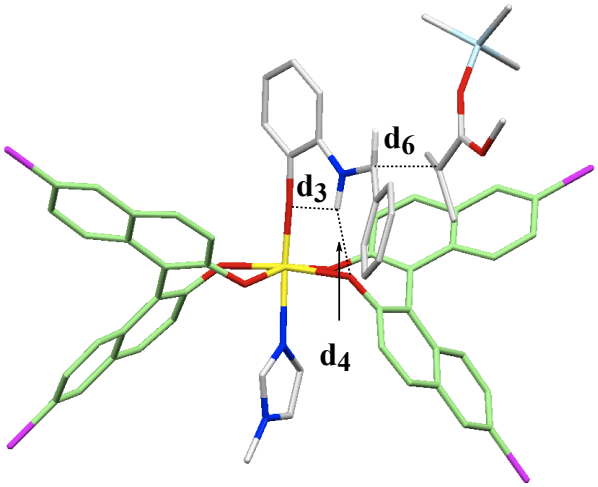

TS3-**487**-*Re*

$\Delta\Delta G^{\ddagger}$ = +0.4

d_3 = 2.24 Å, d_4 = 2.35 Å and d_6 = 2.12 Å

Figure 9.12 cont'd

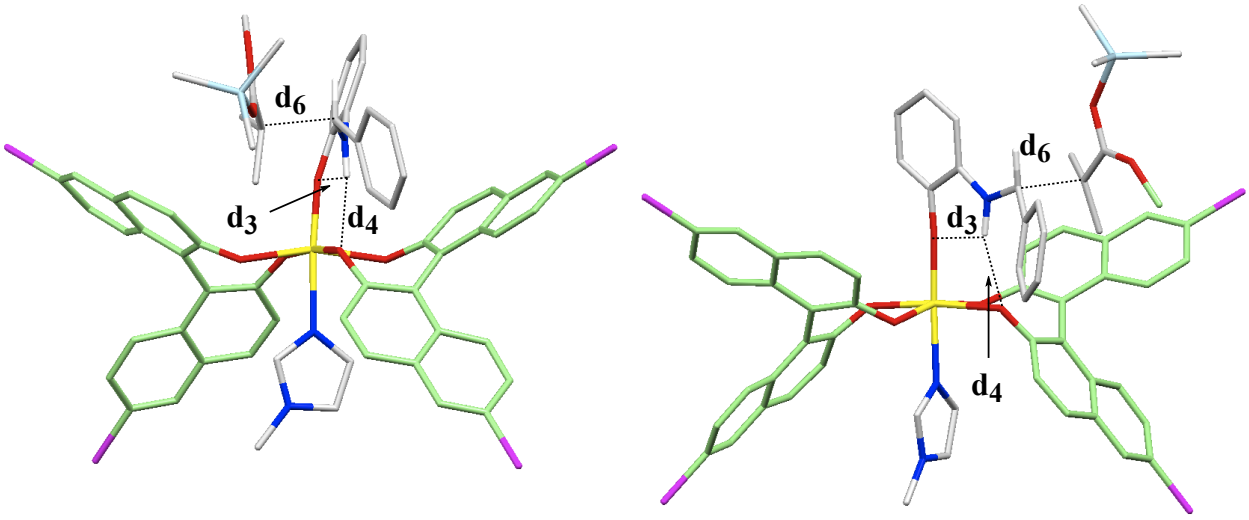

TS4-**488**-*Si*

$\Delta\Delta G^{\ddagger}$ = +3.9

d_3 = 2.42 Å, d_4 = 2.16 Å and d_6 = 2.10 Å

TS4-**488**-*Re*

$\Delta\Delta G^{\ddagger}$ = +1.6

d_3 = 2.22 Å, d_4 = 2.42 Å and d_6 = 2.12 Å

We then decided to include the DFT in the lower level of the ONIOM calculations. Subsequently, the transition states TS1-**485** and TS3-**487** were subjected to the higher level calculations, i.e. ONIOM(B3LYP/DGDZVP:B3LYP/LanL2MB) (Figure 9.13). However, there was no change in the outcome. Therefore, it is likely that there is a difference in the mechanism of the imino-aldol reaction depending on the type of the ligand employed. Consequently, the catalytic cycle II′ (Scheme 9.2A) in the case of (*R*)-6,6′-Br_2-BINOL **459** was not supported by the above described computational analysis since it predicts the wrong enantiomer of the product.

Figure 9.13 Calculated relative free energies of TS1-**485**-*Si*, TS1-**485**-*Re*, TS3-**487**-*Si* and TS3-**487**-*Re*, at ONIOM(B3LYP/DGDZVP: B3LYP/LanL2MB) level. Free energies and bond

Figure 9.13 cont'd

lengths are in kcal/mol and Å respectively. Some interactions are highlighted: d_3 (O^3–H), d_4 (O^4–H) and d_6 (C–C).

TS1-**485**-*Si*

$\Delta\Delta G^{\ddagger}$ = +1.3

d_3 = 2.42 Å, d_4 = 2.17 Å and d_6 = 2.09 Å

TS1-**485**-*Re*

$\Delta\Delta G^{\ddagger}$ = +0.0

d_3 = 2.21 Å, d_4 = 2.46 Å and d_6 = 2.18 Å

TS3-**487**-*Si*

$\Delta\Delta G^{\ddagger}$ = +1.3

d_3 = 2.40 Å, d_4 = 2.21 Å and d_6 = 2.06 Å

TS3-**487**-*Re*

$\Delta\Delta G^{\ddagger}$ = +0.2

d_3 = 2.26 Å, d_4 = 2.35 Å and d_6 = 2.11 Å

Next, we decided to computationally examine the original proposed mechanism by Kobatashi i.e. catalytic cycle III′ (Scheme 9.2B). The division of layers for ONIOM calculations is already shown in Figure 9.11. Similar to the approach for catalytic cycle II′, four different orientations of ketene acetal **460** were examined (Figure 9.14). Three transition states were located and the transition state with the fourth orientation failed to converge irrespective of the method utilized (Figure 9.14). Interestingly, the lowest energy transition state (TS1-**489**-*Si*) leading to the favored enantiomer was found to be 0.9 kcal/mol higher in energy than the lowest energy transition state (TS1-**489**-*Re*) leading to the disfavored enantiomer using ONIOM(B3LYP/LanL2DZ:HF/STO-3G) level of calculations (Figure 9.14). This suggested that either the catalytic cycle III′ does not hold true for the reaction, or the level of calculations is not appropriate. Hence we decided to perform the calculations using DFT in the lower layer and the results are presented in Figure 9.15.

Figure 9.14 (**A**) Different conformations and orientations of silyl ketene acetal **460** used for calculations. (**B**) Calculated 3D structures and relative free energies of TS1-**489** to TS4-**492** at ONIOM(B3LYP/LanL2DZ:HF/STO-3G) level. The structures are visualized by the Mercury program (C, gray; O, red; N, blue; Zr, yellow; Si, light blue; Br, magenta; H, white). Hydrogen atoms are omitted (except O-H and sp^2-C-H of imine) and the ligand is given in green color for clarity. Free energies and bond lengths are in kcal/mol and Å respectively. Some bond distances are highlighted: d_7 (Zr–O), d_8 (Zr–N) and d_9 (C–C).

A

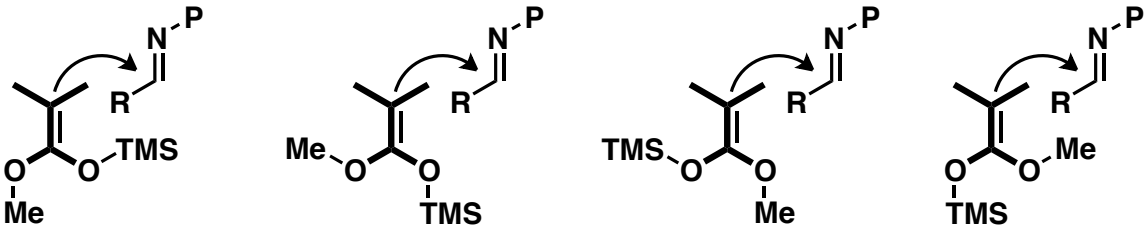

(For TS1-**489**) (For TS2-**490**) (For TS3-**491**) (For TS4-**492**)

B

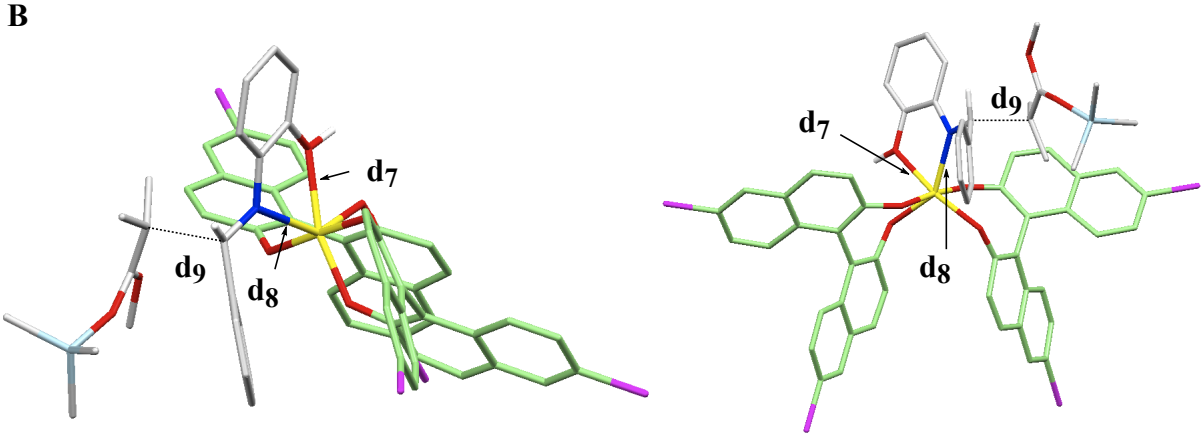

TS1-**489**-*Si*

$\Delta\Delta G^{\ddagger}$ = +0.9

d_7 = 2.25 Å, d_8 = 2.32 Å and d_9 = 2.11 Å

TS1-**489**-*Re*

$\Delta\Delta G^{\ddagger}$ = +0.0

d_7 = 2.23 Å, d_8 = 2.31 Å and d_9 = 2.13 Å

Figure 9.14 cont'd

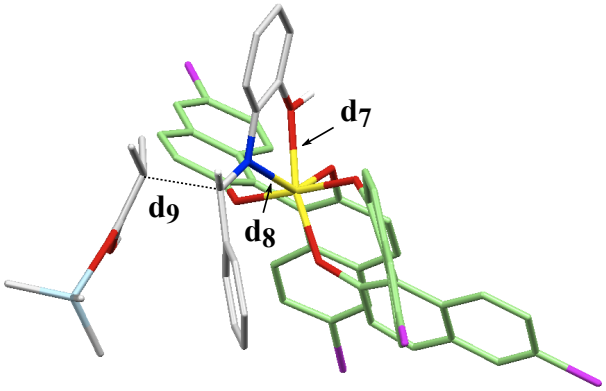

TS2-**490**-*Si*

$\Delta\Delta G^{\ddagger}$ = +3.7

d_7 = 2.24 Å, d_8 = 2.33 Å and d_9 = 2.12 Å

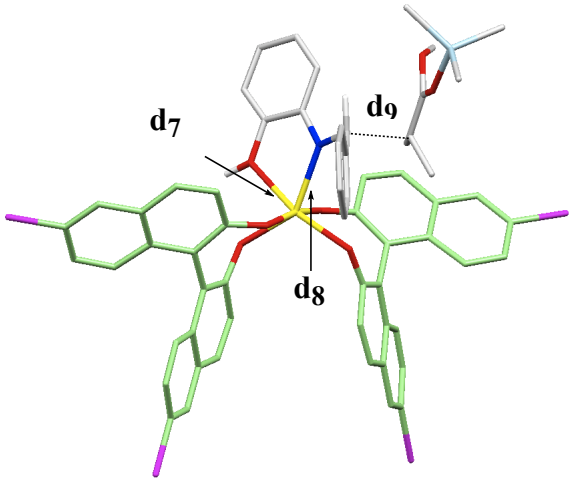

TS2-**490**-*Re*

$\Delta\Delta G^{\ddagger}$ = +5.3

d_7 = 2.24 Å, d_8 = 2.29 Å and d_9 = 2.06 Å

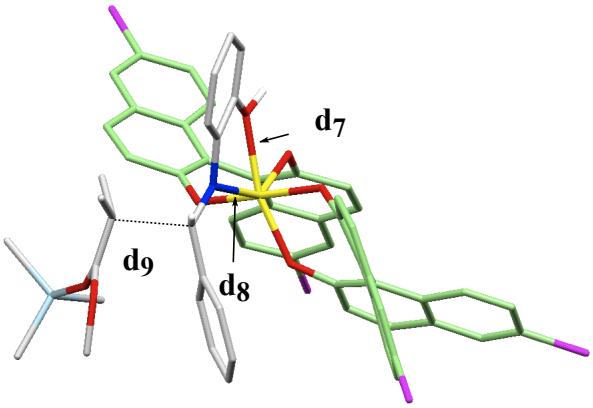

TS3-**491**-*Si*

$\Delta\Delta G^{\ddagger}$ = +1.7

d_7 = 2.24 Å, d_8 = 2.32 Å and d_9 = 2.12 Å

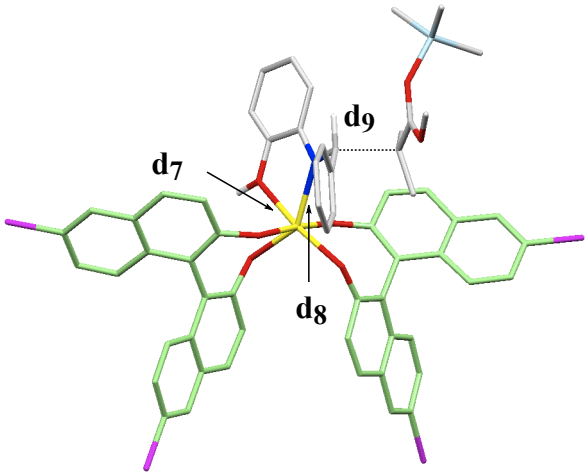

TS3-**491**-*Re*

$\Delta\Delta G^{\ddagger}$ = +2.0

d_7 = 2.23 Å, d_8 = 2.31 Å and d_9 = 2.11 Å

TS4-**492**-*Si*

(no convergence achieved)

TS4-**492**-*Re*

(no convergence achieved)

As stated in last paragraph, TS1-**489** and TS3-**491** were subjected to ONIOM(B3LYP/DGDZVP:B3LYP/LanL2MB) level of calculations (Figure 9.15). The lowest energy transition state leading to the favored enantiomer (*R*) was found to be TS1-**489**-*Si*. Similarly, TS3-**491**-Re was found to be the lowest transition state leading to the disfavored enantiomer (*S*). The observed results with the higher level calculations were found to be consistent with the experimental results. The energy difference between favored transition state TS1-**489**-*Si* and disfavored transition state TS3-**491**-*Re* was determined to be **+1.8** Kcal/mol (Figure 9.15). Also, it must be noted that the *Re* face of the imine **457a** is completely shielded by the naphthalene unit of the (*R*)-6,6′-Br_2-BINOL **459**. Additionally, there is a possible π-π stacking interaction between the phenyl ring of imine and one of the naphthalene rings of the ligand **459**. The reason that the (*S*)-enantiomer is unfavorable is probably due to the steric hindrance between the methyl groups of ketene acetal **460** and the naphthalene ring of the ligand **459** (Figure 9.15).

Figure 9.15 (**A**) Calculated relative free energies of TS1-**489**-*Si*, TS1-**489**-*Re*, TS3-**491**-*Si* and TS3-**491**-*Re*, at ONIOM(B3LYP/DGDZVP:B3LYP/LanL2MB) level. Free energies and bond lengths are in kcal/mol and Å respectively. Some bond distances are highlighted: d_7 (Zr–O), d_8 (Zr–N) and d_9 (C–C). (**B**) Calculated 3D structures and relative free energies of TS1-**489**-*Si* and TS3-**491**-*Re* at ONIOM(B3LYP/DGDZVP:B3LYP/LanL2MB) level. The structures are visualized by the Mercury program (C, gray; O, red; N, blue; Zr, yellow; Si, light blue; Br, magenta; H, white). Hydrogen atoms are omitted (except O-H and sp^2-C-H of imine) and the

Figure 9.15 cont'd

ligand is given in green color for clarity. Free energies and bond lengths are in kcal/mol and Å respectively. Some bond distances are highlighted: d_7 (Zr–O), d_8 (Zr–N) and d_9 (C–C).

A

TS1-**489**-*Si*

$\Delta\Delta G^{\ddagger} = +0.0$

$d_7 = 2.33$ Å, $d_8 = 2.35$ Å and $d_9 = 1.99$ Å

TS1-**489**-*Re*

$\Delta\Delta G^{\ddagger} = +1.9$

$d_7 = 2.30$ Å, $d_8 = 2.34$ Å and $d_9 = 2.04$ Å

TS3-**491**-*Si*

$\Delta\Delta G^{\ddagger} = +0.9$

$d_7 = 2.34$ Å, $d_8 = 2.32$ Å and $d_9 = 2.03$ Å

TS3-**491**-*Re*

$\Delta\Delta G^{\ddagger} = +1.8$

$d_7 = 2.27$ Å, $d_8 = 2.33$ Å and $d_9 = 2.01$ Å

B

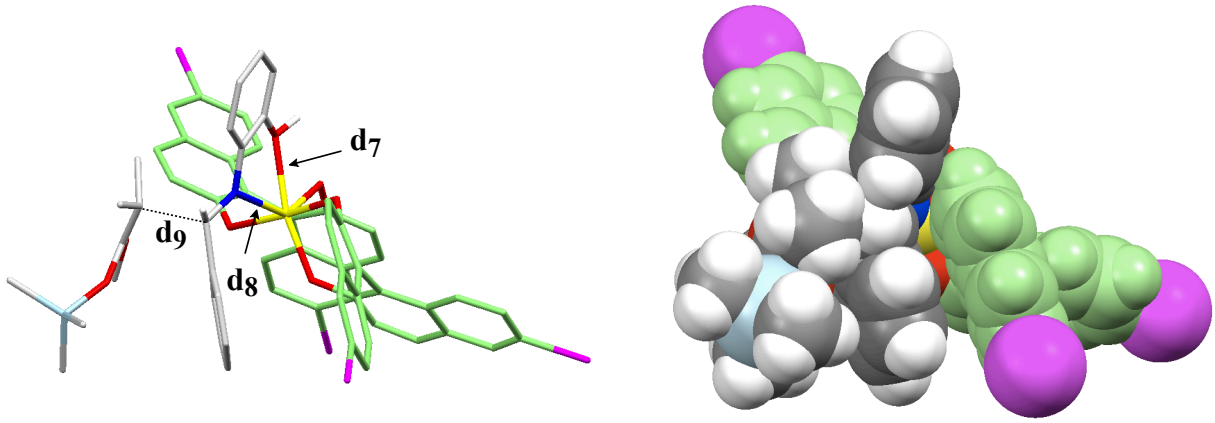

TS1-**489**-*Si*

$\Delta\Delta G^{\ddagger} = +0.0$

$d_7 = 2.33$ Å, $d_8 = 2.35$ Å and $d_9 = 1.99$ Å

Figure 9.15 cont'd

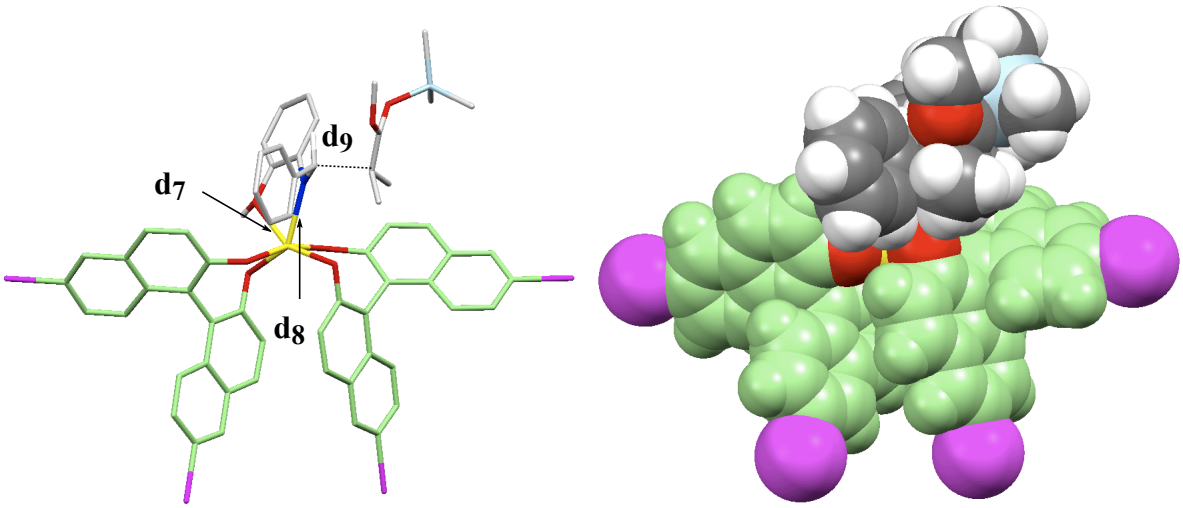

TS3-**491**-*Re*

$\Delta\Delta G^{\ddagger} = +1.8$

$d_7 = 2.27$ Å, $d_8 = 2.33$ Å and $d_9 = 2.01$ Å

9.9 Conclusions

In this chapter, the active site of the catalytic asymmetric imino-aldol reaction has been probed via NMR spectroscopy, computational studies and substrate and catalyst modifications. In the literature, two mechanisms have been proposed. One of them involves the presence of imidazole in the transition state whereas the other one assumes no role of imidazole in the transition state. Both reactions were assumed to be Lewis acid catalyzed reactions. We found that the reaction is actually a Lewis acid assisted Brønsted acid catalyzed reaction (Scheme 9.1, Catalytic cycle II) when (*S*)-VAPOL ligand is used and a Lewis acid catalyzed reaction (Scheme 9.2, Catalytic cycle III') when (*R*)-6,6'-Br_2-BINOL ligand is utilized. The transition states were located using ONIOM level calculations.

APPENDIX

9.10 Experimental

9.10.1 General Information

Same as Chapter 2

9.10.2 Preparation of imine 457a

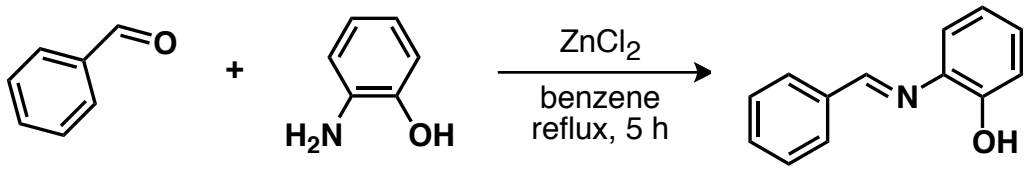

127a **126x** **457a**

(*E*)-2-(benzylideneamino)phenol 457a: To a 250 mL flame-dried round bottom flask filled with argon was added 2-aminophenol **126x** (2.18 g, 20.0 mmol), benzaldehyde **127a** (2.02 mL, 20 mmol), $ZnCl_2$ (100 mg, 0.73 mmol) and dry benzene (100 mL). The reaction mixture was refluxed with a Dean-Stark trap for 5 h, and then cooled to room temperature. The reaction mixture was filtered through Celite and the Celite bed was washed with benzene (10 mL × 3) and then the filtrate was concentrated by rotary evaporation to give the crude imine as a yellow solid. Crystallization (ethanol) and collection of the first crop afforded **457a** as yellow crystals (mp. 91-92 °C) in 85% isolated yield (3.35 g, 17.0 mmol).

Spectral data for **457a**: ^{1}H NMR ($CDCl_3$, 300 MHz) δ 6.92 (ddd, *J* = 7.9, 7.4, 1.4 Hz, 1H), 7.02 (dd, *J* = 8.1, 1.4 Hz, 1H), 7.21-7.18 (m, 1H), 7.25 (s, 1H), 7.32 (dd, *J* = 7.9, 1.5 Hz, 1H), 7.53-7.47 (m, 3H), 7.95-7.91 (m, 2H), 8.71 (s, 1H); ^{13}C ($CDCl_3$, 75 MHz) δ 114.90, 115.62, 118.54, 128.69, 128.81, 129.41, 131.39, 135.41, 135.73, 151.10, 151.22. These spectral data match those previously reported for this compound.[10]

9.10.3 General procedure for the imino-aldol reaction *(Table 9.1-9.2)*

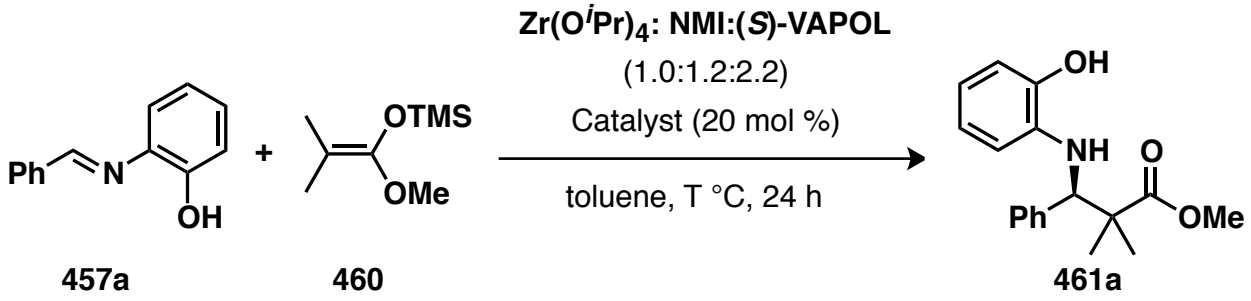

(a) At room temperature (25 ºC):

(*R*)-methyl 3-((2-hydroxyphenyl)amino)-2,2-dimethyl-3-phenylpropanoate 461a: To a 10 mL flame-dried round bottom flask were added (*S*)-VAPOL (59.25 mg, 0.1100 mmol) and Zr(O^{i}Pr)$_4$•^{i}PrOH (19.38 mg, 0.0500 mmol) in toluene (0.9 mL). To this solution was added 1-methylimidazole (4.78 μL, 0.060 mmol) in toluene (0.1 mL) at room temperature. The mixture was stirred for 1 h at the same temperature. A solution of imine **457a** (49.31 mg, 0.2500 mmol) in toluene (1 mL) was added to the flask containing the catalyst and the mixture was stirred for an additional 5 min. This was then followed by the addition of the silyl ketene acetal **460** (62 μL, 0.3 mmol). The resulting reaction mixture was stirred for 24 h at room temperature. Aqueous $NaHCO_3$ (2 mL) was added to quench the reaction. The mixture was extracted with CH_2Cl_2 (10 mL × 2). The combined organic layer was concentrated *in vacuo* to give the crude product. The crude product was then treated with a mixture of THF and aqueous 1N HCl (11 mL, 10:1, v/v) at 0 ºC for 30 min. The hydrolysis was quenched with aqueous $NaHCO_3$ (2 mL) and then extracted with ethyl acetate (10 mL × 2). The combined organic layer was washed with brine and dried with anhydrous $MgSO_4$ and concentrated *in vacuo* to give the crude product

461a. Purification of the crude product by silica gel column chromatography (20 × 280 mm, 5:1 hexanes/EtOAc as eluent) afforded pure ester **461a** in 95% yield (71 mg, 0.24 mmol). The optical purity of **461a** was determined to be 89% *ee* by HPLC analysis (Daicel Chiralpak AD, 90:10 Hexanes/i-PrOH at 222 nm, flow rate: 1.0 mL/min): retention times; R_t = 8.47 min (major enantiomer, **461a**), R_t = 14.73 min (minor enantiomer, *ent*-**461a**).

Spectral data for **461a**: R_f = 0.36 (1:5 EtOAc/hexane); ^{1}H NMR ($CDCl_3$, 300 MHz) δ 1.22 (s, 3H), 1.24 (s, 3H), 3.69 (s, 3H), 4.55 (brs, 1H), 4.87 (brs, 1H), 5.31 (s, 1H), 6.39 (dd, *J* = 7.7, 1.3 Hz, 1H), 6.54 (td, *J* = 7.5, 1.4 Hz, 1H), 6.62 (td, *J* = 7.5, 1.3 Hz, 1H), 6.69 (dd, *J* = 7.5, 1.2 Hz, 1H), 7.32-7.19 (m, 5H); ^{13}C ($CDCl_3$, 75 MHz) δ 19.93, 24.22, 47.27, 52.31, 64.27, 113.18, 114.10, 117.56, 120.79, 127.34, 127.93, 128.32, 135.60, 138.90, 144.03, 177.70. These spectral data match those previously reported for this compound.[5b]

(b) At –45 ºC

(*R*)-methyl 3-((2-hydroxyphenyl)amino)-2,2-dimethyl-3-phenylpropanoate 461a: To a 10 mL flame-dried round bottom flask were added (*S*)-VAPOL (59.25 mg, 0.1100 mmol) and $Zr(O^iPr)_4$•^{i}PrOH (19.38 mg, 0.0500 mmol) in toluene (0.9 mL). To this solution was added 1-methylimidazole (4.78 μL, 0.060 mmol) in toluene (0.1 mL) at room temperature. The mixture was stirred for 1 h at the same temperature. A solution of imine **457a** (49.31 mg, 0.2500 mmol) in toluene (1 mL) was added to the flask containing the catalyst and the mixture was stirred for an additional 5 min. Then the mixture was cooled to –45°C followed by the addition of the silyl ketene acetal (62 μL, 0.3 mmol). The resulting reaction mixture was stirred for 24 h at – 45 ºC.

Aqueous $NaHCO_3$ (2 mL) was added to quench the reaction. The mixture was extracted with CH_2Cl_2 (10 mL × 2). The combined organic layer was concentrated *in vacuo* to give the crude product. The crude product was then treated with a mixture of THF and aqueous 1N HCl (11 mL, 10:1, v/v) at 0 ºC for 30 min. The hydrolysis was quenched with aqueous $NaHCO_3$ (2 mL) and then extracted with ethyl acetate (10 mL × 2). The combined organic layer was washed with brine and dried with anhydrous $MgSO_4$ and concentrated *in vacuo* to give the crude product **461a**. Purification of the crude product by silica gel column chromatography (20 × 280 mm, 5:1 hexanes/EtOAc as eluent) afforded pure ester **461a** in 92% yield (69 mg, 0.23 mmol). The optical purity of **461a** was determined to be 91% *ee* by HPLC analysis (Daicel Chiralpak AD, 90:10 Hexanes/i-PrOH at 222 nm, flow rate: 1.0 mL/min): retention times; R_t = 8.47 min (major enantiomer, **461a**), R_t = 14.73 min (minor enantiomer, *ent*-**461a**).

The ligands **59**, **197** and **482** were also screened using the procedure described above and the results are presented in Table 9.2.

9.10.4 DFT Calculations

All quantum mechanical calculations were performed using the Gaussian '03.[8] The B3LYP[11] and BHandHLYP[9,12] density functional were used along with 6-31G* basis sets. The coordinates of all transition states were provided to Prof. Wulff as a separate file.

REFERENCES

REFERENCES

(1) Mannich, C.; Krösche, W. *Archiv Der Pharmazie* **1912**, *250*, 647-667.

(2) (a) Kobayashi, S.; Mori, Y.; Fossey, J. S.; Salter, M. M. *Chem. Rev.* **2011**, *111*, 2626-2704. (b) Ting, A.; Schaus, S. E. *Eur. J. Org. Chem.* **2007**, 5797-5815. (c) Friestad, G. K.; Mathies, A. K. *Tetrahedron* **2007**, *63*, 2541-2569. (d) Kobayashi, S.; Ueno, M. In *Comprehensive Asymmetric Catalysis*; Jacobsen, E. N., Pfaltz, A., Yamamoto, H., Eds.; Supplement 1; Springer: Berlin, 2003; Chapter 29.5, p 143. (e) Kobayashi, S.; Ishitani, H. *Chem. Rev.* **1999**, *99*, 1069-1094. (f) Arend, M.; Westermann, B.; Risch, N. *Angew. Chem., Int. Ed.* **1998**, *37*, 1044-1070.

(3) (a) KLeinman, E. F. In *Comprehensive Organic Synthesis*; Trost, B. M., Ed.; Pergamon Press: Oxford, 1991; Chapter 2.3, Vol. 2, p 893. (b) Arend, M. *Angew. Chem., Int. Ed.* **1999**, *38*, 2873-2874. (c) *Enantioselective Synthesis of β-amino acids*; 2nd ed.; Juaristi, E.; Soloshonok, V. A., Eds.; John Wiley & Sons: Hoboken, New Jersey, 2005.

(4) (a) Ishihara, K.; Miyata, M.; Hattori, K.; Tada, T.; Yamamoto, H. *J. Am. Chem. Soc.* **1994**, *116*, 10520-10524. (b) Müller, R.; Goesmann, H.; Waldmann, H. *Angew. Chem., Int. Ed.* **1999**, *38*, 184-187.

(5) (a) Benaglia, M.; Biaggi, C.; Annunziata, R.; Rossi, S. *Chirality* **2010**, *22*, 369-378. (b) Akiyama, T.; Katoh, T.; Mori, K.; Kanno, K. *Synlett* **2009**, 1664-1666. (c) Marcel Sickert, C. S. *Angew. Chem., Int. Ed.* **2008**, *47*, 3631-3634. (d) Giera, D. S.; Sickert, M.; Schneider, C. *Org. Lett.* **2008**, *10*, 4259-4262. (e) Yamanaka, M.; Itoh, J.; Fuchibe, K.; Akiyama, T. *J. Am. Chem. Soc.* **2007**, *129*, 6756-6764.

(6) Ishitani, H.; Ueno, M.; Kobayashi, S. *J. Am. Chem. Soc.* **1997**, *119*, 7153-7154.

(7) Xue, S.; Yu, S.; Deng, Y.; Wulff, W. D. *Angew. Chem., Int. Ed.* **2001**, *40*, 2271-2274.

(8) Gaussian 03, Revision D.01 M. J. Frisch, G. W. T., H. B. Schlegel, G. E. Scuseria, M. A. Robb, J. R. Cheeseman, J. A. Montgomery, Jr., T. Vreven, K. N. Kudin, J. C. Burant, J. M. Millam, S. S. Iyengar, J. Tomasi, V. Barone, B. Mennucci, M. Cossi, G. Scalmani, N. Rega, G. A. Petersson, H. Nakatsuji, M. Hada, M. Ehara, K. Toyota, R. Fukuda, J. Hasegawa, M. Ishida, T. Nakajima, Y. Honda, O. Kitao, H. Nakai, M. Klene, X. Li, J. E. Knox, H. P. Hratchian, J. B. Cross, V. Bakken, C. Adamo, J. Jaramillo, R. Gomperts, R. E. Stratmann, O. Yazyev, A. J. Austin, R. Cammi, C. Pomelli, J. W. Ochterski, P. Y. Ayala, K. Morokuma, G. A. Voth, P. Salvador, J. J. Dannenberg, V. G. Zakrzewski, S. Dapprich, A. D. Daniels, M. C. Strain, O. Farkas, D. K. Malick, A. D. Rabuck, K. Raghavachari, J. B. Foresman, J. V. Ortiz, Q. Cui, A. G.

Baboul, S. Clifford, J. Cioslowski, B. B. Stefanov, G. Liu, A. Liashenko, P. Piskorz, I. Komaromi, R. L. Martin, D. J. Fox, T. Keith, M. A. Al-Laham, C. Y. Peng, A. Nanayakkara, M. Challacombe, P. M. W. Gill, B. Johnson, W. Chen, M. W. Wong, C. Gonzalez, and J. A. Pople, Gaussian, Inc., Wallingford CT, 2004

(9) (a) Zhao, Y.; Truhlar, D. G. *J. Chem. Theory Comput.* **2005**, *1*, 415-432. (b) Yu, W.; Liang, L.; Lin, Z.; Ling, S.; Haranczyk, M.; Gutowski, M. *J. Comput. Chem.* **2009**, *30*, 589-600.

(10) López, C.; Caubet, A.; Péreza, S.; Solans, X.; Font-Bardía, M. *J. Organomet. Chem.* **2003**, *681*, 82-90.

(11) (a) Becke, A. D. *Phys. Rev. A* **1988**, *38*, 3098. (b) Lee, C. Y., W.; Parr, R. G. *Phys. Rev. B* **1988**, *37*, 785.

(12) Becke, A. D. *J. Chem. Phys.* **1993**, *98*, 1372-1377.